30th International Conference Ecological Truth & Environmental Research 2023

Proceedings

Editor
Prof. Dr Snežana Šerbula

University of Belgrade, Technical Faculty in Bor

30

ECOTER

30th International Conference Ecological Truth & Environmental Research 2023

Proceedings

Editor
Prof. Dr Snežana Šerbula

PROCEEDINGS

30th INTERNATIONAL CONFERENCE

ECOLOGICAL TRUTH AND ENVIRONMENTAL RESEARCH – EcoTER'23

Editor:

Prof. Dr Snežana Šerbula

University of Belgrade, Technical Faculty in Bor

Editor of Student section:

Prof. Dr Maja Nujkić

University of Belgrade, Technical Faculty in Bor

Technical editors:

Jelena Milosavljević, PhD, University of Belgrade, Technical Faculty in Bor

Asst. prof. Dr Ana Radojević, University of Belgrade, Technical Faculty in Bor

Sonja Stanković, **MSc**, University of Belgrade, Technical Faculty in Bor

Cover design:

Aleksandar Cvetković, **BSc**, University of Belgrade, Technical Faculty in Bor

Publisher: University of Belgrade, Technical Faculty in Bor

For the publisher: Prof. Dr Dejan Tanikić, Dean

Printed: University of Belgrade, Technical Faculty in Bor, 100 copies, electronic edition

Year of publication: 2023

ISBN 978-86-6305-137-9

CIP - Каталогизација у публикацији
Народна библиотека Србије, Београд

502/504(082)(0.034.2)
574(082)(0.034.2)

INTERNATIONAL Conference Ecological Truth & Environmental Research (30 ; 2023)
Proceedings [Elektronski izvor] / 30th International Conference Ecological Truth & Environmental Research - EcoTER'23, 20-23 June 2023, Serbia ; organized by University of Belgrade, Technical faculty in Bor (Serbia) ; co-organizers University of Banja Luka, Faculty of Technology – Banja Luka (B&H) ... [et al.] ; [editor Snežana Šerbula]. - Bor : University of Belgrade, Technical faculty, 2023 (Bor : University of Belgrade, Technical faculty). - 1 elektronski optički disk (CD-ROM) ; 12 cm

Sistemski zahtevi: Nisu navedeni. - Nasl. sa naslovne strane dokumenta. - Preface / Snežana Šerbula. - Tiraž 100. - Bibliografija uz svaki rad.

ISBN 978-86-6305-137-9

а) Животна средина -- Зборници б) Екологија – Зборници

COBISS.SR-ID 118723849

30th International Conference
Ecological Truth and Environmental Research – EcoTER'23

is organized by:

UNIVERSITY OF BELGRADE
TECHNICAL FACULTY IN BOR (SERBIA)

Co-organizers of the Conference:

**University of Banja Luka, Faculty of Technology,
Banja Luka (B&H)**

**University of Montenegro, Faculty of Metallurgy and Technology,
Podgorica (Montenegro)**

University of Zagreb, Faculty of Metallurgy, Sisak (Croatia)

**University of Pristina, Faculty of Technical Sciences,
Kosovska Mitrovica**

Association of Young Researchers Bor (Serbia)

Gold Donor of the Conference

HONORARY COMMITTEE

Dr. Petar Paunović
(Zaječar, Serbia)
Prof. Dr Zvonimir Stanković
(Bor, Serbia)
Prof. Dr Velizar Stanković
(Bor, Serbia)
Prof. Dr Milan Antonijević
(Bor, Serbia)
Dragan Ranđelović, Association of Young Researchers Bor
(Bor, Serbia)
Toplica Marjanović, Association of Young Researchers Bor
(Bor, Serbia)
Mihajlo Stanković, Special Nature Reserve Zasavica
(Sremska Mitrovica, Serbia)

SCIENTIFIC COMMITTEE

Prof. Dr Snežana Šerbula, *President*

Prof. Dr Alok Mittal (India)
Prof. Dr Jan Bogaert (Belgium)
Prof. Dr Aleksandra Nadgórska-Socha (Poland)
Prof. Dr Luis A. Cisternas (Chile)
Prof. Dr Wenhong Fan (China)
Prof. Dr Martin Brtnický (Czech Republic)
Prof. Dr Isabel M. De Oliveira Abrantes (Portugal)
Prof. Dr Shengguo Xue (China)
Prof. Dr Tomáš Lošák (Czech Republic)
Prof. Dr Maurice Millet (France)
Prof. Dr Murray T. Brown (New Zealand)
Prof. Dr Xiaosan Luo (China)
Prof. Dr Daniel J. Bain (United States of America)
Prof. Dr Che Fauziah Binti Ishak (Malaysia)
Prof. Dr Richard Thornton Baker (United Kingdom)
Prof. Dr Mohamed Damak (Tunisia)
Prof. Dr Jyoti Mittal (India)
Prof. Dr Miriam Balaban (United States of America)
Prof. Dr Yeomin Yoon (United States of America)
Prof. Dr Chang-min Park (South Korea)
Prof. Dr Faramarz Doulati Ardejani (Iran)
Prof. Dr Ladislav Lazić (Croatia)
Prof. Dr Natalija Dolić (Croatia)
Prof. Dr Milutin Milosavljević (Kosovska Mitrovica)
Prof. Dr Nenad Stavretović (Serbia)
Prof. Dr Ivan Mihajlović (Serbia)
Prof. Dr Milovan Vuković (Serbia)
Prof. Dr Nada Blagojević (Montenegro)
Prof. Dr Darko Vuksanović (Montenegro)
Prof. Dr Irena Nikolić (Montenegro)
Prof. Dr Šefket Goletić (B&H)
Prof. Dr Džafer Dautbegović (B&H)
Prof. Dr Borislav Malinović (B&H)
Prof. Dr Slavica Sladojević (B&H)
Prof. Dr Nada Šumatić (B&H)
Prof. Dr Snežana Milić (Serbia)

ORGANIZING COMMITTEE

Prof. Dr Snežana Šerbula, *President*

Prof. Dr Snežana Milić, *Vice President*

Prof. Dr Đorđe Nikolić, *Vice President*

Prof. Dr Marija Petrović Mihajlović

Prof. Dr Milan Radovanović

Prof. Dr Milica Veličković

Prof. Dr Danijela Voza

Prof. Dr Maja Nujkić

Prof. Dr Žaklina Tasić

Dr Ana Simonović

Dr Tanja Kalinović

Dr Ana Radojević

Dr Jelena Kalinović

Dr Jelena Milosavljević

Sonja Stanković, MSc

Miljan Marković, MSc

Vladan Nedelkovski, MSc

Aleksandar Cvetković, BSc

PREFACE

The 30th international conference Ecological Truth & Environmental Research – EcoTER'23 kept three areas in focus: ecology, environmental protection and sustainable development. The conference will be held on Mt Stara Planina in hotel Stara Planina, Serbia, 20–23 June 2023. The monograph is published on the occasion of the 30th anniversary of the conference. On behalf of the scientific and organizing committee, it is a great honor and pleasure to wish all the participants a warm welcome to the conference.

The monograph is published on the occasion of the 30th anniversary of the conference.

We hope to convey the message of the conference, which is that a transformation of attitudes and behavior would bring the necessary changes. This is also an opportunity for the participants who are experts in this field to exchange their experiences, expertise and ideas, and also to consider the possibilities for their collaborative research.

The 30th international conference Ecological Truth & Environmental Research – EcoTER'23 is organized by the University of Belgrade, Technical Faculty in Bor, and co-organized by the University of Banja Luka, Faculty of Technology, the University of Montenegro, Faculty of Metallurgy and Technology – Podgorica, the University of Zagreb, Faculty of Metallurgy – Sisak, the University of Pristina, Faculty of Technical Sciences – Kosovska Mitrovica and the Association of Young Researchers, Bor.

These Proceedings 103 papers from the authors coming from the universities, research institutes and industries in 11 countries: Australia, USA, Brazil, Spain, Portugal, Libya, Italy, Bulgaria, Bosnia and Herzegovina, North Macedonia, and Serbia.

As a part of this year's conference, the 5th Student Session – EcoTERS'23 is being held. We appreciate the contribution of the students and their mentors who have also participated in the conference.

The support of the Gold donor and their willingness and ability to cooperate has been of great importance for the success of the EcoTER'23. The organizing committee would like to extend their appreciation and gratitude to the Gold donor of the conference for their donation and support.

We appreciate the effort of all the authors who have contributed to these Proceedings. We would also like to express our gratitude to the members of the scientific and organizing committees, reviewers, speakers, chairpersons and all the conference participants for their support to the EcoTER'23. Sincere thanks go to all the people who have contributed to the successful organization of the EcoTER'23.

Prof. Snežana Šerbula,

President of the scientific and organizing committee

TABLE OF CONTENTS

Plenary Lecture

Invited Lectures

Conference Papers

Environmental monitoring and impact assessment

Student Section

Plenary Lecture

OPTICALLY ACTIVE NANOMATERIALS FOR ENVIRONMENTAL REMEDIATION

Lidija Mančić[1*], Maria Eugenia Rabanal[2], Bojan Marinkovic[3]
[1]Institute of Technical Sciences of SASA, Belgrade, SERBIA
[2]University Carlos III, Madrid, SPAIN
[3]Pontifical Catholic University of Rio de Janeiro, RJ, BRAZIL
[*]*lidija.mancic@itn.sanu.ac.rs*

Abstract

In recent years optically active nanomaterials have opened up a number of frontiers, especially in life science and environmental protection. Novel hybrid nanomaterials based on wide band gap oxides (TiO_2) and Ln^{3+} doped rare earth compounds (down- and up-conversion luminescence materials) obtained through innovative processing will be presented from the viewpoint of their potential application for light harvesting and photocatalysis.

Keywords: luminescence, up-conversion, core-shell, charge-transfer complex, photocatalysis.

INTRODUCTION

The field of nanoscience has made exciting progress in recent decades, particularly regarding the synthesis of optically active nanoparticles that might be able to solve some of the aroused energy and environmental problems. One of the key points in achieving a sustainable low carbon society is development of innovative synthesis routes which could ensure processing of nanomaterials in a controlled manner. The synthesis from solution, such as spray pyrolysis and hydro/solvo-thermal processing, offers many advantages over conventional solid-state synthesis: design of nanomaterials at the molecular level, tuning of their crystallinity, control of morphology and homogeneous doping. While spray pyrolysis comprises formation and decomposition of aerosol in a high temperature tubular flow reactor, hydro/solvothermal processing refers to any homogeneous or heterogeneous reaction in the presence of aqueous or organic solvents at elevated pressure and temperature in a closed vessel. Both methods are successfully developed in the scope of research activities in the Institute of Technical Sciences of SASA [1,2]. The examples from some wide band gap oxides and down- and up-conversion luminescence materials processed using these, will be presented and discussed from the viewpoint of their potential use for environmental remediation.

MATERIALS AND METHODS

YAG:Ce, $Y_{1-x}Gd_xO_3$:Eu, Y_2O_3:Yb and $NaY_{1-x}Gd_xF_4$:Yb co-doped with Er, Tm or Ho, YF_3:Yb,Er, hybrid TiO_2 and TiO_2-based nanoparticles, as well as, Y_2O_3:Eu@Ag and

$NaYF_4$:Yb,Tm@TiO_2-Acac core-shell structures, were synthesised in accordance to the previously published procedures [1–10].

RESULTS AND DISCUSSION

Figure 1 presents typical morphologies of nanoparticles obtained through spray pyrolysis in function of precursor type. The diverse levels of structural, morphological and functional complexity are achieved by appropriate setting of processing parameters, i.e. temperature (which controls volume/surface precipitation in droplets and phase composition) and precursor concentration (which affects particle size and agglomeration degree).

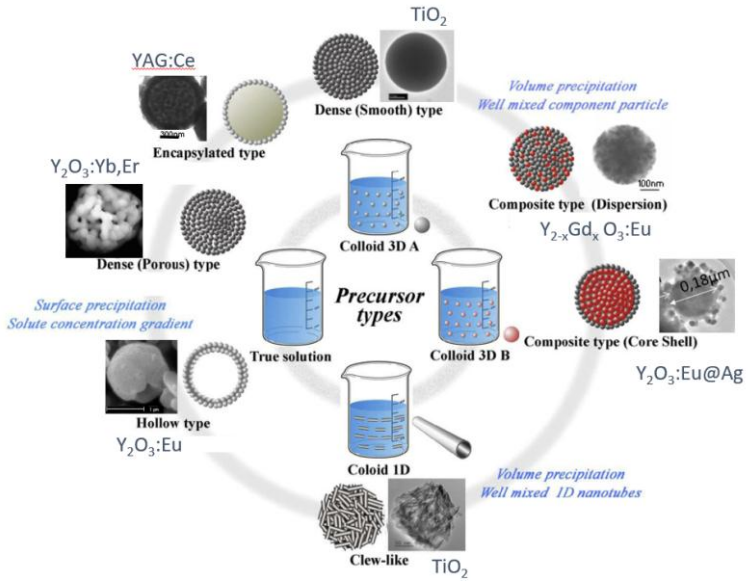

Figure 1 *Morphologies of nanoparticles obtained through spray pyrolysis*

Figure 2 presents typical morphologies of nanoparticles obtained through hydro/solvo-thermal processing. Their structural properties are defined by the main processing parameters, i.e., temperature, pressure, time, pH and precursor/solvent type, while their surface chemistry is tailored by the addition of surfactants (EDTA, PEG, PVP, PLGA, Chitosan).

Both methods belong to the bottom-up building blocks synthesis approach, which enables enhancing a specific functionality through the synergy of properties associated with different structural levels and interactions at their interfaces. As a result, such particles could be used in displays, lighting, photovoltaics and photocatalysis. For lighting application in small devices, besides being used as white emission mercury-free sources, nanophosphors need to have broad range tunability of a multi-colour emission by single wavelength excitation which could be achieved through co-doping. Tuneable absorption in the infrared spectrum and ability to convert a low-energy infrared radiation into high-energy emission, make them attractive for infrared-driven photocatalysis and light harvesting improvement in the state-of-the-art solar cells. This is because the spectral distribution of sunlight at air mass 1.5 Global includes photons with a wide range of wavelengths, ranging from 280 to 2500 nm (0.5–4.4 eV), while

the current generation of photocatalysts and solar cells utilize only a small fraction of the incident photons which energy match their energy bandgap.

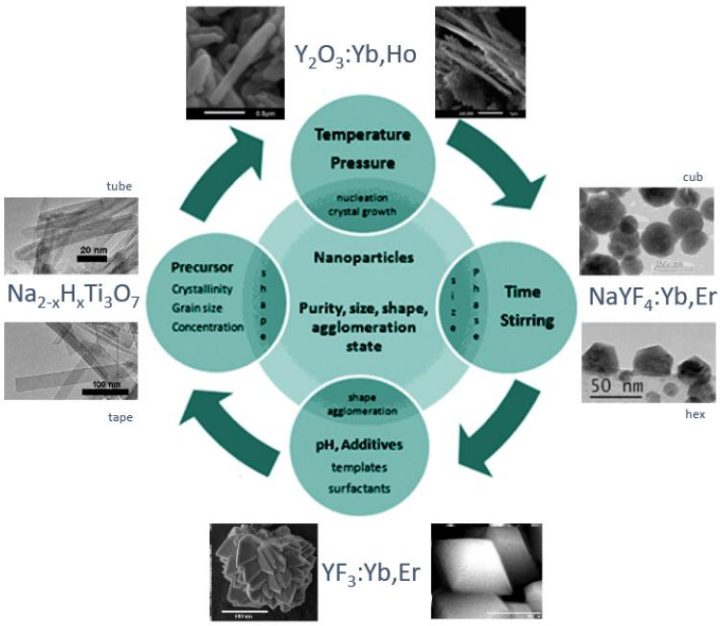

Figure 2 *Morphologies of nanoparticles obtained through hydro/solvo-thermal processing*

Recently we shown that efficiency of the novel hybrid core-shell structure, in which up-converting core $NaYF_4$:Yb,Tm acts as a medium for converting NIR to visible light via multiphoton up-conversion processes while TiO_2-Acetylacetonate shell absorbs the visible light through direct injection of excited electrons from the highest-occupied-molecular-orbital (HOMO) of Acetylacetonate into the TiO_2 conduction band (CB), toward tetracycline degradation is twofold better that of TiO_2-Acetylacetonate solely.

CONCLUSION

The essential principles for rational design of efficient optically active materials were highlighted. Particular emphasis is placed on synthesis methods developed in the Institute of Technical Sciences of Serbia, as well as on hybrid structure materials for future development of infrared-driven photocatalysts and photovoltaics.

ACKNOWLEDGEMENT

The corresponding author is grateful to the Ministry of Science, Technological Development and Innovation of Republic of Serbia for financial support according to the contract with the registration number (451-03-47/2023-01/200175) and Science Fund of the Republic of Serbia (program DIJASPORA, #6421090, COSH-PHOTO).

REFERENCES

[1] Milosevic O., Mancic L., Rabanal M. E., *et al*., Powder Part. J. 27 (2009) 84–106.

[2] Mancic L., Nikolic M., Gomez L., *et al*., Adv. Powder Technol. 28 (2017) 3–22.

[3] Dugandžić I., Jovanović D. J., Mančić L., *et al*., J. Nanoparticle Res. 14 (2012) 1157.

[4] Mancic L., Marinkovic K., Marinkovic B.A., *et al*., J. Eur. Ceram. 30 (2010) 577–582.

[5] Alkan G., Mancic L., Tamura S., *et al*., Adv. Powder Technol. 30 (2019) 1409–1418.

[6] Mancic L., Marinkovic B. A., Jardim P. M., *et al*., Cryst. Growth Des. 9 (2009) 2152–2158.

[7] Habran M., Ponton P. I., Mancic L., *et al*., J. Photochem. Photobiol. A 365 (2018) 133–144.

[8] Dinic I. Z. Mancic L. T., Rabanal M. E., *et al*., Adv. Powder Technol. 28 (2017) 73–82.

[9] Mancic L., Lojpur V., Marinkovic B., *et al*., Adv. Powder Technol. 25 (2014) 1449–1454.

[10] Marković S., Machado T. M., Dinić I., *et al*., Proceedings of the 15th International Conference on Fundamental and Applied Aspects of Physical Chemistry Vol II, on-line (2021) 399–401.

Invited lectures

THE EXTRACTION OF ACTIVE COMPOUNDS FROM PLANT WASTE: THE POTENTIAL IN HUMAN AND INDUSTRIAL APPLICATIONS AS THE CONCEPT OF ZERO WASTE IN THE CIRCULAR ECONOMY

Aleksandra A. Jovanović[1*]

[1]University of Belgrade, Institute for the Application of Nuclear Energy INEP, Banatska 31b, 11080 Zemun Belgrade, SERBIA

[*]*ajovanovic@inep.co.rs*

Abstract

Plant waste contains various active compounds that can be applied in food, pharmaceutical, cosmetic, or other industries. Polyphenols, carotenoids, pectin, aromas, fibers, or enzymes extracted from agri-food waste can be considered ready-to-use without demanding and expensive downstream isolation and purification steps. In the present study, plant extracts were prepared using Thymus serpyllum and Vaccinium myrtillus leaf dust and empty Aloe vera leaves (the matrix without aloe gel). The biological potential of T. serpyllum, V. myrtillus, and A. vera waste extracts with the highest polyphenol yield was investigated. T. serpyllum extract possessed the highest DPPH radical scavenging capacity (1.50±0.02 mg/mL). It also had antimicrobial potential against all examined strains, particularly against Enterococcus faecalis, and showed spasmolytic activities in isolated rat ileum models of spontaneous contractions, acetylcholine- and potassium chloride-induced contractions. V. myrtillus extract showed the highest ABTS radical scavenging potential (48.77±1.47 µmol Trolox equivalents/g of plant material) and significant antimicrobial and skin regeneration activity (percentage of wound healing was 29.2±1.8). However, A. vera extract had the lowest antioxidant capacity and did not show antimicrobial potential, while it showed a significant wound healing influence (30.9±1.7%). Due to showed the biological potential of all prepared waste extracts, they can be potentially used in the food, pharmaceutical, and cosmetic industries. In future experiments, T. serpyllum waste extract will be examined in terms of bronchodilatory activity, whereas all prepared waste extracts will be investigated via effects on enzymes, dying of textile, as well as anticorrosive effects.

Keywords: biological activities, extraction, industrial potential, plant waste.

INTRODUCTION

Plant waste or by-products possess plenty of bioactive compounds that may be applied in various food, functional food, pharmaceutical, or cosmetic formulations. According to Panić *et al*. [1], polyphenol extracts of grape and olive pomace (as food by-products) can be considered ready-to-use in pharmaceutical, food, and cosmetic industries without demanding and expensive processes of isolation and purification. Additionally, distillation liquid residues of several aromatic plants are used for the extraction of antioxidant and antimicrobial agents, including phenolic acids [2]. Due to the establishment of modern extraction techniques, dietary fibers from vegetable and fruit waste, such as onion layers, potato peels, cauliflower stems and florets, carrot and tomato pomace, apple, mango, orange, and peach peel, as well as polyphenol compounds from citrus, pear, apple, peach, and pomegranate peels, can be

successfully extracted and used [2,3]. Tea factories produce a higher amount of waste, including microfined tea dust, tea seeds, winnowings, and floor sweepings. Since the quantity of by-products generated from teas and aromatic plants manufacturing processes shows a significant increase with annual increment of their production over the world, the use of medicinal plants' waste as a low-cost material in different branches of industry has aroused more and more interest for recycling and reuse purposes. Tea dust represents particles lower than 0.5 mm which according to Regulations on the quality of tea, herbal tea, and their products of the Republic of Serbia cannot be an integral part of the tea products for the market, trade, and sale [4]. Examples of such plant waste are *Thymus serpyllum* and *Vaccinium myrtillus* leaf waste. Empty *Aloe vera* leaves (the matrix without aloe gel) also represent plant waste that is rich in carbohydrates, amino acids, lipids, organic acids, chromones, flavonoids, anthraquinones, minerals, vitamins, pigments, and volatile organic components [5].

The next step after the collection of plant waste is the extraction of the target compounds, i.e. the optimization of the extraction process *via* varying solvent types, solid-to-solvent ratio, extraction time, and technique. Furthermore, in recent studies, different methods for the extraction of bioactive compounds were established [6–8]. The extraction techniques vary in nature of the plant matrix, extraction medium, solvent-to-solid ratio, time, temperature, pressure, and pH. Considering that polyphenols, as the most biologically active plant metabolites, are various in structure, it is not simple to establish a standardized extraction process that would extract the majority of polyphenols from each plant matrix. However, traditional extraction procedures possess several disadvantages, such as low extraction yield, long extraction time, a large amount of plant material, high solvent consumption, and negative environmental impact. Hence, in recent time, application of the modern extraction methods have been evaluated, including heat-assisted extraction. Novel procedures provide numerous benefits, including solvent saving, shorter time of extraction, and high extract quality. Additionally, modern techniques support the concept of "green" solvent, which is aimed to minimize the negative environmental impact of the utilization of large amounts of solvents in the extraction process. It has also shown that simple alcohols (e.g. ethanol), as well as alcohol-water mixtures, are more environmentally favorable solvents [8].

Preparation of the extracts with the highest yield of target compounds under the optimized extraction conditions is further followed by their physicochemical characterization and investigation of the biological activities, including antioxidant, antimicrobial, enzyme inhibition, spasmolytic, skin regeneration potential (depending on the presence of the active compounds of the plants).

In this paper, the biological potential of *T. serpyllum*, *V. myrtillus*, and *A. vera* waste extracts with the highest polyphenol yield was represented.

MATERIALS AND METHODS

Plant materials and reagents

T. serpyllum and *V. myrtillus* leaf waste was herbal dust, the particle size of 0.3 mm or lower resulting from the grinding of the initial plant material in the Institute for Medicinal Plants Research “Dr Josif Pančić”, Pančevo, Serbia. *A. vera* was purchased in ASC Garden

d.o.o., Belgrade, Serbia. The aloe gel was removed from the leaves. Subsequently, clean and empty leaves that represent the waste were cut and freeze-dried in Beta 2-8 LD plus (Christ, Germany). Ethanol (Merck, Germany), 2,2'-azino-bis(3-ethylbenzothiazoline-6-sulphonic acid) or ABTS, 6-hydroxy-2,5,7,8-tetramethylchroman-2-carboxylic acid or Trolox, and 2,2-diphenyl-1-picrylhydrazyl or DPPH (Sigma-Aldrich, Germany), dimethyl sulfoxide or DMSO, triphenyltetrazolium chloride or TTC, amoxicillin, fluconazole, sodium dodecyl sulfate, high-glucose Dulbecco's Modified Eagle Medium (DMEM) supplemented with 10% fetal bovine serum (FBS), and thiazolyl blue tetrazolium bromide or MTT (Sigma-Aldrich, USA).

Extraction procedure

Heat-assisted extraction from all types of plant waste for (*T. serpyllum*, *V. myrtillus*, and *A. vera*) was performed at 80°C using the incubator shaker KS 4000i control (IKA, Germany) and 50% ethanol at a solid-to-solvent ratio of 1:30 g/mL for 30 min. The extracts were prepared in the Erlenmeyer flasks covered by aluminum foil to avoid light exposure and evaporation of the solvent. After the extraction, the sample was filtered using filter paper and stored at 4°C until further experiments.

Lyophilization

In order to obtain dried extracts for antimicrobial, skin regeneration, and spasmolytic potential analyses, liquid extracts were lyophilized. The ethanol from the extracts was evaporated using Heizbad Hei-VAP (Heidolph, Germany) at 40–50°C, a pressure of 50 mbar, and a rotation speed of 150 rpm. Subsequently, the sample was frozen in the freezer, at -80°C for 1 h and freeze-dried at -75°C and pressure of 0.011 mbar for 24 h and at -65°C and pressure of 0.054 mbar for one additional hour (Alpha 2-4 LSCplus, Christ, Germany).

Examination of the biological potential of the extracts

Antioxidant activity

The ABTS assay was based on the procedure described by Li *et al*. [9] with a slight modification and the absorbance was measured at 734 nm. The antioxidant activity was expressed as mmol Trolox equivalent per g of plant material (μmol TE/g). The DPPH assay was based on the procedure described by Xi and Jan [10] with a slight modification and the absorbance was measured at 517 nm. The results were expressed as IC_{50} (mg/mL), defined as the concentration of the extract required to scavenge 50% of DPPH free radicals.

All spectrophotometric measurements were performed in a UV-1800 spectrophotometer (Shimadzu, Japan).

Antimicrobial activity

The minimum inhibitory (MIC) and minimum bactericidal or fungicidal concentrations (MBC or MFC) of the extracts were determined by broth micro-dilution assay. Antimicrobial capacity was examined against *Bacillus cereus*, *Enterococcus faecalis*, *Staphylococcus aureus*, *Escherichia coli*, *Salmonella enterica*, and *Candida albicans*. The antimicrobial assay was performed using sterile 96-well microliter plates. The extract was dissolved in 5% DMSO aqueous solution, while 0.0075% TTC was used as a growth indicator. Positive growth control was a 5% DMSO in an appropriate medium. Plates with bacteria were incubated at 37°C for 24 h, whereas plates with fungus were incubated at 32°C for 48 h. The lowest

concentration of extract without any visible growth of microbial strains was considered as MIC value. MBC and MFC were determined by serial sub-cultivation of the samples taken from each well that showed no change in color into microplates containing the appropriate medium. The lowest concentration without any visible growth after repeated incubation was taken as MBC or MFC. Amoxicillin and fluconazole were used as positive control for bacterial and fungal strains, respectively. The antimicrobial analysis was done in triplicate and the highest value was taken as MIC and MBC/MFC, thus the results are not shown as average values of several measurements with standard deviation, but a "stricter criteria" rule was applied, common in antimicrobial assays.

Spasmolytic activity

The examination of the spasmolytic activity of *T. serpyllum* extract was performed using isolated rat ileum and three experimental models, including spontaneous contractions, acetylcholine- and potassium chloride-induced contractions. All experimental procedures were on eighteen male Wistar albino rats. The segments of the ileum (2 cm) were mounted in 10 mL of Tyrode's solution in the organ bath (37°C, pH 7.4, a mixture of 5% carbon dioxide and 95% oxygen), between two stainless steel hooks with continuous air-bubbling. Six segments of isolated rat ileum were tested in each experimental model. The change in intestinal activity was determined using transducer TSZ-04-E and analyzed with a SPEL Advanced ISOSYS Data Acquisition System. The extract and control compounds were added directly to the organ bath; the area under the curve was estimated. First, the influence of extract on spontaneous contractions of isolated rat ileum was examined. After the stabilization period, the segment of the ileum was exposed to the extract, whereas papaverine was used as a positive control. The spasmolytic activity of the sample was expressed as a percentage of the control contractility without extract. Additionally, the increasing concentrations of acetylcholine were added to the organ bath cumulatively in order to obtain the maximum contractile response curve. Further, the acetylcholine induced-contractions were registered in the presence of extract, whereas atropine was used as a positive control. In the third experimental model, the rat ileum contractions were induced using 80 mM KCl solution, while verapamil was used as a positive control; the extract was cumulatively added to the organ bath. The relaxation of the ileum segment in the presence of extract or antagonist was expressed as a percentage of the maximum contractile response induced by acetylcholine or KCl. After each experimental model, the intestinal preparation was flushed with fresh Tyrode's solution and left to adapt for 10 min.

Skin regeneration activity (cell viability and wound-scratch healing assays)

The viability of spontaneously immortalized keratinocyte cells (HaCaT) in the presence of *V. myrtillus* and *A. vera* waste extracts was assessed using the MTT assay. The cells (10^4/well) were seeded in 96-well plates in 100 μL of the complete medium and allowed to adhere overnight at 37°C in a 5% CO_2 incubator. After 24 h of incubation, cells were rinsed with warm, sterile phosphate-buffered saline (PBS) and further cultured in a complete medium in the absence and presence of the extract. The cells were incubated for 24 h at 37°C. and the medium was removed and replaced with 100 μL of fresh complete medium containing MTT and incubated for 3 h at 37°C. Subsequently, 100 μL of 10% sodium dodecyl sulfate was added to each well and the plate was further incubated at 37°C overnight. The absorbance

was measured at 570 nm using a microplate reader. The results were expressed as IC_{50} value, indicating 50% of cell viability when compared with untreated control. Namely, the criterion used to categorize the cytotoxicity of preparations in HaCaT cell line was as follows: IC_{50}≤20 µg/mL=highly cytotoxic, IC_{50} 21–200 µg/mL=moderately cytotoxic, IC_{50} 201–400 µg/mL=weakly cytotoxic, and IC_{50}>401µg/mL=no cytotoxicity.

The HaCaT cells were grown to confluency. The cell monolayer was scraped using a 200 µL tip. The floating cells were washed and grown in DMEM with 1% FBS, 2 mM L-glutamine, 1% antibiotic-antimycotic, and 250 g/mL or IC_{25} concentrations of the extracts. Cell migration was studied after 24 h. Non-treated cells were used as a control. The percentages of wound closure during the extract exposure were utilized to present the results.

Statistical analysis

The statistical analysis (except for the results from the antimicrobial assay) was done by using analysis of variance (one-way ANOVA) and Duncan's *post hoc* test in STATISTICA 7.0. The differences were considered statistically significant at $p<0.05$.

RESULTS AND DISCUSSION

According to the literature data, oxidative stress induced by free radicals has an important role in the development of various chronic diseases, cancer, degenerative neuronal damage, diabetes mellitus, and coronary heart disease [11,12]. Reactive oxygen species (ROS) are a class of unstable chemical compounds that are produced in all cells during normal physiological and biochemical reactions. Excessive free radical generation can induce cellular and tissue damage by nonspecific alteration and disruption of lipids, proteins, and nucleic acids [13]. Therefore, the antioxidant capacity of *T. serpyllum*, *V. myrtillus*, and *A. vera* waste extracts was examined using two antioxidant assays (ABTS and DPPH methods). The results of the ABTS and DPPH radical scavenging capacity of all prepared extracts are shown in Figures 1a and 1b, respectively.

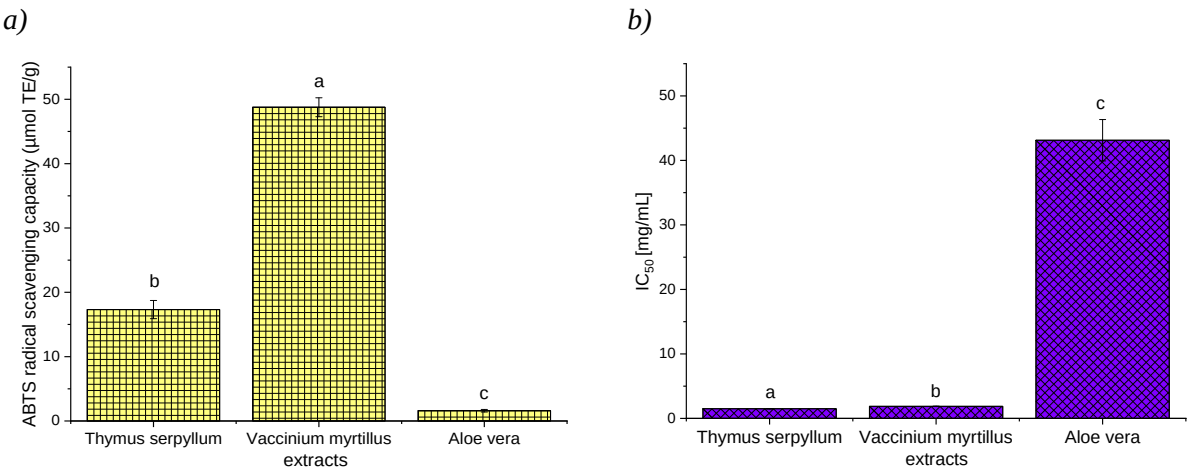

Figure 1 *a) ABTS and b) DPPH radical scavenging activity of Thymus serpyllum, Vaccinium myrtillus, and Aloe vera waste extracts; TE, Trolox equivalent, IC_{50}, concentration of the extract requires to scavenge 50% of free DPPH radicals; values with different letters (a-b) showed statistically significant differences ($p<0.05$; n=3; analysis of variance, Duncan's post-hoc test)*

According to the results from Figure 1a, it can be noticed a statistically significant difference in ABTS radical scavenging potential between *T. serpyllum* and *V. myrtillus* extracts (17.32±1.41 and 48.77±1.47 μmol TE/g, respectively), while *A. vera* extract showed significantly lower antioxidant activity (1.6±1.47 μmol TE/g).

As can be seen from Figure 1b, *A. vera* extract showed the highest IC_{50} value, i.e. the lowest DPPH radical scavenging capacity (43.13±3.21 mg/mL). *T. serpyllum* and *V. myrtillus* extracts had significantly lower IC_{50} values (1.50±0.02 and 1.87±0.03 mg/mL, respectively). However, *T. serpyllum* extract possessed statistically significantly higher DPPH antioxidant potential.

The presented results of ABTS antioxidant potential did not follow the trend of the results obtained in DPPH assays, which can be explained by the fact that various plant secondary metabolites and their synergism significantly influence the overall antioxidant activity of herbal extracts [14]. The mentioned phenomenon can be also explained by the fact that free radical scavenging potential depends on the polyphenol concentration in the extracts and their chemical structure as well. Furthermore, the presence of synergistic or antagonistic reactions among flavonoids should be taken into consideration for the overall antioxidant capacity of the extracts [15,16]. Differences between the antioxidant activity of *T. serpyllum* and *V. myrtillus* extracts can be explained by different reactivity of free radicals, as well as different mechanisms of the reactions. Hence, ABTS free radicals are more reactive compared to DPPH radicals. Additionally, DPPH radicals have a role in the transfer of hydrogen atoms, whereas ABTS radicals interact *via* electron transfer. Thus, the higher reactivity of ABTS radicals resulted in the high radical scavenging potential of *V. myrtillus* extract, while *T. serpyllum* extract possessed the highest DPPH antioxidant potential, i.e. the lowest IC_{50} value. Jovin *et al*. [17] have reported that flavonoid derivates in herbal extracts provide better biological effects. According to the literature data, the extracts with a higher concentration of flavonoid compounds possessed a higher DPPH radical scavenging ability [18] which can be the case with *T. serpyllum* extract. Hirano *et al*. study [19] also showed that the neutralization of DPPH radicals can be due to the reducing ability of flavonoids.

The investigation of antimicrobial properties of the extracts against five bacterial strains and one fungal strain was done and the results are presented in Table 1 (except for *A. vera* samples). *T. serpyllum* and *V. myrtillus* extracts have shown antibacterial activity against all investigated bacterial stains, while *A. vera* extract did not have antibacterial potential. *T. serpyllum* and *V. myrtillus* extracts were the most effective in inhibiting the growth of *E. faecalis* (MIC of 0.313 mg/mL). *V. myrtillus* extract exhibited significant activity against *B. cereus* with a MIC value of 0.625 mg/mL, whereas MIC was higher for *T. serpyllum* extract (1.25 mg/mL). MIC value against *S. aureus* was the same for both extracts and amounted to 1.25 mg/mL). Both extracts showed moderate activity against *E. coli* (MIC of 5 mg/mL). *V. myrtillus* extract inhibited growth of *S. enterica* with MIC of 2.5 mg/mL, while *T. serpyllum* extract exerted the same effect at higher concentrations, 5 mg/mL. According to the results of antifungal potential, both extracts showed inhibition of *C. albicans* strains in relatively high concentration, MIC of 20 mg/mL.

Table 1 *Antimicrobial activity of Thymus serpyllum and Vaccinium myrtillus waste extracts expressed as minimum inhibitory (MIC, mg/mL) and minimum bactericidal or fungicidal concentration (MBC or MFC, mg/mL)*

Microbial strain	*Thymus serpyllum* extract		*Vaccinium myrtillus* extract		Amoxicillin/fluconazole	
	MIC [mg/mL]	MBC/MFC [mg/mL]	MIC [mg/mL]	MBC/MFC [mg/mL]	MIC [mg/mL]	MBC/MFC [mg/mL]
Bacillus cereus	1.25	2.5	0.625	2.5	5.42	21.68
Enterococcus faecalis	0.313	5	0.313	5	0.34	2.71
Staphylococcus aureus	1.25	10	1.25	10	0.17	1.36
Escherichia coli	5	10	5	10	5.42	21.68
Salmonella enterica	5	5	2.5	5	2.71	5.42
Candida albicans	20	/	20	/	12.5	50

Besides growth inhibitory capacity, *T. serpyllum* and *V. myrtillus* extracts also exerted bactericidal potential at a relatively low concentration. The strongest bactericidal capacity of both extracts was observed against *B. cereus* (MBC value of 2.5 mg/mL). Furthermore, both extracts exhibited the same bactericidal potential against *E. faecalis* and *S. enterica* (MBC of 5 mg/mL), whereas bactericidal capacity against *S. aureus* and *E. coli* has been at the higher tested concentration, 10 mg/mL. Both extracts did not show fungicidal activity even at the highest tested concentration. According to the literature data, aromatic plant extracts showed strong antibacterial activity against *S. aureus* and only moderate activity against *E. coli* [20,21]. Several studies have shown that the antibacterial capacity of plant extracts can be attributed to the presence of various types of components, including phenolic acids, flavonoids, and tannins, which possess hydroxyl groups and the ability to form hydrogen bonds with water molecules in bacterial cell [20–22]. Polyphenol compounds can also coagulate the proteins in bacteria cells destroying enzymes involved in bacterial metabolism [20]. However, other compounds apart from polyphenols can be also responsible for the overall antimicrobial potential of plant extract. Due to the increasing incidence of resistant bacteria, including methicilin-resistant *S. aureus* and multi-resistant *E. coli* and *E. faecalis*, in food and clinical settings, these findings can be valuable. Therefore, this research opens the door for medicinal plant extracts to be considered natural, safe, and effective food, cosmetic, and pharmaceutical preservatives.

T. serpyllum plant has traditionally been used in various gastrointestinal disorders, thus the spasmolytic potential of the extract was tested in a model of isolated rat ileum. The results of the spasmolytic activity of *T. serpyllum* extract in spontaneous contractions, acetylcholine- and potassium chloride-induced contractions are shown in Table 2.

Table 2 *Spasmolytic activity of Thymus serpyllum waste extract on spontaneous contractions and acetylcholine- and potassium chloride-induced contractions of the isolated rat ileum*

Samples	Spontaneous contractions	Acetylcholine-induced contractions	Potassium chloride-induced contractions
	EC_{50} [µg/mL]	EC_{50} [nM]	EC_{50} [µg/mL]
Thymus serpyllum extract	$9.16 \cdot 10^3$	$1.25 \cdot 10^3$	$9.17 \cdot 10^3$
Papaverine	0.06	/	/
Atropine	/	28	/
Verapamile	/	/	0.94

T. serpyllum extract significantly inhibited the spontaneous contractions of isolated rat ileum. The EC50 value was $9.16 \cdot 10^3$ mg/mL (Table 2). Papaverine, as a positive control, showed an EC50 value of 0.06 µg/mL (Table 2) due to the inhibition of phosphodiesterase and calcium influx [23]. With the aim to investigate the possible mechanisms of the spasmolytic ability of the tested extract, the contractions of isolated rat ileum were induced by acetylcholine. The extract showed a significant reduction of acetylcholine-induced contractions (Table 2). The extract caused a change in the value of the EC_{50} of acetylcholine from 0.25 nM (in the absence of the extract) to $1.25 \cdot 10^3$ nM (in the presence of the extract).

Acetylcholine causes gastrointestinal smooth muscle contractions by the stimulation of muscarinic receptors, through two different mechanisms: 1) the stimulation of M_2 muscarinic receptors and activation of cationic channels through pertussis toxin-sensitive G proteins, causing membrane depolarization and the influx of Ca^{2+} ions [24], and 2) the activation of M_3 muscarinic receptors and induction of the G_q protein transduction signal, resulting in the activation of phospholipase C, formation of inositol trisphosphate and diacylglycerol, and increment of intracellular calcium concentration, membrane depolarization, and intestinal musculature contraction [25]. The inhibitory effect of the extract on acetylcholine-induced contractions was significantly lower in comparison to atropine, as a non-selective muscarinic receptor antagonist. Additionally, after rinsing, the contractility of the isolated ileum was the same as at the beginning. Thus, the spasmolytic ability of the extract can be attributed to the reversible blockade of muscarinic receptors.

Potassium chloride causes depolarization and tonic contraction of isolated rat ileum by inducing membrane depolarization and opening of voltage-dependent Ca^{2+} channels [23]. The extract has induced significantly the reduction of the potassium chloride-induced contractions with EC_{50} value of $9.17 \cdot 10^3$ µg/mL (Table 2). Verapamil, as an antagonist of Ca^{2+} influx through calcium channels, has shown a significant activity on potassium chloride-induced contractions with an EC_{50} value of 0.94 µg/mL (Table 2). According to Gilani *et al*. study [26], herbal extracts inhibit potassium chloride-induced contractions acting as antagonists of the influx of Ca^{2+} ions. Since the extract possessed a significant effect on smooth muscle relaxation of isolated rat ileum in the presence of a high concentration of K^+ ions, it can be concluded that its spasmolytic activity is related to Ca^{2+} channel blockade.

Since *V. myrtillus* and *A. vera* plants possess skin regeneration potential, both extracts were subjected to cytotoxicity and scratch wound healing assays. As can be seen from Table 3, none of the extracts had an unfavorable effect on the cell line's growth rate. The results

revealed that the extracts were not cytotoxic and their IC_{50} values were larger than 400 μg/mL. The presented results indicate the lack of toxicity of both extracts against skin cells (no harmful impact on HaCaT cells was detected) suggesting their potential use in pharmaceutical and cosmetic industries.

Table 3 *Cytotoxic and scratch wound healing activity of Vaccinium myrtillus and Aloe vera waste extracts on immortalized keratinocyte cells*

Samples	IC_{50} [μg/mL]	Wound healing [%]
Vaccinium myrtillus extract	>400	29.2±1.8[a*]
Aloe vera extract	>400	30.9±1.7[a]
Control	>400	0.10

[*]values with the same letter showed no statistically significant differences (p<0.05; n=3; analysis of variance, Duncan's *post-hoc* test).

Wound healing represents an important component of the skin's defensive and protective activities, thus *V. myrtillus* and *A. vera* waste extracts were included in the wound healing experiment and results are presented in Table 3. When both extracts were applied to immortalized keratinocyte cells with scratched wound gaps, it led to a significant improvement in the wound gap closure, compared to the control. Both extracts exhibited similar effectiveness in helping wound closure (30.9±1.7 and 29.2±1.8%). Wound healing varies in its duration and contains four sequentially overlapped phases, including homeostasis, inflammation, proliferation, and remodeling [27]. The results presented in Table 1 confirmed that *V. myrtillus* and *A. vera* extracts can stimulate keratinocyte growth and migration. Flavonoids and terpenoids are known to aid wound healing due to their antioxidant and antibacterial properties. According to Tsuchiya *et al*. [28], the mentioned abilities can be responsible for wound contraction and an increased rate of epithelialization. Therefore, these findings indicate that both extracts can help in skin wound healing.

CONCLUSION

The presented study investigated the biological potential of *T. serpyllum*, *V. myrtillus*, and *A. vera* waste extracts. *T. serpyllum* extract possessed the lowest IC_{50} value in DPPH radical scavenging assay, i.e. the highest antioxidant capacity, as well as antibacterial, bactericidal, and antifungal potential in the case of all tested bacteria and fungus. Additionally, the mentioned extract significantly inhibited spontaneous contractions and acetylcholine- and potassium chloride-induced contractions. *V. myrtillus* extract showed the highest ABTS radical scavenging capacity and the same antimicrobial activity as *T. serpyllum* extract. Furthermore, *V. myrtillus* extract had no harmful influence on HaCaT cells and exerted a significant wound-healing effect. On the other hand, *A. vera* extract possessed the lowest antioxidant activity in ABTS and DPPH assays and did not show antimicrobial potential against tested strains. However, *A. vera* extract also had no harmful effect on HaCaT cell lines and showed a significant wound-healing effect. In future experiments, *T. serpyllum* waste extract will be examined in terms of bronchodilatory activity, whereas all prepared waste

extracts will be investigated *via* .effects on enzymes, dying of textile, as well as anticorrosive effects.

ACKNOWLEDGEMENT

The authors are grateful to the Ministry of Ministry of Science, Technological development and Innovation of the Republic of Serbia for financial support according to the contracts with the registration numbers 451-03-47/2023-01/200019 and 451-03-47/2023-01/200135.

REFERENCES

[1] Panić M., Radić Stojković M., Kraljić K., *et al.*, Food Chem. 283 (2019) 628–636.

[2] Saha A., Basak B., Ind. Crops Prod. 145 (2020) 111979.

[3] Sagar, N.A., Pareek, S., Sharma, S., *et al.*, Compr. Rev. Food Sci. (2018) 1–20.

[4] Regulations on the quality of tea, herbal tea and their products of Republic of Serbia (2012) (*in Serbian*).

[5] Semerel J., John N., Dehaen W., *et al.*, J. Renew. Mater. 31 (2022).

[6] Both S., Chemat F., Strube J., Ultrason. Sonochem. 21 (2014) 1030–1034.

[7] Dent M., Dragović-Uzelac V., Penić M., *et al.*, Food Tech. Biotech. 51 (2013) 84–91.

[8] Mustafa A., Turner C., Anal. Chim. Acta 703 (2011) 8–18.

[9] Li L., Yang Y., Hou X., *et al.*, Sep. Purif. Technol. 104 (2013) 200–207.

[10] Xi J., Yan L., Sep. Purif. Technol. 175 (2017) 170–176.

[11] Finkel T., Holbrook N. J., Nature 408 (2000) 239–247.

[12] Sen S., Chakraborty R., Sridhar C., *et al.*, Int. J. Pharm. Sci. Rev. Res. 3 (2010) 91–100.

[13] Hunt J. V., Dean R. T., Wolff S. P., Bioche. J. 256 (1988) 205–212.

[14] Jovanović A. A., Petrović P. M., Đorđević V. B., *et al.*, Hrana i ishrana 62 (2021) 15–20.

[15] Ginova A., Mihalev K., Kondakova V., Int. J. Pure App. Biosci. 1 (2013) 38–43.

[16] Hidalgo M., Sánchez-Moreno C., de Pascual-Teresa S., Food Chem. 121 (2010) 691–696.

[17] Jovin E., Toth A., Beara I., *et al.*, Planta Med. 74 (2008) PB65.

[18] Jovanović A. A., Mosurović M., Bugarski B., *et al.*, Lekovite sirovine 42 (2022) 51–59.

[19] Hirano R., Sasamoto W., Matsumoto A., *et al.*, J. Nutr. Sci. Vitaminol. 47 (2001) 357–362.

[20] Fayad N. K., Hamad O., Al-Obaidi S., *et al.*, Inn. Sys. Des. Eng. 4 (2013) 41–51.

[21] Al-Fatimi M., Wurster M., Schröder G., *et al.*, Rec. Nat. Prod. 4 (2010) 49–63.

[22] Ulukanli Z., Cigremis Y., Ilcim A., Eur. Rev. Med. Pharmacol. 15 (2011) 649–657.

[23] Rang H., Dale M., Ritter J., *et al.*, Farmakologija, Data status, Belgrade, Serbia (2005) (*in Serbian*).

[24] Unno T., Matsuyama H., Sakamoto T., *et al.*, Br. J. Pharmacol. 146 (2005) 98–108.

[25] Branković S., Kitić D., Radenković M., *et al.*, J. Food Med. 14 (2011) 495–498.

[26] Gilani A., Khan A., Ghayur M. Nutr. Res. 26 (2006) 277–283.

[27] Gothai S., Arulselvan P., Tan W. S., *et al.*, J. Intercult. Ethnopharmacol. 5 (2016) 1.

[28] Tsuchiya H., Sato M., Miyazaki T., *et al.*, J. Ethnopharmacol. 50 (1996) 27–34.

ELECTROCHEMICAL ADVANCED OXIDATION PROCESSES FOR WASTEWATER TREATMENT: RECENT ADVANCES AND PERSPECTIVES

Tanja Brdarić[1*]

[1]Vinča Institute of Nuclear Sciences-National Institute of the Republic of Serbia, Department of Physical Chemistry, University of Belgrade, Mike Petrovića Alasa 12–14, 11001 Belgrade, SERBIA

[*]*tanja.brdaric@vin.bg.ac.rs*

Abstract

Over the last decades, scientific research is focused on the development of green technologies which would be effectively used for the purification of aquatic environment pollution. Among the various electrochemical technologies, the electrochemical advanced oxidation processes (EAOPs) are promising option that may be applied to remove organic pollutants from wastewater. These methods are based on the electrochemical generation of very powerful oxidizing species, such as the hydroxyl radical (•OH) at the anode surface or in the bulk solutions, which is then able to destroy organics partially or to their total mineralization. This article reviews currently most promising approach of EAOPs technology, introduces its basic principles, and describes the research progress in that field. Both technics of production OH radical are considered, and the role of electrode materials is discussed together with the author's laboratory experiments.

Keywords: electrochemical oxidation, hydroxyl radical, Fenton's reaction.

INTRODUCTION

The waste and pollution of water resources with organic pollutants arising from the anthropogenic factor (through their industrial, agricultural, and urban activity) are a crucial environmental problem worldwide. Therefore, in order to prevent a water crisis and improve the quality of water, it is necessary to develop effective technologies for the purification of industrial or communal wastewater before its discharge to the recipient. Numerous methods have been proposed, such as adsorption [1], photocatalysis [2], biological treatment [3], membrane filtration (reverse osmosis, ultrafiltration, nanofiltration, etc.) [4], and electrochemical methods [5]. Electrochemical techniques are based on the electrolysis of water, with hydrogen evolution on the cathode and oxygen on the anode surface. The conventional electrochemical technology like electrodeposition, electrocoagulation, and electroflotation, have been widely employed in the separation process of real wastewater, for example, landfill leachates [6], printing and dyeing wastewater [7,8], and oil wastewater [9]. However, significant problems with effective application arise, related to the cost, handling of the chemicals, etc. In recent years, scientists have turned their attention to the development of electrochemical advanced oxidation processes (EAOPs) with the aim to totally degrade/mineralize organics pollutants and reduce their toxicity with minimum capital and operational expenditure. EAOPs involve the electrochemical degradation of organic pollutants

via reactive oxygen species (ROS), such as hydroxyl radicals (•OH), which are produced, in electrochemical system by oxidation of water on the anode surface or in the bulk solutions. Various EAOPs are described in the literature [10–12]. Firstly, anodic, or electrochemical oxidation which is basic EAOPs technology, where an organic pollutants are oxidized directly or indirectly via •OH generated on the anode surface. This environmental friendly technology is very interesting for wastewater treatment due to using electrons as a „clean" reagents. Also it is versatile, safe, and highly effective for elimination a large variety of pollutants. Other EAOPs including electro-Fenton (EF), Fered-Fenton (FF), photoelectro-Fenton (PEF), which use •OH produced in the bulk solution. Generally, the purification of wastewater using EAOPs depends on many factors like wastewater composition or nature and concentration of supporting electrolyte, the configuration of the electrochemical reactor (undivided or divided electrochemical cell), anode and cathode characteristics, and applied operational parameters such as applied current density (galvanostatic mode) or potential (potentiostatic regime), stirring rate, temperature, pH etc.

In this study, we present the advances and future perspectives of EAOPs, as well as a general review of laboratory experiments performed in the author's laboratory, related to the application of nanocomposite anodes for purification of synthetic wastewater by electrochemical oxidation. The review involves only hydroxy radical-mediated processes, in which •OH are electrogenerated at the surface anode or in bulk solutions such as electrochemical oxidation, and electro Fenton (and other EAOPs based on Fenton's reaction chemistry).

EAOPs BASED ON PRODUCTION OH RADICAL ON THE SURFACE ANODE

The electrochemical oxidation of organic pollutants in wastewater can occur directly by electron transfer from the electrode to adsorbed organic molecules on the surface anode, or indirectly (mediated) via reactive oxygen species formed at the anode. According to the literature review [13], the direct oxidation of pollutants rarely occurs and it has poor efficiency. The process is theoretically possible to perform at lower potentials than the oxygen evolution potential (OEP), which depends on the electrocatalytic activity of the anode material. On the other hand, adsorbed pollutants and their products can formed a polymeric layer on the anode surface, and consequently, the oxidation process is rapidly blocked, which is commonly called the poisoning effect [14].

The treatment of industrial wastewater by indirect electrochemical oxidation is based on the ROS production, such as •OH which are generated as oxygen intermediates of water oxidation to oxygen Eq. 1–3; and other weaker oxidant agents, such as chlorine, (per)bromate, persulfate, ozone, hydrogen peroxide, percarbonate, which are electrochemically generated from ions in the bulk solutions.

$$H_2O \rightarrow {\bullet}OH_{(aq)} + H^+ + e^- \quad (1)$$

$$2H_2O \rightarrow H_2O_2 + 2(H^+ + e^-) \quad (2)$$

$$H_2O \rightarrow O_2 + 4(H^+ + e^-) \quad (3)$$

•OH is the main oxidant of interest in the electrochemical system. It is generated in large amounts by water oxidation without additional chemicals and has the strongest oxidation power (except for fluorine). Due to its very short half-life (10^{-9} seconds) diffusion of this radical to the bulk electrolyte is obstructed, so the reaction oxidation is occurring on the anode surface, Eq. 4.

$$M + H_2O \rightarrow M(\bullet OH) + H^+ + e^- \quad (4)$$

After •OH is produced, it will be chemically or physically adsorbed on the anode surface (M(•OH)), depending on the nature of the anode materials.

Influence of anode material

A few studies [15,32] performed in the last twenty years have shown the strong influence of the anode material nature on both, degradation efficiency and mechanism of electrochemical oxidation. Also, the mass transfer becomes a very important process that determinate the oxidation rate. Anyway, there is a consensus on the role of OH radical, and its primary role for the high-efficiency degradation of organic pollutants by electrolysis on some types of electrodes. Comninellis *et al*. [15] during a pioneering work of their group, based on the efficiency of the process degradation, had divided electrodes into two types: active and non-active. The no-existence of free •OH on the surface active electrode leads to the partial degradation of organic pollutant along with the formation of persistent species as the final products. On the other hand, on the non-active electrode total degradation occurs, i.e. mineralization of organic pollutants to CO_2, water, and inorganic ions, due to the existence of free •OH on the electrode surface. Later, in numerous works [16,17], it has been stated that oxygen evolution may have a positive effect on the oxidation of organics and may initiate their mineralization. It explains the high percent efficiencies, although the process of organic pollutants degradation is in competition with the oxygen evolution reaction (OER). For instance, a Boron-doped diamond anode (BDD), which is characterized by a very high OEP, can completely mineralize highly polluted wastewater with great efficiency, up to 100% [14]. Comninellis linked results of percent efficiency with OEP which is an electrocatalytic characteristic electrode. Based on OEP, Comninellis [18] additionally explained the differences between two limiting typa, "active" and "non-active" anodes, and predicted two mechanisms of degradation. The active electrode has low oxidation power and low OEP. In this case, the •OH strongly interacts with the anode surface (strong electrode – •OH interaction), during which the adsorbed •OH (M(•OH)) are transformed in chemisorbed "active oxygen" (oxygen in the oxide lattice), and the higher oxide or superoxide (MO) are formed, Eq. 5.

$$M(\bullet OH) \rightarrow MO + H^+ + e^- \quad (5)$$

MO has a weaker oxidizing capacity compared to •OH, and may partially oxidize organic pollutants (R), into intermediate products RO (such as short-chain carboxylic acids, aldehydes, and ketones), Eq.6.

$$MO + R \rightarrow M + RO \quad (6)$$

Platinum (Pt), iridium dioxide (IrO_2), ruthenium dioxide (RuO_2), graphite, and other sp^2 carbon-based electrodes are prominent examples of active anodes that have OEP below 1.8 V/SHE.

The non-active electrode has high oxidation power and high OEP. Due to a weak electrode – •OH interaction, •OH is easy to desorb (physisorbed M(•OH)), and transform to the solvated OH radical $•OH_{(aq)}$ (Eq. 7) which react with organic molecules (R), Eq.8.

$$M(•OH) \rightarrow M + •OH_{(aq)} \quad (7)$$

$$•OH_{(aq)} + R \rightarrow M + CO_2 + H_2O + H^+ + e^- \quad (8)$$

and may totally mineralize organic pollutants, R, to CO_2 and H_2O (Eq.8) and inorganic ions.

Tin dioxide (SnO_2), lead dioxide (PbO_2), and BDD electrodes can be classified as non-active electrodes and their OEP range is from 1.7 to 2.6 V/SHE . In some cases, substoichiometric TiO_2 has been reported as a promising anode material containing several suboxides of TiO_2 (also known as Magneli phases). The best conductive compounds of these series are Ti_4O_7 and Ti_5O_9.

The electrode is the most important component of the electrolytic system for electrochemical oxidation, so the material and performance of the electrode determine a cost and process efficiency. In order to use electrodes for the electrochemical oxidation of organic pollutants they must have good electrochemical properties (electrode surface area, OEP, and electroconductivity), catalytic activity, stability, and satisfactory service life. Various types of electrodes such as graphite and pure metal anodes, dimensionally stable anode (DSA), BDD electrodes, and sub-stoichiometric titanium oxide electrodes have been investigated in many recent studies [19–32]. The latest trends in electrode disignis introducing nanostructure into the anode to improve their properties.

Graphite and pure metal materials are extensively used in wastewater treatment due to excellent electrical properties, low cost, and easy preparation of electrodes. Sivodia *et al*. [19] investigated the degradation of the environmentally persistent cytarabine (CBN) -anticancer drug, using graphite anodes. Under the applied conditions (current density of 10 mA, pH of 3) they obtained a removal rate of CBN of about 95% after 60 min of electrolysis. While Yong *et al*. [20] got an excellent removal effect (98.0%) of methyl orange (MO) from textile wastewater. Al, Fe, Pt, and Ti are metal electrodes usually used in systems for electrochemical oxidation of organic pollutants in industrial or communal wastewater. The problem with their application is the formation of colloidal particles in the electrolyte solution, which must be separated by flocculation or a similar technic [21].

A numerus research studies showed that the BDD electrode has the best removal effect on organic pollutants degradation in wastewater [22–26]. It has excellent characteristics, such as high mechanical strength, corrosion resistance, long service life, high stability, high OEP, a low background current, a low energy consumption, the electrode surface is inert and has low adsorption capacity [27]. However, widely application of BDD electrodes is limited with high price, and complexity of scaled-up preparation technology.

The Magneli phase Ti_4O_7 (class of sub-stoichiometric titanium oxide) electrode is very interesting for applications in electrochemical green technology, due to its remarkable high OEP, strong corrosion resistance, conductivity up to 1500 S cm^{-1}, and long service life. Today, a great number of research groups worldwide are exploring the possibilities of applying this type of electrode for the purification of wastewater by EAOPs [28–30].

Dimensionally stable anode (DSA), or metal oxide electrodes, such as PbO_2, SnO_2, IrO_2, and RuO_2 are used in environmental pollution treatment, for more than 30 years. Due to good conductivity and high OEP (1.8 to 2.0 V vs. SHE), good corrosion resistance and low cost of synthesis, the PbO_2 electrode is a good candidate for organic pollutant degradation. However, its applications seemed to be further restricted by short lifetimes, toxicity and limited catalytic performance. For that reason, the development of electrochemical systems with nanostructured PbO_2 anodes shows a rising research trend. Chen *et al*. [31] fabricated Pb/PbO_2 anode which possessed a stronger oxidation ability than that traditional PbO_2 electrode. The better •OH generation on the newly synthesized PbO_2 anode encouraged the removal of the organic dye Congo red to 68.62%, with the initial concentration of 20 mg/L at 8 mA/cm^2 for 20 min. Savic [32] carried out the degradation of the mixture of phenolic compounds by applying electrochemical oxidation on PbO_2-GNR anodes in potentiostatic conditions at potentials 2.3 V and 3 V. Its concluded that the removal efficiency of phenolic compounds increased with increasing the time of electrolysis and applied potential, up to 78% for 300 min and potential of 3 V.

Tin dioxide (SnO_2) is an n-type semiconducting nanomaterial that has advantages such as low cost of synthesis, chemical stability, non-toxicity and high OEP (1.9 to 2.2 V vs. SHE). Due to poor electric conductivity, the application of pure SnO_2 as anodes is not possible.

Basic electrochemical properties of the these anodes can be changed by modifying morphology and reducing grain size to nanometer dimension, doping with metals or mixing with metal- and carbon-based nanomaterials.

Many researchers most commonly are using Sb as a dopant for SnO_2. Also, the application of other dopants like Ag, B, and Bi is known. For example, Zhou *et al*. [33] achieved a very good degradation efficiency of antiviral drug abacavir (more than 96%, only 10 min at a current density of 0.2 mA/cm^2) using a porous Ti/SnO_2-Sb anode.

Recently, our research group [34] introduced a SnO_2-MWCNT (tin dioxide-multi walled carbon nanotube) nanocomposite anode, which can be successfully used in the electrolytic system for the bis-phenol A (BPA) removal from acidic sulphate-rich wastewater, by electrochemical oxidation. SnO_2-MWCNT nanocomposite was prepared by mixing nanosized SnO_2 (prepared using the sol-gel method) and functionalized MWCNT (using acidic treatment) in mass ratio 3.5:1 (w/w) in dimethylformamide. Electrode preparation was done

by applying previously prepared nanocomposite onto clean SS electrode (surface area of 2 cm^2) and dried under infrared lamp.

Characterized SnO_2-MWCNT nanocomposite by TEM (Figure 1), confirmed the success of the attachment of SnO_2 nanoparticles to MWCNTs (probably via carbonyl (C =O) or hydroxyl (O–H) functional groups of MWCNT). The estimated average particle size of SnO_2 in the nanocomposite is about 15 nm. The electrode has good stability and recyclability. It also had a larger electrochemical active surface area (about 2-times higher) than bare stainlees steel and MWCNT, which indicate better electrochemical performance toward organic pollutant degradation. LSV measurement displays that the potential for the OER (1.89 V vs. RHE) between these two electrodes, pointing to higher electrochemical activity for the degradation of organic molecules.

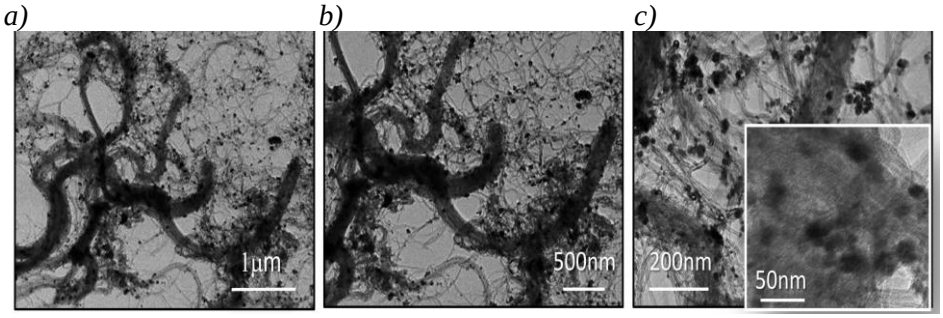

Figure 1 *TEM micrograph of SnO_2 –MWCNT nanocomposite [34]*

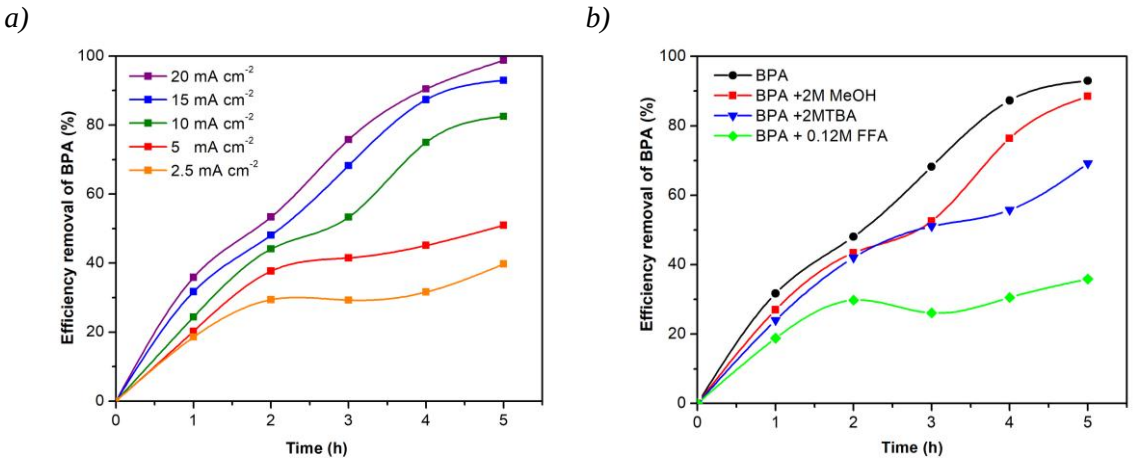

Figure 2 *a) Efficiency removal of 30 mg /L BPA in 0.1 M Na_2SO_4 solution at pH 4.0 during time at different current densities; b) Effect of radical scavengers on BPA removal during electrolytic process (current density 15 mA/ cm^2) [34]*

About 84 % of BPA is completely mineralized after 5 h of treatment at a current density of 15 mA/cm^2 . This implies that BPA was oxidized to other organic compounds before it is fully converted to CO_2 and H_2O. Also, the results of applied free radical quenching tests (Figure 2b) confirmed that the oxidation of BPA occurs indirectly mechanism via •OH, and the removal efficiency of BPA rises with increasing current densities (see Figure 2a). The degradation of BPA fitted well with the pseudo-first-order kinetics. Due to the greater

production of hydroxyl radicals on larger current density, the k has elevated values. Compared to other electrodes, which were employed by Wu *et al*. [35,36] and Cui *et al*. [37], the obtained results of efficiency BPA degradation, for the SnO_2-MWCNT electrode were better (except the BDD electrode). The main benefit of the suggested approach is the low cost and simplicity of the synthesis process of anodic materials without employing expensive chemicals.

EAOPs BASED ON PRODUCTION OH RADICAL IN BULK SOLUTIONS

Development and investigation of EAOPs based on Fenton's reaction chemistry, as a method for wastewater purification, were started at the end of the last century by Brillas' and Oturan's groups [38–40]. Generally, depending on the technique of generation of Fenton reagent (H_2O_2 or Fe) in the electrochemical system, a process can be classified into four categories: classic electro-Fenton (EF), peroxy-coagulation (PC) process, Fered Fenton process (FF), and electrochemical peroxidation (ECP).

The electro-Fenton (EF) process originates from an electrochemically assisted Fenton reaction (Eq. 9), in which a powerful oxidant •OH is formed by a chemical reaction between electrochemically generated H_2O_2 and Fe^{2+} (Fenton reagents) in the acidic medium.

$$Fe^{2+} + H_2O_2 \rightarrow Fe^{3+} + {\bullet}OH + OH^- \quad (9)$$

The EF process comprises: (i) the in situ and continuous electro-generation of H_2O_2 at carbon cathode fed by pure oxygen or air (Eq. 10).

$$O_{2(g)} + 2H^+ + 2e^- \rightarrow H_2O_2 \quad (10)$$

(ii) the addition Fe^{2+} catalyst to the electrolyte solution, and (iii) the reduction of Fe^{3+} to Fe^{2+} on cathode Eq. 11.

$$Fe^{3+} + e^- \rightarrow Fe^{2+} \quad (11)$$

and consequently continuous generation of Fenton reagent and •OH. OH radicals produced in bulk solutions react with organic pollutants leading to their oxidation /mineralization, according to Eq. 12.

$$R + {\bullet}OH \rightarrow \text{oxidation intermediates} \quad (12)$$

$$\text{Intermediates} + {\bullet}OH \rightarrow CO_2 + H_2O + \text{inorganic ions} \quad (13)$$

The main problem of the EF process is parasitic reactions of chemical decomposition (Eq. 14 and Eq. 15) and cathodic reduction (split cell) (Eq. 16 and Eq. 17) or AO (non-split cell) that may destroy the accumulation of H_2O_2 in bulk solutions.

$$2H_2O_2 \rightarrow O_{2(g)} + 2H_2O \quad (14)$$

$$H_2O_2 + 2H^+ + 2\,e^- \rightarrow 2H_2O \quad (15)$$

$$H_2O_2 \rightarrow HO_2\bullet + H^+ + e^- \quad (16)$$

$$HO_2\bullet \rightarrow O_{2(g)} + H + e^- \quad (17)$$

Therefore, the use of optimal operating conditions (acidic pH, ambient temperature, etc.) and an appropriate cathode material are important to obtain better efficiency EF process for the degradation of organic pollutants.

The first used cathode material was mercury [41], their application is aborted due to its toxicity. After that, carbon-based cathodes such as carbon-PTFE-O_2 gas diffusion cathode [42], carbon sponge [43], activated carbon fiber [44], and graphite [45,46] were employed.

The most common used anode is Pt. Recent studies [47] suggested using of BDD anode. In this case, the surface-adsorbed OH radicals on BDD anode, besides OH radicals in bulk solutions, contribute to the efficiency of the EF process.

The peroxi-coagulation (PC) process, proposed by Brillas' group [48] is realized, by simultaneous electro-generation H_2O_2 at carbon cathode with Fe^{2+} produced by anodic iron dissolution Eq. 18.

$$Fe \rightarrow Fe^{2+} + 2e^- \quad (18)$$

During this process, pollutants are oxidized by the attack of •OH in the bulk and their coagulation can also take place via $Fe(OH)_{3(s)}$ formation depending on pH.

The Fered Fenton process (EF) involves the addition Fenton's reagent (Fe^{2+} and H_2O_2) to the solutions which produce the OH radicals in the undivided electrolytic cell, and the ferrous ion is regenerated via the reduction of ferric ion on the cathode Eq. 19.

$$Fe^{3+} + e^- \rightarrow Fe^{2+} \quad (19)$$

The electrochemical peroxidation (ECP) used a sacrificial iron anode for ferrous electro generation Eq. 18, while hydrogen peroxide is externally added. At the inert cathode, hydrogen is produced from water reduction and Fe^{2+} is cathodically regenerated by Eq. 19.

Photo-electro-Fenton (PEF), first developed by Brillas' group [11], involves the treatment of the contaminated solution under EF conditions with simultaneous irradiation with UVA or solar light to accelerate the mineralization rate of organics. •OH is produced from Fenton's reaction (Eq. 9), while the undesired Fe(III) ions are eliminated by:

1. photoreduction of Fe(III)-hydroxy such as $FeOH^{2+}$ at a pH of about 3, Eq. 20.

$$FeOH^{2+} + h\nu \rightarrow Fe^{2+} + \bullet OH \quad (20)$$

2. direct photolysis formed between Fe^{3+} and some organics like carboxylic acids (Eq. 21).

$$Fe^{3+}(L)_n + h\nu \rightarrow Fe^{2+}(L)_{n-1} + L_{ox}\bullet \quad (21)$$

INFLUENCE OF OPERATIONAL PARAMETERS

The purification of wastewater using EAOPs, besides the anode and cathode characteristics previously described, depends on the configuration of the electrochemical reactor, the wastewater composition ie. the nature of the supporting electrolyte (in the case of experimental model-wastewater) and concentration of organic pollutants, and applied operational parameters such as applied current density or potential, temperature, pH, etc.

The EAOPs can be performed in undivided electrochemical cells with two electrodes (anode and cathode) and divided cells (separated cathodic and anodic parts). The EAOPs process can be performed under a galvanostatic (on constant current) or potentiostatic (constant potential) regime. Most commonly, EAOPs are operated in a galvanostatic regime.

Current density is a key parameter in EAOPs since it has direct influence on the produced amount of oxidizing species. It includes the control of the amounts of electrogenerated OH radicals M(•OH) for electrochemical oxidation. For EAOPs based on Fenton's reaction, current density regulates rate of cathodic Fe^{3+} regeneration to Fe^{2+}, the amount of electrogeneration of H_2O_2, and consequently the amount of •OH in the bulk produced from Fenton's reaction. In general, the rate of pollutants degradation rises with increasing current density for all EAOPs since more oxidizing species are formed at a given time [34,49]. However, the rate of parasitic reactions (like the dimerization of M(•OH) to H_2O_2 the anodic oxidation of M(•OH) to oxygen) is also promoted with increasing current density leading to the decrease of current efficiency for degradation organic. On the other hand, energy consumption elevates with the higher current. From the economic perspective, this is a limiting factor for applying all EAOPs technology.

It is well known that solutions with a higher initial concentration of organic pollutants need longer treatment to achieve a given percent degradation [50–52]. Precisely, the using of greater initial pollutants contents leads to the removal of more pollutants per unit of time, i.e. higher pollutants removal rates [53]. This can be explained by the faster oxidation of organics with •OH, inhibiting parasitic reactions.

The nature of the supporting electrolyte, such as sodium sulfate, sodium chloride, potassium chloride, sodium perchlorate, sodium nitrate, and sodium carbonate, can affect to the degradation process of organic pollutants. Exactly, the presence of some ions in solution leads to (i) the formation of strong oxidants such as active chlorine species produced by direct oxidation of chloride at the anode, (ii) the production of toxic by-products like chloro derivatives, which are slowly degraded by •OH (iii) the consumption of H_2O_2 as it happens in the presence of SO_4 and (iv) the generation of complexes with iron like sulfate-iron and chloro-iron complexes [12].

The authors in their scientific works do not have a unified approach regarding the influence of pH on electrochemical oxidation processes. A few studies describe the independency of mineralization rate by changing pH in the 2.0–6.0 or 4.0–10 range [54,55];

another author achieved greater process efficiency at pH 3.0 compared to higher pH values [56]. In contrast, the best pH value for electro-Fenton process is close to 3.0, eventually, 4.0, due to: the absence of iron precipitation, null auto-decomposition rate of H_2O_2 to water and oxygen, typically occurring for pH above 5 [57].

FUTURE PERSPECTIVES AND CONCLUSION

The concept of the scientific research presented in this work is evident proof that EAOPs technology has a great application potential for wastewater purification. From our point of view future perspectives are as follows:

- Research and development of new electrode materials with satisfactory physical and chemical characteristics, with simple and inexpensive synthesis procedures

- In order to wider acceptance of EAOPs treatments additional toxicological assessment of treated wastewater needs to be conducted, so it can be linked to the formation of mostly unknown oxidation intermediates

- Passing from academic research, which was performed on small electrochemical systems, to pilot plants or treatment stations. This conception firstly includes the economic evaluation of the costs of practical application to real wastewater treatment. The modeling of the systems reactors and the process optimization of the operating parameters and prediction the behavior of pollutants can be useful for it.

- Development and research of hybrid systems which can be designed by coupling of existing EAOPs electrochemical systems with conventional (e.g biology treatment) or other advanced oxidation processes.

ACKNOWLEDGEMENT

The author would like to thank the Ministry of Science, Technological Development and Innovation of the Republic of Serbia for the financial support to the research through institutional funding (Contract number 451-03-47/2023-01/200017).

REFERENCES

[1] Ahmaruzzaman M., Adv. Colloid Interface Sci. 143 (2008) 48–67.

[2] Ahmed S., Rasul M., Martens W., *et al*., Desalination 261 (2010) 3–18.

[3] Ferrer-Polonio E., Mendoza-Roca J., Iborra-Clar A., *et al*., J. Ind. Eng. Chem. 43 (2016) 44–52.

[4] Raza W., Lee J., Raza N., *et al*., J. Ind. Eng. Chem. 71 (2019) 1–18.

[5] Moussa D., El-Naas M., Nasser M., *et al*., J. Environ. Manage. 186 (2017) 24–41.

[6] Naje A., Ajeel M., Ali I., *et al*., Water Sci. Technol. 80 (2019) 458–465.

[7] Butler E., Hung Y., Yeh R., *et al*., Water (Switzerland) 3 (2011) 495–525.

[8] Safwat S., Hamed A., Rozaik E., Sep. Sci. Technol. 54 (2019) 183–194.

[9] Andrade A., Costa Marques M., New Technol. Oil Gas Ind. (2012) 3–28.

[10] Malinović B., Markelj J., Gotvajn A., *et al*., Prosen H., Environ. Chem. Lett. 20 (2022)

3765–3787.

[11] Sirés I., Brillas E., Oturan M., *et al*., Environ. Sci. Pollut. Res. 21 (2014) 8336–8367.

[12] Moreira F., Boaventura R., Brillas E., *et al*., Appl. Catal. B Environ. 202 (2017) 217–261.

[13] Moradi M., Vasseghian Y., Khataee A., *et al*., J. Ind. Eng. Chem. 87 (2020) 18–39.

[14] Martínez-Huitle C., Panizza M., Curr. Opin. Electrochem. 11 (2018) 62–71.

[15] Gandini D., Michaud P., Duo I., *et al*., New Diam. Front. Carbon Technol. 9 (1999) 303–316.

[16] Comninellis C., Chen G., Electrochemistry for the Environment, Springer, New York (2010), ISBN: 978-0-387-36922-8.

[17] Martínez-Huitle C., Ferro S., Chem. Soc. Rev. 35 (2006) 1324–1340.

[18] Comninellis C., Electrochim. Acta 39 (1994) 1857–1862.

[19] Sivodia C., Sinha A., Chemosphere 243 (2020) 125456.

[20] Kong Y., Wang Z., Wang Y., *et al*., New Carbon Mater. 26 (2011) 459–464.

[21] Kumari S., Kumar R., Chemosphere 273 (2021) 128571.

[22] Chen L., Lei C., Li Z., *et al*., Chemosphere 210 (2018) 516–523.

[23] Murugananthan M., Yoshihara S., Rakuma T., *et al*., J. Hazard. Mater. 154 (2008) 213–220.

[24] Dirany A., Sirés I., Oturan N., *et al*., Chemosphere 81 (2010) 594–602.

[25] Brosler P., Girão A., Silva R., *et al*., Environments 10 (2023) 15.

[26] Pereira G., Rocha-Filho R., Bocchi N., *et al*., Chem. Eng. J. 198–199 (2012) 282–288.

[27] Qiao J., Xiong Y., J. Water Process Eng. 44 (2021) 102308.

[28] Ioroi T., Yasuda K., J. Power Sources 450 (2020) 227656.

[29] Geng P., Su J., Miles C., *et al*., Electrochim. Acta 153 (2015) 316–324.

[30] Ganiyu S., Oturan N., Raffy S., *et al*., Sep. Purif. Technol. 208 (2019) 142–152.

[31] Chen Z., Xie G., Pan Z., *et al*., J. Alloys Compd. 851 (2021) 156834.

[32] Savić B., Stanković D., Živković S., *et al*., Appl. Surf. Sci. 529 (2020) 147120.

[33] Zhou C., Wang Y., Chen J., *et al*., Chemosphere 225 (2019) 304–310.

[34] Simić M., Savić B., Ognjanović M., *et al*., J. Water Process Eng. 51 (2023) 103416.

[35] Wu W., Huang Z., Lim T., J. Environ. Chem. Eng. 4 (2016) 2807–2815.

[36] Wu W., Huang Z., Hu Z., *et al*., Sep. Purif. Technol. 179 (2017) 25–35.

[37] Cui Y. hong, Li X., Chen G., Water Res. 43 (2009) 1968–1976.

[38] Brillas E., Sauleda R., Casado J., J. Electrochem. Soc. 145 (1998) 759–765.

[39] Brillas E., Calpe J., Casado J., Wat. Res. 34 (2000) 2253–2262.

[40] Oturan M., J. Appl. Electrochem. 30 (2000) 475–482.

[41] Oturan M., Pinson J., Bizot J., *et al*., J. Electroanal. Chem. 334 (1992) 103–109.

[42] Brillas E., Bastida R., Llosa E., *et al*., Electrochem. Sci. Technol. 142 (1995) 1733–1741.

[43] Özcan A., Şahin Y., Savaş K., *et al*., J. Electroanal. Chem. 616 (2008) 71–78.

[44] Wang A., Qu J., Ru J., *et al.* Dye. Pigment. 65 (2005) 227–233.

[45] Pozzo A., Palma L., Merli C., *et al*., J. Appl. Electrochem. 35 (2005) 413–419.

[46] Nidheesh P., Gandhimathi R., Sanjini N., Sep. Purif. Technol. 132 (2014) 568–576.

[47] Oturan N., Brillas E., Oturan M., Environ. Chem. Lett. 10 (2012) 165–170.

[48] Brillas E., Sirés I., Oturan M., Chem. Rev. 109 (2009) 6570–6631.

[49] Antonin V., Garcia-Segura S., Santos M., *et al*., J. Electroanal. Chem. 747 (2015) 1–11.

[50] Hamous H., Khenifi A., Bouberka Z., *et al*., Environ. Eng. Res. 25 (2019) 571–578.

[51] da Costa Soares I., da Silva D., do Nascimento J., *et al*., Environ. Sci. Pollut. Res. 24 (2017) 24167–24176.

[52] Labiadh L., Oturan M., Panizza M., *et al*., J. Hazard. Mater. 297 (2015) 34–41.

[53] Moreira F., Boaventura R., Brillas E., *et al*., Appl. Catal. B Environ. 162 (2015) 34–44.

[54] El-Ghenymy A., Cabot P., Centellas F., *et al*., Electrochim. Acta 90 (2013) 254–264.

[55] El-Ghenymy A., Rodríguez R., Arias C., *et al*., J. Electroanal. Chem. 701 (2013) 7–13.

[56] Garcia-Segura S., Keller J., Brillas E., *et al*., J. Hazard. Mater. 283 (2015) 551–557.

[57] Moreira F., Soler J., Fonseca A., *et al*., Appl. Catal. B Environ. 182 (2016) 161–171.

HUMIC ACIDS IN THE ENVIRONMENT

Mirjana Marković[1*], Svjetlana Radmanović[2], Đuro Čokeša[1], Nebojša Potkonjak[2]

[1]Vinča Institute of Nuclear Sciences, University of Belgrade – National Institute of the Republic of Serbia, P.O. Box 522, 11001 Belgrade, SERBIA

[2]University of Belgrade, Faculty of Agriculture, Nemanjina 6, 11080 Belgrade, SERBIA

[*]*mmmark@vinca.rs*

Abstract

Humic acids, belonging to the humic substances, are the most reactive organic compounds in water, soil and sediments. They are known for their role in processes related to soil structure, biology, and chemistry, as well as for their effects on the behavior of environmental pollutants. The effects of humic acids on the environment are strongly influenced by their composition and structure. Humic acids are used in various fields, especially in agriculture, environmental remediation and medicine. Agricultural fertilizers containing humic acids as additives are often used to improve plant growth and soil fertility. The content of heavy metals, metalloids, radionuclides and various organic pollutants can be reduced by adsorption, complexation, and redox processes involving humic acids. Owing to the ability of humic acids to form composites with inorganic and organic oxides, pollutants are adsorbed and removed from water. In addition, the composites formed exhibit pronounced antibacterial activity in water. Various organic pollutants such as pesticides, microplastics and antibiotics can also be removed from soil and water by adsorption on the composites or humic acids. Various viruses with positively charged glycoproteins can be bound by the negatively charged humic acids, defining them as antivirally active. Currently, the humic acids are isolated from various matrices such as coals, peat and organic wastes. Due to the increasing requirements for the commercial applications of humic acids, their production and utilization are significantly important and trendy tasks. The humic acid production with the higher yield is the focus of research today.

Keywords: humic acids, environmental pollution, remediation.

INTRODUCTION

Humic substances (HS) are the most important organic components in water, soil and sediments and have important environmental functions. Their role in controlling the fate of environmental pollutants and the biogeochemistry of organic C in the global ecosystem is well known [1].

Most of the difficulties in chemically defining the structure and reactivity of HS arise from its extremely pronounced chemical heterogeneity and geographic variability. The complexity of the chemistry of HS is a function of several general characteristics of the ecosystem in which it is formed: vegetation, climate, topography, etc. [1].

Despite the outstanding importance of HS in sustaining life, its basic chemical nature and reactivity remain a fascinating research topic [2]. The structure of HS has been discussed from various aspects, including molecular conformation, molecular aggregation,

macromolecularity, and supramolecular properties [3]. One approach states that HS consists of relatively small molecules held together by weak interactions such as hydrophobic forces and hydrogen bonding [1].

Humic acids (HA), one of the HS fractions, are the most reactive compounds in soil and have the capacity for various chemical and physical reactions in the environment. HA have a complex structure with active functional groups such as carboxyl and hydroxyl, which have an important influence on the transformation and migration of various compounds in soil [4,5]. Humic acids mediate processes related to soil structure, biology and chemistry, thus maintaining vital ecosystem functions [6].

Soil and water contamination by organic and inorganic pollutants is of extreme concern due to their high toxicity and environmental persistence. Due to their ability to interact with these potentially hazardous compounds in soil and water, humic acids strongly influence their mobility and bioavailability [7].

HUMIC ACIDS – SUMMARY OF PROPERTIES

Humic substances account for about 25% of the total organic carbon on earth. These substances represent a class of naturally occurring complex molecular structures formed by aggregation processes in which biomolecules derived from plant and animal residues are progressively transformed through biotic and abiotic pathways. Prior to physicochemical analysis of HS, physical and/or chemical separation from the inorganic components by an extraction process is required. The most efficient separation procedures involve extraction with alkali, yielding three fractions based on their solubility in water: fulvic acids (soluble at all pH values), humic acids (insoluble under acidic conditions, pH < 2, soluble at higher pH values), and humins (insoluble at any pH value) [8].

In general, articles published in the research area are significant indicators of the importance of humic acids. Applying the following keywords: "humic substances", "humic acids", "fulvic acids" and "humins" in the Scopus database, a total of 17,135, 27,622, 9,642 and 573 articles were published, respectively. Under the keyword "humic acids", most articles were published in the field of environmental sciences (26.8%), followed by chemistry (16.1%), agricultural and biological sciences (11.2%), chemical engineering (9.1%), etc. (Figire 1).

Elemental analysis is a useful tool for characterizing nonstoichiometric mixtures such as humic acids. Variations in the elemental composition of humic acids of different origins have been reported [9]. These differences are the result of the HA various molecular structures that affect the behaviour of some inorganic and organic pollutants in the environment. Moreover, the values of H/C and O/C ratio have been used to indicate the degree of aromaticity or aliphaticity [9–11]. The variations of the ratio also depend on the HA source. For example, Rice and MacCarthy [12] statistically analyzed 410 samples of HA. When segregated by source, the differences between humic acids isolated from soil, fresh and sea water are evident (Table 1). The degree of aliphaticity of humic acids decreases in the order sea water > freshwater > soil. In addition to the differences in the origin of each category, obviously pronounced standard deviations indicate the heterogeneity of the HA elemental composition.

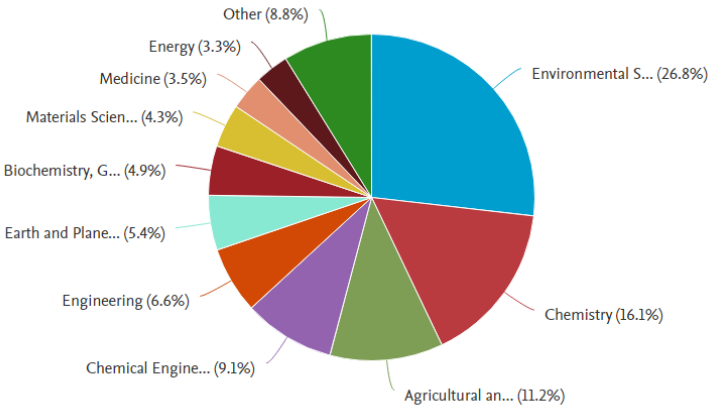

Figure 1 *Overview of published articles, keyword "humic acids" (the 1881–May 18, 2023 period) (source: www.scopus.com)*

Table 1 *Mean and standard deviation for elemental composition of humic acids from various sources, expressed in weight percent; O/C and H/C ratios in atomic percent (ash-free basis) (after Rice and MacCarthy [12])*

Source	C	H	N	O	O/C	H/C
Soil	55.4±3.8	4.8±1.0	3.6±1.3	36.0±3.7	0.50±0.09	1.04±0.25
Freshwater	51.2±3.0	4.7±0.6	2.6±1.6	40.4±3.8	0.60±0.08	1.12±0.17
Sea water	56.3±6.6	5.8±1.4	3.8±1.5	31.7±7.8	0.45±0.08	1.23±0.23

A wide range of optical, spectroscopic, microscopic and chromatographic techniques facilitated the study of the molecular structure of humic acids [13].

Humic acids are complex organic colloidal mixtures whose composition and chemical structure depend on their origin and age. These differences in composition and structure strongly influence their environmental behavior and ecological fate. Accordingly, the molecular structure of HA is not clearly defined [13]. The concepts describing the HA structure originate from the developments in structural chemistry [2]. The traditional view, based on the concept of macromolecularity, considers HA as coiled conformations of slightly cross-linked long-chain molecules [14]. More recent approaches suggest that HA are an aggregation of relatively small molecules held together not only by weak hydrophobic forces and hydrogen bonding [1], but also by stronger near-covalent forces [2,15,16]. The HA aggregation process depends on various environmental conditions (pH, ionic strength, HA concentration, residence time, type and concentration of organic and inorganic ions, presence of solid particles) as well as on the structural properties of HA (size, shape, conformation, functional groups) [17–21].

Chemical reactivity is one of the most important characteristics of HA [13], with antioxidant, acid/alkali, ion exchange, complexation, antibacterial, adsorption, and redox properties considered crucial [22–24].

Regardless of the differences arising from the HA origin, their basic structure includes aromatic rings, peptides or aliphatic groups and various reactive groups such as carboxyl,

alcohol hydroxyl, phenolic, methoxy, carbonyl and quinones [25–26]. Carboxyl and phenolic groups are the most abundant and are mainly responsible for the total acidity of HA [26]. The carboxyl and phenolic groups represent the hydrophilic domain of HA, while aliphatic chains and aromatic rings are hydrophobic in nature [13]. The hydrophilic and hydrophobic parts are responsible for chelating and repelling processes, respectively [27]. The hydrophilic parts form micelles increase the soil water-holding capacity, while the nonpolar parts repel water molecules, reducing water infiltration and improving the stability of soil aggregates [28].

The carboxyl and phenolic groups enable the HA complexation and ion exchange processes. The polar and anionic moieties formed by dissociation of these functional groups form the HA-metal complexes by electrostatic bonding. Thus, hydrogen bonding is confirmed to be the predominant interaction type in the HA-arsenite complex formation (Figure 2) [7].

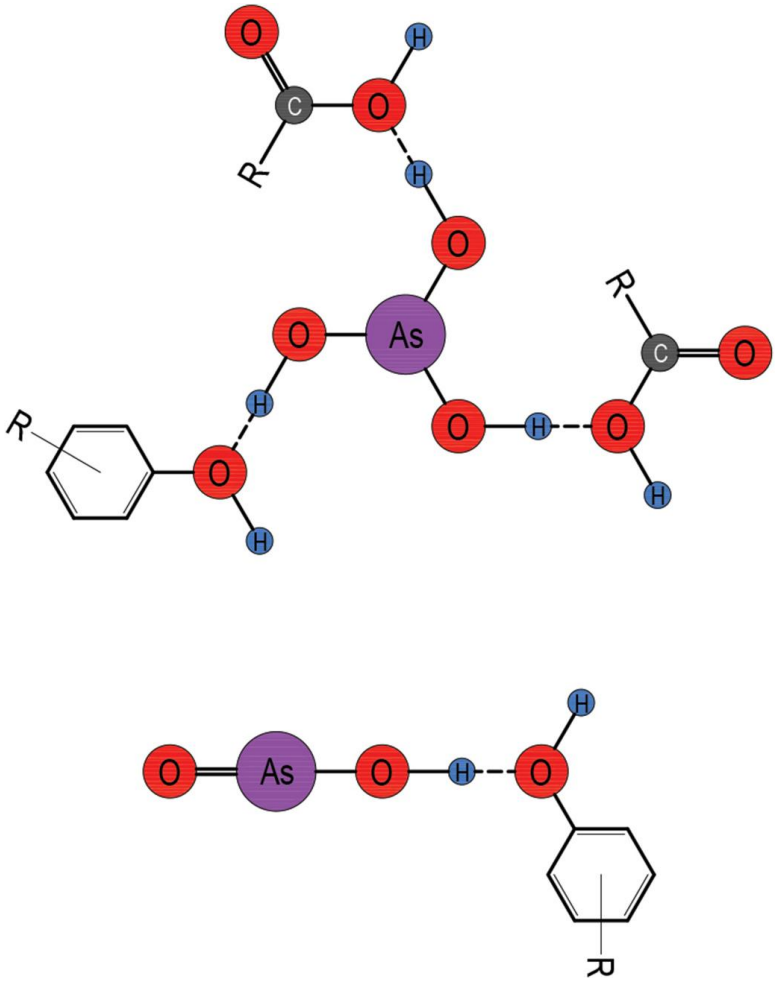

Figure 2 *HA-arsenite hydrogen bonding of $As(OH)_3$ (top) and AsH_2O_2 (bottom) with carboxyl and phenolic groups* [7]

The low molecular weight HA, having more phenol and carboxyl groups, manifest a pronounced chelating ability compared to HA with high molecular weight [26].

Due to their properties, HA are widely used in various fields, especially in agriculture, environmental remediation and medicine [13].

THE HUMIC ACID APPLICATIONS

Using the keywords "humic acids" and "application" (Scopus database) yielded a total of 4,583 articles. Most articles (24.0%) were published in the area of environmental sciences, followed by agriculture and biological sciences (16.2%), chemistry (14.1%), chemical engineering (9.6%), etc. (Figure 3).

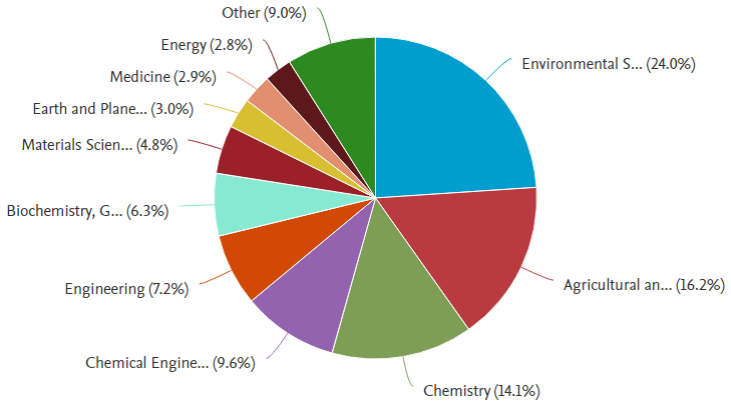

Figure 3 *Overview of published articles, keywords "humic acids" and "application" (the 1914–May 18, 2023 period) (source: www.scopus.com)*

Recently, due to the increasing requirements for commercial HA applications, their production and use are a challenging task [13]. Soil humic acids are not suitable for commercial use due to their low content. Currently, the commercial products of HA are extracted from various sources (coals, peat, animal and plant residues) [27]. More efficient extraction methods that allow higher HA yields are the focus of research. In addition, increasing the content of nitrogen, oxygen and functional groups (carboxyl and phenolic) in the development of the extraction process is very important to improve the bioavailability of HA [29–31].

Humic acids in agriculture

It is known that HA improve soil structure, increase soil water retention capacity and soil cation exchange capacity, improving nutrient utilization by plants [32]. As soil organic matter content decreases, external additions have been studied [27].

Agricultural fertilizers containing HA can be used as biostimulants that improve plant growth and/or soil fertility [33–34].

Physiological plant functions are directly affected when the liquid HA products are introduced into the root zone of plants through a drip irrigation system, increasing the HA concentration in the rhizosphere and promoting plant growth [35–36]. This direct effect results from the HA interaction with cell membranes on the surface of plant roots [35].

In addition to direct, indirect effects also influence pathways between nutrients and the environment, including complementary processes of complex formation and biochemical pathways [35]. During complexation, stable and soluble natural HA-metal complexes (e.g. Fe, Zn, Mn, Cu) are formed, which increase the solubility and bioavailability of micronutrients. The biochemical mode of action of the HA application can improve the mineral nutrition of

plants by activating factors important for the uptake, transport and metabolism of nutrients in plants [37,38]. The main factors activated are nutrient transport proteins, plasma membrane (PM) H+-ATPases, hormones, genes/enzymes for nitrogen assimilation, cell division and development [39].

Humic acids in the remediation

Environmental pollution is caused by anthropogenic activities resulting from industry, agriculture and municipal waste. The released pollutants enter the atmosphere, water, soil and sediments, making them unsuitable as habitats. The most common substances include heavy metals, metalloids, radionuclides, and various organic substances that affect the physiological system of all living organisms [40]. To minimize or remove environmental pollutants, they can be mineralized, reduced, or degraded by adsorption, complexation, and redox processes [41–42]. In particular, the HA functional groups bind heavy metals by complexation or ion exchange processes, while organic pollutants are sorbed by the HA hydrophobic aliphatic groups [43–44]. Mobility and toxicity of pollutants in soil can be changed by their adsorption to the HA-mineral complexes [13].

The molecular weight of humic acids has a great influence on the behavior of heavy metals in the soil. The high molecular weight HA stabilize heavy metals directly by ion exchange and complexation processes and indirectly by affecting soil properties (pH, CEC, organic matter and microorganisms). The low molecular weight HA act as a surfactant mobilizing and removing heavy metals from the soil [45]. The low heavy metal binding affinity to the HA is one of the most important factors for the removal and control of heavy metals in soil [46–47]. Thus, cadmium and copper, which are strongly bound by humic acids, are eliminated from soil more efficiently than lead and nickel, which are only weakly attached to the HA [48]. Metal translocation from soil also depends on the HA concentration, soil pH, equilibration time, and solid/liquid ratio [49,50].

Regarding water, the HA-containing composites are used to adsorb pollutants in order to separate them from water. Currently, the composites are usually prepared by coating iron oxide nanoparticles (hematite, goethite, and magnetite, etc.) on HA [51–53]. The efficient combination of HA and iron oxide can successfully remove various metals [13]. Moreover, the ability of HA, to form composites with inorganic and/or organic oxides makes them antibacterially active substances in water [54–56]. In addition, the composites with antibacterial activity against various pathogens can be used as biocides in air disinfection, food packaging, etc. [56].

Organic pollutants, which are widely distributed in the environment, are of great importance for research and remediation. Various combinations of processes with humic acids are applied to remove organic pollutants from soil and water [57]. Due to the HA hydrophobic structure, the HA-coated hematite adsorb ionisable pentachlorophenol and non-ionizable phenanthrene particularly strongly. Consequently, coating hematite with HA significantly reduces its polarity, inhibiting water adsorption and promoting the formation of hydrophobic interactions between HA-coated hematite and these hydrophobic organic compounds. The HA carboxyl and phenolic groups increase the electron donor-acceptor and hydrogen bonding interactions between HA-coated hematite and the studied organic compounds. Due to the

deprotonation of the HA functional groups, the soil or water pH affects the adsorption process [58].

Micro(nano)plastics, as extremely toxic and resistant pollutants, have become the important subject of many research studies and regulatory rules. The most abundant microplastic comes from packaging materials produced for pharmaceuticals, personal care and cosmetic products, detergents, etc. [59,60], and from fragmentation during weathering and abrasion processes [61]. Nowadays, microplastics are present in large quantities in water, air, soil, and sediments, even in places that are not inhabited [62]. The mutual interaction between microplastics and the HA produces the omnipresent heterogeneous mixture of different organic materials with many functional groups already present in the environment [63].

Humic acids are sorbed by microplastics due to various interactions, including hydrophobic and electrostatic attraction. The most important factors for the sorption process are the properties of the HA (functional groups, molecular weight, etc.), the microplastic (polymer type, size, shape, concentration), and the matrix (pH, salinity, ionic content, temperature) [64,65]. Mechanical, photochemical and biological degradation processes enable the HA migration from microplastics [62] leaching them into ecosystems [66].

Veterinary antibiotics (VA) contaminate soil and water and have potentially detrimental impacts on the ecosystem and health of living organisms. Manure as agricultural fertilizer is the main source of VA in the environment [67]. Among other factors affecting the VA behavior, HA are one of the very important [68–71]. Due to various interactions, including electrostatic, cation exchange, and hydrophobic interactions, HA-VA complexes are formed, which decrease the degradation and mobility of antibiotics [32,72–76].

Humic acids as antiviral agents

The HA antiviral activity is based on the ability of their negatively charged molecules to bind positive viral glycoproteins through a competitive inhibitory mechanism that suppresses viruses to merge with cell membrane receptors. The HA intracellular antiviral mechanism is also present [77]. The antiviral properties were found to be related to the hydrophobic, aromatic [78], carbohydrate and lipophilic [79] parts of the HA molecule, but also dependant on the HA carboxyl groups content [80].

CONCLUSION

Humic acids, belonging to the humic substances, are the most reactive organic compounds in water, soil and sediments. They are known for their role in processes related to soil structure, biology, and chemistry, as well as for their effects on the behavior of environmental pollutants. The effects of humic acids on the environment are strongly influenced by their composition and structure. Humic acids are used in various fields, especially in agriculture, environmental remediation and medicine. To improve plant growth and soil fertility, agricultural fertilizers having humic acids as additives are frequently used.

The content of heavy metals, metalloids, radionuclides and various organic pollutants can be decreased by adsorption, complexation, and redox processes involving humic acids. The

mobilization/removal of heavy metals from the soil can be accomplished by the low molecular weight humic acids, while the high molecular weight humic acids act as stabilizers.

Owing to the ability of humic acids to form composites with inorganic and/or organic oxides, pollutants are adsorbed and removed from the water. Moreover, the formed composites manifest the pronounced antibacterial activity in water. Various organic pollutants, such as pesticides, microplastics and antibiotics, can also be removed from soil and water by adsorption to the composites or humic acids.

Various viruses with positively charged glycoproteins can be bound by the negatively charged humic acids, which define them as antivirally active.

Currently, the humic acids are isolated from various matrices such as coals, peat and organic wastes. Due to the increasing requirements for the commercial HA applications, their production and utilization are significantly important and trendy tasks. The humic acid production with the higher yield is the focus of research today.

Due to the humic acid structure and superior properties, in addition to their traditional use, there is an erasing need for potential innovative applications in industry.

ACKNOWLEDGEMENT

This work was partially supported by the Ministry of Science, Technological Development and Innovation of the Republic of Serbia (Grants no. 451-03-47/2023-01/200017 and 451-03-47/2023-01/200116).

REFERENCES

[1] Piccolo A., Adv. Agronomy 75 (2002) 57–134.

[2] Zavarzina A., Danchenko N., Demin V., *et al*., Eurasian Soil Sci. 54 (12) (2021) 1826–1854.

[3] Schaumann G., J. Plant Nut. Soil Sci. 169 (2006) 145–156.

[4] Wang S., Mulligan C., Chemosphere 74 (2009) 274–279.

[5] Liu Y., Zhi L., Zhou S., *et al*., Sci. Poll. Res. 27 (2020) 18650–18660.

[6] Hoffland E., Kuyper T., Comans R., *et al*., EcoPlant Soil 455 (2020) 1–22.

[7] Čokeša Đ., Radmanović S., Potkonjak N., *et al*., Chemosphere 315 (2023) 137687.

[8] Weber J., Chen Y., Jamroz E., *et al*., Soils Sed. 18 (2018) 2665–2667.

[9] Xiaoli C., Shimaoka T., Qiang G., *et al*., Waste Manage. 28 (2008) 896–903.

[10] Dergachevaa M.., Nekrasovab O., Okoneshnikovac M., *et al*., Problems Ecol. 5 (5) (2012) 497–504.

[11] Klavins M., Purmalis O., J. Mol. Structure 1050 (2013) 103–113.

[12] Rice J., MacCarthy P., Org. Geochemistry 17 (5) (1991) 635–648.

[13] Wei S., Li Z., Sun Y., *et al*., Renew. Sustain. Energy Rev. 170 (2022) 112984.

[14] Stevenson F., Humus Chemistry: Genesis, Composition, Reactions. John Wiley & Sons, Inc., New York (1994) p.512, ISBN: 978-0-471-59474-1.

[15] Wells, M., J. Environ. Qual. 48 (2019) 1644–1651.

[16] Wells M., Stretz H., Sci. Total Environ. 537 (2019) 81–92.

[17] Galicia-Andrés E., Escalona Y., Oostenbrink C., *et al*., Geoderma 401 (2021) 115237.

[18] Jovanović U., Marković M., Cupać S., *et al*., Plant Nutr. Soil Sci. 176 (2013) 674–679.

[19] Jovanović U., Marković M., Živković N., *et al*., Serb. Chem. Soc. 87 (6) (2022) 761–773.

[20] Radmanović, S., Marković, M., Jovanović, U., *et al*., J. Serb. Chem. Soc. 85 (3), 407–419.

[21] Tombácz E., Soil Sci. 164 (1999) 814–824.

[22] Panettieri M., Knicker H., Murillo J., *et al*., Soil Biol. Biochemistry 78 (2014) 70–81.

[23] Jin P., Song J., Yang L., *et al*., Environ. Poll. 233 (2018) 290–298.

[24] Ma B., Ding Y., Li W., *et al*., Chemosphere 197 (2018) 793–802.

[25] Lee J., Yoon H., Cha J., *et al*., Biotech. Adv. 3 (2019) 107416.

[26] De Melo B., Motta F., Santana M., Mater. Sci. Eng. C 62 (2016) 967–974.

[27] Ampong K., Thilakaranthna M., Gorim Y., Front. Agronomy 4 (2022) 848621.

[28] Billingham K., Proceedings of the 27th Annual Conference The Grassland Society of NSW Inc., 24–26 July, Wagga Wagga, Australia (2012) 43–50.

[29] Zara M., Ahmad Z., Akhtar J., *et al*., Energy Source. 39 (2017) 1159–1166.

[30] Boral P., Varma, A., Maity S., Int. J. Coal Sci. Technol. 8 (2021) 1034–1053.

[31] Fatima N., Jamal A., Huang Z., *et al*., Sustainability 13 (2021) 8969.

[32] Yang B., Wang C., Cheng X., *et al*., Water Res. 202 (2021) 117379.

[33] Khaled H., Fawy H., Soil Water Res. 6 (2011) 21–29.

[34] Colpas F., Taron B., Dunoyer A., *et al*., Food Agric. 30 (2018) 941–945.

[35] Olaetxea M., De Hita D., Garcia C., *et al*., Appl. Soil Ecol. 123 (2018) 521–537.

[36] Nardi S., Pizzeghello D., Muscolo A., *et al*., Soil Biol. Biochemistry 34 (2002) 1527–1536.

[37] Jannin L., Arkoun M., Ourry A., *et al*., Plant Soil 359 (2012) 297–319.

[38] Quaggiotti S., Ruperti B., Pizzeghello D., *et al*., J. Exp. Bot. 55 (2004) 803–813.

[39] Nardi S., Schiavon M., Francioso O., Molecules 26 (2021) 2256.

[40] Marcon L., Oliveras J., Puntes V., Sci. Total Environ. 791 (2021) 148324.

[41] Zingaretti D., Lominchar M., Verginelli I., *et al*., Environ. Sci. Poll. Res. 27 (2020) 22225–22234.

[42] Park C., Han J., Chu K., *et al*., J. Ind. Eng. Chem. 48 (2017) 186–193.

[43] Peng X., Gai S., Cheng K., *et al*., J. Hazard. Mater. 435 (2022) 129070.

[44] Yan C., Fan L., Chen Y., *et al*., Colloid. Surface. 602 (2020) 125135.

[45] Zheng X., Li Q., Peng H., *et al*., Sustainability 14 (2022) 13058.

[46] Baken S., Degryse F., Verheyen L., *et al*., Environ. Sci. Technol. 45 (2011) 2584–2590.

[47] Hartley N., Tsang D., Olds W., *et al*., Soil Sediment Con. Int. J. 23 (2014) 599–613.

[48] Borggaard O., Holm P., Jensen J., *et al*., Acta Agric. Scand. B 61 (2011) 577–581.
[49] Tang W., Zeng G., Gong J., *et al*., Sci. Total Environ. 468–469 (2014) 1014–1027.
[50] Zhang S. Y., Wen J., Hu Y., *et al*., J. Hazard. Mater. 366 (2019) 210–218.
[51] Peng H, Liang N, Li H, *et al*., Environ Poll. 204 (2015) 191–198.
[52] Liu J., Zhao Z., Jiang G., Sci. Technol. 42 (2008) 6949–6954.
[53] Xu B., Lian Z., Liu F., *et al*., Environ. Poll. 248 (2019) 929–937.
[54] Kochar C., Taneja L., Yadav P., *et al*., J. Mol. Liq. 380 (2023) 121684.
[55] Taneja L., Kochar C., Yadav P., *et al*., Groundw. Sustain. Develop. 22 (2023) 100954.
[56] Venezia V., Verrillo M., Gallucci N., *et al*., J. Environ. Chem. Eng. 11 (2023) 108973.
[57] Yang F., Tang C., Antonietti M., Chem. Soc. Rev. 50 (2021) 6221–6239.
[58] Fang Q., Chen B., Lin Y., *et al*., Environ. Sci. Technol. 48 (2014) 279–88.
[59] Duis K., Coors A., Environ. Sci. Eur. 28 (2016) 2.
[60] Hernandez E., Nowack B., Mitrano D., Environ. Sci. Technol. 51 (2017) 7036–7046.
[61] Galloway T., Cole M., Lewis C., Nat. Ecol. Evol. 1 (2017) 1–8.
[62] Sun Y., Ji J., Tao J., *et al*., Trends Analyt. Chem. 158 (2023) 116882.
[63] Bolan N., Adriano D., Kunhikrishnan A., *et al*., Adv. Agronomy 110 (2011) 1–75.
[64] Junaid M., Wang J., Crit. Rev. Environ. Sci. Technol. 52 (2022) 4241–4265.
[65] Kumar R., Verma A., Rakib Md. R. J., *et al*., Sci. Total Environ. 856 (2023) 159097.
[66] Rillig M., Leifheit E., Lehmann J., PLoS Biol. 19 (2021) e3001130.
[67] Gbadegesin L., Tang X., Liu C., *et al*., Int. J. Environ. Res. Pub. Health 19 (2022) 1702.
[68] Lian F., Sun B., Chen X., *et al*., Environ. Poll. 204 (2015) 306–312.
[69] Christl I., Ruiz M., Schmidt J. R., *et al*., Environ. Sci. Technol. 50 (2016) 9933–9942.
[70] Pan B., Wang P., Wu M., *et al*., Environ. Poll. 171 (2012) 185–190.
[71] Li Y., Bi E., Chen H., Ecotox. Environ. Saf. 178 (2019) 43–50.
[72] Wang L., Liang N., Li H., *et al*., Environ. Poll. 196 (2015) 379–385.
[73] Xu J., Yu H.Q., Sheng G.P., J. Hazard. Mater. 302 (2016) 262–266.
[74] Wang R., Yang S., Fang J., *et al*., Res. Public Health 15 (2018) 1458
[75] Fan W., Guo T., Gao S., *et al*., Environ. Res. 193 (2021) 110527.
[76] Zhao Y., Gu X., Gao S., *et al*., Geoderma 183–184 (2012) 12–18.
[77] Socol D., Front. Pharmacology 13 (2023) 1018904.
[78] Zhernov Y., Konstantinov A., Zherebker A., *et al*., Environ. Res. 193 (2021) 110312.
[79] Zhernov Y., J. Allergy Cl. Immunology 141 (2018) AB233.
[80] Meerbach A., Neyts J., Balzarini J., *et al*., Antivir. Chem. Chemotherapy 12 (6) (2001) 337–345.

ADVANCED OPTICAL TOOLS APPLIED ON HONEY SAMPLES FOR BEE HEALTH STATUS MONITORING

Mira Stanković[1,2*], Miloš Prokopijević[1], Dragana Bartolić[1,2], Jevrosima Stevanović[3], Filip Andrić[4], Ksenija Radotić[1,2]

[1]University of Belgrade, Institute for Multidisciplinary Research, Kneza Viseslava 1, 11000 Belgrade, SERBIA

[2]University of Belgrade, Center for Green Technologies, Institute for Multidisciplinary Research (IMSI), Belgrade, Kneza Viseslava 1, 11030 REPUBLIC OF SERBIA

[3]University of Belgrade, Faculty of Veterinary Medicine, Bulevar oslobodjenja 18, 11000 Belgrade, SERBIA

[4]University of Belgrade, Faculty of Chemistry, Studentski trg 12–16, 11000 Belgrade, SERBIA

[*]*mira.mutavdzic@imsi.rs*

Abstract

Honey bees have a very important role in pollinating plants, in addition to honey production. Bee diseases are one of the reasons of a significant decrease in bee colonies in the world in recent years. Honey samples originating from hives with different infestations with N. ceranae were analyzed. Total phenolic content and total protein content were determined by the Folin-Ciocalteu assay and the Bradford assay, respectively. Fluorescence spectroscopy combined with PARAFAC was used to determine the spectral components originating from proteins (PFSC1) and phenolics (PFSC2) in honey samples, and their ratios were calculated. Phenols and proteins content in the honey samples, obtained by spectrophotometric quantification, decreases with increasing infestation levels in the respective hives infected with N. ceranae. A negative correlation was obtained for the ratio of PARAFAC components PFSC2/PFSC1 and the level of infestation with N. ceranae in honey samples. These results indicate that fluorescence spectroscopy combined with PARAFAC could be used as an optical tool for non-invasive and rapid screening of honey to estimate bee health status.

Keywords: *Apis mellifera*, *Nosema ceranae*, fluorescence spectroscopy, proteins, TPC.

INTRODUCTION

Honey bees (*Apis mellifera*) are source of unique, natural products of honey, wax, propolis and royal jelly. However, bees have an important ecological role related to the pollination of numerous agricultural and wild plant species, thus the high annual losses of bees in recent years have attracted a lot of public and scientific attention. Consequently, scientists have devoted much of their recent work to uncovering the stresses that affect bees [1,3]. Several studies have focused on assessing the relationship between bee colony health and the effects of multiple biotic (parasites and pathogens) and abiotic (pesticide exposure, poor nutrition, and low temperature) stressors [4,5]. Monitoring the health status of bee colonies can help us identify potential threats to their survival, and take action to protect them.

Special attention of the scientific public is focused on the influence of the parasite microsporidia *Nosema ceranae*, on bee colonies. Research has shown that the infestation with microsporidia *N. ceranae* leads to disturbances in the protein metabolism of bees, a decrease in the amount of protein in the hypopharyngeal glands of bees, then leads to a decrease in the growth of bees and the loss of bee colonies [6,7]. The negative influence of *N. ceranae* on the yield of honey originating from infected bee colonies has been shown in several studies [8,9].

MATERIALS AND METHODS

Samples

Five honey samples were collected during 2018 from the apiary in the yard of the Faculty of Veterinary Medicine in Belgrade. At the moment when the honey was taken for further analysis, the bees were also taken to assess nosema infestation.

Microscopic detection of *N. ceranae* spores and quantification of the infestation level

A microscopic examination of bee samples was performed to detect nosema spores in accordance with the recommendations of the World Organization for Animal Health (World Organization for Animal Health, OIE, 2017). From each hive, 30 adult foraging bees were collected from the hive, and then the bees were frozen. Each bee was macerated with 2–3 ml of water, and then the obtained suspension was examined under a microscope (magnification x400). Figure 1 shows a microscopic examination where the presence of spores of the genus *N. ceranae* was observed. At the moment when the bees were taken for the assessment of nosema infestation, the honey samples were also taken for further analysis. All samples were collected during one season from one apiary.

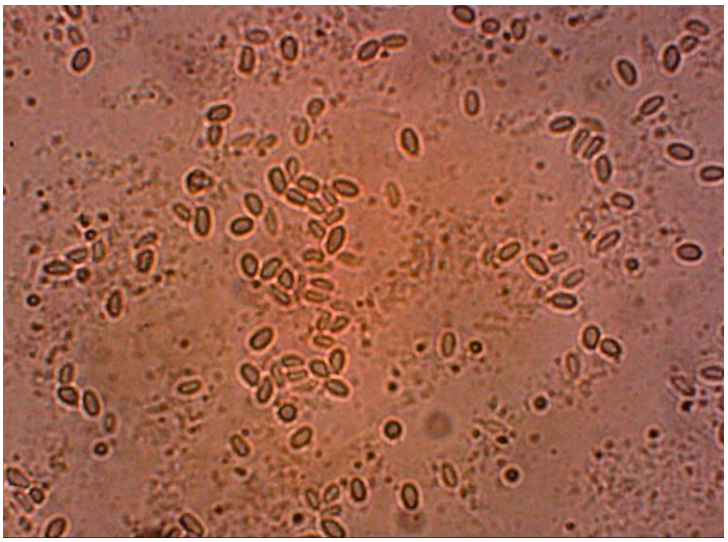

Figure 1 *Microscopic examinations of the macerated bees with the presence of N. ceranae spores*

Determination of Total Phenolic Content (TPC)

Each honey sample (5 g) was diluted with ultrapure water at 50 mL volumetric flask and filled to the mark. The total phenolic content was determined spectrophotometrically by the Folin–Ciocalteu method [10]. The sample solution (0.3 mL) and deionized water (6 mL) were

mixed with Folin-Ciocalteu reagent (0.5 mL) and incubated for 6 min at room temperature. About 3 mL sodium carbonate solution (20 %) was added in the sample solution. Afterwards, the sample was kept at 40 °C for 30 min and the absorbance was measured at 765 nm using a Shimadzu UV-160 spectrophotometer (Kyoto, Japan). Gallic acid was used as the standard, and the calibration curve of gallic acid was prepared in the concentration range between 0 and 250 mg L^{-1}. A mixture of water and Folin–Ciocalteu reagent was used as the blank. The results are expressed as the gallic acid equivalent (GAE) per kg of honey.

Determination of Total Protein Content

The total protein content was determined using the Bradford procedure [11]. Each honey sample (5 g) was mixed with ultrapure water (10 mL). Coomassie Brilliant Blue (200 μL) was added in the honey solution (5 μL). After 5 min of incubation, the absorbance was measured at 595 nm against a standard solution of bovine serum albumin (10–100 μg/0.1 mL). The total protein content was quantified and expressed as g/kg of honey.

Fluorescence measurements

Fluorescence spectra of honey samples were recorded using a Fluorolog FL3-221 spectrofluorimeter (Jobin Yvon Horiba, Paris, France), with the FluorEssence 3.5 software package (Horiba Scientific, Kyoto, Japan); the light source was a xenon lamp 450 W. All measurements were made in the front face configuration at an angle of 35°, with an integration time of 0.1 s, while the width of the opening for passing the excitation and emitted light (slits) was 2 nm. Emission spectra of honey samples were recorded in the range from 280 to 500 nm with excitation wavelengths of 260–380 nm. The wavelength step in the excitation measurements was 5 nm and the emission step was 1 nm.

PARAFAC

The EEMs of honey samples were packed in three-way data arrays for PARAFAC analysis. PARAFAC is able to decompose a three-way data into trilinear components, which number depends on the number of fluorophores in the samples. PARAFAC Components should correspond to the fluorophores in the sample [12].

Correlation analysis

Correlation analysis was performed using basic Data analysis add in the Microsoft office Excel 365, by calculating Pearson's correlation coefficient between PARAFAC scores and the rest of the studied variables. Statistical significance of correlations was estimated by Student's *t*-test.

RESULTS AND DISCUSSION

The results of spectrophotometric quantification of proteins and phenols in honey samples are presented in Figure 2 and Figure 3. It can be observed that the values of total proteins and phenols content in the honey samples decrease with the increase in the infestation *N. ceranae* of the corresponding bee colonies. A high linear dependence is confirmed with R^2 values for proteins and phenols 0.8174 and 0.7423, respectively.

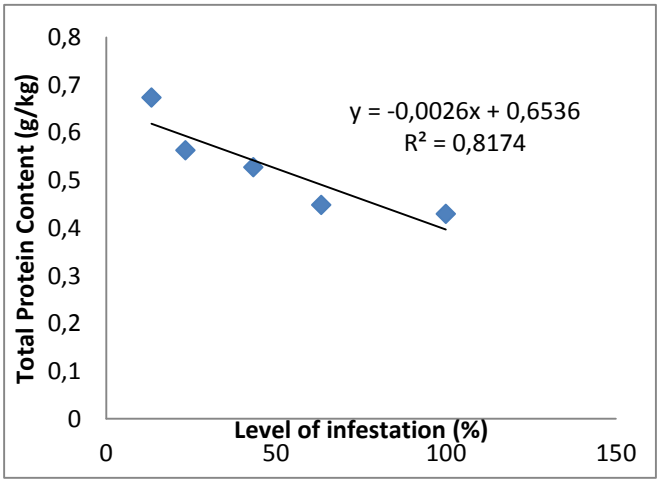

Figure 2 *Dependence of total protein on the level of hives infestation with N. ceranae*

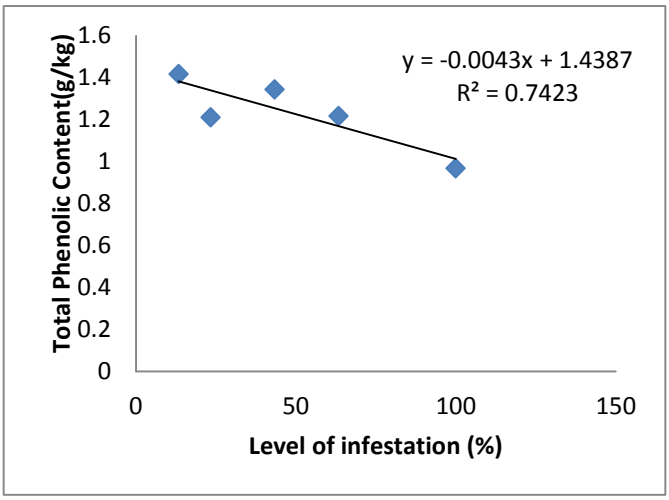

Figure 3 *Dependence of phenolic content on the level of hives infestation with N. ceranae*

Figure 4 shows, as an example, the fluorescence EEM contour map for the honey sample obtained from the beehive with 10% *N. cerenae* infestation. In all honey emission spectra, there were two broad characteristic maxima, the first maximum emission about 340–360 nm assigned to proteins and the second about 400–450 nm assigned to phenolic compounds.

The PARAFAC models were built by successive increase in number of components, from 1 to 5. Investigation of residuals and changes in the core consistency suggested that the spectral data are best described by 2 components. Considering low number of honey samples validation of PARAFAC models by split-half analysis was not possible. The loading vectors of the two PARAFAC components obtained by decomposition of EEMs are given in the Figure 5. These two should represent the inherent pure emission (a) and excitation (b) spectra of the characteristic honey fluorophores.

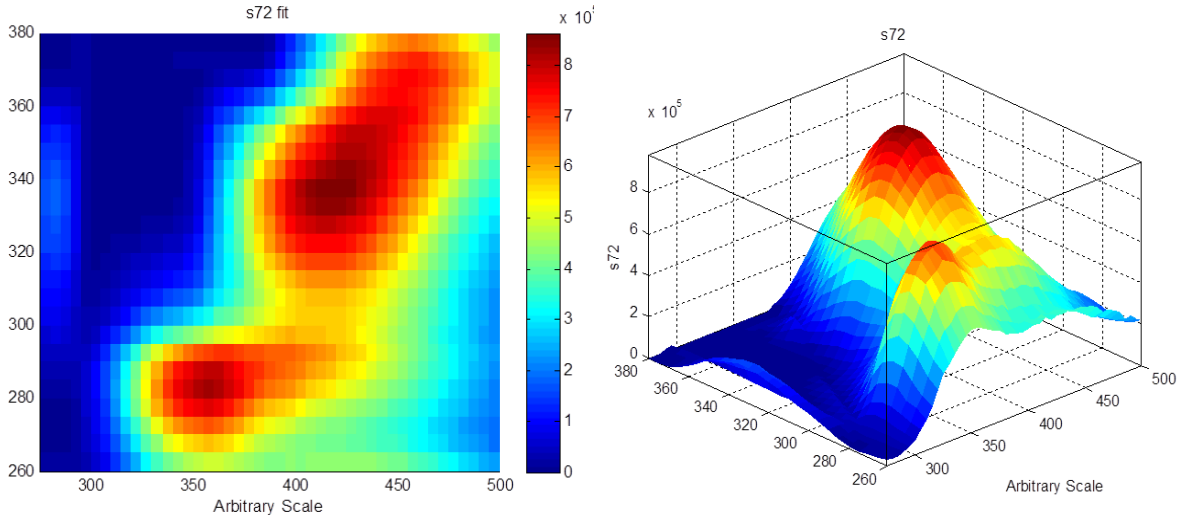

Figure 4 *The Excitation Emission Matrix (EEM) contour map for the raw spectra of the honey sample obtained from the beehive with 10% N. cerenae infestation*

The emission loading vector of the first PARAFAC component (PFC1) has the maximum at 325 nm, while its corresponding excitation loading vector reaches the maximum above 360 nm. According to findings this component can be attributed to the protein fluorophore in honey [13]. In the case of the second component (PFC2) one small emission maximum (at 325 nm) and two prominent emission maxima (in the range of 370–400 nm) are observed. Excitation loading vector of PFC2 shows significant intensity from 260–345 nm. This can be attributed to the phenolic compounds present in honey samples [14].

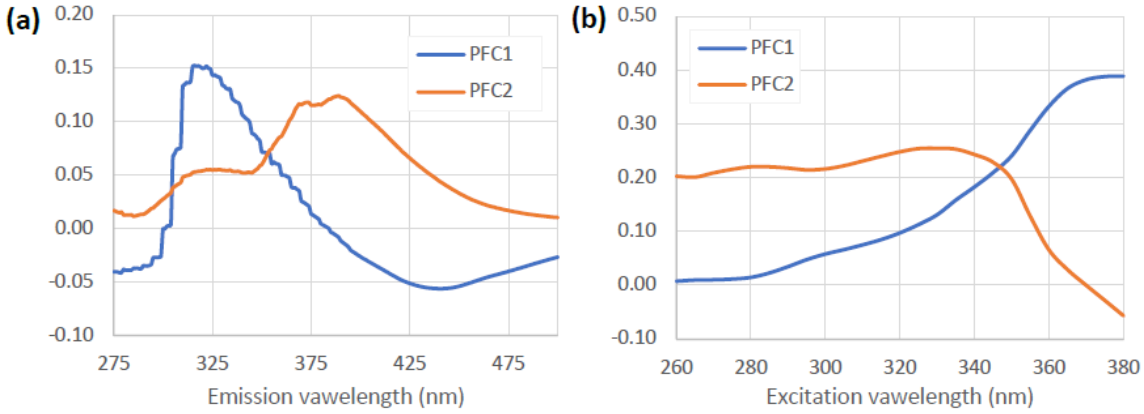

Figure 5 *Emission (a) and excitation (b) loading vectors for the two components (PFC1, and PFC2) PARAFAC model*

In order to explore possible connections of the spectral features with biochemical properties of honey samples, especially the level of infestation (%), a simple correlation matrix, based on Pearson's correlation coefficient was calculated between PARAFAC scores of both components and their ratios (PFSC2/PFSC1). The total proteins and TPC are significantly negatively correlated with the infestation level. Also, a statistically significant

negative correlation (-0. 71, R= -0. 71, p=0.05) between the ratio PFSC2/PFSC1 and the level of infestation was found.

CONCLUSION

The results presented in this research show the relationship between different parameters in honey samples and the infestation of colonies with *Nosema ceranae* as a type of stress of bee colonies. Corresponding protein and phenolic components in the emission spectrum of honey were obtained using the PARAFAC method which was applied to the excitation-emission matrices of honey samples. The ratio of spectral PFSC2/PFSC1 PARAFAC components is a negatively correlated with the level of infestation. It was shown that the contents of total proteins and total phenolics decrease with the level of *N. ceranae* infestation of the corresponding bee colonies, and they are significantly negatively correlated with the infestation level. Observed changes in honey may indicate changes in the state of the bee colony that is exposed to biotic stress, specifically the infestation of colonies with *Nosema ceranae.* Spectrofluorimetric assessment of the relative content of phenols and proteins may have an advantage over the existing methods used for the quantification of proteins and phenols in honey, because it is done without a sample preparation procedure. This method enables the simultaneous determination of proteins and phenols, because their maxima in the emission spectra are clearly separated. The results obtained in this research can be the basis for developing new optical tools applied on honey samples for bee health status monitoring.

ACKNOWLEDGEMENT

This work was funded by the Ministry of Science, Technological Development and Innovation of the Republic of Serbia, the contracts No. 451-03-47/2023-01/200053 with the Institute for Multidisciplinary Research University of Belgrade, No. 451-03-68/2022-14/200116 with Faculty of Chemistry University of Belgrade and No. 451-03-68/2022-14/200143 with Faculty of Veterinary Medicine, University of Belgrade.

REFERENCES

[1] Belsky J., Joshi N. K., Insects 10 (8) (2019) 1–42.

[2] Dainat B., van Engelsdorp D., Neumann P., Environ. Microbiol. Rep. 4 (1) (2012b) 123–25.

[3] Goulson D., Nicholls E., Botías C., *et al*., Science 347 (6229) (2015) 1122–1126.

[4] DeGrandi-Hoffman G., Chen Y., Curr. Opin. Insect. Sci. 10 (2015) 170–176.

[5] Meixner M. D., Le Conte Y., Apidologie 47 (2016) 273–275.

[6] Goblirsch M., Apidologie 49 (2018) 131–150.

[7] Holt H. L., Aronstein K. A., Grozinger C. M., BMC Genom. 14 (2013) 799.

[8] Botías C., Martín-Hernández R., Barrios L., *et al*., Vet. Res. 44 (2013) 1–14.

[9] Emsen B., Guzman-Novoa E., Kelly P. G., Entom. Society of Canada 146 (2013) 236–240.

[10] Singleton V. L., Rossi J. A., Am. J. Enol. Vitic. 16 (1965) 144–158.

[11] Bradford M.M., Anal. Biochem. 72 (1976) 248–254.

[12] Bro R., Chemometr. Intell. Lab. Syst. 38 (1997) 149–171.

[13] Lenhardt L., Bro R., Zeković I., *et al*., Food Chem. 175 (2015) 284–291.

[14] Rodriguez Delgado M. A., Malovana S., Perez J. P., *et al*., J. Chromatogr. A 912 (2001) 249–257.

ESTIMATION OF THE ANTIFUNGAL ACTIVITY OF THE TWO DIFFERENT CARBON DOTS AGAINST *Aspergillus flavus*

Dragana Bartolić[1*], Milica Nikolić[2], Mira Stanković[1], Miloš Prokopijević[1], Manuel Algara[3], Slavica Stanković[2], Ksenija Radotić[1]

[1]University of Belgrade, Institute for Multidisciplinary Research, 11000 Belgrade, SERBIA

[2]Maize Research Institute, Zemun Polje, Slobodana Bajića 1, Belgrade, SERBIA

[3]INAMAT2-Institute for Advanced Materials and Mathematics, Departamento de Ciencias, Universidad Pública de Navarra, Campus de Arrosadía, 31006 Pamplona, SPAIN

[*]*dragana.bartolic@imsi.rs*

Abstract

Environmental occurrence of the pathogenic fungus Aspergillus flavus (A. flavus) has hazardous effects on the health status of plants, humans, and animals. It is important to explore novel antifungal agents to control the growth of this fungus. In this study, we aimed to evaluate the antifungal contact activity of two different types of carbon dots (CD_S) nanomaterials; the one was coated with vitamin B_{12} ($CD_S@VB_{12}$) and the other was obtained from folic acid (FA@CDs). We used fluorescence spectroscopy to obtain their fluorescence fingerprinting profile. The CDs were pipetted on the PDA medium with sterilised filter paper placed in the center of the Petri dish. Then, pure A. flavus cultures were subcultured on PDA and incubated at 25°C for 7 days, and the diameters of mycelium growth were daily evaluated. The percentage of inhibition by $CD_S@VB_{12}$ ranged from 38.09% to 60.9% and from 46.03% to 71.39% for the amounts of 30 µl and 50 µl, respectively. On the other hand, FA@CDs did not show any inhibitory effect on the first day, and after that more progressive growth of A. flavus was noticed. The obtained results showed that $CD_S@VB_{12}$ could be considered as a potential new antifungal material against toxic and pathogenic A. flavus.

Keywords: carbon nanodots, antifungal activity, *A. flavus.*

INTRODUCTION

Aspergillus spp. includes a variety of environmental filamentous fungi found in diverse ecological niches worldwide [1]. *Aspergillus flavus* (*A. flavus*), after *Aspergillus fumigatus*, is the most important Aspergillus species which leads to a variety of allergic reactions and infectious diseases in immunocompromised individuals [1–3]. *A. flavus* grows at temperatures in the range of 12 to 48°C, with an optimum temperature at 37°C, contributing to pathogenicity in humans. Mainly, clinical syndromes related to this fungus include chronic granulomatous sinusitis, keratitis, cutaneous aspergillosis, wound infections and others [2]. Furthermore, *A. flavus* produces aflatoxin B_1 (AFB_1) which have many hazardous health effects to human and animals [4], and has been classified as a first-class human carcinogenic compound [5]. The exposure of humans and animals to this toxic compound mainly occurs via the consumption of contaminated foods, as well as inhalation of toxigenic spores and by dermal contact [6]. The most commonly used methods for determination of aflatoxins are

high-performance liquid chromatography (HPLC) and enzime linked immunosorbent assay (ELISA) [7]. Further, optical methods, such as fluorescence spectroscopy, are widely used for non-invasive screening the aflatoxin-contaminated cereal seeds [8,9]. Different pre and post-harvest strategies are used for preventing and controling fungal growth and their toxic compounds such as aflatoxins [10–12]. Phytopathogenic fungi have mostly been controlled by cheap chemicals which are easily obtained and indiscriminate use [13]. That may cause several problems regarding environmental pollution, disease in humans and animals, ecological imbalances, as well as developing fungi resistance [13,14]. Among the Aspergillus species, *A. flavus* seems to be more virulent and resistant to antifungal drugs [2]. Therefore, there is an urgent need to control the growth of pathogenic fungus. To overcome the fungus resistance, it is crucial to develope novel antifungal agents [13,15]. It has been demonstrated that many kinds of essential oils obtained from plants or herbs exhibit antifungal effects against *A. flavus* [16,17]. Nanomaterials have received great attention in agriculture, medicine and other fields of science [18,19]. Nowdays, different types of nanomaterials are considered a good alternative to chemical fungicides for the growth control of phytopathogenic fungi [13,20]. Carbon-based nanoparticles are known as carbon dots (CDs). They are nanoclusters of amorphous carbon or composed of small crystalline structure, with sizes bellow 10 nm [21]. CD_S have wide applications due to their excellent chemical stability, easy surface modification, high water solubility, good biocompatibility, photoluminescence and low toxicity [21,22].

In this study, we aimed to estimate the contact effects of two different types of CD_S, one coated with vitamin B_{12} and the other synthesized from folic acids, on the growth of the *A. flavus* colony. To our knowledge, the analysed CD_S have not been tested before as antifungal agents on toxigenic fungus. Therefore, obtained results may provide a useful approach for further designing and exploiting carbon dots as new antifungal materials in environmental protection.

MATERIALS AND METHODS

Materials

Folic acid (≥97%), D-Lactose (≥98%), phosphoric acid (85 wt.%, 99.99%) were purchased from Sigma-Aldrich Química (Spain). The Ultrapure Millipore water was used for all measurements. The isolate *A. flavus* No. 4219 was used as a toxigenic strain, and potato dextrose agar (PDA) as growth culture media.

Synthesis of CD_S coated with vitamin B_{12} (CD_S@VB_{12})

A hydrothermal method was used for the sythesis of CD_S@VB_{12}. Briefly, 12 mg lactose was dissolved in 200 µl deoinised water, and than 10 mg vitamin B_{12} and 800 µl 85% H_3PO_4 were added in the Tefon-lined strainless steel vessel and heated at 150°C for 2 h [23].

Synthesis of CD_S obtained from folic acid (FA@CDs)

The synthesis of CD_S from folic acid (FA@CDs) was carried out according to work [24]. The detailed synthesis and characterisation of these CD_S were described in the previous studies [23,24].

Fluorescence spectroscopy

Fluorescence characteristics of CDS@VB_{12} and FA@CDs were determined by FL3-221 spectrofluorimeter (Jobin Yvon Horriba, France), equipped with 450 W Xe lamp. The fluorescence emission spectra of CDs were measured in a right-angle (RA) configuration. All measurements were done at room temperature. Experimental parameters for CD_S@VB_{12} and FA@CDs were done at excitation wavelengths 385 nm and 350 nm, respectively. The emission range for both types of CDs was 365 nm to 650 nm, with an integration time of 0.1 s and bandpass for excitation and emission slits around 2 nm.

Evaluation of the antifungal activities of CD_S@VB_{12} and FA@CDs

A schematic illustration of antifungal test is shown in Figure 1. The pure *A. flavus* culture were subcultured to three places around the filter paper (Whatman No. 4) on the potato dextorse agar (PDA) using a microbiological method. Aliquots of 30 µl and 50 µl of the analysed CD_S were pipetted on the sterilized round filter paper, that was placed in the center of the Petri dish. The PDA medium with sterilised round filter paper without addition of CQDs was used as control. Each CDs was tested in three replicates. Further, the Petri dishes were covered and incubated at 25°C for 7 days in dark. The diameters of mycelium growth were evaluated daily during seven days, and their percentage of inhibition (IG) was calculated by the following formula: IG (%) = [(C−T)/C] × 100 where C and T shows colony diameter of control and CD_S-treated group, respectively [16].

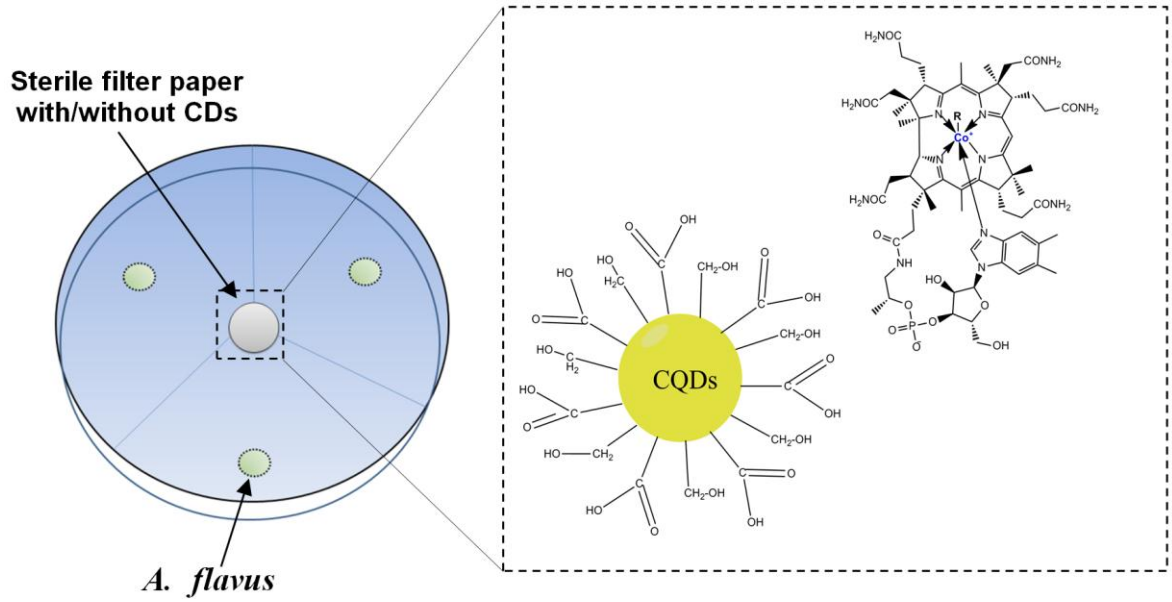

Figure 1 *Schematic illustration of antifungal contact test of A.flavus-CD_S@VB_{12}*

Statistical analyses

All data are expressed as mean values of the three repetitions per treatment. The differences were considered to be statistically significant at $p \leq 0.05$ according to non-parametric Mann-Whitney *U* test.

RESULTS AND DISCUSSION

Figure 2 and 3 shows fluorescence emission spectra of CDs@VB_{12} and FA@CDs, respectively. As displayed in Figure 2, CDs@VB_{12} exhibits two emission maxima at 450 nm and 560 nm in the range from 400 to 600 nm. This result is in agreement with our previous studies [23]. On the other hand, FA@CDs show one emission maximum with a position around 450 nm, similar to the results obtained in the previous study [24]. The observed difference in spectral characteristics results from the difference in their respective structures.

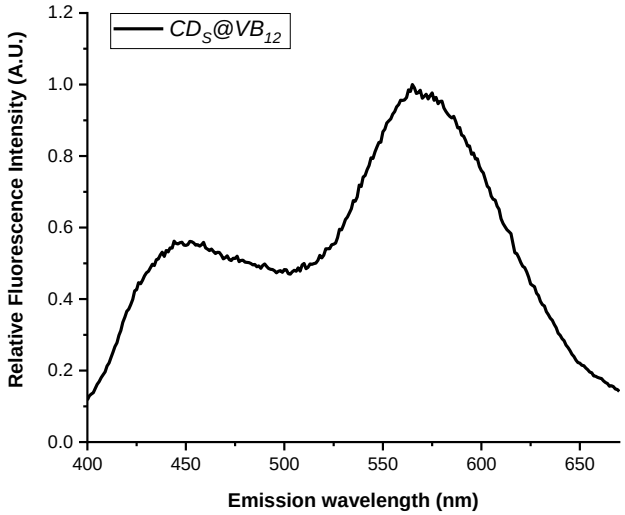

Figure 2 *Fluorescence emission spectrum of CDs@VB_{12}, after excitation at 385 nm*

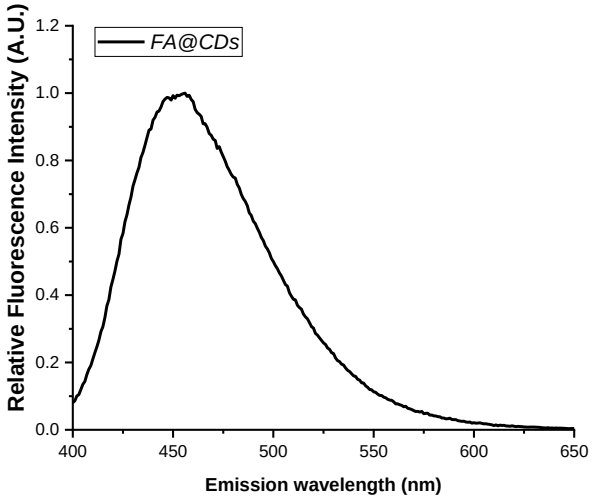

Figure 3 *Fluorescence emission spectrum of FA@CDs, after excitation at 350 nm*

Estimation of contact effect between CDs and *A. flavus*

Representative pictures of the colony morphology of *A. flavus* on PDA without (Figure 4a) and with the treatment (Figure 4b) after seven days of incubation are shown in Figure 4. The results of macroscopic characterisation show yellow-green colour of mycelia of the *A. flavus* [25]. The results related to the diameters of mycelium growth (mm) during seven days are presented in Table 1 and Table 2. During the studied period, one can see that increasing the dose of CDs@VB_{12} leads to a significant decrease of the diameters of mycelium growth. On the other hand, the FA@CDs did not show any significant inhibition effect on fungi growth after the first day. After that, more progressive growth of *A. flavus* was observed. Obtained results indicate that mycelium growth was stimulated with FA@CDs, and is not dependent on the applied doses.

a) *b)*

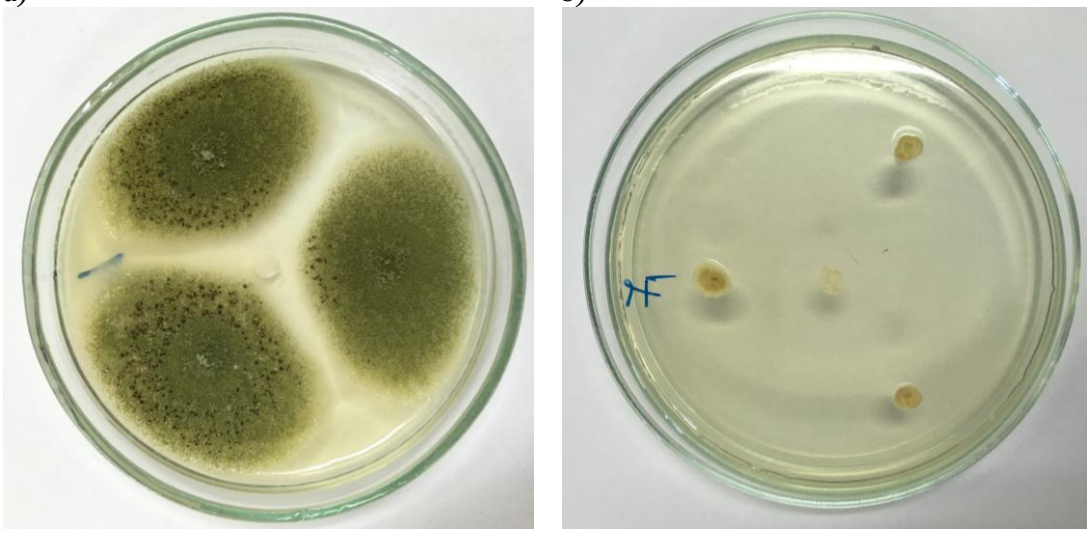

Figure 4 *Representitive pictures of the colony morphology of A. flavus (Isolate No.4219) on PDA a) without and b) with the treatment*

Table 1 *Exposure time of CD_S@VB12 and A.flavus contact during seven days*

Exposure time (days)	**Diameter of mycelium growth (mm)**		
	Control	**CD_S@VB_{12} (30 µl)**	**CD_S@VB_{12} (50 µl)**
1st	7	4.3±0.33	3.8±0.38
2nd	18.3±0.57	9.5±0.6938	7.4±1.1097
3rd	27.6±0.5773	12.7±0.962	9.4±1.2619
4th	35.83±0.763	15.22±1.07	11.3±1.45
5th	43.66±0.577	17.4±0.693	12.61±1.397
6th	49.33±1.155	19.22±1.17	14±1.764
7th	54±3	21.1±0.694	15.4±1.895

**Data are means ± standard (± SD) deviation of the three replicates (n=3).*

Table 2 *Exposure time of FA@CDs and A.flavus contact during seven days*

Exposure time (days)	Diameter of mycelium growth (mm)		
	Control	*FA@CDs* (30 µl)	*FA@CDs* (50 µl)
1st	7#	7±0.33#	7#
2nd	18.3±0.57	20	20
3rd	27.6±0.5773	29.2±0.192	29.2±0.19
4th	35.83±0.763	38.55±1.07	37.8±0.96
5th	43.66±0.577	47.8±0.192	45.6±0.33
6th	49.33±1.155	55.88±0.69	54.3±0.333
7th	54±3	61.4±0.838	60.3±0.66

**Data are means ± standard (± SD) deviation of the three replicates (n=3);*
 # – no significant difference.

As shown in Figure 5, the percentage inhibition by CDs@VB_{12} on *A. flavus* varied from 38.09% to 60.9% for 30 µl, and 46.03% to 71.39% for 50 µl. The calculated IG for *A. flavus* was 1.2-fold higher for 50 µl CDs@VB_{12} than for 30 µl. The studied CDs@VB_{12} reached a maximum value of IG against *A. flavus* on the 5th day. However, similar values of IGs were found with prolonged time exposure (6th and 7th day). The results imply that applied CDs@VB_{12} exhibited antifungal activity to fungus *A. flavus*. Studied FA@CDs did not show inhibitor effects on *A. flavus.* Moreover, it was obvious that after the first day, this CDs lead to stimulative effects of fungus growth (Figure 6). It has been reported that the effect of CDs on microorganisms, and their interaction, appears to be dependent on numerous factors such as surface chemistry, composition, size, and shape among others [21,22]. Further, the mechanism of antimicrobial effects of CDs could be activated under visible natural illumination to promote the generation of high reactive oxygen species [26].

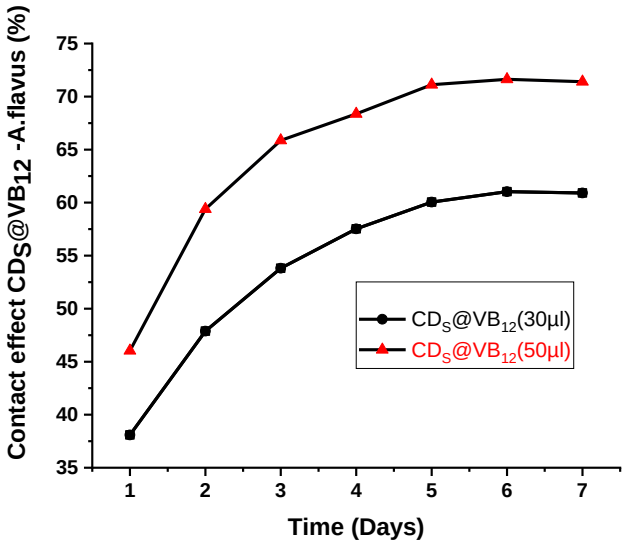

Figure 5 *Contact effect of CD_S@VB_{12} on A. flavus growth during 7 days exposure*

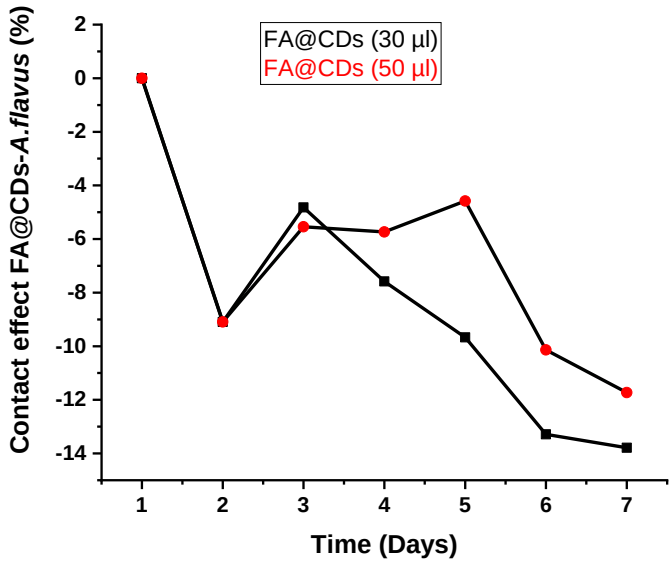

Figure 6 *Contact effect of FA@CDs on A. flavus growth during 7 days exposure*

CONCLUSION

This study provides new information about the contact effects of the two types of carbon dots on *A. flavus*. Our results imply that antifungal effects of studied carbon dots depend on their compositions; however, further research will be needed for a deep understanding of the mechanisms of their actions. The FA@CDs did not show effectiveness against growth *A. flavus*, on the other hand, the CD_S@VB_{12} showed a good inhibitory effect and thus could be considered a promising antifungal agent, with its potential application in agriculture, food and medicine.

ACKNOWLEDGEMENT

This work was supported by the Ministry of Science, Technological Development and Innovation of the Republic of Serbia (Grant No. 451-03-47/2023-01/200053, University of Belgrade, Institute for Multidisciplinary Research).

REFERENCES

[1] Latgé J. P., Clin. Microbiol. Rev. 12 (2) (1999) 310–350.

[2] Hedayati M. T., Pasqualotto A. C., Warn P. A., *et al*., Microbiology 153 (2007) 1677–1692.

[3] Paulussen C., Hallsworth J. E., Álvarez-Pérez S., *et al*., Microb. Biotechnol. 10 (2) (2017) 296–322.

[4] Afsah-Hejri L., Jinap S., Hajeb P., Compr. Rev. Food Sci. Food Saf. 12 (2013) 629–651.

[5] International Agency for Research on Cancer (IARC), Aflatoxins, Lyon: W. H. O. 82 (2002) 171.

[6] Zain M. E. J., Saudi Chem. Soc. 15 (2) (2011) 129–144.

[7] Wacoo A. P., Wendiro D., Vuzi P. C, *et al*., J. Appl. Chem. (2014) 1–15.

[8] Bartolić D., Stanković M., Mutavdžić D., *et al*., J. Fluoresc. 28 (3) (2018) 729–733.

[9] Bartolić D., Mutavdžić D., Carstensen J. M., *et al*., Sci. Rep. 12 (2022) 4849.

[10] Marshall H., Meneely J. P., Quinn B., *et al*., Trends. Food Sci. Technol. 106 (2020) 489–496.

[11] Tsitsigiannis D. M., Dimakopoulou M., Antoniou P. P., *et al*., Phytopathol. Mediterr. 51 (2012) 158–174.

[12] Awuchi C. G., Ondari E. N., Ogbonna C. U., *et al*., Foods 10 (2021) 1279.

[13] Cruz-Luna A. R., Cruz-Martínez H., Vásquez-López A., *et al*., J. Fungi 7 (2021) 1033.

[14] Tian F., Woo S. Y., Lee S. Y., *et al*., Antibiotics 11 (12) (2022) 1727.

[15] Pereira L., Dias N., Carvalho J., *et al*., J. Appl. Microbiol. 117 (2014) 1601–1613.

[16] Hu Y., Zhang J., Kong W., *et al*., Food Chem. 220 (2017) 1–8.

[17] Da Cruz Cabral L., Fernández Pinto V., Patriarca A., Int. J. Food. Microbiol. 166 (1) (2013) 1–14.

[18] Joseph T. M., Kar Mahapatra D., Esmaeili A. *et al*., Nanomaterials 13 (2023) 574.

[19] Algarra M., Bartolić D., Radotić K., *et al*., Talanta 194 (2018) 150–157.

[20] Gómez J. V., Tarazona A., Mateo F., *et al*., Food Control 101 (2019) 58–68.

[21] Bayda S., Amadio E., Cailotto S., *et al*., Nanoscale. Adv. 3 (2021) 5183–5221.

[22] Liu J., Li R., Yang B., ACS Cent. Sci. 6 (12) (2020) 2179–2195.

[23] Jiménez-Jiménez J., Rodríguez-Castellón E., da Silva J. C. G. E., *et al*., Sens. Actuators B: Chem. 239 (2017) 553–561.

[24] Campos B. B., Oliva M. M., Contreras-Cáceres R., *et al*., J. Colloid. Interface Sci. 465 (2016) 165–173.

[25] Nikolic M., Nikolic A., Jaukovic M., *et al*., Genetika 50 (2018) 143–152.

[26] Awak Al M. M., Wang M., Wang P., *et al*., RSC Adv. 7 (48) (2017) 30177–30184.

Conference Papers

RADIOACTIVITY IN SOIL AND MOSSES FROM THE SPECIAL NATURE RESERVE OF ZASAVICA IN 2021

Ana Čučulović[1*], Jelena Stanojković[1], Rodoljub Čučulović[2], Mihajlo Stanković[3]

[1]University of Belgrade, Institute for the Application of Nuclear Energy – INEP, Banatska 31b, 11080 Zemun, SERBIA

[2]University of MB, Faculty of Business and Law, Teodora Drajzera 21, 11000 Belgrade, SERBIA

[3]Pokret gorana, Svetog Save 19, 22000 Sremska Mitrovica, SERBIA

[*]*anas@inep.co.rs*

Abstract

Soil and moss samples were collected in the Special Natural Reserve (SNR Zasavica) in August 2021 from 12 localities. Determination of the specific activity of natural radionuclides (^{226}Ra, ^{232}Th, ^{40}K) and artificial radionuclide (^{137}Cs) was performed using a germanium detector ORTEC-AMETEK, USA. The specific activity (Bq kg^{-1}) of ^{40}K in soil (moss) samples was from 633 (188) to 1022 (530), ^{226}Ra from 27.9 (16.6) to 48.6 (36.6), ^{232}Th from 35.4 (6.5) to 48.5 (25.7) and ^{137}Cs from 3.8 (1.7) to11.1 (65.0). The specific activity of radionuclides in soil and moss in SNR Zasavica were within the range of measured activity in soil and moss in Serbia.

Keywords: SNR Zasavica, radionuclides, soil, moss.

INTRODUCTION

The special natural reserve (SNR) Zasavica was put under state protection in 1997 as a natural reserve of the first category of extreme significance to the Republic of Serbia in order to preserve natural watercourses and wet habitats and its significant variety of flora and fauna. It is situated in Northeastern Serbia, in the region of south Vojvodina and northern Mačva, east of the Drina River and south of the Sava River, on the territory of the municipalities of Sremska Mitrovica and Bogatić, between settlements: Crna Bara, Banovo Polje, Ravnje, Radenković, Zasavica I and II, Salaš Noćajski, Noćaj and Mačvanska Mitrovica. Its area is 1852 ha and it spans the river Zasavica with a length of 33.1 km. The Batar stream runs through, and it includes the Jovac, Prekopac and Bogaz channels (the Bogaz channel links it with the Sava River). Zasavica has a subterraneous water supply from the Drina River and gravitationally from the Cer Mountain. The area of northern Mačva is bordered on the southern side by Cer and Iverak Mountains comprised of remnants of granite melt of magmatic rocks that include pegmatites, greisens and granodiorites composed of rare earth minerals and also uranium and thorium [1]. The reserve enjoys an internationally protected status: Ramsar area (No. 1783), botanically significant area (IPA), area significant for birds (IBA, RS008), and primary area for butterflies (PBA, 40) [2]. It is a member of the Europark federation. The reserve is looked after by the non-governmental organization "Pokret gorana" from Sremska Mitrovica.

All organisms on the planet Earth are exposed to radiation. Natural radioisotopes: ^{40}K, ^{232}Th, ^{226}Ra, ^{238}U, etc. located in the Earth's crust and formed during the nucleosynthesis process with a long half-life (10^5–10^{16} years) contribute the most to gamma irradiation (96%) in the environment. These radionuclides have different geochemical properties, types of radioactive half-life, irradiation intensity, isotopic abundance, expression, migration and geochemical cycles [3]. Radionuclides of an anthropogenic origin (^{131}I, ^{137}Cs, ^{90}Sr, ^{99}Tc, ^{239}Pu, etc.), deriving mostly from splitting heavy nucleus also contribute to gamma radiation. Pollution with these radionuclides usually has a regional character, but it can be wider in the case of strong nuclear explosions (Chernobyl, 26.4.1986) [4]. The Chernobyl accident (Ukraine) released a great amount of radionuclides into the environment of which 3.7×10^{16} Bq ^{137}Cs. Radio-cesium – 137, forms as a fission product or is produced in the production or testing process of nuclear weapons and in nuclear reactors. It is a toxic element and its physicochemical characteristics enable active incorporation into the food chain of humans and animals through plants, as it metabolically replaces potassium [4], has a long physical half-life (30.2 years), and the processed of radio-cesium adoption from the environment can be physical and chemical adsorption and ionic exchange. Land is one of the basic living conditions. Soil is the most significant and sensitive component of the environment and a complex, dynamic system in which different physic-chemical and biological processes occur [5]. Soil has different compositions, chemical, physical and biological properties. One of the physical properties is radioactivity. Natural ionizing radiation in the environment caused by ^{40}K, ^{232}Th, ^{226}Ra and ^{238}U varies from place to place and mainly depends on the geology and concentration of elements in rocks and soil. According to the UNSCEAR report (2000) average specific activities (Bq kg^{-1}) in soil in the World (min-max) are ^{238}U 35 (16–110); ^{226}Ra 35 (17–60); ^{232}Th 30 (11–64) and ^{40}K 400 (140–850) [6].

Moss is characterized with a particular structure (no root, trunk, leaf and they have a large body surface) and a specific ecology in relation to vascular plants. Their longevity, physiological activity and adaptability to different environmental conditions, possible accumulation of many materials in their body and retention of old part, and also wide prevalence make them good bioindicators and biomonitors of polluting substances. The localities of the SNR Zasavica showed the presence of 43 moss taxonomies (41 species and 2 varieties) grouped in 22 genuses and 14 families. Three taxonomies belong to the liverwort class, while 40 are members of real moss (9.09% flora Bryopsida Serbia) [7,8].

Measuring and monitoring activity levels in soil and moss samples from the environment has a great significance from the aspect of ecosystem protection as it is the basis for the formation of criteria for the radiological security of the biosphere. Radioactivity monitoring is necessary and significant to achieve environmental protection and radiological protection of the inhabitants of a certain region.

MATERIAL AND METHODS

Soil (S) and moss (M) samples were collected in the SNR Zasavica in August 2021 from 12 localities: (1) Ravnje, Zovik; (2) Radenković, Batar; (3) Glušci, Bitva, (4) Banovo polje, Trebljevine; (5) Hajdučki potok, Miline; (6) Parloge; (7) Lešnica; (8) Jadarska lešnica; (9) Badivinci; (10) Bradić; (11) Desić and (12) Ladjane. The moss type was not determined.

After the samples were brought to the laboratory they were cleaned to remove noticeable impurities, dried, homogenized and packed in Marinelli vessels with volumes of 0.5 and 1 L that were sealed with paraffin and left for 40 days in order to establish radioactive equilibrium between ^{226}Ra, ^{222}Rn and their short-lived descendants. The moss sample mass was up to 100g, while the soil sample mass was up to 600g. A semiconducting germanium high purity detector of the n-type produced by ORTEC-AMETEK, USA, with 8192 channels, resolution 1.65 keV and relative efficiency of 34% at 1.33 MeV for ^{60}Co was used to determine radionuclide activity levels. Detector calibration was performed using a reference radioactive material: silicon resin matrix, Czech Metrological Institute Praha (ČMI Praha). All samples were measured for 60000 s. Spectral analysis was performed using the Gamma Vision software package 32. The relative sample preparation and measurement uncertainty was up to 10%. The activity level of ^{226}Ra was determined based on the gamma line for: ^{214}Bi (609, 1120 and 1764 keV) and ^{214}Pb (295 and 352 keV), of ^{232}Th on the gamma line ^{228}Ac (338, 911 and 969 keV), of ^{40}K on the gamma line at 1460.8 keV, while for ^{137}Cs it was determined based on the gamma line at 661.6 keV.

RESULTS AND DISCUSSION

The specific activity of ^{40}K, ^{226}Ra, ^{232}Th and ^{137}Cs (Bq kg^{-1}) in soil and moss collected from SNR Zasavica in 2021 is presented in Table 1. From the values shown in Table 1, it follows that the specific activity of ^{40}K in soil samples was from 633 (locality 8) to 1022 Bq kg^{-1} (locality 7) and in moss samples from 188 (locality 9) to 530 Bq kg^{-1} (locality 2). The average value of the specific activity of ^{40}K in soil (moss) was 764 (353) Bq kg^{-1}. The results of this investigation show that the specific activity of ^{40}K in soil (moss) from Zasavica was higher in relation to our previous research 206–654 (130–438) [9,10]. The specific activity of ^{40}K in soil from SNR Zasavica are within the measured range of specific soil activity in Vojvodina (238–1000 Bq kg^{-1}) [11], but somewhat higher than values determined in the World (140–850 Bq kg^{-1}) [6]. The specific activity of ^{226}Ra in soil samples were from 27.9 (locality 4) to 48.6 Bq kg^{-1} (locality 2), and in moss samples from 16.6 (locality 12) to 36.6 Bq kg^{-1} (locality 10). The average value of the specific activity of ^{226}Ra in soil (moss) was 35.5 (22.5) Bq kg^{-1} (Table 1). This research has shown that the specific activity of ^{226}Ra in soil (moss) from investigated localities in Zasavica were higher compared to our previous measurements 32–37 (0.9–13.3) Bq kg^{-1} [9,10], but they are still within the measured values for soil from Vojvodina (9.7–49.1 Bq kg^{-1}) [11] and within the range of the values determined in the World (17–60) [6]. Table 1 follows that the specific activity of ^{232}Th in soil samples was from 35.4 (locality 8) to 48.5 Bq kg^{-1} (locality 7), while in moss samples it was from 6.5 (locality 3) to 25.7 Bq kg^{-1} (locality 2). The average value of the specific activity of ^{232}Th in soil (moss) was 40.3 (16.5) Bq kg^{-1}. This research has shown that the specific activity of ^{232}Th in soil (moss) from the investigated localities in Zasavica were higher when compared to our previous measurements 41–46 (3.9–14.8) Bq kg^{-1} [9,10], but they are within the range of measured values in Vojvodina soil (11.7–70.5 Bq kg^{-1}) [11], but somewhat higher than in the World (11–64) [6]. The specific activity of ^{137}Cs in soil samples was from 3.8 (locality 8) to 11.1 Bq kg^{-1} (locality 4), while in moss samples it was from 1.7 (locality 12) to

65.0 Bq kg^{-1} (locality 11). The average value of the activity of ^{137}Cs in soil (moss) was 7.0 (18.0) Bq kg^{-1}. This research has shown that the specific activity of ^{137}Cs in soil (moss) from the investigated localities in Zasavice was significantly higher than our previous measurements 6.5–13.1 (0.8–5.8) [9,10], but they are within the measured values of soil activity in Vojvodina (3.04–42.6 Bq kg^{-1}) [11]. Analysis of the obtained results enables the conclusion that the substrate collected on locality 7 has the most ^{40}K and ^{232}Th, while the substrate collected on locality 8 has the lowest ^{40}K, ^{232}Th and ^{137}Cs. Moss collected at locality 12 has the lowest ^{226}Ra and ^{137}Cs. Pearson correlation coefficients for ^{40}K-^{226}Ra, ^{40}K-^{232}Th, ^{226}Ra-^{232}Th in soil are 0.903; 0.842; 0.771, respectively and indicate a strong interdependence between the observed radionuclides, while for ^{40}K-^{137}Cs, ^{226}Ra-^{137}Cs and ^{232}Th-^{137}Cs they are -0.150; -0.052; 0.006 and indicate a very weak interdependence. High values of the Person coefficients between radionuclides of the uranium and thorium series in soil indicate their joint origin. Pearson correlation coefficients for ^{40}K-^{232}Th and ^{40}K-^{137}Cs in moss are 0.603; -0.607 and indicate a moderate interdependence between the observed radionuclides, while for ^{226}Ra-^{232}Th, ^{232}Th-^{137}Cs and ^{40}K-^{226}Ra they are 0.207; 0.203 and 0.214, respectively and indicate a weak interdependence, while for ^{226}Ra-^{137}Cs it is -0.008 and indicates a very weak interdependence.

Table 1 *Specific activity of ^{40}K, ^{226}Ra, ^{232}Th and ^{137}Cs in soil (S) and mosses (M) collected in August 2021 in Zasavica and transfer factors (TF)*

Locality	Sample type, TF	^{40}K	^{226}Ra	^{232}Th	^{137}Cs
		(Bq kg^{-1})			
1	S	701	32.1	41.6	7.1
	M	461	19.7	17.1	2.7
	TF	0.66	0.61	0.41	0.38
2	S	953	48.6	41.4	6.4
	M	530	25.6	25.7	2.8
	TF	0.56	0.53	0.62	0.44
3	S	793	43.2	44.1	8.5
	M	309	21.5	6.5	1.9
	TF	0.39	0.50	0.15	0.22
4	S	640	27.9	36.4	11.1
	M	421	20.5	20.2	3.7
	TF	0.66	0.73	0.55	0.33
5	S	728	31.3	37.7	6.2
6	S	641	29.3	37.6	6.7
7	S	1022	43.3	48.5	6.1
8	S	633	28.2	35.4	3.8
9	M	188	22.6	12.7	40.9
10	M	359	36.6	17.8	25.2
11	M	265	17.2	21.4	65.0
12	M	288	16.6	10.3	1.70

The transfer factor (TF) for the introduction of any radionuclide from soil to moss that grows on that soil is defined as the ratio between specific activity of the analyzed radionuclide in moss (Bq kg^{-1}) and the activity level in soil (Bq kg^{-1}) [12]. Transfer of radionuclides from the substrate to moss depends on physical, chemical and biological factors that determine the radionuclide properties, moss type and soil characteristics. The calculated mean values of TF grow in the following order $^{137}Cs < ^{232}Th < ^{40}K < ^{226}Ra$ (0.34 < 0.43 < 0.57 < 0.59).

CONCLUSION

Radionuclides ^{40}K, ^{226}Ra, ^{232}Th and ^{137}Cs are present in all soil and moss samples and they have partly appeared due to discharging from the Cer Mountain. The average value of the specific activity (Bq kg^{-1}) of ^{40}K in soil (moss) was 764 (353), ^{226}Ra 35.5 (22.5), ^{232}Th 40.3 (16.5) and ^{137}Cs 7.0 (18.0). Pearson correlation coefficient for ^{40}K-^{226}Ra, ^{40}K-^{232}Th, ^{226}Ra-^{232}Th in soil are 0.903; 0.842; 0.771, respectively and indicate a strong interdependence between the observed radionuclides and their joint origin. Pearson correlation coefficients for ^{40}K-^{232}Th and ^{40}K-^{137}Cs in moss are 0.603; -0.607 respectively and indicate a moderate interdependence between the observed radionuclides.

ACKNOWLEDGEMENT

The research presented in this work was performed with the financial backing of the Ministry of Science, Technological Development and Innovation of the Republic of Serbia, as part of financing scientific research at the Institute for the Application of Nuclear Energy – INEP, contract number 451-03-47/2023-14/200019.

REFERENCES

[1] Djordjević V., Djordjević P., Milovanović D., Osnovi petrologije, Nauka, Beograd (1991) p.110–111 (*in Serbian*).

[2] Sekulić N., Sinžar J., Emerald ekološka mreža u Srbiji, Ministarstvo životne sredine i prostornog planiranja, Beograd (2010), p.48, (*in Serbian*), ISBN: 978-86-80877-34-1.

[3] Dangić A., Geohemijski procesi u prirodi i radionuklidi *u* Jonizujuća zračenja iz prirode, INN Vinča. JDZZ, Beograd (1995), p.41–56, (*in Serbian*), ISBN: 86-80055-75-1.

[4] IAEA, Construction and use of calibration facilities for radiometric field equipment, Technical Report Series 309, International Atomic Energy Agency (IAEA), Vienna, (1989), ISBN: 92-0-145189-X.

[5] Antić M., Jović N., Avdalović V., Pedologija, Naučna knjiga, Beograd (1980) (*in Serbian*).

[6] UNSCEAR (2000), Ionizing Radiation Sources and Biological Effects, UNSCEAR 2000 Report to the General Assembly, with Scientific Annexes, Vols I and II, New York, (2000).

[7] Stanković M., Medjunarodna i nacionalna vrednost biodiverziteta SRP Zasavica, Naučno-stručni skup Zasavica, Zbornik radova, Sremska Mitrovica, Srbija (2012) 74–80.

[8] Grdović S., Blaženčić Ž., Prilog poznavanju mahovina Rezervata Zasavica, Zasavica 2001, Monografija, PMF, Institut za biologiju, Novi Sad i Goransko-ekološki pokret, Sremska Mitrovica, (2001) 35–41.

[9] Čučulović A., Dželetović Ž., Stanković M., Veselinović D., Ecologica. 74 (2014) 263–266, ISSN: 0354-3285 (*in Serbian*).

[10] Dželetović Ž., Čučulović A., Andrejić G., Stanković M., Veselinović D., Ecologica, 95 (2019) 313–318, ISSN: 0354-3285, (*in Serbian*).

[11] Nikolić V., Radioaktivnost zemljišta Vojvodine, Diplomski rad, Univerzitet u Novom Sadu, PMF, Departman za fiziku, Novi Sad (2011) (*in Serbian*).

[12] IAEA, Quantification of Radionuclide Transfers in Terrestrial and Freshwater Environments for Radiological Assessments, IAEA-TECDOC-1616, IAEA, Vienna, (2009), ISBN: 978-92-0-104509-6.

Chaenomeles × *superba* 'PINK LADY' IN DESIGNING PRIVATE GARDENS IN CONDITIONS OF CLIMATE CHANGE

Djurdja Petrov[1*], Mirjana Ocokoljić[1], Nevenka Galečić[1], Dejan Skočajić[1], Isidora Simović[2]

[1]University of Belgrade-Faculty of Forestry, Kneza Višeslava 1, 11030 Belgrade, SERBIA

[2]BioSense Institute, University of Novi Sad, Dr Zorana Djindjića 1, 21000 Novi Sad, SERBIA

[*]*djurdja.stojicic@sfb.bg.ac.rs*

Abstract

By evaluating the design of 10 private gardens, in the suburban zone of Belgrade, in Ostružnica, this research provided recommendations for the use of certain landscape elements and specifics with Pink Flowering Quince for design or reconstruction in conditions of a changed temperate-continental climate. The effect of climatic variables on phenological patterns of flowering was determined through accumulated cold hours, phenological patterns, and their correlations. The results indicate a significant influence of climatic variables on phenophases and their duration. Genotype 1 is proposed for multiplication, as it stands out with the longest flowering period. The research confirmed that landscape design is not successful without high-quality plant material such as Chaenomeles × superba 'Pink Lady', as well as that when choosing plants, ecological characteristics should be evaluated, and those that ensure the sustainability of the landscape should be selected.

Keywords: Pink Flowering Quince, landscape design, seasonality, phenological observations.

INTRODUCTION

In the context of climate change but also in relation to the challenges of designing private gardens, ornamental vegetation can be singled out as a factor for improving the conditions, quality, and aesthetics of urban and suburban spaces that can provide a living environment [1] of good quality. In light of the growing interest in the impact of climate change on life cycles and phenological patterns and the processes that control them, the phenophases of leafing, flowering, fruiting, color changes, and leaf fall, as well as the arrival and departure of migratory birds have been intensively studied [2–5]. Studying plants' phenological patterns provides information on plant growth and development patterns, as well as environmental influences and selective pressures on flowering and fruiting [6]. Research on phenological patterns in conditions of a temperate-continental climate indicates the dominant influence of seasonal factors: temperature and moisture regime [5,7]. The importance of phenology and phenological patterns lies in their effectiveness as a tool for monitoring the impact of climate on plants and animals [8]. Phenological events are important for biodiversity and ecology, i.e. assessing the impact of mismatches in the timing of phenological events on species interactions and community patterns, as well as for landscape design.

The study aims to determine the impact of the suburban environment, under conditions of climate change on the phenological patterns of flowering and the development of

Chaenomeles × *superba* 'Pink Lady' (Pink Flowering Quince) to implement it in the design practices of private gardens. Phenological patterns applied in garden design can: (1) influence the choice of flower-decorative shrubs, (2) indicate the adequacy of the plant material selection for the site and purpose, (3) provide floristic richness in private gardens (4) enable better visual perception of flowering decorative shrubs as vital elements in gardens and (5) optimize maintenance costs. The subject of the study was the cultivar *Chaenomeles*, whose taxa were cultivated in European gardens at the end of the eighteenth century, and 'Pink Lady' (Pink Flowering Quince) in 1946 [9], due to its large presence in private gardens in the southwestern suburban zone of Belgrade.

MATERIALS AND METHODS

The research area is Ostružnica in the municipality of Čukarica, Belgrade, covering an area of 31,210 ha, on the right bank of the Sava River. Through field research, 10 private gardens were selected where individuals of *Chaenomeles* × *superba* 'Pink Lady' are present. The size of gardens ranges from 32 m^2 to 3741 m^2 and their distance from the Sava River ranges from 148 m to 329 m. Further description of the studied gardens' locations is shown in Table 1.

Table 1 *Description of the research area*

Garden	Latitude φ	Longitude λ	Altitude H (m)	Distance from the Sava river (m)	Aspect	Slope* (°)
1.	44º 43' 22.49 "N	20º 18' 45.96" EGr	88	301	W	3–5 °
2.	44º 43' 51.18" N	20º 18' 56.24" EGr	76	309	N	0–1 °
3.	44º 43' 22.55" N	20º 18' 47.21" EGr	90	329	W	3–5 °
4.	44º 43' 49.98" N	20º 18' 48.78" EGr	77	151	N	5–8 °
5.	44º 43' 37.55" N	20º 18' 43.61" EGr	85	150	W	8–12 °
6.	44º 43' 13.39" N	20º 18' 37.17" EGr	75	149	NW	3–5 °
7.	44º 43' 15.40" N	20º 18' 37.74" EGr	76	157	NW	5–8 °
8.	44º 43' 14.38" N	20º 18' 37.21" EGr	76	148	NW	8–12 °
9.	44º 43' 07.78" N	20º 18' 39.29" EGr	88	200	W	3–5 °
10.	44º 43' 06.58" N	20º 18' 43.15" EGr	97	290	W	3–5 °

*Slope angle: 0–1 ° (flat terrain), 3–5 ° (slightly inclined terrain), 5–8 ° (fairly inclined terrain) and 8–12 ° (slanted terrain).

The specificity assessment of private gardens and their vegetation was carried out by comparing the design of selected gardens, i.e. the application of Pink Flowering Quince according to the Liu method [10].

In order to determine the impact of climate change on this floral decorative taxon, the flowering phenophase was monitored in the period from November 1st, 2022, to the end of the flowering phenophase (April 19, 2023) using the Cosmulescu & Ionescu method [11]. Using the *BBCH* scale [12], phenological observations were made visually, at intervals of 2 to 4 days, noting the dates: blossoming bud breaking – BB (the day when the flower buds began to burst), beginning of flowering – BF (the day when more than 10% of flowers), full flowering – FF (the day when more than 50% of the flowers were open) and end of flowering – EF (the

day when more than 80% of the flowers have bloomed and the plants have fully leafed). During field research, photographic material was collected and garden owners were interviewed (the owner of garden number 7 refused to be interviewed). Climatological data were obtained from the Main Meteorological Station (GMS) Surčin Airport (44º49'27.37" N; 20º17'27.82" EGr; altitude: 99 m) www.hidmet.gov.rs/index.php (accessed on 18 April 2023), RHMZ.

Accumulated cold hours (CH_t) were determined from November 1st, 2022, to the date when flower bud bursting was recorded. The starting date and formula for determining CH were determined according to Cosmulescu and Ionescu [11]. The occurrence of high temperatures before the specified date does not contribute to the accumulation of cold hours for the conditions of a moderate-continental climate (according to the Köppen classification, for the period 1991–2020, Belgrade's climate is labeled C(f)wa – moderately continental, RHMZ). Formula (1) was used:

$$CH_t = \sum_{i=1}^{t} H \qquad (1)$$

if 0°C< T<7°C, then add 1, else 0. Relationships between accumulated CH_t and phenophases were determined by Spearman's correlation coefficient. The software package XLSTAT 2020 was used for data processing.

RESULTS AND DISCUSSION

During the research of 10 private gardens in Ostružnica the following was recorded: the gardens have a different terrain configuration, which is why there is a need for landscape and engineering vertical solutions; 10% of gardens are arranged in a landscape style with only a decorative function, and 90% in a mixed style with decorative-utilitarian functions; landscape design is characterized by a wide range of decorative woody plants; gardens with a decorative and utilitarian orientation are characterized by the presence of auxiliary buildings, a garden for growing vegetables, fruit and berry plantations, which were formed according to the "beautiful + useful" principle. All the detached gardens are characterized by details, conciseness in the zoning of the total area and the presence of Pink Flowering Quince aged 9 to 12 years. Pink Flowering Quince in the analyzed gardens is in use: as a solitary shrub (in garden 1 and 3 – on the central lawns, and in garden 8 are next to the concrete and retaining wall and the transparent wooden fence with *Hedera helix* L.), in pair (garden 4 – on the meadow/lawn), as hedges (garden 2 – protective, monolithic, free-growing, garden 10 – mixed free-growing paravane, and garden 6 – shaped mixed border), binding of sloped terrain (neglected garden 7 and a well-maintained garden 5 in which, after the slope, the supporting stonework with a mixed free-growing hedge is placed) and barrier (from evergreen and deciduous shrubs that were selected so that flowering and ornamentality are continuous throughout the year, and started in 2023 with the analyzed cultivar in garden 9).

Taking into account the frequency and application of the selected cultivar, it is emphasized that the main adaptation of plants to climate changes is a longer vegetation period, earlier appearance of spring and late autumn phenophases [13]. Each taxon has special requirements regarding the accumulated cold hours that are important for exiting the dormancy phase and are the main factor that determines the flowering time, and the need for the use of this species is the result of long-term climatic adaptations of genotypes in different regions [14]. The number of accumulated cold hours from November 1st, 2022, until bud break varied from 623 h (garden 1), over 1140 h (garden 2), and 1481 h (gardens 3, 6, 7, 8 and 10) to 1505 h (gardens 4, 5 and 9). The results of the study confirm the necessity of individual research, as each taxon has certain requirements regarding cold hours and that only after accumulating the necessary cold hours does the beginning of different phenophases of leafing or flowering occur. Flowering depends on the taxon, but also the genotype, their CH_t needs [15], and the heat [5]. Spearman's correlation coefficients were determined with a probability of $p<0.05$, and confirmed: a) complete positive (1.00) CH_t and № of days from November 1st to BB, b) very good positive (0.851) № of days from FF-EF and № of days BF-EF and c) weak negative correlations (-0.690 and -0.670) between № of days from November 1st to BB and № of days FF-EF and № of days from November 1st to BB and № of days BF-EF. Correlation analysis confirmed the importance of the accumulation of cold hours and the expected direct correlation of the increase in the number of CH_t with the increase in the number of days from November 1st, but also that a greater number of days from FF to EF affects the increase in the length of the flowering period. The negative correlations, although weak, indicate that an increase in the number of cold hours affects the number of days from full flowering to the end and the total flowering period. Other correlations were insignificant. Figure 1 shows the phenogram for Pink Flowering Quince in the 10 analyzed gardens.

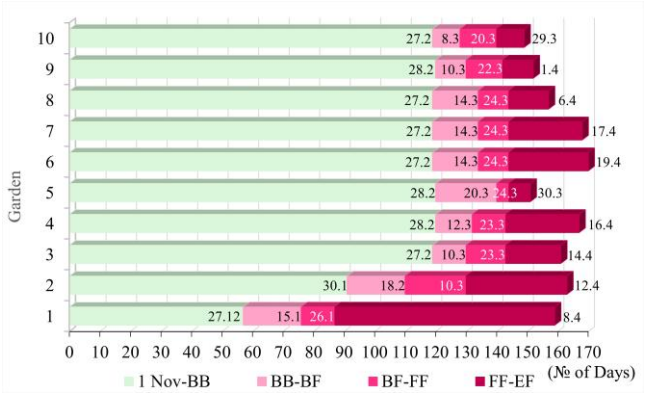

Figure 1 *Phenogram № of day: November 1-BB, BB-BF, BF-FF and FF-EF (December 2022–April 2023) for Pink Flowering Quince in the gardens in Ostružnica*

Evident differences stand out for the genotype in garden 1, where the bursting of flower buds was recorded on 27.12.2022, and the end of flowering on 08.04.2023. The length of the flowering phenophase was 83 days. Only 27.65 m away, there is an individual in garden 3 whose flower buds burst was on 27.02.2023, and on 10.04.2023. flowering ended. The length of the flowering phenophase was 31 days. Considering that the phenophases vary depending on the age of the plants, local climate, abiotic and biotic factors [16] as well as the proximity

of the plants and identical environmental conditions, the differences are related to the genotype. According to the time of flower bud break, but with a 34-day delay, the closest to genotype 1 are the 4 individuals in garden 2 (for the gardens with multiple specimens, the mean value of the recorded dates for all plants was used). In garden 2, flower buds burst on January 30, 2023, and on April 12, 2023, flowering ended. The length of the flowering phenophase was 53 days. The shortest period from the beginning to the end of flowering was in the garden 5 – only 11 days.

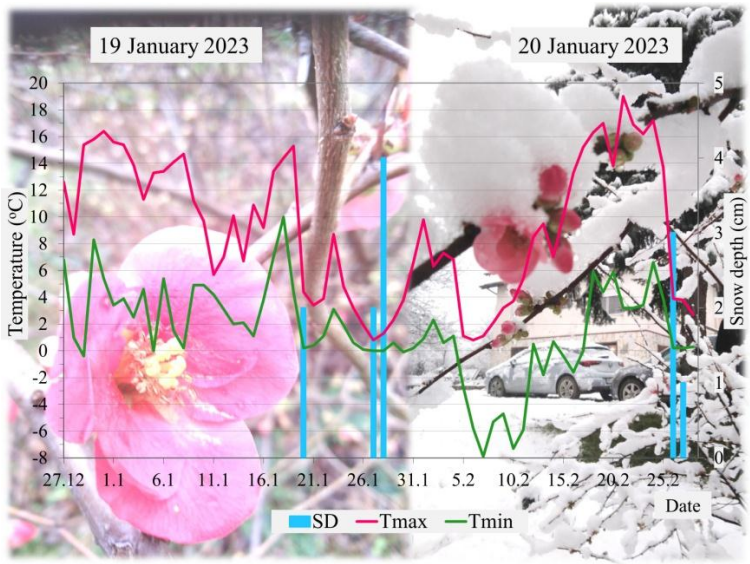

Figure 2 *Minimum and maximum daily air temperatures and thickness of the snow cover in the period from November 1, 2022 to the date of "bursting" of the flower buds of Pink Flowering Quince*

Figure 2 shows the minimum and maximum daily temperatures, as well as the height of the snow cover in the period from 27.12.2022 to 28.02.2023, in which the beginning of the flowering phenophase of bud burst was recorded for all Pink Flowering Quince individuals in the gardens. Genotype 1, in garden 1, was shown on two consecutive days in January, and further monitoring confirmed that there was no damage to the flower after a one-day snow cover. In February, after colder days, minor damage to open flowers, but not flower buds, was recorded. The flowering phenophase continued after the period of temperatures below 0°C and four more days with snow cover (RHMZ). There was no damage to the flower buds even in the plants in garden 2. In the plants in the other eight gardens, the bursting of flower buds and subsequent flowering phenophases were recorded after the cold period. During March 2023, all gardens were in full flowering phenophase. The mean daily air temperature at the beginning of the second decade, according to the percentile method (RHMZ), was in the cold category, while it was very cold in the middle of the third decade. In the warm and very warm categories, it was at the end of the first, middle of the second and middle of the third decade and at the end of the month. Temperatures stand out on 24.03. with T_{max} of 25.3°C, 29.03. T_{min} of -1.1°C, 28.03., when snowfall was recorded in the period of 1–3 hours, and during the day several short-term showers of hail, 28.03. and 29.03. with strong gusts of wind (16.7 m/s).

In April (4th and 5th April 2022), a snow cover of 14 cm and 17 cm was recorded. The snow had a density of 1400 kg/m^3 and 1700 kg/m^3 (RHMZ, www.hidmet.gov.rs/index.php), which caused snowdrifts and avalanches in many taxa in the research area, and the full flowering phenophase of thistle, which is a thermophilic, autochthonous, species [17]. In the observed Pink Flowering Quince, after the aforementioned events in March, the flowering phenophase ended in gardens 5, 9 and 10, and in the other gardens only minor damage to fully opened flowers were noted, and all plants continued with the full flowering phenophase. In April, there was no snow fall and crown deformity, and the flowering phenophase continued until 19.04, which confirmed the resilience of the genotypes in the other 7 gardens.

The obtained results are the basis for the operationalization of garden design, which has a key role in providing environmental sustainability through design interventions [18]. The innovative approach in the work is determining the correlations of the obtained results with the design of private gardens, but also the management of local landscapes and their elements that can be applied to other green and open spaces.

CONCLUSION

Our research confirms, based on the research of 10 private gardens, that the phenophases of Pink Flowering Quince and their duration are influenced by climatic elements, but also conditions in microlocations as well as genotype. Research should continue for several years to determine the impact of climate change on phenophases in the suburban zone. Understanding long-term trends is an essential part of managing and mitigating the effects of climate change through phenological patterns. For the design of private gardens, it is recommended to use compositional models with the analyzed cultivar that is adaptable. The recommendations are contextually appropriate and specific so that the implementation of the design has benefits for people and ecosystems, and the landscape is sustainable.

ACKNOWLEDGMENT

The authors are grateful to the Ministry of Science, Technological Development and Innovation of the Republic of Serbia for financial support of the University of Belgrade – Faculty of Forestry the scientific research work in 2023, the registration number 451-03-47/2023-01/200169.

REFERENCES

[1] Zhang X., Friedl M. A., Schaaf C. B. *et al.*, Geophys. Res. Lett. 31 (2004) L12209.

[2] Menzel A., Dose V., Meteorology. 14 (2005) 429–432.

[3] Gordo O., Sanz J. J., Oecologia. 146 (2005) 484–495.

[4] Cleland E. E., Chuine I., Menzel A., *et al.*, Trends Ecol. Evol. 22 (2007) 357–365.

[5] Ocokoljić M., Petrov Dj., Galečić N., *et al.*, Land 12 (2023) 706.

[6] Zimmerman J. K., Wright S. J., Calderon O., *et al.*, J. Trop. Ecol. 23 (2007) 231–251.

[7] Ting S., Hartley S., Burns K. C., Glob. Ecol. Biogeogr. 17 (2008) 648–657.

[8] Menzel A., Clim. Change 57 (2003) 243–263.

[9] Weber C., Bulletin of popular information of the Arnold Arboretum, Harvard University. Arnoldia. 23 (3) (1963) 17–75.

[10] Liu C., IOP Conference Series: Earth and Environmental Science, 714 (2) (2021) 022030.

[11] Cosmulescu S., Ionescu M., Int. J. Biometeorol. 62 (11) (2018) 2007–2013.

[12] Meier U., BBCH-Monograph. Growth Stages of Plants. [Entwicklungsstadien von Pflanzen. Estadios de las Plantas. Stades De Développement des Plantes]; Blackwell Wissenschafts-Verla: Berlin, Germany; Vienna, Austria (1997) p.622.

[13] Robeson S. M., Clim. Change 52 (2002) 219–238.

[14] Ruiz D., Campoy J. A., Egea, J., Environ. Exp. Bot. 61 (2007) 254–263.

[15] Citadin I., Raseira M. C. B., Herter F. G., *et al.*, HortScience 36 (2001) 305–307.

[16] Denny E., Gerst K. L., Miller-Rushing A. J., *et al.*, Int. J. Biometeorol. 58 (2014) 591–601.

[17] Ocokoljić M., Petrov Dj., Decorative Dendrology, University of Belgrade – Faculty of Forestry, Belgrade (2022) 409, ISBN: 978-86-7299-339-4.

[18] Khoroshkov L., Derevianko N., Sci. Horiz. 24 (3) (2021) 68–74.

ACTIVTY CONCENTRATIONS OF ^{210}Pb, ^{137}Cs, AND ^{40}K IN WILD MUSHROOMS FROM SERBIA AND THEIR EFFECTIVE DOSE TO INGESTION

Mirjana Đurašević[1], Igor Čeliković[1], Irina Kandić[1], Tamara Milanović[1], Aleksandra Samolov[1], Nataša Mladenović Nikolić[1], Aleksandar Kandić[1*]

[1]„Vinča" Institute of Nuclear Sciences, National Institute of Republic of Serbia, University of Belgrade, SERBIA

[*]*akandic@vin.bg.ac.rs*

Abstract

Fourteen samples of nine different species were collected in the region of Fruška gora, the suburban areas of Belgrade, and the vicinity of Vlasina Lake (Serbia) have been analyzed from the radiological point of view. Specific activities of radionuclides ^{210}Pb, ^{137}Cs, and ^{40}K were measured using a semiconductor HPGe spectrometer system in these wild mushroom samples. The activity concentrations of all measured dried wild mushrooms are for ^{210}Pb: between 2.05 Bq/kg and 9.74 Bq/kg; for ^{137}Cs: between < 0.2 Bq/kg and 19.3 Bq/kg; for ^{40}K between 704 Bq/kg and 2530 Bq/kg. The total individual annual effective doses due to ingestion of ^{210}Pb, ^{137}Cs, and ^{40}K radionuclides within a 0.5 kg dry mass of the wild mushrooms is between 3.99 µSv and 10.81 µSv, and are much lower than the recommended level for the public (1 mSv/y).

Keywords: wild mushrooms, radioactivity, annual effective dose.

INTRODUCTION

The environmental contamination caused by global fallout due to atmospheric nuclear weapons testing, which peaked in 1963, as well as various nuclear accidents such as Chernobyl and Fukushima, has contributed to the presence of anthropogenic radionuclides in the environment [1]. Furthermore, the use of radionuclides in everyday life has also led to contamination with anthropogenic radionuclides. On the other hand, it is important to pay attention to the presence of naturally occurring radionuclides, particularly in regions with high levels of radioactivity and near uranium mines.

Mushrooms have the ability to accumulate both anthropogenic and naturally occurring radionuclides, particularly in areas with high levels of radioactive fallout. This is due to the fact that certain species of mushrooms absorb and concentrate radionuclides from the substrate in which they grow. As a result, they are considered excellent bioindicators of environmental pollution within their ecosystem. Studies have found that wild mushrooms typically have higher levels of radioactivity than cultivated mushrooms. However, it is important to note that the accumulation of radionuclides in mushrooms can pose a radiological hazard [2–5].

Measuring the levels of radioactivity in mushrooms allows us to assess the degree of radioactive contamination in the nearby soil and air. The amount of radionuclides found in wild mushrooms can be influenced by several factors, including the composition and moisture

of the soil, climate, radioactive fallout, and natural radionuclides present in the environment. Additionally, the radioactivity levels found in mushroom fruit bodies are dependent on various factors such as the mushroom species, its nutrition and ecology (whether it's saprophytic or mycorrhizal), the depth of the mycelium in the substrate from which the mushroom obtains nutrients and radionuclides, and the vertical distribution of radionuclides in the soil [2,3,6]. In spite of that, it has been observed that even for the same mushroom species in the same location and at the same time, there can be significant variation in the radioactivity concentration recorded [1].

Although various radionuclides have been investigated in mushrooms in different countries worldwide [2,4–10], most attention is given to ^{137}Cs because it is a long-lived radionuclide and chemically similar to potassium. The analysis of the radioactive content of mushrooms reported in the literature was also focused on ^{40}K, as mushrooms contain between 1.5 g and 117 g of potassium per kg of dry matter (d.m.) [2]. On the other, ^{210}Pb has a significantly higher effective dose coefficient (52 times higher than for ^{137}Cs and 91 times higher than for ^{40}K). Therefore, it was the subject of our research.

Guillén and Baeza [5] gave an exhaustive review of the radioactivity levels of mushrooms. According to their findings, the range of radiocesium content in mushrooms worldwide since 1986 varies greatly, spanning nine orders of magnitude from 0.4 Bq/kg d.m. to 50.7 MBq/kg d.m. As potassium is an essential nutrient, its range of variation is limited, spanning only three orders of magnitude, with the most commonly reported values for ^{40}K falling between 1000 Bq/kg d.m. and 2000 Bq/kg d.m., depending on the mushroom species (ranging from 70 Bq/kg d.m. to 3.52 kBq/kg d.m.). Besides, their paper reports that the range for ^{210}Pb falls between 0.75 Bq/kg d.m. and 289 Bq/kg d.m. [5].

The objective of this study is to analyze the content of radionuclides ^{210}Pb, ^{137}Cs, and ^{40}K in fourteen samples of nine different wild mushroom species from three regions of Serbia (Fruška gora, suburban areas of Belgrade, and vicinity of Vlasina Lake). Additionally, the study aims to estimate the individual annual effective dose resulting from ingestion of these mushrooms.

MATERIALS AND METHODS

Fourteen samples of nine different wild mushroom species were collected from three regions in Serbia: Fruška gora, suburban areas of Belgrade, and the vicinity of Vlasina Lake. As a first step, all samples were thoroughly cleaned of impurities. Since mushroom fruit bodies are often consumed completely, the stalks and caps of each sample were initially sundried together for several days and then dried at 105 °C for 24 h in a temperature-controlled oven. Each dried mushroom sample was separately homogenized to a fine powder using a laboratory blender and stored in a suitable standard cylindrical PVC container with a volume of 125 ml prior to analysis. The mass of each individual sample was up to 30 g, adequate to the working standard, which contains dried grass as a matrix. The matrix of dried grass was spiked with a radioactive solution with a common mixture of gamma ray emitters (^{241}Am, ^{109}Cd, ^{139}Ce, ^{57}Co, ^{60}Co, ^{137}Cs, ^{113}Sn, ^{85}Sr, and ^{88}Y) purchased from CMI (Czech Metrology Institute). The working standard was prepared at the Laboratory for Nuclear and

Plasma physics, "Vinča" Institute of Nuclear Sciences, National Institute of Republic of Serbia, University of Belgrade [11,12].

The samples were analyzed using a Canberra GX5019 coaxial HPGe spectrometer with a 55% relative efficiency and 1.9 keV resolution for ^{60}Co at 1332.5 keV, in close detector geometry. The spectra of wild mushrooms samples were recorded and analyzed using Canberra Genie2000 software. To obtain reliable results, the samples were measured for up to 575,000 seconds to ensure acceptable statistical accuracy.

The activity concentrations of radionuclides ^{210}Pb, ^{137}Cs, and ^{40}K in wild mushroom samples were determined directly by analyzing full-energy peaks at 46.54 keV, 661.66 keV, and 1460.82 keV, respectively. Corrections for background were taken into account. It should be noted that the net peak area at 1460.82keV was corrected for the contribution of the ^{228}Ac peak at 1459.13 keV energy. The uncertainty of measurement was determined by applying the general law of propagation of uncertainty. The largest contribution to the total uncertainty was due to the statistical uncertainty (in some samples more than 40% for ^{137}Cs) and efficiency calibration (5%), whereas uncertainty due to measured mass of the sample could be neglected.

The individual annual effective dose, E_{ing}, received by an individual adult due to yearly ingestion of 0.5 kg dry mass of the wild mushrooms is calculated according to the following formula [5]:

$$E_{ing} = \Sigma E_{ingj} = \Sigma A_{sj} H DF_{ingj} \quad (1)$$

where E_{ingj} is the individual annual effective dose due to ingestion of specific radionuclide *j* in the wild mushrooms [Sv], A_{sj} is the activity concentration of specific radionuclide *j* in dried wild mushrooms sample [Bq/kg], *H* is the annual amount of dry mass of the wild mushroom ingested per year by the standard individual [kg], and DF_{ingj} is the effective dose coefficient for ingestion of specific radionuclide *j* [Sv/Bq].

The effective dose coefficients for ingestion of specific radionuclide are: 6.8 10^{-7} Sv/Bq for ^{210}Pb, 1.3 10^{-8} Sv/Bq for ^{137}Cs, and 6.2 10^{-9} Sv/Bq for ^{40}K and [13,14].

RESULTS AND DISCUSSION

The activity concentrations of ^{210}Pb, ^{137}Cs, and ^{40}K radionuclides in fourteen dried samples of nine different wild mushroom species collected in the region of Fruška gora, the suburban areas of Belgrade, and the vicinity of Vlasina Lake (Serbia) with uncertainties of measurement at the confidence level 1 σ, are presented in Table 1.

The activity concentration of radionuclides presented in Table 1. are given for dried wild mushroom samples in order to compare our experimental data with the literature ones obtained for fresh mass. A dry/wet ratio of 0.1 can be used, according to the mean value reported in literature [2,5,15].

Table 1 *^{210}Pb, ^{137}Cs, and ^{40}K specific activities in dried samples of wild mushrooms with uncertainties of measurement at the confidence level of 1σ, and calculated values of total individual annual effective doses due to ingestion of ^{210}Pb, ^{137}Cs, and ^{40}K radionuclides within a 0.5 kg of dry mass of the wild mushrooms*

Mushroom species	**Family**	**Ecology**	**Edibility**	**Location**	A_s **[Bq/kg]**			E_{ing} **[μSv/y]**
					^{210}Pb	**^{137}Cs**	**^{40}K**	
Amanita pantherina	Amanitaceae	m	p	a	5.82 ± 0.63	0.89 ± 0.35	1464 ± 75	6.52
Amanita vittadinii	Amanitaceae	m	u	b	8.67 ± 0.93	1.19 ± 0.35	2530 ± 130	10.81
Cantharellus cibarius	Cantharellaceae	m	e	c	2.76 ± 0.59	7.30 ± 0.98	967 ± 50	3.99
Boletus edulis	Boletaceae	m	e	b	8.19 ± 1.22	1.40 ± 0.31	973 ± 50	5.81
Boletus edulis	Boletaceae	m	e	c	2.87 ± 0.72	19.3 ± 1.3	704 ± 37	5.08
Hypsizygus Tessularus	Lyophyllaceae	s	e	b	6.70 ± 0.88	3.07 ± 0.36	1187 ± 60	5.98
Hypsizygus Tessularus	Lyophyllaceae	s	e	b	3.25 ± 0.40	2.49 ± 0.35	1056 ± 54	4.39
Clytocybe rivulosa	Omphalotaceae	s	p	a	5.53 ± 0.52	1.20 ± 0.21	1380 ± 70	6.17
Clytocybe rivulosa	Omphalotaceae	s	p	b	5.73 ± 0.66	0.95 ± 0.20	1776 ± 90	7.47
Lepiota lilacea	Agaricaceae	s	p	a	5.38 ± 0.56	0.76 ± 0.27	1223 ± 62	5.62
Lepiota lilacea	Agaricaceae	s	p	b	9.21 ± 0.80	< 0.3	1464 ± 74	7.67
Lepiota lilacea	Agaricaceae	s	p	b	9.74 ± 1.06	< 0.2	2010 ± 100	6.52
Macrolepiota procera	Agaricaceae	s	p	a	4.94 ± 0.53	< 0.2	1036 ± 53	4.89
Macrolepiota konradii	Agaricaceae	s	p	b	2.05 ± 0.25	1.18 ± 0.33	1980 ± 100	6.86

m – mycorrhizal fungi, s – saprophytic fungi; p – poisonous, u – unknown, e – edible; a – Fruška gora, b – suburban areas of Belgrade, c – vicinity of Vlasina lake.

The activity concentrations of all measured dried wild mushrooms is for ^{210}Pb: between 2.05 Bq/kg (*Macrolepiota konradii* from suburban area of Belgrade) and 9.74 Bq/kg (*Lepiota lilacea* from suburban area of Belgrade); for ^{137}Cs: between < 0.2 Bq/kg (*Lepiota lilacea* from suburban area of Belgrade and *Macrolepiota procera* from Fruška gora) and 19.3 Bq/kg (*Boletus edulis* from vicinity of Vlasina lake); for ^{40}K between 704 Bq/kg (*Boletus edulis* from vicinity of Vlasina Lake) and 2530 Bq/kg (*Amanita vittadinii* from suburban area of Belgrade).

The activity concentration values of radionuclides presented in Table 1 can be considered to be at very low contamination levels, compared to the specific activity concentration limits set by the international legislation. The limits are: 113 Bq/kg d.m. for ^{210}Pb, 6000 Bq/kg d.m. for ^{137}Cs, and 12581 Bq/kg d.m. for ^{40}K [2,5,16].

The total individual annual effective doses due to ingestion of ^{210}Pb, ^{137}Cs, and ^{40}K radionuclides within a 0.5 kg of dry mass of the wild mushrooms, calculated according Equation (1), with corresponding uncertainties at the confidence level of 1σ are also given in Table 1.

The total individual annual effective doses calculated by Equation (1) are based on the conservative assumption that all species of mushrooms are edible, consumed raw, and the entire radionuclide content in the mushroom can be assimilated by the human body [2].

The individual annual effective doses due to ingestion radionuclides within a 0.5 kg dry mass of the wild mushrooms is for ^{210}Pb: between 0.70 μSv (*Macrolepiota konradii* from suburban area of Belgrade) and 3.31 μSv (*Lepiota lilacea* from suburban area of Belgrade); for ^{137}Cs: between < 1 nSv (*Lepiota lilacea* from suburban area of Belgrade and *Macrolepiota procera* from Fruška gora) and 125 nSv (*Boletus edulis* from vicinity of Vlasina Lake); for ^{40}K between 2.18 μSv (*Boletus edulis* from vicinity of Vlasina Lake) and 7.85 μSv (*Amanita vittadinii* from suburban area of Belgrade).

The total individual annual effective doses due to ingestion of ^{210}Pb, ^{137}Cs, and ^{40}K radionuclides within a 0.5 kg of dry mass of the wild mushrooms is between 3.99 μSv (*Cantharellus cibarius* from vicinity of Vlasina Lake) and 10.81 μSv (*Amanita vittadinii* from suburban area of Belgrade), and are much lower than the recommended level for the public (1 mSv/y) [2,5,17].

CONCLUSION

The total individual annual effective doses due to ingestion were estimated based on measured activity concentration of ^{210}Pb, ^{137}Cs, and ^{40}K in 14 samples of 9 different species of wild mushrooms collected in the region of Fruška gora, the suburban areas of Belgrade, and the vicinity of Vlasina Lake (Serbia). All values of measured can be considered as a very low contamination level, compared to the specific activity concentration set by the international legislation. The calculated total individual annual effective doses resulting from ingestion of ^{210}Pb, ^{137}Cs, and ^{40}K radionuclides within a 0.5 kg of dry mass of the wild mushrooms are significantly lower than the recommended level for the public (1 mSv/y).

ACKNOWLEDGEMENT

This work was financially supported by Serbian Ministry of Science, Technological Development and Innovation (Project number 451-03-47/2023-01/200017).

REFERENCES

[1] Yamada T., Agricultural Implications of the Fukushima Nuclear Accident *in* Mushrooms: Radioactive Contamination of Widespread Mushrooms in Japan, Editors: Nakanishi T. M., Tanoi K., Springer, Tokyo (2013) p.163–176.

[2] Caridi F., Belmusto G., Cogent phys. 4 (2017) 1.

[3] Karadeniz Ö., Yaprak G., J. Radioanal. Nucl. Chem. 285 (2010) 611–619.

[4] Pekşen A., Kurnaz A., Turfan N., *et al*., YYU. J. Agr. Sci. 31 (1) (2021) 30–41.

[5] Guillén J., Baeza A., Food Chem. 154 (2014) 14–25.

[6] Čadová M., Havránková R., Havránek J., *et al*., Radiat. Environ. Biophys. 56 (2017) 167–175.

[7] Castro L.P., Maihara V.A., Silva P.S.C., *et al*., J. Environ. Radioact. 113 (2012) 150–154.

[8] Szymańska K., Falandysz J., Skwarzec B., *et al*., Chemosphere 213 (2018) 133–140.

[9] Barua T., Bhuian A. K. M. S. I., Hossain S., *et al*., J. Radioanal. Nucl. Chem. 322 (2019) 173–182.

[10] Žunić Z. S., Mietelski J. W., Błażej S., *et al*., J. Environ. Radioact. 99 (8) (2008) 1324–1328.

[11] Vukanac I., Djurašević M., Kandić A., *et al*., Appl. Radiat. Isot. 66 (6–7) (2008) 792–795.

[12] Kandić A., Vukanac I., Djurašević M., *et al*., Appl. Radiat. Isot. 70 (9) (2012) 1860–1862.

[13] Scientific Committee on the Effects of Atomic Radiation (UNSCEAR), (2000). Sources and effects of ionizing radiation: sources (Vol. 1). United Nations Publications, New York, ISBN: 92-1-142238-8, *Available on the following link*:

www.unscear.org/unscear/en/publications/2000_1.html.

[14] Eckerman K., Harrison J., Menzel H. G., *et al.* ICRP publication 119: Compendium of dose coefficients based on ICRP Publication 60, Annals of the ICRP 41 (1) (2012).

[15] Baeza A., Hernández S., Guilléna F. J., *et al.* Sci. Total Environ. 318 (2004) 59–71.

[16] European Commission (EC), (2020). Council Regulation No 1158/2020 of 15 August 2020 on the conditions governing imports of agricultural products originating in third countries following the accident at the Chernobyl nuclear power station, *Available on the following link*: https://eur-lex.europa.eu/eli/reg_impl/2020/1158/oj.

[17] ICRP, Compendium of dose coefficients based on ICRP publication 60. ICRP Publication 119 Annals of ICRP 41 (2012), *Available on the following link*: www.icrp.org/publication.asp?id= ICRP%20Publication%20119.

LANTHANUM IMMOBILIZED ONTO GRAPHENE AS A CATALYST DESIGNED FOR ELECTROCHEMICAL APPLICATIONS

Jelena Čović[1], Milan Z. Momčilović[2*], Marjan Ranđelović[1]

[1]University of Niš, Faculty of Sciences and Mathematics, Višegradska 33, 18000 Niš, SERBIA

[2]University of Belgrade, "Vinča" Institute of Nuclear Sciences – National Institute of the Republic of Serbia, P.O. Box 522, 11000 Belgrade, SERBIA

[*]*milanmomcilovic@yahoo.com*

Abstract

Electrochemistry of glassy carbon electrode modified with composite of lanthanum immobilized onto graphene and MWCNT was examined in three-electrode cell regarding its electrocatalytic properties. Red-ox reactions of potassium ferrocyanide in Britton-Robinson buffer solutions as benchmark media were analyzed. SEM revieled shape and dimensions of typical particles of the synthesized material. XRD confirmed the hexagonal phase of $La_2O_3CO_3$ present in the graphene matrix. Cyclic voltammetry evidenced higher current intensities but sluggish electrode kinetics in case of the modified glassy carbon electrode.

Keywords: cyclic voltammetry, glassy carbon electrode, MWCNTs, kinetics.

INTRODUCTION

The commercially available working electrodes such as glassy carbon electrode (GCE) exhibit notable electrical conductivity, mechanical and dimensional stability, resistance to temperature fluctuations, low porosity, and a wide potential range [1]. The performance of this electrode is frequently optimized through deposition of various carbon nanomaterials (e.g. MWCNTs and graphene) which can be beneficial for the electrochemical sensing or electrocatalytical features of the processes taking place at the electrode surface.

MWCNTs are capable of facilitating electron transfer in electrochemical reactions. This phenomenon is ascribed to the presence of edge-plane-like graphite sites located at the CNT ends [2]. The large edge-plane-to-basal-plane ratio of MWCNTs, combined with the enhancement of electrode surface area and porosity, is accountable for their superior sensitivity, reduced detection limit, and faster electron transfer kinetics in comparison with traditional carbon based electrodes [3].

Graphene can be envisioned as a two-dimensional sheet of carbon atoms bonded by sp^2 bonds and have unique mechanical, electrical, thermal, and optical properties [4]. This carbon based material has a large surface area, and shows excellent thermal and electrical conductivity [5]. The broad attraction of graphene as an electrode material can be attributed to its capacity for high heterogeneous electron transfer rates, excellent electrochemical stability

across a broad potential range, and its adaptability for modifying the electrochemical performance by modulating its surface state [6].

Rare earth-based electrocatalytic materials including alloys, perovskites, hybrids, and single atoms and their advantages in electrocatalysis are becoming very important. For instance, Zhang *et al*. [7] synthesized hybrid material, La_2O_3 on carbonaceous microspheres as an efficient bifunctional electrocatalyst for ORR and OER. Weiwei *et al.* [8] reported ORR electrocatalytic activity of the hybrid, $La_2O_2CO_3$ encapsulated La_2O_3 nanoparticles on a carbon black (Vulcan XC-72, Cabot). The unique chemical bonds formed at the interface are beneficial for the development of ORR activity.

In the current study, the as-prepared La-graphene (LaG) material was employed as electrode material for enhancing the performance of bare GCE. Notably, we have used novel material for investigating the well-known electrode red-ox processes of potassium fero-cyanide.

MATERIALS AND METHODS

Synthesis and characterization of LaG

Synthesis of graphene started with mixing the amounts of 6 g glucose and 6 g of $FeCl_3 \cdot 6H_2O$ and dissolution in 10 cm^3 of deionized water. Water evaporation was carried out by heating at 80 ºC for 24 hours. Carbonization of the obtained product was performed at 700 ºC for 3 hours under an inert atmosphere of nitrogen. Subsequently, the material was ground, added in 100 cm^3 of concentrated HCl (36%) and stirred for 6 hours. After that, the suspension was filtered and washed-out with 300 cm^3 deionized water, then washed-out with 80 cm^3 of acetone. The obtained material was dried at 70 ºC for 1 hour.

Introduction of La into graphene structure was carried out in few steps. Initially, 0.04 g of Pluronic® F127 was added into 20 cm^3 of mixture of ethanol and water (*wt*. 1:1) followed by addition of 100 mg of graphene. This suspension was sonicated for 5 minutes. In the next step, 58 mg of La(VI) nitrate was dissolved in 2 cm^3 of deionized water and this solution was mixed with the suspension from the previous step. Then, 0.1 M NaOH was added in drops untill pH 12 is reached. Alkalized suspension was transfered to PTFE lined autoclave and thermally treated at 200 °C for 3 h. After the treatment, pH of the suspension was between 11 and 12. It was centrifugated twice with rinsing in between. An excess of the aqueous layer was discharged and the remaining slurry was dried at 50 °C for several hours, and then transfered into cuvete.

All the chemicals were of analytical grade and were purchased from Sigma-Aldrich. Deionized water of 18.2 MΩ obtained from demineralizator Smart2Pure (Thermo, USA) was used for all experiments.

SEM images were obtained by using Leo Gemini 1530 device from Zeiss with an Everhart-Thornley detector for collecting secondary electrons. The accelerating voltage was 10 kV. Samples were also analyzed on STADI P XRD diffractometer from STOE & Cie GmbH with Mythen1K detector. Cu-Kα-radiation was used at 40 kV and 40 mA.

Electrode preparation

For electrochemical testing of lanthanum graphene hybride, electrode LaG@MWCNT was prepared and glassy carbon technique was applied. Synthesized material was mixed with the same mass of MWCNT (3.5 mg of each) and dispersed in 1 cm^3 of ethanol/water mixture (40*v*/*v*%) followed by homogenization in the ultrasonic bath for 30 min. Before applying the drop of this suspension onto the surface of the glassy carbon electrode (GCE), it was thoroughly polished by the aid of fine cloth containing alumina powder and ultrasonically treated in ethanol for 15 min. Then, 0.01 cm^3 of the LaG@MWCNT suspension was transferred onto the surface of GC electrode (working area was 0.04 cm^2) and dried under nitrogen stream. After the thin carbon layer was dried, it was covered with 0.007 cm^3 of 0.05 *wt*.% Nafion® in ethanol and again evaporated by the nitrogen gas.

RESULTS AND DISCUSSION

Material characterization

Figure 1a displays diverse morphology of the analyzed sample with particles of various shapes and dimensions. At the magnifications of 500 times, crisp like particles can be spotted scattered in various directions and covered with particles of irregular symmetry and of significantly smaller dimensions. From this perspective and at this magnification it is hard to claim in which degree lanthanum based phase is dispersed throughout the graphene structure but it is probably mostly on surface.

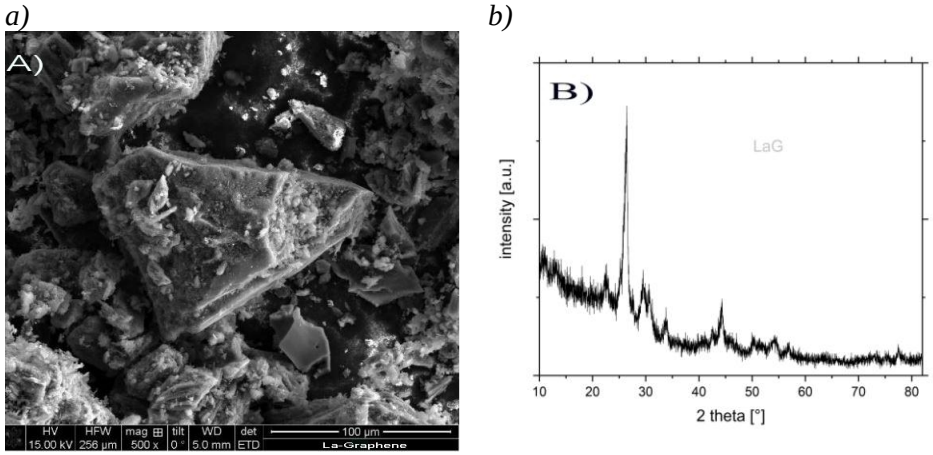

Figure 1 *a) SEM image of LaG at 500x magnification; b) XRD profile of LaG*

The diffraction peak assigned at about 26° is ascribed to the (002) crystal plane of carbon (Figure 1b). The peaks at approximately 27.6°, 33.6°, 42.5°, 44.4°, and 75.6° correspond to the hexagonal phase of $La_2O_3CO_3$ (JCPDS card 37-0804) indicating that the synthesized lanthanum compound is consisted of above phase.

Electrochemical tests

In this study, cyclic voltammetry was employed as a tool to investigate the reversibility of the electrode reactions and aid in elucidating of their mechanisms. Herein, electrochemical oxidation of ferrocyanide ions to ferricyanide and the reverse reduction reaction was carried

out at 3 mm diameter GCE. Figure 2a shows cyclic voltammograms for specific electrodes in 1 mM potassium ferrocyanide ($[K_4Fe(CN)_6]$) with Britton-Robinson (B-R) buffer supporting electrolyte using LaG@MWCNT imobilised onto GCE and bare GCE as working electrodes. Cyclic voltammograms were obtained at different scan rates (5–200 mV/s).

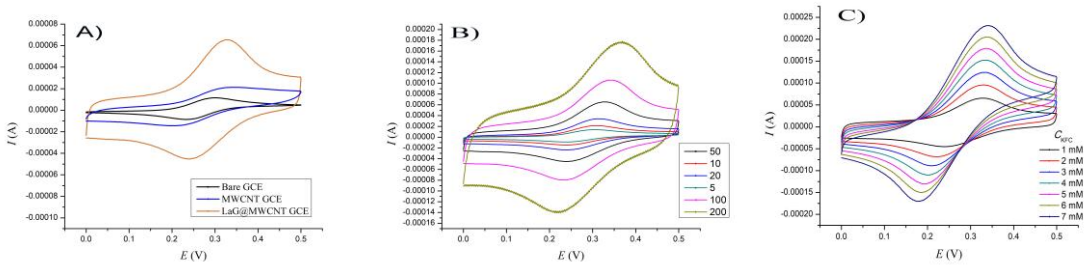

Figure 2 *Cyclic voltammograms of a) three compared electrodes in 1 mM K-ferrocyanide at 50 mV/s; b) LaG@MWCNT at scan rates from 5 to 200 mV/s; c) LaG@MWCNT with diferent ferrocyanide concentrations*

The recognizable, nearly symmetrical shape of the cyclic voltammograms for ferrocyanide electrooxidation-reduction is observed. The E_{pa} and I_{pa} from the voltammograms were measured and collected in Table 1 together with other kinetic parameters. Formal potentials were calculated from the anodic and cathodic peak potentials (E_{pa} and E_{pc}) according to the standard equation ($E^0 = (E_{pa} + E_{pc})/2$), yielding values of 0.285 V, 0.272 V and 0.265 V for LaG@MWCNT, MWCNT GCE and bare GCE, respectively. Calculated values are slightly higher than standard redox potential given in the literature.

A preliminary approach used to evaluate the reversibility of an electrochemical process is reflected in the ratio between the anodic and cathodic peak currents. The peak current ratio (I_{pa}/I_{pc}) was observed to be close to unity (1.038) for bare GCE for 50 mV/s. That is characteristic of an reversible electron transfer reaction with chemically stable generated products. However, the ratio I_{pa}/I_{pc} is greater than unity for MWCNT GCE (1.132) and for LaG@MWCNT GCE (1.569) at 50 mV/s. This indicates the quasi-reversible nature of the electrode process. It seems that LaG@MWCNT GCE seletively promoted oxidation process and indicates adsorption of the reduced species, despite the apparently quasireversible redox behaviour.

For LaG@MWCNT GCE, ΔE_p value of 0.064 V was observed for the lowest scan rate (5 mV/s) which increased slightly with scan rate to 0.138 V at 200 mV/s. These values are typical for most electrodes and normally considered to represent quasireversible behavior. The bare GCE, however, has shown to be more close to theoretically ideal behavior with ΔEp values of 0.062 V. This value slightly changed over the scan rates examined. However, the voltammetric response for the modified electrode is significantly improved in comparison to bare GCE, reflected by the enlargement of the peak currents (Table 1). A plot of the anodic peak current versus the square root of the scan rate ($v^{1/2}$) is shown in Figure 3.

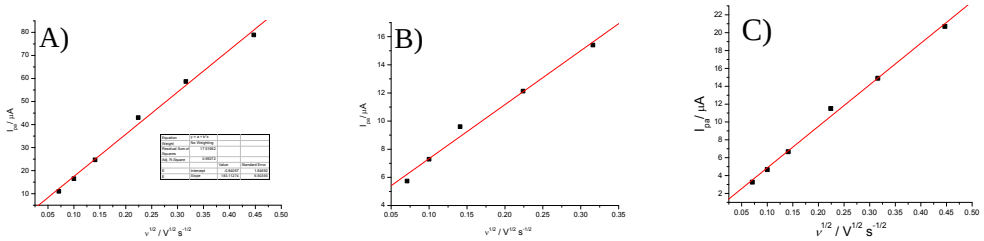

Figure 3 *The linear dependences of I_{pa} vs. square root of the scan rates for a) LaG@MWCNT GCE; b) MWCNT GCE and c) bare GCE*

Here, the obtained data were fitted to a straight line. From the linear dependence in the range from 5 to 200 mV/s it can be concluded that the electrode reaction at sufficient overpotential is diffusion controlled. Generally, the peak current of diffusion controlled reversible or quasi-reversible electrochemical reaction follows Randles-Sevcik equation. As seen in Figure 3, the slope of the I_{pa} versus $v^{1/2}$ fit lines is significantly greater for the modified electrode as compared to the bare GCE and MWCNT modified GCE. That is indicative of an decrease in the apparent diffusivity for the ferro/ferricyanide ions on the LaG@MWCNT GCE.

Heterogeneous electron transfer rate coefficient (k^0) is the key kinetic parameter which was calculated by applying the method of Nicholson. Standard value for the diffusivities of the reduced species ($6.32 \cdot 10^{-6}$ cm^2/s) was used. For the LaG@MWCNT GCE, MWCNT GCE, and bare GCE and, k^0 valuees of 0.007 cm/s, 0.002 cm/s, and 0.02 cm/s were obtained at scan rate of 50 mV/s, respectively, which is comparable to values reported in the literature. It should be noted that these values have been observed to be dependent on pretreatment, amount of Nafion® solution added and polishing method used. It seems that electron transfer is impeded by both contact resistance between catalyst particles, the catalyst and the glassy carbon surface, and by the presence of the Nafion® binder onto the mdified electrode. Additionally, it should be mentioned that the Nicholson method used in calculating k^0 assumes semi-infinite diffusion to the electrode surface (worth for flat disc electrodes and micro-electrodes) which is not the case for a modified electrodes with specific hybrid structures.

Table 1 *Kinetics parameters obtained from cyclic voltammogram and Tafel analysis of 1 mM $[K_4Fe(CN)_6]$ oxidation in B-R buffer (scan rate: 5 mV/s; counter electrode: platinum coil)*

Electrode	E_{on} (mV)	I_0 (μA/cm^2)	E_{eq} (mV)	$n\alpha_a$	Tafel slope (mV/dec^1)	E_{pa} (V)	I_{pa} (μA)
LaG@MWCNT GCE	210	0.924	23	0.543	107.8	0.304	$11.03 \cdot 10^{-6}$
Bare GCE	200	2.77	176	0.863	67.8	0.296	$3.27 \cdot 10^{-6}$

In order to get additional information on the electrochemical kinetics of $[K_4Fe(CN)_6]$ oxidation, the value of $n\alpha_a$ was determined. α_a is the anodic transfer coefficient and n is the number of electrons involved in the rate determining step. The Tafel plot (log I vs. E) was drawn using the data obtained from the rising part of the cyclic voltammograms for the

$[K_4Fe(CN)_6]$ oxidation current and scan rate of 5 mV/s in order to reach steady-state conditions. The Tafel slope for LaG@MWCNT GCE is 108 mV/decade, which is equal to value for the transfer coefficient α_a for $[K_4Fe(CN)_6]$ oxidation of 0.54. The Tafel value obtained for LaG@MWCNT GCE was found to be closer to the theoretical value (118 mV/dec) for one-electron transfer.

The value of α_a is higher than 0.5 which is commonly expected for simple outer-sphere redox reactions. Extrapolation of the Tafel plot to the equilibrium $[K_4Fe(CN)_6]$ redox potential gives an exchange current density value of $9.24 \cdot 10^{-7}$ A/cm^2 for LaG@MWCNT GCE and $2.8 \cdot 10^{-6}$ A/cm^2 for bare GCE which corresponds to the standard heterogeneous rate constant for ferrocyanide oxidation of $9.6 \cdot 10^{-6}$ cm/s and $2.8 \cdot 10^{-5}$ cm/s. These findings are in line with the results obtained by using the method of Nicholson since both methods provide almost the same ratio of heterogeneous rate constants for LaG@MWCNT and bare GCE indicating slower electron transfer kinetics of $[K_4Fe(CN)_6]$ oxidation at LaG@MWCNT.

From the two voltammograms and the values of peak currents, it is evident that with the increase of concentration, the I_{pa} and I_{pc} increases (Figure 2c). This response for both LaG@MWCNT modified and bare GCE shows a direct relationship between peak current and concentration of the electroactive species in solution which confirms the relation in the Randles-Sevcik equation. In spite of some evident kinetics hindrances for ferrocyanide oxidation/reduction at LaG@MWCNT GCE, this material has better voltammetric response with significantly hihger I_{pa} and I_{pc} than bare GCE.

CONCLUSION

Glassy carbon electrode modified with lanthanum doped graphene and MWCNT mixture showed higher peak currents in contrast to unmodified electrode. Interestingly, regardless of this catalytic enhancement modified electrodes resulted in poorer parameters obtained in electrochemical analysis. The sluggish kinetics of the overall activity on modified electrodes can be attributed to various kinetic resistances throughout the layer of applied electrode material and also contribution of adsorption phenomena in complex electrode processes.

ACKNOWLEDGEMENT

The authors are grateful to the Ministry of Science, Technological Development and Innovations of the Republic of Serbia for supporting this study according to the contract with the registration number 451-03-47/2023-01/200017.

REFERENCES

[1] Smarzewska S., Jasinska A., Ciesielski W., *et al*., Electroanalysis 29 (2017) 244–248.

[2] Liu G., Riechers S.L., Mellen M.C., *et al*., Electrochem. Commun. 7 (2005) 1163–1169.

[3] Sipa K., Brycht M., Leniart A., *et al.,* Talanta 176 (2018) 625–634.

[4] Beladi-Mousavi S.M., Salinas G., Antonatos N., *et al.,* Carbon 191 (2022) 439–447.

[5] Martín A., Escarpa A., Trends Anal. Chem. 56 (2014) 13–26.

[6] Inozemtseva A., Sergeev A., Napolskii K., *et al*., Electrochim. Acta 427 (2022) 140901.

[7] Zhang X., Xiao Q., Zhang Y., *et al.*, J. Phys. Chem. C 118 (2014) 20229–20237.
[8] Gu W., Liu J., Hu M., *et al*., ACS Appl. Mater. Interfaces 7 (2015) 26914–26922.

NITROGEN DOPED CARBON MICROSPHERES SUPPORTED ONTO MWCNT AS NOVEL ELECTRODE MATERIAL

Jelena Čović[1], Milan Z. Momčilović[2*], Marjan Ranđelović[1]

[1]University of Niš, Faculty of Sciences and Mathematics, Višegradska 33, 18000 Niš, SERBIA

[2]University of Belgrade, "Vinča" Institute of Nuclear Sciences – National Institute of the Republic of Serbia, P.O. Box 522, 11000 Belgrade, SERBIA

[*]*milanmomcilovic@yahoo.com*

Abstract

This study is focused on the synthesis and electrochemical study of novel modified glassy carbon electrode containing nitrogen doped carbon microspheres deposited on the multi-walled carbon nanotubes (MWCNTs). The results of electrochemical study of bare and modified GCE were obtained by cyclic voltammetry of potassium ferrocyanide in Britton-Robinson buffer solutions. Morphology and structure of the synthesized carbon microspheres were analysed by SEM which showed typical spherical particles. The findings of the electrochemical study are controversial since curent peak intensities are increased in case of the modified electrode despite evident kinetic hindrance proved by the electrochemical analysis.

Keywords: voltammetry, glassy carbon electrode, electrocatalysis, kinetics.

INTRODUCTION

Carbon microspheres (CMS) are a novel class of carbon based materials with particular features including minimal surface energies, controllable sizes, unusual morphology, good thermal stability, and specific electronic and chemical structure. These spherical semi-crystalline or crystalline (graphitic) carbon materials are characterized with solid, hollow or core shell morphology. Diameters of the spheres can range from 10 nm to 10 μm while their specific surface areas are usually from 2 m^2/g to 1500 m^2/g. CMS can be prepared involving techniques such as arch discharge [1], laser ablation [2], plasma processes [3], shock compression techniques [4], chemical vapor deposition [5], and catalytic and non-catalytic hydrothermal treatments in autoclave. The later technique is known as efficient and facile while it gives products in good yield.

The design of carbon materials for catalytic applications has seen significant progress through the optimization of pore size distribution, morphology, and structure. In particular, increasing the number of edge sites has been shown to enhance catalytic performance [6]. Additionally, carbon doping with various chemical species has been found to effectively boost catalytic activity [7]. Incorporating heteroatoms into the carbon bond network induces atomic charge density and/or spin density redistribution, resulting in a significant impact on the catalytic performance of carbon materials.

Incorporating nitrogen atoms into the carbon-based acceptor introduces additional electrons into the graphitic lattice, resulting in metallic or semi-conductive features characterized by a narrow energy gap. Theoretical investigations have demonstrated that nitrogen incorporation can narrow the gap between the highest-occupied molecular orbitals and the lowest-unoccupied molecular orbitals. This reduction in energy gap facilitates electron transfer from the carbon material to adsorbed species, thereby enhancing catalytic performance [8].

In this paper, carbon microspheres synthesized by hydrothermal technique were *in situ* doped with nitrogen and then carbonized in protected atmosphere. This material was used in combination with multi-walled carbon nanotubes (MWCNTs) as an electrode-modifying agent in glassy carbon technique. Cyclic voltammetry was employed to test red-ox reaction of potassium ferrocyanide as a benchmark compound.

MATERIALS AND METHODS

Synthesis and characterization of N-doped carbon microspheres

For the synthesis of carbon microspheres, 2 g of phenol and 7 cm^3 of a formaldehyde (37 wt.%) were dissolved in 10 cm^3 of 0.5 M NaOH solution and stirred at 70 °C for 0.5 h. At the same time, 4 g of Pluronic® F127 (PEO_{106}-PPO_{70}-PEO_{106}) was dissolved in 20 cm^3 of deionized water and later added to the first solution. This suspension was stirred for the next 3 h. The material was doped by introducing 1.5 mmol of hydrazine (H_2N_2) into the probe. Then, content was transferred to the stainless steel autoclave and heated at 100 °C for 12 h. Obtained fragile monolith of dark color was thoroughly washed with deionized water, dried for 3 h at 60 °C and carbonized in the tube furnace at 600 °C for 3 h with ramping rate of x°/min. The pristine (not dopped) carbon microspheres were obtained by the same procedure without adding the nitrogen source.

The morphology of the native and nitrogen doped carbon microspheres was investigated using scanning electron microscope (SEM) Tescan Mira3.

Electrode preparation

Electrochemical behavior of synthesized nitrogen doped carbon microspheres supported onto MWCNT as a basic electrode modifying agent was investigated by applying glassy carbon technique. To use it as an electrode material, 3.5 mg of N-CMSs were weighed with the same mass of MWCNT, dispersed in 1 cm^3 of ethanol/water mixture (40 v/v%), and the suspension was homogenized in the ultrasonic bath for 30 min. The surface of the glassy carbon (GC) electrode was cleaned by polishing on fine cloth containing alumina powder and ultrasonically treated in ethanol for 15 min. Then, 10 μL of the prepared suspension was transferred onto the surface of GC electrode (working area was 0.04 cm^2) and dried under nitrogen stream. After the thin carbon layer was dried, it was covered with 7 μL of 0.05 wt.% Nafion in ethanol. The solvent was removed by evaporation, as well.

Reagents

For the use as supporting electrolytes, Britton-Robinson (BR) buffers were prepared by mixing 2.69 cm^3 of H_3PO_4 (ω=85%, ρ=1.71 g/cm^3), 2.47 g of H_3BO_3, and 2.3 cm^3 of glacial CH_3COOH (≥99%, ρ=1.05 g/cm^3). Final concentration of each component was equal to 0.04

mol/dm^3. All the chemical were purchased from Sigma-Aldrich. All chemicals used were of analytical grade and were used as received without any further purification. For all the experiments, water of 18.2 MΩ obtained in laboratory from the demineralizator Smart2Pure (Thermo, USA) was used.

RESULTS AND DISCUSSION

SEM

Figure 1 displays SEM images of native and nitrogen doped microspheres. In both cases, spherical particles with smaller cubic fragments and/or fragments of irregular shape are notable. If observed separately, the microsphere dimensions slightly differ among themselves, which is typical case as often reported in literature. In addition, fuzzed spherical particles in case of nitrogen doped CMS are also common and probably originate from unfinished process of separation during formation of spheres. The fact is that native spheres are in some degree of greater dimensions in contrast to nitrogen doped spheres which can be told by microscope magnification. In the first case, spheres are visually larger in spite of the fact that around 50% lower magnification was applied. It can be concluded that hydrazine addition during the doping step significantly reduces the final sphere diameter, which might have substantial impact on structural and functional properties of CMS.

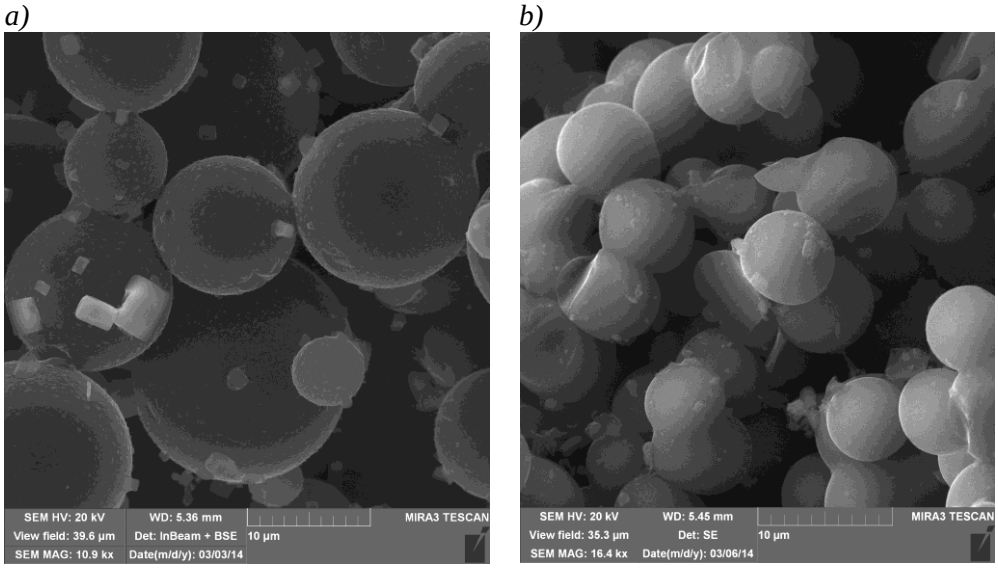

Figure 1 *SEM images of a) native and b) nitrogen doped carbon microspheres*

Electrochemical tests

With mechanistic approach, we used cyclic voltammetry to analyze the reversibility of reactions at the working electrodes. Commercial glassy carbon electrode of 3 mm diameter was applied as a working electrode for electrochemical oxidation of ferrocyanide ions to ferricyanide and the reverse reduction reaction. Three options were tested, including bare GCE, GCE modified with MWCNT, and GCE modified with N-CMS@MWCNT mixture. Voltammograms of these three electrodes recorded for 1 mM potassium ferrocyanide ($[K_4Fe(CN)_6]$) in B-R buffer supporting electrolyte at different scan rates (5–200 mV/s) are

presented in Figure 2a. In all cases, characteristic, nearly symmetrical shape of the cyclic voltammograms for ferrocyanide red-ox reactions is observed.

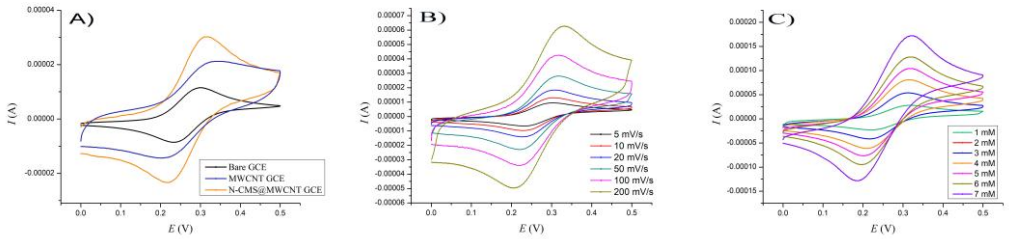

Figure 2 *Cyclic voltammograms of a) three compared electrodes in 1 mM K-ferrocyanide at 50 mV/s; b) N-CMS@MWCNT at scan rates from 5 to 200 mV/s; c) N-CMS@MWCNT with diferent ferrocyanide concentrations*

The values of E_{pa} and I_{pa} were determined from the voltammograms and given in Table 1 together with other kinetic parameters. Formal potentials were calculated to be 0.268 V, 0.272 V and 0.265 V for N-CMS@MWCNT, MWCNT GCE, and bare GCE, respectively, and these values are slightly higher than standard redox potential known from the literature. It is known from theory that in case of electrochemically reversible electrode processes which usually exhibit fast electrode kinetics, cyclic voltammogram results in a peak potential separation of around 60 mV with charge transfer coefficient of approximately 0.5 and a ratio between anodic and cathodic peak currents equal to 1. A preliminary approach used to evaluate the reversibility of the electrochemical process is reflected in the ratio between the anodic (I_{pa}) and cathodic (I_{pc}) peak currents. The peak current ratio (I_{pa}/I_{pc}) was observed to be close to unity (1.038) for bare GCE and for N-CMS@MWCNT modified GCE (1.035) at 50 mV/s which is inherent to reversible electron transfer reaction with chemically stable generated products. Despite the seemingly quasi-reversible redox behaviour, the MWCNT GCE exhibits an I_{pa}/I_{pc} ratio greater than unity (1.132), indicating adsorption of the reduced species.

Lowest scan rate of 5 mV/s applied for examination of N-CMS@MWCNT modified electrode gave ΔE_p value of 0.069 V. This value increased with scan rate and reached 0.121 V at 200 mV/s. This trend is common for most electrodes and normally considered to represent quasireversible behavior for all practical purposes. On the other side, bare GCE exibited behaviour more close to theoretically ideal case with ΔE_p values of 0.062 V with holding to this value over the several applied scan rates. As a contrast, the peak currents of N-CMS@MWCNT modified GCE are higher when compared to bare GCE (Table 1) which contributes to overall voltammetric response. Such diffusion controlled redox processes obey the Randles–Sevcik equation. A plot of the anodic peak current versus the square root of the scan rate ($v^{1/2}$) is shown in Figure 3.

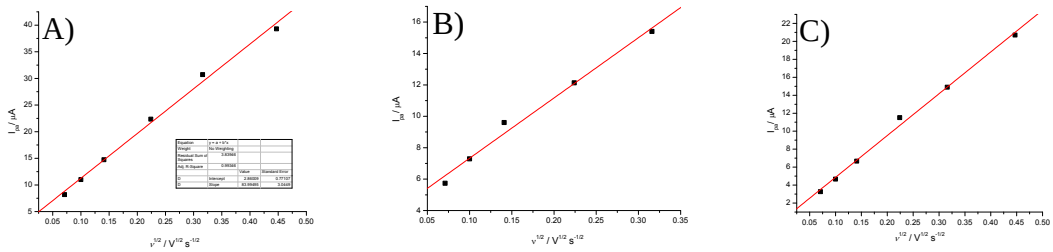

Figure 3 *The linear dependences of I_{pa} vs. square root of the scan rates for a) N-CMS@MWCNT GCE; b) MWCNT GCE and c) bare GCE*

In Figure 3, obtained data were fitted to a straight line and from the linear dependence in the range of applied scan rates, it can be concluded that the electrode reaction at sufficient overpotential is definitely diffusion controlled. Here, the slope of the I_{pa} versus $v^{1/2}$ fit lines is significantly greater for the N-CMS@MWCNT GCE as compared to the MWCNT and bare GCE. For the modified, bare GCE and MWCNT, heterogeneous electron transfer rate coefficient (k^0) values of 0.0065 cm/s, 0.02 cm/s and 0.002 cm/s were obtained, respectively. This is in line with values found in the literature. These values can be dependent on pretreatment, amount of Nafion® solution added and polishing method applied. Also, it should be mentioned that the Nicholson method used in calculating k^0 assumes semiinfinite diffusion to the electrode surface (case for flat disc electrodes and micro-electrodes) which is not the case for a modified electrodes with specific hybrid structures.

Table 1 *Kinetics parameters obtained from cyclic voltammogram and Tafel analysis of 1 mM $[K_4Fe(CN)_6]$ oxidation in B-R buffer (scan rate: 5 mV/s; counter electrode: platinum coil)*

Electrode	E_{on} (mV)	I_0 (μA/cm^2)	E_{eq} (mV)	$n\alpha_a$	Tafel slope (mV/dec)	E_{pa} (V)	I_{pa} (μA)
Modified GCE	205	8.85	161	0.58	99.9	0.301	$8.18\cdot10^{-6}$
Bare GCE	200	2.77	176	0.86	67.8	0.296	$3.27\cdot10^{-6}$
MWCNT	200	4.6	157	0.661	88.5	0.320	$5.74\cdot10^{-6}$

For a deeper electrochemical analysis, the anodic transfer coefficient (α_a) and the number of electrons involved in the rate determining step (n) should be determined. For this, Tafel plot ($log_{\text{current density}}$ vs. potential) was constructed using the data from the rising part of the cyclic voltammograms for the $[K_4Fe(CN)_6]$ oxidation current and scan rate of 5 mV/s. This is the case of steady-state conditions. The Tafel slope for N-CMS@MWCNT GCE is 99.9 mV/dec, which is equal to value for the transfer coefficient α_a for $[K_4Fe(CN)_6]$ oxidation of 0.58. The Tafel value obtained for N-CMS@MWCNT GCE was found to be closer to the theoretical value (118 mV/dec) for one-electron transfer.

The value of α_a is higher than 0.5 which is commonly expected for simple outer-sphere redox reactions. Extrapolation of the Tafel plot to the equilibrium $[K_4Fe(CN)_6]$ redox potential gives an exchange current density value of $8.8\cdot10^{-6}$ A/cm^2 for modified and $2.8\cdot10^{-6}$ A/cm^2 for bare GCE which corresponds to the standard heterogeneous rate constant for

ferrocyanide oxidation of $9.1 \cdot 10^{-5}$ cm/s and $2.9 \cdot 10^{-5}$ cm/s, respectively. These results are different from the results obtained by applying the Nicholson's method. This indicates that kinetics at low scan rates (5 mV/s) is faster at N-CMS@MWCNT GCE due to the fast electron transfer which is very important. Nevertheless, at higher scan rates (50 mV/s) present kinetic hindrance could be ascribed to the possibility that electron transfer is impeded by both contact resistance between catalyst particles, the catalyst and the glassy carbon surface, and by the presence of the Nafion® binder onto N-CMS electrode.

From Figure 2c, it can be seen that with the increase of concentration, I_{pa} and I_{pc} increase with emphasized difference in favour of N-CMS@MWCNT modified electrode. This response for both electrodes shows a direct relationship between peak current and concentration of the electroactive species in solution which confirms the relation in the Randles-Sevcik equation.

CONCLUSION

Nitrogen doped carbon microspheres supported onto MWCNTs and applied as working electrode material in GCE technique showed interesting electrokinetic properties. Evident electrocatalytic effect in case of the modified electrodes is reflected by the higher peak current. However, complex electrode process on modified electrodes, especially in terms of certain kinetic resistances which are related to adsorption phenomena, the existence of Nafion® layer through which diffusion is hindered, as well as a possible weak contact among the particles in the carbon film on the surface of the electrode are responsible for sluggish kinetics of the overall process.

ACKNOWLEDGEMENT

This study has been supported by the Ministry of Science, Technological Development and Innovation of the Republic of Serbia through the contract with the registration number 451-03-47/2023-01/200017.

REFERENCES

[1] Seraphin S., Wang S., Zhou D., *et al.*, Chem. Phys. Lett. 228 (1994) 506–512.

[2] Zhang H., Liang C., Liu J., *et al.*, Carbon 55 (2013) 108–115.

[3] Kang J., Li O. L., Saito N., Carbon 60 (2013) 292–298.

[4] Niwase K., Homae T., Nakamura K.G., *et al.*, Chem. Phys. Lett. 362 (2002) 47–50.

[5] Boudjema A., Mokrani T., Bachari K., *et al.*, Mater. Sci. Semicond. Process. 30 (2015) 456–461.

[6] Pašti I., Gavrilov N., Dobrota A., *et al.*, Electrocatalysis 6 (2015) 498–511.

[7] Ji Y., Du J., Chen A., Transactions of Tianjin University 28 (2022) 292–306.

[8] Chen C., Zhang J., Zhang B., *et al.*, Chem. Comm. 74 (2013).

SUSTAINABLE PECTIN MONOLITH CRYOGELS

Aleksandra Nesic[1], Sladjana Meseldzija[1], Milan Momcilovic[1*]

[1]University of Belgrade, Vinca Institute of Nuclear Sciences – National Institute of the Republic of Serbia, 12–14 Mike Petrovića Street, 11000 Belgrade, SERBIA

[*]*milanmomcilovic@yahoo.com*

Abstract

The subject of this work is synthesis and characterization of pectin-based cryogels obtained by internal crosslinking with calcium ions. The crosslinking reaction was confirmed by FTIR/ATR analysis, while SEM analysis demonstrated that pores of obtained cryogel were in macro range (between 130 and 380 µm). Pectin cryogel had high swelling degree with the value of 800% after 24 h of immersion in distilled water, and high water vapor permeability (E-7 order, g/ m s Pa). In addition, it showed high rate of biodegradation (85%) after exposure of 3 months in the soil. The obtained results suggest that pectin cryogel obtained by internal crosslinking reaction might find applicable potential in food, agriculture and separation technologies, providing an eco-sustainable approach to tackle current ecological and economical stresses.

Keywords: pectin, cryogels, biodegradation.

INTRODUCTION

Development of sustainable materials have become growing need, due to depletion of fossil fuels and negative impact of petroleum-derived materials on environment and human health. Hence, there is a gained interest to identify new raw materials that are from renewable resources and biodegradable, to convert them into multifunctional materials, and to become an eco-replacement for petroleum-derived materials on market.

Pectin is promising natural biopolymer, that can be utilized to obtain multifunctional biodegradable materials. Namely, it can be found in cell walls of most of the plants. It is mostly extracted from citrus and apple fruits but can be derived from peel waste accumulated in juice industry [1,2]. Pectin has ability to gel in the presence of divalent cations. The mechanism is described as “egg box” model, where divalent cations react with carboxylic groups from pectin, taking chain conformations in shape of egg box [3]. Up to date, pectin is commonly used in food industry due to its nontoxicity and gelling ability, as a stabilizer, compatibilizer or gelling additive [4]. Moreover, due to its 3D network formed in the presence of divalent cations, and biodegradability, it has been widely tested as a biobased matrix for drug delivery, in biomedicine, and for sorption processes [5,6]. However, once when hydrogels are dried under ambient/vacuum conditions, the obtained materials are denser and less porous than starting hydrogel, due to pore collapsing because of high capillary pressure. On the other side, freeze-drying procedure is able to maintain open pore structure of the starting hydrogels. The porosity of final material not only depends on route of drying, but also on crosslinking reaction, and crosslinking density of hydrogels. Regarding the pectin, the

most common crosslinker is $CaCl_2$, where hydrogels are obtained by direct dripping of pectin solution into calcium ion aqueous bath [7]. In contrast, water insoluble calcium-salts can be used as an internal crosslinkers, by dispersing them in pectin solution, and allowing uniform distribution before gelation occurs. The release of calcium ions from $CaCO_3$ is stimulated by d-glucono-δ-lactone (GDL), which hydrolyze slowly within the time, lowering the pH of solution, and allowing better internal crosslinking of calcium ions with pectin chains [8].

Hence, the aim of this work is to internally crosslink the pectin chains in the presence of $CaCO_3$ and GDL and freeze-dry to obtain 3D network with preserved porous structure. The obtained material was subjected to several different characterization techniques, in order to evaluate structural, morphological, water-related and biodegradation properties.

MATERIALS AND METHODS

Chemicals

Amidated pectin, with a degree of methylation of 38%, was obtained from Herbstreith & Fox KG, Pektin-Fabriken (Neuenburg, Germany). $CaCO_3$ and GDL were purchased from Sigma Aldrich (St. Louis, MO, USA).

Preparation of pectin cryogel

Calcium carbonate (200 mg) was finely dispersed in 100 mL of water by sonication (Vibracell VC 505, Sonics, Newtown, USA) for 10 min at 500 Hz (50% of amplitude). 1 g of pectin was dissolved in the aqueous suspension. Afterwards, GDL was slowly added in mixture and set down to allow formation of hydrogel. The ratio GLD/Ca^{2+} was 4:1. The resulting mixture was immediately poured into a petri dish (36 mm diameter) and allowed to set in air for 24 h at room temperature. The obtained polysaccharide hydrogel sample was frozen in round bottomed flasks in liquid nitrogen and freeze dried for at least 24 h on an VirTis SP Scientific Sentry 2.0 freeze drier. The drying conditions were as follows: vacuum set to 100 mTorr and a condenser temperature of -80.0 °C.

Characterization

Fourier-transform infrared spectroscopy (FTIR/ATR)

FTIR analysis was performed by a Perkin Elmer Spectrum 100 spectrometer (Waltham, USA) equipped with a diamond crystal Perkin Elmer Universal ATR sampling accessory. Spectra were recorded on pectin and pectin/alginate films as an average of 16 scans in the range 4000–400 cm^{-1}, with a resolution of 4 cm^{-1}.

Scanning electron microscopy (SEM)

The morphology of the obtained cryogel was scanned on FEI Quanta 200 FEG Scanning Electron Microscope (SEM) (Oregon, USA) at accelerating voltage of 10 kV. Prior to the SEM analysis, the cryogels were sputtered with gold (~7 nm).

Water related properties

The swelling degree (SD) of cryogels was determined by gravimetric method. The cryogels were weighed (m_0, g) and placed in 100 mL of distilled water at room temperature (25 ^oC). The cryogels were taken out from water after 24 h; the excess of water from the

surface was removed by filter paper and the weight of the swollen aerogels (m_{t1}, g) was measured. The swelling degree was calculated by the following equation:

$$SD(\%) = \frac{(m_{t1} - m_0)x100}{m_0} \quad (1)$$

The solubility test was determined as the content of dry matter solubilized after 24 h in distilled water. The swollen cryogels were taken out after 24 h and dried until constant weight (mt_2, g) in an oven at 105 °C. The solubility degree (SLD) was calculated according to following equation:

$$SLD(\%) = \frac{(m_0 - m_{t2})x100}{m_0} \quad (2)$$

The water vapour permeability (WVP) trough cryogels was determined gravimetrically by wet cup method according to the ASTM E96 standard. Cryogels were sealed in a 3 mm circular opening of a glass vial-permeation cell containing water (~100% relative humidity inside the cell). The permeation cell was kept in a chamber with controlled relative humidity of 50% at 25 ^{o}C. The change in weight of the permeation cell was followed in period of 24 h. The WVP of the films were calculated using the following equation:

$$WVP = \frac{\Delta G x l}{t x A x \Delta p} \quad (3)$$

where ΔG was the weight change (g), t was the time during which ΔG occurred (h), A was the test area cup (m^2), l (m) was the thickness of the film and Δp was the water pressure difference between both sides of the cryogel (Pa). Measurements were performed in triplicate and average data were used for calculations.

Biodegradation test

The biodegradation test was performed in soil and the weight change of sample was monitored within 3 months. Prior the test, samples were wrapped in nylon mesh to prevent losing of material during experiment. The humidity and temperature of the experiment were maintained constant. The sampling was performed every 2 weeks, and samples were rinsed with distilled water and dried at 50 °C to constant mass. The percentage of biodegradation rate was calculated according to the following equation:

$$Bio\,deg_{rate} = \frac{(m_0 - m\ )x100}{m_0} \quad (4)$$

where $Biodeg_{rate}$ is biodegradation rate, m_o (g) was initial weight of sample and m (g) final weight of sample after exposure to the soil for the period of 3 months.

RESULTS AND DISCUSSION

FTIR/ATR

The FTIR/ATR spectrum of obtained cryogel is presented in Figure 1. Pectin/$CaCO_3$ cryogel shows a broad, intense area of absorption between 3600 and 3000 cm^{-1} related to -OH stretching vibrational modes, due to inter- and intramolecular hydrogen bonding of the galacturonic acid. The presence of moderately intense bands, in the range of 3000–2800 cm^{-1},

is ascribed to CH, CH_2, and CH_3 stretching and bending vibrations. Strong absorption bands occurring at 1745, 1660 and 1600 cm^{-1}, are attributed to the ester carbonyl (-$COCH_3$) groups, amide groups and asymmetrical stretching band of carboxylate ion (COO-), respectively, whereas the COO- symmetric stretching can be detected at 1415 cm^{-1}. In the range of 1360 and 800 cm^{-1}, moderate absorption peaks, commonly referred to as the "finger print" region related to C-O-C and C-C bonds of carbohydrate ring, can be found. From the analysis of spectrum, it is worthy to underline that the intensity of ester groups is lower than that of carboxylated residues; this outcome confirms the pectin low esterification degree, as previously determined by means of titration method.

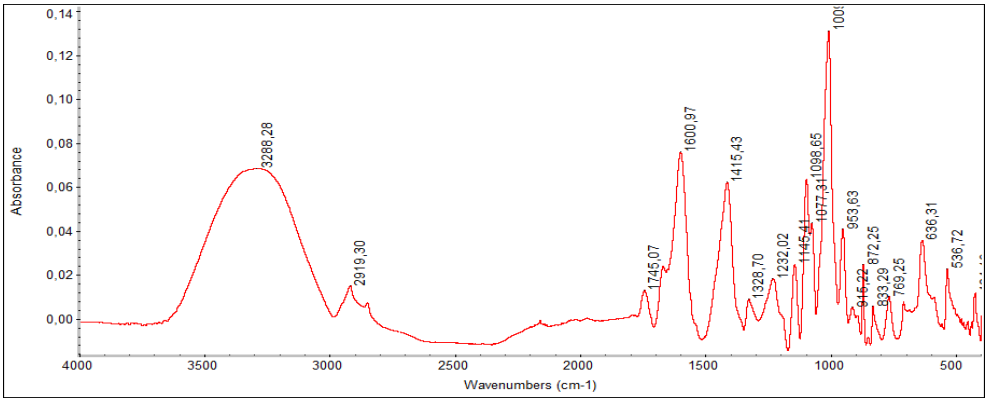

Figure 1 *FTIR/ATR of pectin/$CaCO_3$ cryogel*

SEM

The morphology of pectin/$CaCO_3$ cryogels is displayed in Figure 2. SEM analysis reveals the macroporous system with large number of disconnected voids. The voids diameter ranges between 130 and 380 µm. This result is expected, since this type of structure is common for samples that are freeze-dried for prolonged time, because the longer time of drying promotes growth of crystals. A similar morphology is reported in literature for other pectin cryogels, as well as for starch and alginate cryogels [2,9–11].

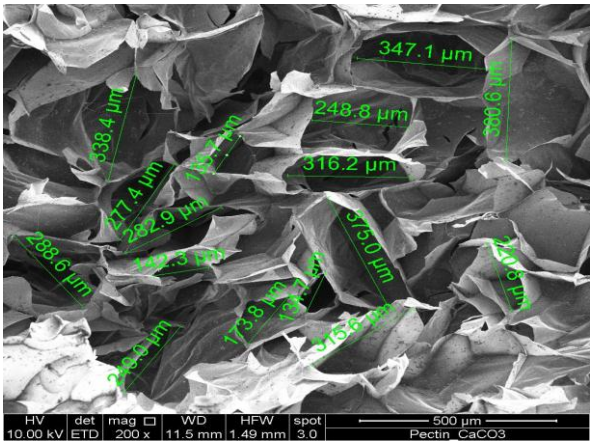

Figure 2 *SEM micrograph of pectin/$CaCO_3$ cryogel*

Water related properties and biodegradation

In order to evaluate the stability of obtained cryogel, solubility, swelling and permeability test in aqueous solutions was performed and results are presented in Table 1. The internal gelation of pectin shows to be efficient, since the solubility of final cryogel is only 5%. On the other side, the obtained cryogel is characterized by high uptake of water, and high water vapor permeability, probably due to voids of large diameters in their structure. Finally, the obtained material demonstrates high level of biodegradation in soil, reaching a value of 85% after 3 months of exposure. There are no published data related to biodegradation rate of pectin cryogels for long exposure time. Chen *et al*. [12] reported 60% of pectin/clay cryogel biodegradation after 1 month of exposure in compost media. On the other side, a biodegradation rate of 63% in a period of 30 days was achieved by the respiratory method for externally crosslinked cryogels [2].

Table 1 *Water related properties*

SD, %	SLD, %	WVP, g/ m s Pa	Biodegradation rate, %
800	5	$1.5 \cdot E^{-7}$	85

CONCLUSION

In this work the pectin was internally crosslinked by calcium ions and additionally freeze-dried in order to obtain porous 3D materials. The FTIR/ATR analysis confirmed the crosslinking reaction between pectin chains and calcium ions. SEM analysis showed macroporous system with uneven size distribution of voids in the range of 130 and 380 μm. The obtained cryogels demonstrated high ability to uptake large amount of water (800%), low solubility in water (5%), high water vapor permeation ($1.5 \cdot E^{-7}$ g/ m s Pa) and high biodegradation rate (85%), implying that these materials might potentially be used in sorption processes (wastewater treatments, or as insertions in food packages for moisture/gas uptake), or for specific release of nutraceuticals and fertilizers in food/agriculture sectors, providing product sustainability.

ACKNOWLEDGEMENT

This work was supported by the Ministry of Science, Technological Development and Innovation of the Republic of Serbia (Contract number 451-03-47/2023-01/ 200017). This work has been realized in the frame of AERoGELS COST Action CA18125–Advanced Engineering and Research of aeroGels for Environment and Life Sciences.

REFERENCES

[1] Meseldzija S., Petrovic J., Onjia A., *et al*., J. Ind. Eng. Chem. 75 (2019) 246–252.

[2] Nesic A., Meseldzija S., Onjia A., *et al*., Polymers (Basel). 14 (2022) 5252.

[3] Gawkowska D., Cybulska J., Zdunek A., Polymers (Basel). 10 (2018) 762.

[4] Nesic A., Trifunovic S., Grujic A., *et al*., Carbohydr. Res. 346 (2011) 2463–2468.

[5] Kedir W., Deresa E., Diriba T., Heliyon. 8 (2022) e10654.

[6] Wang R., Liang R., Dai T., *et al*., Trends Food Sci. Technol. 91 (2019) 319–329.

[7] Nešić A., Onjia A., Davidović S., *et al*., Carbohydr. Polym. 157 (2017) 981–990.

[8] Neves S., Gomes D., Sousa A., *et al*., J. Mater. Chem. B. 3 (2015) 2096–2108.

[9] Groult S., Buwalda S., Budtova T., Eur. Polym. J. 149 (2021) 110386.

[10] Barros A., Quraishi S., Martins M., *et al*., Chemie-Ingenieur-Technik. 88 (2016) 1770–1778.

[11] Ago M., Ferrer A., Rojas O., ACS Sustain. Chem. Eng. 4 (2016) 5546–5552.

[12] Chen H., Chiou B., Wang Y., *et al*., ACS Appl. Mater. Interfaces. 5 (2013) 1715–1721.

INVESTIGATION OF SILICA-LIGNIN INTERACTION. APPLICATION OF AFM AND FLUORESCENCE TECHNIQUES

Daniela Djikanović[1], Olivera Prodanović[1*], Jelena Dragišić Maksimović[1], Jelena Jovanović[1], Aleksandar Kalauzi[1], Dragica Spasojević[1], Ksenija Radotić[1]

[1]University of Belgrade, Institute for Multidisciplinary Research, Kneza Višeslava 1, 11000 Belgrade, SERBIA

[*]*oliverap@imsi.rs*

Abstract

In this study, we investigated, in an in vitro system, the interaction of SiO_2 (as a complex with NH_4OH) with the peroxidase-catalyzed polymerization of lignin monomer into lignin model compound DHP, imitating conditions of the last step of lignin formation in the cell walls. The structure of obtained polymer was monitored using fluorescent spectroscopy and AFM 30 minutes after the start of synthesis. We studied effect of two different Si concentrations, 0.6 mM and 6 mM. Analysis of the DHP fluorescent spectra, and the application of mathematical decomposition clearly shows that structure of lignin model compound depends on Si concentration in the reaction mixture. The amount of Si affects the distribution of electrons in the DHP polymer. When silicon is present at a concentration of 6 mM, the position of the longest-wavelength APD band shifts towards shorter wavelengths compared to the position of the APD band for 0.6 mM Si. This indicates that during polymer synthesis, higher concentration of silicon may inhibit the formation of pi-electronic structures, which are responsible for electron delocalization. AFM images also show differences in the size and regularity of DHP globules.

Keywords: lignin, Silica, fluorescence spectroscopy, deconolution, AFM.

INTRODUCTION

Silicon (Si) holds a significant position in the mineral world as the second most abundant element in the Earth's crust [1]. Silica (SiO_2) is a naturally occurring mineral that can be taken up by plants and incorporated into their tissues, including the cell wall (CWs) [2–5]. Silica exists as silicic acid ($Si(OH)_4$) in the soil (ranging from 0.1–0.6 mM), which can be absorbed by the roots of plants and transported and deposited in the CWs as amorphous silica [6]. Such silica has a non-crystalline form. Plants have developed mechanisms for Si uptake, translocation, and deposition within their tissues. Silica in plant CWs can provide structural support, improve resistance to biotic and abiotic stress, and contributes to plant growth and development. Depending on the plant species, soil properties, Si source and Si amount, Si content in planta can vary from 0.1% (near the detection limit) to 10%, on a dry weight basis [7].

Lignin is a major component of the secondary CWs of many plant species and plays an important role especially in the responses to various types of biotic and abiotic stress and it provides rigidity and strength to the CWs [8–11]. It is a natural phenolic polymer with high molecular weight, complex structure and composition.

Si is predominantly accumulated in CWs, its localization and content being influenced by the chemistry and structure of lignin [12–14]. In this study, we aimed to explore the interaction between Si and the lignin formation process in CWs. Using an *in vitro* system, we examined the interaction between SiO_2 and the peroxidase-catalyzed polymerization of a lignin monomer to create a lignin model compound, thus simulating the conditions of the final step in lignin formation in CWs. DHP is a lignin model compound that allows us to investigate the behavior of lignin, changes in its structure, and its interaction with different molecules.

Fluorescence spectroscopy is a valuable technique for tracking structural changes in complex molecules like DHP throught its autofluorescence. It enables monitoring and analyzing variations in molecular structure with high precision. AFM microscopy complements spectroscopic analysis by providing visual confirmation of structural features. It allows us to obtain detailed imaging and visualization of the analyzed structures, further validating the findings obtained through fluorescence spectroscopy.

Some studies have suggested that silica and lignin may interact in the cell wall, but the exact nature of this interaction is not well understood [15]. The interaction between silicon and lignin holds potential significance for the development of silicon-lignin composites, which could have intriguing applications as hydrogels for drug release or sensors in the field of biomedicine.

MATERIALS AND METHODS

DHP synthesis in presence of Si

The lignin model compound, dehydrogenative polymer (DHP), was synthesized according to the procedure of Radotić *et al*. [16]. DHP was synthesized from coniferyl alcohol, using horseradish peroxidase as an enzymatic catalyst. The reaction mixture contained $5 \cdot 10^{-3}$ M coniferyl alcohol, $5x10^{-3}$ M H_2O_2, and $2.5x10^{-8}$ M horseradish peroxidase (all from Fluka Chemical Corp., New York) in 50 mM phosphate buffer pH 7, in the absence or presence of SiO_2-NH_4OH (in further text SiO_2) in the concentrations 0.1 mM, 0.6 mM and 6 mM. All reaction components were added simultaneously to the mixture. After mixing, the solution was shaken constantly for 24 h. Polymerization occurs in the solution phase, at a temperature of 25 °C. During the reaction, aliquots of the reaction mixture were taken 1 h after the beginning of synthesis and liophilised. After 24 h, the precipitate was washed twice in 50 mM phosphate buffer, and twice in deionized water, and finally dried in a desiccator.

Fluorescence spectroscopy

The fluorescence spectra were collected using an FL3-221P TCSPC (HORIBA Jobin Yvon, France) spectrofluorometer. For each sample, we collected 12 spectra at different excitation wavelengths with a 5-nm step, to record the emission of all fluorophores contained in the polymer. The excitation range was from 360 nm to 415 nm, and the emission range was 380 nm to 600 nm. The obtained spectral series for each sample were analyzed by deconvoluting the original spectra into an optimal number of log-normal components corresponding to different fluorophores in lignin. Non-linear fitting of all fluorescence spectra was performed using Nelder-Mead algorithm implemented in Matlab, as described by Kalauzi

et al. [17]. Thus, the histograms of component maxima were obtained, and the corresponding approximate probability distribution (APD) was calculated by weighted averaging of histogram values for a set of histograms of varying abscissa intervals [17].

Atomic Force Microscopy

The surface topography of samples was characterized by Atomic Force Microscope (NT-MDT Ntegra SPM, Russia) in Semicontact Error Mode. The scanning frequency during the measurement was maintained at 0.5 Hz, while the step size in the recorded images was 7×7 μm, respectively. The cantilever oscillation amplitude (Set Point) during the measurements was 10. The recorded images in the Height mode correspond to the surface topography, while the images in the Mag (Magnitude) mode are related to the error signal which gives higher contrast for sharp objects in the scanned area.

RESULTS AND DISCUSSION

Our investigation focused on the interaction between (Si) and a lignin model compound at the midpoint of synthesis, specifically 30 minutes after start of the reaction. We examined the changes in autofluorescence in samples containing two different concentrations of Si (0.6 mM and 6 mM) (Figure 1).

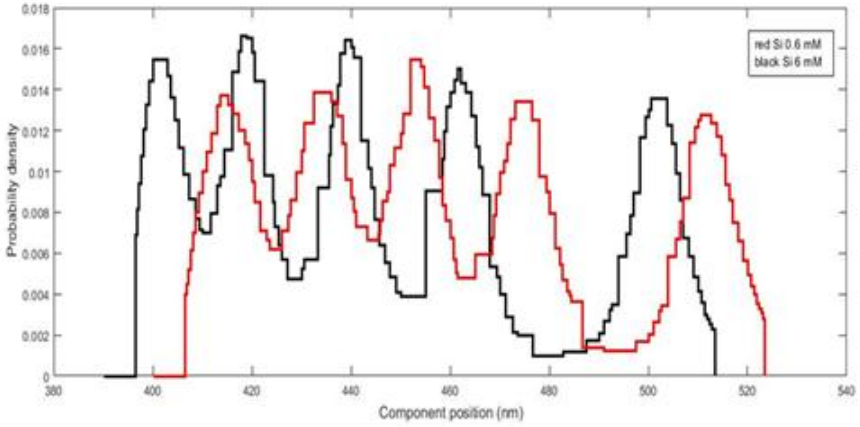

Figure 1 *APD for DHP synthesizes in presence of 0.6 mM (red), and 6 mM (black)* SiO_2

By employing a fluorescent spectroscopy technique and varying the excitation wavelength by 5 nanometers (ranging from 360 nm to 415 nm), we recorded 12 spectra for each sample. Utilizing the Nelder-Mead algorithm implemented in Matlab, we analyzed all spectra and determined the optimal number of components for spectral deconvolution, based on the minimum fitting error. Consequently, a five-component analysis was applied to all the samples.

The final results obtained from the analysis of the emission spectra using the APD technique revealed that higher concentration of silicon exert an inhibitory effect, hindering the formation of double bonds and conjugation in the lignin molecule during the synthesis process. This effect is manifested in the final polymer structure. Notably, the APD results demonstrated a blue-shift in the emission maximum of the green spectral component

(500–520 nm) for the sample with a higher Si concentration (6 mM). Previous research has indicated that lignin fragments containing conjugated -C=C- and -C-C- bonds emit in the green region of the spectrum, and the degree of red shift in their emission maximum is proportional to the length of these conjugated fragments.

Additionally, the AFM images (Figure 2) provided valuable insights into the influence of silicon concentration on the appearance and formation of the lignin model compounds. The microscopic images clearly depicted a more pronounced regularity in the structure and well-defined shape of DHP globules at a silicon concentration of 0.6 mM.

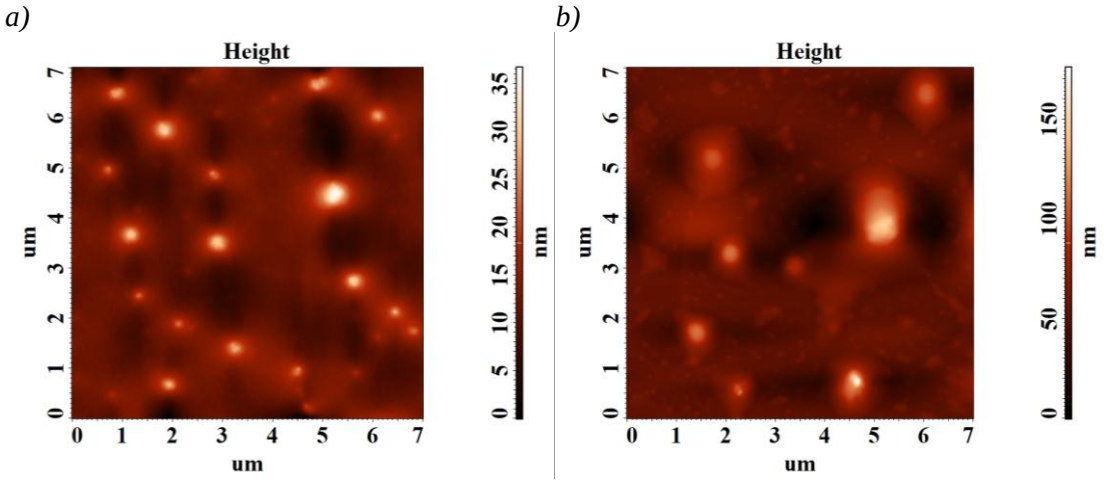

Figure 2 *AFM micrography of DHP synthesized in presence of SiO_2 a) 0.6 mM; b) 6 mM*

CONCLUSION

Our findings highlight the significant role of silicon in shaping the structure of the lignin model compounds during polymer formation. Fluorescence spectroscopy and AFM technique clearly show that structure and arrangement of lignin model compound depend on concentration of Si in the reaction mixture. During polymer synthesis, 6 mM silicon may inhibit the formation of pi-electronic structures, which are responsible for electron delocalization. The obtained results provide an encouraging basis for further exploration of the interactions between silicon and lignin, as well as the effects of silicon on the structure of cell walls (CWs). This opens up opportunities to deepen our current understanding of how silicon influences the overall CW structure.

ACKNOWLEDGEMENT

The authors are grateful to the Ministry of Science, Technological Development and Innovation of the Republic of Serbia for financial support according to the contract with the registration number (Grant No. 451-03-47/2023-01/200053).

REFERENCES

[1] Sommer M., Kaczorek D., Kuzyakov Y., *et al*., J. Plant Nutr. Soil Sci. 169 (2006) 310–329.

[2] Currie H. A., Perry C. C., Ann Bot. 100 (2007) 1383–9.

[3] Ma, J. F., Yamaji, N., Trends Plant Sci. 11 (2006) 392–397.

[4] Ma J. F., Soil Sci. Plant Nutr. 50 (2004) 11–18.

[5] Epstein E., Ann. Appl. Biol. 155 (2009) 155–160.

[6] He C., Wang L., Liu J., *et al*., New Phytol. 200 (2013) 700–709.

[7] Epstein E., Proc. Natl. Acad. Sci. U. S. A. 91 (1994) 11–17.

[8] Boerjan W., Ralph J., Baucher M., Annu. Rev. Plant Biol. 54 (2003) 519–546.

[9] Sarkanen K. V., Ludwig C. H., Lignins: Occurrence, Formation, Structure and Reactions. John Wiley and Sons, New York, (1971), ISBN: 0471754226.

[10] Carpita N. C., Gibeaut D. M., Plant J. 3 (1993) 1–30.

[11] Vanholme R., Demedts B., Morreel K., *et al*., Plant Physiol. 153 (2010) 895–905.

[12] He C., Ma J., Wang L., New Phytol. 206 (2015) 1051–1062.

[13] Sheng H., Chen S., Plant Physiol Biochem. 155 (2020) 13–19.

[14] Soukup M., Rodriguez Zancajo M. V., Kneipp J., *et al*., J. Exp. Bot. 71 (2019) 6807–6817.

[15] Głazowska S., Baldwin L., Mravec J., *et al*., Biotechnol. Biofuels 11 (2018) 171.

[16] Radotić K., Simić-Krstić J., Jeremić M., *et al*., Biophys. J. 66 (1994) 1763–1767.

[17] Kalauzi A., Mutavdzić D, Djikanović D., *et al*., J. Fluoresc. 17 (2007) 319–329.

COMPOSITION OF THE FISH COMMUNITY OF THE RIBNICA RIVER WITH RESPECT TO THE CONSERVATION STATUS

Vesna Djikanović[1*], Jelena Čanak Atlagić[1], Katarina Zorić[1], Stefan Andjus[1], Marija Ilić[1], Vera Nikolić[2], Katarina Jovičić[1]

[1]University of Belgrade, Institute for biological research "Siniša Stanković"- National Institute of the Republic of Serbia, Bulevar despota Stefana 142, 11060 Belgrade, SERBIA

[2]University of Belgrade, Faculty of Biology,Studentski trg 16, 11000 Belgrade, SERBIA

[*]*djiki@ibiss.bg.ac.rs*

Abstract

The aim of the present study was to determine the current status of the fish community structure and composition in the Ribnica River. The Ribnica River, a tributary of the Kolubara River, is classified as a Type 3 watercourse according to the current national regulations. A total of 347 fish specimens were collected and analysed, and seven fish species were identified. Over 60% of the fish community consists of the species Barbus balcanicus and Alburnoides bipunctatus, and the community has high diversity and Evenness. The conservation status of the present fish species was also reviewed, and three identified fish species are protected by national and international regulations. The occurrence of Sabanejewia balcanica is very interesting. This fish species is strictly protected by national legislation as well as by the Bern Convention (Annex III) and the Habitats Directive (Annex II). With the presented study results we would like to point out the importance and conservation of these types of watercourses. As a result of anthropogenic pressures, potential impacts in the form of habitat alteration and degradation are expected, which may lead to threats to local fish populations.

Keywords: fish species, community structure, hill-mountain river, threat status.

INTRODUCTION

Most activities related to the use of water disrupt, degrade and even destroy the functioning of aquatic ecosystems. There are a whole range of factors that affect the biodiversity of fish habitat, the state of fish stocks and their fisheries use in inland waters. According to EIFAC (European Inland Fisheries Advisory Commission), there are three main reasons for the continuous decline of fish stocks in European inland waters and thus for the persistent threat to ichthyofauna biodiversity: 1. insufficient knowledge of the relationships between fish species and their habitats; 2. fishing exploitation of fish stocks in inland waters is not adequately assessed in relation to other forms of water resource use; and; 3. commercial and recreational fishing has traditionally been conducted separately from other water resource users.

For the fish resources of Serbian inland waters, there are no estimates of their size, as well as no good estimates of the impact of current fishing pressure on the biodiversity of ichthyofauna, and it is practically impossible to properly assess the actual status and potential of this resource.

According to the WFD [1], fish represent one of the most important elements of the biological quality of aquatic ecosystems, with species composition, abundance and age structure representing the minimum set of data that should be used in the assessment of ecological status. In addition to various anthropogenic impacts, fragmentation of river courses also has a negative impact on fish, especially migratory species.

According to the Regulation on the Designation of Surface and Underground Waters [2], the Ribnica River is designated as TYPE 3 (MSL up to 500 m, medium and small streams with dominance of hard bed substrate). The riverbed is formed of limestone and granite substrate. The ecological status of this watercourse is assessed as good (II) according to some previous ecological studies [3].

The objective of this study was to determine the current fish community composition of the Ribnica River and to assess whether this habitat harbours endemic or protected fish species that would require future conservation measures.

MATERIALS AND METHODS

Sampling area

The Ribnica is a right tributary of the Kolubara River, which belongs to the Sava river basin. It is formed in Brežđe (Kozomor) by the Paklešnica and Manastirica streams. The Ribnica catchment area is 148.75 km^2 and the river course is 28.38 km long [4].

Methodology

The fish fauna was sampled with standard electrofishing equipment at two locations, site one (Paštrić near the Ribnica monastery) in autumn, and sites one and two (Brežđe village) in spring of 2022/23 (Table 1). A selected section was studied to gain insight into the current fish fauna. The sampled fish were identified on site based on morphological characteristics using identification keys [5,6].

Table 1 *Sampling locality data*

Date of sampling	Sampling site	Coordinates	Altitude (msl)	Watercourse width	Watercourse depth	Researched stretch
01.11.2022.	Paštrić village	N 44.205687 E 20.092431	255m	4-8m	30-90cm	90m
19.04.2023.	Brežđe village	N 44.183509 E 20.075534	255m	3-4m	30-50cm	100m

RESULTS AND DISCUSSION

The middle course of the Kolubara River and some of its tributaries are a typical area dominated by common barbel (*Barbus barbus* L.1758) and grayling species (*Thymallus thymallus* L.1758). The water body of the Ribnica River is characterised as a middle rithron, dominated by Danube barbel and common chub (*Barbus balcanicus* and *Squalius cephalus* L. 1758) [7]. This watercourse is characterised by a high water conductivity and a high dissolved oxygen content, which is typical for many limestone streams.

Table 2 *Recorded fish species, measured body lengths and weights of sampled fish individuals*

Species	English name	Number of individuals	Length (cm)	Weight (g)
CYPRINIDAE				
Alburnoides bipunctatus	Riffle minnow	114	3-11	0,5-17
Barbus balcanicus	Danube barbel	104	4-20	0,5-69
Squalius cephalus	Common chub	17	6-23	3-198
Gobio gobio	Gudgeon	44	4,3-10,2	0,5-12
COBITIDAE				
Sabanejewia balcanica	Balkan spined loach	52	5-8,5	1-4
BALITORIDAE				
Barbatula barbatula	Stone loach	2	5-8,8	1-5
LEUCISCIDAE				
Phoxinus phoxinus	Eurasian minnow	14	4,5-6,3	0,5-3

A total of 347 fish individuals of seven fish species were measured in terms of standard body length and weight (Table 2). The composition and structure of the sampled fish community in the researched area of the Ribnica is shown in Figure 1. More than 60% of the fish community were Danube barbel (*Barbus balcanicus*) and riffle minnow (*Alburnoides bipunctatus*). The species *Sabanejewia balcanica* (Balkan spined loach) and *Gobio gobio* (gudgeon) were represented with a lower percentage. The species *Phoxinus phoxinus* occurred only in the upper part of the watercourse at site two.

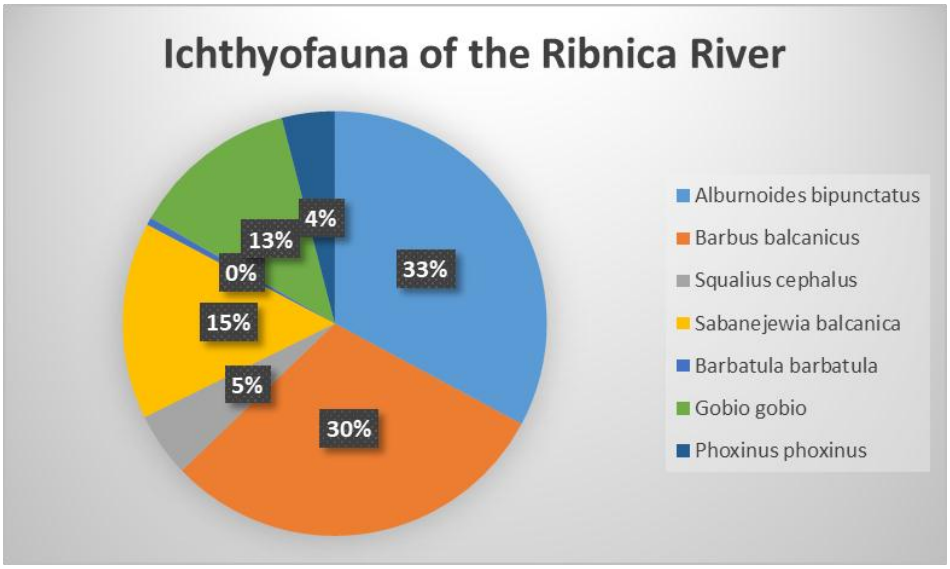

Figure 1 *Illustration of fish community structure at upper section of the Ribnica River based on three electrofishing samples*

Standard biodiversity parameters, diversity indices and evenness were calculated and presented in Table 3. By sampling in the fall and spring, which have different water regimes, we can say that the pooled samples can give a realistic insight into the Ribnica fish community. The river has high fluctuations in water flow with the change of seasons and a

discontinuous course with several smaller concrete weirs. The fish community showed to have high diversity according to the results of Simpsons (0,88) and Shannon-Wiener indices (1,55), and Evenness can also be considered very high (0,8).

Table 3 *Results of applied biological indices*

N (number of species)	D (Simpson)	H (Shannon-Wiener)	Evenness (Pielou)
7	0,88	1,55	0,80

The fish community can be considered typical for this type of water body. The same species and a similar community structure for the Ribnica River were found during the commercial fisheries survey in the Kolubara River catchment [7]. No non-indigenous fish species were found in the surveyed section. Also, no salmonid or migratory fish species were found at the surveyed site during this preliminary survey.

Three of the seven identified species present in researched area are protected by national legislation [8]. *Sabanejewia balcanica* is strictly protected, while *Alburnoides bipunctatus* and *Barbus balcanicus* are protected. In addition, the Balkan spined loach is protected by international legislation, the Bern Convention (III) [9] and the Habitats Directive (II) [10], while the Danube barbel is protected by the Habitats Directive (V). According to the IUCN Red List [11], all identified fish species have conservation status LC. Although classified by the IUCN as LC, the Balkan spined loach is usually present in small numbers and is sensitive to changes in its habitat. It stays in the upper parts of river and may be absent in the lower sections if the habitat is altered, e.g. by slower water flow, more silt and mud (sedimentation) in the riverbed and pollution from industry and agriculture [12]. According to Marešova *et al*. [13], *Sabanejewia balcanica* has been detected in three rivers in Serbia, the Kolubara River, the Kutinska River and the Crni Timok, and may also be present in their tributaries. There are no detailed data on the actual occurrence of this strictly protected species in Serbian waters.

CONCLUSION

The anthropogenic pressure via direct and indirect pollution and reconstruction of the river flow could have potential negative impacts. Changes in water level fluctuations, a decrease in oxygen concentration, and a change in the ecological characteristics of the river ecosystem, as well as fragmentation of the water continuum, may threaten the existence of local populations of fish species, especially protected species. Further research is needed to provide a basis for future conservation action for protected species found in this preliminary survey.

ACKNOWLEDGEMENT

This research was funded by the Ministry of Science, Technological Development and Innovation of the Republic of Serbia, Contract No. 451-03-47/2023-01/200007 and 451-03-47/2023-01/200178.

REFERENCES

[1] WFD (2000). Water framework directive. J. Ref. OJL, 327, 1–73.

[2] Official Gazette of the Republic of Serbia (2010). Regulation on establishment of surface and groundwater bodies. "Official Gazette RS" No. 30/2010 (*in Serbian*).

[3] Official Gazette of the Republic of Serbia (2011). Regulation on the parameters of ecological and chemical status of surface waters and parameters of chemical status and quantitative status of ground waters. "Official Gazette RS" No. 74/2011 (*in Serbian*).

[4] Jović A., Paunović N., Stojanović B., *et al*., Arch. Biol. Sci. 58 (2) (2006) 115–119.

[5] Simonović P., Ribe Srbije. NNK International, Bioloski fakultet & Zavod za zastitu prirode Srbije, Beograd (2001). [Fish of Serbia. NNK International, Faculty of Biology & Agency for Nature Protection of Serbia].

[6] Kottelat M., Freyhof J., Handbook of European freshwater fishes. Publications Kottelat, Cornol and Freyhof, Berlin (2007), p.646.

[7] Simić V., Simić S., Petrović A., *et al.*, Management programm of fishing area „Kolubara" (2017-2026), University of Kragujevac, Faculty of Sciences, (2018).

[8] Official Gazette of the Republic of Serbia (2016) Regulations on declaring and protection of strictly protected and protected wild species of plants, animals and fungi. Appendix 2. Protected wild species. "Official Gazette RS" No. 5/2010, 47/2011, 32/2016 and 98/2016 (*in Serbian*).

[9] Bern Convention (Appendix/Annexe III), Convention on the Conservation of European Wildlife and Natural Habitats, ETS/STE 104, (1979).

[10] NATURA 2000 - EUROPEAN UNION Fish SPECIES (Annex II; IV & V) in Serbia.

[11] IUCN, 2020. The IUCN Red List of Threatened Species. Version 2020-1.

[12] Delic A., Bucar M., Kucinic M., *et al*., Folia biologica 51 (2003) 39–42.

[13] Marešová E., Delić A., Kostov V., *et al*., Folia Zoologica 60 (4) (2011) 335–342.

INDICATIVE ECOLOGICAL STATUS ASSESSMENT OF RIBNICA RIVER (KOLUBARA BASIN) BASED ON AQUATIC MACROINVERTEBRATES

Nikola Marinković[1*], Bojana Tubić[1], Ana Atanacković[1], Nataša Popović[1], Jelena Tomović[1], Maja Raković[1], Momir Paunović[1]

[1]University of Belgrade, Institute for Biological Research "Siniša Stanković", National Institute of the Republic of Serbia, Department of Hydroecology and Water Protection, Bulevar despota Stefana 142, 11060 Belgrade, SERBIA

[*]*nikola.marinkovic@ibiss.bg.ac.rs*

Abstract

This paper aims to present indicative ecological status of the Ribnica River, a tributary to the Kolubara River, based on aquatic macroinvertebrate community. On 7 selected localities a total of 123 taxa were identified. These taxa belong to 14 taxonomic groups. Macroinvertebrate community was dominated by insect groups, mainly Diptera, Trtichoptera and Ephemeroptera, while other groups are less diverse and have lower abundance. Overall water quality was moderate or better with exception of the site located between Paštrić village and Mionica, which showed deterioration in all biological quality indices. This can be explained by the presence of numerous farms in the vicinity which have a negative impact on taxa richness and composition of macroinvertebrate community.

Keywords: benthos, macroinvertebrates, ecological status, Ribnica River.

INTRODUCTION

The Ribnica River is a right tributary of the Kolubara River, formed in Brežje (Kozomor) by the Paklešnica and the Manastirica brooks. The upper part of the river valley is gorge-shaped, while the lower part flows through the Paštrić village and the Mionica before confluence to the Kolubara River. The River Ribnica is categorized as Type 3 watercourse in national legislation [1]. These watercourses are located at altitudes up to 500 masl with domination of hard substratum composed of bedrock, large stones and cobbles. Aquatic habitats of the river Ribnica reflect typical conditions of Type 3 watercourse. The bottom is mainly composed of stones and cobbles with deposits of sand and detritus in sections with slower water flow. Water depth varies from 30 cm to 1 m and water width from 3 m to 10 m. Water levels and flow vary significantly throughout the year. The aim of this study is to provide an assessment of ecological quality of river Ribnica and to provide biodiversity baseline of aquatic macroinvertebrate community.

MATERIALS AND METHODS

For the integrated quality assessment of rivers based on the requirements of Water Framework Directive, benthic macroinvertebrates are the most commonly used component of aquatic communities [2]. For this study samples were collected on 7 selected sites on the entire course of the river Ribnica. Field work was conducted in autumn of 2022. All

investigated sites were located on the main course of the Ribnica River, from its source (Ribnica 7 site), confluence of the Paklešnica and Manastirica brooks, to the most downstream (Ribnica 1 site) before its confluence to the Kolubara River. Locations of sampling sites are presented in Figure 1. Samples were collected using Kick and Sweep method performed following the EN 27828:1994 standardized protocol using a hand net (0.25×0.25 m, mesh size of 500 μm) [3]. For calculation of biological indices Asterics 4.04 software was utilized [4].

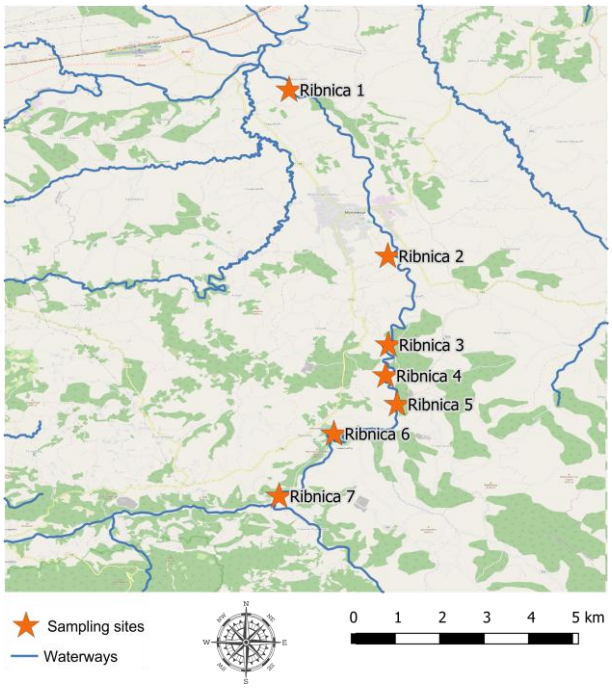

Figure 1 *Sampling sites on the Ribnica river*

RESULTS AND DISCUSSION

A total of 123 taxa from 14 taxa groups were identified during the investigation of the river Ribnica. Taxa richness of macroinvertebrate groups is presented in Figure 2 while the structural composition is presented in the Figure 3. The overall diversity of aquatic macroinvertebrate community of the river Ribnica was high. The community was dominated by aquatic insects, as is expected for this kind of habitats. The most diverse group was Diptera with 42 species which was dominated by the family Chironomidae (non-biting midges) and its 27 species recorded. Beside these groups, large number of species of other insect groups were recorded: Ephemeroptera (18 species), Trichoptera (17) and Coleoptera (8), while Odonata and Plecoptera were represented with 4 and 3 species, respectively. Relatively high number of species (13) was recorded within the Oligochaeta, a group of aquatic worms. Within the molluscs gastropods 8 taxa were recorded, while representatives of Bivalvia were not recorded. Other taxa groups were represented with only one or two species. The highest number of taxa was recorded for the Ribnica 3 site (44) and the lowest for the Ribnica 2 (16). Comparison of taxa richness of investigated sites of the river Ribnica is presented in Figure 4. The diversity of macroinvertebrate community of the river Ribnica reflected through

Shannon-Wiener index was high for all investigated sites. The highest (H') index calculated for the Ribnica 4 and the lowest for the Ribnica 2 site.

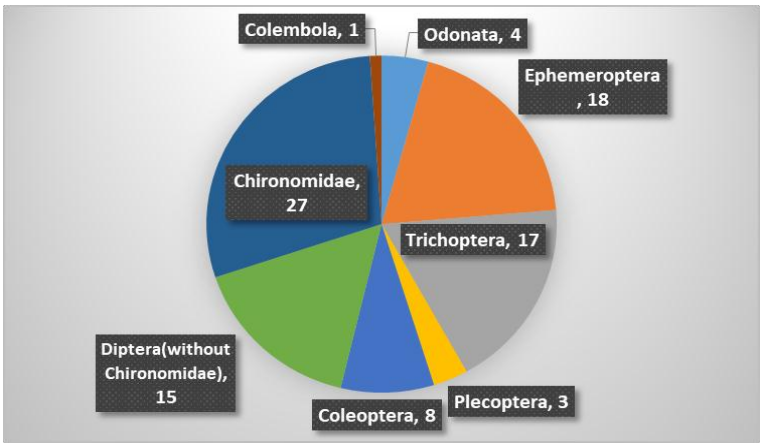

Figure 2 *Taxa richness of different insect groups in the macroinvertebrate community of the river Ribnica*

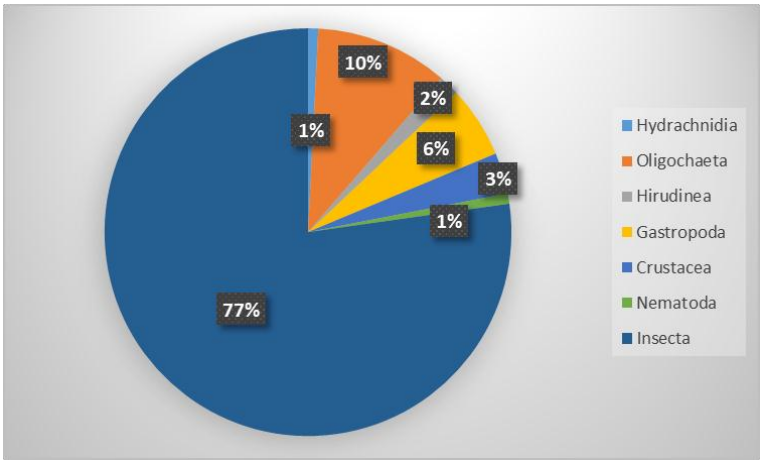

Figure 3 *Structural composition of the aquatic macroinvertebrate community of the river Ribnica based on taxa groups*

All investigated sites belong to river Type 3 in national legislative [1,5]. Following metrics were used for the ecological status assessment: Number of taxa, Saprobic index (Zelnika & Marvan), BMWP score, Average Score Per Taxon (ASPT), Diversity index (Shannon-Wiener), Number of Ephemeroptera (mayflies), Plecoptera (stoneflies) and Trichoptera (cadissflies) species (EPT), number of recorded families, and percentage of family Tubificidae in the community. Indicative ecological status assessment was performed according to procedure proposed by Paunović *et al*. [6,7] and results are presented in the Table 1.

Ecological status based on the number of recorded taxa and high values of the diversity index, was regarded as high (water quality class I-II). The same assessment was made based on ASPT index. Very high number of species from different families indicates that the ecological status was excellent for all investigated sites.

Table 1 *Ecological status of Ribnica River based on macroinvertebrate community*

	Ribnica 1	**Ribnica 2**	**Ribnica 3**	**Ribnica 4**	**Ribnica 5**	**Ribnica 6**	**Ribnica 7**
Number of Taxa	I	II	I	I	I	I	II
Saprobic Index (Zelinka & Marvan)	II	III	II	II	II	II	II
BMWP Score	III	III	II	I	I	II	II
Average score per Taxon	II	II	II	II	II	II	I
Diversity (Shannon-Wiener-Index)	I	II	I	I	I	II	II
EPT	II	IV	III	I	II	III	III
Number of Families	I	I	I	I	I	I	I
Tubificidae %	+	+	+	+	+	+	+
Ecological status	III	IV	III	II	II	III	III

I – excellent, II – good, III – moderate, IV – poor, V – bad; + good status reached.

Good or better ecological status for all sites was reflected by Tubificidae % metrics. BMWP metric evaluates the ecological status of all sites as good or better. The only site that did not reach moderate ecological status is the Ribnica 2 which is located downstream the Paštrić village, and the metric that gave unfavourable result was EPT index. This site was characterized by the overall lower diversity and parameters that are derived from the number of recorded taxa, which could reflect the effects of anthropogenic pressures present in the vicinity (farming, agriculture, waste disposal and stone quarries). Insect groups Ephemeroptera, Plecoptera and Trichoptera are regarded as sensitive taxa, and deterioration in their numbers reflects habitat quality degradation. Previous knowledge on the macroinvertebrate fauna of this river is very limited. Only available publication is Jović *et al*. [8]. Their paper list a presence of 43 taxa for both the Ribnica and the Lepenica rivers. This is a considerably lower number in comparison with this study (123). Couple of notes should be made: Jović *et al*. [8] investigated fewer sites (3) and some groups such as Chironomidae, Oligochaeta and Amphipoda were not identified past the group level.

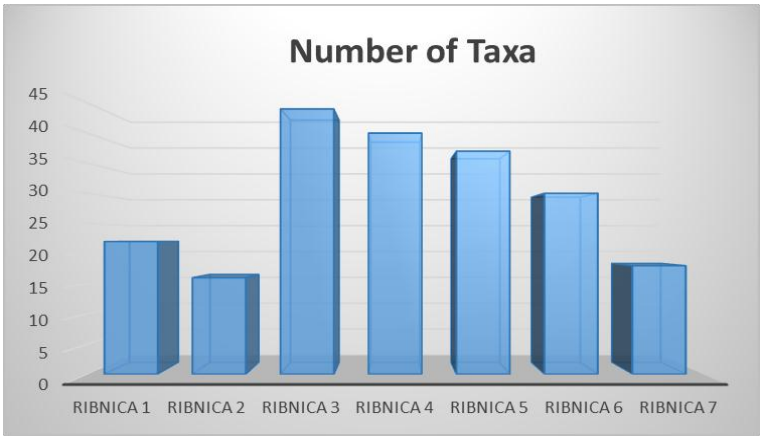

Figure 4 *Species richness of investigated sites of the river Ribnica, sites are arranged based on their location, from the most downstream to the most upstream*

CONCLUSION

This study showed that overall ecological status of the Ribnica River was moderate or better. The majority of biological quality indices showed that the water quality was good or better. The exception was the site in the vicinity of Paštrić village which shows deterioration in water quality. Rich fauna of aquatic macroinvertebrates of the river Ribnica consisting mostly of insect taxa was expected given the type of watercourse, and it reflected preserved habitats and good ecological status of this watercourse mainly in the middle part of the course of the river, while on sites located in the vicinity of human settlements decrease in the diversity of macroinvertebrate community and deterioration of water quality were observed.

ACKNOWLEDGEMENT

Publication of manuscript was supported by Ministry of Science, Technological Development and Innovation of Republic of Serbia (contract number: 451-03-47/2023-01/200007).

REFERENCES

[1] Official Gazette of the Republic of Serbia 30/2010, Regulation on establishment of surface and groundwater bodies.

[2] WFD, Water Framework Directive- Directive of the European Parliament and of the Council 2000/60/EC – Establishing a Framework for Community Action in the Field of Water Policy (2000).

[3] EN 27828:1994, Water quality – Methods of biological sampling; Guidance on handnet sampling of aquatic benthic macro-invertebrates - ISO 7828:1985.

[4] AQEM, Manual for the application of the AQEM system: A comprehensive method to assess European streams using benthic macroinvertebrates, developed for the purpose of the Water Framework Directive. Contract No: EVK1-CT1999-00027 (2002).

[5] Official Gazette of the Republic of Serbia 74/2011, Regulation on the parameters of ecological and chemical status of surface waters and parameters of chemical status and quantitative status of ground waters.

[6] Paunović M., Simić V., Simonović P., *et al*., Biological Quality Elements in WFD implementation in Serbia – typology, reference conditions and ecological status class boundaries, Technical Report, Institute for Biological Research „Siniša Stanković", Beograd (2009).

[7] Paunović M., Simić V., Simonović P., *et al*., Biological Quality Elements in WFD implementation in Serbia – typology, reference conditions and ecological status class boundaries, Technical Report, Contract No.01-772, 14.06.2010, Institute for Biological Research „Siniša Stanković", Beograd (2010).

[8] Jović A., Paunović M., Stojanović B., *et al*., Arch. Biol. Sci. 58 (2) (2006) 115–119.

INFLUENCE OF FREEZING ON NITRATE AND NITRITE CONTENT IN RADISH, PARSLEY LEAF AND CELERY ROOT

Tamara Petronijević[1*], Ivana Kostić Kokić[2], Tatjana Anđelković[2], Bojan Zlatković[1], Kristina Kitanović[1], Danica Bogdanović[2], Nikola Stanković[1]

[1]University of Niš, Faculty of Science and Mathematics, Department of Biology and Ecology, Višegradska 33, 18000 Niš, SERBIA

[2]University of Niš, Faculty of Science and Mathematics, Department of Chemistry, Višegradska 33, 18000 Niš, SERBIA

[*]*tamarapetronijevic994@gmail.com*

Abstract

The vegetables are the majour source of nitrate and nitrite entry in the human body. The present study was conducted to investigate influence of freezing on nitrite and nitrate content in three commonly used vegetables: radish, parsley leaf and celery root. After nitrite and nitrate extraction, determination of these anions was performed using ion chromatography. The highest levels of nitrite and nitrate content before freezing were obtained for samples of radish. Results obtained by analysing samples after freezing showed that the highest content of nitrite ion was determined in samples of celery root, while in samples of radish, nitrite content was not detected. The highest content of nitrate ion in samples after freezing was obtained for samples of radish. Also, all samples of radish and celery root showed higher content of nitrate ion and lower content of nitrite ion after freezing comparing to results before freezing, while results obtained for samples of parsley leaf showed the higher concentrations after freezing in both cases.

Keywords: nitrate, nitrite, vegetables, ion chromatography.

INTRODUCTION

Nitrate and nitrite are present in a wide range of foods and vegetables are known as the major source of nitrate and nitrite. It is estimated that 75–80% of the total nitrate and nitrite daily intake comes from vegetables [1]. Many environmental and biological factors including composition of soil, light intensity, moister, duration of growth period, harvesting time, storage time, and use of nitrogen fertilizer, influence nitrite and nitrate content in vegetables. Nitrite and nitrate content is extremely variable and also varied from country to country and region to region [2]. The nitrate levels in vegetables are very variable and may reach level up to 10 g/kg if they are grown in extreme conditions [1–3].

Nitrates that could be found in vegetables are subjected to certain reactions. Products and metabolites of these reactions, including nitrite, nitric oxide, and N-nitroso compounds, have potentially adverse effects and health implications which are related to the methaemoglobinaemia syndrome, gastric diseases and bladder cancers. Bearing in mind that there is increasing nitrogen fertilizers and additives usage that contain nitrite, human exposure

to nitrogen-containing compounds such as nitrites and nitrates are increasing and it is becoming an important public health issue [4–6].

Various methods are reported to determine nitrites and nitrates in water, food and other matrices. Different analytical techniques, such as potentiometry, spectrophotometry, ion chromatography, as well as high liquid chromatography have been used [7].

In this work, nitrite and nitrate level from samples of radish, parsley leaf, and celery root before and after freezing are reported. The analyses were carried out by ion chromatography.

MATERIALS AND METHODS

Sample preparation

Fresh and frozen plant material

Fresh vegetables including radish, parsley and celery were purchased from local open supermarket. Each vegetable was rinsed with water to remove any soil or wind-borne particles. From the fresh vegetables, subsamples were taken for determination of native nitrite and nitrate content in vegetables. Subsamples taken for determination of nitrite and nitrate content after freezing were putted into snap-lock plastic bags. All subsamples for freezing were labelled and stored in freezer for 3 months.

Sample preparation

About 10 g portion of each vegetable was homogenized by mixer (Bosh, Germany). From each homogenised sample, three subsamples of 1.0 g were weighed out by analytical balance with precision ± 0.00001 g (Kern, Germany). Sample extractions were done as follows for both the nitrate and nitrite concentrations. For each sample extraction, at least 3 g of the homogenized plant tissue were placed into a 100 ml beaker. Then, 5 ml disodium tetraborate ($Na_2B_4O_7 \cdot 10H_2O$) solution and 100 ml hot water (80°C) was added to the beaker and beaker was placed into a boiling water bath for 15 min. After this, 1 ml potassium hexacyanoferrate (II) ($K_4Fe(CN)_6 \cdot 3H_2O$) were added and the solution was shaken. Then, 2 ml zinc acetate ($Zn(CH_3COO)_2 \cdot 2H_2O$) were added to the solution and it was shaken again. This solution was allowed to cool down to room temperature, and it was transferred to a 100 ml volumetric flask. This solution was then filtered through a cellulose filter (port size 0.45 μm), to obtain a clear liquid that as filtrate sample. A dilution with ultrapure water was necessary due to high concentrations of ions. The supernatant was diluted to one twenty-fifth to match the dilution for analysis on ion chromatograph.

Instrumentation

The three replications were analysed for nitrate concentrations as follows. Volume of 5 mL of each filtrate sample was placed into the Dionex AS 50 model autosampler vials. Each of samples was loaded automatically into the ion chromatograph. Separation was achieved using Dionex IonPac AS22 column (4 × 250 mm) with the guard column Dionex IonPac AG22 (4 × 50 mm). The ion chromatograph used mix of 4.5 mM sodium carbonate and 1.4 mM sodium bicarbonate as an eluent at a flow rate of 1.2 mL/min. The concentration of nitrate and nitrite anions in samples was detected by the Dionex AERS 500, Carbonate, 4 mm, conductivity detector. Dionex Seven Anion Standard (Product No. 056933) was used for preparing

standard solutions. The nitrate and nitrite concentration values were calculated automatically based on previous made processing method using Chromeleon 7 software.

RESULTS AND DISCUSSION

After dilution to one twenty-fifth prior to analysis on ion chromatograph, all sample solutions that were analysed on IC successfully met the criterion of availability. Concentration of diluted solutions were between 0.25 and 10 mg/L and after conversion to nitrate content to vegetables, it was ranged from 0 to 3430 µg/kg.

Calibration curves obtained for nitrite and nitrate ion showed good correlation coefficients, 0.99989 and 0.99899, respectively. Figure 1 presents the calibration curves that were used for quantification of nitrite and nitrate ion. Figure 2, 3 and 4 present the chromatograms obtained after analysing samples of radish, parsley leaf and celery root, before and after freezing.

a) *b)*

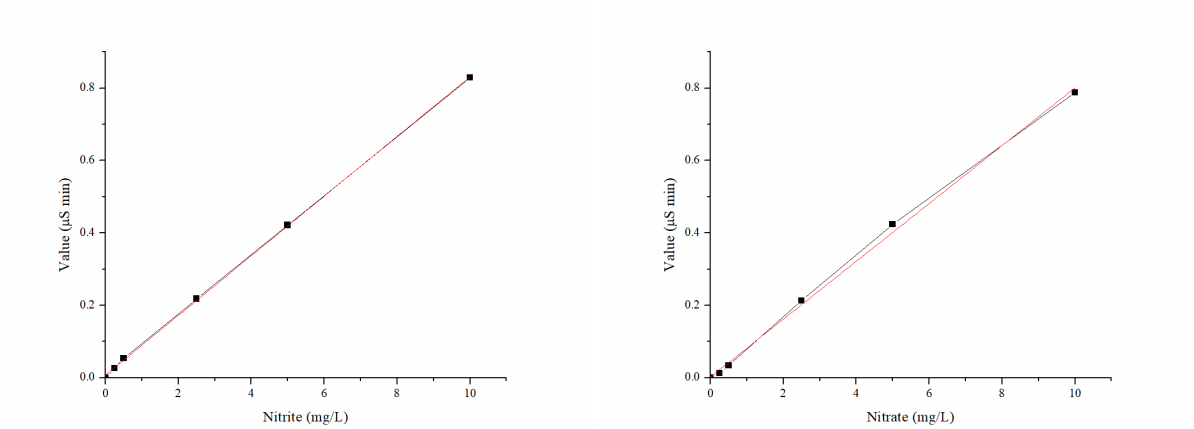

Figure 1 *Standard curves for a) nitrite; b) nitrate*

a) *b)*

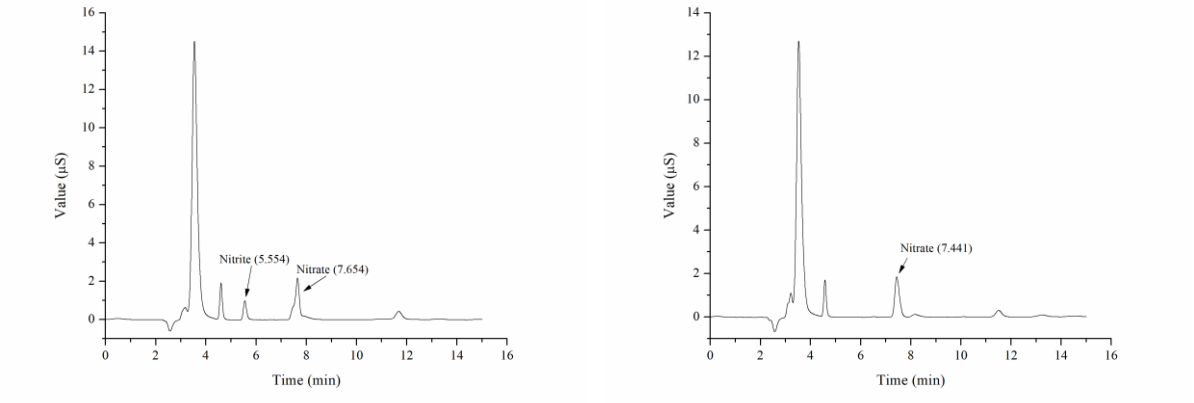

Figure 2 *Chromatogram of radish sample a) before freezing; b) after freezing*

a) *b)*

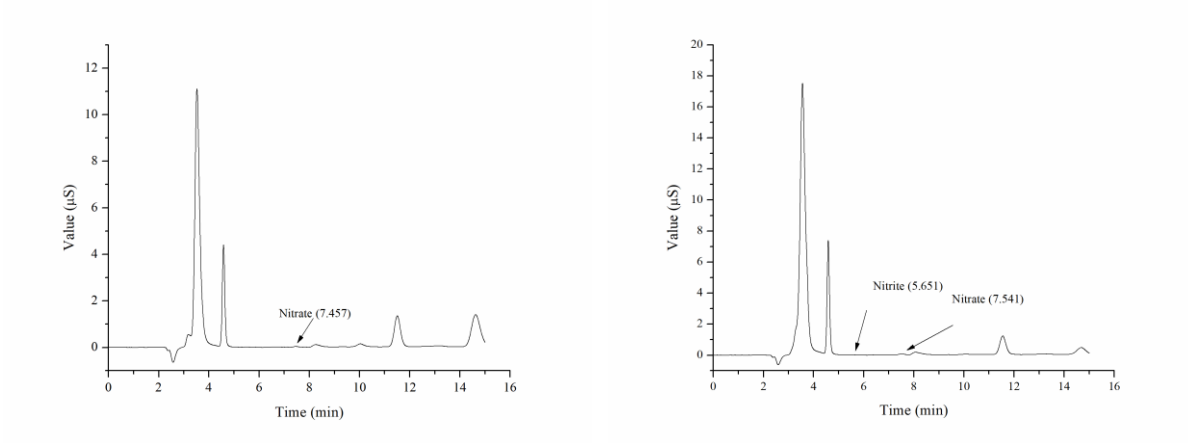

Figure 3 *Chromatogram of parsley leaf sample a) before freezing; b) after freezing*

a) *b)*

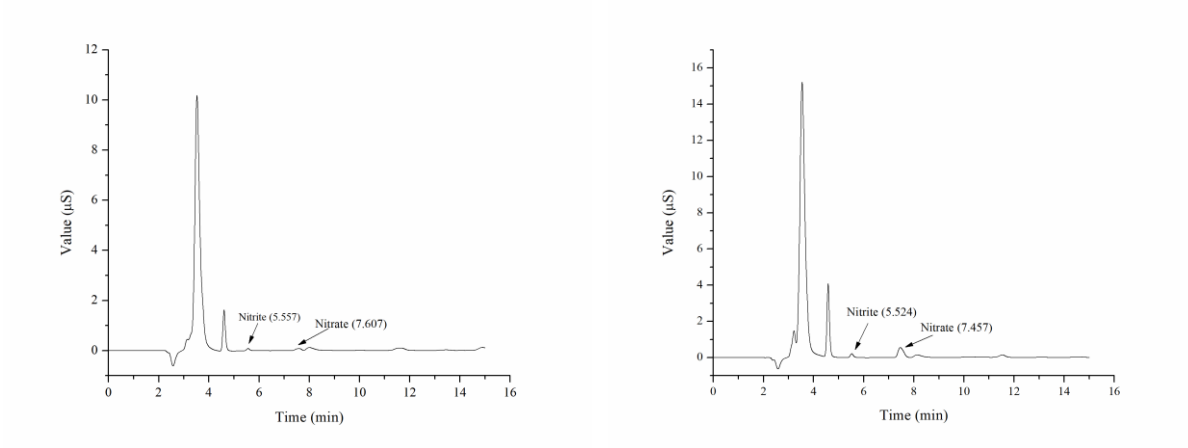

Figure 4 *Chromatogram of celery root sample a) before freezing; b) after freezing*

Results of nitrite and nitrate quantification are presented in Table 1.

The highest level of nitrite content before freezing showed samples of radish (1090.84 µg/kg), while in samples of parsley leaf nitrites were not detected. Samples of celery root showed lower content than samples of radish (739.29 µg/kg). The highest value of nitrate content before freezing also showed samples of radish, 3094.43 µg/kg, while nitrate content in samples of celery root was 382.92 µg/kg. Samples of parsley leaf showed the lowest content of nitrate ion before freezing (242.28 µg/kg). By comparing the results of nitrite and nitrate content in samples before freezing, only samples of celery root showed lower level of nitrate then nitrite content.

Results obtained using samples of vegetables after 3 months of freezing, showed that only samples of parsley leaf and celery root, contain nitrite ions at concentrations 229.62 and 704.78 µg/kg, respectively. In chromatograms obtained by analysing of radish samples, peaks which correspond to the nitrite ion was not detected. The highest level of nitrate content was obtained for the samples of radish, 3428.84 µg/kg, while the lowest value for content of nitrate ions was obtained for samples of parsley leaf, 379.06 µg/kg. The nitrate content that

was obtained for samples of celery root was 1220.96 μg/kg. By comparing the results of nitrite and nitrate content in samples after freezing, all samples showed higher content of nitrate then nitrite ion.

Table 1 *Nitrite and nitrate content in radish, parsley leaf and celery root determined before and after freezing*

Vegetable	Anion	Concentration of ion (μg/kg)	
		Before freezing	After freezing
Radish	NO_2^-	1090.84	/
	NO_3^-	3094.43	3428.83
Parsley leaf	NO_2^-	/	229.62
	NO_3^-	242.28	379.06
Celery root	NO_2^-	739.29	704.78
	NO_3^-	382.92	1220.96

These results indicate that process of conversion nitrite to nitrate ion can occur in freezing conditions. Storage in freezer for 3 months is probably the reason for obtaining results that showed lower content of nitrite ion in samples before freezing, and the higher content of nitrate ion after freezing in case of radish and celery root.

CONCLUSION

The nitrite and nitrate content in three commonly consumed fresh vegetables in Serbia was determined. Reported values indicate that all investigated samples before freezing showed the values of nitrite and nitrate content similar to results that has been found previously in the literature. Samples of radish and celery root showed lower concentration of nitrite after freezing comparing to concentrations obtained before freezing. Only parsley leaf samples showed a higher nitrite content after freezing, i.e. the nitrite content in the fresh sample was not detected. In all analysed samples, nitrate content after freezing was higher than content determined in samples after freezing.

ACKNOWLEDGEMENT

This study was supported by the Ministry of Science, Technological Development and Innovation, Republic of Serbia (Contract Number 451-03-47/2023-01/200124).

REFERENCES

[1] Chang A. C., Yang T. Y., Riskowski G. L., Food Chem. 136 (2013) 995–960.

[2] Bahadoran Z., Mirmiran P., Jeddi S., *et al*., J. Food Compos. Anal. 51 (2016) 93–105.

[3] Chang A. C., Yang T. Y., Riskowski G. L., Food Chem. 138 (2013) 382–388.

[4] Novaes H. B., Vaitsman D. S., Dutra P. B., Quim. Nova 32 (6) (2009) 1647–1650.

[5] Kyriacou M. C., Soteriou G. A., Solla G., *et al*., Food Chem. 285 (2019) 468–477.
[6] Hsu J., Arcot J., Alice Lee N., Food Chem. 115 (2009) 334–339.
[7] Zu T-H., Hsieh S-P., Su C-M., *et al*., Int. J. Anal. Chem. (2018) Article ID 6285867.

DETERMINATION OF PTEs CONTENT IN LIVESTOCK FODDER AND SOIL IN THE VICINITY OF THERMAL POWER PLANTS AND ASH DISPOSAL SITES

Marija Matić[1*], Dragana Pavlović[1], Veljko Perović[1], Dimitrije Sekulić[1], Natalija Radulović[1], Miroslava Mitrović[1], Pavle Pavlović[1]

[1]Department of Ecology, Institute for Biological Research "Siniša Stanković" – National Institute of Republic of Serbia, University of Belgrade, Bulevar Despota Stefana 142, 11060 Belgrade, SERBIA

[*]*marija.pavlovic@ibiss.bg.ac.rs*

Abstract

Potentially toxic elements (PTEs) are present in the environment as a result of natural processes, but also numerous anthropogenic activities. A large part of PTE in the soil originates from industrial plants or from contaminated water used to irrigate agricultural fields. Thus, they are taken up by plants used for human consumption or by plants grown to feed domestic animals (fodder). In order to determine the presence of B, Cu and Ni in the food chain and to evaluate and reduce the risk of growing plants for livestock feed on potentially contaminated soils in the immediate vicinity of coal mines and thermal power plants, samples of alfalfa (Medicago sativa L.) and soil were collected from the territory of municipalities of Obrenovac (village Krtinka) and Lazarevac (village Sokolovo), while the territory of the municipality of Surčin (village Jakovo) was chosen as the control site. Furthermore, the bioconcentration factor (BCF) was calculated, which can provide information about the potential efficiency of the removal of elements from the soil by the plant. The results of the content of the studied elements in fodder were within the usual concentrations for conventional production. However, Ni content in the soil was above the proposed MAC for soils according to the regulations of the Republic of Serbia (50 mg kg^{-1}) and higher than the limit values proposed by the Council Directive of the European Community (30–75 mg kg^{-1}). These results urge caution in the cultivation of fodder at investigated sampling sites.

Keywords: potentially toxic elements, *Medicago sativa*, soil contamination, bioconcentration factor.

INTRODUCTION

Intensive urbanization and industrialization led to the development of new and the expansion of existing cities and industrial areas, the main problem being the pollution of air, water, soil and vegetation. The main sources of pollution in such environments are combustion products from industry, traffic, urban heating plants, domestic heating, construction activities, and improper storage of industrial and municipal waste. Potentially toxic elements (PTEs) are present in the environment, both as a result of natural processes and numerous anthropogenic activities. A large proportion of PTEs and other pollutants in soil and water originate from industrial facilities, as a result of the use of pesticides and mineral fertilizers or from contaminated water used to irrigate agricultural fields. Thus, elements are taken up by plants grown for human consumption or to feed domestic animals. Sometimes

these concentrations can rise to levels that are toxic to plants, animals, and thus to humans who consume food produced on such soils, as they are incorporated into the food chain [1-4].

Regardless of the origin of PTEs in the soil, their concentration, mobility and potential availability to plants depend on the parent substrate, the pH reaction, the proportion of organic matter and clay in the soil, the physical properties of the soil, moisture, the presence of other chemical substances and other factors [4–6].

In order to determine the presence of B, Cu and Ni in the food chain, to assess and reduce the risk of growing plants for animal feed on soils in the immediate vicinity of coal mines and thermal power plants, samples of alfalfa (*Medicago sativa* L.) and soils were collected on the territory of the municipalities of Obrenovac (village Krtinka) and Lazarevac (village Sokolovo). The area of Surčin municipality (village Jakovo) was chosen as the control site without direct industrial activity. In addition, the bioconcentration factor (BCF) was calculated, which can provide information about the potential efficiency of the removal of chemical elements from the soil by the plant.

Medicago sativa is a perennial herb that is one of the most important fodder crops. Apart from feeding livestock, it is also important for improving the physical, chemical and microbiological properties of the soil, as its harvest leaves significant amounts of organic matter in the soil, which is further decomposed. Owing to its deep root system, it helps improve the nitrogen fertility of the soil and protect it from soil erosion. The depth of root system makes it very resistant, especially to droughts [7].

MATERIALS AND METHODS

Sample collection and preparation

Sampling was conducted in three municipalities – Obrenovac (village Krtinka), Lazarevac (village Sokolovo) and Surčin (village Jakovo), in gardens located in the vicinity of the fly ash disposal site of the "Nikola Tesla-A" thermal power plant. At each of the three villages, three sampling sites (gardens) were randomly selected for plant and associated soil sampling. *Medicago sativa* was sampled in the form of hay for livestock feed in the amount of approximately 2 kg. Samples of plant material were dried for 10 days at room temperature, and then in a drying chamber (Binder, Tuttlingen, Germany) to a constant weight. Dried samples were grounded with a stainless-steel mill and sieved through 1.5 mm stainless-steel sieve (Polymix, Kinematica AG). The associated soil at each sampling site was also sampled from three individual sampling points at the depth of 0–20 cm following a harmonised sampling regime. These were then mixed into a composite sample with the total weight of approximately 2 kg. Soil samples were dried at 105 ºC to a constant mass and homogenized. The surface layer of soil was chosen for analysis because PTE deposition in soil mostly occurs in top soil [8].

PTEs and statistical analysis

The concentration of B, Cu and Ni in the collected plant material was measured after digestion with HNO_3 and H_2O_2 (USEPA 3052). Element concentrations were measured by the method of optical emission spectrometry for simultaneous multielemental analysis (ICP-OES, Spectro Genesis), using the reference material beech leaves (BCR-100) for validation of the

analytical procedure and quality control of the laboratory protocol. The analysis was performed in six replicates (n=6). The detection limits (mg kg^{-1}) are as follows: B-0.001, Cu-0.007 and Ni-0.089. The element content in the soil was determined in the same manner as for the plant material, using the USEPA method (3052) and the standard reference material (Loam soil - ERM - CC141) to validate the analytical procedure, with detection limits identical to those of the plant material.

The data from this study was analysed using statistical analysis (ANOVA) and means were separated with a Bonferroni test at a level of significance of $p<0.05$, using the Statistica software package (StatSoft In., Tulsa, USA, 2007).

Based on the obtained element concentrations in soil and plant material, the bioconcentration factor (BCF) was determined, which indicates the potential efficiency of removal of chemical element from soil by plants. This factor defines the ratio between the available amount of a chemical element in the soil and the amount in the plant material ($[Element]_{leaf\ or\ bark}/[Element]_{soil}$] [9,10]. A value of BCF > 1 indicates the potential of plant for phytostabilization of certain soil element.

RESULTS AND DISCUSSION

The concentrations of PTEs in plant material were compared with reference values for the leaves of most herbaceous plants [11], and the maximum allowable concentration of certain elements in fodder that do not adversely affect the diet of domestic animals (Table 1) [12,13].

Table 1 *Limit values of PTEs in plants and fodder (mg kg^{-1})*

	B	Cu	Ni
TL[a]	50–200	20–100	10–100
MAC[b]	/	12–200	50

[a] Critical or toxic levels in leaf tissue for various species [11]; [b] maximum allowable concentration in fodder [13].

The concentrations of PTEs in fodder and associated soil at the investigated sampling sites are shown in Figure 1.

Boron is an essential trace element for higher plants, and its requirement varies from species to species (10–100 mg kg^{-1}, [11]), so the range between B deficiency and its toxicity is smaller than for any other element. Its uptake in plants depends directly on the physical and chemical properties of the soil, but also on the form of B and on plant transpiration [14]. In the literature, B is often cited as one of the most toxic phytonutrients due to its high solubility [15]. In the examined *Medicago sativa* samples normal concentrations of B were measured (18–25 mg kg^{-1}, [11]) (Figure 1a), with statistically significant differences in accumulation capacity determined between all sampling sites (Table 2). Regulation on maximum allowable concentrations of harmful substances and ingredients in livestock fodder does not set permissible concentration for this element (Table 1). Soil boron content ranged from 130–155 mg kg^{-1} (Figure 1b), with the highest values measured in soil samples from Surčin.

Statistically significant differences in B content ($p<0.05^{*}$) were found between the control site in Jakovo and Obrenovac (Table 2).

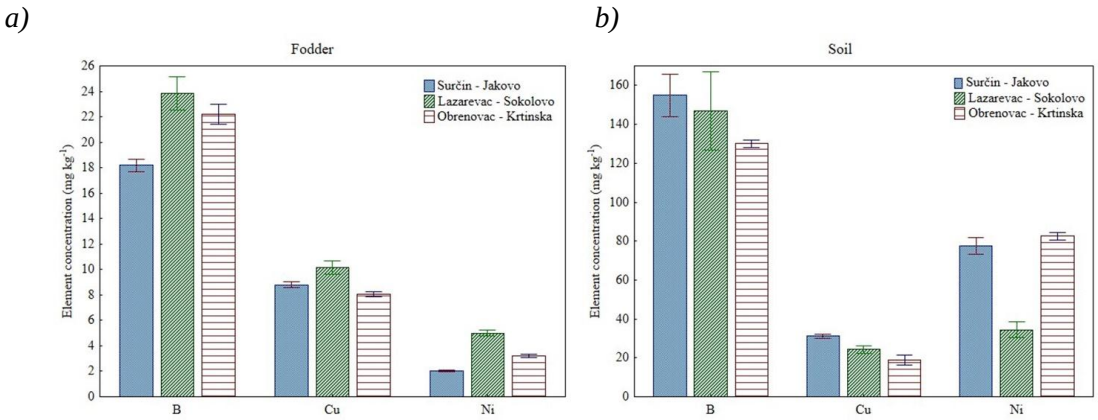

Figure 1 *Potentially toxic elements content in a) fodder and b) associated soil at examined sampling sites (mean values and standard deviation)*

The B content was above the MAC set by the regulations of the Republic of Serbia (50 mg kg^{-1}), at all sites examined, and its increased concentration may be related to coal combustion and ash formation, considering the proximity of thermal power plants [15]. Ash from thermal power plants is characterized by high content of macro and microelements, especially B, which is one of the most important environmental pollutants in the vicinity of thermal power plants and ash landfills due to its high mobility [16]. However, high B content in soil does not necessarily imply a potential risk to the environment, as its transport is affected by numerous soil parameters (texture, organic matter content, $CaCO_3$, type of parent substrate, etc.), but mainly by the pH reaction [17].

Average Cu concentrations in leaves range from 5 to 30 mg kg^{-1} [11], whereas in fodder they can vary from 2 to 69 mg kg^{-1} [12,18]. The Cu content of the studied fodder was in the normal range (8.06–10.16 mg kg^{-1}, Figure 1a), but statistically significant differences were found between all the examined sites (Table 2). Copper content in the examined soils did not exceed the MAC in soil set by regulations of the Republic of Serbia (100 mg kg^{-1}) [19,20] and the limits set by the Council Directive of the European Community (50–140 mg kg^{-1}) [21] and ranged from 18.87 mg kg^{-1} in Obrenovac to 31.2 mg kg^{-1} in Surčin. Statistically significant differences were found between all sampling sites (Table 2).

The lowest Ni content in fodder was measured in Surčin (2.04 mg kg^{-1}) and the highest in Lazarevac (5 mg kg^{-1}) and was within the normal range for plants and below the value specified for animal food ingredients MAC (Table 1). Nickel is accumulated mainly in the roots of plants, and its uptake depends primarily on the characteristics of the soil (OM content, clay, pH), the origin of Ni, and the characteristics of the plant itself. Statistically significant differences were found between all sampling sites in fodder (Table 2). Nickel content in the studied soils was higher than the MAC values for soils according to the regulations of the Republic of Serbia (50 mg kg^{-1}), except at the Lazarevac site (34.37 mg kg^{-1}, Figure 1b), and higher than the limit values proposed by the Council Directive of the European Community (30–75 mg kg^{-1}) [21]. These results are not unexpected,

considering that soils in the Republic of Serbia are characterized by high Ni content due to their geological origin [22,23], but contamination of soils by Ni is possible due to the influence of industry [24].

Table 2 *Difference in PTEs content between sampling sites in fodder and associated soil*

	Fodder			**Soil**		
B (mg kg^{-1})	Surčin	Lazarevac	Obrenovac	Surčin	Lazarevac	Obrenovac
Surčin Jakovo	/	***	***	/	ns	*
Lazarevac Sokolovo	***	/	*	ns	/	ns
Obrenovac Krtinska	***	*	/	*	ns	/
Cu (mg kg^{-1})						
Surčin Jakovo	/	***	**	/	***	***
Lazarevac Sokolovo	***	/	***	***	/	***
Obrenovac Krtinska	**	***	/	***	***	/
Ni (mg kg^{-1})						
Surčin Jakovo	/	***	***	/	***	ns
Lazarevac Sokolovo	***	/	***	***	/	***
Obrenovac Krtinska	***	***	/	ns	***	/

ANOVA, n=5, $^{*}p<0.05$; $^{**}p<0.01$; $^{***}p<0.001$; ns – no statistical significance.

Phytostabilization is the formation of chemical compounds by plants and the immobilization of pollutants, which reduces their availability. The investigated *Medicago sativa* did not prove to be effective in immobilizing the examined PTEs, as all obtained values for BCF were below 1.

CONCLUSION

The concentration of the studied PTEs measured in livestock fodder from the selected sampling sites was within the usual concentrations for conventional production. *Medicago sativa* was found not to be a significant accumulator of B, Cu and Ni, as the values of the bioconcentration factor were below 1, indicating that fodder is not suitable for phytostabilization of these elements in the studied soils. It was found that the highest content of all elements in fodder was measured in the Sokolovo village (Lazarevac) and the lowest in the control site in Jakovo (Surčin). In contrast, the highest concentrations of the examined elements in the soil were measured at the control site, where the Ni values were above the MAC values for soils according to the regulations of the Republic of Serbia (50 mg kg^{-1}) and above the limit values proposed by the Council Directive of the European Community (30–75 mg kg^{-1}). Such results for Ni are not unexpected, considering that soils in the Republic of Serbia are characterized by high Ni content of geological origin, but soil contamination is also possible due to the influence of industry.

Despite the common concentrations of the studied elements in fodder, caution should be exercised in their use, as certain elements are present in the soil in high concentrations. Soil is a dynamic system in which, under suitable conditions (change in pH, redox potential and

salinity), elements can be easily transported to above-ground plant parts, which could lead to significant accumulation.

ACKNOWLEDGEMENT

This work was supported by the Ministry of Science, Technological Development and Innovation of the Republic of Serbia, grant No. 451-03-47/2023-01/200007.

REFERENCES

[1] Madrid F., Biasioli M., Ajmone-Marsan F., Arch. Environ. Contam. Toxicol. 55 (2008) 21–32.

[2] Bielicka-Giełdoń A., Rylko E., Zamojc K., Pol. J. Environ. Stud. 22 (4) (2013) 1013–1021.

[3] Pan L., Ma J., Hu J., *et al*., Environ. Sci. Pollut. Res. 23 (19) (2016) 19330–19340.

[4] Pavlović P., Mitrović M., Degradacija i zaštita zemljišta, Tematski zbornik, Univerzitet u Beogradu, Šumarski fakultet (2016), p.173, ISBN: 978-86-7299-242-7.

[5] Ghrefat H. A., Yusuf N., Jamarh A., *et al*., Environ. Earth Sci. 66 (2012) 199–208.

[6] Gržetić I., Ghariani R. H. A., J. Serb. Chem. Soc. 73 (8-9) (2008) 923–934.

[7] Latrach L., Farissi M., Mouradi M., *et al*., Turk. J. Agric. For. 38 (3) (2014) 320–326.

[8] Pavlović D., Pavlović M., Perović V., *et al*., Int. J. Environ. Res. Public Health. 18 (2021) 9412.

[9] Migeon A., Richaud P., Guinet F., *et al*., Water Air Soil Pollut. 204 (2009) 89–101.

[10] Chen M., Tang Y. L., Ao J., *et al*., Russ. J. Plant Physiol. 59(6) (2012) 772–780.

[11] Kabata-Pendias A., Pendias H., Trace elements in soils and plants, CRC Press, Boca Raton, FL, USA (2001), p.331, ISBN: 0-8493-1575-1

[12] Adams R. S., J. Dairy Sci. 58 (1975) 1538–1548.

[13] Official Gazette of Social Federative Republic of Yugoslavia, No. 2/90 and No. 27/90.

[14] Goldberg S., Lesch S. M., Suarez D. L., Soil Sci. Soc. Am. J. 64 (2000) 1356–1363.

[15] Adriano D. C., Trace elements in terrestrial environments, Springer, New York (2001), p.867, ISBN: 978-1-4684-9505-8.

[16] Pavlović P., Mitrović M., Đurđević L., Environ. Manage. 33 (2004) 654–663.

[17] Padbhushan R., Kumar D., J. Agric. Sci. 155 (7) (2017) 1023–1032.

[18] Simić A., Dželetović Ž., Vučković S., *et al*., Hem. Ind. 69 (5) (2015) 459-467.

[19] Official Gazette of the Republic of Serbia, No.23/94.

[20] Official Gazette of the Republic of Serbia, No. 88/10.

[21] Directive 86/278/EEC, Off. J. Eur. Communities. 1986 (181) 6–12.

[22] Mrvić V., Zdravković M., Sikirić B., *et al*., Harmful and hazardous elements in soil *in* The Fertility and Content of Hazardous and Harmful Substances in the Soils of Central Serbia, Editors: Mrvić V., Antonović G., Martinović L., Institute of Soil Science, Belgrade (2009) 75–144, ISBN: 978-86-911273-1-2.

[23] Kuzmanoski M. M., Todorović M. N., Aničić-Urošević M. P., *et al*., Hem. Ind. 68 (2014) 643–651.

[24] Wei B., Yang L., Microchem. J. 94 (2010) 99–107.

LEAF NITROGEN BALANCE INDEX USED TO MONITOR STRESS RESPONSE TO AIR POLLUTION OF DECIDUOUS TREE SPECIES GROWN IN URBAN ZONE OF BELGRADE

Sonja Veljović Jovanović[1*], Sonja Milić Komić[1], Bojana Živanović[1], Ana Sedlarević Zorić[1], Nikola Šušić[1]

[1]University of Belgrade, Institute for Multidisciplinary Research,
Kneza Višeslava 1, 11030 Belgrade, SERBIA

[*]*sonjavel@imsi.rs*

Abstract

Street trees are important component of urban forest presenting a first barrier between air pollution originated from vehicle traffic and pedestrians. It implies that an improvement of air quality in urban areas greatly depends on green biomass, in short, the bigger and greener tree crown, better for human health and wellbeing. Determination of Leaf Nitrogen Balance Index (LNBI) and chlorophyll concentration (ChlC) by a non-invasive methodology and a user friendly instrument (Dualex 4, Force), widely used in agronomy and horticulture, was tested here for the assessment of tree fitness in urban zones. Investment of energy and resources either in growth or defence according to the trade-off strategy of plants may be indicated by LNBI, which approximately presents a Nitrogen/Carbon ratio. We selected few tree species from Belgrade's streets to determine those two parameters during summer. We also presented the changes in those parameters of the introduced bamboo species within ten years at several urban locations in Belgrade differing in air pollution aiming to evaluate usefulness the LNBI parameter in access of multiyear exposure to the effect of intense vehicle traffic. Numerous limiting factors for development of healthy tree crowns in urban ecosystem, such as low capacity to cope with toxic pollutant, sensitivity to diseases, early senescence and etc., greatly depends on tree species. We propose this methodology may also contribute in the process of choice of the adequate tree species to be planted along streets.

Keywords: LNBI, chlorophyll, epidermal flavonoids, street trees, bamboo, air pollution.

INTRODUCTION

Taking into account that urban areas (city, megalopolis) become everyday environment of the majority of global population, about 55%, and even 80% in EU countries [1], urban forest research received a considerable attention from scientific community with an involvement of both, natural and social science disciplines. Environmental benefits of urban trees for human health and environmental health have been thoroughly analysed elsewhere [2]. Authors of this review emphasized that urban forest planning and management should strategically promote trees as a social determinant of public health. Street trees contribute significantly to urban air quality by forming the closest buffer zone between sources of air pollution originated from vehicles traffic and residential areas. Main benefits provided by rich tree crowns related to environmental protection are amelioration of the effects of greenhouse gasses, adsorption of particulate matters, microclimate change mitigation. Though a releasing oxygen via

photosynthesis by trees – "the lungs of the earth", is the first argument used in urban forest management, the actual effect of urban trees on the oxygen concentration in cities are to be scientifically supported [3,4]. However, gas-exchange measurements of tree canopy are very complex as photosynthetic activity of tree leaves are highly variable depending on leaf genetically heterogeneity, position within crown, which mainly determine their light exposure and hydration, tree age, morphology etc. [5]. In searching for the methodology to best suit study of street trees, we tried to test whether a non-invasive optical measurements of leaf transmittance (375) using a commercial Chl and flavonoid (Flav) meter – Dualex 4 Scientific, proposed to be used in crops surveys and nutrition management [6,7], might be also used for the assessment of tree's physiological status in their natural (urban) environment. Though determination of Chl is widely used as a stress meter (SPAD), this device measures Chl and Flav using leaf clip on the same leaf spot, allowing a generation of nitrogen balance index (NBI) which approximately presents a Nitrogen/Carbon ratio. Based on the hypothesis – the trade-off strategy of plants – that energy and resources are invested either in growth (primary metabolism, proteins, and chlorophyll) or defence (secondary metabolism, phenolic compounds), under the same nitrogen availability LNBI could be used as an indicator of plant metabolic status. Thus, monitoring of LNBI might be good indicator of plant sensitivity to pollutants, high temperature and sunlight or drought, commonly occurring abiotic stressors during summer in urban areas. Aim of this report is to encourage using this optical methodology as an early diagnostic tool of either air pollution or early senescence or species specific response occurring in urban trees as one of the contribution to fostering tree monitoring technologies.

MATERIALS AND METHODS

Experimental design

Various tree species (*Tilia sp*., *Platanus acerifolia*, *Aesculus hippocastanum* L., *Corylus colurna* L., *Fagus sylvatica* L., *Ginkgo biloba* L., *Magnolia x soulangeana* Soul.-Bod., *Pinus wallichiana A.B.Jacks*, *Platanus acerifolia* (Aiton) Willd., *Quercus robur* L.) grown in urban zones in Belgrade municipalities (Arboretum and along main streets) were used to monitor physiological plant status by determining several optically derived parameters: 1) leaf nitrogen balance index – LNBI, 2) chlorophyll concentration – ChlC, and 3) epidermal flavonoids – EFlav. Measurements of Chl fluorescence were obtained from 20 to 30 mature, sun-exposed leaves of each tree or bamboo, about 5 to 7 hours after sunrise. The location of the monitored trees was given by names of city districts and streets. Leaves of bamboo, all exposed to sun and either close to traffic pollution source (Despota Stefana street) or from Košutnjak (Arboretum) were similarly analyzed.

Determination of ChlC, LNBI and EFlav

Total chlorophyll concentration (ChlC), epidermal Flavonoids (EFlav), and the leaf nitrogen balance index (LNBI) were obtained from the same leaf spot with the Dualex (Dx4, FORCE-A, Orsay, France; see Cerović *et al*. [6] for more details). Two laser beams, at 375 and 650 nm, were applied on leaf surface using leaf clip, to excite Chl in the leaf mesophyll. By equalizing Chl fluorescence under visible (650 nm) and UV (375 nm) light excitation, an electronic feedback loop, variable Chl fluorescence is avoided and a precise measurement of

the absorbance of Flav in the UV-A is secured [8,9]. As a non-destructively measured leaf Chl content was used as indicator of N nutrition of crops [e.g. 10,11]. The new index called NBI (nitrogen balance index) derived from the Chl/Flav ratio is an indicator of C/N allocation changes [11]. Also the Chl/Flav ratio would correspond to an LMA-corrected Chl, i.e. Chl on mass basis.

Statistical Analysis

Significant differences in bamboo leaf ChlC, EFlav and LNBI ratio between locations in four years were determined using a two-way ANOVA test. The significance threshold value was set at $P \leq 0.05$. The homogeneity of variance was checked with Levene's test. Following two-way ANOVA analysis, the Tukey post hoc test was used for specific comparisons among experimental groups ($P \leq 0.05$). The experimental data were analysed using the software package Statistica 8.0. To test for significant differences in chlorophyll content and LNBI index between June and August, the Mann–Whitney U/t-test was used, and the significance threshold value was set at 0.05. The experimental data were analysed using software package Statistica 8.0.

RESULTS AND DISCUSSION

Effects of traffic pollution on LNBI

Traffic pollution can have various effects on the LNBI, which is being an indicator of the nitrogen content implies the status of stress impact on plant based on the metabolic strategy defence int leaves. Particulate matter (PM) from vehicle emissions ($PM_{2.5}$, PM_{10}) can settle on leaves and obstruct the metabolism either by closing stomata which can reduce photosynthesis and transpiration or by importing adsorbed toxic heavy metals (12), leading to a decline in the LNBI (Table 1).

Table 1 *Effects of traffic pollution on Leaf Nitrogen Index (LNBI) of the examined plant species. White fields represent trees at unpolluted locations (Košutnjak, Ušće); dark fields represent trees exposed to pollution (Kneza Miloša street, King Aleksander boulevard, Makenzijeva street. Results represent the mean value from 30 leaves ± SE*

Species	LNBI	Species	LNBI
Tilia platyphyllos	46.5 ± 4.9	*Platanus acerifolia* 1	27.8 ± 0.9
Tilia europea 1	46.7 ± 4.2	*Platanus acerifolia* 2	20.9 ± 8.5
Tilia europea 2	40.4 ± 7.1	*Platanus acerifolia* 3	20.1 ± 4.3
Tilia europea 3	64.7 ± 9.9	*Platanus acerifolia* 1	14.5 ± 1.4
Tilia europea 4	68.8 ± 15.7	*Platanus acerifolia* 2	19.8 ± 1.6
Tilia platyphyllos	29.7 ± 0.6	*Platanus acerifolia* 3	18.4 ± 2.4
Tilia cordata 1	29.4 ± 3.5	*Platanus acerifolia* 4	20.4 ± 3.1
Tilia cordata 2	20.4 ± 1.9	*Platanus acerifolia* 5	15.6 ± 2.6
Tilia grandiflora 1	24.5 ± 2.0	*Platanus acerifolia* 6	21.8 ± 2.9
Tilia grandiflora 2	21.2 ± 4.8	*Platanus acerifolia* 7	15.3 ± 2.1
Tilia grandiflora 3	38.1 ± 2.7	*Platanus acerifolia* 8	20.1 ± 1.0
Tilia grandiflora 4	21.1 ± 1.9	*Platanus acerifolia* 9	15.2 ± 1.6
Tilia europea 1	26.2 ± 4.7	*Platanus acerifolia* 10	15.6 ± 1.7
Tilia europea 2	33.9 ± 8.4	*Platanus acerifolia* 11	16.3 ± 1.4
Tilia europea 3	35.1 ± 6.7	*Ginkgo biloba L.*	51.4 ± 10.3
Tilia europea 4	24.1 ± 4.3	*Ginkgo biloba L.*	31.2 ± 4.1

Traffic pollution can also contribute to leaf damage and premature senescence. Traffic pollution often includes emissions of nitrogen dioxide (NO_2) and nitrogen oxides (NO_x). These pollutants can deposit onto plant leaves and negatively impact their nitrogen metabolism, which can affect plant growth and productivity (13). Leaves exposed to high levels of pollutants may exhibit symptoms such as smaller leaf size, abnormal shape, or chlorosis (yellowing). Traffic pollution is often accompanied by other air pollutants, such as sulfur dioxide (SO_2) and ozone (O_3) (14). Elevated ozone levels can increase oxidative stress in plants, leading to nitrogen imbalances and reduced LNBI.

Species specific variation of ChlC, EFlav and LNBI

Total chlorophyll concentration (ChlC) levels varied in different tree species depending on the month during summer season with the greatest effect observed in *P. wallichiana*, *A. hippocastanum*, *M. soulangeana*, *P. acerifolia*, and *Q. robur*, while magnolia had the lowest ChlC. Unique pattern was observed in ginkgo, where the ChlC first increases in June and then gradually decreases until October (Table 2, and data not shown).

Table 2 *Total chlorophyll concentration (ChlC, µg/cm^2) and concentration of epidermal flavonoids (EFlav,* µg/cm^2*) in the leaves of the examined plant species in summer season, measured by Dualex. Results represent the mean value from 30 leaves ± SE. Significant differences in ChlC between June and August according to Mann–Whitney U/t-test in each experiment are indicated (* P < 0.05, ** P < 0.005)*

Species	ChlC (µg/cm^2)		EFlav (µg/cm^2)	
	June	August	June	August
Aesculus hippocastanum L.	27.4 ± 0.6	33.8 ± 1.5*	1.09 ± 0.07	0.96 ± 0.06
Corylus colurna L.	24.8 ± 0.4	21.3 ± 0.5	1.03 ± 0.02	1.30 ± 0.05*
Fagus sylvatica L.	57.8 ± 10.9	26.5 ± 5.3*	1.56 ± 0.19	1.60 ± 0.15
Ginkgo biloba L.	47.0 ± 2.0	38.3 ± 4.0*	0.98 ± 0.24	1.21 ± 0.20*
Magnolia x soulangeana Soul.-Bod. 1	25.9 ± 3.9	28.7 ± 6.3	1.46 ± 0.29	1.32 ± 0.30
Magnolia x soulangeana Soul.-Bod. 2	25.7 ± 3.7	27.9 ± 4.0	1.02 ± 0.43	1.43 ± 0.29*
Pinus wallichiana A.B.Jacks	57.8 ± 10.9	47.1 ± 10.9*	1.73 ± 0.11	1.42 ± 0.11*
Platanus acerifolia (Aiton) Willd.	35.3 ± 1.5	31.7 ± 1.1*	1.51 ± 0.03	1.66 ± 0.01*
Quercus robur L.	18.2 ± 0.6	22.7 ± 0.9*	1.43 ± 0.04	1.46 ± 0.04

The highest accumulation of epidermal flavonoids (EFlav) in April was recorded in *P. wallichiana*, and it was twice less in *A. hippocastanum*, *G. biloba*, and *C. colurna* (data not shown). Furthermore, it was observed that there was a significant accumulation of EFlav in *F. sylvatica*, ginkgo, and *P. acerifolia* during the summer, indicating that these tree species may have an active mechanism for biosynthesis and distribution of flavonoid *sunscreeners* in leaf epidermal layer throughout the growing season (Table 2). In contrast, while the ChlC in magnolia increases during the growing season, there was no change in the level of EFlav. On the other hand, with *A. hippocastanum* and *P. wallichiana*, a linear decrease in EFlav content was observed from spring to autumn, with *P. wallichiana* showing a more significant decrease than *A. hippocastanum* (Table 2).

The accumulation of flavonoids in the epidermal layer of leaf cells is an important mechanism that protects the leaf from photo-oxidation caused by high doses of ultraviolet

radiation, which is especially increased in the summer [15]. The results suggest that plants synthesize flavonoids in the spring, and the level is maintained during the summer months [16]. The accumulation of flavonoids is influenced by a variety of factors, mostly by the level of exposure to sunlight, besides species of the plant, and the metabolic priorities of the plant during different phases of its growth cycle [17]. Accordingly, sun-exposed leaves tend to have higher levels of epidermal flavonoids than shaded leaves, indicating that this protective mechanism against harmful UV radiation.

It was noted that the lowest value for the leaf nitrogen index (LNBI) was observed in beech tree and magnolia, while the highest value was observed in Himalayan pine, indicating tickness of leaf is an important factor to take into account using Dualex4. The biggest initial increase in the LNBI index was seen in beech tree, ginkgo, and magnolia, with values increasing by 2–3 times (Table 3).

Table 3 *Leaf Nitrogen Index (LNBI) of the examined plant species in the period from April to October, measured by Dualex. Results represent the mean value from 30 leaves ± SE. Significant differences in LNBI between June and August according to Mann–Whitney U/t-test in each experiment are indicated (* $P < 0.05$, ** $P < 0.005$)*

Species	LNBI	
	June	August
Aesculus hippocastanum L.	28.3 ± 1.7	36.1 ± 1.1*
Corylus colurna L.	24.5 ± 0.8	17.3 ± 0.9*
Fagus sylvatica L.	36.8 ± 5.4	17.0 ± 4.9**
Ginkgo biloba L.	51.4 ± 10.3	32.6 ± 5.5**
Magnolia x soulangeana Soul.-Bod. 1	18.3 ± 4.5	23.2 ± 8.2*
Magnolia x soulangeana Soul.-Bod. 2	30.5 ± 5.5	20.3 ± 4.6**
Pinus wallichiana A.B.Jacks.	36.8 ± 5.4	29.3 ± 6.8*
Platanus acerifolia (Aiton) Willd.	23.3 ± 1.0	19.4 ± 0.9*
Quercus robur L.	21.6 ± 0.5	29.1 ± 1.1*

The results indicate that in 2012, the ChlC was significantly higher in bamboo leaves from Košutnjak compared to the more polluted location at Despota Stefana street (Figure 1). However, over the next two years, the ChlC became relatively similar at both locations and remained so even after 10 years in 2023. Additionally, there was a significant decrease in ChlC at both locations after 11 years compared to the beginning of the measurement in 2012.

The study also found that the content of EFlav decreased over the four years of the study in bamboo leaves at both locations, with a lower accumulation of EFlav observed in bamboo leaves from the more polluted location (Figure 1). The changes in the content of EFlav were followed by a change in the level of the LNBI. A significantly lower LNBI was measured in bamboo leaves grown in Despota Stefana street, while a decrease in LNBI over the years was recorded only in bamboo leaves from Košutnjak (Figure 1). The more polluted location at Despota Stefana street showed a lower accumulation of EFlav and a lower LNBI compared to the less polluted location at Košutnjak. Overall, these results suggest that both locations

experienced a decrease in the health of the bamboo plants over time, as indicated by the decreasing chlorophyll content, decreasing epidermal flavonoids, and decreasing NBI index.

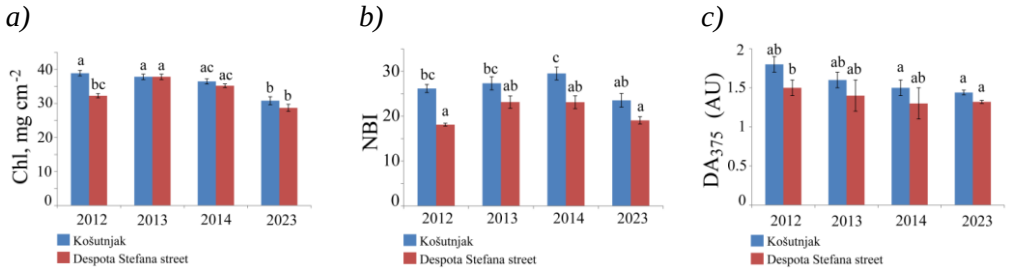

Figure 1 *a) Total chlorophyll concentration (ChlC), b) leaf nitrogen index (LNBI) and c) concentration of epidermal flavonoids (EFlav) of bamboo leaves measured in 2012, 2013, 2014 and 2023 by Dualex. Values are presented as means ± SE (n = 20). Different letters denote significant differences between means according to Tukey HSD post*

CONCLUSION

The coordination of continuous activities by municipality in synergy with academic and social organizations including a continuous monitoring of urban forestry as well as a proper nourishment and selection of the best adaptable tree seedlings in nurseries to these specific environmental conditions, is of crucial importance for further development of green city and maintenance of healthy urban forest. To ascertain the actual human health benefits derived from urban forest, a future research requires an inevitable multidisciplinary approach implemented in the long-termed ecological projects. We present here that use of described technology, adapted measurement of Chl fluorescence from leaf by the Dualex (Dx4, FORCE-A might contribute to the monitoring of plant sensitivity to pollutants, high temperature and sunlight or drought, commonly occurring abiotic stressors during summer in urban areas. Results encourage using this optical methodology as an early diagnostic tool of either air pollution or early senescence or species specific response occurring in urban trees as one of the contribution to fostering tree monitoring technologies.

ACKNOWLEDGEMENT

The authors are grateful to the Ministry of Science, Technological Development and Innovation of the Republic of Serbia for financial support according to the contract with the registration number (451-03-47/2023-01/200053), to the Center for Green Technologies, University of Belgrade, JKP Zelenilo, and Secretariat for Environmental Protection, City of Belgrade.

REFERENCES

[1] Coleman A. F., Harper R. W., Eisenman T. S., *et al*., Forests 13 (11) (2022) 1779.

[2] Wolf K. L., Lam S. T., McKeen J. K., *et al*., Int. J. Environ. Res. Public Health 17 (12) (2020) 4371.

[3] Ramanan S. S., Osman M., Shanker A. K., *et al*., Curr. Sci. 121 (5) (2021) 622.

[4] Wei Y., Wu J., Huang J., *et al*., Environ. Sci. Technol. 55 (12) (2021) 7808–7817

[5] Thomas S. C., Tree Physiol. 30 (5) (2010) 555–573.

[6] Cerović Z. G., Masdoumier G., Ghozlen N. B., *et al.*, Physiol. Plant 146 (3) (2012) 251–260.

[7] Tremblay N., Wang Z., Cerović Z. G., Agron. Sustain. Dev. 32 (2012) 451–464.

[8] Bilger W., Veit M., Schreiber L., *et al*., Physiol. Plant. 101 (4) (1997) 754–763.

[9] Cerović Z. G., Ounis A., Cartelat A., *et al*., Plant Cell Environ. 25 (12) (2020) 1663–1676.

[10] Cartelat A., Cerović Z. G., Goulas Y., *et al*., Field Crops Res. 91 (1) (2005) 35–49.

[11] Huan Y. U., Hua-Song W. U., Zhijie W., Acta Agron. Sin. 36 (5) (2010) 840–847.

[12] Hubai K., Kováts N., Teke G., SN Appl. Sci. 3 (9) (2021) 770.

[13] Xu Y., Xiao H., Wu D., Environ. Pollut.-249 (2019) 655–665.

[14] He K., Huo H., Zhang Q., Annu. Rev. Environ. Resour. 27 (1) (2002) 397–431.

[15] Jansen M. A., Gaba V., Greenberg B. M., Trends Plant Sci. 3 (4) (1998) 131–135.

[16] Agati G., Tattini M., New Phytol. 186 (4) (2010) 786–793.

[17] Winkel-Shirley B., Curr. Opin. Plant Biol. 5 (3) (2002) 218–223.

USE OF BIOCHEMICAL METHODS FOR ASSESING OXIDATIVE STRESS IN TREES IN URBAN AREA DURING GROWING SEASON

Bojana Živanović[1], Sonja Milić Komić[1], Ana Sedlarević Zorić[1], Aleksandra Jelušić[1], Nikola Šušić[1], Sanja Marković[1], Sonja Veljović Jovanović[1*]

[1]University of Belgrade, Institute for multidisciplinary research,
Kneza Višeslava 1, 11030 Belgrade, SERBIA

[*]*sonjavel@imsi.bg.ac.rs*

Abstract

Due to increased urbanization and industrialization, the emission of toxic material into the atmosphere is in expansion, which has a negative impact on the environment and human health. In this research, we monitored the effect of air pollution on the peroxidase (POD) activity and total antioxidant capacity of different tree species during the growing season. The main goal was to determine which tree species developed the highest tolerance to unfavorable environmental conditions at the end of growing season, based on the response of their antioxidative metabolism. The greatest change in POD activity was observed in the Fagus sylvatica L. leaves, where enzyme activity was more than doubled in the autumn, in comparison to spring. On the other hand, decrease in POD activity was the greatest in Cedrus atlantica (Endl.) Manetti ex Carrière needles. Moreover, total antioxidative capacity was altered during growing season in almost all examined tree species. The Magnolia spp. showed the most consistent response to the given environmental pollution with both portrayed parameters induced during growing season. In general, we can conclude that the tree species investigated in this research possess distinctive tolerance potential to air pollutants.

Keywords: urban area, street trees, oxidative stress, peroxidase, antioxidative capacity.

INTRODUCTION

Environmental pollution has a severe ecological and social impact, particularly in industrialized and urban regions. Significant pollutant sources are industry, traffic, households, consumption of low-quality fuels and agricultural production [1]. Also, unorganized urbanization and industrialization have detrimental effect on ecosystems dynamics, especially in developing countries [2]. Among different air pollutants, particulate matter (PM_{10}, and $PM_{2.5}$), heavy metals (predominantly Pb and Cd), nitric oxides, ozone and carbon monoxide have the most negative impact on human health and the environment. In that regard, in urban densely populated areas, planting vegetation (i.e. trees) is one of the main factors in ameliorating the consequences of air pollution [3]. Numerous research papers have shown that trees have the highest pollution removal capacity, and thus a crucial contribution to air quality improvements in comparison to green roofs and green walls. Also, the important benefit of trees in urban areas lies in their capacity to reduce air temperature, which is very important during hot summer months [5]. On the other hand, trees from urban areas are constantly exposed to negative environmental conditions, like pathogen attacks and different abiotic stress factors. Almost all types of stressors cause oxidative damage of

biomolecules (proteins, lipids, carbohydrates, and nucleic acids) by reactive oxygen species (ROS) [6]. On the other hand, ROS can act as secondary messengers involved in the regulation of plant defence by different mechanisms (apoptoses, induction of antioxidants, and retardation of growth) [7]. Plants possess an efficient antioxidant system involved in neutralization of the harmful effects of the ROS excess, via activating various antioxidative enzymes (e.g. superoxide dismutase, catalase, glutathione peroxidase, peroxidase class III, ascorbate peroxidase) or nonenzymatic antioxidants (ascorbate, glutathione, α-tocopherol, flavonoids and carotenoids).

In the present study we investigated the antioxidative capacity as well as POD activity extracted from the leaves of chosen tree species grown in different municipalities of the City of Belgrade (Čukarica, Vračar, Stari grad and Savski venac). All measurements were performed on leaves sampled at the beginning and the end of the growing season, to observe species specific acclimation to harmful environmental conditions [8]. Our goal was to determine which of the commonly grown trees in the urban area of Belgrade can be considered for future planting based on their response to oxidative stress caused by pollution and severe conditions [1].

MATERIALS AND METHODS

Plant material

Trees from four Belgrade municipalities were used for monitoring plant's response to oxidative stress during growing season. Location of all trees were given as GPS coordinates in Table 1. Sampling for biochemical measurements was performed twice, at the beginning and at the end of the growing season.

Table 1 *Location (GPS coordinates) of all trees used for monitoring seasonal variation in biochemical parameters*

Tree species	GPS coordinates	Tree species	GPS coordinates
1. *Ginkgo biloba* L.	44.798430, 20.465322	10. *Taxus baccata* L.	44.782968, 20.420341
2. *Ginkgo biloba* L.	44.790244, 20.440110	11. *Taxus baccata* L.	44.817950, 20.452024
3. *Cupressus arizonica* Greene	44.787843, 20.454914	12. *Taxus baccata* L.	44.817950, 20.452024
4. *Fagus sylvatica* L.	44.785460, 20.449492	13. *Cedrus atlantica* (Endl.) Manetti ex Carrière	44.786608, 20.447019
5. *Fagus sylvatica* L.	44.822933, 20.454354	14. *Quercus robur* L.	44.819501, 20.451536
6. *Pinus wallichiana A.B.Jacks.*	44.791531, 20.432272	15. *Platanus acerifolia* (Aiton) Willd.	44.798904, 20.472900
7. *Magnolia x soulangeana* Soul.-Bod f. *Lennei*	44.787416, 20.454242	16. *Aesculus hippocastanum* L.	44.821523, 20.464327
8. *Magnolia x soulangeana* Soul.-Bod.	44.790242, 20.439805	17. *Corylus colurna* L.	44.821275, 20.450662
9. *Taxus baccata* L.	44.787561, 20.454018		

Five samples of twenty fully developed leaves per tree for biochemical measurements were immediately frozen in liquid nitrogen and stored at -80°C. For both antioxidative capacity and POD activity, leaf samples were finely ground to powder in liquid nitrogen.

Determination of POD activity

Class III peroxidase (PODs, EC 1.11.1.7) was measured according to Kukavica *et al*. [9], with some modifications. Homogenized leaves were extracted in 100 mM sodium phosphate buffer (pH 6.5) with 2 mM EDTA, 2 mM PMSF (phenylmethanesulfonyl fluoride) and 5% (*w*/*v*) insoluble polyvinylpyrrolidine (PVP). Obtained homogenate was centrifuged at 10 000 *g* for 10 min at 4°C. The POD activity was measured spectrophotometrically in a reaction mixture consisting of 100 mM K-phosphate buffer pH 6.5, 20 mM guiacol and aliquots of plant fraction. The reaction was started by addition of 5 mM H_2O_2, and an increase in absorbance at 470 nm was followed. Activity of POD was calculated using the extinction coefficient for guiacol ($\varepsilon = 26.6\ mM^{-1}cm^{-1}$).

Antioxidative capacity

The total antioxidative capacity of leaf samples was analyzed according to the protocol from Cano *et al*. [11]. The reaction mixture contained 2 mM 2,2'-azino-bis (3-ethylbenzothiazoline-6-sulphonic acid) (ABTS), 0.015 mM H_2O_2 and 0.25 µM horseradish peroxidase (HRP) in 50 mM potassium phosphate buffer (pH 7.5) and 50 µl of methanol plant extract. The decrease in absorbance due to the depletion of radical was measured at 730 nm. Ascorbic acid was used as a standard to form a standard curve in order to determine the relative antioxidative capacity of samples.

Statistical analyses

Significant differences in POD and total antioxidative activity between spring and autumn leaf samples were determined using a Student t-test. The significance threshold value was set at $P \leq 0.05$. This test was conducted with IBM SPSS statistics software (Version 268 20.0, SPSS Inc., Chicago, USA).

RESULTS AND DISCUSSION

Monitoring of POD level is an indicative way of determining the plant health status long before the damage becomes visible. Therefore, in this research special attention was brought to measuring activity of PODs in the trees' leaves during growing season [8].

It has been shown that plant species, like *Magnolia spp.* accumulate high levels of heavy metals (Pb, Cd and Cu) in urban areas compared to the suburbs, which implies their tolerant potential to air polluted environment. Consequently, it is recommended to be planted in industrialized urban areas and city parts with heavy traffic conditions [11,12]. In our research, POD activity was elevated by more than 25% in *Magnolia spp.* samples from the autumn in comparison to spring, while the total antioxidant capacity was increased by more than half, Figure 1. Also, increased POD level was also observed in *Fagus sylvatica* L. leaves in the end of the experiment, which is in accordance with induced antioxidative defence [13]. The opposite trend was noticed in *Cedrus atlantica* (Endl.) Manetti ex Carrière needles, where decreased POD activity in autumn was accompanied with decreased total antioxidative activity [14]. In our study an accumulation of antioxidative components in the leaves of

Platanus acerifolia (Aiton) Willd. found in autumn is linked to elevated POD activity in a study which deals with the heavy metal's influence on trees ecophysiological parameters in urban area [15].

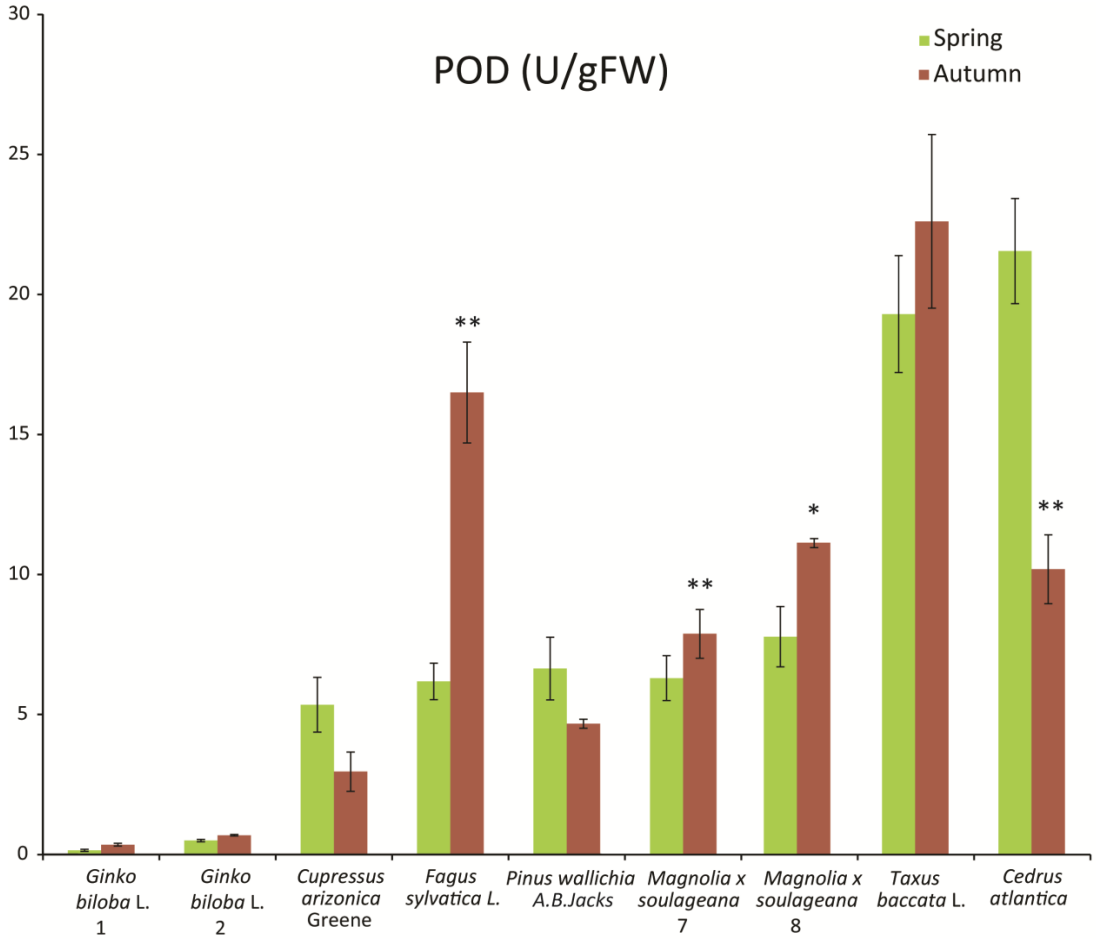

Figure 1 *POD activity in different plant species during growing season. Results represent mean ± SE (n ≥ 5). Significant differences between Spring and Autumn according to the Student's t-test are indicated (*P < 0.05, **P < 0.01)*

Seasonal variations in the antioxidant capacity were investigated in the leaves of *Quercus robur* L. in Hungarian forests during vegetation period [16]. Similarly, in our study, the antioxidative capacity was also reduced by 30% by the end of the growing season, Table 2. Also, decreased antioxidative capacity was noticed in *Aesculus hippocastanum* L. leaves in the end of the experiment [16]. Besides its well-known medicinal, food and pharmaceutical properties, *Ginkgo biloba* L, a living fossil tree, possesses a high potential for absorbing air pollutants. Therefore, in comparison with *Magnolia spp.* and *Cedrus atlantica (Endl.) Manetti ex CarrièreMan.*, *Ginkgo biloba* L. has medium value for metal accumulation index [12]. Moreover, in our research, antioxidative capacity of *Ginkgo biloba* L. leaves in the autumn was doubled.

Table 2 *Total antioxidant capacity (TAC) in extracts of the leaves of the examined plant species shown in equivalents of ascorbic acid in period from April to October. Results represent mean ± SE (n ≥ 5). Significant differences between Spring and Autumn according to the Student's t-test are indicated (*P < 0.05, **P < 0.01, ***P < 0.001)*

Tree species	Spring	Autumn
	TAC [ekq mmol Asc]	
1. *Ginkgo biloba* L.	0.77 ± 0.04	1.21 ± 0.1*
2. *Ginkgo biloba* L.	0.44 ± 0.02	0.99 ± 0.07***
3. *Cupressus arizonica* Greene	3.22 ± 0.08	2.91 ± 0.06***
4. *Fagus sylvatica* L.	1.76 ± 0.05	2.25 ± 0.09***
5. *Fagus sylvatica* L.	1.22 ± 0.31	/
6. *Pinus wallichiana A.B.Jacks.*	2.53 ± 0.07	1.47 ± 0.04***
7. *Magnolia x soulangeana Soul.-Bod forma f. Lennei*	1.07 ± 0.04	1.83 ± 0.08***
8. *Magnolia x soulangeana Soul.-Bod.*	0.61 ± 0.05	0.98 ± 0.09*
9. *Taxus baccata* L.	2.47 ± 0.03	2.74 ± 0.07
10. *Taxus baccata* L.	1.01 ± 0.04	0.92 ± 0.02**
11. *Taxus baccata* L.	0.74 ± 0.04	0.64 ± 0.02**
12. *Taxus baccata* L.	0.79 ± 0.06	0.72 ± 0.10
13. *Cedrus atlantica (Endl.) Manetti ex CarrièreMan.*	2.38 ± 0.07	1.37 ± 0.08***
14. *Quercus robur* L.	1.06 ± 0.04	0.70 ± 0.01***
15. *Platanus acerifolia* (Aiton) Willd.	1.35 ± 0.03	1.42 ± 0.02**
16. *Aesculus hippocastanum* L.	1.05 ± 0.08	0.53 ± 0.06**
17. *Corylus colurna* L.	0.68 ± 0.06	0.76 ± 0.03*

CONCLUSION

Proposed measuring of biochemical parameters is an efficient approach to pinpoint tree species which are more suitable for planting in industrialized urban areas. Leaves of trees are suitable to be used as indicators of the overall fitness of the tree, via these two suggested methods, even before any symptoms of disease or stress are visible. Overall, we can conclude that *Magnolia spp.* and *Fagus sylvatica L.* species are particularly suitable trees for planning urban landscapes, as they proved to be resistant to hazardous environmental conditions.

ACKNOWLEDGEMENT

The authors are grateful to the Ministry of Science, Technological Development and Innovation of the Republic of Serbia for financial support according to the contract with the registration number (451-03-47/2023-01/ 200053), Center for Green Technologies, University of Belgrade and JKP Zelenilo, City of Belgrade.

REFERENCES

[1] Dadkhah-Aghdash H., Rasouli M., Rasouli K., *et al*., Sci. Rep. 12 (1) (2022) 15398.

[2] Alahabadi A., Ehrampoush M. H., Miri M., *et al*., Chemosphere 172 (2017) 459–467.

[3] Morina F., Vidović M., Srećković T., *et al*., Bull. Environ. Contam. Toxicol. 99 (2017) 706–712.

[4] Badach J., Dymnicka M., Baranowski A., Sustainability 12 (3) (2020) 1258.

[5] Ferrini F., Fini A., Mori J., *et al*., Sustainability 12 (10) (2020) 4247.

[6] Munné-Bosch S., Queval G., Foyer C. H., Plant Physiol. 161 (2013) 5–19.

[7] Apel K., Hirt H., Annu. Rev. Plant Biol. 55 (2004) 373–399.

[8] Puccinelli P., Anselmi N., Bragaloni M., Chemosphere 36 (4–5) (1998) 889–894.

[9] Kukavica B., Veljović Jovanović S., Menckhoff Lj., *et al*., J. Exp. Bot, 63 (12) (2012) 4631–4645.

[10] Cano A., Hernández-Ruíz J., García-Cánovas F., *et al.*, Phytochem. Anal. 9 (4) (1998) 196–202.

[11] Zhang P., Liu Y., Chen X., *et al.*, Ecotoxicol. Environ. Saf. 132 (2016) 212–223.

[12] Liang J., Fang H. L., Zhang T. L., *et al*., Urban For. Urban Green. 27 (2017) 390–398.

[13] Kadinov G., Ananieva K., Gesheva E., *et al*., Genet. Plant Physiol. 7 (1–2) (2017) 34–48.

[14] Hofmann T., Visi-Rajczi E., Albert L., Ind. Crops Prod. 145 (2020) 111935.

[15] Baycu G., Tolunay D., Özden H., *et al*., Environ. Pollut. 143 (3) (2006) 545–554.

[16] Tálos-Nebehaj E., Hofmann T., Albert L., Ind. Crops Prod. 98 (2017) 53–59.

30th International Conference Ecological Truth & Environmental Research
20–23 June 2023, Serbia

ACCLIMATION OF PEDUNCULATE OAK SEEDLINGS TO DIFFERENT LIGHT CONDITIONS IN THE FIRST MONTHS AFTER GERMINATION

Nikola Šušić[1], Sonja Milić Komić[1], Bojana Živanović[1], Aleksandra Jelušić[1], Sanja Marković[1], Ana Sedlarević Zorić[1], Sonja Veljović Jovanović[1*]

[1]University of Belgrade, Institute for Multidisciplinary Research, Kneza Višeslava 1, 11030 Belgrade, P.O. Box 33, SERBIA

[*]*sonjavel@imsi.bg.ac.rs*

Abstract

The first months are the most sensitive phase of oak seedling development. Light conditions have an important role in this sense, both from the physiological and management viewpoint. We investigated the response of pedunculate oak seedlings to three growth light intensities (100, 550 and 2000 µmol $cm^{-2}s^{-1}$) during development of the first and second growth flush. The low and high light intensities of PAR are supposed to mimic the effects of solar radiation under extreme natural conditions (closed canopy and open field). The response of seedlings to different light intensities was evaluated by determining the photochemical activity of photosystem II, leaf chlorophyll concentration and epidermal flavonoid accumulation for both growth flushes. At the end of the experiment (after 4.5 months) the effects of different treatments on growth parameters were also determined. We showed here that oak seedlings responded to varying light intensities by modifying their physiological and morphological traits of successive growth flushes. At medium light, seedlings had the highest PSII photochemical activity in the 2nd flush. High light induced very low photochemical efficiency of photosystem II in both growth flushes indicating the development of high non-photochemical quenching of chlorophyll fluorescence as part of photoprotective mechanism. In accordance with high photosynthetic yield at ML, the investment of photosynthates in growth, especially biomass allocation towards root system was confirmed. ML was optimal for seedling development in the first months. The results may contribute to a better understanding of oak seedling development and acclimation and could have importance for oak natural regeneration.

Keywords: growth flush, photochemical efficiency, morphological parameters.

INTRODUCTION

The early stages of oak seedling development are crucial for their establishment and competitiveness with other tree species and herbaceous plants [1]. Although many factors influence seedling growth, light conditions can be considered as one of the most important determinants of oak seedling development [2–4]. Morphological traits were widely used for characterization of oak seedlings development or growth in various studies on different species [4,5]. However, the underlying physiological mechanisms of the morphological changes are of essential importance for understanding acclimation to natural conditions and for application in oak regeneration management [6]. Multi-flush growth is a characteristic morphological trait for pedunculate oak, both in juvenile and adult individuals [6–8] and implies a rhythmic growth pattern that is under strong genetic control [9]. Although this

growth pattern is found in pedunculate oak seedlings in a wide light gradient (from closed canopies with no more than 5% sunlight to full sunlight, in the open areas), it can be stimulated by silvicultural measures in order to increase pedunculate oak competitiveness against surrounding vegetation [1,7].

The aim of this study was to investigate how pedunculate oak seedlings respond in their early phase of development (first 4.5 months) and acclimate to three different light intensities of photosynthetically active radiation (PAR) by assessing: i) photochemical activity of photosystem II (PSII), leaf total chlorophyll (Chl) and epidermal flavonoid (EpFlav) contents during the first two growth flushes and ii) morphological parameters such as fresh weight, dry weight, shoot/root ratio, leaf area and specific leaf area.

MATERIALS AND METHODS

Plant material and experimental design

The acorn was collected in pedunculate oak forest in Morović in a stand that belongs to the Sava-Danube provenance (Serbia). The acorns of good quality and similar size were selected and planted in 12 plastic containers (each with one acorn) at 1–2 cm depth filled with Klasmann Potground H commercial substrate. The seedlings were grown in a growth chamber under controlled conditions: 14/10 h day/night photoperiod, 26 °C temperature and relative humidity of 40–50%.

From the start of the experiment, the seedlings were divided into three groups (four seedlings each) growing in the following light intensities: low light (~100 µmol cm^{-2} s^{-1}, LL); medium light (~550 µmol cm^{-2} s^{-1}, ML) and high light (~2000 µmol cm^{-2} s^{-1}, HL). The plants were grown for about 18 weeks.

Chlorophyll fluorescence measurements, leaf chlorophyll and epidermal flavonoid contents

The photosynthetic yield (YPSII) was derived from measuring modulate pulse chlorophyll fluorescence using Junior PAM portable chlorophyll fluorometer (Gadermann Instruments GmbH, Würzburg, Germany). Measurements of photochemical activity [Y(II)], were calculated using the WinControl software (v3.29; Heinz Walz GmbH, Effeltrich, Germany) as described by Van Kooten and Snel [10] and were performed continuously during 24 h by applying a saturating pulse (10,000 µmol $m^{-2}s^{-1}$) every 20 minutes. Changes in diurnal photosynthetic activity were followed on a mature leaf of each seedling on two development stages [after the formation of the 1^{st} flush (6 weeks after planting) and the 2^{nd} flush (10 weeks after planting)]. Total chlorophyll content (Chl), the content of leaf epidermal flavonoids (EpFlav) and the nitrogen balance index (NBI) were determined using Dualex FLAV (Force-A, Orsay, France; Cerović *et al.* [11]) on the basis of three leaves per plant 14 weeks after planting.

Morphological parameters

Fresh (FW) and dry weight (DW) of stem, roots and leaves were measured 18 weeks after planting. Dry weight data were used for calculation of the shoot/root ratio. Total leaf area per plant (LA) was measured using ImageJ software [12], while specific leaf area (SLA) was expressed as the ratio between leaf area and dry weight per plant.

Statistical analysis

Two-way ANOVA was used to determine the effects of light intensity and growth flush on NBI, Chl and EpFlav mean values. Fisher's LSD test was used for determination of differences between the treatments with a 0.05 significance threshold. The same test was used for determination of significant differences between the mean values of the analysed morphological parameters. The experimental data were analysed using software package Statistica 8.0.

RESULTS AND DISCUSSION

After 6 weeks when the first growth flush was formed, Y(II) was constant during the day with expected variations in the HL treatment. Upon darkening, Y(II) attained their maximal values by a similar rate within the first 80 minutes. Interestingly, ML and HL treatments brought about similar Y(II) throughout the day.

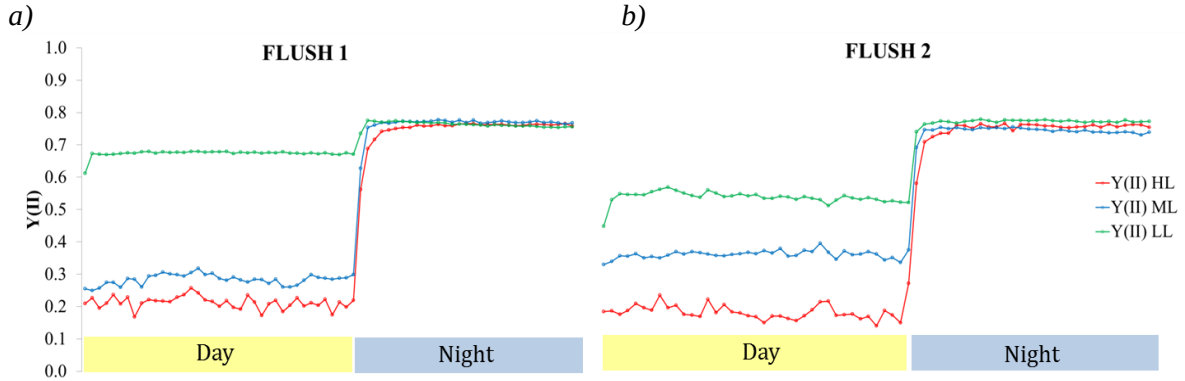

Figure 1 *Diurnal photochemical efficiency of photosystem II [Y(II)] of pedunculate oak seedlings a) 6 weeks (1st flush) and b) 10 weeks (2nd flush) after planting*

After 10 weeks, once the seedlings have developed another growth flush, Y(II) at LL was reduced, while at ML plants showed an increase in photochemical activity (Figure 1). The results show that oak seedlings acclimated in the 2nd flush compared to the 1st flush. By increasing light intensity, root growth was stimulated in the 18-week-period (by 57% in HL and 81% in ML conditions, compared to LL conditions). With increasing light intensity, oak seedlings also showed a tendency to increase the dry weight of leaves and stem, even though this was not confirmed by LSD test. The shoot/root ratio of all oak seedlings showed that the largest part of the biomass was allocated to root (57–64%). Previous research on one- or two-years-old seedlings showed that the shoot/root ratio is generally higher in low light conditions [3,13]. However, this was not confirmed in our study, because of the shorter investigated time span, as the differentiation in the shoot/root ratio between the treatments probably occurs somewhat later in the seedling development. As expected, with increasing light intensity, LA decreases due to higher leaf thickness, as indicated by SLA, that may be explained by acclimatization to high light and multiplication of palisade cells in order to increase CO_2 assimilation [14]. Such morphological plasticity was observed on cork oak seedlings under a

light gradient [4]. The plants in excess light of the HL treatment, which was noticed for some leaves, showed photoinhibition based on observed chlorophyll damage (Figure 2a).

Table 1 *Morphological parameters of pedunculate oak seedlings 18 weeks after planting (different letters indicate significant differences on the basis of LSD test)*

Light intensity	**LL**	**ML**	**HL**
Leaves FW (g)	4.19 ± 0.44 a	6.25 ± 1.09 a	5.39 ± 0.77 a
Stem FW (g)	3.02 ± 0.27 a	5.37 ± 1.20 a	4.34 ± 0.36 a
Roots FW (g)	13.02 ± 2.00 a	20.84 ± 2.11 b	18.01 ± 1.30 ab
Plant FW (g)	20.23 ± 4.04 a	32.47 ± 8.35 b	27.74 ± 3.13 ab
Leaves DW (g)	1.63 ± 0.18 a	2.61 ± 0.43 a	2.44 ± 0.33 a
Stem DW (g)	1.31 ± 0.16 a	2.57 ± 0.61 a	2.09 ± 0.30 a
Roots DW (g)	4.85 ± 0.88 a	8.80 ± 1.02 b	7.63 ± 1.33 ab
Plant DW (g)	7.80 ± 1.80 a	13.98 ± 3.93 b	12.16 ± 2.09 ab
Leaves FW/DW	2.57 ± 0.02 a	2.39 ± 0.07 a	2.35 ± 0.62 a
Stem FW/DW	2.32 ± 0.07 a	2.13 ± 0.06 a	2.11 ± 0.11 a
Roots FW/DW	2.71 ± 0.08 a	2.39 ± 0.07 a	2.46 ± 0.30 a
Shoot/root ratio	0.64 ± 0.11 a	0.57 ± 0.08 a	0.64 ± 0.16 a
LA (m^2)	279.1 ± 18.8 ab	316.8 ± 48.7 b	189.8 ± 22.2 a
SLA ($cm^2g^{-1}DW$)	36.8 ± 4.33 b	22.5 ± 1.01 a	16.31 ± 3.56 a

*Rows with significance differences between some of the treatments are marked grey.

As a result of increasing light intensity, flavonoids accumulated in the epidermal layer of leaves to fulfil their sun protective function (Figure 2). EpFlav are also indicators of higher stimulation of phenylpropanoids biosynthesis, on account of primary metabolites, which was followed by decreasing NBI. These results are in accordance with the changed trade-off strategy of plants.

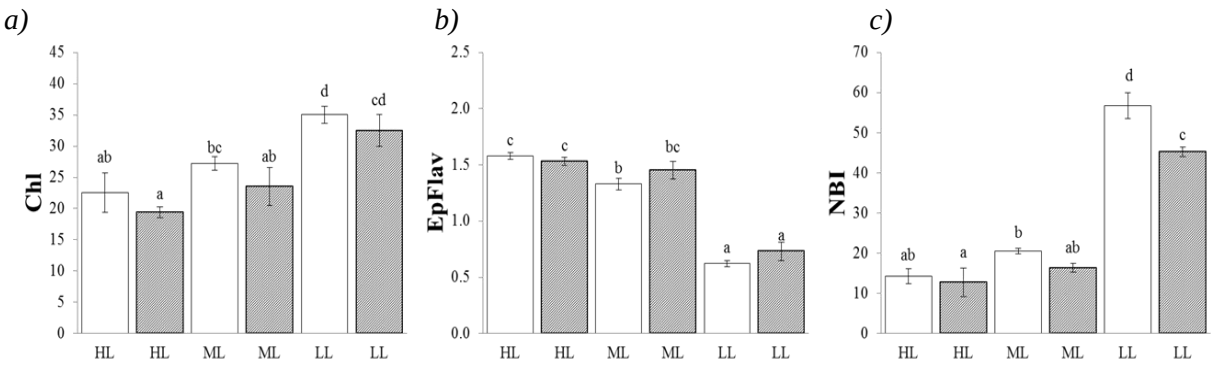

Figure 2 *a) Chlorophyl content (Chl), b) leaf epidermal flavonoid content (EpFlav) and c) nitrogen balance index (NBI) under high (HL), medium (ML) and low light (LL) conditions in first flush leaves (white bars) and second flush leaves (grey bars). Different letters indicate significant differences on the basis of LSD test*

Regardless of light conditions, pedunculate oak produces 2nd growth flush, which is in line with previous research [6,7]. The seedlings employ this 2nd flush to acclimate to the environmental conditions which was confirmed in our research [6].

CONCLUSION

Oak seedlings acclimated to the given environmental conditions by modifying some of the observed morphological and physiological traits in the successive growth flush. We found that optimal growth conditions in the first few months of oak seedling development are in the medium light treatment that corresponds to about 50% of the maximum daily sunlight. In these conditions, pedunculate oak seedlings produced highest total biomass while improving their photochemical efficiency in the second growth flush. In low light (closed canopy conditions), a reduction of photochemical efficiency was noted. Seedlings grown under high light showed a constant, but very low photochemical efficiency of photosystem II in both growth flushes. This, however, may partly be attributed to excessive light for 14 hours a day. The results may contribute to better understanding of oak seedlings development and acclimation that may have importance for oak natural regeneration.

ACKNOWLEDGEMENT

The authors are grateful to the Ministry of Science, Technological Development and Innovation of the Republic of Serbia for financial support according to the contract with the registration number (451-03-47/2023-01/ 200053) and to the Center for Green Technologies, University of Belgrade. We would like to express our gratitude to MSc Andrijana Bauer Živković from Public Enterprise „Vojvodina šume" for providing us with acorn used in the experiment.

REFERENCES

[1] Bobinac M., Ecology and regeneration of hygrophilous common oak Forests of Ravni srem, Hrvatski šumarski institut Jastrebarsko, Institut za šumarstvo, Belgrade, Zagreb (2011), p.294, ISBN: 978-953-98401-9-6.

[2] Sevillano I., Short I., Grant J., *et al*., For. Ecol. Man. 374 (2016) 11–19.

[3] Kolb T. E., Steiner K. C., McCormic L. H., *et al*., For. Ecol. Man 38 (1990) 65–78.

[4] Cardilo E., Bernal C. J., For. Ecol. Man. 222 (2006) 296–301.

[5] Šušić N., Bobinac M., Andrašev S., *et al*., Šum. List 143 (5–6) 221–229.

[6] Jensen A. M., Löf M., Gardiner E. S., EEB 71 (2011) 367–375.

[7] Bobinac M., Šumarstvo 1–2 (47) (1994).

[8] Bobinac M., Batos B., Miljković D., *et al*., Arch. Biol. Sci. 64 (1) (2012) 97–105.

[9] Herrmann S., Recht S., Boenn M., *et al*., JEB 66 (22) (2015) 7113–7127.

[10] Van Kooten O., Snel J. F., Photosynth. Res. 25 (1990) 147–150.

[11] Cerović Z. G., Masdoumier G., Gnozlen N. B., *et al*., Physiol. Plant. 146 (3) (2012) 251–260.

[12] Schneider C. A, Rasband W. S., Eliceiri K. W., Nat. Methods 9 (7) (2012) 671–675.

[13] van Hees A. F. M., Ann. Sci. For. 54 (1997) 9–18.

[14] Givinish T. J., Aust. J. Plant Physiol. 15 (1988) 63–92.

BENTHIC DIATOMS AS PROXY FOR THE ECOLOGICAL CONDITIONS OF THE RIBNICA RIVER, SERBIA

Božica Vasiljević[1*], Jelena Đuknić[1], Nikola Marinković[1]

[1]University of Belgrade, Institute for Biological Research "Siniša Stanković" – National Institute of the Republic of Serbia, Bulevar despota Stefana 142, Belgrade, SERBIA

[*]*bozica@ibiss.bg.ac.rs*

Abstract

Benthic diatoms of the Ribnica River situated in Valjevo karst area were not studied so far. The objective of this paper is to provide base data on diatom community of the Ribnica River, through diversity, abundance, diatom ecological guilds, and to estimate its preliminary ecological status according to national regulations. Phytobenthos sampling and laboratory work was done by national standards. Analysis of diatom community was based on identification, enumeration, and classification into ecological guilds. Indicative ecological status was assessed according to IPS and CEE diatom indices. At the Ribnica River in total 52 diatom taxa were recorded, and also high taxa richness at each locality. The most frequent and numerous were diatoms Achnanthidium minutissimum, A. pyrenaicum and Encyonopsis subminuta. Low profile ecological guild, typical for fast flowing streams with lower nutrient concentrations was dominant in the Ribnica River. Diatom indices IPS and CEE reviled excellent ecological status.

Keywords: epilithic diatoms, ecological guilds, hilly-mountain river, ecological status.

INTRODUCTION

The Ribnica River is located in the western Serbia, and belongs to the Kolubara River basin. It originates at altitude of 300m in the village Brežđe, and after 22 km flows into the Kolubara River, near Mionica. The Ribnica River is an allogeneic watercourse of the Valjevo karst zone. Its river valley consists of canyons and gorges, with erosive widenings occurring [1]. It is positioned in the area where mountainous shifts to hilly region.

Previous data on diatoms of the Ribnica River refer to cave biofilms. Being part of karst relief, the Ribnica River has 12 caves, of diverse sizes and located at different altitudes [1]. Diatom taxa *Nitzschia* Hassall spp. and aerophilous *Hantzschia amphyoxis* (Ehrenberg) Grunow were found only on the entrance of Ribnica Cave floor, in accumulated soil and mud [2], as well as *Humidophila contemnata* (E. Reichardt) Lowe, Kociolek, Johansen, Van de Vijver, Lange-Bertalot & Kopalová and *H. paracontenta* (Lange-Bertalot & Werum) Lowe, Kociolek, Johansen, Van de Vijver, Lange-Bertalot & Kopalová [3].

The objective of this paper is to provide starting point on benthic diatom community of the Ribnica River, through diversity, abundance, diatom ecological guilds, and to estimate its preliminary ecological status according to national regulations.

MATERIALS AND METHODS

Epilitic phytobenthos samples at the Ribnica River were collected from the four localities (Figure 1) [4]. Samples were cleaned in the laboratory using a hot acid method; afterwards permanent slides were prepared [4]. Diatom taxa on slides were observed and photographed using light microscope Zeiss Axio Lab1 with Axiocam ERc 5s camera and ZEN software. Identification was done according to standard taxonomy literature and relative abundance by counting 400 diatom valves at each slide [5]. Identified diatoms were grouped in ecological guilds [6,7]. Indices Shannon diversity index [8], IPS diatom index [9] and CEE diatom index [10] were calculated in OMNIDIA software [11]. Ecological status classes based on IPS and CEE were determined by the guidance of national laws [12,13,14].

RESULTS AND DISCUSSION

During phytobenthos survey at the Ribnica River, 52 diatom taxa were recorded. The greatest number of taxa was identified among genera *Cymbella* (11) and *Nitzschia* (9).

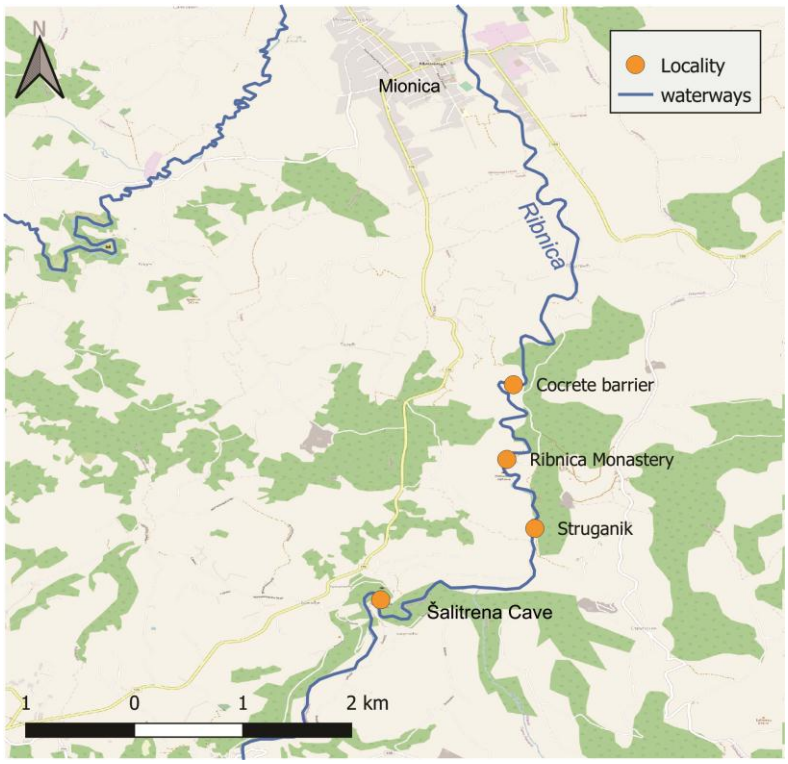

Figure 1 *Phytobenthos sampling sites at the Ribnica River*

Biological integrity status of the Ribnica River was assessed by taxa richness and Shannon diversity index. The highest taxa richness was recorded at the localities Concrete barrier (41) and Struganik (38), with highest values of Shannon diversity index (4.04 and 3.94, respectively). High taxa richness was also noted at locality Šalitrena Cave (35) and Ribnica Monastery (31), nevertheless values of Snannon diversity index were lower (2.82 and 3.06, respectively), due to the uneven distribution of taxa – dominance of two or three species which together attributed with abundance of nearly 70% (Figure 2).

The most frequent diatom taxa, recorded in all samples collected from the Ribnica River were *Achnanthidium minutissimum* (Kützing) Czarnecki, *A. pyrenaicum* (Hustedt) H.Kobayasi, *Cocconeis euglypta* Ehrenberg, *Cymbella compacta* Oestrup, *C. neolanceolata* W. Silva, *Diatoma moniliformis* (Kützing) D.M.Williams, *Encyonema auerswaldii* Rabenhorst, *Encyonopsis subminuta* Krammer & E.Reichardt, *Gomphonema parvulum* (Kützing) Kützing, *Navicula capitatoradiata* Germain, *Navicula cryptotenella* Lange-Bertalot, *Navicula tripunctata* (O.F.Müller) Bory, *Nitzschia dissipata* (Kützing) Grunow, *N. lacuum* Lange-Bertalot and *Ulnaria acus* (Kützing) Aboal. The most abundant species during investigation at the Ribnica River were *Achnanthidium minutissimum* and *A. pyrenaicum* (Figure 2). *A. minutissimum* is generally one of the most frequent diatoms, with very wide ecological amplitude. *A. pyrenaicum* can be found in high numbers in hilly-mountain, calcium-bicarbonate rich, ologotrophic and mesotrophic rivers [15]. Species *Encyonopsis subminuta* and *E. minuta* Krammer & Reichardt, with ecological preferences similar as *A. pyrenaicum*, were also very abundant in the Ribnica River during sampling in 2022 (Figure 2). *Cymbella affinis* Kützing, was the most abundant at the locality Ribnica Monastery (Figure 2). It is common epiphytic species in hilly-mountain, usually mesotrophic watercourses.

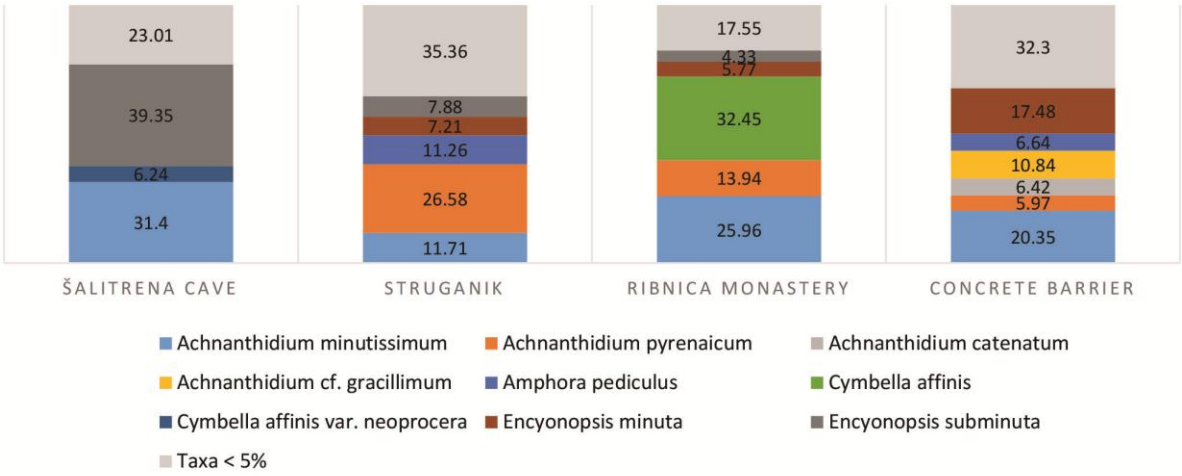

Figure 2 *Relative abundance (%) of diatoms recorded in more than 5% at surveyed localities of the Ribnica River*

Trait-based approaches are useful tool for complementing ecological studies [16], as they provide valuable information on changes in aquatic environment [17]. One of the metrics are ecological guilds – groups of diatom taxa that live in the same habitat, nonetheless they adapt in different ways to predominant abiotic conditions [6,7,17]. In the Ribnica River, the dominant ecological guild was low profile (Figure 3), represented by genera *Achnanthidium*, *Amphora*, *Cocconeis*, *Encyonopsis*, *Reimeria*, *Rhoicosphenia*, smaller *Cymbella* species and *Encyonema procerum* Krammer. This guild includes taxa of short stature, adhering to the substrate with entire valve surface, apically attached parallel or perpendicular to the substrate, as well as slow moving taxa, adapted to high current velocities, and low nutrients concentrations [6,7]. High profile guild comprises large stalked species, or species that form

colonies. These taxa are susceptible to water turbulence, and prefer increase of nutrients concentrations. At the Ribnica River high profile guild is represented by genera *Amphipleura*, *Diatoma*, *Encyonema*, *Gomphonella*, *Gomphonema*, *Fragillaria*, *Ulnaria*, large *Cymbella* species, and *Achnanthidium catenatum* (Bily & Marvan) Lange-Bertalot. Motile guild consists of fast moving species, which are adapted to finer substrate granulation and higher nutrient concentrations [6]. Motile diatoms in the samples from the Ribnica River were *Fallacia* sp., and species belonging to genera *Navicula* and *Nitzschia*. Increased percentage share of high profile and motile guild in diatom community was recorded at locality Concrete barrier (Figure 3). Sample was taken from the part of the watercourse above the barrier, which caused slower current velocity and partly blocked transport of fine fraction substrate, resulting in ecological conditions favorable to diatoms belonging to high and motile guild.

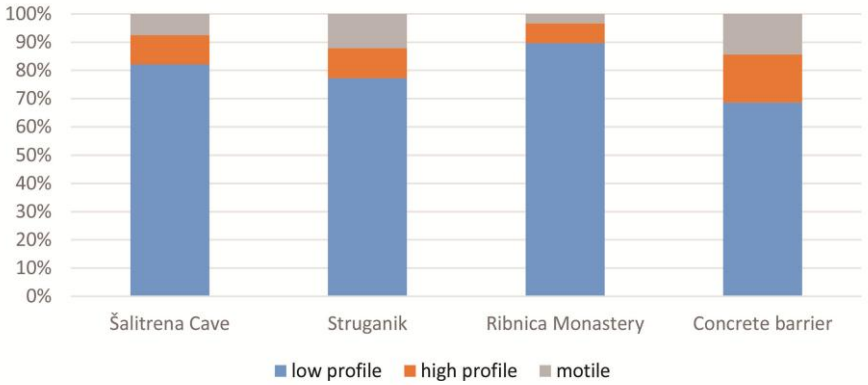

Figure 3 *Percentage share of diatom ecological guilds at surveyed localities of the Ribnica River*

According to national typology [13,14], the Ribnica River belongs to type 3 watercourse, thus ecological status classes are determined by IPS and CEE indices. Both indices values were higher than boundary values set between first and second ecological status classes (Figure 4), and revealed excellent preliminary ecological status at all investigated localities, based on benthic diatom community.

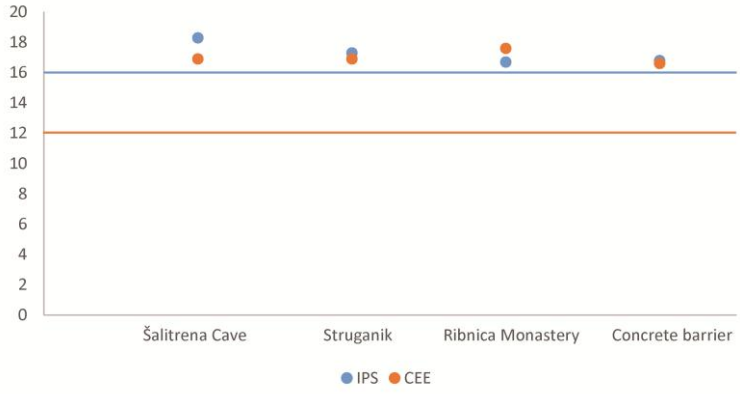

Figure 4 *Values of diatom indices IPS and CEE at surveyed localities of the Ribnica River (dots). Lines represent boundary values between first and second ecological status class [14], for IPS (blue line), and CEE (orange line)*

CONCLUSION

Conducted study mainly included localities in the middle stretch of the Ribnica River. Composition of the benthic diatom community indicated high taxa richness. Classification of diatom ecological guilds clearly described existing ecological conditions. Dominance of low profile guild is typical for fast flowing streams with lower nutrients concentrations. In the part of the flow immediately upstream barrier, rise in the species share belonging to high and motile guild was noted, due to slower water velocity, presence of smaller substrate fractions, and slight increase in nutrient concentrations. Diatom indices IPS and CEE reviled excellent preliminary ecological status.

ACKNOWLEDGEMENT

Work on this paper was supported by Ministry of Science, Technological Development and Innovation of Republic of Serbia (contract number: 451-03-47/2023-01/ 200007).

REFERENCES

[1] Stanojević D. Zbornik radova, Geografski fakultet, Univerziteta u Beograd, 57 (2009) 47–58.

[2] Popović S., Simić G., Stupar M., *et al*., J. Cave Karst Stud. 79 (1) (2017) 10–23.

[3] Nikolić N., Popović S., Vidaković D., *et al*., Arch. Biol. Sci. 72 (2) (2020) 279–289.

[4] SRPS EN 13946:2015. Kvalitet vode – Uputstvo za rutinsko uzimanje uzoraka i pripremu preparata bentosnih silikatnih algi reka i jezera.

[5] SRPS EN 14407:2015. Kvalitet vode – Uputstvo za identifikaciju i utvrđivanje brojnosti bentosnih silikatnih algi iz reka i jezera.

[6] Passy S., Aquatic Botany 86 (2007) 171–178.

[7] Rimet F., Bouchez A., Knowl. Manag. Aquat. Ecosyst. (406) (2012) 01.

[8] Shannon C.E., BSTJ 27 (1948) 379–423.

[9] Cemagref. Etude des methods biologiques d'appré-ciation quantitative de la qualitédes eaux. Rapport Q. E. Lyon, Agence de l'eau Rhöne-Me´diterrane´e-Corse-Cemagref, Lyon, France (1982).

[10] Descy J. P., Coste M., Verhandlung Internationale Vereingung de Limnologie 24 (1991) 2112–2116.

[11] Lecointe C., Coste M., Prygiel J., Hydrobiologia 269/270 (1993) 509–513.

[12] Službeni glasnik Republike Srbije 30/2010. Zakon o vodama.

[13] Službeni glasnik Republike Srbije 96/2010. Pravilnik o utvrđivanju vodnih tela površinskih i podzemnih voda.

[14] Službeni glasnik Republike Srbije 74/2011. Pravilnik o parametrima ekološkog i hemijskog statusa površinskih voda i parametrima hemijskog i kvantitativnog statusa podzemnih voda.

[15] Lange-Bertalot H., Hofmann G., Werum, *et al*., Schmitten-Oberreifenberg: Koeltz Botanical Books (2017), p.942, ISBN: 978-3-946583-06-6.

[16] De Castro-Català N., Dolédec S., Kalogianni E., *et al*., Sci. Total Environ. 742 (2020) 140543.

[17] Peszek Ł., Zgrundo A., Noga T., *et al*., Ecol. Indic. 125 (2021) 107579.

BLASTING MATS FOR THE PROTECTION OF PEOPLE, STRUCTURES AND THE ENVIRONMENT IN PROXIMITY TO THE BLAST SITE

Milanka Negovanović[1*], Lazar Kričak[1], Stefan Milanović[1], Jovan Marković[1], Nikola Simić[1], Snežana Ignjatović[1]

[1]University of Belgrade, Faculty of Mining and Geology, Djusina 7, 11000 Belgrade, SERBIA

[*]*milanka.negovanovic@rgf.bg.ac.rs*

Abstract

The explosive energy released during the detonation process in a blasthole is used to fragment the solid rock mass into fragments of different shapes and sizes, depending on the properties of the rock and the optimization of drilling and blasting parameters. In addition to positive effects of rock blasting, there are certain side effects of each blasting process which may occur, and these are: ground vibration, flyrock, airblast, toxic and suffocating fumes and dust. Flyrock is the uncontrolled throwing out of fragments of blasted rock mass and represents one of the main causes of material damage and harm to people. Blasting mats can be used to cover the blasting site in order to protect the surroundings against damage or serious accidents. Blasting mats provide the best protection from negative effects of rock blasting especially the elimination of flyrock, reduction of shock wave and noise. Blasting mats should be always used during urban blasting, demolition blasting or in rock blasting in surface mines and secondary blasting when there is an increased risk of flyrock.

Keywords: blasting mat, covering, flyrock, blasting.

INTRODUCTION

Flyrock, also called rock throw, is the uncontrolled propelling of rock fragments produced in blasting operation and constitutes one of the main sources of material damage and harm to people [1]. Institute of Makers of Explosives (IME) has defined flyrock as the rock propelled beyond the blast area by the force of an explosion [2]. When the blast propels rock beyond the blast area sometimes the serious injuries can occur related the flyrock, often with a fatal outcome.

Good blast design, generally, is primary method of avoiding flyrock; however, it often is not enough, and the blaster must resort to methods of containing the flyrock: (1) covering the field with heavy blast mats and (2) backfilling [3]. Coverings are all the elements used to cover the blasting site to avoid rock throw or any other material that could harm people, buildings etc. [1]. Generally speaking, any protection system should comply to the following characteristics:

- reduced weight and high resistance,
- ease of union or overlapping of the elements,
- permeability to gases,
- ease in placing and removing,

- economical and reusable,

- good size to cover large areas, etc.

Backfilling is covering a blast with soil, preferably sand, to control or prevent undesirable flyrock. Backfilling is advantageous in that it requires less equipment than blasting mats, it can produce better breakage, and the whole blast can be shot at once. On the other hand, using backfill for blast coverage generally requires more explosives, because the backfill constrains the movement of the rock [3].

BLASTING MATS

Blasting mats are netting of matting constructed of either cable or rubber tires and designed to contain the rock or prevent it from flying when blasted. The main rule for blasting mats is never to blast more holes than can be safely covered with the mats. As with backfilling, great care should be taken to break any leg placing the mats [4]. Blasting mats can be used when explosives are detonated in places such as quarries or construction sites. The mats are placed over the blasting area to contain the blast, suppress noise and dust as well as prevent flyrock from damaging structures, [5] people or the environment in proximity to the blast site [6].

Blasting mats can be used singly or in layers [7] depending on the size of the blast charge, the type of mat and the amount of protection needed. They can be used horizontally on the ground or vertically hanging from cranes or attached to structures. In the vertical capacity the mats are sometimes referred to as blasting curtains [8]. When used in blasting tunnels the mats can be placed in patterns designed to let the mats stabilize each other and to direct the discharge from the explosion out of the tunnel [9]. Blasting mats must be thoroughly inspected before each use to ensure there are no blown out segments or broken cables, by a blaster.

As early as 1960, the blasting mat which comprises a plurality of sections of vehicle tire casings with each section having tire tread, the two side walls of the casing and the bead or rim of each side wall has patented (Figure 1). The sections are arranged in two layers with each layer comprising at least one row of sections disposed side by side with a side wall of one section abutting a side wall of an adjacent section. One of the two layers is superimposed on the other with the tread of the sections of each layer facing outwardly and forming the top and bottom of the mat [10].

The sections of one layer are arranged relative to the sections of the other layer so that abutting side walls of two adjacent sections of one layer are positioned between the two side walls of a section of the other layer. The ends of the tread of the sections in one layer are located substantially at the midportion of the sections of the other layer so as to form an overlapping of one row of sections in one layer with the sections of a row of the other layer [10].

a)

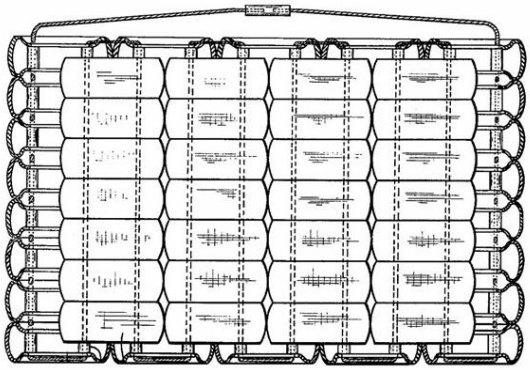

b)

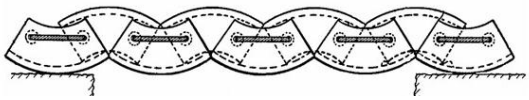

Figure 1 *a) Plan and b) cross-section of blasting mat [10]*

Types of blasting mats and their characteristics

Blasting mats are made of different material and new materials with different properties are constantly being introduced into this field. Table 1 shows different types of blasting mats and their characteristics. The most common materials are strips of old tires held together by steel cables, mats woven from manila rope or wire cables, logs or conveyor belts [4]. Mats made from recycled tires can be fashioned in a number of ways depending on how the tires are cut. Layers of wire netting can also be used [11].

Table 1 *Types of blasting mats and their characteristics [12]*

MANILA ROPE BLASTING MAT 1.5" CUSTOM	
	Blasting mats such as this standard manila mat help shield construction and industrial job sites from the debris generated by explosions and by everyday work. Blasting mats act as curtains to help prevent construction site debris from leaving a contained area. Blasting mats can be equipped with hoisting loops on any side, enabling them to be attached horizontally or suspended vertically for the best protection possible.
RUBBER BLASTING MAT SIDEWALL STYLE 4" THICK 10' X 12'	
	The design of this mat allows harmful gases to escape, so that the mats do not raise as high as most other designs. This design keeps the blast in the hole and keeps the mat closer to the ground. The design: overall thickness: 4 inches; 5/8" new steel core cables spaced 12 inches apart provide a solid internal structure for the mat; drop forged cable clamps; all cables are double clamped for easy handling; approximately 20 lbs per square foot (97.65 kg/m^2); lifting rings are available upon request.

Table 1 *continued*

RUBBER BLASTING MAT TREAD STYLE 10" THICK 10' X 12'	
	Heavy, solid, durable blasting mats. Strong enough for the toughest jobs. The design: overall thickness: 10 inches; 5/8" new steel core cables spaced 12 inches apart provide a solid internal structure for the mat; drop forged cable clamps; all cables are double clamped for easy handling; approximately 50 lbs per square foot (244.12 kg/m^2); heavyweight mat design; lifting rings are available upon request.
WIRE ROPE BLASTING MAT	
	The wire rope blasting mat made an immediate impact on the safety standards of blasting operations in high density urban areas. Wire rope blasting mats are the only blasting mats designed to vent gases which give the blaster more control. Wire rope blasting mats weigh 65 kg/m. They are the most versatile and flexible units on the market today. Extremely durable; built to withstand intensive daily use. They are also fireproof, which offers blasters the ability to use new modern aluminized explosives. The wire rope blasting mat is constructed under ISO 9001:2000 standards and is completely recyclable (Green).

Mostly, blasting mats which are used in blasting come in two basic types: rubber tire mats: typically consist of recycled tires chopped up and bound together with cables ropes or chains and wire rope mats: which have a woven steel construction.

Placement and removal of blasting mats on the blast field

Due to their large weight, the blasting mats are most often placed with a hydraulic excavator. Blasting mats are lifted by the teeth of the excavator bucket or other excavator attachment via lifting rings at the ends of the blasting mats.

Figure 2 shows the placement of blasting mats on the blast field during blasting in urban areas, while Figure 3 shows the removal of blasting mats after blasting from a muck pile with a hydraulic excavator.

Figure 2 *Placement of blasting mats on the blast field during blasting in urban areas [13]*

Figure 3 *Removal of blasting mats after blasting from a muck pile with a hydraulic excavator [13]*

Fields of application of blasting mats

Blasting mats can be used during urban blasting, building demolition, construction blasting, as well as for secondary blasting or blasting in quarries and open-pit mines where there is an increased risk of flying debris.

When blasting is carried out in small ditches and inhabited areas are nearby, a covering of loose and can be used with thicknesses equal to the stemming height, maintaining a minimum of 0.8 to 1 m. Another system consists in overlapping conveyer belts and pinning them down to the ground with sandbags, for example. At the same time metal screening or mesh, nylon nets, rubber tires that overlap [1] or blasting mats can be used.

Secondary blasting is a common source of flyrock. To control this, besides using the protection systems mentioned, it is recommended that the boulders be removed to areas where they do not disturb the operation, and that the blasts be sufficiently closed in by the slopes of the exploitation to eliminate part of the noise produced by the shielding effect of the faces with respect to the fragments of flying rock.

In demolition blasting, the blastholes drilled in the exterior structural elements should be protected by heavy screens made up of hanging conveyor belts. Special pistols are used to nail them in place, and underneath the holding points there should be sufficient space to allow the gases to escape because, if this is not done, the protections would be torn down in the first blasting. Occasionally, the whole perimeter of the structure to be demolished is covered with geotextile sheets which act as complementary protection [1]. Blasting mats can be used in demolition operations, for example when demolishing high structures close to other constructions. In this form, the purpose of the mats is safety and damage prevention [15].

Figures 4 shows blast field covered with blasting mats in urban blasting, while Figure 5 shows the initiation of blasting charges covered with blasting mats in urban blasting.

Figure 4 *Blast field covered with blasting mats in urban blasting [14]*

Figure 5 *Initiation of blasting charges covered with blasting mats in urban blasting [14]*

Blasting mats are not often used in blasting in quarries and surface mines, but only in cases where there is a risk of flyrock to protect people, equipment, and surrounding objects. Figures 6 and 7 show blast field covered with blasting mats and the initiation of blasting charges

covered with blasting mats produced from the most wear resistant parts of recycled truck tires and sewn together with galvanized steel wires in quarry rock blasting [13,14].

Figure 6 *Blast field covered with blasting mats in quarry rock blasting [14]*

Figure 7 *Initiation of blasting charges covered with blasting mats in quarry rock blasting [14]*

CONCLUSION

Blasting mats are mats usually made of sliced-up rubber tires bound together with ropes, cables, or chains. They are used during rock blasting to cover the blast field. Blasting mats are used when explosives are detonated in places such as quarries or construction sites to prevent flying rocks, reduce of shock wave and noise, suppress dust to protect people, structures, or the environment in proximity to the blast site. Blasting mats provide a safer working environment by containing the blast and preventing flying debris. This reduces the risk of injury and property damage and protects workers and equipment from harm.

Blasting mats have the following advantages [16]:

- environmental protection: blasting mats help to suppress dust and debris generated during blasting, which can have a negative impact on the environment,
- cost-effective: using a blasting mat is a cost-effective solution for containing the blast and preventing damage,
- versatility: blasting mats can be used in a variety of settings, from mining and quarrying operations to construction sites and demolition projects,
- durability: blasting mats are made from high-quality raw materials and are designed to withstand the toughest conditions,
- easy to install: blasting mats are easy to install and can be quickly deployed to provide immediate protection,
- compliance: blasting mats are often required by regulatory agencies to ensure the safety of workers and the public during blasting operations.

REFERENCES

[1] Jimeno C. L., Jimeno E. L., Carcedo F. J. A., Drilling and Blasting of Rocks, A. A. Balkema, Rotterdam (1995) p.368, ISBN: 9789054101994.

[2] Institute of Makers of Explosives (IME). Glossary of commercial explosives industry terms, Safety publication, No. 12, Washington, DC, Institute of Makers of Explosives, (1997) p.16.

[3] Tamrock. Handbook on Surface Drilling and Blasting, Painofaktorit, Finland (1984) pp. 172–173.

[4] Pijush P. R., Rock Blasting: Effects and Operations (Illustrated ed.), Boca Raton, Florida: CRC Press (2005) p.29. ISBN: 0-415-37230-5.

[5] Ghose, A. K., Mining, Challenges of the 21st Century. APH Publishing (2000) p.383. ISBN: 8176481580.

[6] Wyllie D. C., Mah C., Rock Slope Engineering (4 ed.), CRC Press (2004) pp. 270–271. ISBN: 0-415-28000-1.

[7] Bulletin – Association for Preservation Technology, Association for Preservation Technology 30–31 (1999) p.70.

[8] Whiteside P. G. D., The role of geology in urban development, Hong Kong: Geological Society of Hong Kong (1987) p.170.

[9] Redmond S., Romero V., Editors, Rapid Excavation and Tunneling Conference Proceedings, Society for Mining, Metallurgy, and Exploration, Inc. (2011), p.276, ISBN: 978-0-87335-343-4.

[10] Hammel, J. R. Jr, *et al*., Blasting Mats, Pittsburgh, United States Patent Office No. 2,926,605, Patented Mar. 1 (1960).

[11] Gustafsson R., Blasting technique, Vienna: Dynamit Nobel (1981) pp. 122–127.

[12] Idealblasting, *Available on the following link*: idealblasting.com/4-x-6-wire-rope-blasting-mat/

[13] T D Bergma Blasting Mats, *Available on the following link:*

www.youtube.com/watch?v=YTYgRqon8lA.

[14] Bergma, *Available on the following link:* www.bergma.no/english/english/blasting-mats.

[15] Jowenko blasting mats, *Available on the following link:* jowenko.com/en/blasting-mats/.

[16] Valuebond blasting mats, *Available on the following link:*

www.valuebond.in/infra/blasting-mats.

INFLUENCES OF EXTREME SOLAR ACTIVITY ON EARTH ENVIRONMENT – CASE STUDY

Aleksandra Kolarski[1], Vladimir Srećković[1], Zoran Mijić[1*]

[1]Institute of Physics Belgrade, University of Belgrade, Pregrevica 118, 11080 Belgrade, SERBIA

[*]*zoran.mijic@ipb.ac.rs*

Abstract

The changes in the Earth environment triggered by the Solar activity can have a significant impact on the functionality of spaceborne and ground-based systems and services, potentially putting human wellbeing at risk. Recent assessment of the European Space Agency pointed out that a single extreme space weather event might have a huge socioeconomic impact on Europe society with its tendency to become even more sensitive in the future years. Many studies indicated significant direct influence of space weather events such as geomagnetic storms and solar flares on human health. As a result, systematic monitoring, and investigation of changes in the atmosphere caused by solar flares have become extremely important over the last decades. The aim of this case study is to investigate the solar flare effects on the ionosphere focusing on the changes that occurred above the European region on 6 September 2017, when one of the strongest solar flares occurred. Simultaneous monitoring of Very Low Frequency radio signals propagation at the Institute of Physics Belgrade station in regular and perturbed ionospheric conditions, enabled retrieving of propagation parameters of sharpness and reflection height during perturbed ionospheric conditions. In addition, numerical simulations reveal changes in electron density profiles showing the increase of several orders of magnitude compared to unperturbed conditions. Obtained findings could be useful for investigation of both atmospheric plasma properties, and prediction of extreme weather impacts on human activities.

Keywords: solar flare, radio signal, environmental impact, atmospheric perturbation.

INTRODUCTION

Through solar-terrestrial interactions between solar activity events of electromagnetic (EM) and corpuscular nature and our planet's outer protective magnetospheric shield, Sun in a great matter influences the near-surface Earth environment. Some of the main inducing agents originating from the Sun are powerful events such as solar flares (SFs), coronal mass ejections (CMEs), energetic proton and electron events etc. Such energetic space weather events can potentially be hazardous to human health [1] and activities, causing radio communication and navigation disturbances such as radio wave blackout [2], directly affecting human crews on space missions and space-born instruments and also producing geomagnetic storms [3].

Energy released during solar flare events, powerful bursts of electromagnetic energy, is well known to penetrate deep into the Earth’s atmosphere. Aside from the Lyman-alpha component, soft-range X-rays with wavelengths of 0.1–0.8 nm reach the lowest of ionospheric regions, the D-region spreading between 50 and 90 km in height that overlaps

with mesospheric region of the atmosphere [4]. Additional incident EM radiation during SFs changes plasma properties within lower ionosphere causing electron density height profile to change as well, following in behaviour input X-ray radiation. Investigation of changes in the atmosphere caused by solar flares and related impacts on the environment have attracted more attention over the last decades. In this paper characteristics of one of the strongest SF events observed are analysed and its impact on lower ionospheric perturbations discussed.

MATERIALS AND METHODS

Case study presented in this work covers X-class SF event X9.3 occurred on September 6th, 2017 (Figure 1) and accompanying CMEs directed towards Earth through ionospheric influences within the near Earth environment. Technology for remote sensing of the lower ionosphere employing artificial man-made Very Low Frequency (VLF) radio signals of frequency range 3–30 kHz is applied [5,6]. Analysis is conducted on data recorded by BEL VLF systems located at the Institute of Physics Belgrade, while X-ray data were taken from GOES database [7]. Retrieving of propagation parameters of sharpness and reflection height during perturbed ionospheric conditions was done according to measured VLF signal perturbations related to X9.3 inducing agent through numerical simulations, with electron density height profile variation during this event obtained based on Wait's empirical approach [6].

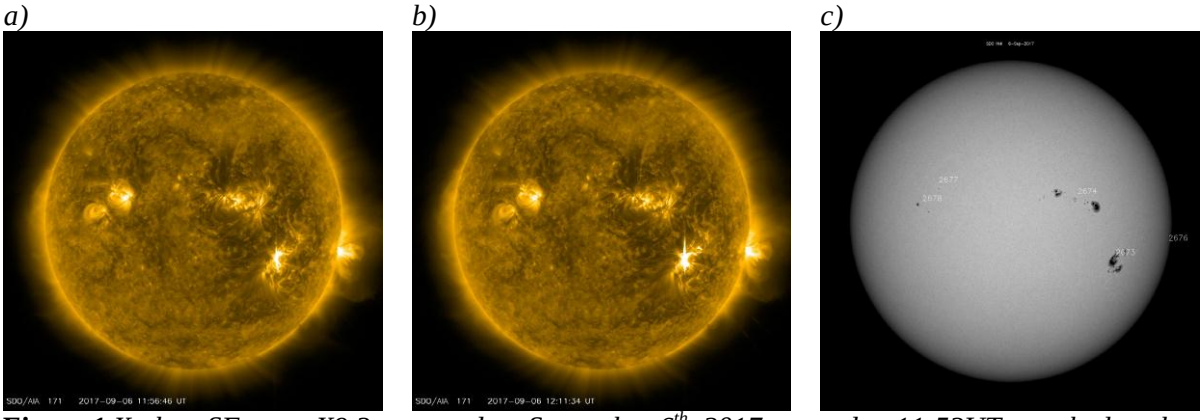

Figure 1 *X-class SF event X9.3 occurred on September 6th, 2017, started at 11:53UT, reached peak at 12:02UT with Ix_{max} = 9.3293·10^{-4} Wm^{-2}, and ended at 12:10UT, which originated from active region 2673, as captured by one of NASA's Solar Dynamics Observatory telescopes: two successive frames of this SF and its active region a) frame at 11:56UT left; b) frame at 12:11UT in the middle; c) active regions on September 6th 2017 (taken from https://www.nasa.gov/)*

Absolute Phase and Amplitude Logger (AbsPAL) station, located in Belgrade (44.85°N; 20.38°E), provided the VLF data used in this analysis. Amplitude and phase perturbations related to case study event of X9.3 SF, were monitored on VLF signal emitted from military transmitter in Skelton (54.72°N; 2.88°W), UK on frequency 22.1 kHz, with code name GQD, arriving in Belgrade from west with Great Circle Path (GCP) in length of about 2 Mm (Figure 2). Methodology used relies on subionospheric VLF signal propagation within Earth-ionosphere waveguide, with lower ionosphere as the upper boundary and Earth's surface as

the lower boundary of this waveguide, and hop-wave theory of radio signal transmitting within the waveguide [5,6,8,9]. Approach involves multi-signal simultaneous monitoring of VLF signals' amplitude and phase in regular and perturbed ionospheric conditions, enabling to retrieve properties of perturbation from measured VLF data, through comparison between unperturbed and perturbed states, using numerical procedures for modelling of ionospheric plasma properties [10–20].

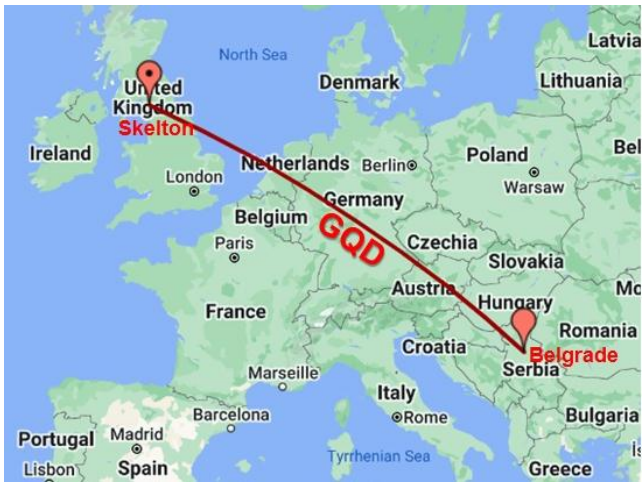

Figure 2 *Great Circle Path (red) of VLF radio signal GQD/22.1 kHz, transmited from Skelton (UK) and registered in Belgrade (Serbia)*

RESULTS AND DISCUSSION

Amplitude and phase perturbations observed on GQD signal recorded in Belgrade during X9.3 SF, with incident soft X-ray irradiance as recorded by GOES-15 satellite, are presented in Figure 3, on middle, lower and upper panel, respectively.

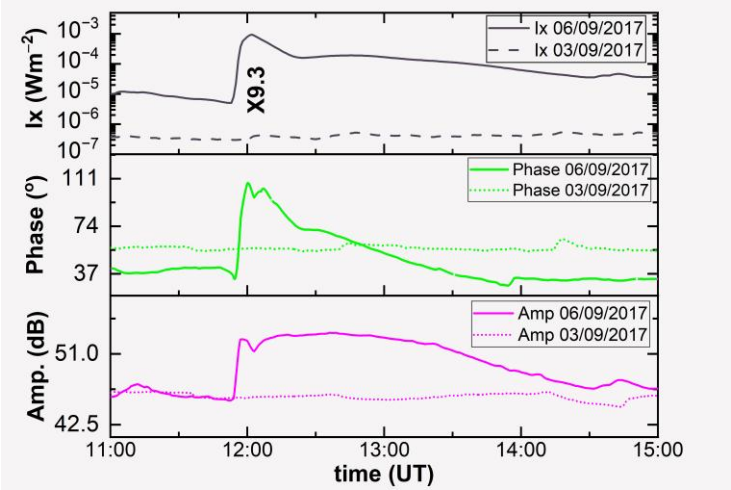

Figure 3 *Simultaneous variations of X-ray flux (perturbed and quiet days in solid and dashed gray, respectively) recorded by GOES-15 satelite, perturbed phase (solid green) and amplitude (solid pink) and quiet signals (dotted green and pink) of GQD/22.10 kHz VLF radio signal during X9.3 SF occurred on September 6th, 2017, recorded by Belgrade VLF station (from upper to lower panel)*

Amplitude and phase perturbations on monitored VLF signals are of relatively simple morphology and pattern, following inducing X-radiation agent with time delay corresponding to the sluggishness of the ionosphere [21,22]. Recorded amplitude and phase perturbation on monitored GQD signal as induced by SF event X9.3 on September 6th, 2017, reached maximal increase of 7.09 dB in amplitude and 52.03° in phase compared to unperturbed values during September 3rd, 2017, corresponding to the peak activity of soft X-ray flux.

Based on amplitude and phase perturbations during X9.3 SF, modelling of ionospheric plasma properties was done through numerical simulations, using Long Wavelength Propagation Capability (LWPC) software [23] and the FlarED' Method and Approximate Analytic Expression application [4,17]. Estimated values of analysed VLF signals' amplitude and phase obtained during modelling through both applied numerical procedures are in good agreement with real values measured by BEL VLF receiving system.

LWPC software utilisation based on Wait's theory application, rely on Wait's parameters β (km^{-1}) and *H'* (km) (lower ionospheric boundary sharpness and VLF signal's reflection height), determined for daytime ionospheric conditions using Equation (1) [6]. Electron densities calculated at the reflection height, when $h = H'$ give profile throughout D-region altitude range (Figure 4).

$$N_e(h, H', \beta) = 1.43 \cdot 10^{13} \cdot e^{(-0.15 \cdot H')} \cdot e^{[(\beta - 0.15) \cdot (h - H')]}, \quad (m^{-3}) \qquad (1)$$

FlarED' Method and Approximate Analytic Expression application, designed for obtaining VLF signal propagation parameters β and *H'* from incident solar X-ray irradiance, gave electron density profiles (Figure 5) calculated by using polynomial Equation (2) [4,17].

$$log\ Ne(h, Ix) = a_1(h) + a_2(h) \cdot log\ Ix + a_3(h) \cdot (log\ Ix)^2 \qquad (2)$$

Estimated electron densities at reference height of 74 km, obtained by both numerical approaches are within one order of magnitude. Obtained results are in line with results from other studies dealing with high class SF events and conducted by observation from mid-latitudinal located VLF receivers [4,15,16,18,24,25].

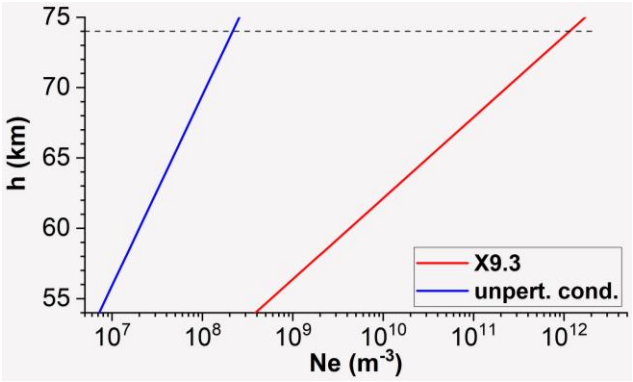

Figure 4 *Electron density height profile for GQD signal at peak intensity of X9.3 SF (red) obtained using Equation (1) and in unperturbed ionospheric conditions (blue); reference height 74 km is indicated by dotted black line*

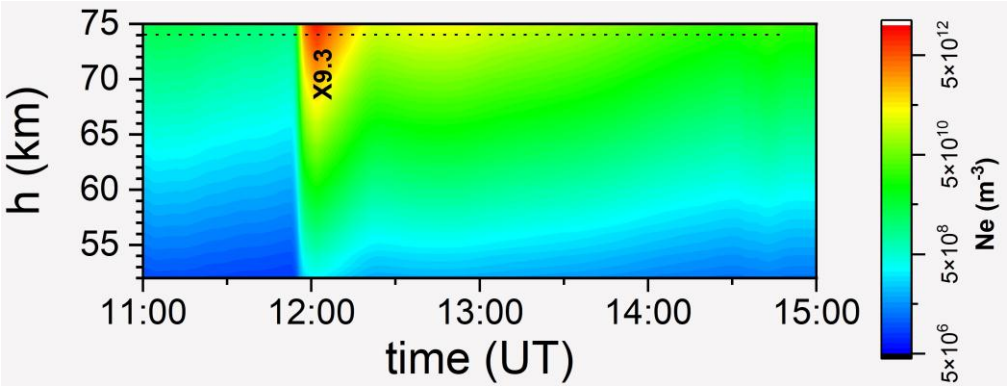

Figure 5 *Electron density height profiles for GQD signal during four hours including peak intensity of X9.3 SF obtained through application of approximative Equation (2); reference height 74 km is indicated by dotted black line*

CONCLUSION

Solar flare events are well-known extraterrestrial driver for lower ionospheric perturbations, inducing change of plasma properties in near Earth environment, that can affect human health and cause serious damage to electronically dependent modern society, causing satellite operation breakdowns, communication blackouts, flight risks especially over polar regions, etc. Ionospheric D-region, as medium for VLF signal propagation in a way "mirrors" disturbances of its plasma properties onto propagation parameters of VLF signals, forcing them to deviate from their regular propagation patterns characteristic for unperturbed ionospheric conditions. In this manner caused amplitude and/or phase perturbations make VLF technique as very efficient and as the technique of choice for this region remote sensing exploration. Lower ionospheric disturbance related to X9.3 solar flare event that occurred on September 6th, 2017, caused perturbations in propagation parameters of VLF signals, that as recorded by Belgrade VLF system and observed on GQD signal, reached several dB in amplitude and few tens of degrees in phase, compared to unperturbed signal on September 3rd, 2017. Accordingly, electron density profiles also changed, following the incident soft X-ray radiation, showing the increase of several orders of magnitude compared to their unperturbed values at the reference height of 74 km, as obtained through conducted numerical simulations.

ACKNOWLEDGEMENT

This work was funded by the Institute of Physics Belgrade, University of Belgrade, through a grant by the Ministry of Science, Technological Development and Innovations of the Republic of Serbia.

REFERENCES

[1] Alabdulgader A., McCraty R., Atkinson M., *et al.*, Sci. Rep. (2018) 2663.

[2] Yasyukevich Y., Astafyeva E., Padokhin A., *et al.*, Space Weather (2018) 1013–1027.

[3] Riley P., Love J. J., Space Weather (2017) 53–64.

[4] Srećković V. A., Šulić D. M., Ignjatović Lj., *et al.*, Appl. Sci. 11 (2021) 7194.

[5] Mitra A. P., Lonospheric Effects of Solar Flares; Springer, Berlin/Heidelberg (1974), p.305, ISBN: 978-90-277-0467-2.

[6] Wait J. R, Spies K. P., Characteristics of the Earth-Ionosphere Waveguide for VLF Radio Waves; US Department of Commerce, National Bureau of Standards, Gaithersburg MD, (1964), p.110.

[7] NOAA National Centre's for Environmental Information, *Available on the following link*: https://satdat.ngdc.noaa.gov/sem/goes/data/avg/.

[8] Budden K., Radio Waves in the Ionosphere, Cambridge University Press, Cambridge (1961), p.542, ISBN: 052111439X.

[9] Wait J. R., Electromagnetic Waves in Stratified Media, Pergamon Press, Oxford (1970), p.620, ISBN: 9781483184258.

[10] Silber I., Price C., Surv. Geophys. 38 (2017) 407–441.

[11] Žigman V., Kudela K., Grubor D., Adv. Space Res. 53 (2014) 763–775.

[12] Nina A., Remote Sens. 14 (2022) 54.

[13] Šulić D., Nina A., Srećković V., arXiv (2014) arXiv:1405.3783.

[14] Grubor D., Šulić D., Žigman V., Ann. Geophys. 26 (2008) 1731–1740.

[15] Kolarski A., Srećković V. A., Mijić Z. R., Appl. Sci. 12 (2022) 582.

[16] Barta V., Natras R., Srećković V., *et al*., Front. Environ. Sci. 10 (2022) 904335.

[17] Srećković V.A., Šulić D.M., Vujčić V., *et al*., Appl. Sci. 11 (2021) 11574.

[18] Kolarski A., Veselinović N., Srećković V. A., *et al*., A. Remote Sens. 15 (2023) 1403.

[19] Kolarski A., Grubor D., Adv. Space Res. 53 (2014) 1595–1602.

[20] Kolarski A., Srećković V. A., Mijić Z. R., Contrib. Astron. Obs. Skaln. Pleso 52 (2022) 105.

[21] Appleton E. V., J. Atmos. Sol.-Terr. Phy. 3 (1953) 282–284.

[22] Žigman V., Grubor D., Šulić D., J. Atmos. Sol.-Terr. Phys. 69 (2007) 775–792.

[23] Ferguson, J. Computer Programs for Assessment of Long-Wavelength Radio Communications, Version 2.0: User's Guide and Source Files, Space and Naval Warfare Systems Center, San Diego (1998).

[24] Thomson N. R., Rodger C. J., Clilverd M. A., J. Geophys. Res. Space Phys. (2005) A06306.

[25] McRae W. M., Thomson N. R., J. Atmos. Sol.-Terr. Phys. 66 (2004) 77–87.

AVAILABILITY OF TOXIC ELEMENTS IN ROADSIDE SOILS (HIGHWAY 75, VOJVODINA, SERBIA): IS THERE ANY SIGNIFICANT CONTAMINATION RISK?

Maja Poznanović Spahić[1*], Aleksandra Gulan[1], Darko Spahić[1], Pavle Tančić[2], Sanja Sakan[3], Srebrenka Petrović[1]

[1]Geological Survay of Serbia, Rovinjska 12, 11000 Belgrade, SERBIA

[2]Department for Catalysis and Chemical Engineering, Institute of Chemistry, Technology and Metallurgy, University of Belgrade, Njegoševa 12, 11000 Belgrade, SERBIA

[3]Centre of Excellence in Environmental Chemistry and Engineering – Institute of Chemistry, Technology and Metallurgy, National Institute of the Republic of Serbia, University of Belgrade, Njegoševa 12, 11158 Belgrade, SERBIA

[*]*maja.poznanovic@gzs.gov.rs*

Abstract

In this paper we provide the observations of a group of toxic elements Cu, Pb, Cr, Co, Ni, Pb, V, Zn, Sb, and Mo, in the soils that are sampled at the distances of 1 m and 5 m (two layers) from the road (Highway 75, north section). The observation of toxic elements are indicating a level of the existing contamination, availability and ecological risk. The mean values of the content of the elements Cr, Cu, Mo, Pb, Sb and Zn are lower with respect to the reference MAC values, whereas the mean and particular values of the content of Co, V, and Ni are higher. The content of the Sb, Pb, Mo, Cr, Cu, V and Zn reach higher values in the surface layer near to the road – at a distance of 5 m. The particular values of Pb, Zn and Cu only in the surface samples, at both distances, at two sampling localities, are indicating the presence of anomaly. However, the results of the content of the elements in most mobile forms are suggesting a presence of insignificant content of the toxic elements, which can easily become available to the environment and spread by streams or groundwater. The results of the Risk assessment code (RAC) confirms that there is a lower risk of contamination of the near-road environment by these toxic elements.

Key words: roadside soils, toxic elements, mobility, risk assessment.

INTRODUCTION

Traffic at regional highways and roads represents the main anthropogenic activity often inducing soil pollution. Traffic can frequently be a source of a number of toxic- or potentially toxic elements: Cu, Cd, Pb, Cr, Co, Ni, Fe, Mn, Pb, V, Zn, Sb, Hg, Ba, and Mo [1–3]. These elements can be emitted from different sources and traffic-related processes: wearing (tire, asphalt pavements, vehicle, banks, brake system etc.), spilling or combustion of fossil fuels, transportation of different materials, etc. The contamination levels of soils can be influenced by a number of factors such are: traffic frequency, vegetation, terrain configuration, wind direction, age of roads. Additionally, mobility of these elements largely depends on soil properties (granulometric composition, pH, cationic capacity, clay content, carbonates, and

organic matter) or forms in which these elements are released etc. Contamination of the surrounding soil by water is referring to the washing of the pavement accounting for activity of streams, draining, splashing, including the infiltration of these elements into deeper sections or layers of the soil [4]. Consequently, the impact of this source of the pollution increases significantly at different distances from roads and different depths. With an increase in the distance from the edge of the road, the concentrations the elements such as Zn, Cu, Pb and Cd decrease exponentially with the distance, reaching up to a distance of 100 m from the pollution source [5].

In the literature, availability of elements is observed as: 1) mobility – content of the elements available in the soil (in mobile forms); 2) bioavailability – the content available to the extent that it can be adopted by the plants, and 3) toxicity – content that causes a toxic effect in organisms [6]. For that reason, ecological effects of the toxic elements are strongly dependable on the content of the elements in mobile forms, rather than the total content [7]. The sequential extraction (SE) methods can be used to investigate the availability – mobility, bioavailability, as well as the risk assessment of the groundwater contamination (here defined as "geoavailability"). The following study discusses the influence of the traffic and road (Highway 75) as a potential pollution source affecting its roadside soils. We discuss a possible geoavailability, whereby we are assessing the risk of soil contamination with the following chosen elements: Cu, Pb, Cr, Co, Ni, Pb, V, Zn, Sb, and Mo.

MATERIALS AND METHODS

The investigated road samples are collected alongside the northern section of the Corridor "X" (Highway 75, Belgrade–Subotica, northern Serbia). Sampling of the soils was planned for fifteen localities (K1–K15) that are distributed alongside the highway itself. Sampling was performed prior its reconstruction in 2012. The soil samples are collected along a single side of the highway (K1–K10; direction Subotica–Belgrade), collected at a length of 20 km. The sampling across the second side of the highway was at a length of 4 km (K11–K15). Sampling was performed at the distance of 1 and 5 m from the edge of the road at all localities. The sampling at the distance of 5 m (or the place of near-road drainage system) was performed in the two separate layers with different near-subsurface depths: surface layer – T (with depths of 0–10 cm) and a subsurface layer – B (depths of 30–50 cm).

The SE method, which is applied onto 45 roadside soil samples, involves the five phases (F1–F5) [8]. The following study is observing the phases which are targeting the forms of the toxic elements: adsorbed and soluble (F1), included or occluded by Fe/Mn hydro-oxides and carbonates (F2). The concentration of the chosen toxic elements in the investigated soil samples is measured by applying the ICP/OES technique (Inductively Coupled Plasma/Optical Emission Spectrometry – iCAP-6500 Duo, Thermo Scientific, UK). The mineralogical characterization of the samples was performed by using the X-ray powder diffraction (XRPD) analysis (PHILIPS powder automatic X-ray diffractometer, PW-1710). The content of organic matter (%) is measured as a loss of ignition after heating the samples at 600°C, in duration of 4 h. The granulometric analysis subdivided the acquired soils samples

into the three grain fractions [9]: sandy (0.25–0.063 mm), silty (0.063–0.005 mm) and clayey (>0.005 mm) fraction.

RESULTS AND DISCUSSION

Mineralogical characteristics and granulometric composition

The most abundant mineral in the soil samples collected out from the surface layer (T) and the subsurface layer (B) is Quartz. Across the majority of the samples collected at all distances, the following minerals were detected: Clay-group minerals, Feldspars and carbonates (Dolomite and Calcite). The Clay minerals are mainly comprised of Illite, Sericite and Chlorite. Only in a few samples, Amphibole minerals are detected in the samples at the distance of 1 m (K4, K11 and K12), and 5 m (K7, K8, K10, K12, K13). Granulometric composition slightly changes with the distance and within the layers itself. Namely, the mean content of the sandy and clayey fractions (in %) has a slight decrease, whereas the silty fraction slightly increases. Within the layers the mean content of the silty and sandy fractions varies slightly, however, the presence of the clayey fraction is unchanged.

Concentration levels and availability of the elements

The results show that the mean values of the following toxic elements Cr, Cu, Mo, Pb, Sb and Zn are lower than the reference values (at the distances of 1 and 5 m from the road; Table 1). The reference values represent the maximum allowed values (MAC) defined by domestic regulative (Official Gazette 88/2010) and modified according to the content of clayey fraction (4.23%) and organic matter (5.19%).

Table 1 *The mean $C_{average}$ and most available content $C_{(F1+F2)}$ of the toxic elements in the samples (at the distances of 1 and 5 m)*

Distance	mgkg^{-1}	Cu	Pb	Zn	Cr	Ni	Co	V	Sb	Mo
	$C_{average}$	24.0	50.0	66.3	32.2	27.8	9.11	27.2	0.47	0.51
1m	St dev	13.4	68.4	42.6	17.9	13.3	2.14	8.08	0.48	0.20
	$C_{(F1+F2)}$	0.09	0.27	3.04	<0.01	0.26	0.13	0.46	<0.05	<0.02
	$C_{average}$	20.9	27.3	56.7	24.9	27.4	7.04	29.7	0.86	0.52
5m (T)	St dev	9.97	26.3	32.5	7.79	10.5	2.22	7.59	0.35	0.21
	$C_{(F1+F2)}$	0.06	0.08	0.97	<0.01	0.26	0.15	0.35	<0.05	<0.02
5m (B)	$C_{(F1+F2)}$	<0.02	<0.03	<0.01	<0.01	0.84	0.63	0.39	<0.05	<0.02
	MAC*	20.7	59.5	70.7	58.6	14.3	3.21	17.2	3.00**	3.00**

*MAC – modified maximum allowed contents; **unmodified values.

The mean and particular values of the content of Co, V, and Ni suggest the presence of the contamination in the roadside soils both at surface and subsurface layer. However, some previous research of the agricultural soils in the area of Vojvodina, indicated an anomaly in the content of the toxic elements such are Co, Ni, and Cr. Especially at the localities that are near the Fruška Gora Mt. complex [10]. The maximum values above the MAC of Cu are registered in the samples K3, K14, K15 (1 m), K12, K14, K15 (5 m T)/K12, K15 (5 m B). The Pb and Zn content values overcome the MAC and are registered in K13, K14, K15 (1 m)

and K14, and K15 (5 m T). Nevertheless, the content of these elements in subsurface layer does not exceeds MAC values. Content of Cr exceeds MAC only in the sample K2 at a distance of 1m away from the road, whereas content of the Sb and Mo does not exceed MAC in any sample. Summary, the most contaminated localities K14 and K15 are placed near the Fruška Gora Mt. complex (exposed bedrock assembly). The localities are labeled as the points with extremely high concentrations in the surface samples of Pb (at the distance of 1 m – 218 and 214 $mgkg^{-1}$), Zn (179 and 135 $mgkg^{-1}$), including elevated values at the distance of 5 m Pb (57.3 and 113 $mgkg^{-1}$) and Zn (124 and 136 $mgkg^{-1}$). The values of Cu content are higher reaching 20.7 $mgkg^{-1}$(1 m – 57.1 and 48.7; 5 m – 40.9 and 41.5 $mgkg^{-1}$).The content of the elements Zn, Cu, Cr, Co in the surface layer are slightly decreasing with the sampling distances. In fact, the content of Pb decreases significantly, suggesting the presence of anthropogenic source, which is almost certainly the road activities itself. On the other hand, the mean content values of Mo, V, Ni are unchanged, being undependable of the distance. Thus, the influence of the road as their source of contamination is ruled out.

As the measure of the geoavailability we have taken into account the sum of the content of the elements occurring in the first two phases (F1+F2, Table 1). According to the results, it can be concluded that an insignificant content of the toxic element can become mobile and available to the environment, likely spreading by local streams or groundwater. That refers, in particular, for the most contaminated localities K14 and K15 (Pb_{F1+F2} 0.70 – 2.98 $mgkg^{-1}$; $Zn_{(F1+F2)}$ 6.87 – 30.2 $mgkg^{-1}$).

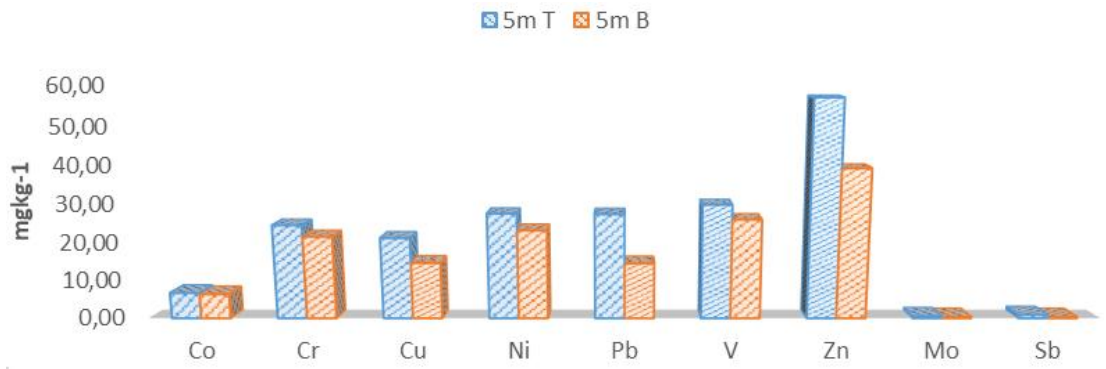

Figure 1 *Distribution of the mean content values of the toxic elements in surface soils (T) and subsurface (B) at the distance of 5 m*

The content of the toxic elements in the soils, at the distance of 5m from the road (Figure 1), shows that the availability and distribution can be observed in the following two aspects: (i) soil profile – due to a possibility of infiltration of contaminant in deeper strata (by rain and stream) and (ii) distribution between the mobile and the immobile forms within strata. The soil profile process is strongly influenced by the following conditions: granulometric composition and presence of components, such are clay minerals or content of organic matter. The granulometric composition, i.e. higher content of sand and larger grains, and lower clay fractions, or more precisely clay minerals, can produce a better permeability of water that is

drained from the highway and is infiltrating into deeper layers (in this case at a distance of 5 m).

The results of the mean values of the toxic elements (Figure 1) may indicate a different distribution of the content of the elements between the two layers. The values of the content of Sb and Pb in the surface layer have three- and two-times higher values. The Wilcoxon ("two-tail") test is confirming that there is a significant difference between the values of Sb and Pb, as well as Mo, Cr, Cu, V and Zn. That further implies the enrichment is more pronounced in the surface layer of the soil, at a distance of 5 m from the road. One of the reasons can be a higher content of the organic matter, and a lower content of the sand, as well as the presence of clayey fraction in the surface samples. Especially it is referring to the sample K15, wherein the content of the clayey fraction reaches 8.0 %; sandy fraction 16.3% and 9.86 % of organic matter in the T layer. The values in the B layer are: 9.50% of clayey fraction; 4.84% of sandy fraction; 5.11% of organic matter. Thus, the values of Pb (24.3 $mgkg^{-1}$) and Zn content are much lower (51.5 $mgkg^{-1}$), by comparing those one in T layer, named above. With regards to the fact that the content of the toxic elements in the subsurface soil samples (T) are lower than in the subsurface (B), it is to expect that the values of the content of available/mobile forms of the elements have a lower amount as well. This hypothesis can be confirmed by the results of their content (F1+F2) (Table 1) in the soils of the B layer. Ergo, in the most contaminated samples K14 and K15 in the subsurface the content values are: for Pb – 0.08 and 0.83 $mgkg^{-1}$; Zn – 7.48 and 6.87 $mgkg^{-1}$; Cu – 0.38 and 0.19 $mgkg^{-1}$, respectively. Additionally, these values are much lower than the MAC reference values.

Contamination risk assessment – Risk assessment code (RAC)

A degree of the potential mobility or availability of toxic elements, and risk of contamination in the investigated soil is represented by the RAC indices, calculated by the following formula:

$$RAC = \frac{C_{(F1+F2)}}{C_{(F1+F2+F3+F4+F5)}} x100 \quad (1)$$

In this equation, $C_{(F1+F2)}$ represents the sum of the contents in the phases F1 and F2 and $C_{(F1+F2+F3+F4+F5)}$, yielding the already observed total content of the elements.

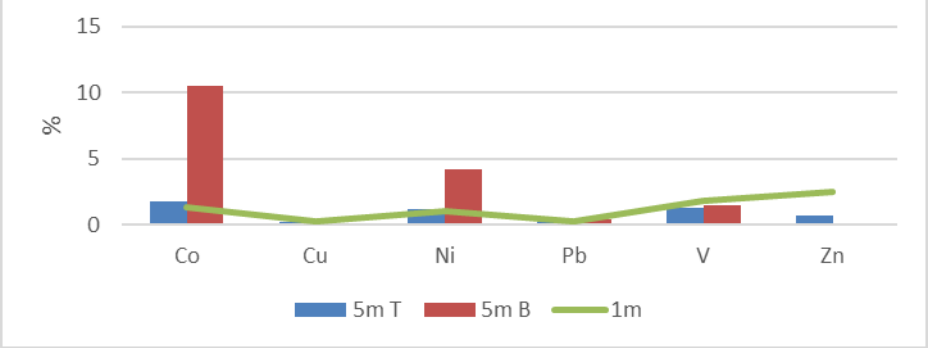

Figure 2 *Mean RAC values of the samples in surface layer (1m and 5m T) and subsurface layer (B)*

According to the results of the average RAC values of Pb, Zn, Cu (Figure 2), these elements are belonging to the group of contaminants having a lower risk of the contamination (RAC< 1). However, in the one of the most contaminated samples K14 (at the distance of 1 m) RAC values of Pb and Cu are indicating a moderate risk level (1.37 and 1.10). The RAC value of Zn, Cu and Pb at the distance of 5 m (T) evaluating a moderate risk level in the samples K14 (6.01) and K15 (5.06). In the case of Cu K14 (1.42) are the lower values for Pb in K15 (0.74). In the subsurface layer, elements like Zn and Pb were not detected in mobile forms, and a lower Cu was calculated at the locality K3 (0.60). A group with the moderate mobility level and ecological risk (1 < RAC< 10) includes the elements: As, Cd, Co, Ni, Zn and V (Figure 2). However, in this case, the content of the elements of the most mobile forms has significantly lower value than MAC. It should be noted here that the highest mean RAC value and mobility of Co and Ni was calculated in the samples collected out from the subsurface layer located at a distance of 5 m (Figure 2).

CONCLUSION

Traffic at regional highways and roads can be the principal source of a number of toxic elements or potentially toxic elements. These elements can often be spread in different manner within soils that is in the vicinity of the roads. These include deeper soil layers. In this paper, we provide the observations of a group of toxic elements in the soils that are sampled at the distances of 1m and 5m from the road, indicating the level of the existing contamination and ecological risk. The mean values of the toxic elements Cr, Cu, Mo, Pb, Sb and Zn have lower values relative to the reference MAC values. These include the particular values of Pb, Zn and Cu that are higher than the MAC in the surface samples. The most contaminated localities by these elements are K14 and K15, with extremely high values of Pb, and Zn. However, observing the results of the content of the elements in most mobile forms, at all localities, the conclusion is that insignificant content of the toxic element can become available to the environment and spread by streams or groundwater. The results of the mean content values of Mo, Cr, Cu, V and Zn; in particular Sb and Pb, indicate its different distribution between two layers. One of the reason can be the conditions – higher contents of the organic matter, a lower content of the sand, and the presence of clayey fraction in the surface samples. In the samples of the subsurface layers, the elements (except Ni and Co) are not detected in the mobile forms or the contents are much lower than MAC. At last, study shows that there is no risk or there is a low risk of the contamination of the environment with Pb, Zn, Cu in soils at the investigated surface and the subsurface roadside soils. This goes even in the localities with a highest content of these elements. The RAC values indicate a moderate ecological risk of the contamination of the soils by As, Cd, Co, Ni, Zn and V. Having said that, the content of the elements of the most mobile forms are significantly lower than MAC, making the risk assessment grouping debatable.

REFERENCES

[1] De Miguel E., Lamas J., Chacon E., *et al*., Atmos. Environ. 31 (17) (1997) 2733–2740.

[2] Yu, Y., Li Y., Li, B., *et al*., Environ. Poll. 216 (2016) 764–772.

[3] Grace B., Bouamar B., Hassan E. H., Mariem L., Int. J. Civ. Eng. Techn. 10 (2019) 1462–1477.

[4] Bohemen H. D. V., De Laak, W. H. V., Environ. Manage. 31 (1) (2003) 50–68.

[5] Turer D. G., Maynard J. B., Clean Technol. Environ. Policy 4 (2003) 235–245.

[6] Baran A., Wieczorek J., Mazurek R., *et al*., Environ. Geochem. Hlth. 40 (2018) 435–450.

[7] Hlavay J., Prohasha T., Weisz M., *et al*., Pure Appl. Chem. 76 (2), (2004) 415–442.

[8] Poznanović Spahić M., Manojlović D., Tančić P., *et al*., Environ. Monit. Assess. 191 (3) (2019) 133.

[9] Konta J., University Karlova, Prague (1973).

[10] Poznanović Spahić M., Sakan S., Trbić-Glavaš B., *et al*., J. Environ. Sci. Health A. 54 (2018) 219–230.

MULTICRITERIA EFFICIENCY ASSESSMENT OF THE PINE TREE POTENTIAL FOR THE PHYTOREMEDIATION OF COPPER

Tanja Kalinović[1*], Ana Radojević[1], Jelena Kalinović[1], Jelena Milosavljević[1], Snežana Šerbula[1]

[1]University of Belgrade, Technical Faculty in Bor, V.J. 12, 19210 Bor, SERBIA

[*]*tkalinovic@tfbor.bg.ac.rs*

Abstract

Special emphasis in this paper was given to the multicriteria efficiency assessment of the phytoaccumulation and exclusion properties of the pine tree, as well as the Cu uptake from the soil by the root system, and further translocation to the needles, in the anthropogenically multi-medium polluted areas. Pine tree did not show the properties of the Cu hyperaccumulator plant under the environmental conditions of the study area, so pine could not be used in phytoextraction of copper from the soil. Pine tree from the sampling sites with the lowest pollution level had the properties of plant excluder of Cu. In the conditions of elevated Cu contents (>1500 mg/kg, the UI and R2 sampling sites) in the soil, pine showed the ability to efficiently translocate Cu to the above-ground parts, which could be the tolerance mechanism to high Cu concentrations in the environment, and especially in the soil. Such fate of Cu throught the soil-plant interface should be further tested in the specific physico-chemical conditions of the soil and Cu soil contents higher than the specified value.

Keywords: pine, copper, phytoremediation, translocation, environmental pollution.

INTRODUCTION

Environmental studies in the anthropogenically multi-medium polluted areas [1,2], are of the great importance from the aspects of human health protection [3] and preservation of natural resources. From the scientific point of view, the surroundings of open pit mines, overburden dumps, flotation tailing ponds and copper smelters, represent the "open air laboratory", for multidisciplinary examinations of fate of polluting substances in the environment. Soil in these areas as the crucial environmental component, is a major sink of heavy metals released from the pollution sources. Change in the chemical and biological characteristics of the polluted soil [4] has huge consequences, and also affects the physico-chemical and metabolic functions of plants. Because of that, polluted soil and plants that exist on it, are the most significant elements in the studies of the possibilities of phytoremediation. Due to the adaption and tolerance to different environmental stresses, naturally abundant species have priority in this method [5]. Different species of *Pinus spp.* had good adaptability in polluted environment, and could be used in the phytoremediation and restoration of polluted soil [6–8].

The aim of this study was the assessment of the pine tree ability to absorb Cu from the soil and translocate it through the plant tissues, upon different soil pollution level. The obtained results were also used in the evaluation of possibilities of using pine tree in phytoremediation.

MATERIALS AND METHODS

Study area and analyses of samples

Sampling of soil and plant material was conducted at ten sampling sites: UI-urban-industrial; U-urban; SU-suburban; I1 and I2 (industrial zone); T1-Brestovac spa and T2-Bor lake (tourist zone); R1-village Oštrelj and R2-village Slatina (rural zone); and B-Gornjane (background, unpolluted zone). It should be noted that impacts of pollution sources at most of the sampling sites are overlapping, because of the close vicinity of the mining and smelting facilities.

Soil from the surroundings of roots, as well as roots and needles of pine were sampled and prepared for chemical analyses according to the methodology described in Kalinovic *et al.* [9]. All chemical analyses were conducted by accredited chemical laboratory, at the Institute of Mining and Metallurgy Bor (Serbia). Samples of soil and plant material were digested according to the U.S. EPA method [10], in a microwave oven. Concentrations of Cu in extracts were determined by simultaneous dual view inductively coupled plasma atomic emission spectrometer (ICP-AES).

Data analyses

Soil and plant Cu concentrations were analysed using SPSS Statistics software. Possibilities of using the pine tree in phytoremediation were defined based on the bioaccumulation factor for roots and washed needles (BAF_{roots}, eqn. (1); $BAF_{needles}$ eqn. (2)), translocation factor (TF, eqn. (3)) [8,11], as well as, by comparing the Cu concentrations in the washed needles with the concentrations which foliar parts of plants hyperaccumulators or excluders should contain [12].

$$BAF_{roots} = \frac{C_{roots}}{C_{soil}} \quad (1)$$

$$BAF_{needles} = \frac{C_{needles}}{C_{soil}} \quad (2)$$

$$TF = \frac{C_{needles}}{C_{roots}} \quad (3)$$

In the specified equations, C_{soil}, C_{roots} and $C_{needles}$ represented Cu concentrations in the samples of soil, roots and needles, respectively.

If at the same time the following criteria are met: the aboveground plant part contain the Cu concentrations which are characteristic for plants hyperacumulators (≥300 mg/kg Cu) [13]; and $BAF_{roots}>1$, $BAF_{needles}>1$ and $TF>1$, then the plant was considered a hyperaccumulator, i.e. the plant had the abilities for being used in phytoextraction [5].

If the values of BAF_{roots}, $BAF_{needles}$ and TF were <1, then the plant had the properties of excluder [5]. However, it should not be omitted that excluder plants certainly uptake necessary quantities of essential elements, which enable their primary metabolic functions [14]. It was suggested that Cu concentrations in excluder plants should not exceed values of

40 mg/kg [12]. Excluder plants can accumulate highest amounts of a certain element in their roots, compared to other parts, but translocation to the aboveground parts is limited. This property is suitable for the use of plants in phytostabilization.

If $BAF_{roots}<1$, $BAF_{needles}<1$ and TF>1, only efficiency of Cu translocation from the roots to needles was considered. If Cu translocation from the roots to needles is efficient, then the roots compared to the washed needles should contain lower Cu concentrations.

The ranges of Cu concentrations in the soil from the sampling sites where the values of TF were <1 and the range of Cu concentrations in the soil from the sampling sites where the values of TF were >1, were compared. In the soil Cu concentration zone of overlapping these values (TF<1 and TF>1), it was considered that Cu soil concentrations did not have dominant effect on the Cu translocation from the roots to needles. This method of analyses of the results indicated the Cu translocation efficiency in the range of lower and in the range of higher Cu concentrations in soil. That was one of the ways to define a strategy that pine tree uses to adapt to the increased Cu concentrations in the soil.

Based on the values of BAF, intensity of absorption of some elements from soil into roots and needles were defined. Depending on the values of the bioaccumulation factors, absorption was classified as follows: 10–100 (intensive absorption), 1–10 (strong absorption), 0.1–1 (average absorption), 0.01–0.1 (weak absorption) and 0.001–0.01 (very weak absorption) [6].

RESULTS AND DISCUSSION

Cu concentrations in the samples of soil and roots and needles from 10 sampling sites, were presented in Figure 1. It should be mentioned that Cu contents of the soil from all the sampling sites exceeded the limit value (LV) for soil of 36 mg/kg, while the remediation value (RV) (190 mg/kg) was not exceeded only in the soil from the B sampling site [15]. These exceedances indicated that the fundamental functions of the soil in the studied area were seriously disturbed and required remediation, recovery and other measures. This is of great importance for the soil in the rural zone, where the agricultural activities of cultivation of food for human and animal consumption took place.

The minimum Cu concentration of 67.89 mg/kg was determined in the soil from the B-unpolluted sampling site. Cu concentration that was marked with asterisk represented extreme Cu content determined in the soil from the UI sampling site that was three times higher than the values which were fell within 75% of the presented Cu soil concentrations.

The contents of Cu in the pine roots ranged from 3.36 µg/g at the UI sampling site, to 44.42 µg/g at the B sampling site, which was not expected due to the environmental and especially soil pollution in the study area (Figure 1b). Neither of the detected Cu concentrations in the roots was statistically characterized as atypical or extreme. Cu concentrations in the needles were in the range of 4.83–164.13 µg/g, where the minimum was detected in the needles from the B sampling site, while maximum was detected in the needles from the UI sampling site. Concentrations of Cu in needles sampled from the T2, R2, U, SU and UI sampling sites were higher than the defined critical for foliar parts of higher plants [16]. There was one atypical Cu concentration detected in the needles from the R2 sampling

site, which was more than 1.5 times greater than the 75% data values. Cu concentration in the needles from the UI sampling site represented extreme value that was three times higher than the 75% data, which was in accordance with the level of the pollution of the specified sites.

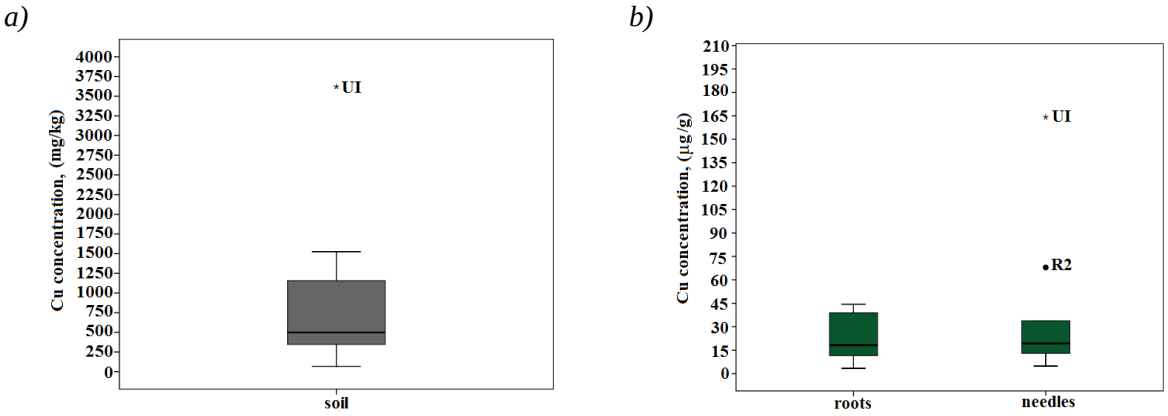

Figure 1 *Box plots of Cu concentrations in the samples of a) soil; b) roots and needles of pine*

Pine sampled from the study area could not be specified as Cu hyperaccumulator plant, because Cu content in the washed needles did not exceed 300 µg/g. The BAF_{roots} and $BAF_{needles}$ at all the sampling sites were <1 (Table 1), which also indicated that pine cannot be used in the phytoextraction of copper, under the physico-chemical soil and air conditions at the studied sampling sites. Because of that, the results were considered from the aspect of the efficiency of the roots and needles Cu uptake from soil, but also the efficiency of their translocation from the roots to needles.

Table 1 *BAF, and TF for Cu in pine tree, depending on the sampling site*

	UI	SU	U	R1	T1	I1	R2	T2	I2	B
BAF_{roots}	0.001	0.034	0.082	0.012	0.059	0.033	0.009	0.034	0.075	0.654
$BAF_{needles}$	0.045	0.089	0.052	0.030	0.020	0.038	0.045	0.022	0.029	0.071
TF	48.833	2.601	0.629	2.462	0.334	1.139	4.835	0.642	0.388	0.109

Absorption of Cu in the roots from the soil at all the sampling sites was weak, except at the UI and R2 sampling sites where the absorption was very weak. Concentrations of Cu in the soil from these sampling sites compared to the rest of the sampling sites were the highest (3620.19 mg/kg and 1524.25 µg/g, respectively). The absorption efficiency of Cu in the needles from the roots was weak at all the sampling sites.

At the U, T1, T2, I2 and B sampling sites, values of TF were <1. The needles from the specified sampling sites had Cu content lower than 40 µg/g, which was defined as one of the requirements which excluder plants s should fulfil [12]. However, for the samples from the U, T1 and T2 sampling sites, the condition that roots should contain higher Cu concentrations compared to the needles, was not met [17]. Higher Cu contents in the roots than in the needles, were only at the sampling sites I2 and B [17], where Cu in the needles (8.66 µg/g and 4.83 µg/g, respectively) did not exceeded the critical value of 20 µg/g [16] for the needles. Because of that, environmental conditions at the I2 and B sampling sites where pine was

sampled favour the pine Cu excluder properties. The Cu concentrations in the soil samples from these sampling sites (67.89 and 298.67 mg/kg, respectively), were lower compared to the concentrations of Cu in the soil from the other sampling sites. Cu concentrations in the pine roots from the U, T1 and T2 sampling sites, where the values of TF were <1, were lower than Cu contents in the washed and unwashed needles.

The values of TF were >1 for the samples from 5 (UI, SU, R1, I1 and R2) out of 10 sampling sites. That means that at these sampling sites, and especially at the UI and R2 (the highest Cu soil contents were detected), Cu was efficiently translocated from the roots to the needles. Concentrations of Cu in the needles from the UI and R2 sampling sites (164.13 µg/g and 67.94 µg/g, respectively), which were higher than the critical, also indicated that pine tree had the ability to efficiently translocate Cu from the soil with the highest Cu contents to the above-ground parts, but the possibility of the Cu absorption into the needles from the atmospheric deposition must not be ignored. These results indicated that the pine trees that were growing at the UI, SU, R1, I1 and R2 sampling sites, possess specific tolerance mechanisms to high Cu concentrations in the environment, and especially in the soil.

The range of Cu concentrations in the pine soil where the values of TF were <1, was 67–1156.33 mg/kg, while the values of TF were >1 at the sampling sites where Cu concentrations were in the range of 345.54–3620.19 mg/kg. These two ranges of the Cu soil concentrations at the sampling sites where TF<1 and TF>1, overlap for some of the Cu soil concentrations. Based on that, it was supposed that in the zone of overlapping, Cu concentrations in soil did not have dominant influence on the translocation of Cu from the roots into the aboveground pine parts, at the environmental conditions that prevailed at the specified sampling sites. According to the obtained results, it could be said that with increasing concentrations of Cu in the pine soil over about 1500 mg/kg, which represented Cu concentration higher than concentrations in zone of overlapping, pine uses mechanism of avoiding Cu toxicity, by translocation of Cu from the roots to the needles. This was the case at the sampling sites R2 and UI, which are the two most polluted areas of the Bor city and the surroundings.

CONCLUSION

The obtained results indicated that soil sampled from all the sampling sites (except the B sampling site) at different distances from the pollution sources such as copper smelter, flotation tailings, tailing ponds, open pit mines, was polluted with Cu, required the remediation, recovery and other measures. The maximum Cu content in the soil and washed needles was determined in the samples from the urban-industrial sampling site, which was previously proven to be the most endangered area in the Bor region. Unlike that, the unexpected lowest Cu content had the roots from the UI sampling site, and the highest Cu content was detected in the roots from the B sampling site. The sampled pine tree did not show the properties of the hyperaccumulator plant, so pine could not be used in phytoextraction of copper, under the environmental conditions of the study area. Pine sampled from the I2 and B sampling sites had the properties of plant excluder. It was noticed that pine tree had the ability to efficiently translocate elevated Cu contents from the soil to the above-ground parts, that could be the specific tolerance mechanism to high Cu concentrations in the

environment, and especially in the soil. Such specific Cu fate in the soil-needles interface was determined for the concentrations of Cu in the pine soil over about 1500 mg/kg (UI and R2 sampling sites). This specific behaviour should be further tested in the conditions of Cu soil contents higher than the specified value.

ACKNOWLEDGEMENT

The authors are grateful to the Ministry of Education, Technological Development and Innovation of the Republic of Serbia for financial support, within the funding of the scientific research at the University of Belgrade, Technical Faculty in Bor (No. 451-03-47/2023-01/200131). Our thanks go to Prof. Mara Ž. Manzalović from the University of Belgrade, Technical Faculty in Bor, for providing language assistance.

REFERENCES

[1] Šerbula S., Stanković V., Živković D., *et al*., Mine Water Environ. 35 (2016) 480–485.

[2] Serbula S. M., Milosavljevic J. S., Kalinovic J. V., *et al*., Sci. Total Environ. 777 (2021) 145981.

[3] Ristić N., Veličković M., Panić M., *et al*., Pol. J. Environ. Stud. 31 (4) (2022) 3287–3296.

[4] Milosavljevic J. S., Serbula S. M., Djuro C. M., *et al*., Eur. J. Soil Biol. 101 (2020) 103232.

[5] Siyar R., Doulati Ardejani F., Norouzi P., *et al.*, Water 14 (2022) 3597.

[6] Favas P. J. C., Pratas J., Prasad M. N. V., Int. J. Environ. Sci. Technol. 10 (2013) 809–826.

[7] Placek A., Grobelak A., Kacprzak M., Int. J. Phytoremediation 18 (6) (2016) 605–618.

[8] Petrova S. T., Environ. Sci. Pollut. Res. 27 (2020) 39490–39506.

[9] Kalinovic T. S., Serbula S. M., Radojevic A. A., *et al.*, Geoderma 262 (2016) 266–275.

[10] US Environmental Protection Agency, 1996. Acid Digestion of Sediments, Sludges, and Solids (3050B), Washington, DC.

[11] Kafle A., Timilsina A., Gautam A., *et al*., Environ. Adv. 8 (2022) 100203.

[12] Mendez M. O., Maier R. M., Environ. Health Perspective 116 (3) (2008) 278–283.

[13] van der Ent A., Baker A. J. M., Reeves R. D., *et al*., Plant Soil 362 (2013) 319–334.

[14] Ernst W.H.O., Geochem. 65 (S1) (2005) 29–42.

[15] Regulation No. 88/10 (2010) The Official Gazette of Republic of Serbia, No. 88/2010: the soil quality monitoring programme using indicators for assessing the risks from the soil degradation as well as the methodology for working out the remediation programme (*in Serbian*).

[16] Radmacher P., Institute for World Forestry, Federal Research Centre for Forestry and Forest Products, Hamburg, (2003).

[17] Kalinović T., Šerbula S., Kalinović J., *et al*., Proceedings of the 28th International Conference Ecological Truth and Environmental Research–EcoTER'20, 16–19.06.2020, Kladovo, Serbia, (2020) 60–65.

ELECTROCHEMICAL SENSING OF FOLIC ACID

Žaklina Tasić[1*], Marija Petrović Mihajlović[1], Ana Simonović[1], Milan Radovanović[1], Milan Antonijević[1]

[1]University of Belgrade, Technical Faculty in Bor, V.J. 12, 19210 Bor, SERBIA

[*]*ztasic@tfbor.bg.ac.rs*

Abstract

The purpose of this article is to analyze the findings from studies on the electrochemical determination of folic acid (Vitamin B9). Folic acid is an important water-soluble vitamin for various biological processes, and its deficiency in human organisms can lead to health problems. Different electrochemical sensors are available for detecting folic acid in various mediums. These sensors provide rapid, selective and sensitive detection of folic acid, making them a valuable tool in analytical research. The results of researchers who used low-cost and environmentally friendly materials to prepare sensors are presented in this study. The limit of detection of one such sensor was 1.8×10^{-10} *mol* dm^{-3} *indicating its good selectivity and sensitivity.*

Keywords: electrochemical sensors, folic acid, vitamins, differential pulse voltammetry.

INTRODUCTION

Vitamins represent essential nutrients that are necessary for normal functioning of the human organism. They are introduced into the body through food or supplements because the body cannot synthesize them [1]. The B group vitamins include eight water-soluble vitamins that play important roles in cell metabolism. They are: B1 (thiamine), B2 (riboflavin), B3 (niacin), B5 (pantothenic acid), B6 (pyridoxine), B7 (biotin), B9 (folate), and B12 (cobalamin). Each B vitamin has its own unique function, but they all work together to help the body convert food into energy and to support the nervous system. Deficiencies in B vitamins can lead to various health problems, such as anemia, neuropathy, and birth defects [2]. Folic acid (vitamin B9) is important for several processes in the human body, including the formation of red blood cells, for cardiovascular health, nucleic acid synthesis, the normal development of the neural tube and to produce neurotransmitters [3]. B vitamins are commonly found in animal products such as meat, fish, and dairy products, as well as in supplements. Spinach, white beans, asparagus, soybeans, oranges and melons are also the important sources of folic acid [2].

There are several analytical methods that can be used to determine the level of folic acid (FA) in a sample, including: high-performance liquid chromatography (HPLC), capillary electrophoresis (CE), spectrophotometry [4]. Despite their high precision and sensitivity, these methods for determining folic acid have drawbacks such as time-consuming procedures, necessary sample preparation, expensive equipment, and complexity of procedures [5]. On the other hand, electroanalytical methods, which are frequently utilized due to their benefits of low cost, simple sample preparation, fast analysis time, high accuracy, and low detection

limits, are increasingly being used as alternatives. Electrochemical sensors can be used to detect folic acid, too. There are several advantages of using electrochemical sensors for the detection of folic acid compared to other analytical methods: sensitivity, selectivity, they are also portable and cost-effective.

Different electrodes were used for the determination of folic acid including glassy carbon electrode, carbon paste, pencil graphite electrode, silver solid amalgam, and mercury drop electrode [5,6]. The significance of the determination of folic acid in different mediums and using different sensors is highlighted in review works by Di Tino *et al*. [4] and Batra *et al*. [7]. Additionally, in the paper of Alizadeh *et al*. [6] the possibilities of using modified carbon-based electrodes for the determination of FA are summarized.

The aim of this paper is to point out the importance of using low-cost materials for developing electrochemical sensors for the determination of folic acid in different matrices.

ELECTROCHEMICAL SENSORS FOR THE DETERMINATION OF FOLIC ACID

In the early 2000s, bismuth-film electrodes (BiFEs) attracted an increasing interest from researchers in electroanalytical investigations, as an adequate replacement for mercury electrodes. Compared to the mercury electrodes, bismuth-based electrodes are non-toxic and have a wide potential window. Bismuth-film electrodes are a type of electrochemical sensor that can be used for the detection of various compounds, including folic acid. They are made by depositing a thin film of bismuth onto a conductive substrate, such as glassy carbon electrodes (GCEs), carbon paste electrodes (CPEs), screen-printed electrodes (SPEs) [8]. Bismuth-film electrodes can be used to detect a wide range of substances, including: heavy metals, and organic compounds (pesticides, vitamins, amino acids).

Pencil graphite electrodes belong to the carbon based electrodes. Carbon based electrodes stand out from other materials due to their properties, such as chemical stability, a large active surface, the ability to modify the surface, and electrocatalytic activity in various oxidation-reduction reactions [9]. In their papers, Tasić *et al*. [10,11] showed the applicability of low-cost electrochemical sensors, such as PGE and an electrochemical sensor prepared using recycled carbon from spent batteries, for the detection of target analytes.

The effectiveness of poly(cystine)/PGE in determining folic acid was studied through the use of differential pulse voltammetry (DPV) and cyclic voltammetry (CV) techniques. The peak current of the unmodified pencil graphite electrode was found to be 0.77 μA. However, the response of folic acid was enhanced to 3.56 μA with the use of poly(cystine)/PGE. This improvement was attributed to the presence of thiol groups in L-cystine, which facilitate electron transfer and enhance the conductive properties of the electrode [5]. The slope of the Ep versus pH plot was calculated to be -35 mV/pH, indicating that the oxidation of folic acid involves a transfer of two electrons and one proton [5].

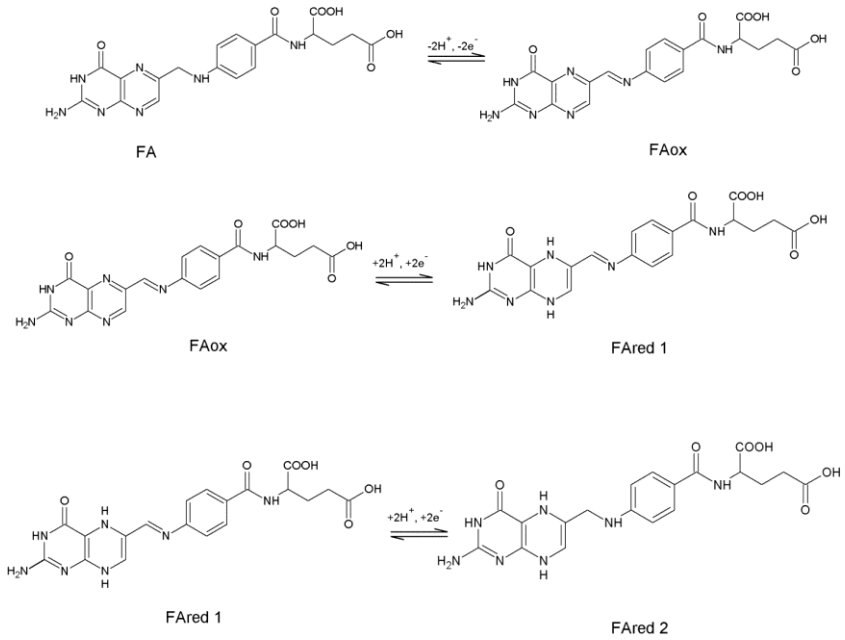

Figure 1 *Proposed mechanism of oxidation and reduction of FA on graphite paste electrode [12]*

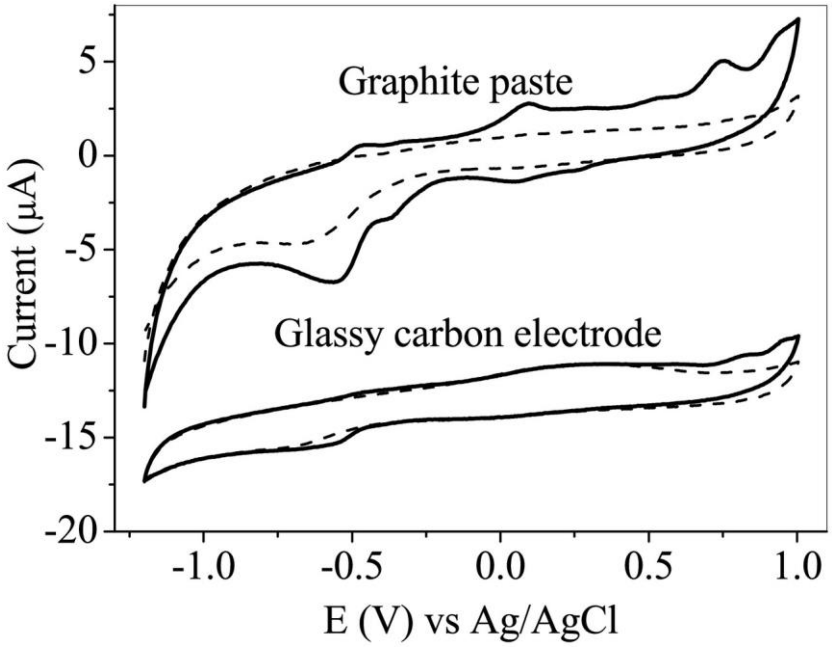

Figure 2 *Cyclic voltammograms obtained for 44.14 mg L^{-1} FA in 0.1 mol L^{-1} acetate buffer as supporting electrolyte at pH 4.5 with v = 50 mV s^{-1}, using graphite paste-based electrode (dashed line – blank solution) and glassy carbon electrode (dashed line – blank solution) [12; https://doi.org/10.1016/j.jelechem.2018.04.043].*

Table 1 summarizes the results obtained by different electrochemical sensors for determining FA.

Table 1 *Electrochemical characteristics of different electrodes as sensor for folic acid detection*

Sensor	Medium	Method	Linear range	LOD	Reference
FA-imp/CNDs/PGE	PBS (pH 6.2) + 0.1 M KCl	CV, DPV	2.2–30.8 ng mL^{-1}	2.02 ng mL^{-1}	[3]
poly(cysteine)/PGE	PBS pH 7	CV, DPV	1.0–100 µmol dm^{-3}	0.43 mol dm^{-3}	[5]
NiZCB-GCE		DPV	0.004–0.22 mg dm^{-3}	1.3 µg dm^{-3}	[13]
Bismuth film electrode		SWAdS	0.5–20 nmol dm^{-3}	0.2 nmol dm^{-3}	[14]
GPE modified with hybrid MIP (poly(methacrylic acid)-SiO_2)	pH 4.5	DPV, SWV	0.005–0.1 µg dm^{-3}	0.72 µg dm^{-3}	[12]
poly tyrosine modified PGE	PBS pH 7	CV, DPV	1µM–85 µmol dm^{-3}	/	[15]
BiFE-GCE	BR pH 2	CV, DCV	$2.5x10^{-8}$–$3x10^{-5}$ mol dm^{-3}	$4.1x10^{-9}$ mol dm^{-3}	[8]
BiFE-GCE	Acetate buffer solution pH 4.5	SWCSV, CV	0.1–10.0 µmol dm^{-3}	$1x10^{-3}$ µmol dm^{-3}	[16]

CV – cyclic voltammetry; DPV – differential pulse voltammetry; SWV – square wave voltammetry; DCV – direct current voltammetry; SWCSV – square wave cathodic stripping voltammetry; PGE – pencil graphite electrode; NiZCB-GCE – Ni-zeolite/carbon black-modified glassy carbon electrode; BiFE-GCE – a bismuth-film electrode prepared on the glassy carbon electrode; FA-imp/CNDs/PGE – folic acid imprinted on a pencil graphite electrode modified with carbon nanodots; PBS – phosphate buffer solution; BR – Britton-Robinson buffer solution; LOD – limit of detection.

Porada *et al*. [13] in their study presented a low-cost and highly specific voltammetric method for measuring vitamins B2, B9, B12, and B3 using a Ni-zeolite/carbon black-modified glassy carbon electrode (NiZCB/GCE). By using an environmentally friendly Ni-exchanged natural zeolite and conductive carbon black (CB) in a one-step modification of the GCE, a highly sensitive sensor capable of accurately detecting individual B-group vitamins, even in the presence of other vitamins, was obtained with a low limit of detection (Table 1). Kuceki *et al*. [12] initially compared the electrochemical responses of folic acid using graphite paste and glassy carbon electrodes (Figure 2). The results showed substantial improvements in both the anodic and cathodic peak currents when using the graphite paste electrode. This improvement may be due to the higher porosity of the graphite paste compared to the glassy carbon electrode, which makes the adsorption process easier [12]. As reported, the oxidation process at +0.8 V occurs on the side-chain, as demonstrated in Figure 1, which results in the loss of two protons and two electrons [12]. The reduction processes at -0.35 V and -0.50 V are likely attributed to the reduction of the pterin moiety of the FA molecule (Figure 1), and the reduction of the side-chain –CH=N–, respectively. According to the data reported by Kuceki *et al*. [12], the inclusion of a low amount (3% w/w)

of molecularly imprinted polymer in the graphite paste electrode enabled the development of a highly sensitive and selective sensor for folic acid without the need for a preconcentration step. Stepankova *et al*. [8] and Vladisavljevic *et al*. [16] used a bismuth-film prepared ex situ on a glassy carbon electrode for the determination of folic acid. No oxidation signal was recorded in Britton–Robinson buffer (pH 5) under the optimised conditions, indicating that the electrode process is irreversible with one reduction peak near -0.55 V [8,16]. The shift in the reduction potential to a less negative value and increasing the intensity of folic acid reduction peak on the BiFE compared to the GCE suggest the electrocatalytic nature of the BiFE. This behaviour was also seen with the BiNWs/GCE and is believed to be due to its high surface-to-volume ratio and uniform pore size that enhance the rapid reduction kinetics of folic acid [16]. Vladisavljević *et al*. [17] prepared BiFE on GCE at different pH, with or without the presence of a complexing agent (EDTA) and used the sensor to determine folic acid and glutathione. The findings in this study show a strong correlation between the bismuth film structure and the electrolyte composition and electrodeposition parameters. Typically, a thick, uniform, non-porous bismuth film was obtained when electrodeposition was carried out in an acetic buffer with a pH of 4.5. However, incorporating the complexing agent ethylenediaminetetraacetic acid (EDTA) into the acetic buffer produced a flake-like, dendritic structure. On the other hand, films produced in HNO_3 had a porous structure and lacked stability. The use of the BiF electrode in the determination of folic acid showed that the film created in the acetate buffer with the addition of EDTA has impressive stripping performance and improved sensitivity. Geca *et al*. [18] demonstrated that the solid bismuth microelectrode is a highly efficient tool for determining folic acid, providing a wide linear range, low limits of detection and quantification, and high selectivity. The lowest reported limit of detection for folic acid was 1.8×10^{-10} mol dm^{-3}. The adsorptive stripping voltammetry method with prepared sensor can be used in pharmaceutical analysis without complicated sample preparation. Furthermore, the solid bismuth microelectrode does not require the addition of Bi^{3+} to the supporting electrolyte, making it an environmentally-friendly alternative to bismuth film electrodes. Overall, the solid bismuth microelectrode is a convenient and superior alternative to previously reported bismuth microelectrode arrays and bismuth film electrodes [18]. According to the results summarized in Table 1, it can be said that the modified PGEs were better in near-neutral solution, while the sensory characteristics of BiFE were better in acidic environments.

CONCLUSION

The importance of folic acid in various vital biological processes, such as nucleic acid synthesis, cell division, fetus growth and development, has led to its widespread use as a supplement to prevent and treat folate deficiency in human organism. As a result, in recent years, there has been a significant effort in the analytical field to create precise and reliable sensors for the determination of folic acid due to its crucial role in human health. Based on a literature review, it can be seen that different prepared electrochemical sensors can be used to determine folic acid. Some of them were better in acidic solutions (BiFEs), while others were better in neutral solutions (modified PGEs). Depending on the experimental conditions and the type of sensor, the detection limits ranged from 1.8×10^{-10} mol dm^{-3} to 0.43 mol dm^{-3}.

In addition, the researchers showed that the modified electrodes have improved sensing capabilities than the unmodified ones. It is still a challenge for researchers to develop a suitable sensor that is sensitive and selective, while being cheap and environmentally friendly.

ACKNOWLEDGEMENT

The authors are grateful to the Ministry of Science, Technological Development and Innovation of the Republic of Serbia for financial support according to the contract with the registration number (451-03-47/2023-01/200131).

REFERENCES

[1] Bas B., Jakubowska M., Górski Ł., Talanta 84 (2011) 1032–1037.

[2] Ribeiro M. V. de M., Melo I. da S., Lopes C., *et al*., Braz. J. Pharm. Sci. 52 (2016) 741–750.

[3] Güney S., J. Electroanal. Chem. 854 (2019) 113518.

[4] Di Tinno A., Cancelliere R., Micheli L., Sensors 21 (2021) 3360.

[5] Dokur E., Gorduk O., Sahin Y., Anal. Lett. 53 (13) (2020) 2060–2078.

[6] Alizadeh M., Nejad F. G., Dourandish Z., *et al*., J. Food Meas. Charact. 16 (2022) 3423–3437.

[7] Batra B., Narwal V., Kalra V., *et al.*, Process Biochem. 92 (2020) 343–354.

[8] Stepankova M., Selesovska R., Janıkova L., *et al*., Monatsh. Chem. 148 (2017) 423–433.

[9] Tasić Ž. Z., Petrović Mihajlović M. B., Simonović A. T., *et al*., Sensors 22 (23) (2022) 9185.

[10] Tasić Ž. Z., Petrović Mihajlović M. B., Simonović A. T., *et al*., Results Phys. 22 (2021) 103911.

[11] Tasić Ž. Z., Petrović Mihajlović M. B., Radovanović M. B., *et al*., Sci. Rep. 12 (2022) 5469.

[12] Kuceki M., Oliveira F. M. de, Segatelli M. G., *et al*., J. Electroanal. Chem. 818 (2018) 223–230.

[13] Porada R., Fendrych K., Kochana J., *et al*., Food Control 142 (2022) 109243.

[14] Rutyna I., Anal. Lett. 48 (2015) 1593–1603.

[15] Santhy A., Beena S., Veena, *et al*., IOP Conf. Series: Mater. Sci. Eng. 872 (2020) 012128.

[16] Vladislavić N., Buzuk M., Buljac M., *et al*., Croat. Chem. Acta 90 (2) (2017) 231–239.

[17] Vladislavić N., Buzuk M., Brinić S., *et al*., J. Solid. State Electrochem. 20 (2016) 2241–2250.

[18] Gęca I., Korolczuk M., Electroanal. 32 (2020) 496–502.

POTENTIAL ENVIRONMENT POLLUTANT – INTERMEDIATE PRODUCT OF THE STEEL PRODUCTION PROCESS

Vanja Trifunović[1*], Snežana Milić[2], Ljiljana Avramović[1], Milan Antonijević[2], Milan Radovanović[2]

[1]Mining and Metallurgy Institute Bor, Zeleni bulevar 35, 19210 Bor, SERBIA

[2]University of Belgrade, Technical Faculty in Bor, V.J. 12, 19210 Bor, SERBIA

[*]*vanja.trifunovic@irmbor.co.rs*

Abstract

As an intermediate product of the steel production process using an electric arc furnace, electric arc furnace dust (EAF dust) occurs. The resulting intermediate product of steel production is considered hazardous industrial solid waste in many countries of the world, given that it contains a large number of heavy metals that can reach the environment due to the action of atmospheric influences if it is not adequately disposed of. In this paper, the physico-chemical characterization of the EAF dust originating from a steel plant in the Republic of Serbia was performed, and Toxicity Characteristic Leaching Procedure (TCLP test) and Leachability Procedure (LP test) were performed in order to define the impact of this material on the environment and human health. The chemical analysis of the tested sample of the EAF dust showed a zinc content of 32.44%, iron – 18.92%, lead – 1.39%, cadmium – 0.04%, chromium – 0.25% and a lower content of a large number of other elements. The results of the LP test showed an increased chloride content in the leaching eluate, above the permitted limits, even for waste disposal at a hazardous waste landfill. In the TCLP eluate, the content of zinc, cadmium and lead are above the permitted limits, thus the sample shows toxic characteristics and danger to the environment and human health. In order to environmental and human health protection, it is necessary to do the treatment of this type of material before disposal at the landfill.

Keywords: EAF dust, environmental protection, TCLP test, LP test.

INTRODUCTION

During the steel production using electric arc furnaces, at a process temperature of 1600°C, during the melting of a batch of scrap iron, some elements evaporate. Volatile elements, together with a part of solid particles, go as a gas phase to the gas purification system, during which one of the intermediate products of this process – electric arc furnace dust (EAF dust) is formed [1,2].

During the production of 1 ton of raw steel, about 10–20 kg of red-brown EAF dust is generated [1,3–9]. Due to the presence of heavy metals in the EAF dust, it is considered officially hazardous industrial solid waste in many countries [3,6–8,10–13].

In this paper, the physico-chemical characterization of the EAF dust originating from a steel plant in the Republic of Serbia was performed, and its toxicity characteristics and leachability were examined in terms of defining its impact on the environment and human health after disposal in a landfill.

POTENTIAL ENVIRONMENTAL POLLUTION WITH EAF DUST

The potential pollution of this type of waste consists in the possibility of leaching of heavy metals, such as: Zn, Cu, Ni, Cd, Cr, Pb, F and Cl, etc., which are in its composition [14]. Inadequate disposal of the EAF dust has a negative impact on the environment [7]. There is still a large amount of EAF dust in the world, the treatment of which should be carried out as soon as possible, and which is accumulated around steel plants or in landfills of this material. Disposal method of the EAF dust is very important. If the EAF dust is inadequately disposed of, and in inappropriate landfills, due to the action of atmospheric influences, self-leaching of heavy metals from the EAF dust may occur. It is necessary to ensure that when the EAF dust is disposed in hazardous waste landfills, it must be protected from rain, in order to prevent the formation of polluted leachate, which could contaminate the surrounding areas [14].

Figure 1a shows a "mountain" of the EAF dust generated from steel production in Egypt [1]. The figure represents a typical inadequate way of disposing of this type of waste, given that the waste is exposed to atmospheric influences. Also, considering that the EAF dust is a material with very fine particles that can spread in the air, this kind of exposure to it due to the action of the wind makes it possible [1,14]. A more adequate way of disposal of the EAF dust from steel production in the Republic of Serbia is shown in Figure 1b. The EAF dust is packed in jumbo bags and stored under a canopy at the landfill around of the steel plant, in the production process of which it is generated.

a) *b)*

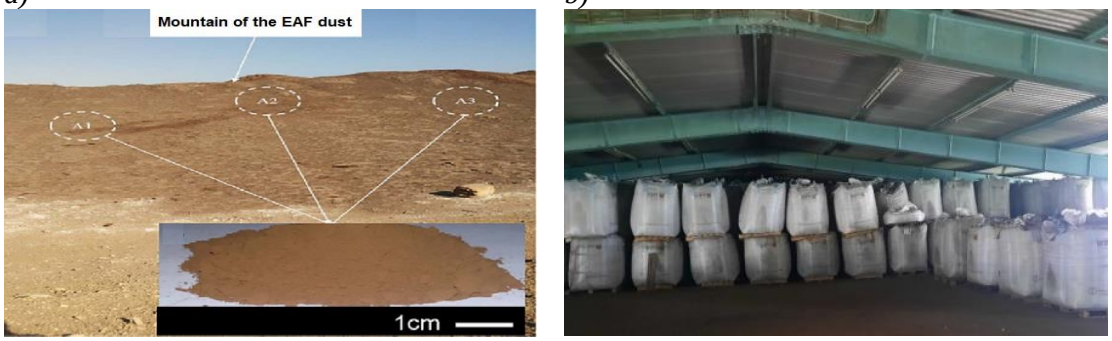

Figure 1 *Method of disposal of the EAF dust in the world and in our country a) landfill in Egypt [1]; b) landfill in the Republic of Serbia*

In order to environmental protection and human health protection from the negative impact of this type of hazardous waste, it is necessary to carry out its treatment in accordance with the legislation of the country where it is located. Before applying any treatment of electric arc furnace dust, it is necessary to carry out its detailed characterization.

Physico-chemical characterization

The results of the physical characterization of the initial representative sample of the EAF dust are as follows: moisture – 0.36%, pH value of the sample – 11.42, density – 4.351 g/cm^3 and bulk mass – 654 kg/m^3.

The chemical composition of a representative EAF dust sample is presented in the Table 1.

Table 1 *Chemical composition of a representative EAF dust sample [15]*

Element	Content, %	Element	Content, %
Zn	32.44	Ca	3.85
Fe	18.92	Co	0.0017
Sn	0.037	Pb	1.39
S	0.51	Ni	0.036
Mo	<0.005	P	0.15
Mn	1.81	Mg	0.93
Si	1.34	Sb	0.022
Cr	0.25	Al	0.73
As	0.0041	K	0.87
Cd	0.04	Na	1.28
Cl	2.85	Hg	0.0001
Bi	0.013	Ag	0.00604
Cu	0.19	Au	0.00004

LABORATORY INVESTIGATIONS OF THE IMPACT ON THE ENVIRONMENT AND HUMAN HEALTH

According to the Rulebook on categories, investigation and classification of waste (Official Gazette of RS 93/2019, 39/2021), with regard to the impact on the environment and human health after its disposal, toxicity and leachability tests of the material were performed on a representative sample of the EAF dust. Laboratory tests were carried out according to accredited standard methods: SRPS EN 12457-2 for testing material leachability, and EPA 1311 for testing material toxicity characteristics.

Leachability Procedure (LP test)

The results of the leachability test (LP test) of a representative EAF dust sample according to the SRPS EN 12457-2:2008 standard are presented in Table 2 [15].

Due to the increased chloride content in the leaching eluate (leaching solution) above the permitted limits, even for waste disposal at a hazardous waste landfill, based on the leachability test results, the EAF dust sample was categorized as hazardous waste in terms of disposal. These results indicate that the EAF dust must undergo pretreatment before final disposal.

Table 2 *Leachability test results for the representative EAF dust sample*

Parameter	Measured value	Reference value for non-hazardous waste[a]	Reference value for hazardous waste[b]
pH	11.31	6–13[c]	-
Conductivity, $\mu S \cdot cm^{-1}$	8288	-	-
Content of dry matter, $mg \cdot kg^{-1}$			

Table 2 *continued*

Elements	Measured value	Reference value for non-hazardous waste[a]	Reference value for hazardous waste[b]
Zn	3.00	50	200
As	<0.20	2	25
Cu	<0.05	50	100
Sb	<0.50	0.7	5
Cd	<0.08	1	5
Mo	4.70	10	30
Ni	<0.07	10	40
Se	<0.33	0.5	7
Pb	10.00	10	50
Cr	<0.05	10	70
V	<0.08	200	-
Hg	<0.005	0.2	2
Ba	2.60	100	300
Ag	<0.05	50	-
Cl^-	**30900**	**15000**	**25000**
F^-	36.30	150	500
SO_4^{2-}	7400	20000	50000
Phenol index	0.24	1000	-

[a,b]Annex 10 of the Rulebook on categories, investigation and classification of waste (Official Gazette of RS 93/2019, 39/2021), Article 2, Parameters for testing waste and leachate from non-hazardous waste landfills[a] and hazardous waste[b]. Ambient temperature 21°C, humidity 52 %, pressure 970 hPa.
[c]Reference value for pH according to the Rulebook 93/2019, 39/2021 Annex 7, H15-Waste that has the property of producing another substance in any way after disposal, e.g. leachate that has any of the following characteristics (H1-H14), is 6–13. The measured pH value is within the allowable range.

Toxicity Characteristic Leaching Procedure (TCLP test)

Table 3 [15] presents the results of the toxic leaching characteristic test (TCLP test) (EPA 1311) of a representative sample of the EAF dust intended for disposal.

The obtained results of the TCLP test show that the EAF dust sample, due to the increased content of zinc, cadmium and lead in the TCLP eluate (leaching solution), which are above the permitted prescribed limits, showed toxic characteristics. This type of hazardous waste requires additional attention and the application of appropriate treatment in order to environmental protection and human health protection.

The treatment of this type of hazardous waste can be performed by hydrometallurgical, pyrometallurgical or combined procedures [1,5,6,10,15]. Considering the highest content of zinc in the EAF dust, compared to all other elements, there is a possibility of its recovery by some of the mentioned procedures, which would also make it possible to make a profit. Apart from the application of the appropriate treatment of the EAF dust, primarily in order to protect the environment from the negative impact of hazardous waste, it is observed that this material can represent a secondary raw material for recovery of zinc.

Table 3 *TCLP test results of a representative EAF dust sample*

Elements	Measured value, mg·dm^{-3}	Reference value for non-hazardous waste[a], mg·dm^{-3}	Elements	Measured value, mg·dm^{-3}	Reference value for non-hazardous waste[a], mg·dm^{-3}
V	<0.008	24	Ag	<0.005	5
Cr	<0.005	5	**Cd**	**13.88**	**1**
Ni	0.068	20	Ba	0.880	100
Cu	0.050	25	Hg	<0.0005	0.20
Zn	**2690.67**	**250**	**Pb**	**61.16**	**5**
Ar	<0.020	5	Mo	<0.007	350
Se	<0.033	1	Sb	<0.050	15

[a]Annex 10 of the Rulebook on categories, investigation and classification of waste (Official Gazette of RS 93/2019, 39/2021), Article 1, Parameters for testing the toxic characteristics of waste intended for disposal.

CONCLUSION

Dust from the electric arc furnace (EAF dust) is generated as an intermediate product of the steel production process by melting secondary raw materials in an electric arc furnace. Due to the fact that the EAF dust contains a large number of heavy metals that can enter the environment due to the action of atmospheric influences, this material is considered hazardous industrial solid waste in many countries of the world. Chemical analysis of a representative EAF dust sample, originating from the Republic of Serbia, determined the content of the following elements: zinc – 32.44%, iron – 18.92%, lead – 1.39%, cadmium – 0.04%, chromium - 0.25% and lower content of a large number of other elements. Laboratory tests of toxicity characteristics (TCLP test) and leachability (LP test) were also performed on a representative EAF dust sample. The results of the TCLP test showed that the content of zinc, cadmium and lead are above the permitted prescribed limits, on the basis of which it can be concluded that the sample shows toxic characteristics and danger to the environment and human health. The results of the LP test showed increased chloride content in the eluate for leaching, above the permitted limits, even for waste disposal at the hazardous waste landfill. In order to protect the environment and human health, it is necessary to do the treatment of this type of material before its disposal in a landfill. The treatment can be performed using hydrometallurgical, pyrometallurgical or combined procedures. Apart from the application of appropriate treatment of the EAF dust, primarily in order to protect the environment from the negative impact of this hazardous waste, this material can also be used as a secondary raw material for zinc recovery, and gaining adequate economic profit.

ACKNOWLEDGEMENT

The authors are grateful to the Ministry of Ministry of Science, Technological Development and Innovation of the Republic of Serbia for financial support according to the contract with the registration number 451-03-47/2023-01/200052 and number 451-03-47/2023-01/200131.

REFERENCES

[1] Wang J., Zhang Y., Cui K., *et al*., J. Cleaner Prod. 298 (2021) 126788.

[2] Trifunović V., Avramović Lj., Jonović R., *et al*., Proceedings of The 52nd International October Conference on Mining and Metallurgy, Bor, Serbia (2021) 209–212.

[3] Khattaba R.M., El-Sayed Selemanb M.M., Zawraha M.F., Ceram. Int. 43 (2017) 12939–12947.

[4] Halli P., Hamuyuni J., Revitzer H., *et al*., J. Cleaner Prod. 164 (2017) 265–276.

[5] Tsakiridis P. E., Oustadakis P., Katsiapi A., *et al*., J. Hazard. Mater. 179 (2010) 8–14.

[6] Kukurugya F., Vindt T., Havlík T., Hydromet. 154 (2015) 20–32.

[7] Hazaveh P. K., Karimi S., Rashchi F., *et al*., Ecotoxicol. Environ. Saf. 202 (2020) 110893.

[8] Laforest G., Duchesne J., J. Hazard. Mater. B135 (2006) 156–164.

[9] Alencastro de Araújo J., Schalch V., J. Mater. Res. Technol. 3(3) (2014) 274–279.

[10] Lin X., Peng Z., Yan J., *et al*. J. Cleaner Prod. 149 (2017) 1079–1100.

[11] Ledesma E. F., Lozano-Lunar A., Ayuso J., *et al*., Constr. Build. Mater. 183 (2018) 365–375.

[12] Commission of the European Communities, Guidance on classification of waste according to EWC-Stat categories, Supplement to the Manual for the Implementation of the Regulation (EC) No 2150/2002 on Waste Statistics, version 2, December 2010.

[13] Environmental Protection Agency, Land Disposal Restrictions for Electric Arc Furnace Dust (K061) - Federal Register Notice, Vol. 56 No. 160, August 19 (1991) 41164.

[14] Norma Brasileira, ABNT 10004:2004, Solid waste Classification (2004).

[15] Trifunović V., Milić S., Avramović Lj., *et.al*., Hem. Ind. 76 (4) (2022) 237–249.

BIOPESTICIDES IN THE ENVIRONMENT

Natalija Ognjanović[1*], Vladan Nedelkovski[1], Sonja Stanković[1], Snežana Milić[1]
[1]University of Belgrade, Technical Faculty in Bor, V.J. 12, 19210 Bor, SERBIA
[*]*onatalija611@gmail.com*

Abstract

Pesticides are substances intended for the prevention, destruction, suppression or reduction of pests. The continuous application of pesticides has led to the development of resistance in plant and animal species and the transfer of microelements through treated plants to the bodies of humans and animals. This can lead to chronic and acute diseases, and even toxic poisoning. In order to avoid the negative impact of pesticides on plant and animal life and to prevent environmental pollution, researchers suggest the use of biopesticides. Biopesticides are an environmentally friendly alternative to synthetic pesticides. They are obtained from natural materials such as microorganisms (fungi, bacteria, viruses, etc.), plants (extracts from plants) and the animal world (nematodes) and some minerals. This paper provides an overview of scientific research on the use of biopesticides instead of pesticides in order to reduce environmental pollution.

Keywords: pesticides, pollutants, biopesticides, environment.

INTRODUCTION

The pollution of ecosystems by pesticides has occurred due to their increased use in agriculture. Western Europe, North America, and Australia are considered highly polluted areas, where contamination is caused by excessive pesticide use. These regions have high-intensity agriculture. In addition to pesticide pollution, a characteristic of these areas is the loss of habitats for many plant and animal species, resulting from substrate homogenization caused by the widespread use of artificial fertilizers [1]. The use of conventional pesticides and fertilizers over several decades has led to their bioaccumulation, with detrimental effects on soil biodiversity and the development of resistance in pests. With the increasing number of plant and animal species that are resistant to typical pesticides, it becomes imperative for researchers to develop new and more effective biopesticides. The demand for more efficient biological pesticides has been growing worldwide in recent years. Due to the various undesirable effects of pesticide application, researchers aim to develop more effective biopesticides that would have targeted efficacy while minimizing harm to non-targeted species and the overall environment. Some authors believe that the use of nanotechnology in the production of biopesticides could enable adequate treatments for targeted species [2].

PESTICIDES AS ENVIRONMENTAL POLLUTANTS

Pesticides represent a group of chemical substances whose application in agriculture is based on the eradication of harmful organisms. The main mechanisms of pesticide action are biomagnification and bioaccumulation [3]. Pesticides are used in agriculture for their protective role against certain plant crops. Their protective function consists of destroying, preventing, or controlling the growth of pests, including insects, rodents, and specific animal species. They also prevent unwanted plant growth, which, together with insects, negatively affects crop yields or damages specific plant species [4]. Pesticides often have a negative impact on the quality and quantity of food produced from plants treated with these chemicals, despite being applied to protect certain plant species. The increased presence of pesticides and other harmful chemicals adversely affects the functioning of organs in all living organisms [3].

Environmental pollutants are toxic substances that contaminate and negatively affect the living world, resulting from industrialization and intensive agriculture [5]. Figure 1 illustrates the movement of pesticide residues in nature. Residual pesticide particles, carried by air and water, can pollute plant and animal life that is not in proximity to the treated crops. Additionally, the retention of pesticide residues in the soil can be toxic to other organisms. The circulation of pesticide residues in nature, through air, groundwater, and surface water, leads to contamination of the entire environment and all living beings within it [6].

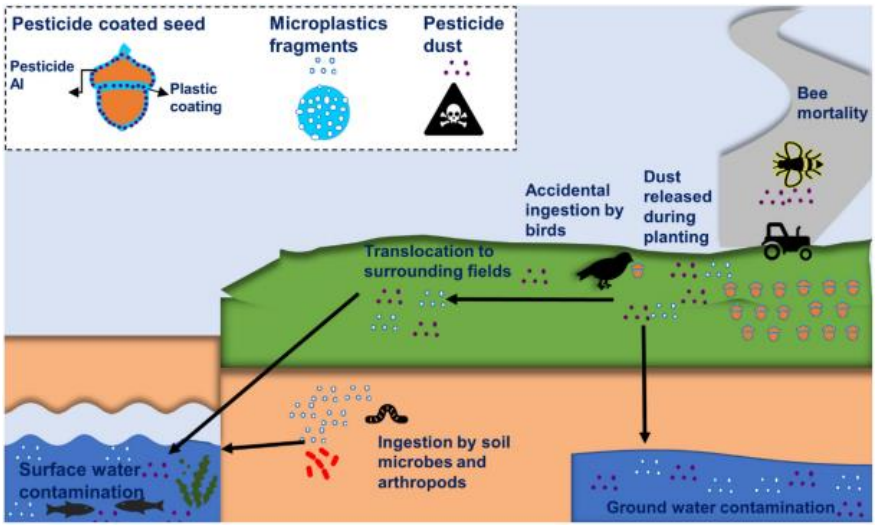

Figure 1 *Schematic representation of pollutant movement in the environment [6]*

It is crucial to accurately assess the current and future ecological state of an environment, as well as the ecotoxicological effects that impact it. This is commonly done by determining the concentrations of specific pollutants in a given environment. Numerous studies have been conducted, using various types of plants, insects, and animals as bioindicators of environmental pollution. When bioindicators are exposed to pesticides, they are simultaneously subjected to significant stress, resulting in morphological and physiological changes, as well as alterations in their behaviour [5]. Figure 2 depicts the environmental circulation of pesticides applied to a specific plant species through the air, water, and soil.

According to the authors Khursheed *et al*. [7], pesticide application leads to contamination of the entire ecosystem.

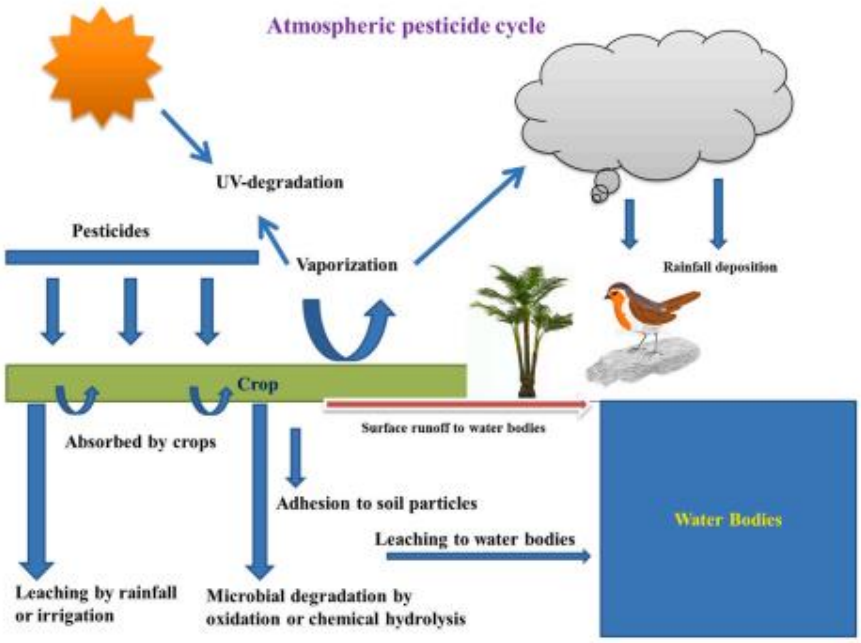

Figure 2 *Ecologic cycle of conventional pesticides [7]*

BIOPESTICIDES IN THE ENVIRONMENT

The mode of action of a biopesticide is crucial for its effectiveness and commercial success. Synthetic pesticides typically consist of a single chemical with specific effects, while biopesticides have more complex mechanisms of action. Biopesticides contain both chemical and biochemical components that modify and control the biochemical, genetic, or structural functions of targeted pests (Figure 3). A large number of biopesticides are composed of bacteria, such as *Bacillus thuringiensis* (Bt), entomopathogenic fungi like *Beauveria bassiana* and *Metarhizium anisopliae*, viruses, single-celled eukaryotes, or entomopathogenic nematodes (EPN). Some biopesticides are derived from microorganisms, such as the neurotoxic insecticide Spinosad, which consists of spinosyns A and D obtained through fermentation of the actinomycete Spinosad, or they can be derived from plants. EF and EPN act by attacking insects through the cuticle, penetrating the host's body, where they reproduce and ultimately kill the host insect, considered a pest. Bacterial control agents, microbial and plant-based products like Spinosad and azadirachtin, are activated after ingestion or through contact, causing rapid death in a wide range of insect pests [8].

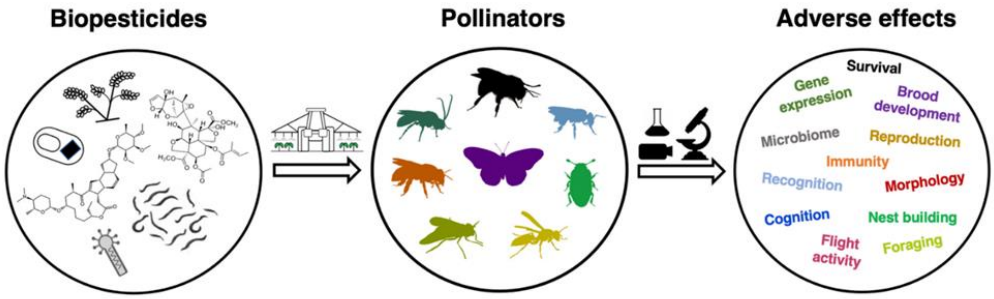

Figure 3 *The impact of biopesticides on target species and the harmful effects resulting from their application [8]*

Implementation of various sorts of biopesticides aiming to reduce environmental pollution

Numerous studies show that synthetic pesticides, which are predominantly used in agriculture, are toxic to non-target plant and insect species, as well as other surrounding organisms, animals, and even humans. Simply put, the entire ecosystem is poisoned by the application of chemical pesticides. Moreover, certain species have developed and continue to develop increasing resistance to synthetic pesticides. By accumulating these chemicals in their bodies, they survive and thrive despite pesticide contamination. Biopesticides are defined as a type of pesticide derived from natural raw materials, such as plants, bacteria, fungi, animals, minerals, etc. They represent an alternative to synthetic pesticides, providing a more natural and healthier solution for the surrounding living world. Biopesticides are more environmentally friendly and serve the same purpose as synthetic pesticides: controlling unwanted plant species, insects, animals, as well as protecting crops from diseases such as viruses, bacteria, fungal infections, and more. In a study conducted by Adhikari and colleagues [9], the efficacy of biopesticides and their impact were evaluated by applying them to potato tubers in order to manage and control the population of moth insects. The biopesticides used in the experiment were *Bacillus thuringiensis*, *Acorus calamus*, *Azadirachta indica*, and *Artemisia vulgaris*. *Bacillus thuringiensis* is a gram-positive bacterium found in the soil and commonly used as a biological insecticide. *Acorus calamus*, also known as sweet flag or calamus, yields essential oil through distillation and is used in the production of plant protection products against insects and parasites. *Azadirachta indica*, commonly known as neem, has strong antiviral, antifungal, and antibacterial properties. *Artemisia vulgaris*, also known as mugwort or black sage, is used in the production of bioherbicides.

During the experiments, the potato tubers were first coated with solutions of biopesticides, *Bacillus thuringiensis*, *Acorus calamus*, *Azadirachta indica*, and *Artemisia vulgaris*, and then bioinsecticides in powder form were applied over the potato tubers. Testing on samples of different potato varieties using the bioinsecticide Acorus calamus demonstrated significant effectiveness [9]. Control research indicates that larval mining was reduced by 88%, while decay loss of the tubers was reduced by 93%. Figure 4 shows a visible difference in the degree of damage to the tubers after treatment with different bioinsecticides: (a) *Azadirachta indica*, (b) *Acorus calamus*, (c) *Bacillus thuringiensis*, (d) *Artemisia vulgaris*,

and (e) the untreated control sample, which serves as a comparison to the controlled test samples.

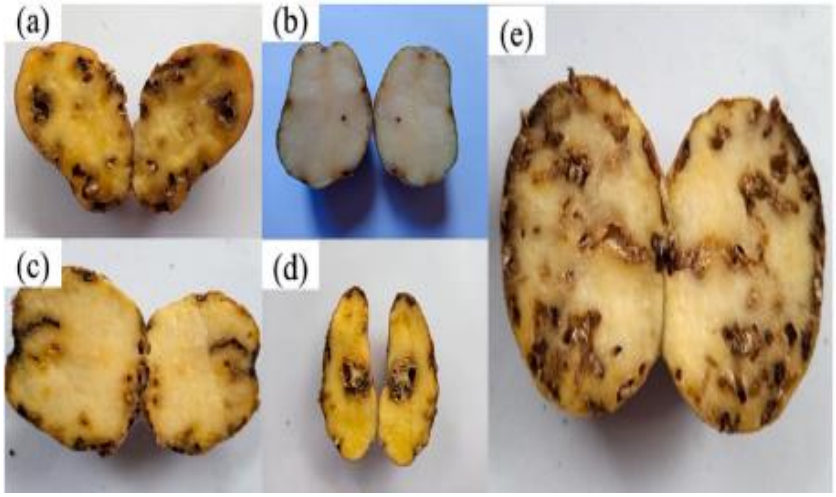

Figure 4 *Samples of different degrees of tuber damage after treatment with bioinsecticides: (a) Azadirachta indica, (b) Acorus calamus, (c) Bacillus thuringiensis, (d) Artemisia vulgaris, (e) untreated control sample [9]*

The research results of Adhikari *et al*. [9] confirmed that the applied biopesticides can be used as alternatives to synthetic pesticides in order to control moths. Their study presented the effects of different types of biopesticides on moth pests in three different regions of Nepal. However, the investigations also confirmed that these biopesticides cannot be used independently, as their effectiveness is lower compared to synthetic pesticides.

CONCLUSION

The mechanism of action of biopesticides is not easily determined experimentally because plants possess numerous enzymes and proteins that affect the target species in various ways. Biopesticides, in fact, still require additional research and investigation to more precisely determine their mechanism of action, which is currently insufficiently understood. The advantage of biopesticides lies in their specific activity and their action on a particular type of target species. Some authors argue that biopesticides exhibit a safe level of toxicity and that their impact on the environment is not negative, while others point out a certain level of toxicity associated with biopesticides. The goal of authors involved in the development and design of new-generation biopesticides is the preservation and protection of the environment. However, certain studies indicate that biopesticides also have negative effects on pollinating insects, causing disturbances and diseases in many pollinators. For these reasons, due to incomplete and contradictory analyses by scientists, it is necessary to constantly conduct experiments and research to assess the environmental risks of biopesticides, as well as their impact on the surrounding plant and animal life. Additionally, it is crucial to continually monitor and adhere to specific regulations prescribed for each type of biopesticide, as mandated by law.

ACKNOWLEDGEMENT

The authors are grateful to the Ministry of Science, Technological development and Innovation of the Republic of Serbia for financial support according to the contract with the registration number 451-03-47/2023-01/200131.

REFERENCES

[1] Schreiner V. C., Link M., Kunz S., *et al*., Water Res. 188 (2021) 116528.

[2] Bapat M. S., Singh H., Shukla S. K., *et al*., Chemosphere 286 (2022) 131761.

[3] Hassaan M. A., Nemr A. E., Egypt. J. Aquat. Res. 46 (3) (2020) 207–220.

[4] Kaushal J., Khatri M., Arya S. K., Ecotoxicol. Environ. Saf. 207 (2021) 111483.

[5] Devillers J., Pham-Deelgue M. H., Honey bees: Estimating the Environmental Impact of Chemicals, London (2002) ISBN: 9780367396329.

[6] Sohail M., Pirzada T., Opperman C. H., *et al*., Green Chem. 24 (2022) 6052.

[7] Khursheed A., Rather M. A., Jain V., *et al*., Microb. Pathog. 173 (2022) 105854.

[8] Cappa F., Baracchi D., Cervo R., Sci. Total Environ. 837 (2022) 155714.

[9] Adhikari A., Shrestha A. K., Timsina S., *et al*., Agric. Res. J. 10 (2022) 100411.

ENVIRONMENTALLY ACCEPTABLE PROCEDURE FOR THE SYNTHESIS OF TETRAETHYLTHIURAMMONOSULFIDE TETS

Goran Milentijević[1], Marko Agatonović[1], Milica Rančić[2], Milutin Milosavljević[1*]

[1]University of Priština, Faculty of Technical Science, Knjaza Miloša 7,
38220 Kosovska Mitrovica, SERBIA

[1]University of Belgrade, Faculty of Forestry, Kneza Višeslava 1, 11030 Beograd, SERBIA

[*]*milutin.milosavljevic@pr.ac.rs*

Abstract

Tetraethylthiuram disulfides (TETD) and tetraethylthiurammonosulfide (TMTS) occupy an important place among the products of organic chemical technology due to the variety of applications. A simple and efficient one-pot synthesis was developed for the preparation of tetraethylthiurammonosulfide (TETS) from diethylamine, carbon disulfide, potassium cyanide and ammonium chloride catalyst, using the isopropanol/water azeotrope as solvent. The isopropanol/water reaction medium is recycled after product removal. Namely, in the first phase of the reaction, the amine salt of diethyldithiocarbamic acid is formed, from which tetraethylthiuram disulfide (TETD) is obtained by oxidation with hydrogen peroxide. In the second phase of the reaction, sulfur is eliminated from the disulfide bond of TETD with the help of potassium cyanide in the presence of ammonium chloride, whereby TETS is formed with the separation of potassium isothiocyanate. Significant features of this protocol are: simplicity of operation, mild reaction conditions, solvent recycling and high product yields, as well as applicability to industrial production level.

Keywords: Tetraethylthiuram disulfides, tetraethylthiurammonosulfide, isothiocyanate.

INTRODUCTION

Due to the variety of applications, tetraethyl thiuram disulfide (TETD) and tetraethyl thiuram monosulfide (TETS) are very often the subject of research synthesis and application. TETD is one of the important accelerators of rubber vulcanization [1], it can also be applied to prevent fungal diseases [2] and for treatment of alcoholism [3]. It can be used for the synthesis of diethyldithiocarbamate and alkyl monosulfide, and recently it was discovered that TETD can act as an irreversible inhibitor of monoglyceride lipase to regulate growth inhibition of prostate and breast cancer cells [4]. Tetraethylthiurammonosulfide (TETS) is an active vulcanization accelerator for natural, butadiene-styrene and butadiene-nitrile rubbers. It gives the mixture good resistance to aging and low-set compression, and can be used for white and colored tires [5]. In addition to being used as an active vulcanization accelerator, TETS is used as a fungicidal active compound [6], in the synthesis of aryl-dithiocarbamates in the reaction with aryl boronic acid in the presence of copper as a catalyst [4], in the synthesis of diaryl sulfides (symmetric thioethers) by reaction with iodobenzenes and phenylboronic acid [7]. Tetraethylthiurammonosulfide (TETS) can be obtained by the reaction of diethylthiocarbamoyl chloride and the corresponding alkaline salt of diethyldithiocarbamic

acid [8,9]. This manuscript presents the one-pot synthesis procedure of TETS from diethylamine, carbon disulfide, hydrogen peroxide and potassium cyanide in isopropanol/water azeotrope (87.3/12.7) as solvent. The reaction mechanism of the synthesis of TETM by the elimination of sulfur from the disulfide bond of TETD with cyanide ion was defined and trial production was carried out under industrial conditions.

MATERIALS AND METHODS

Synthesis of TETS

In the experimental part of the work, the procedure for the synthesis of TETS in one vessel by oxidation of the amine salt of diethyldithiocarbamic acid and subsequent reaction of cyanide in the presence of an ammonium chloride catalyst is described. Also, the procedure for the synthesis of TMTS by the reaction of cyanide in the presence of ammonium chloride on the previously isolated product TETD, which was obtained by oxidation of the amine salt of diethyldithiocarbamine with hydrogen peroxide, is described [10]. The laboratory procedure for the synthesis of sodium diethyldithiocarbamate and diethylthiocarbamoyl chloride, as starting reactants for the synthesis of TETS, is described.

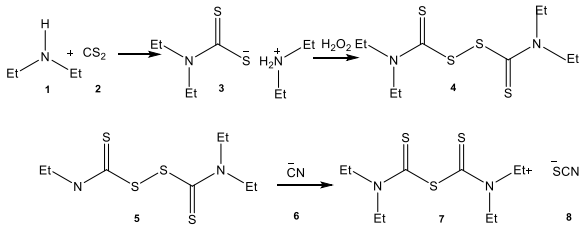

Figure 1 *TETS synthesis reaction*

One-pot laboratory procedure for the synthesis of TETS

Into a 5000 cm^3 three-necked flask equipped with a reflux condenser, dropping funnel, thermometer, cooling jacket and mechanical stirrer, 1540 cm^3 of an azeotropic mixture of isopropyl alcohol-water (87.7–12.3%) and 389.9 cm^3 (4.16 mol) of 70.0% diethyl amine solution, which raises the pH of the solution to 9.5. After starting the stirrer, 256.4 cm^3 (4.16 mol) of 98.0% carbon disulfide was added from a dropping funnel over 0.5 h while maintaining the temperature in the range of 28–35 °C, provided by circulating cooling water. At the end of the reaction, the pH of the reaction mixture was 6.5. At this point, 536.2 cm^3 of a 13.2% hydrogen peroxide solution, prepared by diluting 178.6 cm^3 (2.08 mol) of 35.0% hydrogen peroxide with 406.5 cm^3 of an isopropyl alcohol–water azeotropic mixture (87.7–12.3%) using a dropping funnel for 0.5 h at 35–40 °C. As soon as the reaction took place, the reaction mixture turned yellowish due to the suspended TETD particles. The end of the reaction was tested by sampling the reaction mixture, filtering and adding a few drops of copper(II) sulfate solution to the filtrate. The appearance of a black precipitate indicates that unreacted dithiocarbamate is still present and the reaction has continued [19,20]. At the end of the first phase, 231.11 g (4.16 mol) of ammonium chloride and a 20% aqueous solution of potassium cyanide (285.42 g of potassium cyanide) are added to the suspension of the

obtained TETD (21%) with intensive stirring dissolved in 1068.88 cm^3 of water (4.16 mol). The entire amount of potassium cyanide is added within 2 hours, and then the mixing of the reaction mixture is continued for another hour while maintaining the reaction temperature of 50 °C. The reaction mixture is filtered and the filtrate is used for the next TETS synthesis reaction, the filter cake is washed with water (until negative reaction to NCS^- ion), the crystals are dried in a vacuum dryer at 60 °C until the moisture content is below 0.5%. The obtained crystals are recrystallized from a suitable solvent (benzene, dichloroethane, chloroform, absolute alcohol). Achieved yield 87.57%, melting temperature 70–72 °C, purity: 99.2%. Purity was determined according to the literature method that is used to determine the rest of the dithio compound based on the destruction of sulfuric acid and the absorption of the produced carbon disulfide in a solution of potassium hydroxide – alcohol [21].

Laboratory procedure for the synthesis of TETS from TETD using cyanide ion

In three-necked flask to a 250 cm^3 equipped with a magnetic stirrer, an upright condenser, a thermometer, and a dropping funnel 114 cm^3 of water, 17.00 g (0.057 mol) of 99.2% TETD and 3.21 g (0.057 mol) of ammonium-chloride are added with constant stirring, a prepared 15% aqueous solution of sodium cyanide is added (2.94 g (0.057 mol) of sodium cyanide are dissolved in 16 cm^3 of water). The entire amount of sodium cyanide solution is added during two hours, and then stirring is continued for another hour at constant temperature of 50 °C. Immediately after the addition of the sodium cyanide solution, the formation of yellow crystals of TETS in the reaction mass is observed. The reaction mixture is filtered, the crystals are washed with 200 cm^3 of water (negative reaction to NCS^-ion) and dried in a vacuum dryer at a temperature of 60 °C until the moisture content is less than 0.5%. The resulting crystals are recrystallized to a constant melting temperature from a suitable solvent (benzene, dichloroethane, chloroform, absolute alcohol). The yield of synthesized TETS is 87.6%.

RESULTS AND DISCUSSION

The first series of experiments in this paper presents the definition of a laboratory procedure for the synthesis of TETS in one vessel from diethylamine, carbon disulfide, potassium cyanide and an ammonium chloride catalyst, using the isopropanol/water azeotrope as a solvent. The second series of experiments is represented by experiments on the synthesis of TETS from TETD using cyanide ion as a nucleophile (thiophile) (Figure 1). The reaction of diethylamine (1) and carbon disulfide (2) produces the amine salt of diethyldithiocarbamic acid (3), from which TETD (4) is obtained by oxidation with hydrogen peroxide. The resulting amine salt undergoes oxidation to TETD with the separation of amine (1) which reacts with the present carbon-disulfide (2) in the reaction mixture. During the adding carbon disulfide, one half of the added amount reacts with the amine, and the other remains in the reaction flask due to the consumption of amine to obtain the dithiocarbamate amine salt. When hydrogen peroxide addition started, the amine salt is oxidized to TETD with release of the amine which immediately reacts with the carbon disulfide present to regenerate the amine salt of diethyldithiocarbamic acid. The addition of hydrogen peroxide is continued until complete oxidation of the amine salt in TETD. In the second phase of the reaction, sulfur is eliminated from the disulfide bond of TETD by cyanide ion, whereby TETS is formed with the separation of potassium isothiocyanate. The reaction takes place when the nullophile

performs heterolysis of the disulfide bond in TETD with the release of diethylthiocarbamoyl isothiocyanate (5) and diethyldithiocarbamate anion (6). Dimethyldithiocarbamate anion (6) as a nucleophile, reacts with diethylthiocarbamoyl isothiocyanate (5), resulting in TETS (7) with isolation of isothiocyanate (8).

Results of the synthesis reaction of TETS from TETD using cyanide

The synthesis of TETS was optimized based on three series of experiments by varying the reaction conditions: reaction time, reaction temperature, and reactant concentration. Table 1 shows the results of the dependence of the reaction product yield as a function of temperature, while other parameters are constant: reactant concentration, mixing mode and reaction time.

Table 1 *Dependence of TETS yield as a function of reaction temperature*[(a)]

Exp.	Temperature (°C)	Yield		M. point[(b)] (°C)	Pure (%)
		(mol)	(%)		
1	20	0.047	83.59	70–71	98.9
2	30	0.048	83.81	70–72	99.0
3	40	0.050	84.93	70–72	99.0
4	50	0.052	86.00	71–72	99.3
5	60	0.048	83.50	70–72	98.6
6	70	0.047	80.40	70–71	98.9
7	85	0.046	80.25	70–72	98.9

[(a)]Reaction time 2 h, amount of reactants: TETD 0.057 mol, NaCN 0.057 mol, NH_4Cl 0.057 mol, H_2O 114 cm^3, [(b)]Melting point, literature data 70–72 °C [10].

The influence of the reaction temperature was examined in the range from 20 to 85 °C, and the highest yield of 86.00% was achieved in experiment 4 at a temperature of 50 °C (Table 2) The highest product yield is 87.01%, achieved in a reaction time of 3 hours, with the addition of NaCN lasting two hours and subsequent mixing for another hour. Table 3 shows the results of the yield dependence of the reaction product as a function of the reactant concentration.

Table 2 *Dependence of TETS yield on reaction time*[(a)]

Exp	React. time[(b)] (h)			Yield		M. point (°C)	Pure (%)
	a	b	c	(mol)	(%)		
8	0.5	0.5	1.0	0.039	67.93	70–72	90.3
9	1.0	0.5	1.5	0.050	80.82	70–72	98.9
10	1.5	0.5	2.0	0.055	85.57	70–72	99.1
11	1.0	1.0	2.0	0.051	82.16	70–72	99.1
12	2.0	1.0	3.0	0.055	87.01	71–72	99.2

[(a)]Reaction temperature 50 ^{0}C, quantity of reactants: TETD 0.057 mol, NaCN 0.057 mol, NH4Cl 0.057 mol, H_2O 114 cm^3, [(b)]Reaction time: a – NaCN addition of cyanide, b – additional mixing, c – total reaction time.

Table 3 *TETS yield as a function of reactant concentration*[(a)]

Exp.	Amounts of reactant (mol)			Yield		M. point (°C)	Pure (%)
	TETD	NaCN	NH_4Cl	(mol)	(%)		
13	0.057	0.067	0.057	0.055	86.84	70–72	98.9
14	0.057	0.070	0.057	0.059	87.00	71–72	99.2
15	0.067	0.057	0.057	0.051	81.05	70–72	98.1
16	0.070	0.057	0.057	0.049	75.96	70–72	98.8
17	0.057	0.057	0.067	0.050	86.06	71–72	99.0
18	0.057	0.057	0.070	0.055	86.04	71–72	99.0

[(a)] Reaction temperature 50 °C, reaction time 3 h.

The highest product yield is 87.00%, achieved in experiment 14, where a small excess of sodium cyanide was used. Using an excess of TETD (experiment 16) results in a lower product yield. Most likely, the presence of unreacted TETD in the reaction mixture affects the efficient separation of TETS by recrystallization from ethanol. The cyanide ion is the most reactive nucleophile in the substitution reaction on the S-atom of the S-S bond of TETD, and its reactivity is also high in S_{N2} reactions on the C-atom of methyliodide. In all the presented experiments, the identification of the synthesized products was performed on the basis of the obtained UV, IR and MS spectra.

Industrial process of TMTS production

The industrial procedure for the production of TMTS takes place in the process equipment shown in Figure 2. In a reactor with a volume of 5 m^3 (position 1), 1.5 m^3 of an azeotropic mixture of isopropyl alcohol-water (87.7%/12.3%) is introduced from a dispenser (position 3), and 0.437 m^3 (4.16 kmol) of 70.0% diethyl amine solution from the dispenser (position 5). After starting the stirrer, 0.256 m^3 (4.16 mol) of 98.0% carbon disulfide was added from doser CS_2 (position 4) over 0.5 h while maintaining the temperature in the range of 28–35 °C, provided by circulating cooling water. At the end of the reaction, the pH of the reaction mixture is 6.5. At this point, 0.536 m^3 of 13.2% hydrogen peroxide solution from the H_2O_2 dispenser (position 6) was added to for 0.5 h at 35–40 °C. At the end of the first stage, 231.11 kg (4.16 mol) of ammonium chloride and a 20% aqueous solution of potassium cyanide (285.42 kg of potassium cyanide) are added to the suspension of the obtained TETD (21%) dissolved in 1.068 m^3 of water (4.16 mol)) from the KCN solution dispenser (position 8). The entire amount of potassium cyanide is added over the course of 2 hours, and then the mixing of the reaction mixture is continued for another hour while maintaining the reaction temperature of 50 °C.

After completion of the reaction, the reaction mixture is filtered on a vacuum filter device (position 10). The filtrate is collected in tanks (positions 11 and 12) and used for the next TETS synthesis reaction, and the filter cake is washed with water (negative reaction to NCS^- ion), the crystals are dried in a vacuum dryer (position 13) at 60 °C until the content moisture content below 0.5%. The dried crystals are ground in the mill section (position 14) to the required granulation and forwarded to formulation and packaging. After the filtrate is used as a reaction medium for the next synthesis, it is transferred to rectification (position 15) and stored in a tank (position 9).

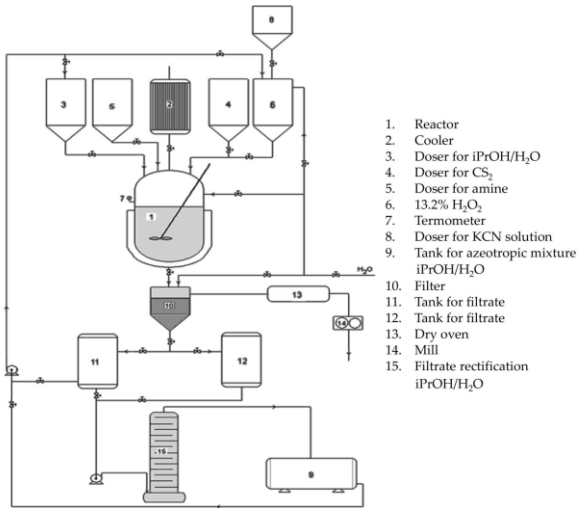

Figure 2 *Technological scheme of TETS production*

CONCLUSION

A new laboratory procedure for the synthesis of TETS was defined by performing the synthesis reaction in one pot that has significant advantages over the previous ones: 1) Using ammonium chloride as a catalyst, generates enough H^+ ions for the reaction to take place and the synthesis in the presence of sulfuric acid, which decomposes both the product TMTS and the reactant TMTD, was avoided; 2) The defined procedure avoids the use of gaseous hydrogen cyanide, which significantly makes the procedure simpler and safer to work with; 3) New TETS synthesis procedure, simpler than the previously known procedures, achieves a significantly higher yield.

ACKNOWLEDGEMENT

The authors are grateful to the Ministry of Science, Technological Development and Innovation of the Republic of Serbia for financial support according to the contract with the Project Number 43007 and 451-03-47/2023-01/200169.

REFERENCES

[1] Scheele W. L., Dummer O. W., Rubber Chem. Technol. 29 (1956) 15–28.

[2] Wang M., Ma N., Catal. Lett. 144 (2014) 1233–1239.

[3] Brewer C., Alcohol Alcohol. 28 (1993) 383–395.

[4] Xu-Ling X., Qi-Long Z., Jin-Quan C., *et al*., Synthesis 54(02) (2022) 475–482.

[5] Hermanus R., Bloemenkamp J., Johannes A., US 6465691 (2002).

[6] Rathore H. S., Varshney G., Mojumdar S. C., *et al*., Therm J. Anal. Calorim. 90 (2007) 681–686.

[7] Ritter E. J., Wyandotte M., US 25240813 (1950)

[8] Hu J. Y., Tian J., Wang K., *et al*., ACS Omega. 5 (37) (2020) 23736–23742.

[9] Shrivash M. K., Adeppa K., Singh R., *et al*., A Novel, Proc. Natl. Acad. Sci., India. Sect. A Phys. Sci. 87 (2017) 189–193.

[10] Liang F., Synthesis 22 (2008) 3579–3584.

[11] Parkinson A. R., US 3992448 (1976).

[12] JP patent 54/61123 (1979).

[13] US patent 3992448 (1976).

[14] JP patent 54/61123 (1979).

[15] Trunta R. Chem. Abstr. 61 (1964) 9408.

[16] Braun J., Stechele, F. Ber. 35 (1963) 2275.

[17] ČČSR patent 134154 (1969).

[19] Silva M. C., Conceicao M. M., Trindade M. F., *et al*., J. Therm. Anal. Calorim. 75 (2004) 583–590.

[20] Rathore H. S., Ishratullah K., Varshney C., *et al*., J. Therm. Anal. Calorim. 94 (2008) 75–81.

[21] Milosavljevic M. M., Marinkovic A. D., Markovic J. M., *et al*., Chem. Ind. Chem. Eng. Q. 18 (2012) 73–81.

TECHNOLOGICAL PROCESSES AS SOURCES OF POLLUTION IN THE ENVIRONMENT

Anđela Stojić[1*], Dejan Tanikić[1], Emina Požega[2]
[1]University of Belgrade, Technical Faculty in Bor, V.J. 12, 19210 Bor, SERBIA
[2]Mining and Metallurgy Institute, Z.B. 35, Bor, SERBIA
[*]*astojic@tfbor.bg.ac.rs*

Abstract

This paper explores the impact of technological processes on environmental pollution. Technological processes are crucial elements of industrial activities, but at the same time, they can be a source of various types of pollution, including air, water, and soil pollution. The aim of this research is to analyze different technological processes and their impact on the environment, as well as to propose possible strategies for reducing negative effects.

Keywords: technological processes, environment, pollution.

INTRODUCTION

Technological processes are an integral part of modern industrial development and play a crucial role in the production of various goods and services. However, while these processes are vital for societal progress, they also have a significant impact on the environment. Environmental pollution has become one of the greatest challenges facing humanity today, and technological processes have been recognized as one of the main sources of this pollution. The aim of this research is to analyze in detail the impact of technological processes on environmental pollution. By studying different industrial sectors and their technological processes, we will investigate how these processes contribute to the emissions of harmful gases, wastewater, toxic substances, and other forms of pollution. This analysis will enable us to gain a better understanding of the scope of the problem and identify key areas where efforts need to be focused to reduce negative impacts. Through a comprehensive overview of the topic, this paper aims to raise awareness about the importance of recognizing technological processes as sources of environmental pollution. We also want to highlight the need for the development and implementation of strategies and practices that will mitigate the negative impacts of technological processes on the environment. Only through such a holistic approach we can build a more sustainable future where technological advancements go hand in hand with environmental protection.

THE IMPACT OF TECHNOLOGICAL PROCESSES ON THE ENVIRONMENT

The development of industrialization worldwide and in our country is achieving increasing results, but at the same time, it is causing harmful consequences to the environment. Technological processes have undeniably transformed the way we live and have brought

significant advancements in various industries [1]. However, these processes also come with a profound impact on the environment. The extensive use of energy and resources, coupled with the release of pollutants and waste, has resulted in various forms of environmental degradation. It is crucial to examine and understand the consequences of these technological processes on the environment to develop sustainable strategies for mitigating their negative effects. One of the primary impacts of technological processes is the emission of greenhouse gases, contributing to climate change. Industries heavily rely on fossil fuels for energy generation, leading to the release of carbon dioxide, methane, and other harmful gases into the atmosphere [2].

These emissions trap heat and disrupt the Earth's climate system, causing rising global temperatures, altered weather patterns, and more frequent extreme weather events. Air pollution is a primary problem in areas where industrialization is developed. It particularly occurs in cities with heavy traffic, where combustion products from motor vehicles contribute to nearly 50% of pollution. Worldwide, there are millions of passenger cars on the roads, each emitting around 600 kg of harmful substances into the atmosphere annually [1].

This pollution poses serious risks to ecosystems, biodiversity, and human health. It can lead to the depletion of natural resources, contamination of drinking water sources, and the disruption of delicate ecological balances. In addition to direct pollution, technological processes also contribute to resource depletion. The extraction and consumption of raw materials, such as minerals, metals, and fossil fuels, for manufacturing and energy production, lead to habitat destruction and loss of biodiversity. Deforestation, mining activities, and unsustainable extraction practices further exacerbate the negative impacts on ecosystems and wildlife. To address these issues, it is crucial to implement sustainable practices and technologies that minimize the environmental footprint of technological processes. This includes transitioning to cleaner and renewable sources of energy, adopting circular economy principles to reduce waste generation and promote recycling, and implementing stricter regulations and standards for emissions and waste management. Additionally, promoting awareness and education about the environmental impact of technological processes can encourage responsible decision-making and drive innovation towards more sustainable practices. In the end, the impact of technological processes on the environment is undeniable. It is imperative to recognize and address these impacts to ensure a sustainable future. By adopting environmentally conscious practices, embracing clean technologies, and promoting responsible consumption and production, we can strive towards a harmonious balance between technological progress and the preservation of our environment.

THE IMPACT OF THE CHEMICAL INDUSTRY ON ENVIRONMENTAL POLLUTION

The chemical industry plays a critical role in driving economic growth and providing a wide range of essential products. However, it also has a significant impact on environmental pollution. The production, use, and disposal of chemical substances can result in various forms of pollution that pose serious risks to ecosystems and human health. One of the primary concerns associated with the chemical industry is the release of toxic substances into the environment. Chemical manufacturing processes often involve the use of hazardous materials,

which, if not properly managed, can contaminate air, water, and soil. Accidental spills, leaks, and inadequate waste management practices can lead to the release of pollutants that have long-lasting effects on ecosystems and can accumulate in the food chain.

Air pollution is a major consequence of chemical industry activities. Emissions of volatile organic compounds (VOCs), nitrogen oxides (NO_x), and sulfur dioxide (SO_2) from manufacturing plants contribute to the formation of smog, acid rain, and the deterioration of air quality [3].

These pollutants have detrimental effects on human health, respiratory systems, and contribute to the greenhouse effect and climate change. Water pollution is another significant concern associated with the chemical industry. Effluents from chemical manufacturing facilities may contain various toxic substances, heavy metals, and other pollutants that, if discharged untreated, can contaminate water bodies. This contamination poses a threat to aquatic ecosystems, disrupts the balance of aquatic life, and affects the quality of drinking water sources. Furthermore, the improper disposal of chemical waste can have long-term consequences. Hazardous chemicals that are not adequately managed or disposed of can seep into the soil, contaminate groundwater, and persist in the environment for extended periods. This contamination not only affects the immediate vicinity of the waste site but can also spread through water systems, leading to far-reaching ecological and health implications.

To mitigate the environmental impact of the chemical industry, it is crucial to prioritize sustainable practices and technologies. This includes implementing stricter regulations and standards for waste management and emissions, promoting the use of cleaner and greener production processes, and investing in research and development of safer alternatives to hazardous chemicals [3].

Additionally, fostering transparency and accountability within the industry is essential to ensure responsible and environmentally conscious practices throughout the supply chain. In the end, chemical industry has a significant impact on environmental pollution. It is imperative to address these issues through proactive measures that prioritize sustainable practices, pollution prevention, and the development of safer alternatives. By promoting responsible chemical management and investing in greener technologies, we can strive for a more sustainable and environmentally friendly future.

THE IMPACT OF THERMAL POWER PLANTS ON ENVIRONMENTAL POLLUTION

The impact of thermal power plants on environmental pollution is a significant concern. These power plants play a crucial role in electricity generation, but their operations often result in various forms of pollution that pose risks to the environment and human health. One of the primary concerns associated with thermal power plants is air pollution.

The combustion of fossil fuels, such as coal, oil, and natural gas, releases harmful emissions into the atmosphere. These emissions include sulfur dioxide (SO_2), nitrogen oxides (NO_x), particulate matter, and greenhouse gases like carbon dioxide (CO_2). They contribute to the formation of smog, acid rain, and climate change, and have detrimental effects on air quality and respiratory health [2].

Thermal power plants also generate large quantities of ash and other solid waste as byproducts. These wastes often contain toxic substances, heavy metals, and other pollutants that can contaminate soil and water when not properly managed. Improper disposal and inadequate treatment of these wastes can lead to soil degradation, groundwater pollution, and the contamination of nearby ecosystems. Water pollution is another significant concern associated with thermal power plants. The cooling processes used in these facilities often involve withdrawing large amounts of water from nearby water bodies, such as rivers or lakes, for cooling purposes [2].

This withdrawal can disrupt aquatic ecosystems and harm fish and other aquatic organisms. Additionally, the discharge of heated water back into the source can lead to thermal pollution, affecting the temperature balance and ecological health of the water bodies. The extraction, transportation, and storage of fossil fuels for thermal power plants also have environmental consequences. These activities can result in habitat destruction, deforestation, and biodiversity loss. The exploration and extraction of fossil fuels can disrupt ecosystems, impact wildlife habitats, and contribute to the depletion of natural resources. To mitigate the environmental impact of thermal power plants, various measures can be implemented. These include adopting cleaner and more efficient technologies, such as advanced pollution control systems, to reduce emissions and improve air quality. Increasing the use of renewable energy sources, such as solar and wind power, can help reduce reliance on fossil fuels. Additionally, implementing proper waste management practices, including the safe disposal or recycling of ash and other solid waste, is crucial to minimize soil and water contamination. Furthermore, strict regulations, monitoring, and enforcement mechanisms are necessary to ensure compliance with environmental standards and promote responsible practices within the industry. Investing in research and development of innovative technologies and promoting energy conservation and efficiency can also contribute to reducing the environmental impact of thermal power plants. In conclusion, thermal power plants have a significant impact on environmental pollution. It is essential to address these concerns through the adoption of cleaner technologies, proper waste management practices, and the promotion of renewable energy sources. By prioritizing environmental sustainability and minimizing the negative impacts of thermal power generation, we can strive for a cleaner and healthier environment.

MEASURES TO REDUCE POLLUTION CAUSED BY TECHNOLOGICAL PROCESSES

Measures to reduce pollution caused by technological processes are essential in promoting sustainable development and preserving the environment. Several strategies can be implemented to minimize the negative impact of these processes on air, water, and soil quality [3]. One effective measure is the adoption of cleaner production technologies. This involves implementing innovative techniques and equipment that minimize the generation of pollutants and waste during the manufacturing and production processes. By optimizing resource utilization and reducing emissions, cleaner production technologies can significantly reduce environmental pollution. Another crucial measure is the implementation of stringent environmental regulations and standards. Governments and regulatory bodies can establish and enforce strict guidelines to limit the release of pollutants into the environment. These

regulations can cover emissions control, waste management, and the use of hazardous substances. Compliance with these standards can help mitigate pollution and ensure that technological processes are conducted in an environmentally responsible manner. Promoting the use of renewable energy sources is another effective measure. By transitioning from fossil fuels to clean and renewable energy sources like solar, wind, and hydroelectric power, the reliance on environmentally harmful energy generation methods can be reduced. This shift not only helps in combating air pollution but also contributes to mitigating climate change. Additionally, waste management plays a crucial role in reducing pollution from technological processes. Implementing proper waste disposal and recycling practices ensures that hazardous materials and byproducts are handled safely and do not contaminate the environment.

Recycling and reusing materials can also reduce the extraction of raw resources and minimize waste generation. Furthermore, fostering awareness and education about the environmental impact of technological processes is essential. By promoting sustainable practices and providing information on the consequences of pollution, individuals and organizations can make informed decisions and take steps to reduce their ecological footprint. In conclusion, implementing measures to reduce pollution caused by technological processes is crucial for preserving the environment. By embracing cleaner production technologies, enforcing stringent regulations, promoting renewable energy, implementing proper waste management, and raising awareness, we can strive for a cleaner and more sustainable future [2].

CONCLUSION

Technological processes are significant sources of pollution in the environment. The extensive use of energy, the release of harmful emissions, and improper waste management contribute to air, water, and soil pollution. To mitigate these negative impacts, it is crucial to adopt cleaner technologies, enforce stricter regulations, promote renewable energy sources, and prioritize responsible waste management. By doing so, we can strive towards a more sustainable future where technological progress and environmental preservation go hand in hand.

REFERENCES

[1] Ruttan V., Am. J. Agric. Econ. 53 (1971) 707–717.

[2] Okafor Dž., Negative Impact of Technology on the Environment, *Available on the following link*: https://www.trvst.world/environment/negative-impact-of-technology-on-the-environment/.

[3] Kwazo H. A., Muhammad M. U., Tafida G. M., *et al*., Acad. J. Interdiscip. Stud. 3 (7) (2014) 1–14.

LONDON PLANE (*Platanus* × *acerifolia* (Aiton) Willd.) IN THE STREET TREE LINES OF THE OLD TOWN IN BELGRADE

Aleksandar Lisica[1*], Nadežda Stojanović[1], Milorad Veselinović[2], Jovana Petrović[1], Nenad Stavretović[1], Mirjana Tešić[1]

[1]University of Belgrade, Faculty of Forestry, Kneza Višeslava 1, 11000 Belgrade, SERBIA
[2]Institute of Forestry, Kneza Višeslava 3, 11030 Belgrade, SERBIA
[*]*aleksandar.lisica@sfb.bg.ac.rs*

Abstract

Street tree lines in the city provide many benefits. The most important among them are ecological, aesthetic, psychological and cultural. However, tree lines on most streets in cities are exposed to many stressful conditions. For that reason, it is important to know the ecological requirements of the tree species from which they are established, as well as their ability to adapt to specific urban conditions. This paper presents an overview of the existing condition of London plane tree lines (Platanus × acerifolia (Aiton) Willd.*) as one of the frequently used tree line species in the area of the central Belgrade municipality – Old Town, in the context to identify the main factors that affect the stability of the population of these street trees. The results of the research are applicable in the process of street tree line management.*

Keywords: London plane tree, street tree lines, arboriculture, tree line management.

INTRODUCTION

Street tree lines are an important component of the city's green infrastructure. In an ecological sense, trees affect the modification of air temperature, alleviate high summer temperatures, increase relative air humidity, reduce insolation, etc. [1]. They also affect on the reduction of city noise levels [2,3] and the reduction of air pollution concentration in the city air [4]. These green spaces also have aesthetic significance in the city because they have the ability to create a visual impression, reviving existing urban solutions, homogenizing and humanizing the street space [5]. Also, tree-lined trees have a psychologically positive effect on the observer thanks to their variety, colour, texture, size and variability over time [6]. Street tree lines, like other objects in the city, can have their own history as well as their own cultural significance. They can represent part of the urban heritage or they can be located in streets that have a certain historical and cultural significance. The special importance of street tree lines in the city is reflected in their ability to connect other categories of urban green spaces (especially larger ones such as great city parks and urban forests) into a unique system - urban green infrastructure [7-9]. City tree lines also serve as habitats for many wild animals [10].

Maintaining a sustainable population of street trees in the city, however, is not simple. Street trees in cities are exposed to many unfavourable conditions such as drought, deficiency

of water in the soil, soil compaction, air pollution, the presence of deicing salt, vandalism, etc. [11–13]. This task becomes even more challenging if the immediate built environment of the city is not favorable for the growth and development of trees, such as, for example, limited space available for the development of underground and above-ground parts of trees, high traffic frequency, urban changes in the city, etc. For this reason, it is important to know the ecological requirements of the tree species from which the street tree lines are established, as well as their ability to adapt to specific urban conditions.

This paper presents an overview of the existing condition of the London plane street tree lines (*Platanus* × *acerifolia* (Aiton) Willd.) as one of the frequently used tree lines species in the area of the central Belgrade municipality - Old Town. The paper aims to identify the main factors that influence the stability of the population of these trees in the street space. The results of the research provide recommendations on how to improve the sustainability of these street tree lines in Belgrade, as well as significant data for programs to establish new and manage existing street tree lines in this area.

MATERIALS AND METHODS

In the area of Belgrade, with problems of space deficiency for the growth and development of tree lines, due to intensive urbanization and inadequate management, almost all existing tree lines are exposed. As a special category, old tree lines composed of species whose dimensions exceed the available space of the streets in which they grow are distinguished. London plane (*Platanus* × *acerifolia* (Aiton) Willd.), which is also one of the most abundant tree species that is traditionally used for street greening, both in Belgrade and in other cities of Serbia [14]. It is a hybrid species that was hybridized by crossing the eastern and western plane (*P. orientalis* L. and *P. occidentalis* L.). This plane species reaches a height of over 40 m and a diameter of the trunk greater than 2.5 m [15]. It is a tree with very large leaves similar to a maple, after which the species got its name. It grows very fast, and it develops the fastest on fresh alluvial soils, but it also grows on poorer substrates. As a species for tree lines, it was qualified due to its high resistance to polluted and dry air, as well as its high resistance in the presence of dust to which tree lines are often exposed [14]. Among the morphological features, the greatest importance of the London plane as a tree species: large leaf plate, favourable density of the crown and peculiarities of the bark of the trunk. Large leaves are important from a microecological point of view, realizing a high intensity of photosynthetic activity, which is very important in urban environments. The density of the crown is not too high, even though it is a species with large leaves. The canopy lets in light and achieves the ideal degree of shading of the city surface. The equable distribution of leaves along the branches allows part of the sun's rays to penetrate through the crown. This species is also characterized by aesthetic qualities due to the shape of the leaf and the colour of the bark, which separates (peels) segmentally, creating an interesting aesthetic detail in the space. One of the dominant characteristics of the London plane as a species is the dimensions it reaches.

The municipality of Old Town, representing the historical centre of Belgrade. The Old Town is specific in relation to other municipalities in terms of its history, architecture and urban structure. It is located on an area of 698 ha and has about 70,000 inhabitants. The border of the investigated area, i.e. the border of the municipality of Old Town, was

determined based on the Statute of the City of Belgrade (Belgrade city official gazette, number 60/19).

The survey of the existing condition of London plane trees was carried out in the I and II order streets in the area of the Old Town municipality (according to the Transport Model of Belgrade, 2015), because they are the most frequent in terms of traffic intensity, ways of use and measures to maintain greenery. For the purposes of this work, in the streets that are the subject of the research, each individual London plane tree was observed and evaluated from the point of view of its morphological and biological characteristic. The data collected in the field are: the number of trees in the street tree lines, the diameter of the trunk, the presence of entomological damages or phytopathological diseases and the assessment of the vitality of the trees. The diameter of the trunk was measured at a standard trunk height of 1.3 m with a forester's crossbar. According to the method Yang. (2012) [16], the vitality of tree-lined trees is evaluated with grades up to 1-5 in relation to the percentage of dry branches in the canopy, according to the scale: grade 1 - dead tree or one about to die (from 76-100% tree damage); grade 2 -bad (31-75%); 3 - good (11-30%); 4 - very good (1-10%) and grade 5 is excellent, without obvious dry branches within the tree canopy. In addition, in the case of the assessment of the vitality of the plane tree lines in the researched area, the impact of the care measure - topping the trunks was taken into account. The mentioned measure is of particular importance because all the tree lines of London plane in the area of the Old Town are located in streets where there is not enough available space for the growth of this species, and as a maintenance measure, the measure of tree topping is applied here.

RESULTS AND DISCUSSION

Through field research, it was determined that there are a total of 39 streets in the area of the Old Town municipality in Belgrade that belong to I and II order. Of this number, 15 streets belong to the order I, and 24 streets to the order II. Tree lines are represented in 8 out of 15 I order and in 14 out of 24 II order streets. London plane (*Platanus* × *acerifolia* (Aiton) Willd.) occur in 4 streets, 3 streets belong to order I and 1 street belongs to order II. In all streets, London plane are positioned on both sides of the street. The total number of recorded trees is 257. The results of the field research are shown in Table 1.

Research indicates that the general condition of the London plane tree lines in the researched area is largely the result of several factors. The most significant are the application of the method of topping the crown as a solution to the issue of controlling the dimensions of the trees, the incompatibility between the space required for the growth of species of these dimensions in the streets where tree lines are established and the insufficient distance between the trees, which leads to the overlapping of their crowns and additional deformations in the crowns and ultimately a decrease in vitality to which the presence of entological and phytopathological pathogens also contributes.

By analyzing the street trees in the field, a disproportion was observed in the relationship between the diameters and the expected dimensions of the crown. A large number of trees have disproportionately small crowns in relation to the diameter of the trunk (Figure 1). This is a consequence of radical methods of pruning the crown, i.e., the application of a care

measure - topping the trees. It was found that 220 (86%) trees out of a total of 237 have a trunk that has been cut (topping).

Table 1 *The existing condition of of London plane trees lines (Platanus × acerifolia (Aiton) Willd.) in the streets of the I and II order in the area of the Old Town municipality in Belgrade*

Street name	Number of trees in the line	Minimum diameter (cm)	Average diameter (cm)	Maximum diameter (cm)	The number of trees on which entomological damage or phytopathological disease was recorded	Medium vitality rating	Number of topping crown trees
Streets of the I order							
Bulevar vojvode Bojovića	16	43	44,5	60	12	3,1	1
Cara Dušana	147	18	58,5	74	147	3,1	137
Džordža Vašingtona	89	17	66	75,0	57	3	81
Streets of the II order							
Simina	5	11	26,2	38	1	4,1	1
Total:	257	22,3	48,6	56,9	217	3,3	220

Figure 1 *Overview of London plane trees in the investigated area: a) tree line in the street (Bulevar vojvode Bojovića) of small width but with enough available surrounding space; b) tree line in the street (Cara Dušana) with insufficient available space; c) topping crown trees; d) tree line in Džordža Vašingtona; e) open trunk rot; f) tree line in Simina street; g) insufficient space for the development of trees*

The consequences of applying the tree topping method in order to maintain acceptable dimensions of old tree lines of London plane are the permanent deformation of the trees a significant reduction of all the functions that these tree lines perform [17]. Anastasijević [14]

especially points out that in a species such as London plane, after applying the measure of topping the trunk, a large number of water shoots are formed, because dormant buds are activated due to the stress that the trees suffer. The result is the formation of water shoots that form irregular branches forming deformed crowns. On the other hand, due to exposure to high stress due to overtopping, trees focus all their energy on restoring the crown and compensating a large amount of their leaf mass, so that such processes additionally exhaust the trees, which in many cases results in a decrease in their overall vitality.

The research determined that the mean vitality rating of tree-lined trees in the researched area is 3.3 (1-5). Trees with reduced vitality are more susceptible to pathogen attacks, and when infestation occurs such trees often suffer great damage. In homogeneous tree lines (composed of one species of trees) this represents an additional threat to the survival of the tree line due to the easy mechanism of pathogen transmission. The speed of the spread of pathogens and the degree of damage they can cause increases in tree lines in which there is a significant overlap between the crowns, as is the case with the tree lines of the researched area. In the investigated lines of trees out of a total of 237 trees, 217 of them (84%) were found to have damage caused by the presence of one of the pathogens. Among the most important pathogens are the fungus that causes powdery mildew *(Microsphaera platani* Hove.) and the apiognomonia blight of leaves and saplings (*Apiognomonia veneta* (Sacc. & Speg.)). Among the insects, the dominant presence is the sycamore lace bug (*Corythucha ciliata* Say).

When the London plane is used as a species for street tree line planting, an important factor for its further growth and survival is the distance at which the trees are planted, as well as the width of the street where the lines of trees is raised. In Belgrade, in a large number of cases, the old tree lines of plane trees have outgrown their positions, and an additional problem in the lack of space for them is the inadequate distance between the trees, i.e. the fact that the majority of tree lines are planted too close in relation to the diameters that their crowns reach during their existence. In the streets of Cara Dušana, Džordža Vašingtona and Simina, the distance between trees ranges is from 5-7 m, which is an extremely small distance for this species of tree. In the research of Anastasijević [14] also states that the distance between London plane trees in some tree lines in Belgrade was only up to 4 m. It is suggested here that in such cases there are two ways to adequately maintain the trees lines - thinning of the trees or corrective pruning of the crown that would ensure that the trees in such tree lines are kept within the dimensions that are acceptable for the space of the street where the tree line is established. London plane trees, which grow in streets with insufficient space in relation to the requirements of this species, can manifest other negative effects, especially during the vegetation period. One of them is the excessive closing of the street canyon with tree crowns. Due to the formation of a dense conformation between the crowns of trees that intertwine fighting for space and light, a tunnel effect is created, which results in difficult and slow ventilation of the street, long retention of polluting gases and dust (Vratuša and Anastasijević, 1995) [18].

CONCLUSION

The following conclusions were established by researching the existing condition of the London plane tree lines in the area of the central Belgrade municipality Old Town are:

- Street tree lines of London plane (*Platanus* × *acerifolia* (Aiton) Willd.) occur in 4 streets, 3 streets belong to I order and 1 street belongs to II order category.
- In the municipality of Old Town, a total of 257 London plane trees were recorded. In all streets, London plane are positioned on both sides of the street.
- It was determined that the existing condition of tree lines is most affected by: methods of topping the crown as a solution to the issue of controlling the dimensions of the trees; the incompatibility between the necessary space for the growth of species of these dimensions in the streets where tree lines are established; and the insufficient distance between the trees, which leads to the overlapping of their crowns and decrease in vitality, which is also contributed by the presence of entological and phytopathological pathogens.
- It was determined that 220 (86%) trees out of a total of 237 have a trunk that has been cut (topping).
- it was determined that the mean vitality rating of street trees in the researched area is 3.3 (1-5).
- Out of a total of 237 trees, 217 (84%) were damaged caused by the presence of one of the pathogens.
- It was determined that in the investigated area, the two-sided rows of London plane trees grow in streets with insufficient space for this species.

REFERENCES

[1] Heisler M., Grant H., Gao W., Agric. For. Meteorol. 120 (2003) 113–126.

[2] Bunuševac T. Šumarstvo, god. XV, 7–9 (1962) 351–374.

[3] Samara T., Tsitsoni T., Noise Control. Eng. J. 59 (2011) 68–74.

[4] Nowak D., Crane D., Stevens J., Urban For. Urban Green. 4 (2006) 115–123.

[5] Anastasijević N., Vratuša V. Monografija, Ekokonferecija 99 (1999) 445–450.

[6] Smardon C., Landsc. Urban Plan. 15 (1988) 85–106.

[7] Tzoulas K., Koprela K., Venn S., *et al*., Landsc. Urban Plan. (2007) 167–178.

[8] Herzog C. P., Landsc. Ecol. Eng. 12 (2016) 41–150.

[9] Stavretović N., Novaković A., Petrović J., *et al*., Acta Herbol. 31 (67–75) (2022) 35–42.

[10] Fernandez-Juricic E., Conserv. Biol. 14 (2000) 513–521.

[11] Close R. E., Nguyen P. V., Kielbaso J. J., J. Arboric. 22 (1996) 144–150.

[12] Jutras P., Prasher S., Mehuys G., Arboric. Urban For. 36 (2010) 1–10.

[13] Nielsen C., Buhler O., Kristoffersen P., Arboric. Urban For. 33 (2007) 231–245.

[14] Anastasijević N., Monography, Faculty of Forestry, (2012) Belgrade.

[15] Vukićević E., Ornamental dendrology, Faculty of Forestry, (1987) Belgrade.

[16] Yang J., Zhou J., Ke Y., *et al*., Urban For. Urban Green. 11 (4) (2012) 432–438.

[17] Mesicek M., Stojanovic N., Anastasijevic N., *et al.* Ecol. (2014) 416–421.

[18] Vratuša V., Anastasijević N., Proceedings of the international conference Preventive Engineering and Living Environment (1995) H3-1-H3-3.

30th International Conference Ecological Truth & Environmental Research
20–23 June 2023, Serbia

APPLICATION OF SPECIES OF THE GENUS *Parthenocissus* L. IN URBAN GREEN INFRASTRUCTURE – STATE AND PERSPECTIVES

Djurdja Petrov[1*], Mirjana Ocokoljić[1], Nevenka Galečić[1], Dejan Skočajić[1]

[1]University of Belgrade - Faculty of Forestry, Kneza Višeslava 1, 11030 Belgrade, SERBIA

[*]*djurdja.stojicic@sfb.bg.ac.rs*

Abstract

This study focuses on selected aspects of the spatial analysis of green infrastructure in Banovo brdo, Belgrade, with the aim of implementing species from the genus Parthenocissus L. on green roofs, walls and rain gardens. Through the analysis of urban green infrastructure, public and private green areas in the compact urban environment, Parthenocissus quinquefolia (L.) Planch. and Parthenocissus tricuspidata (Siebold & Zucc.) Planch. were selected. To highlight the visual perception of the mentioned species, autumn foliage color changes in combination with climatic elements were recorded by phenological observations. Research confirmed the greater presence of Virginia Creeper (75%), but also the identical adaptability of both species in changed climatic conditions. The analyzed specimens of Virginia Creeper were 10 to 12 years old, and the specimens of Japanese Creeper were 15 years old. The invasive nature of both species was recorded in both public and private green areas. The results confirm that both species are suitable for innovative strategies and that they can be used to preserve selected spatial elements with adequate maintenance. Based on the analyses, for the operationalization of landscape design, recommendations were formulated for strengthening the connectivity of the green infrastructure network and implementing new elements with both species in the urban fabric where the number and size of green areas are insufficient.

Keywords: green infrastructure, Virginia Creeper, Japanese Creeper, landscape design.

INTRODUCTION

The formation of green infrastructure network is a holistic approach to connecting natural and artificially formed green areas in the city, which provides a wide range of ecosystem services: improving the quality of life, health and well-being, recreation, access to nature, attracting businesses, tourists and other visitors, maintaining soil quality and adapting to climate change. Elements of green infrastructure have physical, psychological, emotional and socio-economic benefits for individuals and society [1]. According to the study by Klichovski and Patricio [2], a comparative analysis of cognitive sciences and ecological landscape design confirmed that the environment has a positive effect on cognitive functions. Green infrastructure elements are very important, especially implementation of plant material which mitigates environmental problems and the effects of heat islands in urban areas [3]. Therefore, it is necessary to complement gray infrastructure with green, in order to obtain a synergistic effect, namely to reach urban sustainability by implementing green infrastructure [4]. Green infrastructure is not just an alternative description for conventional open spaces but a network that includes parks, open spaces, playgrounds, forests, but also street trees, green plots and private gardens. Likewise, it includes green roofs and walls [5]. The range of benefits

provided by green infrastructure includes essential basis for wildlife and biodiversity, as well as benefits for humans through the visual perception of plant material throughout the year.

In addition to aspects of the spatial analysis of urban green infrastructure in Belgrade, the aim of this research is: (1) identification, state and perspectives of the application of species from the genus *Parthenocissus* L. in public and private green areas in the urban fabric, (2) regeneration of green areas with Virginia Creeper and Japanese Creeper in a compact urban center by using innovative strategies and (3) ecological protection and preservation of selected spatial elements. The focus of the work is also the change of autumn color leaves before winter, which is the result of changes in the metabolism of woody plants that belong to temperate climate [6].

MATERIAL AND METHODS

The study area represents four locations in the territory of Belgrade, Čukarica municipality, Banovo brdo (Figure 1). The locations were chosen to include two public (green areas of city blocks and squares) and two private gardens. *Parthenocissus quinquefolia* (L.) Planch. (Virginia Creeper) (*P. quinquefolia*), allochthonous species from North America, and *Parthenocissus tricuspidata* (Siebold & Zucc.) Planch. (Japanese Creeper) (*P.tricuspidata*), native to Japan and China [7], were identified in study area. Further description of the study sites is included in Table 1.

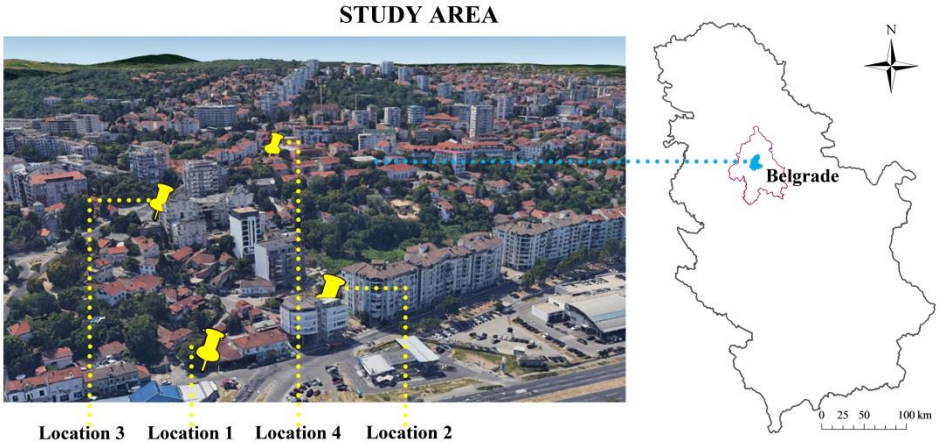

Figure 1 *Location of the study area*

Cartographic materials, planning documents and field research were used to study the spatial distribution of green infrastructure in the urban fabric of Banovo brdo. Green elements were identified based on data from satellite maps, that are according to Simović *et al.* [8] convenient for monitoring vegetation on a local scale. During field research, individual elements of green infrastructure were documented by photographs. The analysis included phenological data which are the result of our phenological monitoring of the dynamics of phenological phases in the period July 2022 – January 2023. Phenological observations were made visually twice a week, on the same day at all locations. The expanded BBCH scale according to Meier [9] was used. Using this scale, the following dates were determined: the

beginning of autumn leaf discolouration (the day when more than 10% of the leaves had autumn colour), the peak of leaf discolouration (the day when 80% of the leaf mass had autumn colour) and the end of discolouration and leaf-fall (the day when there were no more leaves on the plants).

Table 1 *Description of the study areas*

Location	Latitude φ	Longitude λ	Altitude H (m)	Soil type [10]	Aspect	Slope* (°)
1.	44º 47' 11.29 " N	20º 24' 75.89" EGr	72	Haplic Fluvisol (Eutric, Siltic)	NW	7.5
2.	44º 47' 09.39" N	20º 24' 56.63" EGr	81	Haplic Fluvisol (Eutric, Siltic)	NW	6.0
3.	44º 47' 07.37" N	20º 25' 03.07" EGr	98	Luvic Chernozems	NW	5.8
4.	44º 47' 01.18" N	20º 25' 03.75" EGr	109	Luvic Chernozems	NE	1.8

*Slope: 1–3 ° (slightly sloping terrain) and 5–8 ° (sloping terrain).

Climate data were taken from RHMZ - Republic Hydrometeorological Service of Serbia, which were collected at the Meteorological station Belgrade (44º47'54.44" N; 20º27'53.35" EGr; altitude: 132m) (www.hidmet.gov.rs/index.php, accessed on 20 February 2023).

RESULTS AND DISCUSSION

Research on green infrastructure and its relationship to the patterns of the urban fabric is important for the concept of planning and design, both at the city level and in its individual parts. The analysis of selected aspects of the green infrastructure at Banovo brdo indicates a fragmented green infrastructure. The number and size of green areas is insufficient in a dense built-up area, but there are examples of the use of new elements such as green walls, green roofs, rain gardens and plantings along traffic corridors. The most common forms of vegetation at Banovo brdo are trees, bushes and lawns in landscape compositions. Climbers, such as species of the genus *Parthenocissus* L. are present occasionally. *P. quinqefolia* was recorded as a part of rain garden, green roof and hedge (Figure 2a) at location 1. The age of the plants is 10 years. The invasive character and spread to the species were registered in the private garden, which is next to the busy road (Radnička Street) and near the main road Belgrade-Obrenovac. The beginning of the colour change of the leaves was recorded on 10th October 2022, the peak of the colour change on 18th November 2022, and the complete leaf fall on 27th December 2022. Compared to the work of Kalista and Kovalenko [11], in which they state that the leaves change colour in September-October, our research recorded later appearances of red to purple-red colour. The length of autumn-colour foliage that could be seen from a distance of 500 m (open view from Ada Ciganlija), when most of the deciduous plants dropped their leaves, was 70 days. Less than 10% of the leaves were present from the 70th to the 78th day.

P. tricuspidata was recorded in green areas of the city blocks as a green wall and hedge, at location 2 (Figure 2b). The age of the plants is 15 years. The invasive character and spread to street lamp post, traffic signs and to the trunk of the other plants in the city block between Radnička and Visoka Streets was noted. The beginning of the colour change of the leaves was

recorded on 15th October 2022, the peak of the colour change on 13th November 2022, and the complete colour change on 2nd January 2023. The length of autumn-colour foliage that could be seen from a distance of 100 m (the only possible view is towards the Visoka Street green block) was 60 days. Less than 10% of the leaves were present from the 60th to the 79th day.

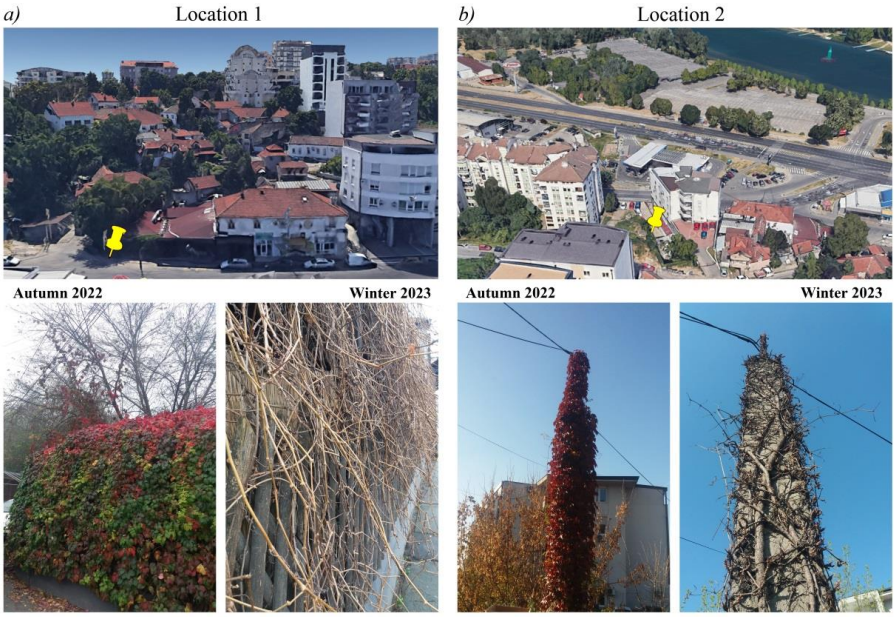

Figure 2 *Analysed specimens during the research period: a) P. quinqefolia and b) P. tricuspidata*

P. quinqefolia was recorded on the square near Kirovljeva street (location 4), where it was placed on the retaining wall based on a project. The age of the plants is 10 years. The occurrence of invasive, uncontrolled spread at this location was also recorded. Figure 3b shows the branches of *P. quinqefolia* over the attractive taxon with orange fruits *Pyracantha coccinea* 'Orange Glow'.

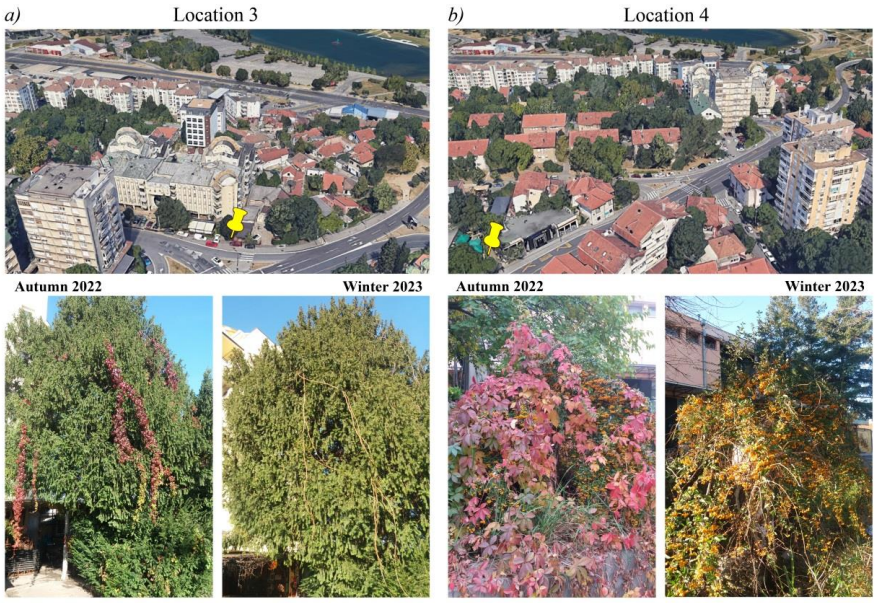

Figure 3 *P. quinqefolia a) at the location 3 and b) the location 4 during research period*

The beginning of the leaf colour change was recorded on 10th October 2022, the peak of the colour change on 15th November 2022, and the full colour change on 5th January 2023. The length of the autumn-colour ornamentality, which can only be seen from close proximity due to the location of the square, was 77 days. Less than 10% of the leaves were present from the 77th to the 87th day.

The recorded colour changes of Virginia Creeper and Japanese Creeper are directly related to the length of day and night, as well as to the decrease in the number of sunny hours per day, temperature and air humidity [6]. The combination of warm, sunny days combined with cool and mild nights stimulates the production of anthocyanin pigments that turn the leaves to red, purple and crimson [12]. Our results are in accordance with the aforementioned, as the autumn of 2022, according to RHMZ, was warm and rainy and the early production of anthocyanins was stimulated by the cold wave recorded at the end of the second and beginning of the third decade of September in Belgrade (www.hidmet.gov.rs/data/klimatologija/ciril/jesen.pdf, accessed on 02/22/2023). The exceptionally long duration of autumn colours during autumn and the beginning of winter 2022/23 is directly related to climatic parameters. According to RHMZ, December 2022 was the warmest month since the beginning of the measurements (www.hidmet.gov.rs/data/klimatologija/ciril/Decem-bar.pdf, accessed on 02/25/2023). Altitude also affects the pace of autumn colour change [12], which was not confirmed in our research, but it should be emphasized that the study is located in the dense urban environment.

Based on the analysis of the arrangement of green areas in the urban fabric and their connection at Banovo brdo, as well as the state of the analysed species of climbers at four locations, the following recommendations are formulated: a) in the urban fabric, it is necessary to create continuity and connection of green infrastructure systems, b) it is necessary to continuously increase the plantings along the pathway system, c) implementation of specific green infrastructure elements in the dense urban environment in which the presence for more than a decade of both species has been recorded by this research is strongly recommended, and according to Ocokoljić and Petrov [7] they have a lifespan of 25–50 years and d) grow both species as new elements of green infrastructure. Their importance and perspectives of use were best illustrated by Darwin [13]: "The gain in strength and durability in a tendril after its attachment is something wonderful. There are tendrils now attached to my house, which are strong, and have been exposed to the weather in a dead state for fourteen or fifteen years. One single lateral branchlet of a tendril, estimated to be ten years old, was still elastic and supported a weight of exactly two pounds…so that after having been exposed during ten years to the weather, it would probably have resisted a strain of ten pound".

CONCLUSION

The analysis of selected elements of green infrastructure in Banovo brdo confirmed that the green infrastructure network is fragmented, and that the number and size of green areas are insufficient in the dense urban fabric. Only a few new elements of green infrastructure were singled out: green walls, green roofs, rain gardens and linear plantings along roads. The main recommendation is to strengthen the interconnection of elements and introduce new elements to improve the environment. Virginia Creeper and Japanese Creeper have confirmed

exceptional adaptability, which is why they have the perspective of application in innovative strategies, in the regeneration and preservation of elements of green infrastructure, but with the adequate maintenance.

ACKNOWLEDGEMENT

The authors are grateful to the Ministry of Science, Technological Development and Innovation of the Republic of Serbia for financial support of the University of Belgrade - Faculty of Forestry the scientific research work in 2023, the registration number 451-03-47/2023-01/200169.

REFERENCES

[1] Kellert S. R., Nature by Design. The Practice of Biophilic Design, Yale University Press, New Heaven (2018), p.224, ISBN-13: 978-0300214536.

[2] Klichowski M., Patricio C., Enhancing Places through Technology – Proceedings from the ICiTy conference, (2017) 223–239.

[3] Supuka J., Životné prostredie 52 (1) (2018) 11–18.

[4] Depietri Y., Curr. Opin. Environ. Sustain. 54 (2022) 101148.

[5] Tóth A., Halajová D., Halaj P., Ecology and Safety 9 (2015) 132–138.

[6] Archetti M., Döring T., Hagen S., *et al*., Trends Ecol. Evol. 24 (2009) 166–173.

[7] Ocokoljić M., Petrov Dj., Dekorativna dendrologija; Univerzitet u Beogradu-Šumarski Fakultet, Belgrade, Serbia, (2022) p. 409. ISBN: 978-86-7299-339-4 (*in Serbian*).

[8] Simović I., Šikoparija, B., Panić, M., *et al.*, Remote Sens. 14 (2022) 6331.

[9] Meier U., BBCH-Monograph. Growth Stages of Plants. [Entwicklungsstadien von Pflanzen. Estadios de las Plantas. Stades De Développement des Plantes]; Blackwell Wissenschafts-Verla: Berlin, Germany; Vienna, Austria (1997), p. 622.

[10] Škorić A., Filipovski G., Ćirić M., Klasifikacija zemljišta Jugoslavije. Akademije nauka i umjetnosti Bosne i Hercegovine. Posebna izdanja knjiga LXXVIII. Sarajevo (1985).

[11] Kalista M. S., Kovalenko O. A., Actual Problems of Botany and Ecology: Proceedings of the International Conference of Young Scientists, September 3–4, Kyrylivka, Ukraine (2018) 45.

[12] Andersen Ø. M., Jordheim, M., Anthocyanins *in* Encyclopedia of Life Sciences (ELS), Encyclopedia of Life Sciences, (2010), ISBN: 9780470015902.

[13] Darwin C., Movements and Habits and Climbing Plants. D. Appleton & Co. New York (1876) p.236, *Available on the following link:* www.biodiversitylibrary.org/item/84398#page/14/mode/1up.

SECOND FLOWERING OF *Philadelphus coronarius* L. IN GREEN-BLUE INFRASTRUCTURE OF BELGRADE

Djurdja Petrov[1*], Mirjana Ocokoljić[1], Nevenka Galečić[1], Dejan Skočajić[1], Isidora Simović[2]

[1]University of Belgrade, Faculty of Forestry, Kneza Višeslava 1, 11030 Belgrade, SERBIA

[2]University of Novi Sad, BioSense Institute, Dr Z. Đinđića 1, 21000 Novi Sad, SERBIA

[*]*djurdja.stojicic@sfb.bg.ac.rs*

Abstract

The study focuses on the analysis of the elements of blue-green infrastructure (BGI) of Belgrade in the Gazela Park and the part of the Topčider Park along the Topčider River. The distance of the Sava River from these green spaces is 557 m and 1295 m respectively. During autumn and the beginning of winter 2022/2023 phenological observations of repeated flowering of European mock-orange, which has a favorable effect on ambient values, were noted in these parks. The phenological patterns of the second flowering and the morphological characteristics of the flowers were analyzed. Research has confirmed greater visual impact and longer duration of flowering in Topčider Park. The evaluation of the spatial structure of green areas provided guidelines for alternatives to the landscape design of BGI elements that would contribute to the increase in the value of ecosystem services.

Keywords: European mock-orange, blue-green infrastructure, second flowering, landscape design.

INTRODUCTION

Blue-green infrastructure (BGI) is a concept that determines the way of living in cities and improves its quality, especially in conditions of climate change. Solutions based on green and blue infrastructure are the basis of the BGI concept. BGI includes natural (rivers, ponds, wetlands) and designed elements (rain gardens, absorbent wells, artificial ponds, underground systems), which provide ecological, landscape, economic, social, and environmental benefits [1]. The term infrastructure in BGI indicates that the role of natural processes (which include vegetation and water features) is essential in providing diverse ecosystem services to urban residents. It should be noted that the proper functioning of plant elements depends on water resources, and that vegetation determines the activity of local hydrological processes [1].

In stabilizing and improving the ecological conditions of BGI, flowering decorative shrubs, among which *Philadelphus coronarius* L. (*P. coronarius*) stands out as one of the most commonly cultivated species in Serbia [2], have a special role. Such abundantly blooming species have a significant place in landscape design for the formation of aesthetically attractive spaces with a beneficial effect on the psychology and emotional state of users. However, the conditions of the urban environment are aggressive for plants and can affect the reduction of their ornamentality [2]. With global warming, plants adapt or are suppressed, which significantly affects the functioning of ecosystems and ecological interactions in BGI.

During these processes, the phenophases of plants, which contribute to the dynamics and quality of space, can provide the most intense visual perception [3].

The paper analyzed a species of wide ecological amplitude (*P. coronarius*) as an element of Belgrade BGI because the species primarily grows in the temperate biome due to the abundant flowering phenophase at the beginning of summer [2,4–7]. The aims of the research are: a spatial analysis of green-blue infrastructure, identification of elements of green infrastructure where repeated flowering of *P. coronarius* was recorded, visual perception of the species during the period of autumn flowering, and determination of measures of environmentall protection and preservation of isolated spatial elements.

MATERIALS AND METHODS

The research area is the BGI of the Belgrade municipality Savski venac (Figure 1), as the central and one of the oldest, whose name symbolically indicates that its territory follows the course of the right bank of the Sava river like a wreath [8]. The Gazela Park with an area of 1.86 ha (bordered by Savska, Drinska, Kneza Miloša Street, and the E75 highway), and the Natural Monument Topčiderski Park with an area of 3.1 ha (in the valley of the Topčider River, surrounded by hills – Part III of the park with an artificial water surface along Vojvode Mišić Boulevard) were selected. On this location, the repeated flowering of *P. coronarius* was recorded during autumn and the beginning of winter 2022/2023. Table 1 shows the descriptive characteristics of both parks.

Figure 1 *Wider context BGI – study areas in Belgrade, Savski venac municipality*

Google Earth images, cartographic materials, and plans were used to investigate the spatial arrangement of the green-blue infrastructure.

Field surveys included recording, phenological monitoring, rating flower abundance, and collecting the flowers of *P. coronarius.* Flowering phenology was monitored twice a week and the BBCH system [9] was applied. The dates of the beginning of the second flowering – BF (the day when <10% of flowers are opened), the full second flowering – FF (the day when

>50% of the flowers are opened), and the end of the second flowering – EF (the day when there are no more open flowers), as well as the duration of flowering in the period of August 2022 to January of 2023, were recorded.

Table 1 *Description of the study areas*

Park	Latitude φ	Longitude λ	Altitude H (m)	Soil type*	Aspect	Slope**
1. Gazela Park	44º47'58.87" N 44º47'57.20" N	20º26'59.73" EGr 20º27'04.65" EGr	74	Haplic Fluvisol (Eutric, Siltic)	W	0–1
2. Topčider Park	44º46'51.70" N 44º47'01.74" N	20º26'17.95" Egr 20º26'23.77" EGr	77	Haplic Fluvisol (Siltic)	NE	1–3

*[10]; **Slope angle: 0–1° (flat terrain), 1–3° (very mildly sloping terrain).

Meteorological data were used from the Main meteorological Station in Belgrade (44º47'54.44" N; 20º27'53.35" EGr; altitude: 132 m) (www.hidmet.gov.rs/index.php, accessed on 24 March 2023).

The abundance of flowering was visually evaluated, according to a scale from 1 to 5; where 1 is an individual with minimal flowering, and 5 is an individual with maximum flowering. The fresh material including floral parts was collected during field research. Measurements were based on 30 flower samples for quantitative analysis. To observe the floral morphological structure, the flower diameter, the calyx diameter, and the number of stamens using UTHSCSA Image tool software. Quantitative parameters were processed using descriptive statistics using the Statgraphics Centurion 19 software package.

RESULTS AND DISCUSSION

The BGI in the Savski Venac consists of larger and smaller green spaces that run through the interior of the site and exit to the river. The territory of the municipality is characterized by a level of urbanization of 66.95%, while artificial surfaces do not include green urban areas and sports and recreational areas as parts of "nature in the city" (land.copernicus.eu/local/urban-atlas/urban-atlas-2018, accessed on 20 March 2023). The creation of green corridors along the banks, roads, and bicycle and pedestrian paths on the site allows a connection between urban green spaces, and an accessible and open attractive network is formed that provides social security and contributes to the aesthetics of the city landscape [11]. BGI also affects the reduction of the vulnerability of the urban environment to the increasingly pronounced negative effects of climate change and extreme weather events [1,11]. Design solutions used in water management systems are proposed for the BGI of the research area: rain gardens, green roofs, vertical greening systems, and permeable pavements. The potential of these elements stems from the possibility of implementing them in a dispersive way that can be adapted to the terrain. The analyzed BGI is also specific for the parks where repeated flowering of *P. coronarius* was recorded.

A repeated flowering was recorded for one individual that was located in the Gazela Park (Park 1), and in the Topčider Park (Park 2) along Vojvoda Mišić Boulevard, in *P. coronarius*

that formed a hedge 48 m long. The average rating of flowering abundance in Topčider Park was 3.5, and in Gazela Park it was 1. Unlike the flowering period stated in the literature [2,4,7], repeated flowering was recorded in the parks 4 months after the first one. The individual in the Gazelle Park had BF noted on the 8th of November 2022, FF on the 12th of November 2022, and EF on the 10th of December 2022, while the individuals in the Topčider park the events were recorded on the following dates: BF on the 1st of November for BF, FF on the 7th of November 2022, and EF on the 19th of December 2022. Flowering in Park 1 lasted 32 days, and 49 days in Park 2. In Gazela Park, only single flowers were noted, and in Topčider Park both individual and clustered inflorescences (2–5). There is a noticeable deviation from the literature that states that five to seven flowers are grouped in inflorescence and form racemes at and near the ends of leafy branches [4,7,12]. The repeated flowering of European mock-orange was recorded for the first time in Belgrade during the fall of 2022, after a 16-year survey [4]. Repeated flowering is explained by climatic parameters: mean daily temperature for BF-FF period of 8.1°C (Gazela Park) and 7.9°C (Topčiderski Park, where there was a longer flowering phenophase). December 2022 was the warmest since 1887 (www.hidmet.gov.rs/ciril/meteorologija/klimatologija_produkti.ph, accessed 03/21/2023) at GMS Belgrade. The recorded differences between the two parks are explained by the influence of the microclimatic conditions of the environment.

Bearing in mind that the visual perception, in addition to the grouping in the inflorescence, the size of the flowers are also influenced by microclimate, and a comparative analysis confirmed that in the Gazela Park flowers size varied the most and included those of the largest but also the smallest dimensions, which is why the average values shown in Table 2 single out the Topčider Park with larger diameter flowers and the number of stamens per flower. According to the literature, in the first flowering at the end of spring, the diameter of one flower is 2.5–3.5 cm [5–7,12], and the research of repeated flowering confirmed the same ranges of the analyzed variables, with the exception of individual flowers that included also the larger dimensions.

Table 2 *Morphometric statistical features of P. coronarius flowers in Belgrade*

Park	Limiting value	$\bar{x} \pm S_{\bar{x}}$	$S \pm S_S$	$V \pm S_V$
the diameter of flowers (mm)				
1. Gazela Park	14–45	29.50 ± 1.47	8.88 ± 4.67	0.30 ± 0.05
2. Topčider Park	29–40	33.67 ± 1.12	3.23 ± 4.34	0.10 ± 0.01
the diameter of calyx (mm)				
1. Gazela Park	8–20	13.40 ± 0.67	4.11 ± 2.12	0.31 ± 0.05
2. Topčider Park	16–18	16.33 ± 0.54	1.09 ± 2.11	0.07 ± 0.01
the number of stamens				
1. Gazela Park	24–48	37.80 ± 1.89	7.21 ± 5.98	0.19 ± 0.03
2. Topčider Park	42–67	54.53 ± 1.82	7.11 ± 7.04	0.13 ± 0.02

The analysis of the state and application of *P. coronarius* in the parks enables the formation of a database in order to operationalize the design of BGI, but also the management and use of protected areas such as Topčider Park. Topčider is characterized by a significant diversity of entomofauna, amphibians, reptiles, and ornitofauna related to wetlands [13]. The

selected part of the park is located near the Topčider River, next to an artificial water surface that was without water at the time of the research. Through *in situ* monitoring, for more than 20 years, the drying up of the artificial water surface was recorded for the first time, which is explained by the influence of climatic factors. According to RHMZ data, the summer and fall of 2022 were rainy, but with a small number of days with precipitation ≥1 mm, which indicates that it was showery and that the precipitations were abundant on a daily basis. Rainwater is collected particularly in the crowns of deciduous plants, and the root system filters and stores water in the soil, reducing runoff [14], which resulted in the pond being without water even in November and December. In addition to the mentioned function, plants such as *P. coronarius* in urban areas create a habitat that attracts wild animals and allows them to complete their life cycle [3,4]. The species is also important during the off-vegetation period due to the loculicidal pods that remain open on the branches of the fruits, which remain on the branches until the following in spring and attract ornithofauna even after seed dispersal [12]. Vitality, flowering and repeated flowering of *P. coronarius* are important elements that allow wide introduction in different environmental conditions because of their resistance, ornamental value, fragrance, but also medicinal properties [3,4,7,12]. In both parks, it is necessary to preserve landscape and ambient values while maintaining the measures aimed at protecting natural values, primarily through adequate maintenance and the creation of good conditions for improving biodiversity without introducing invasive species.

CONCLUSION

The approach presented in this paper focuses on the concept of BGI, which combines issues related to green and blue infrastructure and ecosystem networks. Research has confirmed that a holistic and co-creative approach to the creation of BGI is necessary in modern landscape design to achieve ecosystem services [15]: 1) regulation (air quality, climate regulation, water purification, control of the spread of diseases and pathogenic organisms, pollination, mitigation of extreme events, carbon storage, decomposition of matter), 2) supply (food, drinking water, medical resources, raw materials such as wood, fiber, and other materials), 3) of cultural importance (intangible benefits that people receive from nature – recreation, aesthetic values, religious and spiritual values, mental and physical health, education) and 4) support (supporting services that support all other ecosystem services – they include both human and ecosystem needs: photosynthesis, nutrient cycling, soil formation, water cycling). As well as that more different design and engineering solutions in an area result in greater hydrological, landscape, and social benefits for the urban environment.

European mock-orange in the analyzed parks has confirmed good adaptability and ornamentality, which is why, with adequate maintenance, it can be used to preserve BGI elements. Well integrated into new functions and spaces will contribute to: the development of blue-green infrastructure, the design of a network of green paths starting from the rivers inland, which incorporates greenery into the spaces along the paths and around the buildings, the design of spaces suitable for rest and relaxation and their ecological sustainability.

ACKNOWLEDGEMENT

The authors are grateful to the Science, Technological development and Innovation of the Republic of Serbia for financial support of the University of Belgrade – Faculty of Forestry the scientific research work in 2023, the registration number 451-03-47/2023-01/200169.

REFERENCES

[1] Ghofrani Z., Sposito V., Faggian R., J. Sustain. Dev. Energy Water Environ. Syst. 8 (1) (2020) 213–234.

[2] Ocokoljić M., Petrov Dj., Dekorativna dendrologija, Univerzitet u Beogradu – Šumarski fakultet, Beograd (2022), p.409, ISBN: 978-86-7299-339-4.

[3] Alvey A., Urban For. Urban Green. 5 (2006) 195–201.

[4] Ocokoljić M., Petrov Dj., Galečić N., *et al*., Land. 12 (2023) 706.

[5] Hufford L., Hydrangeaceae *in* Flowering Plants Dicotyledons. The Families and Genera of Vascular Plants, Vol 6, Editor: Kubitzki K., Springer, Berlin, Heidelberg (2004) 202–215, ISBN: 978-3-642-05714-4.

[6] APG IV. An update of the Angiosperm Phylogeny Group classification for the orders and families of flowering plants: APG IV Bot. J. Linn. Soc. 181 (2016) 1–20.

[7] Ocokoljić M., Ninić-Todorović J., Priručnik iz dekorativne dendrologije, Šumarski fakultet, Beograd (2003), p.160. ISBN: 86-7299-084-6.

[8] Mala enciklopedija Prosveta (3 izd.), Beograd, Prosveta (1985), ISBN: 978-86-07-00001-2.

[9] Meier U., BBCH-Monograph. Growth Stages of Plants. [Entwicklungsstadien von Pflanzen. Estadios de las Plantas. Stades De Développement des Plantes]; Blackwell Wissenschafts-Verla: Berlin, Germany; Vienna, Austria (1997) p.622.

[10] Škorić A., Filipovski G., Ćirić M., Klasifikacija zemljišta Jugoslavije. Akademija nauka i umjetnosti Bosne i Hercegovine. Posebna izdanja knjiga LXXVIII. Sarajevo (1985).

[11] Pochodyła E., Glińska-Lewczuk K., Jaszczak A., Landsc. Online 92 (2021) 1–20.

[12] Hu S. Y., J. Arnold Arbor. 35 (1954) 275–333.

[13] Cvejić J., Vasiljević N., Tutundžić A., Tipologija predela Beograda: za potrebe primene Evropske konvencije o predelima. Izdanje Univerziteta u Beogradu Šumarskog fakulteta, (2008), ISBN: 867299146X, 9788672991468.

[14] i-Tree. *Available on the following link*: www.itreetools.org/documents/61/iTree_Eco_Precipitation_Interception_Model_Descriptions.pdf (accessed on12 October 2022).

[15] Reid W., Mooney H., Cropper A., *et al*., Millennium Ecosystem Assessment. Ecosystems and human well-being: synthesis, Island Press, Washington, DC (2005), p.160, ISBN: 9781597260404.

EFFECTS OF SO_2 AND NO_2 ON THE PHOTOSYNTHETIC EFFICIENCY AND CATALASE ANTIOXIDATIVE ENZYME ACTIVITY IN *Betula pendula* Roth

Dragana Pavlović[1*], Marija Matić[1], Veljko Perović[1], Olga Kostić[1], Dimitrije Sekulić[1], Miroslava Mitrović[1], Pavle Pavlović[1]

[1]Department of Ecology, Institute for Biological Research 'Siniša Stanković' – National Institute of the Republic of Serbia, University of Belgrade, Bulevar Despota Stefana 142, 11060 Belgrade, SERBIA

[*]*dragana.pavlovic@ibiss.bg.ac.rs*

Abstract

Air pollution in urban environment is one of the major stressors for vegetation. The aim of the present study was to investigate the levels of sulfur dioxide (SO_2) and nitrogen dioxide (NO_2) in the air in Belgrade and Smederevo and their effects on photosynthetic efficiency and catalase enzyme activity of Betula pendula Roth*. It was found that SO_2 and NO_2 concentrations increased from June to October at both studied sites but did not exceed the limits set by the national regulation. NO_2 concentrations above the limits were measured only in October in Belgrade. It was also found that the values of the parameter of photosynthetic efficiency (Fv/Fm) were within the optimal range determined for deciduous trees, except in June in Belgrade, indicating that birch has optimal photosynthetic efficiency. Average catalase activity increased during the course of season at both sites. The lowest enzyme activity was measured in June in Belgrade and the highest in October in Smederevo. It was be concluded that under the given environmental conditions, the birch trees show no signs of damage and that the basic physiological processes are running at an optimal level. The increase in photosynthetic efficiency and catalase activity in birch leaves in the second part of the season could represent some kind of adaptation mechanism that allows it to survive under unfavorable environmental conditions.*

Keywords: air pollution, photosynthetic efficiency, catalase enzyme activity, *Betula pendula* Roth.

INTRODUCTION

Air pollution is one of the most serious environmental problems, especially in the urban environment where most of the world's population lives. Urban air quality is continuously affected by emissions from stationary and mobile combustion sources, which generate a large number of pollutants whose chemical composition is extremely heterogeneous [1]. Sulphur dioxide (SO_2), nitrogen dioxide (NO_2), carbon monoxide (CO), and ozone (O_3) are the main hazardous air pollutants responsible for acid rain formation, crop yield decline, and ecological damage [2–4]. Sulphur dioxide is known as a primary pollutant that is produced in large quantities from the combustion of coal and other fuels in industry and households [4]. Unlike SO_2, NO_2 belongs to both primary and secondary pollutants and is a precursor of harmful secondary pollutants such as ozone. The major anthropogenic sources of NO_2 are industrial fossil fuel combustion, vehicle exhaust, biomass burning, and electricity generation [4]. At higher concentrations, SO_2 and NO_2 cause oxidative damage to biochemical and physiological

processes in plants. However, plants have several enzymatic and non-enzymatic antioxidant defense mechanisms to prevent oxidative damage [5,6]. Non-enzymatic antioxidants include glutathione, carotenoids, tocopherols, and flavonoids, while catalase (CAT), superoxide dismutase (SOD), ascorbate peroxidase (APX), glutathione reductase (GR), etc. are antioxidant enzymes of plants [6,7].

In this research, the concentrations of SO_2 and NO_2 in the air in Belgrade and Smederevo in June and October were monitored in order to determine whether they exceed the limits set by the Regulation on Monitoring Conditions and Requirements for Air Quality [8] and how these pollutants affect the efficiency of photosynthesis and the activity of catalase enzyme activity in *Betula pendula* trees.

MATERIALS AND METHODS

Sampling and field research

Photosynthetic efficiency and collection of leaf samples of *Betula pendula* Roth for determination of catalase enzyme activity were carried out in urban parks in Belgrade and Smederevo, exposed to different sources of pollution, in June and October 2012. In Belgrade, the samples were taken in the park "Hall Pioneer", which is located near several main roads, where traffic exhaust is a main source of pollution, while in Smederevo the samples were taken in the park "Tri heroja", which is about 7 km away from the main source of pollution "Železara Smederevo".

The data describing SO_2 and NO_2 concentrations in Belgrade and Smederevo during 2012 were obtained from the Serbian Environmental Protection Agency, which summarises data from the network of local air quality monitoring stations in Belgrade and Smederevo.

Photosynthetic efficiency was measured using the method of induced chlorophyll fluorescence kinetics of photosystem II. Measurements were taken with the aid of a portable Plant Stress Meter (BioMonitor S.C.I. AB, Sweden), as described by Krause and Weis [9]. Chlorophyll was excited for 2 s by actinic light with a photon flux density of 200 and 400 μmol m^{-2} s^{-1}. Prior to measuring, samples were adapted to the dark for approximately 30 min. [10–12]. Measurements were performed in thirty repetitions (n=30).

Leaf extract preparation and enzyme activity assays

Birch leaves were placed in liquid nitrogen immediately after sampling and stored at a temperature of -80°C until analysis. For enzyme extraction, the frozen leaf tissue was homogenized in a mortar with pestle and liquid nitrogen and then extracted in ice-cold 0.1 M potassium phosphate extraction buffer (pH 6.5) containing 3% polyvinylpyrrolidine (PVP) and 5% phenylmethanesulfonyl fluoride (PMSF). After homogenization, the crude leaf extracts were centrifuged at 14,000 x g at 4°C for 20 min, and the supernatants obtained were aliquoted and used to measure protein content and enzyme activity. Protein content was determined according to Bradford [13], using bovine serum albumin (BSA) as a standard. Catalase activities were determined spectrophotometrically in duplicate at 20°C using a Shimadzu UV-160 spectrophotometer. Catalase activity was measured by adding 10 μl of the enzyme extract to 1 ml of a reaction mixture containing 50 mM K-phosphate buffer (pH 7)

and 30% H_2O_2 and measuring the changes in absorbance at 240 nm for 3 min [14]. The results of catalase activity were expressed in units per mg of protein (U mg^{-1}).

Statistical analysis

The data from this research was analyzed using statistical analysis (ANOVA) and means were separated with a Bonferroni test at a level of significance of $p<0.05$, using the Statistica software package [15].

RESULTS AND DISCUSSION

Concentrations of SO_2 and NO_2 in Belgrade and Smederevo in June and October 2012 are shown in Figure 1.

Concentrations of SO_2 and NO_2 increased at both study sites during the season. The highest SO_2 concentrations were measured in Belgrade in October (23.69 μg m^{-3}) and did not exceed the limits set by the Regulation on Monitoring Conditions and Requirements for Air Quality (50 μg m^{-3}) [8]. NO_2 concentrations ranged from 10.60 μg m^{-3} in June in Smederevo to 42.56 μg m^{-3} in October in Belgrade, where the limit values (40 μg m^{-3}) [8] were only exceeded during the course of this research. It is clear that the studied birch individuals were exposed to lower concentrations of gaseous pollutants (SO_2 and NO_2) at the beginning of the growing season in relation to at the end of the season. Throughout the season, individuals from Belgrade were significantly more affected than those from Smederevo ($p<0.001$).

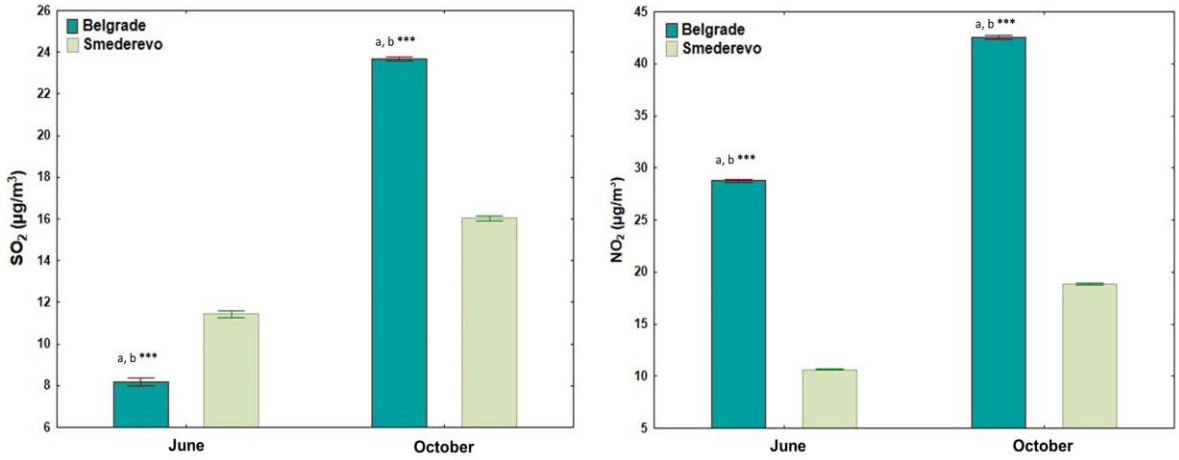

Figure 1 *SO_2 and NO_2 concentrations in Belgrade and Smederevo in June and October of 2012 (Source: Serbian Environmental Protection Agency)*

The variation of photosynthetic efficiency and catalase activity in samples of birch leaves in Belgrade and Smederevo are shown in Figure 2.

The analysis of the parameter Fv/Fm in birch showed a regularity in the seasonal dynamics, with the minimum values measured in June and the maximum in October at both study sites. It was also found that the Fv/Fm values in birch from Belgrade (0.731–0.781) and from Smederevo (0.773–0.783) were within the optimal range for deciduous trees (0.750–0.850) [16], except in June in Belgrade. This result indicates that SO_2 and NO_2 may have negative effects on birch, but not to an extent that would seriously threaten its

functioning. Nevertheless, the higher SO_2 and NO_2 concentrations in Belgrade affected photosynthetic efficiency, resulting in lower Fv/Fm in Belgrade compared to Smederevo in both seasonal periods, whereas this difference was significant only in June ($p<0.001$), Figure 2. Photosynthesis is one of the first processes affected by high SO_2 concentration [17], but when plants are exposed to low SO_2 concentrations, the absorbed SO_2 is oxidized and used to synthesize proteins. NO_2 is also known as a toxic gaseous pollutant that reduces net photosynthetic rate and chlorophyll content and inhibits photosynthesis at elevated concentrations. However, some relevant studies have found that plants exposed to moderate levels of atmospheric NO_2 for extended periods of time exhibit increased absorption and metabolism of nutrients used by plants for growth and development [18–20]. In general, whether SO_2 and NO_2 have adverse effects on plants under certain conditions is species-specific and depends on their concentration, the time period the plant is exposed to them, and the rate at which the plant takes them up [17,20,21].

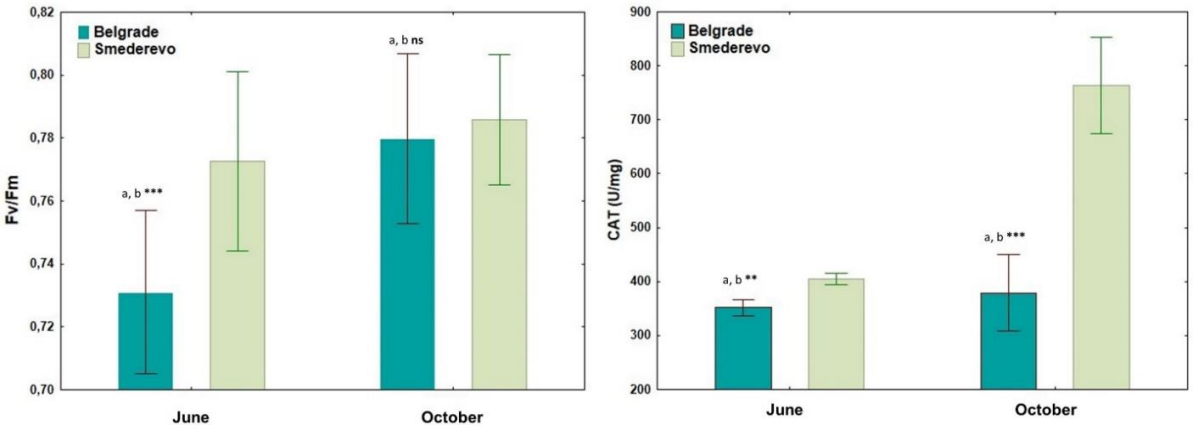

Figure 2 *The variation of photosinthetic efficiency (Fv/Fm) and catalase enzyme activity (CAT) in birch leaves in Belgrade and Smederevo in June and October 2012*

Average catalase enzyme activity increased over the season at both sites. The lowest enzyme activity was measured in June in Belgrade (351.71 U mg^{-1}) and the highest in October in Smederevo (763.55 U mg^{-1}). The increase in enzyme activity during the season can be associated with the increase in SO_2 and NO_2 concentrations. Similar effects of pollution on enzymatic activity of catalase were found by Ghorbanli *et al.* [22] who discovered that the activity level of catalase enzyme was increased in *Nerium oleander* and *Robinia pseudo acacia* leaves collected from the contaminated sampling site compared to the control site, but that increase was not statistically significant. However, from the results presented here, it is also evident that catalase activity is higher in birch trees from Smederevo, although SO_2 and NO_2 levels were lower than in Belgrade. Such result is not unusual, considering that the mechanisms of plant resistance under stress conditions are very complex and include several physiological and biochemical strategies aimed at mitigating the negative effects of various environmental stress factors through their joint action [23]. Prysedskyj [24] studied the influence of the type of complex compounds nitrogen and sulfur on catalase activity of selected tree and shrub species and concluded that the influence of pollutants on catalase activity depends on plant resistance, structure, and duration of pollutant effectiveness. He

found that in contrast to less resistant plants, species resistant to pollution are characterized by the absence of changes in catalase activity, i.e. an increase in catalase function due to the short-term effect of pollutants [24].

CONCLUSION

From the obtained results, it can be concluded that under the given environmental conditions, the birch trees do not show any signs of morphological damage and the basic physiological processes are at an optimal level. The increase in the value of the photosynthetic efficiency parameter and catalase activity in the second part of the vegetation period could be considered as an adaptation mechanism of the birch that allows it to survive in unfavourable site conditions.

ACKNOWLEDGEMENT

The authors are grateful to the Ministry of Science, Technological Development and Innovation of the Republic of Serbia for financial support according to the contract with the registration number (451-03-47/2023-01/200007).

REFERENCES

[1] Fusaro L., Salvatori E., Winkler A., *et al*., Ecol. Indic. 126 (2021) 107707.

[2] Mukherjee A., Agrawal S. B., Agrawal M. Sci. Total Environ. 710 (2020) 136363.

[3] Aghajanzadeh T. A., Otaghsara S. H. T., Jafari N., *et al*., J. Plant Physiol. Breed. 11 (1) (2021) 49–62.

[4] Wang Y., Jin W., Che Y., *et al*., Forests 10 (2019) 312.

[5] Li L., Yi H., Plant Physiol. Biochem. 58 (2012) 46–53.

[6] Hasanuzzaman M., Bhuyan M. H. M. B., Zulfiqar F., *et al*., Antioxidants 9 (2020) 681.

[7] Dumanović J., Nepovimova E., Natić M., *et al*., Front. Plant Sci. 11 (2021) 552969.

[8] OGRS (2010/2013) Regulation on Monitoring Conditions and Requirements for Air Quality. Official Gazette of the Republic of Serbia. No. 11/10; 75/10; 63/13.

[9] Krause H.M., Wei E. Annu. Rev. Plant Physiol. 42 (1991) 313–349.

[10] Mitrović M., Pavlović P., Lakušić D., *et al*., Sci. Total Environ. 407 (2008) 338–347.

[11] Gajić G., Mitrović M., Pavlović P., *et al*., Ecotoxicol. Environ. Saf. 72 (2009) 1090–1101.

[12] Kostić O., Mitrović M., Knežević M., *et al*., Arch. Biol. Sci. 64 (1) (2012) 145–158.

[13] Bradford M.M. Anal. Biochem. 72 (1976) 248–254.

[14] Aebi H. Meth. Enzymol. 105 (1984) 121–126.

[15] SPSS (2007) SYSTAT Version 16: Statistics. SPSS, Chicago, IL.

[16] Björkman O., Demmig B. Planta 170 (1987) 489–504.

[17] Lee H.K., Khaine I., Kwak M. J., *et al*., Hortic. Environ. Biotechnol. 58 (6) (2017) 523–529.

[18] Takahashi M., Nakagawa M., Sakamoto A., *et al*., New Phytol. 168 (2005) 149–154.

[19] Adam S.E.H., Shigeto J., Sakamoto A., *et al*., Botany 86 (4) (2008) 442–442.

[20] Jiechen W., Yue W., Huihui Z., *et al*., J. Plant Interact. 16 (1) (2021) 422–431.

[21] Hu Y., Bellaloui N., Tigabu M., *et al*., Acta Physiol. Plantarum 37 (2015) 39.

[22] Ghorbanli M., Bakand Z., Bakhshi khaniki G., *et al*., Iran. J. Environ. Health Sci. Eng. 4 (3) (2007) 157–162.

[23] Skrypnik L., Maslennikov P., Feduraev P., *et al*., Plants 10 (2021) 1871.

[24] Prysedskyj Y., Biosyst. Divers. 24 (2) (2016) 295–301.

PLANT-SOIL RELATIONSHIPS IN MEDITERRANEAN SPECIES GROWN ON TECHNOSOLS ENRICHED WITH COMPOST

Ermenegilda Vitale[1], Pasquale Napoletano[2*], Carmen Arena[1,3], Anna De Marco[4]

[1]Department of Biology, University of Naples Federico II, 80126 Naples, ITALY

[2]Department of Agricultural, Environmental and Food Sciences, University of Molise, 86100 Campobasso, ITALY

[3]NBFC-National Biodiversity Future Center, 90133 Palermo, ITALY

[4]Department of Pharmacy, University of Naples Federico II, 80131 Naples, ITALY

[*]*pasquale.napoletano@unimol.it*

Abstract

Organic-based amendments are promising, cost-effective, and eco-friendly solutions among soil requalification strategies. This study explored the application of compost to Technosols to improve soil quality and make the substrate suitable for growing typical species of the Mediterranean area, i.e. Malva sylvestris L., Phillyrea angustifolia L., and Quercus ilex L. Chemical soil quality indicators have been assessed after the compost addition. Furthermore, functional leaf characteristics and photochemical efficiency have been evaluated to estimate the relationships between soil characteristics and plant growth. The results showed that compost addition increased soil carbon compounds and C/N over time, which is probably emphasized by plant metabolism. Among species, M. sylvestris rapidly respond to compost addition, showing the best photosynthetic efficiency and a higher carbon investment in photosynthetic tissues (higher leaf area and lower leaf mass per area). Moreover, the growth of P. angustifolia L., and Q. ilex L. on compost for 11 months significantly improved the leaf water content. The results encourage using organic-based amendments in overexploited soil to favour plant growth.

Keywords: Technosol, compost, plant productivity, restoration, urban ecology.

INTRODUCTION

The urban vegetation and the planning of new green spaces can provide the city environment and society with several ecosystem services, such as recreational and aesthetic benefits; pollutant and dust removal from the atmosphere; carbon sequestration balancing the high anthropic carbon emissions; microclimate regulation; restoration of soil quality and services and preservation of plant biodiversity [1]. However, plant growth in the urban environment depends on the relationships between soil quality and plant species selected to cover the soil surfaces.

Several urban soils incorporate anthropogenic materials derived from human activities. They are named Technosols (which are characterized by ≥ 20% of artefacts in the upper 100 cm from the soil surface) and generally present a poor structure, a weak amount of organic matter and nutrients, extreme pH values and minimal biological activity [2].

Soil quality influences plant growth [1]; thus, improving the growth substrate's quality is a prerequisite to obtaining healthy plants. Short or long-term effects of compost on soil have demonstrated that such procedures improve soil fertility, especially in terms of organic compounds and essential nutrient content [3,4]. Based on this evidence, the compost addition to technogenic soils, may improve nutrients enhancing photosynthetic capacity and plant growth. The possibility of utilizing compost to ameliorate soil quality and plant growth is worthy of attention also in the realization of new urban green spaces. However, it requires an accurate choice of the most suitable species to consider the aesthetic value of landscape and plant biodiversity [5].

In this study, three species of Mediterranean maquis *Malva silvestris* L., *Phillyrea angustifolia* L., and *Quercus ilex* L. were grown in experimental mesocosms filled with technogenic soils alone or enriched with compost to assess for one-year the effect of compost addition on plant growth and soil properties. Furthermore, plant species were compared to evaluate their capability to grow on Technosols for greening purposes.

MATERIALS AND METHODS

Experimental site and set-up

The experimental site is in Naples (Campania region, Southern Italy) at the University Campus of Monte Sant'Angelo Federico II (40° 50' 12.63" N, 14° 10' 58.03" E, 122 a.s.l.) and comprises 8 mesocosms (area: 16 m^2, depth: 2 m each) filled with Isolatic Ekranic Technosols [1,2], containing more than 20% of artefacts deriving from cracked building rubble mixed with pyroclastic materials deposed in 2006. In December 2010, the soil substrate was enriched with dry compost (2 kg m^{-2} consisting of green refuse) to a depth of 20–30 cm, and then the soil surface was levelled [6]. The compost was added to 4 mesocosms (CP) while the other 4, without compost, were used as control (NCP). After 7 days from compost addition, specimens of *Quercus ilex* L. (Q) and *Phyllirea angustifolia* L. (Ph), were transplanted. In each mesocosm, 6 plants were placed: 3 for each species, for a total of 12 individuals. The herbaceous species *Malva silvestris* L. (M) was left to grow spontaneously in each mesocosm. During the experimental period, the mesocosms were left undisturbed and irrigated twice a week for two months [7]. Soil analyses were carried out before compost addition (BC) and at 2, 4 and 11 months from compost addition (MFC). Five soil subsamples at different depths (0–10 and 10–20 cm) were collected from each mesocosm. The soil samples were sieved (< 2 mm) to process the following chemical analyses: pH, water content (SWC), carbon (C), nitrogen (N), C/N, soluble fraction of C, N and ratio. As a proxy of plant healthy status and growth, the three species were analyzed on NCP and CP substrate for photochemical activity, C and N leaf content and functional leaf characteristics at 2, 4 and 11 MFC.

Soil analyses

The pH, water content (SWC), carbon (C), nitrogen (N), C/N were evaluated according to the Italian Official Methods of Soil Science [8]. Briefly, pH was evaluated in soil: distilled water (1:2.5=v:v) suspension by electrometric method. Soil water content (SWC) was determined after drying at 105°C until constant weight; C and N were evaluated in oven-dried

and grounded samples by CNS analyser (Thermo Finnigan, EA 112 series) and from these C/N was calculated. Soluble C and N were measured in oven-dried soil (105°C) and leaf (70°C) samples following De Marco *et al.* [9].

Plant measurements

The leaf functional traits, namely leaf area (LA), leaf mass per area (LMA), and leaf water content (LWC) were estimated according to Cornelissen *et al*. [10]. Fluorescence measurements were performed *in vivo* on fully expanded leaves by a pulse amplitude modulate fluorometer (MiniPAM, Walz) under natural conditions of temperature, on 30 min dark-adapted leaves following the procedure reported in Vitale *et al.* [11]. More specifically, the background fluorescence signal, F_0 and the maximal fluorescence in the dark-adapted state, F_m, were used to calculate the F_m/F_0 ratio, an indicator of plant healthy status.

Statistical analysis

The statistical analysis was performed by SigmaPlot_12.2 software (Jandel Scientific, USA) for soils and plants. The normality of the data distribution was assessed by the Shapiro-Wilk test. Comparisons among BC, NCP and CP treatments for soil properties and responses of the three investigated species were tested by One-Way ANOVA.

RESULTS AND DISCUSSION

Technosols characteristics at different soil depths

Table 1 *Soil characteristics for BC, NCP and CP substrate at 2, 4 and 11 MFC, at 0–10 and 10–20 cm: pH, SWC (% d.w.), C (% d.w.), N (% d.w.), C/N, Soluble C (% d.w.), Soluble N (% d.w.), Soluble C/N. Different letters show statistically significant differences for at least p<0.05.*

	Depth (cm)	BC	CP			NCP		
			2 MFC	4 MFC	11 MFC	2 MFC	4 MFC	11 MFC
pH	0–10	7.96 ±0.05^{a}	7.68 ±0.05^{b}	8.06 ±0.10^{a}	7.67 ±0.06^{b}	7.70 ±0.08^{ab}	7.97 ±0.05^{ab}	7.81 ±0.07^{ab}
	10–20	8.30 ±0.05	7.91 ±0.07	8.19 ±0.05	8.05 ±0.12	7.95 ±0.08	8.18 ±0.03	8.00 ±0.09
SWC	0–10	27.7 ±0.98^{a}	30.8 ±1.29^{a}	18.3 ±0.90^{b}	19.7 ±0.13^{b}	29.7 ±0.80^{a}	16.41±1.09^{b}	18.2 ±0.12^{b}
	10–20	21.9 ±0.17^{c}	24.7 ±0.54^{b}	18.2 ±0.37^{e}	21.4 ±0.21^{c}	24.7 ±0.48^{a}	18.01 ±0.94^{e}	20.3±.16^{d}
C	0–10	1.57 ±0.11^{b}	2.14 ±0.33^{ab}	2.26 ±0.11^{a}	2.22 ±0.06^{ab}	1.97 ±0.18^{ab}	1.76 ±0.07^{ab}	1.94 ±0.09^{ab}
	10–20	1.16 ±0.06	1.45 ±0.23	1.54 ±0.10	1.35 ±0.03	1.31 ±0.05	1.41 ±0.04	1.20 ±0.04
N	0–10	0.18 ±0.03	0.11 ±0.01	0.14 ±0.01	0.14 ±0.001	0.10 ±0.01	0.13 ±0.01	0.13 ±0.002
	10–20	0.13 ±0.02^{a}	0.07 ±0.01^{ab}	0.10 ±0.002^{ab}	0.12 ±0.002^{a}	0.05 ±0.01^{b}	0.08 ±0.002^{ab}	0.09 ±0.001^{ab}
C/N	0–10	10.2 ±0.58^{b}	19.8 ±1.30^{a}	16.3 ±2.50^{a}	15.9 ±0.30^{a}	19.2 ±1.24^{a}	12.9 ±0.84^{ab}	14.7 ±0.81^{ab}
	10–20	11.07 ±0.72	22.14 ±2.51	17.66 ±0.34	11.37 ±0.35	25.61 ±2.73	16.99 ±0.58	12.75 ±0.27
Sol C	0–10	0.13 ±0.01^{b}	0.21 ±0.01^{ab}	0.22 ±0.004^{ab}	0.30 ±0.004^{a}	0.21 ±0.01^{ab}	0.20 ±0.01^{ab}	0.21 ±0.01^{ab}
	10–20	0.15 ±0.01^{d}	0.35 ±0.01^{b}	0.38 ±0.01^{a}	0.14 ±0.01^{d}	0.38 ±0.01^{a}	0.21 ±0.01^{c}	0.14 ±0.002^{d}
Sol N	0–10	0.02 ±0.001^{b}	0.07 ±0.002^{a}	0.06 ±0.001^{a}	0.02 ±0.001^{b}	0.06 ±0.001^{a}	0.01 ±0.001^{b}	0.02 ±0.001^{b}
	10–20	0.03 ±0.001^{a}	0.02 ±0.002^{b}	0.04 ±0.002^{a}	0.01 ±0.001^{a}	0.02 ±0.002^{b}	0.03 ±0.002^{a}	0.02 ±0.001^{b}
Sol C/N	0–10	6.86 ±0.38^{d}	3.16 ±0.14^{e}	3.74 ±0.14^{e}	12.8 ±0.64^{b}	3.50 ±0.17^{e}	19.1 ±1.24^{a}	10.0 ±0.18^{c}
	10–20	5.01 ±0.24^{b}	14.4 ±0.60^{a}	10.6 ±0.58^{ab}	14.9 ±1.56^{a}	14.5 ±2.28^{a}	7.74 ±0.64^{ab}	7.41 ±0.39^{ab}

In Table 1, soil pH at 0–10 cm showed lower values for CP treatment at 2 and 11 MFC probably due to both compost addition and plant growth. The soil water content depended more on the specific climate condition than the plant or compost effect. It is likely that compost addition increased C soil content, although the differences were not always statistically significant (Table 1). In detail, the content of C displayed the highest values in CP soils at 4 MFC compared to BC. Moreover, N was particularly abundant in BC and CP 11 MFC at a depth of 10–20 cm, whereas C/N showed higher values after 2, 4 or 11 MFC regardless of the compost addition. It is reasonable that an increase of organic matter complexity may have been influenced by plant metabolism and compost addition [6]. On the other hand, soluble C increased in NCP and CP soils compared to BC at 0–10 cm depth, while more fluctuation was evidenced at 10–20 cm, probably due to the leaching. Compared to BC, soluble N apparently increased only at 2 MFC due to plant uptake or loss of soluble compounds. The higher complexity of soluble compounds affected C/N ratio, which raised overtime [6].

Carbon, nitrogen and functional traits in leaves as affected by compost

The addition of compost determined a significant increase in leaf C content in M plants grown on CP soil compared to NCP at 4 and 11 MFC. No difference was detected in Ph and Q plants. The highest C content was found in Ph leaves on both NCP and CP soils, irrespective of the time (Figure 1a). The nitrogen content was higher in M plants grown on CP substrate compared to NCP and at 4 and 11 MFC. Conversely, the leaf N content in Q plants on CP soil increased only at 2 MFC. Among species, *Malva* showed higher values of leaf N than Ph and Q plants, irrespective of the compost addition, while the lower values were found in Q leaves (Figure 1b).

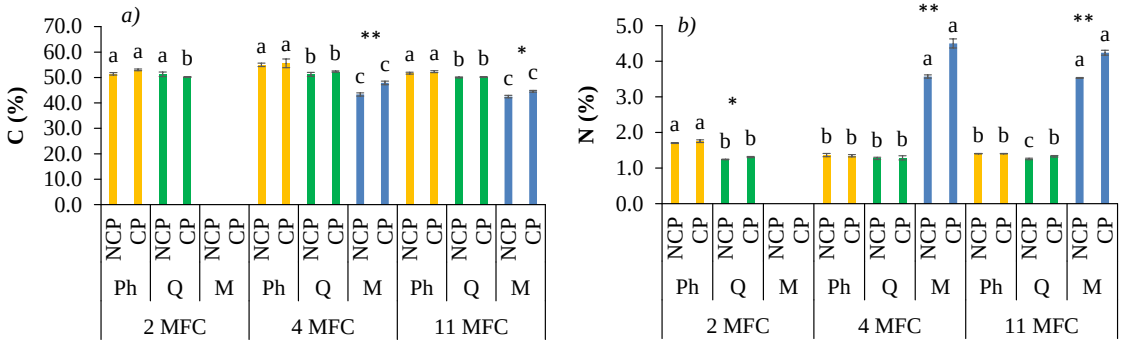

Figure 1 *a) C (%); b) N (%) leaf content in Ph, Q and M plants grown on Technosols NCP and CP at 2, 4 and 11 MFC. Different letters indicate statistically significant differences ($p<0.05$) among the three species grown on NCP or CP. Asterisks represent statistically significant differences between NCP and CP plants within the same species ($^{*}p<0.05$, $^{**}p<0.01$, $^{***}p<0.001$)*

The growth on different substrates did not affect LA in Ph plants. In Q plants, LA was lower on CP at 2 MFC but higher at 11 MFC on NCP. On the other hand, CP-M plants exhibited a significant increase in LA at 4 MFC. Among species, M plants showed the highest LA values on both substrates (Figure 2a). Compost addition significantly affected only Ph plants, as LMA was lower in CP than NCP plants. The lowest LMA values were found in *M.*

sylvestris, regardless of the experimental period and growth substrate (Figure 2b). The LWC increased in only NCP-Q plants compared to CP at 2 MFC. Among species, Ph and Q always showed comparable LWC values, lower than those measured in M plants (Figure 2c).

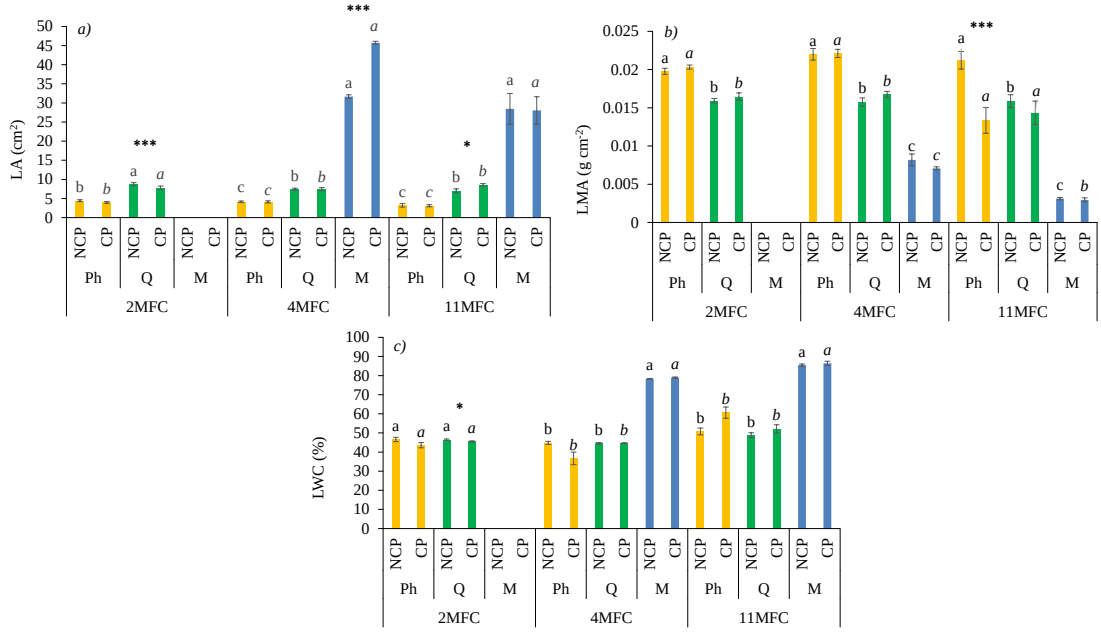

Figure 2 *a) LA; b) LMA; c) LWC in Ph, Q and M plants grown on Technosols NCP and CP at 2, 4, and 11 MFC. Different letters indicate statistically significant differences ($p<0.05$) among the three species grown on NCP or CP. Asterisks represent statistically significant differences between NCP and CP plants within the same species ($^{*}p<0.05$, $^{**}p<0.01$, $^{***}p<0.001$)*

Leaves of *M. sylvestris* plants grown on amended mesocosms showed increased leaf N, C content and lower LMA, suggesting a positive influence of the compost on the Technosols quality. Leaves with high nitrogen levels and low LMA are typical of species presenting high photosynthetic rates, which invest more C and N in photosynthetic machinery and pigments, thus increasing photosynthetic performance and growth. Conversely, sclerophyll plants show a different growth strategy and use of energy and soil resources. Indeed, in *Ph. angustifolia* and *Q. ilex*, foliar C and N did not increase significantly with the addition of compost because they invest more photosynthates in structural carbon. *Q. ilex* and *Ph. angustifolia* also exhibited a different structure of leaves, typical of xeromorphic species, which take advantage in hot and dry environments. Furthermore, after 2 MFC, *Q. ilex* plants grown on NCP substrate showed higher values of LA and LWC, while after 11 MFC, LA also increased in plants grown on Technosols enriched with compost. Considering that LA decreases with the decreasing of water availability [12] and starting from 4 MFC, the soil water content lessened compared to the initial conditions (BC and 2 MFC), it is reasonable to suppose that the amendment of Technosols with compost may have promoted the water conservation within plant tissues. Such effect was evident in *M. sylvestris* CP-plants, as leaves showed an expansion of the leaf lamina already after 4 months from compost addition. Even if SWC and soluble N reduced in all mesocosms after 11 MFC, *Ph. angustifolia* seems to benefit from the compost addition because it showed lower LMA values. This result contrasts with the

literature because a higher LMA is generally associated with plants with longer leaf longevity, growing on dry land and poor soil [13]. In our context, the LMA reduction likely suggests an increase in soil fertility due to the compost addition.

Plant photochemical efficiency

Q plants did not show differences in F_m/F_0 on different substrates. Conversely, F_m/F_0 increased in Ph plants on CP soil at 2 and 11 MFC, and in M plants on CP regardless of the time. M plants maintained higher values of F_m/F_0 compared to Ph and Q plants during the whole experimental period, while Ph exhibited higher values of F_m/F_0 ratio than Q plants (Figure 3).

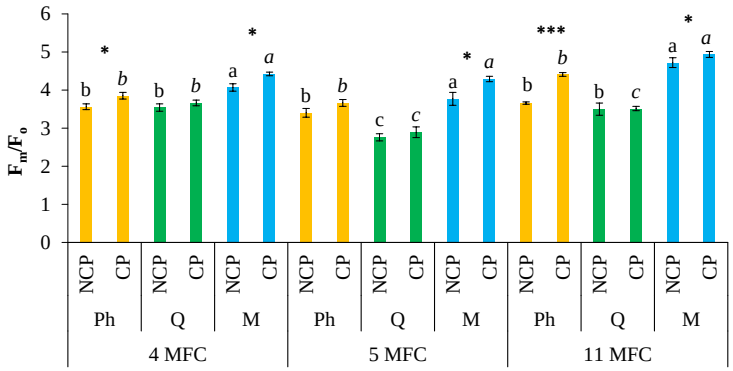

Figure 3 *F_m/F_0 in Ph, Q and M plants grown on Technosol NCP and CP 4, 5 and 11 MFC. Different letters indicate statistically significant differences ($p<0.05$) among the three species grown on NCP or CP. Asterisks represent statistically significant differences between NCP and CP plants within the same species ($^{*}p<0.05$, $^{**}p<0.01$, $^{***}p<0.001$)*

As all the investigated species showed F_m/F_0 ratio values within 3-4 arbitrary units [14], we exclude stressful conditions at photosynthetic apparatus due to an impairment of photosystems. Moreover, excluding from *Q. ilex*, the observed increase of F_m/F_0 ratio in *Ph. angustifolia* and *M. sylvestris* on CP soil might suggest a higher nitrogen investment in leaves towards chlorophyll synthesis. Specifically, in *M. sylvestris*, the nitrogen leaf content seems to be positively influenced by plant growth on Technosols enriched with compost, representing a prompt-available nitrogen source in the soil.

CONCLUSION

The compost addition and plant establishment significantly affected the Technosols quality. Among investigated plants, *M. sylvestris*, a colonizing and fast-growing herbaceous species, takes more advantage from compost addition to soil at the beginning and after almost one year from fertilization. It is likely that sclerophyllous species, investing more photosynthates in structural carbon, need more time to show positive outcomes in terms of growth and functional traits due to soil amendment with compost.

The overall results showed that all species can grow on Technosols amended with compost and could be employed for urban greening areas contributing to ecosystem services in urban contexts.

REFERENCES

[1] Napoletano P., Colombo C., Di Iorio E., *et al*., Sustainability 13 (2021) 9101.

[2] IUSS Working Group WRB: World Reference Base for Soil Resources 2014, Update 2015, World Soil Resources Report No. 106, FAO: Rome, Italy, 2015.

[3] Odlare M., Pell M., Svensson K., Waste Manag. 28 (7) (2008) 1246–1253.

[4] Memoli V., De Marco A., Baldantoni D., *et al*., Ecosphere 8 (2017) 1–12.

[5] Ugolini F., Baronti S., Lanini G.M., *et al*., J. Environ. Manage. 273 (2020) 1111682020.

[6] Panico S. P., Memoli V., Napoletano P., *et al*., Appl. Soil Ecol.138 (2019) 156–159.

[7] Kottek M., Grieser J., Beck C., *et al*., Meteorol. 15 (2006) 259–263.

[8] Colombo C., Miano T., Metodi di analisi chimica del suolo. Ed. Pubblicità & Stampa, Bari, Italy, (2015) ISBN: 978-88-940679-0-3.

[9] De Marco A., Arena C., Giordano M., *et al*., Plant Soil 372 (2013) 473–486.

[10] Cornelissen J.H.C., Lavorel, S., Garnier E., *et al*., Aust. J. Bot. 51 (2003) 335–380.

[11] Vitale L., Arena C., Virzo De Santo A., Plant Biosyst.146 (2012) 443–450.

[12] Wang C., He J., Zhao T.H., *et al*., Front. Plant Sci. 10 (2019) 58.

[13] Wright I. J., Reich P. B., Cornelissen J. H. C., *et al*., Glob. Ecol. Biogeogr. 14 (5) (2005) 411–421.

[14] Lichtenthaler H.K., Buschmann C., Knapp M., Photosynthetica 43 (3) (2005) 379–393.

IMPACTS OF PESTICIDE APPLICATION ON THE ENVIRONMENT

Milica Blažić[1*], Milivoje Milovanović[1],Tatjana Sekulić[1], Vladanka Stupar[1], Zlata Živković[1]

[1]Academy of Applied Technical Studies Belgrade, Colleage of Applied Engineering Sciences, Nemanjina 2, Požarevac, SERBIA

[*]*mblazic@atssb.edu.rs*

Abstract

Increased growth tendency of human population observed during many years was leading to increased food manufacturing. In order to achieve safety level of food supply for fast growing human population and global demand for food it was necessary to increase the yield and reduce the loss in agricultural production. This has led to intensive use of pesticides. Nearly one third of agricultural products had pesticides in their production. The absence of their use would lead to massive loss in food production. According to Tudi et al. the absence of pesticides would cause 78% loss in fruit production, 54% loss in vegetable production and 32% in crops production. They play key role in a food production increase and reduction of the crops diseases, worldwide. As they are chemical substances or mixture of substances for weeds and pest extermination they can have toxic effect on targeted species and as well not targeted species, water, air, soil, leading to global pollution. Pesticides residue can affect human health through environment pollution and food intake. It is very important to predict the risk of their use in a long run. Our study offers a view into scientific information needed for sensible use of pesticides, their influence on environment and human health, and minimization of their use.

Keywords: pesticides, toxicity, agricultural production.

INTRODUCTION

According to definition from United Nations Organization for Food and Agriculture – FAO pesticides are substances or mixtures of substances intended for prevention, destruction, repulsion or reduction of any pest, including carriers of human and animal diseases, unwanted species of plants or animals causing damage during production or interfere in another way with production, treatment, storing, transportation or marketing of food, agricultural products, wood products or animal feed [1]. Pests include insects, mollusca, rodents, nematodes, birds, mammals, microorganisms and weeds [2,3]. Three trillion kilograms of pesticides are used annually worldwide [4], while only 1% of total pesticides are used effectively to control pests on target organisms [5].

The use of pesticides in agricultural production has been a very easy, quick and cheap solution for controlling weeds and pests and increasing crop yields on a global level for centuries. However, their free and unsystematic application has led to serious problems for the environment and human health. There is no part of the environment that is not contaminated by pesticides; their remains are found in the soil, air, surface and underground water, and through the contamination of the environment and food, they indirectly affect

people's health. This paper provides a brief overview of the benefits and negative impacts of pesticide use on the environment and human health on a global level.

BENEFITS OF PESTICIDE APPLICATION

Enormous primary benefits have been achieved by the application of pesticides in various fields, including agriculture and public health [6]. Pesticides are used in everyday life to kill pests, including mosquitoes, ticks and rats in homes and public places. In this way, the transmission of diseases whose carriers are the above-mentioned organisms [7] was significantly reduced. Pesticides are indispensable in agricultural production. The increase in world population in the 20th century would not have been possible without a parallel increase in food production. The factors that influenced the increase in food production included, in addition to the development of better varieties and the use of more modern machines and the use of pesticides, which significantly influenced the reduction of harvest losses caused by weeds, diseases and pests [6]. Close to 1/3 of agricultural products are produced using pesticides. Without the use of pesticides, losses in fruit production would amount to 78%, in vegetable production 54%, and in grain production 32% [8]. Because of this, pesticides play a key role in reducing disease and increasing crop yields around the world, thereby contributing significantly to alleviating hunger in the world population.

There are also secondary benefits of pesticide application that are less obvious but with long-term consequences: improving the quality and safety of food and human health, which improves the quality of life and extends life expectancy. Also, the control of pests on pastures contributes to significant benefits for animal husbandry [9]. Table 1 summarizes the primary and secondary benefits of pesticide application and their interactions.

Table 1 *Primary and secondary benefits of pesticide application*

Primary benefits	Secondary benefits
1. Suppression of pests and carriers of plant diseases	**1. Social benefits**
Improved crop/livestock quality Reduced fuel consumption for weeding Reduced soil disturbance Control of invasive species	Improved human nutrition and health Food safety Increased lifespan Reduced maintenance costs
2. Control of human and animal disease carriers	**2. National benefits**
Saved human lives Reduced level of various disorders in humans Animal suffering reduced Increased quality of livestock	National agricultural economy Increased export income Reduced soil erosion
3. Prevention or control of organisms that harm human activities and structures	**3. Global benefits**
Tree/bush/leaf hazards prevented Protection of recreational lawns Protection of wooden structures	Less pressure on uncultivated land Less introduction of pests elsewhere International income from tourism

* Edited from Cooper and Dobson [10].

NEGATIVE EFFECTS OF PESTICIDE APPLICATION

Although pesticides play a significant role in improving crop yields and producing affordable and high-quality food, their continued use has numerous negative impacts on the environment and human and animal health. In addition to destroying pests and weeds, they can be toxic to a host of other non-target organisms – fish, birds, beneficial insects and non-target plant species. It is estimated that over 98% of insecticides and 95% of herbicides reach non-target species, including soil, water and air [9]. An overview of the negative impacts and consequences of the application of pesticides on the mentioned segments of the environment is given below.

Impact on water

Pesticides can enter water systems in several ways: agricultural runoff, spills, drifts, through industrial wastewater, washing of spraying equipment, aerial spraying, and washing from soil treated with pesticides. The most common way of transferring pesticides from land to water is through runoff or drainage [11]. Runoff from agricultural fields treated with pesticides is the most common way pesticides enter and contaminate water systems. Some of the research has shown that excessive contamination in streams, lakes and coastal waters is the result of pesticide runoff from agricultural land. According to the OECD report from 2001, it was determined that agriculture in the countries of the European Union contributes 40–80% to the total amount of nitrogen and 20–40% to the total amount of phosphorus in polluted surface waters [9]. Important sources of river pollution are industrial waters and runoff from private farms. The key users of pesticides are farmers who use them in huge quantities to protect their crops and increase their yields. Also, the use of pesticides to control pests in private gardens is an important source of water pollution [11]. High concentrations of pollutants are found in river and groundwater rather than lake water, since the detected concentrations of most pesticides follow seasonal variations, with the highest values occurring during spring and summer, with a significant decrease during winter [12].

Contamination of surface and groundwater with pesticides can affect aquatic flora and fauna, as well as human health when water is used for public consumption [13]. One of the most shocking effects of groundwater pesticide contamination occurred in India in 2002, when bottled water was found to contain pesticide residues. Seventeen brands of bottled water sold in New Delhi were contaminated with pesticides. The most common residues found in almost all samples were organochlorines and organophosphates [11]. Long-term and regular use of pesticides leads to bioaccumulation. Level of O_2 are drastically reduced due to the killing of aquatic plants by herbicides, which produce the largest percentage of O_2 in aquatic ecosystems, leading to a lack of O_2 for fish and other aquatic organisms. One of the herbicides, atrazine, indirectly affects the immune system of amphibians and is dangerous for some types of fish. The herbicide glyphosate has been found to cause high mortality rates in tadpoles and young frogs. It has also been shown that small amounts of the accumulated insecticide malathion change the amount and composition of the plankton and periphyton population, which indirectly affects the development of frog tadpoles [14].

Impact on soil

A large part of the pesticides that are used every day accumulates in the soil, where they undergo various processes of degradation, transport and adsorption, which change the

properties of the soil and soil microflora. Degraded pesticides interact with indigenous soil microorganisms, which changes its microbiological diversity, the flow of biochemical reactions and enzymatic activities. Any change in soil microbiological diversity and biomass eventually leads to disturbances in the functioning of the soil ecosystem and loss of soil fertility. The use of pesticides also negatively affects vital biochemical reactions that take place in the soil through microorganisms: nitrogen fixation, nitrification and ammonification. Pesticides also affect the mineralization of organic matter, which is a key property of soil that determines its quality and productivity [3]. In addition to the effect of pesticides on harmful insects, numerous useful members of the soil fauna also suffer, which reduces their positive role in the soil. Microflora breaks down organic matter, and earthworms and microarthropods break it down, crush plant remains and accelerate their decomposition. It was found that the decomposition of plant residues in the soil is reduced by 25%, if microarthropods are eliminated from it by fumigation. Indirectly, the use of pesticides reduces the number of pests, so beneficial insects are left without food, and their population decreases [15].

The persistence of pesticides in soil depends on their physicochemical properties including water solubility, soil sorption constant, octanol/water ratio coefficient, and soil half-life [16]. Pesticides that are strongly bound to soil particles have high values of the octanol/water ratio coefficient as well as soil sorption constants, which results in strong sorption of organic matter in the soil. Therefore, hydrophobic and bioaccumulative pesticides accumulate and persist in the soil for a long period of time [6]. Thus, some organochlorine pesticides, such as the widely used insecticide dichloro-diphenyl-trichloroethane (DDT), are no longer used in some countries due to their high persistence in soil, or people use them despite the fact that they are prohibited. On the other hand, some pesticides that are not persistent in the soil, but because they are subjected to different transformation processes during runoff and leaching through the soil, still represent a threat to aquatic ecosystems and food chains. The behavior of pesticides in the soil also depends on the concentration of organic matter in the soil, its pH value, temperature, humidity, the presence and types of microorganisms, as well as the method of irrigation [9].

Impact on human health

Toxicity caused by pesticides in humans can result from ingestion, inhalation or dermal absorption. Pesticides enter the human body by inhaling polluted air, dust and vapor containing pesticides, by consuming contaminated food, especially fruits and vegetables that are sprayed the most, water, and direct contact through the skin. Acute or single exposure to pesticides in humans causes symptoms such as headache, skin rash, nausea, dizziness, visual impairment, panic attacks, loss of concentration. About three million cases of acute pesticide poisoning are reported worldwide every year [3]. Continuous exposure to pesticides over a long period of time – a chronic effect, in humans can lead to various diseases, some of which are: neurological, psychological and behavioral dysfunctions, hormonal imbalance that can lead to infertility, immune system dysfunction, reproductive system defects, cancer, blood system diseases. Some toxicological studies on animals have shown that a certain number of pesticides to which the human population can be chronically exposed are carcinogens, neurotoxins, reproductive and immunotoxins. It has been shown that pesticides cause mutations in the DNA molecule as well as neurodegenerative diseases. Also, some studies

have shown that they affect biochemical parameters, especially protein metabolism and the endocrine and reproductive systems [2].

Impact on air

During application, 30–50% of the total amount of pesticide applied can be lost to the air, which is one of the main sources of persistent organic pollutants in the atmosphere. It has been shown that pesticides are carried by air and that they can be found in it in three forms: solid, liquid and gaseous. They enter the atmosphere by spraying from pesticide sprayers, evaporation from treated surfaces, degradation pathways (hydrolysis in water and soil, photolysis and reaction with OH radicals in the atmosphere) and aeolian erosion. When they are dispersed in the air and transported by the wind, their further fate is influenced by both their properties and environmental factors such as meteorological conditions [17]. Once they are in the air, they can be transported over long distances by atmospheric processes, thus leading not only to local, but also global atmospheric pollution. Air pollution with pesticides has dangerous consequences for flora and fauna as well as human health.

Impact on non-target organisms

Most pesticides, especially insecticides, which are used to destroy target species, also reach non-target organisms, causing negative consequences. Some of the studies have shown that some of the non-target organisms of pesticides are soil (micro) fauna, natural predators and pollinators [18]. One of the studies showed that the treatment of winter wheat seeds, regardless of whether it is insecticides or fungicides, reduced the surface activity of earthworms [19]. Many of the pollinators are under the influence of environmental stress caused by the use of pesticides. Pesticide application can cause direct loss of pollinating insects and indirect crop loss due to deficiencies in pollinator populations. One of the studies led to the conclusion that the application of pesticides by spraying leads to a change in the species composition and succession of vegetation in areas near arable land where pesticides were applied [20]. In Germany, a study was conducted that showed that pesticides can even affect the migration of juvenile and adult amphibians that migrate through cultivated areas where they are applied [21]. Contamination of the environment with pesticides has led to a reduced diversity of insects, birds and biodiversity in general [22].

CONCLUSION

Due to the growing consumption of food, modern agribusiness includes the daily application of pesticides of the widest spectrum of action. Many of the available and used pesticides can have negative effects on the environment if not used safely and correctly. Their proper use protects all segments of the environment: surface and underground water, soil, air, flora and fauna, as well as human life and health. The data presented in this review can help researchers and farmers to better understand the problems related to the global application of pesticides, their impacts and consequences on the environment.

REFERENCES

[1] Cooper J., Dobson H., Crop Prot. 26 (2007) 1337–1348.

[2] Maksiv I., J. Vasyl Stefanyk Precarpath. Nat. Univ. 2 (2015) 70–76.

[3] Yadav I. C., Devi, N. L., Environ. Sci. Eng. 6 (2017) 140–158.

[4] Hayes T. B., Hansen M., Kapuscinski A. R., *et al*. Elem. Sci. Anth. 5 (2017) 1–24.

[5] Bernardes M. F. F., Pazin M., Pereira L. C., *et al*. InTech. (2015) 195–233.

[6] Aktar W., Sengupta D., Chowdhury A., Interdiscip. Toxicol. 2 (2009) 1–12.

[7] Kim K. H., Kabir E., Jahan S.A., Sci. Total Environ. 575 (2017) 525–535.

[8] Lamichhane J. R., Crop. Prot. 97 (2017) 1–6.

[9] Tudi M., Daniel Ruan H., Wang L., *et al*. Int. J. Environ. Res. Public Health 18 (2021) 1112.

[10] Cooper J., Dobson H., Crop Prot. 26 (2007) 1337–1348.

[11] Srivastava M., Malin B., Srivastava A., *et al*. Agri. Sci. Food Res. 13 (2022) 1000495.

[12] Aydinalp C, Porca M. M., J. Cent. Eur. Agric. 5 (2004) 5–12.

[13] Cerejeira M. J., Viana P., Batista S., *et al*. Water Res. 37 (2003) 1055–1063.

[14] Kumar V., Kumar P., Pesticides in agriculture and environment: Impacts on human health. In: Contaminants in Agriculture and Environment: Health Risks and Remediation, Editor: Kumar V., Kumar R., Singh J., Kumar P, Agricultural and Environmental Science Academy, Haridwar (2019), p.76–95, ISBN: 978-93-5321-003-8.

[15] Ugrenović V., Pesticidi i zemljište (*in Serbian*), *Available on the following link:* serbiaorganica.info/pesticidi-i-zemljiste/.

[16] Zhang F., He J., Yao Y., *et al*., Environ. Monit. Assess. 185 (2013) 6893–6908.

[17] Gil Y., Sinfort C., Atmos. Environ. 39 (2005) 5183–5193.

[18] Ware G. W., Residue Rev. 76 (1980) 173–201.

[19] Van Hoesel W., Fiefenbacher A.,Koning N., *et al*. Front. Plant Sci. 8 (2017).

[20] Nelemans J. B., Van Wijngaarden R. P. A., Roessink I., *et al*. Front. Environ. Sci. 5:10 (2017).

[21] Berger G., Graef F., Pallut B., *et al*. Front. Environ. Sci. 6:6 (2018).

[22] Zaller J. G., Bruhl C. A., Front. Environ. Sci. 7:117 (2019).

GREEN SYNTHESIS OF GEOPOLYMER-POLYURETHANE COMPOSITES FOR EM SHIELDING

George Vuković[1], Danijela Kovačević[2*], Nenad Đorđević[2], Marko Perić[3], Sanja Knežević[3], Milan Nikolić[4], Branislav Vlahović[5], Vera P. Pavlović[6], Goran Rašić[5], Snežana Nenadović[3], Marija Ivanović[3], Miljana Mirković[3], Vladimir B. Pavlović[7]

[1]University of Wisconsin-Madison, USA

[2]The Academy of Applied Technical Studies Belgrade, Belgrade, SERBIA

[3]University of Belgrade, Institute of Nuclear Sciences Vinča, SERBIA

[4]University of Kragujevac, Faculty of Agronomy, SERBIA

[5]North Carolina Central University, Durham, USA

[6]University of Belgrade, Faculty of Mechanical Engineering, SERBIA

[7]University of Belgrade, Faculty of Agriculture, Department for Physics and Mathematics, Belgrade, SERBIA

[*]*dkovacevic@atssb.edu.rs*

Abstract

Development of electromagnetic (EM) shielding materials is vital for controlling EM pollution, protecting human health and its environment, due to advancement in telecommunication and nuclear technologies. The aim of our research was to investigate new green synthesis routes for geopolymer-polyurethane composites production which can be used as polymer matrix for EM shielding materials. Composites were synthesized from fly ash and a recycled bio-polyol substrate. XRF was used to chemically characterize fly ash, while XRD, SEM and EDS analysis have been performed to investigate crystal structure and microstructure of obtained composite.

Keywords: geopolymer, polyurethane, composites, EM shielding, microstructure.

INTRODUCTION

It is well known that prolonged exposure to certain types of electromagnetic (EM) fields can potentially have harmful effects to health [1]. In order to reduce EM pollution, various international standards and regulations for EM shielding (Table 1), set limits for the amount of electromagnetic interference (EMI) that devices can emit [2]. EM shielding provides reduction of the electromagnetic field by blocking the field with barriers made of conductive or magnetic materials. EM shield design and the usage of EMI shielding tests such open field or free space method, shielded box method, shielded room method or co-axial transmission line method, depend on the specific requirements of the application and are based on reflection and absorption mechanisms Figure 1a [2,3]. In recent years, new technologies such as nanomaterials, metamaterials, and conductive coatings, are being developed in order to provide improved shielding performance, lighter weight, or other advantages [4]. The aim of advanced EM shielding materials is to block or limit the passage of electromagnetic fields or

radiation. They can be used for controlling EM pollution, to protect sensitive electronic equipment from external electromagnetic interference (EMI), or to prevent the equipment from emitting EMI that interferes with other electronic devices.

Table 1 *Electromagnetic compatibility standards*

Area	Standard	Details
Aerospace	DO-160	Aircraft EMC requirements
	SAE ARP5412B	Aircraft lightning environment and related test waveforms
	SAE ARP5416A	Aircraft lightning test methods
Automotive	SAEJ1113	General automotive EMC
Commercial	ANSI C63.4	Methods of measurement
	CISPR 11	ISM equipment
	CISPR 16	Methods of measurement
	CISPR 22 FCC	ITE equipment EN 55022
	Part 15B	ITE equipment
	IEC 61000-3-2	Harmonics
	IEC 61000-3-3	Flicker
	IEC 61000-4-2	Electrostatic Discharge, ESD
	IEC 61000-4-3	Radiated immunity
	IEC 61000-4-4	Electrically Fast Transient
	IEC 61000-4-5	Surge (lightning)
	IEC 61000-4-6	Conducted immunity
	IEC 61000-4-8	Magnetic immunity
	IEC 61000-4-11	Voltage dips, interrupts & variations
Medical	IEC 60601-1-2	Medical products
Military	MIL STD 461F	EMC test requirements

Various polymer-based EMI shielding materials and composites such as metal-filled composites, carbon-based composites, intrinsically conducting polymers, magnetic material composites and hybrid composites, can be used in EM shielding (Figure 1b) [4,5]. These materials often consist of a polymer matrix filled with active materials which allow tailoring composite's electromagnetic properties. Although EM shielding composites can offer many advantages for EM shielding, due to their lightweight nature, corrosion resistance, and flexibility in design, they also have some challenges to overcome. This includes ensuring good dispersion and bonding of the fillers in the polymer matrix, and balancing the trade-off between shielding effectiveness and other properties like weight, cost, and mechanical strength.

Polyurethane (PU) based composites have gained significant attention for use in EM shielding due to their good mechanical properties, ease of processing, and excellent adhesion to various substrates. For effective EM shielding, the PU matrix is typically filled with micro or nano-sized conductive or magnetic particles to provide necessary characteristics for reflecting or absorbing EM radiation. It is important to notice that for achieving high shielding effectiveness good dispersion of the filler particles within the PU matrix has to be ensured.

The versatility of PU used as an EM shielding matrix arises from its unique structure and the wide variety of precursors that can be used in its synthesis. Typically, PU is formed by the reaction of a diisocyanate with a compound containing two or more hydroxyl groups such as diol or a polyol. The synthesis involves complex chemistry and requires a careful balance of the different components and reaction conditions to achieve the desired properties of the final product. The most common PU synthesis method is the two-step prepolymer method. The first step of the synthesis is a diisocyanate reaction with a stoichiometric excess of a polyol and formation of a prepolymer with isocyanate groups at the ends. The second part is the linking of prepolimer with a chain extender. As a result the formation of urethane linkages (-NH-(C=O)-O-) with a long chain of alternating flexible segments (formed by the polyol) and rigid segments (formed by the diisocyanate) is enabled. In order to further modify the properties of the PU matrix in addition to the diisocyanate and polyol, other additives can be included in the polyurethane formulation, such as catalysts, surfactants, flame retardants.

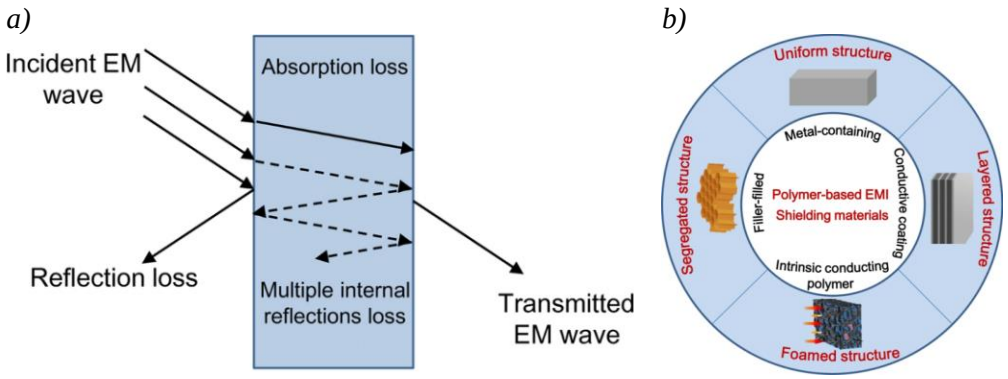

Figure 1 *a) Interaction of EM wave with EM shielding material; b) polymer-based EMI Shielding materials*

It should be noticed that the PU synthesis reactions should be carefully controlled to prevent side reactions and ensure the desired properties of the final product. Although PU synthesis is generally carried out at elevated temperatures and may use a catalyst to speed up the reaction there is another method of the production of PU where all the ingredients are mixed together at once. Although this method is simpler and faster, it gives less control over the PU molecular structure. In order to further improve EM shielding matrix, beside PU, some other polymers can be incorporated into the EMI shielding composite structure as well [5]. A combination of multiphase polymer blend enables formation of phase structures with different filler localization which may overcome some of the problems of poor processability and deteriorating mechanical properties of these materials. Unfortunately production of these materials, especially synthetic polyols, tend to be toxic, non-degradable, and high-cost, thus resulting in health hazards and environmental pollution [6]. Taking this into account the aim of this work is to present the green synthesis of geopolymer-polyurethane composites which can be used as matrix for EM shielding.

MATERIALS AND METHODS

Green synthesis of geopolymer-polyurethane composites has been performed in several steps. For green synthesis of PU based composites we used biopolyols from used vegetable oil and recycled polyethylene terephthalate (PET). Biopolyols were synthesized using the transesterification of the waste oil and PET with diethylene glycol. The mixture of waste vegetable oil, PET grains and diethylene glycol were heated in stainless steel reactor on temperatures of 220–230°C by using 0.3 wt.% of the catalyst (zinc acetate).

We used fly ash taken from thermal power plant Nikola Tesla (Tent A), Obrenovac, Belgrade, Serbia as a raw material for the synthesis of the geopolymer. Water glass, i.e. Sodium silicate (Na_2SiO_3) (manufactured by Galenika-Magmasil, Serbia) and sodium hydroxide (NaOH), were used as alkaline activators. The activator (the ratio of $NaOH:Na_2SiO_3$ = 1:1.6) was used in the synthesis to activate geopolymerization (solid phase/liquid phase = 0.85). Detailed procedure for geopolymer synthesis was described in our previous studies [7,8]. Obtained material was dispersed in the biopolyol, where 80% of the mixture was fly ash and 20% of the mixture was biopolyol; after dispersion, methylene diphenyl diisocyanate MDI44 was added, and then the entire mixture was mixed for about 50 seconds so that MDI44 was well homogenized in that starting mixture. The ratio between biopolyol and MDI44 was maintained at 1:0.75. The mixture of polyol and fly ash made up 90% of the total mixture, while the remaining 10% was made up of the addition of $BaSO_4$. We used XRF for fly ash chemical analysis. The samples were prepared in accordance to standard EN 450–1 [9] and their parameters (Al_to, So, Fo_o, Cano, Mg, SO, Na_bob, $K_o$na Lois of ignition at 950 °C were determined in accordance to standard EN 196–2 [10]. Crystal structure of the composite was characterized by X-ray diffraction analysis (RD.) using an Ultimo IV Riau diffract meter equipped with Cu Kα1,2 radiation and with a generator voltage of 40.0 kV and a generator current of 40.0 mA. Microstructure analysis has been performed on Au-coated samples using a JEOL JSM 6390 LV electron microscope equipped with Oxford Instruments energy dispersive spectroscopy system (EDS).

RESULTS AND DISCUSSION

Geopolymer-polyurethane (GP-PU) composites are a relatively new area of study in the field of EM shielding materials. Depending on the specific formulation and processing conditions, these materials bring together the beneficial properties of both polymers. While geopolymers have high mechanical strength, thermal stability, and chemical resistance, PU can be tailored to possess a range of properties. They can be made to be flexible or rigid, to have good adhesion to various substrates and good impact resistance. GP-PU composite structure generally involves a PU matrix reinforced with geopolymer particles, or a geopolymer matrix filled with PU. In most cases depending of the amount of crystalline and amorphous phase, the geopolymer provides rigidity, chemical resistance and thermal stability, while the PU provides flexibility, impact resistance, and good adhesion.

Table 2 *Chemical parameters of fly ash*

Sample ID	LOI 950°C	SiO_2	Al_2O_3	Fe_2O_3	CaO	MgO	Na_2O	K_2O	SO_3	MnO	TiO_2	P_2O_5	Cr_2O_3
Fly Ash, %	1.80	56.97	25.14	6.73	4.28	2.01	0.31	1.52	0.38	0.07	0.76	0.07	0.05

It is important to notice that the interaction of GP aluminosilicate materials, such as fly ash, metakaolin, or blast furnace slag, with PU matrix are crucial for overall composite performance, since their good adhesion and dispersion can enhance the composite's properties, while poor adhesion or their agglomeration can lead to defects and weaken the composite. Therefore we have analysed chemical composition of fly ash used in GP-PU synthesis process (Table 2) and concluded that it can be classified as siliceous fly ash (< 10% CaO) according to standard EN 197–1 [11].

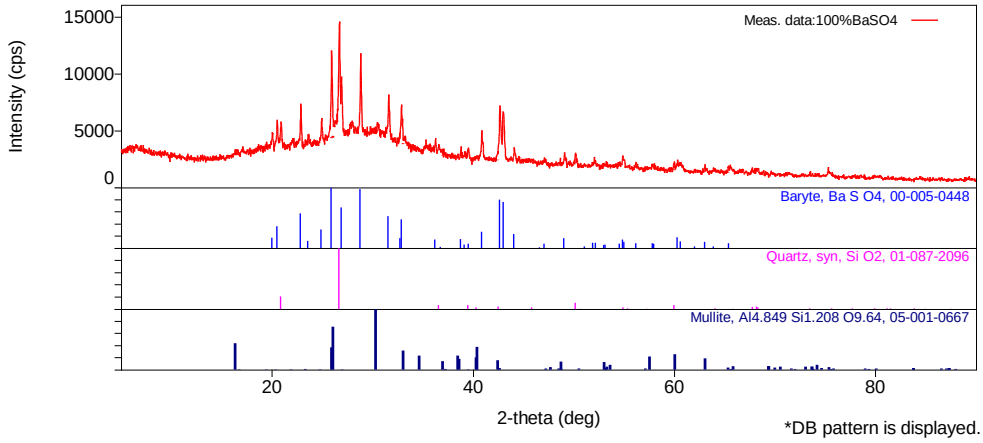

Figure 2 *Geopolymer composite X-ray diffraction pattern*

These results are in agreement with GP XRD analysis presented on Figure 2. This analysis showed significant presence of the amorphous phase, while the most common crystalline phases are quartz, mullite.

a) *b)*

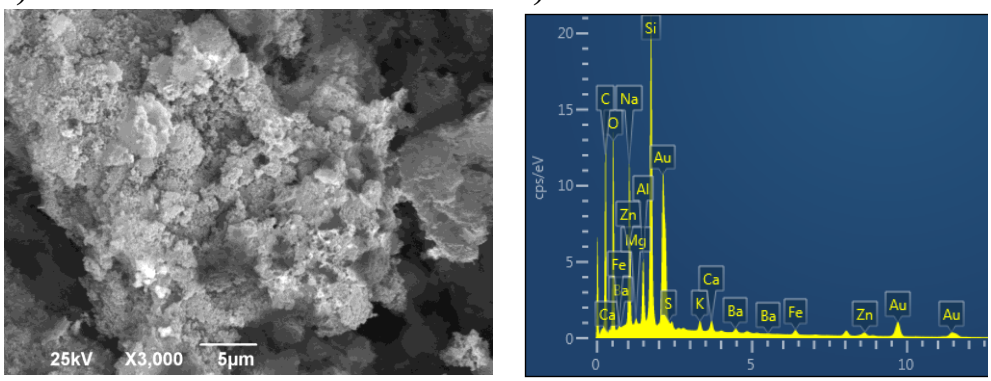

Figure 3 *Microstructure analysis of geopolymer-polyurethane composite a) SEM micrograph of b) EDS spectrum*

Microstructure analysis of the GP-PU composites (Figure 3) pointed out the formation of a complex composite structure where PU matrix is surrounded by geopolymer particles. Furthermore, a microphase separation of PU matrix has been observed. During microphase separation, when hard and soft segments of PU tend to segregate, hard domains, act as physical crosslinks that provide tensile strength and rigidity, while the remaining soft segments form a matrix around these hard domains, grant the material its elasticity.

CONCLUSION

In this study the results of the green synthesis of geopolymer-polyurethane composites which can be used as matrix for EM shielding have been presented. For green synthesis of PU based composites we used biopolyols from used vegetable oil and recycled polyethylene terephthalate, while we used fly ash for the synthesis of the geopolymer. It has been found that geopolymer exhibit significant presence of the amorphous phase, while the most common crystalline phases are quartz, mullite. Microstructure analysis of GP-PU composites pointed out formation of complex structure with the presence of microphase separation of PU matrix.

ACKNOWLEDGEMENT

The research was funded by the Ministry of Science, Technological Development and Innovation of the Republic of Serbia (Record numbers: 451-03-47/2023-01/200105; 451-03-47/2023-01/200116 and 451-03-47/2023-01/200017, US National Science Foundation (Grant: DMR EiR 2101041, NSF DMR PREM 2122044) and US Department of Energy/National Nuclear Security Administration (Grant: NA0003979).

REFERENCES

[1] Li Y., Shen B., Yi D., *et al.*, Compos. Sci. Technol. 138 (2017) 209–216.

[2] Shahapurkar K., Gelaw M., Tirth V., *et al.*, Polym. Polym. Compos. 30 (2022) 1–17.

[3] Yao Y., Jin S., Zou H., *et al*., J. Mater. Sci. 56 (2021) 6549–6580.

[4] Tiwari A. K., Kumar A., Said Z. Micro and Nano Technologies *in* Nanotechnology in the Automotive Industry, Elsevier (2022) 749–772.

[5] Meng Y., Sharma S., Chung J. S., *et al.*, Polymers 14 (2022) 967.

[6] Selvaraj V. K., Subramanian J. A., Polymers 14 (2022) 3344.

[7] Mladenović N., Kljajević Lj., Nenadović, S., *et al.*, J. Inorg. Organomet. Polym. Mater. 554 (2020) 1215.

[8] Trivunac K., Kljajević Lj., Nenadović S., Sci. Sinter. 48 (2016) 209–220.

[9] EN 450–1: Fly ash for concrete - Part 1: Definition, specifications and conformity criteria (2013).

[10] EN 196–2: Method of testing cement - Part 2: Chemical analysis of cement (2013).

[11] EN 197–1: Cement - Part 1: Composition, specifications and conformity criteria for common cements (2011).

APPLICATION OF STATISTICAL METHODS FOR THE ANALYSIS OF WASTEWATER TREATMENT PLANT EFFICIENCY

Ana Vukmirović[1*], Boris Obrovski[1], Srđan Vukmirović[1], Ivana Mihajlović[1]

[1]University of Novi Sad, Faculty of Technical Sciences, Trg Dositeja Obradovića 6, 21000 Novi Sad, SERBIA

[*]*anavuk3001@gmail.com*

Abstract

The paper presents statistical evaluation of data obtained from municipal WWTP in order to examine efficiency of wastewater treatment based on nine selected water quality assurance parameters. More than 1,000 samples were used for statistical evaluation. Statistical data processing and analyses were performed using the software IBM SPSS version 25. Based on the results of the independent sample t test, it can be concluded that the treatment process is efficient. However, the concentrations of BOD, phosphorus, nitrogen and suspended matter in effluent are elevated in relation to the emission limit values for wastewater discharged into the recipient. This indicates the need for improvement the WWTP in order to obtain higher efficiencies in removal of selected water quality parameters.

Keywords: effluent, influent, t-test, descriptive statistics.

INTRODUCTION

Water quality is an important issue for sustaining human existence. The growth of the population and industrial activities adversely affect the aquatic environment and water resources. Low water quality causes many significant problems and adverse effects on ecological and human health. Considering the global water scarcity and water pollution problems, the development of efficient and sustainable wastewater treatment plants (WWTPs) is of crucial importance.

The aim of the wastewater treatment process is to achieve a treated effluent quality that is environmentally safe for discharge into the recipient or for reuse [1]. Numerous WWTPs were constructed in order to improve water quality; however they are not all efficient and functional [2–4]. The main problems are focused on complexity of raw waste water matrix and fate of pollutants in chemical cocktails, which lead to problems in achieving the prescribed limits by national and international regulations. With the increase in population, the number of inhabitants in cities increases, which causes an increase in organic load and an increased amount of wastewater. Additional problems are related to energy consumption, shortage of staff and sludge production.

Understanding the complex phenomena prevailing in large systems of WWTPs is a challenging task. The quality of water in a treatment process, for example, may be affected by several factors which either is not known thoroughly or which have not been verified on an experimental basis. There are many parameters which can be used to measure the quality of

wastewater. However the most widely used are chemical oxygen demand (COD), biological oxygen demand (BOD), suspended matter (SM), nitrogen, and phosphorus compounds.

WWTPs continuously monitor with sensor systems or experimentally measure in laboratory on a daily basis the physico-chemical and biological parameters and collect data from unit processes, but the data are often underutilized. Due to the size and complexity of datasets currently generated by WWTP and the lack of data science background for WWTP professionals, it can be challenging to efficiently collect data and apply statistical evaluation or modelling of data in order to improve management of WWTPs [5].

The aim of this research is statistical evaluation of data obtained from municipal WWTP in order to examine efficiency of wastewater treatment based on water quality assurance parameters. Nine physico-chemical parameters (pH, COD, BOD, ammonium (NH_4^+), sulphate (SO_4^{2-}), sulphide (S^{2-}), total nitrogen (N), total phosphorus (P) and SM) were chosen for statistical evaluation. A big data set (more than 1,000 samples) was used for statistical analysis.

MATERIALS AND METHODS

Statistical data processing and analyses were performed using the software IBM SPSS (Statistical Package of Social Science) version 25. Descriptive statistics and independent sample t test were used to examine the differences in the concentration of parameters of the raw influent wastewater and the final treated effluent. A level of 0.05 was used for the threshold value of significance.

The experimental data used in this study were obtained from the municipal WWTP. A large amount of experimental data (more than 1,000 samples) was used for statistical evaluation. After considering the available options for modelling the treatment plant performance, it was decided to relate the quality of the raw influent wastewater to the quality of the final treated effluent based on nine selected physico-chemical parameters.

The WWTP was designed for 18,000 population equivalent (PE). The amount of waste water is 9,300 m^3/day, and the organic load is 3,500 kg BOD^5/day. WWTP operated since 1985. The treatment plant consists of a water line and a sludge line. The water line consists of: pumping station, mechanical grid, sand-oil separator, primary clarifier, aeration basin, secondary clarifier and recirculation pumps, while the sludge line consists of: primary thickener, digester, secondary thickener, biogas tank and mechanical dehydration. At the water line for biological purification, the process of highly loaded biologically active sludge was applied with the function of reducing organic matter and reduction of sediments. At the sludge line, sludge stabilization takes place through anaerobic digestion in the temperature range of mesophilic bacteria with a retention time of at least 20 days. The resulting biogas is used to maintain the temperature conditions for mesophilic bacteria of the anaerobic digestion process. The treated waste water is discharged into the Danube-Tisa-Danube canal.

RESULTS AND DISCUSSION

The mean values of the raw influent and treated effluent of municipal wastewater from the WWTP were compared with the Regulation on pollutants' emission limit values in waters and the deadline for their achievement in the Republic of Serbia [6]. It was found that the concentrations of all parameters are below the limit values of emissions at the entrance to the wastewater treatment plant (Table 1). The concentrations of BOD, total phosphorus, total nitrogen and suspended matter are elevated in relation to the emission limit values for wastewater discharged into the recipient (Table 2).

Table 1 *Descriptive statistics of raw influent of municipal WWTP*

Water parameters	Unit	Admissible limits	Min	Max	Mean	Standard deviation
pH	-	6.5–9.5	3.20	9.40	7.59	0.77
COD	mg/l	1000	10.66	5,302	987.85	386.43
BOD	mg/l	500	1	1,200	437.52	185.58
NH_4^+	mg/l	100	0.02	1,123	52.70	37.72
SO_4^{2-}	mg/l	400	6.45	567.70	61.02	21.83
S^{2-}	mg/l	5	0.001	1,277	1.14	33.34
N	mg/l	150	0.01	843	77.10	40.98
P	mg/l	20	0.29	53.90	13.09	5.72
SM	mg/l		1.59	11,142	1,042.41	855.23

The research examined whether there is a statistically significant difference in the concentrations of the observed parameters in the water at the entrance to the WWTP and at the exit from the WWTP after treatment. Based on the results of the independent sample t-test, it can be concluded that the treatment process is efficient, since the concentration of seven parameters after treatment is significantly lower compared to the concentration of treated wastewater (Table 3). The sulphide concentration did not significantly decrease in the water treatment (p=0.200). The pH value of the water increased during the water treatment.

Table 2 *Descriptive statistics of treated effluent of municipal WWTP*

Water parameters	Unit	Admissible limits	Min	Max	Mean	Standard deviation
pH	-	-	6.40	9.57	7.93	0.40
COD	mg/l	125	1.71	1280	48.92	53.63
BOD	mg/l	25	1	1,000	42.51	57.65
NH_4^+	mg/l	-	0.01	91.80	6.31	11.72
SO_4^{2-}	mg/l	-	0.03	122	52.59	14.91
S^{2-}	mg/l	-	0.001	13.20	0.03	0.38
N	mg/l	15	0.02	221.70	18.25	14.71
P	mg/l	2	0.10	849	3.73	22.28
SM	mg/l	35	0.083	3566	62.12	178.85

Table 3 *Difference in concentrations of the raw influent and the treated effluent of WWTP*

	Influent	Effluent	t	*p*
	Mean			
pH	7.59 ± 0.77	7.93 ± 0.40	-14.894	<0.0005*
COD	987.85 ± 386.43	48.92 ± 53.63	92.272	<0.0005*
BOD	437.52 ± 185.58	42.51 ± 57.65	72.194	<0.0005*
NH_4^+	52.70 ± 37.72	6.31 ± 11.72	45.112	<0.0005*
SO_4^{2-}	61.02 ± 21.83	52.59 ± 14.91	11.936	<0.0005*
S^{2-}	1.14 ± 33.34	0.03 ± 0.38	1.281	0.200
N	77.10 ± 40.98	18.25 ± 14.71	51.262	<0.0005*
P	13.09 ± 5.72	3.73 ± 22.28	15.608	<0.0005*
SM	1,042. 41 ± 855.23	62.12 ± 178.85	43.206	<0.0005*

CONCLUSION

Descriptive statistics and t test were used in statistical data processing in order to evaluate the effluent water quality parameters and efficiency of WWTP treatment. Even the results of independent sample t test showed that the treatment process is efficient; concentrations of key water quality parameters such as BOD, total phosphorus, total nitrogen and suspended matter are higher than emission limit values for wastewater discharged into the recipient prescribed by national regulation which indicates the need for improvement the wastewater treatment processes.

ACKNOWLEDGEMENT

This research has been supported by the Ministry of Science, Technological Development and Innovation through the project no. 451-03-47/2023-01/200156: "Innovative scientific and artistic research from the FTS (activity) domain".

REFERENCES

[1] Hassen E., Asmare A., Chem. Int. 5 (2019) 87.

[2] Adebayo, M. A., Areo, F. I., Resour. Environ. Sustain. 3 (2021) 100020.

[3] Xiao J., Wang L., Chai N., *et al*., Environ. Pollut. 278 (2021) 116930.

[4] Tang W., Pei Y., Zheng H., *et al*., Chemosphere 295 (2022) 133875.

[5] Newhart K. B., Holloway R. W., Hering A. S., *et al*., Water Res. 157 (2019) 498–513.

[6] "Official Gazette of RS", 67/2011, 48/2012, 1/2016.

COMPARISON OF DIFFERENT SORBENTS IN THE HERBICIDE REMOVAL FROM WATER

Ivana Mihajlović[1*], Ali Hgeig[2], Nevena Živančev[1], Maja Petrović[1], Mladenka Novaković[1]

[1]University of Novi Sad, Faculty of Technical Sciences, Trg Dositeja Obradovića 6, 21000 Novi Sad, SERBIA

[2]Nalut University, College of Engineering, Department of Civil Engineering, LIBYA

[*]*ivanamihajlovic@uns.ac.rs*

Abstract

The aim of the reserach is to examine the process of the linuron herbicide treatment from water using a synthesized material based on coffee waste and comparing it with a commercial material such as zeolite ZSM-5. Coffee waste was used to synthesize activated carbon by impregnation with phosphoric acid at 600 °C. ZSM-5 was used without any modification. During the development of the water treatment procedure, all parameters important for the efficiency of the treatment were optimized (pH value, contact time, adsorbent mass, initial concentration of selected herbicide). The study of the interaction between selected herbicide and adsorbents was modelled using Langmuir, Freundlich and Temkin isotherms. The best fit for linuron adsorption on activated carbon prepared from coffee waste (ACWC) is the Langmuir model, while sorption on ZSM-5 is best defined by the Freundlich isotherm. Adsorption isotherms indicated higher adsorption capacity of ACWC in comparison to ZSM-5. Higher removal efficiency was found when ACWC was used for linuron removal in wastewater sample in comparison to ZSM-5 under optimal conditions.

Keywords: linuron, pesticide, water treatment, coffee waste, zeolite.

INTRODUCTION

Agricultural production depends on the use of pesticides, as protection agents for plant diseases. Only a part of the pesticide concentrations reaches its goals in plant protection, while the rest is distributed in environmental media, which can lead to its transfer to aquatic ecosystems and water pollution.

Linuron is a selective herbicide, applied after sowing and before plant emergence, which is used to control annual broadleaf weed species in corn, sunflower and carrot crops. The commercial names of preparations whose main component is linuron are Linar, which is produced in China, and Hemolin 450 SC, which is produced in the Republic of Serbia. The Linar is also registered in some countries for use in various vegetable species such as celery, parsley, dill, peas, potatoes, beans, asparagus, garlic and onions. It acts on the photosynthesis process, as an inhibitor of electron transport in the photosystem. It is adopted predominantly by the root, although it can also be taken up by the leaf. Linuron is classified by the US Environmental Protection Agency (EPA) as a Restricted Use Pesticide.

The leaching of herbicides from agricultural land is one of the leading reasons for water pollution with herbicides. For this reason, researchers focused their attention on the development of effective treatments for the removal of different types of pesticides from the aquatic media [1–3].

Application of low-cost adsorbents for water treatment based on waste materials is increasingly being investigated due to its importance in the circular economy and sustainable development [1,4,5]. The commercial application of such materials is still at a low level and in the field of laboratory research with aqueous solutions.

The aim of this work is to compare an adsorbent prepared from coffee waste (ACWC) with a commercial adsorbent such as zeolite ZSM-5 in water treatment. The parameters affecting the efficiency of the treatment process were examined. The results were modelled using the Langmuir, Freundlich and Temkin adsorption isotherms. Wastewater sample was used to compare treatment efficiencies of ACWC and ZSM-5 under optimal conditions obtained in previous experiments.

MATERIALS AND METHODS

The rest of the coffee grounds were collected from a coffee machine used by employees of the Department of Environmental Engineering, Faculty of Technical Sciences, University of Novi Sad. The coffee grounds were washed with distilled water to eliminate impurities, dust and water-soluble substances. The material was then dried in an oven (Memmert, Germany) at 60 °C for 24 h before activation. It was impregnated for 24 hours with a solution of phosphoric acid, in a concentration of 30%. The impregnated samples were washed with hot distilled water several times until the pH values were 4.5 to 5 and then dried at 110 °C for 24 hours. Thermochemical activation of coffee waste was performed at 600 °C with phosphoric acid. After cooling at room temperature and washing with distilled water, the material was dried in an oven for 6 hours at 110 °C. The activated coffee waste-based carbon (ACWC) was ready for use as an adsorbent material after crushing and sieving to obtain particles between 100 and 200 μm in size.

The microstructures of the ACWC were determined using a SEM JSM 6460LV instrument (JEOL, USA), equipped with an EDX device. The specific surface was determined by measuring N_2 adsorption, using the BET method and the Autosorb iQ instrument (Quantachrome, USA). The chemical characteristics were studied by FTIR spectroscopy in order to recognize the functional groups on the surface of the adsorbent. FTIR spectra were recorded with a Nexus 670 FTIR/NIR spectrophotometer (Thermo Nicolet, USA), at wavelengths from 400 to 4000 cm^{-1}. Zeolite, type: ZSM-5, was used without any modifications as a reference material for the removal of the selected herbicide.

The influence of key parameters, such as pH, initial linuron concentration, adsorbent mass and contact time were studied in batch experiments. The effect of pH removal was studied in the pH range of 3.0 to 10.0. Linuron solutions with a concentration of 5 mg L^{-1} were in contact with an adsorbent with a concentration of 2.0 g L^{-1} for 30 minutes at room temperature. Adsorption kinetics was studied for different contact times from 5 to 120 min,

while adsorption equilibrium was investigated for initial linuron concentrations from 2 to 15 mg L^{-1}.

The treatment performance was evaluated and reported as percent removal efficiency. The adsorption capacity, q_e and the percentage of linuron adsorbed, %Ads, were calculated using (Eq. (1) and (2)):

$$q_e = \frac{(C_0 - C_e)}{m} * V \quad (1)$$

$$\%Ads = \frac{(C_0 - C_e)}{C_0} * 100 \quad (2)$$

where q_e is the adsorption capacity (mg g^{-1}), C_0 and C_e are the linuron concentrations before and after adsorption, respectively (expressed in mg L^{-1}), V is the solution volume (mL) and m is the adsorbent dosage (g) .

Selected pesticide was analysed using a high-performance liquid chromatograph (HPLC-DAD). Separation was performed with an Eclipse XDB-C18 column (3 x 150 mm, particle size 3.5 µm). Operating conditions were: flow rate 0.4 ml min^{-1}, column temperature 30 °C and sample injection volume 10 µL. The mobile phase consisted of water (A) and acetonitrile (B). The binary gradient elution started with 25% B in the first minute, then increased linearly to 50% B in the 5th minute, and finally the starting condition, 25% B, was applied in the seventh minute. The maximum wavelength of 215 nm was used.

Wastewater sample consisting of complex mixture of industrial and municipal wastewater was spiked with linuron to obtain concentration of 5 mg L^{-1} and treatment efficiency of ACWC and ZSM-5 was studied under optimal conditions obtained in previous batch experiments.

RESULTS AND DISCUSSION

Scanning electron microscopy (SEM) equipped with an EDX device was used to examine the morphology and components of the ACWC surface before and after adsorption. The results showed that the ACWC surface is irregular and porous with various holes and channels. Macro and mesopores were observed on the ACWC surface. The pore structure indicated the adsorption of linuron on the surface of the adsorbent. The FTIR spectrum of activated carbon prepared from coffee waste presents characteristic peaks (3418.6 cm^{-1}, 2922.97 cm^{-1}, 1562.56 cm^{-1}, 1068 cm^{-1}) corresponding to functional groups typical for activated carbon (-OH, C-H, C-O, P-O-C). The synthesized adsorbent has a highly developed BET surface area (803 m^2 g^{-1}) [1]. Zeolite ZSM-5 is a type of "high-silica"-Zeolite, which is responsible for most of its special properties. BET surface area of ZSM-5 is 390 m^2 g^{-1}, while the volume of micropores and mesopores are 0.17 cm^3 g^{-1} and 0.19 cm^3 g^{-1}, respectively.

A significant influence of pH value was observed in the removal of linuron. The highest removal efficiency of linuron was 92.4% at pH=5 using activated carbon prepared from coffee waste. Lower removal efficiency in the range of 77.2% to 87.7% was achieved using zeolite ZSM-5. The highest removal efficiency using ZSM-5 was achieved at pH=3.

The removal efficiency of linuron on ACWC ranged from 21.5% to 91.8%, with an increase in the adsorbent dose from 0.2 to 2.4 g L^{-1}. The optimum mass of 40 g L^{-1} for removal of linuron on ZSM-5 was obtained at pH=3 and contact time of 60 min. The obtained results indicate that the removal percentage of selected pesticide rises from 79.9% to 87.7% with an increment in the adsorbent dosage.

The adsorption of linuron on ACWC was investigated at different contact times with an initial concentration of linuron of 5 mg L^{-1}. The removal efficiency of linuron for a contact time of 20 minutes was 92.13%, at an ACWC concentration of 2.00 g L^{-1} and a pH value of 5. For ZSM-5 removal efficiencies were in range from 78.8% to 87.2% for contact times from 5 to 120 min.

The influence of the initial concentration of linuron was studied in the concentrations range from 2 to 15 mg L^{-1}, while all other parameters, pH of the solution, adsorbent mass and contact time, were set to optimal values. The removal efficiency of linuron was increased from 92.3% to 78.3% by using coffee waste as an adsorbent. Removal efficiency decreased when pesticide concentrations increased. Removal efficiencies ranged from 89.5% to 69.9% for ZSM-5 as the initial linuron concentration increased from 2 to 15 mg L^{-1}.

The results were fitted with Langmuir, Freundlich and Temkin models (Figure 1).

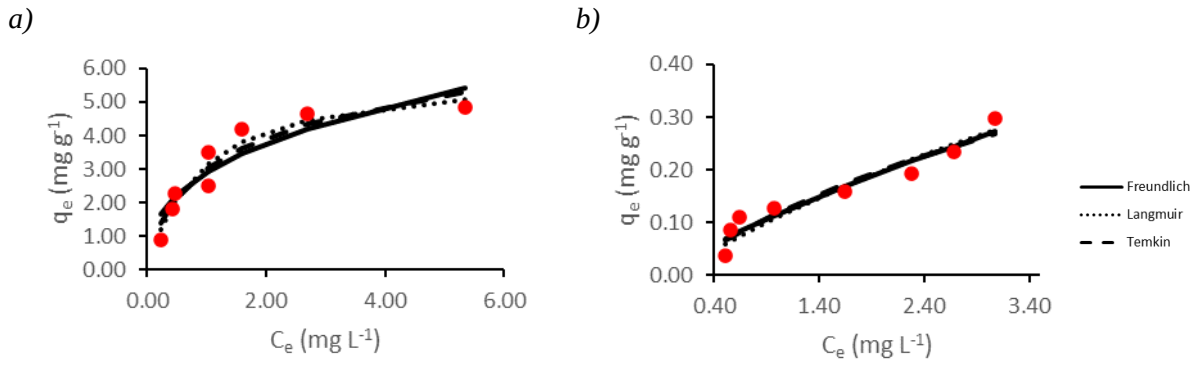

Figure 1 *Adsorption isoterms for linuron removal from water using a) acitvated carbon prepared from coffee waste b) zeolite ZSM-5*

The best fit for linuron adsorption on ACWC is Langmuir model. The maximum adsorption capacity for ACWC calculated from the Langmuir isotherm was 5.96 mg g^{-1} at room temperature. Adsorption of linuron on zeolite, type: ZSM-5, is best defined by the Freundlich isotherm.

The obtained optimum conditions of pH, initial linuron concentration, sorbent dosage and contact time were applied to study treatment efficiency on spiked wastewater. The obtained recovery was higher when ACWC was applied as sorbent (86.1%) than for ZSM-5 (75.3%).

CONCLUSION

Activated carbon prepared from coffee waste and zeolite ZSM-5 were used as adsorbents for investigation of linuron removal from water. The influence of key parameters for water

treatment optimization (pH, initial linuron concentration, adsorbent mass, contact time) was studied in batch experiments. Results indicated higher recoveries when ACWC was used in comparison to ZSM-5. Higher optimum mass of ZSM-5 also results in higher cost of the treatment. On the other hand, the preparation process of ACWC requires the consumption of electricity for drying and annealing, as well as the use of chemicals (phosphoric acid) for chemical activation of adsorbent. Adsorption isotherms indicated higher adsorption capacity of ACWC than of ZSM-5. Removal efficiency of linuron in spiked wastewater sample was also higher when ACWC was used as sorbent in comparison to ZSM-5.

ACKNOWLEDGEMENT

This research has been supported by the Ministry of Science, Technological Development and Innovation through the project no. 451-03-47/2023-01/200156: "Innovative scientific and artistic research from the FTS (activity) domain". Ali Hgeig would like to thank the Ministry of Higher Education in Libya for his PhD grant supporting the research.

REFERENCES

[1] Hgeig A., Novaković M., Mihajlović I., J. Environ. Sci. Health., Part B 54 (2019) 226–236.

[2] Aouada F. A., Pan Z., Orts W. J., Mattoso L. H. C., J. Appl. Polym. Sci. 114 (2009) 2139–2148.

[3] Yedla S., Dikshit A. K., J. Environ. Eng. 134 (2008) 102–109.

[4] Serrano-Gómez J., López-González H., Olguín M.T., *et al*., J. Environ. Manage. 156 (2015) 121–127.

[5] Hameed B. H., J. Hazard. Mater. 161 (2009) 753–759.

VALLME PREPARATION METHOD FOR THE DETERMINATION PHARMACEUTICALS IN WATER

Aleksandar Krstić[1*], Ivan Bracanović[1] , Dragana Vasić Anićijević[1], Ana Kalijadis[1]

[1]University of Belgrade, Vinča Instutute of Nuclear Sciences - National Instutute of the Republic of Serbia, Mike Peterovića Alasa 12–14, Belgrade, SERBIA

[*]*aleksandar.krstic@vin.bg.ac.rs*

Abstract

This study presents the novel VALLME preparation method for determining the selected pharmaceuticals (Carbamazepine, Naproxen, Diazepam and Diclofenac) from water and their validation method. This method is based on the vortex-assisted liquid-liquid microextraction of pharmaceuticals with ethyl acetate, the concentration in the nitrogen stream, and quantification by ultra-high performance liquid chromatography (UPLC). The advantages of this preparation method are the use of a small sample and solvent volume, high extraction efficiency, and small waste production. In order to optimize of VALLME method for pharmaceutical determination by UPLC, the validation study was carried out according to EURACHEM and ICH guidelines. The validation parameters defined by guidelines are: linearity, sensitivity, accuracy, repeatability and reproducibility, limit of detection (LOD) and limit of quantification (LOQ). The spiked surface water with a specified concentration of pharmaceuticals was used as a synthetic water model. The results of the validation study are in accordance with the required criteria and the optimized method for the determination of pharmaceuticals has been successfully validated.

Keywords: pharmaceuticals determination, validation, microextraction, water pollution.

INTRODUCTION

Pharmaceuticals are increasingly recognized as environmental pollutants and cause concern for human health when their residues are due to watercourses and freshwater systems. The increasing rate in the production and diversification of pharmaceuticals exceeds most of the previously recognized impacts of global change, such as increased carbon dioxide concentration in the atmosphere, food pollution, and loss of biodiversity. These led to the spread of active pharmaceutical ingredients in the environment, soil, water, and sediment. One of the most important properties of pharmaceuticals is stability. They are designed to be stable to interact with the target molecule, which means that they degrade very slowly and that their continued uses result in the continuous release into the environment in amounts that exceed the degradation rate [1]. Therefore, there is an increasing demand for the analysis of pharmaceuticals in water samples. The most commonly used sample preparation technique for determining pharmaceuticals in water is liquid-liquid extraction (LLE) [2] and solid phase extraction (SPE) [3,4]. The main disadvantages of LLE are the considerable consumption of organic solvents, which are expensive and toxic. SPE is a demand, time-consuming, and relatively expensive technique. Therefore, efforts have been made to develop new water sample preparation techniques to save time and solvents and improve the overall extraction

efficiency [5]. Microextraction methods have attracted much attention lately due to their accuracy, sensitivity, simplicity, high extraction efficiency, environmentally friendly and compatibility with a wide range of analytes and analytical instruments. Recently, new microextraction methods, such as vortex-assisted liquid-liquid microextraction (VALLME) were proposed to determine various organic compounds [6]. The aim of this work is to develop, optimize and validate the sample preparation method based on vortex-assisted liquid-liquid microextraction to determine and quantify pharmaceuticals (Carbamazepine, Naproxen, Diazepam and Diclofenac) from water samples. Ethyl acetate was used as an extraction solvent. All pharmaceuticals were quantified by ultra-high performance liquid chromatography (UPLC).

MATERIALS AND METHODS

Reagens and chemicals

For validation experiments, the following chemicals were used: analytical standards of pharmaceuticals: Carbamazepine (CBZ), Naproxen (NPR), Diazepam (DZP) and Diclofenac (DKF) from Hemofarm Serbia, all grade >99%, methanol, ethyl acetate from Sigma Aldrich. Ultra High-Performance Liquid chromatography (Waters, Milford, Massachusetts, USA) equipped with a PDA detector was used to detect and quantify pharmaceuticals. The pharmaceuticals were separated on *ACQUITY UPLC BEH C18* column with dimensions (1.7 *μm*, 100 *mm* × 2.1 *mm)* also from *Waters*. Pharmaceuticals were detected by comparing literature UV spectra from experimentally obtained and comparing the retention time of each component with a standard pharmaceutical solution. The mobile phase for stepwise gradient elution consisted of 0.1% triethylamine (TEA) in water, pH 4.0 (TEA), and 100% Acetonitrile (AcN). The TEA/AcN volume ratio was 65:35 at the beginning of the chromatographic run, then changed to 50:50 at 3 min, 35:65 at 5 min, 20:80 at 7 min, and finally 65:35 at 10 min. The eluent flow rate was 0.2 ml/min, and the injection volume was 6 µl. The UPLC detection wavelengths for Carbamazepine, Naproxen and Diclofen were at 230 nm, and for Diclofenac at 220 nm [7].

Sample preparation by VALLME

For all validation experiments, water aliquots were prepared by modified vortex-assisted liquid-liquid microextraction method (VALLME) on the following procedure: 1 ml of sample aliquot was taken, then placed in a glass cuvette, and 2 ml of ethyl acetate was added. Then, the cuvette was vigorously shaken by a vortex agitator (LLG Labware Unitexer, Germany) for 100 seconds at 2000 rpm. After shaking, the organic fraction was carefully withdrawn, transferred to the vial, and evaporated in the stream of nitrogen. Finally, the analytes were reconstituted with 1 ml of methanol and injected into the UPLC unit [7].

Validation parameters

In order to verify the optimized preparation method for the detection and quantification of pharmaceuticals in water samples, a validation study was performed according to the EURACHEM [8] and ICH [9] guidelines. The protocol defined the validation parameters: specificity/selectivity, linearity, sensitivity, accuracy, repeatability and reproducibility, the limit of detection (LOD), and the limit of quantification (LOQ). A surface water sample was

spiked with a specified concentration of pharmaceutical mixture and used as a model sample for validation. The sample for analysis was prepared according to the previously described procedure.

- the specificity/selectivity was determined by analyzing a surface water sample spiked with a mixture of pharmaceuticals at a concentration of 5 ppm. By comparison of the signal retention times from the sample with the retention times from the standard and comparing the literature UV spectra of each pharmaceuticals with the spectra obtained experimentally, the match was confirmed the specificity of the method. The selectivity was confirmed by the components' retention times, which showed no interferences.
- the linearity was determined by preparing and analyzing the standard working solutions of the pharmaceutical mixture at 5 concentration levels (0.05, 0.1, 0.5, 1, and 2 ppm) with an acceptable correlation coefficient ($R^2 > 0.99$).
- the analytical sensitivity was determined from the slope of the calibration curve.
- the accuracy, precision, repeatability, and reproducibility was tested by the recovery test, multiple analysis of a spiked water sample with a mixture of pharmaceuticals at three concentration levels: 0.5, 5, and 50 ppm
- the precision is determined based on repeatability and mean reproducibility. Reproducibility and repeatability was determined by multiple analyses of a spiked sample and determination of other precision parameters: S_k (standard deviation of means); S_v (intra-series standard deviation-reproducibility); S_b (inter-series standard deviation); S_{tot} (total standard deviation-intra-laboratory reproducibility).
- the limit of detection (LOD) and limit of quantification (LOQ) were determined experimentally by injecting 10 samples of water samples pharmaceuticals were not detected, and where the minimum concentration of the standard pharmaceuticals solution was added which the UPLC unit gives a satisfactory response.

RESULTS AND DISCUSSION

The results of the validation method for determining pharmaceuticals from water with vortex-assisted microextraction as a preparation method are presented in Tables 1–4. The linearity test showed satisfactory linearity for all pharmaceuticals (obtained value $R^2<0.999$). Analytical sensitivity ranged from 64291 for Diclofenac to 320594 for Carbamazepine. The limit of detection ranged from 0.010 ppm for diazepam to 0.023 ppm for Diclofenac, while the limit of quantification was in the range of 0.042–0.076 ppm. The precision criteria (Table 1) were satisfied for all pharmaceuticals. The recovery test results ranged from 99-105 % for all spiked concentration levels, which satisfied the accuracy criteria.

Table 1 *Required criteria for accuracy*

Spike Level	Accuracy (%)	Precision (%)
I spike level	95–105 % recovery	3.7
II spike level	97–103 recovery	2.7
III spike level	98–102 recovery	7.3

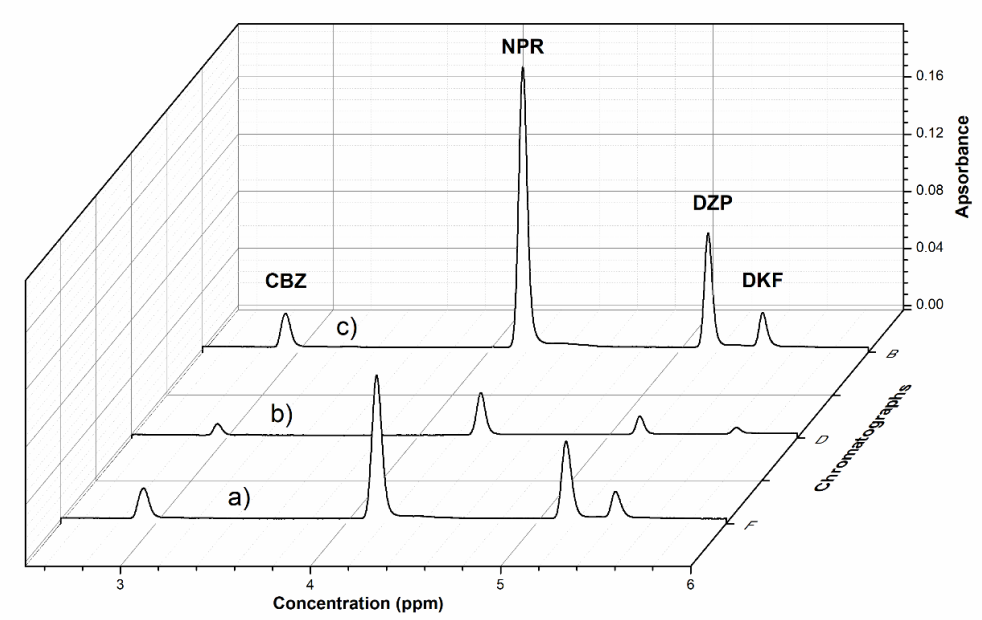

Figure 1 *Chromatographs of a) 5 ppm standard solution of mixture pharmaceuticals; b) water spiked with 0.5 ppm standard of mixture pharmaceuticals; c) water spiked with 5 ppm standard of mixture pharmaceuticals on 230 nm*

Table 2 *The parameters of linearity and analytical sensitivity*

Pharmaceutical	λ (nm)	*Rt* (min)	Regression equation	R^2	Analytical sensitivity (au)
Carbamazepine	230	2.97	y= 72249x+1627,2	0.9994	72249
Naproxen	230	4.38	y=320594x+2613,5	0.9995	320594
Diazepam	230	5.19	y=128193x+1346	0.9992	128193
Diclofenac	220	5.75	y=64291x+43,315	0.9996	64291

Table 3 *The summary parameters of accuracy, precision, repeatability and reproducibility*

Analyte	Spike 0.5 mg/kg Recovery (%)	Spike 5 mg/kg Recovery (%)	Spike 50 mg/kg Recovery (%)	BIAS (%)	Precision (%)	Repetability (%)
Carbamazepine	105	103	102	3.3	2.50	3.32
Naproxen	104	98	101	2.4	1.80	2.90
Diazepam	102	102	98	2.0	2.80	1.95
Diclofenac	99	102	102	2.3	2.92	1.80

Table 4 *Limit of detection and limit of quantification*

Analyte	LOD ppm	LOQ ppm
Carbamazepine	0.016	0.055
Naproxen	0.019	0.064
Diazepam	0.012	0.042
Diclofenac	0.023	0.076

CONCLUSION

Based on obtained validation parameters, it can be concluded that this optimized method was applicable in the range of 0.5–50 ppm of pharmaceuticals. The results of the validation study are in accordance with the required criteria, and it can be concluded that the optimized method for the determination of pharmaceuticals in water samples using vortex-assisted microextraction sample preparation technique and UPLC has been successfully validated.

ACKNOWLEDGEMENT

The authors are grateful to the Ministry of Science of the Republic of Serbia for financial support according to the contract with the registration number (451-03-47/2023-01/ 200017).

REFERENCES

[1] OECD, "Pharmaceutical Residues in Freshwater Hazards and Policy Responses", Paris, (2019) 2–8.

[2] Rodríguez-Llorente D., Pablo Navarro P., Santiago R., *et al*., J. Chem. Eng. 451 (2023).

[3] Madikizela L. M., Chimuka L., Water SA. 43 (2) (2017) 211–220.

[4] Olatunde J. O., Chimezie A., Tolulope B., *et al.*, J. Environ. Chem. Ecotoxicol. 6 (3) (2014) 20–26.

[5] Farajzadeh M. A., Sadeghi Alavian A., Sattari Dabbagh M., Anal. Methods 10 (48) (2018) 5842–5850.

[6] Shalash M., Makahleh A., Salhimi S. M.,Talanta 174 (2017) 428–435.

[7] Krstić A., Lolić A., Mirković M., *et al*., J. Environ. Chem. Eng. 10 (6) (2022).

[8] Magnusson B., Eurachem Guide: The Fitness for Purpose of Analytical Methods – A Laboratory Guide to Method Validation and Related Topics, 2nd ed. (2014) 7–39.

[9] I. C. H. H. T. Guideline, "Validation of analytical procedures: text and methodology Q2 (R1)", IFPMA: Geneva, (2005) 2–13.

REMOVAL EFFICIENCY OF HEAVY METAL IONS FROM AQUEOUS SOLUTION WITH WASTE TREE BIOMASS HYDROCHARS

Marija Koprivica[1*], Jelena Petrović[1], Jelena Dimitrijević[1], Marija Ercegović[1], Marija Simić[1], Mirko Grubišić[1]

[1]Institute for Technology of Nuclear and Other Mineral Raw Materials, 86 Franchet d`Esperey St., 11000 Belgrade, SERBIA

[*]*m.koprivica@itnms.ac.rs*

Abstract

In this study, Paulownia tree leaves hydrochars (PL-HTCs) were used as potential adsorbents for Zn(II), Cd(II) and Mn(II) ions from aqueous solution and their efficiency was investigated. The preliminary adsorption results showed that hydrochars had better affinity for Cd(II) than for Zn(II) and Mn(II) ions removal. In order to improve adsorption capacity, hydrochar obtained at 220°C were activated with NaOH and further investigated only for Cd(II) removal. Alkali activated hydrochar (AH-220) has significantly better efficiency (q=24.05 mg/g, E=52.57%) in removing Cd(II) ions than hydrochar before modification. Adsorption kinetic studies showed that Cd(II) ions sorption at AH-220 surface followed the pseudo-second-order model. This implies that the adsorption process was mostly controlled by the chemical binding.

Keywords: tree leaves hydrochars, adsorption, heavy metals, kinetic studies.

INTRODUCTION

The various, toxic metals can easily be found in the nature since they are extensively use in industry. The most heavy metals are nonessential and cause enormous health problems due their persistency and therefore accumulation in the food chain and environment [1,2]. Diverse conventional techniques are used to remove various organic and inorganic contaminants from wastewaters. Most of them have limited scope of application, due to various shortcomings such as expensive operation costs, production of second pollutants, poor regeneration [3,4]. These disadvantages could be avoided by choosing adsorption as purification strategy. Adsorption is a successful physicochemical method for contaminants removal, if a suitable material is chosen as adsorbents [3,5]. The usage of obtained hydrochar from biowaste as adsorbent have causes growing interests. It is extensively used due to renewable resources, eco-friendly quality, could have high efficiency and possibility to be chemically activated [3,6].

The hydrothermal carbonization (HTC) treatment of biomass is alternative, thermochemical process, which contributes to using of residual waste and convert them into valuable, low-cost materials (hydrochars) [7,8]. According to characteristics of the obtained hydrochars, the application of these materials was investigated in numerous fields [9,10]. Since the structure of hydrochars is porous with reactive, functionalized surface and increased aromatization, one of the fields for application include the adsorption of various contaminants

[4,11]. Additionally, in order to improve the reactivity and/or the selectivity, several methods are applied to further modify the hydrochar [9]. The alkali treatment activates the hydrochar through increasing the oxygen functional groups (OFG) as well as the surface basicity [11]. Also, cold alkaline activation is low-cost and easily treatment thus it is promising method for industrial application [12].

One of the biomasses available in large quantities is tree leaves. Our previous studies showed that *Paulownia* leaves (PL) biomass is very suitable for HTC treatment [11,13]. In this regard, the aim of this paper was to examine the possibility of PL hydrochars (PL-HTCs) as potential and efficient zinc(II), cadmium(II) and manganese(II) ions adsorbents. Thereafter, the selected PL-HTC was alkali modified and investigated for Cd(II) ions adsorption under kinetics study. For this purpose, the pseudo-first-order (PFO), pseudo-second-order (PSO) and Weber Morris intra-particle diffusion kinetic models were applied to experimentally obtained results.

MATERIALS AND METHODS

Materials preparation

The leaves of *Paulownia* tree were collected from park in Belgrade, Serbia, wash with ultrapure water, air-dried for two weeks and grinded, where sieved fraction of 0.5 mm was used in HTC experiments.

The HTC process was carried out in laboratory autoclave (Carl Roth, Model II), where 10 g of leaves powder was stirred with 120 ml of ultrapure water on reaction temperature at 180, 200, 220, 240 and 260ºC constant for 1 h. After that period, the hydrochar was separated from liquid by filtration, rinsed three times with ultrapure water and dried at 105°C for 24 h.

Alkali modification was performed by stirring 3 g of the hydrochar obtained at 220ºC with 300 mL of 2 M NaOH solution for 1 h at room temperature (about 25°C). Thereafter, the obtained modified hydrochar (AH-220) was filtered, rinsed with ultrapure water to the neutral pH value and dried at 105°C.

Preliminary adsorption test

For preliminary adsorption test we used: adsorbents (PL-HTCs) mass 0.020 g, heavy metals solution (Zn(II), Cd(II) and Mn(II)) with initial concentration 50 mg/L in volume 0.020 L, contact time 3 hours and at room temperature (25°C). Solution was separated from adsorbent by filtration and Zn(II), Cd(II) and Mn(II) concentrations before and after adsorption were determined using atomic adsorption spectrophotometer (AAS, PerkinElmer, PinAAcle 900T).

The amount of Zn(II), Cd(II) and Mn(II) ions adsorbed on PL-HTCs surface was calculated using equation:

$$q = (C_0\text{-}C_{eq})/m \times V \quad (1)$$

where q [mg/g] was adsorbent capacity, C_0 and C_{eq} [mg/L] were initial and after adsorption concentration of metal ions, m [g] was amount of adsorbent and V [L] was volume of the metal ions solutions.

The efficiency of Zn(II), Cd(II) and Mn(II) ions removal in percentages (E) was calculated based on the difference in metal concentration in initial solutions (C_0) and in solutions after adsorption (C_{eq}):

$$E = (C_0 - C_{eq})/C_0 \times 100\% \quad (2)$$

Effect of contact time, kinetics studies

The effect of contact time on Cd(II) removal from aqueous solution using alkali activated PL hydrochar (AH-220) was studied. For this experiment 0.020 g AH-220 was mixing with 20 mL Cd(II) solution, initial concentration 50 mg/L at different contact time from 10 to 1080 min. The used kinetic models included the non-linear Lagergren pseudo-first-order (PFO) rate equation [14]:

$$q_t = q_{eq} \times (1 - e^{-k_1 t}) \quad (3)$$

Additionally, the non-linear pseudo-second-order (PSO) rate equation [15]:

$$q_t = q^2_{eq} k_2 t / (1 + k_2 q_{eq} t) \quad (4)$$

where q_{eq} and q_t [mg/g] were the amount of Cd(II) adsorbed by AH-220 at equilibrium and time t [min] calculated from kinetic models. The k_1 [1/min] and k_2 [g/(mg×min)] were the pseudo-first-order and pseudo-second-order constant rate, respectively.

The Weber-Morris intra-particle diffusion model equation [16]:

$$q = k_{id} \times t^{0.5} + C \quad (5)$$

In which q [mg/g] represented the amount of adsorbed Cd(II) in time t [min], k_{id} [mg/(g× $min^{1/2}$)] represented the intra-particle diffusion rate constant and C was the intercept.

RESULTS AND DISCUSSION

Preliminary adsorption test

The preliminary adsorption test showed that hydrochars exhibited similar adsorption ability for Zn(II), Cd(II) and Mn(II) removal (Figure 1). The comparison of the examined ions revealed that Cd(II) ions were the most bound to the hydrochars surface (q ~10 mg/g), while the Mn(II) ions bound the least (q ~5 mg/g). Additionally, the hydrochar formed at 180°C

showed the best efficiency for Zn(II) ions (E = 23.86%), while the hydrochar at 220°C has the higher efficiency for Cd(II) and Mn(II) removal compared to other PL-HTCs (25.49% and 13.59%, respectively). Since the PL-HTC obtained at 220°C exhibited the best adsorption capacity and efficiency for Cd(II) ions, this sample was chosen for alkaline activation with NaOH and further kinetic studies for Cd(II) adsorption.

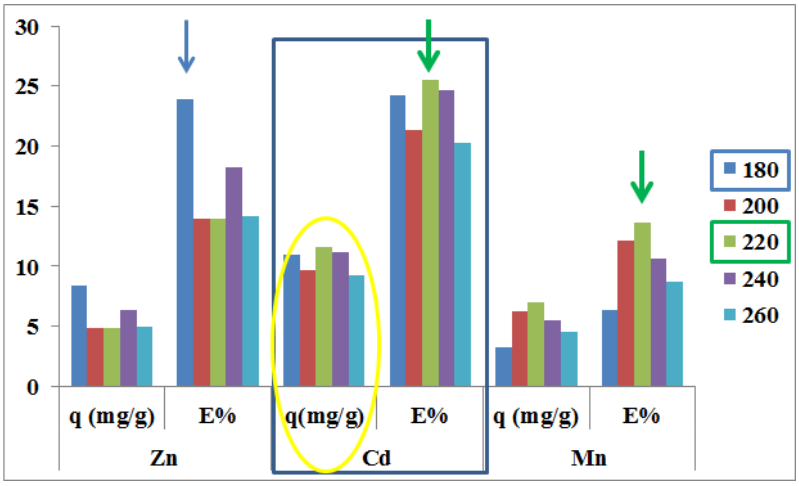

Figure 1 *The preliminary results of the Zn(II), Cd(II) and Mn(II) adsorption onto the PL-HTCs*

Effect of contact time, kinetics studies of Cd(II) sorption at modified hydrochar

In order to define the equilibrium time at the solid-liquid interface, the change in Cd(II) ion concentration during selected time period was monitored (Figure 2). The obtained results revealed that the AH-220 rapidly removed the Cd(II) ions from solution in the initial stage, probably due to plenty of availible active sites on the adsorbent surface [1,2]. After the two hours, a milder increase in capacity is observed and equilibrium was reached by approximately 360 min (Figure 2a).

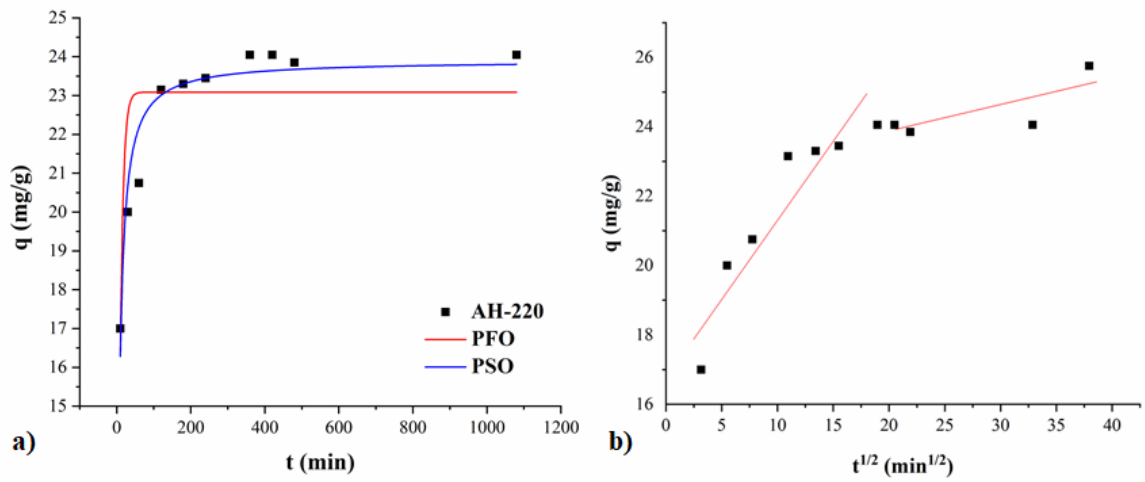

Figure 2 *a) Effect of contact time and non-linear kinetic models; b) Intra-particle diffusion model of Cd(II) adsorption (50 mg/L) on the AH-220*

To assume the adsorption mechanisms of Cd(II) ions binding, the pseudo-first-order (PFO) and pseudo-second-order (PSO) and Weber Morris intra-particle diffusion kinetic models were applied. The calculated kinetic parameters were shown in Table 1. According to these results, it can be concluded that PSO model the best fit with experimental data, R^2 = 0.9307. The calculated equilibrium adsorption value determined by the PSO model ($q_{eq,cal}$ = 23.90 mg/g) was in agreement with the experimentally obtained result ($q_{eq,exp}$ = 24.05 mg/g) (Figure 2a, Table 1). This implies that chemical interaction, such as covalent bonding, the complexation and/or the exchange of electron and ions, is controlling step during Cd(II) ions sorption onto the AH-220 surface [1,2,11]. Also, applied intra-particle model (Figure 2b, Table 1) revealed two different linear zones and indicated that intra-particle diffusion of ions was not the only rate-controlling step and that also some other mechanisms could be included [1,11].

Table 1 *Kinetic parameters for Cd(II) adsorption onto the AH-220*

Adsorbent AH-220	
$q_{eq,\ exp}$ [mg/g]	24.05
Pseudo-First-Order Model	
$q_{eq,cal}$ [mg/g]	23.09
k_1 [1/min]	0.12
χ^2	1.96
R^2	0.6887
Pseudo-Second-Order Model	
$q_{eq,cal}$ [mg/g]	23.90
κ_2 [g/(mg×min)]	0.009
χ^2	0.93
R^2	0.9307
Weber-Morris diffusion Model	
K_{id1} [mg/(g×min$^{1/2}$)]	0.50
C_1 [mg/g]	16.5
R^2	0.8864
K_{id2} [mg/(g×min$^{1/2}$)]	0.10
C_2 [mg/g]	21.39
R^2	0.6472

CONCLUSION

Based on the obtained results, it can be concluded that alkaline activation significantly improves the efficiency of hydrochar in order to adsorb metal ions. The kinetic studies revealed that the sorption of Cd(II) ions onto the alkali modified hydrochar surface followed pseudo-second-order model and that chemical adsorption was controlling step. Additionally, the intra-particle model revealed that adsorption occurred through two simultaneous stages. The results from this work presented that the waste tree leaves biomass had promising potential in further use as feedstock for metal ion adsorbents production.

ACKNOWLEDGEMENT

The authors are grateful to the Ministry of Science, Technological Development and Innovation of the Republic of Serbia for financial support according to the contract with the registration number 451-03-47/2023-01/200023.

REFERENCES

[1] Simić M., Petrović J., Šoštarić T., *et al*., Processes 10 (10) (2022) 1957.

[2] Dimitrijević J., Jevtić S., Marinković A., *et al*., Processes 11 (5) (2023) 1308.

[3] He X., Zhang T., Xue Q., *et al*., Sci. Total Environ. 778 (2021) 146116.

[4] Rasam S., Moraveji M. K., Soria-Verdugo A., *et al*., Chem. Eng. Process 159 (2021) 108236.

[5] Nzediegwu C., Naeth M. A., Chang S. X., J. Hazard. Mater. 412 (2021) 125255.

[6] Jiang Q., Xie W., Han S., *et al*., Colloids Surf. 583 (2019) 123962.

[7] Gallifuoco A., ACS Sustain. Chem. Eng. 7 (2019) 13073–13080.

[8] Holliday M. C., Parsons D. R., Zein S. H., Processes 10 (2022) 1756.

[9] Lang J., Matějová L., Cuentas-Gallegos A. K., *et al*., J. Environ. Chem. Eng. 9 (2021) 105979.

[10] Malool M. E., Moraveji M. K., Shayegan J., J. Taiwan Inst. Chem. E 133 (2022) 104203.

[11] Koprivica M., Simić M., Petrović J., *et al*., Processes 11 (2023) 1327.

[12] Wang C., Wang H., Cao Y., Colloids Surf. A 556 (2018) 177–184.

[13] Koprivica M., Petrović J., Ercegović M., *et al*., Biomass Convers. Biorefin. (2022) https://doi.org/10.1007/s13399-022-02619-6.

[14] Lagergren S., Sven K., Vetensk. Handl. 24 (1898) 1–39.

[15] Ho Y. S., McKay G., Process Biochem. 34 (1999) 451–465.

[16] Weber W., Morris J., J. Sanit. Eng. Div. 89 (1963) 31–60.

HORSERADISH PEROXIDASE IMMOBILIZATION WITHIN MICRO-BEADS OF OXIDIZED TYRAMINE-ALGINATE FOR PHENOL REMOVAL FROM WASTEWATER

Nevena Surudžić[1], Dragica Spasojević[1], Mira Stanković[1], Milica Spasojević[2], Reyadh Gomah Amar Elgahwash[3], Radivoje Prodanović[3], Olivera Prodanović[1*]

[1]University of Belgrade, Institute for Multidisciplinary Research, 11000 Belgrade, SERBIA

[2]University og Belgrade, Innovative Centre of the Faculty of Chemistry, 11000 Belgrade, SERBIA

[3]University of Belgrade, Faculty of Chemistry, 11000 Belgrade, SERBIA

[*]*oliverap@imsi.rs*

Abstract

Natural polymers such as alginate, pectin, chitosan etc. were used as carriers for the immobilization of different types of enzymes. Among investigated enzymes, peroxidases hold a special place. Immobilized enzymes are frequently used in phenol removal reactions. In this research horseradish peroxidase was immobilized within alginate micro-beads. This natural polymer was previously oxidized with sodium periodate and modified with tyramine hydrochloride. Percent of oxidation was varied from 2.5 mol% to 10 mol%, and an increase in specific activity was noticed with increasing the oxidation percent. Immobilized peroxidases showed satisfactory stabilities after 10 days of storage. Phenol concentration in a batch reactor decreased during its oxidation with horseradish peroxidase immobilized on tyramine-alginate hydrogels.

Keywords: phenol removal, alginate, horseradish peroxidase, tyramine, immobilization.

INTRODUCTION

Features of natural polymers such as biodegradability, biocompatibility and non-toxicity qualifies them for the immobilization of different enzymes [1]. Among many carriers with natural origin, alginate, chitosan and agarose, can be marked as the most frequently used ones [2], [3]. Each of these polymers can be applied in the immobilization of different enzymes, meanwhile peroxidases are the ones with the widest use. Horseradish peroxidase (HRP) belongs to the group of oxidative enzymes whose role in phenol oxidation is of great importance in various fields. During this process and as a consequence of interactions between enzyme's active site and products of oxidation reaction (phenoxy radicals), inactivation of enzyme might occur [4]. This major issue can be overcome by immobilization or addition of different reagents such as poly(ethylene glycol) (PEG), whose role is in reduction of amount of HRP needed for phenol oxidation reaction [5]. By immobilization, on the other hand, increased activity and operational stability of immobilized enzyme can be achieved [6].

Enzymes immobilized on natural polymers like alginate have wide application in phenol removal. The concentration of phenol and phenol like compounds in wastewater effluents is

increasing daily, making this environmental problem a priority [7]. For these purposes, many methods have been proposed, but among the most effective, those that involve application of immobilized enzymes have been singled out.

In this work alginate was subjected to oxidation with sodium periodate and reductive amination with tyramine hydrochloride in the presence of sodium cyanoborohydride. Micro-beads with immobilized horseradish peroxidase were used for the removal of phenol.

MATERIALS AND METHODS

Materials

Alginate from brown algae in the form of sodium salt was purchased from Sigma-Aldrich (St. Louise, Mo, USA), as well as following chemicals: horseradish peroxidase (150−250 U/mg), pyrogallol (98%), tyramine hydrochloride (98%), glucose oxidase-type VII (160 U/mg), Triton X-100 (laboratory grade), Span 80, potassium ferricyanide (≥99%), sodium metaperiodate (≥99.8%) and glycerol (98%). From Fluka (Buchs, Switzerland) were purchased 4-aminoantipyrene (p.a.) and sodium cyanoborohydride (95%). Sodium chloride (p.a.), sodium dihydrogen phosphate (>99%) and phenol (p.a.) were obtained from Centrohem (Stara Pazova, Serbia). Ethanol (96%) and glucose (p.a.) were purchased from Zorka (Šabac, Serbia), while hydrogen peroxide (30% (w/w)) was obtained from AppliChem GmbH (Darmstadt, Germany). Tris buffer and calcium chloride (p.a.) were purchased from Serva (Heidelberg, Germany) and Termohemija (Belgrade, Serbia), respectively.

Periodate oxidation and reductive amination of alginate

Prodanović *et al*. [8] previously described the method for oxidation of alginate with sodium periodate and further modification of this oxidized form with tyramine hydrochloride, which was applied in this study. Briefly, sodium alginate was first dissolved in water to a final concentration of 1% (w/v), and afterwards oxidized with sodium metaperiodate to a concentration of 1.25 mmol/L, 2.5 mmol/L and 5 mmol/L. Hereby it was provided that a molarity ratio of periodate to C6 glycoside units was set to 2.5 mol%, 5 mol% and 10 mol%. The reaction was stopped by adding glycerol to a final concentration of 50 mmol/L. Precipitation of oxidized alginate was performed in ethanol with subsequent addition of sodium chloride at 1% (w/v) concentration. This procedure was repeated twice, after it was dissolved in water. Amination was conducted by adding solid tyramine hydrochloride (final concentration of 1.5% (w/v)) to the solution of oxidized alginate in sodium phosphate buffer pH 6. Sodium cyanoborohydride, as a reducing agent, was added to a final concentration of 0.5%. Modified alginate was precipitated in ethanol with sodium chloride addition (1% (w/v) concentration). This procedure was repeated two times. Tyramine-alginates were stored at −20 °C.

Horseradish peroxidase oxidation onto tyramine-alginates

Alginates oxidized in different degrees with sodium periodate and modified with tyramine were dissolved in Tris buffer pH 7 (final concentration of 15%). Emulsion polymerization reaction was used for horseradish peroxidase immobilization (2.89 µL and 34.9 µL; 0.5 U/mL and 6.98 U/mL) within tyramine-alginate micro-beads. Simultaneously with immobilization, production of hydrogen peroxide from glucose and glucose oxidase, was performed.

Enzyme activity studies

For determination of peroxidase activity pyrogallol and hydrogen peroxide were used as substrates. Bound enzyme activity was determined by using 130 µL of bead suspension and 30 µL of hydrogen peroxide (0.97 mmol/L) were added to the pyrogallol solution (13 mmol/L). Reaction mixture was stirred for 7 min, while every 120 s aliquots were taken from the solution, filtrated and absorbance at 420 nm was measured using UV-VIS spectrophotometer (Shimadzu Corporation, UV-2501PC, Japan). One unit of enzyme activity was defined as the amount of peroxidase that produces 1 mg of purpurogallin in 20 s.

Phenol removal studies

For the removal of phenol from batch reactor, horseradish peroxidase immobilized within alginate-beads was used. Internal generation of hydrogen peroxide was enabled by glucose oxidase catalyzed oxidation reaction of glucose. The best relation of these two chemicals was determined in our previous study [9] and applied in this research. Concentration of phenol was monitored by applying a colorimetric assay with 4-aminoantipyrene (20.8 mmol/L) and potassium ferrocyanide ($K_3Fe(CN)_6$) (83.4 mmol/L). Absorbance at 510 nm was measured using UV-VIS spectrophotometry, and calibration curve of soluble enzyme was used for determination of concentration of removed phenol.

RESULTS AND DISCUSSION

Sodium alginate was oxidized with different amounts of sodium periodate and further subjected to amination with tyramine hydrochloride in the presence of sodium cyanoborohydride as reducing agent. Polymers were used for the immobilization of horseradish peroxidase, by applying emulsion polymerization reaction enzyme was entrapped within crosslinked network of phenolic residues present on the surface of modified alginate. Figure 1 is a schematic representation of described method for enzyme immobilization.

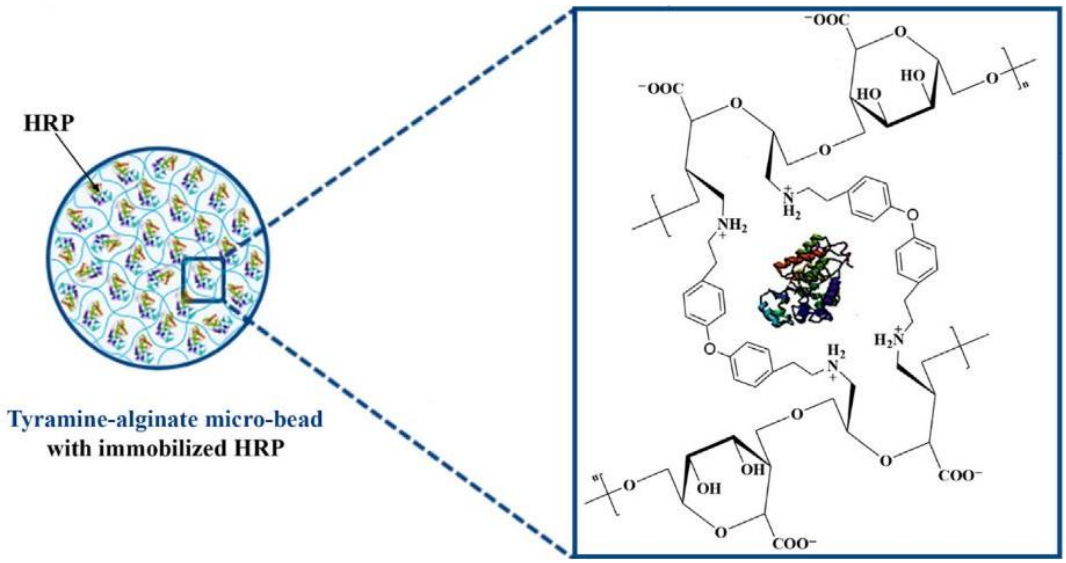

Figure 1 *Entrapment of horseradish peroxidase within tyramine-alginate micro-beads*

Measurements of specific activities of HRP immobilized within tyramine-alginate micro-beads oxidized in different mol% with periodate (2.5, 5 and 10 mol%) showed increasement with the increase of oxidation percent (Figure 2). These findings could be explained with formation of more potential binding sites for enzymes and are corroborated with results previously reported by our group [8].

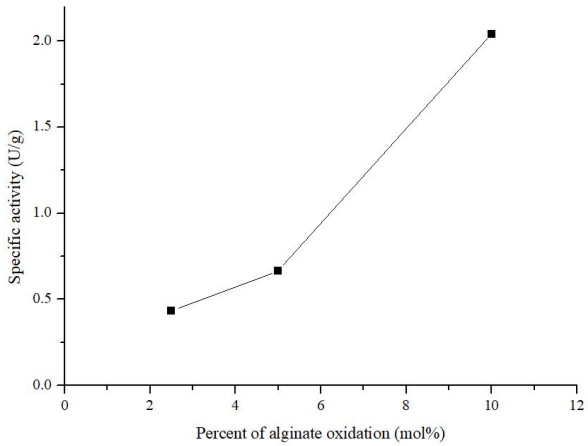

Figure 2 *Specific activity of peroxidase immobilized within tyramine-alginate micro-beads oxidized in different percent with sodium periodate*

Studies of enzyme stabilities in time showed that horseradish peroxidase entrapped within micro-beads of modified alginates oxidized in 2.5 mol% and 5 mol% retains 64.5% and 83% of initial activity, respectively, after 10 days of storage.

HRP immobilized on hydrogel formed with 10 mol% oxidized tyramine-alginate was applied for the removal of phenol in a batch reactor. Results present in Figure 3 show decrease of concentration of remained phenol in a solution with time.

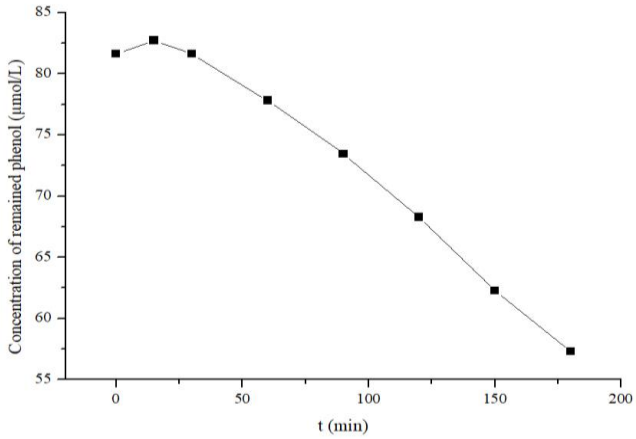

Figure 3 *Dependance of concentration of remained phenol from time*

Within the period of 3 days enzyme was able to remove around 90% of phenol from the reaction mixture.

CONCLUSION

Emulsion polymerization reaction was used for the immobilization of horseradish peroxidase onto micro-beads of modified alginate. Sodium alginate was oxidized with periodate and further subjected to reductive amination with tyramine hydrochloride. Obtained results showed increased specific activity with increasement of oxidation percent. Peroxidase immobilized on 10 mol% oxidized tyramine-alginate was used for the removal of phenol in a batch reactor. Decrease in the concentration of remained phenol was noticed with time.

ACKNOWLEDGEMENT

This work was supported by the Ministry of Science, Technological Development and Innovation of the Republic of Serbia (Grant No. 451-03-47/2023-01/200053, University of Belgrade, Institute for Multidisciplinary Research).

REFERENCES

[1] Monier M., Ayad D. M., Wei Y., *et al*., Int. J. Biol. Macromol. 46 (3) (2010) 324–330.

[2] Caza N., Bewtra J. K., Biswas N., *et al*., Water Res. 33 (13) (1999) 3012–3018.

[3] Quintanilla-Guerrero F., Duarte-Vázquez M. A., García-Almendarez B. E., *et al*., Bioresour. Technol. 99 (18) (2008) 8605–8611.

[4] Alemzadeh I. and Nejati S., J. Hazard. Mater. 166 (2–3) (2009) 1082–1086.

[5] Lai Y. C. and Lin S. C., Process Biochem. 40 (2005) 1167–1174.

[6] Qiu H., Lu L., Huang X., *et al.* Bioresour. Technol. 101 (24) (2010) 9415–9420.

[7] Aguiar L. L., Tonon C. B., Nunes E. T., *et al*., Ecotoxicol. Environ. Saf. 125 (2016) 116–120.

[8] Prodanovic O., Spasojevic D., Prokopijevic M., *et al*., React. Funct. Polym. 93 (2015) 77–83.

[9] Pantić N., Prodanović R., Ilić Đurđić K., *et al*., Environ. Technol. Innov. 21 (2021) 101211.

WASTEWATER TREATMENT BY AMINATED PEROXIDASE IN ALGINATE HYDROGEL

Dragica Spasojević[1], Olivera Prodanović[1*], Nevena Surudžić [1], Daniela Djikanović[1], Jasna Simonović Radosavljević[1], Ksenija Radotić[1], Radivoje Prodanović[2]

[1]University of Belgrade, Institute for multidisciplinary research, Kneza Višeslava 1, 11000 Belgrade, SERBIA

[2]University of Belgrade, Faculty of Chemistry, Studentski trg 12–16, 11000 Belgrade, SERBIA

[*] *oliverap@imsi.rs*

Abstract

Phenols are highly toxic organic compounds found in wastewater due to various industries' pollution. Its removal is of great importance for human and animal health. Enzymatic wastewater treatment has several advantages over traditional methods. Enzyme immobilization onto solid carriers enables its reusability and lowers the cost of treatment. In this work, immobilized horseradish peroxidase on chemically modified alginate hydrogel was tested for phenol removal. The reusability of the tested immobilizate was monitored in repeated cycles. After five consecutive cycles, the remaining activity of the immobilized enzyme was 54%. The obtained result shows the potential for using this immobilizate for wastewater treatment.

Keywords: phenol, alginate, aminated HRP, immobilization.

INTRODUCTION

Phenolic compounds are hazardous substances commonly found in the wastewater of various industries, such as petrochemicals, pharmaceuticals, paper and wood industries, textiles, plastic and paint manufacturing, etc. As it is found highly toxic to human, animal and aquatic life, its removal or neutralization is of great importance. Different methods are developed for dealing with this problem, like adsorption and extraction, membrane separation, bio-degradation, evaporation/distillation, chemical oxidation [1]. Enzymatic wastewater treatment has advantages over conventional treatments. This process is eco-friendly, not dependent on energy, highly selective, and requires mild working conditions. The immobilization of enzymes onto different carriers allows its reusability, which makes this process cost-effective [2].

Peroxidases are well-known enzymes found in all living organisms. Horseradish peroxidase (HRP) is a commercially available and extensively used peroxidase, that first appeared in scientific literature 200 years ago [3]. HRP uses H_2O_2 to oxidase organic substrates. Since green chemistry is one of the main focuses in modern science, HRP found its place as a useful tool [4]. Natural polymers are non-toxic, biocompatible, and biodegradable and therefore are particularly suitable for enzyme immobilization. Alginate is a natural polysaccharide from brown seaweed, composed of two monomeric units: β–D-mannuronic

acid and α–L-guluronic acid. Alginic acid can easily form hydrogels by ionic (in a solution of many divalent cations) or covalent cross-linking methods. Covalent cross-linking improves the physical properties of alginate hydrogels [5].

The aim of this research was to test the chemically crosslinked alginate hydrogel with immobilized HRP for synthetic wastewater treatment. The reusability of obtained immobilizate was monitored in a batch reactor during five repeated cycles.

MATERIALS AND METHODS

Materials

Sodium alginate (medium viscosity), HRP (150–250 U/mg), ethylenediamine dihydrochloride (98%), and sodium borohydride ($NaBH_4$) (≥98.0%) were purchased from Sigma-Aldrich (St. Louise, Mo, USA). Phenol (p.a. 99.5%), was obtained from Centrohem (Stara Pazova, Serbia). 4–aminoantipyrene and potassium ferricyanide were purchased from Fluka (Buchs, Switzerland) MP Hemija (Belgrade, Serbia), respectively.

Chemical modifications and immobilization

Immobilizate of aminated HRP in oxidate alginate beads was prepared as previously described by Spasojevic *et al.* [6]. Briefly, sodium alginate was activated by oxidation with sodium periodate in the dark. Peroxidase was firstly oxidized with periodate and then added into a solution of ethylenediamine. $NaBH_4$ was used as a reducing agent.

A 2% solution of activated alginate in $NaHCO_3$ was made and aminated HRP was added at a concentration of 0.01 mg/mL. After 24 hours Tris buffer was added to quench any remaining noncoupled carbonyl group. Immobilizate was mixed with native alginate to improve the mechanical properties of the gel. The beads were made by dripping the immobilizate solution from a syringe into a 5.5% solution of $CaCl_2$ (in distilled water) and stirring it for 1 h. The obtained beads were stored in a fridge in a HEPES buffer with 5 mM $CaCl_2$.

Phenol assay

Phenol concentrations were determined photometrically in an oxidative coupling reaction with 2.08 mM 4-aminoantipyrine (4-AAP) and 8.34 mM potassium ferricyanide ($K_3Fe(CN)_6$) in bicarbonate buffer pH 8 (Emerson reaction) [7]. After 10 minutes phenols fully reacted with 4-AAP in the presence of ferricyanide ion and form a stable reddish-brown antipyrine dye. Maximum absorbance was measured at 510 nm, and a calibration curve was made with a series of aqueous standards of phenols.

Phenol removal

200 mg of immobilizated HRP–alginate beads (with specific activity 0.43 U/g) was added in 3 mL phenol in water solution (2 mM). The solution with beads was placed on magnetic stirrer and the reaction started with the addition of 2.4 mM H_2O_2. After specified time intervals, aliquots were taken and the concentration of remaining phenol was determined using Emerson's reagent. The elimination efficiencies of phenol were calculated using the initial and residual concentrations. Each cycle lasted 2 hours, after which the beads were

filtered and washed. This procedure was repeated five times in the batch reactor at 25 °C with constant steering.

RESULTS AND DISCUSSION

Obtained immobilizate of aminated HRP onto oxidized alginate beads demonstrates the ability for phenol removal. To test the reusability of the immobilizate, hydrogel beads were separated from the batch reactor after 2 hours, rinsed with water, and used in the next cycle. The immobilized HRP could be easily separated and manipulated during repeated use, which is the main advantage over free enzyme. The phenol contents in the solution were calculated using equation (1) obtained from the standard curve.

$$y = 0.0122x + 0.0138 \quad (1)$$

The enzyme activity obtained in the first cycle is considered to be 100%. After the 5th cycle, the enzyme retained 54% of its original activity (Figure 1), which was similar to or better result compared to some existing studies [8–10].

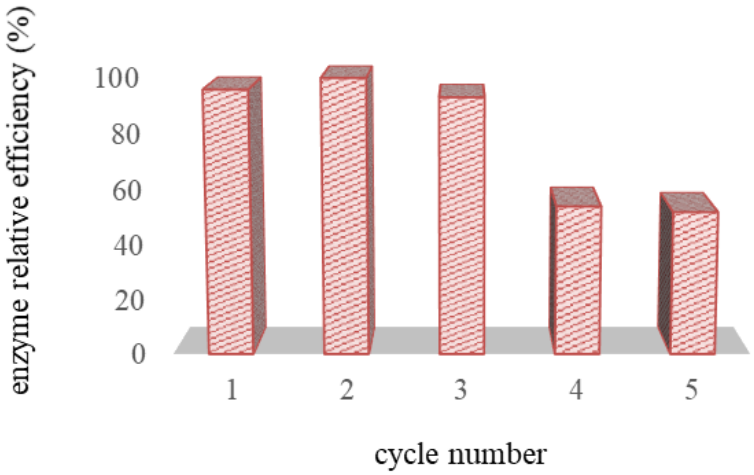

Figure 1 *Reusability of aminated HRP encapsulated within oxidized alginate*

The decrease in enzyme activity, which can be seen during cycles, is probably a result of the accumulation of polymerized phenol products onto alginate beads, which become brown upon utilization (Figure 2). A possible solution to this issue would be washing the hydrogel beads with organic solvents (like ethanol) after each cycle [11].

a) *b)*

Figure 2 *Hydrogel beads with immobilized HRP before a) and after b) reaction with phenol*

CONCLUSION

In this study, we tested the immobilizate of aminated HRP within oxidated alginate, that we have developed in our previous work, for phenol removal and its reusability. The results showed that the immobilized enzyme didn't lose its activity during the 3 cycles, and at the end of the 5th cycle activity loss was 46%. This confirmed that the hydrogel of chemically modified alginate and HRP has the potential for wastewater treatment or other phenolic removing processes. Also, this hydrogel system can be used for the immobilization of various enzymes and for removing pollutants from different mediums.

ACKNOWLEDGEMENT

This work was supported by the Ministry of Science, Technological Development and Innovation of the Republic of Serbia (Grant No. 451-03-47/2023-01/200053, University of Belgrade, Institute for Multidisciplinary Research).

REFERENCES

[1] Villegas, L. G. C., Mashhadi, N., Chen, M. *et al.*, Curr. Pollution Rep. 2 (2016) 157–167.

[2] Al-Maqdi K. A., Elmerhi N., Athamneh K., *et al.*, Nanomaterials 11(11) (2021) 3124.

[3] Krainer, F. W., Glieder, A., Appl. Microbiol. Biotechnol. 99 (4), (2015) 1611–1625.

[4] Lopes G. R., Pinto D. C. G. A., Silva A. M. S., RSC Adv. 4 (2014) 37244–37265.

[5] Lee K. Y., Mooney D. J., Prog Polym Sci. 37 (1) (2012) 106–126.

[6] Spasojević D., Prokopijević M., Prodanović O., *et al*., Hem. Ind. 68 (1) (2014) 117–122.

[7] Emerson E., J. Org. Chem. 8 (1943) 417–428.

[8] Zhang F., Zheng B., Zhang J., *et al*., J. Phys. Chem. C 114 (2010) 8469–8473

[9] Lu Y.-M., Yang Q.-Y., Wang L.-M., *et al*., Soil, Air, Water 45 (2) (2017) 1600077.

[10] Alemzadeh I., Nejati S., J. Hazard. Mater. 166 (2–3) (2009) 1082–1086.

[11] Pantić N., Spasojević M., Stojanović Ž., *et al*., J. Polym. Environ. 30 (7) (2022) 3005–3020.

CONTRIBUTION OF INSTITUTE OF PUBLIC HEALTH OF SERBIA IN MONITORING TRAFFIC-INDUCED AIR POLLUTION IN BELGRADE

Branislava Matić[1*], Mladen Milić[1]

[1]Institute of Public Health of Serbia, Dr Subotića 5, 11000 Belgrade, SERBIA

[*]*brankicam@batut.org.rs*

Abstract

Ambient air pollution is a substantial health issue for mankind, causing around 4.2 million deaths globally per year. The aim of this paper is to show the level of contribution of the Institute of Public Health of Serbia (IPHS) in the process of monitoring air pollution parameters originating from mobile sources of air pollution (TRAP, transport-related air pollution) in the last two consecutive calendar years (2021 and 2022). Parameters monitored were gases (NO_2, NO_x, SO_2, CO) and particles ($PM_{2.5}$; PM_{10}). Broader Belgrade area was divided in 5 different zones according to traffic frequency. Air samplers were positioned at frequent traffic junctions. In 2021 NO_2 mean annual values (MAVs) were beyond 40 µg/m^3 at 8 out of 15 sampling points (53%), ranging from 26.60 µg/m^3 to 59.5 µg/m^3. The highest daily peak concentration for 2021 was 136.5 µg/m^3. In 2022 4 out of 5 NO_2 MAVs were beyond 40 µg/m^3. MAVs of other two gaseous pollutants (SO_2, CO) were moderate. Concerning both PM_{10} and $PM_{2.5}$ MAVs, at all 5 sampling point they were below the national standards, ranging from 26.78 µg/m^3 to 36.68 µg/m^3 (PM_{10}) and from 16.17 µg/m^3 to 23.52 µg/m^3 ($PM_{2.5}$). As expected, all peak daily values for both parameters exceeded daily limit values at all measuring points.

Keywords: traffic, air pollution, intersections, pollutants.

INTRODUCTION

Ambient air pollution is a substantial health issue for mankind, causing around 4.2 million deaths globally per year [1]. High levels of air pollution can cause and worsen cardiopulmonary and respiratory diseases and increase mortality in the exposed population [2], and the elderly, particularly those over 80 years old, are negatively affected by urban air pollution [3]. Urban areas are especially prone to the harmful effects of air pollution given their dense populations, heavy street traffic and various industries. The major urban air pollutants today are nitrogen oxides (NO_x = NO + NO_2), particulate matter (PM), non-methane volatile organic compounds (NMVOCs) and reduced nitrogen compounds (NH_x). Besides the well-studied adverse health effects of PM [4], NO_2 is potentially the most harmful pollutant to humans, even from short-term exposure [5]. Half of humanity (3.5 billion people) lives in cities today, pushing the pressure on urban energy consumption, pollution and congestion to problematic levels. Although cities occupy just 3 per cent of the available land, they account for up to 95% of carbon emissions both through transport and energy sectors. It is forecasted that by 2050, more than 6 billion people, about 70 percent of the global population, will live in urban areas. Many of the urban population currently depend on a car or other motorized vehicles for their mobility. This results in an appalling 1 billion cars worldwide (excl. trucks) many of which are in use in (or near) urban centers. In cities, these

cars are not only the main sources of air pollution (according to the WHO there are 7 million premature deaths annually) but cities are also home to more than half of the world's 1,25 million road traffic fatalities annually [6,7].

A multitude of air contaminants of varying toxicity comes from road transport. These contaminants originate from the tailpipes of vehicles with internal combustion engines, from other vehicle components (such as brake and clutch linings and pads, tires and fuel tanks), and from road-surface wear and treatment materials. Road traffic can be labelled the most important source for some pollutants of great concern, such as nitrogen oxides, benzene and carbon monoxide. Until recently, leaded petrol was an important contributor to exposing the population to lead. Recently, emissions of particulate matter (PM) have attracted much attention, owing mainly to epidemiological findings that suggest that it is a major risk to human health. Besides the pollution sources already mentioned, PM is also formed in the atmosphere, as a secondary pollutant from gases such as nitrogen oxides, sulfur dioxide and volatile organic compounds (VOCs) [7]. TRAP causes the onset and worsening of asthma in children [8,9] and is associated with: all-cause and cardiovascular mortality, cardiovascular disease, the onset of asthma in adults, decreased lung function in people of all ages, lung cancer. Looking into a more detailed linkage to health effects of TRAP, different air pollutants are potentially correlated to a myriad of health effects (Table 1).

Table 1 *Health outcomes associated with TRAP [7]*

Outcome	Associated transport-related pollutants
Mortality	Black smoke, ozone, $PM_{2.5}$
Respiratory disease (non-allergic)	Black smoke, ozone, nitrogen dioxide, VOCs, diesel exhaust, CAPs
Respiratory disease (allergic)	Ozone, nitrogen dioxide, PM, VOCs, diesel exhaust, CAPs
Cardiovascular disease	Black smoke, CAPs
Cancer	Nitrogen dioxide, diesel exhaust
Adverse reproductive outcomes	Diesel exhaust; also equivocal evidence for nitrogen dioxide, carbon monoxide, sulphur dioxide, total suspended particles

PM: particulate matter; $PM_{2.5}$: PM<2.5μm; VOCs: Volatile Organic Compounds (incl Benzene); CAPs: Concentrated Ambient Particles

The aim of this paper is to show the level of contribution of the Public Health Institute of Serbia in the process of monitoring air pollution parameters originating from mobile sources of air pollution (TRAP, transport-related air pollution) in the last two consecutive calendar years (2021 and 2022).

MATERIALS AND METHODS

Of the representative polluting substances originating from mobile sources of air pollution, the concentration of which is measured in Belgrade, IPHS for the City of Belgrade monitors the concentrations of carbon monoxide (CO), nitrogen dioxide (NO_2), sulphur dioxide (SO_2) for several years continuously, at 15 measuring points, while starting from 2022, monitoring is broadened to nitrogen monoxide (NO), nitrogen oxides (NO_x) and particles (PM_{10}, $PM_{2.5}$) [10]. The spatial distribution of measuring points has been reduced to 6 measuring points starting in 2022. For all contracted measurements from 2016 to 2021, a mobile

ecotoxicological automatic measuring unit is used, using standard methods included in the Regulation on monitoring conditions and air quality requirements [11]. Measurements were provided twice a day for 60 minutes during rush hours. All measurements, beginning with 2022, were carried out with a mobile ecotoxicological automatic measuring unit, as continuous 24-hour measurements, in a larger number of cycles (than before), of seven days each. The methods used are standard and accredited. The selection of sampling sites and measurements was carried out in accordance with the current legislation and the Air Quality Control Program for the territory of Belgrade [11,12]. Sampling and measurements in 2021 were carried out at 16 measuring points, distributed in 5 specific *city zones*. Concentrations of pollutants are measured no more than 10 meters from the edge of the sidewalk at a height of 1.5 meters from the ground. In order to have a better insight into the sources of air pollution, due to its geographical distribution, the measuring area has been divided in five zones (2021):

1. *Central urban.* 3 intersections: "London" Kralja Milana/Kneza Miloša; "Tunel" Nušićeva; Kneza Miloša/Bul. k. Aleksandra. It is characterized by canyon-type streets with public city transport and personal traffic as predominant transport mode. The presence of trucks in that zone is prohibited. The special feature of the zone is the traffic congestion due to very narrow streets, providing the increase in the emission of pollutants originating from the motor vehicles exhaust gases [13].

2. *Central urban periphery.* 2 intersections: "Zeleni venac" Brankova/Jug Bogdana/K. Natalije; "Vuk" Ruzveltova/Bul. k. Aleksandra. In this zone, traffic through the two boulevards is carried out with increased dynamics, considering that this zone represents the space through which the central city core is connected to the transit zones. It is dominated by public transport (buses) and individual transport. Measuring point "Franche"– Autokomanda is a traffic hub through which the city commutes with main roads (highway) and other urban units of the wider city zone. Means of public transportation, such as intra-city buses, are directly affected by pollutants generated by traffic because higher volumes of exhaust fumes are released during peak traffic hours in comparison to normal traffic conditions [14]. Pollutants, such as particulate matter (PM_{10}) [15] and CO [16], can have serious detrimental effects on environmental health.

3. *Broader central.* 2 intersections: "Gradska bolnica" Batutova/Dimitrija Tucovića; "Karaburma" Marijane Gregoran/ Vojvode Micka. Characteristics of this measuring points and subjected streets intersections is of the same kind as previously described zone: two traffic congested streets with both public and individual mode of transport, kind of vehicles.

4. *Sava River left bank.* 3 intersections: "Zemun, Glavna" Glavna/Zmaj Jovina; Hotel Hyatt Milentija Popovića; "Studentski grad" Tošin bunar. Measuring points in the "Zone across the Sava River" are located in the central zones of two separate urban units. The measuring point in the historical core of Zemun Municipality (Glavna) is located in a canyon-type street, with dense slow-moving traffic, and has the characteristics of measuring points in the central city zone of Belgrade (zone 1). On the contrary, the intersection where the pollution parameters are monitored in New Belgrade, although it is in its center, due to the application of more modern urban planning standards, has much more favorable conditions for the development of traffic, and above all, a faster flow of vehicles.

5. *City transit zone (presence of heavy traffic).* 5 intersections: "Cvijićeva" Cvijićeva/Bul. Despota Stefana; "Central rail station" Savski trg; "Autokomanda" Bul. Oslobođenja/Franche D`Eperea; Hub "Mostar" Živojina Mišića; Pančevo Bridge Bul. Despota Stefana. Transit zone characteristic is accommodation of traffic flows for entry, i.e. leaving the city, resulting in a large number of trucks operating on diesel fuel for engine propulsion, together with public buses and individual vehicles. Measuring points "Central rail station", "Pančevački most" and "petlja Mostar" we can lable as "transit hubs", while the intersection of Cijićeva Street and Despota Stefan Boulevard represents the intersection of two busy canyon-type streets [13]. Spatial distribution of sampling sites by zones (GIS) is shown in Figure 1.

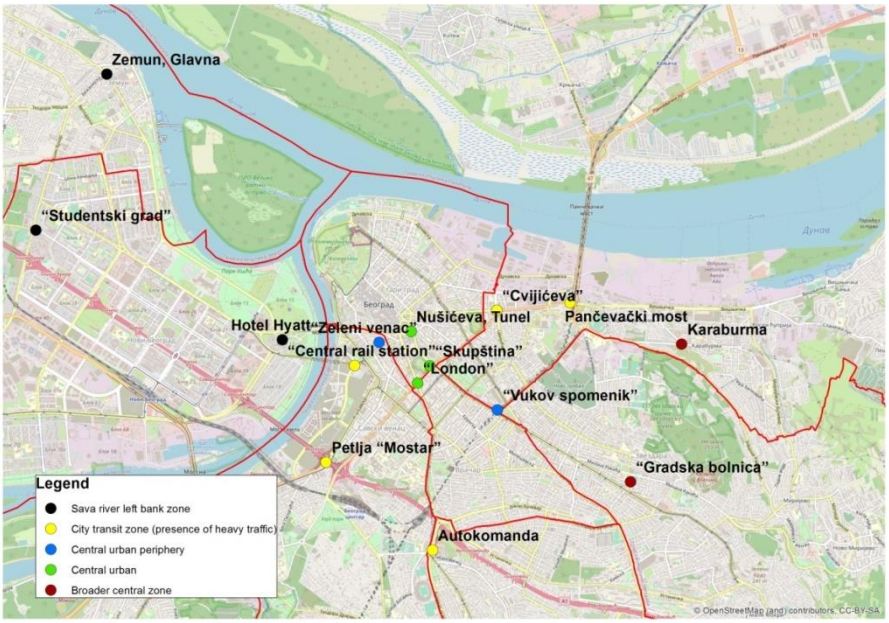

Figure 1 *Spatial distribution of sampling sites by zones (GIS)*

RESULTS AND DISCUSSION

In 2021 NO_2 mean annual values (MAVs) were beyond 40 µg/m^3 (National standard value) at 8 out of 15 sampling points (53%), ranging from 26.60 µg/m^3 (Central rail station) to 59.5 µg/m^3 ("Parliament"). The highest daily peak concentration for 2021 was measured at the "London" junction (136.5 µg/m^3), and at "Zemun, Glavna" in 2022 (129.95 µg/m^3). In 2022 4 out of 5 NO_2 MAVs were beyond 40 µg/m^3. As we expected, the levels of other two gaseous pollutants (SO_2, CO) monitored in the broad Belgrade area were moderate. The mean annual concentration values throughout the whole period of the survey were below the National Standard [11].

Table 3 *Mean annual values of pollutants measured in 2021 and 2022 - Belgrade*

Year	2021 (µg/m^3)		mg/m^3	2022 (µg/m^3)						mg/m^3
Intersection	**NO_2**	**SO_2**	**CO**	**NO_2**	**NO**	**NO_x**	**PM_{10}**	**$PM_{2.5}$**	**SO_2**	**CO**
Hotel Hyatt	**42.2**	32.4	0.91	**42.28**	49.86	121.51	30.68	20.25	14.6	0.80
"**Vuk**"	**44.7**	28.1	1.14	**40.42**	32.18	92.96	27.2	17.28	17.87	0.47
"**London**"	**53.1**	28.8	1.35	**58.12**	48.35	136.05	35.38	20.39	16.77	0.66
"**Tunel**"	**51.8**	35.7	1.35							
Parliament	**59.5**	40.6	1.50	39.11	23.55	77.4	26.78	16.17	17.36	0.57
"**Cvijićeva**"	**48.5**	36.6	1.36							
"**City Hospital**"	32.3	27.5	0.91							
Zemun, Glavna	**46.2**	26.3	1.15	**46.16**	37.79	107.76	36.68	23.52	14.29	0.73
"**Student City**"	34.2	27.6	0.92							
Karaburma	33.6	25.5	0.68							
Zeleni Venac	31.9	28.1	0.77							
Central Rail Stat.	26.6	23.1	0.63							
Franche Autokomanda	31.3	21.8	0.74							
"**Mostar**" **hub**	**45.00**	24.1	1.24							
Pančevo Bridge	35.1	21.3	0.96							
	41.07	**28.5**	**1.05**	**45.52**	**38.35**	**107.14**	**31.34**	**19.52**	**16.18**	**0.65**
ALV	**40.0**	**50.0**	**3.0**	**40.0**			**40.0**	**25.0**	**50.0**	**3.0**

Concerning both PM_{10} and $PM_{2.5}$ values, which have started to be monitored since the beginning of 2022, at all 5 defined sampling point MAVs were below the national standard (PM_{10} 40 µg/m^3; $PM_{2.5}$ 25 µg/m^3), ranging from 26.78 µg/m^3 to 36.68 µg/m^3 (PM_{10}) and from 16.17 µg/m^3 to 23.52 µg/m^3 ($PM_{2.5}$), respectively. As expected, all peak daily values for both parameters exceeded daily limit values at all measuring points [11] (Table 4).

Table 4 *Continuous monitoring at 5 junctions in 2021 & 2022*

Measuring points		**2021**		**2022**					
		NO_2	**SO_2**	**NO_2**	**NO**	**NOx**	**PM_{10}**	**$PM_{2.5}$**	**SO_2**
Hotel Hyatt	C_{max}	120.4	50.1	86.3	191.05	372.57	66.5	54.2	31.61
	C_{sr}	42.2	32.4	42.28	49.86	121.51	30.68	20.25	14.6
"Vuk"	C_{max}	105.8	45.9	94.03	78.46	216.23	59.5	66.4	49
	C_{sr}	44.7	28.1	40.42	32.18	92.96	27.2	17.28	17.87
"London"	C_{max}	**136.5**	49.4	121.7	211.41	376.08	87.4	68.8	39.6
	C_{sr}	53.1	28.8	58.12	48.35	136.05	35.38	20.39	16.77
"Parliament"	C_{max}	134.6	54.2	70.3	89.32	192.67	58.4	47.8	48.6
	C_{sr}	59.5	40.6	39.11	23.55	77.4	26.78	16.17	17.36
Zemun, Glavna St.	C_{max}	110.3	44.4	**129.55**	176.5	352.2	**132.2**	**109.4**	46.1
	C_{sr}	46.2	26.3	46.16	37.79	107.76	36.68	23.52	14.29

The fact that negative health effects of air pollution can be observed even if the air pollutants' concentrations are below the values given by the WHO (before 2021 Guidelines), was confirmed by some authors [17,18]. In the SEARCH (School Environment and Respiratory Health of Children) study [19], almost half (48%) of the investigated children attended schools located either in heavy traffic (31%), or in a very heavy traffic area (17%).

This study was also conducted in 10 Belgrade primary schools. Bronchial symptoms in surveyed children are in statistically relevant correlation only with elevated concentration of ambient air PM_{10} measured in front of the classrooms ($p < 0.001$). On the other hand, they significantly correlate with reduced values of other pollutants, which are otherwise typical for the tailpipe exhaust, such as nitrogen dioxide [19,20]. These results coincide with the results the Netherlands research, where it was proven that the appearance of bronchial hypersensitivity occurs in children studying in schools close to heavy traffic, i.e. vehicles driven by diesel fuel engine, with PM pollution as a dominant by-product of incomplete combustion [21,22].

CONCLUSION

Knowing the fact that even a low-level exposure to TRAP can produce serious health effects, especially in vulnerable population groups (children), urge public health authorities to become involved in programme-based health impact assessment activities, at least in school children attending schools close to streets burdened with frequent and heavy traffic.

REFERENCES

[1] World Health Organisation 2016; Ambient air pollution: a global assessment of exposure and burden of disease. ISBN 978 92 4 151135 3. *Available on the following link*: https://apps.who.int/iris/bitstream/handle/10665/250141/9789241511/9789241511/9789241511353-eng.pdf?sequence=1

[2] C. A. Pope, D. W. Dockery, J. Air Waste Manag. Assoc. 56 (6) (2006) 709–742.

[3] W. Wu, M. Yao, X. Yang, *et al*., Atmos. Environ. (2020) 118098.

[4] M. Kulmala, Nature 526 (2015) 497–499.

[5] R. Chen, E. Samoli, C.-M. Wong, *et al*., Environ. Int. 45 (2012) 32–38.

[6] United Nations Economic Council for Europe, UNECE "A Handbook on Sustainable Urban Mobility and Spatial Planning - Promoting Active Mobility"; UNITED NATIONS PUBLICATION eISBN: 978-92-1-004859-0.

[7] World Health Organization, WHO (2005), "Health effects of transport-related air pollution", Ed. Michal Krzyzanowski, Birgit Juna-Dibbert, Jurgen Schneider; ISBN 978-92-890-1373-4.

[8] M. Brauer, C. Reynold, P. Hystad, University of British Colombia School of Population and Public Health. Traffic-related air pollution and health: a Canadian perspective on scientific evidence and potential exposure-mitigation strategies [Internet]. Ottawa, ON: Health Canada; 2012. *Available on the following link*: http://allergen-nce.ca/wp-content/uploads/pubs/Traffic&Health.pdf

[9] Health Effects Institute. Traffic-related air pollution: a critical review of the literature on emissions, exposure, and health effects. Special report 17 [Internet]. Boston, MA: Health Effects Institute; 2010 [cited 2015 Dec 29]. *Available on the following link*: http://pubs.healtheffects.org/getfile.php?u=553

[10] "Zagađenost urbanog vazduha na teritoriji Republike Srbije merena u mreži institucija javnog zdravlja u 2021.godini" *(in Serbian) Available on the following link*: https://www.batut.org.rs/download/izvestaji/higijena/Zagadjenost%20urbanog%20vazduha%202021.pdf

[11] Uredba o uslovima za monitoring i zahtevima kvaliteta vazduha; "Sl. glasnik RS", br. 11/2010, 75/2010 i 63/2013 (*in Serbian*).

[12] Plan kvaliteta vazduha u Aglomeraciji Beograd, "Sl. list grada Beograda" Br. 46/2021 (*in Serbian*).

[13] L. Ehrnsperger, O. Klemm, Atmos. Environ. 13 (2022).

[14] H. H. Kim, Environ. Sci. Pollut. Res. Int. 27 (29) (2020) 37087–37098.

[15] E. Behrentz, L. D. Sabin, A. M. Winer, *et al*., J. Air Waste Manag. Assoc. 55 (10) 1418–1430.

[16] US EPA, Health and environmental impacts of CO. EPA, U.S.A. (2003). *Available on the following link*: http://www.epa.gov/air/urbanair/co/hlth1.html

[17] WHO Air Quality Guidelines. Global update 2005. Report on a Working Group Meeting, Bonn (2005). *Available on the following link*: https://apps.who.int/iris/bitstream/handle/10665/349878/WHO-EURO-2005-4244-44003-62046-eng.pdf?sequence=1&isAllowed=y

[18] M. Jevtić, N. Dragić, S. Bijelović, *et al*., Int. J. Occup. Med. Environ. Health 27 (2) (2014) 153–164.

[19] P. Rudnai, E. Csobod, E. Vaskovi, *et al*., Epidemiology 23 (5S) (2012).

[20] B. I. Matić, Prediktori respiratornog zdravlja učenika osnovnih škola, Doktorska disertacija, Univerzitet u Kragujevcu, Fakultet medicinskih nauka, (2018). *Available on the following link*:

https://nardus.mpn.gov.rs/bitstream/handle/123456789/10948/Disertacija.pdf?sequence=6&isAllowed=y

[21] N. A. H. Janssen, B. Brunekreef, P. V. Vliet, *et al.*, Environ. Health Perspect. 111 (2003) 1512–1518.

[22] G. Hoek, B. Brunekreef, S. Goldbohm, *et al.*, Lancet. 360 (2002) 1203–1209.

ALTERNATIVE METHODS OF REHABILITATION (SOIL RECOVERY), RECLAMATION AND REMEDIATION OF MINE TECHNOSOLS

Nenad Malić[1*], Una Matko[2], Miladin Trbić[1], Radoslava Pijunović[1], Mihajlo Marković[3]

[1]EFT – Mine and TPP Stanari, 74208 Stanari, Republic of Srpska, B&H

[2]EFT Trade Belgrade, 11000 Belgrade, SERBIA

[3]University of Banja Luka, Faculty of agriculture, 78000 Banja Luka, REPUBLIC OF SRPSKA

[*]*nenad.malic@eft-stanari.net*

Abstract

Mining activity has not only a positive but also a negative side, bringing the consequences for the environment. The effects of mining activities may be permanent (loss of mineral resources and soil, transformation of the landscape) or transient (noise, dust, change of water conditions). The aim of this study was to estimate the adaptive potential of Miscanthus×giganteus Greef & Deu. to grow on Deposol of mine technosol. Before the harvest, the following plant biometric parameters were measured: calorific value, yield of dry mass, number of shoots per rhizome, stem height, etc. The analyzed chemical properties in Deposol and Rekultisol are as follows: soil pH, organic matter content, humus content, C, N, P_2O_5, K_2O. The average value of calorific value of dry mass miscanthus was 18273 kJ kg^{-1}. Use of miscanthus for energy production and reclamation process enables the preservation of primary sources and soil recovery.

Keywords: renewable sources, energy crops, *Miscanthus* sp., calorific value.

INTRODUCTION

Minerals are essential for the economic and civilization development of societies and their acquisition is indissolubly linked with the history of mankind. Mining activity has not only a positive but also a negative side, bringing the consequences for the environment. The effects of mining activities may be permanent (loss of mineral resources and soil, transformation of the landscape) or transient (noise, dust, change of water conditions), which disappear after the cessation of the extraction [1].

Main objective of the reclamation of degraded areas, caused by open pit mine exploitation of the mineral reserves, is to establish the management functions on these newly created technogenic soils (technosols). Soils at the open pits or technogenic soils (mine soil, mine land sites, mine degraded land, antropogeomorfic soil material, technosols) have been created by anthropogenic effect, but seem to be different from the class of anthropogenic soils in many properties. These soils have been created on various substrates that occur to be moved by mining activities in the course of technological process [2].

The ecological restoration of damaged and destroyed ecosystems involves the introduction and cultivation of suitable plant species with the aim of initiating natural processes of re-establishment of an ecosystem's form and functions [3]. Ecological restoration of a specific

ecosystem requires evaluation of the local climate, the physical and chemical properties of the substrate and the selection of the most appropriate plant species. Sustainable managements of technosols (Deposol, flotation tailings, etc.) can be achieved by phytostabilization, reclamation, an economically acceptable and eco-friendly phytoremediation procedure. Phytostabilization reduces the risk of heavy metal contamination of natural ecosystems by immobilizing the pollutants within the soil and decreasing their bioavailability [4]. Plants suitable for phytostabilization are those that develop strong roots with high efficiency in erosion control and heavy metal absorption [5]. Effective biological restoration and phytostabilization of heavy metal polluted soils in temperate climates have already been achieved with grasses belonging to genera Festuca, Poa and Agrostis and legumes such as Medicago and Vicia [6].

Mine technosols and bioenergy crops

The fertility of the Deposol and most other types of technogenic soils is usually low. The concentration of the Deposol with the basic biogenic elements (N, P and K) is within or below the minimum concentrations [7,8]. In addition to the deficit of nutrients, technogenic soils have low content of pedobios and organic matter, and poorly developed adsorptive complex [9]. Shukla *et al*. [10] states the following disorders in technogenic soil: loss of aggregate and soil structure, decrease in soil C concentration, increase in volume, and decrease in porosity.

The results of the past physical and chemical analyzes of Deposol at disposal area for overburden at the Stanari coal basin found that they have favorable physical – mechanical but unfavorable chemical properties [11]. The same authors state that the content of organic matter is very low and acidic chemical reaction make are the biggest problems in Stanari Deposol.

Mixtures of perennial grasses and leguminous can restore the soil quality, biodiversity, and energy flow of degraded ecosystems [12,13]. Perennial grasses provide multiple benefits like improvement in soil structure and quality, reduction in erosion, and increase in biodiversity. The overall genetic resources of the perennial grass family are categorized into (1) wild varieties of the domesticated grass species of same genus, (2) seminatural form of the domesticated grass species, and (3) domesticated populations of the plant adapted in a specific region, also known as ecotype and the cultivars undergoing constant breeding techniques [14].

The first generation bioenergy crops (FGECs) include a few annual and perennial grasses and leguminous. The most suitable from the point of view of agricultural value and improvement of soil properties, in direct biological reclamation were: *Avena sativa* L. *Bromus inermis* Leyss., *Dactylis glomerata* L., *Echinochloa crusgalli frumentacea* W.F. Wight, *Festuca pratensis* Huds., *Hordeum vulgare* L., *Lotus corniculatus* L., *Lupinus luteus* L., *Lupinus plyphyllus* Lindl., *Madicago falcata* L., *Medicago lupulina* L., *Medicago sativa* L., *Melilotus alba* Med., *Melilotus officinalis* L., *Melilotus officinalis* Lam., *Phleum pretense* L., *Secale cereale* L., *Sorghum vulgare sudanense* (Piper) Hitchc., *Trifolium hybridum* L., *Trifolium pretense* L., *Trifolium repens* L. *и Trifolium repens* L. [15,16]. Species: *Dactylis glomerata* L., *Festuca rubra* L., *Festuca arundinacea* Schreb. and *Lotus corniculatus* L. were proposed in a dedicated grass-leguminous mixture for the biological reclamation of Deposol at disposal area for overburden from Raškovac open pit in Stanari coal mine [13].

The second generation bionergy crops (SGECs) include perennial forage crops such as Switchgrass, Phalaris arundinacea L., Medicago sativa L., Pennisetum purpurem Schumach, Cynodon spp, Miscanthus sp. In the practice of mine Deposol reclamation, three bioenergy crops have proven to be ther most promising [17]: American wild millet (*Panicum virgatum* L.), Italian reed (*Arundo donax* L.) and miscanthus (*Miscanthus×giganteus* Greef & Deuter).

Of the species of the genus Miscanthus, the *Miscanthus×giganteus* J. M. Greef & Deuter is the most used. *Miscanthus×giganteus* Greef & Deu. is a triploid hybrid grass native to southeastern Asia originating from the natural crossing of *M. sinensis* and *M. sacchariflorus* [18]. This highly productive, perennial, rhizomatous sterile hybrid is vegetatively propagated by rhizome cuttings. It has a rapidly growing and extensive root system, which is very efficient in nutrient and water supply. Owing to its tolerance to heavy metals, organic pollutants, nutrient deficiency, drought and low temperatures, it remains highly productive in different climatic conditions and on contaminated, degraded and marginal lands [19–21]. It displays large biomass yield and is successfully cultivated worldwide for renewable energy production [22,23].

Meeting the environmental requirements (reduction of CO_2 and NO_2 emissions), producing energy from renewable or CO_2 neutral sources, providing raw materials for biomass fuel production, developing rural areas etc., provide justifiable reasons for growing miscanthus (*Miscanthus×giganteus*) as energy crop. Relations between the environment and energy crops are various as well as complex. It is believed that the effect of biomass crops on the environment should be beneficial rather than detrimental. Use of miscanthus for energy production enables the preservation of primary sources of energy such as petroleum and coal. Amount of 20 t of miscanthus is equivalent to 12 t of hard coal [24]. Biomass such as miscanthus is considered to be CO_2 neutral since the result of its combustion does not influence the increase of atmospheric carbon dioxide due to the absorption of CO_2 during the crops' photosynthesis.

MATERIALS AND METHODS

The coal basin Stanari is located between 44°40' and 44°50' N and 17°45' and 18°00' E, in the northern part of the Republic of Srpska and Bosnia and Herzegovina. Research on biological reclamation of a direct type was carried out at the experimental field (GPS Coordinates: y = 6.486.903.48; x = 4.957.170.11; altitude 230 m a.s.l) within internal disposal area for overburden of the excavation from the open pit Raškovac in the lignite coal basin Stanari: "EFT – Mine and Thermal Power Plant Stanari" (Figure 1).

Pre-grown *M.×giganteus* rhizomes 7–10 cm long were planted in two terms: at the April 2014 and October 2017. They were planted in April 2014 at 8–10 cm depth with a planting density of 3–4 rhizomes per m^2 in (equivalent to 30000-40000 plants ha^{-1}). Rhizomes were planted in October 2017 at 10–15 cm depth with a planting density of 2 rhizomes per m^2 (equivalent to 20000 plants ha^{-1}). Planting was done by hand in the first period and with a partially modified planter in the second planting period. Before planting fertilizing with mineral fertilizer was carried out ($N_{37}P_{37}K_{37}$). Before the harvest, the following plant biometric parameters were measured: yield of dry mass, number of shoots per rhizome, stem

height, etc. The basic elementary and calorific values of the dry weight of miscanthus were done in the lab of the EFT Mine and TPP Stanari.

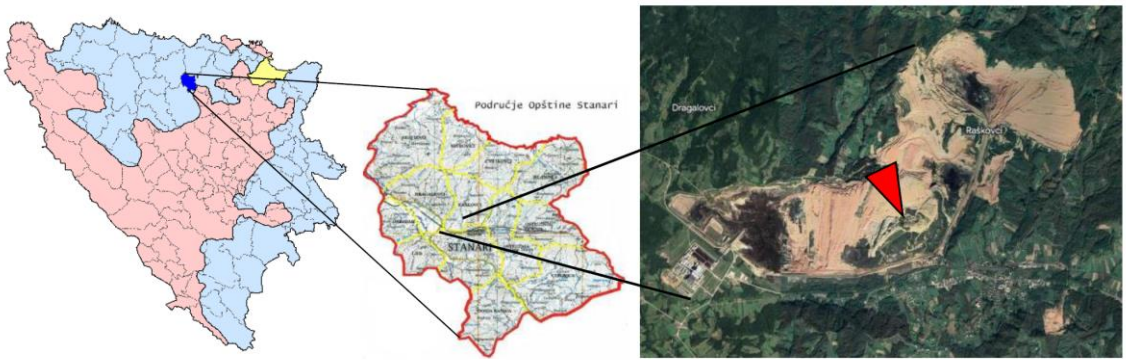

Figure 1 *Experimental filed location*

RESULTS AND DISCUSSION

Average results of the analysis of chemical properties of Deposol and Rekultisol of Stanari coal basin are presented in tables 1 and 3. Results of the elementary and calorific value of miscanthus are presented in Table 2.

Table 1 *Results of the analysis of chemical properties of Deposol*

No. of sample	pH		Organic matter	Humus	Total C	Total N	AL-P_2O_5	AL-K_2O
	H_2O	KCl			%		mg $100g^{-1}$	
1	6.2	4.9	2.1	0.0	0.0	0.0	0.0	1.3
2	5.8	4.5	1.2	0.0	0.0	0.0	0.5	2.2
3	5.2	4.0	1.6	0.0	0.0	0.0	0.6	2.7

The researched Deposol belongs to the class of low and medium content, while there is no pure humus and nitrogen. According to the content of P_2O_5 and K_2O in the Deposol, they are classified as very poorly secured by these elements. The Deposol is characterized by a non-carbonate substrate, a strong unsaturation with base cations, a medium and highly acidic chemical reaction.

Miscanthus planted in spring and fall and biomass produced during the summer are harvested in winter (Figure 2). This growth pattern is repeated every year for the lifetime of the crop, which wil be at least 12–15 years.

a) *b)* *c)*

Figure 2 *Plantation of miscanthus a) rhizomes; b) planting; c) harvesting*

The growth pattern of the crop is simple. It produces new shoots annually and these usually emerge from the soil during May (Stanari location). Frome the second season onwards the crop can start harvest (February–March).

Table 2 *Results of the elementary and calorific value of miscanthus*

No. of sample	Part of plant	Content of moisture	Content of ash	Combustible matter	Volattile matter	C-fix	Total S	Calorific value
		%						kJ kg^{-1}
1	Whole plant	18.12	5.02	76.86	62.97	13.89	0.09	18273
2	Stem	18.37	2.38	79.24	66.39	12.86	0.07	18621
3	Leaf	17.79	6.16	76.05	64.29	11.76	0.10	17995

The results of technical and basic laboratory coal analysis proved that the coal from Raškovac open pit has all characteristics of lignite: high moisture content (36.30–30.01%), variable ash content (1.31–46.95%), average calorific value (8500–9500 kJ kg^{-1}) and extremely low content of S (0.08–0.37%). Miscanthus has higher calorific value than lignite. Amount of 20 t of miscanthus is equivalent to 35–40 t of lignite these characteristics. Amount of 20 t of miscanthus is equivalent to 12 t of hard coal [24].

A critical factor for an energy crop is the moisture content at harvest. The drier the crop, the higher the energy yield and bale value. Moisture contents as low as 15% have been reported in southern Europe. By conditioning and allowing dry in the field, the stem moisture content can be halved from 50% to 25%.

Table 3 *Results of the analysis of chemical properties of Rekultisol under plantation of miscanthus*

No. of sample and year	pH		Organic matter	Humus	Total C	Total N	AL-P_2O_5	AL-K_2O
	H_2O	KCl	%				mg 100g^{-1}	
1 (2018)	5.9	5.9	1.89	0.0	0.0	0.0	1.1	6.6
2 (2019)	5.3	4.2	2.09	0.0	0.0	0.0	2.6	5.3
3 (2021)	5.4	4.2	3.0	1.1	5.45	0.06	1.3	5.3

CONCLUSION

The plantation of energy crops – crops which are grown specifically to be harvested and burnt in power stations or heating systems, develop in response to the need for atmospheric CO_2 abatement and potentially uses soils lower fertility. Planting of miscanthus was done at the experimental field within internal disposal area for overburden of the excavation from the open pit Raškovac. Calorific value of researched of miscanthus is from 17995 to 18621 kJ kg^{-1}. The biological reclamation in researched agro-ecological conditions has been successfully conducted by plantation of miscanthus.

REFERENCES

[1] Uberman R., Ostręga A., AGH J. Min. Geoeng. 36 (2) (2012) 285–297.

[2] Malić N., Lončar S., Matko U., 8th Balkan Mining Congress – Proceedings, September 28–30, Belgrade, Serbia (2022) 708–723.

[3] Dickinson N. M., Baker A. J. M., Doronila A., *et al.*, Int. J. Phytoremediation 11 (2) (2009) 97–114.

[4] Berti W. R., Cunningham S. D., Phytostabilization of metals *in* Phytoremediation of toxic metals: using plants to clean up the environment, Editors: Raskin I., Ensley B. D., New York, Wiley (2000) 71–88.

[5] Andrejić G., Šinžar-Sekulić J., Prica M., Dželetović Ž., Arch. Biol. Sci. (2019) 1–16.

[6] Smith R. A. H., Bradshaw A. D., J. Appl. Ecol. (1979) 595–612.

[7] Pivić R., Stanojković A., Čakmak, *et al.*, Zbornik radova 6. simpozijuma "Reciklažne tehnologije i održivi razvoj", Soko Banja (2011) 307–314.

[8] Sheoran V., Sheoran A. S., Poonia P., Int. J. Soil Sediment Water 3 (2) 13 (2010) 1–20.

[9] Rasulić N., Miličić B. M., Delić D., *et al.*, J. Sci. Agric. Res. 66 (4) (2005) 73–80.

[10] Shukla M., Lal R., Ebinger M. Soil Sci. 169 (2004) 133–142.

[11] Malić N., Marković M., 3rd International and 15th National Congress SOILS FOR FUTURE UNDER GLOBAL CHALLENGES, 21–24 Septembar, Sokobanja, Serbia (2021) 302–312.

[12] Creutzig F., Ravindranath N. H., Berndes G., *et al*., GCB Bioenergy 7 (2015) 916–944.

[13] Malić N. Rekultivacija stanarskih deposola primjenom agromeliorativnih mjera i sjetvom travno-leguminoznih smjesa. Doktorska teza. Poljoprivredni fakultet Univerziteta u Banjoj Luci, (2015), p.165.

[14] Sokolovic D., Babic S., Radovic J., *et al*., Selekcija i semenarstvo 23 (1) (2017) 69–82.

[15] Motorina L. V., Čeklina V. N., Iževskaя T.I., Эkologiя (Moskva) 5 (1971) 20–24.

[16] Lyle E. S. Jr. Surface mine reclamation manual, Elsevier, New York, (1987) p.268.

[17] Dželetović Ž., Simić A., Maksimović J., *et al*., Proceedings of Integrated meeting, May 12–13, Zrenjanin, Serbia (2014) 70–79.

[18] Hodkinson T. R., Chase M. W., Lledó D. M., *et al*., J. Plant Res. 115 (5) (2002) 381–392.

[19] Naidu S. L., Moose S. P., Al-Shoaibi A. K., *et al*., Plant Physiol. 132 (3) (2003) 1688–97.

[20] Purdy S. J., Maddison A. L., Jones L. E., *et al*., Ann. Bot. 111 (5) (2013) 999–1013.

[21] Ježovski S., Buckby S., Cerazy-Waliszewska J., *et al*., Front Plant Sci. 8 (2018) 726.

[22] Brosse N., Dufour A., Meng X., *et al*., Biofuel Bioprod Biorefin. 6 (5) (2012) 580–598.

[23] McCalmont J. P., Hastings A., McNamara N. P., *et al*., Glob. Change Biol. Bioenergy 9 (3) (2017) 489–507.

[24] Lewandowski I., Kicherer A., Vonier P., Biomass Bioenergy 8 (2) (1995) 81–90.

30th International Conference Ecological Truth & Environmental Research
20–23 June 2023, Serbia

PRELIMINARY ECOLOGICAL STATUS ASSESSMENT OF THE GROŠNICA RIVER BASED ON PHYTOBENTHOS

Snežana B. Simić[1*], Kristina A. Markeljić[2]

[1]University of Kragujevac, Faculty of Science, Department of Biology and Ecology, Radoja Domanovića 12, 34000 Kragujevac, SERBIA

[2]University of Kragujevac, Faculty of Agronomy in Čačak, Cara Dušana 34, 32102 Čačak, SERBIA

[*]*snezana.simic@pmf.kg.ac.rs*

Abstract

The research on the Grošnica River was conducted to obtain data on benthic algae diversity and provide a preliminary assessment of water quality due to the absence of prior studies. Benthic algae sampling and analysis were carried out in May 2022. In five selected localities, a total of 28 taxa of benthic algae were detected: Cyanobacteria (3), Rhodophyta (1), Chlorophyta (2), Ochrophyta (Xanthophyceae) (1), and Bacillariophyta (21). A preliminary assessment of the ecological status was carried out according to the guidelines of the Water Framework Directive and national legislation, using the IPS diatom index. In addition, literature data on the indicator properties of observed macroalgae were examined. Based on the obtained values at localities L1, L2, L3 (upper course), a good ecological status was determined, while at locality L4 (middle course) a moderate ecological status was determined, and in at locality L5 (lower course) a good ecological potential of the Grošnica river was determined. The occurrence of massive growth of macroalgae Cladophora glomerata and Vaucheria sp. in the middle (L4) and especially in the lower reaches of the river (L5) indicates an increased amount of nutrients and deterioration of water quality.

Keywords: water quality, benthic algae, diatoms, macroalgae, ecological status assessment.

INTRODUCTION

The Grošnica River flows through the municipality of Kragujevac along its entire course. It is 18 km long and flows from the spring called Hajdučka voda (800 m altitude) in the Gledić Mountains to its confluence with the Lepenica River (187 m altitude). It is the most densely networked river in the Kragujevac basin (1429 m/km^2) [1]. The establishment of a dam on the Grošnica River in 1938 led to the formation of the Grošnica reservoir, which serves as a source of drinking water for a portion of Kragujevac city. Above the dam, many smaller ones have been built on the river to protect against sediment deposition and to slow down the erosion process [2]. According to the National Regulations [3,4], the Grošnica River is classified as a TYPE 3 water body (small and medium-sized rivers, up to 500 m altitude, dominated by large substrate granulation). Although it is a significant tributary of the Lepenica River, it has been poorly studied in terms of water quality [5–9].

According to the Water Framework Directive [10], the National Law [11] and Regulation [4], the assessment of ecological status for this type of water body is based on physical and

chemical parameters and biological elements (phytobenthos and macroinvertebrates). The use of phytobenthos (especially diatoms) is recommended for assessing the ecological status of surface waters, due to the significant bioindicator properties of this community. Although they are not included in national legislation, the use of other groups of benthic algae (non-diatom) as an addition to existing methods is significant. This approach would yield more precise insights into water quality, especially the trophic status [12].

The aim of this study is to present the diversity of benthic algae in the Grošnica River with an assessment of the river's ecological status/potential in accordance with WFD [10], National Law [11] and Regulations [3,4].

MATERIALS AND METHODS

Field research of the Grošnica River was conducted in May 2022 at five localities: L1 - upstream of the small dams (N 43°53'38.9", E 20°54'27.3", 426 m a.s.l.); L2 - downstream of the small dams (N 43°53'58.5", E 20°54'55.1", 387 m a.s.l.); L3 - Trešnjevak (N 43°54'08.3", E 20°54'58.4", 394 m a.s.l.); L4 - Grošnica (N 43°57'34.0", E 20°52'31.1"E, 232 m a.s.l.); L5 - near the confluence with the Lepenica River (N 43°59'32.4", E 20°53'13.7", 194 m a.s.l.). In the upper stream (localities L1, L2), the Grošnica River flows through a forested, sparsely populated area where no pollutants have been identified. In the middle and lower stream, it flows through villages and the industrial part of the city (localities L3, L4, L5).

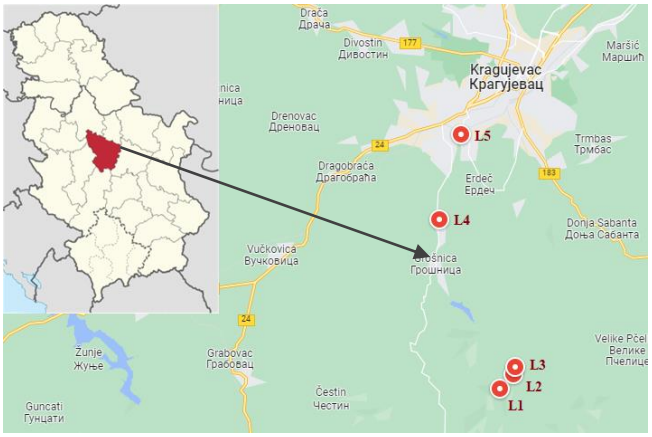

Figure 1 *The Grošnica River Basin with position of investigated localities at the Grošnica River: L1 - upstream of the small dams; L2 - downstream of the small dams; L3 - Trešnjevak; L4 - Grošnica; L5 - near the confluence with the Lepenica River*

Hydro-morphological, physical, and chemical water characteristics were recorded at all mentioned localities, and phytobenthos samples were collected. Physical and chemical parameters (Table 1) were measured directly using set of field laboratory photometer system "AQUALITIC AL450", according to the standard SRPS EN 5667 (1–9) [13].

Sampling in the field, preparation of samples, identification, and quantification of diatoms and macroalgae were carried out in accordance with the methodology presented in Simić *et al.*

[14]. Based on the qualitative and quantitative analysis of diatoms, the IPS (*Pollution Sensitivity Index*) [15] diatom index was calculated in the OMNIDIA software.

The category of surface waters was determined according to Regulations [3,4,16]. The channel and banks of the Grošnica River have been arranged (significantly modified) at location L5. Accordingly, the ecological status was assessed at localities L1–L4, and ecological potential at locality L5.

RESULTS AND DISCUSSION

The measured physical and chemical parameters of the Grošnica River localities are presented in Table 1.

Table 1 *Physical and chemical water parameters of the Grošnica River*

Metric / Locality	L1	L2	L3	L4	L5
Water temperature (°C)	11.5	13.1	13.1	21.7	21.2
Conductivity (µS/cm^3)	380	380	380	450	530
Water hardness ($CaCO_3$) (mg/L)	180	190	190	210	320
pH (0-14)	7.97	8.13	8.13	8.33	7.93
Oxygen concentration (mg/L)	10.33	10.33	10.33	14.6	12.37
Oxygen saturation (%)	99.2	99.2	99.2	171.6	133

Qualitative analysis of the phytobenthos in the Grošnica River in May 2022 recorded a total of 28 taxa, classified into five divisions: Cyanobacteria (3), Rhodophyta (1), Chlorophyta (2), Ochrophyta (Xanthophyceae) (1), and Bacillariophyta (21) (Table 2).

Of all the recorded taxa, the greatest diversity was observed within the division Bacillariophyta (21 species). The highest number was observed at locality L2 (13), while the lowest number of species was found at L1 (6). Quantitative analysis showed that the most domiant species of diatoms at L1 was *Gomphonella olivacea*, at L2 *Cymbella* sp., at L3 *Encyonema lange-bertalotii*, at L4 *Ulnaria ulna*, and at L5 *Cocconeis peduculis*.

Four macroalgae (*Audouinella pygmaea*, *Cladophora glomerata*, *Stigeoclonium tenue*, *Vaucheria* sp.) and two microalgae (*Phormidium breve*, *Chroococcus* sp.) forming macroscopic aggregations were found at the surveyed localities. Of all the recorded macroalgae, only *C. glomerata* was found at all localities, but with significant differences in coverage, length, and color of the filaments. Its coverage was <5% at L1 and L2, 10% at L3 (with filaments length up to 30 cm), 30% at L5, while at L4 it reached a maximum of 80–90% coverage of the riverbed surface (with filaments length up to 1 m). The color change was related to the amount of epiphytic diatoms (*Cocconeis placentula* and *Gomphonema* sp.) that covered the filaments. The green algae *S. tenue* formed macroscopic aggregations on rocky substrates, as well as on filaments of *C. glomerata* at L4. It occurred in traces, with coverage less than 1%. Mats of the macroalgae *Vaucheria* sp. were registered with coverage of 10% at L3 and 70% at L5. The red algae *A. pygmaea* was found at L2, in traces with coverage <1%. The cyanobacterium *P. breve* formed blue-green macroscopic aggregations on rocks at L2 and L3. Orange macroaggregations of the microalga *Chroococcus* sp. were also observed at L3.

Table 2 *List of taxa recorded along the Grošnica River*

Taxa / Locality	L1	L2	L3	L4	L5
Cyanobacteria					
Phormidium breve (Kütz. ex Gomont) Anagnostidis & Komarek		+	+		
Spirulina sp.		+			
Chroococcus sp.			+		
Rhodophyta					
Audouinella pygmaea (Kütz.) Weber Bosse		+			
Chlorophyta					
Cladophora glomerata (Linnaeus) Kütz.	+	+	+	+	+
Stigeoclonium tenue (C. Agardh) Kütz.				+	
Ochrophyta (Xanthophyceae)					
Vaucheria sp.			+		+
Bacillariophyta					
Cocconeis peduculis Ehrenb.					+
Cocconeis placentula Ehrenb.	+	+		+	+
Cyclotella meneghiniana Kütz.				+	+
Cymbella lanceolata (C. Agardh) C. Agardh		+	+		
Cymbella sp.	+	+	+		
Cymbella affinis Kütz.		+			
Diatoma vulgaris Bory			+	+	+
Encyonema sp.		+	+		
Encyonema leibleinii (Agardh) Silva et al.		+	+		
Encyonema lange-bertalotii Krammer		+	+	+	
Gomphonema olivaceoides var. densestriata				+	
Gomphonella olivacea (Hornem.) Rabh.	+	+			+
Gyrosigma attenuatum (Kütz.) Rabenh.		+	+		
Meridion circulare (Grev.) C.Agardh			+	+	
Melosira varians C. Agardh		+	+	+	+
Navicula tripunctata (O. F. Müll.) Bory	+	+	+		
Navicula viridula (Kütz.) Ehrenb.					+
Nitzschia sigmoidea (Nitzsch) W.Sm.	+	+	+	+	
Rhoicosphenia abbreviata (C. Agardh)	+		+		+
Surirella brebissonii Krammer and Lange-		+		+	
Ulnaria ulna (Kützing) Compère				+	+
Total number of taxa: 28	**7**	**17**	**16**	**12**	**11**

By comparing the values obtained by calculating the IPS diatom index [15] at the surveyed localities and the limit values of the classes from the National Regulation [4] for TYPE 3 water bodies, a good ecological status was determined at localities L1, L2, and L3, a moderate ecological status at L4, and good ecological potential at locality L5 of the Grošnica river (Table 3). Estimations of water quality of this river based on algae as indicators were carried out prior to the implementation of the WFD [5–7] and indicated the second class of water quality (β-mesosaprobic). After the implementation of the National Law [11], the Serbian Environmental Protection Agency (SEPA) conducted a water quality assessment of this river, whose results, based on the IPS index values, indicate the second class in the upper course of

the river (year 2015/16) and the third class of ecological status in the lower course of the river (year 2020) [8,9].

Table 3 *Ecological status/potential* assessment of the Grošnica River based on diatom community*

Metric / Locality	L1	L2	L3	L4	L5*
IPS index	15.9	15.6	15.7	13.2	14.5
Ecologial status/potential* assessment	II	II	II	III	II*
Class of ecological status/potential*	good	good	good	moderate	good*

Detected macroalgae can also provide some insight into the water quality status of the Grošnica River. Species *C. glomerata*, an indicator of β-mesosaprobic water according to Sladeček [17], was found in both localities with good and moderate ecological status, with an increasing coverage in areas where the status is worse and where organic pollution is present (L4). The species *S. tenue*, which is known to tolerate significant organic pollution and heavy metal loading [18] and is considered to be an indicator of α-mesosaprobic water [17], was also found at the L4 locality. *Vaucheria* sp. thalli were massively developed in class II water (L3, L5). Generally, species of this genus inhabit weakly polluted streams and rivers, but they can be found in polluted water and in that case, they occur together with *Cladophora* species [19], which was observed in this study. It is generally accepted that red algae inhabit clean, well-aerated, and organic-poor waters [20]. The presence of the red alga *A. pygmaea* only in the upper reaches of the river (L2), where a good ecological status (class II) was determined, confirms this.

CONCLUSION

The ecological status/potential of the Grošnica river, determined according to Regulations [3,4] based on the IPS diatom index, worsens from the upper to the lower course and its confluence with the river Lepenica. The ecological status is assessed as good (class II) in the section passing through sparsely populated areas (localities L1, L2, L3), moderate (class III) in the middle course in the settlement of Grošnica (locality L4). At locality L5, a good (class II) ecological potential has been determined. The extensive development of macroalgae at localities L4 (*C. glomerata*) and L5 (*C. glomerata* and *Vaucheria* sp.), as well as the presence of the species *S. tenue* at locality L4, indicate an increased amount of nutrients in the water, but further research is necessary to determine the exact cause of this phenomenon. In order to obtain a more precise assessment of the ecological status of the Grošnica river in the future, it is necessary to use all biological elements (phytobenthos, macroinvertebrates, macrophytes, fish) and physico-chemical parameters of water quality according to recommendations of WFD [10].

ACKNOWLEDGEMENT

Work on this paper was supported by Ministry of Science, Technological Development and Innovation of Republic of Serbia (451-03-47/2023-01/ 200122).

REFERENCES

[1] Milanović A., Hidrogeografska studija reke Lepenice, Geografski institut „Jovan Cvijić“, SANU, Beograd (2007), p.138, ISBN: 978-86-80029-38-2.

[2] Baračkov Z., Ekološka proučavanja naselja dna Grošničke reke, PMF, Kragujevac (1973).

[3] Službeni glasnik Republike Srbije 96/2010, Pravilnik o utvrđivanju vodnih tela površinskih i podzemnih voda.

[4] Službeni glasnik Republike Srbije 74/2011, Pravilnik o parametrima ekološkog i hemijskog statusa površinskih voda i parametrima hemijskog i kvantitativnog statusa podzemnih voda.

[5] Grupa autora, Stanje, problemi, mogućnosti i mere zaštite i unapredjenja životne sredine na području regiona Šumadije i Pomoravlja, PMF, Kragujevac (1986).

[6] Grupa autora, Studija zaštite životne sredine i razvoja ekoloških sistema grada Kragujevca do 2010. godine, PMF, Kragujevac (1993).

[7] Simić S., Makroalge u tekućicama brdsko-planinskih područja Srbije (Doktorska disertacija), Biološki fakultet, Beograd (2002).

[8] Agencija za zaštitu životne sredine, Rezultati ispitivanje kvaliteta površinskih i podzemnih voda – 2020, Beograd (2020).

[9] Agencija za zaštitu životne sredine, Izveštaj o statusu površinskih voda Srbije u 2015. i 2016. godini, Beograd (2018).

[10] WFD, Water Framework Directive- Directive of the European Parliament and of the Council 2000/60/EC - Establishing a Framework for Community Action in the Field of Water Policy (2000).

[11] Službeni glasnik Republike Srbije 30/2010, Zakon o vodama.

[12] Stancheva R., Sheath G., Knowl. Manage. Aquat. Ecosyst. 417 (2016) 1–15.

[13] SRPS EN 5667 (1-19):2017, Kvalitet vode – Uzorkovanje.

[14] Simić S., Rakonjac A., Čabrić K., *et al*., Kragujevac J. Sci. 45 (2023) 1–22.

[15] Cemagref, Etude des methods biologiques d'appré-ciation quantitative de la qualitédes eaux, Rapport Q.E. Lyon, Agence de l'eau Rhöne-Méditerranée-Corse-Cemagref, Lyon, France (1982).

[16] Denić Lj., Čađo S., Đurković A., *et al.*, Status površinskih voda Srbije, Ministarstvo poljoprivrede i zaštite životne sredine, Agencija za zaštitu životne sredine, Beograd (2015).

[17] Sládecek V., Arch. Hydrobiol. –Beih. Ergebn. Limnol. 7 (1973) 1–218.

[18] Kaštovský J., Hauer T., Geriš R., *et al*., Atlas sinic a řas České republiky 2, Jihočeská univerzita v Českých Budějovicích, České Budějovice (2018), p.480, ISBN: 978-80-7568-125-6.

[19] Entwisle J., Mar. Freshw. Res. 40 (5) (1989) 471–489.

[20] Eloranta P., Kwandrans J., Oceanol. Hydrobiol. Stud. 33 (1) (2004) 47–54.

30th International Conference Ecological Truth & Environmental Research
20–23 June 2023, Serbia

AN ASSESSMENT OF THE ECOLOGICAL POTENTIAL OF ŠUMARICE RESERVOIRS (CENTRAL SERBIA) BASED ON PHYTOPLANKTON

Snežana B. Simić[1*], Nevena B. Đorđević[1]

[1]University of Kragujevac, Faculty of Science, Institute of Biology and Ecology,
Radoja Domanovića 12, 34000 Kragujevac, SERBIA

[*]*snezana.simic@pmf.kg.ac.rs*

Abstract

Investigation of the Šumarice Reservoir was conducted during the 2022 year in order to assess the ecological potential of the reservoir. The Šumarice Reservoir is formed by damming of the Sušica Creek (Type 3 water bodies). The ecological potential is determined on the basis of biological quality element-phytoplankton, supporting physico-chemical quality elements that are defined by the Regulation on the parameters of the ecological and chemical status of surface waters and the parameters of the chemical and quantitative status of groundwaters. An assessment of the ecological potential of the Šumarice reservoir revealed that the water quality was poor and corresponded to class V ecological potential. Monitoring of the reservoir throughout 2022 confirmed the presence of sewage inflow, which introduced significant amounts of nutrients that promote the growth of cyanobacteria. The frequent occurrence of invasive and potentially toxic cyanobacteria species in the reservoir such as Raphidiopsis raciborskii, along with the accompanying adverse effects, emphasizes the urgent need to address the sewage inflow issue to mitigate these harmful effects.

Keywords: reservoir, cyanobacteria, *Raphidiopsis raciborskii*, ecological potential assessment.

INTRODUCTION

Located on the outskirts of the city of Kragujevac in Central Serbia (44°01′49″N; 20°52′28″E) at an altitude of 185 meters above sea level, the Šumarice reservoir was created in 1967 by damming Sušica Creek and is part of the memorial park "October 21". The Sušica Creek basin comprises forests, meadows, agricultural land, and settlements with a partially organized sewage network. On one side of the reservoir, there is a settlement, while the other side has meadow vegetation and forest fragments of the *Quercetum confertae-ceris* Rudski 1949 community [1]. The well-maintained side of the reservoir is suitable for sports activities, and it is the most popular recreational water body in Kragujevac. However, the reservoir is under constant negative influence from sewage water especially during the rainy season, which flows into the stream, ultimately affecting the reservoir. Cyanobacterial blooms and the appearance of invasive species occur in the reservoir during the summer and autumn months [2]. The World Health Organization (WHO) cautions that any population of cyanobacteria should be treated as potentially toxic [3]. In 2014, the reservoir was prohibited for sports and recreational purposes due to a cyanobacterial bloom of the *Aphanizomenon flos aquae* Ralfs ex Bornet & Flahault species. Cyanobacteria of the genus *Aphanizomenon* can produce microcystin, anatoxin, saxitoxin, and cylindrospermopsin, making them potentially toxic. It

was the first occurrence of a cyanobacterial bloom in the reservoir since its formation [2]. Extreme rainfall in May 2014 caused an episodic increase in nutrient concentration, leading to a change in the cyanobacteria community in the Šumarice reservoir [2].

MATERIALS AND METHODS

The sampling of the Šumarice reservoir was conducted between July and August 2022. Sampling of phytoplankton and measurement of environmental parameters were conducted at three locations in the reservoir – the Dam, Center, and Mouth (Figure 1).

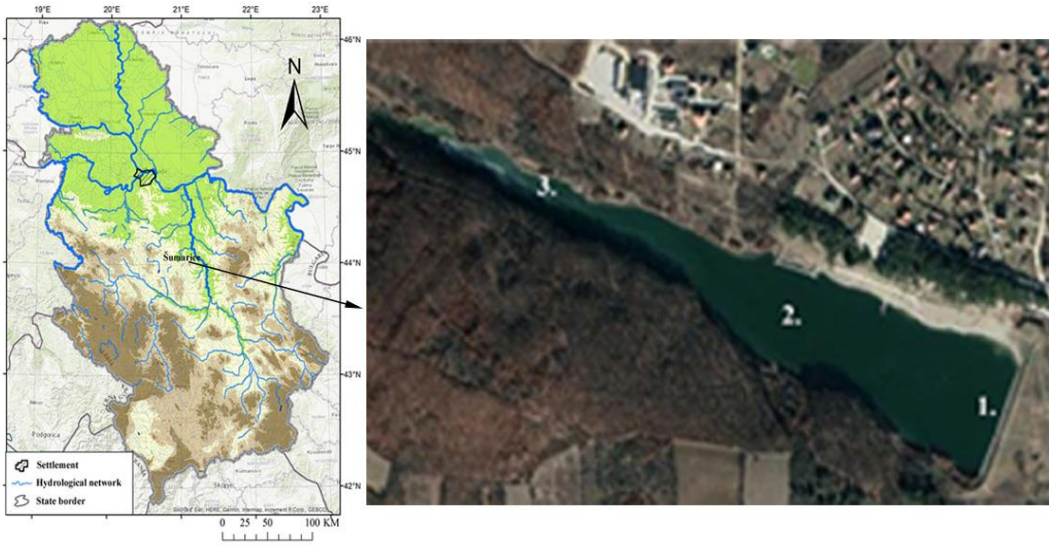

Figure 1 *The location of the Šumarice reservoir and satellite image of the research localities: 1. Dam, 2. Center, 3. Mouth*

In August, water samples for physico-chemical analysis were collected in accordance with the standard SRPS EN ISO 5667-14:2017 [4]. The physico-chemical parameters of water were determined using standard methods according to the APHA [5]. Water temperature (ºC), pH, electrical conductivity (µS/cm), water hardness (mg/L), transparency (m), phosphate concentration (PO_4-P, mg/L), nitrates (NO_3-N, mg/L), and ammonium ions (NH_4-N, mg/L) were measured at each location.

Qualitative phytoplankton samples were taken in July and August, while quantitative analysis of phytoplankton abundance was conducted on samples collected in August. The sampling, preparation, identification, and quantification of phytoplankton were conducted following the methodology described in the research by Simić *et al*. [2].

The assessment of the ecological potential of the Šumarice reservoir was based on the biological element of quality (phytoplankton) according to the national regulations [6,7].

RESULTS AND DISCUSSION

The environmental parameters of Šumarice Reservoir

The results of environmental parameters are presented in Table 1.

Table 1 *The values of environmental parameters measurements at Šumarice Reservoir*

Locality	Mouth	Center	Dam
Water temperature (°C)	27.2	26.6	26
Conductivity (μs/cm)	390	390	380
Hardness (mg/L)	190	190	200
Transparency (m)	0.4	0.7	0.6
pH	8.6	8.4	8.5
NH_4-N (mg/L)	<0.03	<0.03	<0.03
NO_3-N (mg/L)	8.3	9	8.6
PO_4-P (mg/L)	<0.06	<0.06	<0.06
Total P (mg/L)	0.03	0.02	0.03

Based on the environmental parameters, including electroconductivity, pH, water temperature, and water hardness, it has been confirmed that there were no significant variations in the values of these parameters. However, elevated nitrate concentration (NO_3-N) levels were observed in all localities of the Šumarice reservoir (mouth, middle, and dam), accompanied by reduced water transparency across all investigated locations.

Qualitative and quantitative analysis of phytoplankton in the Šumarice reservoir

The qualitative analysis of the Šumarice reservoir revealed the presence of 55 taxa from five divisions of algae: Cyanobacteria (16), Bacillariophyta (17), Dinophyta (4), Euglenophyta (3), and Chlorophyta (15) (Table 2).

Table 2 *The qualitative composition of phytoplankton at investigation localities in the Šumarice Reservoir during July and August 2022*

Locality	Mouth		Center		Dam	
Taxa\Month	VII	VIII	VII	VIII	VII	VIII
CYANOPHYTA						
Aphanizomenon flos-aquae Ralfs ex Bornet & Flahault	+	+	+	+		+
Chroococcus minutus (Kützing) Nägeli		+				
Chrysosporum bergii (Ostenfeld) Zapomelova et al.	+	+	+		+	+
Chrysosporum minus (Kiselev) Komárek	+		+			
*Cuspidothrix issatschenkoi (*Usachev) Rajaniemi et al.		+		+		+
Limnococcus limneticus (Lemmermann) Komárková et al.				+		
Limnothrix redekei (Goor) Meffert	+		+	+		+
Lyngbya sp. C. Agardh ex Gomont		+		+		
Merismopedia sp. Meyen			+		+	
Microcystis aeruginosa (Kützing) Kützing	+	+	+	+		+
Oscillatoria tenuis C. Agardh ex Gomont			+	+	+	+
Oscillatoria sp. Vaucher ex Gomont		+	+	+		
Pseudanabaena limnetica (Lemmermann) Komárek		+		+		
Raphidiopsis raciborskii (Woloszynska) Aguilera et al.	+	+		+		

Table 2 *continued*

Snowella lacustris (Chodat) Komárek & Hindák	+		+		+	
Woronichinia compacta (Lemmermann) Komárek & Hindák	+	+		+		
BACILLARIOPHYTA						
Asterionella formosa Hassall			+	+		+
Aulacoseira granulata (Ehrenberg) Simonsen		+			+	+
Cocconeis placentula Ehrenberg	+	+				+
Cyclotella ocellata Pantocsek	+	+		+	+	+
Cymbella affinis Kützing	+					
Diatoma vulgaris Bory	+	+		+		
Fragilaria crotonensis Kitton				+		
Gomphonema olivaceum (Hornemann) Kützing	+		+			
Melosira varians C. Agardh				+		+
Meridion circulare (Greville) C. Agardh		+		+	+	
Navicula capitatoradiata Germain	+	+				
Navicula sp. Bory		+				
Nitzschia acicularis (Kützing) W.Smith		+	+	+		
Nitzschia palea (Kützing) W. Smith	+	+	+	+	+	+
Nitzschia sp. Hassall	+					
Pinnularia viridis (Nitzsch) Ehrenberg		+	+			
Ulnaria ulna (Nitzsch) Compère		+			+	+
DINOPHYTA						
Ceratium hirundinella (O.F.Müller) Dujardin	+	+	+	+	+	+
Gymnodinium sp. F.Stein	+	+		+	+	+
Peridinium cinctum (O.F.Müller) Ehrenberg	+	+	+		+	+
Peridinium sp. Ehrenberg				+		
EUGLENOPHYTA						
Trachelomonas volvocina Ehrenberg		+		+		
Euglena sp. Ehrenberg	+	+	+			
Phacus sp. Dujardin	+	+		+		
CHLOROPHYTA						
Closterium aciculare West	+	+	+			+
Cosmarium depressum (Nägeli) P. Lundell		+		+	+	
Coelastrum rugosum (Rich) Tsarenko		+				
Eudorina elegans Ehrenberg						+
Golenkinia radiata Chodat		+		+		+
Monoraphidium contortum (Thurs.) Komarkova-Legn.	+	+	+			
Mougeotia sp. C.Agardh		+		+		
Pandorina sp. Bory	+					
Pediastrum boryanum (Turpin) Meneghini	+	+			+	
Pediastrum duplex Meyen	+	+		+	+	+
Pediastrum simplex Meyen	+	+	+			
Spirogyra sp. Link		+		+		
Staurastrum gracile Ralfs ex Ralfs		+		+		
Staurastrum paradoxum Meyen ex Ralfs	+	+	+			
Ulothrix sp. Kützing		+				

+ present taxa

During the month of July, a total of 38 taxa from five divisions of algae were recorded in the Šumarice reservoir: Cyanobacteria (11), Bacillariophyta (14), Dinophyta (3), Euglenophyta (2), and Chlorophyta (8) (Table 2). The dominant species in the phytoplankton community was the cyanobacterium *Chrysosporum bergii* (Ostenfeld) Zapomelova et al., and it was observed in all areas of the reservoir in July.

In August, a total of 49 taxa from five divisions of algae were recorded in the Šumarice reservoir: Cyanobacteria (13), Bacillariophyta (14), Dinophyta (4), Euglenophyta (3), and Chlorophyta (15) (Table 2). Notably, there was an observed increase in the population density of Cyanobacteria during this month. The most abundant species was the cyanobacterium *Aphanizomenon flos-aquae*. Additionally, a species from the Dinophyta section, *Ceratium hirundinella* (O.F.Müller) Dujardin, was also abundant.

The presence and increasing abundance of Cyanobacteria, along with the identification of *Raphidiopsis raciborskii* (Woloszynska) Aguilera et al., in the Šumarica reservoir during 2022, require special attention. Previously regarded as a tropical species, *Raphidiopsis raciborskii* is now recognized as an extremely invasive alga capable of producing toxins like cylindrospermopsin and saxitoxin [8].

In the Šumarice reservoir, the highest phytoplankton abundance in August (56,100 cells/mL) was recorded at the Mouth location, while numbers near the Dam and Center ranged from 43,920 to 47,820 cells/mL. Among the total phytoplankton community in August, cyanobacteria (61%) and Dinophyta algae (23%) were the most numerous, whereas Bacillariophyta and Chlorophyta represented only 7–8% of the entire community. In order to protect human health, the WHO has proposed risk levels based on the number of cyanobacteria cells and microcystin concentrations in recreational waters and water supply [3]. Based on the number of cyanobacteria cells per mL, the water in the Šumarice reservoir in August falls into the medium level of health risk.

Ecological potential assessment of the Šumarice reservoir based on physico-chemical quality elements

The ecological potential of the Šumarice reservoir was evaluated as poor in all surveyed locations, based on the values of the measured physical and chemical parameters. Specifically, the water of the reservoir falls within the IV water class, as shown in Table 3.

Table 3 *Ecological potential assessment of the Šumarice reservoir based on physico-chemical quality elements*

Parameters / Locality	**Mouth**		**Center**		**Dam**	
	value	class	value	class	value	class
NH_4-N (mg/L)	<0.03	II	<0.03	II	<0.03	II
NO_3-N (mg/L)	8.3	IV	9	IV	8.6	IV
PO_4-P (mg/L)	<0.06	II	<0.06	II	<0.06	II
Total P (mg/L)	0.03	II	0.02	II	0.03	II
Transparency (m)	0.4	IV	0.7	IV	0.6	IV
Ecological potential assessment	**IV poor**		**IV poor**		**IV poor**	

Ecological potential assessment of the Šumarice reservoir based on biological quality elements – phytoplankton

The ecological potential of the Šumarice reservoir, determined by the abundance of phytoplankton and the percentage of cyanobacteria, categorizes it as having a class V ecological potential, indicating bad ecological conditions (Table 4).

Table 4 *Ecological potential assessment of the Šumarice reservoir based on biological quality elements-phytoplankton*

Parameters / Locality	**Mouth**	**Center**	**Dam**
Abundance of phytoplankton (cells/mL)	56,100	47,800	43,920
Percentage of cyanobacteria (%)	61	60	61
Ecological potential assessment	V bad	V bad	V bad

CONCLUSION

An assessment of the ecological potential of the Šumarice reservoir revealed that the water quality was bad and corresponded to class V ecological potential. Monitoring of the reservoir throughout 2022 confirmed the presence of sewage inflow, which introduced significant amounts of nutrients that promote the growth of cyanobacteria. Invasive and potentially toxic cyanobacterial species, such as *Raphidiopsis raciborskii*, have emerged, potentially causing negative consequences for the ecosystem. The frequent occurrence of cyanobacteria blooming and the invasive and potentially toxic cyanobacteria species in the reservoir, along with the accompanying adverse effects, emphasizes the urgent need to address the sewage inflow issue to mitigate these harmful effects.

ACKNOWLEDGEMENT

The publication of the manuscript was supported by the Ministry of Science, Technological Development and Innovation of the Republic of Serbia under contract number 451-03-47/2023-01/200122. It is also part of the "Ecological Image of Šumarica Lake" project, which is being implemented by the Association for the Promotion and Ecological Marketing of Natural Values (EKOMAR).

REFERENCES

[1] Ranković B., Simić S., Bogdanović D., Kragujevac. J. Sci. 28 (2006) 107–114.

[2] Simić S., Đorđević N, Milošević Dj., Fundam. Appl. Limnol. 190 (1) (2017) 1–11.

[3] WHO Guidelines for Safe Recreational Water Environments: Coastal and fresh waters, Vol. 1., World Health Organization, p.219, ISBN: 9241545801.

[4] SRPS EN 5667-14:2017 Water quality – Sampling – Part 14: Guidance on quality assurance and quality control of environmental water sampling and handling.

[5] APHA Standard methods for the examination of water and wastewater. 17th ed. Washington: American Public Health Association, (1995).

[6] Official Gazette of the Republic of Serbia 74/2011, Regulation on the parameters of ecological and chemical status of surface waters and parameters of chemical status and quantitative status of ground waters (*in Serbian*).

[7] Official Gazette of the Republic of Serbia 96/2010, Regulation on the establishment of surface and groundwater bodies (*in Serbian*).

[8] Meriluoto J., Spoof L., Codd G., A Handbook of cyanobacterial monitoring and cyanotoxin analysis, Wiley, Chichester (2017), p.548, ISBN: 9781119068686.

FLUORESCENCE CHARACTERISATION OF BISPHENOL A IN VARIOUS SOLVENTS AND DRINKING WATER

Miloš Prokopijević[1*], Mira Stanković[1,2], Dragana Bartolić[1,2], Aleksandra Lj. Mitrović[1,2], Ksenija Radotić[1,2]

[1]University of Belgrade, Institute for Multidisciplinary Research (IMSI), 11030 Belgrade, REPUBLIC OF SERBIA

[2]University of Belgrade, Center for Green Technologies, Institute for Multidisciplinary Research (IMSI), 11030 Belgrade, REPUBLIC OF SERBIA

[*]*milos.prokopijevic@imsi.rs*

Abstract

Environmental safety may be compromised by the presence of hazardous chemical compounds, such as bisphenol A (BPA), which is commonly used in the production of certain types of plastics. BPA is an emerging organic contaminant that could be found in many matrices, such as drinking water, due to anthropogenic activities. Within this study, we used fluorescence spectroscopy to analyse the photoluminescent characteristics of BPA in various solutions and drinking water. The emission spectra of BPA in various solvents are recorded from 280 nm to 380 nm, after excitation wavelength at 230 nm. These results imply that the fluorescence approach can be used for rapid detection and estimation of the level of BPA in water samples and, hence, for non-invasive monitoring of BPA in drinking water is an important concern for public health and environmental protection.

Keywords: bisphenol A, fluorescence, water safety, environmental protection.

INTRODUCTION

Bisphenol A (BPA), 2,2-bis(4-hydroxyphenyl) propane, is an organic compound composed of two phenol rings connected by a methyl bridge and two methyl functional groups attached to the bridge (Inset of Figure 1). BPA is commonly used as a raw material for the production of certain types of plastics such as epoxy resins, polycarbonate, etc. [1]. However, during long term decomposition of plastic materials, BPA can be leached from these plastics and contaminate food products, beverages, and other consumer products, leading to potential health risks [2]. As previously reported, BPA has genotoxicity, neurotoxicity, cytotoxicity, and reproductive toxicity, and is capable of causing endocrine-disrupting effects [3]. The potential risk to human health due to BPA exposure by drinking water is becoming an important topic of concern and a major environmental hazard. It was reported that the leaching of BPA from plastic wastes into the water is causing contamination of the water supply worldwide [4,5].

Sensitive and selective analytical techniques, such as gas chromatography coupled with mass spectrometry and high-performance liquid chromatography with a detector based on fluorescence, UV, or mass spectrometry, have been developed to determine the trace of BPA [3]. These techniques are time-consuming and use expensive equipment. So it is important to

develop rapid and non-expensive tools for screening of BPA in drinking water samples. BPA exhibits its fluorescence with emission at 300 nm and excitation maxima around 220 nm. However, BPA has low quantum efficiency in aqueous solutions. The fluorescence intensity of BPA increases significantly in other solvents such as ethanol, methanol, or acetonitrile [6]. Fluorescence spectroscopy is a non-invasive technique that can be used to detect the presence of BPA in various samples, including food, water, and human biological fluids [7]. To perform BPA fluorescence screening, a sample is first prepared by extracting BPA from the matrix using an appropriate solvent. This study aimed to optimize conditions appropriate for fluorescence detection of BPA in various solvents and drinking water. Furthermore, the detection threshold and the impact of the concentration of BPA on its emission spectra profile was examined.

MATERIALS AND METHODS

Chemicals and materials

Bisphenol A (2,2-Bis(4-hydroxyphenyl)propane, BPA, 97%) standard was purchased from Thermo Fisher Scientific Inc. (Waltham, MA, USA). Methanol (MeOH) (HPLC grade) was purchased from VWR International (Radnor, PA, USA). Ultrapure deionized water (Thermofisher Scientific, Bremen, Germany) was used to prepare samples solutions.

Sample preparation

The proper amounts of standard BPA were dissolved in methanol and deionised water, as well as in drinking water. Concentrations of BPA in methanol, deionised water, as well as spiked drinking water, are given in Table 1. The drinking water was collected from the laboratory tap. Generally, BPA has poor solubility in water, so solutions were stirred at room temperature for 60 min before analysis.

Fluorescence spectroscopy measurements

The fluorescence measurements were performed using an Fl3-221 P spectrofluorometer (JobinYvon, Horiba, France), which is equipped with a 450 W Xe lamp and a photomultiplier tube. The spectra of the samples were measured in the cuvette with 10 mm optical path and 1 ml volume, in the right-angle (RA) configuration at room temperature. The Integration time was set at 0.1 s. The fluorescence emission spectra of the proper amounts of standard BPA in metahnol, acetonitril, deionised water and drinking water were recorded in the range from 280 to 380 nm (increment 1 nm), after excitation at 230 nm. All recorded spectra were normalised.

RESULTS AND DISCUSSION

This study investigated the influence of variation in BPA concentration and usage of different solvents for this compound on the recorded fluorescence emission spectra. The normalised fluorescence emission spectra of different concentration of BPA in methanol are presented in Figure 1. After excitation at 230 nm, all the resulting spectra displayed the characteristic broad emission band from 280 to 380 nm [8]. We observed that increasing

concentrations of BPA in methanol lead to slightly red shifting in the position of their respective emission maxima, such as shown in Figure 1 and Table 1.

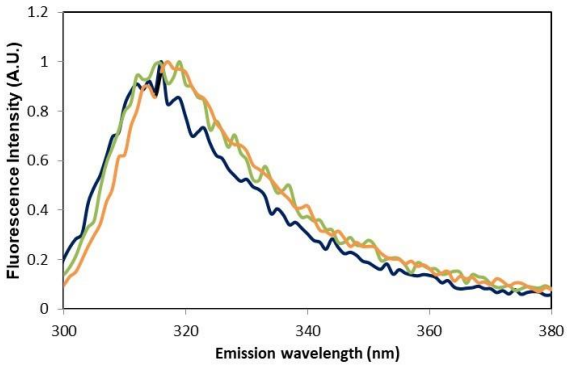

Figure 1 *Overlaid normalised fluorescence emission spectra of the different concentrattions of the BPA in metahnol (blue color coresponds to BPA concentration of 50 mg/L, green coresponds to 250 mg/L and orange to 350 mg/L)*

Table 1 *Position of the Emission maximua of BPA in spiked samples after excitation at 230 nm*

Matrix solvent (solutions)	Spiked level of BPA (mg L^{-1})	Emission maximum (nm)
Methanol	50	316
Methanol	250	318
Methanol	350	320
Methanol	450	322
Deionized water	0.15	316
Drinking water	0.12	317

Further, the fluorescence emission band (280–380 nm) of BPA in drinking water is presented in Figure 2. The observed weak fluorescent signal of BPA in drinking water with a maximum at 317 nm corresponds to the previously published results. It has been reported that fluorescence spectra of BPA are more susceptible to microenvironment changes and solvent polarity [8]. These results imply that BPA in analysed concentrations could be detected in real samples, such as drinking water using fluorescence spectroscopy as a highly sensitive method.

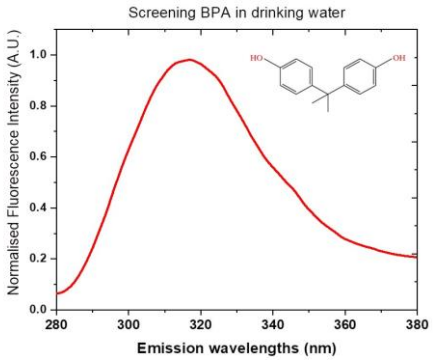

Figure 2 *Fluorescence Emission spectra of BPA in drinking water (0.12 mg/L), after excitation at 230 nm. Inset: Chemical structure of BPA.*

CONCLUSION

Our results indicate that the nature of solvents and concentrations of BPA affect fluorescence emission spectra of this compound, such as spectral width and position of the emission maxima. With increasing concentrations of BPA in methanol, the position of the emission maximum is red-shifted. Overall, the study shows that fluorescence spectroscopy could be used for the non-invasive screening of contaminants like BPA in drinking water. The upcoming research will focus on the fluorescence characterization of the other BPA-contaminated water samples from various environmental sources. Besides, developing a valuable non-invasive, rapid, and non-expensive fluorescence tool for monitoring BPA will increase environmental safety.

ACKNOWLEDGEMENT

The authors are grateful to the Ministry of Science, Technological Development and Innovation of the Republic of Serbia for financial support according to the contract No 451-03-47/2023-01/200053.

REFERENCES

[1] Ćwiek-Ludwicka K., Rocz Panstw Zakl Hig. 66 (4) (2015) 299–307.

[2] Kang J., Katayama Y., Kondo F., Toxicology 207 (2–3) (2006) 81–90.

[3] Dueñas-Moreno J., Mora A., Cervantes-Avilés P., *et al*., Environ. Int. 170 (2022) 107550.

[4] Rosa D. D. S., Nunes L., Bianchi V. N., *et al*., Int. J. Hydro. 2 (3) (2018) 333–336.

[5] Alabi O. A., Ologbonjaye K. I. , Awosolu O., J. Toxicol. Risk Assess. 5 (1) (2019) 021.

[6] Nascimento C. F., Rocha F. R. P., Microchem. J. 137 (2018) 429–434.

[7] Orzel J., Swit P., Int. J. Mol. Sci. 22 (19) (2021) 10569.

[8] Wang H., Zou Y., Li C., *et al*., J. Fluoresc. 23 (2013) 1157–1165.

NOVEL APPROACH IN AIRBORNE POLLEN DISPERSION MODELLING

Slobodan Ničković[1,2], Luka Ilić[1,3], Slavko Petković[2], Goran Pejanović[2], Alfredo Huete[4], Zoran Mijić[1*]

[1]Institute of Physics Belgrade, University of Belgrade, Pregrevica 118, 11080 Belgrade, SERBIA

[2]Republic Hydrometeorological Service of Serbia, 11000 Belgrade, SERBIA

[3]now at Barcelona Supercomputing Center, Plaça Eusebi Güell, 1–3, 08034 Barcelona, SPAIN

[4]School of Life Sciences, University of Technology Sydney, Sydney, NSW, AUSTRALIA

[*]*zoran.mijic@ipb.ac.rs*

Abstract

When exposed to high atmospheric humidity, pollen grains rupture and release large numbers of small allergenic particles. Unlike whole pollen grains, these submicron particles easily enter deep into lungs and can cause a serious asthmatic response. Current operating pollen models predict the concentration of intact (whole) pollen grains but not respirable allergenic fragmented particles. We tested a novel numerical pollen model that predicts the formation and dispersion of sub-pollen allergenic granules released after pollen grains burst in the moist air. We evaluated the model for the case of the November 2016 Melbourne thunderstorm asthma epidemic, which resulted in 10 deaths and thousands of hospital admittances. This episode was triggered by intact grass pollen transported toward the city by a severe storm weather system followed by a 5 hour lag in the arrival of the finer, sub-pollen granules into the city, with a spike in hospital presentations shortly after. The model accurately predicted the observed times, locations and quantities of both fragmented and intact pollen concentrations. The presented modelling system, if operationally implemented, can be used as a prognostic tool for early warning alerts on asthma epidemic occurrences.

Keywords: pollen, numerical modeling, thuderstorm asthma, sub-pollen particles.

INTRODUCTION

Thunderstorms occurring during the pollen season are often associated with an increased number of sub-pollen particles. The conceptual model of thunderstorm asthma (asthma episodes associated with thunderstorms) assumes that a thunderstorm circulation transports the emitted pollen grains into a cloud where grains rupture due to high atmospheric moisture. Each pollen grain release almost one thousand sub-pollen particles [1]. Recently presented direct measurements of sub-pollen concentrations performed for the first time with a novel fluorescence spectroscopic technique show that fragments remain airborne for several hours after pollen rupturing by thunderstorms [2]. These fragmented particles are small enough to enter deep into the lungs and to cause severe asthmatic reaction [3].

During the 21 November 2016, the asthma epidemic episode in Melbourne (Australia), ryegrass pollen was transported to the city from widespread pastures in the region by a strong

wind gusts ahead of fast-moving thunderstorm squall-line front [4]. The city recorded ten asthma-related deaths and almost 500 admissions to the hospital over a short time after this event. The number of hospital visits increased by 992% within 30 h [5]. The Melbourne episode was the worldwide largest asthma epidemic coinciding with pollen presence. Many people had breathing difficulties occurred in such a short interval that it caused extreme pressure on the health system. The sudden increase in observed ruptured pollen counts associated with the frontal passage was assumed to be the major cause of the epidemic [6]. High levels of intact pollen concentrations, observed a day earlier on 20 November from nearby local grass emissions did not cause an asthma epidemic, since stable synoptic conditions prevailing that day were not favourable for pollen fragmentation. In response to the 21 November thunderstorm asthma episode, the local Victorian government recommended the development of a physical pollen model as a key priority in order to fulfil societal needs for a more reliable early warning system.

Currently several physical models available in the community provide short-term prediction of the intact pollen concentration embedded into numerical weather prediction systems [7,8]. However, parameterization of pollen rupturing and dispersion of sub-pollen allergenic particles is still challenging task. In this paper the results of sub-pollen particles prediction obtained by numerical simulation are presented using a novel parameterization scheme for pollen rupturing.

MATERIALS AND METHODS

The numerical model called DREAM-POLL have been developed to predict not only the intact pollen concentration but also the production and dispersion of allergens released from ruptured pollen grains. DREAM-POLL is an Euler-type model in which prognostic pollen concentration equation is embedded on-line into a high-resolution non-hydrostatic weather prediction model. The on-line modelling approach allows the atmospheric and pollen processes to be synchronously simulated. DREAM-POLL mathematically describes the major phases of the atmospheric pollen cycle, including the emission of pollen, its vertical and horizontal transport, and pollen turbulent mixing and deposition.

The model starts emitting pollen from a pre-specified source when near-ground turbulence exceeds a threshold at that source. The emitted pollen is further directed by the turbulence and large-scale dynamics of the atmospheric model driver. At the end of their atmospheric cycle, pollen particles are settled to the ground by precipitation and by near-surface dynamics as predicted by the atmospheric driver. In the newly developed pollen rupturing parameterization, we calculate in every model time step the number of fragmented particles released from ruptured pollen grains whenever the atmospheric humidity of the driver model exceeds a pre-specified threshold of 60% [9]. The intact, ruptured and fragmented particles are driven by the same atmospheric dynamics in the model, except that intact pollen elements are emitted from the ground, and the other two particle categories originate in high moisture cloud conditions. Model experiments presented in this study were performed with horizontal grid spacing of approximately 5 km. At this resolution, convective and non-hydrostatic atmospheric processes are explicitly resolved in the model, which is essential for appropriate simulation of pollen dynamics under thunderstorm conditions. The 50-m resolution Australian

Land Use and Management (ALUM) classification data was used to specify the grass fraction used in the model as potential pollen sources. We tested the model performance by executing it in a real-time prognostic mode for the Melbourne episode, validating its results against available pollen observations.

DREAM-POLL represents a modified version of the DREAM regional dust aerosol atmospheric model [10]. The model domain in this study covers the southwestern region of Australia, and there are 28 model vertical levels spanning from the surface to 50 hPa. The horizontal grid distance is set to 1/20 deg (approximately 5 km). The pollen advection and lateral diffusion are computed every 35 sec, the emission and vertical diffusion are updated every 70 sec, and the convection and large-scale precipitation are calculated every 140 sec.

The model was run over the period 19–22 November 2016 during which the Melbourne episode happened. The initial and boundary conditions for the atmospheric model component were specified using weather prediction parameters of the European Centre for Medium-range Weather Forecast (ECMWF) global model. Since there are no satisfactory three-dimensional pollen concentration observations to be assimilated, the initial state of pollen concentration in the model was defined by the 24-h forecast from the previous day model run. Only for the "cold start" of the model at 00:00 UTC 19 November 2016, the initial pollen concentrations were set to zero.

RESULTS AND DISCUSSION

The synoptic situation on 21 November was characterized by the presence of a cold front over southeast Australia. Northerly winds ahead of the front swept ryegrass pollen from pastures north of Melbourne. A multi-cell thunderstorm squall-line heading the cold front passed the city area between 17:00 and 18:30 AEDT (AEDT – Australian Eastern Daylight Time is the local time, which is UTC+11:00), when surface meteorological parameters abruptly changed their values. From the early afternoon onwards, the observed intact and ruptured pollen concentrations increased as well. At 16:00 AEDT, the simulated horizontal wind convergence line approached the wider city area. The convergence line separated the warmer air on the Melbourne side from the colder maritime air southward. Previously emitted intact pollen north of the city was lifted by warm updrafts to zones of moist air, while cold downdrafts prevailed behind the squall-line. The predicted location, orientation, and intensity of the squall-line agree with satellite data. Its circulation pattern is consistent with conceptual models of squall-line thunderstorm systems. After entering the moist air, pollen rupturing was triggered, but at this time the ruptured grains had not reach the surface. At 22:00 AEDT, after the thunderstorm line moved away from Melbourne, the predicted intact pollen concentrations were reduced to zero (Figure 1a). However, about this time, the surface concentration of ruptured particles achieved its maximum (Figure 1b).

Figure 2 shows the spatio-temporal evolution of the intact and fragmented particles as predicted for the pollen measurement site Burwood (the Deakin University, Melbourne). Being lighter in weight, the fragmented particles progressed much slower than the heavier intact pollen grains, with most sub-pollen particles arriving at the city on 21 November about 5 h later than intact pollen. A time delay of several hours is observed during asthma thunderstorm episodes in the USA as well [2].

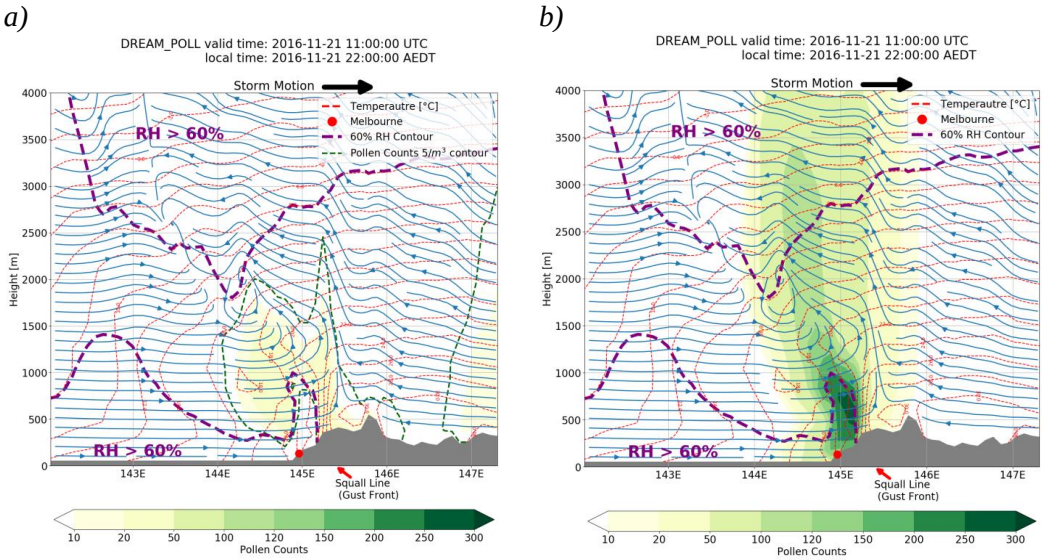

Figure 1 *Predicted intact and ruptured pollen concentration at 22:00 AEDT on 21 November; Vertical cross sections along the normal to the front, with pollen concentration (yellow-to-green palette), streamlines and contours of 60% relative humidity (dashed purple lines); a) intact; b) ruptured pollen; Melbourne is represented by a red dot in each panel.*

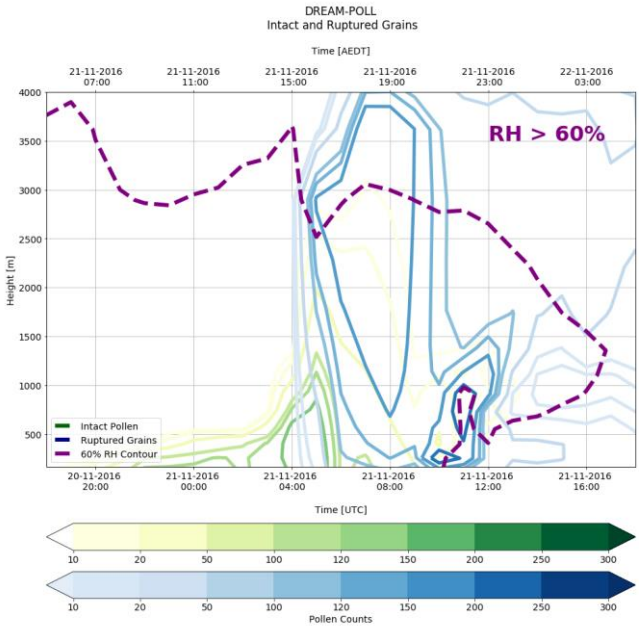

Figure 2 *Predicted intact and ruptured pollen grains above Melbourne; 60% relative humidity contour*

There are two peaks of intact pollen concentrations observed in Melbourne during the 20–21 November period (Figure 3). The first peak on the 20th is attributed to pollen probably emitted from nearby urban sources. During this day, there were no significant ruptured pollen numbers recorded, which indicates that particle fragmentation did not occur under the prevailing stable synoptic conditions. However, on the 21 November both observations and model results show increased numbers of intact and ruptured pollen particles linked with the

passage of the wind gust front. Affected by the passing front, the largest decrease/increase of predicted intact/ruptured particle numbers occurred at approximately 18:00 AEDT. Significant increase in the observed ruptured-to-intact grain ratio after the front passage was reproduced by the model as well.

The predicted intact pollen achieved its largest number several hours before the thunderstorm arrived in Melbourne. Later that afternoon, the arrival of the squall front coincided with a short-term precipitation event [5]. From 15:00 AEDT onwards, the predicted number of pollen fragments (represented with the size of 3.03 μm in the model) started to increase, reaching the maximum concentration of 97,500 particles per m^3 at 21:00 AEDT. This value is within an order of observed magnitudes [2]. A decline in intact pollen before and an increase in fragment numbers after the frontal passage we simulated are consistent with a recently published characterization of airborne pollen dynamics during several thunderstorms [2]. The maximum number of allergenic pollen fragments was predicted to have occurred 2 h before the highest recorded number of asthma-related hospital presentations.

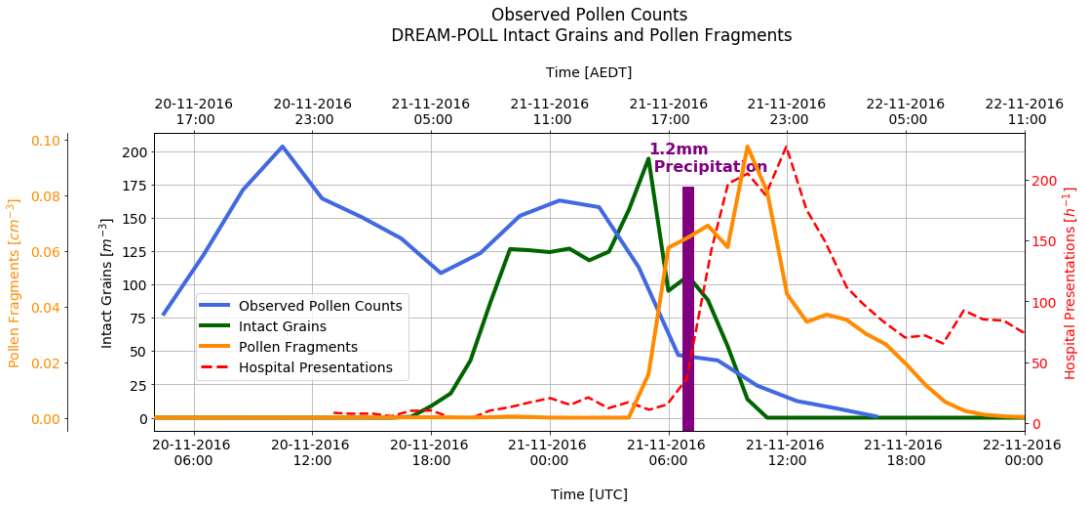

Figure 3 *Pollen concentrations in Melbourne: Observed pollen counts (blue); predicted intact grains (green) and sub-pollen particles (orange); observed 1.2 mm precipitation (purple bar); 1-h hospital presentations (dashed red line)*

CONCLUSION

We presented in this study a numerical modelling approach that enables the prediction of concentration of respirable sub-pollen fragments several days in advance. We demonstrated the effectiveness of this approach by forecasting the Melbourne thunderstorm asthma event 48 h earlier. The proposed method can play a crucial component in an early warning system dedicated to predict time and location of asthma-related outbreaks. DREAM-POLL can be implemented with different model resolutions, over specified geographical domains and for a given pollen type. The availability of such an early-warning system would allow civil authorities to react in a timely manner to asthma epidemics and thus significantly diminish pressure on health services and reduce fatalities and illnesses due to respiratory problems.

However, a numerical parameterization scheme for sub-pollen particles formation from whole grains can be further improved taking into the account not only high humidity but other effects of convective thunderstorm conditions.

ACKNOWLEDGEMENT

The authors acknowledge Prof. Ed Newbigin and Jeremy Silver (the University of Melbourne, Australia) for supplying the pollen observation data and Dr. Elizabeth E. Ebert (Weather and Environmental Prediction, Bureau of Meteorology Melbourne, Australia) for useful discussions. L. Ilic and Z. Mijic acknowledge funding provided by the Institute of Physics Belgrade, through a grant by the Ministry of Education, Science and Technological Development of the Republic of Serbia. Partial support has also been provided by the Republic Hydrometeorological Service of Serbia.

REFERENCES

[1] Taylor P. E., Jonsson H., Curr. Allergy. Asthm. (2004) 409–413.

[2] Hughes D. D., Mampage C. B. A., Jones L. M., *et al*., Environ. Sci. Technol. Lett. 7 (2020) 409–414.

[3] D'Amato G., Annesi Maesano, I., Molino, A., *et al*., J. Allergy Clin. Immunol. 139 (2017) 1786-1787.

[4] Grundstein A., Shepherd M., Miller P., *et al*., J. Appl. Meteorol. Clim. 56 (2017) 1337–1343.

[5] Thien F., Beggs P. J, Csutoros D., *et al*., Lancet Planet Health 2 (2018) e255–263.

[6] Lindstrom J.S., Silver D., Sutherland F., Med. J. Aust. 207 (2017) 235–237.

[7] Siljamo P., Sofiev M., Filatova E., *et al*., Int. J. Biometeorol. 57 (2013) 125–136.

[8] Sofiev M., Siljamo P., Ranta H., *et al*., Int. J. Biometeorol. 57 (2013) 45–58.

[9] Wozniak M.C., Solmon F., Steiner A. L., Geophys. Res. Lett. 45 (2018) 7156–7164.

[10] Nickovic S., Kallos G., Papadopoulos A., *et al*., J. Geophys. Res. 106 (2001) 18113–18130.

THE APPLICATION OF SORBENT SYNTHESIZED USING ULTRASOUND FOR REMOVAL OF TEXTILE DYE

Nena Velinov[1*], Slobodan Najdanović[1], Milica Petrović[1], Miljana Radović Vučić[1], Miloš Kostić[1], Jelena Mitrović[1], Aleksandar Bojić[1]

[1]University of Niš, Faculty of Sciences and Mathematics, Department of Chemistry, Višegradska 33, 18000 Niš, SERBIA

[*]*nena.velinov@yahoo.com*

Abstract

An sawdust obtained from oak tree was modified with alumina by simple sonochemical synthesis method. The performance of sorbents obtained with and without sonication was evaluated using sorption process for removal of textile dye Reactive Blue 19 from aqueous media. The sorption optimization was done and the optimal condition for sorption process, such as: pH, sorbent dose and dye concentration were determined. The application of obtained sorbent present very fast sorption with high removal efficiency of dye.

Keywords: wood sawdust, alumina, ultrasound synthesis, dye sorption.

INTRODUCTION

Dyes are widely employed in the food, textile, pharmaceutical, plastics, cosmetics, photographic and paper industries. It is estimated that over 10,000 different dyes and pigments are used industrially, and over 7 x 10^5 tons of synthetic dyes are annually produced worldwide [1]. The discharge of textile dyes is classified as the most polluting of all the industrial sectors, considering the volume generated as well as the effluent composition. Dyes may have negative effects on water plants, animals, and human [2]. Therefore, the development of different processes and technologies for removal of dyes from water could be very important [3].

There are numerous processes used for dyes removal, but the sorption is one of highly effective and progressive treatment [4]. Sorbents obtained using wood biomass waste as a precursor has many benefits, such as: low cost, ease to access, ubiquitous, renewable, and environmental friendliness [5]. The wood biowaste material has specific reactive centres – functional groups, such as: aliphatic and phenolic hydroxyl, methoxy, carbonyl groups, which can be used as a good base for chemical modification using inorganic oxides, such as alumina, to produce highly efficient sorbents [6]. Therefore, the main aim of this research was usage of ultrasound for modification of the sawdust using alumina. The application of the sorbents was evaluated using textile dye Reactive blue 19. The relationship between the synthesis of sorbent with and without sonication and the sorbent efficiency was discussed and the principal parameters, such as: pH, sorbent dose and dye concentration, were investigate.

MATERIALS AND METHODS

The activation agent – $Al(NO_3)_3 \cdot 9H_2O$ and RB19 were purchased from Sigma-Aldrich. HNO_3 and NaOH were reagent grade (Merck, Germany). All chemicals were used without further purification. All solutions were prepared with deionized water (18 MΩ). The wood residue was collected from furniture manufacture in Eastern Serbia. Firstly, the wood residue was fractionated by size and washed with deionized water, then alkali-treated using NaOH for 60 min [5]. After that, 10 g of wood residue each were added into two solutions containing 2.0 g of $Al(NO_3)_3 \cdot 9H_2O$ in 100.0 cm^3 water. One solution was heated to 100°C for 30 min and the second one was sonicated in the ultrasonic bath for 30 min. The obtained materials were treated by trimethylamine, washed with deionized water, and dried at 55±1ºC for 5 h.

Working model solutions of dye were prepared daily by the appropriate dilution of the stock solutions (1.0 g dm^{-3}). The pH of the solutions was adjusted with 0.1/0.01 mol dm^{-3} NaOH/HNO_3 solutions pH-metrically (Orion Star A214, Thermo Fisher Scientific, USA). All experiments were performed at 25.0±0.2°C. The dye concentration was measured at 569 nm using UV-1800 spectrophotometer (Shimadzu, Japan).

The percent of the removed dye (*RE*, %) was calculated using the equation:

$$RE = \frac{c_0 - c_t}{c_0} \cdot 100 \quad (1)$$

where c_0 is the initial concentrations of the dye and c_t is the concentration of the dye in the solution after time t (mg dm^{-3}). The sorption study was menage to analyze the effects of the pH (2.0–12.0), the sorbent dose (0.5–6.0 g dm^{-3}), and initial dye concentration (10.0–1000.0 mg dm^{-3}) on the dye sorption by synthesized sorbent. All experiments were performed in triplicate and ± SD (error bars) are presented in all graphs.

RESULTS AND DISCUSSION

Based on the results (Figure 1), the modification process of wood using alumina probably enabled the formation of new functional groups or active centers on the wood surface, which can bind the dye molecules and remove them from the solution compared to the unmodified sawdust, which has removal efficiency below 1%.

The results of the experiments also show that among the sorbents synthesized with and without sonication, the sorbent obtained using ultrasound during synthesis possess better sorption ability for the removal of dye. The removal efficiency of sorbent obtained using ultrasound was near 100% and for sorbent obtained without ultrasound was 71.7%.

The use of sonication during synthesis of the sorbents affects not only the sorption efficiency, but also the sorption rate, and the sorption equilibrium time. The sorbent synthesized using ultrasound, requires a shorter time to reach the equilibrium of the sorption process and the dye sorption rate increases. Complete dye removal is achieved for less than 10 min for sorbent synthetised using ultrasound and 20 min for sorbent synthesized without sonication. Also, ultrasonic irradiation spent a lot less energy than electric heating used in the conventional synthesis method confirming that the use of ultrasound during synthesis of the

sorbent is a more efficient, quicker, and greener alternative to conventional synthesis without sonication.

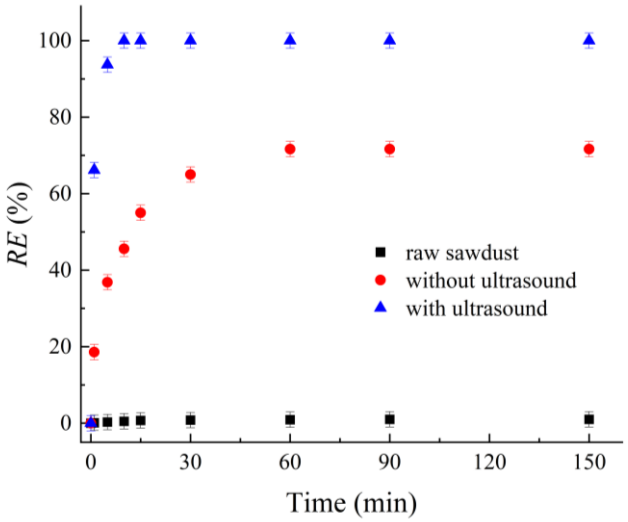

Figure 1 *Effect of ultrasound on sorbent synthesis*

The use of sonication during synthesis of the sorbents affects not only the sorption efficiency, but also the sorption rate, and the sorption equilibrium time. The sorbent synthesized using ultrasound, requires a shorter time to reach the equilibrium of the sorption process and the dye sorption rate increases. Complete dye removal is achieved for less than 10 min for sorbent synthetised using ultrasound and 20 min for sorbent synthesized without sonication. Also, ultrasonic irradiation spent a lot less energy than electric heating used in the conventional synthesis method confirming that the use of ultrasound during synthesis of the sorbent is a more efficient, quicker, and greener alternative to conventional synthesis without sonication.

Optimal parameters for sorption process for sorbent synthetised using sonication, such as: pH, sorbent dose and dye concentration, were investigated. The pH affects the charges on the sorbent surface and the physico-chemical properties of the dye molecule, and also the sorption process and the amount of sorbed dye by synthesized sorbent. To determine the optimal pH for dye sorption, sorption experiments were done in the pH range 2.0–10.0, with other constant parameters (dose 2.0 g dm^{-3} and dye concentration 100.0 mg dm^{-3}). Results show that the dye removal efficiency decrease from 100% to 72.2% with the increase of the pH up to 5.0 (Figure 2). An additional increase of pH up to 10.0 caused a significant decrease of the amount of sorbed dye, removal efficiency is near 2%. The point of zero charge for sorbent synthetised using sonication is 5.41. When the pH is under that value, the charge of the sorbent surface is positive and suitable for sorption of the anions, such as Reactive blue 19 dye, which has negatively charged sulfonic group and therefore the higher attraction with the sorbent surface occurs. On the other hand, with the increase of the pH, the positive charge on surface of the sorbent decreases, so the amount of the sorbed dye also decreases [7]. Consequently, the optimal pH for dye sorption is 2.0, which was used in all further experiments.

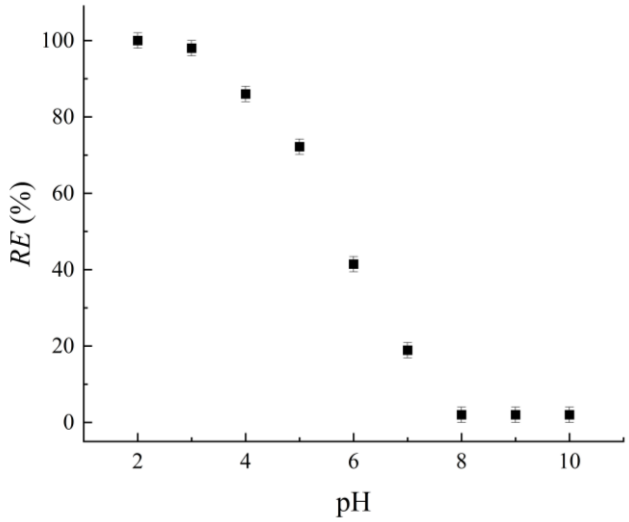

Figure 2 *Effect of pH on dye removal efficiency*

The dye sorption depends on both sorbent dose and dye concentration. The effect of sorbent dose was examined in the range 1–6.0 g dm^{-3}, with other constant parameters (pH 2.0 and dye concentration 100.0 mg dm^{-3}), while the effect of dye concentration was examined in the dye concentration range 100.0–1000.0 mg dm^{-3}, with other parameters constant (pH 2.0 and sorbent dose 2.0 g dm^{-3}). The results show that with the increase of the sorbent dose up to 2.0 g dm^{-3} the dye removal efficiency quickly increases from 40.1 to 100% because the sorbent surface and accessible active sites also increase (Figure 3). The amount of sorbed dye negligibly changed with higher sorbent doses (from 3.0 to 6.0 g dm^{-3}), probably because of higher number of active sites onto sorbent surface regarding the dye amount in the solution [8]. So, the optimal sorbent dose for dye sorption was 2.0 g dm^{-3}, which was used in all other experiments.

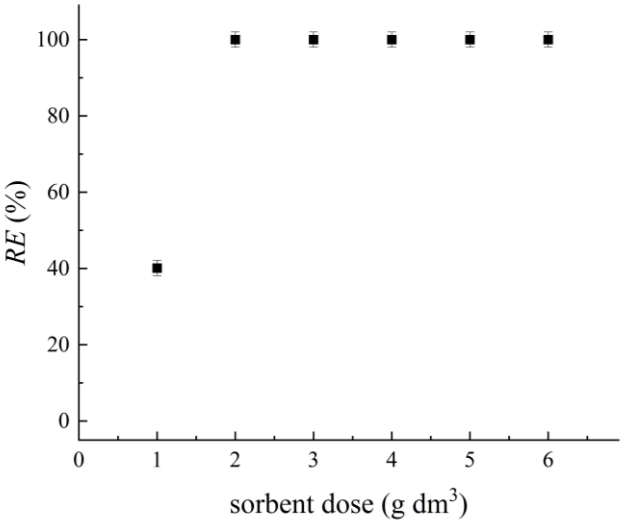

Figure 3 *Effect of sorbent dose on dye removal efficiency*

On the other hand, the results show that with the increase of dye concentration, the dye removal efficiency decrease (Figure 4). Lower tested dye concentrations (100.0–300.0 mg dm^{-3}) show higher removal efficiency values but further increase of the dye concentrations up to 1000.0 mg dm^{-3} led to the increase of the amount of the sorbed dye to a 44.1%. At lower dye concentrations, the number of binding spots for dye sorption on the sorbent surface are much higher so the sorption process does not dependent on dye concentration, but at higher dye concentrations, because of a saturation of the binding spots, the specific amount of dye molecules remains in the solution, so the initial concentration is conditioning dye removal [9].

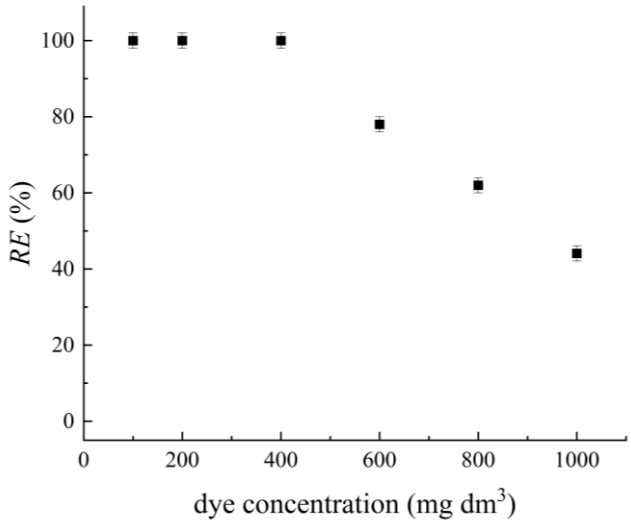

Figure 4 *Effect of initial dye concentration on dye removal efficiency*

CONCLUSION

The use of ultrasound during sorbent synthesis highly affects the sorption characteristics of the obtained sorbent. Obtained sorbent using via sonochemical method possess better sorption ability for the removal of dye with removal efficiency near 100%. The usage of sonication during sorbents synthesis also affects the sorption rate, and the sorption equilibrium time, so complete dye removal is achieved for less than 10 min. The optimal pH value where the amount of sorbed dye has the highest value is 2.0. It can be assumed that the main binding mechanism is ion exchange. The amount of sorbent dye is directly related to the sorbent dose and the optimal value was 2.0 g dm^{-3}. With the increase of initial dye concentration, the dye removal efficiency decreases. The obtained results show that the sorbents synthesized via sonochemical reaction technique present fast sorption with high removal efficiency, which could become potential material for environmental protection.

ACKNOWLEDGEMENT

This work was supported by the Ministry of Science, Technological Development and Innovation of the Republic of Serbia (grant no 451-03-47/2023-01/200124).

REFERENCES

[1] Kaya M., Wood. Sci. Technol. 52 (2018) 245–260.

[2] Leme D. M., de Oliveira G. A. R., Meireles G., *et al*., Toxicol. Environ. Health. Part. A. 78 (2015) 287–300.

[3] Kadhom M., Albayati N., Alalwan H., *et al*., Sustain. Chem. Pharm. 16 (2020) 100259.

[4] Wang J., Chen N., Li M., *et al*., J. Polym. Environ. 26 (4) (2018) 1559–1572.

[5] Mangwandi C., Kurniawan T. A., Albadarin A. B., Chem. Eng. Res. Des. 156 (2020) 251–262.

[6] Monteiro M. S., de Faria R. F., Chaves J. A. P., *et al*., J. Environ. Manage. 204 (2017) 23.

[7] Rambabu K., Bharath G., Banat F., *et al*., Environ. Res. 187 (2020) 109694.

[8] Rafiaee S., Samani M. R., Toghraie D., Synth. Met. 265 (2020) 116416.

[9] da Rocha Ferreira G. L., Vendruscolo F., Antoniosi Filho N. R., Heliyon 5 (3) (2019) e01450.

30th International Conference Ecological Truth & Environmental Research
20–23 June 2023, Serbia

ATMOSPHERIC PRESSURE CORONA PLASMA DEGRADATION OF REACTIVE ORANGE 4 IN DEIONIZED AND RIVER WATER

Milica Petrović[1*], Slobodan Najdanović[1], Nena Velinov[1], Saša Rančev[2], Dragan Radivojević[2], Miljana Radović Vučić[1], Aleksandar Bojić[1]

[1]University of Niš, Faculty of Science and Mathematics, Department of Chemistry, 33 Višegradska str., 18000 Niš, SERBIA

[2]University of Niš, Faculty of Science and Mathematics, Department of Physics, 33 Višegradska str., 18000 Niš, SERBIA

[*]*milicabor84@gmail.com*

Abstract

Degradation of Reactive Orange 4 dye by atmospheric pressure positive pulsating corona plasma self made reactor was examined in deionized and river water. Degradation proceeded via hydroxyl radical, •OH, generated by plasma decomposition of previously plasma generated H_2O_2 in water. Production of H_2O_2 and dye degradation rate were about 30% and 23% lower, respectively, in river water due to the presence of the substances which consumed •OH in competitive reactions. Dye degradation rate was the highest at pH 5.5, slightly lower at pH 3 and significantly lower at pH 10. The fastest degradation was observed at the maximal input voltage of 12 kV and it decreased with the decrease of the input voltage. Total organic carbon removal (TOC) % was about 81% after 150 minutes of the treatment and it practically did not change further.

Keywords: corona discharge, degradation, dye, river.

INTRODUCTION

Textile dyes in natural water pose the environmental threat, particularly due to their high chemical resistance in the environment. However, they can be degraded by the hydroxyl radical, •OH, a strong oxidant which is obtained by so-called advance oxidation processes (AOPs). Plasma degradation, as one of them, is based on the ionization of gas and/or liquid by the high voltage discharge that generates active ion and radical species, like •OH, which further oxidizes and degrades dye molecules [1,2] Various types of discharge were used for this purpose, such as plasma jet [2,3], dielectric barrier discharge (DBD) [4] gliding arc discharge (GAD) [5–7] and atmospheric pressure corona discharge. The advantages of the latest are the ability to operate in open air at atmospheric pressure and ambient temperature, to degrade several pollutants simultaneously and the simplicity of construction and high energy yield in the dye decolorization processes [8].

This work deals with the degradation of Reactive Orange 4 (RO 4) textile dye in model river water by self made atmospheric pressure positive pulsating corona plasma reactor. Role of the plasma generated H_2O_2, as well as the most important degradation parameters were examined.

MATERIALS AND METHODS

Materials

RO 4 was purchased from Sigma Aldrich and used without further purification. The solutions were prepared with deionized water (18 MΩ, Smart2Pure, Thermo Scientific, USA) and with water of Nišava River (Republic of Serbia), taken in the flask in the centre of the city of Niš.

Plasma reactor

Plasma experiments were performed using a self made device, consisting of power supply, DC pulse generator, high voltage output stage, and open chamber. The positive corona discharge was created in the gas phase (air) over the liquid, on the tips of the multipoint anode, made of stainless steel needles of mutually equal dimensions, while the cathode was the liquid surface (dye solution). The reactor cell was a polyvinyl chloride cylinder. The stainless steel contact electrode was centered at the bottom of the reactor cell and connected to the ground potential. The discharge current was controlled by the electronic circuitry of the device, adjusting the voltage at the multipoint anode. Gases produced by the discharge were removed through the exhaust system. The reactor average total current I and discharge voltage U (V) were measured by the multimeter Iskra Unimer 06 and with high voltage probe Tektronix P6015A, respectively. The current and voltage signals were recorded using Digital oscilloscope TDS 2024C. The working frequency was set to 40 kHz and the corona discharge was without sparks and with appearance of low intensity streamers. Some of the streamers reached the liquid surface and extinguished without their transition into sparks. The experimental set-up is schematically shown in Figure 1.

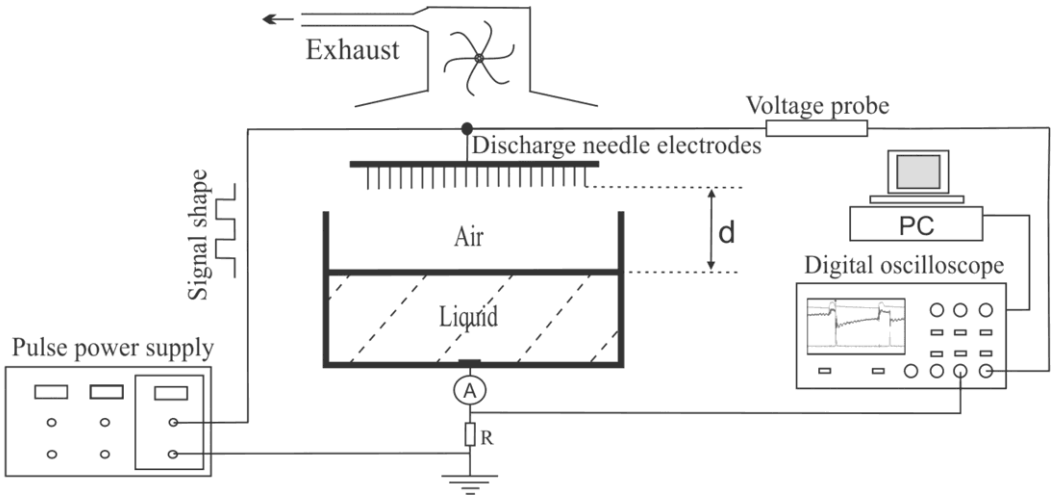

Figure 1 *The experimental set up*

Dye degradation

Working dye solutions were prepared by dissolving the required amount of dye in deionized and river water (stock solutions) and by diluting those solutions to the required concentrations. Prior to that, the river water was filtered 0.45 μm filter. Degradation experiments were done using the described plasma reactor at ambient temperature of

22±01°C at native pH (5.50). Dye concentration was measured by UV-VIS spectrophotometer Shimadzu UV-1650 PC (Japan) at 490 nm. Plasma – formed H_2O_2 was determined spectrophotometrically, by iodometric method. The temperature and pH of the solutions were measured using pH meter (SensIon3, Hach, USA).

RESULTS AND DISCUSSION

Decolorization and role of the plasma generated H_2O_2

Plasma decolorization of 40 mmol dm^{-3} RO 4 proceeded little slower in river than in deionized water (Figure 2). It took about 5.5 and 8.5 minutes for the decolorization of 50% of initial dye amount in deionized and river water, respectively. Complete decolorization in deionized water was achieved in about 30 minutes, while decolorization in river water was about 95% at that point.

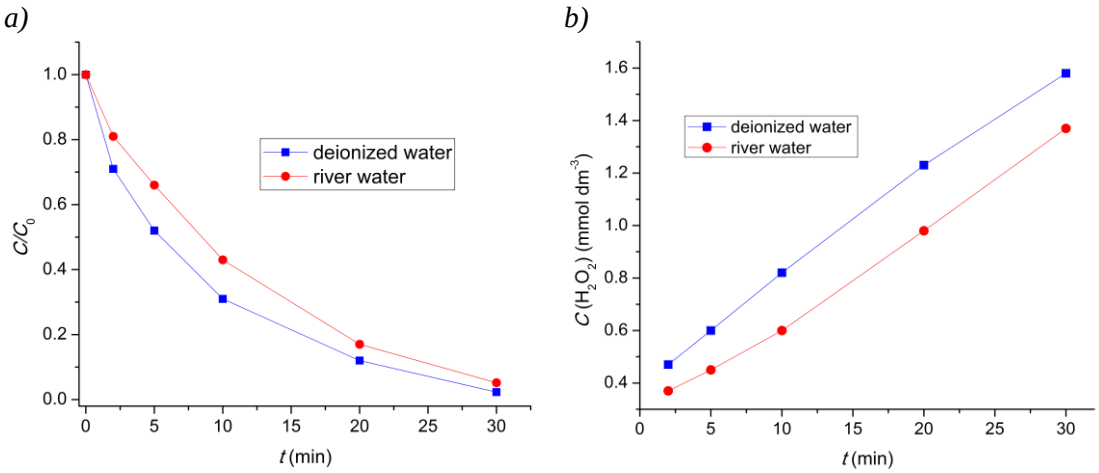

Figure 2 *Comparison of a) decolorization rate and b) H_2O_2 concentration during the plasma treatment of RO 4 solution in deionized and river water*

H_2O_2 was produced both in deionized and river water during their treatment by plasma. It was formed in water when the active species generated by the plasma discharge in air (in this case mostly positive ions and radicals, like •O, •NO, O^+, O_2^+ etc.) and fast electrons, accelerated by the strong electric field, penetrated the water surface and stroke the water molecules. That can be represented by the following equations [3,6,7]

$$O_2 + e^-_{plasma\ generated} \rightarrow O + O + e^- \quad (1)$$

$$O + H_2O \rightarrow 2{\bullet}OH \quad (2)$$

$${\bullet}OH + {\bullet}OH \rightarrow H_2O_2 \quad (3)$$

Once formed, H_2O_2 underwent the plasma decomposition into •OH radical, a strong oxidant, which attacked and destroyed dye molecules:

$H_2O_2 \rightarrow 2{\bullet}OH$ (4)

RO 4 + $\bullet OH \rightarrow$ *degradation products* (5)

That was proven by the addition of isopropanol, an •OH scavenger, to the solutions, which lead to the drop of decolorization rate in both deionized and river water by more than 90%, while some other radical scavengers barely affected it. This strongly indicates that H_2O_2 was consumed during the plasma decolorization as the source of dye degrading •OH radical [9]. Its concentration increased approximately linearly in both deionized and river water, but the increase rate is lower in the later. The reason is the presence of dissolved organic matter and some inorganic ions, such as Na^+, Ca^{2+}, SO_4^{2-}, Cl^-, HCO_3^-, etc., which were detected in the river water. So, part of the plasma-generated •OH radicals reacted with the organic matter and ions which acted like the radical scavengers in the parallel competitive reactions, thus making •OH radicals less accessible for the dye molecules. This reflected in the decolorization efficiency of the process in river water, which is somewhat lower than in deionized one. However, the efficiency of the process did not decreased much and it still remains relatively high [6,7].

Effect of input voltage on decolorization process in the river water

Decolorization rate increased with the increase of the input voltage U (Figure 3). The increase of U provided a stronger electric field in the discharge gap between anode and cathode (solution surface) which increased ionization rate and acceleration of the plasma-generated active species. Thus, higher voltages provided more strikes with higher energy, that lead to creation of more •OH radicals for dye degradation. Degradation rate was the highest at 12 kV and the lowest at 7.5 kV. At the voltages higher than 12 kV the discharge became instable, with the appearance of sparks, and at the ones lower than 7.5 kV, ionization of the gas stopped, with the visible disappearance of corona.

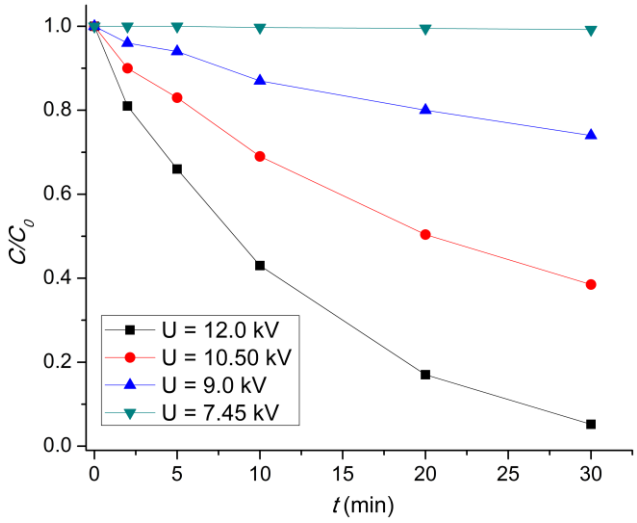

Figure 3 *Effect of the input voltage on the plasma decolorization of river water*

Effect of pH on decolorization process in the river water

Decolorization rate in the river water was the highest at pH 5.5 (Figure 4). It slightly decreased at pH 3 and significantly decreased at pH 10. The decrease of the plasma process efficacy in acidic medium was probably caused by protonation of some reactive species and intermediates and in basic medium it was caused by scavenging effect of OH^- ions [10].

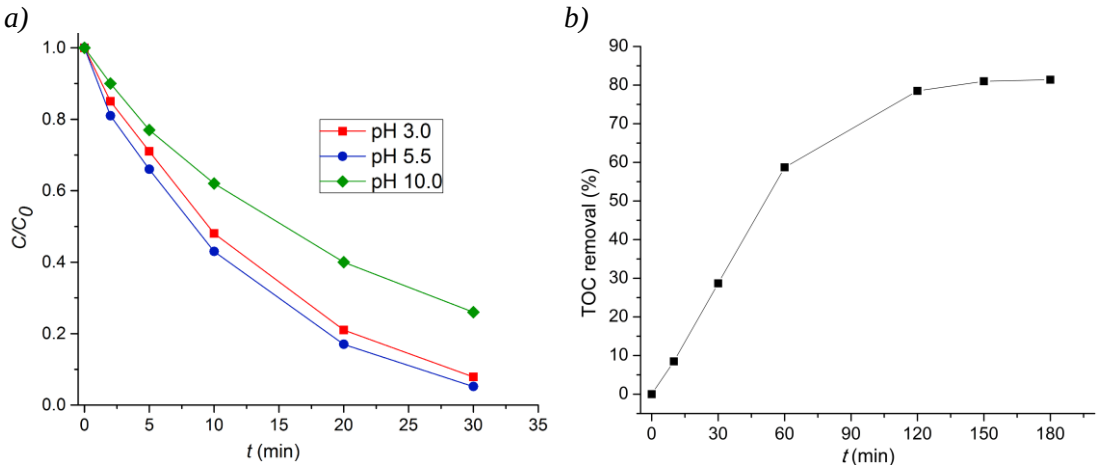

Figure 4 *a) Effect of pH and b) TOC removal % in the process of plasma degradation of river water*

TOC removal

TOC removal % rapidly increased in approximately linear manner during the first 60 minutes of the treatment. After that, the increase rate slowed down, and it attained its maximal value of about 81% after 150 minutes of the treatment. Further increase of the treatment time did not provide significant and industrially justified TOC removal. The attained TOC removal is river water by the plasma treatment is high, meaning that more than 80% of the starting compound was mineralized.

CONCLUSION

Reactive Orange 4 dye was removed from both deionized and river water by atmospheric pressure pulsating positive corona plasma. Dye was degraded via oxidation by the •OH radical, a product of the plasma decomposition of H_2O_2. Peroxide had been previously generated by the electrical discharge which caused the ionization of air in the discharge gap and creation of highly reactive positive ion and radical species, as well as the fast electrons that further stroke the liquid surface and reacted with the water molecules, generating peroxide. Generation of peroxide and consequently, decolorization rate was higher in deionized water due to the presence of organic matter and inorganic ions in river water which react with the •OH radical, making it less accessible for the dye molecules. Decolorization rate in river water increased with the increase of the input voltage. The fastest decolorization was observed at pH 5.5 and it was significantly slower at pH 10. TOC removal % was about 81% and it was attainted after about 150 minutes of the treatment, which indicates a high degree of the mineralization of the starting compound in real water by the atmospheric pressure corona plasma.

ACKNOWLEDGEMENT

The authors would like to acknowledge financial support from the Ministry of Science, Technological Development and Innovation of the Republic of Serbia (Agreement No 451-03-47/2023-01/200124).

REFERENCES

[1] Ma D., Yi H., Lai C., *et al.* Chemosphere 275 (2021) 130104.

[2] García M. C., Mora M., Esquivel D., *et al*., Chemosphere 180 (2017) 239–246.

[3] Pandiyaraj K. N., Vasu D., Ghobeira R., *et al*., J. Hazard. Mater. 405 (2021) 124264.

[4] Meropouli S., Rassias G., Bekiari V., *et al*., Sep. Purif. Technol. 274 (2021) 119031.

[5] Tarkwa J-B., Acayanka E., Jiang B., *et al*., Appl. Catal. B: Environ. 246 (2019) 211–220.

[6] Ghezzar M. R., Abdelmalek F., Belhadj M., *et al*., J. Hazard. Mater. 164 (2009) 1266–1274.

[7] Hentit H., Ghezzar M. R., Womes M., *et al*., J. Mol. Catal. A: Chem. 39 (2014) 37–44.

[8] Kusumandari K., Saraswati T. E., Wulandari S. W., *et al*., Indian J. Phys. 96 (2022) 1001–1008.

[9] Rančev S., Petrović M., Radivojević D., *et al*., Plasma Sci. Technol. 21 (2019) 125501.

[10] Jiang B, Zheng J, Liu Q., *et al*., Chem. Eng. J. 204–206 (2012) 3–39.

THE INFLUENCE OF TYPE OF SOLVENT ON THE ELECTROCHEMICALLY SYNTHESIZED SORBENTS BASED ON BASIC BISMUTH NITRATES

Slobodan Najdanović[1*], Milica Petrović[1], Nena Velinov[1], Miloš Kostić[1], Jelena Mitrović[1], Danijela Bojić[1], Aleksandar Bojić[1]

[1]University of Niš, Faculty of Sciences and Mathematics, Department of Chemistry, Višegradska 33, 18000 Niš, SERBIA

[*]*najda89@gmail.com; slobodan.najdanovic@pmf.edu.rs*

Abstract

In this work, basic bismuth nitrates were synthesized by galvanostatic electrodeposition from solution of bismuth nitrate in nitric acid, followed by thermal treatment of the obtained deposit at 200 ºC. Electrodeposition was performed from different solvents: deionized water, ethanol, propanol, butanol, 96% ethanol, 96% propanol and 96% butanol. The parameters of the electrodeposition process were current density of 150.0 mA cm^{-2} for a duration of 5.0 min. The obtained materials were applied for sorption of textile dye Reactive Blue 19 (RB19). The effect of the solvent used to prepare the electrodeposition solution on the sorption performance of the obtained material was investigated.

Keywords: electrodeposition, textile dyes, Reactive Blue 19, water treatment.

INTRODUCTION

Worldwide production and extensive use of dyes in industries such as textile, paper, printing, leather, food, and cosmetics can generate colored effluent. Dye RB19 is commonly used in the textile and leather industry and may be mutagenic and toxic because of the presence of electrophilic vinyl sulfone groups [1]. Being mutagenic and carcinogenic, most of the dyes are highly toxic to the aquatic biota [2]. Various methods like sorption, chemical oxidation, photocatalytic degradation, ion exchange, ozonation, etc. have been developed to remove dyes from wastewaters. Among all methods, sorption is highly preferred due to its cost-effectiveness, efficiency, reusability of sorbents, and because it requires little technological equipment [2].

Basic bismuth nitrates have been known since the 17th century [3]. They are known under the trade names Magisterium bismuthi and Bismutum subnitricum and are used in medicine as mild antiseptics [4]. Recently, basic bismuth nitrates have been used for sorption and photocatalytic degradation of organic pollutants [5–7]. Also, they are used as precursor for bismuth oxide production [8]. Basic bismuth nitrates are usually obtained by hydrolysis of bismuth nitrate pentahydrate ($Bi(NO_3)_3 \cdot 5H_2O$). Bismuth nitrate pentahydrate is commonly used as a source of bismuth for the preparation of bismuth-based compounds due to its efficiency and availability [5].

The aim of this work is to synthesize basic bismuth nitrates by electrodeposition from bismuth nitrate solution from different solvents and comparation of its efficiencies for RB19 removal. Also, the influence of solution pH on the sorption efficiency was investigated.

MATERIALS AND METHODS

Chemicals

Textile dye RB19 (chemical formula: $C_{22}H_{16}N_2Na_2O_{11}S_3$) was obtained from Sigma-Aldrich (Germany). Bismuth nitrate pentahydrate was obtained from the Acros Organics (USA). Other chemicals such as ethanol, propanol, butanol, nitric acid, sodium hydroxide was purchased from Sigma-Aldrich (Germany). All the chemicals were of analytical grade and used as received without further purification. Deionized water was used for the preparation of all solutions.

Procedure of electrochemical synthesis of materials

The electrochemical procedure of material synthesis is based on cathodic electrodeposition from acidic solution of bismuth nitrate. Electrodeposition was performed from solutions obtained by dissolving appropriate amounts of bismuth nitrate in a nitric acid concentration of 1.0 mol dm^{-3}. The bismuth nitrate concentration in the solutions were 0.1 mol dm^{-3}. As solvents in solutions for electrodeposition were used deionized water, ethanol, propanol, butanol, 96% ethanol, 96% propanol and 96% butanol.

A two-electrode cell with a titanium sheet as the cathode (working electrode) and a stainless-steel sheet as the anode (counter electrode) was used for the electrodeposition experiments. The dimensions of titanium and stainless-steel sheets were 10x20 mm. The distance between them in the electrochemical cell was 15 cm. All electrodes were prepared before use as follows: by polishing with abrasive paper, by degreasing with detergent, and then by cleaning with ethanol and deionized water in an ultrasonic bath. A potentiostat-galvanostat Amel 510 DC (Material Mates, Italy) was used for electrodeposition experiments. The software package VoltaScope was used to set the parameters of the electrodeposition process and to control the potentiostat-galvanostat operation. Cathodic electrodeposition was done in galvanostatic regime at constant current density of 150.0 mA cm^{-2} for 5.0 min. The obtained deposit was then thermally treated at 200 ºC for 90 min. After cooling in air, the obtained material was removed from the titanium electrode, ground into powder and used as such in all experiments.

Sorption experiments

Batch sorption experiments were performed at room temperature in Erlenmeyer flasks. The pH of the initial dye solution was adjusted by adding nitric acid and sodium hydroxide. A sorbent in a dose of 500.0 mg dm^{-3} was added to 50.0 cm^3 of a dye solution of a certain concentration. The mixing speed of the solution was 200 rpm. The samples were collected at desired time intervals and filtered immediately through 0.45 µm membrane filters made of regenerated cellulose. The residual concentration of RB19 in the samples was determined using a UV-Vis spectrophotometer Shimadzu UV-1800 (Japan). The amount of sorbed RB19 dye (q_t, mg g^{-1}) and the removal efficiency (*RE*, %) was determined by using the following equations:

$$q_t = \frac{c_0 - c_t}{m} \cdot V \quad (1)$$

$$RE(\%) = \frac{c_0 - c_t}{c_0} \cdot 100 \quad (2)$$

where c_0 and c_t are the initial and final concentrations of the RB19 (mg dm^{-3}), V is the solution volume (dm^3), and m is the mass of the sorbent (g).

Determination of isoelectric points (pI) of materials

The isoelectric points of the sorbents were determined using the method of adding salt [9]. A solution of $NaNO_3$ (0.1 mol dm^{-3}) was prepared and used as an inert electrolyte. Then a series of test solutions was prepared by measuring 50.0 cm^3 of inert electrolyte and adjusting pH in the range from 2.0 to 11.0. To adjust pH, solutions of HNO_3 (0.01 mol dm^{-3}) and NaOH (0.01 mol dm^{-3}) were used. Then sorbent (0.2 g) was added to each solution, the Erlenmeyer flask was closed, stirred for 24 h, and the final pH (pH_f) was measured. The pH_f values were plotted against the initial pH (pH_i), and the pI was determined from the data where $pH_i = pH_f$.

RESULTS AND DISCUSSION

Sorption performances of materials obtained from different solvents

The solvent, i.e., the medium from which the electrodeposition is performed, has a huge effect on the sorption performances of obtained materials. The results of RB19 removal efficiency are shown in Figure 1.

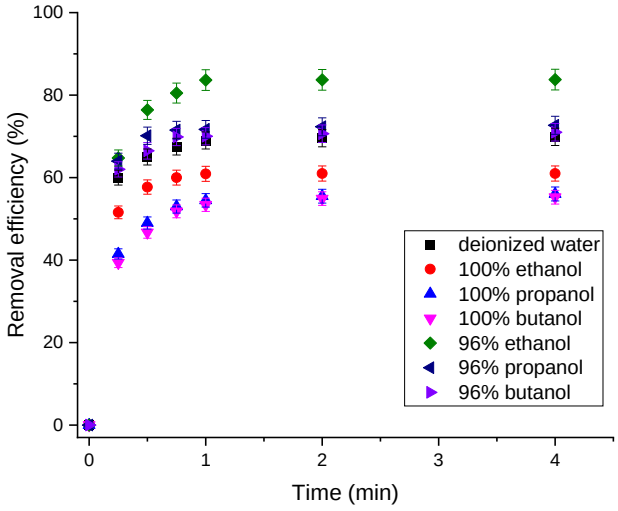

Figure 1 *Comparison of RB19 dye removal efficiency using sorbents synthesized in deionized water, pure and 96% alcohols (ethanol, propanol and butanol): initial dye concentration RB19 600.0 mg dm^{-3}, sorbent dose 500.0 mg dm^{-3}, native pH, mixing speed 200 rpm, temperature 25.0 ± 0.5 ºC*

Due to the high concentration of dye that was applied during the sorption treatments, it can be said that all materials are very effective. However, materials obtained using 96% solvents showed significantly higher efficiency compared to materials obtained from pure solvents. The removal efficiency of RB19 by sorbent synthesized by electrodeposition from 96% ethanol was 83.8%, from 96% propanol 72.8%, and from 96% butanol 71.0%, while the

efficiency of sorbents synthesized from pure solvents was 61.0%, 56.0% and 55.2%, respectively.

Figure 2 shows a comparison of the sorption capacities of the materials. Sorbents synthesized from solvents with a concentration of 96% are about 30% more efficient. By using pure solvents due to the lack of water molecules in the system, the oxidation of deposited Bi is incomplete; since metal Bi has no sorption activity, the obtained materials have poorer sorption performance. The efficiency of materials synthesized from ethanol, propanol and butanol decreases according to the given order in accordance with the decrease of their polarity [10].

The sorbent synthesized from deionized water has a higher removal efficiency (69.9%) than sorbents synthesized from pure solvents, and lower than sorbents obtained from 96% solvents. One of the most important characteristics of materials obtained by electrodeposition from 96% of solvents is their high hydrophilicity, i.e., tendency to solvate which is why they do not float on water. This provides better liquid-solid phase contact, so it can be assumed that this is one of the main reasons for the higher efficiency of these materials in relation to the material obtained from aqueous solution.

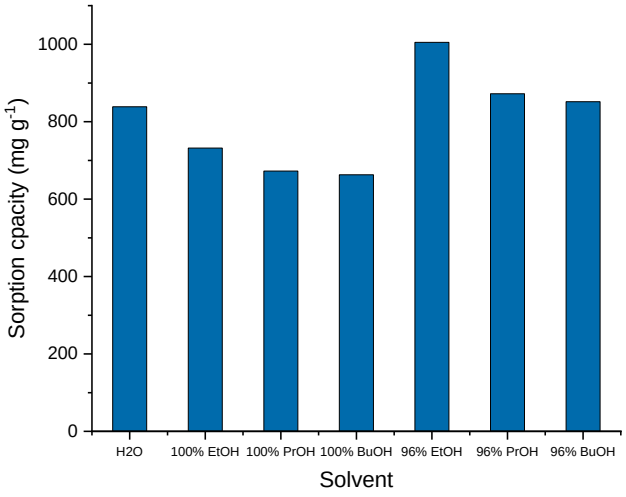

Figure 2 *Comparison of sorption capacities of materials obtained from different solvents: initial dye concentration RB19 600.0 mg dm^{-3}, sorbent dose 500.0 mg dm^{-3}, native pH, mixing speed 200 rpm, temperature 25.0 ± 0.5 ºC*

Effect of pH

Surface charge of a material has a huge impact on its sorption performance. If the pH of the solution is lower than the isoelectric point of the material, its surface will be positively charged. Otherwise, when pH is higher than the isoelectric point, the surface of the material will be negatively charged. This is why the isoelectric points of the materials were determined. The results are shown in Table 1.

Table 1 *The isoelectric points of obtained materials from different solvents*

Solvent	Isolectric point
deionized water	2.12
100% ethanol	2.10
100% propanol	2.14
100% butanol	2.12
96% ethanol	2.09
96% propanol	2.11
96% butanol	2.15

The results show that the isoelectric points of all materials are similar, and their values are extremely low. Based on these results, it can be concluded that the sorption of negatively charged molecules will be more favored at low pH values, while the sorption of positively charged molecules will be more favored at higher pH values.

The effect of solution pH on the efficiency of color removal is the same for all materials. Therefore, the results are shown in Figure 3 only for the most effective material (obtained from 96% ethanol).

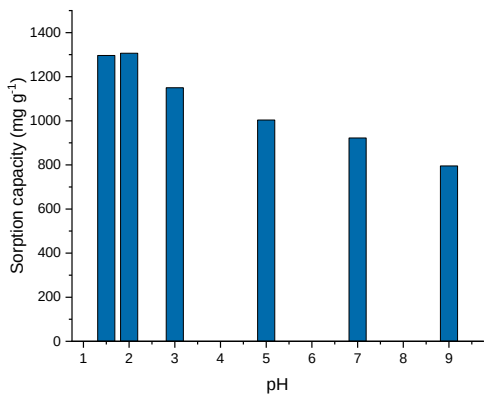

Figure 3 *Effect of solution pH on the maximum sorption capacity of the material obtained from 96% ethanol: initial dye concentration RB19 700.0 mg dm^{-3}, sorbent dose 500.0 mg dm^{-3}, mixing speed 200 rpm, temperature 25.0 ± 0.5 ºC*

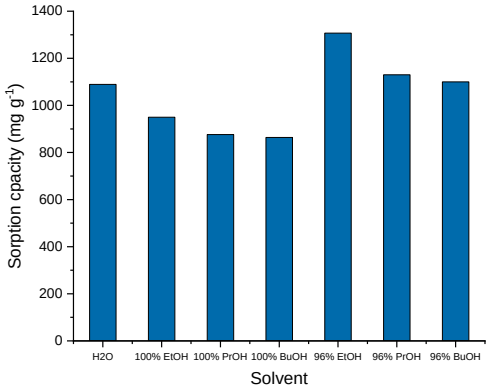

Figure 4 *Comparison of maximum sorption capacities of obtained materials at solution pH 2.0: initial dye concentration RB19 700.0 mg dm^{-3}, sorbent dose 500.0 mg dm^{-3}, mixing speed 200 rpm, temperature 25.0 ± 0.5 ºC*

The results show that the highest sorption capacity is achieved at pH 1.5 and 2.0, and with a further increase in the pH of the solution, the sorption capacity decreases. This can be explained by the low isoelectric point of the material (2.09). Since the dye RB19 is anionic and the surface charge of the material is positive at pH less than 2.09, the strongest electrostatic attraction is at pH ≤ 2.09, and therefore the highest sorption capacity. The maximum sorption capacities for all materials at pH 2.0 are presented in Figure 4.

CONCLUSION

Basic bismuth nitrates were successfully synthesized by electrochemical deposition from an acidic bismuth nitrate solution and further thermal treatment at 200 ºC. Experimental results suggest that materials obtained from different solvents have different sorption efficiencies for RB19. The materials synthesized from 96% solutions have higher sorption efficiencies than material synthesized from 100% solutions. The sorption efficiency of materials synthesized from ethanol, propanol and butanol decreases, respectively, in accordance with the decrease of their polarity. Thus, the most effective material is material synthesized from 96% ethanol. The maximum sorption capacity was obtained at pH 2.0 for all materials, and it is 1307 mg g^{-1} for the most efficient material.

ACKNOWLEDGEMENT

The authors are grateful to the Ministry of Science, Technological Development and Innovation of the Republic of Serbia for financial support according to the contract with the registration number 451-03-47/2023-01/200124.

REFERENCES

[1] Karimifard S., Alavi Moghaddam M. R., Process Saf. Environ. Prot. 99 (2016) 20–29.

[2] Menkiti M. C., Aniagor C. O., Arab. J. Sci. Eng. 43 (5) (2018) 2375–2392.

[3] Henry N. Evain M., Deniard P., *et al*., J. Solid State Chem. 176 (1) (2003) 127–136.

[4] Christensen N. A., Lebech B., Dalt. Trans. 41 (7) (2012) 1971–1980.

[5] Pang J., Han Q., Liu W., *et al.*, Appl. Surf. Sci. 422 (2017) 283–294.

[6] Xiao J., Zhang H., Xia Y., *et al.*, RSC Adv. 6 (46) (2016) 39861–39869.

[7] Gong S., Han Q., Wang X., *et al.*, Cryst. Eng. Comm. 17 (2015) 9185–9192.

[8] Abdullah E. A., Abdullah A. H., Zainal Z., *et al.*, E-Journal Chem. 9 (4) (2012) 1885–1896.

[9] Mahmood T., Saddique M. T., Naeem A., *et al.*, Ind. Eng. Chem. Res. 50 (17) (2011) 10017–10023.

[10] Koizumi N., Hanai T., Bull. Inst. Chem. Res. Kyoto Univ. 33 (1) (1955) 14–20.

APPLICATION OF MICROALGA *Chlorella sorokiniana* IN WASTEWATER BIOREMEDIATION – CASE OF LAKE ROBULE

Milena Dimitrijević[1*], Snežana Kovačević[1], Uroš Jovanović[2], Marina Stanić[1], Miloš Opačić[1], Isidora Santrač[1], Marija Tanović[1], Valentina Ćurić[3], Ivan Spasojević[1]

[1]University of Belgrade, Institute for Multidisciplinary Research, Kneza Višeslava 1, 11030 Belgrade, P.O. Box 33, SERBIA

[2]University of Belgrade – Vinča Institute of Nuclear Sciences, P.O. Box 522, 11001 Belgrade, SERBIA

[3]University of Belgrade-Faculty of Biology, Studentski trg 16, 11000, Belgrade, SERBIA

[*]*milena.dimitrijevic@imsi.bg.ac.rs*

Abstract

Heavy metals remain a major pollutant in waters near mining sites. Water pollution is a current, long-term problem that affects plants and organisms that live in these water systems, and the effect is very harmful not only for individual species and populations, but also for the entire biological community. This study analyzed the potential of the microalga Chlorella sorokiniana in the adsorption of four selected metals: Fe, Cu, Zn and Ni, all present in high amounts in Lake Robule. This pilot study was conducted to evaluate the potential of these microalgae for possible use in future bioremediation treatment of these water. A laboratory study of metal accumulation in lake water samples lasted for 7 days, after which a total decrease in metal concentration was observed, namely Fe ~25%, Cu ~17%, and Zn ~4% on the seventh day. This study confirms the strong potential of microalgae C. sorokiniana to reduce the presence of heavy metals in conditions known for the low pH value of water with a high percentage of Fe and other heavy metals.

Keywords: heavy metals, microalgae, *C. sorokiniana*, Lake Robule.

INTRODUCTION

Pollution of the environment with various compounds, where heavy metals are among the first, is a big problem everywhere. Today, more than before, awareness has been raised about the consequences of water pollution in the vicinity of mines, and monitoring is becoming mandatory, and intensive work is being done on bioremediation projects [1,2]. Microalgae are increasingly attracting the attention of researchers due to their ability to remove heavy metals, inorganic nitrogen, phosphorus and some toxic organic compounds [3–5]. Given the actuality of the mentioned problem and with the aim of maintaining the availability of quality water resources, the biological treatment of wastewater using microalgae stands out as attractive biotechnology. In this field, accelerated development can be observed, which is profitable both economically and ecologically [6–8]. Numerous studies to optimize the growth and productivity of microalgae have focused on the cultivation of microalgae in various wastewater streams, including municipal, industrial and agricultural waste, which, in addition to nutrients, may contain heavy metals, metalloids and various organic pollutants [9]. There is

ample evidence that it is possible to use microalgae in wastewater to achieve several goals at the same time: purification of wastewater, synthesis of valuable metabolic products and accumulation of algal biomass that can be used as fertilizer [3,6].

Here, a study was made on real samples of the accumulation of Lake Robule, which was located next to the copper mining excavations in Bor, Serbia. The goal of the work was to evaluate the potential of using the microalgae *Chlorella sorokiniana* for phytoremediation of mining wastewater, ie for the absorption of heavy metals in a highly acidic environment.

MATERIALS AND METHODS

C. sorokiniana cultivation and experimental design

Chlorella sorokiniana strain CCAP 211/8K was obtained from the Culture Collection of Algae and Protozoa (CCAP), UK. Microalgae inoculum was added to 50 ml of 3N-BBM+V medium in 100 ml Erlenmeyer flasks at an initial density of 0.5×10^6 cells ml^{-1}. The initial pH of the medium was ~7.5. Microalgal cultures were grown at 22 °C on orbital shakers (120 rpm) in a growth cabinet with a continuous photon density of 120 µmol m^{-2} s^{-1}. Volume of the samples was corrected for evaporation on day 15 with sterile deionized water. Growth was monitored spectrophotometrically at 750 nm (OD750), which is proportional to cell density. Microalgae were transferred to Robule Lake water on day 20 (early stationary phase). The entire amount of culture was centrifuged at 5000 g for 5 minutes and resuspended in 50 ml of lake water. The resistance of cultures to lake water was examined by measuring the OD750 of control and samples at 1 h, 24 h, 72 h and 168 h after treatment.

At each time point after sampling, 2 ml aliquots of the cultures were centrifuged at 5000 g for 5 min and the supernatant was collected for heavy metal analysis. 4 µl of 65% HNO_3 per 1 ml was added to the supernatant, filtered through a nylon filter with a diameter of 22 µm and diluted 2 times (for Ni) or 20 times for other metals. Control samples remained in 3N-BBM+V medium. All chemicals were purchased from Sigma-Aldrich (St. Louis, MI, USA).

Chemical analysis of heavy metals

The content of Fe, Cu, Zn and Ni in solutions was determined by using the flame atomic emission spectroscopy (AAS Aanalyst 700/Perkin-Elmer). Standard solution (Merck, Darmstadt, Germany) and 18.2 MΩ water were used for preparing calibration standards.

Statistical analysis

To test for significant effects, Tukey's post hoc test was used to test for significant differences in metal absorbance at different time points among different sample groups. Tukey's post hoc tests were performed using IBM SPSS statistical software (version 20.0, SPSS Inc., Chicago, IL, USA). The significance threshold value was set at 0.05.

RESULTS AND DISCUSSION

The initial metal concentration in the water sample is Cu 48.125 ± 0.006 mg/L: Zn 19.272 ± 0.003 mg/L; Fe 296.550 ± 0.006 mg/L and Ni 0.687 ± 0.033 mg/L. The adsorbed amount of metals shown by time points and for target metals (Table 1) shows that there is a reduction in

water pollution with metals in the presence of microalgae *C. sorokiniana*. The best results were obtained with Fe, where after 7 days (168 h) there was a reduction of more than 25% of the initially present amount of metal and for Cu ~17%, and Zn ~4% in the same, 7 day.

Table 1 *The decrease in the amount of Fe, Cu, Zn and Ni in the Lake Robule water after treatment with microalgal culture. The amount of aforementioned metals was measured after 1 h, 24 h, 72 h and 168 h (7 days)*

Amount of adsorbed metals in [mg/L]	**1 h**	**24 h**	**72 h**	**168 h**
Cu	0.480 ± 0.009	7.610 ± 1.320	4.229 ± 0.105	8.453±0.050
Zn	0.423 ± 0.005	4.050 ± 0.053	1.939 ± 0.021	8.453±0.050
Fe	16.870 ± 3.150	68.635 ± 7.245	48.580 ± 2.940	73.350±1.320
Ni	/	/	/	/

The percentage values shown in Figures 1–3 (decrease of each metal in water of Lake Robule after treatment with microalgal culture at different time points) are percentages calculated in relation to the measured values of metals in the water before treatment and the values measured at a given time point. The decrease is expressed as the percentage of the metal amount in untreated water and can be attributed to adsorption and/or absorption of metal by microalgal cells.

The Figures below (Figure 1 and Figure 3) show that Cu and Fe are absorbed in the same way; the greatest effect of absorption is in the first 24 hours, while it then decreases to return in seven days to the same value as in 24 hours. In the case of zinc (Figure 2), the absorption dynamics are different. It reaches a maximum of 24 hours, while after that it only reaches a decrease in the value of the absorbed amount of metal.

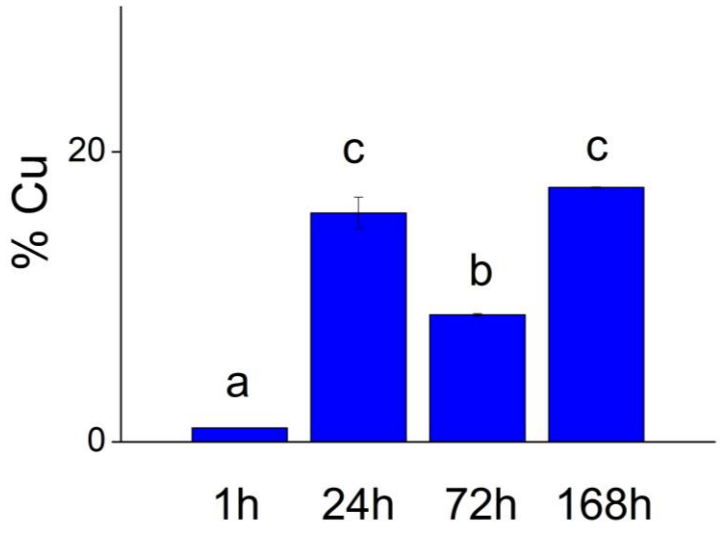

Figure 1 *Amount of absorbed Cu and/or absorbed expressed as a percentage by time points. Different letters indicate significant differences based on Tukey's test*

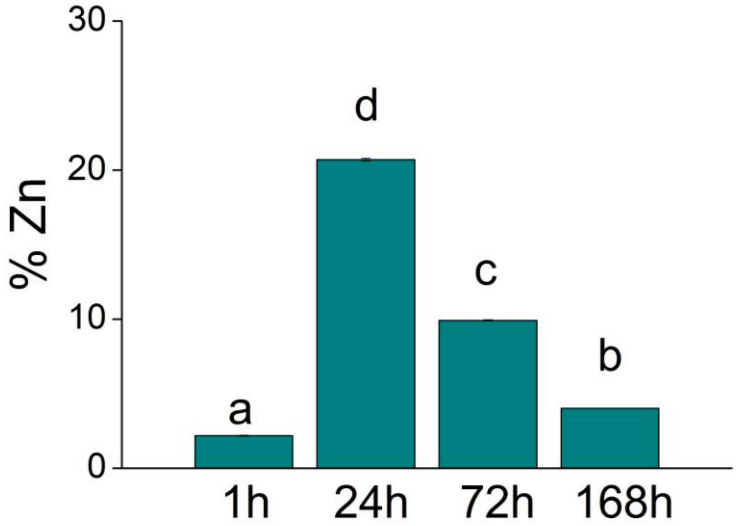

Figure 2 *Amount of absorbed and/or absorbed Zn expressed as a percentage by time points. Different letters indicate significant differences based on Tukey's test*

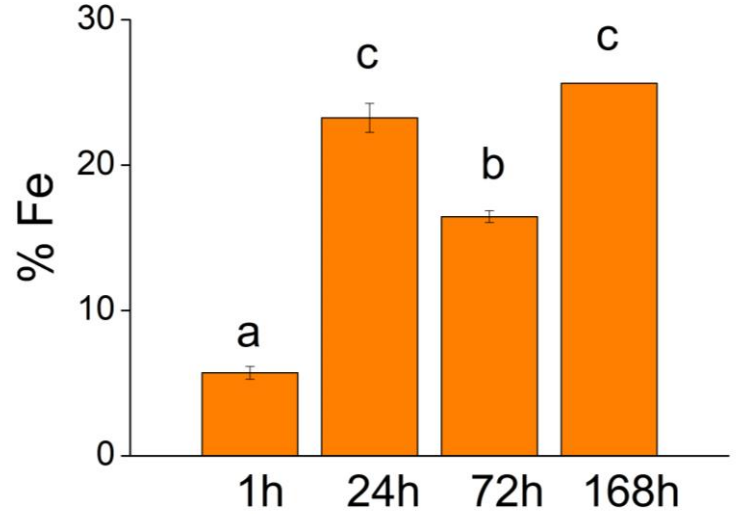

Figure 3 *Amount of absorbed and/or absorbed Fe expressed as a percentage by time points. Different letters indicate significant differences based on Tukey's test*

Figure 4 shows the percentage share of target metals Fe, Cu, Zn and Ni based on the percentage presence of those four metals, which are absorbed by phytoremediation with algae *C. sorokiniana* followed in the actual sample of Lake Robule.

Based on the presented data, that is, the different presence of metals, it can be seen that there is also competition in the adoption of metals, which is also a promising result. Although nickel is present in the smallest amount, it is not removed from the water for seven days.

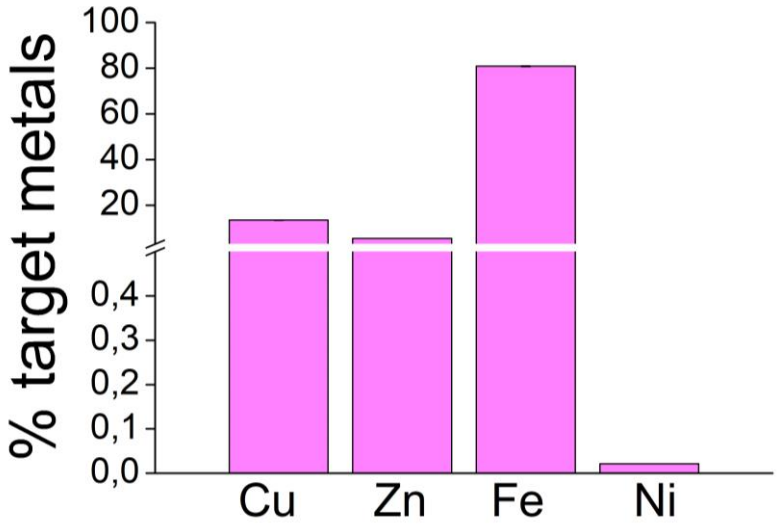

Figure 4 *Percentage of each target metal adsorbed to and/or absorbed in the biomass. Iron dominates, which is expected, as it is the metal most represented in the lake water. It is followed by copper and zinc, and lastly nickel, which is the least abundant in the lake water itself*

CONCLUSION

The decrease in the amount of metals in the water of Lake Robule shows that the microalgae *C. sorokiniana* is a good candidate for natural bioremediation of acidic wastewater. For Cu and Fe, 24 h was the optimal time for maximum removal, because on the seventh day there is a slight additional metal removal. Although Zn had different removal dynamics, but reached the maximum in 24 h. These results show the need to examine and optimize the treatment of each polluted site depending on the composition of polluting metals.

ACKNOWLEDGEMENT

The authors are grateful to the Ministry of Science, Technological Development and Innovation of the Republic of Serbia for financial support according to the contract with the registration number (451-03-47/2023-01/200053).

REFERENCES

[1] Silkina A., Ginnever N. E., Fernandes F., *et al*., 12 (14) (2019) 2772.

[2] Stefan D., Proceedings of the International Symposium, 24–28 Apr 2023, Vienna, Austria (2023).

[3] Vojvodić S., Dimitrijević M., Žižić M., *et al*., 74 (3) (2023) 1107–1122.

[4] Vojvodić S., Stanić M., Zechmann B., *et al*., 177 (2021) S102.

[5] Lugo L. A., Thorarinsdottir R. I., Bjornsson S., *et al*., 12 (11) (2020) 3144.

[6] Whitton R., Ometto F., Pidou M., *et al*., 4 (1) (2015) 133–148.

[7] Hom-Diaz A., Jaén-Gil A., Bello-Laserna I., *et al*., 592 (2017) 1–11.

[8] Wang Y., Ho S. H., Cheng C. L., *et al*., 222 (2016) 485–497.

[9] Li K., Liu Q., Fang F., *et al*., 291 (2019) 121934.

ADSORPTION ISOTHERMS FOR COPPER IONS BIOSORPTION ONTO ONION PEELS

Milan Gorgievski[1*], Miljan Marković[1], Nada Štrbac[1], Vesna Grekulović[1], Milica Zdravković[1]

[1]University of Belgrade, Technical Faculty in Bor, V.J. 12, 19210 Bor, SERBIA

[*]*mgorgievski@tfbor.bg.ac.rs*

Abstract

Langmuir, Freundlich, and Temkin isotherm models were used to study the equilibrium and mechanism of biosorption of copper ions onto onion peels under batch conditions. Isotherm parameters were calculated from the line graphs according to each model. The results obtained on the basis of correlation coefficients, show that the Freundlich isotherm model (R^2 = 0.964) is in good agreement with the analyzed experimental data. This model assumes that the surface energy of the adsorbent is heterogeneous, strong binding sites are occupied first, and that the binding energy decreases as the number of occupied adsorbent sites increases.

Keywords: Adsorption isotherms, copper ions, onion peels, biosorption.

INTRODUCTION

Water is making up more than 70% of the Earth's surface, and it is our most valuable natural resource, without which life would not be possible [1]. However, as a result of the continuous population growth, agricultural activities, industrialization, and other geological, environmental, and global changes, water pollution is increasing and, in many parts of the world, safe drinking water is not available [2]. Due to the great importance of water for our everyday life, the need for continuous improvement and preservation of water quality is constantly increasing [3]. Water whose physical, chemical, or biological properties have been altered by the presence of certain substances that make it unsafe, for example, consumption, is considered wastewater [4].

Many industries, such as metallurgy processing plants, metal finishing plants, electronic industry, electroplating, phytopharmaceutical plants, and many others, release heavy metals along with their wastewater, polluting the environment [5].

Many biological waste materials, such as fungi, algae, peat, yeasts, and different agricultural wastes have been tested as potential adsorbents for heavy metal ions adsorption from water solutions [6].

Adsorption isotherms are used to obtain information about the mechanism of the adsorption process, and the maximum adsorption capacity. There are several adsorption isotherm models that are usually used in relevant literature to describe the adsorption equilibrium, such as Langmuir, Freundlich, Temkin, Sips, Brunauer, Emmett and Teller (BET) model [7,8].

MATERIALS AND METHODS

Adsorption isotherm data was obtained by performing the following experiment: 0.5 g of onion peels (granulation -1 + 0.4 mm) was brought into contact with 50 mL of synthetic solutions containing different initial concentrations of copper ions, ranging from 50 to 500 mg dm^{-3}. The suspension was stirred by a magnetic stirrer for 60 min, considered a process time long enough to reach the equilibrium between phases [9]. The suspension was then filtered and the filtrate was analysed on the residual amount of copper ions.

RESULTS AND DISCUSSION

Adsorption isotherm for copper ions biosorption onto onion peels

The obtained adsorption isotherm for copper ions biosorption onto onion peels is shown in Figure 1.

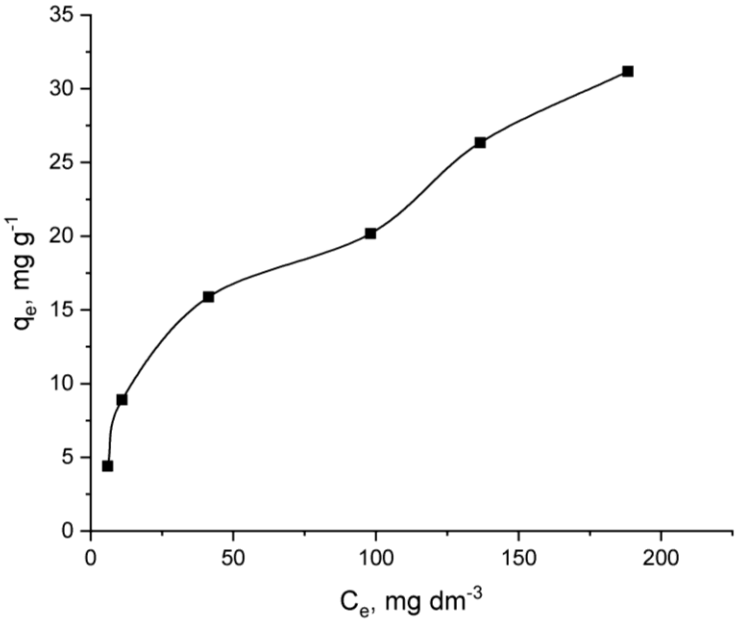

Figure 1 *Adsorption isotherm for copper ions biosorption onto onion peels*

According to Figure 1, the adsorption capacity increases with increasing the concentration of copper ions.

Langmuir model

The Langmuir model assumes that adsorption takes place in a monolayer and that the surface of the adsorbent consists of active sites with constant adsorption energy [10].

The Langmuir model can be written by the following equation:

$$q_e = \frac{q_m K_L C_e}{1 + K_L C_e} \quad (1)$$

Linearisation of Eq. (1) the following equation is obtained:

$$C_e / q_e = \frac{1}{K_L q_m} + \frac{1}{q_m} C_e \quad (2)$$

where C_e is the equilibrium concentration of metal ions (mg dm^{-3}), q_e is the equilibrium adsorption capacity (mg g^{-1}), q_m is the maximum adsorption capacity (mg g^{-1}) and K_L (dm^3 g^{-1}) is the Langmuir equilibrium constant.

Graphical dependence of C_e/q_e in function of C_e gives the straight-line with the slope $1/q_m$ and the intercept $1/K_L q_m$ which is shown in Figure 2.

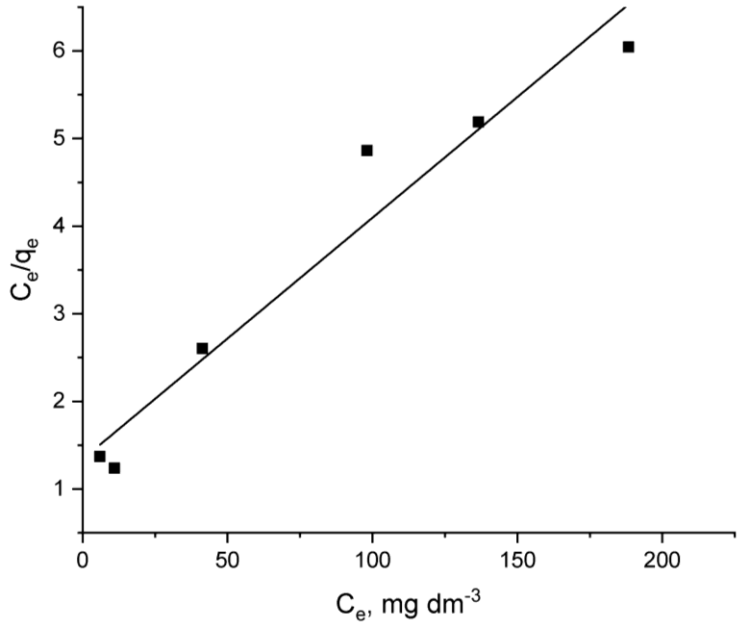

Figure 2 *Langmuir adsorption isotherm model for copper ions biosorption onto onion peels*

Freundlich model

The Freundlich adsorption isotherm model is based on the assumptions that the surface energy of the adsorbent is heterogeneous, that strong binding sites are occupied first, and that binding energy decreases with the increase in the number of occupied adsorption sites [10].

This model is represented by the following equation:

$$q_e = K_f C_e^{1/n} \quad (3)$$

Linear form of Eq. (3) is given as:

$$\log q_e = \log K_F + \frac{1}{n} \log C_e \quad (4)$$

where C_e is the equilibrium concentration of copper ions in the solution (mg dm^{-3}); q_e is the adsorbent capacity defined as mass of the adsorbed metal per unit mass of the adsorbent (mg g^{-1}) at equilibrium; K_F is the Freundlich equilibrium constant ((mg g^{-1}) (dm^3 $mg^{-1})^{1/n}$), and $1/n$ is the coefficient of heterogeneity in the Freundlich adsorption isotherm equation.

Graphical dependence of *log* q_e in function of *log* C_e gives the straight line, with the slope $1/n$ and the intercept K_F which is shown in Figure 3.

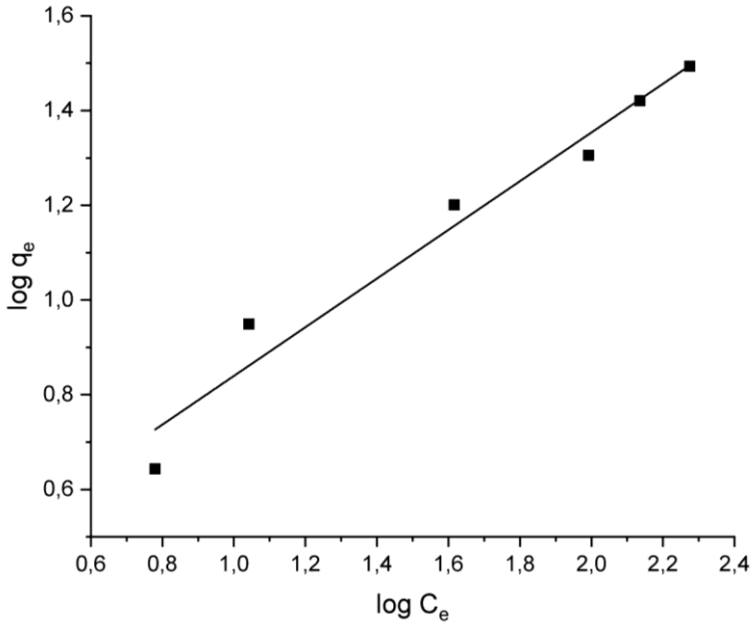

Figure 3 *Freundlich adsorption isotherm model for copper ions biosorption onto onion peels*

Temkin model

Temkin adsorption isotherm model is based on the assumption that, due to the interactions between the adsorbent and the absorbate, the adsorption heat of all adsorbed molecules decreases linearly with the degree of surface coverage, as well as that the binding energy distribution is uniform, up to some maximum energy [11].

Temkin isotherm model is represented by the following equation:

$$q_e = B \ln\left(K_T C_e\right) \tag{5}$$

Linear form of the Eq. (5) is given as:

$$q_e = B \ln K_T + B \ln C_e \tag{6}$$

where $B = RT/b$ is the Temkin constant, which refers to the adsorption heat (J mol^{-1}); b is the variation of adsorption energy (J mol^{-1}); R is the universal gas constant (J mol^{-1} K^{-1}); T is the temperature (K); K_T is the Temkin equilibrium constant (dm^3 g^{-1}); q_e is the adsorption capacity

defined as mass of the adsorbed metal per unit mass of the adsorbent (mg g^{-1}) at equilibrium; C_e is the equilibrium concentration of copper ions in the solution (mg dm^{-3}). Constants B and K_T can be determined from the graph $q_e = f(ln\ C_e)$ (Figure 4), where B is the slope, and K_T the intercept.

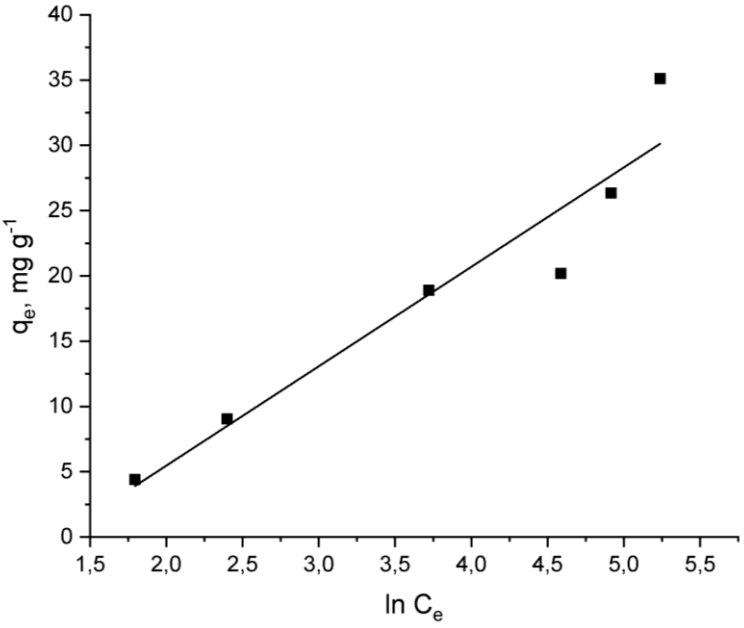

Figure 4 *Temkin adsorption isotherm model for copper ions biosorption onto onion peels*

The obtained experimental data, shown on Figure 1, was fitted using Langmuir, Freundlich and Temkin adsorption isotherm models. Equilibrium parameters for the considered models were determined using the Equations (2), (4) and (6), and, along with the correlation coefficient R^2, are given in Table 1.

Table 1 *Obtained parameters for Langmuir, Freundlich and Temkin adsorption isotherm models for copper ions biosorption onto onion peels*

Langmuir				**Freundlich**			**Temkin**		
K_L $dm^3\ mg^{-1}$	q_{exp} mg g^{-1}	q_m mg g^{-1}	R^2	K_F	1/n	R^2	B J mol^{-1}	K_T $dm^3\ g^{-1}$	R^2
0.021	31.16	36.28	0.949	2.117	1.945	0.964	7.613	-9.759	0.917

CONCLUSION

Onion peels were used as a biosorbent for copper ions biosorption from synthetic copper ion solutions. The adsorption equilibrium data were analysed using the Langmuir, Freundlich, and Temkin adsorption isotherm models. Obtained results indicate that the Freundlich model best fits the analysed experimental data, with the correlation coefficient R^2 = 0.964. This means that the surface energy of the adsorbent is heterogeneous, strong binding sites are

occupied first, and that binding energy decreases with the increase in the number of occupied adsorption sites.

ACKNOWLEDGEMENT

The research presented in this paper was done with the financial support of the Ministry of Science, Technological Development and Innovation of the Republic of Serbia, within the funding of the scientific research work at the University of Belgrade, Technical Faculty in Bor, according to the contract with registration number 451-03-47/2023-01/ 200131.

REFERENCES

[1] Vijayaraghavan K., Yun Y. S., Biotechnol. Adv. 26 (2008) 266–291.

[2] Ali I., Gupta V. K., Nat. Protoc. 1 (6) (2007) 2661–2667.

[3] Ramachandra T. V., Ahalya N., Kanamadi R. D., CES Tech. rep. 110, 7 (4) (2005) 1–34.

[4] Amoatey P., Bani R., Waste Water - Evaluation and Management, Department of Agricultural Engineering, Faculty of Engineering Sciences, University of Ghana, (2011), 380–382.

[5] Perez-Lopez R., Nieto J. M., Almodovar G. R., Appl. Geochemistry 22 (2007) 1919–1935.

[6] Nemes L. N., Bulgariu L., Open Chem. 14 (2016) 175–187.

[7] Hamdaoui O., Naffrechoux E., J. Hazard. Mater. 147 (2007) 381–394.

[8] Mohammed-Ridha M. J., Ahmed A. S., Raoof N. N., NJES 20 (2017) 298–310.

[9] Gorgievski M., Božić D., Stanković V., Štrbac N., Šerbula S., Ecol. Eng. 58 (2013) 113–122.

[10] Yousef R. I., El-Eswed B., Al-Muhtaseb A. H., Chem. Eng. J. 171 (2011) 1143–1149.

[11] Kumar P. S., Ramalingam S., Senthamarai C., *et al*., Desalination 261 (2010) 52–60.

MECHANISM AND KINETICS OF ELECTROCATALYTIC OXIDATION OF PHENOL

Sonja Stanković[1*], Vladan Nedelkovski[1], Milan Radovanović[1], Snežana Milić[1]
[1]University of Belgrade, Technical Faculty in Bor, V.J. 12, 19210 Bor, SERBIA
[*]*sstankovic@tfbor.bg.ac.rs*

Abstract

Phenols are toxic, carcinogenic, organic compounds present in the wastewater of numerous industrial facilities. Improper disposal of industrial wastewater poses a risk to the environment and human health, as the presence of phenolic compounds, even in low concentrations, can cause a range of harmful effects. In order to protect the environment and preserve human health, it is necessary to remove phenol and its derivatives from industrial wastewater before their release into the environment. Since the use of conventional methods in the treatment of phenolic wastewater is limited by low efficiency and high costs, in recent years there has been an increasing interest in the application of advanced oxidation processes in wastewater treatment. Among the numerous advanced oxidation processes, electrocatalytic oxidation has attracted a lot of attention due to its practicality and high efficiency. This paper presents the mechanism of electrocatalytic oxidation of phenol in aqueous solutions, as well as a literature review of the influence of process parameters on phenol oxidation.

Keywords: phenol, electrooxidation, applied potential, pH, initial concentration.

INTRODUCTION

Phenol is one of the most dangerous organic pollutants, which by releasing industrial wastewater, ends up in aquatic ecosystems [1–3]. The maximum allowable concentration of phenolic compounds in industrial wastewater is 2 mg/dm^3. However, the wastewater from numerous industrial facilities contains phenolic compounds in significantly higher concentrations than allowed (50-2000 mg/dm^3) [4]. 80% of wastewater, of which 28% is industrial wastewater, are discharged into the environment without any kind of prior treatment. Because of that, contamination of aquatic ecosystems represents a growing problem worldwide [5–7].

The presence of phenolic compounds in water is harmful to the environment and human health and can lead to a range of unwanted symptoms and health problems [4,8,9]. According to the Environmental Protection Agency (EPA), short-term exposure to water containing phenols, can cause skin, eye and mucous membrane irritation, while long-term exposure could eventually lead to bleeding and liver damage [10]. In addition, phenol can cause damage to the central nervous system, kidney disease, and the formation of various tumors. Therefore, the removal of phenol and its derivatives is significant in protecting the environment and preserving human health [11].

Conventional methods such as biological degradation, chemical oxidation, and adsorption can be used for purifying phenolic wastewater [7,12]. However, wastewaters containing high concentrations of phenol (>5 mg/dm^3) cannot be treated by biological methods due to their toxicity towards microorganisms [13]. The use of traditional methods such as adsorption on activated carbon and chemical oxidation can achieve phenol degradation, but their application in the process of purifying industrial wastewater is limited by high costs [2,13].

Due to their practicality and high efficiency, Advanced Oxidation Processes (AOPs) are attracting lots of attention from researchers. Unlike conventional methods, use AOPs can achieve complete degradation of phenol and its derivatives. In addition, the use of advanced oxidation processes in the treatment of wastewater does not result in secondary pollution [14]. Advanced oxidation processes include electrocatalytic oxidation, photocatalysis, ozonation, Fenton reaction and enzymatic treatment.

Electrocatalytic oxidation is an environmentally friendly and efficient method, which is based on redox reactions of organic compound and strong oxidants [9,12]. By using this method, complete oxidation of organic matter to CO_2 and H_2O can be achieved [9]. This paper presents the mechanism and kinetics of electrocatalytic oxidation of phenol.

MECHANISM OF ELECTROCATALYTIC OXIDATION OF PHENOL

A large number of research teams have investigated the mechanism of electrochemical oxidation of phenol and its derivatives [3,11,15–18]. The mechanism of phenol degradation is shown in Figure 1. The oxidation of phenol begins with electron transfer, which leads to radical reactions [18]. Free-radical reactions result in the formation of benzoquinone. It is assumed that benzoquinone is the main intermediate compound in the process of phenol oxidation [17–19]. Hydroxyl radicals generated by the electrolysis of water react with benzoquinone, leading to the opening of the aromatic ring and the formation of maleic acid and ethene. The formed maleic acid is reduced to succinic acid (reaction pathway IIIa) at the cathode, followed by the oxidation of succinic acid to malonic acid, further to acetic acid, and finally to CO_2. In parallel with the reduction of maleic acid to succinic acid, the oxidation of maleic acid to oxalic acid via hydroxyl radicals takes place (reaction pathway IIIb). The formed oxalic acid is easily oxidized to CO_2 [18]. Tasić *et al.* [3] emphasize that the reaction of phenol oxidation is controlled by the diffusion of phenol molecules on the surface of the anode. However, Li *et al.* [18] emphasize that the rate of phenol degradation is controlled by the rate of opening of the aromatic ring and the oxidation of maleic acid.

In the absence of strong oxidizing free radicals, the accumulation of hydroquinone and benzoquinone occurs, leading to the formation of a layer of polymeric compounds (reaction pathway II) that blocks active sites on the surface of the anode, preventing further oxidation of phenol [3,18]. Polymerization and aromatic ring opening reactions often occur simultaneously. If the aromatic ring opening reaction and formation of carboxylic acids are faster than polymerization, a small amount of benzoquinone and polymeric compounds will be formed on the surface of the anode. Nevertheless, if polymerization is faster than the aromatic ring opening reaction and formation of carboxylic acids on the surface of the anode, a significant amount of polymeric compounds will be formed [18].

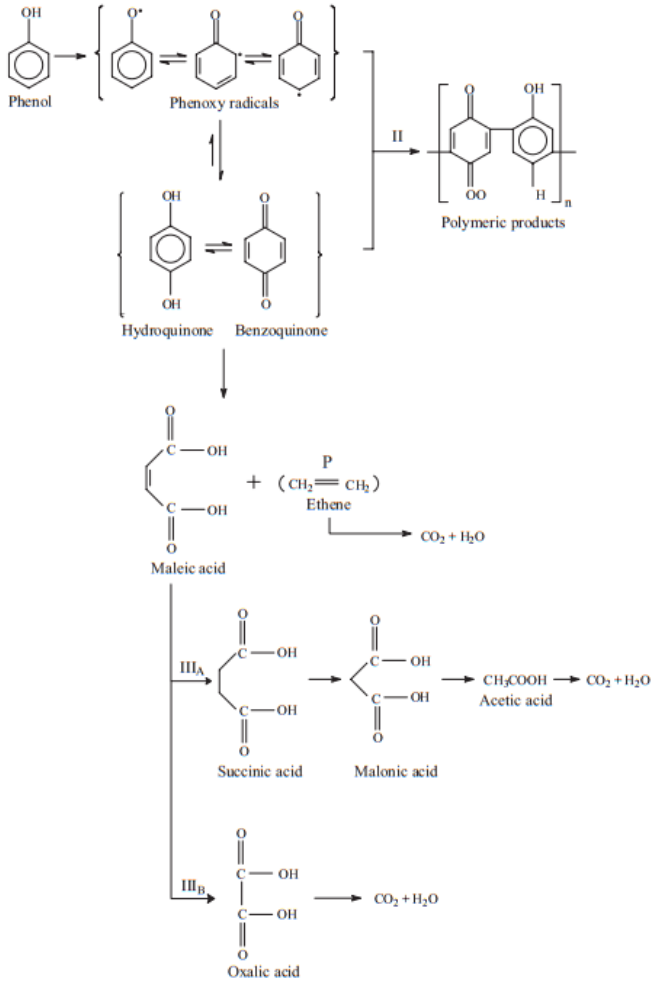

Figure 1 *Mechanism of electrocatalytic phenol degradation [18]*

KINETIC PROCESS PARAMETERS

Understanding the impact of process parameters is of great importance in selecting a sustainable and efficient method for treating phenolic wastewater. The mechanism and kinetics of phenol oxidation depend on a number of variables such as electrolyte pH, initial phenol concentration, current density, anodic material, electrolyte flow rate through the electrochemical cell, etc. [6].

Current density

Current density is the most important operating parameter that affects the efficiency and speed of electrocatalytic oxidation of phenol [11,17,19–23].

Zhu *et al.* [17] investigated the effect of current density (10–50 mA/cm^2) on the electrocatalytic degradation of phenol using a Ti/Sb_2O_3-SnO_2 anode and a stainless-steel cathode. Experimental results indicate that the efficiency of electrocatalytic phenol degradation in acidic, neutral, and basic media increases with increasing current density. After 12 hours of electrolysis, nearly 100% TOC removal was achieved at a current density of 40 mA/cm^2. Loloi *et al.* [19] confirmed in their work that increasing current density from 10 to 40 mA/cm^2 leads to an increase in phenol degradation efficiency. Ghanim and Juda [11]

investigated the effect of current density (30, 50, and 70 mA/cm^2) on the electrocatalytic degradation of phenol using a graphite and β-PbO2 anode. The highest degree of phenol degradation of 74.4% for graphite and 83.7% for β-PbO_2 were achieved at a current density of 70 mA/cm^2, an initial phenol concentration of 100 mg/dm^3, and a flow rate of 12 L/h.

Gao *et al.* [21] studied the impact of higher current densities (100-700 mA/cm^2) on the rate and efficiency of phenol degradation (500 mg/dm^3) using a Ti/IrO_2-Ta_2O_5 anode. Increasing the current density promotes electron transfer and •OH generation on the electrode surface, resulting in increased efficiency degradation of phenol and intermediates. However, higher current density leads to greater energy consumption. Gao *et al.* [21] point out that the optimal current density for electrocatalytic phenol degradation using a Ti/IrO_2-Ta_2O_5 anode, would be 500 mA/cm^2.

Initial concentration

In terms of practical application, of core research importance is to understand the influence of initial phenol concentration on removal efficiency and electrocatalytic oxidation kinetics [24]. The literature review of the impact of the initial concentration on the efficiency of electrocatalytic phenol degradation is provided in Table 1.

Table 1 *The impact of initial phenol concentration on the efficiency of electrocatalytic degradation*

Electrode	Current density (mA/cm^2)	Initial concentration (mg/dm^3)	Removal efficiency (%)	Reference
Ti/SnO_2-Sb_2O_5	20	50	96	[19]
		200	72	
Graphite	70	100	74.7	[11]
		500	58.9	
PbO_2	70	100	83.7	[11]
		500	74.3	
Ti/TiO_2NTs/NiO/Ce-PbO_2	40	50	98.1	[24]
		250	70	
SnO_2-Sb_2O_3/Ti	40	460	98.7	[17]
		550	97.2	
		620	95.4	
		710	94.3	

Based on the reviewed literature [11,17,19,23,24] it can be concluded that as the initial concentration of phenol increases, the efficiency of degradation decreases. As the initial concentration of phenol increases, the need for strong oxidizing agents (•OH) also increases. However, under constant testing conditions, the number of (•OH) formed on the surface of the electrode remains constant. In that case, the number of formed (•OH) is not sufficient to oxidize phenol at higher concentrations. Therefore, with the increase in pollutant concentration, at a constant current density, the efficiency of electrocatalytic phenol degradation decreases [19].

Gui *et al.* [25] investigated the effect of initial phenol concentration on the kinetics of electrocatalytic phenol oxidation. The results of the study are presented in Table 2 and indicate that the value of the reaction rate constant decreases with increasing concentration and that the phenol degradation reaction follows pseudo-first-order kinetics. Wang *et al.* [24], Kornienko *et al.* [26], Park *et al.* [27], Makgae *et al.* [28] and Zhu *et al.* [17] have also confirmed in their works that the electrocatalytic oxidation of phenol follows pseudo-first-order kinetics.

Table 2 *The effect of initial phenol concentration on the rate constant of phenol degradation [25]*

Electrode	Initial concentration (mg/dm^3)	k (min^{-1})
ZnO/Co(II)-PbO_2	50	$7.78 \cdot 10^{-3}$
	100	$7.69 \cdot 10^{-3}$
ZnO/PEG-Co(II)-PbO_2	50	$9.49 \cdot 10^{-3}$
	100	$9.17 \cdot 10^{-3}$
	460	$2.91 \cdot 10^{-3}$
	550	$1.67 \cdot 10^{-3}$
	620	$8.30 \cdot 10^{-4}$
	710	$6.67 \cdot 10^{-4}$

pH

Numerous research teams have investigated the effect of electrolyte pH on the efficiency of electrocatalytic oxidation of phenol [19,23,28–30].

Wu *et al.* [29] investigated the effect of electrolyte pH (4.68, 7.2, and 11) on the electrocatalytic degradation of phenol using a Ti/SnO_2-Sb_2O_5/PbO_2 anode. After 12 hours, complete phenol degradation was achieved only in an alkaline environment (pH 11). The results are consistent with those obtained by Loloi *et al.* [19] and Makgae *et al.* [28] and suggest that phenol degradation is favored in an alkaline environment. The high degree of phenol degradation in an alkaline environment can be attributed to the large amount of hydroxyl radicals formed according to reactions (1) and (2) [29]. The formed hydroxyl radicals participate in the oxidation of phenol.

$$2H_2O - 2e^- \rightarrow 2^{\cdot}OH + 2H^+ \quad (1)$$

$$OH^- - e^- \rightarrow {}^{\cdot}OH \quad (2)$$

Kornienko *et al.* [23] investigated the kinetics of the indirect oxidation of phenol mediated by reactive oxygen species on a Pb/PbO_2 anode in acidic and neutral media. The results of the study are presented in Table 3 and indicate that a higher rate and efficiency of phenol degradation are achieved in acidic than in neutral media. The oxidation reaction of phenol follows pseudo-first-order kinetics.

Table 3 *The effect of pH on the rate and efficiency of electrochemical oxidation of phenol (Co=200 mg/*dm^3*) [23]*

pH	Current density (A/m^2)	Oxidation efficiency (%)	Rate reaction constant k (h^{-1})
2–3	500	84	1.4
	1000	92	1.8
7	500	48	0.66
	1000	77	1.47

The positive effect of low pH on the rate of phenol degradation was confirmed by Li *et al.* [31], Gao *et al.* [21] and Loloi *et al.* [19]. Li *et al.* [31] point out that H^+ ions promote the formation of H_2O_2 and •OH and inhibit the release of oxygen. In an acidic environment, phenol is adsorbed on the surface of the electrode and donates an electron to the anode, forming a phenoxy radical, which is oxidized in the presence of hydroxyl radicals (Loloi et al., 2016).

CONCLUSION

Electrocatalytic oxidation is an efficient and environmentally friendly technology suitable for treating phenolic wastewater. Using this method, complete oxidation of phenolic compounds to CO_2 and H_2O can be achieved. The efficiency and rate of electrocatalytic oxidation of phenol depend on the nature of the anodic material, current density, pH value of the electrolyte, initial phenol concentration, and flow rate of the electrolyte through the electrochemical cell.

- Current density is one of the most important factors that affect the efficiency and rate of electrocatalytic degradation of phenol. Increasing the current density increases the rate of electrocatalytic degradation of phenol. However, it is necessary to consider the economic feasibility of the process, as the use of high current densities requires additional costs.
- Increasing the initial concentration of phenol can negatively affect the efficiency of electrocatalytic oxidation.
- The pH value of wastewater can greatly affect the efficiency and rate of electrocatalytic oxidation of phenol. The highest degree of phenol degradation is achieved in an alkaline, then acidic and neutral environment.

ACKNOWLEDGEMENT

The authors are grateful to the Ministry of Science, Technological Development and Innovation of the Republic of Serbia for financial support according to the contract with the registration number 451-03-47/20223-01/200131.

REFERENCES

[1] Seid L., Lakhdari D., Berkani M. *et al*., J. Haz. Mat. 423 (2022) 126986.

[2] Jin P., Chang R., Liu D., *et al*., J. Environ. Chem. Eng. 2 (2014) 1040–1047.

[3] Tasić Ž., Gupta V. K., Antonijević M. M., Int. J. Electrochem. 9 (2014) 3473–3490.

[4] Silerio-Vazquez F., Alarcon-Herrera M. T., Proal-Najera J.B. ESPR 29 (2022) 42319–42330.

[5] Mao G., Han Y., Liu X., *et al*., Chemosphere 288 (2022) 132483.

[6] Jiang Y., Zhao H., Liang J. *et al*., Electrochem. commun. 123 (2021) 106912.

[7] Mohamed A., Yousef S., Nasser W. *et al.* ESEU 32 (1) (2020) 1–8.

[8] Wu Z., Jing J., Zhang K., *et al*., Appl. Catal. B. 307 (2022) 121153.

[9] Hu C., Zhao Q., Zang G.L. *et al*., Electrochim. Acta 405 (2022) 139758.

[10] Karavasilis M. V., Theodoropoulou M. A., Tsakiroglou C. D., Nanomaterials 12 (2022) 1–21.

[11] Ghanim A. N., Juda Z. M., JETT 9 (3) (2021) 667–674.

[12] Zhou P., Wan J., Wang X., *et al*., J. Appl. Electrochem. 51 (2021) 653–667.

[13] Espinoza-Montero P. J., Vasquez-Medrano R., Ibanez J. G., *et al*., J. Electrochem. Soc. 160 (7) (2013) G3171–G3177.

[14] Zhou M., Wu Z., Wang D. J., Environ. Sci. Health A. (2022) 1263–1275.

[15] Massa A., Hernandez S., Ansaloni S., *et al*., Electrochim. Acta 273 (2018) 53–62.

[16] Feng Y., Cui Y., Logan B., *et al*., Chemosphere 70 (2008) 1629–1636.

[17] Zhu K., Zhang W., Wang H., *et al*., Clean 36 (1) (2008) 97–102.

[18] Li X., Cui Y., Feng Y., *et al*., Water Res. 39 (2005) 1972–1981.

[19] Loloi M., Rezaee A., Aliofkhazraei M., *et al*., ESPR 23 (19) (2016) 19735–19743.

[20] Öztürk H., Barışçı S., Turkay O., *et al*., J. Environ. Eng. 145 (5) (2019) 04019014.

[21] Gao J., Yan J., Liu Y., *et al*., Water Sci. Technol. 76 (3) (2017) 662–670.

[22] Berenguer R., Sieben J. M., Quijada C., *et al*., Appl. Catal. B. 199 (2016) 394–404.

[23] Kornienko V. L., Chaenko N. V., Kornienko G. V., Russ. J. Electrochem. 43 (11) (2007) 1243–1248.

[24] Wang Z., Xu M., Wang F., *et al*., Electrochim. Acta 247 (2017) 535–547.

[25] Gui L., Chen Z., Chen B., *et al*., J. Haz. Mat. 399 (2020) 123018.

[26] Kornienko G. V., Chaenko N. V., Maksimov N. G., *et al*., Russ. J. Electrochem. 47 (2) (2011) 225–229.

[27] Park H., Vecitis C. D., Hoffmann M. R., J. Phys. Chem. 113 (2009) 7935–7945.

[28] Makgae M. E., Klink M. J., Crouch A.M., Appl. Catal. B. 84 (2008) 659–666.

[29] Wu D., Liu M., Dong D., *et al*., Microchem. J. 85 (2007) 250–256.

[30] Zhou M., Wu Z., Wang D. J., Environ. Sci. Health A. 37 (7) (2002) 1263–1275.

[31] Li P., Cai W., Xiao Y., *et al*., Int. J. Electrochem. Sci. 12 (2017) 2777–2790.

ECOENZYMATIC STOICHIOMETRY AS AN EMERGING METHOD IN THE ASSESSMENT OF SOIL HEAVY METAL POLLUTION

Jelena Milosavljević[1*], Snežana Šerbula[1], Ana Radojević[1], Tanja Kalinović[1], Jelena Kalinović[1]

[1]University of Belgrade, Technical Faculty in Bor, V.J. 12, 19210 Bor, SERBIA

[*]*jmilosavljevic@tfbor.bg.ac.rs*

Abstract

Environmental pollution with heavy metals is one of the most important problems that should be addressed worldwide. Thus, efforts have been made in the development and evaluation of different soil pollution indicators. Among them, soil enzyme activity is regarded as the most prominent indicator, considering its enrolment in soil organic matter decomposition and the soil nutrient cycling. Special emphasis is given to the ecoenzymatic stoichiometry, which is regarded as an emerging method in soil pollution assessment. Based on the ratio of the enzyme activity, the ecoenzymatic stoichiometry can be used to assess the soil microbial metabolic limitation under various environmental disturbances. Taking into account different methods for ecological resorting of the contaminated environment, phyotremediation is considered as ecological and cost effective. Thus the evaluation of possible application of ecoenzymatic stoichiometry in the assessment of the impact of phytoremediation on soil structure and function is of great importance.

Keywords: heavy metals, soil pollution, soil enzyme activities, microbial limitations.

INTRODUCTION

Soil pollution with heavy metals has become a global problem due to their environmental persistence which led to degradation of soil quality and functions. Anthropogenic activities, such as mining, smelting, industrialization, and urbanization, are considered as the greatest sources of these non-biodegradable contaminants. Accumulation of heavy metals in soil could be harmful to human health through the soil-plant systems. Considering this, special emphasis is given to the selection of suitable indicators for soil heavy metal pollution assessment [1–3].

Soil extracellular enzymes secreted by plant and microbial cells, have a critical role in decomposition of the soil organic matter and the soil nutrient cycling [4–7]. Soil enzyme activities are regarded as powerful biological indicators due to the fact that they are one of the first soil properties that are altered under environmental disturbances. Thus, they are recognized as an early warning tool for the soil quality assessment, which integrate information about microbial status and soil physico-chemical properties [4,7].

Soil enzyme activity is related to both abiotic and biotic stressors [5]. The enzymes may respond differently to the environmental disturbances, so the use of different enzyme-based indicators may be required in the soil quality assessment [8]. The assessment of soil heavy metal pollution, using soil enzyme activities, include single enzyme index, combined enzyme index, enzyme-based functional diversity index, microbiological stress index, etc. [7]. Among

the methods employing the enzymatic activity, ecoenzymatic stoichiometry (which is based on the ratio of the enzyme activity) is a promising methodology which can be used to assess the soil microbial metabolic limitation under various environmental managmements or disturbances [6,7]. Extracellular enzyme stoichiometry reveals nutrient requirements of microorganisms and environmental nutrients supply, whereby its evaluation facilitates the understanding of the soil nutrient circulation and balance [5]. Thus, this paper focuses on the application of ecoenzymatic stoichiometry, as an emerging method, in the environmental studies, especially for the assessment of heavy metal pollution after phytoremediation.

SOIL ENZYME ACTIVITY AND ECOENZYMATIC STOICHIOMETRY

Soil enzymes have a crucial role in nutrient biogeochemistry, whereby the nutrient cycling between plants and soil is mediated by microbes which secrete extracellular enzymes to degrade different organic compounds [9,10]. Thus, microbes provide plants with nutrients, however in the case of nutrient deficiency, microbes compete with roots for nutrients [10]. Taking into account that microbes have a competitive advantage compared to plants when it comes to acquiring nutrients, if microbes are limited by a certain soil nutrient, plants should also be limited [11].

By combining basics of biological, chemical and physical principles, ecological stoichiometry can be a useful tool for understanding the nutrient cycling in ecosystems. The central concept of ecological stoichiometry is stoichiometric homeostasis, which can be defined as the ability of organisms to maintain nutrient composition relatively constant, irrespective of changing nutrient status in the environment [12].

The activities of soil enzymes can reflect microbial nutrient demand, while the stoichiometric relationships between enzyme activities reflect the ability of microorganisms to use different resources (i.e. C, N, O, P and S) from environments [9]. As an emerging methodology, ecoenzymatic stoichiometry includes different parameters associated with enzyme activities into specific microbial characteristics (i.e. microbial metabolic limitations) [2]. Among soil enzymes, C-, N- and P-acquiring enzymes are of crucial importance since they have a significant contribution in energy flow and nutrient release [11].

The most-frequently analyzed soil enzyme activities linked to the microbial metabolism include [9,13]:

C-acquiring enzymes:

- β-glucosidase (BG) – catalyzes the terminal reaction in degradation of cellulose,
- β-1,4-N-acetylglucosaminidase (NAG) – catalyzes the terminal reaction in degradation of chitin;

N-acquiring enzymes:

- leucine aminopeptidase (LAP) – catalyzes the hydrolysis of leucine and other hydrophobic amino acids from the N-terminus of the polypeptides;

P-acquiring enzymes:

- acid or alkaline phosphatase (ACP or ALP) – catalyzes the hydrolysis of phosphate esters (i.e. phosphomonoesters, phosphodiesters, or phosphosaccharides) that release phosphate.

Specific activity of soil enzymes (i.e. activity g^{-1} soil organic matter) is used for the stoichiometric analyses [14]. Stoichiometric analyses of enzyme activity on the example of β-N-acetylglucosaminidase (NAG), leucine aminopeptidase (LAP), β-glucosidase (BG) and acid phosphatase (ACP) is conducted as [15]:

$$C{:}N_{EEA} = \ln BG/\ln (LAP + NAG) \quad (1)$$

$$C{:}P_{EEA} = \ln BG/\ln ACP \quad (2)$$

$$N{:}P_{EEA} = \ln (LAP + NAG)/\ln ACP \quad (3)$$

where $C{:}N_{EEA}$ represents the ecoenzymatic C to N ratio; $C{:}P_{EEA}$ the ecoenzymatic C to P ratio; and $N{:}P_{EEA}$ the ecoenzymatic N to P ratio.

Obtained ratios could reflect microbial C-limitations (or C-shortage) relative to N (increased BG: (LAP + NAG) ratio), C-limitations (or C-shortage) relative to P (increased BG:ACP ratio) or N-limitations (or N-shortage) relative to P (increased (LAP + NAG):ACP ratio) [13].

Microbial nutrient limitation analyzed by the vector analysis (length, L; angle, A) of the ecoenzymatic stoichiometry on the example of BG, NAG, LAP, ACP activities can be calculated with the equations (4) and (5) as suggested by Li *et al*. [15]:

$$\text{Vector } L = \sqrt{(\ln BG/\ln[NAG + LAP]^2 + (\ln BG/\ln ACP)^2} \quad (4)$$

$$\text{Vector } A = \text{Degrees } (\text{ATAN2}(\ln BG/\ln ACP), (\ln BG/\ln[NAG+LAP])) \quad (5)$$

Vector L represents C limitation (longer vector L indicates greater C limitation); vector A denotes N and P limitation (vector A >45° indicates P limitation and <45° indicates N limitation) [15].

Sinsabaugh *et al*. [14] conducted a global-scale meta-analysis using data from 40 ecosystems, and found that, for hydrolases, the ratios of specific C, N, and P acquisition activities are close to 1:1:1. The C:N:P ratio of enzyme activities is influenced by different environmental factors, as well as anthropogenic disturbances [9].

ASSESSMENT OF SOIL HEAVY METAL POLLUTION BY ECOENZYMATIC STOICHIOMETRY

High concentrations of heavy metals in soil can be toxic to soil microbes since heavy metals can inhibit enzymes by reacting with the active catalytic sites (direct inhibition) or with groups involved in maintaining the enzyme structure (indirect inhibition). Thus, special emphasiz is given to understanding the relations between heavy metals, environmental factors and soil microbial activities [8]. Monitoring and assessment of soil heavy metal pollution can be performed by ecoenzymatic stoichiometry with a special focus on a nutrient cycling and microbial limitations in rhizospheric soil during phytoremediation [2,3].

Rhizosphere represents a hotspot where nutrient cycling among the soil, microbes and plants takes place. This cycling is mediated by enzymes that are produced by soil microorganisms and plant roots. It is estimated that up to 40% of photosynthetically fixed carbon is provided to microbes by plants, resulting in higher microbial activity in rhizospehere compared to the bulk soil. Also, the presence of plant roots affects soil nutrient cycling and C decomposition through altering soil physical properties and heavy metal availability by releasing protons and organic acids [3,15].

The ecoenzymatic stoichiometry can be used for determination of nutritional status and microbial nutrient limitations, or responses of microorganisms to the environmental changes. Cui *et al*. [16] denoted that enzyme stoichiometry method could be used to predict the response of soil microbial structure and element cycling to different long-term fertilization regimes. In the study by Zhang *et al*. [5] the effects of vegetation restoration on soil ecoenzymatic stoichiometry was evaluated. The vegetation and soil from one farmland and two restored land-use types were assessed, and the activity of β-glucosidase, β-1,4-*N*-acetylglocosaminidase, leucine aminopeptidase and alkaline phosphatase were determined. Soil ecoenzymatic C:N:P acquisition ratios deviated from the 1:1:1 ratio and was dependant on the nutrient availability and microbial nutrient demand. The results provided useful knowledge about nutrient cycling and microbial limitation in the restored ecosystems.

It should be pointed out that soil enzyme activities are regarded as sensitive indicators of soil microbial metabolism and nutrient cycling changes, which can be used to assess the impact of phytoremediation on soil structure and function [3].

Soil ecoenzymatic stoichiometry could be employed to study nutrient cycling and microbial limitation during phytoremediation. Duan *et al*. [3] performed a study to improve the assessment of ecological risks in soil polluted by heavy metals (Cu, Zn, Pb and Cd) and to give a theoretical basis for improvement of phytoremediation efficiency. The ecoenzymatic stoichiometry was used to examine the microbial limitation in soil near the copper mine. The activities of soil C- acquiring enzymes (β-glucosidase, cellobiohydrolase), N-acquiring enzymes (*N*-acetylglocosaminidase, leucine aminopeptidase), and P-acquiring enzyme (alkaline phosphatase) were analyzed in the rhizospheric and bulk soil of different plants (*Medicago sativa, Halogeton arachnoideus* and *Agropyron cristatum*). The vector analysis of soil enzyme activities showed that microbial C limitation was significantly less in the rhizospheric compared to the bulk soil, due to the root excretions and rhizodeposition. Also, rhizospheric soil was characterized with low P limitations. The higest ratios of N- and P-acquiring enzyme activities were observed in *Medicago sativa* (both rhizospheric and bulk

soil) indicated low P limitation. The obtained results have shown that soil heavy metal content had negative effect on P limitation and positive effects on C limitations.

Wang *et al*. [2] stated that extracellular enzyme stoichiometry can successfully be used as a methodology for the soil heavy metal contamination assessment. Five-year phytoremediation experiment (*Lolium perenne* L., *Brassica napus* L., *Artemisia argyi*, *Silphium, Taraxacum, Populus*, and a control experiment) was performed in the vicinity of a smelter. The analysis included soil heavy metals content (Cu, Cd, Zn and Pb) and enzyme activities determination. The activities of enzymes involved in C (β-1,4-glucosidase, β-D-cellobiosidase), N (β-1,4-N-acetylglucosaminidase, L-leucine aminopeptidase) and P (alkaline phosphatase) cycling were further used for microbial nutrient limitation analysis. According to the enzymatic stoichiometry, *Lolium* treatment had the lowest microbial C limitation, which was indicative of the lowest heavy metal content. Soil heavy metal content (except Cu) was significantly negatively correlated ($p<0.05$) with microbial P limitation, whereby microbial C limitation was significantly positively correlated ($p<0.01$) with heavy metal content. Microbial C limitation was emphasized as a more appropriate indicator in assessing soil pollution compared to the P limitation.

Ecoenzymatic stoichiometry was emphasized as a promising methodology for heavy metal pollution evaluation in the study by Xu *et al*. [17], which was performed around Pb-Zn mine. The contents of Cd, Pb and Zn were determined in the soil, along with the activities of C-acquiring enzymes (β-1,4-glucosidase, β-D-cellobiosidase), N-acquiring enzymes (β-1,4-N-acetylglucosaminidase L-leucine aminopeptidase) and P-acquiring enzyme (alkaline phosphatase). By calculating the vector lengths and angles, microbial C and P limitation were quantified. Microbial C limitation was significantly positively correlated with Cd, Pb and Zn soil content, which was confirmed with decreasing trend of the vector length. Based on the obtained results, Xu *et al*. [17] stated that microbial metabolic limitation may be used as an index for evaluation of the effects of heavy metal pollution of soil.

The presence of heavy metals in the soil stimulates microbial C metabolism, which can be explained with the fact that microbes consume additional C sources to alleviate HMs toxic effects. On the other hand, heavy metals have negative effects on the growth and reproduction of microorganisms, thus reducing the limitation of P metabolism. Furthermore, the increased soil microbial C metabolism, due to heavy metal stress, affects the soil organic matter decomposition, thus releasing more available P from the organic matter. Also, metal ions (which are positively charged) can form complexes with the negatively charged functional groups (carboxyl and amino groups) on the surface of microorganisms, thus reducing microbial P demand [2,3].

CONCLUSION

Soil pollution with heavy metals has become a worldwide problem due to their environmental persistence and non-biodegradable nature. Bearing this in mind, efforts have been made for the development of indicators which could be used for monitoring and assessment of soil heavy metal pollution. Biological indicators which can be used for soil pollution monitoring, are of great importance since they respond rapidly to the environmental

changes compared to the soil physico-chemical properties. The assessment of soil heavy metal pollution by soil biological properties could be performed by both single and combined enzyme indices. Ecoenzymatic stoichiometry, based on the soil enzyme activity, has been intensively studied as an indicator of the microbial nutrient demand and limitations. Microbial metabolic limitation was defined as a promising indicator for evaluation of soil heavy metal pollution, especially after phytoremediation.

ACKNOWLEDGEMENT

The authors are grateful to the Ministry of Science, Technological Development and Innovation of the Republic of Serbia for financial support, within the funding of the scientific research work at the University of Belgrade, Technical Faculty in Bor, according to the contract with registration number 451-03-47/2023-01/ 200131. Our thanks also go to English language teacher Mara Z. Manzalovic from the University of Belgrade, Technical Faculty in Bor, for providing language assistance.

REFERENCES

[1] Tang J., Zhang J., Ren L., *et al*., J. Environ. Manage. 242 (2019) 121–130.

[2] Wang X., Cui Y., Zhang X., *et al*., Sci. Total Environ. 738 (2020) 139709.

[3] Duan C., Wang Y., Wang Q., *et al*., Environ. Pollut. 300 (2022) 118978.

[4] Kooch Y., Ehsani S., Akbarinia M. Ecol. Eng. 131 (2019) 99–106.

[5] Zhang W., Xu Y., Gao D., *et al*., Soil Biol. Biochem. 134 (2019) 1–14.

[6] Chen Z., Jin P., Wang H., *et al*., Sci. Total Environ. 838 (2022) 156532.

[7] Cui Y., Wang X., Wang X., *et al*., Soil Ecology Letters 3 (3) (2021) 169–177.

[8] Li H., Yao J., Min N., *et al*., Sci. Total Environ. 812 (2022) 152326.

[9] Xu Z., Yu G., Zhang X., Soil Biol. Biochem. 104 (2017) 152–163.

[10] Cui Y., Fang L., Guo X., *et al*., Sci. Total Environ. 648 (2019) 388–397.

[11] Guan H. L., Fan J. W., Lu X., Appl. Soil Ecol. 169 (2022) 104253.

[12] Xiao L., Bi Y., Du S., *et al*., J. Arid Environ. 184 (2021) 104298.

[13] Mori T., Soil Biol. Biochem. 146 (2020) 107816.

[14] Sinsabaugh R. L., Lauber C. L., Weintraub M. N., *et al*., Ecol. Lett. 11 (11) (2008) 1252–1264.

[15] Li Q., Liu Y., Gu Y., *et al*., Sci. Total Environ. 704 (2020) 135413.

[16] Xu M., Cui Y., Beiyuan J., *et al*., Soil Ecology Letters 3 (3) (2021) 230–241.

[17] Cui J., Zhang S., Wang X., *et al*., Geoderma 426 (2022) 116124.

30th International Conference Ecological Truth & Environmental Research
20–23 June 2023, Serbia

ORCHIDS OF THE ZASAVICA SPECIAL NATURE RESERVE

Mihajlo Stanković[1*]
[1]Pokret gorana Sremska Mitrovica, SERBIA
[*]*trogloxen@gmail.com*

Abstract

Eight taxa of orchids were recorded in the area of the reserve, one of which is a natural hybrid. The most widespread taxon in the reserve is E. helleborine with 16 finds, followed by C. damasonium with four finds. The largest number of individuals was found in E. helleborine, a total of 48 and in C. damasonium, a total of 47 individuals. The rarest orchid in the reserve is A. palustris, found only in 2010 with a small number of specimens. The endangered status of orchids in the Zasavica reserve shows that one taxon, A. palustris, is in the endangered species category (EN), while the others have a low level of endangered.

Keywords: orchids, Zasavica, Macva.

INTRODUCTION

Terrestrial orchids belong to the cryptophyte-geophyte life form, because they survive unfavorable periods in the form of tuberoids or rhizomes [1]. Non-photosynthesizing orchids (*Neottia nidus-avis*) remain completely mycoheterotrophic even as adults, while some orchids are photosynthesizing and replenish their carbon supply through ectomycorrhizae. Orchids of the genus *Epipactis* form communities with ectomycorrhizal fungi of the genus *Tuber*, which enter ectomycorrhizae with trees [2]. Feeding with the help of mycorrhizal fungi, they remain underground for years, and when the conditions improve, they reappear on the surface. Orchids have the ability to enter a state of secondary dormancy, when they have an underground lifestyle [3], due to drought, deep freezing of the soil or injury. In Europe, orchids occur in forests, meadows and pastures, in bogs and swamps, which is also the case in the reserve [4], and some inhabit anthropogenic habitats (tailings and ash dumps, embankments of railway tracks, and around roads). The orchid flora in Serbia has a total of 72 taxa, of which there are 57 taxa in Western Serbia (79.17%) and it is an area of moderate richness of orchids [5–7]. Out of a total of 57 taxa of orchids recorded in Western Serbia, 29 taxa grow in the part of Northwestern Serbia [7].

MATERIALS AND METHODS

The orchids in the reserve were created using standard botanical methods, by searching the terrain in their potential habitats. In the locations where orchids were found, the number of specimens per area was counted, the height of the above-ground part of the plant was measured, individuals in flower or fruit and those without flower or fruit were counted, and

other plants in their immediate vicinity were listed. The determination was made according to the literature [7–9].

Site overview with GPS coordinates according to Google Earth Pro.

Locations	X	Y
Banovo polje, Trebljevine	44°55'31.96"N	19°26'37.07"E
Salaš Noćajski, Ostrovac	44°57'54.49"N	19°33'09.07"E
Ravnje, Staniševac	44°55'58.95"N	19°24'45.83"E
Ravnje, Prekopac	44°55'18.52"N	19°25'19.53"E
Radenković, Batar	44°55'42.16"N	19°28'33.53"E
Radenković, Pačija bara odel.35	44°56'30.29"N	19°29'49.40"E
Radenković, Vrbovac odel.35	44°56'26.80"N	19°29'54.07"E
Radenković, Vrbovac odel.34	$44^0$57’04.00"N	$19^0$29’18.92"E
Banovo polje, Duge njive	44°55'40.31"N	19°27'48.25"E
Zasavica II, Lađine	44°57'52.66"N	19°31'53.45"E
Glušci, Češljuška bara-Bitva	44°54'41.14"N	19°31'47.65"E
Glušci, Bitva	44°54'08.52"N	19°33'26.15"E
Radenković, Vrbovac	44°57'10.03"N	19°28'09.65"E
Zasavica II, Turske livade	44°57'42.09"N	19°31'24.00"E
Metković-Belotić	44°50'13.50"N	19°33'21.42"E

RESULTS AND DISCUSSION

Eight were recorded in the area of the reserve orchid taxa, of which 7 are pure taxa and one is a natural hybrid.

Overview of orchids in the reserve with basic information:

- ***Anacamptis palustris*** (Jacq.) R. M. Bateman, Pridegeon & M. W. Chase agg. [syn. *Orchis laxiflora ssp. palustris*]: Banovo polje: Trebljevine, 2010., (CQ77), forest, Σ= 5;
- ***Cephalanthera damasonium*** (Mill.) Druce [syn. *C.alba*]: Salaš Noćajski: Ostrovac, 05.08.2012., forest, Σ=13; Banovo polje: Trebljevine, 04.08.2013., forest, Σ=47; Ravnje: Staniševac, 07.08.2020., forest, Σ=5; Prekopac, 25.07.2003., reedbeds, (herbarium collection);
- ***Cephalanthera longifolia*** (L.) Fritsch: Radenković: Batar, 03.08.2010., forest;
- ***Cephalanthera x schulteicam****:* Radenković: Batar, 03.08.2010., forest, Σ=1 (herbar. collect.);
- ***Epipactis helleborine*** (L.) Ceantz: Radenković: Batar (forest in old oak trees), 03.08.2011., forest, Σ=7; Pačija bara odel. 35, 04.08.2016., forest, P=5x5m Σ=9 (6 in bloom); 04.08.2016., forest, Σ=55; 05.08.2016., forest, Σ=45; 05.08.2017., forest, Σ=48; Pačija bara odel. 34, 06.08. 2021., forest, Σ=11; Vrbovac odel. 34, 05.08.2017.,

forest, Σ= 45; 07.08.2021., forest, Σ= 11; Vrbovac, 06.08. 2021., forest, Σ=13; Banovo polje: Trebljevine, 03.08.2013., forest, Σ=10; 04.08.2013., forest, Σ=1 (herbar. collect); 04.05.2021., forest, Σ=30 on the P=4x5 m; 04.08.2021., forest, P=4x5 m Σ=30; Duge njive, 08.08.2020., forest, Σ=14; Ravnje: Staniševac, 07.08.2020., forest, Σ= 5; Zasavica II, Lađine, 04.05.2021., forest Σ= 2; Glušci: Češljuška bara-Bitva, 07.08.2021., forest, Σ=3; Bitva, 07.08.2021., forest Σ=5;

- ***Neottia sp.*** **(*Neottia ovata*** ??) [*Listera* sp.-(*Listera ovata* ??)]: Zasavica II: Turske livade, 07.08.2012., forest, Σ=1; Metković-Belotić, 13.06.2015., forest, Σ=1 (foto);
- ***Neotinea tridentata*** (Scop.) R. M. Bateman Pridegeon & M. W. Chase [syn. *Orchis tridentata]*: Banovo polje: Trebljevine, 25.07.2010., reedbeds, Σ=5;
- ***Neottia nidus-avis*** (L.) Rich.: Banovo polje: Trebljevine, 04.08.2021., forest, Σ=37.

A total of 57 taxa of orchids were recorded in Western Serbia, of which 3 taxa are from the genus *Cephalanthera* and *Neottia*, 6 taxa are from the genus *Anacamptis*, while the most represented genus is *Epipactis* with 9 taxa. Out of a total of 57 taxa of orchids recorded throughout Western Serbia, 29 taxa grow in Northwestern Serbia [7]. The most widespread taxon in the reserve is *Epipactis helleborine* with 16 finds, followed by *Cephalanthera damasonium* with four finds and *Listera* sp. with two findings, while the remaining taxa had one finding each. All taxa except *Neotinea tridentata* and *Anacamptis palustris* were found in the forest, and *N. tridentata* and *A. palustris* were found in the rushes (the contact of the emergent zone and the forest when there is no water). There are two taxa (*E. helleborine* and *N. tridentata*) in the first level of protection, and the largest number of finds was in the second and third level. A small number of individuals were found in most orchids. The largest number of individuals was found with *E. helleborine* in Pacija bara, ward 35, in 2017, a total of 48 individuals, and with *C. damasonium* in the forest on Trebljevina in 2013, a total of 47 individuals. In the temperate climate zone, orchids occur in forest, meadow and pasture habitats, as well as in bog and swamp ecosystems, which is also the case in the reserve [4], and the largest numbers of species are in forests. Analyzing the summary distribution, we see that it's least wealth and diversity is in Mačva [7]. Eight taxa in the reserve represent 27.50% of the orchid flora of Northwestern Serbia or 14.03% of the orchid flora of Western Serbia or 11.10% of the orchid flora of Serbia. In relation to altitude, according to [7], of the 8 taxa recorded in the reserve, three taxa prefer an altitude of 0-100 m, namely *C.damasonium, C.longifolia, E.helleborine*. In relation to the type of habitat according to the EUNIS classification, grassy habitats and tall sedge habitats are preferred by the taxa *Anacamptis laxiflora, A. palustris, C. longifolia, N. tridentata*, forests and woodland habitats and other forested areas are preferred by the taxa *C. damasonium, C. longifolia, E. helleborine, N. tridentata, N. nidus-avis* and heaths, shrub habitats and tundra *N. tridentata*.

Of the mentioned habitats, heathland and tundra are the only ones that are not represented in the area of the reserve. The genus *Epipactis* and *Orchis* also inhabit anthropogenic habitats, such as tailings and ash dumps, embankments of railway tracks, as well as the vicinity of roads [10,11], and here in the reserve we have a case of the perennial occurrence of *Epipactis helleborine* in a semi-natural anthropogenic habitat what is the culture of the hybrid Euro-

American poplar, where there is inter-row processing by truncation and occasional trampling by heavy machinery. In the flora of Western Serbia according to Đorđević [7], as the most widespread taxa, i.e. which are registered in a large number of localities, 13 taxa stand out, of which four taxa *C. damasonium, C. longifolia, E. helleborine, N. nidus-avis* are present in the reserve, and of which *E. helleborine* is the most represented in the area of the reserve, otherwise it is present in both lowland and high mountain areas [4,12]. The wide distribution of these taxa can be explained by their great adaptability and plasticity, as well as the large representation of the habitats they inhabit, but the wide distribution of individual orchids can be explained by a lower degree of specialization towards pollinators, as for example in *E. helleborine* [13]. Among the rarest orchids of western Serbia, i.e. which were found in the smallest number of localities is 11 taxa, and the rarity of these orchids can be explained primarily by their specific habitat requirements [4], such as e.g. specific types of wet meadows and heaths, including *A. palustris*, found in Zasavica, only in 2010 with a small number of specimens. Orchids spread slowly because they are weak competitors, but once they occupy some space they stay there for many years. If environmental conditions change, e.g. due to an increase in light and a decrease in humidity after cutting down trees or an increase in shading due to the growth of trees and shrubs, orchids can switch to an underground lifestyle. Feeding with the help of mycorrhizal fungi, they remain underground for years, only to reappear on the surface when conditions improve. The strongest competitors of orchids in the fight for space and resources are representatives of the families *Cyperaceae* and *Poaceae* [3], which are very often present in the forests of the reserve. Overgrowth of parts of meadows by competing species *Filipendula ulmaria* and *Deschampsia caespitosa* can completely suppress orchids from those meadows [7]. It is important to emphasize that orchids often inhabit habitats along meadow-forest ecotones, as well as microhabitats that are less populated by other plant species, such as the edge zones of forest and meadow habitats, as well as the surroundings of forest paths, an example of these situations in the reserve is part of the species findings *E. helleborine* and *C. damasonium*.

An overview of orchids of the reserve with belonging to basic horological groups and subgroups and floral elements according to Đorđević [7], is given in Table 1.

Table 1 *Overview of orchids with affiliation to basic horological groups and subgroups and floral elements*

SPECIES	Horological group and subgroup and floral elements
Anacamptis laxiflora	MEDSUBMED MED-SUBMED Atl(S)-Med-submed(W-E)
Anacamptis palustris	EAS EAS(W-C) (tempsubmerid)Atl(S)-SE(W-E)-Eux-Cauc-Pont-Irano-Turan-Aralo-Casp
Cephalanthera damasonium	SESE-CAUC-(Medsubmed)Atl-Med-submed(W-E)-SE(W-E)-Pont) W)-Cauc-Iran(N)
Cephalanthera longifolia	EAS EAS(W-C)Atl-Med-submed(W-E)-SE(W-E)-Cauc-Himal (W)
Epipactis helleborine	EAS EAS(W-E) (tempsubmerid) Atl-Med-submed(W-E)-SE(W-E)-Cauc-Pont(W)-Sib(W-E)-Alt-Him(W-C)
Neottia nidus-avis	SE SE-CAUC Atl-Se(W-E)-Cauc
Neotinea tridentata	MEDSUBMED MED-SUBMED sl (Medsubmed-SE-Cauc-Pont) Med-submed(W-E)-SE(S)-Cauc-Eux-Pont(w)-Krim

In Western Serbia, the Central European horological group (SE) is most represented with 21 taxa from 11 genera, of which four genera (*Cephalanthera, Epipactis, Neottia, Orchis*) are present in the reserve [7]. The Mediterranean-sub-Mediterranean group (MED-SUBMED) includes two genera (*Anacamptis, Orchis*), which are also present in the reserve. Non-photo-synthesizing orchids such as *N. nidus-avis* remain completely mycoheterotrophic and provide the necessary nutrients through ectomycorrhizae. Some species from the genus *Epipactis* form communities with ectomycorrhizal fungi from the genus *Tuber*, which enter ectomycorrhizae with trees [2], which can be connected with the findings of the orchid *E. helleborine* and the locality of found truffles [14]. The property of orchids to go into a state of secondary rest, i.e. to an underground way of life [3], due to drought, deep freezing of the soil or injury to individuals was also recorded in the area of the reserve with *C. damasonium* and *E. helleborine* in the form of their periodic appearance with multi-year breaks. According to the data of Đorđević [7], the northernmost find for *N. nidus-avis* in North-Western Serbia so far is Vladimirci, Kaona. Our orchid finds in the reserve are now the northernmost find in Northwestern Serbia and new data for the flora of Serbia. In the orchid flora of Western Serbia, the closest locality for *Listera* sp. is the vicinity of Valjevo and Sokolska mountains, and determination of the species was not possible because no flowers appeared that year.

Threat status of orchids in the Zasavica reserve

The threat status of orchids in the Zasavica reserve is given in Table 2.

Table 2 *Overview of the endangered status of orchids in the Zasavica reserve*

SPECIES	IUCN (2012)	IUCN (E)	CITES	PZDV	PPPT
Anacamptis palustris	EN B2ab(iii); D		II	I	VII
Cephalanthera damasonium	LC	LC	II	II	VIII
Cephalanthera longifolia	LC	LC	II	II	VIII
Epipactis helleborine	LC	LC	II	II	VIII
Neotinea tridentata	LC	LC	II	II	VI, VIII
Neottia nidus-avis	LC	LC	II	II	VIII

IUCN (E) – IUCN category of threat on the Red List of the Flora of Europe; **IUCN (2012)** – endangered category and criteria (western Serbia); **CITES II** – a species that is not threatened with extinction, but whose trade must be controlled; **PZDV** – Rulebook on the declaration and protection of strictly protected and protected wild species of plants, (I – strictly protected species, II – protected species); **PPPT** - Rulebook on cross-border traffic and trade in protected species (II – plant species from Appendix B of the Regulation, VI – plant species from Annexes I and II of the PPPT Rulebook whose entry into the Republic of Serbia is prohibited, VII – plant species from Appendix I of the **PZDV** Rulebook, VIII – species of plants from Appendix II of the PZDV rulebook).

Threatening factors of orchids in the Zasavica reserve

The conversion of natural habitats into agricultural areas threatens the largest number of orchids in western Serbia. Urbanization and infrastructure construction are in second place, while tourism is in third place. This is followed by pollution of habitats and pastures and mowing, felling of forests that are not ecologically designed and forest management, as well as afforestation with non-native species or ecologically inadequate species. The factors that threaten the smallest number of species and subspecies of orchids are: over-exploitation of orchids (21 taxa), invasive and non-native species (19 taxa) and changes in the hydrological

regime (17 taxa) [7]. All the mentioned factors are present in the reserve to a greater or lesser extent.

CONCLUSION

Eight taxa of orchids were recorded in the reserve area, of which 7 are pure taxa and one is a natural hybrid. According to the protection regimes, two taxa (*E. helleborine* and *N. tridentata*) were found in the regime of protection level I, while the largest number of findings was in the regime of level II and III. A small number of individuals were found in most orchids. The most widespread taxon in the reserve is *E. helleborine* with 16 finds, followed by *C. damasonium* with four finds and *Listera* sp. with two findings, while the remaining taxa had one finding each. All taxa, except *N. tridentata* and *A. palustris*, were found in the forest, while these two taxa were found in rushes, i.e. the contact of the emergent zone and the forest at the time when the water receded from the terrain. The largest number of individuals was found in *E. helleborine*, a total of 48 individuals, and in *C. damasonium*, a total of 47 individuals. The rarest orchid in the reserve is *A. palustris*, found only in 2010 with a small number of specimens. The endangered status of orchids in the Zasavica reserve shows that one taxon, *A. palustris*, is in the endangered species category (EN), while the others have a low level of endangered.

REFERENCES

[1] Ellenberg H., Mueller-Dambois D., A key to Raunkiaer plant life forms with revised subdivisions – Ber. Geobot. Inst., ETH, Zurich 37 (1967) 56–73.

[2] Selosse M. A., Faccio A., Scappaticci, *et al*., Microb. Ecol. 47 (2004) 416–426.

[3] Molnár A., Sulyok J., Vidéki R., Vadon élö orchideak. – Kossuth Könyvkaidó, Budapest (1995).

[4] Delforge P., Orchids of Europe, North Africa and the Middle East. – A. & C. Black Ltd, London, (2006), ISBN13: 9780713675252.

[5] Diklić N., Fam. Orchidaceae. *in* Josifović M., editor, Flora SR Srbije VIII. –SANU, Beograd (1976) 36–116.

[6] Djordjević V., Tsiftsis S., Lakušić D., *et al*., Wulfenia 24 (2017)143–162.

[7] Đorđević D. V., Prostorna distribucija i ekologija orhideja (Orchidaceae) Zapadne Srbije (Doktorska disertacija), Univerzitet u Beogradu, Biološki fakultet, Beograd, 1–709 (2018).

[8] Javorka S., Csapody V., Kozep-europa delkeleti reszenek floraja kepekben Iconographia florae partis austro-orientalis europae centralis, (ed. priszter, sz.), Akademiai kiado. Budapest (1975).

[9] Gajić M., Karadžić D., Flora ravnog Srema sa posebnim osvrtom na Obedsku baru, Šumarski fakultet Beograd i Šumsko gazdinstvo Srem. Mitrovica (1991) 31–322.

[10] Adamowski W., Pol. Bot. Stud. 22 (2006) 35–44.

[11] Rewicz A., Zielińska K. M., Kiedrzyński M., *et al*., Arch. Biol. Sci. 67 (2015) 119–130.

[12] Baumann H., Künkele S., Lorenz R., Die Orchideen Europas. Mit angrenzenden Gebieten. – Eugen Ulmer KG, Stuttgart, (2006) 333.

[13] Rewicz A., Jaskuła R., Rewicz T., *et al*., PeerJ 18 (5) (2017) e3159.

[14] Stanković M., Zbornik radova Naučno-stručnog skupa o biodiverzitetu i drugim vrednostima rezervata Zasavica „ZASAVICA 2017.“ sa međunarodnim učešćem, (2017) 65–70.

CLIMATIC BALANCE OF THE WATER FOR THE SOIL OF THE KRUŠEVAC REGION IN CENTRAL SERBIA

Gordana Šekularac[1*], Miroljub Aksić[2], Tatjana Dimitrijević (ex. Ratknić)[3], Milica Vranešević[4], Nebojša Gudžić[2], Mihailo Ratknić[5]

[1]University of Kragujevac, Faculty of Agronomy, Cara Dušana 34, 32000 Čačak, SERBIA

[2]University of Priština, Kosovska Mitrovica, Faculty of Agriculture, Kopaonička nn, 38219 Lešak, SERBIA

[3]Institute of Forestry, Kneza Višeslava 3, 11000 Belgrade, SERBIA

[4]University of Novi Sad, Faculty of Agriculture, Dositeja Obradovića 8, 21000 Novi Sad, SERBIA

[5]Earthe Climate Change Team (ECCTeam), New Jersey, USA

[*]*gordasek@kg.ac.rs*

Abstract

The paper was aimed at analyzing the climatic water balance of the soil of the Kruševac region in the Central Serbia. There were used the average monthly long–term (30 years) data on the mean air temperatures (T), the mean precipitations (P) and the mean potential evapotranspiration (PE) for the coordinates of the meteorological station of the area studied. The highest mean air temperatures were recorded in July (21.8°C), then in August (21.5°C) and in June, (20.0°C), respectively, whereas the highest precipitations were recorded in June and in May (86 mm and 79 mm, respectively). The potential evapotranspiration was the highest in July (129 mm), to drop in August (116 mm) and in June (114 mm), respectively. On average, the real evapotranspiration (RE) was reported to be the highest in June (114 mm), followed by those reported in May (99 mm) and in July (92 mm), respectively. The average water deficit (WD) in the soil was evidenced as the highest in August (71 mm), lower in July (37 mm), September (34 mm) and the lowest in October (8 mm), respectively, when the soil needed irrigation. The analysis denoting to the average water surplus (WS) recorded in January (30 mm) and in February (17 mm) suggested that drainage be needed.

Keywords: climate, water balance, soil, evapotranspiration.

INTRODUCTION

Soil irrigation is referred to as the water use in the plant production for more intensively utilized environmental conditions of the particular area, thereby relating nor only to the plant but also to the agricultural production in a wider sense. Water gives life in the desert and semi–desert areas, while in the regions of a moderate climate with sensible and expert management, it can provide abundance and safety.

The most significant factors of water irrigation are considered to be climatic–meteorological characteristics, soil features plant requirements for water due to which, they ought to be studied for each area. Within this type of analysis, the water balance

of the soil meaning the quantitative changes in the water content during a particular period of time on a particular area is considered to be a highly significant indicator of using soil reclamation measures, irrigation and drainage, too. When defining the soil water balance of the particular area, all the elements of water stored and consumed along with all the resulting changes in its content are taken into consideration [1]. The most important factors of the soil water balance of a certain area are considered to be precipitations as a natural item and the potential evapotranspiration, i.e. plant requirements for water as a consumption item [2]. Eagleson [3] describes water balance as a quantitative relation among long–term averages of the partition of precipitation and evapotranspiration, which are the most critical parameters. Those parameters are typically computed as the average values from a time–series data set. Also, according to Milly and Fischer and Du Toit **[**4,5], the long–term water balance is determined by the interaction of precipitation and potential evapotranspiration and is regulated by the soil water storage.

Therefore, this paper aims at showing the results of the analysis made on the soil water balance for the region of Kruševac.

MATERIALS AND METHODS

For achieving the climatic soil water balance of the Kruševac region (middle/southern part of central Serbia, 43°35'00" N 21°19'36" E, 137 m.a.s.l.) (Figure 1), the elements favouring both, water inflow into and its outflow from the soil, i.e. it loss, are considered to be air temperatures (1981–2010) and the average precipitation sums (1961–1990) [6] as well as the average values of evapotranspiration following the method of Penman–Montheit (1971–2000) [7].

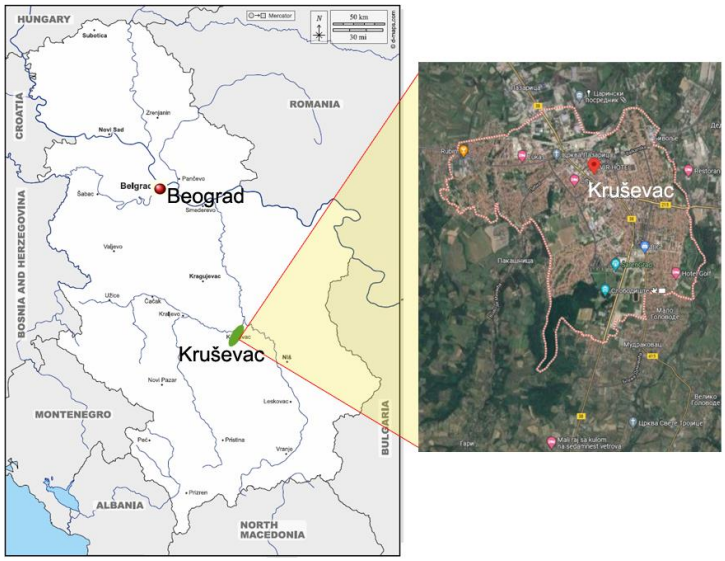

Figure 1 *Kruševac area*

Water balance in the soil was calculated after the method of Thornthwaite [8], assuming that the soil containing 100 mm of the readily available water in the rhizosphere zone was

entirely saturated. Evapotranspiration seemed to be quite constant until 100 mm of the water stored was consumed whereas the remaining water amounts ran off, being the water surplus,. In there was no water reserve in the soil, the evapotranspiration would be equal to zero, with the water deficit prevailing till the new rainfalls.

In addition to the water deficits and surpluses, the soil water balancing also established the values of the real evapotranspiration within the real natural conditions of the area studied.

RESULTS AND DISCUSSION

According to the data collected for the period from 1961 to 1990, the annual air temperature for the republic of Serbia averaged 10.1°C, with January being the coldest and July the hottest month averaging 19.9°C [9]. In addition, the normal annual precipitations averaged 734 mm and those in the valley of the Velika Morava 650 mm, with their higher decreasing intensity noticed over the last series of 35 and 30 years, respectively.

Kruševac is characterised by the annual air temperature (T) of 11.4°C, with the maximum mean monthly values evidenced in July and in August (21.8°C and 21.5°C, respectively) and the minimum one of 0.2°C in January (Figure 2).

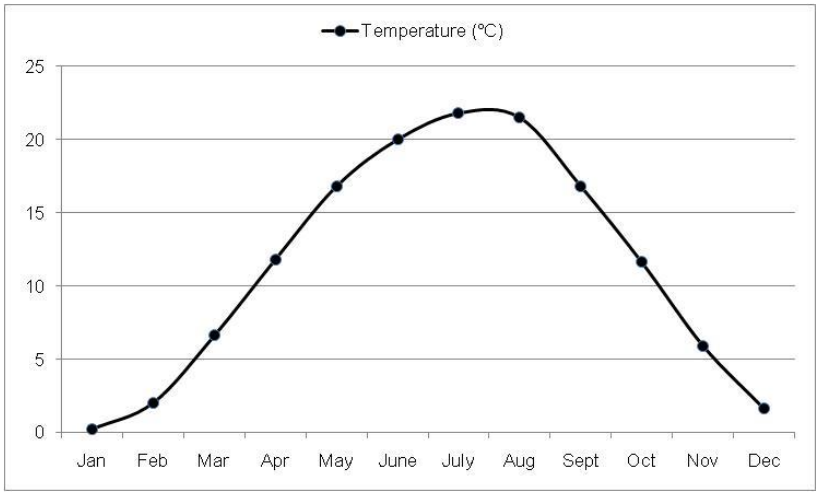

Figure 2 *Average monthly temperatures (T)*

The annual precipitation (P) sum of the Kruševac region amounted to 647 mm, with its maximum reported in June (86 mm) and that in May (79 mm) and the minimum over the winter months (Figure 3). Practically speaking, the period during which the average annual air temperatures increased most was accompanied by that when the average annual precipitations began to decrease (Figures 2 and 3).

Within the climatic conditions of Kruševac, as the average plant requirement for water, the average annual potential evapotranspiration (PE) amounted to 776 mm (maximum in July 129 mm, August 116 mm and in June 114 mm, respectively) (Figure 3).

Water balancing procedure helped determine water deficit and surplus in the soils of the Kruševac region. Water deficit in the soil takes place when the required water (PE) is higher than the available water. The mean annual value of the water deficit (WD) for the soil of the

region Kruševac was found to amount to 150 mm, with the most expressed deficit established in August (71 mm), followed by those found in July (37 mm), September (34 mm) and in October (8 mm), respectively (Figure 4).

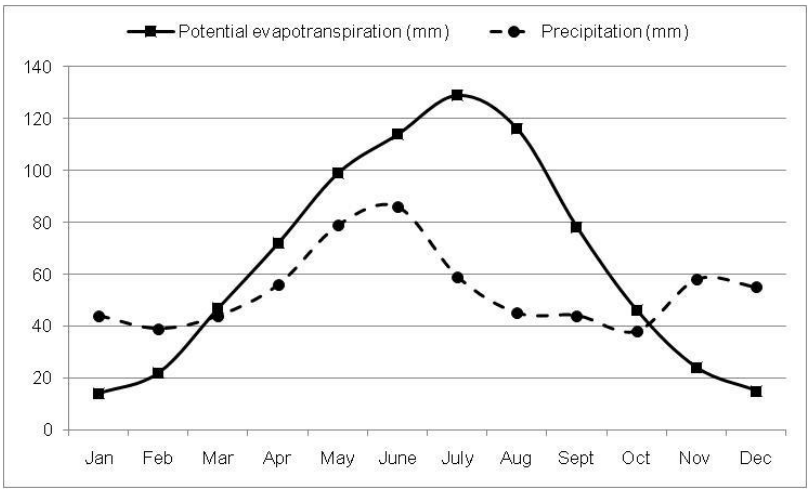

Figure 3 *Average monthly precipitation (P) and potential evapotranspiration (PE)*

Water surplus (WS) in the soil of the area concerned takes place when the water entirely available to evapotranspiration (the existing water reserve in the soil form the rainfalls, i.e. the readily available water reserve, REAV) is higher than the real requirement for water (PE). When the part of the available water was used for the water reserve renewal (REAV) of 100 mm, then the water surplus was exhibited in it [10]. The mean annual value of the WS for the area of Kruševac amounted to 47 mm of which 30 mm was recorded in January and 17 mm in February (Figure 4), noticing that while controlling the average annual water balance for an insight in the calculations reliability, the water surplus of 26 mm, which would be carried over and added to the next period of calculation, occurred.

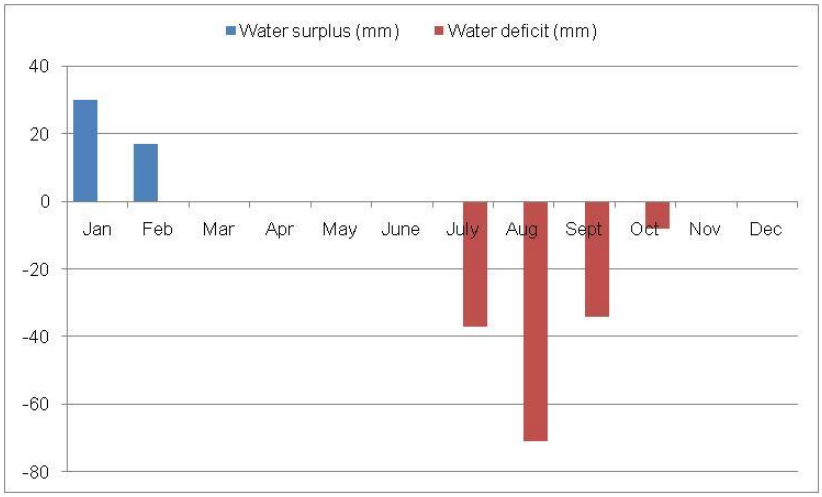

Figure 4 *Average monthly water deficit (WD) and water surplus (WS)*

Thus, the mean annual value of the real evapotranspiration (RE) indicated the real amount of the water availability in the soil depending on the environmental conditions [1], which amounted to 626 mm for the region of Kruševac (Figure 5). The maximum RE was revealed in June (114 mm), and the minimum in December (15 mm).

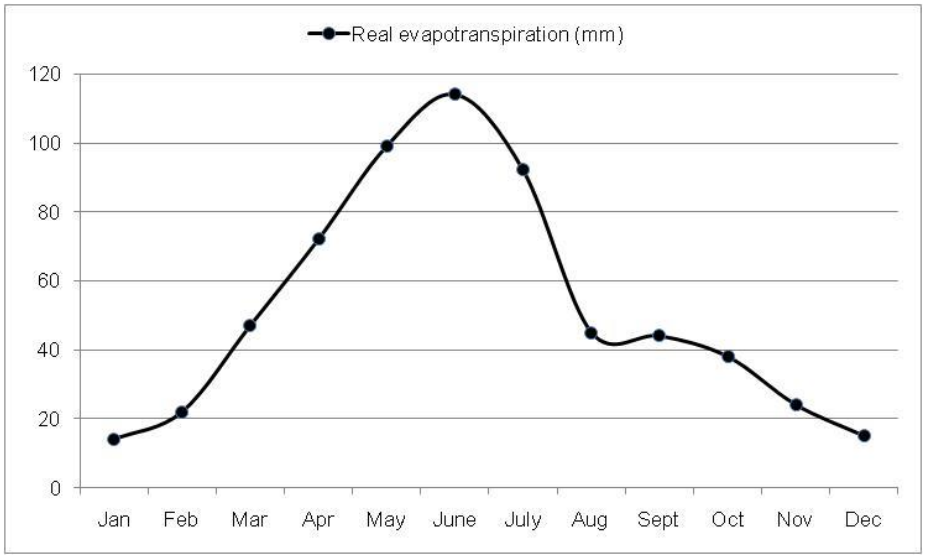

Figure 5 *Average monthly real evapotranspiration (RE)*

For comparison, the research results for the soil of the Middle Podunavlje through Vojvodina (1964–2007) can be mentioned, with the mean values of the rainfalls recorded to be 693.90 mm, the potential evapotranspiration 725.53 mm, the total water deficit averaging 115.91 mm, its surplus being 84.28 mm, along with the real evapotranspiration amounting to 609.62 mm [11].

CONCLUSION

The aim of the paper was to analyze the climatic water balance in the soil of the Kruševac region using the long–term series of values obtained for all the elements over the balancing procedure in order to establish water deficit for the purpose of irrigation as a regular practice, alleviate the impact of consequences of drought on the plant as well as determine the water surplus for drainage. On average, water deficit was exhibited from July to October and its surplus from January to February, with an extra surplus of water of 26 mm carried over to the following period of calculation.

ACKNOWLEDGEMENT

The authors are grateful to the Ministry of Science, Technological Development and Innovation of the Republic of Serbia for financial support (contracts no. 451-03-47/2023-01/200088; 200189 and 451-03-47/2023-01/200027) as well as by the Provincial Secretariat for Higher Education and Scientific Research activity of the Vojvodina (contract no. 142-451-3114/2022-01/2).

REFERENCES

[1] Vučić N. Navodnjavanje poljoprivrednih kultura. Univerzitet u Novom Sadu, Poljoprivredni fakultet, Novi Sad (1976), pp. 46–62.

[2] Rajić M., Ann. Agron. 27 (1) (2003) 160–168.

[3] Eagleson P. S. Ecohydrology – Darwinian expression of vegetation form and function, Cambridge University Press, Cambridge (2002), p.170, ISBN(eBook):0–511–04083–0.

[4] Milly P. C. D., Water Resour. Res. 30 (7) (1994) 2143–2156.

[5] Fischer P. M., Du Toit B., iForest 12 (1) (2019) 51–60.

[6] Republički Hidrometeorološki zavod Srbije, Meteorološki godišnjak–klimatološki podaci. *Available on the following link*:

www.hidmet.gov.rs/latin/meteorologija/klimatologija_godisnjaci.php.

[7] Republički Hidrometeorološki zavod Srbije. Prosečne sume potencijalne evapotranspiracije po metodi Penman – Montheit–a (1971–2000). *Available on the following link*: www.hidmet.gov.rs/latin/meteorologija/pros_pet.php.

[8] Thornthwaite C.W., Geogr. Rev. 38 (1948) 55–94.

[9] Popović T., Radulović E., Jovanović M., Koliko nam se menja klima, kakva će biti naša buduća klima? *Available on the following link*: www.sepa.gov.rs/download/5_web.pdf.

[10] Vlahinić M. Navodnjavanje, Univerzitet u Sarajevu, Poljoprivredni fakultet, Sarajevo (1982), p. 10.

[11] Pekeč S., Orlović S., Ivanišević P. *et al*., Topola 187–188 (2011) 5–13.

30th International Conference Ecological Truth & Environmental Research
20–23 June 2023, Serbia

INFLUENCE OF IRRIGATION METHOD ON THE OCCURRENCE AND INTENSITY OF THE GRAY MOLD OF LETTUCE

Gordana Šekularac[1*], Miroljub Aksić[2], Tatjana Dimitrijević (ex. Ratknić)[3], Milica Vranešević[4], Slaviša Gudžić[2], Nebojša Gudžić[2], Mihailo Ratknić[5]

[1]University of Kragujevac, Faculty of Agronomy, Cara Dušana 34, 32000 Čačak, SERBIA

[2]University of Priština, Kosovska Mitrovica, Faculty of Agriculture,
Kopaonička nn, 38219 Lešak, SERBIA

[3]Institute of Forestry, Kneza Višeslava 3, 11000 Belgrade, SERBIA

[4]University of Novi Sad, Faculty of Agriculture, Dositeja Obradovića 8,
21000 Novi Sad, SERBIA

[5]Earthe Climate Change Team (ECCTeam), New Jersey, USA

[*]*gordasek@kg.ac.rs*

Abstract

The experiment on fungicide efficiency when controlling lettuce grey mold in dependance of irrigation mode, was made in the greenhouses in 2021. Under conditions of drip irrigation, the lowest percent (1.2%) of the diseased plants was revealed on the variant treated with the fungicide Switch. Of the treated variants, the highest infestation percent was recorded in the variant treated with Folio Gold (3.7%) whereas on the control variant without chemical treatment, 10.5% of the diseased plants was recorded. The disease intensity caused by B. cinerea on the control variant in the greenhouse experimental area with micro sprinkler greenhouse irrigation was 15.7%. The infection intensity with the chemically treated variants was reported to be the strongest on the variant treated with Teldor (7.0%) and the weakest on that treated with the fungicide Switch (3.2%). Thus, the most efficient fungicide for lettuce protection from B. cinerea proved to be Switch (88.1%). Comparatively highly efficient with grey mold control was also Signum (80.1%). Somewhat lower level of efficiency was exhibited by Folio Gold (64.3%) and Teldor (69.1%). The fungicide Switch showed the best results with grey mold control in lettuce (79.4%). Signum was also quite efficient (73.0%), with lower efficiency recorded on the variants treated with Folio Gold (61.9%) and Teldor (55.5%).

Keywords: irrigation, lettuce, *B. cinerea*.

INTRODUCTION

An intensive vegetable production is possible only under irrigation conditions. Thus, the properly chosen irrigation method for lettuce is of paramount importance for achieving an optimal soil moisture, which is the basic precondition for the proper lettuce growth and development. Lettuce has rather shallow root system [1]. Therefore, water is a highly important factor for its optimal growth sustainment during the whole vegetation, both, for germination and sustainment of a high rate of photosynthesis [2].

Irrigation in agriculture will face big challenges in the future. Increase in the world`s food production will primarily depend on the quantity and quality of irrigation water [3]. Drip

irrigation system is considered to be a noticeably more advantaged method than the other irrigation methods and, hence, the most efficient mode of plant supply with water and nutrients, which, not only saves water, but also increases crop yield [4]. Thus, an efficient water use through an improved irrigation technique is of prior importance to agriculture [5]. Drip irrigation enables a uniform water distribution and fertilizers uptake by the root system zone, which results in higher crop yields [6]. It is exceptionally significant to determine the time of irrigation in order to utilise the irrigation system most efficiently whereas inadequate irrigation measures may cause stress and lower production [7]. A rational irrigation regime should fulfill the requirements of lettuce for water and thus exclude the potential risks of an excessive soil moisture, which may lead to crop diseases. One of the biggest challenges lettuce producers are facing with is regarded the protection from pests. Thus, the decrease in lettuce yield results most commonly from the destructive crop diseases [8], with the yield losses varying from 1% to nearly 75% [9].

The research goal was, therefore, to establish the impact of lettuce irrigation method on the onset and intensity of *Botrytis cinerea.* In addition, the degree to which the applied fungicides have proved efficient in *B. cinerea* control, will also be determined.

MATERIALS AND METHODS

The experiment on fungicide efficiency when controlling lettuce grey mold in dependance of irrigation mode, was made in the greenhouses in 2021. The greenhouses are situated in the village of Batušinac, the municipality of Merošina (south-east Serbia) (43°26'11" N 21°82'28" E). The lettuce was sown in hotbed greenhouse on the 22nd of January. The seed of Sunny cultivar was used. The lettuce transplant was produced under controlled conditions, the air temperature, soil temperature and a relative air humidity were measured, too. The lettuce was sown on a permanent place in the greenhouse on the 25th of February, sowing spacing of 25×25 cm. Irrigation was done through micro sprinkler and drip irrigation. Tensiometer was used to determine watering time, the irrigation started when the soil moisture capillary potential was 20 kPa. After the soil chemical analysis, the basic fertilisation prior to planting with NPK combination of 8:16:24 in the amount of 50 g/m^2, was performed. Through the irrigation system, the lettuce was fertilised with NPK fertilisers in the ratio of 15:15:35, being: I fertilisation of 10 days upon the planting in the amount of 6 g/m^2 and, II fertilisation, 15 days upon the first fertilisation in the amount of 6 g/m^2. The trial was set up as a block design fitted to the irrigation conditions, 5 variants with 4 replications each. The four variants were treated with chemical means and the fifth one was the control variant. Each replication comprised 100 plants. Intensity assessment of *B. cinerea* onset was made through five categories ranking from 0 to 4 [10].

After the infestation intensity of *B. cinerea* had been classified, the disease index calculated by the formula of Mc Kinney supposed to indicate the mean value of the disease attacking a particular area (Equation 1):

$$I = \frac{\Sigma(n \times k)}{N \times K} \times 100 \quad (1)$$

was put forward: I – disease index in %, n – plant number within a category, k – number of single categories, N – total plant number and, K – total number of the categories.

The efficiency of fungicides (Table 1) was calculated using the formula of Abbott (Equation 2), being:

$$E = \frac{C - T}{C} \times 100 \quad (2)$$

was put forward: E – efficiency of the fungicide studied, C – plant number on the untreated variant and, T – plant number on the treated variant.

Table 1 *Overview of the fungicides tested*

Fungicide	Formulation	Active substance	Dose
Switch 62.5	WG	Fludioksonil 250 g/kg + Ciprodinil 375 g/kg	0.6 kg/ha
Folio Gold 537.5	SC	Metalaksil–m 37.5 g/l + Hlorotalonil 500 g/l	2.5 l/ha
Signum	WG	Piraklostrobin 67 g/l + Boskalid 267 g/l	1.5 kg/ha
Teldor 500	SC	Fenheksamid 500 g/l	1.0 l/ha

RESULTS AND DISCUSSION

Further, the results obtained for disease intensity of lettuce caused by *B. cinerea* while using drip irrigation, are presented in the Table 2.

Table 2 *Intensity of B. cinerea infection on lettuce drip – irrigation*

Variant	Fungicide	Number of infected plants per repetition				Infected plants (%)
		I	II	III	IV	
V_1	Switch	2	1	1	1	1.2
V_2	Folio Gold	5	4	4	2	3.7
V_3	Signum	2	3	1	2	2.0
V_4	Teldor	3	2	5	3	3.2
V_5	Control	11	12	9	10	10.5

The lowest percent (1.2%) of the diseased plants was revealed on the variant treated with the fungicide Switch. Of the treated variants, the highest infestation percent was recorded in the variant treated with Folio Gold (3.7%) whereas on the control variant without chemical treatment, 10.5% of the diseased plants was recorded.

The disease intensity caused by *B. cinerea* on the control variant in the greenhouse experimental area with micro sprinkler greenhouse irrigation was 15.7% (Table 3). The infection intensity with the chemically treated variants was reported to be the strongest on the variant treated with Teldor (7.0%) and the weakest on that treated with the fungicide Switch

(3.2%). The percent of the diseased lettuce plants was higher with micro sprinkler irrigation in all the variants than being with drip irrigation (Figure 1). It was also found out that the consistently less intensity of the disease onset in lettuce using drip subirrigation could favour the long–term sustainability of this irrigation method in practice when coping with diseases [11]. Lettuce was less affected by this disease with drip irrigation whereas no significant effect of different irrigation methods on the disease onset intensity, was noticed [12].

Table 3 *Intensity of B. cinerea infection on lettuce – micro – sprinkler irrigation*

Variant	Fungicide	Number of infected plants per repetition				Infected plants (%)
		I	II	III	IV	
V_1	Switch	3	4	2	4	3.2
V_2	Folio Gold	6	7	5	6	6.0
V_3	Signum	5	5	3	4	4.2
V_4	Teldor	7	8	7	6	7.0
V_5	Control	16	14	16	17	15.7

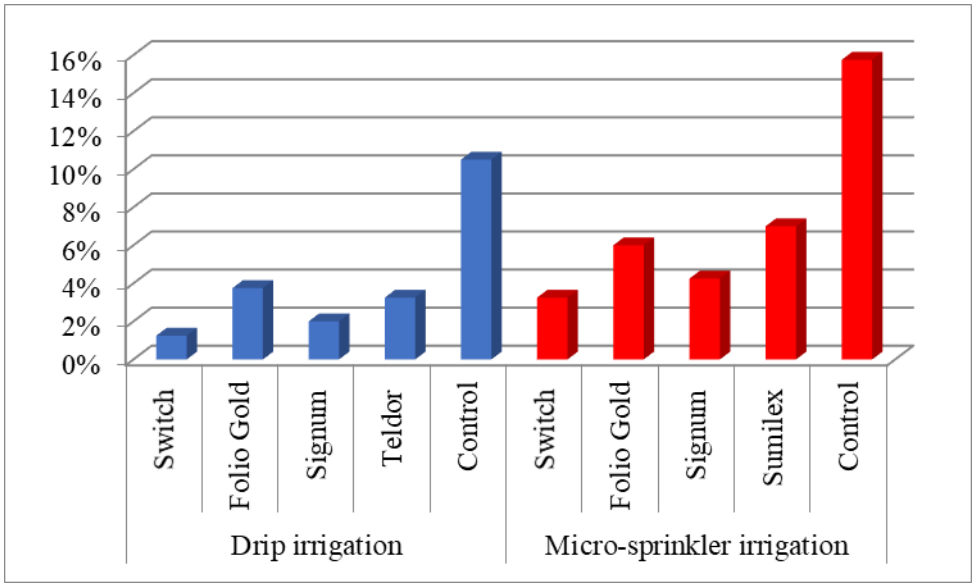

Figure 1 *Intensity of B. cinerea infection on lettuce*

The results of the investigated effciency of the four fungicides on *B. cinerea* control with lettuce under drip irrigation conditions, are given in the Table 4. Thus, the most efficient fungicide for lettuce protection from *B. cinerea* proved to be Switch (88.1%). Comparatively highly efficient with grey mould control was also Signum (80.1%). Somewhat lower level of efficiency was exhibited by Folio Gold (64.3%) and Teldor (69.1%). As regards the fungicide Switch 62.5 WG and the mixture of Switch 62.5 WG + Megafol, they proved efficient from 70.9% to 86.5% in grey mold control from *B. cinerea* [13].

Table 4 *Effectiveness of fungicides in controlling B. cinerea – drip irrigation*

Variant	Fungicide	Infected plants (%)	Efficiency (%)
V_1	Switch	1.2	88.1
V_2	Folio Gold	3.7	64.3
V_3	Signum	2.0	80.1
V_3	Teldor	3.2	69.1
V_5	Control	10.5	–

The assessment of fungicide efficiency with lettuce protection from *B. cinerea* under micro sprinkler irrigation conditions, is presented in the Table 5.

Table 5 *Efficacy of fungicides in controlling B. cinerea – micro – sprinkler irrigation*

Variant	Fungicide	Infected plants (%)	Efficiency (%)
V_1	Switch	3.2	79.4
V_2	Folio Gold	6.0	61.9
V_3	Signum	4.2	73.0
V_4	Teldor	7.0	55.5
V_5	Control	15.7	–

The fungicide Switch showed the best results with grey mold control in lettuce (79.4%). Signum was also quite efficient (73.0%), with lower efficiency recorded on the variants treated with Folio Gold (61.9%) and Teldor (55.5%). On comparing the fungicides sought for protection from lettuce grey mold caused by *B. cinerea*, a weakened disease intensity was spotted on the lettuce plants treated with Switch [14]. It was also established that lettuce control of *B. cinerea* with the fungicides was, on the average, more efficient under drip irrigation (75.4%) than that under the micro sprinkler irrigation (67.45%) (Figure 2).

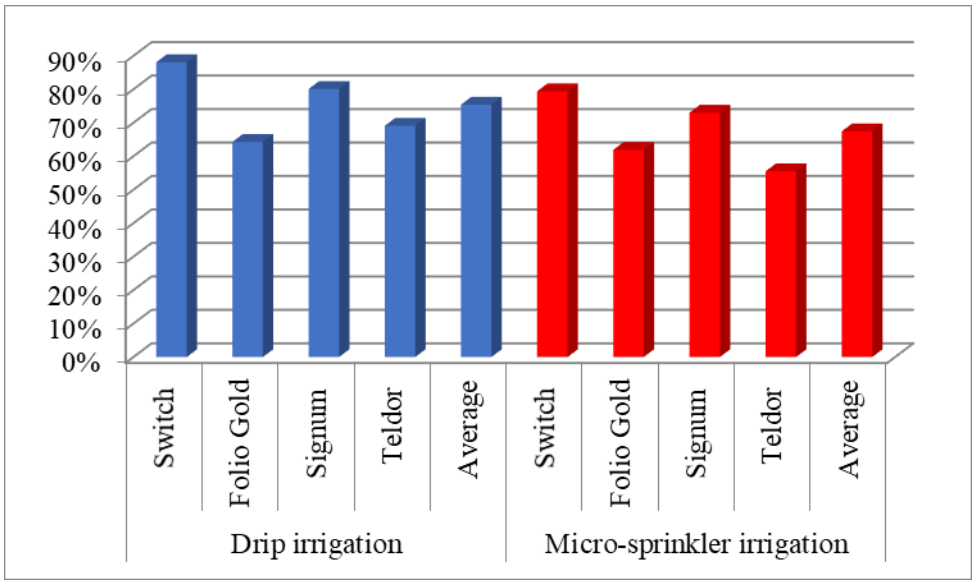

Figure 2 *Efficacy of fungicides in controlling B. cinerea*

CONCLUSION

Throughout the current study, the symptoms of grey mold affecting lettuce were identified in the greenhouse experiment. The percent of the infested lettuce plants was higher with micro sprinkler irrigation in all the variants than it was with drip irrigation. Fungicide control of *B.cinerea* on the lettuce was, on the average, more efficient under drip irrigation (75.4%) than that under micro sprinkler irrigation (67.45%). Therefore, it may be inferred that economic and ecological benefits of the lettuce production with drip irrigation would be higher if the fungicide use was reduced.

ACKNOWLEDGEMENT

The authors are grateful to the Ministry of Science, Technological Development and Innovation of the Republic of Serbia for financial support (contracts no. 451-03-47/2023-01/200088; 200189 and 451-03-47/2023-01/200027) as well as by the Provincial Secretariat for Higher Education and Scientific Research activity of the Vojvodina (contract no. 142-451-3114/2022-01/2).

REFERENCES

[1] Dasberg S., Or D. Practical applications of drip irrigation *in* Drip irrigation, Springer, Berlin, Heidelberg (1999), pp. 125–138.

[2] Kirnak H., Taş I., Gökalp Z. *et al*., Curr. Trends Nat. Sci. 5 (9) (2016) 145–151.

[3] Najafı P., Tabatabaei S. H., Irrig. Drain. 56 (2007) 477–486.

[4] Thompson T. L., Doerge T. A., Soil Sci. Soc. Am. J. 60 (1996) 163–168.

[5] Nalliah V., Sri Ranjan R., Kahimba F., Biosyst. Eng. 102 (3) (2009) 313–320.

[6] Acar B., Paksoy M., Türkmen Ö. *et al*., Afr. J. Biotechn. 7 (24) (2008) 4450-4453.

[7] Yazgan S., Ayas S., Demirtas C. *et al*., J. Food Agric. Environ. 6 (2) (2008) 357–361.

[8] Hao J. J., Subbarao K. V., Plant Dis. 89 (2005) 717–725.

[9] Purdy L. H., Phytopathol. 69 (8) (1979) 875–880.

[10] Gudžić S. Praktikum iz fitopatologije, Poljoprivredni fakultet, Univerzitet u Prištini, Kosovska Mitrovica–Lešak, (2006), p.160, ISBN 86–80737–07–0.

[11] Subbarao K. V., Hubbard J. C., Schulbach K. F., Phytopathol. 87 (1997) 877–883.

[12] Gonzaga N. R., Gonzaga A. B. Jr., Octavio R. *et al*., Int. J. Agric. Technol. 18 (2) (2022) 525–534.

[13] Vuković S., Brzaković N., Lazić S. *et al*., Biljni lekar 47 (3) (2019) 147–156.

[14] Matheron M. E., Porchas M., Veg. Report (P-152) (2008) 20–22.

THE IMPACT OF IRRIGATION ON THE QUALITY OF THE ENVIRONMENT AND WATER RESOURCES

Aleksandar Stevanović[1*], Tatjana Sekulić[1], Milica Blažić[1], Nataša Radić[1], Ana Popović[1], Vladanka Stupar[1]

[1]Academy of Applied Technical Studies Belgrade, Colleage of Applied Engineering Sciences, Nemanjina 2, Požarevac, SERBIA

[*]*astevanovic@atssb.edu.rs*

Abstract

The rapid growth of the human population also dictates the development of agriculture, as well as food production, in which irrigation systems play a significant role. Irrigation is a key factor in securing food supplies in developed countries. According to Pescod, 17 percent of the total arable land in the world is irrigated, which accounts for 34% of the world's total yields. Irrigation systems put a great deal of pressure on water resources, and therefore must be optimized to avoid social, economic, and environmental problems. To achieve this goal, and to preserve water as a natural resource, contaminated wastewater is more often in use for irrigation. Wastewater is an important source of water and nutrients for irrigation in developing countries, especially for those in arid and semi-arid areas. The use of wastewater is widespread and represents about 10% of the total irrigated areas. In this paper are analyzed the positive and negative impacts of the implementation of the sustainable use of waste water in irrigation on the environment and human health.

Keywords: irrigation, waste water, environmental protection.

INTRODUCTION

Irrigation represents an alteration of the natural conditions of the landscape by extracting water from an available source, adding water to fields, and introducing man-made structures and features to extract, transfer and dispose of water (Figure 1) [1]. The environmental impact of irrigation systems depends on the nature of the water source, the quality of the water, and how water is delivered to the irrigated land [2].

Global change is evident during the last decade, including climate change, population growth, urbanization, income growth, improvements in living standard, industrialization, and energy, and represent a challenge to water management. Climatic models predict an increase or decrease in the amount of rainfall or a change in rainfall frequency and distribution [3–5]. The hydrological cycle has strong impact on agriculture and environment, which are sensitive to different rainfall patterns and this indicate changes in vegetation flowering season and soil properties. This is particularly expressed in regions which are characterized by scarcity of water resources, because having adequate moisture in the root zone of a plant during the growing season is very important for its good growth [6].

Figure 1 *Irrigation, an essential factor in crop production [1]*

One of the first reasons for water scarcity is that the fraction of water available for the human consumption, in rivers, streams, lakes, and groundwater, is not distributed uniformly around the world [7]. As a consequence, 40% of the total land area is dry and includes climate zones classified as arid, semiarid and dry subhumid [8]. The increasing need of fresh water resources is a consequence of the demographic growth, the economic development and the improvement of living standards, climate change and pollution [9]. Therefore, the use of freshwater has been exceeding the minimum recharge levels, leading to the desiccation of water streams and depletion of groundwater. Water scarcity and droughts are emerging as major issues worldwide, not only in dry lands, but also in world regions where freshwater is abundant [10]. It is estimated that more than 40% of the world's population will face water stress or scarcity within the next 50 years, a serious incentive to achieve sustainable management options of the water resources [11].

In many arid and semiarid regions, the demand for drinking water and other domestic uses is constantly growing due to demographic growth and increasing standard of living. Therefore, less freshwater is available for agricultural irrigation and new water sources are needed. The most appropriate irrigation method can be determined by looking at the natural and climatic conditions and the state of water resources [12]. A renewable water source for irrigation is provided by the use of treated waste water. Treated wastewater already serves as an important water source for irrigation and is an increasingly common practice which usage will further be extended.

Disposal of waste water to agricultural sites offers an economic alternative to disposal into surface waters and it contributes to nutrient cycling, although pollutants may accumulate in the soils and cause a potential risk to soil quality and productivity in the long term [13]. Related to its high loads with nutrients, salts and organic materials its use as irrigation water can have major effects on the environmental health, such as soil salinity, land degradation, land cover change, water quality issues, loss of biodiversity and risks to public health [14].

The aim of this paper is to analyze the positive and negative impacts of the implementation of the sustainable use of waste water in irrigation on the environment and soil properties, and consequently on the human health.

EFFECTS OF LONG-TERM WASTE WATER IRRIGATION ON THE ENVIRONMENT

A comparative review of the literature so far has in detail discussed the effects of long-term waste water irrigation on the environment, first of all on soil organic matter and soil microbial biomass. The use of sewage effluents for irrigating agricultural land is a worldwide practice [15], and it is especially common in developing countries, where water treatment costs cannot yet be afforded.

Changes in soil biological characteristics caused by irrigation, may be very good indicators of soil quality and health, since they are more dynamic and diverse, and often more sensitive than physical or chemical soil properties, even observing in short time periods. The effects on soil microorganisms populations of the addition of sewage sludge to soils, either agriculture or natural, have been studied so far [16–18], and there are also examples of the activities of enzymes such as dehydrogenase, laccase, cellulase, protease and urease [19,20]. These effects are probably due to the stimulation of microbial growth and activity, boosted by the organic matter and nutrients supplied by wastewater [21].

According to certain literature data, it is argued that, wastewater reuse and nutrient capture can contribute towards climate change adaptation and mitigation [14]. Benefits from this are saving freshwater and energy, fertilizers, phosphorous capture and prevention of mineral fertilizer extraction from mines, that can reduce “carbon footprint”.

Impact on soil microbial populations

Because wastewater irrigation has the potential to cause variation in those physicochemical parameters, possible effects on the environment, soil properties and microbiota will be discussed.

The direct impact of wastewater on soil microbial communities in the worst case scenario, would lead to the elimination of autochthonous microorganisms by competition, or the indirect effects, may contribute to change the physicochemical soil properties and, there- fore, induce microbial community disturbances. On the other hand, the studies of Goyal *et al*. [22] showed that application of waste water containing organic matter and nutrients increase total soil microbial biomass and bacteria, fungi and actinomycetes. According to Friedel *et al*. [13] the predominant effect of long term usage of wastewater irrigation was an increase in microbial biomass and its activities due to the addition of easily decomposable organic material and nutrients and a more humid water regime. Giving consideration to these results, we may conclude that wastewater irrigation can provide the increase of the biogenicity of soil due to increase of microbial biomass.

The occurrence of pathogens in treated domestic wastewater is well documented [23] and their transmission to humans through the food chain is of concern. The risks posed to humans by pathogens transmitted through wastewater irrigation are difficult to estimate, but are mostly dependent on the survival of pathogens in the environment, the infective dose, and the host immunity. Also, another possible adverse effect of wastewater irrigation is the introduction of phytopathogens in the soils.

However, the most evident outcome of the literature search is that the effects on soil microbiotical communities are neglected in the majority of studies on irrigation with waste water.

Impact on soil organic matter

Long-term additions of organic matter, nutrients, and pollutants like salts and heavy metals through long-term waste water irrigation are comparable to those of sewage sludge applications [13]. The complexities of implications of waste water irrigation on soil organic matter are dependent on the concentration and composition of organic matter and on soil texture. Although most of the studies report an increase on organic matter due to waste water irrigation, some did not detect significant variations [24].

Irrigation, while enhancing the carbon input through larger amounts of plant residues, could additionally improve the conditions for microorganisms in soil, causing higher decomposition rates. Thus, the increased input of carbon could be decomposed completely.

Impact on human health

The risks of waste water irrigation for human health are a very important question of any discussion regarding wastewater reuse. These risks cannot be precisely estimated at this moment, but must be paid much attention to. The evidences according to the literature data so far, as well as the critical analyses of some experimental approaches highlight the importance of the accumulation of biological contaminants and pollutants in soils due to waste water irrigation [24]. Human and animal pathogens, phytopathogens and antibiotic resistant bacteria, as well as their genes are important biological agents that can be transported by waste water through the soil ecosystem, and get involved in the trophic food chains. Also numerous chemical substances, such as xenobiotics, pharmaceuticals agents and heavy metals, can threaten the environment, natural and agricultural ecosystems, and their soil properties, and consequently on the human health through the food we consume. The mixture of these contaminants may have unpredictable consequences in both environmental and human health.

CONCLUSION

Increasing production efficiency is a main subject for farmers in order to maintain or increase their economic return in an competitive global market. In the case of irrigated agriculture, producers must also take in consideration the increase in public concern about conservation of water resources, water quality, and environmental protection.

According to the studies so far, a long term wastewater irrigation may cause the significant effects on the environment, and consequently on human health by using the crops growing under these conditions. Irrigation with wastewater may have implications at two different levels: effect the physical, chemical and microbiological properties of the soil and/or introduce and contribute to the accumulation of chemical and biological contaminants in soil.

Long-term use of wastewater for irrigation, in nowday scarcity of fresh water, will lead to conservation of water resources.

The sustainable wastewater reuse in agriculture should prevent effects on the soil and environment in general, requiring an integrated risk assessment. Changes in soil management and enviromnet due to useage of waste water for irrigation, are leading to increased mineralization rates and in long term period may increase the availability and mobility of pollutants adsorbed to the soil organic matter.

Waste water reuse in agriculture enchanses activities such as higher crop yields and changes in cropping patterns, which reduce global carbon footprint. However, there is a need to better investigate waste water reuse for irrigation in order to effectively assess the challenges and potentials of this vital water resource for environmental and health protection.

REFERENCES

[1] Trost B., Prochnow A., Drastig K., *et al*., Agron. Sustain. Dev. 33 (4) (2013) 733–749.

[2] Stockle C.O., IV International Congress of Agricultural Engineering (2001).

[3] Whetton P. H., Fowler A. M., Haylock M. R., *et al*., Clim. Change 25 (3–4) (1993) 289–317.

[4] Timmermann A., Oberhuber J., Bacher A., *et al*., Nature 398 (1999) 694–697.

[5] Alpert P., Osetinsky I., Ziv, B., *et al*., Int. J. Climatol. 24 (8) (2004) 1001–1011.

[6] Li Q., Chen Y., Zhou X. ve Songlie Y., International Conference on New Technology of Agricultural (2011) 305–308.

[7] Shiklomanov I.A. World fresh water resources *In*: Gleick, P. H. (Ed.), Water in Cri- sis: A Guide to the World's Fresh Water Resources. Oxford University Press, New York (1993) p. 13–24.

[8] FAO Drylands, people and land use *In*: Koohafkan, P., Stewart, B. A. (Eds.), Water and Cereals in Drylands. Food and Agriculture Organization of the 21 United Nations (FAO), Roma (2008), p. 5–16, ISBN: 978-92-5-1060520.

[9] FAO Coping with water scarcity. An action framework for agriculture and food security. FAO Water Reports, Food and Agriculture Organization of the United Nations (FAO), Rome (2012), ISBN: 978-92-5-107304-9.

[10] Bixio D., Thoeye C., De Koning J., *et al*., Desalination 187 (2006) 89–101.

[11] Baltić J., Sekulic T., Zbornik radova VTŠSS, Požarevac, Srbija (2018).

[12] Johar R., Bensenouci A. ve Bensenouc, M. A., 15th Learning and Technology Conference (L&T) (2018) 147–152.

[13] Friedel J. K., Langer T., Siebe C., *et al*., Biol. Fertil. Soils 31 (2000) 414–421.

[14] Hanjra M. A., Blackwell J., Carr G., *et al*., Int. J. Hyg. Environ. Health 215 (3) (2012) 255–269.

[15] Feigin A., Ravina I., Shalhevet J. Irrigation with treated sewage effluent. Management for environmental protection, Springer, Berlin Heidelberg New York (1991).

[16] Chander K, Brookes P. C. Soil Biol. Biochem. 23 (1991) 927–932.

[17] Fliessbach A., Martens R., Reber H. H. Soil Biol. Biochem. 26 (1994) 1201–1205.

[18] Kandeler E., Kampichler C., Horak O. Biol. Fertil. Soils 23 (1996) 299–306.

[19] Chevremont A. C., Boudenne J. L., Coulomb B., *et al*., Water Res. 47 (2013) 1971–1982.

[20] Reddy G. B., Faza A, Bennett R. J. Soil Biol. Biochem. 19 (1987) 203–205.

[21] Morugán-Coronado A., Arcenegui V., García-Orenes F., *et al*., Solid Earth 4 (2013) 119–127.

[22] Goyal S., Chander K., Kapoor K. K. Environ. Ecol. 13 (1995) 89–93.

[23] Varela A. R., Manaia C. M. Environ. Sci. Pollut. Res. 20 (2013) 3550–3569.

[24] Becerra-Castro C., Lopes A. R., Vaz-Moreira I., *et al*., Environ. Int. 75 (2015) 117–135.

BIOPREPARATIONS IN THE FUNCTION OF ORGANIC AGRICULTURE IN FRUIT GROWING AND VITICULTURE

Aleksandar Stevanović[1], Markola Saulić[1], Milica Blažić[1], Vladanka Stupar[1*], Darko Stojićević[1], Zlata Živković[1]

[1]Academy of Applied Techical Studies Belgrade, Colleague of Applied Engineering Sciences, Nemanjina 2, Požarevac, SERBIA

[*]*vstupar@atssb.edu.rs*

Abstract

Given that environmental pollution is one of the main problems facing humanity at the global level, and that it is the leading cause of the increasing occurrence of certain human and animal diseases, organic production in fruit growing and viticulture as a sustainable system combines tradition and new technical and technological solutions in the prevention of environmental pollution, both from the aspect of biological diversity of flora and fauna in the agrobiotope, as well as from the aspect of nutritional values and the absence of pesticide residues in plant and animal products, with the aim of producing quality (nutritional and safe) food while protecting biodiversity and the environment. An important determinant of organic agriculture in fruit growing and viticulture is the exclusion of the application of mineral fertilizers and pesticides, due to the potential negative effects that can be caused by their uncontrolled application. In organic production, mainly organic nutrients and biological preparations are used, which accelerate the decomposition of crop residues and the release of plant assimilatives. In recent times, the possibilities of using allelopathic substances and secondary metabolites of plants as growth regulators and natural herbicides in sustainable agriculture are expanding, while the most important alternative to mineral fertilizers are microbiological fertilizers - biopreparations. In this paper, the importance and extent of application of microbiological fertilizers in modern fruit and viticultural agricultural production and the obtaining of health-safe food are considered.

Keywords: organic agriculture, fruit growing and viticulture, biodiversity, biopreparations, healthy food.

INTRODUCTION

Organic farming is one of the most important practices in fruits production, in the context of modern agriculture [1]. Approximately a third part of the world's organic production is located in Europe, and the total area under organic cultivation in the EU-28 has risen from just over 4 million ha in 2002, to 12 million ha in 2016 [2]. Nowdays organic fruit growing and viticulture is considered to be one of the fastest growing activity within the organic farming, and currently organic agriculture is actively developing in more than 150 countries.

It is possible to manage soil health by changing various agronomic practice, such as: tillage, crop rotation, fertilization, compost, manure, various pesticides, and biogenicity of agriculture soil is studied have been studied so far [3]. The question of biodiversity and soil health is the main basis in organic agriculture.

According to economists, the turnover in the field of organic agriculture is worth 85–90 billion US dollars a year. Developers of biological products pay great attention to the creation of complex biofertilizers, which contribute to a stable 20–25% increase in yield, with a significant reduction of plant damage [4].

Over the past decade, many new products used in organic production have been invented: bioproducts, biopreparations, biostimulants and microbial inoculants, which are used to enhance plants health, vigor, growth and yield and to protect them against abiotic and biotic stress factors, and also from plant pathogens.

Biopreparations are any product obtained from a living organism or its metabolic activities, and are used to inhibit the growth of pathogenic fungi or bacteria. Bioproducts or bio-based products are materials, chemicals, and energy from renewable biological resources [5].

Biopreparations can be made from a variety of bioproducts obtained from natural sources. This includes plant extracts, humic substances, polysaccharides, e.g. chitosan [6]. Biopreparations can also contain a great variety of beneficial microorganisms, bacteria or fungi. It has been found that in many cases they may be at least as efficient in biocontrol of fruit pathogens as conventional, commercially available products [7]. It is important to remember, that the efficacy of biopreparations varies and is highly dependent on many factors such as soil and air humidity or rainfalls [8]. It should be pointed out that different species of the pathogen genus may not be sensitive to identical biopreparation to the same extent [9].

The aim of this paper is to analyze the importance and extent of application of microbiological fertilizers in modern fruit and viticultural agricultural production, while obtaining the health-safe food.

A REVIEW OF BIOPREPARATIONS

Plant natural extracts have been used by humans for many centuries because of their ability to inhibit fungal and bacterial pathogens, but these properties were largely determined by the plant species from which the biopreparations were obtained. So far, many papers on the antimicrobial activity of plant extracts including essential oils have been published [10–14].

Antimicrobial activity of plant extracts results mainly from the presence in their composition of biologically active substances capable of inhibiting the development of microorganisms, mainly bacteria and fungi.

Plants are known for the production of aromatic secondary metabolites such as phenols, phenolic acids, quinones, flavones, flavonoids, flavonols, tannins, coumarins, terpenoids, saponins, and glycosides [10–16]. Some of the substances such as carvacrol, eugenol or thymol may inhibit the growth of the pathogens due to their phenolic structures. This compounds represent a part of plants defence mechanisms because they have an antimicrobial properties [17,18]. Garlic extract – allicin, is one of the most common used in biocontrol.

There are many of biopreparations and bioproducts used in organic fruit production e.g. Micosat F, Biosept 33 SL. They are based on different active ingredient such as microbial inoculum (e.g. *Pythium oligandrum*), plant extracts (e.g. *Allium sativum*—garlic, grapefruit extract-the pulp and the seeds of grapefruit (*Citrus paradise*)), or substances derived from

animals (e.g. chitosan) [6]. The scheme of biopreparations, biostimulants and microbial inoculants is shown in Figure 1.

Those biopreparations are valued by farmers due to their effectiveness and safety not only for plants themselves but also for animals.

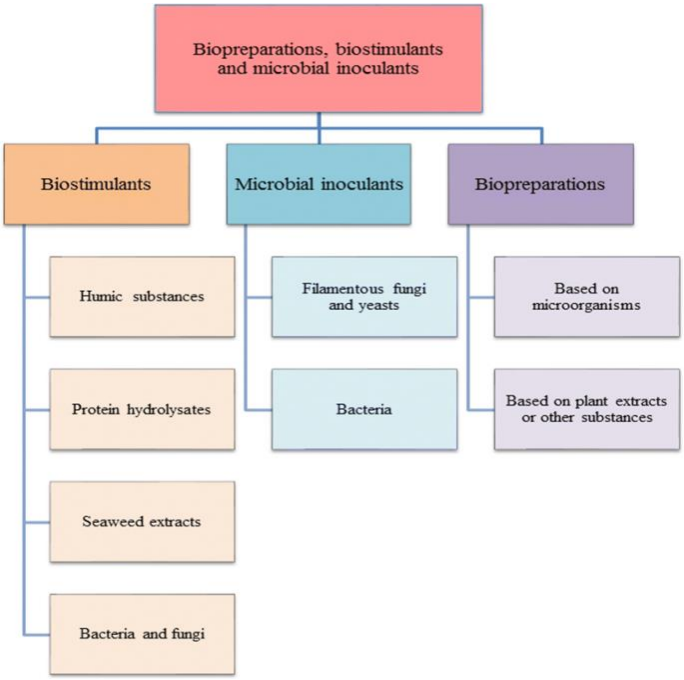

Figure 1 *Presentation of biopreparations, biostimulants and microbial inoculants [6]*

The qualitative and quantitative composition of biopreparations may vary according to the species of plant from which it was prepared. This is confirmed by Nostro *et al.* [19] studies, which showed that the composition of plant preparations was varied and depended mainly on the plant species.

ADVANTAGES OF USE BIOPREPARATIONS

A comparative review of the literature so far has in detail discussed the applicability and benefits of using microbiological fertilizers and plant extracts in organic farming. Practical industrial production and use of biological preparations have been studied by numerous foreign and Ukrainian scientists [20–22].

One of the purposes of using biopreparations is to increase soil biodiversity. According to Escobar and Solarte [23], the use of both organic fertilizers and biopreparations can have positive effects on the soil and the plants.

Biotechnologies based on the use of microbial biopreparations made of the active biomass of hydrocarbon-oxidizing microorganisms are used to solve many environmental problems. For such microorganisms, hydrocarbons are a natural source of nutrition, therefore, in the process of vital activity, they multiply, using different pollutants until that are completely removed from the soil [24].

It is shown in the study of Akhmetov *et al.* [24] that the number of a variety of groups of soil microorganisms (spore forming bacteria, mycelial fungi, actinomycetes) increased after the introduction of a complex organomineral fertilizer (manure, bird droppings, nitroammophos, ammonium nitrate).

Nitrogen fixing bacteria which create a biotic symbiontic relationship with roots of higher plants, have ability to fix molecular nitrogen from the atmosphere (N_2), the synthesis of hormonal and fungitoxic substances, and the mobilization of sparingly soluble soil phosphates. Biopreparations based on the use of these groups of microorganisms are very important chain in the development of eco-friendly farming technologies in order to increase plant productivity and establish biocontrol over the development of plant diseases, reduce the chemical load on the soil, and increase its fertility. Micosat F is a biopreparation produced of arbuscular mycorrhizal fungi: *Glomus* species, *Trichoderma viride*, and rhizosphere bacterial species (*Bacillus subtilis*, *Pseudomonas fluorescens* and *Streptomyces spp.*). These microorganisms live in symbiosis with a wide variety of cultivated crops and enhance plant's nutrient uptake. Furthermore they reduce the influence of environmental damage on ecosystems, such as drought. The research into the influence of this biopreparation onto the growth of fruits in organic farming was conducted and revealed that the biopreparation enhances the growth of apple trees ('Topaz') and sour cherry ('Debreceni Bötermö') [25].

Plant extracts are, as well as microbial bioprepartions, eco-friendly and bio-degradable, so they can be used in modern and organic fruit and viticultural agricultural production. One of the most important advantages of their usage is that they are often cheaper than conventional fungicides.

Analysis of the literature indicates that the use of biopreparations increases plant productivity and promotes the implementation of genotypic traits of varieties and hybrids. The issue of widespread use of biological preparations in modern organic agriculture is given considerable attention in most economically developed countries: France, Great Britain, Germany, Switzerland, the United States, and others [26].

CONCLUSION

The most effective, economically profitable and environmentally friendly way of producing organic food is associated with replacing agrochemicals and pesticides with biological and organic biological products and fertilizers. The primary problem is overuse of pesticides and herbicides in modern agriculture which led to a serious environmental hazard.

Properly prepared, tested and used biopreparations may be the future of nature and as well organic agriculture. The function of biopreparations is to contribute maintaining a good soil structure, high content of organic matter (humification processes in soil), increased water retention, or an increase in the number of populations of beneficial soil microorganisms. Reducing the amount of mineral fertilizers and chemical fungicides can contribute to increase of biodiversity in arable areas.

Biopreparations are valued by farmers due to their effectiveness and safety not only for plants themselves but also for animals. By using products of organic farming, first of all

biopreparations, traditional agriculture can be made more sustainable and environmentally friendly.

Taking everything into consideration, future research should focus on developing new bioproducts, new biopreparations, and formulations, as well as testing their effect in practice.

REFERENCES

[1] Barłowska J., Wolanciuk A., Idec J. Przegl. Hod. 2 (2017) 2–5 (*in Polish*).

[2] McEldowney J., Organic farming legislation revision of regulation on organic production and labelling of organic products. CAP reform post-2020 - Setting the scene. Eur Parliam Res Serv: (2018) 1–11, *Available on the following link:* www.europarl.europa.eu/RegData/etudes/BRIE/2018/614743/EPRS_BRI(2018)614743_EN.pdf

[3] Sekulić T., Stupar V., Stevanović A., *et al*., Not. Bot. Horti Agrobot. 51 (1) (2023) 13115.

[4] Aipova R., Abdykadyrova A. B., Kurmanbayev A. A., Plant Breed. Biotech. 2 (4) (2019) 31–46.

[5] Singh S. P., Ekanem E., Wakefield T., *et al*., Int. Food Agribus. Manag. Rev. 5 (2003) 1–15.

[6] Pylak M., Oszust K., Frac M., Rev. Environ. Sci. Biotechnol. 18 (2019) 597–616.

[7].Wagner A., Hetman B., J. Agric. Sci. Technol. B 6 (2016) 295–302.

[8] Pačuta V., Rašovský M., Černý I., *et al*., List Cukrov a Řepařské 11 (2018) 368–371.

[9] Hussein M. A. M., Hassan M. H. A., Abo-Elyousr K. A. M., World Appl. Sci. J. 32 (2014) 522–526.

[10] Hammer K. A., Carson C. F., Riley T. V., J. Appl. Microbiol. 86 (1999) 985–990.

[11] Barbour E. K., Al Sharif M., Sagherian V. K., *et al*., J. Ethnopharmacol. 93 (2004) 1–7.

[12] Mayachiew P., Devahastin S., LWT Food Sci. Technol. 41 (2008) 1153–1159.

[13] Preethi R., Devanathan V. V., Loganathan M., Adv. Bio. Res. 4 (2010) 122–125.

[14] Ismail A. M., Mohamed E. A., Marghany M. R., *et al*., J. Saudi Soc. Agric. Sci. 15 (2019) 112–117.

[15] Sen A., Batra A., Int. J. Curr. Pharm Res. 4 (2012) 67–73.

[16] Shihabudeen M. S., Priscilla D. H., Thirumurugan K., Int. J. Pharm Sci. Res. 1 (2010) 430–434.

[17] Das K., Tiwari R. K. S., Shrivastava D. K., J. Med. Plants Res. 4 (2010)104–111.

[18] Gurjar M. S., Ali S., Akhtar M., *et al*., Agric. Sci. 3 (2012) 425–433.

[19] Nostro A., Germano M.P., D'angelo V., *et al*., Lett. Appl. Microbiol. 30 (2000) 379–384.

[20] Krutyakova V., J. Agric. Sci. Technol. 7 (2017) 179–186.

[21] Lamichhane J. R., Bischoff-Schaefer M., Blumel S., *et al*., Pest Manag. Sci. 73 (2017) 14–21.

[22] Van Lenteren J. C., Bolckmans K., Köhl J., *et al*., BioControl 63 (2018) 39–59.

[23] Escobar N., Solarte V., Int. J. Biosci. Biochem. Bioinform. 5 (2015) 70–79.

[24] Akhmetov L. I, Puntus I. F., Narmanova R. A., *et al*., Processes 10 (3) (2022) 549.

[25] Grzyb Z. S., Sas-Paszt L., Piotrowski W., *et al*., J. Life Sci. 9 (2015) 221–228.

[26] Vozhehova R., Marchenko T., Piliarska O., *et al*., Economic Engineering in Agriculture and Rural Development 21 (4) (2021) 611–620.

IRRIGATION – IMPACT ON SOIL AS AN ENVIRONMENTAL FACTOR

Vladanka Stupar[1*], Tatjana Sekulić[1], Milica Blažić[1], Nataša Radić[1], Ana Popović[1], Aleksandar Stevanović[1]

[1]Academy of Applied Technical Studies Belgrade, College of Applied Engineering Sciences, Nemanjina 2, Požarevac, SERBIA

[*]*vstupar@atssb.edu.rs*

Abstract

Intensive irrigated agriculture significantly modifies the hydrological cycle and often has major environmental impacts by causing major changes in basic soil regimes. An increase in soil moisture changes the soil climate, reducing the temperature, stimulating the development of fungal and bacterial microflora, contributing to the emission of greenhouse gases such as CO_2 and N_2O from the soil, reducing structural stability, organic carbon content and leading to a higher degree of mineralization of organic matter. A special problem is soil salinization in arid and semi-arid regions of the world (China, Pakistan, Australia, Africa etc.). According to Khan and Cui, globally about 10 Mha of agricultural land is lost annually to salinization of which about 1.5 Mha is in irrigated areas. In these areas, the main problems in irrigation are: soil salinity, lack of adequate water resources and groundwater management. Data from the Republic Institute of Statistics indicate that in 2021, 52,236 ha of agricultural land was irrigated in the Republic of Serbia (which is 3% of the total arable land), with arable land and gardens accounting for 94%, orchards for 5% and other agricultural land for with a share of 1%. The Ministry of Agriculture, Forestry and Water Management of Serbia, in cooperation with the European Bank for Reconstruction and Development (EBRD) and the Food and Agriculture Organization of the United Nations (UN FAO), has started the implementation of a joint project to develop the National Irrigation Strategy for the period 2022–2031 and the five-year Action and Investment Plan. Having this in mind, the aim of this paper is to examine the impact of irrigation on soil as an environmental resource and factor in agricultural production.

Keywords: microbiological activity, structure, mineralization of organic matter, salinity.

INTRODUCTION

Agriculture production today is one of the most challenging human activities. The world population will grow from 6.9 billion people in 2010 to an estimated 9.15 billion people in 2050 [1]. At the same time, the individual food suplly will increase from 2,850 to 3,130 kcal per capita and day [2]. Observing these nowday trends, human population is facing a serious problem which consider a great pressure on natural resources needed for agricultural production, such as soil, water and energy, and increase in greenhouse gas emissions from agriculture. The situation is expected to be aggravated further by global change in climate [1]. The hydrological cycle has strong impact on agriculture and environment, which are sensitive to different rainfall patterns and this indicate changes in vegetation flowering season and soil properties.

Irrigation is the most important tool in agriculture to ensure water supply for crop production and to increase water scarcity due to climate change. This is particulary expressed in regions which are characterized by scarcity of water resources, because having adequate moisture in soil, especially in the root zone of a plant during the growing season is very important for its good growth [3].

On the other hand, irrigation itself might affect climate by altering the capacity of soils to apsorb greenhouse gases, in particular, CO_2 and N_2O [4]. Related to its high loads with nutrients, salts and organic materials, water use for irrigation can have major effects on the environmental health, such as soil salinity, land degradation, land cover change, water quality issues, loss of biodiversity and risks to public health [5].

By using good quality water for irrigation with low amounts of dissolved salts can be one of the solutions to overcome this problem, but only when used in productive soils. However, with increasing salt concentration in the water, decreasing crop growth and yield are excepted and have been observed in many literature data so far.

The objective of this review is to examine the impact of irrigation on soil as an environmental resource and factor in agricultural production.

SOIL STRUCTURE UNDER IRRITAGION

Soil structure is one of the most important properties affecting crop production because it determines the depth that plant roots can reach and the amount of water that can be apllied in the soil by irrigation. Soil structure is defined as heterogeneous formation of soil particles bound together as aggregates of different sizes, and also the soil pores and their continuity, which enable soil physical processes such as continiuos movement of water and air [6].

Pores are the most important soil physical feature because most soil processes that have immediate consequences for soil biological activity or soil conservation occur either within pores or on the surfaces of the particles that form their walls. Aggregate size and stability can affect the ability of soil to transfer essential nutrients, such as liquids and gases, which are crucial for crop production and ecosystem health [7]. Breakdown of larger aggregates into smaller ones occurs as a result of mechanical mechanisams such as by tillage implements, or water application by irrigation, when the applied force exceeds the bonding strength of the particle linkage.

This phenomenon does not always destroy soil structure, but can change soil structural forms which may not necessarily affect soil physical conditions important for agricultural production. However, the swelling and dispersion of clay particles from aggregates by the interaction of water molecules introduced in soil by irrigation with clay surfaces, destroys all the hierarchical orders in the soil structure [8,9]. This proccess significantly degrades soil physical properties.

Impact of irrigation on soil organic carbon and microbial populations

The effects of irrigation on soil organic carbon content are very dependent on the decrease or increase in soil moisture, composition of organic matter and on soil texture, but also on the interaction with other factors like fertilisation, tillage or the activity of soil organisms.

Although most of the studies report an increase on organic matter due to irrigation, some did not detect significant variations. Irrigation, while enhancing the carbon input through larger amounts of plant residues, could additionally improve the conditions for microorganisms in soil, causing higher decomposition rates. Thus, the increased input of carbon could be decomposed completely.

Since irrigation provides more constant humidity in soil throughout the year than just naturally rainfed agriculture, microbial activity in irrigated fields may generally be enhanced. Application of water by irrigation containing organic matter and nutrients has been found to increase total soil microbial biomass [10] and bacteria, fungi and actinomycetes. According to Matei *et al.* [11] the increased number of microorganisms and very active physiological processes in irrigated soil were sustained by microflora with higher taxonomic diversity than in non-irrigated soil. Dissolved organic matter, which is adeded in soil by irrigation, may be the most important C source in soils since all microbial uptake mechanisms require an aqueous environment.

Impact of irrigation on salinity of soil

Salinity of irrigation water may lead to the accumulation of salts in soil layers above a threshold level and impact on crops by osmotic and ion toxicity effects [12]. According to Khan and Cui [13], globally about 10 Mha of agricultural land is lost annually to salinization of which about 1.5 Mha is in irrigated areas. A salinity problem in irrigated areas evolves if salt accumulated from applied water in the crop root zone rises up to a concentration that causes a loss in yield. Yield reductions occur when the salts accumulate in the root zone to such an extent that the crop is no longer able to extract sufficient water from the salty soil solution, resulting in a water stress for a significant period of time. If water uptake is appreciably reduced, the plant slows its rate of growth. The plant symptoms are similar in appearance to those of drought, such as wilting, or a darker, bluish-green colour and sometimes thicker, waxier leaves. Symptoms vary with the growth stage, being more noticeable if the salts affect the plant during the early stages of growth.

Salts accumulate in a soil layer up to 2 metres of the surface and frequently become an important additional source of salt that moves upward into the crop root zone. Control of this is thus essential to salinity control and to successful long-term irrigated agriculture.

Impact of irrigation on CO_2 and N_2O emission processes

Irrigation may influence the CO_2 and N_2O emissions of arable land through out several processes. An continius water supply by irrigation leads, on the one hand, to an increased biomass in soil and therefore to a higher input of carbon, in the form of roots and dead plant material [14,15]. On the other hand, the application of water and consequently higher soil moisture enhances soil microbial activity, and this may result in an increased decomposition of soil organic matter and therefore in rising CO_2 emissions [16].

N_2O is also an important greenhouse gas influenced by irrigation, and nitrification and denitrification are the main processes for N_2O formation [17]. Improved living conditions for microorganisms by increased soil moisture may cause enhanced activity of nitrifying bacteria [18], but an increase in water-filled pore volume over 70% may lead to reduced soil aeration resulting in low oxygen concentrations to anaerobic conditions which suitable for

denitrification [19]. A complex multidisciplinary analysis are necessary to assess the impact of irrigation on greenhouse gas emissions.

NATIONAL IRRIGATION STRATEGY OF SERBIA

The Ministry of Agriculture, Forestry and Water Management of Serbia, in cooperation with the European Bank for Reconstruction and Development (EBRD) and the Food and Agriculture Organization of the United Nations (UN FAO), has started the implementation of a joint project to develop the National Irrigation Strategy for the period 2022–2031 and the five-year Action and Investment Plan [20].

Agriculture plays an important role in Serbia's economy, representing around 9% of gross domestic product (including food processing) and about 17% of employment. The Vojvodina region accounts for 47% of the country's agricultural land, 60% of irrigated areas and 80% of farms over 50 hectares [20]. To date, only around 120,000 hectares are equipped with irrigation facilities. Currently, the actual irrigated area is about 60,000 hectares (Table 1), including over 58,000 hectares in Vojvodina [21].

Table 1 *Area equipped for irrigation (thousand ha) [21]*

COUNTRY	2000	2005	2010	2015	2020
World	289,344	310,291	322,835	337, 892	348,503
Africa	13,189	14,169	15,123	16,408	16,899
Americas	47,617	49,459	51,711	54,565	56,697
Asia	199,144	217,189	227,477	237,627	245,390
Europe	26,712	26,381	25,284	25,994	26,205
Oceania	2,682	3,093	3,241	3,298	3,312
Serbia			88	77	63

The National Irrigation Strategy for the period of 2022–2031 is accompanied by seven briefs in the following areas: 1. water resources availability, distribution and accessibility, including a SWOT analysis of irrigation development potential; 2. governance structure around irrigation and water management in the country, including a detailed analysis of the national and international policy framework; 3. a comparative analysis of the Serbian situation with successful institutional and governance set-ups in similar contexts (e.g. in specific European countries and Turkey); 4. water pricing practices in Serbia, including the description of possible scenarios to optimize and develop irrigation pathways progressively; 5. geospatial analysis and mapping of agricultural areas with potential for irrigation development; 6. key risks, economic opportunities and value drivers of public and private investment in irrigation for select value chains; 7. technology and infrastructure needs for sustainable and profitable irrigation development in Serbia; 8. strategic assessment of social, environmental and climate considerations of irrigation development in Serbia and development of mitigation measures to ensure that investments consider sustainability of

water resources, water quality, climate change and do not negatively affect biodiversity, natural resources and communities [20].

The Irrigation Strategy of the Republic of Serbia will be accompanied by a five-year Action Plan for its implementation, to guarantee a demand driven approach to irrigation development and identify the necessary reforms.

CONCLUSION

In most cases, irrigation leads to significantly higher soil organic carbon contents, which also increase total soil microbial biomass, in arid, semi arid soils and in deserts. For humid climates areas and on soils with higher initial soil organic carbon content, irrigation has no significant effects on soil organic carbon contents. Emissions of N_2O gases, and soil salinity, are proven to increase under irrigation.

Irrigated agriculture is nowdays faceing the most important and serious challenge - to maintain sustainability and to minimise the environmental impacts. Quantifying both positive and negative impacts of different irrigation areas represent a main issue in irrigation management. Negative environmental impacts, such as green house gas CO_2 and N_2O emission processes, salinity, water pollution (by abuse of pesticides), algal blooms etc, especially in intensive crop production systems, should be main concern in reaching sustainability of agriculture.

The most cost-effective option may be to increase water use efficiency and reduce negative impacts on the environment. There is a need to radically rethink sustainability of food production, rational pricing and sharing of water and commodities to justify investment that will maintain and enhance ecosystem function within irrigated areas.

REFERENCES

[1] Alexandratos N., Bruinsma J. (2012) World agriculture towards 2030/2050: the 2012 revision. ESA Working paper, Rome, FAO, No. 12–03.

[2] Bruinsma J., Proceedings of a technical meeting of experts. Food and Agriculture Organization of the United Nations (FAO), Rome, Italy (2009).

[3] Li Q., Chen Y., Zhou X. ve Songlie Y., International Conference on New Technology of Agricultural (2011) 305–308.

[4] Lal R., Science 304 (2004) 1623–1627.

[5] Hanjra M. A., Blackwell J., Carr G., *et al*., Int. J. Hyg. Environ. Health 215 (3) (2012) 255–269.

[6] Rengasamy P., Agronomy 8 (5) (2018) 72.

[7] Muršec M., Leveque J., Chaussod R., *et al*., Plant Soil Environ. 64 (2018) 20–25.

[8] Essington M. E., Soil and Water Chemistry: An Integrative Approach, 2nd ed., CRC Press, Taylor and Francis Group, Boca Raton, FL, USA (2015) p. 633.

[9] Hu F., Liu J., Xu C., *et al*. Geoderma 320 (2018) 43–51.

[10] Goyal S., Chander K., Kapoor K. K., Environ. Ecol. 13 (1995) 89–93.

[11] Matei G. M, Matei S., Seceleanu I., *et al*., J. Environ. Prot. Ecol. 12 (4) (2011) 2101–2109.

[12] Munns R., Tester M., Annu. Rev. Plant Biol. 59 (2008) 651–681.

[13] Khan S., Cui Y., Can irrigation be sustainable? Agricultural Water Managamnet 80 (1) (2006) 87-99.

[14] Entry J. A., Mills D., Mathee K., *et al*., Appl Soil Ecol 40 (2008) 146–154.

[15] Kochsiek A. E., Knops J. M. H., Walters D. T., *et al*., Agr. Forest Meteorol. 149 (2009) 1983–1993.

[16] Jabro J. D., Sainju U., Stevens W. B., *et al*., J. Environ. Manage. 88 (2008) 147–1484.

[17] Phillips R. L., Agron. Sustain. Dev. 28 (2008) 87–93.

[18] Jha P. B., Singh J. S., Kashyap A. K., Plant Soil 180 (1996) 277–285.

[19] Amha Y., Bohne H., Biol. Fert. Soils 47 (2011) 293–302.

[20] *Available on the following link:* www.navodnjavanje.info/en/strategy/irrigation-strategy/.

[21] FAO 2022 FAOSTAT: Land Use *In*: FAO. Rome., *Available on the following link:* www.fao.org/faostat/en/#data/RL.

A RENEWABLE ENERGY SOURCES AND SUSTAINABLE DEVELOPMENT EQUATION

Milan Nedeljković[1*], Srba Mladenović[1], Jasmina Petrović[1]
[1]University of Belgrade, Technical Faculty in Bor, V.J. 12, 19210 Bor, SERBIA
[*]*mnedeljkovic@tfbor.bg.ac.rs*

Abstract

Natural resources are an essential part of our planet, providing us with everything from food and medicine to energy and building materials. Oil, metals, ores, minerals, plants and animals, water, air, land, etc. are all examples of natural resources. A nation's wealth, status in the world economy, power, and political influence are determined by its natural resources. Natural resources are a universal good and a common resource. Their use, economic implementation and economic exploitation should be committed and well planned. Human activities such as overconsumption, pollution, and deforestation are placing increasing stress on these resources. To ensure that we can continue to rely on them in the future, we must use natural resources according to the principles of sustainable development. The process of meeting the needs of the present without compromising the ability of future generations to meet their own needs is called sustainable development. It involves striking a balance between economic growth and the protection of the environment and the conservation of biodiversity. By sustainably conserving natural resources, we can reduce the impact of climate change and ensure that ecosystems continue to perform important functions such as pollination, carbon sequestration, and air and water purification.

Keywords: sustainable, biodiversity, greenhouse.

INTRODUCTION

The most important principle of sustainable development is the protection of the natural environment. This includes the conservation of biodiversity (diversity of life on Earth) and ecosystems. Biodiversity and ecosystems are critical to the functioning of our planet because they provide us with various needs, such as food, medicine, and purification of air and water. However, human activities such as deforestation and pollution are placing increasing stress on these systems. We can help reduce these impacts and ensure that ecosystems continue to provide these essential services by conserving natural resources in a sustainable manner [1].

Sustainable development also includes ensuring that economic growth is transparent and equitable so that everyone benefits. This includes reducing poverty and promoting social equity. Natural resources are an important source of income and employment in many developing countries, and sustainable development can help ensure that these resources are used in ways that benefit local communities [2].

The use of renewable energy sources is one way to achieve sustainable development. The fossil fuels currently used for energy production are limited, and they are also the main source of harmful gas emissions. Renewable energy sources such as solar panels, wind turbines, and

hydroelectric power plants are unlimited and do not emit harmful gases, making them ideal for long-term development [3]. Solar energy, together with other renewable energy resources, is a promising and accessible energy source for dealing with long-term concerns in the energy crisis.

SUSTAINABLE ENERGY SOURCES

Solar and wind energy

Two forms of renewable energy that generate electricity by harnessing the power of natural resources are solar and wind energy. They are abundant, green, silent, and renewable sources of energy [4,5].

Solar energy is a renewable energy source that is derived from the sun's radiation. It is captured via a variety of technologies, including solar panels or photovoltaic (PV) cells (Figure 1). These panels use semiconductor materials to directly turn sunlight into electricity. When sunlight reaches the solar panels, photons (light particles) are absorbed and an electric current is generated [6].

Figure 1 *Photovoltaic cells [6]*

Figure 2 *Wind turbines [6]*

Wind energy is generated by converting the kinetic energy of the wind into electricity using wind turbines (Figure 2) [6].Wind turbines generate electricity by using the wind to turn blades that drive a generator. They come in various sizes, from small turbines for domestic use to large turbines for commercial use [4,5].

Both solar and wind energy have significant advantages over more traditional energy sources like fossil fuels. They don`t emit greenhouse gases and are less harmful to the environment than fossil fuels. They are also becoming more competitive, making them available to more and more people. However, there are some limitations to both solar and wind energy. They are weather dependent, and output varies depending on the time of day and weather conditions. They also require a lot of land and space to generate a large amount of energy, which can be difficult in densely populated areas.

It is expected that the use of solar and wind energy will increase in the future as the technology improves and the cost continues to decrease [4,5].

Geothermal energy

Geothermal energy is a type of renewable energy that generates electricity by using heat from the earth's core. It is a clean and sustainable energy source with low environmental impact that can provide a reliable source of energy. Geothermal energy is generated by using the heat that is naturally produced in the earth's core. This heat is captured by geothermal power plants and used to generate steam, which in turn generates electricity. There are two types of geothermal power plants. Dry steam power plants, which use steam directly from geothermal reservoirs to drive turbines, and flash steam power plants, which use hot water from geothermal reservoirs to produce steam and generate electricity [7].

Compared to other energy production methods, geothermal energy has a number of advantages. As a renewable energy source, it can be produced indefinitely. It also has a lower environmental impact than fossil fuels and emits no greenhouse gases. Unlike solar and wind energy, which are dependent on the weather, it provides a steady and constant source of energy. This makes it a reliable source of energy.

Geothermal energy is also used in industry to pasteurize milk, dry fruits and vegetables, dry clothing, and heat and cool buildings. It has the potential to significantly reduce dependence on non-renewable energy sources (Figure 3) [8].

Geothermal energy also has some limitations. It necessarily requires access to special geological conditions, such as geothermal reservoirs, which are not available in all areas. In addition, the initial investment required to establish a geothermal power plant can be significant, and there is also the risk of seismic activity if not properly managed.

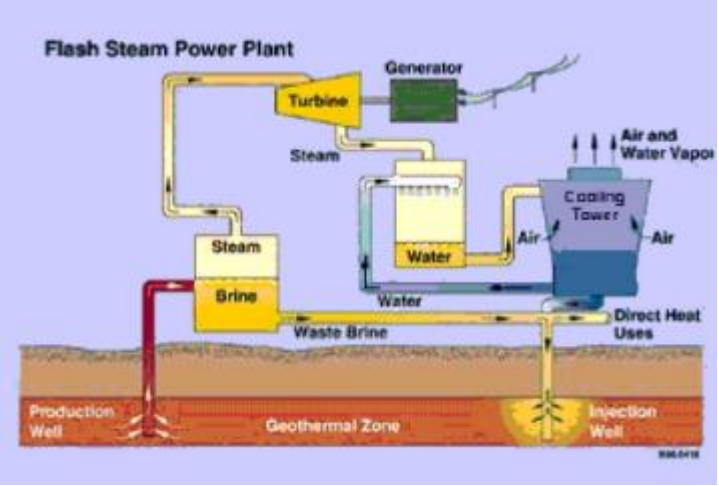

Figure 3 *Geothermal Power Plant [8]*

Hydroelectric power

Hydroelectric power plants (HPP) generate environmentally safe energy and are in line with modern efforts to achieve sustainability because they are powered by renewable energy sources.

HPP is a form of renewable energy in which electricity is generated by absorbing the kinetic and potential energy of water (Figure 4). It is one of the most widely used forms of renewable energy and has several advantages over other energy generation methods [9].

The kinetic energy of water is used to drive turbines, which then spin generators to produce electricity. There are two types of hydroelectric power plants: impoundment power plants and diversion power plants. Impoundment plants, also known as dammed hydroelectric power plants, store water and release it through a turbine with the help of a dam. A diversion power plant, sometimes called a "run-of-river" facility, channel part of the river through a turbine and return the remaining water to the river downstream [10].

Hydropower is the cheapest way to generate electricity today. It is a renewable energy source and provides nearly one-fifth of the world's electricity. It also generates electricity from a renewable natural resource and accounts for six percent of the world's energy supply or about fifteen percent of the world's electricity [11].

A hydropower plant with a dam and reservoir is a flexible source because the amount of electricity generated can be increased or decreased in seconds or minutes as electricity demand changes. Once built, a hydroelectric plant produces no direct waste and almost always emits significantly less greenhouse gases than a fossil fuel power plant. Hydropower has several advantages over other forms of energy production [12].

In addition, generation costs are low and it can be used for irrigation and flood control. However, hydropower also has some disadvantages. It requires access to certain geographic conditions, such as a good water source and a large difference in elevation. The construction of hydropower plants, especially dams, can have serious environmental consequences, such as habitat loss and disruption of river ecosystems. Local communities may also be displaced as a result [13].

Figure 4 *Hydroelectric power plants [12]*

CONCLUSION

Significantly faster development and increasing levels of production and industrialization have led to much faster exploitation and consumption of natural resources. Under the conditions of increased exploitation, environmental problems occur, which also affect the environment. Natural resources are a necessary element for the functioning of society in the modern world. Basically, every form of human activity is based on the use of natural resources in some form. Sustainable development is an essential issue for humanity and means empowering all citizens to acquire the knowledge, skills, habits, values and awareness

to participate in making choices that improve their quality of life without compromising the satisfaction of the needs of future generations.

Finally, conserving natural resources based on the principles of sustainable development is critical to the well-being of our planet and future generations. We can ensure that resources are used in ways that meet the needs of the present without compromising the ability of future generations to meet their own needs by balancing economic growth with environmental protection and biodiversity conservation. Adopting sustainable development principles in the use of natural resources can help mitigate the effects of climate change, promote social equity and poverty reduction, and ensure that ecosystems continue to provide important services such as air and water purification, pollination, and carbon sequestration.

ACKNOWLEDGEMENT

The research presented in this paper was done with the financial support of the Ministry of Science, Technological Development and Innovation of the Republic of Serbia, within the funding of the scientific research work at the University of Belgrade, Technical Faculty in Bor, according to the contract with registration number 451-03-47/2023-01/ 200131.

REFERENCES

[1] Østergaard P. A., Duic N., Noorollahi Y., *et al*., Renew. Energy 146 (2020) 2430–2437.

[2] Magdalinović N., Magdalinović-Kalinović M., Mihajlović D., 3rd Inter. Conf. on Sustainable Development Indicators in the Min. Ind., Milos island, Greece (2007).

[3] Harris J. M., Roach B., Environmental and natural resource economics: A contemporary approach, ME Sharpe (2013).

[4] Bergin M. H., Ghoroi C., Dixit D., *et al*., Environ. Sci. Technol. Lett. 4 (8) (2017) 339–344.

[5] Al-Hasan A. Y., Renew. energy 12 (3) (1997) 291–301.

[6] Al-Dousari A., Al-Nassar W., Al-Hemoud, *et al*., Energy 176 (2019) 184–194.

[7] Kulasekara H., Seynulabdeen V., 2019 5th International Conference on Advances in Electrical Engineering (ICAEE) IEEE, September (2019) 223–228.

[8] Kumar S., Gupta S. K., Rawat M., Materials Today: Proceedings 26 (2020) 1660–1665.

[9] Yah N. F., Oumer A. N., Idris M. S., Renewable and Sustainable Energy Rev. 72 (2017) 228–239.

[10] Singh V. K., Singal S. K., Renewable and Sustainable Energy Rev. 69 (2017) 610–619.

[11] Shahgholian G., J. Renew. Sustain. Energy 7 (3) (2020) 14–28.

[12] Sawin J. L., Martinot E., Barnes D., *et al*., (2013) renewables 2011-Global status report.

[13] Bagher A. M., Vahid M., Mohsen M., *et al*., Am. J. Energy Res. 2 (2) (2015) 17–20.

FORGING A SUSTAINABLE FUTURE: THE CIRCULAR ECONOMY IN THE FASHION INDUSTRY

Tatjana Miljojčić[1*]

[1]University of Belgrade, Vinca Institute of Nuclear Sciences, M.P.A. 12–14, 11351 Belgrade, SERBIA

[*]*tatjana.miljojcic@vinca.rs*

Abstract

The fashion industry's impact on the environment and society has led to the emergence of sustainable alternatives as a response to the dominance of fast fashion. This paper explores the concepts of slow fashion and the circular economy and their significance in promoting a more sustainable future in the fashion industry. Slow fashion advocates departure from disposable fashion by prioritizing quality, durability, and timeless style. It emphasizes transparency, fair trade practices, and waste reduction throughout the supply chain, aiming to minimize the environmental consequences associated with excessive resource consumption and textile waste. The circular economy concept seeks to create a closed-loop system, decoupling economic growth from resource depletion. It encourages practices such as recycling, upcycling, and reusing materials to maximize resource value and minimize waste generation. By prolonging the utilization of products and materials, the circular economy reduces the fashion industry's environmental footprint. Slow fashion and the circular economy share common principles that reinforce each other. Slow fashion promotes durable and timeless garments that align with the circular economy's focus on extending product lifespans. By valuing quality over quantity, slow fashion encourages responsible consumer behavior, urging individuals to invest in well-made, long-lasting items that can be repaired or repurposed. The circular economy complements slow fashion by providing the necessary infrastructure and systems to facilitate material reutilization and recycling. By embracing slow fashion and the circular economy, the fashion industry can transition towards a more sustainable and ethical future, which is a necessary step towards creating a sustainable fashion industry.

Keywords: slow fashion, fast fashion, recycling, circular economy, environment.

INTRODUCTION

The fashion industry has a significant impact on the environment and society. The rise of fast fashion, characterized by the production of cheap, trendy clothing at an accelerated pace, has resulted in the depletion of natural resources, pollution, and poor working conditions for laborers. This unsustainable model of fashion production and consumption has led to the emergence of alternative approaches, such as slow fashion and the circular economy, as a response to the fashion industry's negative environmental and social impact [1].

Slow fashion represents a shift towards conscious and responsible fashion production and consumption. It focuses on creating high-quality, timeless garments that are made to last and that prioritize social and environmental values. The principles of slow fashion emphasize ethical labor practices, transparency, and a reduction in waste throughout the supply chain. By

embracing slow fashion, consumers can make more mindful purchases, choosing quality over quantity, and investing in durable and sustainable clothing [2].

The circular economy is another approach that has gained momentum in the fashion industry. It seeks to minimize resource consumption and waste generation by promoting a closed-loop system. The circular economy encourages the reuse, recycling, and repurposing of materials, keeping them in use for as long as possible. By implementing the principles of the circular economy, the fashion industry can reduce its environmental impact by reducing waste, conserving resources, and minimizing pollution [3].

Slow fashion and the circular economy are not mutually exclusive concepts, but rather complementary approaches that reinforce each other's principles. Slow fashion focuses on creating durable, timeless garments that are made to last, aligning with the circular economy's goal of extending product lifespans. The circular economy provides the infrastructure and systems necessary to facilitate material reutilization and recycling, complementing slow fashion's emphasis on transparency and reducing waste throughout the supply chain [4].

An increasing number of popular fashion brands have embraced slow fashion and the circular economy, setting an example for the industry. They have implemented repair and reuse programs, adopted sustainable materials, and designed garments with longevity in mind. Through these actions, they have demonstrated that it is possible to create sustainable and ethical fashion without sacrificing style or profitability [5].

Embracing slow fashion and the circular economy is crucial to creating a more sustainable and ethical fashion industry. These approaches prioritize responsible consumption and production practices, reducing the environmental and social impact of the fashion industry. By choosing quality over quantity, investing in durable clothing, and adopting circular economy principles, consumers and fashion brands can shift towards a more sustainable future [6].

THE ENVIRONMENTAL IMPACT OF FAST FASHION

The fast fashion industry has been identified as a major contributor to environmental degradation. The production, transportation, and disposal of clothing all have significant impacts on the environment. One of the biggest environmental concerns associated with fast fashion is the high level of greenhouse gas emissions that result from the production and transportation of clothing. The production of synthetic fibers, such as polyester, commonly used in fast fashion, requires large amounts of fossil fuels and emits significant amounts of carbon dioxide and other greenhouse gases. Furthermore, the transportation of clothing from factories in countries like China and Bangladesh to retail outlets worldwide generates additional emissions [7].

Fast fashion also causes water pollution. Textile production requires significant amounts of water, much of which becomes contaminated with toxic chemicals such as dyes and bleaches. The treatment of this contaminated water is difficult and can have long-term negative impacts on both ecosystems and human health. In addition to water pollution, fast fashion contributes significantly to textile waste. Clothing trends change rapidly, leading to many clothing items being worn only a few times before being discarded. The majority of these items end up in

landfills, where they can take decades to decompose. The decomposition of textiles in landfills also releases methane, a potent greenhouse gas [8].

The fashion industry has a responsibility to take steps to reduce its environmental impact. One approach is to invest in sustainable materials such as organic cotton, recycled polyester, and biodegradable textiles. Companies can also implement environmentally friendly production processes, such as minimizing water and energy use and adopting closed-loop systems to minimize waste [9].

However, consumers also play a critical role in reducing the environmental impact of fast fashion. Consumers can choose to purchase clothing made from sustainable materials, buy fewer clothing items overall, and properly dispose of unwanted clothing items by donating them to charity or recycling them. Additionally, advocating for policy changes, such as regulations that require companies to disclose the environmental impact of their products, can also promote sustainability in the fashion industry [10].

The Circular Economy in Practice

The circular economy is an economic model that aims to minimize waste and promote sustainability by keeping resources in use for as long as possible. In practice, the circular economy is characterized by a focus on reducing waste, maximizing the use of resources, and promoting the regeneration of natural systems. One example of the circular economy in practice is the concept of closed-loop production. In a closed-loop system, products are designed to be reused or recycled at the end of their useful life. This can involve designing products with recyclable materials, using renewable energy in production processes, and reducing waste throughout the supply chain [11].

Another example of the circular economy in practice is the rise of circular business models. These models aim to promote sustainability by creating new value from waste or by-products. This can involve repurposing waste materials to create new products, refurbishing and reselling used products, or providing services rather than selling products.

The circular economy is also being put into practice through initiatives aimed at promoting a more sustainable fashion industry. One example of this is the rise of clothing rental services, which allow consumers to rent clothing for a limited time rather than buying new items. Another example is the use of recycled materials in clothing production, which helps to reduce waste and promote the use of existing resources [12].

Governments and organizations are also promoting the circular economy through policy and funding initiatives. For example, the European Union has developed a Circular Economy Action Plan, which aims to promote sustainable growth and create new economic opportunities through the circular economy [13]. In addition, organizations such as the Ellen MacArthur Foundation are working to promote the circular economy by providing resources and support to businesses and policymakers [14].

Overall, the circular economy is a model that is being increasingly put into practice in a variety of industries and contexts. By promoting sustainability and minimizing waste, the circular economy offers a way to create a more environmentally friendly and socially responsible economy.

Slow fashion movement

The slow fashion movement is a growing trend that seeks to promote a more sustainable and ethical approach to fashion. The movement is characterized by a focus on quality over quantity, an emphasis on ethical production practices, and a commitment to reducing waste. At the heart of the slow fashion movement is a belief that clothing should be produced in a way that is mindful of the environment and the people involved in its production. Slow fashion brands often use sustainable materials, such as organic cotton or recycled polyester, and prioritize the use of natural dyes and other eco-friendly production techniques [15].

In addition to using sustainable materials, slow fashion brands also prioritize quality over quantity. Instead of producing large quantities of cheap clothing that is designed to be quickly discarded, slow fashion brands produce high-quality garments that are designed to last. This approach not only reduces waste but also promotes a more sustainable and mindful approach to consumption. The slow fashion movement also seeks to promote ethical production practices. This means that brands strive to ensure that the people involved in the production of their clothing are treated fairly. Slow fashion brands often prioritize transparency in their supply chains, allowing consumers to know exactly where their clothing comes from and who made it [16].

The slow fashion movement is not just about clothing, but also encompasses other aspects of the fashion industry, such as accessories and footwear. It also emphasizes the importance of repairing and upcycling clothing, rather than discarding it, in order to reduce waste. Overall, the slow fashion movement represents a shift towards a more sustainable and mindful approach to fashion. By prioritizing quality, sustainability, and ethics, the slow fashion movement seeks to promote a more responsible and environmentally friendly fashion industry.

RESULTS IN THESE FIELDS

The circular economy and slow fashion movements have been gaining momentum in recent years, and there have been several promising results in both fields. In the circular economy, there have been several successful initiatives aimed at reducing waste and promoting sustainability. For example, the EU's Circular Economy Action Plan has set a target of reducing waste generation by 30% by 2030, while also promoting the use of renewable energy and sustainable products [17]. Additionally, several companies have embraced closed-loop production, designing products with recyclable materials and reducing waste throughout the supply chain.

In the field of slow fashion, there has been a growing demand for sustainable and ethically produced clothing. Furthermore, many established fashion brands have also started to embrace sustainable practices, such as using organic or recycled materials and reducing waste [18]. One of the key benefits of the circular economy and slow fashion is the reduction of waste and pollution [19]. By promoting sustainable practices and reducing the use of non-renewable resources, these movements are helping to create a more environmentally friendly and socially responsible economy.

Moreover, the circular economy and slow fashion are also creating new economic opportunities [20]. For example, the recycling and repurposing of materials can create new jobs in waste management and product design. Similarly, sustainable fashion brands are able to differentiate themselves from their competitors and attract consumers who are willing to pay a premium for ethically produced clothing. Overall, the circular economy and slow fashion movements are creating positive change in a variety of industries and contexts [21]. While there is still much work to be done to create a truly sustainable economy, the results seen so far are encouraging and suggest that these movements will continue to grow in the future.

CONCLUSION

In conclusion, the slow fashion and circular economy movements have emerged as vital initiatives towards creating a more sustainable and socially responsible economy. These movements aim to reduce waste, promote ethical and sustainable practices, and create new economic opportunities.

The circular economy approach offers the potential to reduce the negative environmental impacts of fast fashion by reducing the amount of textile waste that ends up in landfills, incinerators, or the environment. By adopting closed-loop systems, recycling, and repurposing of materials, businesses can reduce their environmental footprint and extend the lifespan of products. Meanwhile, the slow fashion movement encourages consumers to invest in high-quality, timeless garments made from sustainable materials that are designed to last longer and have a lower impact on the environment.

However, the successful implementation of these concepts relies on collaboration between all stakeholders, including policymakers, businesses, and consumers. Governments can incentivize circular and sustainable practices, while businesses can incorporate circular economy principles into their operations and supply chains. Consumers can support these efforts by making informed choices and investing in sustainable and ethical fashion.

In conclusion, the circular economy and slow fashion movements offer a promising way to address the environmental challenges posed by the fast fashion industry. Through concerted efforts and collective actions, we can create a more sustainable and equitable economy that benefits everyone.

ACKNOWLEDGEMENT

The research presented in this paper was completed with the financial support of the Ministry of Science, Technological Development and Innovation of the Republic of Serbia, with the funding of scientific research work at the University of Belgrade, Vinca Institute of Nuclear Sciences (Contract No. 451-03-47/2023-01/200017).

REFERENCES

[1] Nguyen H. T., Le D. M. D., Ho T. T. M., *et al*., Soc. Responsib. J. 17 (4) (2020) 578–591.

[2] Fletcher K., Fash. Practice 2 (2) (2010) 259–265.

[3] Geng Y., Sarkis J., Bleischwitz R. Nature 565 (7738) (2019) 153–155.

[4] Machado M. A. D., Almeida S. O. de, Bollick L. C., Bragagnolo G., J. Fash. Mark. Manag. 23 (3) (2019) 382–395.

[5] Joy A., Sherry J. F., Venkatesh A., *et al*., Fash. Theory 16 (3) (2012) 273–295.

[6] Puspita H., Chae H., J. Glob. Fash. Mark. 12 (2) (2021) 133–145.

[7] Niinimäki K., Peters G., Dahlbo H., *et al*., Nat. Rev. Earth Environ. 1 (4) (2020) 189–200.

[8] Bailey K., Basu A., Sharma S., Water 14 (7) (2022) 1073.

[9] Jacometti V., Laws 8 (4) (2019) 27.

[10] Collett M., Cluver B., Chen H. L., Res. J. Tex. Appar. 17 (2) (2013) 61–68.

[11] Geissdoerfer M., Savaget P., Bocken N. M., *et al*., J. Clean. Prod. 143 (2017) 757–768.

[12] Murray A., Skene K., Haynes K., J. Bus. Ethics 140 (2017) 369–380.

[13] Mhatre P., Panchal R., Singh A., *et al*., Sustain. Prod. Consum. 26 (2021) 187–202.

[14] MacArthur E., J. Ind. Ecol. 2 (1) (2013) 23–44.

[15] Khandual A., Pradhan S., Fashion Brands and Consumers Approach Towards Sustainable Fashion *in* Fast Fashion, Fashion Brands and Sustainable Consumption, Editor: Muthu S. S., Springer (2019), 37–54.

[16] Henninger C. E., Alevizou P. J., Oates C. J., J. Fash. Mark. Manag. 20 (4) (2016) 400–416.

[17] Tisserant A., Pauliuk S., Merciai S., *et al*., J. Ind. Ecol. 21 (3) (2017) 628–640.

[18] Gam H. J., Banning J., Cloth. Text. Res. J. 29 (3) (2011) 202–215.

[19] Dissanayake D. G. K., Weerasinghe D., Circular Economy and Sustainability (2021) 1–21.

[20] Elf P., Werner A., Black S., BSE 31 (6) (2022) 2682–2699.

[21] De Brito M. P., Carbone V., Blanquart C. M., Int. J. Prod. Econom. 114 (2) (2008) 534–553.

CITRATE BUFFERED QuEChERS *vs* SIMPLIFIED SAMPLE PREPARATION METHOD: COMPARATIVE LC/MS ANALYSIS OF PESTICIDES IN APPLES

Darko Anđelković[1], Milica Branković[2*]

[1]University of Niš, Faculty of Agriculture, Kosančićeva 4, 37000 Kruševac, SERBIA

[2]University of Niš, Faculty of Sciences and Mathematics, Department of Chemistry, Višegradska 33, 18000 Niš, SERBIA

[*]*milica.chem@outlook.com*

Abstract

Quantitative chromatography-based analysis with the QuEChERS sample preparation procedure predominates in the multiresidue pesticides analysis in complex matrices. The QuEChERS is time effective and less prone to errors, but at the same time it is less cost-effective than the usual sample preparation procedures, since it implements the usage of sorbents. The objective of this study was to assess if the QuEChERS can be simplified and shortened in order to be more cost-effective, but to preserve best performances. Performances in terms of trueness and precision of the first step of the QuEChERS sample preparation procedure, that is the extraction with acetonitrile, were evaluated for 5 pesticides in 3 matrices – whole apple fruit, apple peel and pulp, by analyzing pesticides procedural standards. These performances were than compared to those of the citrate buffered QuEChERS and relevant conclusions were made.

Keywords: mass spectrometry, fungicides, solvent extraction.

INTRODUCTION

Many fruits production, as well as apple production, is nowadays very dependent on pesticides application. In humid agricultural areas pesticide usage ensure satisfactory crop yields. However, frequent application, with associated health risk keep the need for continuous pesticides residue monitoring in crops and food.

Mass spectrometry currently stands for most used analytical technique in many scientific fields. As highly selective and sensitive, it is the leading technique for both qualitative and quantitative analysis. When it comes to the multiresidue pesticides analysis in complex matrices, quantitative chromatography-based analysis with the QuEChERS sample preparation procedure predominates. Owing to the simple steps, QuEChERS is time effective and less prone to errors, thus it represents a streamlined approach to assess pesticides residues in food. However, it is less cost-effective than the usual sample preparation procedures, since it implements the usage of sorbents.

Non-QuEChERS sample preparation methods and simple solvent extraction methods are less frequent. Some examples of such methods include gas-liquid microextraction technique (GLME) coupled to a d-SPE [1] and classic solid-liquid extraction with acetonitrile for the analysis of chlorpyrifos and acetamiprid in tomato peel [2,3].

The objective of this study was to assess if the QuEChERS can be simplified and shortened in order to be more cost-effective, but to preserve best performances. Performances regarding trueness and precision of the simplest possible sample preparation method, which for LC/MS analysis is a solvent extraction, were evaluated and compared to the same performances of the citrate buffered QuEChERS. The method was developed for five pesticides mostly used in apple production in Serbia – pyrimethanil, cyprodinil (fungicides, anilino-pyrimidines), boscalid (fungicide, pyridine-carboxamides), trifloxystrobin (fungicide, strobilurin) and bifenthrin (insecticide, pyrethroids) and for apple matrices (peel, pulp and the whole fruit).

MATERIALS AND METHODS

Chemicals and appliances

High purity standards of pyrimethanil and cyprodinil were purchased from AccuStandard®, USA. Formic acid (98%) and high purity standards of boscalid, trifloxystrobin and bifenthrin were purchased from Sigma-Aldrich®, Germany. HPLC grade methanol and acetonitrile were produced by J.T. Baker, USA; ammonium-formate (98%) and HPLC grade deionized water were produced by Carlo Erba, Italy. Prepacked QuEChERS extraction pouches (1 g of NaCl, 4 g of $MgSO_4$, 1 g of trisodium citrate dihydrate and 0.5 g disodium hydrogen citrate) and dispersion kits (25 mg PSA and 150 mg $MgSO_4$) were produced by Hillium, USA. Syringe microfilters (Nylon Hydrophilic 0.22 µm) were produced by Membrane Solutions, USA.

For high purity standards weighing procedures analytical balance Sartorius BP110S (Germany) was used. In sample preparation procedure following appliances were used: peeler and slicer (China), balance (acc. ± 0.01 g) KB 2000-2N KERN (Germany), kitchen blender 0.9L BL142A TEFAL (France), centrifuge Jouan C4i Thermo Scientific (USA), syringe microfilter Nylon Hydrophylic 0.22 µm, Membrane Solutions (USA). Apples of Granny Smith variety were purchased in a local supermarket.

Instruments and instrumental parameters

LC/MS analysis was performed on instrumental configuration comprising autosampler Surveyor (Thermo Finnigan, USA), MS pump Accela 1250 (Thermo Scientific, USA) and LTQ XL mass spectrometer equipped with ESI probe and linear ion trap analyzer.

10 µL of the sample was loaded on column (Hypersil GOLD™, 3 µm, 175 Å, 150mm×2.1mm, Thermo Fisher Scientific, USA) in a partial loop injection mode and eluted with a mixture of: eluent A (solution of 0.30 % of FA and 0.01 % of AMF in water) and eluent B (MeOH) following the gradient: 0 min (50 % B), 0-13 min (50–75 % B), 13-15 min (75 % B), 15-16 min (75–100 % B), 16-19 min (100 % B), 19-20 min (100–50 % B), 20-25 min (50 % B) with flow equal to 300 µL min^{-1}. Mass analysis was performed in full scan mode (scan range m/z 150–600) under optimized parameters of ion source, ion optic and ion detection system of mass spectrometer. Chromatographic peaks of analytes were integrated after the extraction of analyte characteristic ions (Table 1) from the total scan range.

Table 1 *Main structural and LC/MS characteristics of investigated pesticides*

Pesticide	Class	Structure	MRL[a], mg kg^{-1}	Molecular mass	Log K_{ow}	Retention time, min	Base ion observed in the MS[1] spectra, *m/z*
Pyrimethanil	Fungicide	Anilinopyrimidine	15.0	199.25	2.84	4.63	200.4
Cyprodinil	Fungicide	Anilinopyrimidine	2.0	225.28	3.59	6.71	226.4
Trifloxystrobin	Fungicide	Strobilurin	0.7	408.37	4.50	17.11	408.7
Bifenthrin	Insecticide	Pyrethroid ester	0.01	422.86	6.00	20.04	439.6
Boscalid	Fungicide	Pyridine-carboxamide	2.0	343.20	2.96	9.43	342.9

[a] Maximum residual level (the highest level of a pesticide residue that is legally tolerated in or on food or feed when pesticides are applied correctly (acc. to *Good Agricultural Practice*).

Procedures

Stocks preparation

Single-pesticide stock solutions (1 mg mL^{-1} each) were prepared by dissolving high purity pesticide standards in ethanol. Multi-pesticide solutions were prepared by mixing and diluting single stocks in ethanol.

Sample preparation

One kilogram of apples was peeled, peel and pulp were separately homogenized, then mixed in appropriate proportion (1:10) to represent the fruit sample. Ten replicates of 10-grams portions of each matrix (peel, pulp and fruit) were weighted in Falcon tubes. Portions were spiked with pesticides (50 mg kg^{-1}). Half of the replicates were treated according to the simplified sample preparation procedure; another half was treated according to the citrate buffered QuEChERS procedure.

Procedure 1 – simplified procedure. Ten grams of sample were extracted with 10 mL of acetonitrile. The mixture was centrifugated (5 min/3000 rpm). The supernatant was microfiltered (0.22 µm) prior to instrumental analysis.

Procedure 2 – Citrate buffered QuEChERS. Ten grams of sample were extracted with 10 mL of acetonitrile, after which an extraction pouch was added. The mixture was immediately vortexed for one minute and centrifuged (5 min/3000 rpm). A supernatant aliquot was subjected to a dispersive extraction by the addition of one dispersion kit per mL of supernatant. The mixture was vortexed for one minute and centrifuged (5 min/3000 rpm). The supernatant was microfiltered (0.22 µm) prior to instrumental analysis.

RESULTS AND DISCUSSION

Spiked samples of apple peel, pulp and fruit were analyzed by methods with simplified sample preparation procedure and with the established sample preparation procedure (QuEChERS), that possess acceptable performances regarding trueness and precision. Trueness of the method with simplified sample preparation was evaluated by comparing the areas of analytes chromatogramic peaks in pesticides procedural standard (50 mg kg^{-1}) subjected to both sample preparation procedures.

For the same matrix type (peel, pulp or fruit), these areas are mutually comparable (Table 2). Peak areas of pyrimethanil, cyprodinil and bifenthrin measured in apple peel analyzed by simplified method express about 13–15% of difference to peak areas measured in peel analyzed by the established method. This percentage is around 6.0 for boscalid and 0.6 for trifloxystrobin. The differences in pulp and fruit range from 14 to 20% and from 4 to 13%, respectively. Negligible variation in measured areas suggests the simplified method has very similar trueness to the QuEChERS's.

Precision in terms of repeatability (coefficient of variation, RSD, %) calculated on the basis of 5 replicates is excellent; it ranges from 2.08 to 7.96% for samples analyzed by simplified method, that is from 1.76 to 7.63% for samples analyzed by the QuEChERS. It suggests that samples analysis by both methods is highly precise and consistent.

Table 2 *Chromatographic peaks analytes areas measured in spiked samples of Granny Smith peel, pulp and fruit (50 mgkg^{-1}, n=5), analyzed with method with simplified and the QuEChERS sample preparation*

Sample type	**Peel**	**Pulp**	**Fruit**
Method	**Simplified sample preparation**		
Pyrimethanil	6.54×10^{7} (4.36)*	6.85×10^{7} (5.38)	7.13×10^{7} (3.86)
Cyprodinil	9.60×10^{7} (7.96)	1.11×10^{8} (6.65)	1.10×10^{8} (4.35)
Boscalid	2.49×10^{6} (2.85)	2.61×10^{6} (2.24)	2.62×10^{6} (3.55)
Trifloxystrobin	2.94×10^{7} (2.08)	3.04×10^{7} (4.06)	3.06×10^{7} (2.64)
Bifenthrin	7.37×10^{6} (2.88)	6.97×10^{6} (7.52)	7.26×10^{6} (4.13)
Method	**Citrate buffered QuEChERS**		
Pyrimethanil	7.74×10^{7} (2.27)	8.73×10^{7} (1.76)	8.27×10^{7} (3.16)
Cyprodinil	1.15×10^{8} (2.84)	1.33×10^{8} (2.16)	1.23×10^{8} (3.02)
Boscalid	2.64×10^{6} (4.53)	3.15×10^{6} (2.45)	2.93×10^{6} (4.74)
Trifloxystrobin	2.96×10^{7} (3.45)	3.54×10^{7} (1.92)	3.18×10^{7} (1.86)
Bifenthrin	8.54×10^{6} (7.63)	8.70×10^{6} (3.53)	8.09×10^{6} (4.47)

*relative standard deviation (RSD, %) *n*=5

CONCLUSION

Performances in terms of trueness and precision of the first step of the QuEChERS sample preparation procedure, that is the extraction with acetonitrile, were evaluated for 5 pesticides in 3 matrices – whole apple fruit, apple peel and pulp, by analyzing pesticides procedural standards. These performances were compared to those of the citrate buffered QuEChERS. Minor variation in pesticides signal measured in samples analyzed by both methods, testifies to the comparable performances of the methods. Therefore, the simplified sample preparation procedure can be used instead of the QuEChERS, as a cost-effective alternative for reliable pesticides analysis in apples.

ACKNOWLEDGEMENT

The authors are grateful to the Ministry of Science, Technological development and Innovation of the Republic of Serbia for financial support (contract numbers 451-03-47/2023-01/200124 and 451-03-47/2023-01/200383).

REFERENCES

[1] Jin X., Kaw H. Y., Liu Y., *et al*. Food Chem. 367 (2022) 130774.

[2] Hegazy A. M., Abdelfatah R. M., Mahmoud H. M., *et al*. Food Chem. 306 (2020) 125640.

[3] Martins Moura A. C., Neves Lagoa I., Fernandes Cardoso C., *et al*. Food Chem. 310 (2020) 125928.

APPLICABILITY OF THE QuEChERS IN NON-CHROMATOGRAPHY-BASED PESTICIDE ANALYSIS IN APPLES

Darko Anđelković[1], Milica Branković[2*]

[1]University of Niš, Faculty of Agriculture, Kosančićeva 4, 37000 Kruševac, SERBIA

[2]University of Niš, Faculty of Sciences and Mathematics, Department of Chemistry, Višegradska 33, 18000 Niš, SERBIA

[*]*milica.chem@outlook.com*

Abstract

The QuEChERS is time effective and less prone to errors, thus it represents a streamlined approach for the assessment of pesticides residues in food. It is predominantly implemented in quantitative chromatography-based pesticides analysis. The aim of this study was to launch a non-chromatography-based flow-injection ESI/MS method designed for fast qualitative pesticides screening in fruit and to investigate the applicability of the QuEChERS in such method. The method was developed for five pesticides mostly used in apple production in Serbia and with apple peel as the fruit matrix. The results of the investigation showed the QuEChERS sample preparation procedure expresses some limitations, mainly due to the lack of chromatography.

Keywords: LOOP injection, apple peel, 3D ion trap.

INTRODUCTION

In a multiresidue pesticides analysis in complex matrices, quantitative chromatography-based analysis with the QuEChERS sample preparation procedure still predominates [1–5]. The QuEChERS is time effective and less prone to errors, thus it represents a streamlined approach to assess pesticides residues in food. The original version was developed in 2003. Organic phase separation was performed by the addition of $MgSO_4$ and NaCl. In later attempts, the method has been modified to expand both analytes and commodity range by introducing buffers, which led to better recovery of some pH-sensitive analytes. Consequently, two buffered versions have been established, the acetate-buffered version or AOAC 2007.01 certified method and the citrate-buffered version or EN 15662 certified method. The last step of the QuEChERS is the dispersive solid phase extraction (d-SPE), originally performed with primary-secondary amine (PSA) as a sorbent for impurities collection. Nowadays, there are numerous combinations of PSA and other sorbents.

The aim of this study was to launch a non-chromatography-based flow-injection ESI/MS method designed for fast qualitative pesticides screening in fruit. Flow-injection is in fact a variation of the LC injection technique in which the chromatography separation is omitted. Also, an automatic injection of a software predefined sample volume via an autosampler is replaced by a semiautomatic injection of a LOOP volume predefined sample volume. Flow-injection configuration can use LOOPs of various volumes (5, 10, 20 µL etc.); it is usually termed the LOOP injection technique.

The method was developed for five pesticides mostly used in apple production in Serbia - pyrimethanil, cyprodinil (fungicides, anilino-pyrimidines), boscalid (fungicide, pyridine-carboxamides), trifloxystrobin (fungicide, strobilurin) and bifenthrin (insecticide, pyrethroids).

MATERIALS AND METHODS

Chemicals and appliances

High purity standards of pyrimethanil and cyprodinil were purchased from AccuStandard®, USA. Formic acid, FA (98%) and high purity standards of boscalid, trifloxystrobin and bifenthrin were purchased from Sigma-Aldrich®, Germany. HPLC grade acetonitrile was produced by J.T. Baker, USA; ammonium-formate, AMF (98%) and HPLC grade deionized water were produced by Carlo Erba, Italy. Prepacked QuEChERS extraction pouches (1 g of NaCl, 4 g of $MgSO_4$, 1 g of trisodium citrate dihydrate and 0.5 g disodium hydrogen citrate) and dispersion kits (25 mg PSA and 150 mg $MgSO_4$) were produced by Hillium, USA. Syringe microfilters (Nylon Hydrophilic 0.22 µm) were produced by Membrane Solutions, USA.

For high purity standards weighing procedures analytical balance Sartorius BP110S (Germany) was used. In sample preparation procedure following appliances were used: peeler and slicer (China), balance (acc. ± 0.01 g) KB 2000-2N KERN (Germany), kitchen blender 0.9L BL142A TEFAL (France), centrifuge Jouan C4i Thermo Scientific (USA), syringe microfilter Nylon Hydrophilic 0.22 µm, Membrane Solutions (USA) and 500 µL glass syringe, Unimetrics (USA). Apples of Idared variety were purchased in a local supermarket.

Instruments and instrumental configuration for screening analysis

Surveyor LC pump (Thermo Finnigan, USA) and LCQ Advantage mass spectrometer (Thermo Finnigan, USA) with 3D ion trap analyzer, were used. Data were acquired and analyzed by Xcalibur™ software, version 1.4 SR1.

Samples were injected directly into the MS source by the LOOP injection technique. LOOP was filed with 5 µL of the sample, after which the sample was transferred to the source by the constant flow of the mobile phase (0.30 % of FA and 0.01 % of AMF in water; flow rate – 50 µL min^{-1}). Syringe-LOOP capillary branch length was 58 cm, LOOP-source capillary branch length was 20 cm. Samples were analyzed in full scan mode (scan range *m*/*z* 197-500) under optimized parameters of the ion source, ion optic and ion detection system of mass spectrometer. Chronogramic peaks of analytes were identified after the extraction of analyte characteristic ions (Table 1) from the total scan range.

Procedures

Stocks preparation

Single-pesticide stock solutions (1 $mgmL^{-1}$ each) were prepared by dissolving high purity pesticide standards in ethanol. Multi-pesticide solutions were prepared by mixing and diluting single stocks in ethanol.

Sample preparation

Blank extract of Idared apple peel was prepared according to the following procedures:

Procedure 1 – QuEChERS sample preparation procedure without the clean-up step. One kilogram of apples was peeled and homogenized by blending. A sub-portion (10 g) was transferred to Falcon tube (50 mL) after which sample extraction with acetonitrile (10 mL) was performed. Then a QuEChERS extraction pouch was added, and the extraction proceeded for two more minutes. Sample extract was centrifuged (5 min/3000 rpm) and the supernatant was separated and microfiltered (0.22 µm Nylon microfilter).

Procedure 2 – QuEChERS sample preparation procedure with the clean-up step. Into a specified volume of supernatant, obtained according to the previously described procedure, a QuEChERS dispersion kit was added (1 kit per 1 mL of supernatant). Extraction by shaking was performed (1 min), the extract was centrifuged (5 min/3000 rpm) and the supernatant was separated and microfiltered (0.22 µm Nylon microfilter).

Post-extraction fortified standards preparation

Two series of post-extraction fortified standards were prepared in the concentration range 0.10–5.00 µg mL^{-1}. One series was prepared by the dilution of appropriate volume of the multi-pesticide stock in blank peel extract obtained according to the procedure 1, another series was prepared in the same manner, by diluting the pesticide stock in blank peel extract obtained according to the procedure 2.

Table 1 *Main structural and MS characteristics of investigated pesticides*

Pesticide	Class	Structure	MRL[a], mg kg^{-1}	Molecular mass	Log K_{ow}	Base ion observed in the MS^1 spectra, *m/z*
Pyrimethanil	Fungicide	Anilinopyrimidine	15.0	199.25	2.84	200.4
Cyprodinil	Fungicide	Anilinopyrimidine	2.0	225.28	3.59	226.4
Trifloxystrobin	Fungicide	Strobilurin	0.7	408.37	4.50	408.7
Bifenthrin	Insecticide	Pyrethroid ester	0.01	422.86	6.00	439.6
Boscalid	Fungicide	Pyridine-carboxamide	2.0	343.20	2.96	342.9

[a] Maximum residual level (the highest level of a pesticide residue that is legally tolerated in or on food or feed when pesticides are applied correctly, acc. to *Good Agricultural Practice*).

RESULTS AND DISCUSSION

Characterization of blank QuEChERS extracts

Mass spectra presented in Figures 1 and 2 represent an average of 10–20 scans around the highest point of sample chronogramic peak, of which the background spectra (mobile phase only) were subtracted. The resulting mass spectra show ions that exclusively originate from apple peel QuEChERS extracts. These spectra reveal that ions from the samples are detected in scan range above *m/z* 280. When mutually compared, spectra reveal practically the same ions are present in both cleaned-up and not cleaned-up peel extract.

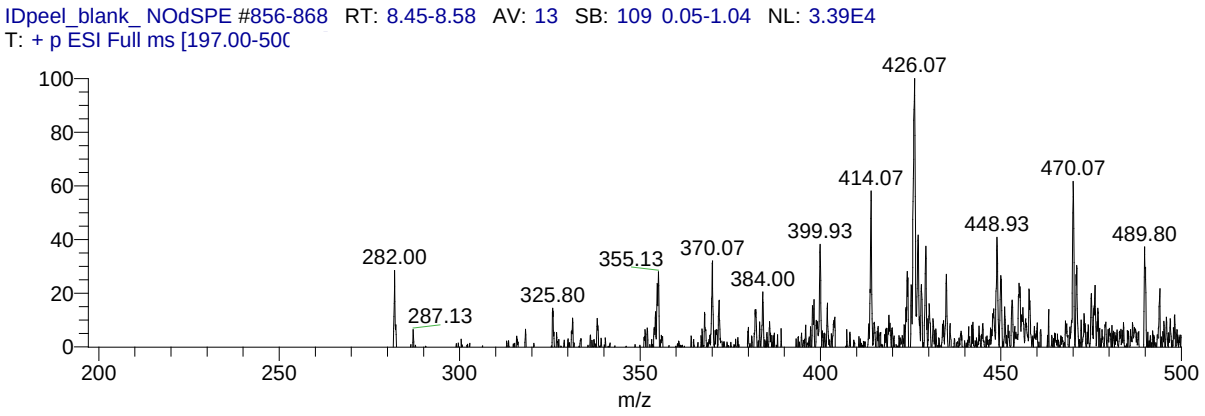

Figure 1 *Background subtracted mass spectrum of Idared peel blank extract prepared to the QuEChERS procedure with no clean-up step*

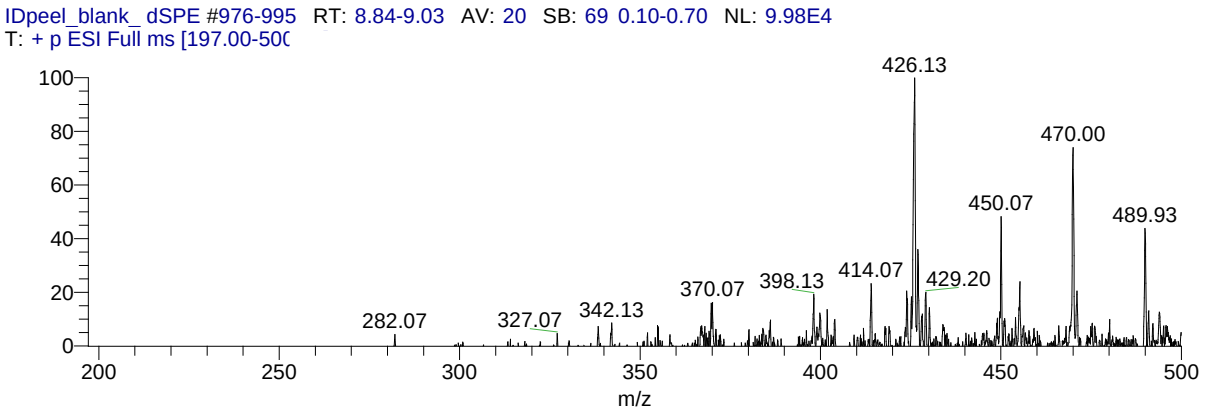

Figure 2 *Background subtracted mass spectrum of Idared peel blank extract prepared to the QuEChERS procedure with the clean-up step*

Analysis of pesticides post-extraction fortified standards

In non-cleaned QuEChERS extracts, it is only possible to identify peaks of trifloxystrobin. Chronogramic peak areas for this pesticide correlate very well with pesticide concentration in the extract. Peaks of pyrimethanil, cyprodinil, boscalid and bifenthrin cannot be observed after the extraction of pesticides characteristic ions from the total scan range; the probable reason is the matrix effect in non-cleaned extract, additionally fortified by the lack of chromatographic separation. Figure 3 illustrates this trend on the example of cyprodinil.

In cleaned QuEChERS extract it is possible to identify peaks of all investigated analytes. Peaks of boscalid, bifenthrin and trifloxystrobin can be identified over the entire concentration range, while the identification and integration of pyrimethanil and cyprodinil peaks start to be a challenge bellow 1.00 µg mL^{-1}. Consequently, peaks of boscalid, bifenthrin and trifloxystrobin were auto integrated (ICIS integration); peaks of cyprodinil and pyrimethanil were however integrated manually.

Chronogramic peaks integrated area of pyrimethanil, cyprodinil and trifloxystrobin correlate very well with pesticides spiked concentration, while such correlation is weak for boscalid and bifenthrin (Table 2). The correlation coefficient ranges from 0.9504 for pyrimethanil, to 0.9922 for trifloxystrobin.

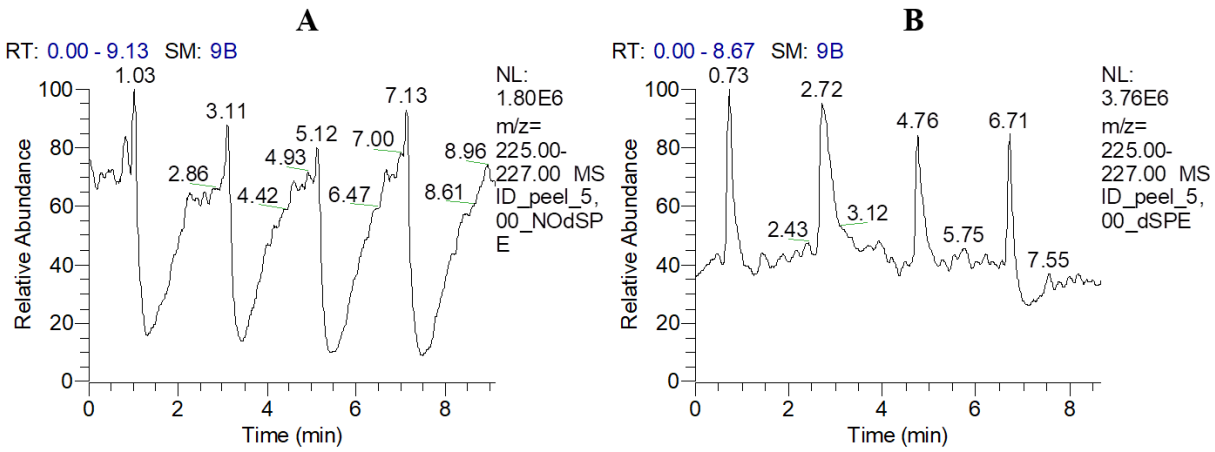

Figure 3 *Extract ion chronograms of cyprodinil acquired after 4 consecutive injections of spiked Idared peel extract (5.00 µg mL^{-1}) prepared to the Procedure 1 (A) and to the Procedure 2 (B)*

Table 2 *Calibration performances in cleaned and non-cleaned QuEChERS extracts (0.10–5.00 µg mL^{-1})*

Analyte	Non-cleaned-up extract	Cleaned-up extract*
Pyrimethanil	/	$y = 1.72\times10^{6}x + 5.64\times10^{6}$, $R^2 = 0.9504$
Cyprodinil	/	$y = 2.88\times10^{6}x + 5.22\times10^{6}$, $R^2 = 0.9617$
Trifloxystrobin	$y = 4\times10^{6}x + 2\times10^{6}$, $R^2 = 0.9963$	$y = 14.25\times10^{6}x + 3.83\times10^{6}$, $R^2 = 0.9922$
Boscalid	/	/
Bifenthrin	/	/

*Parameters for pyrimethanil and cyprodinil are for the narrowed concentration range (0.50–5.00, pyrimethanil and 1.00–5.00 µg mL^{-1}, cyprodinil), since the identification of pesticide peaks was not possible at concentration levels lower than the stated.

CONCLUSION

Applicability of the citrate buffered QuEChERS sample preparation procedure was tested for non-chromatography-based LOOP injection pesticides analysis in apple peel. To assess the significance of the clean-up, the identification of analytes and calibration performances were evaluated in both types of the QuEChERS extract, that is in non-cleaned extract (d-SPE step was omitted) and cleaned extract (d-SPE was done with PSA). In the non-cleaned extract, only one analyte could be identified and correlated with its concentration. In the cleaned extract all tested analytes could be identified, but 3 of 5 correlated with the in-extract concentrations. QuEChERS sample preparation procedure expresses some limitations, mainly due to the lack of chromatography.

ACKNOWLEDGEMENT

The authors are grateful to the Ministry of Science, Technological Development and Innovation of the Republic of Serbia for financial support (contract numbers 451-03-47/2023-01/200124 and 451-03-47/2023-01/200383).

REFERENCES

[1] Kowalska G., Pankiewicz U., Kowalski R., Appl. Sci. 12 (3) (2022).

[2] Liu X., Liu Z., Bian L., *et al*., Food Chem. 387 (2022) 132915.

[3] Pszczolińska K., Shakeel N., Barchanska H., J. Food Comp. Anal. 114 (2022).

[4] Tu F-Q., Yang M., Anal. Letters 55 (3) (2022).

[5] Cha K. H., Lee J., Lee J., *et al*., Food Chem. 374 (2022) 131626.

ESI *vs* APCI IN SELECTED PESTICIDES MS DETECTION IN APPLES

Darko Anđelković[1], Milica Branković[2*]

[1]University of Niš, Faculty of Agriculture, Kosančićeva 4, 37000 Kruševac, SERBIA

[2]University of Niš, Faculty of Sciences and Mathematics, Department of Chemistry, Višegradska 33, 18000 Niš, SERBIA

[*]*milica.chem@outlook.com*

Abstract

ESI and APCI are types of atmospheric pressure ionization. Although both are a soft ionization technique, APCI is more applicable in the analysis of thermostable, volatile and non-polar compounds, while ESI is more applicable in the analysis of thermolabile and polar compounds. The aim of the study was to investigate ESI and APCI ionization efficiency of selected pesticides and applicability of such ionization types for pesticides analysis in apples. ESI proved to be a better choice for the selected pesticides analysis, than the APCI. Moreover, ESI ionization efficiency can be additionally improved by the electrospray heating.

Keywords: heated electrospray, corona discharge.

INTRODUCTION

Electrospray ionization (ESI) is classified as a soft ionization technique. It is one kind of the atmospheric pressure ionization (API). The construction of an electrospray ionization source includes a needle within the ionization probe, an evaporation chamber and an evacuated interface to the MS analyzer. When the liquid sample flows through the ESI probe the needle, set at high voltage (3–8 kV), along with the nebulizer gas promotes sample dispersion and formation of the charged droplets. The droplets emerge from what is known as a Taylor cone formed by the elongation of the electrolyte solution at the needle tip as like-charged ions are repelled from the needle [1]. Liquid phase evaporation leads to a higher charge concentration within a droplet, ultimately resulting in droplet disintegration and in the formation of a single molecular ions, in most cases protonated molecular ions. Formed ions are then focused to the MS analyzer.

Atmospheric pressure chemical ionization (APCI) is another kind of API. The construction of an APCI source includes a probe and a corona needle set at high voltage. Unlike the ESI needle, which is incorporated into the ESI probe, the corona needle is separated from the probe (Figure 1). The role of the needle is to produce a discharge current and to induce solvent ionizations, after which the generated solvent reagent ions react with analyte molecules via gas-phase ion/molecule reactions and produce analyte ions [2]. Like the ESI, protonated molecular ions are formed. Unlike the ESI, molecular fragments can be formed as well, due to a thermal degradation of thermolabile compounds. In general, APCI is more applicable in the analysis of thermostable, volatile and non-polar compounds. Contrary to the

ESI, the ion formation process in APCI is separated from solvent evaporation process, allowing the use of solvents unfavorable for ion formation, such as low-polarity solvents [2].

The aim of the study was to investigate ESI and APCI ionization efficiency of selected pesticides and applicability of such ionization types for pesticides analysis in apples. The method was developed for five pesticides mostly used in apple production in Serbia – pyrimethanil, cyprodinil (fungicides, anilino-pyrimidines), boscalid (fungicide, pyridine-carboxamides), trifloxystrobin (fungicide, strobilurins) and bifenthrin (insecticide, pyrethroids).

MATERIALS AND METHODS

Chemicals and appliances

High purity standards of pyrimethanil and cyprodinil were purchased from AccuStandard®, USA. Formic acid (98%) and high purity standards of boscalid, trifloxystrobin and bifenthrin were purchased from Sigma-Aldrich®, Germany. HPLC grade methanol and acetonitrile were produced by J.T. Baker, USA; ammonium-formate (98%) and HPLC grade deionized water were produced by Carlo Erba, Italy. Syringe microfilters (Nylon Hydrophilic 0.22 µm) were produced by Membrane Solutions, USA

For high purity standards weighing procedures analytical balance Sartorius BP110S (Germany) was used. In sample preparation procedure following appliances were used: peeler and slicer (China), balance (acc. ± 0.01 g) KB 2000-2N KERN (Germany), kitchen blender 0.9L BL142A TEFAL (France), centrifuge Jouan C4i Thermo Scientific (USA), syringe microfilter Nylon Hydrophylic 0.22 µm, Membrane Solutions (USA). Apples of Granny Smith variety were purchased in a local supermarket.

Instruments and instrumental parameters

LC/MS analysis was performed on instrumental configuration comprising autosampler Accela (Thermo Scientific, USA), MS pump Accela 1250 (Thermo Scientific, USA) and TSQ Quantum Ultra mass spectrometer equiped with ESI/APCI probe and triple quadrupole analyzer.

10 µL of the sample was loaded on column (SunFire™ C18, 3.5 µm, 100 Å, 150 mm × 2,1 mm, Waters, USA) in a partial loop injection mode and eluted with a mixture of: eluent A (solution of 0.30% of FA and 0.01% of AMF in water) and eluent B (MeOH) following the gradient: 0 min (50% B), 0–13 min (50–75% B), 13–15 min (75% B), 15–16 min (75–100% B), 16–19 min (100% B), 19–20 min (100–50% B), 20–25 min (50% B) with flow equal to 200 µL min^{-1}.

Mass analysis was performed in full scan mode (scan range *m/z* 150–600) under optimized parameters of ion source, ion optic and ion detection system of mass spectrometer. Chromatographic peaks of analytes were integrated after the extraction of analyte characteristic ions from the total scan range.

Procedures

Stocks preparation

Single-pesticide stock solutions (1 mg mL^{-1} each) were prepared by dissolving high purity pesticide standards in ethanol. Multi-pesticide solutions were prepared by mixing and diluting single stocks in ethanol.

Sample preparation

One kg of apples was peeled; peel was homogenized by blending. A sub-portion of peel (10 g) was extracted with acetonitrile (10 mL). After the extraction the mixture was centrifuged (5 min/3000 rpm), the supernatant was microfiltered (0.22 µm, Nylon microfilter) and used in additional procedures.

Comparison of the ESI and APCI ionization efficiency

One set of pesticides standards was prepared in methanol in the concentration range 0.10–5.00 µg mL^{-1}. Another set of pesticides standards in the same concentration range was prepared in blank acetonitrile extract of Granny Smith peel. Both sets were analyzed by 3 instrumental methods designated as MET-01, MET-02 and MET-03, that differed only in the type of implemented ionization probe or in the heated ESI temperatures (Figure 1). Chromatographic peaks integrated areas along with calculated linear regression function parameters were compared.

Method designation	Ionization source parameters
MET-01	ESI (0 °C) or APCI ionization probe
MET-02	HESI (200 °C) ionization probe
MET-03	HESI (350 °C) ionization probe

Figure 1 *Configuration of ESI (1,2) and APCI probe (3,4) within the MS source housing and source parameters implemented into investigation*

RESULTS AND DISCUSSION

ESI *vs* APCI ionization efficiency

Ionization efficiency for each tested analyte is much better in ESI than in APCI ionization mode (Figure 2) for both investigated matrices (solvent and apple). Pesticides ESI chromatographic peak integrated area is much higher than the corresponding APCI integrated area over the entire concentration range. The slope of the linear regression can indicate changes in ionization efficiency with ionization mode, for the entire concentration range. For solvent-based calibration standards, the slope reveals about 20-, 40- and 100-times better ionization of pyrimethanil, cyprodinil and trifloxystrobin, respectively, in ESI than in APCI ionization mode. The comparison could not be performed for boscalid and bifenthrin, since these analytes were not detected by LC-APCI/MS over the tested concentration range.

Slopes comparisons for apple extract-based calibration standards led to a similar conclusion (Figure 2). The ionization efficiency in ESI mode for pyrimethanil, cyprodinil and trifloxystrobin was about 20-, 40- and 50-times better, respectively. Once again, the comparison could not be performed for boscalid and bifenthrin, since these analytes were not detected by LC-APCI/MS due to an inferior ionization efficiency in APCI ionization mode.

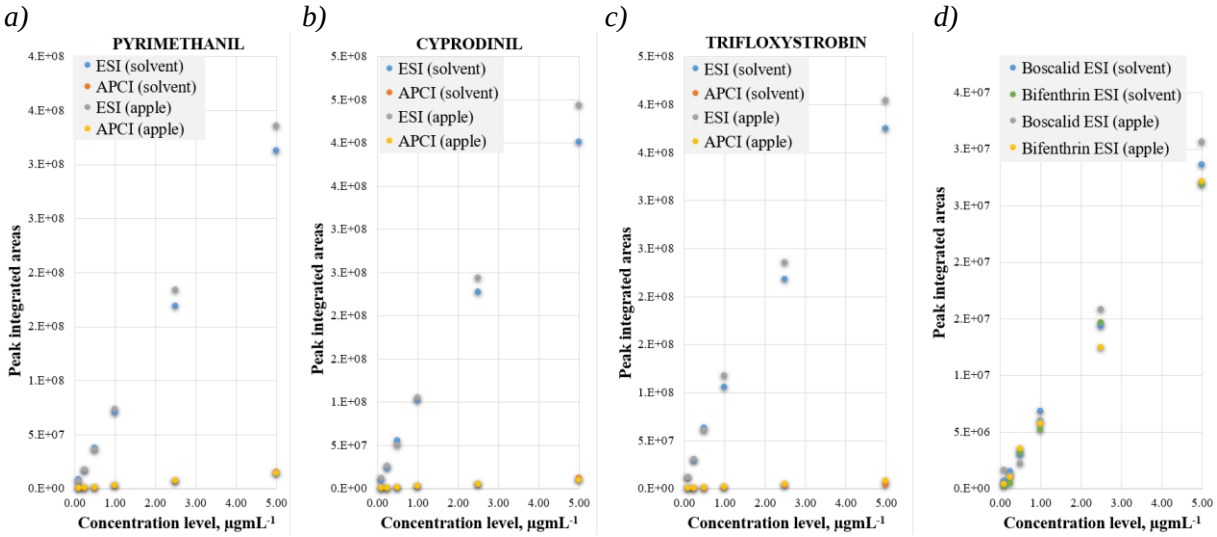

Figure 2 *ESI vs APCI ionization efficiency of pyrimethanil (a), cyprodinil (b), trifloxystrobin (c) and boscalid and bifenthrin (d) over 0.10–5.00 µg mL^{-1} concentration range in solvent and apple peel extract*

ESI *vs* HESI ionization efficiency

Slightly better ionization efficiency over the entire concentration range was observed for pyrimethanil and cyprodinil when shifting from ESI to the HESI ionization mode (Figure 3). Better ionization efficiency becomes notably observable at higher concentrations (higher than 1.00 µg mL^{-1}) and in HESI ionization mode with vaporizer temperature set at the highest tested temperature of 350 °C. When shifting from ESI to the HESI (350 °C), slopes of calibration functions were enhanced by 13% and 29%, for pyrimethanil and cyprodinil, respectively.

Ionization efficiency for boscalid and trifloxystrobin is notably better for the HESI over the entire concentration range, starting from the lowest concentration level. The slope of boscalid calibration functions is about 50% and 200% higher in HESI at 200 °C and HESI at 350 °C, respectively than in ESI ionization mode. Similar percentages of slope enhancement were observed for trifloxystrobin. When shifted from ESI to the HESI ionization mode, the slope was enhanced by 65% (HESI 200 °C) and 200% (HESI 350 °C).

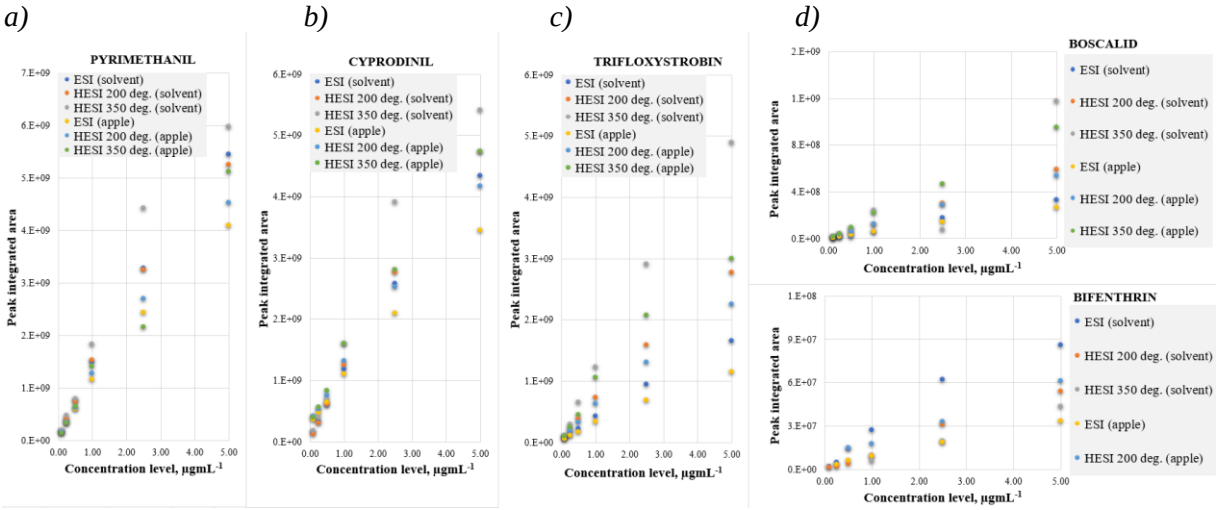

Figure 3 *ESI vs HESI ionization efficiency of pyrimethanil (a), cyprodinil (b), trifloxystrobin (c) and boscalid and bifenthrin (d) over 0.10–5.00 µg mL^{-1} concentration range in solvent and apple peel extract*

Electrospray heating reduces the chromatographic signal of bifenthrin adduct *m/z* 440. This phenomenon is illustrated in Figure 4. Slope of bifenthrin calibration function was calculated in narrower range (1.00–5.00 µg mL^{-1}). Its comparison for different ionization modes reveals ionization efficiency deterioration for 21% and 35%, when the electrospray was heated to 200 and 350 °C, respectively.

Ionization efficiency in peel extracts is better in HESI than in ESI ionization mode for 4 of 5 tested analytes. Ionization efficiency is slightly enhanced for pyrimethanil and cyprodinil when the electrospray is heated to 350 °C. The percentage of slope enhancement is 18 and 28 for pyrimethanil and cyprodinil, respectively.

Slope enhancement for boscalid and trifloxystrobin is much higher. When the temperature of electrospray is 200 °C, the slope is enhanced by 51% (boscalid) and 49% (trifloxystrobin). When the temperature is 350 °C, the slope is enhanced by 72% (boscalid) and 63% (trifloxystrobin).

For Bifenthrin, the slope comparison in ESI and HESI at 200 °C was performed for narrowed concentration range (1.00–5.00 µg mL^{-1}); bifenthrin was not detected in apple extracts when HESI at 350 °C was used. The assumption is that the negative matrix effect and electrospray heating in a combination lead to a significant bifenthrin signal suppression.

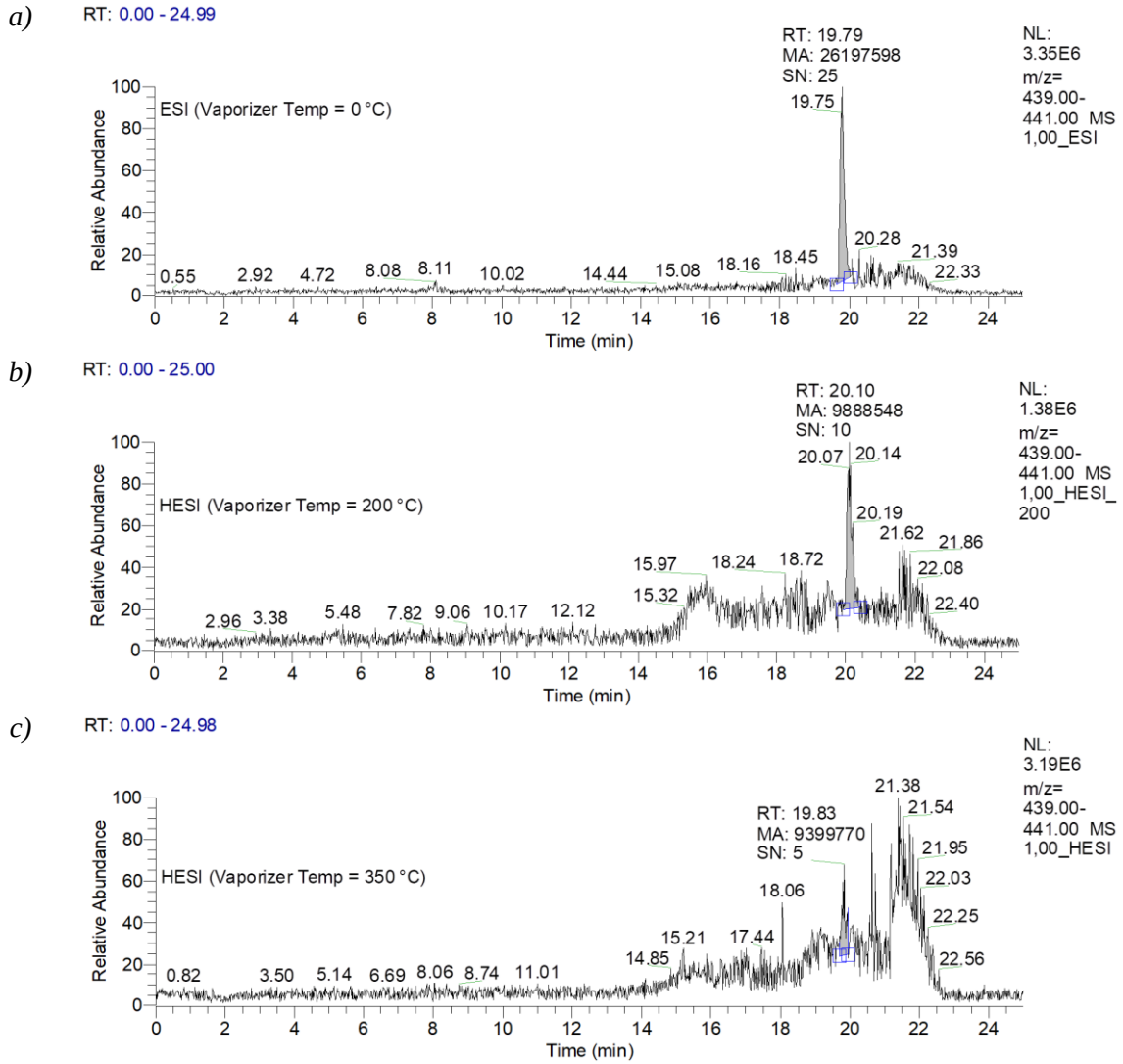

Figure 4 *Extract ion chromatograms of bifenthrin (m/z 440) standard (1.00 µg mL^{-1}) with: a) ESI (vaporizer temp. 0 °C), b) HESI (vaporizer temp. 200 °C) and c) HESI (vaporizer temp. 350 °C)*

CONCLUSION

Electrospray ionization proved to be a better choice for the selected pesticides analysis, than the atmospheric pressure chemical ionization. ESI ionization efficiency was up to a hundred times better than the APCI. Moreover, two of five investigated pesticides were not detectable by the APCI/MS.

ESI ionization efficiency can be additionally improved by the electrospray heating. Significantly better ionization efficiency was observed for all analytes when the electrospray was heated. The contribution of heating to the ionization efficiency was higher for boscalid and trifloxystrobin, than for pyrimethanil and cyprodinil. However, the ionization efficiency of bifenthrin was deteriorated in HESI regimes, probably due to pesticide degradation at higher temperatures.

ACKNOWLEDGEMENT

The authors are grateful to the Ministry of Science, Technological Development and Innovation of the Republic of Serbia for financial support (contract numbers 451-03-47/2023-01/200124 and 451-03-47/2023-01/200383).

REFERENCES

[1] Downard K. The Mass Spectrometer *in* Mass Spectrometry A Foundation Course, Royal Society of Chemistry (2004), pp. 22–66, ISBN-10: 0854046097.

[2] Chen G., Zhang L.-K., Pramanik B. N. LC/MS: Theory, Instrumentation, and Applications to Small Molecules *in* HPLC for pharmaceutical scientists, John Wiley & Sons, Inc. (2007), pp. 281–346, ISBN: 9780470087954.

DIFFERENT GROWTH RESPONSES OF SELECTED REPRESENTATIVES OF PHYTOPLANKTON TO THE PRESENCE OF THE ANTIBIOTIC VANCOMYCIN

Tamara Petronijević[1*], Ivana Kostić Kokić[2], Djuradj Milošević[1], Milica Stojković Piperac[1], Nikola Stanković[1], Tatjana Anđelković[2]

[1]University of Niš, Faculty of Sciences and Mathematics, Department of Biology and Ecology, Višegradska 33, Niš, SERBIA

[2]University of Niš, Faculty of Sciences and Mathematics, Department of Chemistry, Višegradska 33, Niš, SERBIA

[*]*tamarapetronijevic994@gmail.com*

Abstract

Vancomycin is an antibiotic that interferes with the production of peptidoglycan in the cell walls of gram-positive bacteria. Additionally, it moderately inhibits RNA synthesis in the cytoplasm. Due to its widespread use, vancomycin can enter freshwater ecosystems and potentially threaten vital aquatic organisms such as green algae and cyanobacteria. These primary producers play a vital role in the food chain of aquatic systems, making it essential to monitor the presence of vancomycin in the water to prevent any harmful impact on the ecosystem. In this research we monitored the influence of four vancomycin concentrations (6.25, 12.5, 25, and 50 mg/L) on the growth of Chlorella sp., Scenedesmus sp., Anabaena variabilis and Microcystis sp. by determining the concentration of chlorophyll a. The results showed that vancomycin significantly inhibited the growth of A. variabilis at all concentrations, while only higher concentrations (25 and 50 mg/L) caused significant growth inhibition for Microcystis sp. On the other hand, no concentration of vancomycin significantly affected the growth of Scenedesmus sp., while concentrations of 12.5 and 25 mg/L significantly stimulated the growth of Chlorella sp. We concluded that the ecotoxic impact of vancomycin is species-specific, with varying levels of toxicity observed among different phytoplankton species. This finding presents valuable insights into the environmental impact of this antibiotic.

Keywords: vancomycin, phytoplankton, growth, chlorophyll *a*.

INTRODUCTION

Nowadays, the use of antibiotics in human and veterinary medicine is increasing [1]. Due to their wide application, these pharmaceutical products can be found in large quantities in aquatic ecosystems. Although antibiotics aim to fight pathogenic bacteria, once they reach freshwater ecosystems, they can adversely affect other non-target organisms, including microorganisms, green algae and cyanobacteria [2]. In this way, they can negatively influence the decomposer bacteria and the primary producers, representing a risk to the ecosystem. As primary producers in aquatic food chains, algae maintain the structural and functional balance of aquatic ecosystems. They are indicator organisms for assessing the quality of water and the toxic effects of chemicals. Although algal species exhibit varying sensitivity to antibiotics, the underlying biological processes that manage this sensitivity are poorly understood. Several

studies have investigated this topic, including research on the sensitivity of algal species to antibiotics and the factors that influence their sensitivity [2–5].

Vancomycin is a glycopeptide antibiotic commonly used to treat severe infections caused by susceptible Gram-positive bacteria [6]. The presence of vancomycin, its metabolites, and degradation products in the aquatic environment can have harmful ecological effects that could endanger the environment or produce adverse consequences [7]. Vancomycin may be toxic to many aquatic organisms, including algae [7]. Therefore, it is critical to examine the effects of vancomycin on selected representatives of phytoplankton to understand better its impact on these essential organisms in freshwater ecosystems. However, current data regarding the concentrations and biological fate of vancomycin in the environment must be more consistent and sufficient to comprehend the ecological risks associated with this antibiotic fully.

Phytotoxicity tests are continually employed to evaluate the adverse effects of pollutants on algae, which employ growth inhibition as a primary indicator [8]. Research has shown that chlorophyll *a* can be used as a reliable measure of the toxic effects caused by pollutants [8-9]. Due to their high sensitivity to toxic substances, *Scenedesmus* sp. and *Chlorella* sp. are considered relevant species for ecotoxicological tests [10]. In addition, these two types of green algae are among the most common species found in freshwater ecosystems, so the question arises as to what effect antibiotics, specifically vancomycin, have on them. In addition, examining the response of cyanobacteria to antibiotics is also essential as they serve as primary producers and possess a prokaryotic structure, making them highly vulnerable to the impact of antibiotics.

This study aims to examine the response of *A. variabilis*, *Microcystis* sp., *Chlorella* sp., and *Scenedesmus* sp. to several concentrations of vancomycin in the growth medium and its effect on growth rate of these phytoplankton species. Also, in addition to the main objective, the purpose of this study is to determine whether there is a difference in response between these two groups of phytoplankton and whether there is a difference in response within the same group.

MATERIALS AND METHODS

Antibiotic, phytoplankton cultures and cultivation conditions

Vancomycin hydrochloride was purchased from HiMedia Laboratories (assay > 80.00%).

Chlorella sp., *Scenedesmus* sp., and *Microcystis* sp. were isolated from a freshwater pond in southeastern Serbia and cultivated in the laboratory of the Department of Biology and Ecology, Faculty of Science and Mathematics in Niš.

Trichormus variabilis 0441 (heterotypic synonym *Anabaena variabilis*) was isolated from the Danube River in the Vojvodina region (Serbia) and were cultivated in the laboratory at the Department of Biology and Ecology in Novi Sad (NSCCC).

All cultures were prepared in 250 ml Erlenmeyer flaks at 24℃, under cool LED lighting (26.81 μmol/s/m^2) for a 16-h photoperiod with constant aeration. Standard BG11 liquid medium was used to cultivate all species, except *A. variabilis* for which modified BG11 medium (without nitrogen source) was used for cultivation.

Experiment setup

In order to examine the influence of vancomycin on several phytoplankton species, we conducted a study on the growth rate of *A. variabilis*, *Microcystis* sp., *Chlorella* sp., and *Scenedesmus* sp. over 14 days. Different concentrations of vancomycin (6.25, 12.5, 25 and 50 mg/L) were used, with each strain tested at each concentration in triplicate, along with controls.

The experiment was carried out in sterile glass test tubes, with 10 ml of liquid medium BG11 and 2 ml of a culture of each strain added to the specific vancomycin concentration. The controls were monitored to ensure the validity of the assay.

The growth of the phytoplankton species as monitored by determining the concentration of chlorophyll *a* spectrophotometrically. The tubes were incubated at 24°C under cool LED lighting for a 16-hour photoperiod for 14 days.

During the 14-day experiment period, previously vortexed, 1 ml of the culture was placed into cuvettes, and the optical density at 678, 720 and 750 nm was determined spectrophotometrically. The chlorophyll *a* concentration was calculated according to the formula [11]:

$$Chl\ a\,(\mathrm{m}g\times ml^{-1}) = 14.96 \cdot (OD678 - OD750) - 0.616 \cdot (OD720 - OD750)$$

Statistical analysis

ANOVA, followed *post hoc* Tukey HSD test, was used to test any significant difference in growth parameters between treated and control groups of algae between all concentrations. The statistical analyses were performed using IBM SPSS Statistics. The results were considered significant at the level of $p < 0.05$.

RESULTS AND DISCUSSION

This study showed that different phytoplankton species exhibit varying levels of sensitivity to vancomycin in their growth medium.

A. variabilis was the most sensitive, as all concentrations of vancomycin tested caused a significant ($p < 0.05$) inhibition in growth, noticeable within just two days of the experiment. Additionally, the concentration of chlorophyll *a* was significantly lower ($p < 0.05$) in the treated samples compared to the control group.

Compared to *A. variabilis*, *Microcystis* sp. showed tolerance to lower levels of vancomycin exposure (6.25, 12.5 mg/L) without any significant impact on growth. However, exposure to higher concentrations (25 and 50 mg/L) resulted in significant growth inhibition ($p < 0.05$) from the second day of exposure, with notable suppression of chlorophyll *a* production in treated samples compared to control samples.

Vancomycin is an antibiotic that targets pathogenic bacteria by acting on their cell wall. Due to the structural similarity of the cell wall in cyanobacteria to that of bacteria, it was assumed that vancomycin would inhibit the growth of cyanobacteria. We consider that the prokaryotic structure of cyanobacteria is the primary reason for the inhibitory effect of

vancomycin. Our study revealed that *A. variabilis* is more susceptible to vancomycin than *Microcystis* sp., highlighting differences in sensitivity among cyanobacterial species.

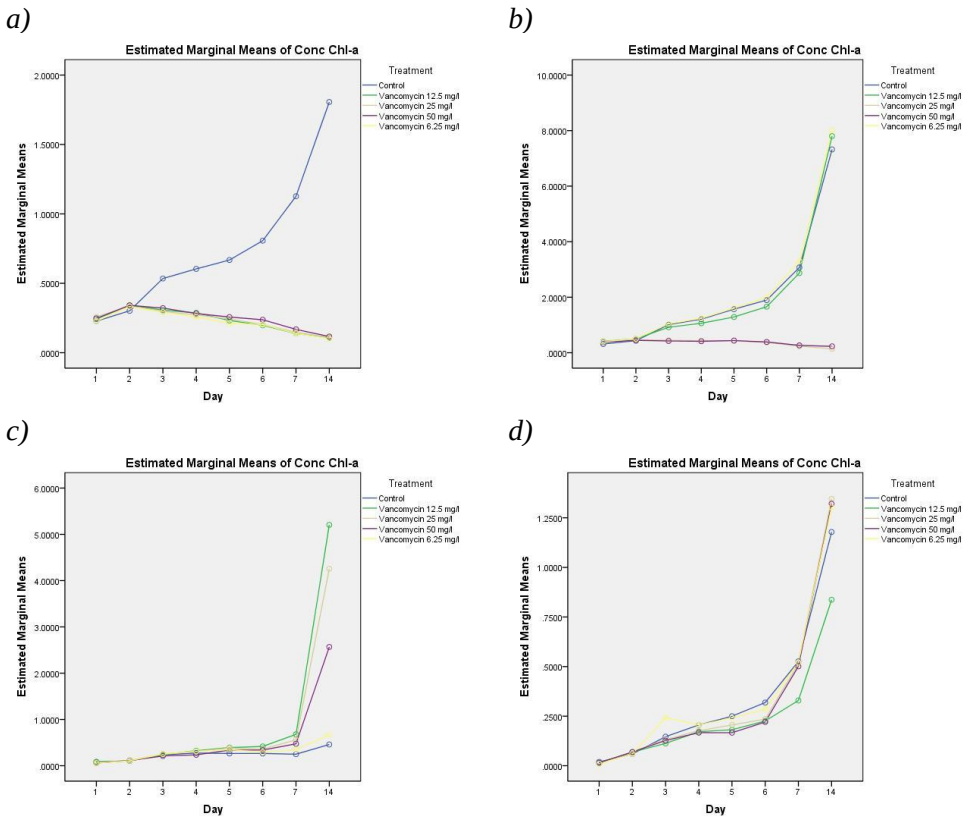

Figure 1 *Spectrophotometric comparison of the growth of a) Anabaena variabilis, b) Microcystis sp., c) Chlorella sp., and d) Scenedesmus sp. in the presence of vancomycin, compared to the growth of the same strains in control conditions (without vanomycin)*

Green algae had a completely different response to the presence of vancomycin in the growth medium than cyanobacteria.

Results showed that all concentrations of vancomycin stimulated the growth rate of *Chlorella* sp. Significant stimulation of chlorophyll *a* production was observed at concentrations of 12.5, and 25 mg/L ($p < 0.05$). In contrast, when examining *Scenedesmus* sp., it was found that the application of vancomycin at various concentrations did not significantly impact the production of chlorophyll *a*. However, a slight inhibition of growth was observed at a concentration of 12.5 mg/L.

The absence of the growth inhibition of green algae by can be attributed to the eukaryotic structure of these organisms. Green algae have unique cell walls that consist of cellulose, hemicellulose, and occasionally chitosan [12]. Unlike bacteria, they do not contain peptidoglycan in their cell walls [12]. Therefore, it is evident that vancomycin, which explicitly targets peptidoglycan synthesis, does not affect cell wall synthesis in green algae.

Previous study have demonstrated that antibiotics can enhance chlorophyll production in *Chlorella* sp. [10]. However, the underlying mechanism by which antibiotics promote the growth of green algae remains unclear. There is a possibility that active communities of

heterotrophic bacteria were present in the test medium alongside the tested phytoplankton strains. These accompanying bacteria may have influenced the growth of *Chlorella* sp., resulting in suboptimal chlorophyll *a* production. Therefore, it is possible that the introduction of antibiotics promoted the growth of *Chlorella* sp. by inhibiting these accompanying bacteria.

While *Chlorella* sp. was found to be resistant to vancomycin, it is possible that the antibiotic had adverse effects on other biological parameters of this species. Furthermore, our findings suggest that vancomycin in natural aquatic environments can potentially lead to increased proliferation of *Chlorella* sp., disrupting the ecosystem's regular processes.

CONCLUSION

Based on the obtained results, we conclude that vancomycin can modulate the growth of certain representatives of phytoplankton, causing both inhibition of cyanobacteria and stimulation of green microalgae, which depends on the exposed strains. The impact of vancomycin on phytoplankton can be influenced by various factors, such as the duration of exposure, concentration, and the types of phytoplankton being tested. As phytoplankton plays a crucial role in aquatic ecosystems, it is imperative to limit the use of antibiotics in these environments to prevent potential disruptions to the balance of the ecosystem and the populations of phytoplankton. Our future study will investigate further biological parameters of phytoplankton that the use of vancomycin may influence.

ACKNOWLEDGEMENT

This work was financially supported by the Ministry of Science, Technological Development and Innovation, Republic of Serbia, Contract No. 451-03-47/2023-01/200124.

REFERENCES

[1] González-Pleiter M., Gonzalo S., Rodea-Palomares I., *et al*., Water Res. 47 (6) (2013) 2050–2064.

[2] van der Grinten E., Pikkemaat M. G., van den Brandhof E., *et al*., Chemosphere 80 (1) (2010) 1–6.

[3] Taylor F. J., Microbiology 39 (2) (1965) 275–284.

[4] Lai H. T., Hou J. H., Su C. I., *et al*., Ecotoxicol. Environ. Safety 72 (2) (2009) 329–334.

[5] Guo J., Selby K., Boxall A. B., Arch. Environ. Con. Tox. 71 (2016) 589–602.

[6] Carvalho I. T., Santos L., Environ. Int. 94 (2016) 736–757.

[7] Cao M., Feng Y., Zhang Y., *et al*., Sci. Rep. 8 (1) (2018) 1–13.

[8] Zhang W., Zhang M., Lin K., *et al*., Environ. Toxicol. Pharmacol. 33 (2) (2012) 344–352.

[9] Wang W. C., Freemark K. Ecotoxicol. Environ. Safety 30 (3) (1995) 289–301.

[10] Zhang W., Sun W., An S., *et al*., Water Environ. Res. 85 (8) (2013) 725–732.

[11] Stankovic R. N., Phytoplankton influence on benthic macroinvertebrates of freshwater ecosystems in multistress conditions: laboratory testing of the toxic effect of cyanobacteria and green microalgae on individuals of the species *Chironomus riparius*, Doctoral dissertation, University of Niš, Faculty of Mathematics and Natural Siences (2020).

[12] Matsuhashi M., Furuyama M., Maruo B., Agr. Biol. Chem. 33 (12) (1969) 1758–1760.

DETERMINATION OF SEVEN ANIONS IN WATER LETTUCE GROWN IN A NATURAL UNPOLLUTED HABITAT BY ION CHROMATOGRAPHY

Tamara Petronijević[1*], Ivana Kostić Kokić[2], Tatjana Anđelković[2], Bojan Zlatković[1], Dajana Stajić[1], Danica Bogdanović[2], Nikola Stanković[1]

[1]Department of Biology and Ecology, University of Niš, Faculty of Science and Mathematics, Višegradska 33, 18000 Niš, SERBIA

[2]Department of Chemistry, University of Niš, Faculty of Science and Mathematics, Višegradska 33, 18000 Niš, SERBIA

[*]*tamarapetronijevic994@gmail.com*

Abstract

In this study, content of seven selected anions in aquatic plant Pistia stratiotes was grown in a natural unpolluted habitat was determined. Selected anions were: fluoride, chloride, nitrite, bromide, nitrate, phosphate and sulphate. During 3 months, 15 individuals of plant were sampled from Ostrovica thermal spring. After anion extraction, determination was performed using ion chromatography. The highest average content was determined in the case of chloride, 143.19 mg/g in individuals sampled in December, while the lowest average content of anions was determined in the case of bromide, 0.027 mg/g in individuals sampled in November. Nitrate content was the highest in individuals sampled in January and the value was 2 times higher than values obtained for individuals sampled in November and December, while in all other cases, the anion content was higher in individuals sampled in December compared to individuals sampled in November and January. The biggest difference in the individual anion content was determined for the nitrite content. The average nitrite content in individuals sampled in December is even 80 times higher than the content determined in individuals sampled in November, that is, 30 times higher than the content determined in individuals sampled in January.

Keywords: anions, aquatic plant, *Pistia stratiotes*.

INTRODUCTION

Clean water is extremely important for human and one of the major concerns is the toxicity of wastewater, because it may contain many harmful chemical compounds (heavy metals, detergents, etc.). However, nutrients in the effluents of wastewater can cause eutrophication, especially nitrogen and phosphorous, which can induce a bloom in microalgal populations. One of the best methods are used to decontaminate wastewater involves using low-cost, sustainable, and green technologies such as bioremediation. Phytoremediation involves the potential of plants to remove organic or inorganic pollutants [1–2]. Floating aquatic macrophytes have potential for removing and recovering nutrients in wastewaters. The high productivity and nutrient removal capability of these plants increasing interest in their use for wastewater treatment and resource recovery [3].

Pistia stratiotes (water lettuce) belong to the family Araceae (Figure 1). It is a monocotyledonous, free-floating aquatic plant which leaves form rosettes. Rosettes are sessile, light dull green in colour, hairy and thick. The adventitious roots are light coloured and feathery and arise at the base in cluster [4]. The whole life cycle leads like a floating plant without roots whose only root system is submerged, while the leaves are above the water surface. *Pistia stratiotes* L. is an invasive aquatic species and now *Pistia stratiotes* L is widespread in many parts of the world compared to its natural distribution. In Serbia, the species occurs in several localities, in thermal springs, as well as in fresh waters, and is considered a naturalized, non-invasive species [5].

Figure 1 *Pistia stratiotes*

Among the aquatic plants, *Pistia stratiotes* has been widely used for the treatment of agricultural, domestic and industrial wastewater due to their availability, resilience in a toxic environment, bioaccumulation potentials, invasive mechanism and biomass potentials [6].

Recent years performed studies have shown that the mechanisms of nutrient uptake from wastewater could be advanced based on physiological, biological and physiochemical behaviours of aquatic plants. The capacity of aquatic plants in nutrients uptake is used in the management of eutrophication in freshwater ecosystems. Nitrogen is primarily responsible for eutrophication and considered as the limiting factor of primary growth. However, high amount of phosphorous often leads to cyanobacterial bloom triggering in many aquatic ecosystems ecological. Submerged macrophytes have a high capacity to absorb phosphorous (P) and plays significant roles in the restoration of freshwater ecosystem. However, the extent to which submerged macrophytes retain P and N content in their tissues at different levels and corresponding influence factors is still not very clear. It depends on many factors, such as natural content of these elements in native plants [7–8].

The objective of the current study was to analyze content of seven anions in aquatic plant *Pistia stratiotes* grown in a natural unpolluted habitat.

MATERIALS AND METHODS

Sampling and extraction

Plant materials sampling

Healthy, well-developed plants of *P. stratiotes* of uniform size, mass and root length and with similar growth stage were collected from a thermal spring in locality Ostrovica (Niš,

Serbia, 43.32680, 22.11117) during November and December 2021, and January 2022. Selected plants were firstly washed thoroughly in a running tap water and then with distilled water to remove the impurities and left to dry indoor at ambient temperature until complete dryness.

Extract Preparation from Plant Tissues

Whole plants were firstly chopped and then portions (0.1000 g) of plant tissues were suspended in 10 mL distilled water, kept at 80°C for 30 min. After this step, samples were put into microwave bath for 30 min and then filtered through Whatman No. 40 filter paper. Extracts were filtered through microfilter (0.45 μm) and analyzed immediately or within 24 h after extraction. Extracts were stored at 4°C.

Instrumentation

The three replications were analysed for anion concentrations as follows. Volume of 2.5 mL of each filtrate sample was placed into the Dionex AS 50 model autosampler vials. Each of samples was loaded automatically into the ion chromatograph. Separation was achieved using Dionex IonPac AS22 column (4 × 250 mm) with the guard column Dionex IonPac AG22 (4 × 50 mm). The ion chromatograph used mix of 4.5 mM sodium carbonate and 1.4 mM sodium bicarbonate as an eluent at a flow rate of 1.2 mL/min. The concentration of nitrate and nitrite anions in samples was detected by the Dionex AERS 500, Carbonate, 4 mm, conductivity detector. Dionex Seven Anion Standard (Product No. 056933) was used for preparing standard solutions. The anion concentration values were calculated automatically based on previous made processing method using Chromeleon 7 software.

RESULTS AND DISCUSSION

All extracts were diluted to one twenty-fifth prior to analysis on ion chromatograph. All sample solutions analysed on IC successfully met the criterion of availability. Concentration of diluted solutions were between 0.25 and 10 mg/L, all in the range of calibration curve. Calibration curves obtained for anions showed good correlation coefficients, between 0.99899 and 0.99989.

Table 1 presents the water quality parameters in which the plant was grown. Monitored parameters were pH, temperature of water, conductivity, and potassium-permanganate consumption.

Figures 1, 2 and 3 presents anion content in all individuals of investigated plant sampled in November 2021, December 2021 and January 2022, respectively.

Obtained results showed decrease of pH value from first to third month. Conductivity of water was lower in December and January in comparing to November, and values for these two months were the same (624 μS/cm). Values of potassium permanganate consumption showed increasing from first to third month, and value determined in January was more than twice higher than value determined in November. Values of temperature were pretty the same for all investigated months (18.5 to 18.9), what was expected bearing in mind that individuals were taken from thermal spring.

Table 1 *Water quality parameters*

Parameter	November 2021	December 2021	January 2022
pH	8.25	7.44	7.19
t (°C)	18.5	18.9	18.8
κ (μS/cm)	639	624	624
$KMnO_4$ (mg/dm^3)	2.89	3.65	6.09

Figure 1 *Anion content in all individuals of investigated plant sampled in November 2021 (mg/g)*

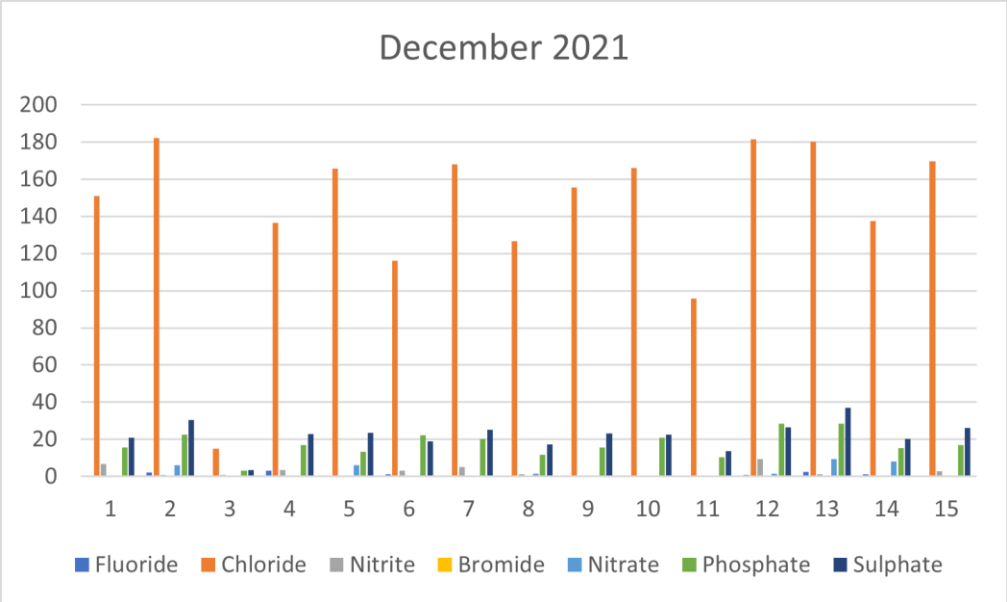

Figure 2 *Anion content in all individuals of investigated plant sampled in December 2021 (mg/g)*

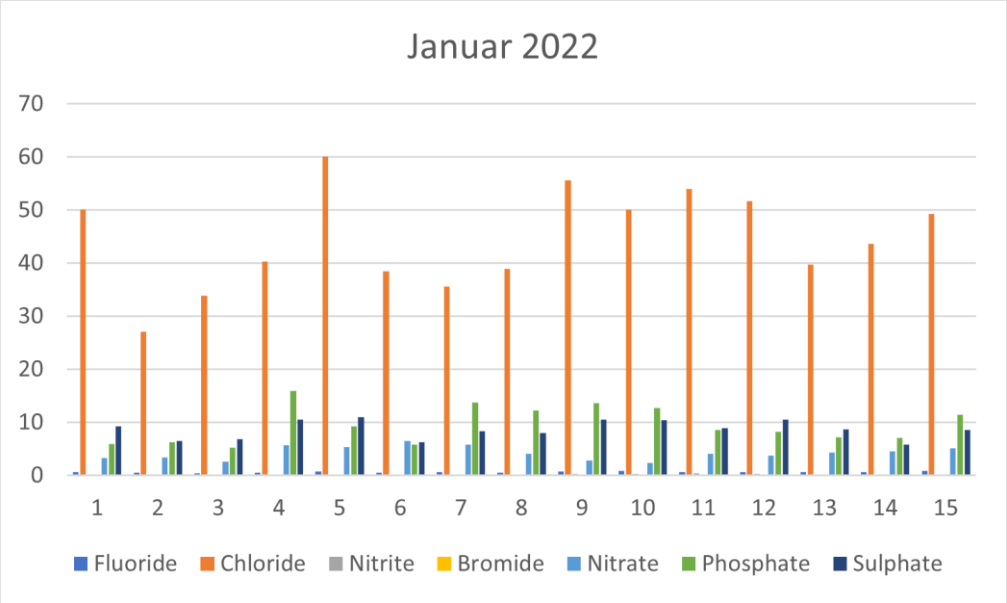

Figure 3 *Anion content in all individuals of investigated plant sampled in January 2022 (mg/g)*

The obtained results show that the average content of anions in plant specimens is the highest in individuals sampled in December, except for nitrate anion. The highest average nitrate content was determined in individuals sampled in January.

Comparing the determined content of all investigated anions, the highest content was determined in the case of chloride, 143.19 mg/g in individuals sampled in December, while the lowest average content of anions was determined in the case of bromide, 0.027 mg/g in individuals sampled in November. Bromide content was not detected in the individuals sampled in January.

The greatest difference in anion content was found between samples sampled in November and December. The values obtained for the content of fluoride, chloride bromide, phosphate and sulphate in the individuals sampled in December are 3 to 5 times higher than the values obtained in the individuals sampled in December. The values obtained from the individuals sampled in January are lower than the values obtained from the individuals sampled in December, but this difference is smaller, and range was from 1.5 to 3 times lower.

The biggest difference in the individual anion content was determined for the nitrite content. The average nitrite content in individuals sampled in December is even 80 times higher than the content determined in individuals sampled in November, that is, 30 times higher than the content determined in individuals sampled in January. Nitrate content was the highest in individuals sampled in January and the value was 2 times higher than values obtained for individuals sampled in November and December.

Bearing in mind that December is the month with the fewest hours of sunshine, as well as that individuals of *Pistia stratiotes* can cover the water surface and thereby additionally block the penetration of sunlight, there is a decrease in primary production, and an increase in the content of nitrites and phosphates.

CONCLUSION

Content of seven anions in aquatic plant *Pistia stratiotes* grown in a natural unpolluted habitat and sampled from November 2021 to January 2022 was determined. The highest average content was determined in the case of chloride, 143.19 mg/g in individuals sampled in December, while the lowest average content of anions was determined in the case of bromide, 0.027 mg/g in individuals sampled in November. Bromide content was not detected in the individuals sampled in January. The biggest difference in the individual anion content was determined for the nitrite content, and established difference was 80 times higher value determined in individuals sampled in December than individuals sampled in November, and 30 times higher value than individuals sampled in January. Nitrate content was the highest in individuals sampled in January and the value was 2 times higher than values obtained for individuals sampled in November and December. In all other cases, the anion content was higher in individuals sampled in December compared to individuals sampled in November and January.

ACKNOWLEDGEMENT

This study was supported by the Ministry of Science, Technological Development and Innovation, Republic of Serbia (Contract Number 451-03-47/2023-01/200124).

REFERENCES

[1] Mustafa H., Hayder G., Ain. Shams. Eng. J. 12 (2021) 355–365.

[2] Buta E., Borsan I. L., Omota M., *et al*., Horticulturae 9 (2023) 503–518.

[3] Ali S., Abbas Z., Rizwan M., *et al*., Sustainability 12 (2020) 1927–1960.

[4] Akpor O. B., Muchie M., Int. J. Phys. Sci. 5 (2010) 1807–1817.

[5] Zlatković B. K., Bogosavljević S. S., Weed Res. 60 (2020) 85–95.

[6] Ahila K. G., Ravindran B., Muthunarayanan V., *et al*., Sustainability 13 (2021) 329–342.

[7] Zhou X., Wang G., Yang F., Desalination 273 (2–3) (2011) 366–374.

[8] Li W., Li Y., Zhong J., *et al*., Front. Plant Sci. 9 (2018) 1–9.

THE COPPER CORROSION IN CHLORIDE MEDIUM WITH ADDITION OF BLACKBERRY LEAF EXTRACT

Milica Zdravković[1*], Vesna Grekulović[1], Nada Štrbac[1], Jasmin Suljagić[2], Ivana Marković[1], Milan Gorgievski[1], Miljan Marković[1]

[1]University of Belgrade, Technical Faculty in Bor, V.J. 12, 19210 Bor, SERBIA

[2]University of Tuzla, Faculty of Technology, Dr. Tihomila Markovića 1, Tuzla, BOSNIA AND HERZEGOVINA

[*]*mboskovic@tfbor.bg.ac.rs*

Abstract

The influence of blackberry leaf extract (BLE) on copper corrosion in 0.5 M NaCl solution was investigated. The extract was made as evaporated blackberry leaf water extract. The cyclic voltammetry (CV) was performed in a blank solution and a solution with the addition of 15 g/L BLE. Surface characterization was performed using scanning electron microscope with energy dispersive X-ray spectroscopy (SEM-EDS). The copper surface characterization was performed on copper specimens after 1 day of immersion in a blank solution and in a solution with the addition of 15 g/L BLE. Three anodic current peaks and two cathodic current peaks were observed on the cyclic voltammogram without the addition of BLE. The CV results show that there was a reduction of anodic and cathodic current peaks in the presence of BLE, which clearly confirms that BLE reduced the amount of corrosion products. SEM-EDS results confirm that a smaller amount of copper oxide and chloride occurs on the copper surface in the presence of BLE in relation to the copper surface in the blank solution. The results show that BLE acts as a good copper corrosion inhibitor in a chloride environment.

Keywords: green inhibitor, blackberry leaf, copper, corrosion, SEM-EDS.

INTRODUCTION

Blackberry leaf is a concentrated source of valuable nutrients and bioactive constituents. It contains vitamins, steroids, and lipids in seed oil and minerals, flavonoids, glycosides, terpenes, acids, and tannins in the aerial parts. The aeral parts have pharmacological activities such as antioxidant, anti-carcinogenic, anti-inflammatory, antimicrobial, anti-diabetic, anti-diarrheal, and antiviral [1,2]. According to a survey conducted in 2005, Serbia had the largest area in the world and accounted for 69% (5300 ha) of Europe's blackberry area. Also, Serbia had the fourth-highest production in the world, with 90% of its production processed and exported [3]. Considering the importance of sustainable development and the replacement of previously toxic substances with environmentally friendly ones, blackberry leaf can be considered as an environmentally friendly corrosion inhibitor. Research shows that blackberry leaves contain caffeic acid, which is already a known copper inhibitor [4,5].

Copper is used in industrial facilities where it is exposed to seawater, chlorine-containing solutions, and hydrochloric acid used to remove rust [6,7]. It is important to note that chlorine

has a negative effect on copper corrosion, so natural corrosion inhibitors can be applied to protect this highly used metal [8,9].

The influence of blackberry leaf extract (BLE) on the copper corrosion behavior in 0.5 M NaCl was previously investigated [5]. The results have shown that BLE acts as a mixed type of copper inhibitor (97.19% IE). The best results were obtained with the addition of 15 g/L BLE. For further understanding of the corrosion mechanism, this paper shows how the presence of 15 g/L BLE in a 0.5 M NaCl solution affects the protection of copper from corrosion by using cyclic voltammetry (CV). Also, surface characterization (SEM-EDS) was performed to show the difference between the copper surface after standing in a pure solution and a solution with the addition of BLE. Based on this, blackberry leaf, as a by-product of blackberry production, can be part of progress towards sustainable development and environmental protection.

EXPERIMENTAL

Solution and material preparation

The starting component for obtaining blackberry leaf extract is a dry blackberry leaf produced by "Adonis", Serbia. Water extract was obtained by pouring hot water over dry leaves. The ratio of solid to liquid components was 1 kg:7.5 L. After 12 hours, filtering was performed on filter paper No. 1. The aqueous extract was evaporated in a rotary evaporator "Buchi R-210". As an output product, a dark colored resin-like substance was obtained, representing blackberry leaf extract (BLE).

The solution of 0.5 M NaCl was prepared using distilled water and NaCl salt p.a. purity manufactured by "Zorka Pharma", Šabac, Serbia. A solution containing 15 g/L BLE was prepared by adding an adequate amount of evaporated extract in a 0.5 M NaCl. Fresh solutions were prepared before each experiment. A rectangular piece of copper Cu-DHP (99.97% Cu, 0.0198% P, 0.0005% Pb) sheet was used to prepare the working electrode. It was sealed with epoxy resin to obtain a cross section of 0.06 cm^2. The copper coupons Cu-DHP for SEM-EDS analysis were made by cutting a copper sheet to dimensions of 1x1 cm.

Electrochemical experiments

The three-electrodes electrochemical cell was used for performing electrochemical experiments. The working electrode was made of copper Cu-DHP, counter electrode was made of platinum sheet, and saturated calomel electrode was used as reference electrode. Experiments were performed at room temperature. The working electrode surface was polished before experiments using a polishing cloth with alumina slurry (0.3 μm), washed with distilled water and ethanol. The "Gamry interface 1010e potentiostat/galvanostat/zra" (Gamry instruments, USA) was used for conducting experiments. The BLE influence on copper corrosion in a chloride medium was investigated using cyclic voltammetry. The cyclic voltammograms were recorded in 0.5 M NaCl without and with the addition of 15g/L BLE in a potential range from -1 V to +1 V (SCE), with a scan rate of 20 mV/s. The "Gamry Framework software" was used for setting parameters and performing experiments, while

"Gamry Echem Analyst" was used for analyzing output data, as well as for drawing graphics (both Gamry instruments, USA).

Metal surface characterization

The copper surface was characterized using scanning electron microscope with energy dispersive X-ray spectroscopy (SEM-EDS "VEGA 3 LMU", Tescan, USA). The copper specimens were immersed in the solution after preparing the surface. The analysis was performed after standing for 1 day in a blank solution and in a solution with the addition of 15 g/L BLE.

RESULTS AND DISCUSSION

Cyclic Voltammetry (CV)

Cyclic voltammograms obtained for copper in 0.5 M NaCl solution with and without the addition of 15 g/L BLE are shown in Figure 1.

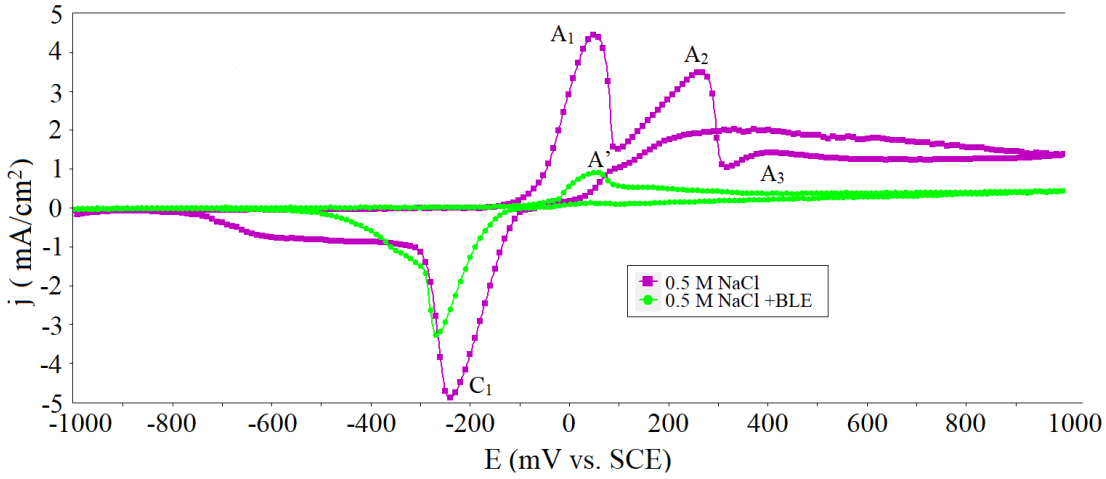

Figure 1 *Cyclic voltammograms obtained for copper in 0.5 M NaCl solution with and without the addition of 15 g/L BLE*

The following current peaks were observed on the cyclic voltammogram obtained in 0.5 M NaCl solution without the addition of BLE: A_1, A_2, A_3, A', and C_1. Copper dissolution starts around E = -150 mV vs. SCE followed by peaks A_1 and A_2. According to the literature, it can be assumed that current peaks A_1 and A_2 correspond to the formation of CuCl and $CuCl_2^-$ [11–15]. The mechanism of copper corrosion takes place starting with the following reaction [16]:

$$Cu + Cl^- \leftrightarrow CuCl + e^- \quad (1)$$

after which it is adsorbed or deposited on the surface of Cu-DHP. Further, this molecule is transformed into a complex [16]:

$$CuCl + Cl^- \leftrightarrow CuCl_2^- \quad (2)$$

The anodic current peak A_3 can be attributed to the formation of copper oxide [17–19]. This additional oxidation of copper is assigned to the current peak A' [17]. These reactions can be represented as follows [16]:

$$CuCl_2^- \rightarrow Cu^{2+} + 2Cl^- + e^- \quad (3)$$

$$2CuCl_2^- + 2OH^- \rightarrow Cu_2O + Cl^- + H_2O \quad (4)$$

$$Cu_2O + 1/2\,O_2 + Cl^- + H_2O \rightarrow Cu_2(OH)_3Cl + OH^- \quad (5)$$

The cathodic peak C_1 observed on the CV curve for blank solution indicates the reduction of corrosion products [20].

Comparing the CV curve obtained in the presence of BLE with the CV curve without the addition, it can be observed that the area under the anodic polarization curve decreases in the presence of BLE. Surface reduction indicates the formation of smaller amounts of corrosion products [19]. The anodic peak A_1 is significantly smaller. Other anodic peaks were not detected in the presence of BLE. This indicates that the presence of inhibitor significantly reduces the formation of copper chloride, while the formation of oxides is completely prevented. The obtained results indicate that BLE molecules adsorb on the copper surface and prevent copper corrosion [5,16,19]. The decrease of cathodic current peak C_1 indicates that the reduction process is taking place but with a much lesser extent than in 0.5 M NaCl solution without the addition [20]. The results obtained by cyclic voltammetry indicate that BLE affects both the cathodic and anodic processes. There is a greater influence on the oxidation process, especially on the process of copper oxide formation.

Metal surface characterization

The backscattered electron (BSE) images were obtained by scanning electron microscopy. Micrographs were obtained from the copper surface after immersion in 0.5 M NaCl solution for 1 day in the absence (Figure 2a) and presence of 15 g/L BLE (Figure 2b). The chemical composition of each surface was determined by EDS for the entire surface as shown in Figure 2. The chemical composition of the elements is shown in Table 1 and expressed in atomic percentages. Spectrum 1 refers to the copper surface in 0.5 M NaCl, while the values for Spectrum 2 refer to the copper surface after standing in a solution with the addition of BLE.

The presence of oxygen and chlorine in the corresponding Spectrum 1 confirms the existence of corrosion products on the Cu-DHP surface after standing in blank solution. In contrast, in the presence of BLE, the copper surface is well protected from corrosion (Figure 2b). Also, the Spectrum 2 of the copper surface in the presence of BLE shows that there is no chlorine detected on the surface. The amount of oxygen is significantly lower, which may be a consequence the inhibitor organic components adsorbed on the copper surface. The presence of BLE molecules on the copper surface is additionally confirmed by the presence of carbon in Spectrum 2 [20]. The earlier research of BLE chemical composition shows that BLE contains caffeic acid, quercetin-3-O-glucoside and kaempferol-3-Oglucoside [5]. SEM-EDS analysis confirms that inhibitor molecules adsorb on the copper surface and protect the metal from corrosion in the presence of chloride ions.

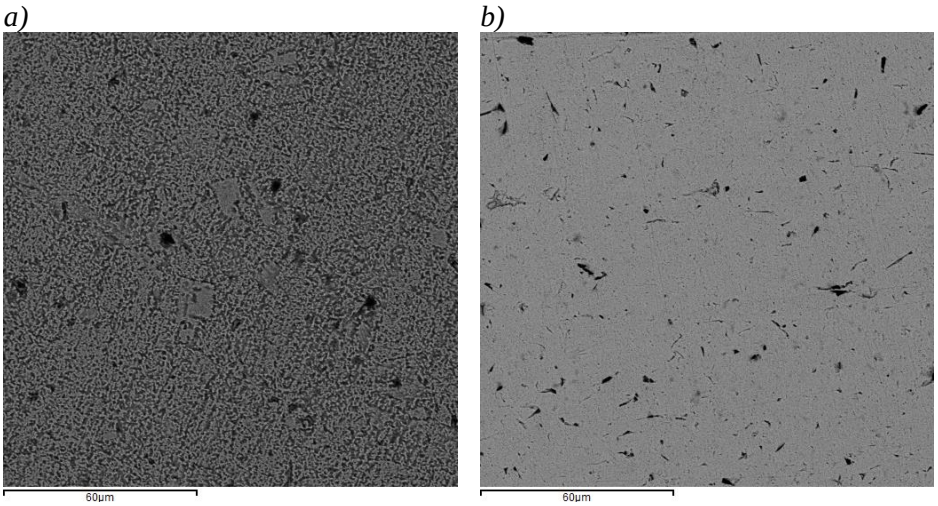

Figure 2 *BSE SEM images of copper specimens after 1 day of immersion in 0.5 M NaCl a) without and b) with 15 g/L BLE*

Table 1 *Chemical composition of copper after standing for 1 day in 0.5 M NaCl solution (Spectrum 1) and in a solution with the addition of 15 g/L BLE obtained by EDS (Spectrum 2)*

Spectrum	Elements, at%			
	O	Cl	Cu	C
1	50.82	1.33	47.85	-
2	11.65	-	38.35	49.99

CONCLUSION

Based on the investigated electrochemical behavior of the Cu-DHP in a 0.5 M NaCl solution, without and with the addition of blackberry leaf extract, the following can be concluded: The results obtained by cyclic voltammetry show that tree current peaks were detected on the anodic polarization curve and two current peaks were detected on the cathodic polarization curve for copper in 0.5 M NaCl. The anodic peaks correspond to the formation of CuCl, $CuCl_2^-$ and Cu_2O. The cathodic peaks correspond to additional oxidation of copper and reduction of corrosion products. With the addition of 15 g/L BLE, the surface area below the polarization curves is smaller than the surface area below the polarization curve recorded without the addition of BLE. Since BLE affects both anodic and cathodic peaks, it can be concluded that it acts as a mixed type of copper inhibitor in chloride medium. SEM and EDS results show that there is no chloride in the presence of BLE, and oxygen amount is significantly reduced. The presence of carbon unequivocally confirms the presence of adsorbed BLE molecules on the copper surface.

ACKNOWLEDGEMENTS

The research presented in this paper was done with the financial support of the Ministry of Science, Technological Development and Innovation of the Republic of Serbia, within the funding of the scientific research work at the University of Belgrade, Technical Faculty in Bor, according to the contract with registration number 451-03-47/2023-01/200131.

REFERENCES

[1] Zia-Ul-Haq M., Riaz M., De Feo V., *et al*., Molecules 19 (8) (2014) 10998–11029.

[2] Riaz M., Ahmad M., Rahman N., J. Med. Plant Res. 5 (24) (2011) 5920–5924.

[3] Strik B. C., Clark J. R., Finn C. E., *et al*., J. Am. Soc. Hortic. 17 (2) (2007) 205–213.

[4] Vrsalović L., Gudić S., Kliškić M., *et al*., Int. J. Electrochem. Sci. 11 (2016) 459–74.

[5] Zdravković M., Grekulović V., Suljagić J., *et al*., Bioelectrochemistry 151 (2023) 108401.

[6] Trabanelli G., Corrosion 47 (1991) 410–419.

[7] Syrett B. C., Corrosion 32 (1976) 242–252.

[8] Hack H. P., Pickering H. W., J. Electrochem. Soc. 138 (1991) 690–695.

[9] Al-Mobarak N. A., Khaled K. F., Hamed M. N. H., *et al*., Arab. J. Chem. 4 (2011) 185–193.

[10] Grudić V., Bošković I., Gezović A., Chem. Biochem. Eng. Q. 32 (3) (2018) 299–305.

[11] Thompson W. T., Kaye M. H., Bale C. W., *et al*., Pourbaix diagrams for multielement systems, Centre for research in computational thermochemistry, Royal military college of Canada, Ecole Polytechnique, Montreal, Quebec, Canada, 2003.

[12] Rajčić-Vujasinović M., Grekulović V., Stamenković U., *et al*., Mater. Test. 59 (6) (2017) 517–523.

[13] Kosec T., Milosev I., Pihlar B., Appl. Surf. Sci. 253 (22) (2007) 8863–8873.

[14] Otmačić H., Telegdi J., Papp K., *et al*., J. Appl. Electrochem. 34 (2004) 545–550.

[15] Mamas S., Kıyak T., Kabasakaloglu M., *et al*., Mater. Chem. Phys. 93 (1) (2005) 41–47.

[16] Li J., Du C. W., Liu Z. Y., *et al*., Int. J. Electrochem. Sci. 11 (2016) 10690–10705.

[17] Grekulović V., Rajčić-Vujasinović M., Corrosion 68 (2) (2012) 025003-1-025003-8.

[18] Rajčić-Vujasinović M., Nestorović S., Grekulović V., *et al*., Corrosion 66 (10) (2010) 105004–105004-5.

[19] M. Zdravković, V. Grekulović, M. Rajčić Vujasinović, *et al*., Prot. Met. Phys. Chem. Surf. 58 (2022) 811–821.

[20] Silva E. F., Wysard J. S., Bandeira M. C. E., *et al*., Corr. Sci. 191 (2021) 109714.

PHOSPHOLIPID LIPOSOMES AS A CARRIER FOR *Aloe vera* WASTE EXTRACT

Aleksandra A. Jovanović[1*], Muna Rajab Elferjane[2,3], Marija Gnjatović[1], Branko Bugarski[2], Aleksandar Marinković[2]

[1]University of Belgrade, Institute for the Application of Nuclear Energy INEP, Banatska 31b, 11080 Zemun Belgrade, SERBIA

[2]University of Belgrade, Faculty of Technology and Metallurgy, Karnegijeva 4, 11000 Belgrade, SERBIA

[3]University of Misurata, Faculty of Nursing and Health Sciences, Misurata, LIBYA

[*]*ajovanovic@inep.co.rs*

Abstract

Aloe vera L. leaf waste contains biologically active compounds, including polyphenols, anthraglycosides, free anthraquinones, resins, mono- and polysaccharides, polypeptides, terpenoids, sterols, chromones, lectins, fatty, amino and organic acids, enzymes, saponins, vitamins, and minerals. However, the application of the mentioned bioactive components is rather limited because of their low solubility, stability, integrity, permeability, and consequently bioavailability. Thus, the encapsulation of the active principles of A. vera into liposomes can be advantageous. In the present study, A. vera waste extract-loaded liposomes were developed and characterized via the determination of particle size, polydispersity index (PDI), zeta potential, conductivity, mobility, storage stability, density, surface tension, and viscosity. The particle size of liposomes with A. vera extract amounted to 335.0±20.5 nm, while the PDI was 0.505±0.056. The zeta potential, conductivity, and mobility were 1.81±0.32 mV, 0.485±0.013 mS/cm, and 0.142±0.026 µmcm/Vs, respectively. The vesicle size and PDI changed during 21 days of storage. The zeta potential, conductivity, and mobility did not vary in the liposomal suspension during the stability study. The density, surface tension, and viscosity were 0.991±0.003 g/mL, 22.8±0.2 mN/m, and 22.9±0.1 mPa·s, respectively. The beneficial effects of bioactive principles from A. vera on human health highlight the application of liposomes as a carrier for A. vera leaf waste extract and their potential implementation in food, functional food, pharmaceutical, and cosmetic formulations.

Keywords: *Aloe vera*, encapsulation, extract, liposomes, waste.

INTRODUCTION

Aloe vera L. (Liliaceae) and its leaf waste (plant material without aloe gel) contains biologically active compounds, including polyphenols (flavonoids, tannins, and phenolic acids), anthraglycosides, free anthraquinones, resins, mono- and polysaccharides, polypeptides, terpenoids, sterols, chromones, lectins, fatty, amino and organic acids, enzymes, saponins, vitamins, and minerals [1,2]. Nevertheless, the application of the mentioned bioactive compounds is rather limited because of their low solubility, stability, integrity, permeability, and consequently bioavailability [3]. Therefore, the encapsulation of the active principles of *A. vera* leaf waste can be advantageous. Liposomes, micro- or nanovesicles usually constituted by phospholipids (but different kinds of other lipids can be used), can be

used for encapsulation of various hydrophilic, lipophilic, or amphiphilic compounds [4,5]. Liposomes have been widely used due to their high structural integrity, stability during storage, and controlled release capability. Additionally, they are easy to prepare and readily functionalized for active targeted delivery. Also, liposomal particles have long been perceived as the ideal drug delivery vehicles because of their superior biocompatibility. Namely, a liposomal bilayer is an analog of a biological membrane and can be prepared from both natural and synthetic phospholipids [6].

In the present study, phospholipid liposomes with *A. vera* leaf waste extract were developed and characterized via particle size, polydispersity index (PDI), zeta potential, conductivity, mobility, storage stability, density, surface tension, and viscosity.

MATERIALS AND METHODS

Plant material and reagents

A. vera leaf waste was purchased in ASC Garden d.o.o., Belgrade, Serbia. The aloe gel was removed from the leaves. Subsequently, clean and empty leaves that represent the waste were cut and freeze-dried in Beta 2-8 LD plus (Christ, Germany). Ethanol (Merck, Germany) and Phospholipon 90 G (unsaturated diacyl-phosphatidylcholine) (Lipoid GmbH, Germany) were also used. Distilled water was purified through a Simplicity UV® water purification system (Merck Millipore, Merck KGaA, Germany).

Extraction procedure

Heat-assisted extraction of bioactive principles form *A. vera* leaf waste was performed at 60°C using the incubator shaker KS 4000i control (IKA, Germany) at a solid-to-solvent ratio of 1:25 g/mL, 50% ethanol, as an extraction medium for 30 min. The extract was prepared in the Erlenmeyer flasks covered by aluminum foil to avoid light exposure and evaporation of solvent. After the extraction, the sample was filtered using filter paper and stored at 4°C until further experiments.

Preparation of extract-loaded liposomes

Phospholipid liposomes containing *A. vera* leaf waste extract were obtained using the proliposome method and a mixture of phospholipids (Phospholipon) [7]. Phospholipids (4 g) and ethanol *A. vera* extract (50 mL) were stirred at 50°C with the aim to homogenize a mixture and evaporate ethanol. After cooling to 25°C, ultrapure water (20 mL) was added and the formulation was stirred at 800 rpm for 1 h.

Determination of particle size, PDI, zeta potential, conductivity, and mobility

The measurements of particle size, PDI, zeta potential, conductivity, and mobility were performed using photon correlation spectroscopy in Zetasizer Nano Series, Nano ZS (Malvern Instruments Ltd., UK). The measurement was repeated on the 1st, 3rd, 5th, 7th, 14th, and 21st days after the liposomal preparation with the aim to monitor their stability at 4°C. Each sample was diluted 500 times and measured in triplicate at room temperature.

Measurement of density, surface tension, and viscosity

The density and surface tension of the extract-loaded liposomes were determined using Force Tensiometer K20 (Kruss, Germany). The sample (20 mL) was examined three times at room temperature.

The viscosity of the sample was examined using Rotavisc lo-vi device (IKA, Germany). The sample (6.7 mL) was examined three times at room temperature.

Statistical analysis

The statistical analysis of the results obtained in storage stability study was done by using analysis of variance (one-way ANOVA) and Duncan's *post hoc* test in STATISTICA 7.0. The differences were considered statistically significant at $p<0.05$.

RESULTS AND DISCUSSION

A. vera extract-loaded liposomes was developed and particle size, PDI, zeta potential, conductivity, mobility, density, surface tension, and viscosity of the sample were determined. The results are presented in Table 1 (the values measured after the liposomal preparation). In addition, storage stability study was performed and the results are shown in the graphs of Figure 1.

Table 1 *Particle size, polydispersity index (PDI), zeta potential, conductivity, and mobility of phospholipid liposomes with Aloe vera leaf waste extract measured immediately after the liposomal preparation*

Variables	Liposomes with extract
Particle size [nm]	335.0±20.5
PDI	0.505±0.056
Zeta potential [mV]	1.81±0.32
Conductivity [mS/cm]	0.485±0.013
Mobility [μmcm/Vs]	0.142±0.026
Density [g/mL]	0.991±0.003
Surface tension [mN/m]	22.8±0.2
Viscosity [mPa·s]	22.9±0.1

As can be seen in Table 1, the particle size of extract-loaded liposomes was 335.0±20.5 nm, whereas the PDI, as a measure of particle size distribution in the liposomal formulation, was 0.505±0.056. The measured values of vesicle size are in agreement with the literature, where phospholipid liposomes had a diameter of ~400 nm [8]. The particle size of liposomes is significantly affected by the type of lipids, the method used for the liposomal formulation, as well as the physicochemical properties of the encapsulated molecules [7,9]. The obtained PDI values indicate the existence of a non-uniform system (0.505±0.056). The zeta potential, conductivity, and mobility were 1.81±0.32 mV, 0.485±0.013 mS/cm, and 0.142±0.026 μmcm/Vs, respectively. The zeta potential was very low indicating the presence

of a very unstable system. According to Lidgate *et al*. [10], a lower capture volume corresponds to an increase in conductivity. Namely, a lower amount of ions are removed as liposome capture volume decreased with decreasing lipid concentration, thus conductivity of the liposome dispersions increased as the lipid concentration decreased. Also, conductivity values increase in the case of leakage of encapsulated compounds [10]. In the case of *A. vera* extract-loaded liposomes, a higher amount of the added extract resulted in a higher value of conductivity. According to the literature, the mobility of liposomal particles represents a function of particle size, total charge, and composition of the liposomal membrane [11]. Additionally, some liposomes are fluid, flexible, and deformable, whereas others are rigid that depend on the bilayer composition, as well as entrapped components. Their fluidity/rigidity and deformable properties also significantly impact mobility [12,13]. The density, surface tension, and viscosity of the liposomes were 0.991±0.003 g/mL, 22.8±0.2 mN/m, and 22.9±0.1 mPa·s, respectively (Table 1). A higher viscosity of the liposomes is an indication of smaller vesicle size [14] which was the case with the obtained *A. vera* extract-loaded liposomes.

In order to examine the stability of phospholipid liposomes with *A. vera* leaf waste extract, particle size, PDI, zeta potential, conductivity, and mobility were measured during 21 days of storage at 4ºC (Figure 1).

As can be seen from Figure 1a, the particle size and PDI did not change in the first 5 days of storage, whereas a slight increase appeared after the 7th day and continued to increase up to the 21st day. The obtained results were expected due to very low values of zeta potential and a high probability of particle fusion. The zeta potential and mobility did not vary and kept low values in the liposomal suspension during the stability study (Figure 1b). Considering that there was no increase in the conductivity of the liposomes (Figure 1c), it can be concluded that there was no leakage of encapsulated compounds from the liposomal bilayer.

a)

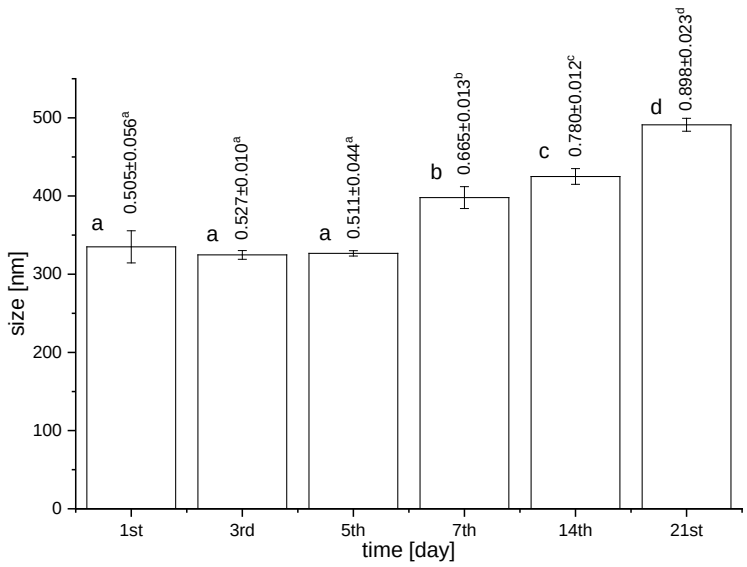

b)

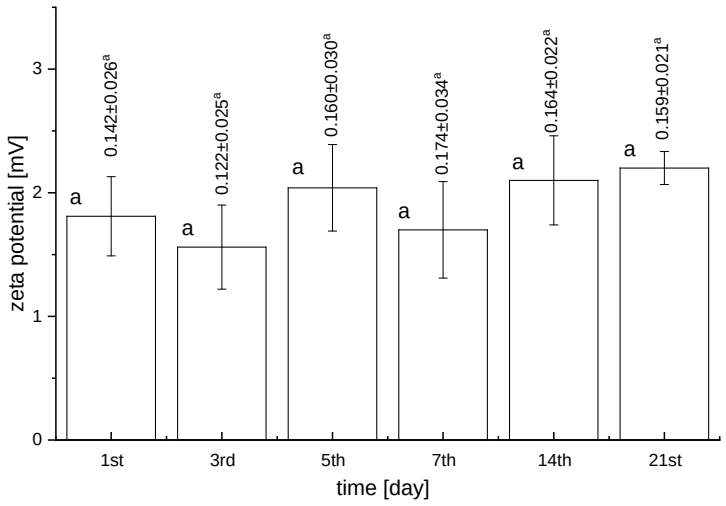

c)

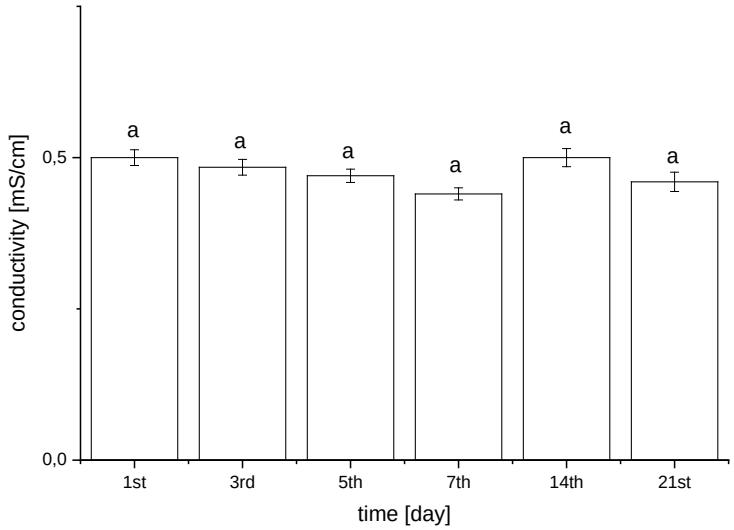

Figure 1 *a) Particle size – bars and polydispersity index – numbers above bars, b) zeta potential – bars and mobility – numbers above bars (µmcm/Vs), and c) conductivity of phospholipid liposomes with Aloe vera leaf waste extract for 21 days; values with different letters (a–c) showed statistically significant differences (p<0.05; n=3; analysis of variance, Duncan's post-hoc test)*

CONCLUSION

In the present study, *A. vera* waste extract-loaded liposomes were developed and characterized in terms of physical properties. The results indicate the existence of nanoparticles and a non-uniform system with very low values of zeta potential and mobility. The results of the stability study showed that particle size and PDI values increased during storage, while zeta potential, conductivity, and mobility did not change. The beneficial effects of bioactive principles from *A. vera* on human health highlight the application of liposomes as a carrier for *A. vera* leaf waste extract and their potential implementation in food, functional

food, pharmaceutical, and cosmetic formulations. However, future experiments and perspectives should be directed toward the improvement of liposomal stability.

ACKNOWLEDGEMENT

The authors acknowledge their gratitude to the Ministry of Education, Technological Development and Innovation of Serbia, contract numbers 451-03-47/2023-01/200019 and 451-03-47/2023-01/200135.

REFERENCES

[1] Khan I. A., Abourashed E. A. Leung's encyclopedia of common natural ingredients: used in food, drugs and cosmetics, John Wiley & Sons, New York (2011), p.25, ISBN: 978-0-471-46743-4.

[2] Hęś M., Dziedzic K., Górecka D., *et al*., Plant Foods Hum. Nutr. 74 (2019) 255–265.

[3] Fang Z., Bhandari B. Trends Food Sci. Technol. 21 (2010) 510–523.

[4] Ribeiro H., Schuchmann H., Engel R., *et al.*, Encapsulation of carotenoids *in* Encapsulation technologies for active food ingredients and food processing, Editors: Zuidam N. J. and Nedović V., Springer, New York (2010), 211–252, ISBN: 978-1-4419-1007-3.

[5] Ricci, M., R. Oliva, Del Vecchio P., *et al*., Biochim. Biophys. Acta. 1858 (2016) 3024–3031.

[6] Hadinoto K., Sundaresan A., Cheow W. S. Eur. J. Pharm. Biopharm. 85 (2013) 427–443.

[7] Isailović B., Kostić I., Zvonar A., *et al*., Innov. Food Sci. Emerg. Technol. 19 (2013) 181–189.

[8] Jovanović A., Petrović P., Ćujić D., *et al*., Proceedings of the VIII International Congress "Engineering, Environment and Materials in Process Industry", 20–23 March, Jahorina, Bosnia and Herzegovina (2023).

[9] Jovanović A., Balanč B., Djordjević V., *et al*., Colloids Surf. B. 183 (2019) 110422.

[10] Lidgate D., Hegde S., Maskiewicz R. Int. J. Pharm. 96 (1993) 51–58.

[11] Duffy C., Gafoor S., Richards D., *et al*., Anal. Chem. 73 (2001) 1855–1861.

[12] Pysher M., Hayes M. Langmuir 20 (2004) 4369–4375.

[13] Jovanović A., Balanč B., Ota A., *et al*., Eur. J. Lipid Sci. Technol. 120 (2018) 1–41.

[14] Shashidhar G. M., Manohar B. RSC Adv. 8 (2018) 34634–34649.

Vaccinium myrtillus LEAF WASTE EXTRACTS WITH NATURAL DEEP EUTECTIC SOLVENT

Aleksandra A. Jovanović[1*], Muna Rajab Elferjane[2,3], Milena Milošević[4], Marija Gnjatović[1], Aleksandar Marinković[2]

[1]University of Belgrade, Institute for the Application of Nuclear Energy INEP, Banatska 31b, 11080 Zemun, Belgrade, SERBIA

[2]University of Belgrade, Faculty of Technology and Metallurgy, Karnegijeva 4, 11000 Belgrade, SERBIA

[3]University of Misurata, Faculty of Nursing and Health Sciences, Misurata, LIBYA

[4]University of Belgrade, Institute of Chemistry, Technology and Metallurgy, National Institute of the Republic of Serbia, Njegoševa 12, 11000 Belgrade, SERBIA

[*]*ajovanovic@inep.co.rs*

Abstract

Vaccinium myrtillus leaf waste extracts were prepared using lactic acid+amonium acetate and maceration, heat- and ultrasound-assisted extractions (HAE and UAE, respectively). The obtained extracts were characterized via analysis of total polyphenol content (TPC), pH, zeta potential, conductivity, density, surface tension, viscosity, and antioxidant potential. The TPC was the highest in the extract prepared in HAE (53.0±0.9 mg GAE/g), whereas the extracts from maceration and UAE possessed significantly lower TPC (50.4±0.7 and 49.5±0.4 mg GAE/g). The ABTS radical scavenging potential was the highest in the extract prepared in HAE (38.4±1.1 µmol TE/g), followed by the extract obtained using UAE (33.7±1.5 µmol TE/g) and maceration (30.2±1.7 µmol TE/g). The DPPH antioxidant capacity followed the same trend: HAE>UAE>maceration. The zeta potential was low in all extracts (2.66±0.48 mV for macerate, 2.57±0.20 mV for HAE, and 3.17±0.13 mV for UAE), while the conductivity was in the range of 1.87±0.13 and 1.84±0.11 mS/cm (maceration and HAE) to 2.10±0.11 mS/cm (UAE). The density varied from 1.105±0.009 g/mL for macerate to 1.122±0.006 and 1.117±0.001 g/mL for HAE and UAE extracts. There were no statistically significant differences in the surface tension and viscosity (~23.5 mN/m and ~5.5 mPa·s). The highest TPC and antioxidant potential were measured in the extract obtained using HAE, whereas the extract prepared by ultrasound waves possessed the highest zeta potential and conductivity. Therefore, the extraction technique should be chosen depending on the future application of V. myrtillus extract.

Keywords: extract, natural deep eutectic solvent, *Vaccinium myrtillus*, waste.

INTRODUCTION

Vaccinium myrtillus L. (Ericaceae) possesses significant economic importance due to the application of its fruits and sometimes leaves in different food, functional food, pharmaceutical, cosmetic, and health-care formulations [1]. The plant contains anthocyanins, phenolic acids, fatty acids, stilbenes, iridoid glycosides, dietary fibers, vitamins, and minerals, while leaf extracts have astringent, antibacterial, antioxidant, anti-inflammatory, lipid-

lowering, hypolipidemic, and hypoglycemic activities [1–3]. Additionally, the extraction of the mentioned bioactive compounds from different plant parts can be a good alternative to the valorization of plant waste [4]. Maceration, as a traditional extraction method, is adequate for the extraction of thermosensitive compounds and does not require a complicated and expensive device. However, it has a lower extraction yield, prolonged extraction time, and a large quantity of plant material and extraction solvents causing an environmentally negative impact [5,6]. Therefore, the implementation of novel extraction techniques, such as heat- and ultrasound-assisted extractions (HAE and UAE, respectively) has been established. Their advantages include a lower solvent consumption, shorter extraction time, and a high extraction yield while supporting the concept of a "green" solvent with the aim to minimize a negative impact on the environment [5]. According to the literature, natural deep eutectic solvent (NADES) is used to enhance the recovery of polyphenol compounds from the herbal matrix and overcome the limitations of conventional and toxic organic extraction mediums [7,8]. NADES is environmentally friendly, relatively safe, less hazardous, and biodegradable due to its composition containing primary metabolites, including sugars, organic bases, plant and amino acids [7,9,10].

In the present study, *V. myrtillus* leaf waste extracts were prepared using lactic acid+amonium acetate, as NADES, and maceration, HAE, and UAE. The extracts were characterized in terms of analysis of total polyphenol content (TPC), zeta potential, conductivity, pH, density, surface tension, viscosity, and antioxidant capacity.

MATERIALS AND METHODS

Plant material and reagents

V. myrtillus leaf waste was herbal dust, the particle size of 0.3 mm resulting from the grinding of the initial plant material in the Institute for Medicinal Plants Research ”Dr Josif Pančić”, Serbia. Folin-Ciocalteu reagent and gallic acid (Merck, Germany), sodium carbonate (Fisher Science, UK), 2,2'-azino-bis(3-ethylbenzothiazoline-6-sulphonic acid) or ABTS, 6-hydroxy-2,5,7,8-tetramethylchroman-2-carboxylic acid or Trolox, and 2,2-diphenyl-1-picrylhydrazyl or DPPH (Sigma-Aldrich, Germany), lactic acid and ammonium acetate (Fisher Bioreagents, Belgium) were used.

Preparation of natural deep eutectic solvent

The mixture of lactic acid and ammonium acetate (3:1) with water was prepared at 60°C with constant mixing for approximately 20 min until a stable transparent liquid was formed. In order to evaporate water from the mixture and to create NADES, the mixture was placed in a rotary evaporator, Heizbad Hei-VAP (Heidolph, Germany) at 60°C, pressure of 50 mbar and rotation speed of 200 rpm for 2 h. Subsequently, NADES was diluted using water (1:1).

Extraction procedures

Maceration

Maceration was performed at 25°C using the incubator shaker KS 4000i control (IKA, Germany) at a solid-to-solvent ratio of 1:30 g/mL, lactic acid+amonium acetate with 50% of water for 60 min.

Heat-assisted extraction

HAE was performed at 80°C using the incubator shaker KS 4000i control (IKA, Germany) at a solid-to-solvent ratio of 1:30 g/mL, lactic acid+amonium acetate with 50% of water for 30 min.

Ultrasound-assisted extraction

UAE was performed using an ultrasound bath, Sonopuls (Bandelin, Germany) at a solid-to-solvent ratio of 1:30 g/mL, lactic acid+amonium acetate with 50% of water for 20 min.

All extracts were prepared in the Erlenmeyer flasks covered by aluminium foil to avoid light exposure and evaporation of water. After the extraction, the samples were filtered using filter paper and stored at 4°C until further analyses.

Determination of total polyphenol content

The total polyphenol content (TPC) was determined spectrophotometrically at 765 nm using the modified Folin-Ciocalteu method [11]. The results are expressed as milligrams of gallic acid equivalents per gram of plant material (mg GAE/g).

Determination of antioxidant capacity (ABTS and DPPH tests)

The ABTS assay was based on the procedure described by Re *et al*. [12] with a slight modification and the absorbance was measured at 734 nm. The antioxidant activity was expressed as mmol Trolox equivalent per g of plant material (mmol TE/g). The DPPH assay was based on the procedure described by Horžić *et al*. [13] with a slight modification and the absorbance was measured at 517 nm. The results were expressed as IC_{50} (mg/mL), defined as the concentration of the extract required to scavenge 50% of DPPH free radicals.

All spectrophotometric measurements were performed in an UV-1800 spectrophotometer (Shimadzu, Japan).

Determination of pH, zeta potential, and conductivity

pH value of the extracts was determined using pH meter HI 2211 (Hanna Instruments, USA). Each sample was measured three times at room temperature.

The measurements of zeta potential and conductivity were performed using photon correlation spectroscopy in Zetasizer Nano Series, Nano ZS (Malvern Instruments Ltd., UK). Each extract was measured three times at room temperature.

Measurement of density, surface tension, and viscosity

The density and surface tension of the extracts were determined using Force Tensiometer K20 (Kruss, Germany). Each extract (20 mL) was examined three times at room temperature.

The viscosity of the extracts was examined using Rotavisc lo-vi device (IKA, Germany). Each extract (6.7 mL) was examined three times at room temperature.

Statistical analysis

The statistical analysis was done by using analysis of variance (one-way ANOVA) and Duncan's *post hoc* test in STATISTICA 7.0. The differences were considered statistically significant at $p<0.05$.

RESULTS AND DISCUSSION

The impact of three extraction procedures (maceration, HAE, and UAE) on TPC, pH, zeta potential, conductivity, density, surface tension, viscosity, and antioxidant capacity of *V. myrtillus* leaf waste extracts prepared using NADES was examined and the results are shown in Table 1.

Table 1 *Total polyphenol content (TPC), antioxidant capacity (ABTS and DPPH tests), pH, zeta potential (ζ), conductivity (G), density (ρ), surface tension (γ), and viscosity (η) of Vaccinium myrtillus leaf waste extracts prepared using maceration, heat- and ultrasound-assisted extractions (HAE and UAE, respectively), and lactic acid+amonium acetate*

Variables	Maceration	HAE	UAE
TPC [mg GAE/g][x]	50.4±0.7[b*]	53.0±0.9[a]	49.5±0.4[b]
ABTS [mmol TE/g][§]	30.2±1.7[c]	38.4±1.1[a]	33.7±1.5[b]
DPPH IC_{50} [mg/mL][£]	6.15±0.06[c]	5.55±0.25[a]	5.99±0.05[b]
pH	1.59±0.03[a]	1.63±0.02[a]	1.66±0.04[a]
ζ [mV]	2.66±0.48[b]	2.57±0.20[b]	3.17±0.13[a]
G [mS/cm]	1.87±0.13[b]	1.84±0.11[b]	2.10±0.11[a]
ρ [g/mL]	1.105±0.009[b]	1.122±0.006[a]	1.117±0.001[a]
γ [mN/m]	23.2±0.8[a]	23.7±0.5[a]	23.5±0.7[a]
η [mPa·s]	5.52±0.10[a]	5.54±0.12[a]	5.50±0.07[a]

[x]GAE, gallic acid equivalents; [§]TE, Trolox equivalents; [£]IC_{50}, concentration required to neutralize 50% of DPPH radicals; [*]values with different letters (a-b) in each row showed statistically significant differences ($p<0.05$; n=3; analysis of variance, Duncan's *post-hoc* test).

As can be seen from Table 1, the TPC was the highest in the extract prepared in HAE (53.0±0.9 mg GAE/g), while the extracts obtained in maceration and UAE possessed significantly lower TPC (50.4±0.7 and 49.5±0.4 mg GAE/g). Therefore, the extraction technique had a statically significant influence on the polyphenol yield that is in agreement with the literature data [5]. Namely, the application of a higher temperature provides better extraction efficiency by disruption of cellular structures, increment of cell membrane permeability, and breakdown of polyphenols-lipoproteins interactions that result in the increase in the solubility and mass transfer of polyphenol compounds [14]. On the other hand, in UAE, there is a potential degradation of polyphenols through the production of free radicals by ultrasound waves. Additionally, the presence of a higher amount of plant particles contributes to the ultrasound waves attenuation and the restriction of their active part [14].

The ABTS radical scavenging capacity was the highest in the extract prepared in HAE (38.4±1.1 μmol TE/g), followed by the extract obtained using UAE (33.7±1.5 μmol TE/g) and maceration (30.2±1.7 μmol TE/g). The DPPH antioxidant potential followed the same trend: HAE>UAE>maceration (5.55±0.25, 5.99±0.05, and 6.15±0.06 mg/mL, respectively). The results of the antioxidant potential of the extracts are in correlation with TFC values which is in agreement with the literature data where the concentration of flavonoids (as a

large group of polyphenols) significantly influenced free radical scavenging of the extracts [15].

pH ranged from 1.59 in macerate to 1.63 and 1.66 in HAE and UAE extracts. The zeta potential was low in all *V. myrtillus* extracts (2.66±0.48 mV for macerate, 2.57±0.20 mV for HAE, and 3.17±0.13 mV for UAE), while the conductivity was in the range of 1.87±0.13 and 1.84±0.11 mS/cm (maceration and HAE) to 2.10±0.11 mS/cm (UAE). Measurement of the zeta potential of herbal extracts is important from the aspect of their further applications, including encapsulation into various carriers and coagulation or flocculation in the treatment of drinking water or wastewater. According to the literature data, plant extracts with a higher conductivity have the better antioxidant potential [16]. However, it was not the case with *V. myrtillus* extracts because ions in the extracts originated from NADES and plant matrix can impact the conductivity without improving their antioxidant potential. Thus, the performing of antioxidant assays is necessary in the case of *V. myrtillus* leaf waste extracts.

The density varied from 1.105±0.009 g/mL for macerate to 1.122±0.006 and 1.117±0.001 g/mL for HAE and UAE extracts. Florindo *et al*. study [17] reported that the density of eutectic solvent strongly depended on its composition and temperature. Therefore, it can explain minor differences between the samples because all extracts contain the same extraction medium and all measurements were performed at room temperature. As can be seen from Table 1, there were no statistically significant differences in the surface tension and viscosity of the extracts (~23.5 mN/m and ~5.5 mPa·s, respectively). Since the used NADES contained 50% of water, all extracts possessed a higher surface tension. Namely, it can be explained by a relatively high interaction of water molecules through hydrogen bonds. The viscosity of eutectic solvents was in the range from 0.05 to 50 mPa·s, whereas their composition and temperature significantly impact the viscosity of the extracts [17,18]. The obtained results of the lower viscosity of *V. myrtillus* leaf waste extracts are expected due to higher water content in NADES because the extract's viscosity is affected by the strength of the hydrogen bonding and van der Walls interactions.

CONCLUSION

The aim of the present study was the physicochemical characterization and investigation of the antioxidant capacity of *V. myrtillus* leaf waste extracts prepared using NADES, as an extraction medium, and maceration, HAE, and UAE. The extract obtained in HAE possessed the highest polyphenol yield and radical scavenging capacity. On the other hand, the extract prepared by ultrasound waves possessed the highest zeta potential (as a predictor of the potential application in water treatment) and conductivity (as a potential predictor of antioxidant capacity). Thus, the extraction technique should be chosen depending on the future application of *V. myrtillus* leaf waste extract.

ACKNOWLEDGEMENT

The authors acknowledge their gratitude to the Ministry of Education, Technological Development and Innovation of Serbia, contract numbers 451-03-47/2023-01/200019, 451-03-47/2023-01/200135, and 451-03-47/2023-01/200026.

REFERENCES

[1] Vrancheva R., Ivanov I., Dincheva I., *et al.*, Plants 10 (2021) 94.

[2] Jensen H. D., Krogfelt K. A., Cornett C., *et al.*, J. Agric. Food Chem. 50 (2002) 6871–6874.

[3] Riihinen K., Jaakola L., Karenlampi S., *et al.*, Food Chem. 110 (2008) 156–160.

[4] Nobre B. P., Gouveia L., Matos P. G. S., *et al.*, Molecules 17 (2012) 8397–8407.

[5] Jovanović A., Đorđević V., Zdunić G., *et al.*, Sep. Purif. Technol. 179 (2017) 369–380.

[6] Vuleta G., Milić J., Savić S., Farmaceutska tehnologija, Faculty of Pharmacy, University of Belgrade, Belgrade (2012) (*in Serbian*).

[7] Chemat F., Abert-Vian M., Fabiano-Tixier A. S., *et al.*, TrAC. 118 (2019) 248–263.

[8] Hikmawanti N. P. E., Ramadon D., Jantan I., *et al.*, Plants 10 (2021) 2091.

[9] Dai Y., van Spronsen J., Witkamp G. J., *et al.*, Anal. Chim. Acta. 766 (2013) 61–68.

[10] Singh P., Singh S., J. Pharm. Innov. 7 (2018) 238–245.

[11] Galván d'Alessandro L. G., Kriaa K., Nikov I., *et al.*, Sep. Purif. Technol. 93 (2012) 42–47.

[12] Re R., Pellegrini N., Proteggente A., *et al.*, Free Radic. Biol. Med. 26 (1999) 1231–1237.

[13] Horžić D., Režek Jambrak A., Belščak-Cvitanović A., *et al.*, Food Bioproc. Tech. 5 (2012) 2858–2870.

[14] Jovanović A., Petrović P., Đordjević V., *et al.*, Lek. sir. 37 (2017) 45–49.

[15] Hirano R., Sasamoto W., Matsumoto A., *et al.*, J. Nutr. Sci. Vitaminol. 47 (2001) 357–362.

[16] Jurinjak Tušek A., Benković M., Valinger D., *et al.*, Ind. Crops Prod. 126 (2018) 449–458.

[17] Florindo C., Oliveira F. S., Rebelo L. P. N., *et al.*, ACS Sustain. Chem. Eng. 2 (2014) 2416–2425.

[18] Abbott A., Boothby D., Capper G., *et al.*, J. Am. Chem. Soc. 126 (2004) 9142–9147.

MORPHOLOGICAL INVESTIGATION OF PVDF/MAGNETITE@NC/$BaTiO_3$ SEMI-SPHERICAL COMPOSITE MATERIALS FOR OIL REMOVAL

Danijela Kovačević[1*], Nenad Đorđević[1], Slađana Glišić[2], Branislav Vlahović[3], Vladimir B. Pavlović[4]

[1]The Academy of Applied Technical Studies Belgrade, Belgrade, SERBIA

[2]University of Belgrade, Faculty of Technology and Metallurgy, Belgrade, SERBIA

[3]North Carolina Central University, Durham, USA

[4]University of Belgrade, Faculty of Agriculture, Department for Physics and Mathematics, Belgrade, SERBIA

[*]*dkovacevic@atssb.edu.rs*

Abstract

The aim of this research has been morphological investigation of new semi-spherical composite structures for potential use in oil removal. Piezoelectric matrix polyvinylidene fluoride (PVDF) has been filled with $BaTiO_3$ and magnetite/nanocellulose (NC) composites with different NC loadings and hydrophobic semi-spherical structures have been obtained by drop casting method. Detailed SEM and EDS investigation of the prepared composite structures, depending on the NC loadings, has been conducted. SEM micrographs revealed variation in morphology and microfibrils formation of samples having different amount of NC. Sample containing 8 wt.% of NC (highest content) showed most uniform filler distribution, based on EDS mapping.

Keywords: PVDF, composites, nanocelullose, EDS, SEM.

INTRODUCTION

The piezoelectric polymer PVDF have shown promising features in the area of oil/water separation, oil absorption, ultrafiltration and recovery. The superhydrophobic features and reusability distinguish PVDF as an excellent candidate for oil separation and oil absorption whether the polymer itself is used or in the form of composite/hybrid materials with organic/inorganic fillers [1]. The main benefit of hydrophobic PVDF membranes use for oil removal is that enables oil permeation at almost zero pressure [2]. Superhydrophobic and superoleophilic PVDF aerogels have been fabricated for oil/water separation and rapid oil absorption. The PVDF aerogel showed moderate oil absorption capacity and oil–water separation was achieved in the case of surfactant-free and as well in surfactant-stabilized water-oil emulsions [1]. Beside aerogels, PVDF foams also demonstrated high potential for oil/solvent recovery [3].

PVDF composite material having organic/inorganic fillers also demonstrated excellent properties in oil removal from water/solvent-oil mixtures and emulsions. The group of authors synthesized exceptionally porous PVDF modified with expanded graphite able to achieve oil absorption of up to 12 g/g and showed excellent reusability [4]. Nano silicon carbide (SiC) was used for modification of foamed PVDF and resulting material demonstrated

superhydrophobic characteristics. PVDF/SiC foam achieved the maximum absorption capacity of 21.5 times of its original weight and high oil/solvent absorption [5]. PVDF/barium titanate (PVDF/$BaTiO_3$) composite material has been reported for ultrafiltration of oily bilge water. The authors prepared piezoelectric membrane and used alternating current (AC) signal in order to prevent membrane fouling. The results indicated that oil concentration in outflow was below 14 ppm [6]. Two different membranes containing PVDF as a matrix polymer have been produced by phase inversion process [7,8]. In the first case, the iron alkoxide was a novel pore-forming additive (PFA) used in production of the high porosity PVDF membranes. The best performance in oil removal from a surfactant-stabilized oil-water emulsion demonstrated untreated PVDF/PFA membranes [7]. In the second paper, Yi *at al.* [8] fabricated TiO_2/Al_2O_3/PVDF ultrafiltration membranes and studied adsorption mechanism in oil emulsion-membrane system.

In some recent studies, magnetite has shown its effectiveness in oil separation and recovery. Magnetite (Fe_3O_4) functionalized with silica was used for preparation of magnetic demulsifier (MD) which effectively recovered oil from oil-water emulsion [9]. The superhydrophobic magnetic cellulose sponge (SMCE) has been successfully used for separation of oil in water-oil mixtures (surfactant free) and as well as in surfactant-stabilized water-oil emulsions. The authors reported that magnetite deposited on the cellulose also contributed to increased roughness of the SMCE surface [10].

The aim of this study was and morphological and elemental characterization of PVDF based inorganic/organic hybrid material for implementation in the field of oil adsorption. The detailed investigation of magnetite/nanocellulose (NC) composites was conducted and already presented [11]. This study is directed toward morphological properties and elemental composition (distribution) of PVDF/magnetite@NC/$BaTiO_3$ semi-spherical composite material. The SEM and EDS analysis of samples having different content of NC will be shown.

MATERIALS AND METHODS

Materials

Nanocellulose was obtained from commercially available cellulose. The solvents, acetone and N,N-dimethylformamide (DMF) were purchased from Sigma-Aldrich, while $FeSO_4 \cdot 7H_2O$ and $FeCl_3 \cdot 6H_2O$ were purchased from Merck NC washing, aqueous solution preparation, and dishwashing were all done with deionized water (DW) with a resistivity of 18 MΩ cm.

Preparation of PVDF/magnetite@NC/$BaTiO_3$ semi-spherical composite

Preparation of NC/Fe_3O_4 has been detailed described in ours previous publication [11]. Preparation of PVDF/magnetite@NC/$BaTiO_3$ was conducted by dissolution of PVDF in a mixture of acetone/DMF (1:1) in order to obtain 20 wt.% solution of polymer. $BaTiO_3$ was sonicated in DMF for 30 min, and subsequently added to the dissolved PVDF in an amount of 4 wt.% with respect to the polymer content and this mixture was stirred for 6h. Nanocelulose/magnetite composites, with different content of NC, were dispersed by sonication in DMF for 30 min and added to PVDF/$BaTiO_3$ mixture, resulting in a composite with four different concentrations of NC. Samples used in this study: SNC1 with 1 wt.% of

NC, SNC2 with 2 wt.% of NC, SNC4 having 4 wt.% of NC and SNC8 with 8 wt.% of NC) The concentrations of $BaTiO_3$ (4 wt.%) and Fe_3O_4 (4 wt.%) have remained the same during the experiment. The semi-spherical structure have been prepared by solution casting technique directly in to the water. The micropipette containing 30 µl of composite material was placed above glass container (250 ml DI water) and composite poured directly in to the water. Semi-spherical structures with the edges curled inwards were then separated from the water and dried for 5 days at room temperature and 8 h at 60 ºC in a vacuum oven.

Characterisation of PVDF/magnetite@NC/$BaTiO_3$ semi-spherical composite

The morphological properties of semi-spherical composite structures was investigated by scanning electron microscopy (SEM, Tokyo, Japan, model: JEOL JSM 6610LV) equipped with energy dispersive X-ray analysis (EDS).

RESULTS AND DISCUSSION

The Figure 1 presents SEM micrographs of the inside and the curled edges forming microfibrils of semi-spherical composite samples with different content of NC.

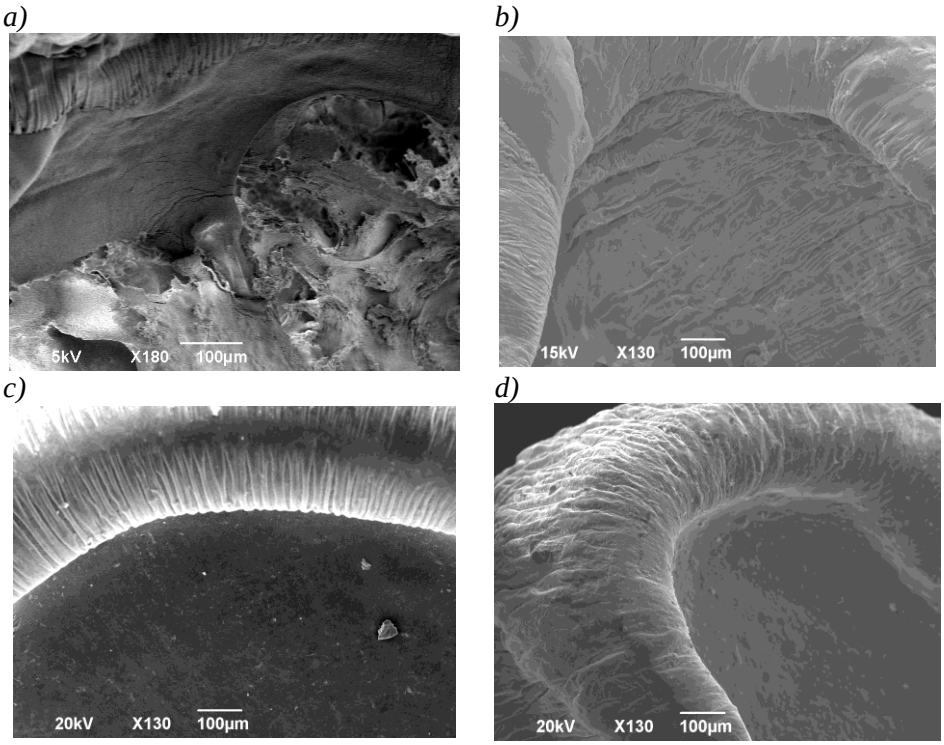

Figure 1 *SEM micrographs of the composite samples with different content of NC: a) SNC1; b) SNC2; c) SNC4; d) SNC8*

The samples having lowest content of NC (SNC1) demonstrated porous rough structure of the inside, while the curled edges with microfibrils formation, to a certain extent resemble to the remaining three samples. In addition, partially rough fibrous inner structure can be observed in the case of the sample SNC2, while the semi-spherical composite samples with higher content of NC–SNC4 and SNC8 have a smooth inner surface in combination with curled edges of a semi-sphere.

The elemental composition of all four samples has been investigated in order to get inside in the filler distribution across PVDF matrix. The results of EDS mapping are presented on the Figures 2–5. It can be observed the uniform distribution of Fe_3O_4 on the surface of composite sample SNC1 (Figure 2a), while the agglomeration of $BaTiO_3$ on the edges of the wrinkle microfibril structures occurs. The EDS spectra of the selected (distinctive) area are presented on the Figure 2b.

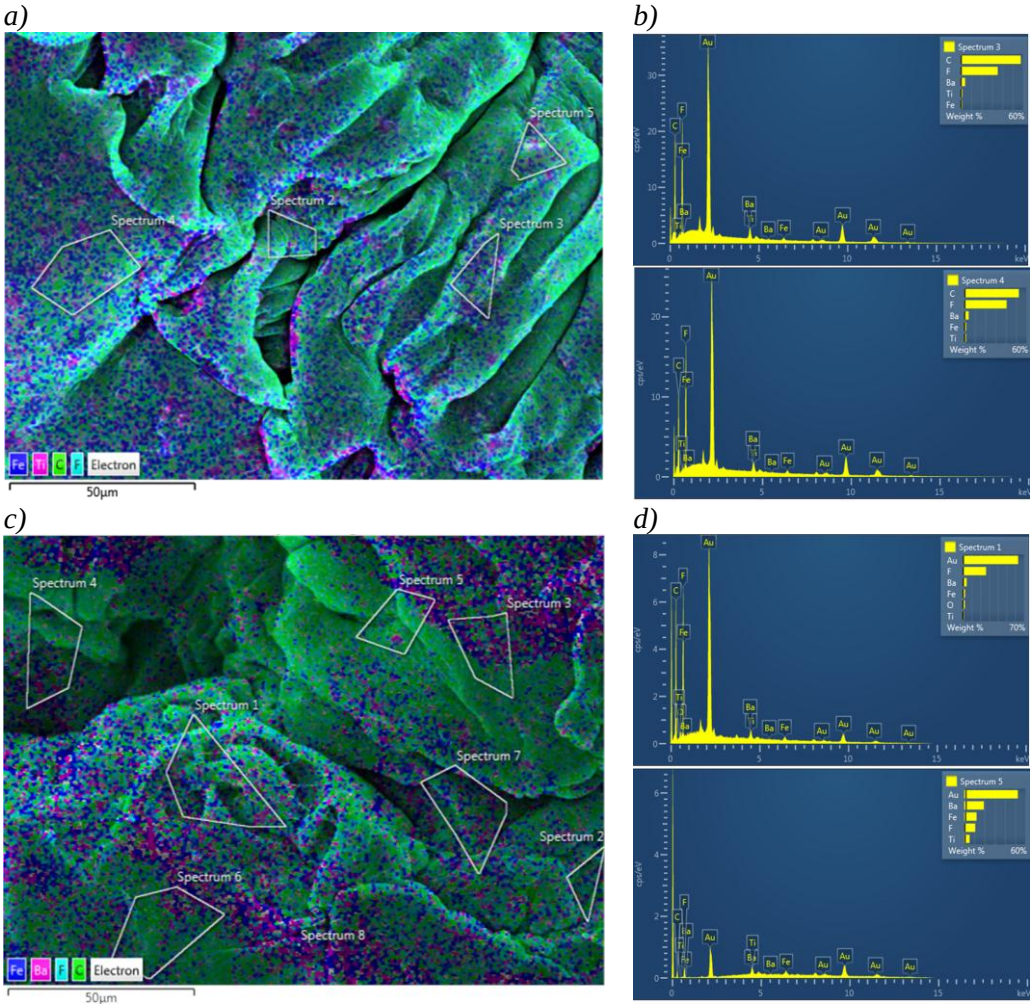

Figure 3 *a) EDS mapping of SNC2 and b) EDS spectrum of the selected areas*

Furthermore, increased amount of NC to 2 wt.% (Figure 3) contributed to more uniform distribution of $BaTiO_3$ even though it is not the most uniform distribution across the polymer surface, considering the existence of the regions with a lower or higher filler concentration. The following sample (SNC4) shows extremely high concentrations of both fillers ($BaTiO_3$ and NC/magnetite) in a certain areas, indicating the lowest degree of filler dispersion. In some areas, agglomeration of $BaTiO_3$ prevails (Figure 4).

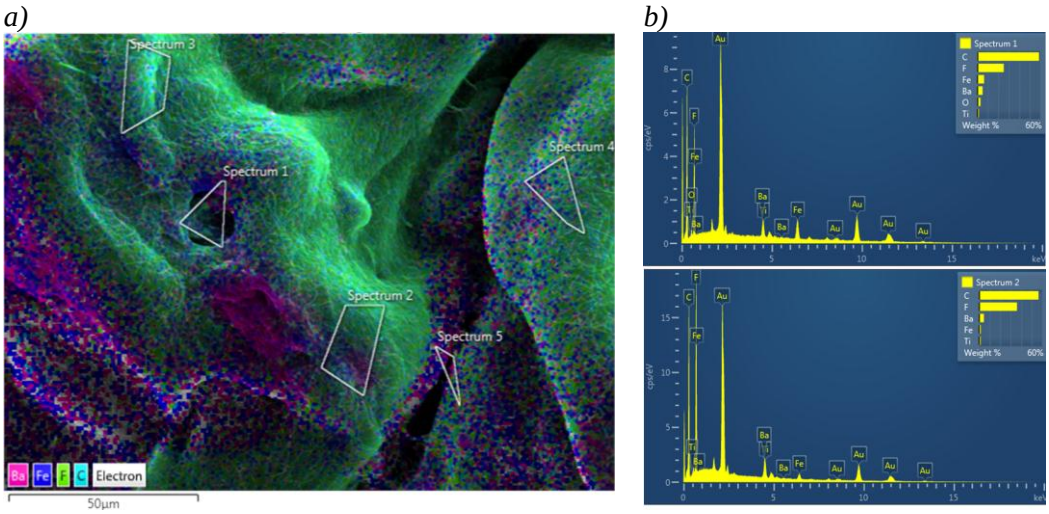

Figure 4 *a) EDS mapping of SNC4 and b) EDS spectrum of the selected areas*

The sample with higest content of NC (8 wt.%) demonstrated the most uniform distribution of $BaTiO_3$ and NC/magnetite inside PVDF matrix (Figure 5). It turned out to be the most optimal content of NC for synthesis of composite in a semi-spherical form according to the EDS mapping.

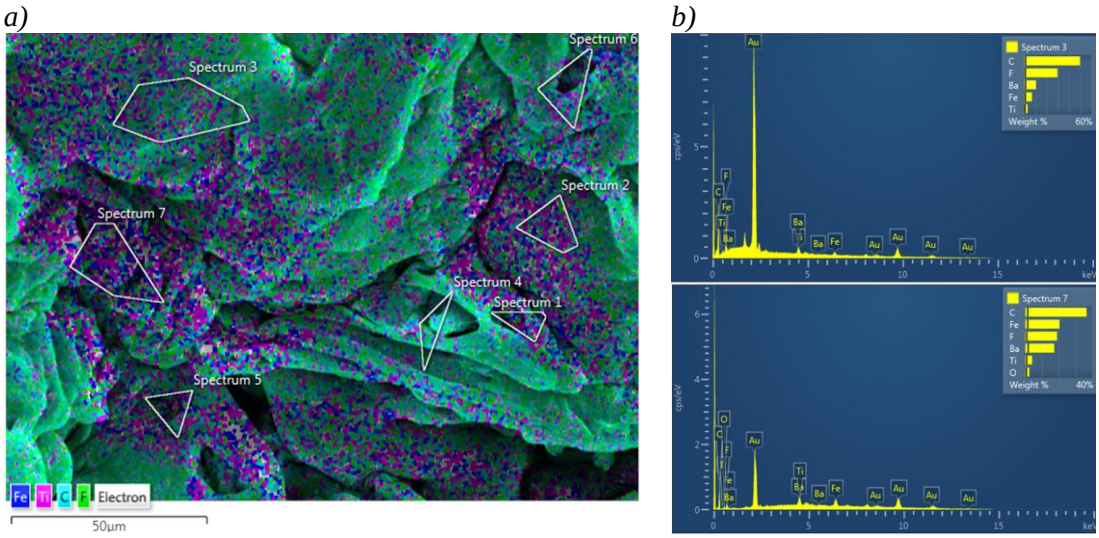

Figure 5 *a) EDS mapping of SNC8 and b) EDS spectrum of the selected areas*

CONCLUSION

The presented study investigated influence of nanocellulose content on morphological properties of polyvinylidene fluoride/$BaTiO_3$/magnetite/nanocellulose composite material prepared in a specific semi-spherical form. Variation of morphological properties and filler dispersion in PVDF matrix showed dependence on the nanocellulose amount. The highest degree of filler agglomeration has been noticed in the case of composite having 4 wt.% of NC, while it is the most optimal distribution observed in a composite sample containing 8 wt.% of nanocellulose.

ACKNOWLEDGEMENT

The research was funded by the Ministry of Science, Technological Development and Innovation of the Republic of Serbia (Record numbers: 451-03-47/2023-01/200105; 451-03-47/2023-01/200116), US National Science Foundation (Grant: DMR EiR 2101041, NSF DMR PREM 2122044) and US Department of Energy/National Nuclear Security Administration (Grant: NA0003979).

REFERENCES

[1] Chen X., Liang Y. N., Tang X.-Z., *et al*., Chem. Eng. J. 08 (2017) 18–26.

[2] Kong J., Li K., Sep. Purif. Technol. 16 (1999) 83–93.

[3] Udayakumar K. V., Gore P. M., Kandasubramanian B., Chem. Eng. J. Adv. 5 (2021) 100076.

[4] Bentini R., Pola A., Rizzi L.G., *et al*., Chem. Eng. J. 372 (2019) 1174–1182.

[5] Arora R., Balasubramanian K., RSC Adv (4) (2014) 53761–53767.

[6] Tana Z., Chen S., Mao X., *et al*., Water. Sci. Technol. 85 (10) (2022) 2980–2992.

[7] Muthukumar K., Kaleekkal N. J., Shanthana Lakshmi D., *et al*., J. Appl. Polym. Sci. 136 (24) (2019) 47641.

[8] Yi X., Zhu Y., Wang D., *et al*., Langmuir 34 (34) (2018) 9907–9916.

[9] Faisal Elmobarak W., Almomani F., Chemosphere 265 (2021) 129054.

[10] Peng H., Wang H., Wu J., *et al*., Ind. Eng. Chem. Res. 55 (3) (2016) 832–838.

[11] Janićijević A., Pavlović V. P., Kovačević D., *et al*., Polymers 14 (9) (2022) 1819.

DEGRADATION OF PHENOL AND SUBSTITUTED PHENOLS: INFLUENCE OF APPLIED POTENTIAL

Branislava Savić[1*], Danka Aćimović[1], Marija Ječmenica Dučić[1], Marija Simić[1], Dragana Vasić Anićijević[1], Tanja Brdarić[1]

[1]Vinča Institute of Nuclear Sciences-National Institute of the Republic of Serbia, Department of Physical Chemistry, University of Belgrade, Mike Petrovića Alasa 12–14, 11001 Belgrade, SERBIA

[*]*branislava@vin.bg.ac.rs*

Abstract

This study investigates the influence of the applied potential (2.3 V and 3.0 V) during electrochemical oxidation using PbO_2-GNR anode on the efficiency of phenol and substituted phenols degradation in base media, as well as on the electricity consumption and the profitability of the process. It can be noted that with an increase in potential, there is an improvement in the efficiency of the electrolytic degradation process and the electricity consumption grows. However, the profitability of the electrochemical treatment, apart from the applied potential, also depends on the duration of the process and its efficiency.

Keywords: phenols, electrooxidation, applied potential.

INTRODUCTION

Direct or indirect discharge of wastewater from industry or households into water bodies leads to pollution of watercourses with phenolic compounds. One of the most important characteristics of pollution prevention is the detection and determination of phenolic compounds in wastewater in very low concentrations. Developing appropriate techniques for the effective removal of these compounds will not only eliminate problems of negative consequences for the environment but also problems directly related to population health. Phenols have a peroxidative capacity, they are hepatotoxic and hepatotoxic, and they can cause mutagenesis and carcinogenesis in humans and other living organisms.

Various researches are conducted in order to develop techniques for reducing and eliminating phenolic compounds from wastewater. Electrochemical anodic oxidation is one of the advanced techniques for removing phenolic compounds from wastewater.

In recent years, more attention is paid to the synthesis of new materials that will increase the efficiency of electrochemical degradation. An important class of potential materials for the degradation of organic chemicals from wastewater are nanostructured materials, including metal, metal oxides, and metal-organic composites [1,2].

Lead-based oxides have long been known as an anode material for the oxidation of organic compounds in wastewater, especially with the addition of different forms of graphene. Among others, many different processes have been developed for the synthesis of graphene

nanoribbons (GNRs) [3]. It has been proven that PbO_2-GNR is a good anode material for the degradation of phenol and its compounds in a base environment [4].

The aim of the presented research is to investigate the influence of the applied potential (2.3 V and 3.0 V) during electrochemical oxidation using PbO_2-GNR anode on the efficiency of phenol and substituted phenols degradation in base media, as well as on the electricity consumption and the profitability of the process. The phenols studied in the work were selected based on the frequency of detection in wastewater samples.

MATERIALS AND METHODS

Preparation of nanocomposite

The PbO_2-GNR nanocomposite was get by mixing synthesized PbO_2 nanoparticles, obtained by the hydrothermal method using synthesized PbO nanoparticles [5] with GNR (commercial) in a ratio of 3:1 (v/v%) on a magnetic stirrer for 3 hours.

Electrode modification

Stainless steel electrodes were washed (acetone, ethanol, deionized water) and 30 min dried at room temperature. PbO_2-GNRs nanocomposites were dispersed in dimethylformamide (Sigma-Aldrich) by sonification for 2 h (5 mg mL^{-1}) and were dripped onto a stainless steel electrode [6].

Electrooxidation of phenol compounds

Electrolytic oxidation was performed in a closed, undivided, thermostated cell with two electrodes. A stainless steel electrode was used as the counter electrode. The modified steel electrode with PbO_2-GNR had the function of working electrode. The experiments were performed at room temperature, 25 ± 1 °C. Electrodes with an area of 2 cm^2 (dimensions 1x2 cm) are placed in the electrolytic cell in a vertical plane, parallel to each other at a fixed distance of 2 cm.

RESULTS AND DISCUSSION

Effect of potential change on the degradation of phenol and substituted phenols

A comparative presentation of phenol and phenolic compounds degradation efficiency during anodic electrooxidation at potentials of 2.3 V and 3.0 V is given in Figure 1. In accordance with literature data, with the increase in electrolysis time, the efficiency of degradation also enhances at a potential of 2.3 V, as well as at 3.0 V [4]. By comparing degradation efficiency at different applied potentials, it can be noted, when potential is rising, electrolytic degradation efficiency of individual phenolic compounds increases. After 60 min of electrolysis at a potential of 2.3 and 3.0 V, efficiency of degradation is substantially better at higher potential, and amounts to about 80%. Based on the results presented in Figure 1, it can be seen that the biggest difference in efficiency is for phenol (about 10 times), and the smallest for 2,4-dimethyl phenol (about 2.6 times). Even if the electrolysis time is extended to 300 minutes at a lower potential of 2.3 V, the obtained results are still deficient compared to a shorter electrolysis at a higher potential.

A drastic jump in efficiency by applied potential of 3.0 V can be explained by the fact that with an increase in potential, the speed of the chemical reaction grows as well as the mobility of electroactive species in the electrolytic system, thus accelerating the electrochemical process of anodic oxidation.

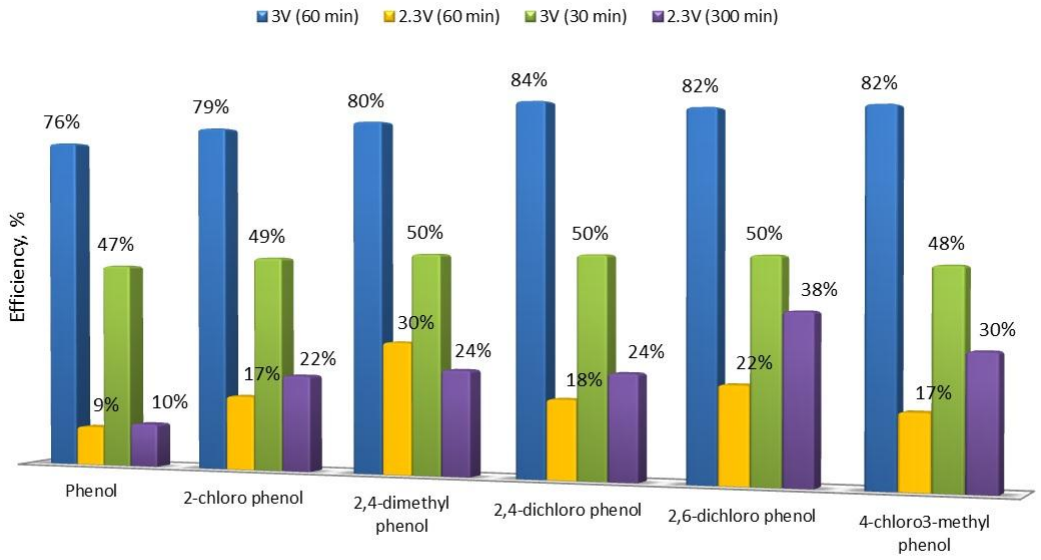

Figure 1 *Comparative presentation of the degradation efficiency of phenolic compounds at potentials of 2.3 V and 3.0 V*

Electricity consumption

The main economic problem is the consumption of electricity during the electrochemical decomposition of pollutants. The electricity consumption (E) during electrochemical oxidation of phenol and phenolic compounds was calculated by following equation (1):

$$E = \frac{V \cdot I \cdot t_E}{V_S} \cdot 10^{-3} \quad (1)$$

where E is electricity consumption (kWh m^{-3}), V is applied potential (V), I is electrical current (A), t_E is time of electrochemical treatment and V_S represents volume of treated solution [7].

Considering the average price of kWh in Serbia (0.103 €), cost of electrochemical treatment with PbO_2-GNR electrode at a potential of 2.3 V and 3.0 V, is 0.019 € and 0.025 € for m^3 of treated solution, respectively.

Overall, for the complete decontamination of wastewater polluted by phenolic compounds using electrochemical treatment, under a constant depletion of pollutan concentration, the consumption of electricity at 2.3 V would amount to 0.864 kWh m^{-3} and it would be necessary to allocate 0.09 € per m^3 of treated solution, while at a potential of 3.0 V electricity consumption is 0.313 kWh m^{-3}, i.e. the price is 0.03 € per m^3 of treated solution (Table 1).

Table 1 *Overview of electricity consumption during electrochemical treatment at different potentials*

U (V)	E(kWh m^{-3}), after 60 min	E(kWh m^{-3}), complete treatment	Cost (€ m^{-3})	jo (A cm^{-2})
2.3	0.19	0.86	0.09	$5.12 \cdot 10^{-8}$
3.0	0.25	0.31	0.03	$6.88 \cdot 10^{-8}$

Base on these findings, it turns out that the more profitable electrochemical treatment is at a higher potential due to greater efficiency, which is also reflected in the shorter duration of the treatment.

Also, electricity consumption during the electrochemical treatment using PbO_2-based anode material was proven to be lower compared to the values obtained by Li *et al*. [8].

CONCLUSION

The obtained results imply that with an increase in the potential, there is an improvement in the efficiency of the degradation of phenol and substituted phenols. Also, an increase in electricity consumption can be observed with a rise of the applied potential. Based on the presented results, it is concluded that the profitability of the electrochemical treatment, apart from the applied potential, also depends on the duration of the process and its efficiency.

ACKNOWLEDGEMENT

The authors would like to thank the Ministry of Science, Technological Development and Innovation of the Republic of Serbia for the financial support to the research through institutional funding (Contract number 451-03-47/2023-01/ 200017).

REFERENCES

[1] Reddy C., Reddy I., Harish V., *et al*., Chemosphere 239 (2020) 124766.

[2] Shetti N., Malode S., Nayak D., *et al*., Appl. Surf. Sci. 496 (2019) 143656.

[3] Higginbotham A, Kosynkin D., Sinitskii A., *et al*., ACS Nano 4 (4) (2010) 2059–2069.

[4] Savić B., Stanković D., Živković S., *et al*., Appl. Surf. Sci. 529 (2020) 147120.

[5] Alagar M., Theivasanthi T., Raja A., J. Appl. Sci. 12 (2012) 398–401.

[6] Stanković D., Ognjanović M., Espinosa A., *et al*., Electrocatalysis 10 (2019) 663–671.

[7] Kariyajjanavar P., Jogttappa N., Nayaka Y., J. Hazard. Mater. 190 (2011) 952–961.

[8] Li J., Li M., Li D., *et al*., Chemosphere 248 (2020) 126021.

30th International Conference Ecological Truth & Environmental Research
20–23 June 2023, Serbia

DEGRADATION OF DYES MIXTURE BY ELECTROCHEMICAL OXIDATION USING STAINLESS STEEL ELECTRODE

Marija Ječmenica Dučić[1*], Danka Aćimović[1], Branislava Savić[1], Marija Simić[1], Aleksandar Krstić[1], Dragana Vasić Anićijević[1], Tanja Brdarić[1]

[1]Vinča Institute of Nuclear Sciences-National Institute of the Republic of Serbia, Department of Physical Chemistry, University of Belgrade, Mike Petrovića Alasa 12-14, 11001 Belgrade, SERBIA

[*]*marija.jecmenica@vin.bg.ac.rs*

Abstract

This paper presents the impact of current density on the degradation efficiency of a dyes mixture (bromocresol green, cresol red and thymol blue) by electrochemical oxidation on stainless steel electrodes. The electrochemical oxidation was performed in galvanostatic mode applying current densities of 10 and 30 mA/cm^2 in 0.1 M Na_2SO_4. Experimental results have shown that the degradation efficiency elevated with increasing of applied current density and electrolysis time. After 170 minutes of electrolysis, the degradation efficiency was 30% and 85% on current densities 10 and 30 mA/cm^2, respectively. The degradation of the dyes mixture fitted well with the pseudo-zero-order kinetics.

Keywords: electrooxidation, degradation, due mixture.

INTRODUCTION

Due to extensive use in many fields of everyday life organic dyes can be introduced into the aqueous system from various sources such as municipal wastes, agricultural runoff, and industrial effluent. Their persistence in the environment, recalcitrant nature, toxicity, and stability to natural decomposition make of them a potential environmental pollutant which has a great negative impact on living organisms. Therefore, the implementation and development of technologies for degradation and detoxification of wastewaters polluted with organic dye could have a substantial environmental significance in recent years. Some of the processes proved effective in the treatment of high due concentration in aqueous solutions are precipitation, ion exchange [1], adsorption on various supports [2] and photocatalytic oxidation [3,4]. Electrochemical methods including electrochemical oxidation also have been successful in efficient treatment of dyes [5,6]. Anodic material has a great influence on the efficiency of the electrochemical process, as well as on the mechanism of degradation of organic pollutants [7,8]. Low oxidation power anodes such as carbon, graphite or platinum partially oxidize the organic pollutants. On the contrary, anodes with metallic oxide coating of PbO_2, SnO_2–Sb_2O_3, and SnO_2–Sb_2O_4 are known to oxidize organic molecules totally to CO_2 and water.

In this work, we present results for the electrochemical degradation of dyes mixtures which were treated in the electrochemical cell using stainless steel electrodes. We were investigated

the effect of different parameters on efficiency, like: the influence of applied current density and electrolysis time on the degradation rate.

MATERIALS AND METHODS

Preparation of Dyes Mixture Solution

For the electrochemical degradation of the dyes mixture, following colors were selected: bromocresol green (BCG), cresol red (CR), and thymol blue (TB). The indicator dyes in the form of powder were dissolved in 0.1 M Na_2SO_4, and the final concentration of dyes mixture was 15 ppm. For each dye in the mixture solution, mass concentration has been equally represented (5ppm).

Degradation of dyes mixture was carried out in a two-electrode electrolytic cell, where stainless steel electrodes were used both as working and counter electrodes. The area of each stainless steel electrode was 2 cm^2 (1 x 2 cm). The starting electrolyte was 15 ppm dyes mixture in 0.1 M Na_2SO_4, volume 60 mL. Electrooxidative oxidation was performed in the chronopotentiostatic regime, at constant current densities of 10 and 30 mA/cm^2 for 6 hours at room temperature. The device used for these set of experiments is Gamry Instrument-Interface 1000 Potentiostat/Galvanostat/ ZRA06230.

Degradation of dyes mixture solution

In order to confirm oxidation of dyes in aqueous solutions and to define the potential range in which oxidation occurs, a preliminary chronopotentiostatic experiments were done at current density of 10 mA/cm^2 for 150 minutes on 15 ppm dyes mixtures in 0.1 M $NaSO_4$. The degradation of the solution during electrolysis was monitored using a UV-Vis spectrophotometer Lambda 35 (Perkin Elmer, Waltham, MA, USA). The absorption spectra were recorded in the range of 200–700 nm, while the maximum absorbance peak (at 615 nm) was used to track the degradation of the dyes mixture. Along with the degradation process, mineralization of dyes was monitored by the abatement of total organic carbon (TOC) and measured on a TOC-LCPH analyzer (Shimadzu Co., Kyoto, Japan).

RESULTS AND DISCUSSION

The applied current density on electrolytes plays an important role in the process of electrochemical degradation of organic pollutants. Spectroscopic studies presented on Figure 1 indicate that electrochemical oxidation is a promising technology for the treatment of sulfate-based wastewaters.

The absorption spectrum of the dye mixture has two absorbance peaks positioned at 450 and 615 nm and isosbestic point at 420 nm which is better defined at 10 mA cm^{-2} current density. By increasing the electrolysis time, the peaks reduce in intensity suggesting the supposed degradation occurs. Due to the proximity of isosbestic point to the absorbance peak at 450 nm, quantitative tracking of process degradation is not reliable. Therefore, absorbance peak (at 615 nm) was used for quantitative tracking of dyes mixture degradation.

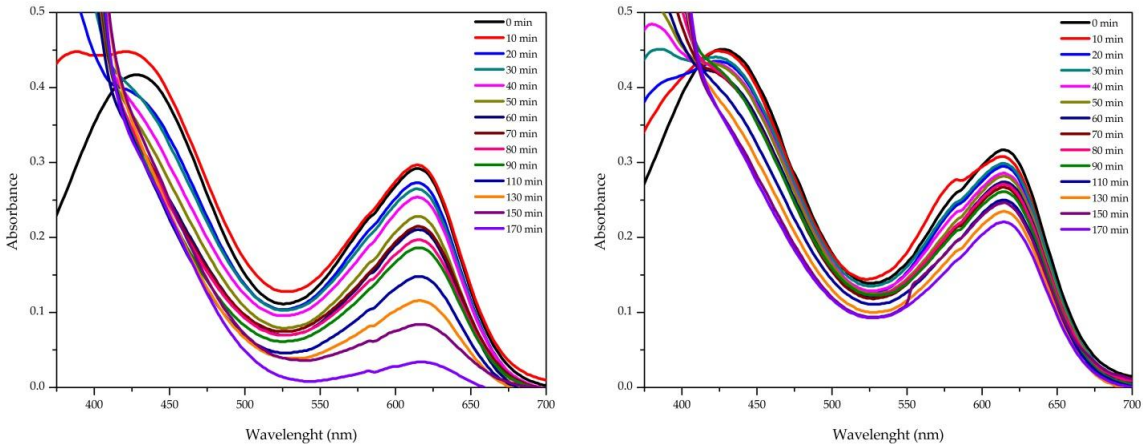

Figure 1 *UV-Vis absorption spectra of the electrolyzed solutions (15 ppm dyes mixture in 0.1 M Na_2SO_4) at current densities of 30 mA cm^{-2} (left) and 10 mA cm^{-2} (right)*

Figure 2 shows the degradation efficiency of 15 ppm dyes mixture on stainless steel electrode at applied current densities of 10 and 30 mA cm^{-2}. As expected, with increasing of applied current density, the degradation efficiency improves. After 170 minutes of electrolysis process the degradation efficiency on current densities of 10 and 30 mA cm^{-2} was 30% and 85%, respectively.

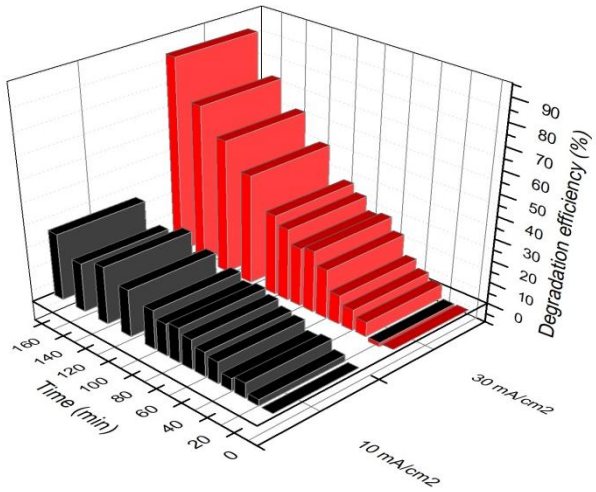

Figure 2 *The degradation efficiency of 15 ppm dyes mixture*

These results can be explained by increased production of reactive hydroxyl radicals (•OH) at higher current densities. Generally, oxidation of water, oxygen evolution, electrooxidation, and electropolymerization of organic compounds can occur at the anode surface during the electrolysis process. The electrooxidation of organics is associated with the oxidation of water and the production of hydroxyl radicals on the anode surface. Previous research by Panizza [8], had explained the role of hydroxyl radicals in organic wastewater treatment. Accordingly, the electrodes with lower oxygen evolution potential, such as stainless steel electrodes, have higher electrocatalytic activity for the oxygen evolution reaction and have "active" behavior for the oxidation of organic pollutants. Therefore organic molecules has been degraded via

•OH which is produced by the oxidation of water molecules. Due to strong interaction of •OH with the surface of "active" electrodes higher oxides or superoxides-MO are produced, which further oxidizes organic pollutants-R (Eqs. (1)–(2)):

$$M(\bullet OH) \rightarrow MO + H^+ + e^- \quad (1)$$

$$MO + R \rightarrow M + RO \quad (2)$$

Thus, a higher concentration of OH radicals at greater current densities at the same electrolysis time contributes to improvement of degradation efficiency. On the other hand, the lower percentage of mineralization (TOC about 30%) is an additional confirmation of the proposed mechanism.

The degree of mineralization is changed poorly with the increase of current density from 10 to 30 mA cm^{-2} (only 1-2%). This is consistent with what has been found in previous studies by Feng and Li [9], who demonstrated that current density has no effect on the reduction of TOC upon phenol electrooxidation. Additionally, dyes degradation efficiency is constant with a further increase of electrolysis time, probably due to the electropolymerization of the electrode surface by phenol-like compounds and their oxidation products which are blocking the surface of anode.

The kinetics rate constant of the due degradation process, k, followed the pseudo-zero-order reaction (see Figure 3). The k values were $5.73 \cdot 10^{-8}$ and $1.43 \cdot 10^{-7}$ mol dm^{-3} min^{-1} at the current densities of 10 and 30 mA cm^{-2}, respectively. Due to higher current density, production of OH radicals is greater, which directly affects the increase in the k value.

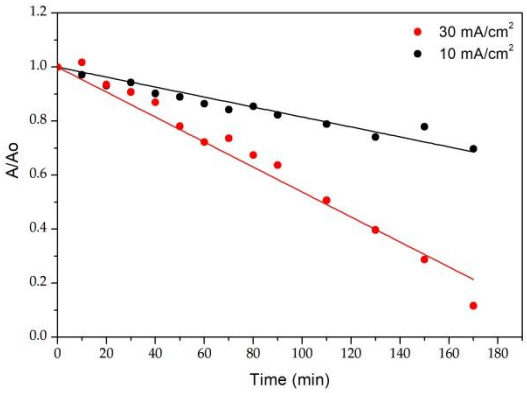

Figure 3 *Linear fits of 15 ppm dyes mixture degradation rate at stainless steel electrode to pseudo-zero-order kinetics 30 mA cm^{-2} and 10 mA cm^{-2}*

CONCLUSION

Stainless steel electrodes were applied for electrochemical degradation of a dyes mixture in aqueous solution. Particularly, the results indicated that the current density is an important factor and has a significant effect on the electrochemical oxidation efficiency. These results

provide a starting point for further research related to the electrochemical degradation of various pollutants including organic molecules on anode materials.

ACKNOWLEDGEMENT

The authors would like to thank the Ministry of Science, Technological Development and Innovation of the Republic of Serbia for the financial support to the research through institutional funding (Contract number 451-03-47/2023-01/ 200017).

REFERENCES

[1] Yang Y., Ladish C., Ladish M. R., J. Microb. Tech. 10 (1988) 632–636.

[2] Specchiar V., Ruggeri B., Gianetto, Chem. Eng. Comm. 68 (1988) 99–117.

[3] Seraghni N., Dekkiche B. A., Debbache N., *et al*., J. Photochem. Photobiol. A. Chem. 420 (2021) 113485.

[4] Hankarea P. P., Patil R. P., Jadhava A. V., *et al*., Appl. Catal. B: Environ. 107 (3–4) (2011) 333–339.

[5] Mahmoudian F., Nabizadeh Chianeh F., Sajjadi S. M., J. Electroanal. Chem. 884 (2021) 115066.

[6] Ječmenica Dučić M., Krstić A., Zdolšek N., *et al*., Crystals 13 (1) (2023) 125.

[7] Kapalka A., Fóti G., Comninellis C., Basic Principles of the Electrochemical Mineralization of Organic Pollutants for Wastewater Treatment. In Electrochemistry for the Environment, Comninellis C., Chen G., Springer, New York (2010), p. 1–23, ISBN: 978-0-387-68318-8.

[8] Panizza M., Importance of Electrode Material in the Electrochemical Treatment of Wastewater Containing Organic Pollutants. In Electrochemistry for the Environment, Comninellis C., Chen G., Springer, New York (2010), p. 25–54, ISBN: 978-0-387-68318-8.

[9] Feng Y. J., Li X. Y., Water Res. 37 (10) (2003) 2399–2407.

THE OXYGEN EVOLUTION REACTION AT TIN DIOXIDE-CARBON-BASED ELECTRODES

Marija Simić[1*], Danka Aćimović[1], Branislava Savić[1], Marija Ječmenica Dučić[1], Ivana Perović[1], Dragana Vasić Anićijević[1], Tanja Brdarić[1]

[1]Vinča Institute of Nuclear Sciences-National Institute of the Republic of Serbia, Department of Physical Chemistry, University of Belgrade, Mike Petrovića Alasa 12–14,

11001 Belgrade, SERBIA

[*]*marija.simic@vin.bg.ac.rs*

Abstract

This study presents the effect of pH and the modification of the SnO_2 electrode with multiwall carbon nanotubes on the kinetic parameters of the oxygen evolution reaction (OER) in sodium sulfate electrolyte. Linear sweep voltammetry (LSV) and Tafel plots analysis were used to determine kinetic parameters (Tafel slopes, exchange current density (j_0), and the potential for OER). Obtained results indicate that the potential for OER are higher with decreasing of medium pH values. Also, compared to the pure SnO_2 electrode, the carbon-based modified SnO_2 electrode showed a slightly change in electrocatalytic activity to the OER.

Keywords: OER, SnO_2 electrode, MWCNT.

INTRODUCTION

The oxygen evolution reaction (OER) is a crucial anode reaction that turned out to be significant for the development and implementation of energy conversion and storage technologies as well as for environmental technologies related to the wastewater treatment.

The electrocatalysts with low overpotentials for OER like RuO_2 and IrO_2 [1,2] are most efficient in water splitting, fuel cells, dinitrogen/carbon dioxide fixation, and metal-air batteries. On the other hand, due to favoring of the total mineralization of the organic compounds to CO_2 and H_2O, anodes with high overpotential for OER (i.e., anodes that are poor catalysts for the OER), are ideal for wastewater treatment by electrochemical oxidation.

Tin dioxide (SnO_2) is an n-type semiconducting nanomaterial, inexpensive and non-toxic. The literature review [3] showed that SnO_2 electrodes are typical examples of electrodes with high overpotential for OER (1.9 to 2.2 V vs. SHE depending of pH) and it is ideal anode material for use in electrochemical oxidation purification technology. However, applications of pure SnO_2 in the field of electrochemical oxidation technology are restricted by its poor electric conductivity and instability of electrodes. This problem can be overcomed by doping with carbon-based nanomaterial [4].

Because of combination of large surface area, high electrical conductivity and good stability, carbon materials are most widely used as supports in electrocatalysis, for example,

in fuel cell applications. At the same time, on the high potentials OER can occur and carbon will be oxidized to CO_2, which makes it inconvenient as a catalyst support.

The aim of this work is to estimate the influence of pH on the potential for OER on SnO_2 electrodes, to determine and compare the basic kinetic parameters for OER on SnO_2 and SnO_2-MWCNT anodes in base medium, at pH 11. The results can be useful as the proposal for using SnO_2-MWCNT electrodes in energy conversion and storage technologies or in environmental technologies.

MATERIALS AND METHODS

The synthesis, characterization, and preparation of SnO_2 and SnO_2-MWCNT electrodes were presented in our previous paper [4].

Linear sweep voltammetry measurements were performed on the Gamry Instrument – Interface 1000 Potentiostat/Galvanostat (Warminster, Pennsylvania, USA), and a three-electrode electrochemical cell was employed. Ag/AgCl was used as a reference electrode and the Pt mesh as a counter electrode, while the pure SnO_2 and SnO_2-MWCNT electrodes (2 cm^2, surface area (1 x 2 cm)) served as the working electrodes. The measurements were done between 0.0 and 3.0 V (vs. Ag/AgCl) at a scanning rate of 10 $mV \cdot s^{-1}$ in 0.1 $mol \cdot L^{-1}$ Na_2SO_4 with the addition H_2SO_4 and NaOH (0.5 M) to adjust pH.

RESULTS AND DISCUSSION

As can be seen (Figure 1), the potential for OER on SnO_2 electrodes rises with decreasing of pH, from 2.90 V at pH 11 to 1.88V at pH 4. Moreover, the potential for OER in neutral system was also lower than in acid system, probably due to the minor concentration and availability of OH^- Also, it can be noted a high interfacial diffusion resistance for the electron transfer from the electrode via the active sites to absorbed OH species. In agreement with literature [5] the OER is highly pH-sensitive. OER mechanism is widely presented as a four-electron-transfer step in both acidic and alkaline media.

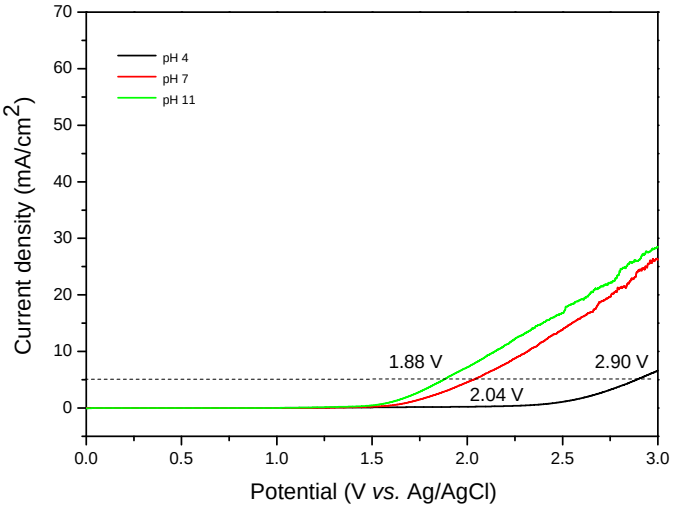

Figure 1 *Linear sweep voltammograms of the SnO_2 electrode in 0.1 $mol \cdot L^{-1}$ Na_2SO_4 at pH = 4, pH = 7, pH = 11, scan speed 10 $mV \cdot s^{-1}$*

The overall water oxidation reaction under acidic condition is denoted by the following equation:

$$2H_2O\ (l) \rightarrow O_2 + 4H + 4e^- \quad (1)$$

Generally, reaction can be represented in 4 steps (Eqs (2–5)):

$$H_2O\ (l) + * \rightarrow *OH + H + e^- \quad (2)$$

$$*OH \rightarrow *O + H + e^- \quad (3)$$

$$H_2O\ (l) + *O \rightarrow *OOH + H + e^- \quad (4)$$

$$*OOH \rightarrow * + O_2\ (g) + H + e^- \quad (5)$$

where „*“ is defined as the active site of the catalyst, (g) refers to the gas phase, (l) refers to liquid phase, and *OH, *O, and *OOH represent the species adsorbed on the active site.

In contrast to under acidic conditions, Eq (1), the water oxidation reaction under alkaline conditions is given by Eq (6).

$$4OH^- \rightarrow O_2\ (g) + 2H_2O\ (l) + 4e^- \quad (6)$$

Usually reaction (6) is assumed to proceed in following steps (Eqs (7–9)):

$$* + OH^- \rightarrow *OH + e^- \quad (7)$$

$$*OH + OH^- \rightarrow *O + H_2O\ (l) + e^- \quad (8)$$

$$*O + OH^- \rightarrow *OOH + e^- \quad (9)$$

$$*OOH + OH^- \rightarrow * + O_2\ (g) + H_2O\ (l) + e^- \quad (10)$$

Figure 2 shows linear sweep voltammograms and Tafel fitting curves of pure SnO_2 and SnO_2-MWCNT electrode in the basic supported electrolyte at pH 11.

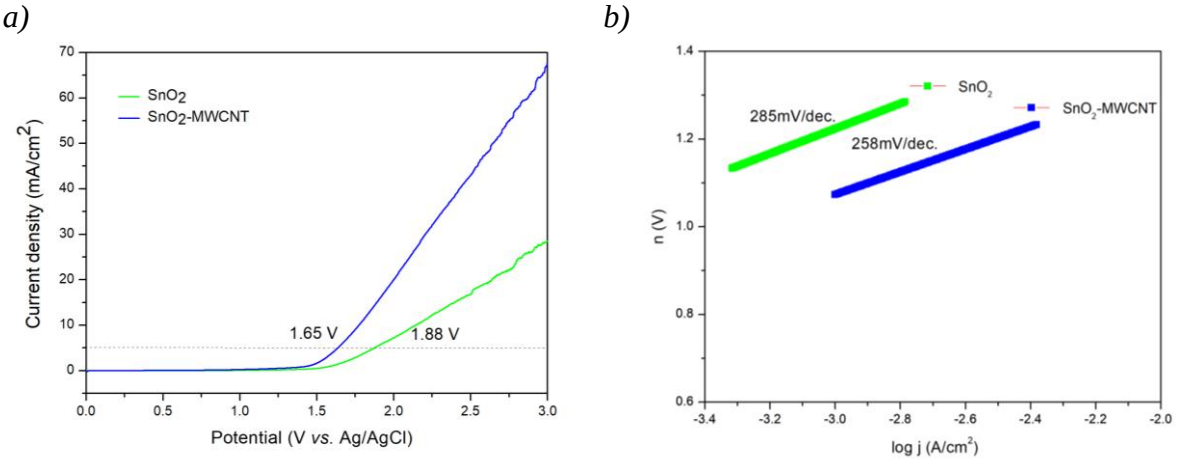

Figure 2 *Linear sweep voltammograms (a) linear fitting curves (b) of the SnO_2 and SnO_2-MWCNT electrode in 0.1 mol·L^{-1} Na_2SO_4 at pH = 11, scan speed 10 mV·s^{-1}*

With the addition of carbon materials to SnO_2, the potential for OER at 5 mA·cm^{-2} was 1.65 V at pH 11, which is a lower than the 1.88 V observed on pure SnO_2 electrodes at the same pH values. At the same potentials, pure SnO_2 electrode shows a lower current density compared to SnO_2 doped with MWCNT. MWCNT, as carbon material with excellent

electrical conductivity, leads to increased current density and better electrical conductivity of SnO_2-MWCNT electrode.

Table 1 *Kinetic parametres of OER at pH 11*

Electrodes	a (V)	b ($V \cdot dec^{-1}$)	log j	j_0 ($A \cdot cm^{-2}$)
SnO_2	2.078	0.285	-7.29	$5.12 \cdot 10^{-8}$
SnO_2-MWCNT	1.848	0.258	-7.162	$6.88 \cdot 10^{-8}$

The exchange current density (j_0) can be used to present the extent to which electrode reactions are blocked. Generally, a larger exchange current density (j_0) value and the smaller Tafel slope (b) imply that OER is more likely to occur. As can be seen from Table 1 the higher j_0 and smaller b which means SnO_2-MWCNT electrode show the greater electrocatalytic activity to OER.

CONCLUSION

Investigation of the effect of pH and comparative analysis of OER kinetic parameters obtained by SnO_2 and tin dioxide-carbon based anodes in sulphate electrolyte at pH 11 was performed. Particularly, the results indicated that modification SnO_2 electrode with carbon-based materials leads to an intensive increasing electric conductivity and slightly affects the parameters of OER. Consequently, it can be predicted that the application of SnO_2-MWCNT electrodes could be more successful in environmental protection technologies rather, than in energy conversion and storage technologies.

ACKNOWLEDGEMENT

The authors would like to thank the Ministry of Science, Technological Development and Innovation of the Republic of Serbia for the financial support to the research through institutional funding (Contract number 451-03-47/2023-01/ 200017).

REFERENCES

[1] Zagalskaya A., Alexandrov V., ACS Catal. 10 (2020) 3650–3657.

[2] Zhipeng Y., Junyuan X., Yifan L., *et al*., J. Mater. Chem. A (2013) 1–10.

[3] Moradi M., Vasseghian Y., Khataee A., *et al*., J. Ind. Eng. Chem. 87 (2020) 18–39.

[4] Simić M. D., Savić B. G., Ognjanović M. R., *et al*., J. Water Process Eng. 51 (2023) 103416.

[5] Liang Q., Brocks G., Bieberle-Hütter A., J. Phys. Energy 3 (2021).

OPTIMIZATION OF THE HELICHRYSUM ARENARIUM EXTRACT OBTAINED WITH ULTRASOUND-ASSISTED EXTRACTION

Drita Abazi Bajrami[1*], Mirko Marinkovski[2], Kiril Lisichkov[2], Stefan Kuvendziev[2]

[1]Mother Teresa University, Faculty of Technological Sciences, st. Mirçe Acev n. 4 – floor VII 1000 Skopje, NORTH MACEDONIA

[2]University Ss. Cyril and Methodius, Faculty of Technology and metallurgy, Bul. Goce Delcev, n.9, 1000, Skopje, NORTH MACEDONIA

[*]*drita.abazi@unt.edu.mk*

Abstract

In this paper, the optimization of the ultrasound extraction process was investigated. The extract obtained from H. arenarium has various pharmacological properties. In addition, the essential oil isolated from the flowers of H. arenarium has been confirmed to have better antimicrobial activities. The aim of this study was to express the effect of some specific parameters such as: extraction time, solvents and temperature in order to obtain higher extraction yield. The extraction was carried out in twelve extraction cycles of 2 to 180 min and temperatures of 20°C, 30°C and 40°C. During the development of the process, all the used factors have a positive impact, increasing the extraction rate by recovering higher amounts of extraction yield from Helichrysum arenarium. The results show that the maximum extraction yield is obtained using petrol ether as solvent followed by 55% ethanol, 70% ethanol, 96% ethanol, methanol and the lowest yield is obtained with methylene chloride. From the results it can be seen that the yield of H. arenarium gradually increases with increasing extraction time. Also, it is observed that the extraction yield increases with increasing temperature which is the result of the increased solubility at higher temperature, the viscosity of the solvent decreases, which can help the solvent to diffuse into the cells and improve the desorption of the desired compound from the cells of the plant. Petroleum ether was found to be the best solvent for the process as compared to the others solvent used in the extraction process.

Key words: bioactive components, *H. arenarium*, extraction, ethanol, ultrasound.

INTRODUCTION

Ultrasound assisted extraction was used to obtain bioactive substances from different types of plants [1]. The acquisition of bioactive substances that are inside the plant tissues occurs by breaking down the cell walls and enhancing overall mass transfer of cell contents. Acoustic cavitation is the main mechanism for the increases of extraction efficiency of bioactive compounds [2].

Ultrasound extraction is one of the most used techniques due to the short extraction time, the low amount of the used solvent, decreased energy consumption, increasing the yield of the extraction and improve the quality of extracts. Extraction with this technique can be carried out at a lower temperature and thermal degradation of the extracts is avoided when the process is done in lower temperature [3]. All these parameters contribute that this technique to be considered as environmentally friendly [2,4–7]. This technique has been developed to be a

green extraction method. Ultrasonic assisted extraction is a process that yields products that are widely used for pharmaceutical and cosmetic purpose as well they are used in food industries and for environmental purposes [8].

Modeling and optimization of a process can contribute for increasing the yield of the extract. Various mathematical modeling, methods and experimental studies are used to facilitate optimization, simulation, design, and process control and contribute to energy, time and solvent use [5,9].

In this study, the optimization of the ultrasound extraction process has been developed. The purpose of this work is to obtain bioactive substances with ultrasound assisted extraction from *H. arenarium* using solvents with different polarity, in different temperatures and different period of time. The aim was to ensure the highest yield of the obtained extracts, as well as the comparison of the extraction efficiency of the extraction solvents for the plant material which is *H. arenarium*.

MATERIALS AND METHODS

The working material was bought in pharmacy, produced from Alkaloid AD in Skopje and was packed in a 100 g package. *H. arenarium* was used for the extraction of the bioactive components.

The solvents used were ethanol (96%) and methanol which are produced by the pharmaceutical company Alkaloid AD – Skopje. Petroleum ether, n-hexane and methylene chloride were used also and were produced by Carlo Erba Reagents S.r.l and by Merck. All the solvents were of a high degree of analytical purity.

Ultrasound-assisted extraction

For the extraction process was used an ultrasonic bath with a tank capacity of 30 l and a nominal ultrasonic generator with power of 240 W, with a frequency of 40 kHz. The ratio of mass of the working raw material and the volume of solvent was 1:50.

H. arenarium extraction experiments were carried out at temperatures of 20°C, 30°C and 40°C for 0, 2, 5, 10, 15, 20, 30, 45, 60, 75, 90, 120, 180 minutes. The obtained results were used to examine the kinetics and modeling of the ultrasonic extraction process in order to determine the optimal working conditions.

RESULTS AND DISCUSSION

Dependence of total yield during ultrasonic extraction of *H. arenarium* with different solvents at different temperatures

The effect of different solvents on the extraction yield at different temperatures was investigated and the results are shown in Figure 1.

The results show that the maximum extraction yield is obtained using petroleum ether as solvent followed by 55% ethanol, 70% ethanol, 96% ethanol, methanol and the lowest yield is obtained with methylene chloride. The solubility of the solute in the solvent plays an important role in the extraction process. It is well known that the solubility of the solute increases with increasing temperature and thus the extraction yield increases which is

consistent with the results shown in Figure 1. Different extraction efficiency of these solvents is attributed to their different polarities and viscosities. There are several parameters such as solvent viscosity, surface tension, and vapor pressure that affect cavitation and thus the extraction yield [3].

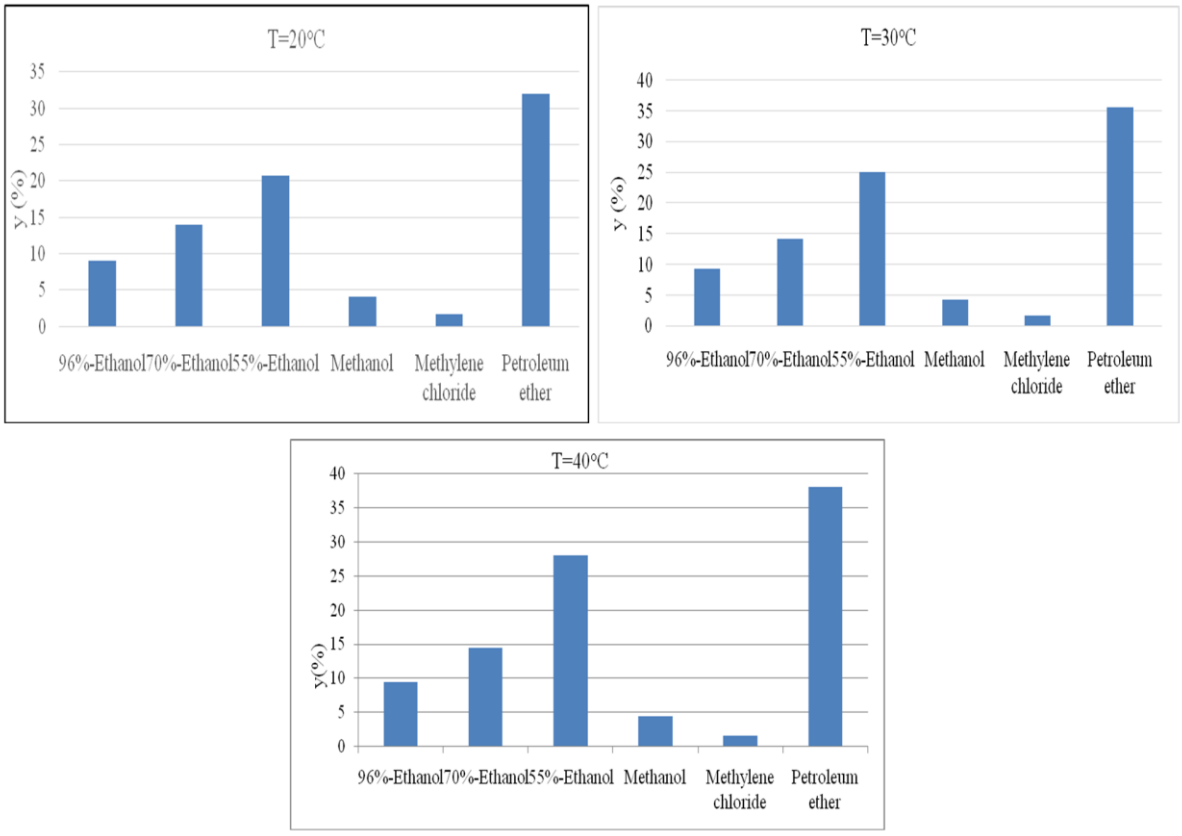

Figure 1 *Dependence of total yield during ultrasonic extraction of H. arenarium with different solvents at a temperature of 20°C, 30°C and 40°C*

Dependence of yield on time during ultrasonic extraction of *H. arenarium* with different solvents at different temperatures

To identify the time equilibrium of the extraction process, the effect of time on the extraction yield with different solvents was studied. The duration of time can also affect the extraction yield. As illustrated in the pictures it can be seen that the yield of *H. arenarium* gradually increases with increasing extraction time. The rate of increase in yield may be a result of the increase in contact time between the solvents and the plant material. Another reason for the gradual increase in yield may be because the inner part of the plant is not easily accessible. Ultrasonic radiation for a long time can damage the quality of heat-sensitive materials. In terms of costs, long extraction times are not cost-effective due to their high energy consumption [10].

The dependence of the yield on time during the ultrasonic extraction of *H. arenarium* with different solvents at a temperature of 20°C, 30°C and 40°C are given in the figure 2. Where it can be seen that the highest yield is obtained in the time period of 180 minutes: with petroleum ether (32%) and with 55% solution of ethanol (20.66667%), followed by 70%

solution of ethanol (14%) while the lowest yield is obtained with 96% solution of ethanol (9%), methanol (4%) and methylene chloride (1.61%). When the process was done in 30°C show that higher yield is obtained when petroleum ether is used as a solvent (35.5%), followed by 55% solution of ethanol (25%) and 70% solution ethanol (14.2%), while the lowest yield is obtained with 96% solution of ethanol (9.2%), methanol (4.2%) and methylene chloride (1.62%). The same case we have in 40°C, with the increasing of the extraction time was obtained higher yield, with petroleum ether (38%) over a period of 180 minutes, 55% solution of ethanol (28%) and 70% solution of ethanol (14.5%) while the lowest yield is obtained with 96% solution of ethanol (9.5%), methanol (4.5%) and methylene chloride (1.63%).

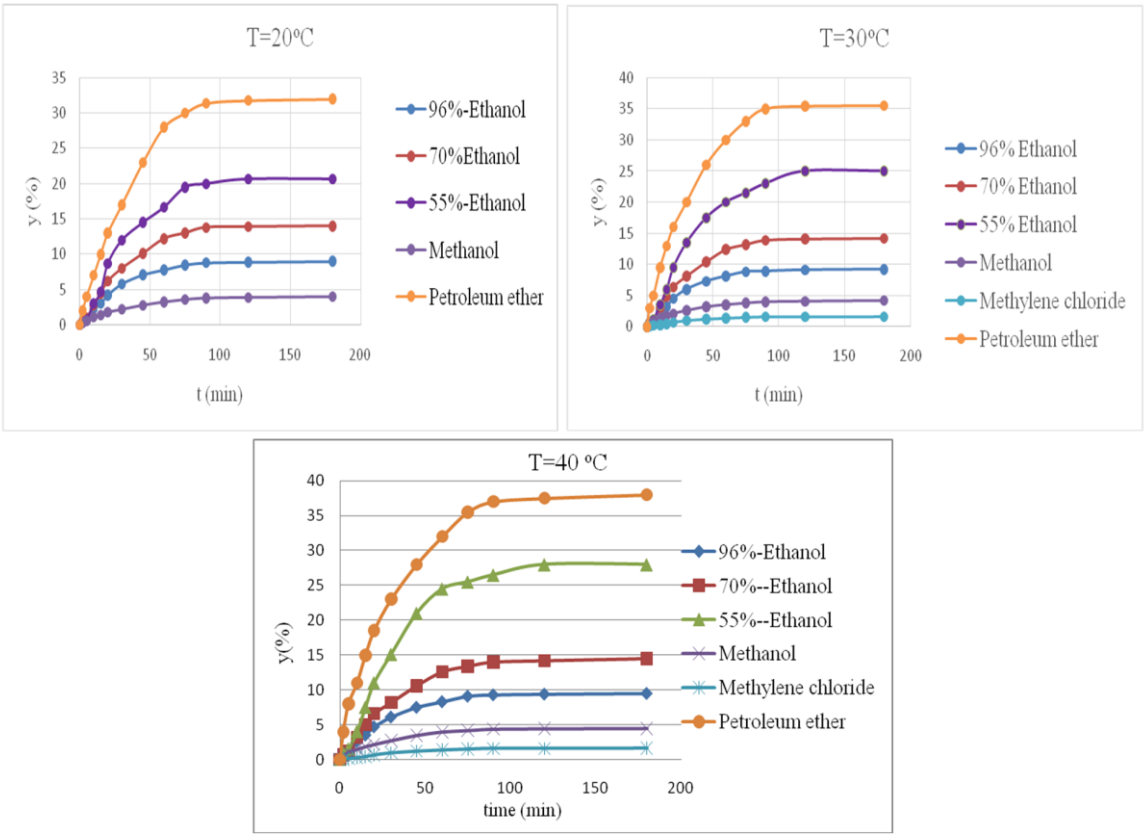

Figure 2 *Dependence of yield on time during ultrasonic extraction of H. arenarium with different solvents at a temperature of 20°C, 30°C and 40°C*

Comparison of total yield for different temperatures of separate solvents

The extraction temperature is an important parameter in ultrasonic extraction because it largely determines the solvent power, analyzing physical properties and the effects of ultrasonic cavitation, which in turn greatly affects the extraction efficiency [11]. The extraction was carried out at different temperatures, 20°C, 30°C and 40°C.

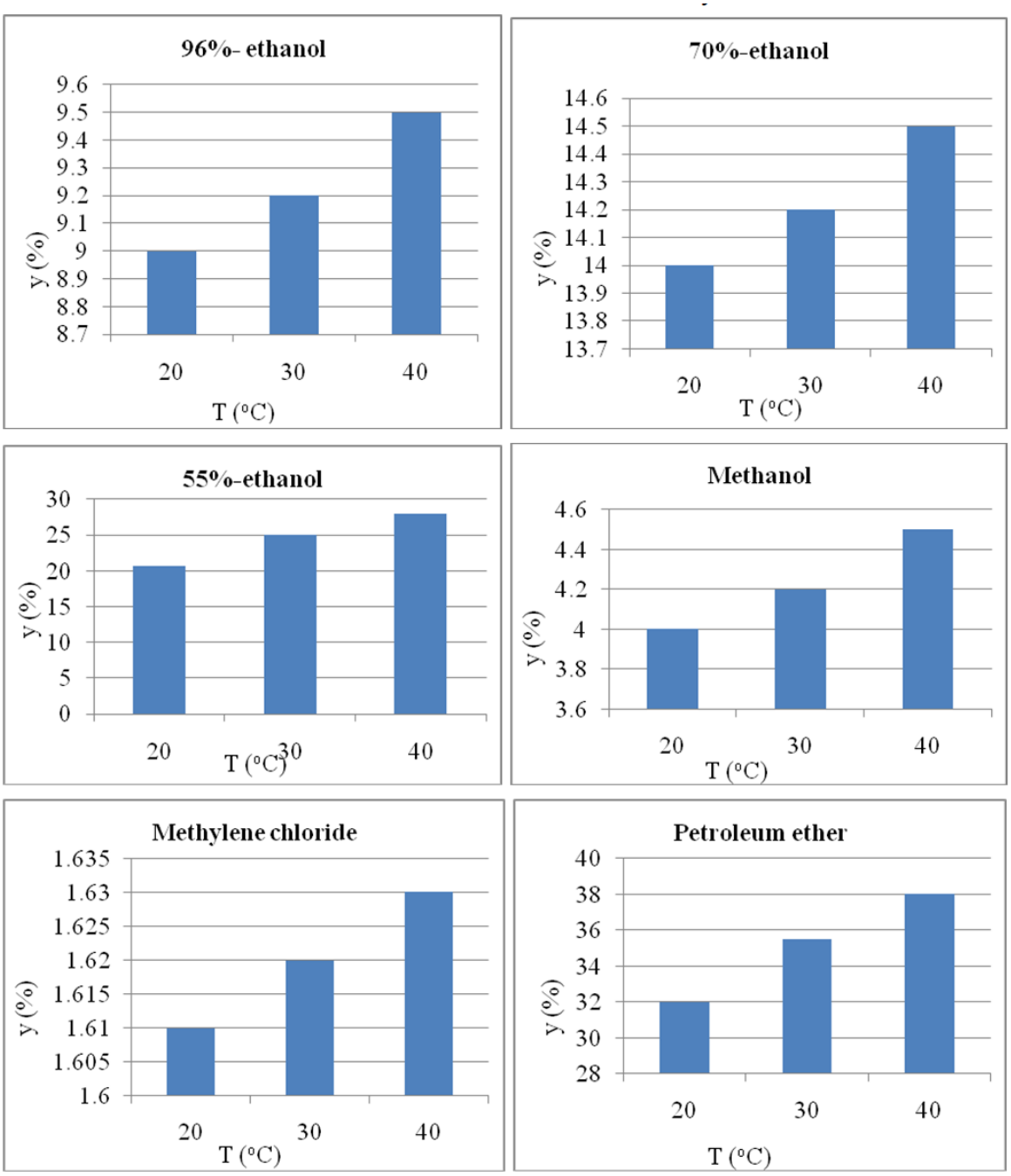

Figure 3 *Comparison of total yield for different temperatures of 96% ethanol, 70 % ethanol, 55% ethanol, methanol, methylene chloride and petroleum ether as solvents*

The effect of ultrasonic extraction at temperature 20°C, 30°C and 40°C on the extraction yield of *H. arenarium* was investigated when 96% ethanol, 70% ethanol, 55% ethanol, methanol, methylene chloride, petroleum ether were used as solvents, and the results are shown in Figure 3. By increasing the ultrasonic extraction temperature from 20°C, up to 40 °C, the extraction yield for *H. arenarium* showed a gradual increase of 9%, 9.2% and 9.5%. With 70% ethanol the extract yield of 14% at 20°C increases to 14.2% at 30°C and 14.5% at 40°C. The change in the extraction yield can be significantly observed when 55% ethanol was used as a solvent, with an increase in temperature from 20 to 30°C, the yield increases from

20.6667% to 25%, while when a temperature of 40°C is used, the yield is higher compared to yields at 20°C and 30°C. The yield does not increase much when methanol was used as a solvent, the difference in yield growth is very small, 4% at 20°C to 4.2% at 30°C and 4.5% at 40°C. The change in extraction yield was marginal at 20°C, 30°C and 40°C, when methylene chloride was used as solvent. At a temperature of 20°C the yield is 1.61%, at a temperature of 30°C the yield is 1.62% while at a temperature of 40°C the yield is 1.63%. With petroleum ether at temperature of 20°C the yield was 32%, at 30°C the yield increases to 35.5% and the largest amount is obtained at 40°C and that is 38%.

In general, from the presented results, it can be concluded that with an increase in the temperature in the solvent-raw material system during ultrasonic extraction, the total extract yield also increases. The order of solvents from highest to lowest yield is: petroleum ether > 55% ethanol > 70% ethanol > 96% ethanol > methanol > methylene chloride.

CONCLUSION

Different operating parameters affecting the ultrasound assisted extraction of *H. arenarium* were optimized based on the maximum yield extracted from the plant material. The best conditions for the ultrasound assisted extraction were obtained at temperature of 40°C, extraction time of 180 min and petroleum ether and 55% ethanol as a solvent. Petroleum ether gives slightly better oil yield compared to 55% ethanol.

REFERENCES

[1] Veličković D. T. *et al*., Ultrason. Sonochem. 13 (2) (2006) 150–156.

[2] Tao Y., Zhang Z., Sun D.-W., Ultrason. Sonochem. 21 (4) (2014) 1461–1469.

[3] Charpe T. W., Rathod V. K., Braz. J. Chem. Eng. 33 (4) (2016) 1003–1010.

[4] Nashrulmillah I. N. A., Sulaiman,A. Z., Chem. Eng. Trans. 56 (2017) 78–786.

[5] Milićević N., *et al.* Ultrason. Sonochem. 79 (2021) 105761.

[6] Zahari N. A., *et al.* Processes 8 (3) (2020) 322.

[7] Zeng G., *et al.* Int. J. Environ. Res. Public Health 19 (3) (2022) 1555.

[8] Simeonov E., Yaneva Z., Chilev C., Green Process Synth. 7 (1) (2018) 68–73.

[9] Susanti *et al*., Processes, 7 (11) (2019) 837.

[10] Ma Y.-Q., *et al*., J. Agric. Food Chem. 56 (14) (2008) 5682–5690.

[11] Zhang H.-F., *et al*., IFSET 10 (1) (2009) 54–60.

VIBRATION ISOLATION

Berina Sejdinović[1*]
[1]University of Zenica, Fakultetska 3, 72000 Zenica, BOSNIA & HERZEGOVINA
[*]*berina.sejdinovic.21@dl.unze.ba*

Abstract

Vibration is a mechanical phenomenon where oscillations occur around a balance point. Due to the many extremely negative effects of vibrations on structures and the human body, there is an effort to reduce (reduction) of vibrations. The aim of the work was to familiarize ourselves with vibrations, what they can be, when they occur and how we can isolate them. Among the various methods for reducing vibrations, the following are mentioned in the paper: avoidance of resonance of the object's own vibrations and excitation vibrations; installation of dynamic, hydraulic or friction dampers and installation of dynamic compensators. The basic results are given through vibration isolation materials, such as deformable elements for building isolation and vibration damping materials. However, the emphasis is on the best materials for vibration isolation: StP Aero Plus; vibration damping material Stp Silver 3mm; sound insulation pad – vibration SoundGuard VibroStop 25; SoundGuard Vibro DUO vibration carrier and sound – vibration isolation. In the considerations, problems with vibration isolation are described, such as: application, selection of isolation means and an example of calculation of vibration isolation. At the end, short conclusions are given regarding the proper selection of insulation materials, and since the correct selection is made once, it should be left to engineers of various professions and experts, in order to fulfill our desire to live healthier and protect the environment.

Keywords: vibration, vibration isolation, StP Aero Plus.

INTRODUCTION

Vibration is a mechanical phenomenon where oscillations occur around a balance point. The word comes from the Latin vibrationem ("shaking, waving"). Oscillations can be periodic, like the movement of a pendulum – or random, like the movement of a tire on a dirt road. Vibrations can be desirable: for example, the movement of a reed in a woodwind instrument or an accordion, a cell phone, or a speaker cone.

However, in many cases the vibrations are undesirable, waste energy and create unwanted sound. For example, the vibrational movements of an engine, electric motor or any other mechanical device in operation are usually unwanted. Such vibrations can be caused by imbalance in rotating parts, uneven friction, or meshing of gear teeth. Careful design usually reduces unwanted vibrations.

Sound and vibration studies are closely related. Sound or pressure waves are generated by vibrating structures (e.g. vocal cords); these pressure waves can also induce vibrations of structures (eg the ear drum). Therefore, attempts to reduce noise are often associated with vibration problems [1].

Vibrations are mechanical oscillations of a system with small amplitudes, while oscillations are generally periodic motions of any amplitude [2].

In periodic motions, the same or very similar displacements of the moving mass are repeated in the same time periods. Most often, the term vibration refers to harmonic motion. Harmonic motion is a motion in which the position, speed, and usually the acceleration of a mass change according to the sinusoidal or cosinusoidal law. Harmonic motion is the simplest form of vibrational motion. The study of vibrations is of great importance in mechanical engineering, construction, shipbuilding, aircraft construction and other branches of technology. The branch of mechanics that deals with the study of vibrations is called vibration theory. A system is said to be vibrating if it consists of a vibrating mass and an elastic element, in real systems there are also elements such as damping and disturbance force [3].

Free vibrations occur when a mechanical system is started with an initial input and allowed to vibrate freely. Examples of this type of vibration are pulling a child on a swing and letting it go, or hitting a fork and letting it ring. The mechanical system vibrates at one or more of its own frequencies and continues until it is stationary.

Forced vibrations occur when a time-varying disturbance (load, displacement or speed) is applied to a mechanical system. A disturbance can be a periodic and steady input, a temporary input or a random input. A periodic input can be harmonic or non-harmonic disturbance. Examples of these types of vibrations include shaking of a washing machine due to imbalance, vibrations in transport caused by the engine or rough road, or vibrations of a building during an earthquake. For linear systems, the steady-state frequency of the vibrational response resulting from the application of a periodic, harmonic input is equal to the frequency of the applied force or motion, with the magnitude of the response depending on the actual mechanical system.

When the energy of a vibrating system is gradually dissipated by friction and other resistances, the vibrations are said to be damped. The vibrations gradually decrease or change in frequency or intensity or stop and the system rests in its equilibrium position [4].

Vibration isolation

Vibration isolation is the process of isolating an object, such as a piece of equipment, from a source of vibration.

Vibrations are undesirable in many domains, primarily designed systems and habitable spaces, and methods have been developed to prevent the transmission of vibrations to such systems. Vibrations are propagated by mechanical waves, and certain mechanical connections conduct vibrations more efficiently than others. Passive vibration isolation uses materials and mechanical joints that absorb and dampen these mechanical waves. Active vibration isolation includes sensors and actuators that produce disruptive interference that cancels out incoming vibrations [4].

VIBRATION REDUCTION METHODS

There are many examples of the harmful effects of vibration: most vehicles have vibration problems due to engine imbalance, diesel engine imbalance can produce shock waves strong enough to be a nuisance in urban areas. At high speeds, the wheels of the locomotives can be

separated from the rails by more than a centimetre due to imbalance. In turbines, vibrations cause spectacular mechanical failures. In general, vibration results in faster wear and failure of engine parts such as mounts and wheels, and also creates loud noise. Nowadays, a lot of research is being carried out with the aim of eliminating vibrations that occur in engine bearings. Whenever the natural frequency of vibration of a motor or structure coincides with the frequency of an external stimulus, a phenomenon called resonance occurs [2].

It can cause disturbances in the operation of the machines and break the structure. Because of the negative impact that vibrations have on machines and structures, vibration testing and monitoring has become a standard procedure in the design and development of most engineering systems.

VIBRATION ISOLATION MATERIALS AND METHODS

Vibration isolation of buildings

Strong vibrations that occur inside buildings cause strong noise in the air. To reduce the amplitude of such noises, special deforming elements are used, which are installed between the structure (apartment, house) and the source of strong vibrations. Thanks to their use, vibrations resulting from the operation of pipelines, air ducts and other sources of strong noise are reduced. The question of such insulation is especially relevant for cellulose, which are located near metro lines, highways. The following are used for vibration isolation of houses [5]:

- Special supports and suspensions;
- Spring vibration insulators, multiple springs and also suspended type;
- Soft materials in the form of rolls and sheets.

Vibration damping materials

Vibration damping materials absorb and dissipate most of the various noises and vibrations. They are able to protect the structure or any structure from the impact of structural, impact and air noise. As a rule, they are used in production and for protection against vibrations, noise, living rooms, rooms, houses. Vibration dampening panels are very popular among consumers.

In addition, they excellently dampen both sound and impact noise (the average reduction in noise output values when using these panels is approximately 20 dB) [5].

RESULTS AND DISCUSSION

Most of the best vibration damping materials are made on a so-called rubber base. In their appearance, they are very similar to liquid rubber, which was previously actively used for tire repair. Some vibration isolation materials are additionally covered with a special metallized coating that vaguely resembles foil in its appearance. The advantage of materials that absorb vibrations is their ability to quickly dampen and reduce the amplitude of various vibrations that occur as a result of the operation of equipment and vehicles [5].

StP Aero Plus

It is used to reduce the amplitude of noise and vibrations in the vehicle. The front side of this vibration damping material is covered with aluminium foil using embossing technology. Due to the presence of such a coating, the vibration isolation is not destroyed by external stimuli. In addition, StP Aero Plus is made on a bituminous base with an adhesive layer. Thanks to this, it has sealing properties, does not absorb moisture and is not subject to decomposition processes.

This vibration isolation can be used in places where the car is most heavily loaded. It is suitable for finishing the floor and trunk. It is a single-layer product based on a polymer composite. The length of one sheet of StP Aero Plus is 75 cm, and the width is 47 cm. The thickness of this material is 3 mm. The operating temperature range is from -45 to +100 °C [5].

Advantages [5]:

- It dampens the vibration amplitude well;
- Noise protection;
- Can be used for soundproofing cars;
- Large range of operating temperatures;
- Good resistance to mechanical damage;
- Reasonable price (2075 rubles);
- Complete set (supplied in a package of 5 pieces);
- Good mechanical loss factor (0.45).

Defects [5]:

- Only suitable for finishing car floors and trunks;
- Before gluing, the work surface must be pre-treated (degreased, cleaned).

Vibration damping material Stp Silver 3mm

Inexpensive sound insulation material suitable for surface installation on doors, bonnet and trunk lids. It consists of a layer of aluminum foil, protective paper and an adhesive polymer layer. It can be applied to a dry, clean surface with a complex configuration. Before application, the work surface must be cleaned of accumulated dirt with water and neutral detergents that do not contain organic solvents and bases.

It should be noted that this material has excellent anti-corrosive and sealing characteristics. It does not decay and repels moisture that accumulates on its surface. During application to the surface, it does not need to be heat treated beforehand. The application temperature range is from -45 to +100 °C. It can withstand temperatures up to +190 °C for a short time. Supplied in a pack of 5 sheets (75x47 cm). The thickness of one sheet is 3 mm [5].

Advantages [5]:

- Acceptable cost (average price is 1425 rubles);
- Technical data;
- Easy installation.

Does not require pre-heating before applying to the work surface.

Defects [5]:

- It is difficult, if necessary, to disassemble;
- Does not withstand strong mechanical stress.

Sound insulation pad – vibration SoundGuard VibroStop 25

According to its appearance, it is a canvas in the production of which an elastic membrane was used. It is used to reduce the amplitude of impact noise in the floating floor system. It can also be used as an elastic layer that divides vibrations and sound. This material is packaged using UV stabilized film. Can be delivered individually or in bulk. The size of the canvas is 1200 x 270 x 270 mm, and the country of origin is Russia [5].

Advantages [5]:

- Acceptable cost (2019 rubles);
- It copes well with reducing the amplitude of impact noise;
- Can be used as additional sound insulation of the room.

Defects [5]:

- Subject to mechanical damage;
- Unpleasant smell (after laying this material, it is recommended to ventilate the room).

SoundGuard Vibro DUO vibration carrier

This anti-vibration support is used during the installation of partitions. Made on the basis of material – elastomer. It is a strong support for vibration isolation, which is equipped with devices for various soundproof vibration fences, partitions, for which a double spaced frame is used.

This attachment consists of a high-strength metal supporting frame, as well as 2 U-shaped elements that are necessary for installation work and the installation of the element on the partition. Available in green and brown shades.

Advantages [5]:

- Acceptable cost;
- Good technical characteristics;
- Made of quality material;
- It dampens the amplitude of vibrations well and protects against vibrations.

Defects [5]:

- Difficult to assemble;
- It takes a long time to install;
- Does not withstand serious mechanical damage.

Sound-vibration isolation

It is a multifunctional, universal insulating agent that has good sound absorption and impact absorption characteristics. It is used to reduce vibration amplitudes and sound insulation of floors, walls and ceilings. It consists of a special needle-punched fiberglass canvas that is pressed and sealed in a protective spunbond sheath. It can be used in rooms and buildings of different types, as well as for purposes during repairs, decoration or construction work. During floor insulation, it is used as a base with vibration damping properties. It is installed directly under the screed itself.

It can also be used as a shock absorption and sound insulation layer for walls and ceilings. These mats are produced in sheet form (1.5 x 5 m). Most often, this material is used in both civil and industrial construction. It can be actively used in rooms with all levels of fire resistance. The operating temperature range of this product is from -100 to +140 °C [5].

Advantages [5]:

- Technical data;
- Versatility (can be used in various construction areas);
- Removes vibrations and other people's noise well;
- Ease of installation.

Defects [5]:

- Cost (2592 rubles per package);
- During installation, you must monitor the integrity of the material.

CONCLUSION

Vibration is a mechanical phenomenon where oscillations occur around a balance point. The word comes from the Latin vibrationem ("shaking, waving").

Vibrations can be: desirable and undesirable. For example, the movement of the reed in a woodwind instrument or harmonica is desirable, and for example, the vibrational movements of an engine, electric motor or any other mechanical device in operation, which consume energy and create unwanted sound, are undesirable.

We distinguish several types of vibrations: free vibrations, forced vibrations and damped vibrations. Free vibrations occur when a mechanical system is started with an initial input and allowed to vibrate freely. Forced vibrations occur when a time-varying disturbance (load, displacement or speed) is applied to a mechanical system, while damped vibrations occur when the energy of the vibrating system is gradually dissipated by friction and other resistances.

Vibrations are undesirable in many domains, that's why vibration isolations are used: passive vibration isolation uses materials and mechanical joints that absorb and dampen these mechanical waves, and active vibration isolation includes sensors and actuators that produce disruptive disturbances that cancel incoming vibrations.

Due to the many extremely negative effects of vibrations on structures and the human body, there is an effort to reduce (reduce) vibrations using different methods, such as: avoiding the resonance of the object's own vibrations and excitation vibrations, installing dynamic, hydraulic or friction dampers, installing dynamic compensators, using special isolators.

In addition to the silencer system, simpler variants in the form of components such as: springs, pneumatic silencers, hydraulic silencers, air springs, various polymer elements are installed.

The best materials for dampening vibrations are made on a so-called rubber base, and StP Aero Plus stands out among them, which is used to reduce the amplitude of noise and vibrations in the vehicle; vibration damping material Stp Silver 3mm, cheap sound insulation

material suitable for surface installation on doors, engine cover and trunk lids. Sound-vibration insulation pad SoundGuard VibroStop 25 is used to reduce the amplitude of impact noise in the floating floor system, and SoundGuard Vibro DUO vibration support, anti-vibration support is used during partition installation. Sound – vibration isolation is a multifunctional, universal isolation agent that has good sound absorption and impact absorption characteristics. It is used to reduce vibration amplitudes and sound insulation of floors, walls and ceilings.

Vibration isolation is actively used to protect against noise and vibrations of both cars and buildings, and is often used to protect against strong vibrations of engineering equipment.

However, you should know that no insulation material is ideal, because each has its own advantages and disadvantages.

For the proper selection of insulation material, it is necessary to know its physical and chemical properties, as well as its advantages and disadvantages, and once the correct selection is made, it should be left to engineers of various professions and experts, in order to fulfil our desire to live healthier and to protect the environment.

REFERENCES

[1] *Available on the following link:* https://hr.upwiki.one/wiki/Vibration

[2] Tehnička enciklopedija, Vibracije , Sv. 13, Leksikografski zavod Miroslav Krleža, Zagreb (1997) 462–467.

[3] Matejiček F., Kinetika sa zbirkom zadataka, Strojarski fakultet u Slavonskom Brodu (2006) 167–192.

[4] *Available on the following link:* https://hr.upwiki.one/wiki/Vibration_isolation

[5] *Available on the following link:* https://best-hr.designuspro.com/luchshie-vibroizolyaczionnye-materialy

THE INFLUENCE OF AGEING ON THE THERMAL PROPERTIES AND MICROSTRUCTURE OF THE EN AW-6082 GREEN ALUMINIUM ALLOY

Uroš Stamenković[1*], Ivana Marković[1]

[1]University of Belgrade, Technical Faculty in Bor, V.J. 12, 19210 Bor, SERBIA

[*]*ustamenković@tfbor.bg.ac.rs*

Abstract

The purpose of this work is to investigate the influence of ageing on the thermal properties and microstructure of the EN AW-6082 green aluminium alloy. The heat treatment of the alloy included annealing, solution heat treatment, and ageing at different temperatures and times. Samples were annealed at 550 °C for 6 h and cooled in air in order to remove asfabricated state. After that, solution heat treatment was done at 550 °C for one hour, followed by quenching in ice water in order to obtain a supersaturated solid solution. Samples were aged after quenching at three different temperatures (160 °C, 230 °C, and 330 °C) for 30 and 60 minutes, respectively. After each step in the heat treatment process, samples were separated and investigated. The investigation of the samples included the measurement of the thermal properties and the microstructural investigation of the aged sample. After the ageing treatment, an initial decrease in thermal diffusivity and thermal conductivity was followed by a gradual increase. A microstructural investigation showed the existence of a finely dispersed metastable phase after ageing, causing an increment in thermal diffusivity and thermal conductivity values.

Keywords: EN AW-6082, thermal conductivity, thermal diffusivity, SEM/EDS analysis.

INTRODUCTION

Aluminium alloys from the 6000 series are common industry materials thanks to their good mix of properties such as good ductility, high strength-to-weight ratio, formability, corrosion resistance, recyclability, and non-toxicity [1,2]. Alloys from this series are often used for the production of heat sinks due to their good electrical conductivity, high strength, and good thermal properties [3–8]. For the production of heat sinks the EN AW-6082 aluminium alloy can be a good candidate. Alloys from this series are commonly heat treated in various ways to alter the microstructure and enhance the alloys' characteristics. Precipitation hardening, also known as ageing, is often used to strengthen aluminium alloys from these series. Besides strengthening, ageing process alters the thermal properties as well. Solution heat treatment, quenching to room temperature or below room temperature, and ageing - either natural (at room temperature) or artificial (at higher temperatures) - are all integral parts of this process [9]. As the alloy ages (at different temperatures and times), different types of precipitates appear in the microstructure. Sometimes, those precipitates are very fine and evenly dispersed thus hindering the movement of dislocations, causing the changes in the alloys' microstructure. Many authors had their focus on investigating the influence of different heat treatments on mechanical and electrical properties [3–5,10]. Some authors were investigating the change in thermal properties of the Al-Mg-Si alloy during precipitation

hardening at different temperatures and times [6–8,11,12]. The literature review concludes that ageing is defined primarily by temperature and time during the ageing process. The aim of this study was to better understand the influence of ageing at different temperatures and times, on the thermal diffusivity, thermal conductivity, and microstructure of the EN AW-6082 alloy.

MATERIALS AND METHODS

For this experimental investigation, the EN AW-6082 alloy was chosen. The extruded rectangular bars were delivered in peak aged condition by "AlCu metali d.o.o.". The chemical composition of the alloy (Table 1) was determined using an optical emission spectrometer Belec Compact Port. The samples were annealed in the Heraeus K-1150/2 electric resistance furnace for 6 hours at 550 °C to remove a fabricated state. After that, supersaturated solid solution (α_{ssss}) was obtained by heating the samples to 550 °C for 1 hour and quenching in ice water. Ageing was performed on quenched samples at three different temperatures (160 °C, 230 °C, and 330 °C) for 30 and 60 minutes, respectively. After each step in the heat treatment process, samples were separated and investigated. After quenching (Temper T-W) and after ageing (Temper T6). The investigation of the samples included metallographic phase investigations, as well as the distribution of phases, by using the TESCAN Vega 3 LMU scanning electron microscope equipped with an EDS X-act detector by Oxford Instruments. Preparation of the samples included wet grinding on a series of SiC papers, and polishing with alumina suspension with two different granulations of Al_2O_3: particle sizes of 0.3 μm and 0.05 μm. Dix-Keller solution was used for the etching of the samples by immersion to reveal the microstructure.

On the TA Instruments DXF 500 thermal conductivity meter, the xenon flash method was applied to determine the thermal diffusivity of the investigated samples after different heat treatments by irradiating the disc-shaped specimens with a diameter of 12.7 mm with the xenon lamp in a nitrogen atmosphere. The thermal conductivity as a function of temperature was calculated according to the equation:

$$\lambda(T) = \rho(T) \times c_p(T) \times \alpha(T) \quad (1)$$

where, λ - thermal conductivity; (W/m·K), ρ – density; (kg/m^3), c_p – specific heat capacity; (J/kg·K), α - thermal diffusivity; (mm^2/s), T – temperature; (°C).

Table 1 *Chemical composition of the investigated alloy, mass.%*

Si	***Fe***	***Cu***	***Mn***	***Mg***	***Cr***	***Ni***	***Zn***
0.807	0.354	0.042	0.453	0.696	<0.012	0.012	0.115
Ti	***Pb***	***V***	***Co***	***Sn***	***Zr***	***Al***	
0.025	0.01	<0.003	0.006	<0.003	<0.003	97.45	

Figure 1 *Samples for a) microstructural analysis; b) measurement of thermal properties*

RESULTS AND DISCUSSION

The first step in investigating process was the measurement of thermal properties after quenching and after ageing. The presented results demonstrate that ageing influences the thermal properties.

After being aged at 160 °C, 230 °C, and 330 °C for 30 minutes and 60 minutes, thermal diffusivity and thermal conductivity were measured at room temperature. These three ageing temperatures were picked to address three distinct stages in the precipitation sequence. At the lowest temperature, G.P. zones appear; metastable phases were formed at the medium chosen temperature while over-ageing is detected at the highest chosen temperature. Figures 2 and 3 depict the measured values of thermal diffusivity and thermal conductivity as a function of a heat treatment procedure, respectively.

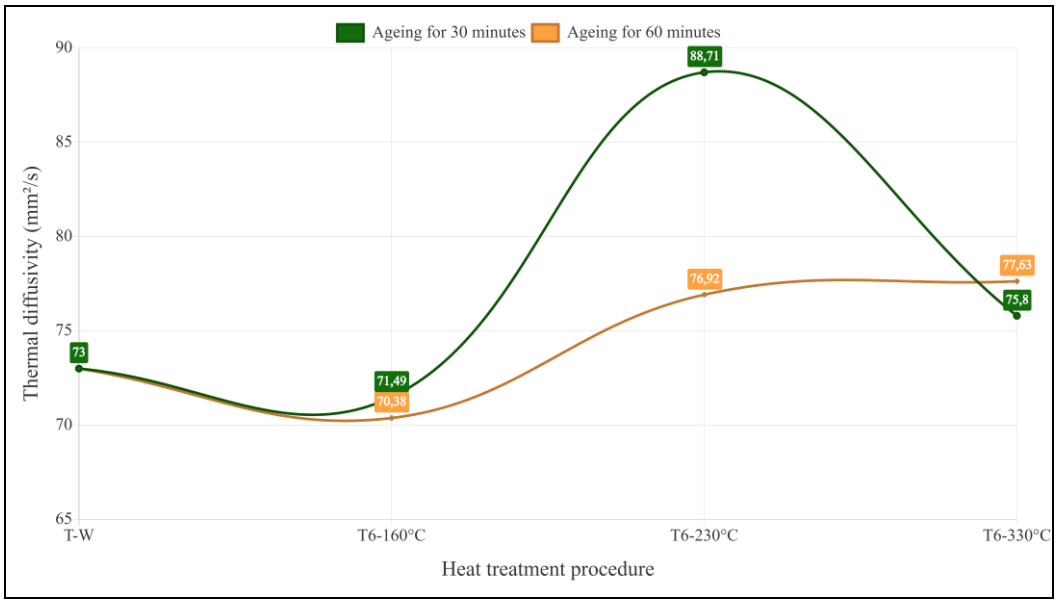

Figure 2 *Thermal diffusivity as a function of heat treatment procedure*

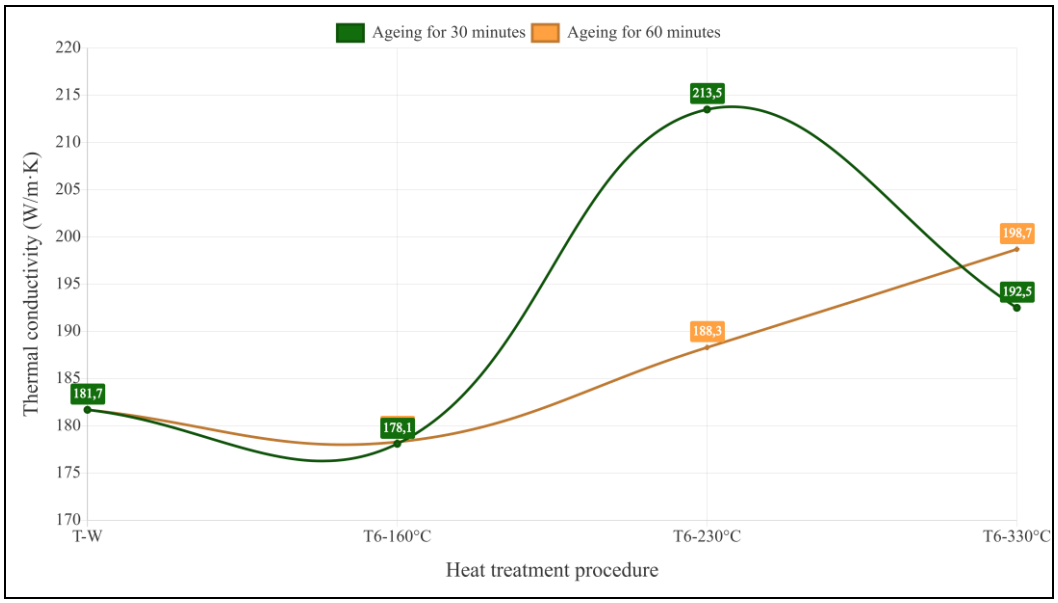

Figure 3 *Thermal conductivity as a function of heat treatment procedure (T-W represents the quenched condition and T6 represents the aged condition)*

Thermal diffusivity and thermal conductivity values were lower after aging at 160 °C than they were in the quenched condition. This is explained by the high electron scattering effect brought on by the production of fine early-stage precipitates and closely spaced G.P. zones [5,11,13,14]. The values of thermal diffusivity and thermal conductivity of the aged samples are greater in comparison to the quenched sample after ageing at 230 °C for both ageing times. The appearance of a metastable semi-coherent phase is a result of increased ageing temperature, which also causes more intense precipitation, transformation, and breakdown of G.P. zones. These processes are causing the activation and faster mobility of electrons, thus raising the thermal diffusivity values. A continued increase in ageing temperature should lead to a higher release of the alloying elements from the matrix and easier movement of electrons, which leads to an increase in thermal properties, which is evident at an ageing time of 60 minutes, but not after ageing for 30 minutes.

The SEM/EDS investigation was carried out to complete the examination in greater depth and examine the structural change during the ageing. Figure 4 shows a SEM microphotograph with EDS analysis of a sample subjected to artificial aging at 230 °C for 60 min. It can be considered that finely dispersed precipitates of the metastable β" phase covers the microstructure of the aged samples, which is shown by the rectangular scanned area in spectrum 4 (S4) in Figure 4. Also, some other metastable phases appear in the microstructure, like AlFeMnSi and AlMgSiMnFe, represented by the spectrums S1-S3.

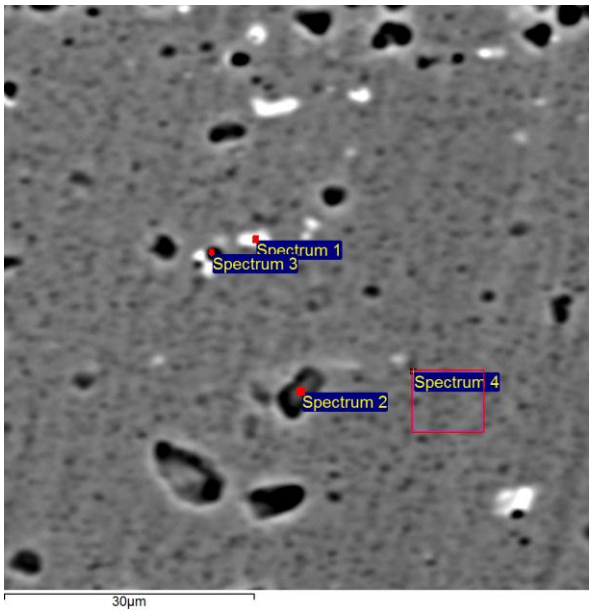

Spectrum	*Mg*	*Al*	*Si*	*Mn*	*Fe*	*Cu*
S1		86.59	5.12	2.83	5.46	
S2	0.57	98.07	1.08	0.13		0.15
S3	0.47	97.85	1.19	0.22	0.27	
S4	0.56	98.38	0.89	0.18		

**All values are in atomic %*

Figure 4 *SEM/EDS analysis of the EN AW-6082 alloy after ageing at 230°C for 60 minutes*

CONCLUSION

The conclusion in this paper can be summarized as follows: after the ageing treatment, an initial decrease in thermal diffusivity and thermal conductivity due to the formation of G.P. zones was followed by a gradual increase. The formation of metastable phases, which resulted in the matrix becoming less saturated, was responsible for the observed rise in values of thermal diffusivity and thermal conductivity. Microstructural investigation showed the existence of a finely dispersed metastable phase after ageing, which can be considered to be β'' causing the increment of thermal diffusivity and thermal conductivity values.

ACKNOWLEDGEMENT

The research presented in this paper was done with the financial support of the Ministry of Science, Technological Development and Innovation of the Republic of Serbia, within the funding of the scientific research work at the University of Belgrade, Technical Faculty in Bor, according to the contract with registration number 451-03-47/2023-01/200131.

REFERENCES

[1] Teichmann K., Marioara C.D., Marioara K.O., *et al*., Mater. Sci. Eng. A 565 (2013) 228–235.

[2] Kolar M., Pedersen K.O., Gulbrandsen-Dahl S., *et al*., Mater. Trans. 52 (7) (2011) 1356–1362.

[3] Karabay S., Mater. Design. 27 (10) (2006) 821–832.

[4] Birol Y., Trans. Nonferr. Metal. Soc. China 23 (7) (2013) 1875–1881.

[5] Cui L., Liu Z., Zhao X., *et al*., Trans. Nonferr. Metal. Soc. China 24 (7) (2014) 2266–2274.

[6] Choi S. W., Kim Y. M., Lee K. M., *et al*., J. Alloys. Compd. 617 (2014) 654–659.

[7] Choi S. W., Cho H. S., Kang C. S., *et al*., J. Alloys Compd. 647 (2015) 1091–1097.

[8] Kim Y. M., Choi S. W., Kim Y. C., *et al*., Appl. Sci. 8 (11) (2018) 2039.

[9] Pogatscher S., Antrekowitsch H., Leitner H., *et al*., Acta Mater. 59 (2011) 3352–3363.

[10] Abid T., Boubertakh A., Hamamda S., J. Alloys Compd. 490 (1–2) (2010) 166–169.

[11] Zhang C., Du Y., Liu S, *et al*., Thermochim. Acta. 635 (2016) 8–16.

[12] Vishwakarma D. K., Kumar N., Padap A. K., Mater. Res. Express. 4 (4) (2017) 046502.

[13] Edwards G. A., Stiller K., Dunlop G. L., *et al*., Acta Mater. 46 (11) (1998) 3893–3904.

[14] Lumley R. G., Deeva N., Larsen R., *et al*., Metall. Mater. Trans. A. 44 (2) (2013) 1074–1086.

MICROSTRUCTURAL AND THERMAL CHARACTERIZATION OF Bi-Sb-Sn ALLOYS FOR ECOLOGICAL APPLICATION

Ljubiša Balanović[1*], Dragan Manasijević[1], Ivana Marković[1], Uroš Stamenković[1], Marijana Petrić[2]

[1]University of Belgrade, Technical Faculty in Bor, V.J. 12, 19210 Bor, SERBIA

[2]Serbia Zijin Copper Branch TIR, Đorđa Vajferta 29, 19210 Bor, SERBIA

[*]*ljbalanovic@tfbor.bg.ac.rs*

Abstract

Bi-Sb-Sn alloys have gained attention as potential replacements for lead-tin (Pb-Sn) alloys due to their desirable properties and reduced environmental impact. These alloys offer a combination of low toxicity, low melting point, good solder ability, and mechanical strength, making them suitable for various applications in electronics and soldering. This work carried out the microstructural and thermal characterization of three-component alloys from the Bi-Sb-Sn system. Microstructural characterization of lead-free solder is essential as it provides crucial insights into the composition, distribution, and morphology of phases within the solder material. Thermal characterization of Bi-Sb-Sn alloys involves evaluating their thermal properties, including thermal diffusivity, specific heat capacity, and thermal conductivity. These properties play a crucial role in determining the performance and suitability of these alloys for various applications. Ongoing research and development in this field are expected to uncover further ecological applications for these alloys.

Keywords: Bi-Sb-Sn, lead-free solder, microstructural characterization, thermal diffusivity.

INTRODUCTION

Lead-free alternatives have become a significant area of research and development due to the harmful effects of lead on human health and the environment [1–4]. Bi-Sb-Sn alloys have gained considerable attention recently due to their potential ecological applications [5–11]. These alloys offer several environmentally friendly characteristics and find utility in various fields [7,9–12].

One of the primary motivations for exploring Bi-Sb-Sn alloys is their potential to replace lead-based solder materials [5,8,9,11,13]. Lead is a toxic element that poses severe health risks and environmental hazards [3,4]. Implementing lead-free solders has become crucial due to environmental concerns regarding the toxicity of lead-based solder materials [12,14]. Bi-Sb-Sn alloys offer a promising alternative, exhibiting low melting points, desirable mechanical properties, and good wetting behaviour on different substrates [10,12,15–18].

Bi-Sb-Sn alloys have been used in low-temperature applications, such as cryogenic systems and superconducting devices [19,20]. These alloys can exhibit good mechanical and thermal properties at extremely low temperatures, making them useful in research, medical, and space-related applications.

Bi-Sb-Sn alloys are relatively non-toxic compared to lead and other heavy metals. This property makes them suitable for applications where human and environmental safety is concerned. Using these alloys helps minimize the release of harmful substances into the ecosystem [12,21,22].

Bi-Sb-Sn alloys also possess good thermoelectric properties. Thermoelectric materials can convert waste heat into valuable electrical energy, offering sustainable energy generation and waste heat recovery opportunities [11,16,20,23,24].

Understanding the microstructure of Bi-Sb-Sn alloys is essential for evaluating lead-free solder's performance, reliability, and suitability in various applications [5–7,10,11,25,26]. On the other hand, thermal diffusivity is an important property to consider in solder materials as it influences their thermal management capabilities and ability to dissipate heat from electronic devices [27,28].

MATERIALS AND METHODS

The raw metals used in the study (Bi, Sb, and Sn, with a purity of 99.999 wt.%) were melted in an induction furnace with an argon atmosphere to prevent oxidation and contamination. After the melting and cooling process, the alloys from the Bi-Sb-Sn system were further processed by pressing them into the shape of a disk. The specific dimensions of the disk were a thickness of 2.50 mm and a diameter of 12.70 mm. The samples were annealed at a temperature of 100°C for three hours to eliminate internal stresses and further enhance the homogeneity of the alloy. The prepared sample's total mass was approximately 6 g. Investigated samples (S1, S2, and S3) from the Bi-Sb-Sn ternary system were with composition 0, 40, and 60 at.% of Sb and ratios Bi/Sn=1. Two sets of each sample were prepared. One set was used for microstructural characterization, and the other for thermal diffusivity measurements. Samples intended for microstructural analysis were prepared by grinding on papers with different granulations, mechanical polishing with aqueous alumina suspension, and etching with aqueous ferric chloride solution. For measuring thermal diffusivity, the upper and lower surfaces of the samples were covered with a thin layer of graphite to prevent heat dissipation and better heat absorption on the lower surface of the sample.

The microstructural properties of the alloys were investigated using scanning electron microscopy – SEM (TESCAN VEGA3 LMU) in combination with energy-dispersive X-ray spectroscopy – EDS (Oxford Instruments X-act). The thermal diffusivity of the investigated alloys was determined using the xenon-flash method at temperatures of 25°C, 50°C, and 100°C. This method is a well-established technique for measuring thermal conductivity [29]. The thermal diffusivity measurements were conducted on the Discovery Xenon Flash (DXF) 500, TA Instruments. The specific heat capacity can be determined using differential scanning calorimetry (DSC) or heat flow calorimetry. The temperature difference can determine the specific heat capacity for unknown materials, that is, by comparing the increase in the temperature of the samples with the increase in the temperature of the reference sample of known specific heat capacity. Both samples must be tested in the same differential mode [28,29]. Thermal conductivity describes the ability of a substance to conduct heat; that is, the

higher the thermal conductivity, the greater the amount of heat that can be transferred through the same cross-section at the same time [30]. As defined by Parker et al. [28,30], thermal conductivity, for homogeneous materials, after measuring the thermal diffusivity and determining the specific heat capacity, can be calculated as $\lambda = \alpha \cdot \rho \cdot Cp$. Where: λ is thermal conductivity (W/m·k), α is thermal diffusivity (m^2/s), ρ is density (kg/m), and Cp is specific heat capacity (J/kg·K).

The specific details of the experimental procedures for microstructural characterization and thermal conductivity measurements can be found in previous papers [28,31]. Combining SEM-EDS for microstructural characterization and the Xenon-flash method for thermal conductivity measurements provides valuable insights into the microstructure and thermal properties of the studied Bi-Sb-Sn alloys.

RESULTS AND DISCUSSION

Microstructural Characterization

The following figures show SEM microphotographs of investigated alloys S1, S2, and S3 at different magnifications a) 200x, b) 500x, c) 1000x, d) 2000x.

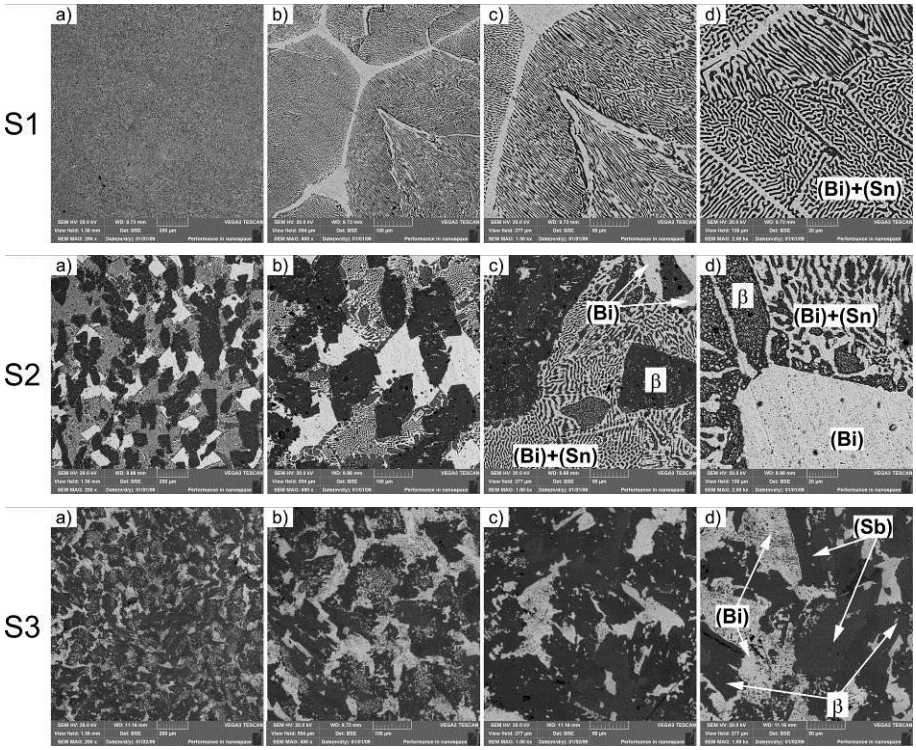

Figure 1 *SEM microphotographs of the investigated alloy S1, S2 and S3 at different magnifications a) 200x, b) 500x, c) 1000x, d) 2000x*

The provided SEM microphotographs of the investigated Bi-Sb-Sn alloys (S1, S2, and S3) reveal essential insights into the microstructure and phase composition. Based on the observed microstructural features and the EDS analysis of the present phases, the following observations can be made. A lamellar eutectic structure is evident in the SEM

microphotographs of alloy S1 at 200x magnification. This structure consists of alternating light lamellae rich in bismuth (Bi) and dark lamellae rich in tin (Sn). The lamellar structure becomes more clearly visible at higher magnifications (500x, 1000x, and 2000x), indicating well-defined boundaries between the different phases. In the SEM microphotographs of alloy S2, the microstructure reveals the presence of three distinct phases. The dark gray phase corresponds to the β phase, the light gray phase represents a solid solution based on bismuth (Bi), and the lamellar eutectic crystal composed of the bismuth and tin (Bi)+(Sn) is also observed. In the SEM microphotographs of alloy S3, a microstructure with three phases is observed. The dark gray phase corresponds to a solid solution based on antimony (Sb), the black β phase is present, and the light gray phase represents a solid solution based on bismuth (Bi). Based on the composition of the present phases determined by EDS analysis and theoretically calculated, we note a higher solubility of bismuth 10.89 at.% in solid solution based on antimony, and also higher solubility of bismuth 3.28 at.% and antimony 55.47 at.% in the β phase.

Thermal Characterization

Table 1 shows experimentally obtained thermal diffusivity results, specific heat capacity, and thermal conductivity for alloys.

Table 1 *Obtained results of thermal diffusivity, specific heat capacity, and thermal conductivity for investigated alloys S1, S2, and S3 at 25 ℃, 50 ℃, and 100 ℃*

Properties	**Samples / Temperature**	**S1**	**S2**	**S3**
Thermal diffusivity (cm^2/s)	25°C	0.0847	0.1227	0.1427
	50°C	0.0962	0.1364	0.1584
	100°C	0.1098	0.1511	0.1661
Specific heat capacity (J/(kg·K)	25°C	159.9689	167.4150	184.9377
	50°C	161.8067	169.2722	186.8094
	100°C	166.2126	173.4360	190.3570
Thermal conductivity (W/m·k)	25°C	11.2549	16.5539	20.3573
	50°C	12.9299	18.6063	22.8257
	100°C	15.1597	21.1186	24.3899

Based on the provided data from Table 1, the thermal diffusivity, specific heat capacity, and thermal conductivity of the examined Bi-Sb-Sn alloys (S1, S2, and S3) can be analyzed, and the following observations can be made. The thermal diffusivity values range from 0.0847 cm²/s to 0.1661 cm²/s in the examined alloys. Alloy S1 exhibits the lowest thermal diffusivity at 25°C, with a value of 0.0847 cm²/s. On the other hand, alloy S3 shows the highest thermal diffusivity at 100°C, with a value of 0.1661 cm²/s. The specific heat capacity values range from 159.9689 J/kg·K to 190.3570 J/kg·K in the examined alloys. Alloy S1 exhibits the lowest measured specific heat capacity at 25°C, with a value of 159.9689 J/kg·K. In contrast, alloy S3 shows the highest specific heat capacity at 100°C, with a value of 190.3570 J/kg·K.

The thermal conductivity values show a similar trend to the thermal diffusivity and specific heat capacity. The lowest calculated thermal conductivity value is 11.2549 W/m·K at 25°C for alloy S1, while the highest thermal conductivity value is 24.3899 W/m·K obtained for alloy S3 at 100°C. Figure 2 presents the dependence of thermal diffusivity, thermal conductivity, and specific heat capacity on the antimony content in investigated alloys.

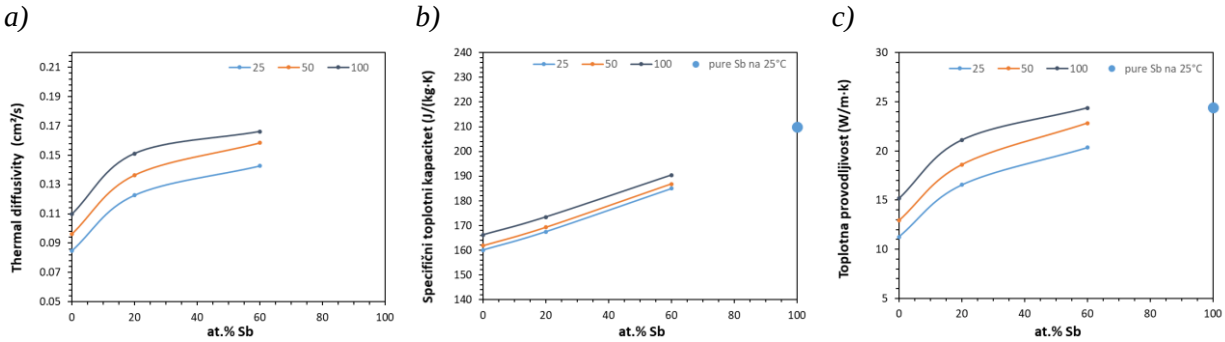

Figure 2 *Dependence of a) thermal diffusivity, b) thermal conductivity, and c) specific heat capacity on antimony content in investigated alloys S1, S2, and S3 at 25 ℃, 50 ℃, and 100 ℃*

With an increase in the antimony content in investigated alloys, it is concluded that there is an increase in the value of thermal diffusivity, and the specific heat capacity also increases, as well as the thermal conductivity. This aligns with the known thermal conductivity values of the constituent elements. Antimony has a relatively high thermal conductivity of 24.4 W/m·K, bismuth has a lower value of 8.2 W/m·K, and tin has the highest thermal conductivity of 67 W/m·K. The higher thermal conductivity of antimony compared to bismuth contributes to the overall increase in thermal conductivity as the antimony content in the alloys increases.

CONCLUSION

The microstructure and thermal properties of the Bi-Sb-Sn ternary alloys were studied in this work. The provided SEM microphotographs of the investigated Bi-Sb-Sn alloys reveal essential insights into the microstructure and phase composition. Based on the composition of the present phases determined by EDS analysis and theoretically calculated, we note a higher solubility of bismuth 10.89 at.% in solid solution based on antimony, and also higher solubility of bismuth 3.28 at.% and antimony 55.47 at.% in the β phase. Regarding the thermal properties, the study found that increasing the antimony content in the Bi-Sb-Sn alloys led to an increase in thermal diffusivity, specific heat capacity, and thermal conductivity. The higher thermal diffusivity indicates improved heat transfer capabilities, while the increased specific heat capacity suggests a more remarkable ability to store thermal energy. Moreover, the higher thermal conductivity implies better heat conduction within the alloys. Bi-Sb-Sn alloys offer significant ecological advantages, including low toxicity, RoHS compliance, sustainable sourcing, soldering process and thermal interface efficiency, low melting point, and lead-free. By embracing Bi-Sb-Sn alloys, we can support environmental sustainability by reducing toxic materials, minimizing environmental impact, and promoting resource efficiency.

ACKNOWLEDGEMENT

This work has been financially supported by the Ministry of Science, Technological Development and Innovation of the Republic of Serbia, with the funding of the scientific research work at the University of Belgrade, Technical Faculty in Bor, according to the contract with registration number 451-03-47/2023-01/200131.

REFERENCES

[1] Directive 2002/95/EC, OJEU, L 37 (2003) 19–23.
[2] RoHS 2 Directive 2011/65/EU, OJEU, L 174 (2011) 88–110.
[3] Puttlitz K., Galyon G., Impact of the ROHS directive Part I, J. Mater. Sci. Mater. Electron. 18 (1) (2007) 331–346.
[4] Puttlitz K., Galyon G., Impact of the ROHS directive Part II, J. Mater. Sci. Mater. Electron. 18 (1) (2007) 347–365.
[5] Yamauchi A., Kurose M., Mater. 15 (3) (2022) 884.
[6] Paixão J. L., Gomes L. F., Reyes R. V., *et al.*, Mater. Charact. 166 (2020).
[7] Manasijević I., Balanović L., Stamenković U., *et al.*, Mater. Test. 62 (2) (2020) 184–188.
[8] Wang F., Chen H., Huang Y., *et al.*, J. Mater. Sci. Mater. Electron. 30 (4) (2019) 3222–3243.
[9] Yamauchi A., Ida K., Fukuda M., *et al.*, Tensile properties of Sn-Bi lead-free solder alloys, in: Solid State Phenomena (2018) 72–76.
[10] Li J. G., Ma X., Zhou M. B., *et al*., Proceedings of ICEPT, 8–11 August, Shanghai, China (2018) 457–461.
[11] Yang F., Zhang L., Liu Z.Q., *et al.*, Adv. Mater. Sci. Eng. 2016 (2016).
[12] Puttlitz K. J., Stalter K. A., Handbook of Lead-Free Solder Technology for Microelectronic Assemblies, Taylor & Francis (2004), ISBN: 9780824752491.
[13] Zhang C., Liu S. D., Qian G. T., *et al.*, Trans. Nonferrous Met. Soc. China 24 (1) (2014) 184–191.
[14] Subramanian K., Lead-Free Electronic Solders: A Special Issue of the Journal of Materials Science: Materials in Electronics, Springer US, (2007), ISBN: 9780387484334.
[15] Abtew M., Selvaduray G., Mater. Sci. Eng. R Rep. 27 (5) (2000) 95–141.
[16] Combe E., Funahashi R., Takeuchi T., *et al.*, J. Alloys Compd. 692 (2017) 563–568.
[17] Watanabe H., J. Japan Inst. Electron. Packag. 8 (3) (2005) 183–187.
[18] Hu L., Zeng M., Shen B., Mod. Electron. Tech. 32 (16) (2009)
[19] Sidorenko N., Parashchuk T., Maksymuk M., *et al.*, Cryogenics 112 (2020) 103197.
[20] Yim W. M., Amith A., Solid State Electron. 15 (10) (1972) 1141–1165.
[21] Suganuma K., Curr. Opin. Solid State Mater. Sci. 5 (1) (2001) 55–64.
[22] Menon S., George E., Osterman M., *et al.*, J. Mater. Sci. Mater. Electron. 26 (6) (2015) 4021–4030.
[23] Hor Y. S., Cava R. J., J. Alloys Compd. 479 (1–2) (2009) 368–371.
[24] Martin-Lopez R., Dauscher A., Scherrer H., *et al.*, Appl. Phys. A 68 (5) (1999) 597–602.
[25] Okamoto K., Nomura K., Doi S., *et al*., Proceedings of the 46th IMAPS, 30 September–3 October, Orlando, United States (2013) 104–108.
[26] Xu K. K., Zhang L., Gao L. L., *et al.*, Sci. Technol. Adv. Mater. 21 (1) (2020) 689–711.
[27] Cowan R. D., J. Appl. Phys. 34 (4) (1963) 926–927.
[28] Parker W. J., Jenkins R. J., Butler C.P., *et al.*, J. Appl. Phys. 32 (9) (1961) 1679–1684.
[29] Gaal P. S., Thermitus M.-A., *et al.*, J. Therm. Anal. Calorim. 78 (1) (2004) 185–189.
[30] Aksöz S., Öztürk E., Maraşlı N., Meas. 46 (1) (2013) 161–170.
[31] Aksöz N., Öztürk E., Bayram Ü., *et al.*, J. Electron. Mater. 42 (12) (2013) 3573–3581.

OPTIMIZATION OF PHENOL ELECTROCHEMICAL OXIDATION USING MODIFIED Ti/SnO_2-TYPE ANODES

Vladan Nedelkovski[1], Sonja Stanković[1], Milan Radovanović[1], Žaklina Tasić[1], Snežana Milić[1]

[1]University of Belgrade, Technical Faculty in Bor, V.J. 12, 19210 Bor, SERBIA

[*]*vnedelkovski@tfbor.bg.ac.rs*

Abstract

In this paper, optimization of phenol electrochemical oxidation process using modified Ti/SnO_2-type dimensionally stabile anodes (DSA) is further discussed. This type of anodes can be modified by doping with different transition metals, rare earth elements, metal oxides, carbon nanotubes, etc.; in order to achieve specific anode surface morphology, crystal structure, electrocatalytic properties and prolonged service life. In order to increase the service life of Ti/SnO_2-Sb anodes, the formation of interlayers and modifications in the synthesis methods represent suitable options, alongside the elements through which oxide layers can be reached. These electrodes are applied in the removal of biocides, phenolic compounds, dyes, pharmaceutical products, surfactants, petrochemical compounds, etc. The following factors have the greatest influence when using these electrodes: pH, temperature, current density, and electrolyte selection.

Keywords*:* phenol, electrooxidation, modifications, optimization.

INTRODUCTION

Technological procedures based on the oxidation of organic compounds in the presence of hydroxyl radicals are collectively known as Advanced Oxidation Processes (AOPs) and are increasingly attracting the attention of researchers due to their efficiency, cost-effectiveness, and numerous other advantages such as ease of implementation and process control, automation possibilities, and combination with other purification methods, etc. [3]. The overpotential of the oxygen evolution reaction is actually a decisive factor when considering the catalytic performance of anodes in electrochemical oxidation processes, as it directly depends on the type of anodic material. When decomposing polluting organic substances in these processes, it is necessary for the overpotential of the oxygen evolution reaction to be higher (more positive) than the overpotential of the decomposition reaction of the specific organic compound. This avoids a situation where the reaction of water molecule decomposition becomes the dominant process in the system [4].

Ti/SnO_2-Sb TYPE ANODES IN ELECTROOXIDATION OF POLLUTANTS

DSA electrodes based on RuO_2 and IrO_2, despite numerous positive characteristics, are characterized by a weaker stability of the oxide layer on the substrate and high charge transfer resistance. They also possess lower overpotentials for the oxygen evolution reaction. On the other hand, PbO_2-based anodes can lead to secondary lead pollution due to the degradation of the oxide layer. For these reasons, and due to their high electrocatalytic activity, DSA

electrodes based on SnO_2 are considered more suitable [5]. In contrast to BDD (boron-doped diamond) anodes, which have an overpotential of 2.7 V for the oxygen evolution reaction compared to the standard hydrogen electrode, Ti/SnO_2 anodes have an approximate value of 1.8 V. This results in relatively lower efficiency in removing certain compounds and high electrical energy consumption [6]. However, despite the chemical stability and high catalytic ability (the ability to form hydroxyl radicals necessary for electrochemical oxidation), the high cost and the difficulty in selecting suitable materials for obtaining BDD anodes limit their broader industrial application [7]. Ti/SnO_2-Sb type DSA electrodes can be obtained using various synthesis methods such as thermochemical decomposition, electrodeposition, hydrothermal synthesis, ultrasonic spray pyrolysis, sol-gel process, self-assembly process, etc. [6].

In order to improve the performance and stability of DSA anodes, researchers are focusing on synthesizing nanostructured DSA anodes, which involve forming nanostructures of different shapes and compositions (TiO_2 nanotubes, carbon nanotubes, IrO_2, Au, Pt, etc.) with the aim of enhancing electrocatalytic activity. Antimony is the most common accompanying element in tin-based DSA anodes, and its incorporation into the tin oxide layer achieves improved charge transfer capability and facilitates the generation of hydroxyl radicals to a greater extent [8].

Montilla *et al*. [1] determined that platinum doping of Ti/SnO_2-Sb anodes leads to the formation of a more compact layer. By doping with platinum in relatively small amounts (3 at.%), an increase in the anode's lifespan is also achieved. Sun *et al*. [9] synthesized a Ti/SnO_2-Sb anode doped with palladium using the method of thermochemical decomposition. The doped anode had a lifespan of 150 hours, while the undoped anode (synthesized using the same method) had a lifespan of 2.8 hours, confirming the positive effect of doping. Liang *et al*. [8] found that molybdenum-doped Ti/SnO_2-Sb anode possesses a more compact oxide layer, contributing to a 36.6% longer lifespan compared to the undoped anode. Chen *et al*. [10] synthesized a Ti/SnO_2-Cu anode with an overpotential value for the oxygen evolution reaction of 2.7 V (determined relative to the standard hydrogen electrode), significantly higher than that of undoped DSA anodes based on tin and antimony.

PROCESS PARAMETERS IN ELECTROCHEMICAL OXIDATION

The factors used to assess the cost-effectiveness of a process are energy consumption (EC) and specific energy consumption (EEO) - the electrical energy required to achieve a reduction in the concentration of the compound being removed in 1 m^3 of water/solution. The electrical energy consumption (EC) can be determined using the following expressions [11,12]:

$$EC\ (kWh(g\ TOC)^{-1}) = \frac{E_{cell} It}{(\Delta TOC)_t V_s} \quad (1)$$

$$E_{EO}\ (kWhm^{-3} order^{-1}) = \frac{E_{cell} It}{V_s \log(C_0/C_f)} \quad (2)$$

In expressions (1) and (2), the following are defined: E_{cell} – the average cell voltage, I – current intensity (A), t – process duration (h), $(\Delta COD)_t$ and $(\Delta TOC)_t$ – reductions in COD (mg O_2/l) and TOC (mg C/l) after a certain time t, Vs – electrolyte volume (dm^3), C_0 – initial concentration of phenol, and C_f – final concentration of phenol [11].

To select the optimal current density, it is necessary to consider not only the oxidation/decomposition time but also the degree of current utilization. In addition, the parameter MCE (Mineralization Current Efficiency) is also present in the investigations as a direct indicator of the efficiency of the current invested in complete mineralization of a specific compound in the corresponding solution in the mineralization reaction, and it is expressed as [11]:

$$MCE = \frac{nFV_s \Delta(TOC)_t}{4,32 \cdot 10^7 mIt} 100 \ (\%) \tag{3}$$

In the expression (3), the following variables are defined: n – (theoretical) number of electrons exchanged in the decomposition, F – Faraday's constant (96485 C/mol), V_s – volume of the solution (dm^3), $\Delta(TOC)_t$ – reduction in total organic carbon content during electrochemical oxidation (mg/l), $4.32 \cdot 10^7$ – conversion factor (= 3600 s/h · 12000 mgC/mol); m – number of carbon atoms in the given compound; I – current intensity (A) and t – time (h) [11].

Table 1 *Parameters determined during the electrooxidation of phenol under different conditions [12]*

Parameter		Phenol degradation efficiency t_{10min} (%)	k (min^{-1})	Total organic carbon (%)	EC (kWh/ gTOC)	E_{EO} (kWhm^{-3} $order^{-1}$)	MCE (%)
NaCl concentration (mol/dm^3)	0	12.75	0.012	20.9	2.09	47.76	14.34
	0.01	84	0.208	22.5	2.32	3.29	18.20
	0.03	100	0.592	52.9	0.8	0.81	58.35
	0.05	100	0.555	45.8	0.75	0.76	24.7
	0.07	99.7	0.422	39.4	0.55	0.67	13.04
pH	2	99.7	0.627	50	2.01	1.6	61.2
	10	99.6	0.563	38	1.52	1.77	34.18
E (V)	6	35.6	0.041	4	1.02	1.31	1
	10	95.8	0.316	34	0.51	0.72	13.2
Initial phenol concentration (mg/l)	10	99.4	0.509	55	0.71	0.21	7.9
	100	52.9	0.086	20	0.93	5.67	13.2

By analysing the data in Table 1, it was concluded that the addition of NaCl reduces energy consumption to minimum values of 0.55 kWh/gTOC and 0.67 kWh/m^3 for a NaCl

concentration of 0.07 mol/dm^3. This can be explained by the increased conductivity of the electrolyte. However, at a NaCl concentration of 0.03 mol/dm^3, the fastest removal of phenol, i.e., total organic carbon, is achieved, which is consistent with the MCE value of 58.35%. The obtained MCE values reflect the influence of pH on the process efficiency, confirming that in acidic conditions, hypochlorous acid is the primary chemical species with higher oxidation capacity than hypochlorite ions, which are the primary species in alkaline conditions [12]. Increasing the potential to 8 V eventually results with maximum removal of total organic carbon, while further increase up to 10 V leads to a reduction in the polluting substance removal percentage due to the competitiveness of oxygen evolution and chlorine evolution reactions [13]. Table 2 shows the removal efficiency – EU (%) of certain pollutants using modified electrodes under different process parameters: Time τ (min), pH values, temperature (°C), initial phenol concentration (g/l), current density j (A/cm^2), i.e., cell voltage U (V) or current intensity I (A).

Table 2 *Phenol removal efficiency using Ti/SnO_2-type electrodes under different process parameters*

Electrode	τ (min)	j (A/cm^2) *U (V)	t (°C)	Electrolyte	C_0 (g/l)	pH	EU (%)	Reference
Ti/SnO_2-Sb	<20	*8	25	0.03 M NaCl	0.05	6	100	[12]
Ti/Sb-SnO_2-La	120	1	30	0.25 M Na_2SO_4	0.1	/	86.7	[13]
Ti/Mn/Sb-SnO_2-La							81.9	
Ti/Fe-Mn/Sb-SnO_2-La							67.3	
Ti/Ce-Mn/Sb-SnO_2-La							88.8	
Ti/SnO_2-Sb-RuO_2/α-PbO_2/β-PbO_2	360	20	30	0.014 M Na_2SO_4	0.5	/	86	[14]
Ti/SnO_2-Sb-RuO_2/α-PbO_2/β-PbO_2		40					73	
Ti/SnO_2-Sb-RuO_2/α-PbO_2/β-PbO_2		100		0.5 M H_2SO_4	1		77	
Ti/SnO_2-Sb	60	0.01	25	0.34 M NaCl	0.1	7	90	[15]
Ti/SnO_2–Sb_2O_4	>60	0.04	25	0.25 M NaCl	0.1	10.5	99	[16]
Ti/SnO_2-Sb	300	0.02	25	0.25 M Na_2SO_4	0.49	5.3	100	[17]
Ti/SnO_2–Sb_2O_3–Nb_2O_5/PbO_2	120	0.02	20	0.05 M Na_2SO_4	0.5	7	78.6	[18]
				0.36 M NaCl			97.2	

At higher potential values, a greater removal of phenol is achieved, while the process rate at lower potential values is influenced by mass transfer degrees. When the process is limited by mass transfer, increasing the potential promotes the occurrence of undesired reactions (RSK). Increasing the potential up to 8 V leads to maximum removal of total organic carbon, while further increase up to 10 V results in a decrease in the removal percentage due to the competitiveness of oxygen evolution and chlorine evolution reactions. Therefore, a potential value of 8 V is considered optimal, with the lowest energy consumption and the highest achieved removal of total organic carbon. Higher initial concentrations of phenol have shown a decrease in removal efficiency.

CONCLUSION

In addition to the widespread use of DSA electrodes in laboratory tests and industrial wastewater treatment processes, the use of this type of electrode limits electrochemical oxidation processes due to disadvantages in terms of shorter working life and/or potential leaching of cations of toxic metals in highly acidic solutions. Based on a large number of studies on the decomposition of poorly soluble compounds, it was found that DSA anodes exhibit better performance at higher temperatures and in acidic environments, which is consistent with the fact that the oxidation ability of reactive species is largely determined by the pH value. Electrochemical oxidation as a purification process has numerous advantages in industrial application, such as automation, absence of additional chemicals, the possibility of treating cloudy and colored wastewater, relatively low operating costs, etc. In order to achieve the complete application of DSA anodes for the electrochemical oxidation of poorly soluble organic compounds, researchers are increasingly directed towards examining the mechanisms of decomposition and the role of reactive chemical species in the oxidation itself, more economical but - effective methods of preparation and synthesis (for the purpose of obtaining DSA electrodes with the desired physical and chemical properties), as well as the possibility of coupling with other technological purification procedures - in order to reduce the costs of the electrochemical oxidation process and increase degradation efficiency of many toxic organic compounds.

ACKNOWLEDGEMENT

The authors are grateful to the Ministry of Science, Technological Development and Innovation of the Republic of Serbia for financial support according to the contract with the registration number 451-03-47/20223-01/200131.

REFERENCES

[1] Montilla F., Morallón E., De Battisti A., *et al*., J. Phys. Chem. B. 108 (2004) 5036–5043.

[2] Wu W., Huang Z., Lim T., Appl. Catal. 480 (2014) 58–78.

[3] Santos D. H. S., Duarte J. L. S., Tavares M. G. R., *et al*., Chem. Eng. Process. 153 (2020) 107940.

[4] Shao C., Zhang F., Li X., *et al*., J. Electroanal. Chem. 832 (2019) 436–443.

[5] Duan Y., Chen Y., Wen Q., *et al*., J. Electroanal. Chem. 768 (2016) 81–88.

[6] Chen A., Xia S., Ji Z., *et al*., Appl. Surf. Sci. 471 (2019) 149–153.

[7] Li X., Yan J., Zhu K., J. Electroanal. Chem. 878 (2020) 30373-30383.

[8] Liang J., Geng C., Li D., *et al*., JMST 31 (2015) 473–478.

[9] Sun, Y., Cheng, S., Yu, Z., *et al*., J. Alloys Compd. 834 (2020), 155184.

[10] Chen, A., Zhu, X., Xi J., *et al*., J. Alloys Compd. 683 (2016), 501–505.

[11] Brillas E., Sirés I., Oturan M. A., Chem. Rev. 109 (2009) 6570–6631.

[12] Santos G. O. S., Dória A. R., Vasconcelos V. M., *et al*., Chemosphere 259 (2020) 127475.

[13] Bi Q., Wang Z., Dang C., *et al*., J. Alloys Compd. (2020) 158033.

[14] Zheng Y., Su W., Chen S., *et al*., J. Chem. Eng. 174 (2011) 304–309.

[15] Santos I. D., Gabriel S. B., Afonso J. C., *et al*., Mater. Res. 14 (2011) 408–416.

[16] Loloi M., Rezaee A., Aliofkhazraei M., *et al*., ESPR 23 (2016) 19735–19743.

[17] Li X. Y., Cui Y. H., Feng Y. J., *et al*., Water Res. 39 (2005) 1972–1981.

[18] Yang X., Zou R., Huo F., *et al*., J. Haz. Mat. 164 (2009) 367–373.

INFLUENCE OF SUBSTITUTES ON THE EFFICIENCY OF ORGANIC CORROSION INHIBITORS

Aleksandar Cvetković[1*], Žaklina Tasić[1], Marija Petrović Mihajlović[1], Ana Simonović[1], Milan Radovanović[1], Maja Nujkić[1], Milan Antonijević[1]

[1]University of Belgrade, Technical Faculty in Bor, V.J. 12, 19210 Bor, SERBIA

[*]*acvetkovic@tfbor.bg.ac.rs*

Abstract

In this paper, a comparison of different organic compounds and their derivatives regarding the effectiveness of corrosion inhibition was made. The following derivatives of organic compounds were taken in consideration: triazole, imidazole, thiophene, hydrazine, thiosemicarbazone and semicarbazone. All of the organic compounds possess one or more heteroatoms in their structure such as oxygen, nitrogen, phosphorus and sulfur. It was found that there is no one given corrosion inhibitor which is the best for all investigated situations. Hence, according to the conditions in which the corrosion takes place, a potential organic corrosion inhibitor should be tested.

Keywords: corrosion, inhibition, organic, inhibition efficiency.

INTRODUCTION

Corrosion is a process of material degradation, most common in aqueous solutions with a large number of potential corrosion agents. Corrosion presents a big risk for human life and leads to large economic losses due to degradation of the infrastructure. Hence corrosion should be prevented or slowed down. One of the many methods used in the corrosion inhibition of metals is the application of organic compounds, known as organic corrosion inhibitors. Prevention and reduction of corrosion is a big area of research in material science. The main benefit is the reduction of economic loss as well the prevention of human casualties as a consequence of structural failure caused by corrosion. The inhibition efficiency of organic molecules is rated by their ability to cover a large percent of a metal surface. These values can be obtained by theoretical methods such as quantum chemical calculations or with experimental procedures and depend on the chemical structure of the investigated compound and medium in which the inhibitor is tested. In order for an organic compound to be classified as a good choice for corrosion inhibition it must contain at least one or more heteroatoms in its structure. In addition to heteroatoms such as nitrogen, oxygen, phosphorus and sulfur, an organic corrosion inhibitor can possesses one or more atomic functional groups and aromatic rings [1–10]. The inhibitive property is correlated with the strength of the bond between the metal surface and the organic compound, consequently the best inhibitors possess some heteroatoms like sulfur, oxygen, nitrogen or phosphorous that introduce a good binding point to the metal surface. In the literature, the most common parameters to be observed, when it comes to corrosion inhibition efficiency, are the highest occupied molecular orbital (E_{HOMO}), the lowest unoccupied molecular orbital (E_{LUMO}) energy as well as the dipole moment and

other parameters that are the result of the structure of a given organic compound. The value of corrosion inhibition efficiencies are first looked at through theoretical methods as quantum chemical calculations and later proven with experimental methods such as electrochemical impedance spectroscopy (EIS), electrostatic force microscopy (EFM), mass loss method and other potentiometric methods [1–3,6,10–12].

This paper is a literature review of inhibition efficiencies of following organic compounds: triazoles, imidazole, thiophene, hydrazine, thiosemicarbazone and semicarbazone. Their values of inhibition efficiencies as well as the solution and metal surface were presented in a tabular form [2–10].

RESULTS AND DISCUSSION

Properties of organic compounds as corrosion inhibitors

Triazole and its derivatives as corrosion inhibitors

A triazole is a five-membered organic compound with three nitrogen atoms in the structure [7,13–15].

Mohamed *et al*. [7], Garcia-Ochao *et al*. [13], Sherif *et al*. [14] and Mert *et al*. [15] in their works conclude that triazoles can bind to the metal surface both with physisorption and chemisorption through one or more of their nitrogen atoms. Beside that the main orientation of triazoles is vertical and can make a polymer like chain on the surface of the metal. With different methods, the researchers have obtained different results of corrosion inhibition properties for few triazole derivatives (Table 1).

Table 1 *Inhibition efficiencies of triazole and its derivatives*

Name	E_{HOMO} (eV)	E_{LUMO} (eV)	Metal	Solution	IE% (min–max)	References
5-amino-1,2,4-triazole	-12.653	-6.068	Copper	/	56*	[7]
	/	/	Steel	0.5M HCl	77–94	[13]
3-amino-1,2,4-triazole-5-thiol	/	/	Brass	3% NaCl	94.7–98.97	[16]
	/	/	Aluminum	0.5 NaCl	76.2–86.1	[14]
	-5.948	-0.6721	Carbon steel	0.5 HCl	43.1–97.7	[15]
5-amino-1,2,4-triazole-3-thiol	-9.905	-6.504	Copper	/	95*	[7]

*values from the literature obtained using theoretical methods

Imidazole and its derivatives as corrosion inhibitors

Imidazole is an aromatic organic compound containing two nitrogen atoms in a five-membered ring [9,17].

In the papers by Stupnišek-Lisac *et al*. [17], El-Haddad *et al*. [18], Otmačić *et al*. [19], Larabi *et al*. [20] and Benali *et al*. [21] different findings for imidazole and its derivatives as the corrosion inhibitors are presented. There are various ways for imidazoles to bind to the

metal surfaces but the most dominant is physisorption through the nitrogen atoms. The results that the researchers have obtained using different theoretical and experimental metodes are presented in Table 2.

Table 2 *Inhibition efficiencies of imidazole and its derivatives*

Name	E_{HOMO} (eV)	E_{LUMO} (eV)	Metal	Solution	IE% (min–max)	References
Imidazole	-9.497	-0.704	Aluminum	0.5 HCl	20.1–70.7	[18]
	/	/	Copper	0.5M H_2SO_4	22–63	[17]
	/	/	Copper	3% NaCl	49.79–67.14	[19]
2-methyl-imidazole	-9.700	-0.574	Aluminum	0.5 HCl	21.4–76	[18]
4-methyl-imidazole	/	/	Copper	3% NaCl	37.13–63.41	[19]
4-methyl-1-phenyl-imidazole	/	/	Copper	0.5M H_2SO_4	6.8–94.3	[17]
	/	/	Copper	3% NaCl	57.68–94.34	[19]
4-methyl-1-toluene-imidazole	/	/	Copper	0.5M H_2SO_4	2–89	[17]
	/	/	Copper	3% NaCl	27.84–93.03	[19]
2-thiol-1-methyl-imidazole	/	/	Copper	0.5-1M HCl	41.07–87.5	[20]
	/	/	Copper	0.5M H_2SO_4	60.44–80.94	[21]

Thiophene and its derivatives as corrosion inhibitors

Thiophene is a heterocyclic compound that contains a sulfur hetero atom in its structure. The sulfur atom represents the place of the highest charge in the structure of the molecule. Hence, beside the aromatic ring, this hetero atom represents the most likely site of interaction with the metal surface. The authors agreed that most thiophene derivatives bond to the metal surface horizontally which makes them good corrosion inhibitors [10,12,22].

Fauda *et al*. [10], Allal *et al*. [12], Khaled *et al*. [22] and Boulkroune *et al*. [23] used various theoretical and experimental methods to determine the corrosion inhibition efficiencies of thiophene and its derivatives on different metals. The values for inhibition efficiencies are given in the Table 3.

Table 3 *Inhibition efficiencies of thiophene and its derivatives on different metals*

Name	E_{HOMO} (eV)	E_{LUMO} (eV)	Metal	Solution	IE% (min–max)	References
Thiophene	/	/	Copper	2M HNO_3	32.8–80.6	[10]
	-6.5889	-0.5481	Aluminum	/	73*	[12]
	-8.709	-0.1924	Steel	0.5M H_2SO_4	35.5–43.57*	[22]
2 -thiophene carboxylic acid	/	/	Copper	2M HNO_3	50.6–74.2	[10]
	-9.3557	-1.439	Steel	0.5M H_2SO_4	62.1–78.28*	[22]
2-thiophenyl ethanol	/	/	Copper	2M HNO_3	75.4–83.6	[10]
2-acetylthiophene	-6.8874	-1.9635	Aluminum	/	86*	[12]
thiophene carbo aldehyde	-7.0024	-2.1369	Aluminum	/	92*	[12]
	-9.1906	-1.412	Steel	0.5M H_2SO_4	67.1–69.23*	[22]
	/	/	Steel	1M H_3PO_4	27.22–97.29	[23]

*values from the literature obtained using theoretical methods

Hydrazine derivatives as corrosion inhibitors

Hydrazine contains two nitrogen atoms that are connected with a double bond. In this paper, a few hydrazine derivatives are mentioned, mostly hydrazines with two functional groups such as thiophene, pyrrole, pyridine and furan. The functional groups distribute the electric charge around the molecule which makes their inhibition efficiencies differ. Hydrazines tend to bind to the metal surfaces in the vertical form which is not ideal for corrosion inhibitors [5,11].

Azzouzi *et al*. [5] and Belghiti *et al*. [11] have done both theoretical and experimental investigation of hydrazine with two functional groups of thiophene, pyrrole, pyridine and furan on their inhibition efficiencies on steel. The results are given in Table 4.

Table 4 *Inhibition efficiencies some hydrazine derivatives on steel*

Name	E_{HOMO} (eV)	E_{LUMO} (eV)	Metal	Solution	IE% (min–max)	References
1,2 - bis(thiophen-2-yl methylene) hydrazine	-5.9529	-2.3333	Steel	2M H_3PO_4	85.75*	[11]
	-7.7033	-4.5146	Steel	1M HCl	50.3–64.2	[5]
1,2 - bis(pyrrol-2-yl methylene) hydrazine	-5.4642	-1.8155	Steel	2M H_3PO_4	84.93*	[11]
	-7.5986	-4.2467	Steel	1M HCl	86.7–95.7	[5]
1,2 - bis(pyridin-2-yl methylene) hydrazine	-6.5020	-2.4688	Steel	2M H_3PO_4	82.04*	[11]
1,2 - bis(furan-2-yl methylene) hydrazine	-5.8718	-2.1695	Steel	2M H_3PO_4	79.5*	[11]

*values from the literature obtained using theoretical methods

Thiosemicarbazone and semicarbazone derivatives as corrosion inhibitors

In semicarbazones and thiosemicarbazones, the main role of binding to the metal surface is performed by the azomethyl group as well as nitrogen atoms. Thiosemicarbazones have better corrosion inhibition efficiency compared to semicarbazones due to the presence of sulfur in place of oxygen atoms in their structure [4,6,24,25].

Goulart *et al*. [4] and Khaled *et al*. [13] performed experimental analysis of thiosemicarbazones and semicarbazones with pyridine as a functional group. The results of their findings are given in Table 5.

Table 5 *Inhibition efficiencies of some tiosemicarbazones and semicarbazones derivatives*

Name	E_{HOMO} (eV)	E_{LUMO} (eV)	Metal	Solution	IE% (min–max)	References
2-pyridine carbaldehyde thiosemicarbazone	-8.525	-0.625	Carbon steel	1M HCl	44–92	[4]
	-8.9898	0.7565	Aluminum	1M HNO_3	20.5–91.2	[24]
2-pyridine carbaldehyde semicarbazone	-9.208	-0.408	Carbon steel	1M HCl	14–38	[4]

CONCLUSION

The various substitutes play a different role in the strength of binding to the metal surface which correlates to the inhibition efficiency of organic compounds. The general trend for good corrosion inhibitors is that they possess one or more atoms of nitrogen, oxygen, sulfur or phosphorus. Beside those atoms, the organic corrosion inhibitor performs better when it has aromatic rings and additional functional groups in its structure.

According to the mentioned facts, the selection of an organic compound as a corrosion inhibitor should be made in relation to the conditions under which corrosion occurs as well as the type of metal.

ACKNOWLEDGEMENT

The authors are grateful to the Ministry of Science, Technological Development and Innovation of the Republic of Serbia for financial support according to the contract with the registration number (451-03-47/2023-01/200131).

REFERENCES

[1] Verma D. K., Aslam R., Aslam J., *et al*., J. Mol. Struct. 1236 (2021) 130294.

[2] Khalil S. M., Ali-Shattle E. E., Ali N. M., Z. Naturforsch (2013) 581–586.

[3] Bedair M. A., J. Mol. Liq. 219 (2016) 128–141.

[4] Goulart C. M., Esteves-Souza A., Martinez-Huitle C. A., *et al*., Corros. Sci. 67 (2013) 281–291.

[5] El Azzouzi M., Aouniti A., Tighadouin S., *et al*., J. Mol. Liq. 221 (2016) 633–641.

[6] Zaidon F. H., Kassim K., Zaki H. M., *et al*., J. Mol. Liq. 329 (2021) 115553.

[7] Awad M. K., Mustafa M. R., Abo Elnga M. M., Journal of Molecular Structure: THEOCHEM 959 (2010) 66–74.

[8] Jamalizadeh E., Jafari A. H., Hosseini S. M. A., Journal of Molecular Structure: THEOCHEM 870 (2008) 23–30.

[9] Costa S. N., Almeida-Neto F. W. Q., Campos O. S., *et al*., J. Mol. Liq. 326 (2021) 115330.

[10] Fouda A. S., Wahed H. A., Arab. J. Chem. (2011).

[11] Belghitia M. E., Echihic S., Dafali A., *et al*., Appl. Surf. Sci. 491 (2019) 707–722.

[12] Allal H., Belhocine Y., Zouaoui E., J. Mol. Liq. (2018).

[13] Lavari L., Benali O., Mekelleche S. M., *et al*., Appl. Surf. Sci. 253 (2006) 1371–1378.

[14] Benali O., Larabi L., Harek Y., J. Saudi Chem. Soc. 14 (2010) 231–235.

[15] Khaled K. F., Corros. Sci. 52 (2010) 2905–2916.

[16] Ebenso E. E., Ekpe U. J., Ita B. I., *et al*., Mater. Chem. Phys. 60 (1999) 79–90.

[17] Garcia-Ochao E., Genesca J., Surf. Coat. Technol. 184 (2004) 322–330.

[18] Sherif E. M., J. Ind. Eng. Chem. (2013).

[19] El-Haddad M. N., Fouda A. S., J. Mol. Liq. 209 (2015) 480–486.

[20] Omašić H., Stupnišek-Lisac E., Electrochim, Acta 48 (2003) 985–991.

[21] Mert B. D., Mert M. E., Kardas G., *et al*., Corros. Sci. 53 (2011) 4265–4272.

[22] Damej M., Chebabe D., Abbout S., *et al*., Heliyon 6 (2020).

[23] Khaled K. F., Al-Mobarak N. A., Int. J. Electrochem. Sci., 7 (2012) 1045–1059.

[24] Boulkroune M., Chibani A., Chem. Sci. Trans. (2012) 355–364.

[25] Lisac E. S., Gazivoda A., Madžarac M., Electrochim. Acta 47 (2002) 4189–4194.

MODIFIED MEMBRANES WITH GRAPHENE OXIDE – REMOVAL OF DYES FROM WASTEWATER

Sonja Stanković[1*], Maja Nujkić[1], Žaklina Tasić[1], Dragana Medić[1], Aleksandra Papludis[1], Snežana Milić[1]

[1]University of Belgrade, Technical Faculty in Bor, V.J. 12, 19210 Bor, SERBIA

[*]*sstankovic@tfbor.bg.ac.rs*

Abstract

Improper disposal of wastewater containing synthetic dyes, due to carcinogenic, teratogenic and mutagenic effects, poses a danger to the environment and human health. Synthetic dyes form wastewater can be effectively removed by membrane separation processes. However, during wastewater treatment, contamination of the membranes can occur and increase the costs of wastewater treatment. Membrane contamination can be overcome by modifying the membranes with graphene oxide. Therefore, the modification of conventional membranes has attracted the attention of numerous researchers in the past few years. This paper provides an overview of scientific research on methods of membrane modification with graphene oxide and the effectiveness of removing synthetic dyes from wastewater.

Keywords: modified membranes, graphene oxide, synthetic dyes, wastewater treatment.

INTRODUCTION

Synthetic dyes are widely used in various industrial sectors, for dyeing paper, leather, textiles, plastics, etc. [1,2]. Contamination of aquatic ecosystems with synthetic dyes is a growing problem worldwide, because about 20% of the total amount of produced dyes is released into the environment without adequate treatment [3,4]. The presence of dyes in surface waters can reduce solar air infiltration and negatively affect photosynthetic activities [1,3]. In addition, consumption of water contaminated with synthetic dyes can lead to kidney disease, liver disease and damage to the central nervous system [1]. Therefore, the removal of synthetic dyes from industrial wastewater is important in protecting the environment and preserving human health.

Membrane separation processes represent an efficient and economical method for dyes removal, because they not require the use of flocculants, coagulants, etc. and do not lead to the formation of toxic by–products and secondary pollution of wastewater [1,5,6]. The main disadvantage of membrane separation processes is membrane contamination [7]. In order to overcome these shortcomings and avoid additional costs, numerous research teams propose the modification of conventional membranes with carbon–based nanomaterials.

MODIFICATION OF MEMBRANES WITH GRAPHENE OXIDE

Membrane modification with carbon–based nanomaterials (carbon nanotube, graphene, graphene oxide, etc.) can improve membrane performance and prevent contamination [8].

Graphene oxide (GO) is considered as the most suitable inorganic material for modification of membranes, because its structure contains specific functional groups (epoxy, hydroxyl, and carboxyl groups) that can increase hydrophilic, selectivity, and reduce pollutant permeability by reducing the membrane pore size and changing their surface charge [8–10]. In addition, the introduction of GO nanosheets can limit the migration of polyelectrolyte chains and improve membrane stability [9]. Modification membranes with graphene oxide can be carried out in two ways: by applying nanosheets of GO on the surface of the membrane (membranes surface modification with GO) or by incorporating nanosheets of graphene oxide into the polymer matrix of the membrane (GO–blended membranes).

Membranes surface modification with GO

Layer by layer (LBL) is an environmentally friendly, simple and most commonly applied method for membrane surface modification [9,11]. The principle of membrane modification by the LBL method is based on the adsorption of oppositely charged nanosheets on the membrane surface [9]. GO nanosheets are negatively charged due to the ionization of carboxyl groups and it is necessary to use positively charged polymers. Nanosheets of GO and other compounds can be applied by pressure–assisted filtration, vacuum filtration or immersion of the membrane into the modifying solution. Depending on the last applied layer, the modified membrane can be used to remove cationic or anionic dyes [1].

Numerous researchers [5,9,12–15] have investigated the possibility of modifying membrane surfaces using the LBL method. For example Ding *et al.* [12] modified a polyethersulfone membrane (PES) with GO and TiO_2. PES membrane was synthesized by the phase inversion method and immersed in an aqueous solution of GO@TiO_2 for 1h. After that, the membrane was washed with deionized water to wipe off the redundant solution and then dried. The results of the investigation conducted by Ding *et al.* [12] indicated that after the membrane modification, the contact angle decreased from 71.4° to 34.9°, which indicates that the hydrophilicity of the modified membranes is significantly improved. As already mentioned, GO contains hydroxyl and carboxyl groups that interact with water molecules, thus increasing the hydrophilicity of the membranes. Similar results and observations were obtained by Gu *et al.* [13] and Homem *et al.* [5].

In addition to hydrophilicity, the thermal and mechanical stability of membranes can be improved by modifying the membrane surface with graphene oxide [12]. The results of Fourier–transform infrared spectroscopy, given by Ding *et al.* [12], indicate that GO@TiO_2 nanosheets are bound to the surface of the PES membrane by interfacial interactions, improving its mechanical and thermal stability.

Homem *et al.* [5] modified polyethersulfone microfiltration membrane (mPES) with polyethyleneimine (PEI) and graphene oxide. A layer of polyethylenimine, then graphene oxide, and finally a layer of polyethylenimine were applied to the surface of the membrane using pressure filtration. The results of the study conducted by Homem *et al.* [5] indicate that the performance of the modified mPES membrane compared to the unmodified membrane is significantly improved. By modifying the mPES membrane with GO, the efficiency of removing sea blue colour from aqueous solutions increased from 11.8% to 92.4–97.8%, depending on the concentration of the GO solution used for membrane modification.

A summary of selected studies evaluating efficiency of removing synthetic dyes from aqueous solutions using GO modified membranes can be found in Table 1.

Table 1 *Efficiency of removal of synthetic dyes from wastewater using surface modified GO membranes*

Membrane	Dye	Efficiency (%)	References
GO/α–$Ni(OH)_2$ (6L)	Methylene blue	99.9	[14]
GO/α–$Ni(OH)_2$ (4L)	Victoria blue	99.7	[14]
$(PEI/GO)_3$	Rose Bengal	99.9	[9]
	Brilliant Blue B	98.1	
	Eosin Y	94.7	
	Methylene blue	85.1	
MLn (n– odd number)	Congo red	>99.0	[13]
	Methyl blue		
MLn (n– even number)	Methyl violet	>99.5	[13]
LBL_3(GO)	Methyl blue	79.0	[15]
$mPES/PEI_{3.0}+GO_{0.025}+PEI_{1.5}$	Dark blue	96.1	[5]

Based on the reviewed literature [5,9,13–15] and the data shown in Table 1, it can be concluded that with the use of modified membranes, a high removal efficiency of synthetic dyes from wastewater can be achieved. The high removal efficiency of synthetic dyes is achieved thanks to an efficient barrier that is formed on the surface of the membrane by applying GO nanofilms [5].

Wang *et al.* [9] investigated the effect of GO concentration (0.50–1.25 g/L) on the removal efficiency of Methylene blue (MB). As the concentration of GO increases from 0.5 to 1.0 g/L, defects on the membrane surface decrease, which leads to an increase in MB removal efficiency. However, with increasing GO concentration, the thickness of the films deposited on the membrane surface also increases, which leads to a decrease in membrane permeability. Li *et al.* [14] investigated the influence of the number of GO nanosheets on the flux of permeate. The test results indicate that with an increase in the number of applied layers of GO (1–6), permeate flux decreases from 92.6 L $m^{-2}h^{-1}MPa^{-1}$ to 6.4 L $m^{-2}h^{-1}MPa^{-1}$. Similar results were obtained by Gu *et al.* [13], Yan *et al.* [15] and Homem *et al.* [5]. Yan *et al*. [15] point out that the decrease in permeate flux occurs due to the reduction of membrane pores or due to their complete covering with a GO nanosheets. In order to increase the selectivity of the membrane, and maintain the permeate flux at an adequate level, it is necessary to optimize the parameters of the membrane modification process [1]. In research conducted by Ding *et al.* [12] the water flow through the optimized PES/GO@TiO_2 membranes was more than 4 times higher than through the unmodified PES membrane.

GO–blended membranes

Conventional membranes can be modified by incorporating graphene oxide into the polymer matrix of the membrane, which improves the hydrophilicity, resistance to contamination, mechanical and thermal stability of the membrane. The most commonly used method for membrane matrix modification is the phase inversion method. Within this method, there are two modification techniques: on–solvent induced phase separation (NIPS) and thermally induced phase separation (TIPS). The NIPS technique is suitable for the modification of membranes that will be used in wastewater treatment. By applying this technique, membranes with asymmetric morphology, a restricted pore size range and reduced mechanical strength are obtained. The TIPS technique produces membranes with a highly porous, symmetrical structure. By adjusting the process parameter, the morphology of the membrane can be changed depending on the desired mechanical properties, pore size and desired permeate flux [1].

GO–blended membranes are widely used in the treatment of wastewater containing synthetic dyes [1]. In summary, removal efficiency of dyes using GO-blended membranes is listed in in Table 2. Based on the data shown in Table 2, it can be concluded that a high degree of removal synthetic dyes can be achieved using GO–blended membranes.

Table 2 *Efficiency of removal synthetic dyes from wastewater using GO–blended membranes*

Membrane	Dye	Efficiency (%)	References
PES–0.5 wt% CeO2/GO	Reactive red 195	88.0	[16]
	Reactive red 43	93.0	
	Yellow 105	98.0	
CS/PAAm–DADMAc/GO	Methylene blue	99.0	[17]
	Congo red		
PVDF – 0.5 wt% GO NP	Rhodamine B	67.8	[18]
Fe/GO–TA20	Mixture of dyes	99.0	[19]
0.1 wt.% rGO/TiO_2/PES	Reactive Blue 21	81.4	[20]
0.1 wt.% GO/PES		69.7	
0.1 wt.% TiO_2/ PES		73.5	
GO/PAN/PEG	Acid Red 18	99.8	[21]
	Methyl Blue	100.0	
MMGO/PES/PVP	Direct Red 16	99.0	[22]

Modifying the membranes with graphene oxide, a higher efficiency of removing synthetic dyes from aqueous solutions can be achieved. Kadhim *et al.* [23] investigated the effect of modification PES membrane with GO nanoparticles on the efficiency of acid black removal and the performance of the newly synthesized membrane. The results of the investigation indicate that after the modification of the PES membrane with graphene oxide, the efficiency of acid black removal increased from 88% to 99%. By incorporating 0.5 wt% GO nanoparticles, the porosity of the membrane increases, while the contact angle is reduced from

60.82° to 39.21°, which indicates that the hydrophilicity of the membrane surface is improved. Zhu *et al.* [18] confirmed the positive impact of incorporating 0.5 wt% GO on membrane performance. Kadhim *et al.* [23] point out that with an increase in the concentration of GO from 0.5 to 1.5 and 2 wt%, the contact angle increases, without a significant decrease in the hydrophilicity of the membrane, which indicates that there has been an aggregation of GO nanoparticles, a decrease in the effective surface area of the particles, and thus a decrease in the number of GO functional groups on membrane surface.

Safarpour *et al.* [16] modified the PES membrane with a CeO_2/GO nanocomposite. The test results indicate that the modified membrane is characterized by greater hydrophilicity and porosity. In addition, with the introduction of CeO_2/GO nanocomposite, the resistance of the membrane to contamination increased from 39 to 69%.

Januario *et al.* [1] point out that the main disadvantage of membrane modification with GO is the reduction of permeate flux, due to the reduction of the pore size. However, the results of the study conducted by Safarpour *et al.* [16] indicate that the incorporation of CeO_2/GO nanocomposite into the polymer matrix of the PES membrane increases the permeate flux. With an increase in the mass fraction of nanocomposite from 0.01 to 0.2 wt%, the permeate flux increases. The permeate flux through the modified membrane containing 0.2 wt% CeO_2/GO nanocomposite was 64% higher than the pure water permeation through the unmodified PES membrane. The introduction of CeO_2/GO nanocomposite increases the number of hydrophilic groups on the surface of the membrane and the porosity, which resulted in an increase in permeate flow through the membrane. Similar results and observations were reached by Kadhim *et al.* [23] and Zhu *et al.* [18].

CONCLUSION

Based on previous researches, it can be concluded that the hydrophilicity, selectivity and stability of the membrane can be improved by modifying the membranes with graphene oxide. The modification of membranes with GO can be carried out in two ways: applying GO nanosheets on the surface of the membrane or incorporating GO nanosheets into the polymer matrix of the membrane. The modification of the membrane surface is based on the adsorption of nanosheets of GO and other compounds on the membrane surface, whereby there is a reduction or complete covering of the membrane pores, a change in the charge of the membrane, an improvement in the hydrophilicity, selectivity and stability of the membranes. Using surface–modified membranes can achieve high efficiency in removing synthetic dyes from aqueous solutions. However, due to covering the pores of GO membranes, the flow of pure water through the membrane is reduced, which is the main drawback of this method of membrane modification. Conventional membranes can be modified by incorporating GO nanosheets into the polymer matrix of the membrane. Applying this method of modification increases the porosity, hydrophilicity and selectivity of the membrane, as well as the permeate flow.

ACKNOWLEDGEMENT

The authors are grateful to the Ministry of Science, Technological Development and Innovation of the Republic of Serbia for financial support according to the contract with the registration number 451–03–47/2023–01/200131.

REFERENCES

[1] Januario E. F. D., Vidovix T. B., de Camargo Lima Beluci N., *et al*., Sci. Total Environ. 789 (2021) 147957.

[2] Zhou Y., Lu J., Zhou Y., *et al*., Environ. Pollut. 252 (2019) 352–365.

[3] Collivignarelli M. C., Abba A., Miino M. C., *et al*., J. Environ. Manage. 236 (2019) 727–745.

[4] Yao L., Zhang L., Wang R., *et al*., J. Hazard. Mater. 301 (2016) 462–470.

[5] Homem N. C., de Camargo Lima Beluci N., Amorim S., *et al*., Appl. Surf. Sci. 486 (2019) 499–507.

[6] Ahlawat W., Dilbaghi N., Kumar S., Mater. Today 45 (2021) 5500–5505.

[7] Vatanpour V., Khadem S. S. M., Dehqan A., *et al*., Chemosphere 263 (2021) 127892.

[8] Mosadegh M., Mahdavi H., JICS 18 (2021) 2883–2896.

[9] Wang C., Park M. J., Gonyales R. R., *et al*., Desalination 549 (2023) 116357.

[10] Mahlangu O. T., Nackaerts R., Thwala J. M., *et al*., J. Membr. Sci. 524 (2017) 43–55.

[11] Wang L., Wang N., Li J., *et al*., Sep. Purif. Technol. 160 (2016) 123–131.

[12] Ding C., Qin X., Tian Y., *et al*., J. Membr. Sci. 659 (2022) 120789.

[13] Gu Y. H., Yan X., Chen Y., *et al*., 2d Mater. 7 (2020).

[14] Li Y., Wang X., Xi W., *et al*., Mater. Lett. 341 (2023) 134289.

[15] Yan X., Huo L., Ma C., *et al*., PSEP, 130 (2019) 257–264.

[16] Safarpour M., Najjariyad–Pezvasti S., Kahataee A., *et al*., J. Environ. Chem. Eng. 10 (2022) 107533.

[17] Lincy V., Prasannan A., Jayachitra R., *et al*., J. Clean. Prod. 368 (2022) 133094.

[18] Zhu Z., Wang L., Xu Y., *et al*., J. Colloid Interface Sci. 504 (2017) 429–439.

[19] Xu D., Liang H., Yhu X., *et al*., Desalination 487 (2020) 114503.

[20] Safarpor M., Vatanpour V., Khataee A., Desalination 393 (2016) 65–78

[21] Qiu Z., Ji X., He C., J. Hazard. Mater. 360 (2018) 122–131.

[22] Abdi G., Aliyadeh A., Yinadini S., *et al*., J. Membr. Sci. 552 (2018) 326–335.

[23] Kadhim R. J., Al–Ani F. H., Al–shaeli M., *et al*., Membranes 10 (2020) 366.

HUMAN HEALTH RISK ASSESSMENT OF PTEs IN ELECTROFILTER ASH AND CHRONOSEQUENCE FLY ASH FROM „TENT A“ DISPOSAL SITES

Olga Kostić[1*], Dragana Pavlović[1], Milica Marković[1], Zorana Miletić[1], Natalija Radulović[1], Miroslava Mitrović[1], Pavle Pavlović[1]

[1]Department of Ecology, Institute for Biological Research ‘Siniša Stanković’ – National Institute of the Republic of Serbia, University of Belgrade, Bulevar Despota Stefana 142, 11060 Belgrade, SERBIA

[*]*olgak@ibiss.bg.ac.ra*

Abstract

The aim of the present study was to evaluate the health risk of potentially toxic elements (PTEs) As, B, Cr, Cu, Mn, Ni and Zn in electrofilter ash (EFA) and fly ash (FA) from chronosequential FA lagoons L0, L1 and L2 (with weathering and revegetation duration of 0, 3 and 11 years, respectively) for the health of residents (children and adults) in the vicinity of Nikola Tesla A Thermal Power Plant (TENT A), Obrenovac, Serbia. Namely, spreading FA on the surrounding agricultural land, roadside and residential areas may expose the surrounding population to the harmful effects of PTEs and endanger their health through direct ingestion, dermal contact or inhalation. Health risk analysis has shown that oral ingestion of EFA and FA poses the highest potential risk to both adults and children. Children are more susceptible to the health effects of PTE compared to adults, and As poses a potential noncarcinogenic risk to children from ingestion, especially in the case of EFA and raw FA from L0 , while the noncarcinogenic risk potential of Cr in EFA is present in both children and adults. The cumulative noncarcinogenic effect of all tested elements was present in children in the case of ingestion of both EFA and FA from L0 and L1, while for adults only in the case of ingestion of EFA. On the other hand, the carcinogenic risk of EFA and FA from all lagoons was within acceptable limits. The results of this study could be useful to obtain basic information about the health risk status of people living in these areas.

Keywords: fly ash; potentially toxic elements; health risk.

INTRODUCTION

Fly ash (FA), a byproduct of coal combustion, is a hazardous material that is stored in landfills in the open because of its low utilization. The content of potentially toxic elements (PTEs) in FA is often excessive, so the possibility of fine particles from FA being dispersed into surrounding habitats means that these landfills are a constant source of pollution and a serious global environmental and ecological threat to air, water, and soil, which can also affect public health [1]. Human exposure to PTEs occurs through ingestion, inhalation, and dermal contact [2,3], and any high concentration of PTEs that enters body tissues threatens human health and leads to serious health risks [4]. Unfortunately, research on the effects of FA on human health is limited and mostly based on animal testing. However, some studies have shown that workers in thermal power plants have a higher risk of malignancy, cytogenic damage and chromosomal aberrations, while studies on parents' perceptions of children's

health have shown that 85% of parents report harmful effects of coal FA on respiratory organs, emotional and behavioral disorders in their children [5]. For these reasons, the main objective of this study was to evaluate the noncarcinogenic and carcinogenic health risks of PTEs (As, B, Cr, Cu, Mn, Ni, and Zn) for children and adults through different exposure pathways based on the content of PTE in electrofilter ash (EFA) and ash from three ash landfill lagoons where the ash was deposited and exposed to weathering and vegetation influence for 0 (L0), three (L1), and 11 (L2) years.

MATERIALS AND METHODS

Sampling and PTEs analysis

Nikola Tesla A thermal power plant (TENT A) is located in the municipality of Obrenovac (44°30' N, 19°58' E, average altitude 80 m) on the right bank of the Sava River, 41 km upstream from Belgrade, the capital of the Republic of Serbia. TENT A consists of 6 generator units with a total capacity of 1726.5 MW. Approximately 2.2–2.5 × 109 kg FA is produced annually, deposited in three lagoons on an area of 400 ha. The studies were conducted on samples of electro filter ash (EFA) and FA from all three lagoons (from a depth of 0–10 cm) characterised by ash of different ages: active lagoon – raw ash (L0), passive lagoon weathered and revegetated for 3 years (L1), and passive lagoon weathered and revegetated for 11 years (L2). Total concentrations of PTEs (As, B, Cr, Cu, Mn, Ni, and Zn) in the FA samples were analysed using inductively coupled plasma optic emission spectrometry (ICP-OES, Spectro Genesis, Spectro-Analytical Instruments GmbH, Kleve, Germany). The obtained concentrations of PTEs, which were the subject of health risk assessment, are described in detail in Kostić *et al*. [6]. In the EFA (As, B, Cr, Cu and Ni) as well as in FA from L0 (As, B, Cr and Ni) and in the two passive lagoons L1 and L2 (Ni), the concentrations of some hazardous and harmful substances exceeded the maximum permissible values in soil [7].

Health risk assessment

Noncarcinogenic risks (HQs) of PTEs to children and adults in residential areas by ingestion ($HQing$), dermal absorption ($HQder$), and inhalation ($HQinh$), and carcinogenic risks (CRs) are calculated according to USEPA recommendations [8,9] using the following equations (1)–(8):

Noncarcinogenic risk:

$$HQing = [(C \times IngR \times RBA \times EF \times ED)/(BW \times AT \times RfDo)] \times 10^{-6} \quad (1)$$

$$HQder = [(C \times SA \times AF \times ABS \times EF \times ED)/ (BW \times AT \times RfDo \times GIABS)] \times 10^{-6} \quad (2)$$

$$HQinh = [(C \times InhR \times EF \times ED)/(BW \times AT \times RfC \times PEF)] \quad (3)$$

Carcinogenic risk:

$$CRing = (C * IFS * RBA * CSFo)/AT) \times 10^{-6} \quad (4)$$

$$IFS = (EF \times EDa \times IngR\ a/BWa) + (EF \times EDc \times IngR\ c/BWc) \quad (5)$$

$$CRder = [(C \times DFS \times ABS \times CSFo)/(AT \times GIABS)] \times 10^{-6} \quad (6)$$

$$DFS = (EF \times EDa \times SAa \times AFa/BWa) + (EF \times EDc \times SAc \times AFc/BWc) \quad (7)$$

$$CRinh = C \times EF \times ED \times IUR \times 1000/AT \times PEF \quad (8)$$

The total noncarcinogenic risk for each of the three exposure pathways was assessed using the hazard index ($HI = HQing + HQder + HQinh$), which is the sum of the HQs for all exposure pathways for each PTE. The total carcinogenic risk ($TCR = CRing + CRder + CRinh$) is calculated using the same principle as the noncarcinogenic risk. Cumulative values (CHQs and CCRs) were calculated to obtain the total impact of all tested elements for each exposure route and the impact of all elements through all exposure routes together (CHI and CTCR). If the values for the noncarcinogenic risk HQ and HI are below 1, no adverse health effects are expected, whereas an increase in these values increases the possibility of adverse noncarcinogenic effects [3,10,11]. The carcinogenic risks that are between 10–4 and 10–6 are considered acceptable [3,11,12]. The values and units associated with these equations are listed in Table 1.

Table 1 *Description and values of all parameters related to health risk assessment for PTEs*

Symbol	Parameters (units)	Values	Ref.
C	PTE concentration (mg/kg)	Site specific	
IngR	Ingestion (mg/day)	200 (child) 100 (adult)	[8]
InhR	Inhalation rate (mg/day)	7.63 (child) 20 (adult)	[8]
EF	Exposure Frequency (days/year)	350 (adult, child)	[8]
ED	Exposure Duration (years)	6 (child) 38 (adult)	[8]
BW	Body Weight (kg)	15 (child) 80 (adult)	[8]
AT	Averaging time (days)	365 x ED; 365*LT=27740 (Carcinogenic) Site specific	[8]
SA	Exposed skin area (cm^2)	2373 (child) 6032 (adult)	[8]
AF	Skin adherence factor (mg/cm^2)	0.2 (child) 0.07 (adult)	[8]
ABS	Dermal absorption factor	0.03 (As) 0.001 (all other PTE)	[9]
RfD_o	Reference Dose – Oral (mg/kg-day)	0.0003 (As); 0.2 (B); 0.003 (Cr); 0.04 (Cu); 0.024 (Mn); 0.02 (Ni); 0.3 (Zn)	[9]
RfC	Reference Concentration – Inhalation (mg/m^3)	0.000015 (As); 0.02 (B); 0.0001 (Cr); 0.0024 (Cu); 0.00005 (Mn); 0.00009 (Ni); 0.0353 (Zn)	[8,13]
GIABS	Fraction of contaminant absorbed in gastrointestinal tract (unitless)	1.0 (As, B, Cu, Zn); 0.025 (Cr); 0.04 (Mn, Ni)	[9]
PEF	Particulate Emission Factor (m^3/kg)	1.36 x 10^9(region-specific)	[8]
RBA	Relative bioavailability factor	0.6 (As); 1 (all other PTE)	[8]
IFS	Resident Soil Ingestion Rate (mg/kg)	Calculated using the age adjusted intake factors equation 44625	[8]
CSFo	Oral Slope Factor $(mg/kg\text{-}day)^{-1}$	1.5 (As); 0.5 (Cr); 0.84 (Ni)	[9,13]
DFS	Resident soil dermal contact factor (mg/kg)	Calculated using the age adjusted intake factors equation 136641.4	[8]
IUR	Inhalation Unit Risk $(\mu g/m^3)^{-1}$	0.0043 (As); 0.084 (Cr); 0,0003 (Ni)	[9,13]
LT	Life time (years)	76 Site specific	

RESULTS AND DISCUSSION

Noncarcinogenic and carcinogenic risks were determined for the respective PTEs in EFA and FA of L0, L1, and L2 for both adults and children via different pathways, whereas carcinogenic risk was quantified only for the elements with defined slope factor (As, Cr, and Ni). The highest HQs, HIs, CHQs, and CHIs were found in EFA and decreased in the following order: EFA > L0 > L1 > L2, which is consistent with the fact that the concentrations of PTE in the studied samples were the highest in EFA [6]. These results

suggest that the risk of non-carcinogenic toxicity decreases with decreasing PTE content and aging of FA during exposure to weather conditions and the influence of vegetation. The risks of noncarcinogenic toxicity from ingestion of EFA and FA from all three lagoons were greater than those from dermal contact or inhalation (HQing > HQder > HQinh) for both children and adults (Tables 2 and 3), suggesting that ingestion is the most important route of exposure in terms of health risks [11,14]. In children, considering all three exposure routes of PTE, the noncarcinogenic risk was the highest for As and decreased in the following order: As > Cr > Mn > Ni > B > Cu > Zn, while in adults it decreased as follows: HQing Cr > As > Mn > Ni > B > Cu > Zn; HQder As > Cr > Mn > Ni > B > Cu > Zn; and HQinh As > Mn > Cr > Ni > Cu > B > Zn.

Table 2 *Noncarcinogenic risk (HQ, CHQ, HI and CHI) to children from ingestion, inhalation and dermal contact*

HQing	**As**	**B**	**Cr[a]**	**Cu**	**Mn**	**Ni**	**Zn**	**CHQing**
EFA	**4.04**	6.26×10^{-2}	**1.32**	4.22×10^{-2}	2.02×10^{-1}	7.80×10^{-2}	4.56×10^{-3}	**5.75**
L0	**1.54**	5.95×10^{-3}	6.38×10^{-1}	2.54×10^{-2}	1.78×10^{-1}	5.48×10^{-2}	2.75×10^{-3}	**2.44**
L1	5.53×10^{-1}	2.56×10^{-3}	3.18×10^{-1}	1.48×10^{-2}	1.16×10^{-1}	3.97×10^{-2}	1.68×10^{-3}	**1.05**
L2	4.83×10^{-1}	1.84×10^{-3}	2.48×10^{-1}	1.24×10^{-2}	1.14×10^{-1}	3.79×10^{-2}	1.51×10^{-3}	8.98×10^{-1}
HQder	**As**	**B**	**Cr[a]**	**Cu**	**Mn**	**Ni**	**Zn**	**CHQder**
EFA	4.79×10^{-1}	1.49×10^{-4}	1.25×10^{-1}	1.00×10^{-4}	1.20×10^{-2}	4.63×10^{-3}	1.08×10^{-5}	6.22×10^{-1}
L0	1.83×10^{-1}	1.41×10^{-5}	6.05×10^{-2}	6.04×10^{-5}	1.05×10^{-2}	3.25×10^{-3}	6.53×10^{-6}	2.57×10^{-1}
L1	6.56×10^{-2}	6.07×10^{-6}	3.02×10^{-2}	3.52×10^{-5}	6.90×10^{-3}	2.36×10^{-3}	3.99×10^{-6}	1.05×10^{-1}
L2	5.73×10^{-2}	4.37×10^{-6}	2.35×10^{-2}	2.95×10^{-5}	6.74×10^{-3}	2.25×10^{-3}	3.59×10^{-6}	8.99×10^{-2}
HQinh	**As**	**B**	**Cr[a]**	**Cu**	**Mn**	**Ni**	**Zn**	**CHQinh**
EFA	3.78×10^{-3}	1.76×10^{-5}	1.11×10^{-3}	1.97×10^{-5}	2.73×10^{-3}	4.86×10^{-4}	1.10×10^{-6}	8.14×10^{-3}
L0	1.44×10^{-3}	1.67×10^{-6}	5.37×10^{-4}	1.19×10^{-5}	2.39×10^{-3}	3.42×10^{-4}	6.62×10^{-7}	4.72×10^{-3}
L1	5.17×10^{-4}	7.18×10^{-7}	2.67×10^{-4}	6.94×10^{-6}	1.57×10^{-3}	2.48×10^{-4}	4.04×10^{-7}	2.61×10^{-3}
L2	4.52×10^{-4}	5.16×10^{-7}	2.08×10^{-4}	5.81×10^{-6}	1.53×10^{-3}	2.36×10^{-4}	3.64×10^{-7}	2.43×10^{-3}
HI	**As**	**B**	**Cr[a]**	**Cu**	**Mn**	**Ni**	**Zn**	**CHI**
EFA	**4.52**	6.28×10^{-2}	**1.45**	4.23×10^{-2}	2.17×10^{-1}	8.31×10^{-2}	4.57×10^{-3}	**6.38**
L0	**1.72**	5.97×10^{-3}	6.99×10^{-1}	2.55×10^{-2}	1.91×10^{-1}	5.84×10^{-2}	2.76×10^{-3}	**2.71**
L1	6.19×10^{-1}	2.57×10^{-3}	3.48×10^{-1}	1.49×10^{-2}	1.25×10^{-1}	4.23×10^{-2}	1.69×10^{-3}	**1.15**
L2	5.41×10^{-1}	1.84×10^{-3}	2.71×10^{-1}	1.25×10^{-2}	1.22×10^{-1}	4.04×10^{-2}	1.52×10^{-3}	9.90×10^{-1}

HQ—hazard quotient; CHQ—cumulative HQ; HI—hazard index; CHI—cumulative HI. Values > 1 are in bold. [a] Cr(VI).

Table 3 *Noncarcinogenic risk (HQ, CHQ, HI, and CHI) to adults from ingestion, inhalation, and dermal contact*

HQing	**As**	**B**	**Cr[a]**	**Cu**	**Mn**	**Ni**	**Zn**	**CHQing**
EFA	3.79×10^{-1}	5.87×10^{-3}	**1.24**	3.96×10^{-3}	1.90×10^{-2}	7.31×10^{-3}	4.28×10^{-4}	**1.65**
L0	1.44×10^{-1}	5.58×10^{-4}	5.98×10^{-1}	2.38×10^{-3}	1.66×10^{-2}	5.14×10^{-3}	2.58×10^{-4}	7.67×10^{-1}
L1	5.18×10^{-2}	2.40×10^{-4}	2.98×10^{-1}	1.39×10^{-3}	1.09×10^{-2}	3.72×10^{-3}	1.58×10^{-4}	3.66×10^{-1}
L2	4.53×10^{-2}	1.72×10^{-4}	2.32×10^{-1}	1.17×10^{-3}	1.06×10^{-2}	3.55×10^{-3}	1.42×10^{-4}	2.93×10^{-1}
HQder	**As**	**B**	**Cr[a]**	**Cu**	**Mn**	**Ni**	**Zn**	**CHQder**
EFA	8.00×10^{-2}	2.48×10^{-5}	2.09×10^{-2}	1.67×10^{-5}	2.00×10^{-3}	7.72×10^{-4}	1.81×10^{-6}	1.04×10^{-1}
L0	3.05×10^{-2}	2.36×10^{-6}	1.01×10^{-2}	1.01×10^{-5}	1.76×10^{-3}	5.42×10^{-4}	1.09×10^{-6}	4.29×10^{-2}
L1	1.09×10^{-2}	1.01×10^{-6}	5.03×10^{-3}	5.87×10^{-6}	1.15×10^{-3}	3.93×10^{-4}	6.66×10^{-7}	1.75×10^{-2}
L2	9.57×10^{-3}	7.28×10^{-7}	3.92×10^{-3}	4.92×10^{-6}	1.12×10^{-3}	3.75×10^{-4}	5.99×10^{-7}	1.50×10^{-2}
HQinh	**As**	**B**	**Cr[a]**	**Cu**	**Mn**	**Ni**	**Zn**	**CHQinh**
EFA	1.86×10^{-3}	8.64×10^{-6}	5.46×10^{-4}	9.69×10^{-6}	1.34×10^{-3}	2.39×10^{-4}	5.34×10^{-7}	4.00×10^{-3}
L0	7.08×10^{-4}	8.20×10^{-7}	2.64×10^{-4}	5.84×10^{-6}	1.18×10^{-3}	1.68×10^{-4}	3.23×10^{-7}	2.32×10^{-3}
L1	2.54×10^{-4}	3.53×10^{-7}	1.31×10^{-4}	3.41×10^{-6}	7.69×10^{-4}	1.22×10^{-4}	1.97×10^{-7}	1.28×10^{-3}
L2	2.22×10^{-4}	2.54×10^{-7}	1.02×10^{-4}	2.86×10^{-6}	7.51×10^{-4}	1.16×10^{-4}	1.77×10^{-7}	1.20×10^{-3}
HI	**As**	**B**	**Cra**	**Cu**	**Mn**	**Ni**	**Zn**	**CHI**
EFA	4.61×10^{-1}	5.91×10^{-3}	**1.26**	3.98×10^{-3}	2.23×10^{-2}	8.32×10^{-3}	4.30×10^{-4}	**1.76**
L0	1.76×10^{-1}	5.61×10^{-4}	6.08×10^{-1}	2.40×10^{-3}	1.96×10^{-2}	5.85×10^{-3}	2.60×10^{-4}	8.13×10^{-1}
L1	6.30×10^{-2}	2.41×10^{-4}	3.03×10^{-1}	1.40×10^{-3}	1.28×10^{-2}	4.24×10^{-3}	1.58×10^{-4}	3.85×10^{-1}
L2	5.51×10^{-2}	1.73×10^{-4}	2.36×10^{-1}	1.17×10^{-3}	1.25×10^{-2}	4.04×10^{-3}	1.43×10^{-4}	3.09×10^{-1}

HQ—hazard quotient; CHQ—cumulative HQ; HI—hazard index; CHI—cumulative HI. Values > 1 are in bold. [a] Cr(VI).

Compared with children, non-cancer risk values for adults were significantly lower for all three exposure pathways, which is in accordance with previous studies [3,14]. Higher risk values for children may be the result of higher ash intake (200 mg/day), lower body weight, longer outdoor play time, hand-to-mouth activities, intentional consumption of contaminated foods, and a less developed immune system [15]. The HQ and HI values for both children and adults were found to be lower than 1 for B, Cu, Mn, Ni, and Zn in all analyzed samples, indicating that exposure to these elements doesn't pose a significant noncarcinogenic health risk (Tables 2 and 3). However, HQing and HI, which are higher than 1 for As and Cr in EFA and FA from L0 for children and Cr in EFA for children and adults, indicate that these elements in EFA and FA from L0 pose a significantly higher noncarcinogenic risk compared with the other PTE tested.

Table 4 *Carcinogenic risk (CR, CCR, TCR and CTCR) to residents from ingestion, inhalation and dermal contact*

CRing	**As**	**Cr** [a]	**Ni**	**CCRing**
EFA	2.29×10^{-4}	2.49×10^{-4}	8.29×10^{-5}	5.61×10^{-4}
L0	8.72×10^{-5}	1.20×10^{-4}	1.16×10^{-4}	3.23×10^{-4}
L1	3.13×10^{-5}	6.00×10^{-5}	8.40×10^{-5}	1.75×10^{-4}
L2	2.74×10^{-5}	4.67×10^{-5}	8.01×10^{-5}	1.54×10^{-4}
CRder	**As**	**Cr** [a]	**Ni**	**CCRder**
EFA	8.55×10^{-5}	3.05×10^{-5}	6.35×10^{-6}	1.22×10^{-4}
L0	3.26×10^{-5}	1.47×10^{-5}	8.87×10^{-6}	5.62×10^{-5}
L1	1.17×10^{-5}	7.35×10^{-6}	6.43×10^{-6}	2.55×10^{-5}
L2	1.02×10^{-5}	5.72×10^{-6}	6.13×10^{-6}	2.21×10^{-5}
CRinh	**As**	**Cr** [a]	**Ni**	**CCRinh**
EFA	2.77×10^{-7}	1.06×10^{-5}	7.51×10^{-9}	1.09×10^{-5}
L0	1.06×10^{-7}	5.13×10^{-6}	1.05×10^{-8}	5.25×10^{-6}
L1	3.79×10^{-8}	2.56×10^{-6}	7.61×10^{-9}	2.60×10^{-6}
L2	3.32×10^{-8}	1.99×10^{-6}	7.26×10^{-9}	2.03×10^{-6}
TCR	**As**	**Cr** [a]	**Ni**	**CTCR**
EFA	3.14×10^{-4}	2.91×10^{-4}	8.93×10^{-5}	6.94×10^{-4}
L0	1.20×10^{-4}	1.40×10^{-4}	1.25×10^{-4}	3.85×10^{-4}
L1	4.30×10^{-5}	6.99×10^{-5}	9.04×10^{-5}	2.03×10^{-4}
L2	3.76×10^{-5}	5.44×10^{-5}	8.62×10^{-5}	1.78×10^{-4}

CR—carcinogenic risk; CCR—cumulative CR; TCR—total CR; CTCR—cumulative TCR; [a] Cr(VI).

Moreover, the cumulative noncarcinogenic effect of all tested elements (CHQing and CHI) in children was also present in the case of FA from L1, indicating an increased sensitivity of children to the effects of PTEs [3,12].

In our study, CCR values decreased for all three exposure pathways in the following order: CCRing > CCRder > CCRinh, and when comparing the studied samples, it can be seen that EFA has the highest potential risk for the development of cancerous diseases in residents near TENT A, which decreased in the order EFA > L0 > L1 > L2 (Table 4). The highest CR values were found for As and Cr, and it is known that chronic exposure to As can cause skin, lung, and bladder cancer in humans [16], and Cr(VI) is classified in the A group of carcinogens. elements [17]. However, the carcinogenic risks of EFA and FA from all tree lagoons were within acceptable limits of 1×10^{-4} to 1×10^{-6}, indicating that carcinogenic risks to residents around TENT A were not expected.

CONCLUSION

The potential health risks of PTEs (As, B, Cr, Cu, Mn, Ni, and Zn) in elecrtofilter ash (EFA) and fly ash (FA) from chronosequence disposal lagoons to residents near TENT A, Obrenovac, Serbia, were evaluated using a model developed by USEPA. The health risk analysis showed that children are more susceptible to the health effects of PTE compared to adults and that the main route of adverse effects is ingestion. The noncarcinogenic risks of the tested samples were in the acceptable range for all tested PTEs, except for As in EFA and FA from L0 for children and Cr in EFA for both children and adults, while the cumulative noncarcinogenic effect of all tested PTEs was present in children and adults in case of ingestion of EFA, while it was also present in children in case of ingestion of FA from L0 and L1. Although the results show that the total potential carcinogenic risk for residents near TENT A is in the acceptable range, the potential for the development of carcinogenic diseases is the highest in the case of EFA ingestion and decreases with decreasing concentration of PTEs (EFA > L0 > L1 > L2). Finally, the results of this study may be useful in providing baseline information on the health risk status of people living near TENT A.

ACKNOWLEDGEMENT

This work was supported by the Ministry of Science, Technological Development and Innovation of the Republic of Serbia, grant no. 451-03-68/2023-14/200007.

REFERENCES

[1] Weber J., Kocowicz A., Debicka M., *et al*., J. Soils Sediments 17 (2017) 1852–1861.

[2] Singh P. K., Shikha D., Saw S., Environ. Sci. Pollut. Res. 30 (2023) 7752–7769.

[3] Pavlović D., Pavlović M., Perović V., *et al*., Int. J. Environ. Res. Public Health 18 (2021) 9412.

[4] Paithankar J. G., Saini S., Dwivedi S., *et al*., Chemosphere 262 (2021) 128350.

[5] Kravchenko J., Lyerly H. K., N. C. Med. J. 79 (5) (2018) 289–300.

[6] Kostić O., Jarić S., Gajić G., *et al*., Catena 163 (2018) 78–88.

[7] OGRS (1994), Regulation about allowable quantities of hazardous and harmful substances in the soil and methods for their investigation. Official Gazette of the Republic of Serbia (Sluzbeni glasnik RS) 23/94 (*in Serbian*).

[8] USEPA (2020a), Regional Screening Levels (RSLs)—User's Guide. *Available on the following link*: www.epa.gov/risk/regional-screening-levels-rsls-users-guide.

[9] USEPA (2020b), Regional Screening Levels (RSLs)—Equations. Available *on the following link*: www.epa.gov/risk/regional-screening-levels-rsls-equations.

[10] USEPA (2001), Supplemental guidance for developing soil screening levels for superfund sites. Peer Rev. Draft. OSWER 2001, 9355, 4–24.

[11] Pazalja M., Salihivić M., Sulejmanović J., *et al*., Sci. Rep. 11 (2021) 17952.

[12] Baltas H., Sirin M., Gökbayrak A. E., Chemosphere 241 (2020) 125015.

[13] USDOE (2011), The risk assessment information system (RAIS). U.S. Department of Energy's Oak Ridge Operations Office (ORO).

[14] Tao X-Q., Shen D-S., Shentu J-L., *et al*., Environ. Sci. Pollut. Res. 22 (2015) 3558–3569.

[15] Guney M., Zagury G. J., Dogan N., *et al*., J. Hazard Mater. 182 (2010) 656–664.

[16] USEPA (1999), Integrated Risk Information System (IRIS) Chromium (VI) U.S. Environmental Protection Agency, National Center for Environmental Assessment *Available on the following link*: https://iris.epa.gov/static/pdfs/0144_summary.pdf.

[17] Hong Y. S., Song K. H., Chung J. Y., J. Prev. Med. Public Health 47 (5) (2014) 245–252.

30th International Conference Ecological Truth & Environmental Research
20–23 June 2023, Serbia

EFFECT OF EXTRACT *Ecklonia maxima* ON CONDITION OF AGRICULTURAL CROPS

Markola Saulić[1*], Vladan Trajić[2], Darko Stojićević[1], Aleksandar Stevanović[1], Zlata Živković[1]

[1]Academy of Applied Technical Studies Belgrade, College of Applied Engineering Sciences, Nemanjina 2, Požarevac, SERBIA

[2]STR "Mali Trg", Gandijeva 15, 12313 Kobilje, SERBIA

[*]*msaulic@atssb.edu.rs*

Abstract

Kelpak® (SL – a water soluble concentrate) is manufactured from the kelp species Ecklonia maxima, which grows only in the clean, cold waters off the Atlantic Coast of southern Africa. This seaweed concentrate made is used worldwide as a biostimulant for a number of agricultural crops. Concentrate contains auxins, cytokinins, polyamines, gibberellins, abscisic acid, and brassinosteroids which are known to have a positive effect on plant growth. In this study, the influence of Ecklonia maxima extract on the growth and condition of the agricultural crop (sunflower and tulip) was described. During 2020/2021, research was conducted in an agricultural farm in the village of Brežane. Immediately before planting, the tulip bulbs were treated with a 1% Kelpak® solution, and the second treatment was done 14 days after planting. In sunflower, the concentrate was applied foliar, when the crop had 3 pairs of leaves. In both cases the treated plants had better condition compared to the control. Kelpak® showed positive effect on the growth of tulip bulbs and the fitness of the sunflower. These preliminary results encouraged to continue this type of research on the other cultivated plants.

Keywords: *Ecklonia maxima*, Kelpak®, tulip, sunflower, biostimulant.

INTRODUCTION

Seaweed extract (SE) application is a contemporary and sustainable agricultural practice used to improve and quality of agriculture and vegetable crops. The main types of algae from which components are extracted for the production of biostimulators, all macroalgae, are classified into three groups based on their color: *Phaeophita* more familiar as brown algae, *Rhodophita* known as red algae and *Chlorophita* or green algae. Among the brown algae, *Ascophillum nodosum*, *Ecklonia maxima*, *Macrocystis pyrifera*, *Durvillea potatorum*, *Fucus vesiculosus*, together with some species of the genus *Laminaria*, are mostly used as a raw material for the production of commercial extracts.

Ecklonia maxima (Phaeophiceae) brown alga grows abundantly on the west coast of South Africa and it's used for the production of alginate, animal feed, nutritional supplements and fertilizers [1]. Their extracts are commercially available in various forms and have been applied to many crops for their growth-promoting effects. The supplementation made of seaweed extract *E. maxima* through a solution of mineral nutrients, enhanced plant growth

and improved yield and many morphological and physiological traits (biomass accumulation, leaf expansion, stomatal conductance, water use efficiency, nitrogen use efficiency, etc.) [2]. Plant biostimulants, such as seaweed extracts, represent interesting tools for reducing the use of chemicals and improving crop tolerance to stresses caused by various abiotic factors [3].

Kelpak liquid seaweed extract (SL – water-soluble concentrate) is the name of a product based on seaweed extract *E. maxima*. Scientific trials proved that Kelpak's unique activity has provided consistent and significant benefits to farmers for four decades [4]. Application of biostimulant Kelpak SL significantly reduces the content of cellulose, hemicellulose and lignin and significantly increased non-structural carbohydrates in plants [5]. Also, auxins as one of the main regulators of plant growth contained in extracts of *E. maxima* affects root growth and its development, increasing root size and vitality [6]. and significantly enhances yield parameters, mineral profile, nutritional and functional features and nitrogen use efficiency (NUE) [7].

From *E. maxima* have been isolated two more phenolic compounds 4-(3,5-dihydroxyphenoxy) dibenzo-p-dioxin-1,3,6,8-tetrol (Eckol) and benzene-1,3,5-triol (phloroglucinol: PG) (Figure 1). PG has been documented to have numerous applications in micropropagation, and Eckol is mainly valued for its therapeutic potential [8].

Figure 1 *Structural formula of phenolic acids 4-(3,5-dihydroxyphenoxy) dibenzo-p-dioxin-1,3,6,8-tetrol, Eckol (a) and benzene-1,3,5-triol, phloroglucinol (b) isolated from Ecklonia maxima and tested [1]*

The aim of the preliminary research in this paper was to monitor the effects of Seaweed Extract *Ecklonia maxima* in the form of Kelpak Liquid Seaweed Extract on the growth and development of tulips and sunflowers.

MATERIALS AND METHODS

Preliminary research was carried out on the agricultural farm of the Trajić family, in the village of Brežani, Požarevac municipality, Braničevo district (S 44° 38′ 35″, E 21° 04′ 21″) during the winter of 2020/2021 in tulip production and in the spring of 2021 in sunflower field. Healthy and well-developed tulip bulbs (*Tulipa sp.)* were selected for this research. The first treatment was carried out immediately before planting by immersing the bulbs in 1% preparation Kelpak® (SL – water-soluble concentrate) for 2 hours. After described treatment,

the bulbs were planted in pots and nurtured in a sheltered area under controlled conditions. Control bulbs were also planted in parallel. The second treatment of the bulbs was carried out 14 days after planting with the same product. At the time of shoot emergence, control and treated bulbs were removed from the soil substrate and compared.

In the sunflower, treatment with Kelpak was carried out in the phase of 3–4 pairs of leaves at a dose of 3 L ha^{-1}. After 15 days, the condition of the plants was monitored and a randomly selected area in the middle of the plot was dug with an axe to a depth of 1.20 m. The development of the sunflower root system was observed.

RESULTS AND DISCUSSION

The rhizosphere is the soil area under the influence of root activity. Plants have developed different morphological, physiological and molecular adaptation mechanisms to adapt to the lack or excess of nutrients. Different concentrations of nutrients in the rhizosphere area can affect the processes in the rhizosphere and thus the growth of the root system, which increases the ability to absorb nutrients and the productivity of plants.

Application of *Ecklonia maxima* seaweed extract affected the growth and development of the root system in tulip bulbs, by increasing the size of the root and its absorption power. Also, these extracts influenced the formation of lateral roots, increasing the total volume of the root system. The effect of algae was also reflected in the number and size of root hairs on bulbs. Seaweed extracts contributed to improved nutrient sorption through the root system resulting in improved water and nutrient efficiency, thereby causing enhanced overall plant growth, vigor and plant fitness (Figure 2).

Figure 2 *Control tulip bulb (left) and bulb treated with seaweed extract Ecklonia maxima (right)*

In sunflower plantation, after 15 days of application of the seaweed extract *Ecklonia maxima*, it was observed that the plants were well developed and of good fitness, and digging to a depth of 1.20 m revealed a deep well-developed root system with a large number of long root hairs (Figures 3 and 4).

The preliminary data coincided with the literature where it is stated that *Ecklonia maxima* extracts improved seedling quality and promoted shoot and root growth, i.e. that intensive growth is influenced by auxin. Compared commercial biostimulant based on *E. maxima* extract and synthetic auxins NAA (1-naphthaleneacetic acid) it was established that tomato

seedlings treated with 100 µg L^{-1} of natural auxins from *E. maxima* extract produced the tallest plants (+22%), with a higher leaf number (+12%), a wider leaf area (+44%), and a stronger stem (+12%), whereas lettuce seedling growth was promoted by all the treatments, but with a greater effect by increasing auxin supplementation [6].

Figure 3 *Sunflower plant treated with seaweed extract Ecklonia maxima*

Figure 4 *Sunflower root treated with seaweed extract Ecklonia maxima*

Research of comparative study of Kelpak and isolated phenolic compounds Eckol and PG from *Ecklonia maxima* suggested that all three compounds have a positive effect on the growth and development of *Eucomis autumnalis*, but isolated phenolic compounds generally exerted higher growth stimulatory effects and remarkable stimulatory effect on the underground organs [1]. Application of the positive effect of Kelpak was observed in grasses (*Dactylis glomerata* and *Festulolium brauna*). *F. brauna* had a better nutritional value than *D. glomerata* as it was lower in cellulose, hemicellulose and lignin, but higher in non-structural carbohydrates compared with orchard grass [5]. Plant of *Brassica rapa* L. subsp. *sylvestris* L. Janch. var. *esculenta* Hort. treated with seaweed extracts of *E. maxima* showed the better crop performance which was associated with an improvement of their nutritional status (higher P and K and lower Na concentrations), higher photosynthetic rate and chlorophyll content in plants [3]. On the other hand, combination *E. maxima* SE treatment and Mo supply can improve spinach production and quality (head fresh weight (FW), ascorbic acid, polyphenols, N, P, K, Mg and nitrogen use efficiency) [7].

CONCLUSION

The application of seaweed extract (SE) is a modern and sustainable agricultural practice used to improve the yield and quality of vegetable crops. Further research may be valuable to elucidate the stimulatory effects of *Ecklonia maxima* extract, to explore the effect of this biostimulant on the growth and development of other agricultural plants.

Benefits of using seaweed extract:

- Stimulates the growth of the primary root tip and enhances the growth of lateral roots;
- Nutrients and water sorption;
- Plant development;
- Fruit and berry size;
- Fruit color and quality;
- Resistance to abiotic stresses;
- Development of leaf surface and improved process of photosynthesis;
- Better absorption of nutrients.

REFERENCES

[1] Aremu A. O., Nqobile A. M., Kannan R. R. R., *et al*., Planta 241 (2015) 1313–1324.

[2] Miceli A., Vetrano F., Moncada A., *et al*., Horticulturae 7 (440) (2021) 1–24.

[3] Di Stasio E., Rouphael Y., Colla G., *et al*., Eur. J. Hortic. Sci. 82 (6) (2017) 286–293.

[4] *Available on the following link:* www.kelpak.com.

[5] Ciepiela G. A., Godlewska A., Jankowska J., Environ. Sci. Poll. Res. 23 (2016) 2301–2307.

[6] Moncada A., Vetrano F., Esposito A., *et al*., Agronomy 12 (329) (2022) 1–19.

[7] La Bella S., Consentino B. B., Rouphael Y., *et al*., Plants 10 (2021) 1139.

[8] Kannan R. R. R., Aderogba M. A, Ndhlala A. R., *et al*., Food Res. Int. 54 (2013) 1250–1254.

SUITABILITY OF THE SOILS IN THE MUNICIPALITY OF KOVACHEVTSI, BULGARIA FOR GROWING ON EINKORN WHEAT (*Triticum monococcum*)

Metodi Mladenov[1*]

[1]University of Chemical Technology and Metallurgy, Faculty of Chemical Technology, 1756, 8 bul. St. Kliment Ohridski, Sofia, BULGARIA

[*]*mladenov@uctm.edu*

Abstract

Agro-ecological characteristics are of main importance for the cultivation of agricultural produce in a given area. The appropriate relationships between: climatic conditions, soil characteristics and the requirements of the crops to the particularities of the environment, determine the potential for maximally good growth and development of the particular crop and the possible yield. In this article, an analysis of soils from the municipality of Kovachevtsi, Republic of Bulgaria was made with a view to determining their suitability for growing einkorn wheat (Triticum monococcum). Seven soil samples were examined regarding the content of humus, pH, electrical conductivity, content of nutrients and heavy metals. The results show that the soil characteristics are suitable for the cultivation of einkorn (Triticum monococcum), according to the requirements of this ancient type of soft angiosperm wheat growing on different soil types. Based on the conditions and climatic characteristics, it is assumed that the obtained product should be of extremely good quality and safe for consumption.

Keywords: soil, nutrients, einkorn wheat *(Triticum monococcum)*, safety food.

INTRODUCTION

Due to the fact that it possesses the property of fertility and that the production of food products is associated with it, soil is the main means of production in agriculture and the main condition for human existence. Soil fertility is the result of the interaction of all the constituent parts and properties of the soil (physical, chemical and biological), which create the water, air, heat and nutrition regime in it. Fertility is measured by the yield of cultivated plants, and productivity by the yield of certain plants under certain climatic conditions and certain agricultural techniques [1,2].

The considered territory of the municipality of Kovachevtsi is located in the western part of Republic of Bulgaria on an area of about 140 km^2. The relief in the municipality is mainly hilly with a mountainous and semi-mountainous character. The climate in the lowest parts of the municipality with an average altitude of about 735 m refers to the temperate-continental region. In the higher parts up to 1150 m above sea level, it passes into mountain. The basin-like nature of the relief causes spring and early autumn frosts. The mountain-basin relief has a strong influence on the annual precipitation and the temperature characteristics, which show that the duration of sunshine for the year exceeds 1700 hours. The period of keeping the temperature above 10 degrees has an average duration of 130–200 days. The average annual amount of precipitation is 450 mm per square meter, and the average annual snow retention is

about 51 days. Relative humidity ranges from 58% in August to 79% in December. North-west and north-east winds prevail, the strength of which is moderate [3].

The soil cover on the territory of the municipality is diverse – gray and dark gray forest soils occupy the largest area and are the main soil type. They are deeply carbonated. The thickness of the humus horizon is on average 30–35 cm for dark gray and 65 cm for gray soils. Their mechanical composition is heavy sandy-clay and difficult to process. They are suitable for growing wheat, barley, oats, corn, rapeseed, sunflower, fodder peas, and under favorable climatic conditions, vines and some fruit species – plums, pears, strawberries, cherries, peaches – grow well on them [3]. Soil salinization is below the standard for the country, and with regard to content of heavy metals, such is not found.

The einkorn appear as a natural alternative for farmers, whose inclusion in the crop rotation would guarantee stable incomes in conditions of sudden climate changes [4]. Single-grain einkorn (*Triticum monococcum*) is extremely suitable due to its unpretentiousness, as it can be sown on different soil types. Einkorn wheat is a plant of the long day, but at the same time the crops withstand temperatures of minus 25 ^{o}C. It has an average demand for moisture, and the critical period in this regard is the grading and pouring of the grain. According to Hidalgo and Brandolini [5], this type of wheat generally has some nutritional advantages over polyploid wheats – it is poor in dietary fiber but rich in proteins, lipids, fructans and trace elements (including zinc and iron). It contains sufficient amounts of antioxidants, which further contribute to the excellent nutritional properties of produced flour.

The aim of the present work is to evaluate the suitability of the soils of the municipality of Kovachevtsi for the cultivation of einkorn wheat (*Triticum monococcum*).

MATERIALS AND METHODS

Sampling and sample preparation

The soil samples were taken from the territory of the municipality Kovachevtsi – six from the land of the village of Lobosh, in 2018 and one from the land of the village of Kalishte, in 2020. They are taken according to standard БДС 17.4.5.01 [6]. The sampling depth is 0–25 cm. Each sample is placed in a plastic box and labeled.

Pre-treatment for preparation for physico-chemical studies was carried out according to the requirements of БДС ISO 11464 [7]. The sample preparation of the samples for the analysis of the content of K, Na, Ca and Mg and heavy metals was carried out according to the standard methodology – БДС 16174 [8].

Instrumentation and measurement conditions

Conductivity measurements and pH determinations were performed with combined pH meter PCE-PHD1 (PCE instruments), according to standards methodology: БДС EN 15933 [9] and БДС ISO 11265 [10]. Phosphorus was determined spectrophotometrical [11]. The content of K, Na, Ca and Mg was determinated by FAAS, after decomposition in "aqua regia". Contents of the elements Al, Co, Cu, Fe, Zn, Ni, Cd, Mn, Pb, Cr, As, Se, and Bi were determinated by ICP-MS ("X SERIES 2"– Thermo Scientific).

Reagents

The following reagents were used to carry out the experimental work: HCl (37% suprapur, Fluka), HNO_3 (65% suprapur, Merck), H_2SO_4 (98%, pure for analysis, Valrus) and Milli-Q water (0.01 μS/cm).

RESULTS AND DISCUSSION

The established pH values of all samples (see Table 1) are in the range 6.90–7.23, which defines them as extremely favorable for the development of plants.

Table 1 *Physicochemical parameters*

Sample №	pH	Conductivity (mS/cm)
1	7.15	0.113
2	7.23	0.163
3	7.06	0.155
4	7.05	0.121
5	7.07	0.146
6	6.95	0.612
7	6.90	0.237

The determination of electrical conductivity is done in order to determine the presence of mobile forms of the elements in the solution, and usually high values for conductivity indicate the presence of a large amount of these mobile forms, mainly metals. The measured values for this indicator (see Table 1) characterize the investigated soils as poor in mobile ions of the elements, with the highest values found in sample 6, respectively 0.612 mS/cm.

Plants obtain phosphorus from the soil, where it is found in the form of organic and mineral compounds in relatively small quantities – in interval 0.05–0.25%. The amount and distribution of phosphorus compounds in the soil depend mainly on the phosphorus content of the soil-forming rock and on the conditions of soil formation. The results regarding the total content of phosphorus in the studied soil samples show that they can be characterized as poorly stocked.

Table 2 *Nutritional element content*

Element, % in dry matter	Sample №						
	1	2	3	4	5	6	7
P	0.07	0.07	0.08	0.07	0.07	0.16	0.11
K	0.44	0.73	0.57	0.70	0.42	0.61	0.55
Na	0.062	0.067	0.071	0.066	0.054	0.056	0.053
Ca	0.46	0.40	0.71	0.34	0.46	0.71	0.55
Mg	0.65	0.59	0.69	0.62	0.70	0.61	0.64
C*	3.54	3.79	4.41	4.0	4.02	4.01	3.94

* expressed as humic acids content.

The carbon content in the soil is mostly in the form of so-called humic compounds, that is why in practice it is accepted to determine the content of total carbon, and most often this indicator for brevity is designated as humus. The average content of humus in the soils in Bulgaria ranges from 2–4%. The comparison of the obtained results (Table 2) with these values show again a good stocking in the studied samples. The highest value was found in sample 3.

The elements Na, Ka, Ca and Mg serve as a source of cation nutrition for plants and belong to the group of so-called exchangeable cations. The results of their analysis show that the content of magnesium ions prevails (the exception is samples 3 and 6 where the highest values were found for the element calcium). Also the results for the sodium content of all samples are in the range of 0.05–0.75% and classified them as nonsalinized. Regarding the element K, the results (see Table 2) fall in the interval 0.4–0.7% and show a good supply of this nutrient.

The results of the analysis for the content of heavy metals carried out by means of ICP-MS are given in table 3.

Table 3 *Content of heavy metals (in dry mass)*

Concentration, mg·kg^{-1}	**Sample №**						
	1	**2**	**3**	**4**	**5**	**6**	**7**
Cr	62.5	56.8	62.6	63.2	58.6	55.0	52.3
Mn	644.2	643.0	804.0	710.5	613.2	652.1	647.1
Fe·10^3	18.3	16.0	21.1	34.4	22.6	20.4	22.7
Al·10^3	50.1	31.5	48.3	50.1	28.1	32.2	30.8
Co	15.6	11.9	15.4	19.0	12.94	12.0	11.9
Ni	43.1	33.7	41.8	37.5	35.7	32.2	34.1
Cu	47.2	39.5	43.4	45.2	37.5	38.7	34.4
Zn	76.5	68.5	76.4	74.0	72.0	73.9	62.7
As	2.4	2.7	11.6	6.3	7.8	9.4	8.7
Pb	< 0.5	< 0.5	< 0.5	< 0.5	< 0.5	< 0.5	< 0.5
Se	< 0.5	< 0.5	< 0.5	< 0.5	< 0.5	< 0.5	< 0.5
Bi	< 0.5	< 0.5	< 0.5	< 0.5	< 0.5	< 0.5	< 0.5
Cd	< 0.25	< 0.25	< 0.25	< 0.25	< 0.25	< 0.25	< 0.25
Sb	< 0.5	< 0.5	< 0.5	< 0.5	< 0.5	< 0.5	< 0.5

* Values for these elements showed with "<" represent the detection limits values.

The values obtained for the heavy metals Pb, Se, Bi, Cd and Sb are below the detection limits of the equipment used. The comparison of the results for the examined samples for the content of heavy metals with the available normatively established values for the elements As, Cu, Cr, Ni, Zn and Hg [12] show that in all soil samples, they are below the maximum permissible concentrations.

CONCLUSION

The obtained data show that the studied soils are characterized by a neutral reaction, contain optimal amounts of humus, have a low phosphorus reserve, high potassium reserve and a content of heavy metals below the maximum permissible concentrations. These characteristics show that the studied soil samples from the land of the Kovachevtsi municipality have the necessary agro-ecological prerequisites for the cultivation of einkorn wheat (*Triticum monococcum*) and for production of biological products.

ACKNOWLEDGEMENT

The author would like to thank of Petar Nikolov for its help for specifying the soil-sample points and the Science and Research Sector of the UCTM – Sofia for the financial support (Contract № 12364/2023).

REFERENCES

[1] Брощилова М., Замърсяване на почвите и въздействие върху екосистемите, Университет „проф. д-р Асен Златаров” – Бургас, 2001.

[2] Малинова Л., Почвознание и замърсяване на почвите, Издателска къща при ЛТУ-София, 2010.

[3] http://kovachevtsi.com – официален сайт на община Ковачевци.

[4] https://nivabg.com – национален сайт за земеделие.

[5] Hidalgo A., Brandolini A., J. Sci. Food Agric. 94(4) (2014) 601–612.

[6] БДС 17.4.5.01 – 85. Опазване на природата. Почва. Общи изисквания към вземането на проби.

[7] БДС ISO 11464:2012 – Soil quality. Preliminary preparation of samples for physico-chemical analysis.

[8] БДС EN 16174:2012, Утайки, обработени биоотпадъци и почви. Усвояване на разтворими в царска вода фракции и елементи.

[9] БДС EN 15933: 2012. Утайки, обработени биоотпадъци, почви и отпадъци. Определяне на pH.

[10] БДС ISO 11265: 2002. Качество на почвите. Определяне на специфичната електрическа проводимост.

[11] БДС ISO 11263: 2002. Качество на почвите. Определяне на фосфор. Спектрометрично определяне на фосфор, разтворим в разтвор на натриев бикарбонат.

[12] Наредба № 3 от 1 Август 2008 г. за нормите за допустимо съдържание на вредни вещества в почвите, обн. ДВ бр. 71/2008.

INFLUENCE OF EFFECTIVE MICROORGANISMS ON THE BASIC PARAMETERS OF SOIL BIOGENICITY IN THE PRODUCTION OF WHEAT AND CORN

Gorica Cvijanović[1*], Vesna Stepić[2], Marija Bajagić[3], Vojin Cvijanović[4], Jelena Marinković[5], Nenad Đurić[6]

[1]University of Kragujevac, Institute of Information Technologies Jovana Cvijića bb, 34000 Kragujevac, SERBIA

[2]Municipal Administration Department of Agriculture in Vladimirci, Sv. Save 38, 15225 Vladimirci, SERBIA

[3]University of Bijeljina, Faculty of Agriculture, RS, Pavlovića put bb, Bijeljina, BOSNA and HERZEGOVINA

[4]Institute for Science Application in Agriculture, Boul. Des. Stefana 68b Belgrade, 11000 Belgrade, SERBIA

[5]Institute of Field and Vegetable Crops, Maksim Gorki 39, 21000 Novi Sad, SERBIA

[6]Institute of vegetable growing, Karađorđeva 71, 11420 Smederevska Palanka, SERBIA

[*]*cvijagor@yahoo.com*

Abstract

In modern directions of food production, it is necessary to apply measures that would reduce the possibility of soil degradation. The aim of the work was to determine the influence of effective microorganisms on the basic parameters of soil biogenicity in the production of wheat and corn. The experiment with wheat was carried out in 2019 and the experiment with maize in 2017. Agroecological conditions in 2019 were optimal for wheat production. In 2017, unfavorable agrometeorological conditions for maize production were recorded. In both experiments, the microbiological preparation EM Aktiv with effective microorganisms was used. With wheat, it was applied twice foliarly with 6 l ha^{-1}. In the case of maize, EM Aktiv was introduced into the soil before sowing at 20 l ha^{-1} and foliarly applied twice at 6 l ha^{-1}. The rhizosphere soil was analyzed. The total number of microorganisms and the abundance of Azotobacter in wheat were determined. In the case of corn, the total number of microorganisms and the number of ammonifiers were determined. In both experiments, an increase in the number of tested groups of microorganisms was found. The percentage increase in abundance depended on the genotype of wheat and corn. Based on the results, it was concluded that the application of effective microorganisms is necessary and that in sustainable food production systems it should be a mandatory measure to preserve the basic resources for food production.

Keywords: Microorganisms, wheat, corn, soil, biogenicity.

INTRODUCTION

In the era of satisfying food needs, the negative impact of agricultural production on the ecosystem is increasing. Inputs in agricultural production in the form of fertilizers, pesticides

and agricultural mechanization have increased, which has led to higher yields, but also increased air, water, soil pollution and loss of biodiversity. Greenhouse gases from agriculture contribute to climate change. According to Tian *et al.* [1] in anthropogenic warming with greenhouse gases, nitrogen oxides from agriculture contribute 8%. The application of intensive agrotechnical measures most often leads to disruption of physical, chemical and biological properties. Intensive application of chemical inputs leads to soil contamination with heavy metals, radionuclides, and a decrease in the biodiversity of the soil microbiome. Soil pollution is estimated to contribute to more than 500,000 premature deaths worldwide each year [2], the largest percentage through food. With the development of sustainable systems of agricultural production (integral and organic), it is necessary to introduce methods that favor processes in accordance with the bio-geo-ecosystem into food production technology. The central place in these systems belongs to microorganisms. In agricultural production, in addition to bacteria that promote plant health (PHPR, Plant Health Promoting Rhizobacteria) or bacteria that promote nodulation (NPR, Nodule Promoting Rhizobacteria) [3,4], preparations with effective microorganisms (EM) are introduced.

Effective microorganisms are mixed cultures of beneficial microorganisms isolated from nature that can be used as inoculants to increase the yield of cultivated plants and the microbial diversity of the soil ecosystem. They consist mainly of photosynthesizing bacteria, lactic acid bacteria, yeasts, actinomycetes and fermenting fungi. When introduced into the soil, they participate in improving the structure, increasing the water capacity and fertility of the soil [5]. Chan *et al.* [6] found that the presence or absence of these beneficial microorganisms in any soil system accurately distinguishes "living" from "dead soil". Vals and Lorenzo [7] determined that the regular application of effective microorganisms can reduce the use of chemical fertilizers and pesticides, which results in a reduction of environmental pollution. Dourado [8] showed that the application of EM and its metabolites can reduce the population of phytopathogenic fungi *Fusarium sp.* on corn seeds from 21–67%. Iriti *et al.* [9] suggest that the use of EM can improve photosynthetic efficiency and thereby increase yields.

Large amounts of mineral fertilizers are used in the intensive production of basic agricultural crops. The constant use of mineral fertilizers leads to a decrease in soil fertility, a decrease in the biodiversity of soil microbes, leaching of nitrate nitrogen and eutrophication of waters. Wheat and corn occupy significant areas of the world, because they are the most common in human nutrition. Considering the large production of organic matter and yields of wheat and corn grains, large amounts of nitrogen are necessary. In intensive production, which is the most common form of production, complex mineral and nitrogen fertilizers are mainly applied.

Due to the current public concern about the side effects of agrochemicals, there is a growing interest in improving the understanding of the activities of microbial interactions among rhizosphere microbes and how they can be effectively used to benefit agriculture and the environment [10,11].

The aim of the work was to show the advantages of using effective microorganisms to change the abundance of the most important groups of microorganisms in the rhizosphere of different genotypes of wheat and maize.

MATERIALS AND METHODS

In the conducted research, the impact of effective microorganisms applied with the preparation EM Aktiv (trade name) on the total number of microorganisms, the abundance of *Azotobacter* and ammonifiers in the rhizosphere soil of cultivated plants was determined. Standard microbiological methods, a series of dilutions on agar plates, determined the basic parameters of biogenicity of the rhizosphere soil of cultivated plants. Microorganisms in the rhizosphere form complex communities, which are strongly influenced by products from plant roots and which have a great influence on the promotion of plant growth and soil fertility.

In 2019, an experiment with different wheat genotypes (Ratarica and Pobeda domestic selection, Nogal and Apache French selection) was conducted at the location of Padinske Skele. The plants were sown at a density of 500 plants per m^2. For the planned grain yield, the plants are provided with 129 N, 60 P_2O and 60 K_2O kg·ha^{-1}. In the phenological phase of flowering, EM Aktiv was applied twice in the amount of 6 l·ha^{-1}. In the phenological phase of pouring wheat grains, the rhizosphere soil was sampled.

In 2017, at the Šabac location, there was an experimental trial with different genotypes of corn where treatment with EM aktiv was applied. The plants were provided with 160 kg·ha^{-1} of nitrogen before sowing. Also, 20 l·ha^{-1} of EM Aktiv was introduced into the soil and during the growing season it was applied foliarly (2 x 6 l·ha^{-1}, in the phenological stages of development of 5–7 leaves and after 15 days). Rhizosphere soil was sampled in the phenological phase of intensive vegetative growth.

Given that agroecological factors are decisive for stable production, temperatures and precipitation in the vegetation were measured during the experiment. In 2019, agroecological factors were favorable for wheat production. The average temperature was within the optimum range of 10.9ºC, the amount of precipitation was 537.3 mm, with a relatively good distribution. In 2017, the average temperature determined was 18.3ºC, which is within the optimal range. The total amount of precipitation was 360.3 mm, which is below optimal needs. In addition, an unfavorable distribution of precipitation in the vegetation was determined Figure 1.

a) *b)*

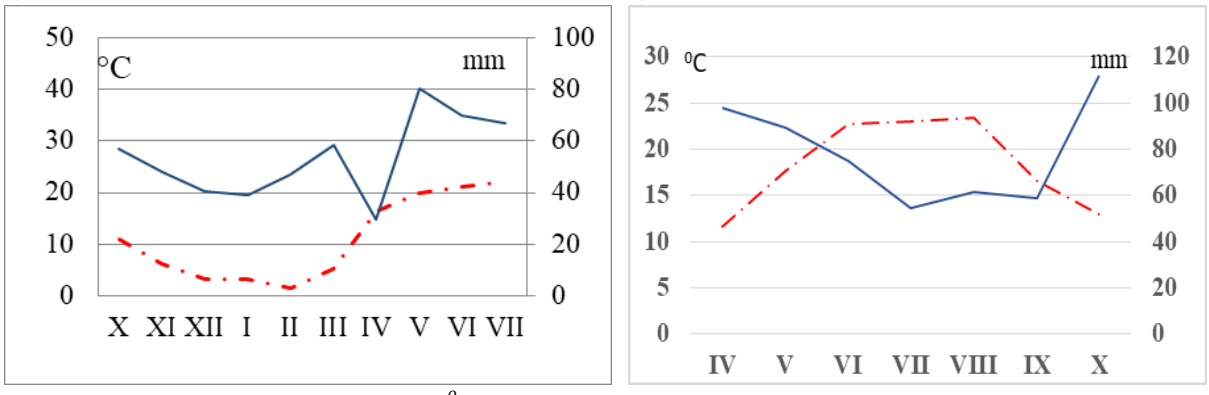

Figure 1 *Average air temperature (^0C) and sum precipitation (mm) in vegetation a) in 2019 year-wheat, b)-in 2017. year -corn*

RESULTS AND DISCUSSION

The level of soil fertility depends on the abundance and activity of different groups of microorganisms as indicators that define changes in soil quality. Given the fact that conditions in the rhizosphere are very dynamic (as a result of the day/ night cycles of photosynthesis and assimilation, and the dynamic growth of roots), thus, plant-associated microbial communities are highly variable in space and time. Research into the dynamics of changes in certain groups of microorganisms in the soil is a good indicator of changes. Changes in soil microbial balance can serve as an "early warning" for negative and positive changes in soil conditions long before they could be detected by classical chemical methods. Today, many studies are devoted to the composition of the microbial community in the soil from the aspect of its preservation [12,13].

Microorganisms, as the most numerous group of organisms in the soil, are under the direct influence of all substances introduced into the soil. Soil microorganisms participate in the degradation of organic and inorganic compounds, in the immobilization of heavy metals, in the biodegradation of slowly degradable compounds such as polycyclic aromatic compounds (PAH), as well as in processes related to the increase and quality of soil fertility. Their enzymatic activity, number, and diversity are bioindicators of the toxic effect of pollutants that reach the soil. Due to their specificities, they can be used as biosensors of soil toxicity [14]. Also, certain groups of microorganisms can be used in plant nutrition as a substitute or supplement for mineral fertilizers.

Based on the results of the experiment with wheat, it was determined that there is a significant influence of genotype and treatment with EM Table 1. In the rhizosphere of all tested wheat genotypes, there was an increase in the total number of microorganisms by 12.23% when treated with EM compared to the control. The PKB Ratarica variety had the best interaction relationship, and the Nogal variety had the weakest. The abundance of Azotobacter on average for all genotypes was increased by 9.14%. A decrease in the number of this group of bacteria was found in the Nogal variety, which indicates that there was probably no competitive relationship with the activity of other groups of microorganisms.

Table 1 *Total number of microorganisms (×·10^7 CFU·g^{-1} absolutely dry soil) and the number of Azotobacter (×·10^1 CFU·g^{-1} absolutely dry soil) in the rhizosphere of wheat*

Treatment (B)	**Total number of microorganisms**			***Number of Azotobacter***		
Genotype (A)	**Control**	**EM**	**Control =100 %**	**Control**	**EM**	**Control =100 %**
Ratarica	222.33	319.67	43.78	85.00	89.67	5.49
Pobeda	175.67	195.67	10.75	95.67	160.33	67.58
Nogal	259.67	255.67	15.64	320.67	312.67	-2.49
Apach	184.67	199.67	8.12	194.33	196.67	1.20
Average	**210.58**	**242.67**	**15.23**	**173.92**	**189.83**	**9.14**
	A**	B**	AxB**	A**	B**	AxB**
F test	0.00	0.03	0.00	0.00	0.00	0.00
$LSD_{0.05}$	12.39	16.69	33.39	6.66	5.05	10.10
$LSD_{0.01}$	16.61	22.87	45.75	8.93	6.92	13.84

In the experiment with corn, Table 2 shows the high significance of genotype and treatment on the total number of bacteria, while treatment with EM had a significant effect on the number of ammonifiers. The total number of microorganisms on average was higher by 23.52% when treated with EM, while the number of ammonifiers was higher by 14.86%. In the rhizosphere of hybrid ZP 548, the highest total number of microorganisms and ammonifiers was determined, so it can be said that it had the best interaction relationship with EM. The hybrid ZP 684 had the weakest interaction relationship. Given that a water deficit was determined in the period before rhizosphere soil sampling, it can be said that the application of EM can alleviate the stress of plants in unfavorable conditions for development.

Table 2 *Total number of microorganisms (× 10^7 CFU g^{-1} absolutely dry soil) and the number of ammonifiers (× 10^1 CFU g^{-1} absolutely dry soil) in the rhizosphere of maize*

Treatment (B)	**Total number of microorganisms**			***Number of ammonifiers***		
Genotype (A)	**Control**	**EM**	**Genotype (A)**	**Control**	**EM**	**Genotype (A)**
ZP 427	161.43	165.33	2.41	41.33	53.80	30.17
ZP 548	130.88	254.63	94.55	36.74	50.83	38.35
ZP 684	274.42	280.12	2.07	72.09	67.84	-5.89
Average	**188.91**	**233.36**	**23.52**	**50.05**	**57.49**	**14.86**
	A**	B**	AxB**	A	B**	AxB**
F test	0.00	0.38	0.00	0.10	0.00	0.00
$LSD_{0.05}$	9.53	10.19	24.57	7.66	5.53	9.58
$LSD_{0.01}$	13.36	11.83	32.61	10.74	7.34	12.72

CONCLUSION

The advantages of applying this form of plant production is that in this way the soil is enriched in organic matter, and the autochthonous microbial population is also activated, and oxidation-reduction processes in the soil are accelerated, which affects the yield and quality of cultivated plants.

Considering that microorganisms are effective only when they are provided with optimal conditions for physiological processes, often their effects are not clearly expressed. However, it can be said that microbial technologies are applicable for solving various agricultural and environmental problems with significant success in recent years, and such research should be continued.

ACKNOWLEDGEMENT

The authors are grateful to the Ministry of Science and Technological development of the Republic of Serbia for financial support according to the contract with the registration number 451-03-47/2023-01/200378.

REFERENCES

[1] Tian H., Lu, C., Ciais, P. *et al*., Nature 531 (7593) (2016) 225–228.

[2] Landrigan P. J., Fuller R., Acosta N. J., *et al*., The lancet 391 (10119) (2018) 462–512.

[3] Sturz A. V., Nowak, J. Appl. Soil Ecol. 15 (2000) 183–190.

[4] Shoebitz M., Ribaudo C. M., Pardo M. A., *et al*., Soil Biol. Biochem. 41 (2009) 1768–1774.

[5] Kengo Y., Hui-lian X. J. Crop Prod. 3 (1) (2000) 255–268.

[6] Chan L., Gu X., Wong J. Adv. Environ. Res. 7 (2003) 603–607.

[7] Valls M., Lorenzo V., FEMS Microbiol. Rev. 26 (2002) 327–338.

[8] Dourado E. D. R. Microrganismos Eficientes (EM) no tratamento de sementes de milho (2018).

[9] Iriti M., Scarafoni A., Pierce S., *et al*., Int. J. Mol. Sci. 20 (9) (2019)

[10] Barea J. M., Pozo M. J, Azcon R., *et al*., Journal Exp. Bot. 56 (2005) 1761–1778.

[11] Lucy M., Reed E., Glick B. R., Intern. J. Gener. Molec. Microbiol. 86 (2004) 1–25.

[12] Lauber C. I., Hamady M., Knight R., *et al*., Appl. Environ. Microbiol. 75 (2009) 5111–5120.

[13] Vestergaard G., Schulz S., Schloter A., Schloter M., Biol. Fertil. Soils 53 (2017) 479–484.

[14] Milošević N., Sekulić P., Tintar B., *et al.*, Proceedings of the International Symposium, Ecological Truth, 01–04 June, Sokobanja, Serbia (2008) 276–280.

APPLICATION OF CLASSIC THIN LAYER CHROMATOGRAPHY METHOD FOR QUALITATIVE DETERMINATION OF SYNTHETIC FOOD COLORS

Vojkan Miljković[1*], Radomir Ljupković[2], Milena Miljković[2]

[1]University of Niš, Faculty of Technology, Bulevaroslobođenja 124, Leskovac, SERBIA

[2]University of Niš, Faculty of Sciences and Mathematics, Department of Chemistry, Višegradska 33, Niš, SERBIA

[*]*vojkan@tf.ni.ac.rs*

Abstract

Food additives are substances that are added to the food during the production, transport, design, processing and storage of food. The use of food colours, as additives, in the food production process aims to correct the natural colour products, as well as making products with an attractive appearance with high quality sensory characteristics that indicates as the colour of the product. The use of all food additives, including colour, is controlled by appropriate legal regulations. Colours used in the food industry, as well as other additives, must be listed in the list of ingredients used in the manufacture of the product, stating the name of the colour and/or the relevant E number. In order to assess and analyses of the risks of consuming food dyes and their classification according to the safety of their use, the international committee Joint FAO/WHO Expert Committee of Food Additives (JECFA) determined the values for acceptable daily intake (Acceptable Daily Intake – ADI). Acceptable Daily Intake for each food colouring the use allowed is based on experimental toxicological studies, which are carried out on animals and data from various clinical studies. Additives can be associated with allergic reactions, migraine and asthma attacks, obesity and behavioural disorders, especially in children. The danger of harmful effects additives on health is especially important in children - in the child's body, additives more easily modulate the processes of growth and development.

Keywords: additives, food, toxicity.

INTRODUCTION

Colour is a physical experience of the human eye, however, the path from the refraction of light to the creation of the experience of colour is complex. It cannot be explained by only one branch of science, but can be explained by the cooperation of fundamental sciences, physics, chemistry, physiology and psychology. H. Helmholz, H. Munsell, J. C. Maxwell and others made a significant contribution to the intensive development of colour science, but W.Ostwaldis considered the true founder [1].

There are several different definitions of colour, of which the following should be mentioned:According to Webster's Dictionary: “Colour is a property of an object or substance, related to the light reflected by the object, and usually determined visually by measuring the hue, saturation, and brightness of the reflected light” [2].

Food colours are additives used in food industry with a purpose to increase a sensation of taste associated with aroma of food product [3]. They are widely used in food industry in

production of processed food, drinks, and candies, and are labelled with letter "E" before a number [4,5]. Candies are industrial products made from candy mass with the addition of various colours, flavours, acids (for fruit candies) and special additives (sesame, peanuts, milk, etc.). It is reported by Food and Drugs Administration that total use of food colours has increased by 5-fold since 1950 [6].

The natural colour of the product is in most cases unstable and subject to degradation [7]. During food processing, different chemical and physical treatments may lead to partial degradation of pigments. Such colour changes are undesirable and affect the reduction of product quality and visual experience [8]. To the loss or destruction of someone's natural colour of a food product can also occur during it's thermal processing or storage. Colour darkening during production and storage of products affects the reduction of their sensory quality. The degree of darkening depends on presence of oxygen, metal ions, pH value, temperature and activity of various enzymes [9].

It is possible to use many analytical techniques for colour identification [10]. Considering the time needed for analysis, financials and technical skills thin layer chromatography is a method of choice [11]. Thin layer chromatography (TLC) is fast and economic chromatographic method that uses a thin layer (0.10–0.25 mm) of absorbing material such as silica gel, alumina, or cellulose, which is applied to a support, which can be made of glass, plastic, or aluminium. This is actually the purpose of this method, to identify individual components of a paint mixture or individual sample, based on the path travelled, by imaging under ultraviolet radiation (UV) [2].

The aim of this paper is to present the results of applying fast and efficient method of thin layer chromatography in identification of colours used in candies.

MATERIALS AND METHODS

For this experiment, 4 different candies with chocolate glaze of domestic manufacturer were used. However, the principal manager didn't allow us to mention full name of candy product which we analysed.

The methodology used is thin layer chromatography, which enabled the separation and quantitative determination of substances that are structurally similar and have similar chemical properties.

The samples were dissolved in a suitable solvent and applied in the form of droplets to the surface of the plate. The plate was then introduced into the chamber at the bottom of which there was a separator that passes through the adsorbent by capillary forces, carrying with it the components of the sample, which are distributed at different distances on the plate, starting from the starting line. The bottom of chamber was filled with solvents mixture consisting of n-butanol, distilled water and acetic acid in ratio 20:12:5.The determination of Rf value (the distance travelled by sample in relation to the distance travelled by standard colours) was done. Standard solutions of colours 1% were used [4]. The Rf values of colours from samples were compared to the Rf values of standards.

RESULTS AND DISCUSSION

As the first step, a chromatogram of the primary colours was created with standards in order to obtain a sample for comparison with the candies sample. The chromatogram is shown in Figure 1.

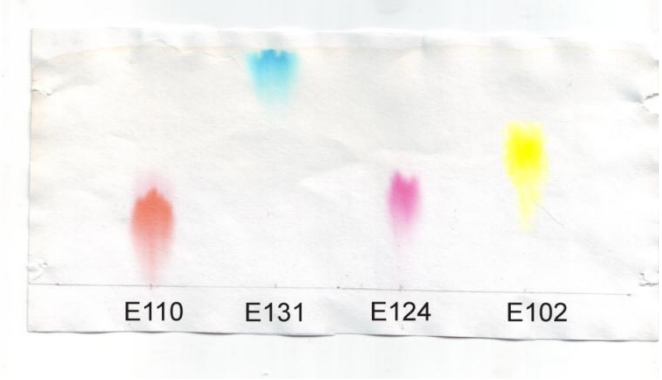

Figure 1 *Chromatogram made with standards*

From the obtained chromatogram, the Rf values of the basic colours were determined and their numerical values shown in Table 1.

Table 1 *Rf values of standard colour samples*

Colour	Rf value
E110	0.46
E131	0.96
E124	0.49
E102	0.65

The obtained Rf values were used to identify the colours isolated from the candies. It can be observed that the dyes E131, E124 and E102 give clearly defined and rather compact stains. Colour E110 gives a slightly stretched orange stain with reddish transitions at the ends of the stain.

By developing a chromatogram of the colours isolated from 4 different chocolate glazed candies, the following chromatogram was obtained:

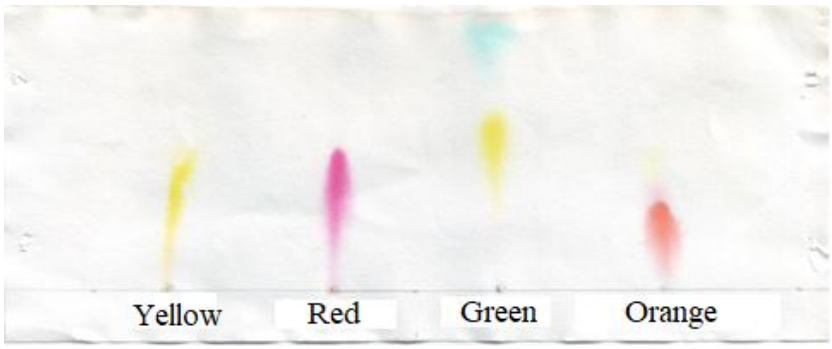

Figure 2 *Chromatogram of colours isolated from a candy sample*

The chromatogram shows that the green colour of the candy consists of two components, blue and yellow. Other colours consist of one component. The Rf values of the isolated colour components are shown in the Table 2.

Table 2 *Rf values obtained from samples of candies*

Candy colour –component	Rf value
Yellow	0.53
Red	0.41
Green (blue, yellow)	0.94, 0.62
Orange	0.36

CONCLUSION

Based on the experimental work and the results obtained, the following conclusions can be drawn:

• The candies contain food dyes labelled: E102, E110, E124 and E131;

• The composition of the isolated colours corresponds to the content on the product declaration (white candies were not analysed - colouring from titanium dioxide);

• The present colors are permitted for use according to domestic and foreign regulations;

• Based on the proportion of glaze in the mass of the product that the amount of colors in the product is within the prescribed and allowed concentrations.

ACKNOWLEDGEMENT

The authors are grateful to the Ministry of Science, Technological Development and Innovation of the Republic of Serbia for financial support according to the contract with the registration number (451-03-47/2023-01/200133).

REFERENCES

[1] Ostwald W., The Color Primer, De Gruyter (1969), ISBN: 9783112528082.

[2] Wolford J., Historical Development of Food Coloration *in* Developments in Food Colors, Applied Science publishers, London, UK, 1 (1980) 1–25.

[3] Miric M. O., Sobajic S. S., Health safety of foods, Institute for textbooks and teaching aids, Belgrade, Serbia (2002).

[4] Farzianpour F., Khaniki G. J., Younesian M., *et al*., Am. J. App. Sci. 10 (2) (2013) 172–178.

[5] Vinković Vrček I., Lerotić D., Additives in food – Guide to e-numbers, School book, Zagreb, Croatia (2010).

[6] Stevens L. J., Burgess J. R., Stochelski M. A., *et al*., Clin. Pediatr. 54 (4) (2014) 309–321.

[7] Radojković-Veličković M., Mijin D., Organic colors and pigments, Tehnološko-Metalurški Fakultet, Belgrade (2001).

[8] Rakić V. P., Indexing and spectroscopic identification of food colors in foodstuffs, Master's thesis, Faculty of Science in Niš, Department of Chemistry (2006).

[9] Novakovic B., Mirosavljev M., Food Hygiene, University of Novi Sad, Medical faculty, Novi Sad, Serbia (2005).

[10] Milosavljević S. M., Structural Instrumental Methods, Faculty of Chemistry, Belgrade, Serbia (1994).

[11] Shakila R. J., Vasundhara T. S., Kumudavally K. V., Food Chem. 75 (2001) 255–259.

NOVEL CARBON MATERIAL FOR OER IN VARIOUS ELECTROLYTE SOLUTIONS

Snežana Brković[1], Nikola Zdolšek[1], Ivana Perović[1*], Gvozden Tasić[1], Mina Seović[1], Stefan Mitrović[1], Jelena Georgijević[1]

[1]University of Belgrade, Vinča Institute of Nuclear Sciences, National Institute of the Republic of Serbia, Mike Alasa 12–14, 11351 Vinča, SERBIA

[*]*ivanaperovic@vin.bg.ac.rs*

Abstract

In this study, a novel carbon material was synthesized from a deep eutectic solvent (DES) and evaluated as an electrocatalyst for the oxygen evolution reaction (OER) in various electrolytes. The DES-derived carbon material showed superior OER activity and stability compared to traditional carbon materials due to the high degree of heteroatom doping and surface functionalization. The carbon material exhibited low overpotentials and Tafel slopes in acidic, neutral, and alkaline electrolytes, highlighting its versatility and potential for use in renewable energy conversion and storage technologies. Our findings demonstrate the promising application of DESs as green solvents for the synthesis of efficient carbon-based electrocatalysts for the OER in diverse electrolytes.

Keywords: OER, DES, carbon electrocatalyst, Tafel analysis.

INTRODUCTION

The oxygen evolution reaction (OER) is a key reaction in many renewable energy conversion and storage technologies, including water splitting, rechargeable metal-air batteries, and regenerative fuel cells. Carbon-based materials have emerged as promising electrocatalysts for the OER due to their low cost, high abundance, and tunable properties [1]. However, the synthesis of carbon materials with high activity and stability for the OER remains a challenge. Deep eutectic solvents (DESs), a new class of ionic solvents formed by mixing hydrogen bond donors and acceptors, have recently emerged as promising alternatives to traditional solvents for the synthesis of carbon materials [2]. DESs offer several advantages, including low toxicity, low cost, and high solubility for a variety of precursors. In this study, we present a novel carbon material synthesized from a DES composed of choline chloride, urea and hydrochinon. The synthesis method involves a simple, one-pot pyrolysis process and offers several advantages, including facile scalability and tunable properties by varying the DES composition and pyrolysis conditions [3]. Our results indicate that the DES-derived carbon material exhibits superior OER activity and stability compared to traditional carbon materials due to the high degree of heteroatom doping and surface functionalization. Our findings highlight the potential of DESs as a promising solvent for the synthesis of efficient and cost-effective carbon-based electrocatalysts for the OER in various electrolytes, paving the way for the development of sustainable energy conversion and storage technologies.

MATERIALS AND METHODS

Synthesis of Carbon material

A deep eutectic solvent (DES) was prepared by blending choline-chloride (purity 99% from Acros Organics), urea (purity 99.5% from Sigma Aldrich), and hydroquinone (from Sigma Aldrich) at a 3:2:1 molar ratio of choline-chloride : urea : hydroquinone. The mixture was stirred on a magnetic stirrer at 80℃ for 6 hours. Subsequently, the Ch-Urea-HQ carbon material was obtained by carbonizing the prepared DES in a furnace at 800°C under N_2 atmosphere. The furnace was heated at a rate of 5°C per minute until the desired temperature was reached, which was held constant for an hour and then cooled down to room temperature under N_2 flow. The surface morphology of the resulting Ch-Urea-HQ carbon material was examined by scanning electron microscopy (SEM).

Electrode preparation and electrochemical measurement

In order to test the activity of obtained sample, three component ink was prepared. Ch-Urea-HQ, 5% Nafion (Sigma Aldrich) and Ethanol (96%, p.a.) were mixed and sonicated for an hour. The surface of freshly cleaned and polished glassy carbon electrode (GCE) was coated with prepared catalyst and then dried at 80 ℃ for 1 h. This electrode was used as a working electrode, while a Pt mesh was used as counter electrode. Saturated calomel electrode (SCE) was used as a reference electrode for electrochemical measurements. All measurements were performed using Gamry 1000E potentiostat/galvanostat in three-electrode electrochemical cell.

With the idea of better determining the possibilities and activities of synthesized catalyst, its activity was assessed in three different electrolytes, varying in pH: alkaline, acidic, and neutral. For alkaline media, 6M KOH was used considering that it most closely reflects the conditions with which the catalyst meets in industrial-scale electrolysis. On the other hand, 1 molar sulfuric acid (1M H_2SO_4) was used as an acidic electrolyte. And in the end, as a representative of a neutral environment, 2M $NaNO_3$ was used as electrolyte.

For electrochemical characterization of this material, linear sweep voltammetry (LSV) was used, and from obtained polarization curves Tafel analysis was performed to determine the slope values in all three electrolytes.

RESULTS AND DISCUSSION

Morphological analysis using the scanning electron microscopy (SEM) technique was performed immediately after the material synthesis. Based on the obtained micrographs, which are shown below (Figure 1), it can be observed that the material shows a smooth morphology with extremely sharp edges. Due to the noticeable scaly structure of the surface, at higher magnifications, much smaller carbon forms can be observed that only further contribute to the increase of the active surface.

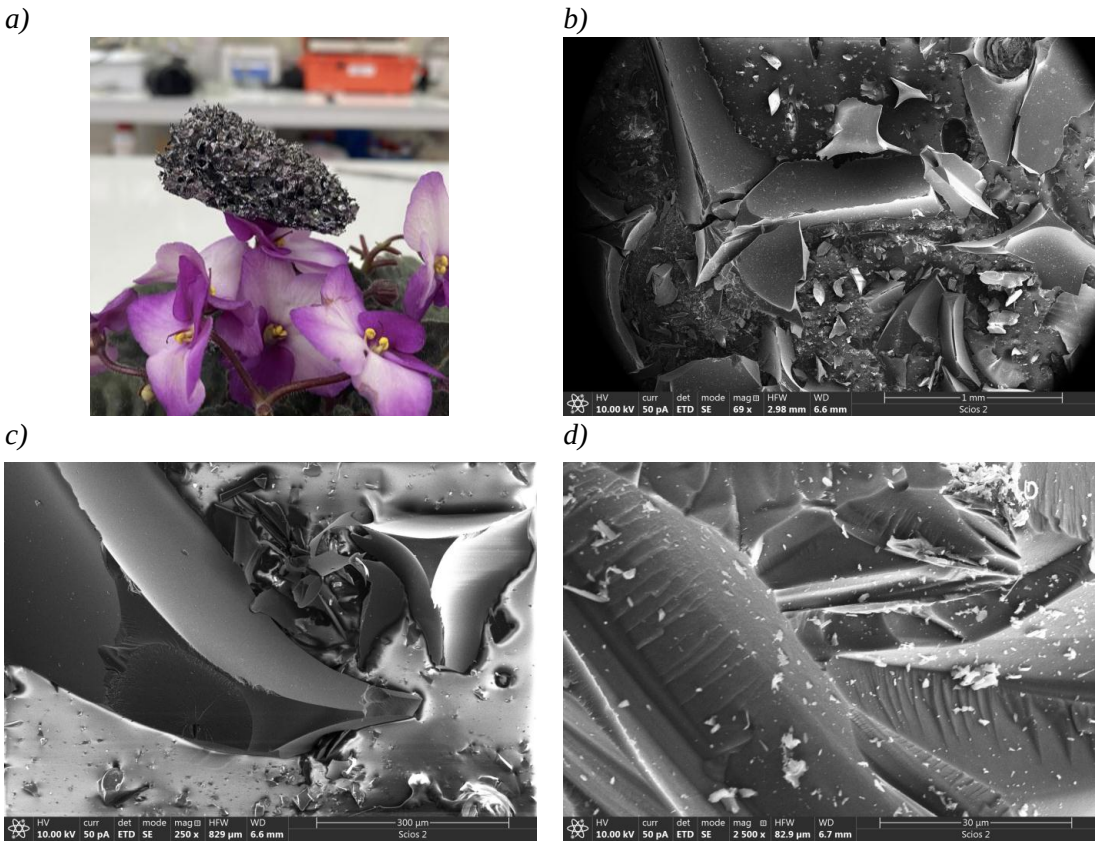

Figure 1 *a) Picture of synthesized material; b)–d) SEM images of synthesized material at different magnifications*

Polarization curves and kinetic parameters determined based on them give us a direct insight into the activity of this material for the oxygen evolution reaction (OER), and also a comparison of the activity in different electrolytes. In order to directly compare activity of synthesized catalyst, linear sweep voltammetry was conducted and recorded polarization curves are presented below (Figure 2a).

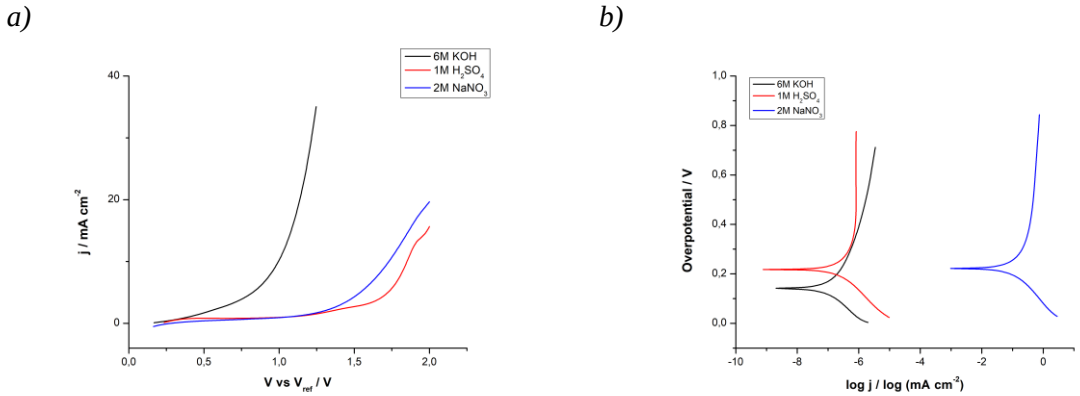

Figure 2 *a) LSV curves and b) Tafel plots*

The polarization curve obtained from the alkaline electrolyte exhibits highest activity, achieving the necessary potential for the onset of the oxygen evolution reaction (OER) faster

than the other electrolytes. The second-best activity of the synthesized material was observed in the neutral electrolyte, while the acidic electrolyte performed worse. This can also be additionally confirmed by observing the potential value at certain reached current density values, as shown in Table 1. Observed at two characteristic current density values, 5 and 10 mA/cm^2, it can be seen that the lowest required potential value to reach these selected current density values is in the alkaline electrolyte, then in the neutral, and finally in the acidic.

Based on the data obtained by recording the polarization curves, a Tafel analysis was performed. The kinetics of these systems, i.e. the oxygen evolution reaction, in different electrolytes, can be discussed based on the obtained Tafel slope values (Table 2). A high Tafel slope shows that the bandgap energy is high which leads to a high overpotential due to the large amount of energy required to achieve activity. Also, Tafel slope gives information about the rate-determining step of the electrochemical reaction. In this case, based on very high values, it can be assumed that the determining step of the reaction is diffusion-controlled [4].

Table 1 *Comparison of potentials at two different current density values*

Electrolyte	Current density j ($mA\ cm^{-2}$)	Potential V (V)
6M KOH	10	0.995
1M H_2SO_4	10	1.850
2M $NaNO_3$	10	1.729
6M KOH	5	0.827
1M H_2SO_4	5	1.725
2M $NaNO_3$	5	1.511

Table 2 *Tafel slope values for the synthesized catalyst in different electrolytes*

Electrolyte	Tafel slope ($mV\ dec^{-1}$)
6M KOH	363
1M H_2SO_4	320
2M $NaNO_3$	468

CONCLUSION

The synthesized material shows a crystalline morphology with a smooth surface area and noticeable scaly structure. The polarization curves show that the material exhibits the highest activity for the oxygen evolution reaction (OER) in the alkaline electrolyte, followed by the neutral and acidic electrolytes. The Tafel analysis indicates that the oxygen evolution reaction kinetics in different electrolytes are diffusion-controlled, and the obtained Tafel slope values suggest that a high overpotential is required for achieving activity due to the high bandgap energy. Therefore, the synthesized material has potential as a catalyst for the oxygen evolution reaction in the alkaline electrolyte.

ACKNOWLEDGEMENT

This work was supported by the Ministry of Science, Technological Development and Innovation of the Republic of Serbia; grant number 451-03-47/2023-01/200017.

REFERENCES

[1] Guo D., Shibuya R., Akiba C., *et al*., Science 351 (6271) (2016) 361–365.

[2] Smith E., Abbott A., Ryder K., Chem. Rev. 114 (21) (2014) 11060–11082.

[3] Demirbas A., Gönenç A., Energy Sources 24 (5) (2002) 471–482.

[4] Shinagawa T., Garcia-Esparza A. T., Takanabe K., Scientific reports 5 (1) (2015) 13801.

THE EFFECT OF DIFFERENT TYPE OF ELECTROLYTES ON THE DISCHARGE CAPACITY OF Zn-AIR BATTERIES

Nikola Zdolšek[1*], Ivana Perović[1], Snežana Brković[1], Mina Seović[1], Jelena Georgijević[1], Stefan Mitrović[1], Petar Laušević[1]

[1]University of Belgrade, "Vinča" Institute of Nuclear Sciences – National Institute of the Republic of Serbia, Department of Physical Chemistry, Belgrade, SERBIA

[*]*ivanaperovic@vin.bg.ac.rs*

Abstract

Zinc-air batteries have emerged as promising energy storage systems owing to their numerous advantages over the commonly used lithium-ion (Li-ion) batteries. Electrolyte, which is at the core of Zn-air batteries, plays a critical role in determining the performance and, more importantly, the stability of the Zn anode. In this study, the electrochemical behavior of Zn-air batteries was examined using IrO_2+Pt/C as the cathode material and Zn anode in three different electrolytes: 1) 6 M KOH+0.2 M Zn-acetate, 2) 6 M KOH+0.2 M choline chloride, and 3) deep eutectic solvent consists of choline chloride: urea: Zn-acetate. Among these, the electrochemical cell Zn//6M KOH+0.2M Zn-acetate//IrO_2+Pt/C exhibited the highest discharge capacity, followed by the cell using 6 M KOH+0.2 M choline chloride electrolyte.

Keywords: deep eutectic solvents, Zn-air batteries, new electrolytes.

INTRODUCTION

Rechargable Zn-air batteries (ZABs) due to their low cost, high safety and environmental friendliness attracted enormous attention. Therefore, in the last few years, rechargeable ZABs have been the focus of many research groups, as well as the battery industry. ZABs shows high energy density (1086 Wh kg^{-1}), which is four times higher than lithium ion batteries (LIBs) [1]. Also, zinc is abundant, cheap, environmentally friendly and recyclable element. Furthermore, aqueous electrolytes in ZABs are non-flammable (compare to electrolytes in LIBs) and safety issues are obvious.

ZABs consist of a zinc anode, alkaline electrolyte and air cathode with a bifunctional electrocatalyst, which can catalyse oxygen reduction (ORR) and evolution (OER) reactions [2]. During discharge of ZAB, zincate ions are formed in the alkaline electrolyte via the zinc oxidation reaction, where OH^- ions are generated via ORR. During this process, zincate ions will further decompose into insoluble ZnO and deposit onto the Zn-anode surface. On the other side, upon recharge ZnO will be reduced back to Zn and OER will take place at the cathode. Zn deposit is uneven and dendrites are also formed, therefore battery capacity is reduced [2].

According to mentioned, mass-scale application of rechargeable ZABs is limited due to several issues. One of the most important limitations in the application of rechargeable ZABs is mentioned deterioration of the Zn anode. This deterioration is caused by a parasitic reaction

in electrolyte. In ZABs, KOH electrolyte is usually used. But despite the low cost, high conductivity and perfect electrochemical performances, KOH is an aggressive electrolyte for Zn electrode.

According to this, different electrolyte additives have been used in ZABs in order to stabilise the Zn anode and increase or maintain battery capacity. In the first line, zinc acetate is the most used aditive (in 6 M KOH electrolyte) in ZABs. Besides zinc acetate, other additives were also used [3]. Organic additives such as formaldehyde, DMSO, ethanol, different surfactants, citric and tartaric acid etc. Organic additives reduce dendrite formation and increase the potential required for hydrogen evolution reaction, therefore enhancing battery perfomances.

In this paper we investiagated two types of electrolytes for ZABs. First, two types of electrolytes with KOH and additives such as Zn-acetate and choline chloride were investigated. Secondly, the discharging performances of ZABs was evaluated using nove deep eutectic solvent based on choline chloride:urea: Zn-acetate.

MATERIALS AND METHODS

Gas diffusion layer (GDL) preparation

GDL was prepared using carbon paper and electrocatalyst ink. Electrocatalyst ink was prepared using IrO_2 and Pt/C (10% Pt on carbon), nafion (Sigma Aldrich) and absolute ethanol (Sigma Aldrich). 10 mg of IrO_2 and 10 mg of Pt/C were mechanically mixed and dispersed in 20 µL of Nafion and 980 µL of absolute ethanol. Obtained dispersion was sonicated at room temperature for 1 hour. A drop casting technique was used to prepare the cathode (i.e. GDL), a certain amount of dispersion was added onto carbon paper (surface 0.78 cm^2) to form GDL. Carbon paper with catalyst was dried at 80°C for one hour. The catalyst load was 4 mg cm^{-2}.

Deep eutectic solvent electrolyte preparation

The deep eutectic solvent was synthesised by mixing choline chloride (abbrev. ChCl) (Sigma Aldrich) with urea (Sigma Aldrich) in a molar ratio 2:1. Both precursors were mixed at constant temperature (80°C) until the clear ionic liquid was formed. After this, Zn-acetate was added to the mixture with continuous mixing at 80°C for the next four hours. Obtained deep eutectic solvent was dried *in vacuo* using rotary evaporator. Molar ratio of choline chloride:urea:Zn-acetate was 2:1:0.2 and this deep eutectic solvent was noted as ChCl:Urea:Zn-acetate.

Zinc-air battery assembly

Battery performance was tested using a homemade zinc-air battery assembly. GDL with the catalyst prepared as previously described was used as a cathode with nickel mesh as the current collector. Anode was a Zn plate, with a thickness of 0.8 mm. The anode and cathode were separated with an electrolyte reservoir (7 ml of electrolyte). Three electrolytes were investigated: 1) 6 M KOH + 0.2 M Zn-acetate; 2) 6 M KOH + 0.2 M ChCl and 3) ChCl:Urea:Zn-acetate.

Electrochemical measurements

All electrochemical measurements were performed using Gamry interface 1000 potentiostat/galvanostat (Gamry, Philadelphia, PA, USA). Discharge curves were recorded at 50 mA cm^{-2}.

RESULTS AND DISCUSSION

Herein we investigated three types of electrolytes for zinc-air batteries using IrO_2+Pt/C cathode electrocatalyst. In the first line, we investigated standard electrolyte 6 M KOH + 0.2 M Zn-acetate. As can be seen from Figure 1, the discharge capacity was 735 mAh g^{-1}. Obtained value falls in the range for other reported data.

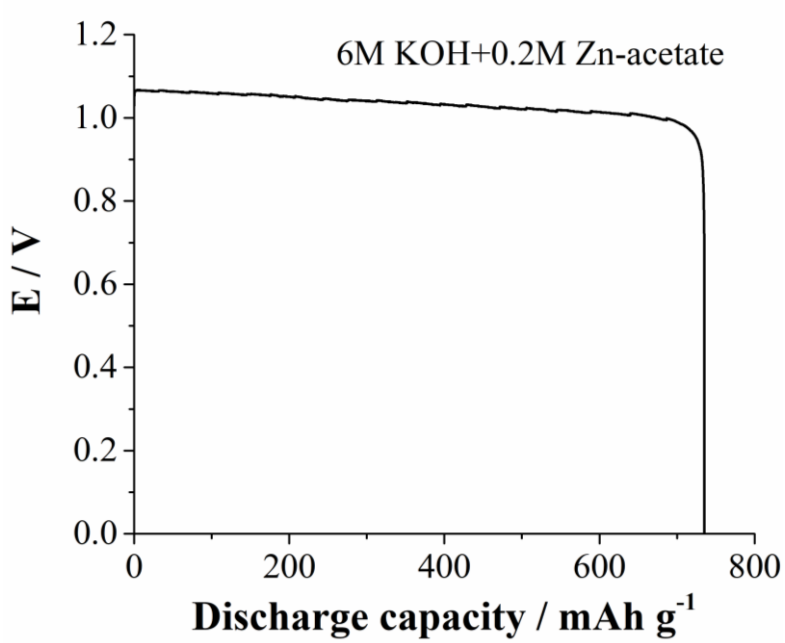

Figure 1 *Discharge profile of Zn-air battery cell with 6 M KOH + 0.2 M Zn-acetate electrolyte*

This high discharge capacity is the consequence of high electrical conductivity of 6M KOH. While Zn-acetate dissolved formed discharging products [4]. High conductivity of electrolyte with a possibility to dissolve discharge products leads to increase battery performances.

In further investigation, Zn-acetate was changed with organic salt, i.e. choline chloride and electrolyte consisting of 6 M KOH + 0.2 M ChCl was investigated.

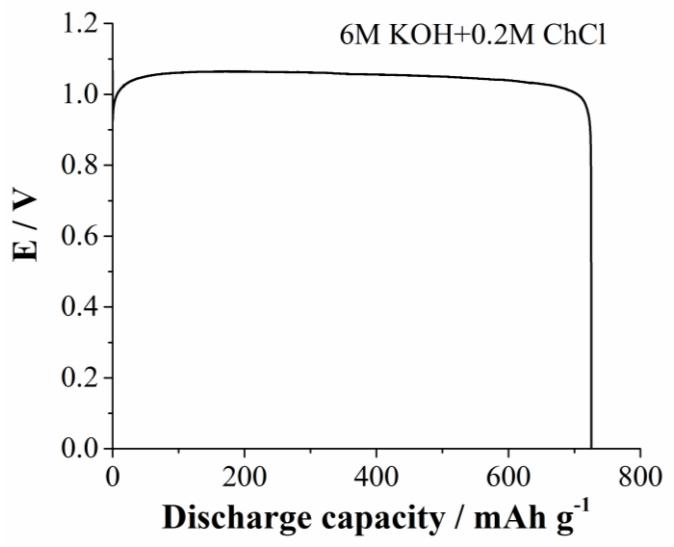

Figure 2 *Discharge profile of Zn-air battery cell with 6 M KOH + 0.2 M ChCl electrolyte*

Upon mixing choline chloride and KOH, choline hydroxide and potassium chloride is generated in situ [5]. This resultant mixture which acts as co-electrolyte was further investigated in ZAB. Figure 2 shows the discharge profile of ZAB with 6 M KOH + 0.2 M ChCl electrolyte. The calculated discharge capacity was 725 mAh g^{-1}. Discharge capacity was slightly lower when compared to ZAB with Zn-acetate as an additive. This could be a consequence of the higher (high alkalinity of choline hydroxide) pH of the used electrolyte, since alkaline electrolytes lead to deterioration of Zn-anode.

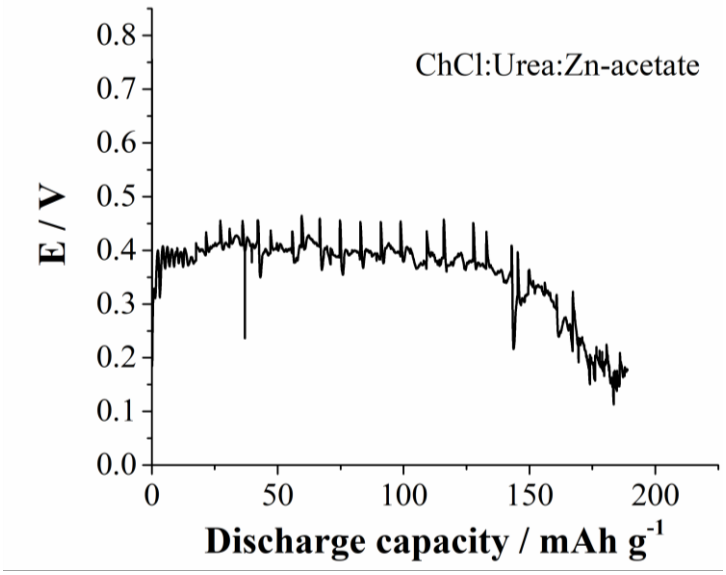

Figure 3 *Discharge profile of Zn-air battery cell with ChCl:Urea:Zn-acetate as electrolyte*

On the other side, deep eutectic solvents represent potential electrolytes for electrically rechargeable ZAB. Deep eutectic solvents can dissolve a range of metal oxides and provide excellent dissolution characteristics. Furthermore, deep eutectic solvents have low or

negligible toxicity, low volatility, high thermal stability, chemical inertness with water and so on. Figure 3 represents the discharge profile of ZAB with deep eutectic solvent (consists of ChCl:Urea:Zn-acetate) as electrolyte. First, it can be noted that potential is several times lower when compared to cell with two other investigated electrolytes (~0.4 V versus ~1.5 V). Secondly, potential fluctuation and instability are obvious, while discharge capacity is significantly lower. These could be a consequence of the very high viscosity of deep eutectic solvents (and the inability for ORR), as well as low conductivity.

CONCLUSION

Three different types of electrolytes were used and investigated for application in Zn-air batteries. Electrolytes based on KOH and two different additives (Zn-acetate and choline chloride) showed high discharge capacities (both around 700 mAh g^{-1}). On the other side, using deep eutectic solvent as electrolyte showed lower performances due to low conductivity and high viscosity. Using additive in KOH electrolytes open up a new possibility for improving the performances of Zn-air batteries.

ACKNOWLEDGEMENT

The authors are grateful to the Ministry of Science, Technological Development and Innovation of the Republic of Serbia for financial support according to the contract with the registration number (451-03-47/2023-01/200017).

REFERENCES

[1] Wu W., Yan X., Zhan Y., Chem. Eng. J. 451 (2023) 138608.

[2] Leong K., Wang Y., Ni M., *et al.,* Renew. Sustain. Energy Rev. 154 (2022) 111771.

[3] Hosseini S., Soltani S. M., Li Y. Y., Chem. Eng. J. 408 (2021) 127241.

[4] Sun W., Küpers V., Wang F., *et al.*, Angew. Chem. 134 (38) (2022) e202207353.

[5] Wadekar P. H., Khose R. V., Pethsangave D. A., *et al.*, EEM 3 (3) (2020) 429–435.

IRON, COBALT DUAL DOPED CARBON ELECTROCATALYST FOR EFFICIENT WATER SPLITTING

Jelena Georgijević[1], Jadranka Milikić[2], Nikola Zdolšek[1], Ivana Perović[1*], Snežana Brković[1], Stefan Mitrović[1], Biljana Šljukić[2,3]

[1]University of Belgrade, Vinča Institute of Nuclear Sciences, National Institute of the Republic of Serbia, Mike Petrovića Alasa 12–14, 11351 Vinča, SERBIA

[2]University of Belgrade, Faculty of Physical Chemistry, Studentski trg 12–16, Belgrade, SERBIA

[3]Center of Physics and Engineering of Advanced Materials, Laboratory for Physics of Materials and Emerging Technologies, Chemical Engineering Department, Instituto Superior Técnico, Universidade de Lisboa, 1049–001 Lisbon, PORTUGAL

[*]*ivanaperovic@vin.bg.ac.rs*

Abstract

Ionic liquids containing iron and copper were carbonized to produce Fe,Cu-dual doped carbon material. This material was then explored for catalysis of electrolytic water splitting, i.e., for oxygen evolution as anodic reaction and hydrogen evolution as cathodic reaction in alkaline medium using linear scan voltammetry. FeCu-C showed remarkable performance during OER with low onset potential of -1.485 V and current density reaching 160 mA cm^{-2} at 2 V vs RHE. Conversly, lower performance was observed during HER with current density of ca. 4 mA cm^{-2} at -0.4 V vs RHE. Lower charge-transfer resistance under OER conditions determined from the electrochemical impedance spectroscopy measurements corroborates the higher activity compared to the HER conditions.

Keywords: transition metals, ionic liquid, direct carbonization, hydrogen evolution reaction, oxygen evolution reaction.

INTRODUCTION

The ever growing energy demand has urged the need for novel chemical fuels to achieve a sustainable energy system. In this context, water electrolysis, which splits water molecule into hydrogen and oxygen, has emerged as a promising approach for producing chemical fuels, particularly hydrogen that can be used in a variety of applications such as fuel cells and transportation. The hydrogen evolution reaction (HER) as the anodic reaction and the oxygen evolution reaction (OER) as the cathodic reaction represent a simple method for obtaining oxygen and hydrogen through the electrochemical water splitting. The efficiency of these reactions largely depends on the performance of the electrocatalyst. Electrocatalysts based on Pt are considered the most efficient for HER, while Ir/Ru oxides are considered the best for OER. However, the high cost and unavailability of precious metals has prompted research to find economically accessible and highly active electrocatalysts for HER and OER. Among the various electrocatalysts explored to date, copper [1] and iron-based [2] materials have attracted significant attention due to their low cost, earth-abundant nature, and good

electrocatalytic properties. Ionic liquids are used in the most diverse fields of science due to their unique physical and chemical properties, and in this regard, they can be used for the development of electrocatalysts by direct carbonization [3].

MATERIALS AND METHODS

Synthesis of carbon material

In this work, FeCu-dual doped carbon material was prepared by direct carbonization of two ionic liquids: $[Bmim]_2[CuCl_4]$ and $[Bmim]_2[FeCl_4]$. Ionic liquids were carbonized in a nitrogen atmosphere at 800 °C for 1 h. After treatment at 800 °C, the material was allowed to cool at room temperature.

Electrochemical measurements

The working electrode was prepared by uniformly coating the catalytic ink on the glassy carbon electrode. Catalytic ink was made by mixing Fe,Cu-C electrocatalyst powder with polyvinylidene fluoride (PVDF) binder in N-methyl-2-pyrrolidone. All electrochemical measurements were performed using an Ivium V01107 potentiostat/galvanostat (Eindhoven, The Netherlands) in a 40 cm^3 glass cell with a three-electrode system. A saturated calomel electrode (SCE) was used as a reference electrode and graphite rod as a counter. All electrode potentials are shown relative to the reversible hydrogen electrode (RHE). Electrocatalyst was explored for hydrogen evolution reaction (HER) and oxygen evolution reaction (OER) in alkaline medium (8 M KOH) by linear cyclic voltammetry (LSV) at scan rate of 2 mV s^{-1} for HER, and at scan rate of 5 mV s^{-1} for OER at temperature of 25 °C. Electrochemical impedance spectroscopy (EIS) was carried out in 8 M KOH in the frequency range of 100 kHz to 0.1 Hz

RESULTS AND DISCUSSION

Fe,Cu-C was first evaluated as electrocatalyst for OER in alkaline media having in mind that OER limits the rate and efficiency of the whole electrolytic water splitting process. Activity for OER was evaluated in 8 M KOH as this concentration corresponds to the concentration used in industrial alkaline electrolysers. Figure 1 shows voltammogram of Fe,Co-C recorded in the potential range from the open circuit potential (OCP) to 2 V at a scan rate of 5 mV s^{-1}. Onset potential, determined as potential to reach 1 mA cm^{-2}, was found to be as low as 1.485 V. High activity of the studied material is further clearly evidenced by high current densities reached under OER polarisation conditions (ca. 160 mA cm^{-2} at 2 V). Next, Tafel analysis was performed; Tafel plot was constructed from the polarisation curve and analysed using the equation (1):

$$\eta = a + b \times \log j \quad (1)$$

where a is the intercept related to the exchange current density j_0 and b is the Tafel slope. Tafel slope reflects the rate of increase of current density j with increase of overpotential η and it was determined to be 134 mV dec^{-1}.

Next, activity of FeCu-C for HER in alkaline media was also investigated. Figure 1 shows voltammogram of FeCu-C recorded in the potential range from OCP to -0.4 V at a scan rate of 2 mV s^{-1}. Under the conditions of cathodic polarization, the electrocatalyst showed some activity for HER reaching the current density value of -4.2 mA cm^{-2} at potential of -0.4 V. Onset potential was observed to be -0.335 V. Tafel slope value for HER was determined to be -151 mV dec^{-1} indicating that HER at FeCu-C proceeds via Volmer-Heyrovsky mechanism. Namely, anodic reaction usually starts with electrochemical hydrogen adsorption on the electrode surface (MH_{ads}) (equation 2), followed by electrochemical desorption (equation 3) and/or catalytic recombination (equation 4) [4].

$$M + H_2O + e^- \leftrightarrow MH_{ads} + OH^- \quad \text{Volmer reaction} \quad (2)$$

$$MH_{ads} + H_2O + e^- \leftrightarrow H_2 + M + OH^- \quad \text{Heyrovsky reaction} \quad (3)$$

$$MH_{ads} + MH_{ads} \leftrightarrow H_2 + 2M \quad \text{Tafel reaction} \quad (4)$$

The overall reaction takes place through two possible stages: Volmer - Heyrovsky or Volmer - Tafel. The value of the Tafel slope is 120, 40 or 30 mV dec^{-1} at a temperature of 25 ^oC for the Volmer, Heyrovsky or Tafel step being the rate-determining step, respectively.

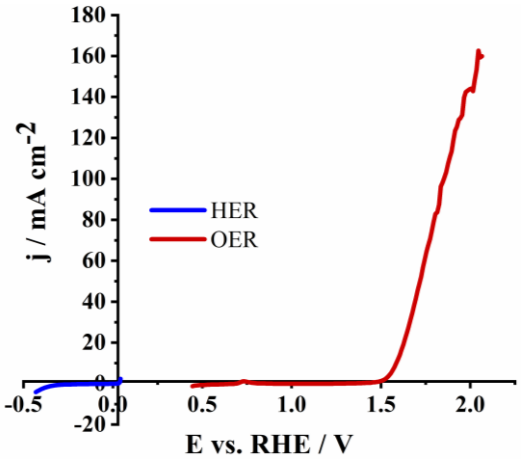

Figure 1 *LSV curves of FeCu-C in 8 M KOH under HER and OER conditions at temperature of 25 °C*

Table 1 summarizes the calculated kinetic parameters for the HER and OER at FeCu-C. Current density j_{400} at the overpotential of 400 mV was notably higher during OER. Similarly, exchange current density j_0, that reflects material's intrinsic activity and rate of charge transfer, was higher in case of OER.

Table 1 *Parameters of HER and OER activity of FeCu-C in 8 M KOH at 25 °C* [*]

Reaction	E_{onset} / V	j_{400} / mA cm^{-2}	b / mV dec^{-1}	j_0 / 10^{-2} mA cm^{-2}
HER	-0.335	2.73	-151	1.42
OER	1.485	24.78	134	2.50

[*] E_{onset} = onset potential, j_{400} = current density at overpotential of 400 mV, b = Tafel slope, j_0 = exchange current density.

Nyquist plots for FeCu-C were recorded in 8 M KOH at potential of -1.4 for HER and 0.6 V for OER at temperature of 25 °C (Figure 2). Nyquist curves provide the charge-transfer resistance R_{ct} value of a material that is equal to the diameter of the recorded semicircle. Thus, it was observed that R_{ct} in OER conditions was around 35 Ω, while in HER conditions the value was around 50 Ω. Lower charge-transfer resistance under anodic polarisation conditions contributes to the recorded higher current densities and higher activity towards OER.

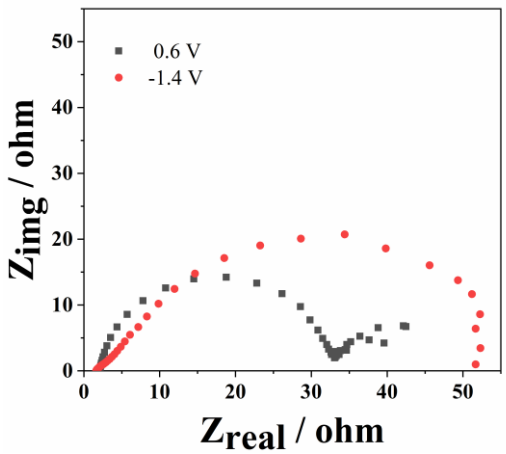

Figure 2 *Nyquist plots at potential of -1.4 V and at potential of 0.6 V at temperature of 25 °C*

CONCLUSION

In this work, FeCu-C electrocatalyst was prepared by direct carbonization of ionic liquids containing Fe and Cu. It was subsequently tested for hydrogen evolution and oxygen evolution in 8 M KOH. According to the presented results, FeCu-C shows exceptional activity for OER with low onset potential and current density as high as 160 mA cm^{-2} at 2 V. On the other hand, activity towards HER was notably lower with current density of -4.2 mA cm^{-2} at -0.4 V. Such notably difference in activity under anodic and cathodic polarisation conditions might be partially explained by the difference in charge-transfer resistance. Namely, charge-transfer resistance under cathodic polarisation was observed to be almost double that under anodic polarisation conditions.

ACKNOWLEDGEMENT

The authors are grateful to the Ministry of Science, Technological Development and Innovation of the Republic of Serbia for financial support according to the contract with the registration number 451-03-47/2023-01/ 200017 and 451-03-47/2023-01/200146. B.Š. is grateful to the Fundação para a Ciência e a Tecnologia (FCT, Portugal) for financial support according to the contract with the registration number IST-ID/156-2018.

REFERENCES

[1] Sun H., Kim H., Song S., *et al*., Materials Reports: Energy 2 (2) (2022) 100092.

[2] Chakraborty B., Beltrán-Suito R., Hausmann J. N., *et al*., Adv. Energy Mat. 10 (30) (2020) 2001377.

[3] Zdolšek N., Vujković M., Metin Ö., *et al*., Int. J. Hydrogen Eng. 47 (33) (2022) 14847–14858.

[4] Santos D. M. F., Amaral L., Šljukić B., *et al*., J. Electrochem. Soc. 161 (4) (2014) F386.

EFFECTS OF CLIMATE CHARACTERISTICS ON THE DIAMETER INCREMENT OF RED OAK IN THE CITY OF BELGRADE (SERBIA)

Tatjana Dimitrijević[1], Gordana Šekularac[2*], Mihailo Ratknić[3], Miroljub Aksić[4]

[1]Institute of Forestry, Kneza Višeslava 3, 11000 Belgrade, SERBIA

[2]University of Kragujevac, Faculty of Agronomy,
Cara Dušana 34, 32000 Čačak, SERBIA

[3]Earthe Climate Change Team (ECCTeam), New Jersey, USA

[4]University of Priština, Kosovska Mitrovica, Faculty of Agriculture,
Kopaonička nn, 38219 Lešak, SERBIA

[*]*gordasek@kg.ac.rs*

Abstract

The paper presents the results of research dealing with the influence of climatic factors on the size of earlywood and latewood and the total diameter increment of red oak (Quercus rubra L.). Samples taken from 30 trees at a height of 1.3 m were used in the analysis. The values were correlated with the mean monthly air temperature and precipitation sums (from April to September). In addition, the tree age expressed in years was included as an important factor. The analysed parameters explained 54.1% of the current diameter increment, 32.9% of the latewood and 49.4% of the earlywood share.

Keywords: red oak, earlywood, latewood, diameter increment, climatic factors.

INTRODUCTION

Climate change has intensified the issue of introducing non-native tree species as part of an adaptive forest management strategy [1]. Changing climate has become a tough challenge for forests and forestry [2]. Although the extent of climate change is difficult to predict at the regional level [3], it is beyond any doubt that the forests of southern Europe, especially in the Balkans, will be strongly affected by climate change with unforeseeable consequences [4]. One of the solutions is to establish mixed stands of tree species that are more adaptable to warm climatic conditions characterized by a reduced amount of soil moisture during the growing season [5]. Based on climate models and changes in forest ecosystems [4], most autochthonous tree species are assumed not to be able to adapt to future climatic conditions. Therefore, allochthonous species should be introduced into the urban forests of Belgrade. As these species are more adapted to future climatic conditions than autochthonous species, they are expected to increase the number of species in this area. A species commonly recommended for the Belgrade area is the red oak.

The red oak is native to North America and is distributed in the eastern and central United States (from the northern end of the Great Lakes, east to Nova Scotia, south to Georgia, Mississippi, Alabama, and Louisiana, and west to Oklahoma, Kansas, Nebraska, and

Minnesota) [6] as well as in south-eastern and south-central Canada. Table 1 shows the characteristics of red oak in natural habitats.

Table 1 *Characteristics of red oak in natural habitats*

Regions	ST	SM	pH	RG	L	NR	PS
Algonquin park region, Ontario	I	d		r	M	vd	S
Southern Ontario	M-I	d-m		r-a	S	e	P
New York and New England	I	m	N	r	L	e	S

Symbols: Shade tolerance (ST): intolerant (I), medium (M); Soil moisture (SM): dry (d), medium (m); Soil reaction (pH): neutral (N); Rate of growth (RG): rapid (r), average (a); Longevity (L): medium (M), short (S), long (L); Natural regeneration (NR): very difficul (vd), easy (e); Place in succession (PS): pioneer (P), subclimax (S).

Introduced to Europe in the 1700, it has been naturalized in most of western and central Europe [7]. Across western and central Europe, northern red oak has become the fourth most important invasive species, colonizing several regions across Belgium, Germany, northern Italy, Lithuania, Poland, Ukraine, European Russia [7], the Urals and Western Siberia. The wide distribution of red oak is based on its economic productivity. On the other hand, considering its impact on the habitats it is introduced to, it is identified as an invasive species that can change the structure of forest ecosystems [8].

MATERIALS AND METHODS

The research was performed in an artificially raised Atlas cedar stand in Šuplja Stena near Belgrade (Serbia). The investigated stand was established in 1961 in the site of (*Quercetum farnetto-cerris aculeatetosum*). It is located at an altitude of 293 m with a slope of 5º and a western aspect. It grows in eutric cambisol, 60 cm deep, overlying serpentine bedrock. The stand has a complete canopy closure and is well preserved.

We used statistical modeling to determine the relationship between stand characteristics and growth elements, on the one hand, and site factors, on the other. The ability of the model to adapt to the character it describes was the criterion used to select the most appropriate model. For this purpose, we used an improved forward "STEPWISE" regression.

In the models obtained using "STEPWISE" regression, the effect of individual independent variables on the values of diameter increment was determined using the net regression calculation procedure.

RESULTS AND DISCUSSION

General data on the artificially established cedar stand are shown in Table 2. As can be seen, the total number of trees is 508 per ha. The maximum number of trees (or 33.5%) is in the diameter degree of 37.5 cm. The mean stand height amounts to 22.3 m, and the mean diameter is 38.9 cm. It has a tree distribution line typical of even-aged stands. The volume distribution line is also typical of even-aged stands. The total basal area is 56.17 m^2 ha^{-1} and the total wood volume is 658.5 m^2 ha^{-1}. The distribution of tree volume by diameter class

results from the distribution of the number of trees. The maximum is in the diameter class of 37.5 cm.

Table 2 *General data on the artificially-established cedar stand*

Diameter class (cm)	N		H_{mean}	G		V (m^3)	
	1 ha	%	(m)	(m^2 ha^{-1})	%	1 ha	%
22.5	17	3.3	19.9	0.68	1.2	6.6	1.0
27.5	68	13.4	21.4	4.04	7.2	41.9	6.4
32.5	153	30.1	22.9	12.69	22.6	139.2	21.1
37.5	170	33.5	24.2	18.78	33.4	215.9	32.8
42.5	34	6.7	25.3	4.82	8.6	57.8	8.8
47.5	15	3.0	26.5	2.66	4.7	33.0	5.0
52.5	17	3.3	27.5	3.68	6.6	47.3	7.2
57.5	34	6.7	28.5	8.83	15.7	116.9	17.7
∑	508	100.0	/	56.17	100.0	658.5	100.0

The dependence of the current diameter increment and the width of earlywood and latewood on climatic characteristics (monthly precipitation sums and mean monthly air temperature in the growing season – from April to September) was examined (Table 3). The independent variables were:

- precipitation sums in April (AP_P), May (MA_P), June (JU_P), July (JL_P), August (AU_P) and September (SE_P) and
- mean air temperature in April (AP_T), May (MA_T), June (JU_T), July (JL_T), August (AU_T) and September (SE_T).

A linear regression model of the effects of age and the analyzed climatic factors on the current diameter increment (Zi), the share of latewood (Ka) and the share of earlywood (Ra) was constructed. The parameters of the model are given in Table 3. Applying the stepwise regression procedure, we determined a negative effect of September precipitation (SE_P), June temperature (JN_T) and July temperature (JL_T) (on the total volume increment (Zi), a negative effect of temperature on the width of the latewood in August (AV_T) and a negative effect of July precipitation (JL_P) and temperature (JL_P) on the width of earlywood (Table 4).

Table 3 *The influence of age and analysed climatic factors on current diameter increment (Zi), share of latewood (Ka) and share of earlywood (Ra)*

Independent variable	Dependent variable					
	Zi		Ka		Ra	
	Parameters	Error	Parameters	Error	Parameters	Error
CONSTANT	16.73000	6.01027	5.05060	3.07033	11.67940	3.40557
Year	-0.11618	0.02611	-0.05094	0.01334	-0.06524	0.01480
AP_P	-0.00238	0.00812	0.00215	0.00415	-0.00452	0.00460
MA_P	0.00049	0.00504	-0.00034	0.00258	0.00083	0.00286

Table 3 *continued*

JU_P	-0.00127	0.00490	-0.00110	0.00250	-0.00017	0.00278
JL_P	-0.00027	0.00449	0.00048	0.00229	-0.00075	0.00254
AU_P	-0.00741	0.00675	-0.00354	0.00345	-0.00387	0.00383
SE_P	-0.01239	0.00703	-0.00479	0.00359	-0.00760	0.00398
AP_T	0.09820	0.13833	0.07004	0.07067	0.02816	0.07838
MA_T	0.06641	0.16823	0.04136	0.08594	0.02504	0.09532
JU_T	-0.19403	0.18393	-0.06782	0.09396	-0.12621	0.10422
JL_T	0.05533	0.20030	0.09928	0.10232	-0.04394	0.11349
AU_T	-0.06043	0.17596	-0.08316	0.08989	0.02272	0.09970
SE_T	-0.32218	0.14883	-0.11072	0.07603	-0.21145	0.08433
R		0.87		0.82		0.88
R^2		75.81		66.53		77.97
Standard error		1.2957		0.6619		0.7341
F-test		8.19		5.20		9.26

Table 4 *Influence of age and analysed climate factors on current diameter increment (Zi), share of latewood (Ka) and share of earlywood (Ra) (Stepwise regression)*

Independent variable	**Dependent variable**					
	Zi		**Ka**		**Ra**	
	Parameters	**Error**	**Parameters**	**Error**	**Parameters**	**Error**
CONSTANT	31.49920	3.81984	7.77490	1.28520	16.41900	2.08272
SE_P	-0.01640	0.00767				
JN_T	-0.43537	0.15989				
JU_P					-0.00679	0.00269
JU_T	-0.38190	0.17473			-0.57903	0.08750
AV_T			-0.26744	0.05633		
SE_T	-0.45459	0.15454				
R		0.74		0.57		0.70
R^2		54.13		32.88		49.37
Standard error		1.58630		0.80581		0.96750
F-test		12.69		22.54		21.94

The net regression equations are presented in Table 5 and Figure 1.

Table 5 *Net regression equations for total diameter increment, latewood and earlywood*

Net regression equations for		
Total diameter increment	**Latewood**	**Earlywood**
5.30111 – 0.01640 * SE_P	7.77490 – 0.26744 * AV_T	15.97358 – 0.57903 * JU_T
13.55918 – 0.43537 * JN_T		3.10132 – 0.00679 * JU_P
13.15657 – 0.38190 * JU_T		
12.60095 – 0.45459 * SE_T		

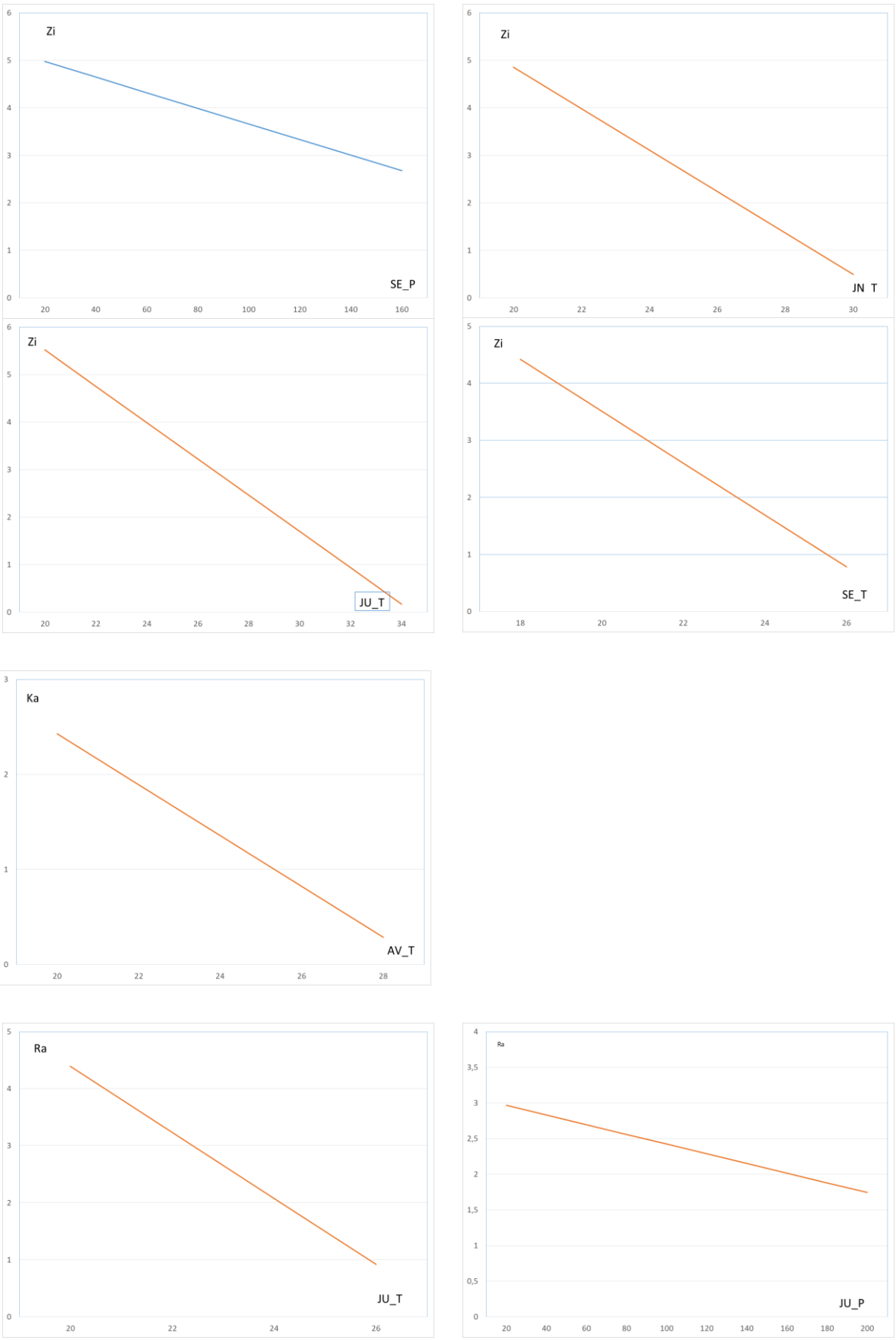

Figure 1 *Net regressions*

CONCLUSION

The study of the impact of climate factors on the diameter increment of introduced species (size of earlywood, latewood and total increment) provides the necessary information about the adaptability of the species to new conditions.

According to the obtained regression models, September precipitation and June, July and September temperatures have a negative statistically-significant impact on the total diameter increment. These factors account for 54.13% of the variability.

The size of the latewood is most negatively affected by the temperature in August which accounts for 32.88% of the variability. The size of earlywood is negatively affected by the sum of precipitation and air temperature in June. This model explains 49.37%.

Bearing in mind that the red oak is distinguished as an invasive species susceptible to the adverse effects of climate factors, its introduction into natural habitats within forest ecosystems should be reconsidered.

ACKNOWLEDGEMENT

The authors are grateful to the Ministry of Science, Technological Development and Innovation of the Republic of Serbia for financial support (451-03-47/2023-01/ 200027, 451-03-47/2023-01/200088 and 200189).

REFERENCES

[1] Ennos R., Cottrell J., Hall J., *et al*., Forest Ecol. Manag. 432 (2019) 718–728.

[2] Lindner M., Maroschek M., Netherer S., *et al.*, Forest Ecol. Manag. 259 (4) (2010) 698–709.

[3] Hemery G. E., Int. Forest Rev. 10 (2008) 591–607.

[4] Ratknić, T. Application of adaptive measures in the adaptation of forest ecosystems to climate change in the City of Belgrade, Final Report, Institute of forestry, Belgrade (2021).

[5] Milad M., Schaich H., Konold W., Biodivers. Conserv. 22 (5) (2013) 1181–1202.

[6] Forbes R. D. Forestry handbook, Ronald Press, New York (1955), ISBN-10: 1114202614; ISBN-13: 978-1114202610.

[7] Quercus rubra, European Forest Genetic Resources Programme, *Available on the following link*: https://www.euforgen.org/species/quercus-rubra/.

[8] Stanek M., Piechnik L., Stefanowicz A., Forest Ecol. Manag. 472 (2020) 118253.

GREENHOUSE EFFECT AND GLOBAL CLIMATE CHANGE – IMPACT ON AGRICULTURE

Milica Blažić[1*], Tatjana Sekulić[1], Vladanka Stupar[1], Zlata Živković[1]

[1]Academy of Applied Technical Studies Belgrade, College of Applied Engineering Sciences, Nemanjina 2, Požarevac, SERBIA

[*]*mblazic@atssb.edu.rs*

Abstract

Climate change and global warming are topics that never ceased to intrigue scientists and public over the last two centuries. Global warming has intensified as a result of increased gas emission and greenhouse effect caused by excessive burning of fossil fuels since industrial revolution in 18th century. Climate change caused by global warming can have negative effect on many levels including agriculture. This can jeopardise safety in human food supply. Despite opinion that there is enough food for entire human population, more than 10% of population is malnourished. It is estimated that climate change will exacerbate current situation by rise in food price and reduction of agricultural production. This study offers summary view on consequences and influence from climate change on global level rather than focus view on certain regions or selected effects, in order to create wide view on risk assessment of global food production. As well, some strategies of adjusting agricultural production to these changes are presented.

Keywords: global warming, greenhouse gases, agriculture

INTRODUCTION

The greenhouse effect implies an increase in the temperature of the Earth's surface due to the heating of the lower layers of the atmosphere as a result of the accumulation of greenhouse gases. These are gaseous components of the atmosphere that absorb and emit radiation in the infrared part of the spectrum [1]. The most represented, in order of importance - the percentage they contribute to the appearance of the effect are: water vapour, carbon dioxide (CO_2), methane (CH_4), nitrogen oxides (N_xO) and ozone (O_3) [2]. Water vapor contributes to the appearance of the effect with 60%, carbon dioxide with 26%, and all other gases together with 14% [3]. The greenhouse effect results in a gradual increase in the global mean annual air temperature, and it has irreversible consequences such as climate change and global warming [4]. According to data from the Intergovernmental Panel on Climate Change - IPCC, the global mean annual air temperature increased by 0.4˚C to 2.6˚C in the second half of the 21st century, and is expected to increase by 1.8–4˚C until the end of it [5]. The greenhouse effect is a natural process, however, due to human activity, it has been strongly intensified in the last two centuries. The production of electricity and thermal energy by burning fossil fuels is one of the most important causes of the increased concentration of greenhouse gases in the atmosphere. Fossil fuel combustion is by far the largest contributor to global climate change, accounting for over 75% of total global greenhouse gas emissions and nearly 90% of total CO_2 emissions [6]. In addition to this, important causes of the emission of

harmful greenhouse gases are the production and construction industry, mining, transport (road, water or air), deforestation and extensive agriculture.

Global warming and the climate changes caused by it have consequences in all segments of people's lives, including agriculture. Agriculture is one of the most sensitive branches of the economy given that climate is a crucial factor in agricultural productivity that directly affects food production worldwide. The consequences of climate change on agriculture have a direct impact on the lives of 1.2 billion people [7]. Global climate changes lead to changes in mean annual temperatures, patterns and amounts of precipitation, sea level rise, increase in atmospheric CO_2 concentration and ultimately indirectly affect outbreaks of diseases and crop pests [8]. The aim of this paper is to provide a concise overview of the most significant impacts and consequences of global climate change on agriculture at the global level.

DIRECT IMPACTS OF CLIMATE CHANGES ON AGRICULTURE AND THEIR CONSEQUENCES

(i) Change in mean annual temperatures

Productivity

An increase in mean annual temperatures affects crop productivity [9]. It is believed that it will increase and spread northward in crops grown in areas of middle and high latitudes, which is especially true for cereals and seed crops [10]. Growing crops prevalent in southern Europe, such as maize, sunflower and soybeans, in more northern areas and at higher altitudes could increase yields by as much as 30% by 2050 [10,11]. On the other hand, in areas experiencing temperatures close to plant physiological maxima, such as seasonally arid and tropical regions, higher mean annual temperatures can be detrimental to crops due to increased heat stress and evaporative water loss. A temperature increase of 2˚C in mid-latitude areas could increase wheat production by almost 10%, while in low-latitude areas it could lead to a yield reduction of the same percentage [12]. Lobell and Field [13], considering the relationships between temperatures, vegetation, precipitation and global average yield for six major crops, estimated that global warming since 1981 resulted in annual yield losses of 40 million tons. Total global agricultural productivity is projected to decline by 3–16% by 2080.

The length of the growing season

Many studies [14–16] have shown that the increase in mean annual temperatures also affects the length of the vegetation period of crops. Thus, the increase in temperatures in the northern regions of the world leads to an increase in the length of the vegetation period [14]. Also, one of the important consequences of the increase in temperature during the growing season is the change in the starting and ending temperature of 0˚C as well as the temperature of 5˚C, which is considered the temperature basis for the growth of crops in cold areas [15]. A reduction in the length of the growing season leads to a reduction in crop yields, given that a shorter growing season shortens the time required for plants to reach full maturity. On the other hand, increasing the length of the growing season provides opportunities for growing crops earlier, providing enough time for plants to reach full maturity, which can then be reflected in the increase in yield [16].

Precipitation

The global increase in temperature affects the annual amount of precipitation, its distribution during the growing season, changes in its duration, as well as when it occurs and when it stops [15]. As water is vital for plant growth, different precipitation patterns have a significant impact on agriculture, especially in non-irrigated areas. More than 80% of the total agricultural production depends on rainfall [17,18]. According to IPCC projections, global warming leads to a general increase in precipitation at higher latitudes, especially in winter, and an overall decrease in many tropical and subtropical areas [19]. Rainfall is not the only influence on water availability. Increased evaporation due to rising temperatures and longer growing seasons could increase crop irrigation needs globally by 5 to 20% by 2070s or 2080s [20].

(ii) Climate variability and extreme weather conditions

Extreme temperatures

Changes in short-term temperature extremes can be critical, especially if they coincide with key stages of crop development. Only a few days of extreme temperatures (higher than 32˚C) in the flowering phase of many crops can drastically reduce yield [21]. Wollenweber *et al*. [22] found that temperatures of 35˚C during the flowering period of plants contributed to a significant reduction in yield. On the other hand, some studies have shown that extreme temperatures during the vegetative phase did not have a significant impact on crop growth and development. In the long term, temperature extremes will affect carbon assimilation, and thus growth rates and final yield.

Drought

Studies have shown that agricultural areas affected by drought increased from 20% to 28% during the 20th century. As a result of climate change, drought is expected to worsen the current state of agricultural production in much of the world. Dry areas will be the most vulnerable. From the year 2100s, areas affected by drought are expected to increase from 15.4% to 44%. Also, it is certain that dry lands will lose more than half of their food production by 2050s, and even more than 90% by 2100s [23].

(iii) Increase in atmospheric CO_2 concentration

The two most significant direct effects of elevated atmospheric CO_2 concentrations are on the process of photosynthesis and transpiration in plants. An increase in CO_2 concentration results in higher rates of photosynthesis. On the other hand, higher concentrations of CO_2 reduce the rate of transpiration, as plants reduce their stoma openings, which has direct influence on efficiency of water use. All this results in an increase in biomass and crop yield [8]. In experimental conditions, it was shown that doubling the concentration of atmospheric CO_2 increases the rate of photosynthesis by 30–50% in C3 and 10–25% in C4 plants. The increase in crop yield is somewhat lower - in C3 plants, an increase in atmospheric CO_2 concentration up to 550 ppm can increase yields by 10-20%, and in C4 plants up to 10% [24]. However, the effects of increased CO_2 concentrations have been measured under experimental conditions and require evaluation of crop responses in the field. An increased level of CO_2 can also cause direct inhibition of breathing at night temperatures higher than 21˚C [25]. The impact of higher CO_2 concentrations on crop yield also depends on the

geographical location of the region for which the assessment is being made. It is predicted that due to increased CO_2 concentrations caused by climate change, Europe and North America will benefit at least in the short term, while arid regions, such as Africa and India, will have up to 5% loss by 2050s [12].

INDIRECT IMPACTS OF CLIMATE CHANGES ON AGRICULTURE AND THEIR CONSEQUENCES

(i) Sea level rise

As a consequence of global warming, the sea level rises. It is caused by the expansion of the already existing ocean mass and the creation of additional water due to the melting of the ice. As a result, flooding of coastal land masses can be expected. Crop productivity is thought to be most threatened in areas where lowland coastal agriculture exists. A rise in global mean sea level may lead to inundation of agricultural lands and salinization of groundwater in the future, although these impacts may not be visible for several centuries to come, as it takes time for huge ice masses to melt [12].

(ii) Diseases and pests

The main factors of climate change that indirectly affect crop productivity through the influence on the spread of plant diseases and pests are increased CO_2 concentration, heavy and unseasonal precipitation, increased humidity, drought, hurricanes and warmer winters. Due to climate change, there are changes in the type of crops, the land on which they are grown, as well as changes in the natural habitats of plants and animals, which indirectly affect the resources that are necessary for pathogens and pests [15]. Some studies have shown that pests, such as aphids and weevil larvae, respond positively to increased CO_2 concentrations [26]. Warmer temperatures that occur earlier in the spring can cause pest populations to expand during sensitive stages of plant growth and development. They also increase the growing season in temperate regions which then allow insect pests to produce an additional generation and thus consequently increase the pest population [15]. Increasing temperatures reduce the mortality of pests during wintering, thus allowing them to spread earlier and more widely. Climate change is also affecting pest migration patterns. They can also affect the resistance of crops to specific diseases through the increased pathogenicity of organisms, which is conditioned by mutations caused by environmental stress [12].

STRATEGIES FOR MITIGATION AND ADAPTATION AGRICULTURE TO CLIMATE CHANGE

Some of the proposed adaptation strategies according to Mahato and Mozaffari [8,15] that the agricultural sector can implement to mitigate current and face future climate change are: changes in sowing dates, selection of varieties with different duration of growing period, change of crop rotation, development of varieties resistant to high temperatures, drought and soil salinity, development of cultivars with a short duration of the growing season, selection of genotypes that have a higher yield per day - as a potential to reduce yield loss due to heat-induced reduction of the growing period, better use of crop residues and weed management, improvement of soil drainage, better control of diseases and pests, implementation of new or

better crop irrigation systems (maintenance of soil moisture - mulching), changes in grazing and pasture rotation, developing early warning systems and protective measures for natural disasters, providing more funding to strengthen research on adaptation and mitigation of climate change impacts on agriculture.

CONCLUSION

The accelerating pace of climate change caused by greenhouse gas emissions and global warming combined with global population growth threatens food security on a global scale. Agriculture is extremely sensitive to climate change. The global increase in mean annual temperatures reduces the yields of desirable crops, and at the same time affects the spread of diseases and pests. Changes in rainfall patterns and duration increase the likelihood of short-term crop failures and affect long-term declines in agricultural production. Although in some regions of the world, especially the northern ones, there will be an increase in production and crop yields, it is expected that the overall impacts of climate change on agriculture will be negative, threatening global food security and the survival of the human population.

REFERENCES

[1] Edenhofer Y., Pichs-Madruga E., Sokona S., *et al*. IPCC 2014: Climate Change 2014: Mitigation of Climate Change, Contribution of working group III to the fifth assessment report of the Intergovernmental panel on climate change, Editor: O. R. Edenhofer, Cambridge University Press, Cambridge, United Kingdom and New York, NY, USA (2015), ISBN: 978-92-9169-142-5.

[2] Kiehl J., Trenberth K., Bull. Amer. Meteor. Soc. 78 (1997) 197–208.

[3] Ahrens C.D., Hensens R. Meteorology Today. USA: Cengage Learning, *Available on the following link*: www.cengage.com/global2014.

[4] Huang S. K., Kuo L., Chou K. L., J. Clean. Prod. 127 (2016) 59–71.

[5] Devasirvatham V., Tan D.K.Y., Trethowan R.M., Breeding strategies for enhanced plant tolerance to heat stress. In: Advances in plant breeding strategies: agronomic, abiotic and biotic stress traits. Editors: Al-Khayri J., Jain., Johnson D., Springer, Dodrecht (2016), p.447–469, ISBN: 978-3-319-22518-0.

[6] United Nations, Causes and Effects of Climate Change, *Available on the following link*: https://www.un.org/en/climatechange/science/causes-effects-climate-change.

[7] Bhattacharya A., Global Climate Change and Its Impact on Agriculture. In: Changing Climate and Resource Use Efficiency in Plants, Editor: Amitav Bhattacharya, Academic Press, Massachusetts (2019), p.1–50, ISBN: 9780128162095.

[8] Mahato A., Int. J. Sci. Res. 4 (2014) 1–11.

[9] Battisti D.S., Naylor R.L., Science 323 (2009) 240–244.

[10] Olesen J.E., Carter T.R., Diaz-Ambrona C.H., *et al*. Clim. Change 81 (2007) 123–143.

[11] Audsley E., Pearn K.R., Simota C., *et al*. Environ. Sci. Policy 9 (2006) 148–162.

[12] Gornall J., Betts R., Burke E., *et al*. Phil. Trans. R. Soc. B. Biol. Sci. 365 (2010) 2973–2989.

[13] Lobell D.B., Field C.B., Environ. Res. Lett. 2 (2007) 1–7.

[14] Linderholm H.W., Agric. For. Meteorol. 137 (2006) 1–14.

[15] Ali Mozaffari G., Climate change and its conseguences in agriculture. The nature, causes, effects and mitigation of climate change on the environment, IntechOpen, *Available on the following link*: https://www.intechopen.com/chapters/79716.

[16] Chen X., Schwartz M.D., Xu C., Int. J. Biometeorol. 44 (2000) 97–101.

[17] Olesen J.E., Bindi M., Eur. J. Agron. 16 (2002) 239–262.

[18] Reilly J., Tubiello F., McCarl B., Clim. Change 57 (2003) 43–69.

[19] Solomon S., Qin D., Manning M., *et al*. IPCC 2007: Climate Change 2007: the physical science basis, Contribution of Working Group I to the Fourth Assessment Report of the Intergovernmental Panel on Climate Change, Editor: Cambridge University Press, Cambridge, United Kingdom and New York, NY, USA (2007), p.996, ISBN 978-0-521-88009.

[20] Fischer G., Tubiello F., Van Velhuizen H., *et al*. Technol. Forecasting Soc. Change 74 (2006) 1083–1107.

[21] Wheeler T.R., Craufurd P.Q., Ellis R.H., *et al*. Agric. Ecosyst. Environ. 82 (2000) 159–167.

[22] Wollenweber B., Porter J.R., Schellberg J., J. Agron. Crop Sci. 189 (2003) 142–150.

[23] Ladrera R.C., Cagasan U.A., Eurasian J. Agric. Environ. Sci. 6 (2022) 52–61.

[24] Ainsworth E.A., Long S.P., New Phytol. 165 (2005) 351–371.

[25] Baker J.T., Allen L.H., Boote K.J., Glob. Chang. Biol. 6 (2000) 275–286.

[26] Newman J.A., Global Change Biol. 10 (2004) 5–15.

GLOBAL CLIMATE CHANGES: GREENHOUSE GASSES, CITIES AND PLASTICS

Vojkan Miljković[1*], Ivana Gajić[1], Ljubiša Nikolić[1]
[1]University of Niš, Faculty of Technology, Bulevar oslobođenja 124, Leskovac, SERBIA
[*]*vojkan@tf.ni.ac.rs*

Abstract

Greenhouse gasses such as water vapour, CO_2, CH_4, nitrous oxides, halocarbons are significantlymore present in Earth's atmosphere than before global industrialization process started and as a result global climate changes are happening. Increased temperature is just one of a consequence.Also, the impact of plastic materials on eco system is evident, and not only during production of plastic but also even in recycling process. Global plastic production reached 390.7 million tons (MT) in 2021, with 32.5 Mt from post consumer recycled plastics and 5.9 Mt Bio-based plastics. China isstill the largest global plastic producer with share of 32%, followed by North America 18% and Europe with 15%, Africa and Middle East 8%, Latin America 4%, CIS 3%, Japan 3% and rest of Asian countries 17%.The Intergovernmental Panel on Climate Change (IPCC) provides a detailed methodological framework in order to collect data on greenhouse gases emission. Contrary to expectations of many people, urban areas with conscious government that is aware of global climate changes could be a solution for problem. The consequences of global climate changes are evident and it is important that people on position of decisions makers at all levels implement measures for lowering greenhouse gasses emission.

Keywords: global climate changes, greenhouse gasses, plastics.

INTRODUCTION

The climate changes on Earth happen naturally. Changes in the intensity of sunlight reaching the Earth is causing warming and cooling of atmosphere which is a part of Earth's climatic history. The solar cycles (i.e. four glacial-interglacial swings in past 400,000 years) last for long time and have amplitudes of 5°C to 6°C. But for the past 10,000 years the Earth has been in warm interglacial phase of such a cycle. It can be said that there is a balance in that process and concluded that because of industrialization process and burning fossil fuels more greenhouse gasses are added into atmosphere. By increasing the amount of greenhouse gasses in atmosphere, the warming capability of the natural greenhouse is enhanced. The consequences of climate change that can be seen are: sea level rise, flooding, hotter summers and wetted winters [1].

The impact of plastics on water ecosystem is serious and it threatens to that extent that it affects warming on Earth by releasing greenhouse gasses CO_2, CH_4 and N_2O. The concentration of greenhouse gasses in Earth's atmosphere has increased since the great industrial revolution. More precisely, compared to the concentrations of mentioned gasses before industrialization the concentrations increased by 41%, 160% and 20%, respectively [2]. In the period of 1951–2010, greenhouse gases contributed to increment of the global average temperature by 0.5–1.3°C, and with constant emission this process will continue [3].

The big cities are usually the first to blame for greenhouse effect and global warming. Some believe that cities generate most of the world's greenhouse gasses emission. The fact is that city hall and local governments are authorized to implement mitigation programs. It should be on mind that local public transportation system is under their control [4].

The aim of this review paper is to get familiarize reader with situation about global climate changes and greenhouse effect, their relation with cities and plastics.

Climate changes

Earth is heated by sunlight, and just like as glass greenhouse construction keeps heat in, Earth's atmosphere keeps the heat, primarily by heat-trapping properties of greenhouse gases. This natural system that regulates temperature on Earth is called greenhouse effect.

One part of the heat energy goes in a direction through the atmosphere to Earth's surface in order to warm it and other from Earth to space as infrared radiation. In this direction it gets absorbed by clouds and molecules of greenhouse gases in the lower atmosphere. At this point energy gets radiated in all directions where other molecules higher up can absorb the energy again. Until energy escapes from the atmosphere this process is repeated. As a result of this repetition huge amount of heat energy is getting in direction of Earth's and rises temperature at surface which is even higher with higher concentration of greenhouse gasses in the atmosphere. This natural process is what is called as the greenhouse effect [1] and it is showed in Figure 1.

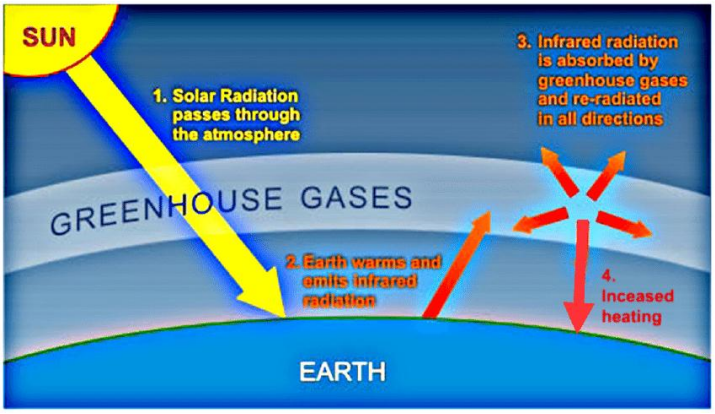

Figure 1 *Greenhouse effect due to greenhouse gasses [5]*

Greenhouse gasses are: water vapour – the most common greenhouse gas, CO_2 – considered as main contributor to climate changes and the most significant greenhouse gas released by human activities, mostly through the burning of fossil fuels, CH_4 – arises after agricultural waste is burned, from garbage dumps and cows and other livestock, nitrous oxides – are results of human activities and also are released after chemical fertilizers and manure are used in agriculture, halocarbons – are group of chemicals that include chlorofluorocarbons (CFCs) and they are damaging the ozone layer along with chemicals that contain chlorine and fluorine. They are effective at absorbing heat escaping from the Earth and in practice it takes only small amounts of these gases to significantly change the properties of the atmosphere [5]. The concentration of greenhouse gases in atmosphere has

been relatively stable over the past 10,000 years, but due to industrialization concentrations began to increase [1].

Greenhouse gasses emission in cities

The Intergovernmental Panel on Climate Change (IPCC) provides a detailed methodological framework in order to collect data on greenhouse gases emission. By this is meant all the greenhouse gases generated from four main sectors: energy; industrial processes and product use; agriculture, forestry and other land use and waste [6]. This provides data at global level of greenhouse gasses emissions and is very useful for making further steps in lowering their emission. Also, they are used for measuring a success in implementation of local and international treaties.

From a detailed work of Dodman it can be seen that, with the exception of Beijing and Shanghai, all the cities that were part of this research are generating smaller volume of carbon oxide equivalents (CO_2eq) per capita than the countries in which they belong: Barcelona, Glasgow, London, District of Columbia, New York City, Toronto, Rio de Janeiro, Sao Paolo, Seoul, Tokyo, Ankara, Bologna, Copenhagen, Miami, Denver, Hanover, Heidelberg, Helsinki, Minneapolis, Portland, Saarbrucken, San Jose, Toronto City, Toronto Metro. The explanation can be found in transition to service based urban economies in cities. In addition, cities with high concentration of people and industries in cities gives an opportunity for easier implementation of new technological innovations, more efficient utilization of power and energy generated from waste, and transport system can cost less [7].

Plastics as source of greenhouse gasses emission

By definition, plastics are synthetic organic polymers with a backbone consisting entirely of C–C bonds, and the raw materials needed for production mainly come from fossil fuel, coal, oil and natural gas. They are one of the most commonly used materials in almost every industrial branch (plastics bags, packages, clothes, building materials). Plastic packing is one of the most problematic types of plastic waste, because it is designed for single use, omnipresent and difficult to be recycled because of low grade multilayered design of plastic packages [8]. Additives such as colorants and other fillers in production process makes recycling even more difficult and low-grade plastic waste such as multilayer plastic packing. Because this material is difficult to degrade naturally it is accumulating in land, fresh water and natural environment in general. It has to be on mind that ocean plants and animals are necessary for microbial carbon pump that filters carbon from the atmosphere [9].

By relevant data, global plastic production increased by 4% compared to previous year and in 2021 it reached 390.7 million tons (Mt) from which 352.3 Mt came from fossil based plastics, 32.5 Mt from post consumer recycled plastics and 5.9 Mt Bio-based plastics [10]. China is still the largest global plastic producer with share of 32%, followed by North America 18% and Europe with 15%, Africa and Middle East 8%, Latin America 4%, CIS 3%, Japan 3% and rest of Asian countries 17%. Just to know Walker & King pointed the fact: "Many of the countries in the western world have dodged their own carbon dioxide emissions by exporting their manufacturing to China. Next time you buy something with "Made in China" stamped on it, ask yourself who was responsible for the emissions that created it." [11]. More precisely, in same year distribution of the global plastic products by application

was: 44% packaging, building and construction 18%, automotive 8%, electrical and electronics 7%, household, leisure and sports 7%, agriculture, farming and gardening 4% [10].

In more details, the European share was approximately 57 million tons of which 5.5 million tons were from circular and climate-neutral plastics industry. These 5.5 million tons of plastics that were reused in new products represents a share of 10% and is 20% increase compared to 2018 considering reused plastics [10].

Despite all, recent paper showed that that greenhouse gases are getting released during the degradation of plastics [12]. In addition, data are showing the fact that greenhouse gas emissions consequence have to be controlled by implementation of strategies and policy that have to be applied.

Plastic waste management practically means: recycling, incineration, sanitary landfill and others. Recycling is the most needed but actually only a small percentage of "recyclable" plastic is getting recycled into the original products, but incineration with releasing of CO_2 can provide energy for industry. Sanitary landfills are up till now the main treatment method for plastic packing waste. By applying this method, green-house gas emissions mainly come only from organic waste. Up to now, there is no record of greenhouse gas emissions from plastic landfills [9].

Low prices of new plastics are not favouring mentioned pathways of plastic waste management and whatever treatment method is used plastic waste will have harmful effect on living environment [9].

CONCLUSION

The climate changes are happening and their impact is evident. There are consequences for living organisms as well as the economy of many countries that are agricultural based economies. No relation between urbanized areas such as cities with high population and high levels of greenhouse gasses emission can be found. Practically in life, there is an opportunity for well planned and managed cities that can be well organized to carry the fight against global climate changes. The impact of plastics on environmental pollution and climate changes cannot be neglected. Greenhouse gasses emission from plastic industry is growing and will it is consuming a significant amount of carbon budget. It is important that principal managers and people on position of decisions makers at all levels make a deal a measures for cutting down greenhouse gasses production.

ACKNOWLEDGEMENT

The authors are grateful to the Ministry of Science, Technological Development and Innovation of the Republic of Serbia for financial support according to the contract with the registration number (451-03-47/2023-01/200133).

REFERENCES

[1] Adedeji O., Reuben O., Olatoye O. J., Geosci. Environ. Prot. 2 (2014) 114–122.

[2] Working Group I of the IPCC, Contr. Work. 43 (2013) 866–871.

[3] Moss R.H., Edmonds J.A., Hibbard K.A., *et al*., Nature 463 (2010) 747–756.

[4] Parker P., Rowlands I., Local Environ. 12 (5) (2007) 505–518.

[5] Thorstein S., Borgar T.O., NPJ Clim. Atmos. Sci. 10 (2) (2020) 168–185.

[6] Intergovernmental Panel on Climate Change (IPCC) (2006), Guidelines for National Greenhouse Gas Inventories, Cambridge University Press, Cambridge.

[7] Dodman D., Environ. Urban. 21 (1) (2009) 185–201.

[8] *Available on the following link*: https://plasticseurope.org/wp-content/uploads/2022/10/PE-PLASTICS-THE-FACTS_V7-Tue_19-10-1.pdf.

[9] Shen M., Huang W., Chen M., *et al*., J. Clean. Prod. 254 (2020) 120138.

[10] https://plasticseurope.org/wp-content/uploads/2021/10/2016-Plastic-the-facts.pdf.

[11] Walker G., King D., The Hot Topic: How to Tackle Global Warming and Still Keep the Lights On, Bloomsbury Publishers, London (2008).

[12] Royer S.J., Ferron S., Wilson, S.T., *et al*., PLoS One 13 (8) (2018) e0200574.

30th International Conference Ecological Truth & Environmental Research
20–23 June 2023, Serbia

ROLE OF NUTRIENTS IN CONTROLLING PLANT DISEASES AND PATHOPHYSIOLOGICAL ALTERATIONS IN PLANTS IN SUSTAINABLE AGRICULTURE. A REVIEW

Zlata Živković[1*], Markola Saulić[1], Darko Stojićević[1], Milica Jevtić[1], Vladanka Stupar[1]

[1]Academy of Applied Technical Studies Belgrade, College of Applied Engineering Sciences, Nemanjina 2, Požarevac, SERBIA

[*]*zzivkovic@atssb.edu.rs*

Abstract

In recent years, sustainable agriculture is considered imperative when it comes to the future of agricultural production. While conventional agriculture is driven solely by productivity and profit, sustainable agriculture integrates biological, chemical, physical, ecological and economic aspects in a comprehensive manner, in order to develop new agricultural practices that are safe and do not degrade the environment. Control of plant diseases using conventional pesticides often leads to resistance of the pathogens themselves and has a great impact on food safety and environmental quality, which leads to the need for alternative techniques to control plant diseases. In addition, soil quality and available nutrients can influence plant resistance to pathogens. Plants require sixteen essential nutrient elements including oxygen, hydrogen and carbon potentially derived from hydrosphere, lithosphere and atmosphere while remaining thirteen are chlorine, molybdenum, boron, copper, manganese, zinc, iron, sulphur, magnesium, calcium, potassium, phosphorous and nitrogen that are supplied either through soil organic matter and soil minerals or by inorganic and organic fertilizers. In most cases, it is more cost-effective and environmentally friendly to control plant diseases with an adequate amount of nutrients and without or with less use of pesticides. This review article summarizes the latest information on the influence of macro- and microelements on plant yield, the occurrence of plant diseases and the induction of pathophysiological alterations in plants.

Keywords: plant diseases, sustainable agriculture, nutrients, pathophysiological alterations.

AGRICULTURE'S STATE

According to FAO [1], agriculture employed 874 million people in 2020, or 27% of the global workforce. In 2019, the global agricultural land area was 4.8 billion hectares (ha). One third of the total agricultural land was cropland (1.6 billion ha in 2019). The global land area equipped for irrigation reached 342 million ha in 2019. Total agricultural use of inorganic fertilizers, expressed as the sum of the three nutrients nitrogen (N), phosphorus (expressed as P_2O_5) and potassium (expressed as K_2O), was 189 million tonnes in 2019, of which 57% was nitrogen. Fertilizer use increased in all regions between 2000 and 2019. The total for the three nutrients went up 33 million tonnes. Global pesticides use increased during the period 2000–2019 by 36 percent, to 4.2 million tonnes in 2019. Total production of primary crops (cereals, sugar crops, vegetables and oil crops) increased by 53 percent between 2000 and 2019, to a record high of 9.4 billion tonnes in 2019. This represents 3.2 billion tonnes more

than in 2000. According to these figures, more food must be produced to feed the world's current population of more than 8 billion people. Agricultural production is essential for human survival, but it is also an important factor that contributes to the negative impact on the environment. Biodiversity has been significantly impacted by long-term soil, water, and air contamination brought on by intensive agriculture employing large inputs like pesticides and fertilizers [1–4]. One feature of conventional agricultural production is the dominance of annual plants grown in monocultures. Such crops result in ecological degradation, soil erosion, and a rise in pests and weeds that have adapted to the cultivated crop. Large doses of different pesticide active ingredients are required to control them due to the development of resistance, which becomes an additional problem in monocultures [4]. Compared to conventional agriculture, sustainable agriculture produces a large amount of food without using a lot of input or harming the environment. These include low input agriculture, organic farming, crop rotation, diversified crop and animal farming, integrated pest control strategies, and limited use of chemical pesticides, and fertilizers [5,6].

CONTROL OF PLANT DISEASES IN SUSTAINABLE AGRICULTURE

One of the major problems of agriculture is plant diseases, which cause great economic damage. The disastrous results of widespread crop disease infestation are well documented in agricultural science history. Despite the availability of more dependable techniques for protecting plants, plant diseases continue to have a significant negative impact on agriculture. For example, the development of phytophthora may cause the loss of half or more of the crop of potatoes, while the tomato may not yield at all under its damage [7]. Chemical pesticides are most frequently employed to treat plant diseases and other harmful organisms, especially in underdeveloped countries [8]. Globally 4.6 million tons of chemical pesticides are annually sprayed into the environment [9]. Pesticides can cause pesticide resistance in some pests, reduction of biodiversity and nitrogen fixation, destruction of marine and birds' life and/or genetic defects in their next generations [10]. Pesticides designed to suppress the fungi, viruses, and bacteria that cause plant diseases are fungicides. Most fungicides have a direct effect by acting on the parasite itself, but some fungicides also have an indirect effect on the host plant by stimulating it to produce substances (phytoncides) that have a harmful effect on the parasite [11]. During the last decades there has been a global awareness that excessive and improper use of chemical fungicides is hazardous to the health of humans, animals, and the environment [8]. Sustainable agriculture aims at reducing the incidence of pests and diseases to such a degree that they do not seriously damage crops without upsetting nature's balance [12] using natural organic pesticides as an alternative to synthetic pesticides [13]. Today, about 83% of the known infectious diseases of plants is caused by fungi, 9% by virus and more than 7% by bacteria. Biofungicides are the common name for preparations derived from microorganisms and their vital products and used against plant diseases. These products have minimal toxicity and a wide range of effects on various pathogens, as well as increase the resistance of plants to adverse factors [7]. Some of the biocontrol organisms that are in use or can be used for environmental protection against plant disease agents *Bacillus subtillis* QST 713 against *Rhizoctonia*, *Pythium*, *Phytophthora* and others phytopathogenic fungi [7,14]. Bacillus subtillis GB03 for Leaf spots, Powdery mildew, *Botrytis*, bacterial diseases,

Rhizocotonia, *Pythium*, *Phytophthora*, extracts of cinnamon and clove as potential biofungicides against strawberry grey mould [15], species of the genus *Trihoderma* against *Rhizoctonia, Pythium, Fusarium, Cylindrocladium, Thielaviopis* [7,16]. *Trichoderma* is one of the most widespread biological agents currently used in agriculture to control different plant diseases and its present in more than 60% of registered biological pesticides worldwide [16]. In addition, it has been shown that plant extracts, essential oils, gums, resins, etc. they exhibit biological activity against plant fungal pathogens and can be used as bio-fungicidal products [8,17]. Plants like *Mentha piperita*, *Lavandula angustifolia*, *Melaleuca leucadendron*, *Pelargonium roseum*, *Juniperus virginiana* and *Artemesia vulgaris*, are also efficient [18]. Many experimental evidences indicate that plant diseases can be controlled by treating plant surfaces with various water-based compost preparations, i.e. – compost teas [19].

PLANT MINERAL NUTRITION, PATHOPHYSIOLOGICAL ALTERATIONS AND DISEASE RESISTANCE

As the plant organism produces a natural habitat for the parasites' growth and development, plants are constantly at danger from their attacks [20,21]. Plants have evolved an array of defenses against pathogens [20,22]. Plant cells response to any harm, whether it is brought on by mechanical, chemical, or parasitic causes. The infection causes biochemical, structural, and physiological alterations in the cells that are infected, which help to identify the injury's root cause. Phytoalexins and phytoncides are two cellular biochemical compounds that are particularly significant because of their protective function [23]. In a damaged plant cell, phytoalexins are phenolic byproducts of metabolism that have an antibacterial effect on the cause of the injury. Phytoncides are compounds that are found in healthy plants' metabolic byproducts and have an active antibiotic impact on phytoparasitic organisms [20,21,23]. Plant parasites can significantly affect the circulation of mineral substances in the processes of plant nutrition, by exploiting mineral substances in the rhizosphere, reducing root absorption, reducing the ability of conducting vessels to transport these substances and reducing the ability of plants to actively use these substances. Plant infections influence the mineral nutrition of plants as well as their photosynthesis, respiration, and cell membrane permeability, all of which have a significant impact on how well plants absorb nutrients and behave in general. Plant parasites with their ferments, toxic and mechanical effects cause chemical and structural alterations in membranes, which lead to their partial or complete non-functionality [20]. Due to the direct involvement of mineral elements in plant defense, the nutrition of the plant impacts its resistance or susceptibility to diseases and the ability to survive pathogens. This nutrition functions as the plant's first line of defense [24].

Plants have evolved a number of defense mechanisms over the course of evolution that enable them to fend against and withstand pathogen invasion [25]. According to Velasquez *et al.* [26]. mineral nutrients may help sustain the health of plants. One of the most essential macronutrients, **nitrogen (N)** has an important impact on the host-pathogen axis. N negatively affects the plant’s physical defense along with the production of antimicrobial compounds. **Potassium (K)** is an essential nutrients for plants and, in adequate amounts, can raise the concentration of polyphenols in the plant, which are crucial to the plant's defense responses

[21,24]. **Phosphorus (P)** has significance because it helps plants survive cold temperatures and diseases, it affects yield amount and quality, and a deficiency results in chlorosis and stunted plant growth [21]. Plants showing **calcium (Ca)** deficiency are observed to be more prone to disease infection, and element exogenous supply has been shown to alleviate the plant's resistance response toward the pathogen. **Magnesium (Mg)** deficiency during plant growth can reduce the energy production necessary for defense functions eventually leading to pathogen metabolites inactivation. An essential macronutrient for plants, **sulfur (S)** plays a crucial part in plant disease resistance. The sulfur-containing amino acid cysteine plays a key function in plant disease resistance and serves as a precursor to numerous biomolecules. The zinc (Zn), boron (B), copper (Cu), manganese (Ma), silicon (Si) and iron (Fe) are very significant micronutrients that plants require in relatively little amounts, but their absence reduces the plants' ability to fend off pathogens – the organisms that cause plant diseases – when they attack [21,24].

Biofertilizers are the natural fertilizers of which the main constituents are living microbial inoculants including algae, fungi, and bacteria which have ability to enhance the availability of nutrients in soil for plants. They have an ability to convert macro- and micronutrients in the soil from unusable form to the usable form by their microbial activities including phosphate solubilization, nitrogen fixation, excretion of plant growth hormones, and biodegradation in the soil [27]. Rhizobia are the soil habitat bacteria that have ability to fix much of free nitrogen [28]. Legumes in cropping systems increase biological nitrogen fixation and improving soil physical conditions and biodiversity [29].

CONCLUSION

Agriculture is vital to the existence of humans and to any human activity because it can reliably produce food and other resources for a population that is growing all over the world. It is essential for conventional agriculture to innovate, become more efficient, and use new agronomic methods in order to produce adequate food for the growing global population while limiting the adverse effects on the environment. On the other side, sustainable agriculture is gaining relevance since it may help address issues including land degradation, climate change, poverty reduction, hunger, health, and biodiversity management while also having a positive effect on the production of healthy food. Although sustainable plant breeding produces lower yields than conventional agriculture, it is essential to achieve system sustainability in order to preserve food supplies and natural resources for future generations. Due to the dangerous effects of the majority of synthetic fungicides, their usage will need to be rigorously restricted in the near future, which could result in a rise in needing biological plant protection solutions like those based on plants. The development of biopesticides stimulates modernization of agriculture and will, without doubt, gradually replace chemical pesticides.

REFERENCES

[1] FAO (2022). Food and Agriculture Organization of the United Nations. FAO's Statistical Yearbook for 2022 goes live. *Available on the following link*:

https://www.fao.org/publications/home/fao-flagship-publications/the-state-of-food-and-agriculture.

[2] Horrigan L., Lawrence R. S., Walker P., Environ. Health Perspect. 110 (5) (2002) 445–456.

[3] Chen H., Yada R., Trends Food Sci Technol, 22 (11) (2011) 585–594.

[4] Crews T. E., Carton W., Olsson L., Glob. Sustain. 1 e11 (2018) 1–18.

[5] James H. S., Agric Human Values. 23 (4) (2006) 427–438.

[6] Velten, S., Leventon, J., Jager, N., *et al.*, Sustain Sci. 7 (6) (2015) 7833-7865.

[7] Khakimov, A., Omonlikov, U., Utaganov,U., GSC biol. pharm. sci. 13 (3) (2020) 119–126.

[8] Zaker, M., Agric. Syst. 14 (1) (2016) 134–141.

[9] Zhang, W. Jiang, F. Ou J., Proceedings of the international academy of ecology and environmental sciences, 28 August, Kowloon Bay, Hong Kong 1 (2) (2011) 125.

[10] Saravi S., Shokrzadeh M., Role of pesticides in human life in the modern age: a review. Editor: Stoytcheva M. Publisher InTech, Rijeka, Croatia (2011) 3–12. ISBN: 978-953-51-4425-0.

[11] Stević, M., Fungicides. University of Belgrade, Faculty of Agriculture, Belgrade (2020). *(In Serbian).* ISBN: 978-86-7834-356-8.

[12] Dubey, K., Shukla, R., Kumar, A., *et al.*, Curr. Sci. 98 (4) (2010) 479–480.

[13] Mfarrej, M., Rara, F., Sheng Tai Xue Bao. 39 (2) (2019) 145–151.

[14] Lahlali, R., Peng, G., McGregor, L., *et al.*, Biocontrol Sci Technol. 21 (11) (2011) 1351–1362.

[15] Šernaitė, L., Rasiukevičiūtė, N., Valiuškaitė, A., Plants. 9 (5) (2020) 613.

[16] Mulatu, A., Alemu, T., Megersa, *et al.*, Microorganisms. 9 (8) (2021) 1675.

[17] Arshad Z., Hanif M. A., Qadri R. W. K., *et al*., Int. j. chem. biochem. 6 (2014) 11–17.

[18] Kordali S., Cakir A., Mavi A., *et al*., J. Agric. Food Chem. 53 (2005) 1408–1416.

[19] Van Bruggen A. H., Gamliel A., Finckh M. R., J Pest Sci. 72 (1) (2016) 30–44.

[20] Šutić D. Anatomy and physiology of diseased plants, University of Belgrade, Faculty of Agriculture, Belgrade (1995) (*in Serbian*). ISBN: 86-19-01422-6.

[21] Stikić S., Jovanović R., Physiology of plants, Second edition, University of Belgrade, Faculty of Agriculture, Belgrade (2017) (*in Serbian*). ISBN: 978-86-6021-088-5.

[22] Karasov, L., Chae, E., Herman, J., *et al.*, Plant J. 29 (4) (2017) 666–680.

[23] Duka, R., Ardelean, D. Arad Medical Journal 13 (3) (2010) 19–25.

[24] Tripathi R., Tewari R., Singh K. P., *et al*., Front. Plant Sci. (2022) 3116.

[25] Sun, Q., Liu, X., Yang, J., *et al.*, Mol plant. 11 (6) (2018) 806–814.

[26] Velásquez, C., Castroverde, M., He, Y. Curr. 28 (10) (2018) R619-R634.

[27] Kalsoom, M., Rehman, U., Shafique, T. *et al.*, Innovare J. Life Sci 8 (6) (2020) 1–4.

[28] Mia, B., Shamsuddin, H., Afr. J. Afr. J. Biotechnol. 9 (37) (2010) 6001–6009.

[29] Peix, A., Ramírez-Bahena, H., Velázquez E., *et al.*, CRC Crit Rev Plant Sci. 34 (1–3) (2015) 17–42.

THE WAY OF MANAGING PLANT DISEASES IN SUSTAINABLE AGRICULTURE

Zlata Živković[1*], Markola Saulić[1], Darko Stojićević[1], Milica Jevtić[1]

[1]Academy of Applied Technical Studies Belgrade, College of Applied Engineering Sciences, Nemanjina 2, Požarevac, SERBIA

[*]*zzivkovic@atssb.edu.rs*

Abstract

In recent years, sustainable agriculture has gained more importance. Agriculture is changing fast and with it the landscape through which disease spreads. The use of fungicides is considered the primary way to control plant pathogens. In large parts of the world, intensively managed farms are getting bigger, crops are grown in monocultures that deplete the soil as an environmental resource and at the same time create favorable conditions for the continued emergence of recurring plant pathogens. By using them, the occurrence of diseases in cultivated crops is reduced and thus, yields increase. However, conventional pesticides are not environmentally friendly. Their continuous use leads to the appearance of pathogen resistance to the chemicals used. In addition, pesticides contain various chemicals such as ethylated, methylated and aromatic substances also adversely affect and pollute the atmosphere and water, thereby harming fish, beneficial insects such as bees, non-target organisms such as rhizobacteria that promote plant growth and fungi that promote plant growth (PGPF). From the perspective of the environment and sustainable agriculture, biological control agents (BCAs), natural enemies of plant pathogens, are a strong candidate to replace conventional methods. Given that the future imperative in the agricultural sector is to increase yields and minimize plant diseases, this paper summarizes the latest information on environmentally friendly ways to control plant diseases in sustainable agriculture.

Keywords: plant diseases, sustainable agriculture, pesticides.

CONVENTIONAL AGRICULTURE

The world's population is constantly increasing, currently numbers more than 8 billion people, and it is estimated that food production will have to double by 2050. According to the Food and Agriculture Organization (FAO) of the United Nations nearly 40% of Earth's land is used by agriculture [1]. According FAO (2022) the production of primary crops, such as sugarcane, maize, wheat and rice grew by 52% from 2000 to 2020. The production of all other raw materials in human nutrition also increased by several tens of percent. The rapid growth of the human population is accompanied by an increase in the area under agricultural crops. In 2019, the global agricultural land area was 4.8 billion hectares (ha) of which one-third was arable land and approximately two-thirds was used for permanent meadows and pastures. The global land area equipped for irrigation reached 342 million ha in an increase of 18% from the 289 million ha of 2000. Global pesticides use per cropland area went up 28% in the 2000s [2]. It has been projected that in each year, approximately 2.5 million tons of pesticides have been used on crops [3]. Although agriculture is imperative for human survival as it provides food for a growing world population, it is also a major source of environmental

degradation. It is considered one of the main factors affecting climate change as it leads to depletion of fresh water resources, fish die-off, land degradation and affects biodiversity at all levels [2,4–6]. Crops grown intensively in monocultures additionally deplete the soil and at the same time create favorable conditions for the continued appearance of recurring plant pathogens. For their suppression, conventional fungicides are most often used, the use of which reduces the occurrence of diseases in cultivated crops, and thus increases yields. Conventional pesticides are not environmentally friendly because they contain various chemicals such as ethylated, methylated and aromatic substances that pollute the atmosphere and water, harm fish, beneficial insects such as bees, non-target organisms such as plant growth-promoting rhizobacteria and growth-promoting fungi plants (PGPF) and their continuous use leads to the emergence of pathogen resistance to the chemicals used [4,5,7,8].

PLANT DISEASES, NUTRITION AND SUSTAINABLE AGRICULTURE

It is estimated that diseases, insects and weeds together disrupt production annually and destroy 36.5% of crop production [9]. One of the characteristics of conventional agricultural production is the dominance of annual plants grown in monocultures, which in the long term leads to soil erosion, ecosystem degradation and an increase in the number of pests and weeds that have adapted to cultivated culture [6]. For control, large amounts of different active substances of pesticides are used, the excessive and improper application of which has led to significant residues in agricultural products, the creation of plant resistance to phytopathogens and the reduction of the amount of beneficial microorganisms in the soil [10]. Conventional agriculture provides higher yields and the chance for a larger number of people to get food, as the main resource necessary for the survival of the human population [2,11]. On the other hand, a sustainable approach in agriculture advocates the need to balance economic with environmental and social goals, to the point of reducing profitability [12]. Sustainable agriculture comprises a range of practices that include integrated pest management (which may include pesticide applications), nonintensive livestock production, crop rotations for pest, disease, and erosion control, and alternative tillage and planting practices to reduce soil erosion [13]. To ensure the sustainability of agriculture, disease management that reflects the dynamics of pathogen population structure is necessary [14,15]. Natural plant products have been found effective in plant disease managements. It is estimated that there are more than 250,000 higher plant species on earth that can be evaluated for their antimicrobial bioactive chemical compounds. Plant extracts, essential oils, gums, resins etc. have been shown to exert biological activity against plant fungal pathogens and can be used as bio-fungicidal products [3,16]. Plants like *Mentha piperita*, *Lavandula angustifolia*, *Melaleuca leucadendron*, *Pelargonium roseum*, *Juniperus virginiana* and *Artemesia vulgaris*, are also efficient together with a variety of fungal pathogens and insects [17]. Cinnamon, clove, oregano, palmarosa and lemongrass oils, tea tree oil, common thyme, cinnamon leaf and aniseed oils, sweet basil, neem, eucalyptus, datura, garlic and oleander extracts are also effective in controlling some plant pathogens [16]. Biological control agents (BCAs), i.e. natural enemies of plant pathogens, represent a good potential that could replace conventional methods, as well as the use of microorganisms that represent an untapped natural resource for long-term and sustainable control of pests and diseases [18]. Many experimental evidences indicate that

plant diseases can be controlled by treating plant surfaces with various water-based compost preparations, i.e. – aqueous fermented compost extracts or compost teas. To improve natural pest and disease control, increased habitat diversity is used – planting trees, shrubs, wild grasses and flowering plants [19]. One of the ways to control plant diseases is the possibility of using antagonistic action of agents for biocontrol of bacteria and fungi, such as production of antibiotics, siderophores, secretion of enzymes, competition for nutrition, stimulation of plant growth by microorganisms from the rhizosphere [10]. New biotechnological products based on stimulation of the plant defense response, and on the use of plant-beneficial bacteria for biological control of plant diseases (biopesticides) and for plant growth promotion (biofertilizers) are largely being developed [19,20].

In addition to the above, the nutrition of a plant determines in large measure its resistance or susceptibility to disease and the virulence or ability of pathogens to survive and represents the first line of plant defense due to the direct involvement of mineral elements in plant protection [19]. Mineral nutrients are most commonly applied to boost crop yields and improve overall plant health and quality [15,21–24]. There are 18 nutrient elements required to grow crops. Plants uptake the following mineral nutrients for a healthy growth: the primary macronutrients, nitrogen (N), phosphorus (P), and potassium (K); the three secondary macronutrients, calcium (Ca), sulfur (S), and magnesium (Mg); and the micronutrients/trace minerals, boron (B), chlorine (Cl), manganese (Mn), iron (Fe), zinc (Zn), copper (Cu), molybdenum (Mo), and nickel (Ni) [15,21–23,25]. Some nutrients have a greater effect on plant diseases than others. Likewise, a certain nutrient can have the opposite effect on different diseases in different environments, that is, the same nutrient can increase the frequency of one disease, but at the same time reduce the frequency of others [17]. Mineral nutrition can influence plant resistance to pathogens by forming mechanical barriers, primarily through the development of thicker cell walls, or by synthesizing natural defense compounds, such as phytoalexins, antioxidants and flavanoids, which provide protection against pathogens [15,25]. Nitrogen (N) is an essential macronutrient required for the normal growth and development of the plants [21]. Most plants absorb nitrogen from the soil in mineral form (i.e. NO_3^- and NH_4^+). In the soil, most of the nitrogen is in the form of organic compounds (humus 90–95%), which can be used as a source of nitrogen for plants only after the mineralization process. Because of its importance for physiological processes, nitrogen deficiency has serious consequences on plant growth and development, yield and yield quality. Nitrogen deficiency leads to changes in root morphology, chlorosis on older leaves, drastically reduced leaf area and reduced plant growth [15,21,25]. Phosphorus (P) is thought to be the second most commonly applied nutrient after nitrogen in crops [25]. Phosphorus plays an important role because many metabolic processes cannot be realized without its compounds and plants cannot complete their cycle of growth and development. Phosphorus is also significant because it contributes to the resistance of plants to low temperatures and diseases, the quantity and quality of yield is affected, as well as the germination of seeds and the growth of shoots and roots. Deficiency causes reduced plant growth as well as chlorosis [15,21,25]. Potassium (K) is an essential nutrient widely distributed in nature, which, in addition to nitrogen and phosphorus, is the most abundant in plant tissues. Plants take it in a large amount, so it must be compensated by fertilizing. Lack of potassium can lead to slowing

down or complete stoppage of plant growth, plant decline and wilting, chlorosis that starts on the edges of the leaves, reduced root length of the root system. Calcium (Ca) is an essential element, serving as one of the cell wall and membrane constituents and thereby contributing to the cell structure along with upholding the physical barriers against invading pathogens [26]. Plants absorb it from the soil solution. Problems in supplying plants with calcium can be caused by its lack in the soil or an increased concentration of other cations (H^+, K^+, Mg^{2+}, Nh^+). Its deficiency in plants can result in the decline of flowers, the appearance of small fruits and dark spots on the fruits of plants [15,21,25]. Magnesium plays an extremely important role in almost all physiological processes in plants. Its deficiency is most often manifested on plants through the characteristic yellow chlorotic peugeot line, while the leaf veins are green [21,25]. Iron is an essential micronutrient. His deficiency manifests itself as chlorosis in young leaves, reduced growth and slowed development [25,27]. In Boron (B) deficient conditions, plant cell walls tend to swell and split, resulting in weakened intercellular space, which eventually weakens the physical barrier to the initial infection. Plants with low copper (Cu) content show an increased disease incidence as a result of reduced lignification [28]. Copper is a plant protection essential part of controlling oomycetes, fungi, and bacteria for over a century [21]. Cu fertilization in plants reduces the severity of fungal and bacterial diseases associated with cell wall stability and lignification. Plants with inadequate manganese (Mn) nutrition are observed to be unable in restricting the fungal hyphae penetration into the root tissues [27]. Silicon (Si) is not essentially a micronutrient but stands out in its potential for decreasing several pathogens' severity in varied crops belonging to the different plant families [29]. Zinc (Zn) deficiency is widespread among plants grown in highly weathered acid soils and in calcareous soils. The most characteristic visible symptoms of Zn deficiency in dicotyledonous plants are stunted growth due to shortening of internodes ('rosetting') and a drastic decrease in leaf size ('little leaf') [28]. In addition to the above, taking appropriate activity against weed plants that host certain pests – carriers of phytopathogenic microorganisms, can contribute to reducing the occurrence of plant diseases. The influence of pH value on the uptake of macro- and micronutrients is another important segment when it comes to controlling plant diseases. If the pH value is not within the optimal limits, the absorption of certain elements decreases, and therefore the resistance of plants to the causes of plant diseases also weakens.

CONCLUSION

Balanced nutrition leads to a better plant fitness, which reduces disease susceptibility and infection. In addition with plant phenophase, it is important to provide balanced nutrition and apply nutrients through mineral fertilizers with aim of high level effectively absorption and indirect control the occurrence of plant diseases. Nowadays, biocontrol agents assume a significant role in the field of agriculture. In order to improve the defense mechanism of plants against disease-causing agents, it is necessary, in addition to mineral nutrition, to pay attention to avoiding growing crops in monoculture, growing varieties and hybrids that are more resistant to diseases, and planting autochthonous varieties that are characteristic for a specified area. Crop rotation can decrease the appearance of the disease. Instead of conventional ones - use biopesticides that are environmentally acceptable and pay special

attention to the time of their application, in order to promote and maintain sustainability in agriculture.

REFERNCES

[1] FAO (2015). Food and Agriculture Organization of the United Nations Statistics Division. *Available on the following link*: https://www.fao.org/faostat/en/.

[2] FAO (2022). Food and Agriculture Organization of the United Nations. FAO's Statistical Yearbook for 2022 goes live. *Available on the following link*: https://www.fao.org/publications/home/fao-flagship-publications/the-state-of-food-and-agriculture.

[3] Arshad Z., Hanif M. A., Qadri R. W. K., *et al*., Int. j. chem. biochem. 6 (2014) 11–17.

[4] Horrigan L., Lawrence R. S., Walker P., Environ. Health Perspect. 110 (5) (2002) 445–456.

[5] Chen H., Yada R., Trends Food Sci Technol 22 (11) (2011) 585–594.

[6] Crews T. E., Carton W., Olsson L., Global Sustainability 1 e11 (2018) 1–18.

[7] Finn J. A., Kirwan L., Connolly J., *et al.*, J Appl Ecol 50 (2) (2013) 365–375.

[8] Gouda S., Kerry R. G., Das G., *et al*., Microbiol. Res. 206 (2018) 131–140.

[9] Prajapati S., Kumar N., Kumar S., *et al*., J. pharmacogn. phytochem. 9 (2) (2020) 1514–1523.

[10] Tariq M., Khan A., Asif M., *et al*., Acta Agric Scand B Soil Plant Sci 70 (6) (2020) 507–524.

[11] Qaim M., Appl Econ Perspect Policy 42 (2) (2020) 129–150.

[12] James H. S., Agric Human Values 23 (4) (2006) 427–438.

[13] Mason J., Sustainable agriculture, Landlinks Press, Collingwood Vic, Australia (2003).

[14] Zhan J., Thrall P. H., Burdon J. J., Trends Plant Sci.19 (9) (2014) 570–575.

[15] Gupta N., Debnath S., Sharma S., *et al*. Role of nutrients in controlling the plant diseases in sustainable agriculture *in* Agriculturally Important Microbes for Sustainable Agriculture, Editors: Vijay S. M., Jaideep K. B., Pankaj K. M., Arunava P., ICAR-Vivekananda Institute of Hill Agriculture, Almora, Uttarakhand, India (2017), p.217–262. ISBN: 978-981-10-5588-1.

[16] Zaker M., The Agriculturists 14 (1) (2016) 134–141.

[17] Kordali S., Cakir A., Mavi A., *et al*., J. Agric. Food Chem. 53 (2005) 1408–1416

[18] Cook R. J., Bruckart W. L., Coulson J. R., *et al*., Biological control 7, 0102 (1996) 333–351

[19] Van Bruggen A. H., Gamliel A., Finckh M. R., Pest Manag. Sci. 72 (1) (2016) 30–44.

[20] Montesinos E., Bonaterra A., Badosa E., Int. Microbiol. 5 (2002) 169–175.

[21] Tripathi R., Tewari R., Singh K. P., *et al*., Front. Plant Sci. (2022) 3116.

[22] Huber D. M., Haneklaus S., Managing nutrition to control plant disease. OpenAgrar, LANDBAUFORSCHUNG-GER (2007), 57 (S) p.313–322. *Available on the following link*: https://www.openagrar.de/receive/timport_mods_00032245

[23] Dordas C., Agron. Sustain. Dev. 228 (2008) 33–46.

[24] Šutić D. Anatomy and physiology of diseased plants, University of Belgrade, Faculty of Agriculture, Belgrade (1995) (*in Serbian*). ISBN: 86-19-01422-6.

[25] Stikić S., Jovanović R., Physiology of plants, Second edition, University of Belgrade, Faculty of Agriculture, Belgrade (2017) (*in Serbian*). ISBN: 978-86-6021-088-5.

[26] White P. J., Broadley M. R., Ann. Bot. 92 (4) (2003) 487–511.

[27] Marschner H., Kirkby E. A., Cakmak I., J. Exp. Bot. 47 (1996) 1255–1263.

[28] Broadley M., Brown P., Cakmak I., *et al.*, Function of nutrients: micronutrients *in* Marschner's mineral nutrition of higher plants, Editors: Marschner's, Academic Press, Oxford (2012), pp.191–248. ISBN: 978-0-12-384905-2

[29] Pozza E. A., Pozza A. A. A., Botelho D. M. D. S., Rev. Ceres 62 (2015) 323–331.

THE ROLE OF PLANTS IN BIOECONOMY AND CIRCULAR ECONOMY

Dragan Ugrinov[1], Magdalena Nikolić[2*]

[1]Institute of Public Health, Pancevo, Pasterova 2, Pancevo, SERBIA
[2]School of Engineering Management, University Union Nikola Tesla,
Bulevar vojvode Misica 43, 11000 Belgrade, SERBIA
[*]*magdalena.nikolic@fim.rs*

Abstract

Bioenergy plays an important role in both the bioeconomy and circular economy. In the bioeconomy, bioenergy refers to the use of renewable biological resources such as energy crops, and organic municipal waste to produce energy. This helps to reduce reliance on fossil fuels and provides a sustainable source of energy that can be used to power homes, businesses, and industries. Moreover, phytoremediation can help this process by removing pollutants from the soil. In the circular economy, bioenergy can be used as a way to close the loop of waste by using organic waste materials to generate energy. This further supports the circular economy by creating a closed loop of resource use. Overall, bioenergy can play a significant role in both the bioeconomy and circular economy by providing a renewable, sustainable source of energy while also contributing to the reduction of pollution, waste, and greenhouse gas emissions. This paper present bioenergy used in Serbia comapared to other sources of energy. Also, plants beside their importance in bioenergy production are capable to remove heavy metals from soils and biowaste percentage in renewable energy production.

Keywords: energy plants, biofuel, phytoremediation, circular economy, bioeconomy.

INTRODUCTION

Globally we are facing climate change, loss of biodiversity, and loss of fossil fuels that we still depend on. The valorization of waste materials into biodiesel has its path through reusing and recycling biowastes. In this respect, Nikolić *et al*. [1] provide a comprehensive overview of the utilization of plants in phytoremediation and then turn them into biofuel. We hope that this aproach will reduce the carbon footprint of fossil fuels, to increase the delivery of green energy, thereby improving resistance to global warming. Circular economy and bioeconomy practices and policies are becoming key elements for the sustainability of cities. Today, cities generate roughly 85% of the world's GDP, and their consumption of materials is expected to skyrocket by 125% between 2010 and 2050, from 40 to 90 billion tons per year. Urban municipal waste is expected to increase from 1.3 to 2.2 billion tons of waste annually between 2012 and 2025, and the total solid municipal waste will be around 3.4 billion tons in 2050. It is obvious that with such an increase, the traditional practice of municipal solid waste management through sanitary landfills and waste-to-energy plants, although very important as starting points, are unable to absorb the growing wave of urban waste. Hence the need to implement the circular economy and bioeconomy and waste prevention measures as central to

the life of cities. Urbanization, supply and price risks, ecosystem degradation, environmental responsibility, consumer behavior, and digital progress are discussed as key drivers of circular economy implementation in cities [2]. This paper aims to present bioenergy used in Serbia comapared to other sources of energy. Also, plants beside their importance in bioenergy production are capable to remove heavy metals from soils and biowaste percentage in renewable energy production.

MATERIALS AND METHODS

The framework of the article is built aroundpercent of bioenergy used in Serbia and the multiple roles of plants in the green economy. Each section is only a part that contribute to a sustainable environment. Therefore the result can be watched through complete soil cleaning and total use of biowaste in bioenergy production.

Phytoremediation

Phytoremediation is a process that involves using plants to clean up contaminated soil, water, and air. The term "phyto" refers to plants, while "remediation" means the process of fixing or correcting a problem. Phytoremediation is a sustainable and cost-effective alternative to traditional methods of environmental cleanups, such as excavation or incineration.

Phytoremediation has been used successfully to clean up contaminated sites around the world, including areas affected by oil spills, industrial pollution, and agricultural runoff. It is a promising technology for environmental cleanup, as it is non-invasive, relatively low-cost, and can be used in combination with other remediation techniques [3–5].

Bioenergy and biomass

The energy obtained from these sources is called "renewable energy" and is defined as energy that is exploited at the same rate as it is naturally renewed. With about 6% of the world's population, the countries of the European Union use about 14–15% of the world's energy sources. To solve the energy crisis, it is necessary to find an answer to two questions: how to ensure a sufficient amount of energy in the future and how to reduce the negative impacts on the environment caused by the use of traditional energy sources. The energy, ecological and economic crisis led to the acceptance of the concept of limited resources and limited capacity of the environment at the global and local levels [1,2,5,6].

Waste biomass from agricultural areas is used for heating the living spaces of individual households, and recently the use of waste biomass for industry has been noticeable, for example: Industrial waste wood boiler "Tarket" – Bačka Palanka, biomass boiler in "Mitrosrem" in Sremska Mitrovica, on wheat straw, corn or sunflower harvest residues. Several objects and facilities that use biomass from the industrial process in Sombor and Šid have been built. Briquetting and pelletizing of biomass is less common, except in individual sporadic cases.

Bioeconomy

The bioeconomy refers to an economic system that uses renewable biological resources, such as plants, animals, and microorganisms, to produce goods and services. It involves the

sustainable use of natural resources and the development of new technologies to create a more efficient and environmentally friendly economy. Biofuels are fuels that are produced from renewable biological resources, such as crops, wood, and waste. Biofuels can be used to replace traditional fossil fuels, such as gasoline and diesel, and can help to reduce greenhouse gas emissions and dependence on foreign oil.

RESULTS AND DISCUSSION

The bioeconomy is the "green engine" of the circular economy. Therefore, the bioeconomy is circular, using all parts of renewable resources and storing the carbon recycled during the life cycle of the product. While the circular economy is focused on "keeping the value of products, materials, and resources in the economy as long as possible", many elements of the bioeconomy go beyond this goal, including aspects focused on product functionality [2]. Energy efficiency in Serbia is not at the appropriate level, as evidenced by the following facts [2,6–9]:

• the level of development of the domestic economy has been constantly declining, as evidenced by the drastic decline of the gross domestic product in the period from 1989 to the present day;

• according to the level of annual electricity consumption per capita of 3400 kWh, Serbia is at the level of medium-developed European countries;

• electricity consumption per $1000 GDP, 1700 kWh in Serbia is the highest in Europe; according to total energy consumption per capita, Serbia is among the last in Europe;

• losses in the transmission and distribution of electricity, amounting to 19%, are among the highest in Europe;

• the price of electricity is several times lower than in Europe;

• consumption of electricity in households increased from 35% to 62%, and in industry, it decreased from 37% to 29%, which is a consequence of the stagnation and decline of economic activity and the corresponding disparity in the prices of certain forms of energy.

The problem is the transition from fossil fuels to renewables. In the previous text the issue is presented, therefore in Table 1 and Table 2 the total energy consumption price is presented.

Table 1 *Total energy cost in Serbia*

Energy/Energy source	Average unit price (EUR)	Unit
Electricity	0.047	kWh
Heat energy	0.633	m^2
Natural gas	0.329	m^3
LPG	0.570	l
Gasoline	1.085	l
Diesel D-2	0.909	l
Euro dizel	0.987	l
Fuel oil	0.380	kg
Biodiesel BD 100	**0.909**	l
Firewood	41.139	m^3
Hard coal	103.797	t
Lignite	46.835	t

Also as it can be seen, hard coal is the most present energy source, then firewood, both extremely harmful to the ennvironment. While, biomass, biogas, and biofuel are jet to show potential in Serbia.

Table 2 *Where is biomass in total renewable sources in Serbia*

Renewables	Total potencial (ktoe/a)	Heat energy (TJ/a)	Electricity (GWh/a)
Biomass (1/3 solid)	**768**	**35000**	**360**
Biogas	**3**	**90**	**20**
Biofuel	**150**		
Wind (300 MW)	65		750
Geotermal	22	1800	
Municipal waste	158	6600	56
Small hydro potential	7.77		90
Big hydro potential	85.0		990
Solar	34	1400	
Total	**1293**	**44890**	**2266**

Also, phytoremediation as a pollutant removal method by energy plants can clean soil from heavy metals and then be used as a material for biofuel production. In a way that strengthens the bio-economy. Table 3 is a good example of energy plants used to clean soil contaminated with toxic heavy metals [1].

Table 3 *Bioaccumulation potential of energy plants*

Plant species	Bioaccumulation potential
Miscanthus × giganteus J.M. Greef & Deuter	*Hg, Cd, Zn, Pb, Cu, Mn, Ti, As, Fe, and Zr*
Miscanthus sinensis	*Hg, Cd, Zn, and Cr*
Miscanthus sacchariflorus	*Zn, Cd, Pb, Fe, Mn, Mo, B, Ba, Sr, As, Sn, Li, Ti*
Miscanthus floridulus	*Zn, Cr, and Cd*
Beta vulgaris L.	*Cd, DTPA-extractable Cd, and Ni*
Saccharum officinarum L.	*Cu, Cd, Se, Pb, Mn, gamma-HCH or lindane, gamma-HCH or lindane, F^-, Fe, PCBs and Cd, Cu, Sn, and Pb/Zn*
Saccharum spontaneum L.	*Cu, Sn, and Pb/Zn*
Saccharum munja	*Zn, Pb, Cu, Ni, Cd, and As*
Saccharum arundinaceum	*Cu, Zn, Pb, and Cd*
Ricinus communis L.	*Cd, Ni, Zn, Fe, Pb, B, and tolerate Cu, Fe, Mn, and Zn*
Prosopis juliflora (Sw.) DC	*Cd, Co, Cr, Fe, Mn, Ni, Pb, and Zn*
Prosopis juliflora (Sw.) DC	*F*
P. laevigata	*Al, Fe, Ti, and Zn*
P. laevigata inoculated with Bacillus sp.	*Cr*
Arundo donax L.	*As,Ni, Cd, Cu, As, Zn, Pb, V, Hg, Se, and NO_3^-*

CONCLUSION

The circular economy represents a different economic model that strives for long-lasting products and the return of all biowaste materials to production processes, implying efficient use of resources and reduced environmental pollution while achieving financial savings and creating new business opportunities.

The solutions offered by this concept are based on the processes that take place in nature every day, whereby the waste of one industry is a raw material for another industry. The role of the circular economy and bioeconomy is biowaste prevention. Therefore, plants that have capabilities to remove heavy metals from the environment can be afterwards use as fuel to multiple purposes.

REFERENCES

[1] Nikolic M., Tomasevic V., Ugrino, D., Chem. Ind. 76 (4) (2022) 209–225.

[2] Nikolic M., Tomasevic V., Ugrinov D., Održivo upravljanje otpadom u cirkularnoj ekonomiji i bioekonomiji, Beograd, Fakultet za inženjerski menadžment (2023). ISBN: 978-86-89691-27-6 (*in Serbian*).

[3] Nikolic M., Circular bioeconomy application towards energy safety, The Second International Scientific Conference Circular and Bioeconomy, CIBEK 2019, Belgrade, Serbia (2019) 142–153.

[4] Nikolic M., Stevovic S., Urban For. Urban Green. 14 (2015) 782–789.

[5] Nikolic M., Tomasevic V., Pol. J. Environ. 30 (1) (2021) 523–534.

[6] Krstić V., Nikolić M., Ugrinov D., Circular economy in industrial symbiosis a mechanism for implementing the concept of industry 4.0. The Third International Scientific Conference Circular and Bioeconomy, CIBEK 2022, Belgrade, Serbia (2022) 70–77.

[7] Ugrinov D., Komatina-Petrović S., Stojanov A., Zaštita materijala 53 (4) (2012) 379–385.

[8] Ugrinov D., Stojanov A., Zaštita materijala 51 (4) (2010) 237–244.

AGRICULTURAL WASTE IN SUSTAINABLE AGRICULTURE

Vojkan Miljković[1*], Ivana Gajić[1], Ljubiša Nikolić[1]
[1]University of Niš, Faculty of Technology, Bulevar oslobođenja 124, Leskovac, SERBIA
[*]*vojkan@tf.ni.ac.rs*

Abstract

Millions of tons of agricultural waste is getting generated every year and therefore it attracts moreattention of scientists as the future of planet Earth is questionable. Most of it is getting burned andgenerate air pollutants. In this work are considered 28 different plant wastes. By chemical reactions itis possible to obtain cellulose from agricultural waste in first step and in second carboxymethylcellulose, a substance that is needed for production of superabsorbent hydrogels. Superabsorbenthydrogels found application in agriculture, for example superabsorbent hydrogel containing onlycarboxymethyl cellulose has a swelling ratio ~450 g/g and act as a water reservoir in field.Superabsorbent hydrogels with carboxymethyl cellulose are biodegradable. By production ofsuperabsorbent hydrogel from agricultural waste the circle of sustainability is created. Agriculturalwaste present valuable source for agricultural industry and has its place in circular agriculturaleconomy.

Keywords: agricultural waste, circular economy, carboxymethyl cellulose, superabsorbent hydrogel.

INTRODUCTION

Agricultural waste receives more attention as existence on planet Earth increases [1]. The generation of millions of tons of agricultural wastes each year presents challenge for sustainability. Economy of many countries in the world is basically agro-based, for example, most South Asian countries are producing oil palm, coconut, cocoa and sugarcane. Therefore, those industries generate large amount of agricultural waste. There is an opportunity to create biodegradable polymer from annually renewable crops and agro industrial waste. That should be a reason to accept the concept “wealth from waste” which means converting plant wastes, that is in reality getting burned and by that generate air pollutants, having lignocellulose as constituent into useful products. The lignocellulose consists of cellulose (38%), hemicellulose (32%) and lignin (17%) [2].

Many regions in the world have a serious problem with lack of water and desertification [3]. The conversion of plant waste into useful product such as superabsorbent hydrogels would bridge this problem and provide “greener” diopter because plant wastes consists of more than 90% of carbohydrate polymers (polysaccharides) [4].

Cellulose is a basic material of plant mass and by that the most widely present natural polymer. It’s structure with reactive hydroxyl groups of the glucosyl units at positions 2, 3 and 6 provides many options for creating useful chemical derivatives [5]. The most widely used cellulose ether today is carboxymethyl cellulose (CMC), with huge range of applications

such as in detergents, food exploration, paper, textiles, pharmaceutical [6] and agricultural industry [7]. All reactions are operated at atmospheric pressure which makes production of CMC simplier than other cellulose ethers [8].

Cellulose based superabsorbents are in focus because of resource that is abundant (cellulose is more abundant than starch and chitosan), biodegradability and low productions cost [9]. The characteristic of superabsorbent hydrogels based on CMC is that they can absorb and hold significant amounts of water [10,11]. After application superabsorbent hydrogel acts as a reservoir of water. With this, regions with insufficient water and rainfalls can overcome this problem. Since CMC is substrate for microorganisms and hydrolytic enzymes these superabsorbent hydrogels have biodegradable feature [5].

The aim of this work is to change the optic of watching on agricultural waste as pollutant into valuable resource.

MATERIALS AND METHODS

Materials

In this work were considered 28 different agricultural wastes (in alphabetical order): almond shells, almond stems, *Asparagus officinalis*stalk end, black tea leaves, barley straw, Cavendish banana pseudo steam, cashew tree gum, coconut fibers, corn cob, cotton gin, cotton linters, dried duckweed, durian rind fruit, fig stems, *Mimosa pigra*peel, oil palm fibers, orange peel, palm bunch, palm kern cake, papaya peel, pineapple peel, rice hull, rice stubble, sago pulp, sugarcane bagasse, sugar beet pulp, sugarcane straw, wheat straw.

Methods

In order to obtain cellulose from agricultural waste, which will be chemically modified into CMC afterwards, pretreatment with acid-chlorite and alkaline is getting performed. By reacting with acid-chlorite called delignification or bleaching, most of lignin and other components is eliminated with a mixture of water, acetic acid and sodium chlorite. The mixture solution with waste material needs to be stirred at 70–80 °C for 4–12 h, and after this process, the solid products of the chemical reaction (holocellulose, consisting dominantly of cellulose and hemicellulose) are washed wish distilled water until pH = 7 and then dried in oven at 50 °C. Then, the solid products need to be treated with an alkaline solution (4–20% (v/v) sodium hydroxide) for 1–5 h in order to remove the amorphous polymer of hemicellulose and residual lignin. The final solid products obtained after washing with distilled water until pH = 7 and dried in an oven at 50 °C consist mostly of cellulose [12].

After cellulose is obtained etherifying reaction with sodium monochloroacetate follows as easy to handle and efficient substance for this purpose. The chemical reaction of CMC production is etherification of hydroxyl groups with sodium monochloroacetate in the presence of alkali. The reaction is [13]:

$$\text{Cell–OH} + \text{ClCH}_2\text{COONa} \rightarrow \text{Cell –O– CH}_2\text{COO-Na}^+ \text{ (CMC)} + \text{NaCl} + \text{H}_2\text{O} \quad (1)$$

RESULTS AND DISCUSSION

Carboxymethyl cellulose that can be obtained from agricultural wastes by chemical reactions as described is essential substance for preparation of superabsorbent hydrogels, three-dimensional network structures of hydrophilic polymer formed by crosslinking [11]. These superabsorbent hydrogels are practically water reservoir.

The composition of superabsorbent hydrogels with CMC can be different and each hydrogels possess different swelling ration. For this purpose, the most interesting one is superabsorbent hydrogel formed only with CMC because it does not consists of other substances that can interfere and therefore contribute to swelling ratio which is in this case of CMC only ~450 g/g [14].

As the CMC molecule is biodegradable circle of sustainability is created and presented in Figure 1.

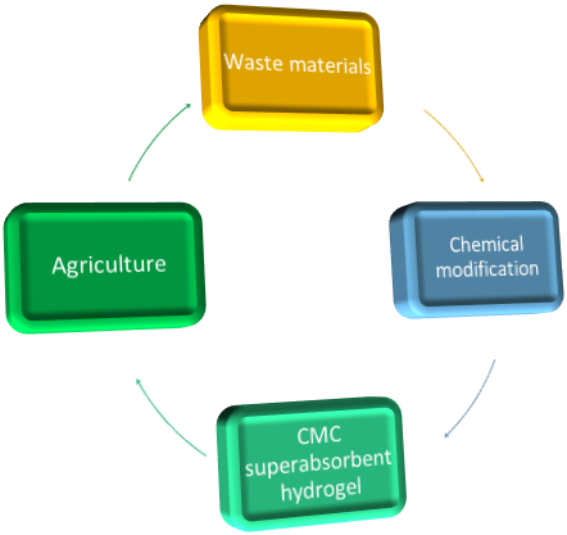

Figure 1 *Sustainability circle of waste materials in agriculture*

CONCLUSION

In this work is shown that fate of plant waste material does not have to be to be burnt, by chemical modification it can be transformed into CMC superabsorbent hydrogel. By that, it present a valuable resource that can find it's place in industry of agriculture. Besides financial benefits, characteristics of superabsorbent hydrogels which contributes to improvement of yield in agriculture also recommend this concept of sustainable agriculture to be implemented in circular agricultural economy.

ACKNOWLEDGEMENT

The authors are grateful to the Ministry of Science, Technological Development and Innovation of the Republic of Serbia for financial support according to the contract with the registration number (451-03-47/2023-01/200133).

REFERENCES

[1] Dai H., HuangY., Huang H., Carbohydr. Polym. 185 (2018) 1–11.

[2] Huang C.M. Y., Chia P.X., Lim C.S.S., *et al*., Cellulose Chem. Technol. 51 (7–8) (2017) 665–672.

[3] Puoci F., Iemma F., Spizziri U.G., et al., Am. J. Agric. Biol. Sci. 3 (1) (2008) 299–314.

[4] Xiquan L., Tingzhu Q., Shaoqui Q., Acta Polym. 41 (1990) 220.

[5] Wach A.R., Mitomo H., Yoshii F., *et al*., J. Appl. Polym. Sci. 81 (2001) 3030–3037.

[6] Methacanon P., Chaikumpollert O., Thavorniti P., *et al*., Carbohydr. Polym. 54 (2003) 335–342.

[7] Stamps R.H., Savage H.M., Horttechnology 22 (6) (2012) 766–760.

[8] Dahlman O., Jacobs A., Sjoberg J., Cellulose 10 (2003) 325–334.

[9] Chang C. Y., Duan B., Cai J., *et al*., Eur. Polym. J. 46 (2010) 92–100.

[10] Pourjavadi A., Ghasemzadeh H., Soleyman R., J. Appl. Polym. Sci. 105 (2007) 2631–2639.

[11] Wang W., Wang A., Carbohydr. Polym.461 (2010) 83–91.

[12] Phanthong P., Reubroycharoen P., Hao X., *et al*., Carbon Resour. Convers. 1 (2018) 32–43.

[13] Rachtanapun P., Kasetsart J. – Nat. Sci. 43 (2009) 259–266.

[14] Fekete T., Borsa J., Takács E., *et al*., Cellulose 21 2014 4157–4165.

30th International Conference Ecological Truth & Environmental Research
20–23 June 2023, Serbia

RECYCLING OF Li-ION BATTERIES FROM THE END-OF-LIFE VEHICLES: OPPORTUNITY OR LIABILITY IN THE FUTURE?

Ana Radojević[1*], Jelena Milosavljević[1], Snežana Šerbula[1], Tanja Kalinović[1], Jelena Kalinović[1]

[1]University of Belgrade, Technical Faculty in Bor, V.J. 12, 19210 Bor, SERBIA

[*]*aradojevic@tfbor.bg.ac.rs*

Abstract

The presence of precious metals with much higher content and purity compared to the corresponding ores, the end-of-life lithium-ion batteries (LIBs), used in electric vehicles (EVs), are known as "urban mine" and have become a research hotspot. The growing demand for the EVs will result in generation of significant quantities of waste LIBs, containing both economically and environmentally targeted materials. If not recycled, traction LIBs could be linked to the depletion of scarce metal reserves, such as lithium and cobalt. Low recycling rate, amounting to less than 5%, is currently affecting profitability of the recycling process. Two main recycling routes for LIBs – pyrometallurgy and hydrometallurgy, have numerous advantages and disadvantages. However, research studies have shown that different processes developed on a laboratory scale could result in good recycling outcomes, considering high recovery rates, achieved purity of products, profitability and eco-friendliness of the recycling process.

Keywords: Li-ion batteries, recycling, end-of-life vehicles, electric vehicles.

INTRODUCTION

The lithium (Li) market is predominantly oriented towards the production of all kinds of batteries for portable devices and electric vehicles, with 80% of the global share, followed by the production of ceramic and glass (7%) and lubricating greases (4%). In recent years, Li consumption for battery production considerably increased mostly due to the fast-growing market of electric vehicles (EVs) [1]. The EVs have a great potential to contribute to the significant reduction of the air pollution emissions in the mobility sector if they are powered on the renewable energy. However, traction Li-ion batteries (LIBs) may become problematic from a sustainability point of view, because of high need for scarce metals [2,3]. The most common nonferrous metals used in the production of the LIBs are Ni, Cu, Co, and Li, among which the Co and Li are denoted as a critical raw material since their resources are limited. According to the reports of the US Geological Survey, the majority of Li production comes from a few countries in the world: Australia, Brazil, Argentina, Chile, China, and smaller operations located in Canada, Portugal, the USA, and Zimbabwe [1,4]. More than half of cobalt production in the world originates from Congo, while China controls about 70% of graphite production, which is also needed for the LIB production [5]. Owing to continuing exploration, the total identified Li resources worldwide are around 98 million tons, mostly located in Bolivia ($21 \cdot 10^6$ t), Argentina ($20 \cdot 10^6$ t), the USA ($12 \cdot 10^6$ t) and Chile ($11 \cdot 10^6$ t). Nevertheless, Blomeke *et al.* [2] showed that the industrial recycling routes are both

economically and environmentally advantageous over the production of the battery components from the raw materials.

At the start of 2019, more than 5.6 million EVs in the world were in use, which is an increase of 64% compared to 2018. By 2040, it is expected that the EVs will account for 58% of all globally sold automobiles [6]. If the LIBs from the end-of-life (EOF) vehicles are hoarded or dumped, non-renewable natural resources are irretrievably wasted. Since the enormous size of the EV´s batteries (e.g. the Tesla Model 3 Long Range battery weighs 480 kg) [6], a substantial amount of waste with high economic value will be produced every year, reaching 21 million tons in the period 2015–2040 [5]. The profit of LIB recycling is up to 3300 €/t, with avoided impacts of emitted 5–7 t of $CO_{2(eq)}$ per tonne of EOF LIBs [6]. The current amount of EOL LIBs affects the profitability of the recycling process. However, the number of EOL LIBs is projected to increase by 2030 due to the rising number of the EVs that will reach their EOL [2], since the average usage of the LIBs is 8 to 10 years [5]. According to Wasesa *et al*. [7], the price of waste LIBs must be less than $227/t in order to be profitable at the lowest incentive condition, while the LIB recycling cost should be $1803/t at the highest incentive scenario. The variety of active cathode materials and the mixing of unknown elements from the production and utilization are the main reasons for difficult and expensive recovery processes [8]. Nevertheless, the reuse of recovered materials in manufacturing of traction LIBs would cause a reduction for all the considered environmental impacts [9]. According to the European legislation, EOL LIBs need to be recycled with a minimum recovery rate of 65% by 2025, which is the medium level of ambition option of the European Commission proposal. Furthermore, the material-specific recovery rates are also set for the valuable components, such as Co, Ni, and Cu, amounting to 90% as well as for Li amounting to 35% of the recovery rate from the EOL LIBs [10].

The paper aims to analyse the main aspects of available recycling processes for the recoverable materials from the EOL LIBs.

RESULTS AND DISCUSSION

Composition of the LIBs

The main components of the LIB structure are battery shell, cathode, anode, separator, and electrolyte. The battery shell is composed of stainless steel, aluminium or plastic. The cathode consists of conductive carbon, binder polyvinylidene fluoride, Al-foil, and active material. There are five types of cathode active material: lithium nickel manganese cobalt oxide ($LiNi_xCo_yMn_zO_2$), lithium iron phosphate ($LiFePO_4$), lithium cobalt oxide ($LiCoO_2$), lithium manganate ($LiMn_2O_4$) and lithium nickel cobalt alumina ($LiNi_xCo_yAl_zO_2$). The anode is usually composed of binder polyvinylidene fluoride, Cu-foil, graphite or conductive carbon, while the electrolyte consists of organic solvents, Li-conductive salts ($LiPF_6$, $LiBF_4$ or $LiClO_4$) and additives [8,11,12].

Available recycling technologies for the EOL LIBs

There are three feasible options for the EOL EVs batteries, depending upon their design, quality, and state of condition: remanufacturing, repurposing, and recycling. Remanufacturing and repurposing extend the usage of the LIBs, while recycling closes the loop [5].

The selection of the recycling process for the EOL LIBs is driven by the difference between the profit of the recycled products and the sum of the costs of the recycling process, other than the recycling rate efficiency and the environmental impact of the process [8]. Dunn *et al*. [13] showed that 15–18% of Co, 9–11% of Li, and 15–17% of Ni demand in 2035, could be met by the closed-loop recycling of the EOL LIBs. As the most valuable component of the LIB, the cathode active materials account for more than 1/3 of the total battery cost [14]. However, if organic solvents and lithium salts are completely recovered from the electrolytes, the profit with a total value of $3345/t of electrolyte could also be gained [15].

Recycling of cathodes could be done *via* smelting in pyrometallurgy, *via* leaching in hydrometallurgy, or without destruction of the crystalline structure of the electrode active material *via* direct recycling. Combination of the given processes could also be employed, such as co-precipitation route, which is a process between hydrometallurgy and direct recycling. The outcomes of the recycling process can differ considerably regarding the recovered materials, achievable purities of the recycled metals, recovery rates, required infrastructure, process emissions, investments, costs, and revenues [2,14,16].

The metallurgy-oriented methods are widely used on the industrial level, while the direct recycling is still in the research stage, but considered as a promising method during which the cathode active materials from the EOL LIBs are directly regenerated [14]. By November 2022, 44 companies in Canada and the USA, and 47 companies in Europe were already involved in recycling or planning to recycle the LIBs [1]. The pyrometallurgical route is implemented mainly in Europe, Japan and North America, while hydrometallurgical route has been mostly commercialized in China [14]. Latini *et al*. [16] reported the plant capacities of most of the recycling facilities in Europe, North America, and Asia. In Table 1, the data is given for the largest ones, according to the recent capacities.

Table 1 *The location, capacities and recycling technology of some LIB recycling facilities [16]*

Company (Location)	Capacity (t/year) for specific year	Recycling technology
Umicore (Begum)	7000 (2020)	Pyro/hydrometallurgy
Glencore* (Norway)	7000 (2020)	Pyrometallurgy
Nortvolt AB (Norway)	8000 (2022)	Mechanical/hydrometallurgy
Stena (Sweden)	10000 (2023)	Mechanical/hydrometallurgy
Neometals (Germany)	10000 (2022)	Mechanical/hydrometallurgy
Erasteel Recycling* (France)	20000 (2020)	Pyrometallurgy
INMETCO* (USA)	6000 (2020)	Pyrometallurgy
Glencore (Canada)	7000 (2020)	Pyrometallurgy
Li-Cycle (USA)	60000 (2023)	Hydrometallurgy/co-precipitation
Nippon Recycle Centre Corp.* (Japan)	5000 (2020)	Pyrometallurgy
SungEel Hi Tech (South Korea)	8000 (2020)	Mechanical/hydrometallurgy
Guanghua Sci-Tech (China)	10000 (2020)	Mechanical/hydrometallurgy
Highpower International* (China)	10000 (2020)	Mechanical, pyro/hydrometallurgy
GEM* (China)	30000 (2020)	Mechanical/hydrometallurgy
Huayo Cobalt (China)	65000 (2020)	Mechanical/ hydrometallurgy

* Facility is recycling batteries other than Li-ion batteries, such as Ni-metal hydride battery, NiCd, etc.

The pyrometallurgical route can utilize different LIB chemistries, as well as geometries, without pre-sorting. However, Li could not be recovered unless the formed slag is subsequently refined. The hydrometallurgy-based processes are more chemistry-specific, but necessarily require pre-treatment [16]. More advantages and disadvantages of pyro- and hydrometallurgical-oriented processes are listed in Table 2.

Table 2 *The key advantages and disadvantages of the pyro- and hydrometallurgical routes for recycling of end-of-life LIBs [2,8,12,16]*

Pyrometallurgy		**Hydrometallurgy**	
Advantages	Disadvantages	Advantages	Disadvantages
Versatile process	Valuable materials are burnt	High recovery rates	Sorting or pre-treatment needed
High capacity of facilities	Downcycling for Li	Recycling of the electrolytes	Lower capacity of facilities
No sorting or pre-treatment needed	Waste gases treatment needed	High purity of obtained products	Generation of wastewaters
High recovery rates for Co, Ni and Cu	High energy consumption (up to 1700 °C)	Lower energy consumption (up to 100 °C)	High operating costs
Industrial application	Low purity of metals	Low emission of waste gases	Complexity of process
Simple process	Further processing of slag is needed	Recovery of the most LIB components	Wastewater treatment needed

Pyrometallurgy is based on smelting of whole batteries in a furnace at extremely high temperatures in order to recover an alloy of precious metals, such as Ni, Co and Cu. The electrolyte is evaporated in the low-temperature zone of the furnace and proceeded to energy recovery unit, while plastics and graphite parts are burnt in the high-temperature zone. The slag, consisted of Li, Al, Mn, and partly of Fe, is typically forwarded to the low-quality markets, although it could be refined via hydrometallurgy to obtain high-purity metals [12].

Hydrometallurgy is based on the leaching in strong inorganic acids (e.g. H_2SO_4, HCl, HNO_3) or alkalis (NaOH), with an additional reducing agent (e.g. H_2O_2), for dissolving the cathode active materials, in order to recover them as single-phase metal salts through crystallization, selective precipitation, solvent extraction, or by electrochemical methods. As an environmentally friendly option, the LIBs could be treated by bio-hydrometallurgy (e.g. microbiological metal dissolution or fungal bioleaching), leached with organic acids (e.g. citric, ascorbic, oxalic or malic acid) or with water because Li-salts are soluble in water [12,17,18]. However, some methods are far from the industrial application. Prior to hydrometallurgical route, a pre-treatment is usually applied in order to increase the recovery rate and reduce the high costs [12]: (a) mechanical separation of electrode materials encapsulated in iron and plastic, including crushing, grinding, gravity and magnetic separation; (b) thermal treatment (e.g. vacuum pyrolysis) in which organic additives and binders are pyrolyzed at high temperatures in order to liberate electrode materials from the foils; (c) mechano-chemical treatment, as a grinding technique, is used to decompose the

crystal structure of metal active materials, extracting Co and Li by an acid leaching process at the room temperature; and (d) dissolution treatment used to weaken the adhesive substance by organic solvents. The electrochemical methods (such as electrolytic deposition, electrodialysis, aqueous electrolysis, and molten salt electrolysis), could replace the traditional chemical leaching of the EOL LIBs. In these methods, the recycling efficiency is greatly improved, and at the same time high reagent consumption and environmental hazards are reduced, which are the main disadvantages of the leaching process. However, many of the electrochemical methods are developed only on a laboratory scale [8,17].

The direct recycling consists of separating and regenerating the cathode and anode active materials without decomposing them into elements. The Li-inventory, lost during battery usage, is restored by keeping the particle morphology and crystalline structure, thus recycled product can be directly reused in new LIBs [12]. The direct recycling has the potential to be environmentally and economically sustainable because the energy and water consumption, as well as the emissions of greenhouse gasses and SO_x are much lower compared to the virgin production of the LIB components and pyro/hydrometallurgical recycling routes. Beyond the challenge of repairing the crystal structure of electroactive materials, there are still many obstacles facing the practical application of the direct recovery [19]. Solid-state sintering, hydrothermal regeneration, eutectic molten salts, and thermal, hydrothermal and electrochemical lithiation are some of the methods, mostly developed at the laboratory scale [16,19].

Zhang *et al*. [20] proposed the concept of carbothermal reduction in combination with three-stage leaching as easy and eco-friendly approach to recycle Li from the LIBs with high Al content, with the comprehensive recovery rate of 87.15%. According to Chakraborty and Saha [6], the optimum choice for the LIB recycling is blending of mechanical shredding, electrolyte extraction, electrode dissolution and Co electrochemical reduction. According to the available data, Dunn *et al*. [13] showed that the recycling of LIBs is less expensive in China than in the USA, neither by conducted transport by truck nor train. Blomeke *et al*. [2] emphasized that, in order to manage the high costs associated with transport of spent batteries as hazardous goods, it is crucial to establish a flexible and scalable recycling infrastructure that can meet the needs for the future market growth and utilization. Makwarimba *et al*. [17] concluded that the focus in the future should be on the development of abundant and non-toxic anode, cathode and electrolyte materials for the LIB production, as well on the new battery designs. Despite the progress made in upscaling conventional methods, there are still few medium to large-scale recycling facilities in the world.

CONCLUSION

In future years, it is crucial to establish a sustainable recycling system that will ensure infrastructure readiness and support the needs for much greater volumes of the LIBs – the valuable, but also hazardous kind of waste. The aim of further research must be feasible connection of a complex relationship among recycling companies, manufacturers of the LIBs, and suppliers of the raw materials on a global scale. If the concept of circular economy is applied on LIBs, the loop could be closed, by combining the supply chain management, sustainability assessment, and innovative engineering. Both, the pyro- and hydrometallurgy-

oriented processes have major drawbacks, such as low purity of the recycled products and downcycling of Li, or high complexity and smaller capacity of the processes, respectively. On the other hand, outcomes of various recycling processes on the laboratory scale, have confirmed that recycling of EOL LIBs is a great opportunity, but also a huge liability for the future.

ACKNOWLEDGEMENT

The authors are grateful to the Ministry of Education, Technological Development and Innovation of the Republic of Serbia for financial support, within the funding of the scientific research at the University of Belgrade, Technical Faculty in Bor (No. 451-03-47/2023-01/200131). Our thanks go to English language teacher, Mara Ž. Manzalović from the University of Belgrade, Technical Faculty in Bor, for providing language assistance.

REFERENCES

[1] Mineral commodity summaries 2023: U.S. Geological Survey, *Available on the following link*: pubs.er.usgs.gov/publication/mcs2023.

[2] Blomeke S., Scheller C., Cerdas F., *et al*., J. Clean. Prod. 377 (2022) 134344.

[3] Chen Q., Lai X., Hou Y., *et al*., Sep. Purif. Technol. 308 (2023) 122966.

[4] Critical Raw Materials for Strategic Technologies and Sectors in the EU – A Foresight Study 2020, Publications Office of the European Union, ISBN: 978-92-76-15336-8.

[5] Chen M., Ma X., Chen B., *et al*., Joule 3 (11) (2019) 2622–2646.

[6] Chakraborty S., Saha A.K., J. Energy Storage 55 (2022) 105557.

[7] Wasesa M., Hidayat T., Andariesta D. T., *et al*., J. Clean. Prod. 379 (2022) 134625.

[8] Li X., Liu S., Yang J., *et al*., Energy Storage Mater. 55 (2023) 606–630.

[9] Jiang S., Hua H., Zhang L., *et al*., Sci. Total Environ. 811 (2022) 152224.

[10] European Commission, 2020. Proposal for a Regulation of the European Parliament and of the Council Concerning Batteries and Waste Batteries, Repealing Directive 2006/66/EC and Amending Regulation (EU), No. 2019/1020.

[11] Mishra G., Jha R., Meshram A., *et al*., J. Environ. Chem. Eng. 10 (2022) 108534.

[12] Wei Q., Wu Y., Li S., *et al*., Sci. Total Environ. 866 (2023) 161380.

[13] Dunn J., Kendall A., Slattery M., Resour. Conserv. Recycl. 185 (2022) 106488.

[14] Fan Y., Kong Y., Jiang P., *et al*., Chem. Eng. J. 463 (2023) 142278.

[15] Vanderburgt S., Santos R. M., Chiang Y. W. Resour. Conserv. Recycl. 189 (2023) 106733.

[16] Latini D., Vaccari M., Lagnoni M., *et al*., J. Power Sources 546 (2022) 231979.

[17] Makwarimba C. P., Tang M., Peng Y., *et al*., iScience 25 (2022) 104321.

[18] Tian G., Yuan G., Aleksandrov A., *et al*., Sustain. Energy Technol. Assess. 53 (2022) 102447.

[19] Wu J., Zheng M., Liu T., *et al*., Energy Storage Mater. 54 (2023) 120–134.

[20] Zhang G., Yuan X., Tay C. Y., *et al*., Sep. Purif. Technol. 314 (2023) 123555.

30th International Conference Ecological Truth & Environmental Research
20–23 June 2023, Serbia

CRYSTALLIZATION CHARACTERISTICS OF BIOACTIVE POLYPHOSPHATE GLASSES

Vladimir Topalović[1*], Srđan Matijašević[1], Veljko Savić[1], Jelena Nikolić[1], Jovica Stojanović[1], Snežana Zildžović[1], Snežana Grujić[2]

[1]Institute for Technology of Nuclear and Other Mineral Raw Materials (ITNMS), 86 Franchet d'Esperey St., 11000 Belgrade, SERBIA

[2]Faculty of Technology and Metallurgy, University of Belgrade, 4 Karnegijeva St., 11000 Belgrade, SERBIA

[*]*v.topalovic@itnms.ac.rs*

Abstract

The essence of this paper is to present the effect of adding TiO_2 and SrO to the crystallization characteristics of polyphosphate glasses. The crystallization of glasses has been studied by using DTA, HSM and XRD methods. Sintered phosphate glass-ceramics containing bioactive β-CaP_2O_6, and β-$Ca_3(PO_4)_2$ phases were successfully prepared. The increasing presence of Sr (1-5%), as well as Ti at the expense of phosphate mole fraction in polyphosphate bioactive glass increases the density of these glasses, transformation temperature and resistance to crystallization.

Keywords: polyphosphate glass, bioactive glass-ceramic, sinter-crystallization.

INTRODUCTION

Because of their promising application in biology, medicine, pharmacy and agriculture, different types of polyphosphate glasses are being widely studied [1,2]. The polyphosphate glasses have recently been examined as drug carriers and also their effect on bone regeneration was documented [3]. The addition of strontium is considered to have a therapeutic effect [4,5].

Furthermore, β-tricalcium phosphate (β-$Ca_3(PO_4)_2$ doped with lanthanum using a precipitation technique was developed. The anti-bacterial efficacy of the modified β-$Ca_3(PO_4)_2$ was confirmed by its effect on Staphylococcus aureus and Escherichia coli [6]. The parent multicomponent phosphate glasses were derived from the basic CaO-P_2O_5-Na_2O system. With the addition of Sr, and Ti as a nucleator [7], new glasses were obtained by standard melt-quenching method: $46P_2O_5{\cdot}40CaO{\cdot}SrO{\cdot}10Na_2O{\cdot}3TiO_2$ (mol%) (GSSr1) and $42P_2O_5{\cdot}$ $40CaO{\cdot}5SrO{\cdot}10Na_2$ $\cdot 3TiO_2$ (GSSr5). The analysis of the crystallization process was carried out by DTA, HSM and XRD methods. Sintered phosphate glass-ceramics containing bioactive β-CaP_2O_6, α-$Ca_2P_2O_7$ and β-$Ca_3(PO_4)_2$ phases were successfully prepared.

MATERIALS AND METHODS

The starting materials used for glass synthesis were high purity reagents $(NH_4)_2HPO_4$, Na_2CO_3, $CaCO_3$, $SrCO_3$ and TiO_2. These reagents were homogenized and prepared in an

agate mortar. To avoid foaming of the melts, the samples were thermally treated at 190 °C during 3 h. The appropriate compositions of the prepared mixtures were melted at 1250 °C in Carbolite BLF 17/3 furnace for 0.5 h in a Pt crucible, after which the melts were poured onto a steel plate and cooled in air.

The chemical analysis was performed using spectrophotometer AAS PERKIN ELMER Analyst 703. The method of atomic absorption spectrophotometry (AAS) was used to determine the content of oxides, CaO, Na_2O, TiO_2, P_2O_5, SrO in glass, after destruction of the sample by NaOH, the composition was determined by analyzing the content of their cations in the solution. The measurement uncertainly is 0.86%.

The DTA-SDT Q600 TGA/DSC/TA Instruments, USA, with Al_2O_3 powder as the reference material, was used to test the non-isothermal crystallization of the glass samples. Powder samples (10 mg) were prepared by crushing and grinding pieces of cast glasses in an agate mortar with a pestle and sieving the prepared samples to the appropriate granulation (<0.048 mm). The glasses were observed in a temperature range of T=20-800 °C at a heating rate of v=10 °C min^{-1}. Before the DTA experiment, the device was calibrated with quartz standard purity of 99.995% of known crystallization temperature. The characteristic temperatures of the tested glasses were determined from the DTA curve.

The sintering behavior of the glass powders was observed by Hot Stage Microscopy (HSM) (Misura – HSML 1400 Expert System Solutions). The glass powder samples (<0.048 mm) were pressed into cylinders and heated in HSML at a heating rate of 10°C min changes in the shape of cylindric samples during heating are monitored and the changes in the area of the samples at the different temperatures were calculated. The shrinkage of the samples was calculated as a ratio A/A_o, where A_o is the initial area and A is the area at temperature T.

The XRD method was used to identify the phase composition of crystallized glass samples. The samples were crystallized at the appropriate temperature according to DTA analysis. XRD diagrams were obtained using an automated diffractometer Philips PW-1710 (PANalytical, The Netherlands) which uses a Cu tube operating at a voltage of 40 kV and a current of 32 mA. The instrument is equipped with a graphite monochromator and a xenon proportional counter. Diffraction data were collected at a 2θ Bragg angle of 5-70 °, with a scanning step of 1 s. The standard database (JCPDS database) for XRD pattern is used for phase identification.

RESULTS AND DISCUSSION

The glass mixture for obtaining the selected glass composition was melted in an electric furnace. The samples of the obtained glasses were transparent, without visible remaining gas bubbles. X-ray diffraction analysis of the powders confirmed that an amorphous structures were obtained. No peaks attributed to any crystallized compound could be identified except a broad diffraction halo (amorphism of between 20° and 35°), which is attributed to the glassy amorphous phase (figure not shown).

The results of the chemical analysis of the investigated glasses are listed in Table 1.

Table 1 *Chemical compositions of the glasses*

Sample	Composition [wt%]					
	P_2O_5	CaO	Na_2O	TiO_2	SrO	Σ
GSSr1	67.07	23.04	6.39	2.46	1.06	100
GSSr5	62.21	23.41	6.47	2.50	5.41	100

Figure 1 shows the DTA/HSM curve of the powdered glass samples (<0.048 mm) recorded at a constant heating rate of 10 °C min^{-1}.

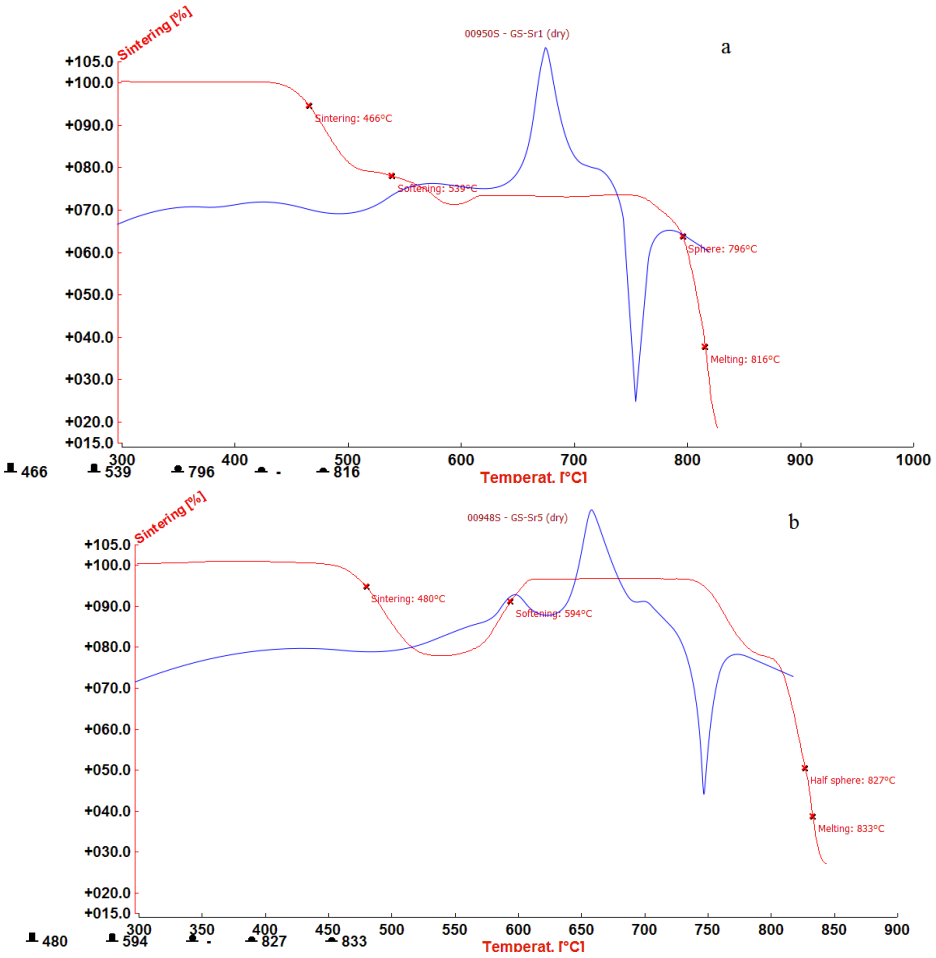

Figures 1 *show comparative thermal analyses of the examined glass samples a) GSSr1 and b) GSSr5 on a DTA (blue line) and HSM (red line)*

The crystallization of the selected glasses is shown on the DTA curve by the exothermic peaks with the temperatures of the beginning of the crystallization processes in T_x = 625-635 °C range and the maximum crystallization temperatures in T_p = 660-675 °C range. Pronounced endothermic peaks, which represent the melting of the glass samples, were observed after the crystallization process.

The onset melting temperatures (T_{om} ~ 700-730 °C) and the maximum liquidus peak temperatures (T_m = 745-755 ºC) can be observed on the DTA curve. The bends that correspond to the temperature ranges of glasses transformation T_g = 420-425 °C can also be

seen on the curve. In this area a solid body begins to behave like a viscoelastic body when heated. Hruby proposed the use of the K_H parameter to assess the resistance of glass to the crystallization process based on DTA analysis [8].

$$K_H = \frac{T_x - T_g}{T_m - T_x} \quad (1)$$

Glasses with high K_H values should show higher resistance to crystallization, and therefore their ability to vitreously solidify the melt during cooling should be higher. The obtained glasses with the addition of strontium have a lower tendency to crystallize than the parent phosphate glass, and the value of the Hruby parameter ranges from 2.53 (GSSr1) to 2.89 (GSSr5).

Thermal properties, viscosity and sinterability of oxide glasses are strictly dependent on their composition. The almost even shift of the characteristic temperatures of transformation T_g, crystallization T_p and melting T_m, of the obtained glasses can be explained by the influence of replacing the oxide P_2O_5 in the starting glass with SrO in the derived glasses.

Namely, the density of P_2O_5 is 2.30 g cm^{-3}, and of the added SrO 4.70 g cm^{-3}. Increasing the density of these glasses by adding strontium oxide to the glass mixture also affects the increase in viscosity and the increase in transformation temperatures, softening temperatures and sinterability (Figure 1).

Temperatures corresponding to the characteristic values of the viscosity of the tested glasses were determined: first sample shrinkage (T_{fs}), maximum shrinkage (T_{ms}), softening (T_d), sphere (T_s), half-ball (T_{hb}) and viscous flux (T_f). Sample sintering occurs in the 466 °C (GSSr1) - 480 °C (GSSr5) range, softening of the samples occurs in the 539 °C (GSSr1) -594 °C (GSSr5) range, and crystallization in the 625 - 730 °C range. Based on the comparative analysis (Figure 1), we can conclude that the sintering and crystallization processes are independent in the obtained glasses. Bearing in mind the possible application, this is significant data.

Based on the value (0.60) of reduced glass transition temperature $T_{rg} = T_g/T_m > 0.58$ it can be assumed that surface crystallization takes place in these glasses [9].

Activation energies for the crystallization process were determined by the method of Kissinger (E_a) because it was determined that the samples crystallize by surface mechanism [10]. The relatively low energies for the crystallization process of the obtained glasses can be attributed to the presence of a nucleator (TiO_2) added to the composition of the starting mixture to control the crystallization process in each glass. TiO_2 is considered an intermediate oxide that affects the chemical stability of glass.

The prepared glass samples for X-ray analysis were isothermally heated in a Carbolite 13/13 furnace with a heating rate regulator and a temperature accuracy of ± 1 ˚C, at crystallization temperatures previously determined on DSC, 665-695 °C for 3 h. The phase composition of the sample was determined by XRD analysis and the results are shown in Figure 2.

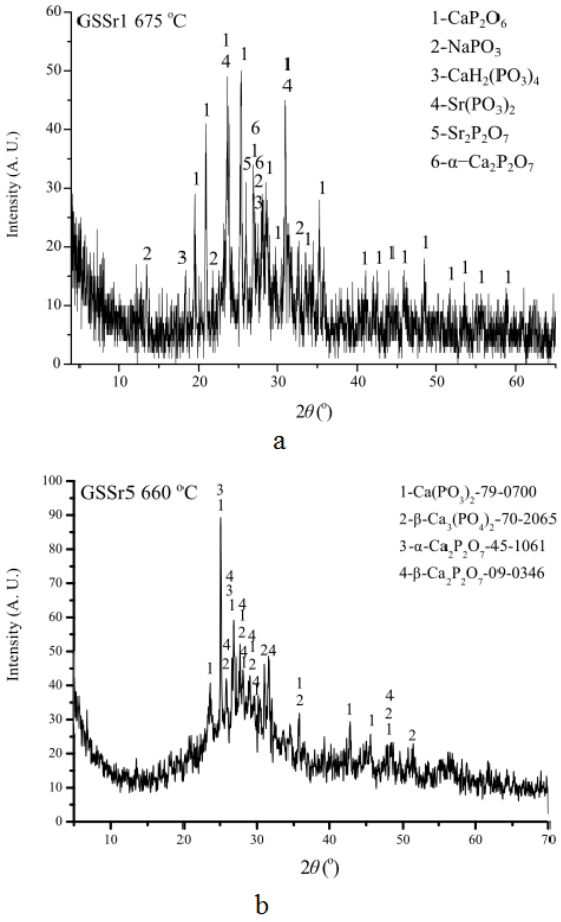

Figure 2 *XRD analyses of the crystalized samples: a) GSSr1 and b) GSSr5*

XRD analyses of the powder samples showed that during thermal treatment glass particles crystallized as opaque glass-ceramics white in color and the presence of crystalline phases was determined, among others: β-CaP_2O_6, α-$Ca_3(PO_4)_2$, β-$Ca_3(PO_4)_2$, $Ca_2P_2O_7$, and $NaPO_3$.

Tricalcium phosphate ($Ca_3(PO_4)_2$, TCP) and β-calcium phosphate (β-CaP_2O_6) found in the analyzed glass-ceramic samples are one of the most compatible materials used as a substitute for human bones in the field of bioceramics. Also, TCP can be used as a replacement for tissues in the bone defects regeneration.

We can conclude that the increasing presence of doped elements Sr (1-5%), as well as Ti at the expense of phosphate mole fraction in polyphosphate bioactive glass increases the density of these glasses (viscosity), transformation temperature and resistance to crystallization.

CONCLUSION

The obtained glasses with the addition of strontium have a lower tendency to crystallize than the parent phosphate glass. The even shift of the characteristic temperatures of transformation T_g, crystallization T_p and melting T_m, of the obtained glasses can be explained by the influence of replacing the oxide P_2O_5 in the starting glass with SrO in the derived glasses. Increasing the density of these glasses by adding strontium oxides to the glass mixture also affects the increase in viscosity and the increase in transformation temperatures,

softening temperatures and sinterability. The relatively low energies for the crystallization process of the obtained glasses can be attributed to the presence of a nucleator (TiO_2). XRD analyses of the powder samples showed the presence of β-CaP_2O_6, β-$Ca_3(PO_4)_2$, $Ca_2P_2O_7$ and $NaPO_3$ crystalline phases, among others. Based on the comparative DTA and HSM analysis, we can conclude that the sintering and crystallization processes are independent in the obtained glasses.

ACKNOWLEDGEMENT

The authors are grateful to the Ministry of Science, Technological Development and Innovation of the Republic of Serbia for financial support according to the contract with the registration number (451-03-47/2023-01/200023 and 451-03-47/2023-01/200135).

REFERENCES

[1] Sharmin N., Rudd C. D., J. Mater. 52 (2017) 8733–8760.

[2] Hazra G., Sustain. Environ. 1 (1) (2016) 54–70.

[3] Hoppe A., Mourino V., Boccaccini A. R., Biomater. Sci. 1 (2013) 254–256.

[4] Mourino V., Cattalini J. P., Boccaccini A.R., J. R. Soc. Interface. 9 (2012) 401–419.

[5] Ni G., Chiu K., Lu W., *et al*., Biomaterials 27 (2006) 4348–4355.

[6] Meenambal R., Singh R. K., Kumar P. N., *et al*., Mater. Sci. Eng. 43 (1) C (2014) 598–606.

[7] Dias A. G., Tsuru K., Hayakawa T., *et al*., Glass Technology 45 (2) (2004) 78–79.

[8] Kozmidis-Petrovic A., Šesták J., J. Therm. Anal. Calorim. 110 (2012) 997–1004.

[9] Matijašević S., Grujić S., Topalović S., *et al*., Sci. Sinter. 50 (2) (2018) 193–203.

[10] Topalović V., Nikolić J, Matijašević S., *et al*., J. Therm. Anal. Calorim.148 (3) (2023) 721–734.

ASSESSING THE COMPOSITION OF MUNICIPAL SOLID WASTE IN ŠID

Isidora Berežni[1*], Tijana Marinković[1], Bojan Batinić[1]
[1]Department of Environmental Engineering, Faculty of Technical Sciences,
University of Novi Sad, Novi Sad, 21000, SERBIA
[*]*isidoraberezni@uns.ac.rs*

Abstract

Solid waste management (SWM) represent one of the main issue faced by transition countries, since the increasing amounts of waste generated and improper handling of this waste creates a risk for the environment and human health. For developing sustainable municipal solid waste management system detailed information about waste amount and composition are crucial. This research was done to analyses representative samples of municipal solid waste in Šid municipality, following the Waste Amount and Composition Survey (WACS), in order to determine waste generation rates, physical composition and apparent specific gravity of waste by types of generation sources. WACS is considered as one of the most important surveys in SWM planning because based on the obtained results total amount of waste to be generated in the area is estimated, so methods of technical systems in the SWM such as waste haulage, recycling and final disposal can be planned.

Keywords: municipal solid waste, waste composition survey, waste amount survey, transition countries.

INTRODUCTION

Due to the rapid population and economic growth, generation of solid waste worldwide has increased over time. It is expected that the growth rate of 1.5% will lead to the production of 3 billion tons of municipal solid waste (MSW) in 2030 [1]. Since solid waste management (SWM) has an impact on environment and public health, it became one of main challenges for both national and municipal governments [2].

Information about waste composition and characteristics are crucial for designing a sustainable waste management for many reasons such as determination of the potential of waste resources for recycling, reuse, and recovery processes; estimation of solid waste generation sources or designing treatment facilities [3]. However, cities in transition countries generally do not have these informations, so waste-related decisions are often made based on national average rates which may completely deviate from the real local situation [4].

For determination of solid waste characteristics there is no international standard methodology, so most countries developed their own guidelines which will suit local conditions and reflect the technological and financial limitations for the implementation of the study [5,6]. In industrialized countries, to obtain highly accurate results, very specific methodologies are used, but require extensive resources, while in developing and transition countries these studies are mostly conducted only for major cities, where methodology is based on simplicity in the procedures rather than data reliability [7].

In this work, we present the results of a study conducted with the aim of evaluating the characteristics of waste composition and generation rates of municipal solid waste of Šid city. The next sections presents the methodology used, results of the study and discussion about main findings as well as some key policy implications and ways forward.

MATERIALS AND METHODS

The study area

The municipality of Šid is located in the southwest of Vojvodina and belongs to the Srem district. Compared to other municipalities, Šid belongs to the group of 10 largest in the autonomous province (AP) of Vojvodina. On its territory there are 19 settlements (Adashevci, Bačinci, Batrovci, Berkasovo, Bingula, Vašica, Višnjićevo, Gibarac, Erdevik, Bikić Do, Ilinci, Jamena, Kukujevci, Ljuba, Molovin, Morović, Privina Glava, Sot, Šid). According to latest data, 32,348 inhabitants live in the municipality, which is 0.46% of the total population in Serbia. According to population density, the municipality of Šid with 58.6 people/km^2 is almost twice less populated (1.6 times) than the AP Vojvodina (94.5 people/km^2). Agriculture is still the dominant branch and one of the carriers of economic development. In addition to agriculture in this municipality, industry, trade services and traffic are also developed. The agricultural-industrial complex and the chemical industry are well-known.

Preparation for WACS

Implementation of the Waste Amount and Composition Survey (WACS) consists of four stages: (I) selection of target generation sources, (II) arrangement of necessary tools and equipment, (III) workplace, (IV) explanation and preliminary data collection.

The most important task is selecting target generation sources due to the fact that the total generation amount in the target area is estimated based on the results obtained from them. The target generation sources are selected based on the types of activities and their sizes and locations. The categories of generation sources defined for WACS are: (1) households, (2) shops, (3) restaurants, (4) schools, and (5) factories. A total of 66 households, 17 shops, 7 schools, 5 shops and 5 factories each were taken as a representative sample.

All the necessary items for implementing the survey were prepared (plastic bags, hand scale, electronic scale, personal protective goods etc.), including the vehicles that were used for sampling collection. Sufficient attention was paid to preparation of sample bags. In order not to confuse among samples of waste to be collected from the target sources throughout the implementation of the survey, different colours of bags were prepared for different generation sources (yellow for households, green for shops, black for factories etc.). Beside this, code relating to the sample is marked onto the sample bag in advance.

WACS was conducted outdoor where all the measures have been taken to prevent from the impact of wind and rain so that the sample will not be affected by externalities. Based on the request, public utility company (PUC) provided space for work at municipal landfill site in Šid.

Before commencement of the survey, each selected source must have understood the purpose of the survey and gained sufficient knowledge about the cooperation required from them. Therefore, visits to the target sources were organized in advance to gain knowledge for

using proper bags for each day throughout the implementation period and to transfer all waste generated by them in same bags during the survey period. At the same time with the explanation, basic information about generation units in each of the target sources were collected and pre-arranged sample bags were distributed to them.

Implementation of WACS

The survey is implemented within 8 days. The samples collected on the first day were not used in the analysis of WACS as it might include waste generated through several days. Therefore, the purpose of the 1st day's collection is to ensure that no waste is remained at target sources so that the waste to be generated on the next day will be 1 day's waste and can be used for the analysis. Samples were collected every day throughout the implementation period from all the target sources. To ensure the collection efficiency sample collection routes were planned in advanced based on the location of the target sources. Map of all locations of target sources is given in Figure 1. The locations were divided between three teams that collected samples daily. All samples collected from target sources were weighted on site and results were record in the appropriate waste amount survey (WAS) record sheets.

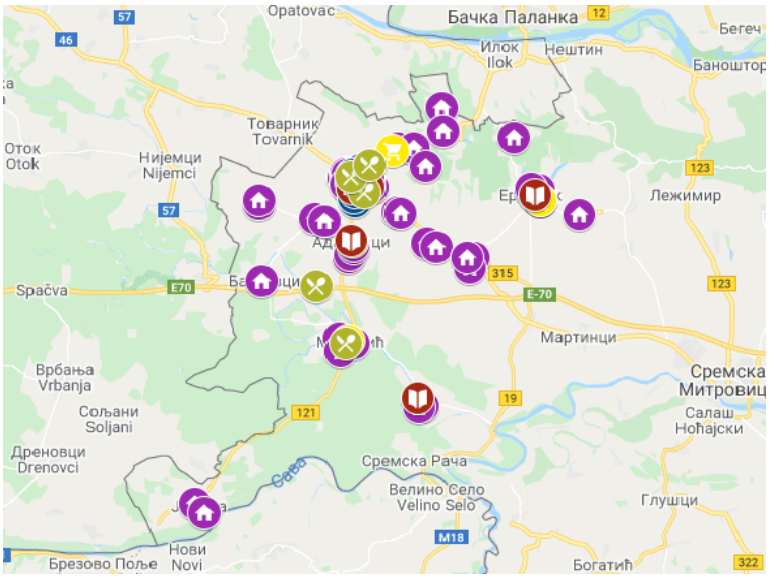

Figure 1 *Map of all locations of target sources*

Waste composition survey (WCS) should be implemented immediately after WAS as composition of waste changes along with the time. Since all samples collected for WAS were the target of WCS, it was also conducted for 8 days. However, the 1st day's sample was excluded from the analysis like that of WAS. The total weight of all waste collected from a same type of generation source is measured, put out of their bags, and prepared in accordance with the following two ways depending on the amount:

1) When amount of waste was too big, it was reduced to an appropriate level (an amount of waste appropriate for WCS is approximately 40 litres). First the waste was mixed completely and then reduction is done based on Method of Quartering to avoid possible changes in the composition of the initial waste. The reduction steps are the following: **Step 1**: Mixing: In order to ensure complete or even mixture, bigger wastes should be cut into small pieces

before mixing. However, there are many items that cannot be cut or broken into pieces or dangerous when cutting or breaking. These items should be picked prior to mixing and put separately from those to be mixed; **Step 2**: Dividing: Once the waste is mixed well, it is divided into four segments of approximately the same size; **Step 3**: Reduction: The two segments of waste diagonally opposite each other are removed and the remaining waste is mixed again; **Step 4**: The above steps are repeated until the volume of the remaining waste is reduced in size to approximately 40 litres.

2) When the amount of waste was less than 40 litres, bigger wastes that cannot be cut or broken into pieces was picked and separated from other waste. Then, mixing and reducing the unpicked waste was not necessary since all the waste was used in WCS processes.

RESULTS AND DISCUSSION

Generation rates (WAS)

Total generation units were counted throughout the period of concern (last 7 days out of the 8) and the total amount of waste was estimated for each single source; and then, for each type of generation sources. Results of estimated waste generation rates are given in Table 1.

Table 1 *Estimating generation rates*

Type of generation sources	Selected sources	Total generation units		Total waste (kg)	Generation rate (g/unit/day)	
a	b	c		d	e	
Households	66	1328	person*day	622.54	469	g/person/day
Shops	17	105	shop*day	53.02	505	g/shop/day
Restaurants	5	35	restaurants*day	129.75	3707	g/restaurant/day
Schools	7	1986	Students*day	83.14	41.9	g/student/day
Factories	5	26	factory*day	101.31	3900	g/factory/day

Analysed target amount (WCS)

The data in the column "WCS total" in Table 2 are amount of waste before picking and reduction by each type of target sources. The column "Picked Total" shows all picked waste, while "Unpicked Total" is the amount of unpicked waste before reduction; the data for this column are estimated by subtracting the "Picked Totals" from the "WCS Totals". These amounts are the initial amounts of waste collected for the WCS, but not the final target from which composition and specific gravity was estimated.

As it is the unpicked waste remained at the final step of sample preparation, its amount does not necessarily match that of "Unpicked Total" since some of the waste is reduced before sorting. The amounts of "Picked Targets" are estimated by the formula Picked Target = (Picked Total) x (Unpicked Target) / (Unpicked Total). The addition of the Picket Target and Unpicked Target is the Analysed Target Amount from which composition and specific gravity will be estimated.

Table 2 *Estimating analysed target amount*

No	Code	Types of generation sources	WCS total (kg)			Analysed target amount (kg)		
			Picked total	Unpicked total	WCS total	Picked target	Unpicked target	Total analysed
		a	b	c	d	e	f	g
1	HH	Households	126.71	495.83	622.54	13.62	51.18	64.80
2	SP	Shops	32.115	20.905	53.02	32.12	20.905	53.02
3	R	Restaurants	57.57	72.18	129.75	26.91	34.06	60.96
4	SH	Schools	35.78	47.36	83.14	23.10	27.86	50.96
5	F	Factories	57.41	43.90	101.31	37.89	25.725	63.61

Physical composition (WCS)

Physical Composition is estimated through 3 steps. These are:

Step 1: Estimating breakdowns of the Picked Target (section "a" in Table 3). Breakdowns of "Picked Target" are the types of waste included in it and estimated for each type of generation sources by multiplying on the total amount of "Picked Target" (data in the column "e" of Table 3) with shares of waste types in the "Picked Total". The shares of waste types in "Picked Total" are estimated by each type of generation sources from the base data using the weights of all the picked waste.

Step 2: Estimating breakdowns of Total Target Waste (section "b" in Table 3). It is estimated by adding the counterpart types in the Picked Target and Unpicked Target. The breakdowns of the Unpicked Target are those taken directly from the base data.

Step 3: Estimating physical composition (section "c" in Table 3). The composition is represented by the shares of each waste type in the total amount of the target waste.

Table 3 *Estimating physical composition (HH: Households)*

No.	Types of waste	a			b			c
		Breakdown of picked target			Breakdown of total target			Physical composition (%)
		Picked total (kg)	Share in the total (%)	Picked target (kg)	Picked (kg)	Unpicked (kg)	Total (kg)	
1	Kitchen waste	12.29	10%	1.32	1.32	34.17	35.49	55%
2	Papers	27.445	22%	2.95	2.95	2.42	5.37	8%
3	Textile	6.8	5%	0.73	0.73	0.865	1.60	2%
4	Plastic	48.74	38%	5.24	5.24	2.745	7.98	12%
5	Grass & Wood	0	0%	0.00	0.00	0.77	0.77	1%
6	Rubber & Leather	2.475	2%	0.27	0.27	0.1	0.37	1%
7	Metal	7.395	6%	0.79	0.79	0.53	1.32	2%
8	Glass & Bottle	17.685	14%	1.90	1.90	3.465	5.37	8%
9	Ceramic & Stone	3.875	3%	0.42	0.42	0.265	0.68	1%
10	Earth & Ash	0	0%	0.00	0.00	3.93	3.93	6%
11	Other	0	0%	0.00	0.00	1.92	1.92	3%
	Grand total	126.705	100%	13.62	13.62	51.18	64.80	100%

The same was done for other four generation sources and the results are given in Figure 2.

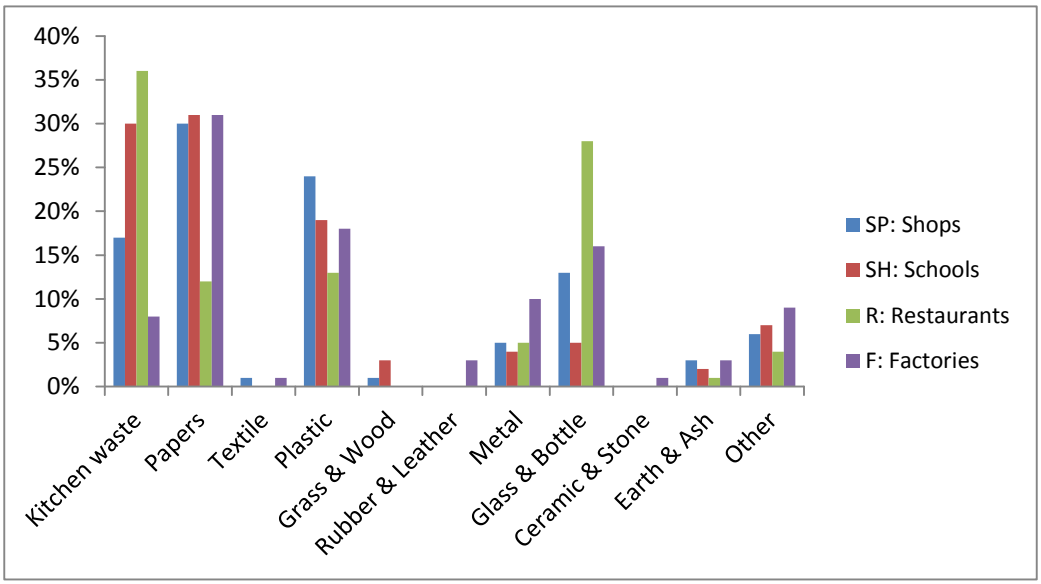

Figure 2 *Physical composition for other generation sources*

Specific gravity

Based on the data of total weight and total volume of the analysed target waste, the specific gravity is estimated. The following results were obtained: 93.49 kg/m^3 for households; 50.53 kg/m^3 for shops; 47.43 kg/m^3 for schools; 52.90 kg/m^3 for restaurants and 57.25 kg/m^3 for factories.

CONCLUSION

The analysis of waste characteristics is a basic tool for long-term sustainable planning and development. As the characteristics of the waste depend on various factors, it is important to conduct analyses for each area so that the results show the real situation and, accordingly, an adequate management system can be implemented. This research has produces estimates of the composition of municipal solid waste in the city of Šid following the WACS procedure. Results showed that the organic fraction in waste is dominant, especially from households, where it makes more than 50% of the total amount. Paper and plastic are the other two categories that are found in a higher percentage, especially in a large percentage coming from stores and factories. For restaurants, in addition to organic waste, paper and plastic, there is also a significant amount of glass and bottles. All this points to the potential for reducing the amount of waste going to landfills. As agriculture is present in the city of Šid, there is potential to return organic waste to use, for example in the form of compost, while for recyclable materials such as glass, plastic and paper it is necessary to establish a system of separate collection and transport to recycling facilities. Future research is needed that will consider social, economic and technical factors in order to find the best solution for establishing an adequate waste collection system in the Šid and possible solutions for reuse and recycling, in order to reduce the amount that is disposed of in landfills.

ACKNOWLEDGEMENT

This research was supported and carried out in the framework of Japan International Cooperation Agency (JICA) project named „Capacity Development for Solid Waste Management in the Republic of Serbia", together with Japanese Expert Team – Kokusai Kogyo Co., as partner.

REFERENCES

[1] Čepić Z., Bošković G., Ubavin D., Batinić B., Pol. J. Envrion. Stud. 31 (2022) 4579–4588.

[2] Ghinea C., Dragoi E. N., Comanita E. D., *et al*., J. Environ. Manage. 182 (2016) 80–93.

[3] Teshome Y. M., Habtu N. G., Molla M. B., Ulsido M. D., Global J. Environ. Sci. Manage. 9 (2023) 227–240.

[4] Miezah K., Obiri-Danso K., Kádár Z., Fei-Baffoe B., Mensah M.Y., Waste Manag. 46 (2015) 15–27.

[5] Sahimaa O., Hupponen M., Horttanainen M., Sorvari J., Waste Manag. 46 (2015) 3–14.

[6] Villalba L., Donalisio R. S., Cisneros Basualdo N. E., Noriega R. B., Resour. Conserv. Recycl. 152 (2020) 104530.

[7] Krause M. J., Townsend T. G., Int. J. Waste Resour. 04 (2014) 2–7.

30th International Conference Ecological Truth & Environmental Research
20–23 June 2023, Serbia

SYNTHESIS AND CHARACTERISATION OF CARBON NANOMATERIAL USING HYDROTERMAL CARBONISATION METHOD

Ivan Bracanović[1], Aleksandar Krstić[1*], Ana Kalijadis[1]

[1]University of Belgrade, Vinča Institute of Nuclear Sciences – National Institute of the Republic of Serbia, Mike Petrovića Alasa 12–14, Belgrade, SERBIA

[*]*aleksandar.krstic@vin.bg.ac.rs*

Abstract

This work aimed to compare surface characteristics of synthesized carbon-based material using the hydrothermal carbonization (HTC) method with a commercially used multi-walled carbon nanotubes that were functionalized in acid solution (f-MWCNT). Precursor for HTC material synthesis was 3M fructose solution. Both materials were characterized using Fourier transform infrared spectroscopy (FTIR), X-ray diffraction analysis (XRD), and scanning electron microscopy (SEM). Obtained results showed that structurally and in terms of morphology examined materials are significantly different unlike generated surface functional groups which are oxygen-based for both materials. With the HTC method, we could synthesize material with abundant content of oxygen surface functional groups in one step.

Keywords: fructose, hydrothermal carbonisation, MWCNT, funcionalization, characterisation.

INTRODUCTION

Carbon nanomaterials [1] were discovered in 1999 as a new allotropic modification of carbon. They consist of nanotubes (CNT) [2] which can be single (SWCNT) and multi-walled (MWCNT), graphene [2] as graphene oxide (GO) [2] and quantum nanodots (GQD) [2]. They have excellent mechanical, electromagnetic and chemical properties because of their unique structure [1]. These properties give CNTs various applications in medicine, engineering, and technology [3].

Hydrothermal carbonization [4] is a thermochemical process that uses heat and self-generated pressure to convert biomass and organic matter into carbon-based material that already possesses oxygen-containing surface functional groups such as hydroxyl, carboxyl, carbonyl, epoxy, etc. These surface functional groups are crucial for functionalization of carbon materials to better adapt their use [5].

MATERIALS AND METHODS

Materials

For this research we used commercially purchased MWCNT (Carbon nanotube, multi-walled; 50-90 nm diameter, >95% carbon basis, 25 g, Sigma-Aldrich), Fructose

(D-(−)-Fructose, ≥99%), H_2SO_4 (ACS reagent, 95.0-98.0%, Sigma-Aldrich) and HNO_3 (puriss. p.a., 65.0-67.0%, Sigma-Aldrich).

Methods

MWCNT functionalization

Pristine MWCNTs (2 g) were added to the mixture containing conc. H_2SO_4 and conc. HNO_3 (3:1 volume ratio). The reaction mixture was left to stir for 24 h at room temperature. After 24 h, the mixture was diluted with distilled water, and the dispersion was kept overnight. Water was decanted, and the remaining dispersion was separated with Buchner and washed with deionized water until the pH reached 7. The residue was dried at 80 °C to get carboxylate MWCNTs (marked as f-MWCNT) [5].

Hydrothermal carbonisation (HTC)

25 cm^3 of 3M fructose solution was poured into a Teflon tube. After that, the tube was placed in a device for hydrothermal carbonization. The device placed in the electric furnace and heated at 160 °C for 4h and then rapidly cooled. To generate the pure solid, obtained dispersion was washed with deionized water until the pH of water reached 7 and centrifuged at 18000 rpm. The obtained HTC material (marked as F160) was dried overnight at 100 ° C.

RESULTS AND DISCUSSION

FTIR spectra are presented in Figure 1. Spectra for all samples show a broad peak between 3700 and 3100 cm^{-1} attributed to the O−H stretching of the hydroxyl groups [7]. The area between 3000 and 2800 cm^{-1} is attributed to the C−H stretching for sp^2 and sp^3 hybridizations [7]. The peak between 1700 and 1600 cm^{-1} and at 1050 cm^{-1} in Figure 1a and 1b can be assigned to the C−O stretching of the carboxyl groups. The peak between 1150 cm^{-1} and 1000 cm^{-1} refers to the C−OH and C−O stretch [7]. The peak between 1700 cm^{-1} and 1600 cm^{-1} Figure 1c is assigned to C=C for MWCNT and for others it's covered with C-O stretching of the carboxyl groups [6,7]. These results indicate that the surface of the material has mostly oxygen-containing groups, including hydroxyl ($^-$OH) and carboxylic ($^-$COOH) functional groups.

Comparing spectra in Figure 1, we can see that intensity of the broad peak attributed to the O−H stretching is stronger for spectra in Figure 1a and 1b, which indicates that F160 and f-MWCNT possess more hydroxyl groups on their surface than MWCNT [7]. The existence of this peak in Figure 1c for MWCNT can be attributed to the possible existence of moisture in the sample because it does not possess a peak between 1150 and 1000 cm^{-1} that is characteristic for hydroxyl group [7]. All spectra in Figure 1 also possess a peak between 1700 and 1600 cm^{-1}, with varying intensity, indicating that they came from different functional groups [7]. For MWCNT that group is alkene and for F160 and f-MWCNT is carboxyl. This can be confirmed by the existence of peaks between 1150 and 1000 cm^{-1} for F160 in Figure 1a and f-MWCNT in Figure 1b that does not exist for MWCNT in Figure 1c [7].

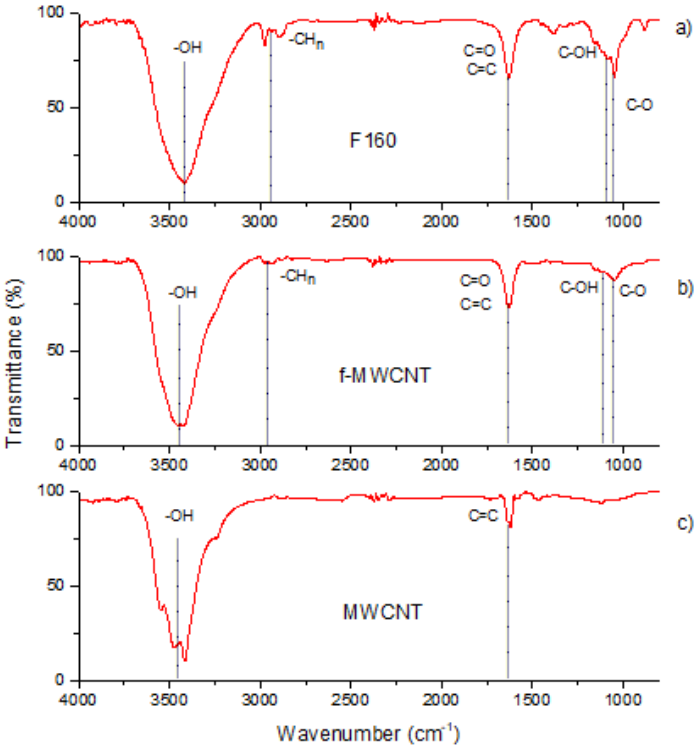

Figure 1 *FTIR spectra of a)F160, b)f-MWCNT and c)MWCNT*

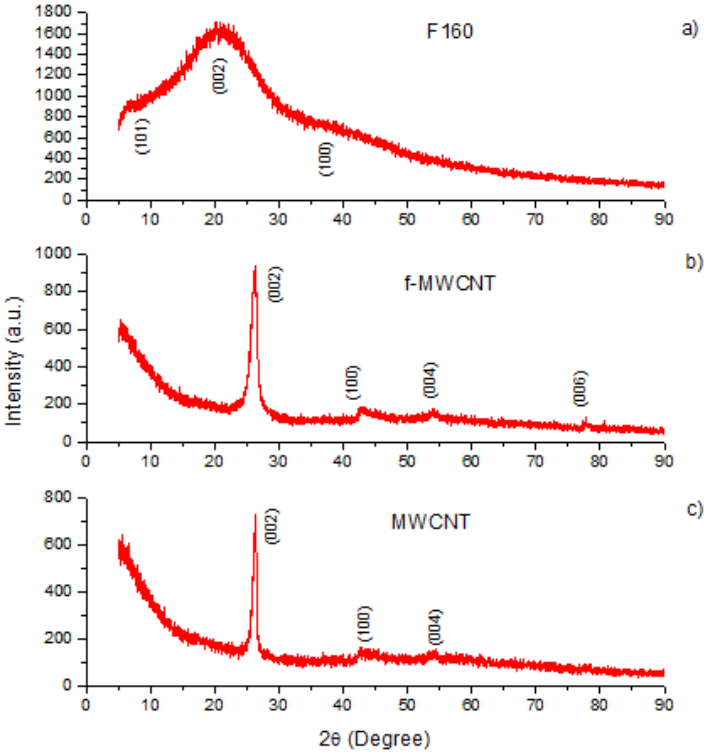

Figure 2 *XRD of a) F160, b) f-MWCNT and c) MWCNT*

The XRD patterns are shown in Figure 2. The X-ray diffraction patterns in Figure 2a display diffraction peaks of the amorphous carbon structure. Diffraction patterns at 2θ values

of approximately 21 and 40 corresponding to (002) and (100) reflection of a turbostratic carbon structure [7]. Both X-Ray diffractograms for MWCNT and f-MWCNT reveal one distinctive peak at 26 degree, which accurately depicts the (002) reflection of graphitic carbon [6]. The peak at 42 degree defining in-plane regularity (100) for both MWCNT and f-MWNCT [6].

Figure 3 shows SEM photograph of: a) F160 and b) f-MWCNT. In Figure 3, we can see that F160 and f-MWCNT have different morphologies that differ in shape and size. F160 characterize spherical shape with a diameter of particles between 1-5 μm, while MWCNT Figure 3b has a straw-like shape with particles length from 3–5 μm.

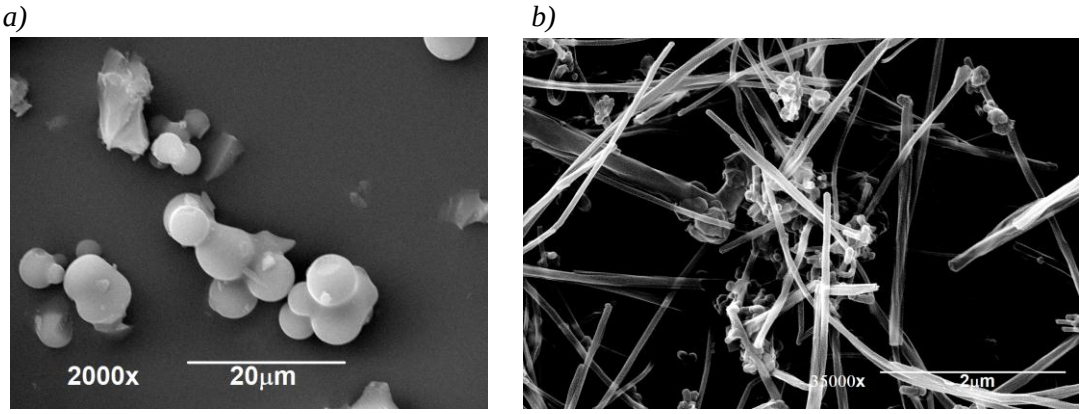

Figure 3 *SEM of a) F-160 and b) f-MWCNT*

CONCLUSION

In this paper they were compared two carbon-based materials: F160 and f-MWCNT. Both materials have similar surface groups, dominantly hydroxyl (-OH) and carboxyl (-COOH) functional groups. The main difference in morphology was in the shape and size of the particles. F160 has a spherical shape, while f-MWCNT has a straw-like shape. Using HCT, we can synthesize material from low-cost precursors with abundant content of oxygen-based function groups in one step.

ACKNOWLEDGEMENT

The authors are grateful to the Ministry of Science of the Republic of Serbia for financial support according to the contract with the registration number (451-03-47/2023-01/ 200017).

REFERENCES

[1] Špitalsky Z., Matejka L., Šlouf M., Polym. Compos. 30 (10) (2009) 1378–1387.

[2] Maiti D., Tong X., Mou X., Front.Pharmacol. 9 (2019) 1–16.

[3] Sahoo G. N., Bao H., Pan Y., Chem. Comm. 47 (2011) 5235–5237.

[4] Jung D., Zimmermann M., Kruse A., ACS Sustainable Chem. Eng. 6 (11) (2018) 13877–13887.

[5] Kumar M., Sharma G., Misra C, Mater Sci. Eng. C Mater. Biol. Appl. 89 (2018) 274–282.
[6] Das R., Hamid S. B. A., Md. Ali E., Curr. Nanosci. 11 (1) (2015) 23–35
[7] Gale M., Nguyen T., Moreno M., J. Am. Chem. Soc., 6 (15) (2021) 10224–10233.

30th International Conference Ecological Truth & Environmental Research
20–23 June 2023, Serbia

RETROSPECTIVE OF THE PLANNED ACTIVITIES FOR THE REHABILITATION OF THE DAMAGED AREA OF THE FORMER SURFACE MINE ČUBRIĆ

Hamid Husić[1], Senad Čergić[1*], Vahidin Aganović[1]
[1]Brown Coal Mines "Banovici", 75290 Banovici, BOSNIA AND HERZEGOVINA
[*]*senadcergic@hotmail.com*

Abstract

The period of coal exploitation in the surface mine „Čubrić" lasted from 1977 to 2011. As a consequence of coal mining, large areas of degraded land were created in the excavated area (mine crater) and the area where the tailings material was disposed of. With the completion of the coal mining works in 2011, total areas of degraded land were formed, some of which were partially recultivated during the mining works, in the amount of 3 258 422 m^2. Pursuant to legal regulations, the Mine is obliged to bring such spaces and surfaces to their appropriate purpose and use.

Keywords: rehabilitation, reclamation, disposal, planning.

INTRODUCTION

Brown coal deposit „Banovići" is located in northeastern Bosnia and is one of the largest coal deposits in Bosnia and Herzegovina. There are two production organizational units within the mine, namely: „Surface Coal Mining" Mine and „Underground Coal Mining" Mine. As part of surface exploitation, there are two active surface mines, „Turija" and „Grivice". The third surface mine„ Čubrić" ended its exploitation at the end of 2011. As part of the underground exploitation, the „Omazići" pit is actively working.

The annual production of the Mine is about 1 700 000 t of separated coal, which is distributed for industry, wide and general consumption and about 12 000 000 (m^3 solid masses) overburden (tailings).

Realization of the aforementioned production degrades large areas of land as well as disrupts underground and surface water. Degraded areas of the land make up the excavation area and the area where the tailings material is disposed of.

In this paper will give an overview of the state of the degraded areas of mine „Čubrić" twelve years after the end of exploitation, as well as the planned activities aimed at the final rehabilitation and recultivation of the degraded land.

GENERAL INFORMATION ABOUT SURFACE MINE „ČUBRIĆ"

The surface mine Čubrić belongs to the southern part of the Banovići coal basin. Extraction of overburden and coal in this surface mine was carried out using classic cyclic machinery and the adopted work technology associated with it. Excavation and loading (dredging) of overburden and coal was carried out by cyclic excavators, and transport by

dumper trucks. Overburden disposal during the period of exploitation was carried out in the eastern and western landfills, which gradually moved to the inner ones [1].

Excavated quantities of overburden and coal from opening to the end of exploitation

From the annual reports on the realized production at the „Čubrić" surface mine, obtained from the "Mining Technical Preparation" service, the total amounts of overburden and coal that were mined in the period from the moment of opening 1977 until the end of coal exploitation in 2011. By comparing the determined and planned amounts of overburden and coal on the one hand and the actual ones, it can be seen that there is a relatively small difference in the amount of coal and a relatively significant difference in the amount of overburden. 492 008 tons of coals were mined, less than the amount of coal planned and determined by the project documentation, or expressed as a percentage of 2.99%. A total of 119 089 015 cubic meters was excavated and deposited at the Čubrić open pit overburden, which is for 13 889 015 (m^3 solid masses) more than the quantities provided for in the project documentation or expressed as a percentage of 13.2%.

Such a large difference between the planned and realized quantities of overburden is the result of:

- errors in the initial data,
- sliding masses from the final slopes,
- temporary disposal of masses in temporary internal landfills.

Table 1 *Projected amounts of overburden and coal at mine „Čubrić"*

Part of the mine	**Coal quantities (tons $_{pit\ coal}$)**	**Amount of overdraft (m^3 $_{solid\ masses}$)**
The central part	14 748 000	92 970 000
Western part	1 700 000	12 200 000
TOTAL:	16 448 000	105 170 000

Contouring of landfill areas at mine „Čubrić"

The planned technology of coal mining and exploitation at mine „Čubrić" until its closure led to the formation of new surfaces with changed morphological, geological, pedological and other characteristics. With the completion of coal mining, surfaces were formed on landfills and the excavated area and the pit crater. The approximate structure of the surfaces at mine „Čubrić", some of which were partially recultivated during mining operations, is presented in Table 2 [2].

Table 2 *Survey of surfaces created at the former Čubrić mine*

Space	**Area (m^2)**
Excavation area mine „Čubrić"	787 365
Eastern part of Ravne	379 007
Western part of internal landfill	1 574 255
North part	517 795
TOTAL AREAS	3 258 422

a) *b)*

Figure 1 *Satellite image mine „Čubrić" in 2011 (a) and (b) 2023*

Display of the current state

During the period of permanent suspension of works on mine „Čubrić", the lowest elevation in the mine crater was 336 m (Figure 1).

By calculating the safety factors of the final slopes, which were calculated using Bishop's and Janbu's methods, the instabilities of the pit crater slopes were determined. Given that the instability of the slopes does not affect the prescribed protection measures, additional work on their stabilization is not recommended, given that the slopes will eventually take on a state of natural balance and stability. In addition, the instability of the slope had an impact on the smaller amount of accumulated water in the pit crater [2].

The excavated area of mine „Čubrić" is 787 365 m^2. A water reservoir with an elevation of 399.72 m and an area of 573 216 m^2 was formed in the pit crater. Technical recultivation has not been carried out on the remaining part of the land outside the water reservoir and it is evident that vegetation has grown on the land [2].

The eastern part of the internal landfill of mine „Čubrić" occupies an area of 379 007 m^2. It consists of a planum and a slope of the landfill. The landfill site is used by the local population for agricultural purposes, so it can be said that biological reclamation has been carried out on this landfill site. The slope of this landfill is due to the existence of groundwater in motion, occupying a natural slope, so work on this part is not possible [3].

The western part of the internal landfill of mine „Čubrić" covers an area of 1 574 255 m^2. Within this part of the landfill, the existence of four plateaus with different elevations is evident. The western part is at an altitude of 440 m, the eastern part at 425 m, the southern part at 435 m and the northern part at 420 m. The local population uses most of the landfill for agricultural purposes, so it can be said that biological reclamation has been carried out on certain segments of this landfill.

The northern part of the internal landfill occupies an area of 517 795 m^2. It consists of a planum and a slope of the landfill. The landfill site is used by the local population for agricultural purposes, so it can be said that biological reclamation has been carried out on this landfill site [4] (Figure 3). The landfill slope is located on the northern side above the Banovići-Lukavac road, so work on this part is not possible (Figure 2).

Figure 2 *View of the western and northern disposal area of the former Čubrić mine*

Figure 3 *Presentation of planum and landfill slopes that have been biologically recultivated by agricultural works on them*

DIRECTIONS FOR FURTHER ACTIVITIES IN THE REMEDIATION OF THE DAMAGED SPACE

In accordance with the legal provision, project documentation was created, which defined that the overburden from mine „Turija" should be disposed of on the premises of mine „Čubrić". The approved project defined that overburden transport and disposal should be carried out by a combined complex that includes discontinuous transport of overburden to the crushing plant, followed by continuous transport by rubber conveyors to the dumper [5].

According to the project documentation, overburden disposal will be done in two stages: the first phase, the tailings will be disposed of in the crater of the mine, that is, from the bottom of the mine (the lowest level...) to the level of 400 m above sea level, where the installation of the disposal conveyor and dumper was carried out at the level of 384 m. Disposal of overburden and filling of the disposal area will be carried out using continuous technology during the first phase in two stages. The figure 5 shows the layout of the landfill at the end of the first phase of development with the development stages marked and the directions of rotation of the landfill conveyors, which are placed at the level of 384 m [5].

The second phase of disposal and landfill development takes place in three stages. Disposal will be done in the deep part of the floor 420/400 m and the upper part of the floor 420/436 m.

After the planned disposal works are implemented, project documentation for rehabilitation, technical and biological reclamation will be prepared. The Figure 5 shows the appearance of the disposal site and the disposition of the equipment engagement at the end of

the third stage of the second phase, the completion of disposal up to the level of 436 meters above sea level and leaving space for slag and ash at the level of 420 m above sea level [5].

Figure 4 *Current state of works in the area of the former Čubrić mine*

a)

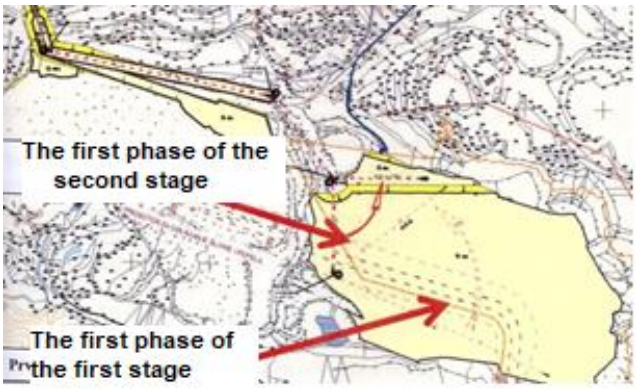

b)

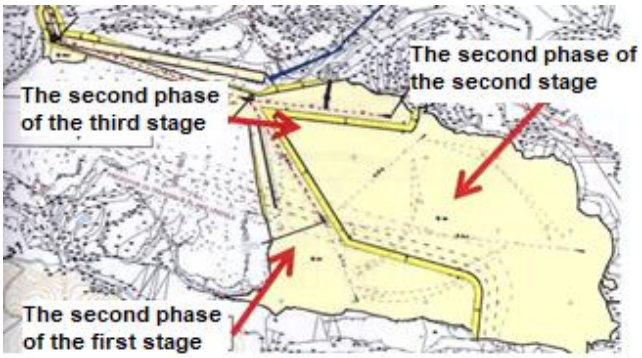

Figure 5 *Projected state of disposal by stages*

CONCLUSION

As a consequence of the surface method of exploitation at the BMC Banovići site, external and internal overburden disposal sites are formed and large craters remain in the exploitation areas. These areas, that is, the so-called „mining lands" are recultivated after the end of exploitation, that is, the land is brought to some other purpose.

The provisions of the Law on Environmental Protection regulate, among other things, the preservation, protection, restoration of the ecological quality and capacity of the environment, measures and conditions for the management, preservation and rational use of natural resources.

According to the provisions of the Law on Mining of the Federation of Bosnia and Herzegovina, after obtaining a license to stop the exploitation of mineral raw materials, the company must carry out the final rehabilitation of the land and recultivation of the environment and remove the consequences caused by the performance of mining works.

Accordingly, this paper analyzed a set of engineering and technical measures that have the task of integrating the damaged area into the natural environment and recultivating it.

The research refers to the factual situation on the ground, whereby the techno orography of the degraded area would be regulated.

The development projects of the local community and the Mine could lead to changes in the techno-orography of the treated terrain for reclamation. The changes would relate primarily to planning for the disposal of slag from the future thermal power plant Banovići. Those possibilities are in the testing phase and will be regulated by special project solutions.

Also, the deepening of active surface mines as well as the constant increase in diesel fuel prices require a change in overburden transport technology. These changes include the transition to the continuous transport of overburden by rubber bands from the Turija surface mine to the area of the former Čubrić open pit mine, and in this way the overburden from the Turja mine will be used to rehabilitate the area of the former Čubrić mine.

REFERENCE

[1] DRP druge etape razvoja PK Turija RMU Banovići Primjena kombinovanog sistema za otkrivku sa polustacionarnim drobiličnim postrojenjima, transporterima sa gumenom trakom Rudarski institut Tuzla d.d., Tuzla (2013).

[2] DRP trajna obustava rudarskih radova na eksploataciji uglja PK „Čubrić" RMU Banovići, Univerzitet u Tuzli, Rudarsko geološko građevinski fakultet, Tuzla, mart (2012).

[3] Čergić M., Husić H., Redžanović Dž., *et al*., Proceedings of the XV Balkan Mineral Processing Congress, 12–16 June, Sozopol, Bulgaria (2013) 974–978.

[4] Čergić S., Husić H., Proceedings of the 27th Internacional Conference Ecological Truth and Environmental Research Eco TER'19, 18–21 June, Bor, Serbia (2019) 166–171.

[5] DRP odlaganje otkrivke sa PK "Turija" u prostor PK "Čubrić" RMU "Banovići" primjenom tračnog transporta otkrivke" Rudarski institut Tuzla d.d., Tuzla (2018).

30th International Conference Ecological Truth & Environmental Research

2023

Student section

Editor
Prof. Dr Maja Nujkić

ENVIRONMENTAL AND HEALTH RISK OF CO_2 IN INDOOR ENVIRONMENTS

UTICAJ POVIŠENIH KONCENTRACIJA CO_2 NA LJUDSKO ZDRAVLJE U ZATVORENIM PROSTORIJAMA

Students: Ana Smiljković, Isidora Sujić

Mentor: Maja Nujkić*

University of Belgrade, Technical Faculty in Bor, V.J. 12, 19210 Bor, SERBIA

*mnujkic@tfbor.bg.ac.rs

Abstract

This paper, indoor CO_2, aims to describe the problems associated with poor air quality and to demonstrate the potential of CO_2 to purify indoor air while generating a renewable carbon stream that can replace conventional carbon sources as a building block for chemical production, contributing to circular economy. The work includes concrete examples and studies on the presence, guidelines and standards related to CO_2 concentrations. There are large fluctuations in the amount of CO_2 concentration in closed spaces, the paper presents analyzes related to the monitoring of CO_2 concentration in the school environment, offices and underground transportation. The research showed that in Spain, all classrooms under investigation had periods with higher CO_2 concentrations than the French, Portuguese and British groups. Analyzes of office space have yielded data that the indoor concentration of CO_2 in offices is often between two and three times higher than the atmospheric concentration of CO_2. Underground public transport systems make up a large percentage of the urban infrastructure of more developed countries. During the use of underground transport with inadequate ventilation, residents are exposed to CO_2 concentrations. In other experiments, subjects were exposed to CO_2 concentrations of 3000 ppm for 2-3 hours, from 1000 to 2500 ppm, and up to 1400 ppm for 8 hours. In addition to some physiological effects such as diastolic blood pressure, all studies showed similar results, with significant reductions in cognitive function and decision-making ability for exposure CO_2 levels of 945–1400 ppm. Furthermore, exposure to CO_2 concentrations above 2000–3000 ppm, together with other bio effluents, can cause health symptoms (headache, drowsiness, fatigue) that reduce cognitive performance. All analyzes deal with the comparison of results from several areas as well as the presentation of the importance of the ventilation system as a system for reducing the amount of CO_2 concentration in closed spaces.

Various technological achievements offer the possibility of solving and reducing this problem, while the decisive factor towards minimizing this problem is the development of human awareness of the surrounding environment and the application of everyday short-term solutions (for example, choosing a means of transport that does not affect CO_2 emissions), which will eventually condition long-term results.

Keywords: climate change, air pollutants, air quality, CO_2 capture, indoor spaces

ACKNOWLEDGEMENT

The research presented in this paper was financial supported by the Ministry of Education, Science and Technological Development of the Republic of Serbia, within the funding of the scientific research work at the University of Belgrade, Technical Faculty in Bor, according to the contract with registration number 451-03-47/2023-01/ 200131.

REFERENCES

[1] Shriram S., Ramamurthy, K., Ramakrishnan, S., Build. Environ. 149 (2019) 58–67. https://doi.org/10.1016/j.buildenv.2018.12.015.

[2] Becerra J. A., Lizana J., Gil M., *et al*., J. Clean. Prod. 242 (2020). https://doi.org/10.1016/j.jclepro.2019.118420.

[3] López L. R., Dessì P., Cabrera-Codony A., *et al*., Sci. Total Environ. 856 Part 2 (2023) 159088, https://doi.org/10.1016/j.scitotenv.2022.159088.

ANTHROPOGENIC MERCURY IN THE ENVIRONMENT: GLOBAL EMISSIONS AND RECYCLING POSSIBILITIES

ŽIVA U ŽIVOTNOJ SREDINI: GLOBALNE EMISIJE I MOGUĆNOST RECIKLAŽE

Student: Avram Kovačević*

Mentor: Uroš Stamenković

University of Belgrade, Technical Faculty in Bor, V.J. 12, 19210 Bor, SERBIA

*akovacevic@tfbor.bg.ac.rs

Abstract

Mercury is a toxic heavy metal that is released into the environment through anthropogenic activities such as metal production, stationary combustion, and waste disposal. The accumulation of mercury in the environment can have a major negative impact on both human health and the ecosystem. The release of mercury into the environment has been increasing over the last few decades, resulting in a significant accumulation in air, water, and soil leading to the long-term contamination of food chains. The bioaccumulation of mercury in seafood has led to recommendations for limiting consumption, particularly during pregnancy. Because of its negative influence on public health, the recycling of mercury-containing products has become an important topic in environmental research.

An estimated 2220 tons of mercury are emitted annually from different anthropogenic sources. Research has shown that the burning of fossil fuels (primarily coal) is the largest single source of emissions from human activities, accounting for about 45% of the total anthropogenic emissions. Small-scale gold mining was responsible for about 18%, with industrial gold production accounting for an additional 5–6% of global emissions from human activities. Other mining and metal production activities are responsible for about 10% of global anthropogenic releases to the atmosphere. Emissions from waste burning and product-use sources could be higher than the 7.5% of global emissions.

Safe disposal and recycling methods for mercury-containing products are available. These methods involve the proper collection, handling, and treatment of waste to prevent the release of mercury into the environment. Some of the methods are applicable on an industrial scale. Recycling mercury-containing products also helps to reduce the need for primary mercury, which is obtained through mining. This study will review the current situation of anthropogenic mercury in the environment. Methods for mercury recovery and proper disposal are discussed along with recommendations for safe and effective management of this hazardous material.

Keywords: mercury, recycling, waste management, public health, mercury processing

ACKNOWLEDGEMENT

The research presented in this paper was done with the financial support of the Ministry of Science, Technological Development and Innovation of the Republic of Serbia, within the funding of the scientific research work at the University of Belgrade, Technical Faculty in Bor, according to the contract with registration number 451-03-47/2023-01/200131.

REFERENCES

[1] Pacyna E. G., Pacyna J. M., *et al*., Atmos. Environ. 44 (2010) 2487–2499.

[2] Pacyna E. G., Pacyna J. M., *et al*., Atmos. Environ. 40 (22) (2006) 4048–4063.

[3] Anselm O. H., Cavour O., *et al*., Environ. Monit. Assess. 193(7) (2021).

[4] Schuster P., Krabbenhoft D., *et al*., ES&T 36 (11) (2002) 2303–2310.

[5] Aucott M., McLinder M., *et al*., J. Air Waste Manag. Assoc. 53 (2) (2003) 143–151.

[6] Haridasn K., Aswin R., *et al*., Int. Res. J. Eng. Technol. 3 (1) (2016) 1315–1319.

[7] Srivastava RK., Hutson N., *et al*., ES&T 40 (5) (2006) 1385–1393.

[8] Sadasiva K., Rayar S., *et al*., J. Pharm. Bioallied. Sci. 9(2017) 79–81.

THE INFLUENCE OF COOLING RATE ON MECHANICAL PROPERTIES AND MICROSTRUCTURE OF C45 CARBON STEEL

UTICAJ BRZINE HLAĐENJA NA MEHANIČKE I STRUKTURNE OSOBINE C45 UGLJENIČNOG ČELIKA

Student: Petar Milanović*

Mentors: Uroš Stamenković, Avram Kovačević

University of Belgrade, Technical faculty in Bor, VJ 12, Bor, SERBIA

*p.milanovic2521@gmail.com

Abstract

Carbon steels, besides tool steels, stainless steels and cast iron are one of the most used materials in the world. Medium-carbon steels are used for different applications where a good combination of ductility and strength are required i.e. for various heavy-duty machinery, tractors and mining equipment. C45 steel is often used in quenched and tempered state for screws, forgings, wheel tyres, shafts, sickles, axes, knives, wood working drills, hammers, etc. Different heat treatments have a great influence on the mechanical, thermophysical and structural properties of C45 carbon steel. By combining different types of heat treatment, it is possible to obtain a range of different structures. Steels in general, including C45 steel, are very sensitive to the cooling rate after heating at high temperatures. With different cooling rates, different properties of the steel can be obtained, along with different structures. In this case, it is very useful to have continuous cooling transformation (CCT) diagrams, which are widely used when heat treating steels and represent which type of phase will occur in a material as it is cooled at different cooling rates.

The aim of this paper was to investigate the influence of cooling rate on the mechanical properties and microstructure of C45 carbon steel. The investigation was carried out in several steps. Firstly, the samples of C45 steel were normalized at 900 °C for one hour in order to remove the fabricated state. After normalization heat treatment, the samples of C45 steel were cut to adequate dimensions. Subsequently, the samples were heated in the austenite region at a temperature of 900 °C for 30 minutes and cooled at five different rates. Cooling was done from the slowest to the fastest cooling rate: in the furnace, on still air, quenching in oil, quenching in water, and quenching in a 20% NaCl solution. After every step, hardness was measured, and tensile strength was calculated from hardness values. Metallographic studies were performed on every sample and analysed. Results show an increase in hardness values and tensile strength values with the increase in cooling rate, which is in agreement with the literature data. The microstructure of the differently cooled samples changes from the typical ferrite-pearlite microstructure after slow cooling to the martensitic microstructure after quenching.

Keywords: C45 steel, heat treatment, microstructure, cooling rate

ACKNOWLEDGEMENT

The research presented in this paper was done with the financial support of the Ministry of Science, Technological Development and Innovation of the Republic of Serbia, within the funding of the scientific research work at the University of Belgrade, Technical Faculty in Bor, according to the contract with registration number 451-03-47/2023-01/200131.

REFERENCES

[1] Askeland D. R., Fulay P. P., Essentials of Materials Science and Engineering Second Edition, Cengage Learning, Toronto (2008), p.493, ISBN: 0495244465.

[2] Nishimura N., Murase K., Onda T., *et al*., Evaluation of dynamic collapse in thin-walled composite members. Journal of Physics: Conference Series, 451 (2013).

[3] Ivanov S., Stanojević B. Termička obrada metala, Tehnički fakultet u Boru, Bor (2018), ISBN: 978-86-6305-004-4.

[4] Vidojević N. Termička obrada metala, Tehnološko-metalurški fakultet, Belgrade (1981).

[5] Lakhtin Y. Engineering, physical metallurgy and heat-treatment, English translation from Russian by Nicholas Weinstein, Mir Publishers, Moscow (1983), ISBN: 5030017410.

[6] World Material, Available on the following link: https://www.theworldmaterial.com/1-0503-material-c45-steel/.

[7] Jovanović M., Lazić D., Adamović N., *et al*., Mašinski materijali, Mašinski fakultet u Kragujevcu, Kragujevac, 2003, ISBN: 86-80581-55-0.

[8] ASM Handbook: Volume 4: Heat Treating, ASM International, Cleveland (1991) ISBN: 0871703793.

[9] Ray B. C., Prusty R., K., Nayak D., Phase Transformations and Heat Treatments of Steels, CRC Press, Milton (2020) ISBN: 0367028689.

[10] Zordao L. H., Oliveira V. A., *et al*., ICHMT, 140 (2019), 807–818.

[11] Totten G. E., Bates C. E., Clinton N. A., Handbook of quenchants and quenching technology, ASM International, Cleveland (1993), ISBN: 087170448X.

[12] SIJ Group, Availavle on the following link: https://steelselector.sij.si/data/pdf/C45.pdf.

AIR POLLUTION WITH CARCINOGENIC SUBSTANCES

ZAGAĐENJE VAZDUHA KANCEROGENIM MATERIJAMA

Student: Milica Denić*
Mentor: Jelena Kalinović
University of Belgrade, Technical Faculty in Bor, V.J. 12, 19210 Bor, SERBIA
*milicaddenic@gmail.com

Abstract

Carcinogenic substances, mixtures or agents are substances that can cause cancer or increase the risk of cancer. Air quality is a basic indicator of the general quality of the environment. Air pollution in large cities and industrial centres is not only a local but also a regional and global problem. Air pollution can directly affect human health in many ways depending on various factors such as: time of exposure, the intensity of pollution, the type of pollutants that people are exposed to, as well as the general health status of the population. Different pollutants can affect the human body in many ways by changing the normal functioning of different parts of the body. The rates of heart attacks, respiratory diseases and lung cancer are significantly higher in the population exposed to polluted air, compared to those living in a relatively cleaner environment. In Hebei province, one of the most polluted provinces in China, during the heating and non-heating seasons, the concentrations of chromium, arsenic, and cadmium exceeded the levels proposed by the World Health Organization (arsenic – 0.02 μg/g, hexavalent chromium 0.01 μg/g, cadmium 1.3 μg/g). The results indicate that the elements found in suspended particles originate from coal burning, dust, traffic, iron smelting, oil burning, as well as from other industrial sources. Ferrous metallurgy, oil and coal burning are the dominant sources of chromium, arsenic and cadmium. Arsenic showed the biggest non-carcinogenic and carcinogenic effects, followed by cadmium. The most exposed to risk are children, and the most common way of introducing these heavy metals into the body is by ingestion. It can be concluded that the concentration is significantly increased when it comes to the heating season and that the highest concentration of heavy metals comes from ferrous metallurgy and oil burning, as well as coal burning. All three groups of respondents (children, women and men) are slightly equally exposed to the risk, but children are the most exposed to the risk of cancer. This study also indicated that attention should be paid not only to PM 2.5 quantity, but also to compounds related to PM 2.5, especially heavy metals and metalloids, to reduce health risks in the future.

Keywords: air pollution, PM 2.5, carcinogenic substances, health risk

ACKNOWLEDGEMENT

The authors are grateful to the Ministry of Education, Technological Development and Innovation of the Republic of Serbia for financial support, within the funding of the scientific research at the University of Belgrade, Technical Faculty in Bor (No. 451-03-47/2023-01/200131).

REFERENCES

[1] Canadian Centre for Occupational Health and Safety; *Available on the following link:* https://www.ccohs.ca/oshanswers/diseases/cancer/occupational_cancer.html?fbclid=IwAR3TSaa2fT%20qoYjuxqa6bNSm_EBpP-0beUzv-ElAxAPEaVWV0KK2-Dt7yTfk

[2] Šerbula S., Air quality, aerosol and biomonitoring, Nova science Publishers, Inc., New York (2017), ISBN: 978-1-53610-428-8.

[3] Singh A., Impact of Air Pollutants on Plant Metabolism and Antioxidant Machinery, Chapter 4 *in* Air Pollution and Environmental Health, Editor: Saxena P., Srivastava A., Springer, Delhi (2020) pp. 62–77, ISBN 978-981-15-3480-5.

[4] Li X., Yan C., Wang C., *et al.*, Sci. Total Environ. 806 (1) (2022) 150440.

ACID RAIN AND SMOG – CHEMICAL REACTIONS

KISELE KIŠE I SMOG – HEMIJSKE REAKCIJE

Student: Gordan Mišić*
Mentor: Jelena Kalinović
University of Belgrade, Technical Faculty in Bor, V.J. 12, 19210 Bor, SERBIA
*ggmisic@gmail.com

Abstract

In the last several hundred years, the expansion of fossil fuels consumption and extensive alteration of the biosphere led to a dramatic rise of gases and particle levels in the atmosphere, causing acid rain and smog formation. Acid rain is a natural phenomenon that causes concern and affects environmental problems, such as water and soil acidity, forest declines, biodiversity loss, soil degradation, and building damage. Acid rain is caused by emissions of acid gases (sulfur dioxide and nitrogen oxides) from anthropogenic sources such as coal-burning processes, cars, homes, industries, etc, as well as from natural sources, such as volcanic eruptions, and organic decomposition. Acid gases react in the atmosphere with atmospheric water resulting the acid rain. The effects of acid rain are huge, due to their influence on every aspect of our planet. Under the influence of acid rain, heavy metals are leached into water streams and lakes, which is toxic to many aquatic species. The negative impact of acid rain on plants is reflected through reduced photosynthesis and growth, as well as damaging the delicate plant's root system. The harmful effects of acid rain on the environment could be reduced by implementing adequate measures, such as the usage of high-quality equipment (chimneys), and scrubbing the waste gases to reduce their concentration in the air. Many chemicals that are included in the formation of acid rain also form smog. The term smog represents the combination of the words smoke and fog. Smog is formed through chemical reactions in the atmosphere between sulfur dioxide, nitrogen oxides, atmospheric water, and under the influence of sunlight. Some of its components are emitted from natural sources, but the majority are from anthropogenic sources, and some are the product of reactions that occur in the lower layers of Earth's atmosphere, such as the troposphere. Smog formation is strongly affected by meteorological conditions, influencing the rate of a chemical reaction or the transport of chemicals. Smog gives the sky a hazy orange color and reduces visibility, but the biggest problem of smog occurrence is the toxicity of fine particulate matter and ozone, as well as the primary compounds that lead to their formation (nitrogen oxides, volatile organic compounds, and sulfur dioxide).

Fine particulate matters such as PM_2, PM_{10}, and NO_x cause concern for children and adolescents' health, because they have lower lung capacity and weaker immune systems. They spend more time outside, and pollutants from the air have a much higher influence on them

than on adults. Some of the solutions for this problem can be coal burners with environment-friendly energy sources, free public transport, ecological education, development of the municipal heating network, and limiting car traffic in city centers.

Keywords: acid rain, smog, $PM_{2.5}$, PM_{10}, NO_x, SO_2

ACKNOWLEDGEMENT

The authors are grateful to the Ministry of Education, Technological Development and Innovation of the Republic of Serbia for financial support, within the funding of the scientific research at the University of Belgrade, Technical Faculty in Bor (No. 451-03-47/2023-01/200131).

REFERENCES

[1] Sivaramanan S., Environmental Officer, Environmental Impact Assessment unit, Environmental Management and Access division, Central Environmental Authority, Battaramulla, Sri Lanka. (2015) doi: 10.13140/RG.2.1.1321.4240/1

[2] Geddes A. J., Murphy G. J., Metropolitan Sustainability (2012) 205–230.

[3] Góra D., Ecological Engineering & Environmental Technology 22 (1) (2021) 60–73.

MEDICAL WASTE MANAGEMENT

UPRAVLJANJE MEDICINSKIM OTPADOM

Student: Milica Denić*
Mentor: Ana Radojević
University of Belgrade, Technical Faculty in Bor, V.J. 12, 19210 Bor, SERBIA
*milicaddenic@gmail.com

Abstract

The World Health Organization (WHO) has defined medical waste as waste generated by various health care activities, ranging from used needles and syringes to soiled dressings, body parts, diagnostic samples, blood, chemicals, pharmaceuticals, medical devices and radioactive materials. This type of waste represents a heterogeneous mixture of municipal and hazardous waste. The dangerous faction of the medical waste is divided into following groups: sharps waste, infectious waste, pathological waste, pharmaceutical waste, cytotoxic waste, chemical waste, and radioactive waste. However, only 15% of medical waste should be classified as hazardous – potentially infectious, toxic and radioactive waste, as well as waste that could cause other environmental and health risks. According to the WHO, between 75% and 90% of the waste produced by health-care providers is comparable to domestic waste and usually called "non-hazardous" or "general health-care waste". It comes mostly from administrative, kitchen and may also include packaging waste and waste generated during maintenance of health-care buildings. Non-hazardous fraction of the medical waste (food, paper, glass, clothes, etc.) could be disposed at sanitary landfills or recycled. However, if non-hazardous medical waste is mixed with hazardous, it must be classified and treated as hazardous medical waste. At hospitals and other healthcare facilities, waste is generally sorted into color-coded bins, which denote different waste streams and waste management.

Pretreatment of medical waste mainly consists of mechanical processes such as shredding, grinding, mixing, liquid-solid separation, agitation, pelletization, and crushing. The aim of pretreatment is to decrease the total volume of the waste but does not eliminate infectious pathogens. Steam sterilization, microwaving, reverse polymerization, dry heat treatment, carbonization, converter biotechnology, incineration, pyrolysis, gasification, irradiation, chemical disinfection, immobilization, landfilling, nanotechnology, and thermal plasma are technologies used for the treatment of solid medical waste.

However, incineration, including waste-to-energy, pyrolysis, plastic chemical recycling and related technologies, can be harmful to human health and the environment. Some recycling companies refuse to collect and recycle waste from hospitals, primarily from fear of contaminated materials. Carcinogenic, mutagenic, toxic, or hazardous substances should be

excluded from products and services used in healthcare, and materials containing hazardous chemicals should not be recycled to prevent contamination of new products.

The volume of waste generated by the healthcare sector recently increased as a result of the COVID-19 outbreak due to intensive use of personal protection equipment. The disinfection technologies — incineration, chemical and physical processes, could effectively treat COVID-19 medical waste. A large amount of medical waste mainly consists of polyethylene, polypropylene, polystyrene, polyethylene terephthalate, and nylon, which can be converted into valuable energy products like oil, gas and char through the pyrolysis process. For example, Wang *et al*. proposed upcycling of medical plastic waste into activated carbon for CO_2 capture as part of sustainable "waste-to-resource" and zero-waste strategies.

Advanced healthcare waste-related activities must be implemented and monitored at local, regional and national levels. Dharmaraj *et al*. propose that current methods must be examined and treated to save environment and human health.

Keywords: medical waste, waste management, health care, recycling

ACKNOWLEDGEMENT

The authors are grateful to the Ministry of Education, Technological development and Innovation of the Republic of Serbia for financial support, within the funding of the scientific research at the University of Belgrade, Technical Faculty in Bor (No. 451-03-47/2023-01/200131).

REFERENCES

[1] World Health Organization (WHO), Safe management of wastes from health-care activities, 2nd Edition, Geneva, Switzerland, ISBN: 978-92-4-154856-4.

[2] Sustainable healthcare waste management in the EU Circular Economy model (2020), *Available on the following link:* https://noharm-europe.org/documents/sustainable-healthcare-waste-management-eu-circular-economy-model.

[3] Windfeld E. S., Brooks M. S.-L., J. Environ. Manage. 163 (2015) 98–108.

[4] Mazzei G. H., Specchia S., J. Environ. Chem. Eng. 11 (2023) 109309.

[5] Dharmaraj S., Veeramuthu A., Pandiyan R., *et al*., Chemosphere 275 (2021) 130092.

[6] Wang J., Li S., Deng S., *et al*., Curr. Opin. Environ. Sci. Health 33 (2023) 100470.

ENVIRONMENTAL POLLUTION BY PET PACKAGING

ZAGAĐENJE ŽIVOTNE SREDINE PET AMBALAŽOM

Student: Gordan Mišić*

Mentor: Ana Radojević

University of Belgrade, Technical Faculty in Bor, V.J. 12, 19210 Bor, SERBIA

*ggmisic@gmail.com

Abstract

Plastics as highly versatile materials have been a part of the prosperity of modern societies. The series of applications, starting with packaging and construction to transport and agriculture is enabled by its high usefulness. Polyethylene terephthalate (PET) is one of the most used polyester for production of bottles, because of characteristics such as transparency, lightweight, gas and water barrier properties, and impact strength. PET bottles accounted for about 67% of beverage packaging in 2015 resulting in accumulation of 141 Mt of waste on the global scale. The single-serve beverage packaging in the US in 2021 was 44.7% of the bulk waste, which represented 12% of global solid waste. Nowadays, the non-selective use of PET products is causing enormous environmental pollution since these kinds of polymers take a very long time to be broken down naturally. The weight of the plastic is not the primary problem because of the much higher volume, which lowers the available space and raises the need for opening the new landfills. The formation of "the Great Pacific Garbage Patch" – an island formed by the surface accumulation of plastic waste in the Pacific Ocean, represent visual, as well as environmental problem for the marine life.

One of the biggest problems of PET is the "Linear Economy Model" which is based on the single use of plastic products. On the other hand, the European Strategy for Plastics of the "Circular Economy Model", adopted in January 2018, is designed to reduce the impact of the extensive exploration of resources through sustainable usage of materials. According to the Strategy, all the plastic used, throughout the design to manufacturing and packaging phases, needs to be recyclable by 2030. However, the multiple recycling of plastics showed that there is a certain number of recycling loops after some mechanical properties of the plastic cannot be maintained. The highest application-specific quality requirements are associated with food-grade recycled materials, such as bottle-to-bottle recycling of PET.

PET by nature is considered safe and inert, but under exposure to ozone and solar radiation its structure will change resulting in emission of microscopic particulates, i.e. microplastics. Today, microplastics are found in every part of the Planet, at the highest parts – like in snow on the Mount Everest to deep-marine ecosystems. Thought the aquatic food chain, soli pollution and drinking water, microplastics could get to humans. Also, the presence of microplastic in human placenta was reported recently.

One way to combat the problem of huge quantities of PET waste is incineration with the benefits like more space at landfills and utilization of energy released in the process. The downside of the method is emission of air pollutants.

The promising alternative to petro-plastics is bio-based plastics obtained from biomass, such as corn and sugar cane, which are not disposed of or recycled but instead composted. However, the recycling of PET is most desired method. Many countries are trying to reduce the usage of PET and other plastic and enhance the recycling rate. The returnable bottle system is a sustainable way to reduce the amount of disposable plastic waste.

Keywords: PET, waste management, environmental pollution, microplastics

ACKNOWLEDGEMENT

The authors are grateful to the Ministry of Education, Technological Development and Innovation of the Republic of Serbia for financial support, within the funding of the scientific research at the University of Belgrade, Technical Faculty in Bor (No. 451-03-47/2023-01/200131).

REFERENCES

[1] Vlasopoulos A., Malinauskaite J., Zabnienska-Gora A., *et al*., Energy 277 (2023) 127576.

[2] Shamsuyeva M., Endres H., JCOMC 6 (2021) 100168.

[3] Torres-Huerta M. A., Palma-Ramírez D., Domínguez-Crespo A. M., *et al*., Eur. Polym J. 61 (2014) 285–299.

[4] Benyathiar P., Kumar P., Carpenter G., *et al*., Polymers 14 (2022) 2366.

[5] Djapovic M., Milivojevic D., Ilic-Tomic T., *et al*., Chemosphere 275 (2021) 130005

[6] Miranda N. M., Sampaio J. M., Tavares B. P., *et al*., Sci. Total Environ. 796 (2021) 148914

COPPER CORROSION IN ARTIFICIAL ACID RAIN SOLUTION IN PRESENCE OF 5-PHENYL-1-TETRAZOLE

KOROZIJA BAKRA U RASTVORU VEŠTAČKIH KISELIH KIŠA U PRISUSTVU 5-FENIL-1-TETRAZOLA

Student: Marija Stanković*

Mentor: Ana Simonović

University of Belgrade, Technical Faculty in Bor, V.J. 12, 19210 Bor, SERBIA

*stankovicmarija829@gmail.com

Abstract

This paper focuses on the effects of acid rain on copper surface and the inhibitory properties of 5-phenyl-1-tetrazole in this case. Acid rain is one of the major problem today. The composition of acid rain as it is, leads to a highly aggressive impact on infrastructure, plant life, and animal life. Laboratory experiments were conducted using a solution of artificial acid rain, prepared with Na_2SO_4, $NaHCO_3$, and $NaNO_3$, while the acidity of the solution was adjusted to pH 3,2 using a 0,2M H_2SO_4. Special attention was given to the acid rain solution with the addition of chloride ions in the form of 0,5M NaCl, which revealed that its presence further increases the corrosive effects on copper surface.

Assuming that 5-phenyl-1-tetrazole would be a good inhibitor under these circumstances, cyclic voltammetry (CV), open circuit potential (OCP), and linear sweep voltammetry (LSW) were performed. The investigations demonstrated that 5-phenyl-1-tetrazole behaves very effectively as an inhibitor in this environment. When the acid rain solution came into contact with the copper surface, pitting corrosion occurred, which is highly damaging and can cause significant issues. Therefore, it is necessary to reduce it to a minimum in an economical and sustainable way. When using organic substances, it is crucial to pay attention to the concentrations and extent of their use due to their toxic effects on the environment. At very low concentrations, in this case 10^{-3}M, 5-phenyl-1-tetrazole yields very good results. In the solution of artificial acid rain, in the presence of the inhibitor 5-phenyl-1-tetrazole, the inhibition efficiency was 92,5%, while in the solution of artificial acid rain with the addition of chloride ions, in the presence of the same inhibitor, the inhibition efficiency was 88,36%. Therefore, based on the previous investigations, we can conclude that 5-phenyl-1-tetrazole would be a suitable inhibitor for protecting copper surface from external factors, specifically acid rain.

Keywords: acid rains, 5-phenyl-1-tetrazole, copper corrosion.

ACKNOWLEDGEMENT

The authors are grateful to the Ministry of Education, Technological development and Innovation of the Republic of Serbia for financial support, within the funding of the scientific research at the University of Belgrade, Technical Faculty in Bor (No. 451-03-47/2023-01/200131).

REFERENCES

[1] Simonović A., Tasić Ž., Radovanović, M., *et al*., ACS Omega 5 (2020) 12832–12841.

[2] Zucchi F., Trabanelli G., Fonsati M., Corros. Sci. 38 (1996) 2019–2029.

[3] Tan B., Zhang S., Liu H., *et al*., J. Taiwan Inst. Chem. Eng. 102 (2019) 424–437.

[4] Sherif E. M., Erasmus R. M., Comins J. D., Journal of Applied Electrochemistry 39 (2009) 83–91.

[5] Sherif E. M., Erasmus R. M., Comins J. D., Corros. Sci. 50 (2008) 3439–3445.

[6] Szocs E., Vastag Gy., Shaban A., *et al*., Corros. Sci. 47 (2005) 893–908.

[7] Subramanian R., Lakshminarayanan V., Corros. Sci. 44 (2002) 535–554.

Author index

L

Lj

M

N

O

P

R

S

Š

T

U

V

Z

Ž

Authors are responsible

for the content of their papers.

Gold Donor of the Conference

eco.tfbor.bg.ac.rs ISBN 978-86-6305-137-9 tfbor.bg.ac.rs